Eastern Economy Edition

REFRIGERATION *and* AIR CONDITIONING

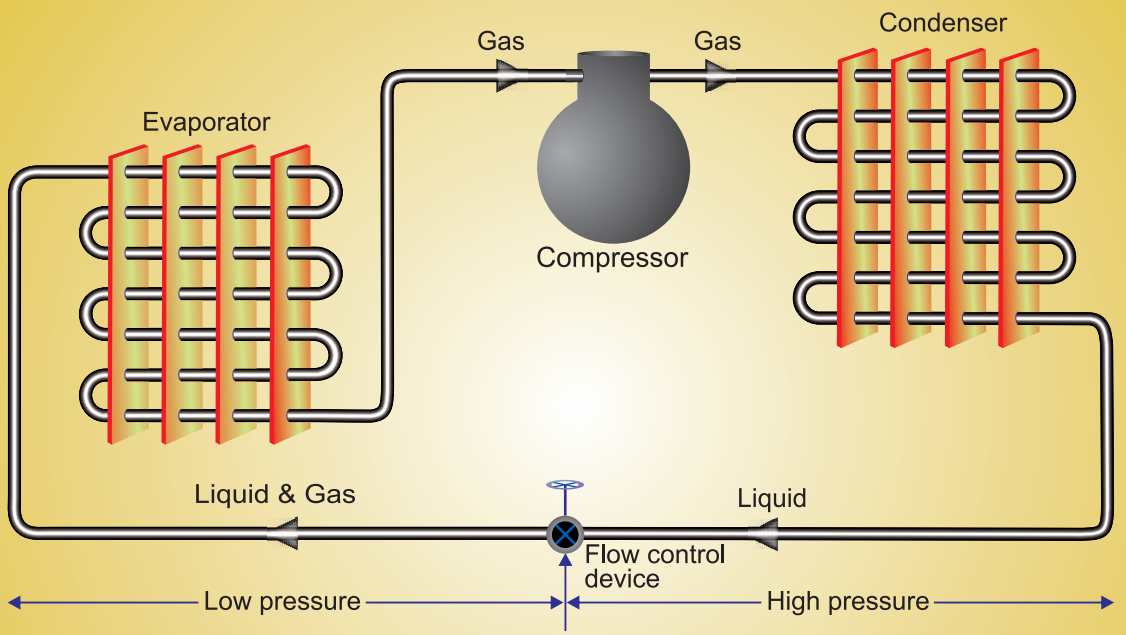

RAMESH CHANDRA ARORA

REFRIGERATION AND AIR CONDITIONING

About the Author

Late (Dr.) Ramesh Chandra Arora served as Professor of Mechanical Engineering at Indian Institute of Technology Kharagpur from 1987 to 2005. He received his B.Tech. and M.Tech. degrees in mechanical engineering from Indian Institute of Technology Kanpur in 1967 and 1969, followed by a Ph.D. (Fluid Mechanics and Heat Transfer) in 1975 from Case Western Reserve University, Cleveland, Ohio, USA. His research areas included fluid mechanics, heat transfer, refrigeration and air conditioning, alternative refrigerants and thermodynamic cycles to highlight a few.

Professor Arora had patents pending for "Design of facility for generation of mono-disperse test aerosols with size control", "Design of low temperature drying system for seed grains", and "A novel methodology of energy optimization for variable-air-volume air conditioning systems".

Professor Arora also held several administrative assignments during his 30 years of tenure at Indian Institute of Technology Kharagpur (1975–2005). These included Deputy Director (Acting); Founder member and Head of Department, School of Medical Science and Technology; Dean of Students Affairs; Chairman, Hall Management Committee; Coordinator, Master's programme in Medical Science and Technology; Professor-in-Charge, Refrigeration and Air Conditioning Laboratory of Mechanical Engineering Department; Chairman, Undergraduate Programme Evaluation Committee Mechanical Engineering Department; Coordinator, Postgraduate and Research Committee of Mechanical Engineering Department; Faculty Advisor, Mechanical Engineering Society of Mechanical Engineering Department.

Professor Arora was a highly respected subject matter expert in academia and industry alike. A few of his responsibilities and associations included: Member, National Advisory Committee of ISHTM-ASME, Joint Heat and Mass Transfer Conference; Member, Engineering Science Committee of Council of Scientific and Industrial Research, New Delhi, Govt. of India; Member, Cryogenics Committee of the Department of Science and Technology, New Delhi, Govt. of India; Reviewer: J. of Institution of Engineers; Reviewer: Indian J. of Engineering and Material Science, CSIR, New Delhi; Member, Board of Governors, Regional Engineering College, Durgapur; Member, Expert Committee to suggest improvement in operation of cold storages, Govt. of West Bengal.

Professor Arora was also the recipient of several outstanding teacher awards, national scholarships, merit awards, graduate fellowship. He is credited with 91 research publications, 8 technical reports, 19 industrial projects and 3 pending patents. He guided 12 researchers towards their Ph.D. degrees, and 29 students towards their M.Tech. degrees, apart from being a constant anchor and mentor for numerous undergraduate students across departments.

REFRIGERATION AND AIR CONDITIONING

RAMESH CHANDRA ARORA
Formerly Professor
Department of Mechanical Engineering
Indian Institute of Technology Kharagpur

PHI Learning Private Limited
New Delhi-110001
2010

Rs. 495.00

REFRIGERATION AND AIR CONDITIONING
Ramesh Chandra Arora

ISBN-978-81-203-3915-6

Published by Asoke K. Ghosh, PHI Learning Private Limited, M-97, Connaught Circus, New Delhi-110001 and Printed by Rajkamal Electric Press, Plot No. 2, Phase IV, HSIDC, Kundli-131028, Sonepat, Haryana.

Contents

Preface

The science and practice of creating controlled thermal conditions, collectively called refrigeration and air conditioning, is an exciting and fascinating subject that has wide-ranging applications in food preservation, chemical and process industries, manufacturing processes, cold treatment of metals, drug manufacture, ice manufacture and above all in areas of industrial air conditioning and comfort air conditioning. The subject of refrigeration and air conditioning dates back to centuries when refrigeration was achieved by natural means such as the use of ice or evaporative cooling. Refrigeration, as it is known these days, is produced by artificial means. Based on the working principle, the present-day refrigeration systems can be classified into (i) mechanical vapour compression refrigeration systems, (ii) absorption refrigeration systems, (iii) gas cycle refrigeration systems, (iv) steam jet refrigeration systems, (v) thermoelectric and magnetic refrigeration systems, and (vi) vortex tube refrigeration systems. Most of the present-day air conditioning systems use either a vapour compression refrigeration system or a vapour absorption refrigeration system.

This textbook on refrigeration and air conditioning is an outcome of 30 years' teaching experience of late Professor (Dr.) Ramesh Chandra Arora at the Indian Institute of Technology Kharagpur. It is intended to lead students to a deeper understanding and a firm grasp of the basic principles of this fast-growing subject area. The text is ideally suited for undergraduate education in mechanical engineering programmes and specialized postgraduate education in thermosciences. The book is designed to typically appeal to those who like a more rigorous presentation.

The presentation of the subject is divided into two areas, i.e. refrigeration topics in Chapters 1 to 14 and air conditioning topics in Chapters 15 to 23. Chapter 2, however, may be treated as common between these areas as it comprehensively reviews the basic principles of thermodynamics, heat transfer and fluid mechanics which constitute the three pillars of refrigeration and air conditioning.

After recapitulation of the basic foundations of refrigeration, the follow-on chapters are devoted to exhaustive coverage of principles, applications and design of several types of refrigeration

systems and their associated components such as compressors, condensers, evaporators, and expansion devices. Refrigerants too, are studied elaborately in an exclusive chapter. The study of air conditioning begins with the subject of psychrometrics being at the heart of understanding the design and implementation of air conditioning processes. The design practices followed for cooling and heating load calculations and methods of duct designing, are discussed elaborately in separate chapters.

The publisher sincerely hopes that this presentation based on the author's extensive lifetime experience of teaching and industrial consultancy, will contribute to the knowledge of the students. The presence of late Professor Ramesh Chandra Arora will be sadly missed but constantly felt as a mentor in the form of this book. Let us all hope that he would approve of what has been done.

Publisher

Acknowledgements

Late (Dr.) Ramesh Chandra Arora completed a large part of the manuscript for this book during his brave 1½ years fight against cancer. The urgency shown by him in penning this book showed an undying sense of responsibility and an attempt to ensure that knowledge was duly transferred. He will live on in our hearts and minds through this book, and probably for ever.

On behalf of the author, I would like to duly acknowledge some of the people who he would have definitely included in this section, though I am aware, that if he were writing this section, it would have been a longer list of acknowledgements. I apologize to those, whose names I might have inadvertently missed.

Mrs. Neeta Arora
w/o. Late Dr. Ramesh Chandra Arora

His teachers and guide from
IIT Kanpur and Case Westren Reserve, Cleveland, Ohio, USA

Dr. M. Ramgopal
Dept. of Mechanical Engineering, IIT Kharagpur

Dr. K.L. Chopra
Director, IIT Kharagpur

Dr. S.K. Som
Dept. of Mechanical Engineering, IIT Kharagpur

Dr. Amitava Ghosh
Director, IIT Kharagpur

Dr. A.K. Chattopadhyay
Dept. of Mechanical Engineering, IIT Kharagpur

Dr. S.K. Dube
Director, IIT Kharagpur

Dr. R.K. Brahma
Dept. of Mechanical Engineering, IIT Kharagpur

Dr. Damodar Acharya
Director, IIT Kharagpur

Dr. P.K. Das
Dept. of Mechanical Engineering, IIT Kharagpur

Late Dr. A.K. Mohanty
Dept. of Mechanical Engineering, IIT Kharagpur

Dr. G.L. Datta
Dept. of Mechanical Engineering, IIT Kharagpur

Dr. Souvik Bhattacharya
Dept. of Mechanical Engineering, IIT Kharagpur

Dr. R.N. Maiti
Dept. of Mechanical Engineering, IIT Kharagpur

Dr. B. Maiti
Dept. of Mechanical Engineering, IIT Kharagpur

Dr. Soumitra Paul
Dept. of Mechanical Engineering, IIT Kharagpur

Dr. A. Mukherjee
Dept. of Mechanical Engineering, IIT Kharagpur

Dr. M.N. Faruqui
Dept. of Mechanical Engineering, IIT Kharagpur

Dr. V.V. Satyamurthy
Dept. of Mechanical Engineering, IIT Kharagpur

Dr. B.N. Shreedhar
Dept. of Aerospace Engineering, IIT Kharagpur

Dr. P.P. Chakraborty
Dept. of Computer Science, IIT Kharagpur

Dr. A.K. Mazumdar
Dept. of Computer Science, IIT Kharagpur

Dr. V.K. Jain
Dept. of Mathematics, IIT Kharagpur

Dr. B.K. Mathur
Dept. of Physics, IIT Kharagpur

Dr. S.L. Sharma
Dept. of Physics, IIT Kharagpur

Dr. Satish Bal
Dept. of Agricultural Engineering, IIT Kharagpur

Dr. Ajay Chakrabarty
IIT Kharagpur

I humbly request the Department of Mechanical Engineering, IIT Kharagpur, to take forward all the future editions of this book.

Ankur Arora
(S/o Late Dr. Ramesh Chandra Arora)

1

History of Refrigeration

LEARNING OBJECTIVES

After studying this chapter the student should be able to:

1. Understand the purpose of refrigeration and air conditioning systems.
2. Identify and describe the working principles of various natural methods of refrigeration.
3. Understand the underlying principles of various artificial methods of refrigeration.
4. Name the important landmarks in the history of refrigeration.
5. Name the important historical landmarks in the development of refrigerants.

1.1 INTRODUCTION

The purpose of refrigeration is to attain and maintain a temperature below that of the surroundings, the aim being to cool some product or space to the required temperature. This can be achieved by transferring heat from the product to another medium, which is at a temperature lower than the product. The age-old method of achieving this is by the use of ice. In earlier times, ice was either transported from colder regions, stored during winter for summer use, or made during night by nocturnal cooling. In Europe, America and Iran, a number of icehouses were built to store ice with indigenous insulating materials like sawdust or wood shavings, etc. which were later replaced by cork. Ice was loaded into these houses during winter for summer use. Beazley and Watt (1977) describe these icehouses. Literature reveals that ice has always been available at least to those who could afford it. According to Gosney (1982), it appears that the aristocracy of seventeenth and eighteenth centuries could not survive without the luxury of ice. In India, the Moughul emperors enjoyed the luxury of ice for cooling during the harsh summers in Delhi and Agra.

Frederic Tudor, who was later called ice king, started the mass scale ice trade in 1806. He cut ice from the Hudson River and ponds of Massachusetts and exported it to various countries including India. In India, Tudor's ice was cheaper than the locally ice manufactured by nocturnal cooling.

The ice trade in North America was a flourishing business. Ice was transported to southern states of America by train compartments insulated with 0.3 m thick cork insulation. It was shipped to the rest of the world including China and Australia. The details of American ice trade are available in Cummings (1949) and Anderson (1953).

1.2 NATURAL COOLING PROCESSES

The use of natural ice for cooling has been described above. Ice was transported from colder regions or stored in icehouses during winter for summer use. In the following section, the other processes of natural cooling that do not require any mechanical means or work input for cooling are described.

1.2.1 Art of Ice Making by Nocturnal Cooling

The art of making ice at night time was perfected in India about 2500 B.C. A thin layer of water, a few millimetre thick, was kept in shallow earthen trays and exposed to the cloudless night sky. The trays were insulated by compacted hay of 0.3 m thickness. The temperature of the stratosphere (11 km above the earth's surface) is –55°C. The trays exposed to sky loose heat by radiation to the stratosphere, and by the early morning hours the water in the trays freezes to ice. Initially, evaporative cooling also cools the water to some extent. The sky should be cloudless and the trays should see the sky only and not see the surrounding trees and buildings, which are at a higher temperature. If the wind velocities are high, then convective heat transfer losses prevent the formation of ice. This method of ice production was very popular in India.

1.2.2 Evaporative Cooling

Evaporative cooling has been used in India for centuries. The process of cooling water by storing it in earthen pots, is still used all over India. The water permeates through the pores of the earthen vessel to the outer surface where it evaporates to the surrounding air absorbing its latent heat in part from the vessel and in part from the surrounding air. The cooled walls of the vessel cool the bulk of the water contained in it. Evaporative cooling of the houses by placing wet straw mats on the windows is still very common in India. The straw mats are made from the stems of a special plant called *khus*, which freshens the air and adds its inherent perfume to it. The mats block the direct and diffuse solar radiation incident on glass windows, thereby reducing the cooling load. Nowadays, desert coolers are used in warm and dry climate to provide evaporative cooling in summer.

Human beings have the most elaborate and a unique natural cooling arrangement. Humans dissipate energy consumed by metabolic and other processes. If this energy cannot be dissipated by convection and radiation, then human beings start to perspire and dissipate this energy by evaporative cooling. Other living forms do not have this natural cooling system. The dogs bring out their tongue for evaporative cooling and elephants cool themselves by using their ears as fans. The dark and light colour stripes of Zebra get differentially heated up and induce convection currents for cooling. The hippopotamuses and buffaloes coat themselves with mud for cooling their bodies through the process of evaporative cooling.

The first air-cooled building was also built in India. It is said that Patliputra University situated on the bank of the river Ganges used to induce the evaporative-cooled air from the river. The air in the rooms becomes warm by coming into contact with persons, its density reduces and it rises up. Its upward flow was augmented by suitably locating chimneys in the rooms of Patliputra University in order to induce fresh cold air from the river.

1.2.3 Cooling by Salt Solutions

Cooling to some extent can be obtained by dissolving salt in water. The salt absorbs its heat of solution from water and cools it. Theoretically, NaCl can yield temperatures up to –20°C and $CaCl_2$ up to –50°C in properly insulated containers. The salt, however, has to be recovered if the process is to be cyclic. The recovery of salt requires the evaporation of water from the solution, which requires an enormous amount of energy compared to heat of solution. Solar energy may be used for salt recovery to a limited extent.

1.3 MECHANICAL COOLING PROCESSES

Evaporative cooling, nocturnal cooling and cooling by naturally occurring ice are the natural processes. These depend upon the season and meterological conditions that cannot be relied upon for year round applications. The minimum temperature that can be obtained by evaporative cooling is the wet-bulb temperature of air and the minimum temperature obtained by melting of ice is 0°C. This temperature can be reduced to –20°C by adding salts like NaCl or $CaCl_2$ to ice. However, cooling by ice is rather an inconvenient process—the ice has to be replenished and water has to be disposed of, and also heat transfer from the ice surface is difficult to control.

Refrigeration, as it is known these days, is produced by artificial means. The history of refrigeration is very interesting since every item, the availability of refrigerants, the prime movers, and the developments in compressors and the methods of refrigeration all are part of it. We describe the history under the headings of (i) Mechanical Vapour Compression Refrigeration, (ii) Absorption Refrigeration, (iii) Solar Refrigeration Systems, (iv) Gas Cycle Refrigeration, and (v) Electrical Methods.

1.3.1 Mechanical Vapour Compression Refrigeration

The ability of liquids to absorb enormous quantities of heat as they boil and evaporate, is the basis of modern refrigeration. The normal boiling point of water is 100°C. Therefore, at room temperature water does not boil during evaporative cooling. It evaporates into unsaturated moist air by a slow process since this is controlled by diffusion and air motion.

It is well known that when a volatile liquid like ether is put on the skin, it cools the skin by evaporating and absorbing the latent heat from the skin. The normal boiling point of ether is around 34.5°C, which is the same as the skin temperature. This process can be made more effective by removing the vapours as they are formed, and thereby increasing the evaporation rate. Professor William Cullen of the University of Edinburgh demonstrated this in 1755 by placing some water in thermal contact with ether under a receiver of a vacuum pump. The evaporation rate of ether increased due to the removal of vapour by the vacuum pump and the water thus could be frozen.

The two thermodynamic concepts involved here are the *vapour pressure* and the *latent heat* which is called the *enthalpy of evaporation* nowadays. If a liquid in a container does not have any other gas present over it, then given sufficient time it comes to equilibrium with its own vapour at a pressure called the *saturation pressure*, which depends on the temperature alone. At this pressure, the escaping tendency of the molecules from liquid is the same as the condensing rate of the vapour molecules. The saturation pressure increases as the temperature increases. The water at atmospheric pressure boils at 100°C. If the pressure is increased, for example in a pressure cooker, the water boils at a higher temperature. The second concept is that the evaporation of liquid requires latent heat. It is called latent since it cannot be sensed, as the temperature of the liquid does not change during evaporation. If latent heat is extracted from the liquid, the liquid will be cooled. However, if sufficient heat is absorbed from the external sources, for example water, then the temperature of ether will remain constant but water will freeze. The temperature of ether will remain constant as long as the vacuum pump maintains a pressure equal to saturation pressure at the desired temperature, that is, it removes all the vapours formed. If a lower temperature is desired, then a lower saturation pressure will have to be maintained by the vacuum pump. The component of the modern day refrigeration system where cooling is produced by this method is called the *evaporator*.

If this process of cooling is to be made continuous, a large quantity of ether will be required unless the vapours are recycled by condensation to the liquid state. The condensation process requires heat rejection to a medium at a temperature lower than that of the vapours. The ether cannot be condensed since it requires a medium at a temperature lower than that it produced. It is known that the saturation temperature increases as the saturation pressure increases. Hence, it can be condensed at atmospheric temperature by increasing its pressure to saturation pressure at atmospheric temperature. The process of condensation was learned in the second-half of the eighteenth century. U.F. Clouet and G. Monge liquefied SO_2 in 1780 while van Marum and van Troostwijk liquefied NH_3 in 1787. Hence, a compressor is required to increase the pressure so that the evaporating vapours can condense at a temperature higher than that of the surroundings. In fact, the compressor will also maintain low pressure in the evaporator in a closed system for the evaporation of liquid, dispensing with vacuum pump. The pressure of the condensed liquid is high. An expansion valve reduces this so that the refrigerant can evaporate at low pressure and temperature. This system is called the vapour compression refrigeration system. The schematic flow diagram of this system is shown in Figure 1.1.

Figure 1.1 is a schematic flow diagram of a basic vapour compression refrigeration system that shows the functioning of its main components—a flow control valve or expansion valve, an evaporator, a compressor, and a condenser. The cooling or refrigeration effect is obtained when the refrigerant flows through a heat exchanger called the evaporator. Heat is extracted from the fluid to be cooled and transferred to the refrigerant. This causes vaporization of the refrigerant in the evaporator, i.e. the refrigerant leaving the evaporator is a gas at a low temperature and low pressure. The gas is compressed in the compressor to a high pressure, also resulting in its temperature increasing to greater than the ambient or any other heat sink. Hence, now when this high pressure, high temperature refrigerant flows through the condenser, condensation of the vapour into liquid takes place by removal of heat from it to the heat sink. The refrigerant therefore condenses to a liquid, at which stage it is relatively at a high pressure and high temperature. This high pressure liquid is now made to flow through an expansion valve, where it pressure and temperature decrease.

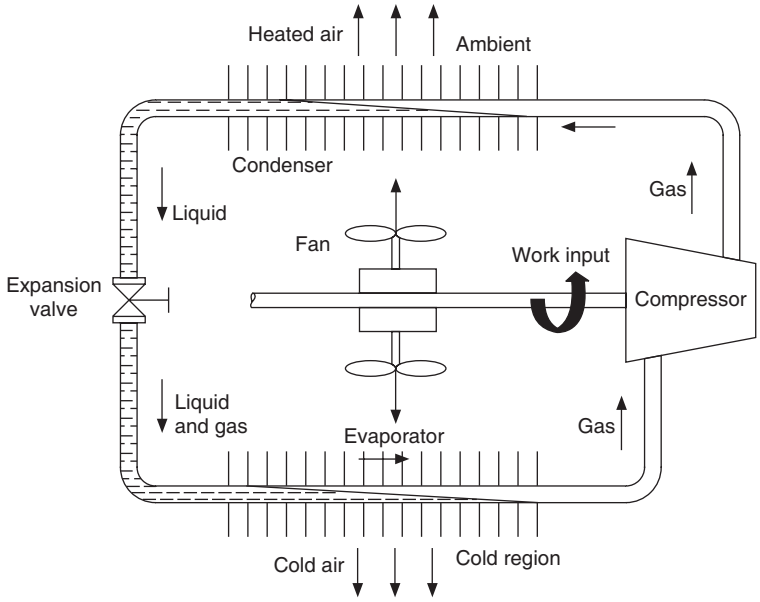

Figure 1.1 Schematic illustration of a basic vapour compression refrigeration system.

The resulting low pressure and low temperature refrigerant is made to evaporate again in the evaporator to take heat away from the cold region. The closed cycle thus provided continuously extracts heat from a cold space and rejects heat to a high temperature sink.

Oliver Evans in his book *Abortion of a Young Steam Engineer's Guide* published in Philadelphia in 1805, described a closed refrigeration cycle to produce ice by ether under vacuum. But the book did not go beyond proposing such a system. Later, Jacob Perkins, an American living in London actually designed such a system in 1834. This is shown in Figure 1.2.

In his patent Jacob Perkins stated *I am enabled to use volatile fluids for the purpose of producing the cooling or freezing of fluids, and yet at the same time constantly condensing such volatile fluids, and bringing them again into operation without waste*. John Hague made Perkins's design into a working model with some modifications. The working fluid, although claimed to be sulphuric (ethyl) or methyl ether, was actually Caoutchoucine—a product obtained by distillation of India rubber (Caoutchouc). This was pointed out in 1882 by Sir Frederick Bramwell who described the hand-operated Perkins's machine which remained unknown for fifty years. John Hague made Perkins design into a working model with some modifications. This is shown in Figure 1.3.

The earliest vapour compression system used either sulphuric (ethyl) or methyl ether. Alexander Twining received a British patent in 1850 for a vapour compression system by use of ether, NH_3 and CO_2. In 1850 his ethyl ether machine could freeze a pail of water and in 1856 his new model could produce 2000 pounds of ice in 20 hours in Cleveland, Ohio.

The man responsible for making a practical vapour compression refrigeration system was James Harrison who took a patent in 1856 for a vapour compression system using ether, alcohol or ammonia. Oldham (1947) gives a good description of the history of these developments. Harrison also patented a shell-and-tube type brine chiller using ethyl ether. He set up ice works in Geelong and then in Melbourne, Australia. Charles Tellier of France patented in 1864, a refrigeration system

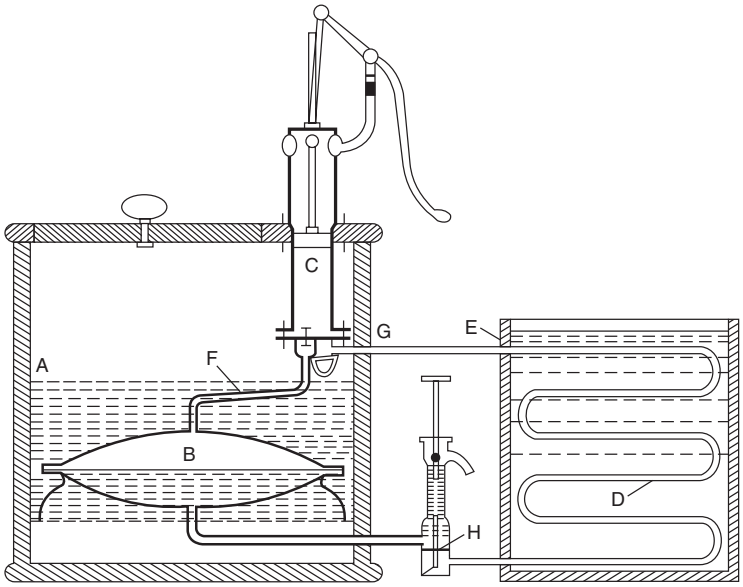

Figure 1.2 Apparatus described by Jacob Perkins in his patent specification of 1834. The refrigerant (ether or other volatile fluid) boils in evaporator B taking heat from surrounding water in container A. The pump C draws vapour away and compresses it to higher pressure at which it can condense to liquid in tubes D, giving out heat to water in vessel E. Condensed liquid flows through the weight-loaded valve H, which maintains the difference of pressure between the condenser and evaporator. The small pump above H is used for charging the apparatus with refrigerant.

Figure 1.3 Perkins machine built by John Hague.

using dimethyl ether with a normal boiling point of –23.6°C. The most famous of his machine was used in the ship Le Frigorifigue that transported meat from France to South America and back. The normal boiling point (that is at atmospheric pressure) of ether is 34.5°C. Hence, its evaporation at lower temperatures requires vacuum. This makes it prone to leakage of air and moisture into the system, and such a mixture of ether and air becomes an explosive mixture. The pressure in the condenser was, however, low and this did not require a strong construction.

Carl von Linde in Munich showed that the mechanical vapour compression system is more efficient than the absorption refrigeration system. He introduced NH_3 as refrigerant in 1873, first with a vertical double acting compressor and then with a horizontal double acting compressor. It required a pressure of more than 10 atmospheres in the condenser. Its normal boiling point (NBP) is – 33.3°C; hence it does not require vacuum in the evaporator. Since then, ammonia is widely used in large refrigeration plants.

David Boyle, in fact, made the first NH_3 system in 1871 in San Francisco. John Enright had also developed a similar system in 1876 in Buffalo N.Y. Franz Windhausen developed a CO_2 vapour compression system in Germany in 1886. This required a pressure of 80 atmospheres and therefore a very heavy construction. Linde in 1882 and T.S.C. Lowe in 1887 tried similar systems in the USA. The CO_2 system is a very safe system and was used in ship refrigeration until 1955. Raoul Pictet in Geneva used SO_2, also known as sulphurous acid (NBP, –10°C), in 1875. Its lowest pressure was high enough to prevent the leakage of air into the system. The SO_2 compressor did not require any lubricant since the liquid SO_2 itself acted as a lubricant. This system did not require an oil separator. However, it forms sulphurous acid immediately upon reacting with moisture, which seizes the compressor. Although it is a toxic substance, it was used for more than 60 years in household refrigerators. Its noxious odour makes it a safe refrigerant since even a small quantity causes coughing and stinging of eyes, which makes the human beings run away from it.

Methyl chloride (chloromethyl) was conventionally used as anesthesia. C. Vincet used it in a two-stage refrigeration system in 1878 in France. Glycerin was used as the lubricant in this system. Glycerin absorbed moisture and clogged the valves. It was replaced by valvoline as the lubricant, which took care of lubrication problems. Servel Company used it in household refrigerators from 1922 onwards. It has delayed toxic effects. SO_2 leaks were sensational with people making a mad rush for outdoors, but CH_3Cl leaks were fatal when these occurred at night. It had another problem in that it reacted with aluminium causing corrosion and making combustible products.

Palmer used C_2H_5Cl in 1890 in a rotary compressor. He mixed it with C_2H_5Br to reduce its flammability. Edmund Copeland and Harry Edwards used isobutane in 1920 in small refrigerators. It disappeared by 1930 when it was replaced by CH_3Cl. Dichloroethylene (dielene or dieline) was used by Carrier in centrifugal compressors in 1922–26. Carrier also used methylene chloride (dichloromethane, trade name CARRENE) in centrifugal compressors in 1926–33.

1.3.2 Household Refrigeration System

The first domestic refrigerator was an icebox (using natural ice) invented in 1809 and was used for almost 150 years without much alteration. It was made of wood with suitable insulation. Ice was kept on top of the box so that the cooled heavy air settled down in the box and set up natural convection current to cool the contents of the box. A dripper was provided to collect the water from the melted ice. It had the disadvantage that the ice had to be replenished and the minimum

temperature was limited. If a particular year had a warmer winter, then there used to be shortage of ice in that year. Hence starting from 1887, efforts were made to develop domestic refrigerator using mechanical refrigeration.

Refrigeration practice underwent a drastic change when the need of small household refrigeration units was felt. The development of household refrigerators was made possible by the development of automatic refrigerant controls, better shaft seals, developments in AC power systems and induction motors. Automatic Controls built in two features: firstly to regulate the refrigerant flow through the expansion valve to match the evaporation rate in the evaporator and secondly the thermostat to switch off the power supply to the compressor motor when the cold space had reached the desired temperature. General Electric introduced the first domestic refrigerator in 1911, followed by Frigidaire in 1915. Kelvinator launched the domestic mechanical refrigerator in 1918 in the USA. In the beginning, these refrigerators were equipped with open-type, belt-driven compressors. General Electric introduced the first refrigerator with a hermetic compressor in 1926. Soon the open-type compressors were completely replaced by the hermetic compressors. Initially, the refrigerators used water-cooled condensers, which were soon replaced by air-cooled condensers. The domestic refrigerator, based on absorption principle as proposed by Platen and Munters, was first made by Electrolux Company in 1931 in Sweden. In Japan the first mechanical domestic refrigerator was made in 1924. The first dual temperature (freezer-refrigerator) domestic refrigerator was introduced in 1939. The use of mechanical domestic refrigerators grew rapidly all over the world after the Second World War. Today, a domestic refrigerator has become an essential kitchen appliance. The initial domestic refrigerator used sulphur dioxide as refrigerant. Once the refrigerator became a household appliance, the refrigerant problem too, became a household problem.

1.3.3 Air Conditioning Systems

Refrigeration systems are also used for providing cooling and dehumidification in summer for personal comfort (air conditioning). The first air conditioning systems were used for industrial as well as comfort air conditioning. Eastman Kodak installed the first air conditioning system in 1891 in Rochester, New York for the storage of photographic films. An air conditioning system was installed in a printing press in 1902 and in a telephone exchange in Hamburg in 1904. Many systems were installed in tobacco and textile factories around 1900. The first domestic air conditioning system was installed in a house in Frankfurt in 1894. A private library in St Louis, USA, was air conditioned in 1895, and a casino was air conditioned in Monte Carlo in 1901. Efforts have also been made to air condition passenger rail coaches using ice. The widespread development of air conditioning is attributed to the American scientist and industrialist Willis Carrier. Carrier studied the control of humidity in 1902 and designed a central air-conditioning plant using air washer in 1904. Due to the pioneering efforts of Carrier and also due to simultaneous development of different components and controls, air conditioning quickly became very popular, especially after 1923. At present, comfort air conditioning is widely used in residences, offices, commercial buildings, airports, hospitals and in mobile applications such as rail coaches, automobiles, and aircraft, etc. Industrial air conditioning is largely responsible for the growth of modern electronic, pharmaceutical and chemical industries, etc. Most of the present-day air conditioning systems use either a vapour compression refrigeration system or a vapour absorption refrigeration system. The capacities vary from few kilowatts to megawatts.

1.3.4 Refrigerants

The refrigerants used in the earlier days were either toxic, flammable or smelled horrible. Leakage of refrigerants caused panic and poisoning when these occurred at night time. Frigidaire Corporation of Dayton Ohio, USA, thought about it and concluded that *the refrigeration industry needed a new refrigerant if they ever expected to get anywhere*. Frigidaire asked General Motors research laboratory to develop a safe , chemically inert, stable, high vapour density, and low normal boiling point refrigerant. Thomas Midgly, Jr. who had the knack of looking at Periodic Table to solve his problems, invented chlorofluorocarbons now known as CFCs. The work started in 1928 but they found all CFCs before filing a patent in April 1930 and announcing it in the Atlanta meeting of American Chemical Society. These are fluorinated compounds. Thomas Midgly, Jr. found that the fluoride bonds were the most stable amongst the halogens, and the addition of fluoride decreased the NBP. The fluorination process was perfected by Swartz in Belgium around 1890. Antimony trifluoride was the fluorinating agent and CCl_4 was the starting material. It was observed by Swartz that the addition of the small amount of antimony to antimony trifluoride increased the rate of the fluorination process.

The interesting part of the history is that when Thomas Midgley, Jr. started the synthesis of CFCs, only five bottles of antimony trifluoride were available in the USA. Starting with CCl_4, CCl_3F was made by this process. A guinea pig exposed to CCl_3F survived. However, when the experiment was repeated with the remaining four bottles, the guinea pigs did not survive each time. Had this happened with the first bottle itself, Midgly would have stopped his search for this class of refrigerants and saved the humanity of ozone depletion. Some bottles of antimony trifluoride were procured from Europe and the guinea pigs survived again. The four bottles contained some water, which caused some phosgene to be made, and that is what killed the guinea pigs.

Thomas Midgley, Jr. made many fluorinated compounds and finally settled on CCl_2F_2 as the most promising refrigerant. It has an NBP of –29.8°C. It had a problem of leak detection and moisture. Initially, 8% SO_2 was added to it since it could be detected by its odour and by ammonia–water swab. This practice was dispensed with once halide torch was developed. Adding small amounts of methyl alcohol to CCl_2F_2 controlled the moisture. This practice was replaced by the use of $CaCl_2$ filter/dryer, which has now been replaced by silica gel drier. This refrigerant was found to be the most suitable for small refrigeration systems. Reciprocating compressors are prone to leakage from the cylinder head and at the point from where the rotating crankshaft comes out of the body of the reciprocating compressor for connection with the drive pulley. A stuffing box or gland or oil seal is used at this point. However, leakage of refrigerant is a nuisance that requires frequent replenishments. To take care of this problem, the hermetically sealed compressor was introduced in the early 1930s where the motor is directly coupled to the compressor and the two are sealed inside a housing to prevent the leakage of refrigerant. Refrigerant comes into direct contact with motor windings; hence a refrigerant like CCl_2F_2 which has a high value of dielectric constant, is well suited for hermetically sealed compressors.

$CHClF_2$ (NBP –40.8°C) was introduced in 1936. It had a higher compressor discharge temperature, which created problems in small systems. Now it is extensively used in small and large air-conditioning systems and marine systems. $CClF_3$ with NBP of –81.4°C was introduced in 1945 for ultra low temperature systems.

Carrier Corporation introduced an azeotropic mixture of CCl_2F_2 and $C_2H_4F_2$ called R500 in 1950 for small air conditioning systems. This gave the same cooling capacity if a 50 Hz motor was

used instead of 60 Hz motor in a $CCl_2.F_2$ refrigeration system. Another azeotrope of $CHClF_2$ and $CClF_5$ called R502 has a NBP of -45.4^oC and its adiabatic temperature rise is lower than that of $CHClF_2$. This can be used for food freezing without using a two-stage compressor as required for $CHClF_2$.

Numerous other CFCs have been developed during the last few decades, but most of them have been sparingly used and have remained in experimental stage only. CFCs were thought to be safe in all respects, and their number was so large that there was always a refrigerant available for a specific application. These are dense gases and have no odour; hence if they leak in enclosed spaces, they will stay near the floor and may cause suffocation. These CFCs were doing very well until 1974, when Rowland and Molina published their famous ozone depletion hypothesis. They claimed that CFCs diffuse to stratosphere where the intense energy of ultraviolet (UV) solar radiation breaks them down to release chlorine atoms that catalytically destroy ozone in a chain reaction. This would increase the intensity UV radiation (0.29–0.32 μm) incident upon the earth's surface with adverse implications on human health and other biological systems. An ozone hole of the size of European continent has been observed over Antarctica. Thus, the inertness and stability of the halogen bonds act as a double-edged sword. These bonds are very stable and cannot break down in troposphere. The CFCs cannot be dissolved in water; as a result these cannot be washed down by rain. These do not have any natural cycle in atmosphere; hence if these leak into the atmosphere they will remain in the atmosphere for all times. In the atmosphere, these gases rise upwards due to atmospheric turbulence and reach stratosphere that is located at heights of 11 km above the sea level. The chlorine and bromine bonds can be broken by UV radiation in the stratosphere; the fluorine bonds cannot be broken by UV radiation. The UV radiation breaks the CFC into a radical and a chlorine atom. The chlorine atom reacts with ozone to form a ClO molecule and an oxygen atom. ClO reacts with another ozone molecule to yield an oxygen atom and a chlorine atom, which causes further ozone depletion in a never-ending chain reaction. Hence, the chlorine and bromine containing CFCs cause ozone depletion. The presence of hydrogen atoms in the CFC lets them break in the lower atmosphere; therefore the hydrogen containing CFCs have a lower ozone depletion potential. These are called HCFCs.

The ozone depletion over the Antarctic zone occurs mainly in the months of September–October when the sun rises over Antarctic after a night of six months. During this period a peculiar feature of this region is that stratospheric clouds make their appearance at stratospheric heights. These clouds provide an enormously large amount of sites where the reaction between ozone and CFCs takes place and ozone depletion occurs at a very fast rate. Similar and more intense reactions occur with bromine containing refrigerants. Bromine containing refrigerants are sparingly used in refrigeration systems. These are more popular as fire-retardants.

The finding of ozone hole and the role of CFCs have alarmed the world; as a result the users and the manufacturers have agreed to reduce the chlorinated CFCs as per Montreal Protocol of 1987.

Hence, substitutes are being sought for such chlorine containing CFCs. CFCs containing hydrogen and fluorine atoms are considered safe. CF_3CFH_2 is being used as a substitute for the most popular refrigerant CCl_2F_2, that was used for small refrigeration systems. Hydrocarbons like propane, isobutane and their mixtures are also being used as substitutes for CCl_2F_2. The inorganic compounds like NH_3 and CO_2 are safe refrigerants. Carbon dioxide has a very high working pressure requiring high pressure equipment. Recent developments indicate that CO_2 may become a popular refrigerant.

The boiling point of a mixture of refrigerants does not remain constant during boiling, similarly the temperature of a product being cooled also decreases during the cooling process. The product and the refrigerant can be arranged in a counterflow heat exchanger in such a way that the temperature difference between the boiling mixture and the product remains constant throughout the length of the heat exchanger giving rise to minimum irreversibility. Also, the mixtures of refrigerants offer better properties than the pure refrigerants. A number of such mixtures have been standardized and their properties are available in *ASHRAE Handbook*.

1.3.5 Absorption Refrigeration

In Collin's experiment with ether and water, the ether evaporates and absorbs heat from water and cools it. John Leslie in 1810 kept H_2SO_4 and water in two separate jars connected together. H_2SO_4 absorbs water vapour and this becomes the principle of removing water vapour evaporating from the water surface, thus requiring no compressor or pump. However, a vacuum pump is used to accelerate the evaporation rate. In this method, H_2SO_4 is an absorbent that has to be recycled, by heating to get rid of the absorbed water vapour, for continuous operation. This was the principle of the refrigeration system designed by Windhausen in 1878, which worked on H_2SO_4. It was used to produce ice or chilled water by evaporation of water. Ferdinand Carrie invented the Aqua–Ammonia absorption system in 1860, water being a strong absorbent of ammonia. If NH_3 kept in a vessel is exposed to another vessel containing water, the strong absorption potential of NH_3 will cause evaporation of NH_3, thus requiring no compressor to drive the vapours. The strong NH_3 solution thus formed is passed through a liquid pump to increase its pressure. The strong solution is then heated and passed through a rectification column to separate the water from ammonia. The ammonia vapour is then condensed and recycled. The schematic diagram of this system is shown in Figure 1.4. The liquid pump requires only a negligible amount of work compared to that performed by the compressor; hence the system runs virtually on low-grade energy used for heating the strong solution to separate the water from ammonia. These systems were initially run on steam. Later on, oil and natural gas-based systems were introduced. In 1922, Balzar von Platen and Carl Munters, two students at the Royal Institute of Technology Stockholm, invented a three-fluid system that did not require a pump. A heating-based bubble pump was used for the circulation of strong and weak solutions and H_2 was used as a non-condensable gas to reduce the partial pressure of NH_3 in the evaporator. Geppert in 1899, gave this original idea but was not successful since he used air as the non-condensable gas. The bubble pump was based on the coffee percolator principle, where the bubbles rising in a tube trapped some liquid (weak solution) between them and the liquid also rose up to the top of boiler. This raised the strong solution to the top of the boiler and above the level of the absorber. The vapour rose to the rectifier and the weak solution was drained to the absorber by hydrostatic pressure. It absorbed ammonia vapour from the evaporator and became a strong solution.

Lithium bromide–water absorption system is used for chilled water air-conditioning system. This is a descendent of Windhausen's machine with LiBr replacing H_2SO_4. LiBr is the absorbent and water is the refrigerant. This system works at vacuum pressures. The condenser and the generator are housed in one cylindrical vessel and the evaporator and the absorber are housed in the second vessel. This system also runs on low-grade energy requiring a boiler or process steam.

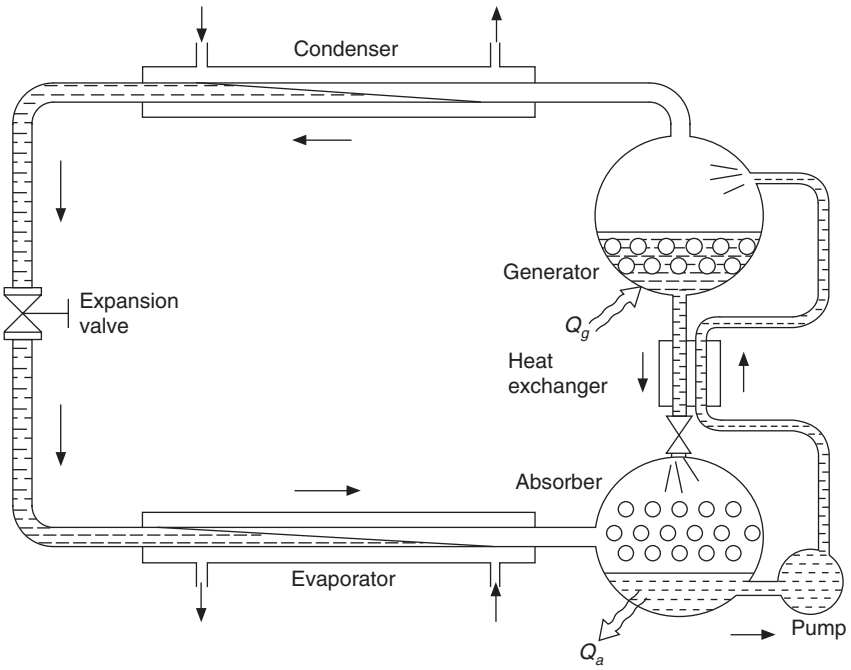

Figure 1.4 Schematic diagram of a basic vapour absorption refrigeration system.

1.3.6 Solar Energy Based Refrigeration Systems

Attempts have been made to run refrigeration systems by solar energy using concentrating and flat plate solar collectors. This work started in several countries around 1950s. In 1953, a solar system using a parabolic mirror type concentrating solar collector of 10 m^2 area could produce 250 kg/day ice in Tashkent USSR. F. Trombe installed an absorption machine with a cylindro-parabolic mirror of 20 m^2 at Montlouis France to produce 100 kg of ice per day. Energy crisis gave some impetus to research on solar refrigeration systems. LiBr–water based systems have been developed for air-conditioning purpose since these do not require a large temperature difference. University of Queensland, Australia was the first to install a solar air conditioning system in 1966. After that, many systems have been successfully used all over the world. There were 500 solar absorption systems in the USA alone.

Solar energy based intermittent adsorption system is another success story. These systems too, do not require a compressor. These systems use an adsorbent and a refrigerant. The solar collector has a bed, which contains the adsorbent. The refrigerant vapour is driven by the adsorption potential of the adsorbent when nocturnal cooling cools the collector. At night-time the refrigerant evaporates giving refrigeration and is adsorbed in activated charcoal or zeolite, and during daytime the refrigerant is driven off by solar energy, condensed and stored in a reservoir for night-time use.

Efficiency is rather poor requiring a large collector area but these systems find applications in remote areas where electricity is not available. These systems use sodium thiocynate, activated charcoal, and zeolite as adsorbents, and the ammonia, alcohols or fluorocarbons as refrigerants.

1.3.7 Gas Cycle Refrigeration

If air at high pressure expands and does work to move the piston or rotate a turbine, its temperature will decrease. This was known as early as 18th century. Dalton and Gay Lusac studied it in 1807. Sadi Carnot mentioned it in 1824. Dr. John Gorrie, a physician in Florida, developed one such machine in 1844 to produce ice for the relief of his patients suffering from fever. This machine used compressed air at two atmosphere and produced brine at –7°C which produced ice. Alexander Carnegie Kirk in 1862 made an air cycle cooling machine, which worked on the reverse Stirling cycle. This machine used steam engine to run its compressor. In fact, Phillips air liquifier is based on this principle. Paul Giffard in 1875, perfected the open type of machine. This machine was further improved by T.B. Lightfoot, A. Haslam, Henery Bell and by James Coleman. This was the main method of marine refrigeration for quite some time. Frank Allen in New York, developed a closed cycle machine employing high pressures to reduce the volume flow rates. This was named dense air machine. These days air cycle refrigeration is used only in aircraft whose small turbo compressor can handle large volume flow rates. The schematic diagram of an open type air cycle refrigeration system is shown in Figure 1.5. A compressor draws air from a cold chamber and compresses it. The hot and high pressure air from the compressor rejects heat to the heat sink (cooling water) in the heat exchanger. The warm but high pressure air expands in the expander, where it is cooled. The cold air is sent to the cold chamber for refrigeration. The compressor and the turbine (expander) are mounted on the same shaft so that the compressor uses the power output of the turbine.

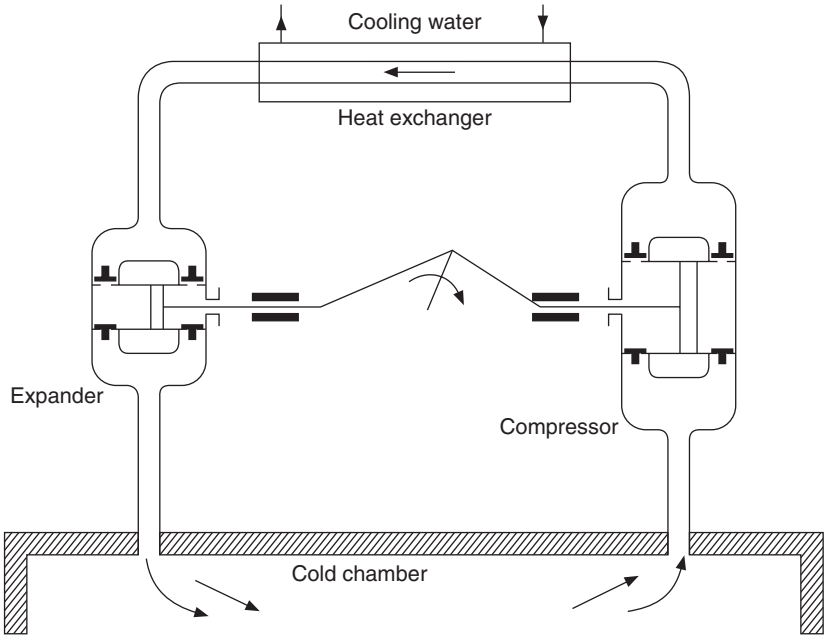

Figure 1.5 Schematic diagram of an open-type air cycle refrigeration system.

1.3.8 Steam Jet Refrigeration System

This system produces cooling by flashing of water, that is, by spraying water into a chamber where a low pressure is maintained. A part of the sprayed water evaporates at low pressure and cools the remaining water to its saturation temperature at the pressure in the chamber. Obviously, lower temperature will require lower pressure but temperature lower than 4°C cannot be obtained with water since water freezes at 0°C. Essentially, it is an evaporative cooling process. In an absorption refrigeration system, the strong absorption potential between H_2SO_4–H_2O or LiBr–H_2O was used to draw water vapour. In this system, high velocity steam is used for this purpose. High-pressure motive steam passes through either a convergent or a convergent-divergent nozzle where it acquires either sonic or supersonic velocity and low pressure of the order of 0.009 kPa corresponding to an evaporator temperature of 4°C. A stream or jet moving with high velocity imparts its kinetic energy to the surrounding fluid, that is, it entrains it or causes it to move along with it. The high velocity steam because of its high momentum entrains or carries along with it the water vapour evaporating from the flash chamber. Because of its high velocity it moves the vapours against the increasing pressure gradient up to the condenser where the pressure is 5.6–7.4 kPa corresponding to the condenser temperature of 35–45°C. Both the motive steam and the evaporated vapour are condensed and recycled as shown in Figure 1.6. Maurice Leblanc developed this system in Paris around 1910. This system requires a good vacuum to be maintained. Sometimes, a booster ejector is used for this purpose. This system is also driven by low-grade energy, that is, by process steam in chemical plants or a boiler. This is not an economical process, and hence it has been replaced by steam-driven LiBr systems in most places.

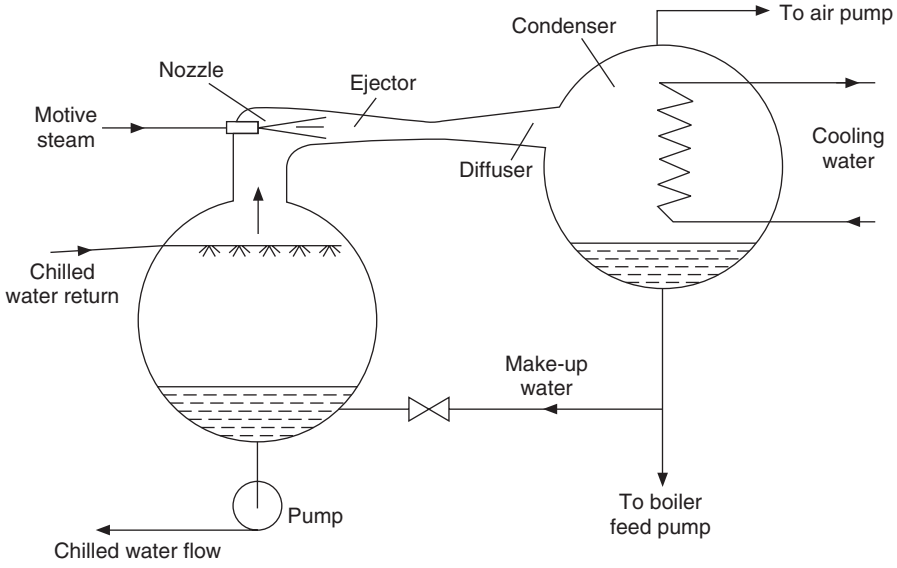

Figure 1.6 Schematic diagram of a steam jet refrigeration system.

A patent for the compression of steam by means of a jet of motive steam was granted in 1838 to the Frenchman Pelletan. The credit for constructing the steam jet refrigeration system goes to the French engineer, Maurice Leblanc, who developed the system in 1907–08. In this system,

ejectors were used to produce a high velocity steam jet (≈ 1200 m/s). The first commercial system was made by Westinghouse in 1909 in Paris based on Leblanc's design. Even though the efficiency of the steam jet refrigeration system was low, it was still attractive as water is harmless and the system could be run using exhaust steam from a steam engine. From 1910 onwards, steam jet refrigeration systems were used mainly in breweries, chemical factories, warships, etc. In 1926, the French engineer Follain improved the machine by introducing multiple stages of vaporization and condensation of the suction steam. Between 1928–1930, there was much interest in this type of systems in the USA where they were mainly used for air conditioning of factories, cinema theatres, ships and even railway wagons. Several companies such as Westinghouse, Ingersoll Rand and Carrier started commercial production of these systems from 1930 onwards. However, gradually, these systems started getting replaced by more efficient vapour absorption systems using LiBr–water. Nonetheless, some East European countries such as Czechoslovakia and Russia continued to manufacture these systems as late as 1960s. The ejector principle can also be used to provide refrigeration using fluids other than water, i.e. refrigerants such as CFC11, CFC21, CFC22, CFC113, CFC114, etc. The credit for first developing (around 1955) these closed vapour jet refrigeration systems goes to the Russian engineer, I.S. Badylkes. Using refrigerants other than water, it is possible to achieve temperatures as low as −100°C with a single stage of compression. The advantages cited for this type of systems are simplicity and robustness, while difficult design and economics are its chief disadvantages. This type of system is still used for vacuum cooling of foodstuff where the water from the foodstuff evaporates, absorbing its latent heat from it and cooling it. Forester (1954) and Vahl (1966) give more details of the steam jet refrigeration system.

1.3.9 Thermoelectric and Magnetic Refrigeration Systems

In 1821, a German scientist T.J. Seebeck reported that when two junctions of dissimilar metals are kept at two different temperatures, an emf is developed which results in flow of current. The emf is proportional to temperature difference. In 1934, a Frenchman, Jean Peltier observed the reverse effect, that is, thermal effect of cooling and heating of two junctions of dissimilar materials when direct current is passed through them, the heat transfer rate being proportional to the current. In 1857, William Thomson (Lord Kelvin) proved by thermodynamic analysis that Seebeck effect and Peltier effect are related and he discovered another effect, that is now called Thomson effect after his name. According to this, when current flows through a conductor of a thermocouple that has an initial temperature gradient in it, then the heat transfer rate per unit length is proportional to the product of the current and the temperature.

As the current flows through a thermoelectric material, it gets heated due to its electrical resistance. This is called the Joulean effect. Further, heat is transferred by conduction heat transfer from the hot junction to the cold junction. Both these heat transfer rates have to be compensated by the Peltier effect if some cooling is to be produced.

Insulating materials give poor thermoelectric performance because of their small electrical conductivity, as a result the Joulean effect masks the Peltier effect. On the other hand, metals fail because of their large thermal conductivity where the conduction heat transfer masks the thermoelectric effect. Hence for a long time the thermoelectric cooling remained a laboratory curiosity. The best thermoelectric effects are obtained with semiconductors. A pile of junctions is used in actual practice with the cold junction kept indoors to absorb heat and the warm junction kept outside to reject heat.

Lenz is said to be the first person to have made a small amount of ice by this method by using antimony and bismuth in 1838. This experiment could not be repeated. It has now been established that it was because of impurities in bismuth and antimony, which acted like semiconductors and the thermoelectric effect could be observed. This method had to wait for the semiconductors to be developed in 1949–1950. Most of the work has been done in Russia by A. F. Ioffe (1957). Several domestic refrigerators based on thermoelectric effect were made in USSR as early as 1949. However, since 1960s these systems are mainly used for storing medicines, vaccines, etc and in electronic cooling. Developments also took place in many other countries. In the USA, domestic refrigerators, air conditioners, water coolers, air conditioned diving suits, etc. were made using these effects. System capacities were typically small due to poor efficiency. However, some large refrigeration capacity systems such as a 3000 kcal/h air conditioner and a 6 tonne capacity cold storage were also developed. By using multistaging, temperatures as low as –145°C were obtained. These systems due to their limited performance (limited by the materials) are now used only in certain niche applications such as electronic cooling, mobile coolers, etc. Efforts have also been made to club thermoelectric systems with photovoltaic cells with a view to developing solar thermoelectric refrigerators.

According to *ASHRAE Handbook of Fundamentals* (1967), materials used for thermoelectric cooling include alloys of bismuth, tellurium, and antimony for p-type elements, and alloys of bismuth, tellurium and selenium for n-type elements.

The thermoelectric method is used only for small refrigeration systems since its efficiency is low and a large value of direct current is required. Further development of this system requires better materials. Temperatures very near the absolute zero may be obtained by adiabatic demagnetization of certain paramagnetic salts. Each atom of the paramagnetic salt may be considered to be a tiny magnet. Normally the atoms or the magnets are randomly oriented such that the net magnetic force is zero. If exposed to a strong magnetic field, the atoms will align themselves to the direction of the magnetic field. Now if the magnetic field is suddenly removed, the atoms will come back to their original random orientation. This requires work to be done at the expense of the internal energy. Consequently the salt will be cooled.

1.3.10 Vortex Tube

George Ranque (1931) based upon his observation of low temperature in cyclone separators devised a "vortex tube" to yield low temperature air. Air at high pressure was fed to it tangentially at one end, creating a vortex with low velocity near the core and high velocity at the periphery. A valve was provided at the opposite end of the tube to create some back pressure. In counterflow arrangement an outlet was provided near the core of the tube at the inlet end. If the kinetic energy can be removed from the stream, its temperature will decrease just like what happens in a turbine. Vortex tube is a device that separates the stream into two parts, a high kinetic energy stream and a low kinetic energy stream. The low kinetic energy stream is removed from one end and the high kinetic energy stream moves to the other end. During the passage of the stream to the long end, the wall friction and the dissipation of kinetic energy raise its temperature further. Hence a warm stream comes out from the long end.

The tube can be arranged such that both the cold and warm streams come out from the same end. Hilsch (1946) studied the vortex tube further and recommended optimum dimensions for its performance. Since then many improvements have been reported.

REFERENCES

Anderson, O.E. (1953): *Refrigeration in America : A History of a New Technology and Its Impact*. Princeton University Press.

Beazley, E. (1977): Technology of Beautiful Simplicity: Iranian Icehouses, *Country Life*, **162**, 1229–31.

Bramwell, F. (1882): Ice making, *Journal of the Royal Society of Arts*, **30**, December 8, 76–77. Raol Pictet's sulphurous acid ice machine (1878), *Nature* (London), 30 March, 432–434.

Cummings, R.O. (1949): *The American Ice Harvests: A Historical Study in Technology*, 1800–1918, University of California Press, Berkeley.

Downing, R. (1984): Developments of Chlorofluorocarbon Refrigerants, *ASHRAE Transactions*, vol. 90, Pt. 2, 481–491.

Forester, L.L. (1954): Steam Jet Refrigeration, *Proc. Institution of Refrigeration*, **59**, 119–152.

Gosney, W.B. (1982): *Principles of Refrigeration*, Cambridge University Press, Cambridge.

Harrison, James (1857): British Patent 747, Producing cold by the evaporation of volatile liquid in vacuo.

Hilsch, R. (1946): Die Enpansia von Gasen, in *Zentrifugalfeld als Kalteprozess Z.f.*, *Naturfarchung*, **1**, 208–14.

Ioffe, A.F. (1957): Semiconductor Thermoelements and Thermoelectric Cooling , *Infosearch*, London.

Midgley,T. Jr. and Henne, A.L. (1930): Organic fluorides as refrigerants, *Industrial and Engineering Chemistry*, **22**, p. 542

Midgley,T. Jr. (1937): From the Periodic Table to Production, *Industrial and Engineering. Chemistry*, **29**, 241–244.

Oldham B.C. (1947): Evolution of machine and plant design, *Proc. Institution of Refrigeration*, **43,** 59–82.

Perkins Jacob (1834): British Patent 6662, Improvements in the apparatus and means for producing ice and cooling fluids.

Ranque, G.J. (1933): Experimences sur la détente giratoire avec production simultance d'un echappement d'air chaud et d'un echappement d'air frod, *J. de Physique* (et Le Rachum) **7**, no. 4, 112–118.

Vahl, L. (1966): Dampfstrahl – Kaltemaschinen, In *Handbuch der Kaltetenik*. Ed., R. Plank, vol. 5, 393–432. Springer-Verlag, Berli.

REVIEW QUESTIONS

1. How was natural ice made in ancient India?
2. The thermal conductivity of compacted hay is 0.2 W/m-K, the stratosphere and air temperatures are –55°C and 25°C respectively, convective heat transfer coefficient

for still air is 5.0 W/m^2-K and the thickness of compacted hay used for natural ice manufacture is 0.3 m. Show that the net heat transfer from water at 0°C is 26.527 W/m^2 if the emmissivity of water is taken as 0.9. Neglect the thermal conduction resistance of the earthen pot.

3. Suppose (a) the convective heat transfer coefficient in Question 2 increases to 10.0 W/m^2-K due to wind velocity and (b) the tray does not see the sky fully (as a result its shape factor with respect to sky is 0.5) and the temperature of surrounding objects is 25°C, then in both the cases find the heat transfer rates and predict if the ice can be made.
4. The convective heat transfer coefficient and the mass transfer coefficient are 10 W/m^2-K and 0.01 kg/m^2-s respectively. The humidity ratio of air at 35°C, 40% relative humidity is 0.014 kgw/kga and the humidity ratio of saturated air is 0.020107. The latent heat of water at 25°C is 2442.5 J/kg. Neglecting radiation, show that the net heat transfer rate from a wetted earthen pot will be 6.18 W/m^2.
5. What is the difference between boiling and evaporation? How does water evaporate from a wetted surface at room temperature?
6. Explain the principle of evaporative cooling and its limitations.
7. Explain the principle of cooling by dissolving salts in water.
8. Evaporation of a refrigerant produces cooling, then why is condensation required and how is it done?
9. Why are two pressures required in a vapour compression refrigeration system?
10. What was the refrigerant used in Perkins hand-operated refrigeration machine?
11. What are the advantages and disadvantages of SO_2 as a refrigerant?
12. Why did Thomas Midgley land up with the choice of chlorofluorocarbons as refrigerants?
13. What was the process used by Thomas Midgley to make CCl_2F_2?
14. What were the main applications of R500 and R502?
15. Who gave the ozone depletion hypothesis?
16. What are the advantages of the absorption refrigeration system?
17. What is the principle of steam jet refrigeration system? Why is the motive steam required—for condensation or for entrainment?
18. Why is gas cycle refrigeration not very common and where does it find applications?
19. Why are semiconductors used in thermoelectric refrigeration?
20. What is the principle used to approach absolute zero temperature?
21. What is the principle of operation of vortex tube?

2

Thermal Principles—A Review of Fundamentals

LEARNING OBJECTIVES

After studying this chapter the student should be able to:

1. Define the concept of thermodynamic *system* and explain what is meant by a *closed system* and on *open system*.
2. Understand the concept of *heat* and *work*, and write the definitions of specific heat, specific kinetic energy, potential energy, power, and explain the meaning of refrigeration capacity.
3. State the four laws of thermodynamics.
4. Explain the concepts of flow work and enthalpy.
5. Define the first and second law of thermodynamics.
6. Understand the reversible and irreversible processes and define the thermodynamic property called *entropy* and explain Clausius inequality.
7. Define fundamental relations of thermodynamics, Gibbs and Helmholtz functions, and Maxwell's relations.
8. Define what a perfect gas is and what an equation of state is.
9. Evaluate the thermodynamic properties of pure substances on *T–s* and *p–h* charts.
10. Explain Fourier's law of heat conduction, understand the concept of thermal conductivity and heat transfer resistance to conduction.
11. Write the basic equations for heat conduction, considering one-dimensional heat transfer.
12. Explain Fick's law and write the convective mass transfer equation.
13. Explain the concept of blackbody and understand the laws governing emission of radiation from a blackbody.
14. Write the basic equations for radiation heat transfer, and estimate radiative exchange between surfaces.
15. Explain how convection heat transfer takes place between a fluid and a solid surface.

16. Write the convection heat transfer equations, explain convective and mass transfer coefficients and various non-dimensional numbers which are related to fluid properties, geometry and physical dimensions of flow.
17. Define 'condensation heat transfer' and 'boiling heat transfer'.
18. State the analogy between heat, mass and momentum transfer.
19. Derive expressions for multi-mode heat transfer through multi-layered walls, composite cylinders, etc. using heat transfer networks and the concept of overall heat transfer coefficient.
20. Perform basic calculations on heat exchangers.
21. Explain the phenomenon of mass transfer for incompressible and steady flows.
22. Write Bernoulli's equation and define pressure, velocity and static pressures and heads.
23. Write the modified Bernoulli's equation for fluid flow through a duct to account for friction losses and the presence of a fan or pump.
24. Evaluate friction pressure drops and minor losses for steady, fully developed, laminar incompressible flow in ducts.
25. Explain the various cooling processes used in refrigeration systems.

2.1 INTRODUCTION

Refrigeration and air conditioning involves transfer of heat and work apart from fluid flow. It is assumed that the reader has studied courses in engineering thermodynamics, fluid mechanics and heat transfer. This chapter reviews some of the fundamental concepts of these subjects pertinent to refrigeration and air conditioning.

2.2 THERMODYNAMIC PROPERTIES

A thermodynamic property is an observable, measurable or calculable attribute of the system in the state of thermodynamic equilibrium. Thermodynamic state is determined by the thermodynamic properties. Thermodynamic equilibrium refers to mechanical, thermal and chemical equilibrium, that is, the absence of unbalanced forces, the absence of heat and mass transfer, and the absence of chemical reactions respectively. Thermodynamics deals with the change in system from one state of equilibrium to another state of equilibrium. Say, we have an insulated container filled with 1 kg of gas at uniform temperature of 30°C. Suppose the specific heat of gas is 1 kJ/kg-K and 10 kJ of heat is transferred to the left corner of cylinder by a flame, and then the flame is removed. The temperature of the gas in the left corner will rise and kinetic energy will increase. With the passage of time the kinetic energy of the molecules in the left corner will be transferred to all the molecules and eventually the temperature of the gas everywhere in the container will become uniform and it will have a unique value of 40°C. *This state is called the new state of equilibrium of gas and the uniform temperature is a thermodynamic property measured in the state of equilibrium.* If a temperature history of the gas as a function of x, y, z were taken, it will vary with time and from place to place in the cylinder. This certainly will require a lot of data. To economize on this

description, a single temperature in the state of equilibrium for the whole 1 kg of gas is sufficient to determine the heat transfer. Thermodynamic properties are defined only in the state of equilibrium. A complete description of thermodynamic state requires a few more properties. For example, for a gas two such properties like temperature and pressure, temperature and volume and pressure and volume are required to fix the thermodynamic state.

2.3 CLOSED AND OPEN SYSTEMS

In thermodynamics, certain mass or volume in space is identified for consideration of analysis and this is called *system*. The boundary of this system is called the system boundary or control volume and whatever is outside it, is called *surroundings*. Accordingly, two kinds of systems are defined in thermodynamics, namely the *closed system* and the *open system*.

A closed system is one that contains the same matter at all times. Its mass remains constant and energy transfers in the form of heat transfer and work occur across its boundary. The concept of thermodynamic closed system is schematically illustrated in Figure 2.1(a).

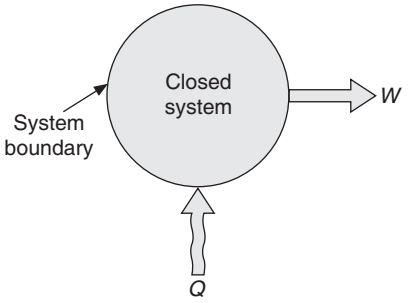

Figure 2.1(a) A closed system.

An open type of system is one in which some mass (for example fluid flow) also crosses its control volume apart from energy transfer in the form of heat transfer and work. An open system is usually a fixed volume in space and its boundary is called control volume. An open system is shown schematically in Figure 2.1(b) where fluid enters the control volume with mass flow rate $\dot{m}_1$ and internal energy u_1 at point 1 and leaves at point 2 with internal energy u_2. Some work is

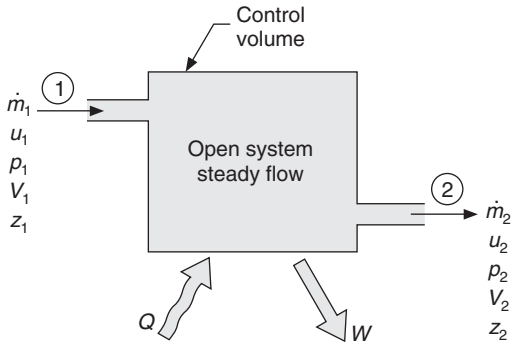

Figure 2.1(b) A steady flow open system.

required to push the fluid into the control volume against the system pressure, p_1, at the inlet. Similarly, some work is done by the system to push the fluid out of the control volume at the outlet at pressure p_2. These works are called *flow work*. The fluid entering the system may have kinetic energy and potential energy as well, as shown in the figure.

2.4 UNITS

All measurable attributes of the system have some dimensions. The FPS system of units has been prevalent in refrigeration and air conditioning. The MKS system of units was also popular in some countries. Now to maintain uniformity, the engineering community all over the world uses the Systéme Internationale D'unites abbreviated SI system of units.

Systéme Internationale D'unites

The international system of units, called SI units, is adopted in this book. In this system, the basic unit of length is metre (m), mass is expressed in kilogram (kg) and time is expressed in second (s). The temperature, the current and the luminous intensity are expressed in kelvin (K), ampere (A) and candela (Cd) respectively. The units of force, pressure, energy, power, etc. are derived units, which are described below.

2.4.1 Force

Force is defined by Newton's second law of motion as follows:

$$F = k\, m\, a \tag{2.1}$$

where m is the mass in kilogram, and a is acceleration in m/s^2. In the SI system, the unit of force is newton (N), which is the force required to accelerate 1 kg mass by an acceleration of 1 m/s^2. The constant k in this system is unity and has the dimensions of [N-s^2/(kg-m)], that is,

$$1\ \text{N} = 1\ \text{kg}\left(1\ \frac{\text{m}}{\text{s}^2}\right) = 1\ \frac{\text{kg-m}}{\text{s}^2}$$

Therefore the dimensions (usually written within square brackets) of newton are: $\text{N} = \left[\frac{\text{kg-m}}{\text{s}^2}\right]$

In the FPS system of units, length, mass and time are in feet (ft), pound mass (lbm) and second (s) respectively. The unit of force is pound force (lbf) which is the force required to accelerate one pound mass by 32.17 ft/s^2. Here 32.17 ft/s^2 is the standard acceleration due to gravity. In Eq. (2.1), the constant k has the value (1/32.17) [lbf-s^2/lbm-ft], hence it reduces to

$$1\ \text{lbf} = \frac{1}{32.17}(1\ \text{lbm})\left(32.17\ \frac{\text{ft}}{\text{s}^2}\right)$$

Similarly, in the MKS system of units, kgf is the unit of force required to accelerate 1 kg mass by 9.80665 m/s^2. The constant k in Eq. (2.1) by analogy with the FPS system is (1/9.80665) [kgf-s^2/kg-m].

1 kgf = 1 kg (9.80665 m/s^2) = 9.80665 kg-m/s^2 = 9.80665 newton = 2.2049 lbf

1 lbf = 1 lbm (32.17 ft/s^2) =1 lbm (0.45359237 kg/lbm) (32.17 ft) (0.3048 m/ft)/s^2

= 4.44766 newton = 0.453535 kgf

1 N = 0.224837 lbf = 0.10197 kgf

The weight of a body at any location where acceleration due to gravity is g, is given by

$$W = \frac{mg}{9.80665} \text{ kgf}$$

If the acceleration due to gravity has the standard value of 9.80665 m/s^2, then the magnitude of weight and mass are the same, which happens to be the case since g does not vary significantly on earth's surface.

2.4.2 Specific Volume and Density

Specific volume is the volume per unit mass and is expressed as m^3/kg. Density is mass per unit volume and is expressed as kg/m^3. The specific volume of vapour (near saturated states) is affected by temperature as well as pressure and is found from a table of properties. For gases (well above the critical temperature), it may be calculated by perfect gas equation. The liquid density is dependent mainly upon temperature; its variation with pressure is negligibly small.

The specific gravity of a liquid is defined as the weight of the given liquid to the weight of equal volume of water at some standard temperature. The standard temperature is usually taken as 4°C. The density of water at 4°C is 1000 kg/m^3. The specific gravity of mercury is 13.6; hence its density is 136,000 kg/m^3. The conversion factors in various units are as follows:

1 ft^3 = 0.028217 m^3 and 1 m^3 = 35.3147 ft^3

1m^3/kg = 35.3147/2.2046226 = 16.0185 ft^3/lbm and 1 ft^3/lbm = 0.062428 kg/m^3

1 kg/m^3 = 0.062428 lbm/ft^3 and 1 lbm/ft^3 = 16.0185 kg/m^3

2.4.3 Pressure

It is the force per unit area exerted by a substance on its boundaries. Pressure is a thermodynamic property. Pressure may be designated as absolute, gauge or vacuum pressure. Gauge pressure is the pressure measured by a gauge relative to atmospheric pressure. This is the difference between absolute pressure and atmospheric pressure; therefore absolute pressure is equal to sum of gauge pressure and atmospheric pressure. This is more than atmospheric pressure. Vacuum pressure is the difference between the atmospheric pressure and the absolute pressure; hence the absolute pressure is equal to atmospheric pressure minus the vacuum pressure. This is less than the atmospheric pressure.

A variety of units are used for expressing pressure, e.g. N/m^2 or pascal, mm of water, mm of mercury and torr. The density of water varies with temperature, however, the pressure in mm of water refers to standard density of 1000 kg/m^3 and specific gravity of mercury is taken as 13.6.

Pressure = force/area = N/m^2

N/m^2 is called pascal, abbreviated Pa.

1 kilopascal = 1000 Pa and 1 bar = 100000 Pa = 100000 N/m^2 = 10 N/cm^2

1 mm of water is equal to the weight of one mm high column of water.

$$1 \text{ mm of water} = \rho\, gh = 1000 \text{ (kg/m}^3\text{)} \times 9.80665 \text{ (m/s}^2\text{)} \times 0.001 \text{ (m)}$$
$$= 9.80665 \text{ Pa} \approx 9.81 \text{ Pa}$$
$$1 \text{ torr} = 1 \text{ mm of Hg} = 13.6 \text{ mm of } H_2O$$
$$= \rho_{Hg}\, gh = 13.6 \times 1000 \text{ (kg/m}^3\text{)} \times 9.80665 \text{ (m/s}^2\text{)} \times 0.001\text{(m)}$$
$$= 133.37044 \approx 133.37 \text{ Pa}$$

Standard atmospheric pressure = 1.01325 bar = 14.696 psi
In MKS system,

$$1 \text{ kgf/cm}^2 = 1 \text{ ata} = 9.81 \text{ Pa}$$

In FPS system,

$$1 \text{ psi} = 1 \text{ lbf/(inch)}^2$$
$$1 \text{ bar} = 10 \text{ N/cm}^2 = 10/9.80665 = 1.02 \text{ kgf/cm}^2 = 1.02 \text{ ata}$$
$$1 \text{ bar} = 10 \text{ N/cm}^2 = [10(2.54)^2]/[4.44766] = 14.5 \text{ psi}$$

2.4.4 Temperature

Temperature may be expressed in absolute or relative units. In FPS system, Fahrenheit is used while in SI system Celsius is used. At 1.01325 bar pressure the melting point of ice and boiling point of water are 0°C (32°F) and 100°C (212°F) respectively.

According to the second law of thermodynamics the lowest possible conceivable temperature is absolute zero, which is −459.69°F or −273.16°C. The temperature measured from this datum is called absolute temperature. The absolute Celsius scale is called Kelvin scale and absolute Fahrenheit scale is called Rankine scale. The absolute temperature is normally indicated by the uppercase letter *T* and relative temperature is indicated by the lowercase letter *t*. The relations between absolute and relative scales are as follows:

$$T_F = t_F + 459.69 \approx t_F + 460$$
$$T_C = t_C + 273.16 \approx t_C + 273$$

The ice point of water is 32°F, which is equal to 0°C. And 100°C is equal to 180°F. Hence the conversion between the two scales is

$$t_C = (t_F - 32)\ (100/180) = (t_F - 32)\ (5/9)$$

2.4.5 Heat and Work

Heat is defined in transit only; it cannot be stored in the body. Energy is stored in the body. Heat is transferred from one body to another body because of temperature difference. According to second law of thermodynamics it can be transferred spontaneously only from higher temperature to lower temperature. Work and heat, both are forms of energy. The energy, according to first law of thermodynamics, cannot be destroyed, it only changes its form. All the work transfer can be dissipated as heat while there are restrictions on the extent of conversion of heat transfer into work transfer. Being two forms of energy, both heat and work have the same unit in the SI system. In the

FPS and MKS systems, the unit of work is different from that of heat transfer and then a Mechanical Equivalent of heat transfer is defined to relate the two.

2.4.6 Heat Transfer

In the FPS system, heat transfer is expressed in British Thermal Unit which is the quantity of heat transfer required to raise the temperature of 1 lbm of water by 1°F. Similarly in the MKS system, heat transfer required to raise the temperature of 1 kg of water by 1°C is called 1 kilocalorie. Both the units have been coined in terms of heating of the most commonly available substance, i.e. water.

2.4.7 Specific Heat

The specific heat of a substance is the heat transfer required to raise the temperature of unit mass of substance by 1 degree. In the FPS system the unit of specific heat is Btu/lbm-°F and in the MKS system it is kcal/kg-°C. Since both these units are defined for water, their magnitude must be the same, that is,

$$1\,\frac{\text{Btu}}{\text{lbm-°F}} = 1\,\frac{\text{kcal}}{\text{kg-°C}} \qquad \therefore \quad 1\text{ kcal} = \frac{\text{kg}}{\text{lbm}}\,\frac{\text{°C}}{\text{°F}}\,\text{Btu} = 2.2 \times \frac{9}{5} = 3.968\text{ Btu}$$

The specific heat of most substances varies with temperature, however over a small temperature range, a constant average value may be used for it. Heat can be transferred to gases either at constant pressure or at constant volume. Accordingly, two specific heats are defined for gases, namely specific heat at constant pressure, c_p, and specific heat at constant volume, c_v, depending upon whether the heat is transferred at constant volume or constant pressure respectively. For liquids the difference between two specific heats is negligibly small, hence only one specific heat c is defined.

If the temperature of mass m changes from t_1 to t_2, then heat transfer is expressed as

For liquids:	$Q_{12} = mc(t_2 - t_1)$
For a gas at constant pressure:	$Q_{12} = mc_p(t_2 - t_1)$
For a gas at constant volume :	$Q_{12} = mc_v(t_2 - t_1)$

2.4.8 Work

Work involves transfer of energy between the system and surroundings when a force moves through a distance or say a fluid flows against a pressure, or a weight is raised in gravitational field. Since the units of mass and distance are different in FPS and MKS systems, the units of force in FPS and MKS system are ft-lbf and m-kgf respectively. According to the first law of thermodynamics the work done and heat transfer are two different forms of energy; hence these are related and the relation is called mechanical equivalent of heat transfer, denoted by J. The values of J are:

1 Btu = 778 ft-lbf or mechanical equivalent J = 778 ft-lbf/Btu in FPS system

1 kcal = 427 m-kgf or mechanical equivalent J = 427 m-kgf/kcal in MKS system

In the SI system, the unit of work is N-m which is the work done in moving a distance of one metre against a force of one newton. This is called joule too. This is also the unit of heat transfer in

the SI system of units. Obviously, unit of heat transfer in SI system is not defined in terms of heating one kilogram of water by one °C, which is one kcal any way.

For a closed system, typically in a piston and cylinder arrangement shown in Figure 2.2(a), the expression for reversible work can be derived as follows. If p [Pa] is the pressure acting on a piston of area A, then the force F on piston is pA [newtons]. If the gas moves the piston by an infinitesimal distance dx in the direction of force, then the work done dW is given by

$$dW = pA\, dx = p\, d\mathbb{V}$$

where, $d\mathbb{V}$ is the infinitesimal volume change during the motion of the piston. The pressure may change during this process. It is assumed that the process of expansion is carried out very slowly so that at each instant of time the system is in equilibrium. Typically, such a process is called reversible. Therefore, we can write

$$đW_{rev} = p\, d\mathbb{V} \tag{2.2}$$

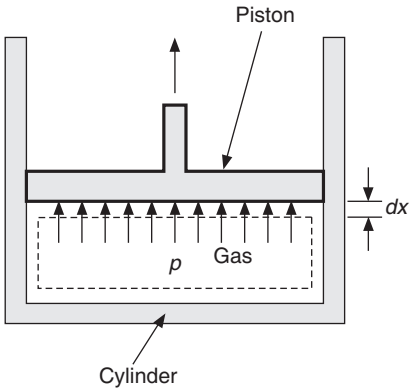

Figure 2.2(a) A piston and cylinder arrangement.

This equation may be integrated between the states 1 and 2 if there exists a relation between p and $\mathbb{V}$, i.e.

$$W_{12} = \int_1^2 p\, d\mathbb{V} \tag{2.3}$$

This is a function of path followed by process 1–2, therefore, the differential in Eq. (2.2) is denoted by $đ$. The work done W_{12} is equal to the area projected 1–2–*b*–*a*–1 on the volume axis in p–$\mathbb{V}$ coordinates as shown in Figure 2.2(b).

For an open system it can be shown by considering the first law of thermodynamics or by considering the flow work required to push the fluid into and out of the control volume that the work done is equal to the projected area 1–2–*d*–*c*–1 projected on the pressure axis. This is given by

$$W_{12} = -\int_1^2 \mathbb{V}\, dp \tag{2.4}$$

For proof, the student may refer to some standard textbook on Thermodynamics.

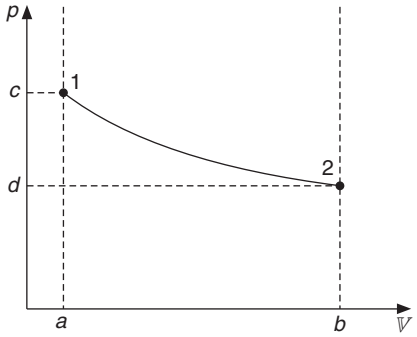

Figure 2.2(b) The work done between the states 1 and 2.

2.4.9 Signs of Work and Heat Transfer

Most thermodynamics books consider the work done by the system to be positive and the work done on the system to be negative. The heat transfer to the system is considered to be positive and the heat rejected by the system is considered to be negative.

By using the conversion factors between newton, lbf and kgf, we find the relations between kcal, Btu and joule.

1 kcal = 427 m-kgf = 427(9.80665) = 4186.8 N-m = 4186.8 J = 4.1868 kJ

Also, 1 kcal = 3.968 Btu

Therefore, 1 Btu = 4.1868/3.968 = 1.05514 kJ = 0.252 kcal

1 kJ = 0.94774 Btu = 0.238846 kcal

1 ft-lbf = 1.35565 N-m = 0.0138237 m-kgf

1 m-kgf = 9.80665 N-m = 7.2339 ft-lbf

1 N-m = 0.73765 ft-lbf = 0.10197 m-kgf

2.4.10 Kinetic Energy

An object of mass m moving with a velocity V is said to have kinetic energy of $mV^2/2$. Similarly, a fluid moving with velocity V has specific kinetic energy of $V^2/2$. Energy in all forms is the capacity to do work, hence in SI units the unit of kinetic energy is also joule.

$$[mV^2] = [\text{kg-m}^2/\text{s}^2] = [\text{kg-m}/\text{s}^2]\text{-m} = \text{N-m} = \text{joule}$$

Similarly, specific kinetic energy V^2 has the unit joule per kg.

2.4.11 Potential Energy

An object of mass m at a height h (from datum) in a gravitational field has the capacity to do mgh joule of work; hence it is said to have potential energy of mgh, where g is the acceleration due to gravity. Similarly, fluid at height h has specific potential energy of gh. The unit of potential energy is also joule.

$$[mgh] = [\text{kg-}(\text{m}/\text{s}^2)\text{-m}] = [\text{kg-m}/\text{s}^2]\text{-m} = \text{N-m} = \text{joule}$$

2.4.12 Power

Power is the time rate of doing work. It is expressed as ft-lbf per minute in FPS system, m-kgf per second in MKS system and kJ per second or kilowatt in SI system. The unit of electric power is also kilowatt. Horsepower is also used as unit of power. By definition,

$$1 \text{ hp} = 33{,}000 \text{ ft-lbf per minute} = (33{,}000/778) \times 60 = 2545 \text{ Btu per hour}$$

$$= 2545 \times 1.05514/3600 = 0.746 \text{ kW}$$

$$1 \text{ kJ} = (1/1.05514) \text{ Btu} \quad \therefore \quad 1 \text{ kW} = (3600/1.05514) = 3413 \text{ Btu/h}$$

$$= (3413/2545) = 1.34 \text{ hp}$$

In the MKS system the unit of horsepower has been rounded off as follows.

$$1 \text{ hp} = 33000 \text{ ft-lbf per min} = 33000 \times 0.138237 \text{ m-kgf /min} = 76.0306 \text{ m-kgf/s}$$

The value 76.0306 has been rounded off to 75.0

$$\therefore \quad 1 \text{ hp} = 75 \text{ m-kgf/s} = 75 \times 9.80665 = 736 \text{ watts}$$

2.4.13 Refrigeration Capacity

This has been defined in terms of ice production rate since this was the main application of refrigeration in earlier times. One ton of Refrigeration (1 TR) is the cooling capacity to produce 1 US ton of ice at 32°F from water at 32°F in twenty-four hours. This involves essentially removal of latent heat of fusion from water at its freezing point, which is 144 Btu/lbm. Therefore,

$$1 \text{ TR} = \frac{1 \times 2000 \text{ lbm} \times 144 \text{ Btu/lbm}}{24 \times 60 \text{ min}} = 200 \text{ Btu / min} \tag{2.5}$$

This is an integer, which makes it convenient to remember and that is why its usage has continued. In the MKS and SI systems it may be written as

$$1 \text{ TR} = 200/3.968 = 50.403 \text{ kcal/min}$$

In the enthusiasm to obtain an integer number in the MKS system it has been rounded off to

$$1 \text{ TR} = 50 \text{ kcal/min}$$

or

$$1 \text{ TR} = 200 \times 1.05514 = 211.028 \text{ kJ/min} \approx 211 \text{ kJ/min} \tag{2.6}$$

2.5 THE FOUR LAWS OF THERMODYNAMICS

Engineering thermodynamics is based upon four empirical principles called zeroth, first, second and third laws of thermodynamics. These cannot be proved but no exceptions to these have been observed; hence these are accepted as laws. These laws define thermodynamic properties, which are of great importance in understanding the thermodynamic principles. The zeroth law defines *temperature*; the first law defines *internal energy*; the second law defines *entropy* and the third law states that *absolute zero temperature* cannot be achieved.

2.6 ZEROTH LAW OF THERMODYNAMICS

This law defines temperature. Suppose there are three systems A, B and C. If system A is in thermal equilibrium with system B and also in thermal equilibrium with system C, then by shear

logic, the system B should be in thermal equilibrium with system C independently. For this thermal equilibrium to exist, the three systems should have some property in common between them to invoke thermal equilibrium. This property is temperature. The three systems should have the same temperature in order to exist in equilibrium with each other. The temperature of a system is measured by bringing a thermometer to be in thermal equilibrium with the system.

2.7 FIRST LAW OF THERMODYNAMICS

This law does the bookkeeping of energy and defines a property called internal energy. According to it, if some heat or work is added to the system or removed from the system, none of this is destroyed or created in the system. In fact, a hypothetical machine that creates energy out of nothing is called perpetual motion machine of first kind (PMM of first kind) and it violates the first law of thermodynamics. Also, according to this law the heat transfer and work transfer are interconvertible.

To illustrate it, a cyclic process shown by 1–*a*–2–*b*–1 in Figure 2.3 is considered. Say the system has some initial state 1 defined by pressure p_1 and temperature T_1. If in this process $\oint đQ$ amount of heat is transferred and $\oint dW$ amount of work is done such that the process returns to its initial state of p_1 and T_1, then such a process is called the cyclic process. The symbol $\oint$ denotes a cyclic process. Since the heat transfer and work transfer are (i) two forms of energy, (ii) these cannot be destroyed and (iii) they change from one form to another, we have for a cyclic process 1–*a*–2–*b*–1,

$$\oint đQ = \oint dW \qquad \text{or} \qquad \oint (đQ - dW) = 0 \tag{2.7}$$

Figure 2.3 shows another cyclic process 1–*a*–2–*c*–1 between the same two points 1 and 2. Equation (2.7) is valid for this process as well. Hence, the integrand of this integral is independent of the path followed by the process, namely 1–*a*–2–*b*–1 or 1–*a*–2–*c*–1. Both the processes start at 1 and end at 1.This is possible only if the integrand ($dQ - dW$) is a function of the thermodynamic state at point 1 , say defined by p_1 and T_1. A quantity that depends upon the thermodynamic state is called point function and is a thermodynamic property. This property is called internal energy, and is denoted by U. Therefore, on difference basis,

$$dU = dQ - dW \tag{2.8}$$

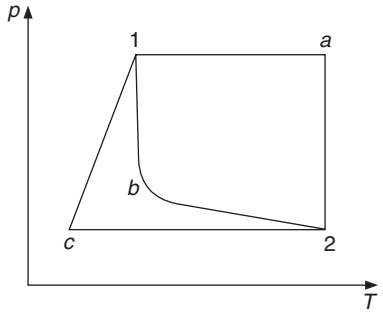

Figure 2.3 Cyclic processes.

It is observed that if work is done by the system, that is dW is positive, the internal energy of the system dU will decrease since work will be done at the expense of it. If heat dQ is transferred to the system, which is considered to be positive then the internal dU energy will increase.

Hence, the first law defines internal energy, which increases if heat is transferred to the system or work is done on the system. The internal energy of a system is the sum total of all forms of energy—nuclear, atomic, molecular, vibrational, rotational, lattice and thermal, etc.

2.7.1 First Law for a Closed System

Let the internal energy of a closed system be U_1 in the initial state 1. If Q_{12} kJ of heat is transferred across its boundary, W_{12} kJ work is done by the system and the system is allowed to come to an equilibrium state 2, then integration of Eq. (2.8) yields

$$U_2 - U_1 = Q_{12} - W_{12} \tag{2.9}$$

If m is the mass of the system and u denotes the specific internal energy of the system in kJ/kg, then,

$$m(u_2 - u_1) = Q_{12} - W_{12} \tag{2.10}$$

or

$$u_2 - u_1 = q_{12} - w_{12}$$

where, q_{12} and w_{12} are heat transfer and work done per unit mass of the system.

2.7.2 Flow Work

In an open system some matter, usually fluid, enters and leaves the system. It requires flow work for the fluid to enter the system against the system pressure and at the same time flow work is required to expel the fluid from the system. Referring to the schematic diagram in Figure 2.4, the velocity of the fluid entering at inlet 1 is V_1, the area of the inlet duct is A_1 and the pressure in the control volume is p_1. In time δt, the fluid in the hypothetical extended length $V_1\delta t$ of the duct is pushed into the control volume against pressure p_1.

$$\text{Work done in time } \delta t = dW = \text{Force} \times \text{distance} = p_1A_1(V_1\delta t) = p_1A_1V_1\delta t \tag{2.11}$$

If v_1 is the specific volume of the fluid at inlet and $\dot{m}_1$ is the mass flow rate, then

$$\dot{m}_1 = V_1A_1 / v_1 \qquad \therefore \quad V_1A_1 = \dot{m}_1v_1$$

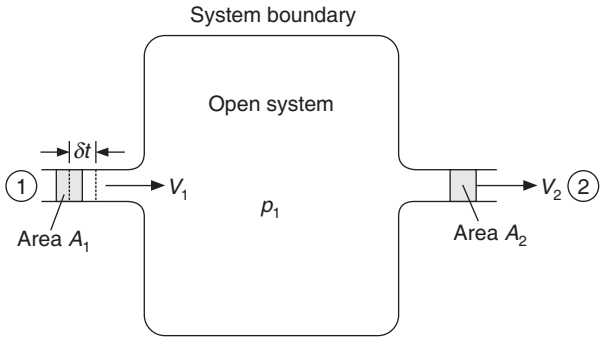

Figure 2.4 Flow work of fluid entering and leaving an open system.

Eq. (2.11) reduces to

$$dW = \dot{m}_1 p_1 v_1 \, \delta t \quad \therefore \quad \text{Rate of flow work} = dW/dt = \dot{m}_1 p_1 v_1 \tag{2.12}$$

Similarly, at the outlet 2, flow work $\dot{m}_2 p_2 v_2$ will be required to expel the fluid.

It can thus be seen that the specific flow work is given by the product of pressure p and specific volume v, i.e. flow work = pv.

2.7.3 Enthalpy

It is convenient to combine the specific flow work $p_1 v_1$ with internal energy u_1 at the inlet since both of them increase the energy of the system. Similarly, at the outlet also specific internal energy u_2 and flow work $p_2 v_2$ can be combined together since while leaving the system these decrease the energy of the system. The sum of specific internal energy and specific flow work is called enthalpy. This quantity is denoted by symbol h and is given by

$$h = u + pv \tag{2.13}$$

Hence, for an open system, it becomes convenient to consider enthalpy instead of internal energy of the fluid at the inlet and outlet so that flow work is included in it.

2.8 FIRST LAW OF THERMODYNAMICS FOR OPEN SYSTEMS

In the system shown in Figure 2.1(b), the inlet and outlet are at heights z_1 and z_2 respectively with reference to a datum, hence the fluid at inlet and outlet possesses specific potential energy of gz_1 and gz_2 respectively where g is the acceleration due to gravity. At inlet and outlet the specific kinetic energy is $V_1^2/2$ and $V_2^2/2$ respectively. Total specific energy of the fluid at inlet is equal to sum of enthalpy, kinetic energy and potential energy, that is $(h_1 + V_1^2/2 + gz_1)$ and at the outlet it is $(h_2 + V_2^2/2 + gz_2)$. If the rate of work done by the system is $\dot{W}$ and heat transfer rate to the system is $\dot{Q}$ and rate of change of energy of the system is $d(E_{\text{system}})/dt = \dot{E}_{\text{system}}$, then energy conservation for the control volume yields

$$\dot{E}_{\text{system}} = \dot{m}_2 (h_2 + V_2^2/2 + gz_2) - \dot{m}_1 (h_1 + V_1^2/2 + gz_1) + \dot{W} - \dot{Q} \tag{2.14}$$

2.8.1 First Law for an Open System in Steady State

In a steady state process, the time rate of change of all the quantities is zero, and mass is also conserved. As a result, the total energy of the system does not change with time, that is

$$\dot{E}_{\text{system}} = 0$$

Mass conservation yields

$$\dot{m}_1 = \dot{m}_2 = \dot{m}$$

Therefore, Eq. (2.14) reduces to

$$(h_2 + V_2^2/2 + gz_2) - (h_1 + V_1^2/2 + gz_1) = (\dot{Q}/\dot{m}) - (\dot{W}/\dot{m}) = \dot{q} - \dot{w} \tag{2.15}$$

where, $\dot{q}$ and $\dot{w}$ are heat transfer and work done per unit mass flow rate.

2.8.2 Perpetual Motion Machine of First Kind (PMMFK)

This is a hypothetical device which gives constant work output without any interaction with the surroundings. An example could be a clockwork device that would periodically wind itself up using some of its own work output. It would thus operate indefinitely. Equation (2.7) indicates that if heat is not supplied during a cycle, no work output will be obtained. This device would create energy out of nothing and its existence would violate the first law of thermodynamics which states that the energy is conserved.

2.9 SECOND LAW OF THERMODYNAMICS

This law is a limit law. It gives the upper limit of efficiency of a system. It also gives the direction that processes will follow. It further defines the property called *entropy*.

It is common sense that heat will not flow spontaneously from a body at lower temperature to a body at higher temperature. In order to transfer heat from lower temperature to higher temperature continuously (that is, to maintain the low temperature) a refrigeration system is needed which requires work input from an external source. This is one of the principles of the second law of thermodynamics, which is known as the *Clausius statement of the second law* that is stated as follows.

2.9.1 Clausius Statement of Second Law

It is impossible to transfer heat in a cyclic process from low temperature to high temperature without work from an external source.

It is also a fact that all the energy supplied to a system as work can be dissipated as heat transfer. On the other hand, all the energy supplied as heat transfer cannot be continuously converted into work giving a thermal efficiency of 100%. Only a part of heat transfer at high temperature in a cyclic process can be converted into work, the remaining part has to be rejected to surroundings at lower temperature. If it were possible to obtain work continuously by heat transfer with a single heat source, then an automobile will run by deriving energy from atmosphere and a ship will propel itself by deriving energy from the ocean, both at no cost. A hypothetical machine that can achieve this feat is called Perpetual Motion Machine of second kind. This fact is embedded in the *Kelvin–Planck Statement of the Second law* that is stated as follows.

2.9.2 Kelvin–Planck Statement of Second Law

It is impossible to construct a device (*engine*) *operating in a cycle that will produce no effect other than extraction of heat from a single reservoir and convert all of it into work.*

It is also implied in the above statement that the potential of work output from heat transfer depends upon the temperature at which it is available. The higher the temperature of the heat source and lower the temperature of the heat sink (surroundings), the higher will be the efficiency of the device.

2.9.3 Reversible and Irreversible Processes

This is a very important concept in determining the efficiency of refrigeration systems and the heat engines, or for that matter in finding the efficiency of any thermal device.

A process is reversible with respect to the system and surroundings if the system and the surroundings can be restored to their respective initial states by reversing the direction of the process, that is, by reversing the heat transfer and work transfer. The process is irreversible if it cannot fulfil this criterion.

If work is done in the presence of friction, say motion of a system, movement of piston in a cylinder, etc. then a part of the work is dissipated as heat and it cannot be fully recovered if the direction of the process is reversed. Similarly, if heat is transferred through a temperature difference from a higher temperature T_H to a lower temperature $T_H - \Delta t$, its direction cannot be reversed since heat transfer from the lower temperature to the higher temperature T_H would require external work input. In fact, one can run a reversible heat engine through a temperature difference Δt and obtain some work output and transfer heat back to T_H. This work is lost if heat transfer occurs through a temperature difference and such a process cannot be reversed.

Reversible process is possible if it is carried out in a large number of infinitesimal steps, very slowly so that the system passes through a set of equilibrium states and at each step the process can be reversed by an infinitesimal change.

Reversible process is a hypothetical process in which work is done in the absence of friction and heat transfer occurs isothermally. Irreversibility leads to loss in work output and loss in availability and useful work. In fact, if heat transfer Q_H is available at temperature T_H and the temperature of the surroundings is T_C, then a reversible engine will give a work output of $Q_H (T_H - T_C)/T_H$—this is called the availability and a part of this is lost due to irreversibility.

2.9.4 Entropy

The second law of thermodynamics is used to define a property called entropy. Figure 2.5 shows that if Q_{12} heat is transferred and W_{12} work is done on the system, it will move from initial state 1 to state 2. The internal energy of the system will change from U_1 to U_2 such that

$$U_2 - U_1 = Q_{12} + W_{12}$$

If the signs of Q_{12} and W_{12} are reversed, the internal energy will change from U_2 to U_1, however the system will not come back to state 1 unless the heat and work transfer are reversible. The first law is valid, however, during the irreversible process 1–2. The description of state 2 is not complete. Something has changed so that we cannot bring back the system to state 1 by reversing the signs of heat and work transfer. This is not reflected by internal energy, hence a property is required to give the measure of this irreversibility. This property is called *entropy*.

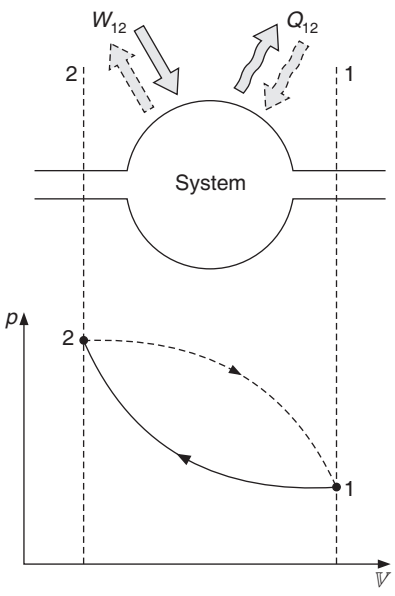

Figure 2.5 An irreversible process.

Let us consider Carnot heat engine for illustration. This is schematically shown in Figure 2.6(b) and its pressure–volume diagram is shown in Figure 2.6(a). It consists of four reversible processes, namely:

(i) 1–2 : isentropic compression
(ii) 2–3 : isothermal heat addition Q_H, actually this gives the work output too.
(iii) 3–4 : isentropic expansion
(iv) 4–1 : isothermal heat rejection Q_C, in actual practice this requires work input.

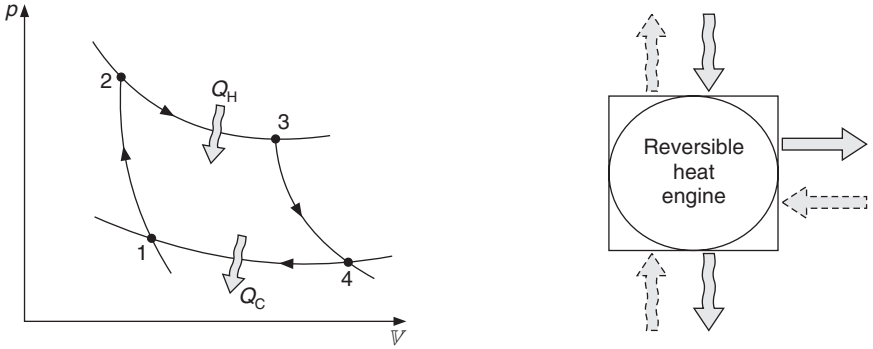

(a) The p–$\mathbb{V}$ diagram (b) Schematic diagram

Figure 2.6 Carnot heat engine.

If a perfect gas is considered as the working fluid, then along the isothermal processes 2–3 and 4–1, the temperature is constant; as a result the internal energy remains constant, therefore from the first law, we have

$$Q_{23} = W_{23} \quad \text{since } U_{23} = 0 \quad \therefore \quad Q_H = W_{23}$$

Similarly, $$Q_{41} = W_{41} \quad \text{since } U_{41} = 0 \quad \therefore \quad Q_C = W_{41}$$

Work requirement for isothermal processes in open systems is given by

$$W_{23} = -\int_2^3 \mathbb{V}\, dp = -RT_H \ln \frac{p_3}{p_2} \quad \therefore\ Q_H = RT_H \ln \frac{p_2}{p_3}$$

Similarly,

$$W_{41} = -\int_4^1 \mathbb{V}\, dp = -RT_C \ln \frac{p_1}{p_4} \quad \therefore\ Q_C = RT_C \ln \frac{p_4}{p_1}$$

Also,

$$\frac{p_2}{p_1} = \left(\frac{T_H}{T_C}\right)^{\gamma/(\gamma-1)} = \frac{p_3}{p_4}$$

Therefore,

$$\frac{Q_H}{T_H} = \frac{Q_C}{T_C}$$

or $$\frac{Q_H}{T_H} - \frac{Q_C}{T_C} = 0 \qquad \text{or for a cyclic reversible process } \oint \frac{dQ}{T} = 0 \tag{2.16}$$

Therefore $\left(\frac{dQ}{T}\right)_{rev}$ does not change in a cyclic process, that is, it is a function of the thermodynamic state only. Therefore, it is the change in a thermodynamic property. This property is called entropy, denoted by S. Therefore,

$$dS = \left(\frac{dQ}{T}\right)_{rev} \quad \text{or} \quad (dQ)_{rev} = T\,dS \tag{2.17}$$

On per unit mass basis, Eq. (2.17) is written as

$$ds = (dq/T)_{rev} \tag{3.18}$$

where, s is the specific entropy. The unit of specific entropy is kJ/kg-K. For a finite reversible process between states 1 and 2

$$s_2 - s_1 = \int_1^2 \frac{dq}{T} \tag{2.19}$$

Entropy at states 1 and 2 is a function of thermodynamic states at point 1 and 2. Hence, the difference $s_2 - s_1$ will be independent of the path followed by the process between 1 and 2. Therefore, it becomes convenient to find the entropy difference $s_2 - s_1$ for a reversible process instead of the relatively undefined irreversible process.

Entropy, like enthalpy, is a thermodynamic property. It cannot be evaluated by direct measurements. It is very useful in engineering calculations involving isothermal and reversible adiabatic processes. It is also used as criterion for equilibrium.

For an actual process which is not reversible,

$$ds > \left(\frac{dq}{T}\right) \tag{2.20}$$

For an irreversible cyclic process, the cyclic integral can be shown to be less than zero. The proof of this is available in standard thermodynamics textbooks. This is also a corollary of second law of thermodynamics known as Clausius inequality.

2.9.5 Clasius Inequality

The Clausius inequality is a mathematical form of the second law of thermodynamics for a closed system undergoing a cyclic process. It is given by:

$$\oint \frac{dQ}{T} \leq 0 \tag{2.21}$$

This is a very useful form of the second law of thermodynamics. We will use the second law in the form of Clausius inequality to derive the maximum efficiency and COP of heat engines and refrigeration systems.

It has been shown that for real processes (irreversible processes) the entropy always increases. This is stated as a corollary of the second law of thermodynamics: This corollary is proved for an isolated system that is one, which does not involve any heat transfer, mass transfer and work

transfer. Any system along with its surroundings (that is universe) can also be considered as isolated system. Then this corollary of second law is stated as follows:

The entropy of an isolated system either increases or remains constant.

The second law of thermodynamics is also known as limit law. It gives the upper bound of efficiency of heat engine and the coefficient of performance of refrigeration system. This also gives the direction that a process can follow.

2.10 FUNDAMENTAL RELATIONS OF THERMODYNAMICS

There are some general thermodynamic relations, which are useful for the determination of several thermodynamic properties from the measured data on a few properties.

Using the definition of entropy and the first law of thermodynamics as follows, we can derive two important relations of thermodynamics. We have from Eqs. (2.2) and (2.17),

$$dQ_{rev} = T\,dS \quad \text{and} \quad dW_{rev} = p\,d\mathbb{V}$$

Substituting these relations in Eq. (2.8) for the first law of thermodynamics, we get

$$dU = T\,dS - p\,d\mathbb{V}$$

or
$$T\,dS = dU + p\,d\mathbb{V} \tag{2.22}$$

Also,
$$H = U + p\mathbb{V} \quad \text{or} \quad dH = p\,d\mathbb{V} + \mathbb{V}\,dp$$

Substituting this relation in Eq. (2.22), we get

$$T\,dS = dH - \mathbb{V}\,dp \tag{2.23}$$

Equations (2.22) and (2.23) are called the first and second fundamental relations of thermodynamics. On per unit mass basis these equations are as follows:

First fundamental relation of thermodynamics

$$T\,ds = du + p\,dv \tag{2.24}$$

Second fundamental relation of thermodynamics

$$T\,ds = dh - v\,dp \tag{2.25}$$

These fundamental relations have been derived by using the definitions of work and entropy for reversible processes. However, these are valid in general for all processes since these are relations between thermodynamic properties, which are point functions and do not depend upon the path followed by the processes.

2.10.1 Gibbs and Helmholtz Functions

Apart from the two fundamental Eqs. (2.24) and (2.25), Gibbs function and Free energy or Helmholtz function are also useful, and yield another two useful equations. The Gibbs function g and Helmholtz function f are defined as follows.

$$g = h - Ts \tag{2.26}$$

and
$$f = u - Ts \tag{2.27}$$

Differentiating these equations and substituting from Eqs. (2.24) and (2.25), we get

$$dg = v\,dp - s\,dT \tag{2.28}$$

$$df = -p\,dv - s\,dT \tag{2.29}$$

Also assuming that g is a function of pressure and temperature while f is a function of volume and temperature, that is,

$$g = g(p, T) \quad \text{and} \quad f = f(v, T)$$

or
$$dg = \left(\frac{\partial g}{\partial T}\right)_p dT + \left(\frac{\partial g}{\partial p}\right)_T dp$$

and
$$df = \left(\frac{\partial f}{\partial v}\right)_T dv + \left(\frac{\partial f}{\partial T}\right)_v dT$$

Comparing these relations with Eqs. (2.28) and (2.29), we get

$$s = -\left(\frac{\partial g}{\partial T}\right)_p, v = \left(\frac{\partial g}{\partial p}\right)_T \quad \text{and} \quad p = -\left(\frac{\partial f}{\partial v}\right)_T, s = -\left(\frac{\partial f}{\partial T}\right)_v \tag{2.30}$$

These equations can be used to determine entropy, specific volume and pressure if g and f are known.

2.10.2 Maxwell's Relations

It is known from mathematical relations that if a complete differential is given such as

$$dA = M\,dx + N\,dy, \qquad \text{then } \left(\frac{\partial M}{\partial y}\right)_x = \left(\frac{\partial N}{\partial x}\right)_y$$

Equations (2.24), (2.25), (2.28) and (2.29) are complete differentials; hence the following four relations known as Maxwell's relations may be derived.

$$\begin{aligned}
\left(\frac{\partial v}{\partial T}\right)_p &= -\left(\frac{\partial s}{\partial p}\right)_T \\
\left(\frac{\partial T}{\partial p}\right)_s &= -\left(\frac{\partial v}{\partial s}\right)_p \\
\left(\frac{\partial p}{\partial T}\right)_v &= -\left(\frac{\partial s}{\partial v}\right)_T \\
\left(\frac{\partial T}{\partial v}\right)_s &= -\left(\frac{\partial p}{\partial s}\right)_v
\end{aligned} \tag{2.31}$$

These relations are very useful in defining relations between various properties and determining them. The following matrix conveniently represents this.

$$\begin{pmatrix} p & T \\ s & v \end{pmatrix}$$

One has to take the negative sign while taking derivatives along columns, that is,

$$\left(\frac{\partial T}{\partial v}\right)_s \quad \text{and} \quad \left(\frac{\partial v}{\partial T}\right)_p$$

2.11 THIRD LAW OF THERMODYNAMICS

This law gives the definition of absolute value of entropy and also states that absolute zero cannot be achieved. Another version of this law is:

The entropy of perfect crystals is zero at absolute zero.

This statement is attributed to Planck. This is in line with the concept that entropy is a measure of disorder of the system. If W is the probability of achieving a particular state out of a large number of states, then entropy of the system is equal to ln (W). The transitional movement of molecules ceases at absolute zero and the position of atoms can be uniquely specified. In addition, if we have a perfect crystal, then all of its atoms are alike and their positions can be interchanged without changing the state. The probability of this state is unity, that is $W = 1$ and ln (W) = ln (1) = 0.

For imperfect crystals, however, there is some entropy associated with configuration of molecules and atoms even when all motions cease, hence the entropy in this case does not tend to zero as $T \rightarrow 0$, but it tends to a constant called the entropy of configuration.

The third law allows absolute entropy to be determined with zero entropy at absolute zero as the reference state. In refrigeration systems we deal with entropy changes only, the absolute entropy is not of much use. Therefore entropy may be taken to be zero or a constant at any suitably chosen state, which serves as a reference. Evaluation of entropy requires correlations for specific heats and latent heats as function of temperature.

Another consequence of third law is that absolute zero cannot be achieved. One tries to approach absolute zero by magnetization to align the molecules. This is followed by cooling and then demagnetization, which extracts energy from the substance and reduces its temperature. It can be shown that this process will require infinite number of cycles to achieve absolute zero. In a later chapter it will be shown that infinitely large amount of work is required to maintain absolute zero if at all it can be achieved. For many interesting problems related to these laws the reader is referred to *Thermodynamics* by J.E. Lay (1963).

2.12 PERFECT GAS

The molecular forces of attraction between gas molecules are small compared to those in liquids. In the limit when these forces are zero, a gas is called a perfect gas. In addition, the volume of the molecules should be negligible compared to total volume for a perfect gas. An equation expressing a relation between pressure, temperature and volume of a substance is called *Equation of State*. A large number of such equations have been proposed for fluids based upon validation by experimental data. In case of perfect gas, this relation has the simplest form, namely

$$pv = RT \tag{2.32a}$$

$$p\mathbb{V} = mRT \tag{2.32b}$$

$$p\mathbb{V} = n\bar{R}T \tag{2.32c}$$

$$p\bar{v} = \bar{R}T \tag{2.32d}$$

where, p is the absolute pressure in kPa, v is the specific volume in m^3/kg, $\mathbb{V}$ is volume in m^3 and $\bar{v}$ is molal volume in m^3 per kgmole. T is the temperature in kelvin. $\bar{R}$ is universal gas constant in kJ/kgmole-K and R is gas constant for a particular gas in kJ/kg-K.

$$\bar{R} = 8.314 \text{ kJ/kgmole-K} \tag{2.33}$$

and $R = \bar{R}/M$, M being the molecular weight of gas in kg/kgmole

Equation (2.32) is a good approximation for gas at temperatures well above the critical temperature and at low pressures, where the intermolecular forces are negligibly small.

According to another definition of perfect gas, *it is a gas, for which the internal energy is a function of temperature only, that is,*

$$u = u(T) \tag{2.34}$$

$$h = u + pv = u(T) + RT = h(T) \tag{2.35}$$

Hence, the enthalpy of perfect gas is a function of temperature only.

A large number of useful relations for various properties can be derived using the perfect gas relations and specific heats, for example, change in internal energy and enthalpy between states 1 and 2 is given by

$$u_2 - u_1 = c_v (t_2 - t_1) \tag{2.36}$$

$$h_2 - h_1 = c_p (t_2 - t_1) \tag{2.37}$$

Integrating Eqs. (2.24) and (2.25) between states 1 and 2, we get

$$s_2 - s_1 = c_v \ln (T_2/T_1) + R \ln (v_2/v_1) \tag{2.38}$$

$$s_2 - s_1 = c_p \ln (T_2/T_1) + R \ln (p_2/p_1) \tag{2.39}$$

In a constant volume heat transfer process, the work done $w_{12} = 0$. Hence from first law,

$$q_{12} = u_2 - u_1 = c_v (t_2 - t_1)$$

Similarly for a constant pressure process, by definition

$$q_{12} = h_2 - h_1 = c_p (t_2 - t_1)$$

2.13 MIXTURE OF IDEAL GASES

While dealing with moist air and mixture of refrigerants, one has to consider mixture of gases. Here, we consider a mixture of ideal gases, say A and B. The molecular forces of attraction between the molecules of each constituent gas, that is, A–A and B–B molecules are zero if these are ideal gases. For the mixture to be treated as a perfect gas, the molecular forces between molecules of different gases, that is, A–B should also be zero.

We first consider a given volume $\mathbb{V}$ of the mixture of gases A and B at pressure p and temperature T. Each of the gases is assumed to follow the ideal gas relation, i.e. Eq. (2.32). If m_A and m_B are the masses of constituent gases and m is the mass of the mixture, then mass conservation yields

$$m = m_A + m_B \tag{2.40}$$

The partial pressure p_A of species A is defined as the pressure that species A would exert if it alone occupied the whole volume $\mathbb{V}$. Since there are no forces of interaction between two gases, the sum of partial pressures of the two gases is equal to the total pressure, p. This is known as Dalton's law of partial pressures and is expressed as

$$p = p_A + p_B \tag{2.41}$$

From Eq. (2.32), we have

$$p_A \mathbb{V} = m_A R_A T, \quad p_B \mathbb{V} = m_B R_B T \quad \text{and} \quad p \mathbb{V} = mRT \tag{2.42}$$

where R is the gas constant for the mixture and is given by

$$R = (m_A R_A + m_B R_B)/m \tag{2.43}$$

If the gases are mixed adiabatically without any change in kinetic and potential energy, and without any work output, then according to first law of thermodynamics, in steady state the initial and final enthalpies are the same, therefore the mixture enthalpy is given by

$$h = (m_A h_A + m_B h_B)/m \tag{2.44}$$

or in differential form,

$$mdh = m_A dh_A + m_B dh_B$$

For a perfect gas $dh = c_p dt$, therefore the specific heat of the mixture is given by

$$c_p = (m_A c_{pA} + m_B c_{pB})/m \tag{2.45}$$

Similarly, the internal energy of the mixture is given by

$$u = (m_A u_A + m_B u_B)/m \tag{2.46}$$

and

$$c_v = (m_A c_{vA} + m_B c_{vB})/m \tag{2.47}$$

The entropy of a mixture is not equal to the sum of entropies of individual components; the entropy of mixing (which is an irreversible process) has to be included.

2.14 REAL GAS AND VAPOURS

The relation between various thermodynamic properties is called the equation of state since these properties help in uniquely fixing the thermodynamic state of a system in equilibrium. Various equations of state have been proposed to model the real gas and the vapours in which the forces of attraction between molecules are not negligible. One of the earliest attempts to improve upon the ideal gas equation was the van der Wall's equation.

2.14.1 van der Wall's Equation

$$\left(p + \frac{a}{\bar{v}^2}\right)(\bar{v} - b) = \bar{R}T \tag{2.48}$$

In this equation, $a/\bar{v}^2$ accounts for the forces of attraction between molecules and b accounts for the finite volume of the molecules. The constants a and b are found by looking at the isotherm passing through the critical point which is supposed to have a point of inflection there. Here, $a = (27/64)\bar{R}^2T_c^2 / p_c$ and $b = \bar{R}T_c/(8p_c)$ where T_c and p_c are the critical temperature and pressure respectively. Four more equations are as follows:

2.14.2 Dieterici Equation

$$p(\bar{v} - b)\exp(a/\bar{v}\,\bar{R}T) = \bar{R}T \tag{2.49}$$

where, $a = 4\bar{R}T_c^2/(e^2 p_c)$ and $b = \bar{R}T_c/(e^2 p_c)$ and $e = 2.718$

2.14.3 Beattie Bridgman Equation

$$p = \bar{R}T(1-\varepsilon)(\bar{v} + B)/\bar{v}^2 - A/v^2 \tag{2.50a}$$

where, $B = B_0(1 - b/\bar{v})$, $\varepsilon = c/\bar{v}T^3$ and $A = A_0(1 - a/\bar{v})$

or $$p\bar{v}^2 = \bar{R}T[\bar{v} + B_0\{1 - b/\bar{v}\}][1 - c/(\bar{v}T^3)] - A_0(1 - a/\bar{v}) \tag{2.50b}$$

2.14.4 Benedict–Webb–Rubin (BWR) Equation

$$p = \frac{\bar{R}T}{\bar{v}} - \frac{B_0\bar{R}T - A_0 - C/T^2}{\bar{v}^2} + \frac{\bar{R}T(b-a)}{\bar{v}^3} + \frac{a\alpha}{\bar{v}^6} + \frac{C}{T^2\bar{v}^3}\left(1 + \frac{\gamma}{\bar{v}^2}\right)\exp(-\gamma/\bar{v}^2) \tag{2.51}$$

where A_0, B_0, C_0, a, b, c, a and γ are constants for a gas. This equation is good for predicting the properties of light hydrocarbons.

2.14.5 Redlich–Kwong Equation

This equation has only two constants. The BWR equation has eight constants, hence extensive experimental data points are required to determine these constants. In case of the gases for which experimental values are available at only a few points, the *RK* equation gives a better approximation than that given by van-der Wall's equation.

$$p = \frac{\bar{R}T}{\bar{v} - b} - \frac{a}{\sqrt{T}\,\bar{v}(\bar{v} + b)} \quad \text{where } a = \Omega_a\bar{R}^2T_c^{2.5}/p_c \text{ and } b = \Omega_b\bar{R}T_c/p_c \tag{2.52}$$

Here Ω_a and Ω_b are determined from the values at two points where the experimental data is available. When no p,v,T experimental data is available, then these constants may be chosen as, $\Omega_b = 0.0867$ and $\Omega_a = 0.4278$. This equation does not give so good an accuracy.

2.14.6 Peng–Robinson Equation

$$p = \frac{RT}{v - b} - \frac{a}{v^2 + 2bv - v^2} \tag{2.53}$$

where

$$a = \frac{0.45724 RT_c^2}{p_c}[1 + f(\omega)(1 - \sqrt{(T/T_c)})]^2 \quad \text{and} \quad b = 0.0778\, RT_c/p_c$$

Another popular equation is Martin–Hu equation of state, which is as follows:

2.14.7 Martin–Hu (MH) Equation

$$p = \frac{RT}{v - b} + \sum_{i=2}^{5} \frac{A_i + B_i + C_i \exp(-kT/T_c)}{(v - b)^i} \tag{2.54}$$

The constant $k \approx 4.2$ for most gases and is an adjustable constant.

This equation has been used in Du Pont tabulated properties of refrigerants.

The values of constants A_i, B_i, C_i and b are available for various refrigerants.

Another equation of state is virial equation of state, which has been used to predict the properties of moist air. This equation is described below.

2.14.8 Virial Equation of State

$$\frac{p\bar{v}}{\bar{R}T} = 1 + A_2(T)p + A_3(T)p^2 + A_4(T)p^3 + \cdots \tag{2.55}$$

Another form of this equation is

$$\frac{p\bar{v}}{\bar{R}T} = 1 + C_2(T)\rho + C_3(T)\rho^2 + C_4(T)\rho^3 + \cdots \tag{2.56}$$

where, density is used on the right hand side for convenience. NEL tables for refrigerant R12 are based upon this equation with up to 15 terms. The virial equation requires more terms than than those in BWR or MH equation, but power series is easier to evaluate than the terms in BWR and MH equations.

2.15 DRY AIR

In air conditioning we consider moist air to be a mixture of dry air and water vapour, since the control of latter is one of the aims of air conditioning. On volume basis, standard air is considered to consist of 78.08% N_2, 20.95% O_2 and traces of about fifteen other gases. The molecular weight and gas constant of dry air are

$$M = 28.966 \text{ kg/kgmole} \tag{2.57}$$

$$R = 0.2871 \text{ kJ/kg-K}$$

Precise measurements indicate that perfect gas approximation is correct at sufficiently low pressures and temperatures well above the critical temperature. For other cases, a reliable equation of state may be derived from statistical mechanics. This equation is called *virial equation of state* and is given by a power series in pressure. One may take as many terms as possible depending upon the degree of accuracy desired. This equation is as follows:

$$\frac{pv}{RT} = 1 + A_2(T)p + A_3(T)p^2 + A_4(T)p^3 + \cdots = Z \tag{2.58}$$

where, A_2, A_3, etc are called virial coefficients. These are functions of temperature and are determined experimentally. Z is called the compressibility factor. The variation of Z with temperature and pressure is available in standard textbooks on thermodynamics. At atmospheric pressure, Z is essentially unity between –75°C and 100°C, hence in this range it behaves like a perfect gas. The specific heat of dry air varies between 1.0048 and 1.013 between –75°C and 100°C.

In the air conditioning range of temperatures from 0 to 50°C, the following values are used:

$$c_p = 1.005 \text{ kJ/kg-K}, \quad c_v = 0.7179 \text{ kJ/kg-K}$$

2.16 Properties of Pure Substance

A pure substance is one whose chemical composition does not change during thermodynamic processes. Water and refrigerants are pure substances. Nowadays, emphasis is on the use of mixture of refrigerants. The understanding of properties of mixtures also requires a sound knowledge of the properties of pure substances.

Water is a substance of prime importance in refrigeration and air conditioning. It exists in three states, namely, ice, water and water vapour and undergoes transformation from one state to another. Steam and hot water are used for heating of buildings while chilled water is used for cooling of buildings. Hence, an understanding of its properties is essential for air conditioning calculations. Substances which absorb heat from other substances or space, are called refrigerants. These substances also exist in three states. These also undergo transformations usually from liquid to vapour and vice-versa during heat absorption and rejection respectively. Hence, it is important to understand their properties as well.

If a liquid (pure substance) is heated at constant pressure, the temperature at which it boils is called *saturation temperature*. This temperature will remain constant during heating until all the liquid boils off. At this temperature, the liquid and the associated vapour at the same temperature are in equilibrium and are called *saturated liquid* and *saturated vapour* respectively. The saturation temperature is a function of pressure only. At atmospheric pressure, the saturation temperature is called *normal boiling point*. Similarly, if the vapour of a pure substance is cooled at constant pressure, the temperature at which the condensation starts, is called the *dew point temperature*. For a pure substance, the dew point and the boiling point are same at a given pressure.

Similarly, when a solid is heated at constant pressure, it melts at a definite temperature called *melting point*. Similarly, cooling of a liquid causes freezing at the *freezing point*. The melting point and freezing point are same at same pressure for a pure substance and the solid and liquid are in equilibrium at this temperature.

For all pure substances there is a temperature at which all the three phases exist in equilibrium. This is called the *triple point*.

The liquid–vapour phase diagram of a pure substance is conveniently shown in temperature–entropy diagram or pressure–enthalpy diagram or p–v diagram. Sometimes, three-dimensional p-v-t diagrams are also drawn to show the phase transformation. In most of the refrigeration applications except dry ice manufacture, we encounter liquid and vapour phases only.

Figure 2.7 shows a typical temperature–entropy diagram for a pure substance in three phases. Line S–S'–S'' indicates the saturated solid states. T_r indicates the triple point. T_r–L–L' indicates saturated liquid in equilibrium with saturated solid states along S–S'–S''. Mixture of solid and liquid exists between the line S'–S'' and the line T_r–L'. The state to the left of line S–S'–S'' is solid state. Line T_r–G is the triple point line. We have a mixture of solid and vapour state below it and a mixture of liquid and vapour above it. Similarly, to the right of line S–S' and to the left of G'–G it is a mixture of solid and vapour states.

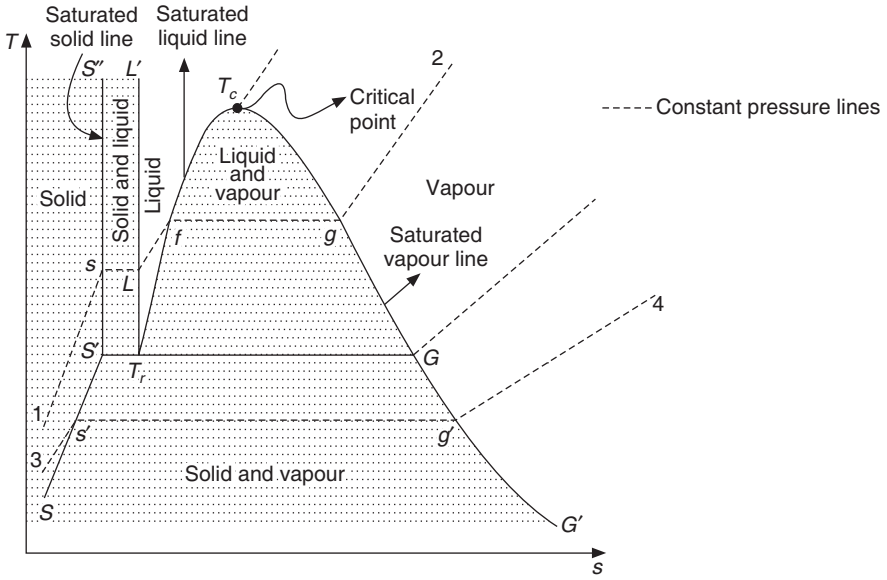

Figure 2.7 Typical *T*–*s* diagram for a pure substance.

Next we look at the liquid–vapour dome T_r–T_c–G, which is of considerable importance in refrigeration system analysis. The top point of this dome is called the *critical point*.

The line T_r–T_c is the *saturated liquid line* and G–T_c is called the *saturated vapour line*. The line 1–s–L–f–g–2 represents a constant pressure line. The solid at s is in equilibrium with liquid at L. The liquid at f is in equilibrium with vapour at g. Portion 1–s is in subcooled solid state and portion L–f is in subcooled liquid state. Portion g–2 is in superheated state. Hence, in general, the states between lines S'–S'' and T_r–L' are in subcooled state and the states to the right of T_c–G are in superheated state.

The line 3–s'–g'–4 is another constant pressure line where the pressure is less than the triple point pressure. The portion 3–s' is subcooled solid state, s'–g' is a mixture of solid and vapour and g'–4 is superheated vapour state. It is observed that upon heating at pressures below the triple point pressure the solid at g' straightaway goes into vapour phase without melting to liquid phase. This process is called *sublimation process*.

Critical point

The states at critical point are denoted by t_c, p_c and v_c. The liquid below this pressure when heated first becomes a mixture of liquid and vapour and then becomes saturated vapour. At the critical

point there is no distinction between the saturated liquid state f and the saturated vapour state g; these two states merge together at the critical point. At constant pressure greater than p_c when liquid is heated in supercritical region, there is no distinction between liquid and vapour; as a result if heating is done in a transparent tube, the meniscus of liquid and vapour does not appear as the transformation from liquid to vapour takes place. Otherwise, at pressures below the critical pressure, when a liquid is heated there is a clear-cut meniscus between the liquid and the vapour, until all the liquid evaporates.

For water:	Triple point : 0.1°C, 0.006112 bar
	Critical point: 221.2 bar, 647.3 K and 0.00317 m^3/kg
For Dry Ice (CO_2) :	Triple point: 5.18 bar, –56.6 °C
	Critical point: 73.8 bar, 31°C

2.16.1 *T–s* and *p–h* Diagrams for Liquid–Vapour Regime

These are of great importance in refrigeration cycle calculations. Figures 2.8(a) and 2.8(b) show the typical *T–s* diagram and *p–h* (Mollier) diagram respectively for a pure refrigerant. The *T–s* diagram shows two constant pressure lines for pressures p_1 and p_2 where $p_1 > p_2$. The constant pressure line 1–2–3–4 is for pressure p_1. The portion 1–2 is in the subcooled region, 2–3 is in wet region, that is mixture of liquid and vapour, and 3–4 is in superheated region. A frequent problem in refrigeration cycle calculations is to find the properties of subcooled liquid at point a shown in Figure 2.8(a). The liquid at pressure p_1 and temperature T_a is the subcooled liquid. The liquid at state a' is saturated liquid at lower pressure $p_{a'}$, but at the same temperature. We have from Eq. (2.24),

$$Tds = du + pdv$$

If the liquid is assumed to be incompressible then $dv = 0$ and

$$Tds = du$$

For liquids, the internal energy may be assumed to be function of temperature alone, that is,

$$u_a = u_{a'} \quad \therefore \quad s_a = s_{a'} \text{ since } T_a = T_{a'}$$

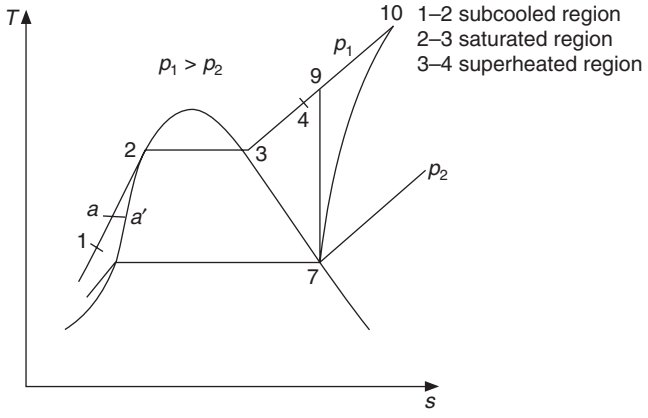

Figure 2.8(a) Typical *T–s* diagram for a pure refrigerant.

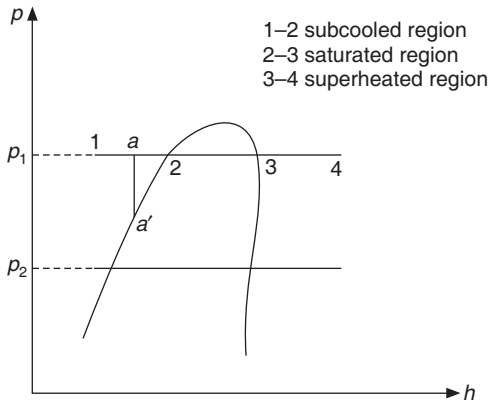

Figure 2.8(b) Typical *p–h* diagram for a pure refrigerant.

Therefore the states a and a' are coincident.

Also, from Eq. (2.25),

$$Tds = dh - vdp$$

The specific volume v is small for liquids, hence $v\,dp$ is also negligible, therefore, $h_a = h_{a'}$.

That is, the enthalpy of the subcooled liquid is equal to the enthalpy of the saturated liquid at liquid temperature. For all practical purposes the constant pressure lines are assumed to be coincident with the saturated liquid line in the subcooled region. This is a very useful concept.

The *T–s* diagram gives a lot of information about the refrigeration cycle. It was observed in Eq. (2.17) that for a reversible process, the heat transfer is related to the change in entropy as follows.

$$(dQ)_{\text{rev}} = T\,ds \quad \text{or} \quad \int_3^4 dQ_{\text{rev}} = Q_{34} = \int_3^4 T\,ds \tag{2.59}$$

The integral on the right hand side represents the area under the line 3–4 on *T–s* coordinates by the very definition of integral. *Therefore, according to this equation the heat transfer for a process is equal to the area under the line on T–s diagram.*

Also, $$Tds = dh - vdp$$

Therefore, for a constant pressure process, $Tds = dh$

Therefore for an isobaric process the area under the curve is equal to change in enthalpy on T–s diagram. Along the constant pressure line 3–4,

$$\int_3^4 T\,ds = h_4 - h_3$$

Isentropic lines are vertical lines on *T–s* diagram. The entropy will increase along all irreversible processes. Line 7–9 on Figure 2.8(a) is an isentropic compression line. Along this line $s_7 = s_9$ and

$$\int_7^9 v\,dp = h_9 - h_7 = \text{specific work}$$

Line 7–10 is a real non-isentropic compression process on this plot.

The pressure–enthalpy diagram in Figure 2.9 shows three constant entropy lines. It is observed that these are not parallel to each other, but are divergent. This divergence is of great use in reheat process for steam turbines and results in saving of compressor work in multistage compression processes. Three isotherms are also shown on this diagram. The pressure scale in this diagram may be a linear scale or logarithmic scale. In logarithmic scale the dome becomes very flat to the critical point. Isotherms shown in the supercritical region have a typical change in curvature.

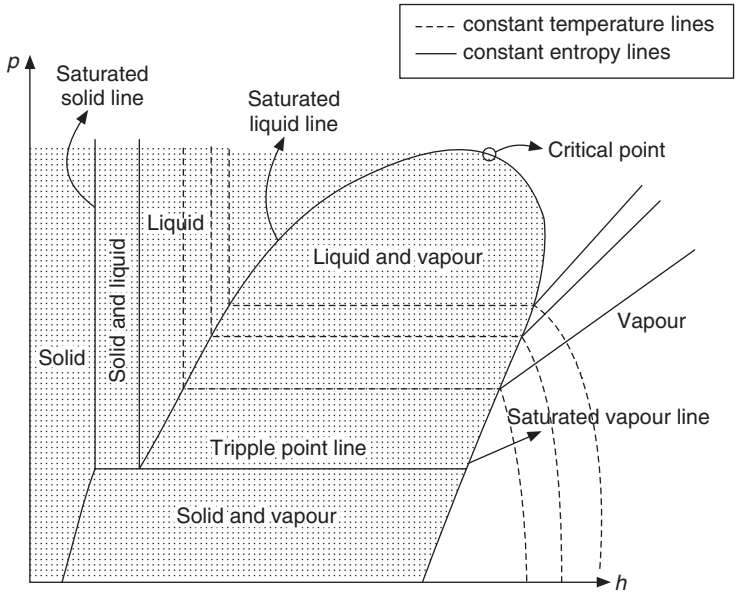

Figure 2.9 *p–h* diagram for a pure substance.

2.16.2 Properties at Saturation

The properties of refrigerants and water for saturated states are available in the form of tables. The properties along the saturated liquid line f–T_c (Figure 2.7) are indicated by subscript f. For example v_f, u_f, h_f and s_f indicate specific volume, internal energy, enthalpy and entropy of saturated liquid respectively. The corresponding saturated vapour states along g–T_c are indicated by subscript g. For example, v_g, u_g, h_g and s_g respectively. All properties with subscript fg represent the difference between the saturated vapour and saturated liquid states. For example,

$$h_{fg} = h_g - h_f \quad \text{(It is called the enthalpy of evaporation or the latent heat.)}$$

Also, $$v_{fg} = v_g - v_f$$

The specific volume, internal energy, enthalpy and entropy of the mixture in a two-phase region may be found in terms of quality, x, of the mixture. The quality, x, of the mixture denotes the mass (kg) of the vapour per unit mass (kg) of the mixture. That is, there is x kg of vapour and $(1 - x)$ kg of liquid in one kg of the mixture. Therefore the properties of the mixture can be expressed as:

$$v = xv_g + (1 - x)v_f = v_f + xv_{fg} \tag{2.60a}$$

$$u = xu_g + (1 - x)u_f = u_f + xu_{fg} \tag{2.60b}$$

$$h = xh_g + (1 - x)h_f = h_f + xh_{fg} \tag{2.60c}$$

$$s = xs_g + (1 - x)s_f = s_f + xs_{fg} \tag{2.60d}$$

The table of properties at saturation is usually temperature based. For each temperature, the table lists the values of saturation pressure (p_{sat}), v_f, v_g, h_f, h_g, s_f and s_g. Two reference states or datum are used in these tables. In ASHRAE, reference $h_f = 0.0$ kJ/kg and $s_f = 1.0$ kJ/kg-K at -40^oC. In IIR, reference $h_f = 200.00$ kJ/kg and $s_f = 1.0$ kJ/kg-K at 0^oC.

The properties in the superheated region are given in separate tables. The values of v, h and s are tabulated along constant pressure lines (that is, at saturation pressures corresponding to, say 0^oC, 1^oC, 2^oC, etc.) at various values of degree of superheat.

2.16.3 Low Pressure Water Vapour

The properties of low-pressure water vapour are of particular significance in air conditioning since in the atmosphere air, water vapour exists at pressures of less than 7 kPa. At this low pressure it is observed that water vapour may be approximated as perfect gas. Figure 2.10 shows the constant enthalpy lines in the superheated region. At pressure of 1 bar the constant enthalpy lines are distinctly curved. Hence, enthalpy at points *a*, *b*, *c* and *d* varies with temperature as well as pressure. At lower pressures, the lines become almost horizontal, that is, enthalpy is independent of pressure. At points *e*, *r* and *s* the pressure is different but temperature, *T*, is the same and enthalpy is same at all these points. Hence, enthalpy is a function of temperature alone; it is independent of pressure. This is typical of perfect gas behaviour. Also,

$$h_e = h_r = h_s = h_g(t) = \text{enthalpy of saturated vapour at temperature, } t$$

Further $h_g(t)$ may be approximated as

$$h_g(t) = (2500 + 1.88t) \text{ kJ/kg, where } t \text{ is in } ^oC \tag{2.61}$$

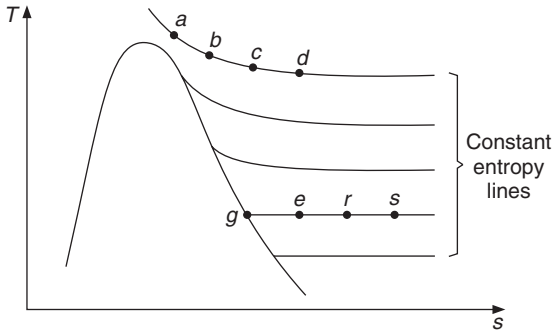

Figure 2.10 At lower pressures, constant enthalpy lines coincide with constant temperature lines in the superheated vapour region of water.

2.16.4 Clapeyron Equation

The Clapeyron equation represents the dependence of saturation pressure on saturation temperature (boiling point). This is given by

$$\frac{dp_{\text{sat}}}{dT} = \frac{h_{fg}}{(v_g - v_f)T} \tag{2.62}$$

Some useful relations can be derived by using Eq. (2.62). The specific volume of liquid is very small compared to that of vapour, hence it may be neglected and then the perfect gas relation $pv_g = RT$ may be used to yield

$$\frac{dp_{\text{sat}}}{dT} = \frac{h_{fg}}{(v_g - v_f)T} = \frac{h_{fg}}{v_g T} = \frac{p_{\text{sat}} h_{fg}}{RT^2}$$

This relation may be integrated between states 1 to an arbitrary state p_{sat}, T to yield

$$\int_{p_1}^{p} \frac{dp_{\text{sat}}}{p_{\text{sat}}} = \frac{h_{fg}}{R} \int_{T_1}^{T} \frac{dT}{T^2} \quad \text{or} \quad \ln \frac{p_{\text{sat}}}{p_1} = \frac{h_{fg}}{R}\left(\frac{1}{T_1} - \frac{1}{T}\right) \tag{2.62a}$$

If p_1 is chosen as standard atmospheric pressure of, say, one atmosphere, and p_{sat} is measured in atmospheres then $T_1 = T_{nb}$ is the normal boiling point of the substance, we therefore obtain from Eq. (2.62a),

$$\ln p = -h_{fg}/(RT) + h_{\text{fg}}/(RT_{nb})$$

Therefore if ln p is plotted against $1/T$, the saturated vapour line will be a straight line.

Also, it has been observed that for a set of similar substances the product Mh_{fg}/T_{nb}, called **Trouton number**, is constant. If we denote this product by N_{trouton}

$$N_{\text{trouton}} = \frac{Mh_{fg}}{T_{nb}} \approx 85 \text{ kJ/kgmol-K} \tag{2.63}$$

where M is the molecular weight in kg/kgmole. Therefore, $\dfrac{h_{fg}}{RT_{nb}} = \dfrac{85}{MR} = \dfrac{85}{\bar{R}}$

$$\ln p = \frac{h_{fg}}{RT} + \frac{N_{\text{trouton}}}{\bar{R}} = \frac{h_{fg}}{\bar{R}T} + \frac{N_{\text{trouton}}}{\bar{R}} \tag{2.64}$$

where, h_{fg} is the molal enthalpy of evaporation.

2.17 CORRELATIONS FOR PROPERTIES OF REFRIGERANTS

2.17.1 Vapour Pressure

Equation (2.64) is modified to include more terms so as to improve the accuracy of representing vapour pressure of refrigerants. The following equation is used.

$$\ln p = c_1 + c_2/T + c_3 \ln T + c_4 T^n \tag{2.65}$$

where c_1, c_2, c_3, c_4 and n are constants for a specific refrigerant.

2.17.2 Liquid Density

Liquid density varies linearly with temperature over a narrow range of temperature. An accurate expression for this is of the form

$$\rho_f = \sum_{i=0}^{n} D_i (1 - T/T_c)^{i/3} \tag{2.66}$$

where T_c is the critical temperature in K

2.17.3 Specific Heat of Vapour

This is also represented as a polynomial

$$c_v = \sum_{i=0}^{n} E_i T^i \tag{2.67}$$

and $c_p = c_v + R$.

Internal energy and enthalpy

The expressions for the variation of internal energy and enthalpy with temperature and pressure are obtained by considering Eqs. (3.24), (3.25) and the Maxwell's relations Eq. (3.31). These are:

$$\begin{aligned}
du &= c_v dT + \left[T\left(\frac{\partial p}{\partial T}\right)_v - p \right] dv = c_v dT + \frac{T^2}{v}\left[\frac{\partial (pv/T)}{\partial T}\right]_v dv \\
dh &= c_p dT - \left[T\left(\frac{\partial v}{\partial T}\right)_p - v \right] dp = c_p dT + \frac{T^2}{p}\left[\frac{\partial (pv/T)}{\partial T}\right]_p dp \\
ds &= c_p \frac{dT}{T} - \left(\frac{\partial v}{\partial T}\right)_p dp \\
ds &= c_v \frac{dT}{T} - \left(\frac{\partial p}{\partial T}\right)_v dv
\end{aligned} \tag{2.68}$$

The refrigerant properties may be determined by integrating these equations, specific heat correlation and one of the equations of state.

2.18 HEAT TRANSFER

'Refrigeration and air conditioning' involves heat transfer, hence a good understanding of the concepts of heat transfer is of vital importance to the student of this subject. The fundamental concepts of heat transfer will now be dealt with and special applications mentioned wherever required.

In general, heat is transferred by three modes, namely, conduction, convection and radiation. In most applications, usually two and often all the three modes are involved in the overall heat transfer problem.

2.19 CONDUCTION

Conduction heat transfer involves flow of heat from one part of the body to another part at a lower temperature by way of free electrons or from molecule to molecule by vibration and rotation of

molecules about their lattice positions. It requires direct contact if flow of heat occurs from one body to another, for example, from a heated solid to a liquid or from one solid to another solid. Heat transfer also occurs in liquids and gases by direct contact with surfaces and by way of energy transfer from molecule-to-molecule. The fundamental law governing conduction heat transfer is an empirical law, called the Fourier's law of heat conduction.

2.19.1 Fourier's Law of Conduction Heat Transfer

According to Fourier's law, heat transfer rate by conduction is proportional to the temperature gradient and the area of heat transfer, i.e.

$$Q_x = -kA\frac{dT}{dx} \tag{2.69}$$

where Q_x is the heat transfer rate in the x-direction, A is the area perpendicular to the x-direction (y–z plane) and dT/dx is the temperature gradient in the x-direction. The proportionality constant k is called the *thermal conductivity*. The negative sign indicates that heat is transferred down-hill, that is, from a high temperature to a low temperature. The thermal conductivity is determined experimentally. It is highest for metals and very low for insulating materials. For isotropic materials it is same in all directions but for materials like wood, it is different along the grain and across the grain. It depends upon temperature. Therefore, it is a function of spatial coordinates in a temperature field and also for non-homogeneous materials it a function of spatial coordinates. Equations similar to (2.69) may be written for y and z directions as well, for example,

$$\left.\begin{aligned} Q_y &= -kA\frac{dT}{dy} \\ \text{and}\quad Q_z &= -kA\frac{dT}{dz} \end{aligned}\right\} \tag{2.70}$$

The unit of thermal conductivity is W/m-K and typical values for some of the materials are shown in Table 2.1.

Table 2.1 Thermal conductivity values of some materials

Material	*Thermal conductivity, k* (W/m-K)
Air	0.023
Polyurethane foam (PUF)	0.025
Expanded polystyrene	0.035
Mineral wool	0.04
Wood	0.225
Glass	0.7
Water vapour	0.021
Water	0.56
Ammonia	0.54
R12 vapour	0.075
Lead	34.6
Steel	45.0
Aluminium	208.0
Copper	380.0

2.19.2 Conduction Equation

Considering energy balance for an elemental control volume and Fourier's law of heat conduction, it can be shown that

$$\frac{\partial T}{\partial \tau} = \alpha \left[\frac{\partial^2 T}{\partial x^2} + \frac{\partial^2 T}{\partial y^2} + \frac{\partial^2 T}{\partial z^2} \right] \tag{2.71}$$

This is known as *conduction equation*. In this equation $\alpha = k/\rho c_p$ is called *thermal diffusivity*. The time variable is denoted by τ and the unsteady term on left hand side indicates the storage of energy in the control volume with time. In case there is no storage of energy and boundary conditions are also independent of time, the temperature does not change with time and such a situation is called steady state. In steady state Eq. (2.71) using the Laplacian operator ∇^2, reduces to

$$\nabla^2 T = \frac{\partial^2 T}{\partial x^2} + \frac{\partial^2 T}{\partial y^2} + \frac{\partial^2 T}{\partial z^2} = 0 \tag{2.72}$$

Equations (2.71) and (2.72) are linear partial differential equations that can be solved easily by separation of variables, Laplace Transform and Fourier Transform methods.

In many practical steady state situations, considering one-dimensional heat transfer gives satisfactory results. Considering a slab of thickness L in x-direction and of very large dimensions in y- and z-directions shown in Figure 2.11, one-dimensional steady state heat transfer equation in x-direction and the boundary conditions are

$$\frac{d^2 T}{dx^2} = 0 \tag{2.73}$$

$$\text{At } x = 0,\ T = T_1 \quad \text{and} \quad \text{at } x = L,\ T = T_2$$

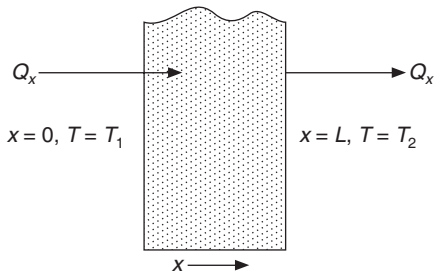

Figure 2.11 One-dimensional, steady state heat conduction.

The solution to Eq. (2.73) is

$$T = T_1 + (T_2 - T_1)\frac{x}{L} \quad \text{and} \quad Q_x = -kA\frac{dT}{dx} = kA\left(\frac{T_1 - T_2}{L}\right) \tag{2.74}$$

Now in the case of a long hollow cylinder, the steady state conduction equation in radial direction and the boundary conditions at inner radius r_1 and outer radius r_2 are as follows:

$$\frac{d^2 T}{dr^2} + \frac{1}{r}\frac{dT}{dr} = \frac{1}{r}\frac{d}{dr}\left(r\frac{dT}{dr}\right) = 0 \tag{2.75}$$

Boundary conditions are given by:

$$\text{At } r = r_1,\ T = T_1 \text{ and at } r = r_2,\ T = T_2$$

The temperature distribution is given by

$$T = T_1 - (T_1 - T_2)\frac{\ln (r / r_1)}{\ln (r_2 / r_1)} \tag{2.76}$$

The heat transfer rate is given by

$$Q_r = -kA\frac{dT}{dr} = -2kL\pi\frac{(T_1 - T_2)}{\ln (r_2 / r_1)} \tag{2.77}$$

where the surface area of the cylinder has been taken to be $2\pi rL$, L being the length of the cylinder.

2.19.3 Electrical Analogy

The temperature difference is the driving force for the heat transfer just as the electrical potential is the driving force for current flow. Hence, heat transfer rate may be considered equivalent to flow of current. Following this analogy between conduction heat transfer and flow of current, a thermal conduction thermal resistance, R, is defined for conduction heat transfer and it is expressed as

$$Q = (T_1 - T_2)/R \tag{2.78a}$$

For heat transfer in the x-direction, we have from Eq. (2.74)

$$R = \frac{L}{kA} \tag{2.78b}$$

Similarly, from Eq. (2.77) in radial coordinates,

$$R = \frac{\ln (r_2 / r_1)}{2\pi Lk} \tag{2.79}$$

2.20 FICK'S LAW OF DIFFUSION

This law deals with the transfer of mass within a medium due to the difference in concentration between the various parts of it. It is very similar to Fourier's law of heat conduction. It is also by molecular diffusion processes. Let us say that we have a mixture of two species and the concentration of one of them is c kg/m^3 while that of the other will be $1 - c$. According to Fick's law, mass transfer rate $\dot{m}$ kg/s by diffusion is proportional to the concentration gradient and the area of mass transfer, i.e.

$$\dot{m} = -DA\frac{dc}{dx} \tag{2.80a}$$

where, D is called the *diffusion coefficient* and it has the units of m^2/s just like those of thermal diffusivity α and the kinematic viscosity of fluid ν for momentum transfer. In problems dealing with diffusion of water vapour, humidity ratio, W will be used instead of concentration. Humidity

ratio is non-dimensional and the product $\rho_a W$ denotes the density of water vapour, hence the density of dry air ρ_a is used along with D in Eq. (2.80a), that is,

$$\dot{m} = -\rho_a DA \frac{dW}{dx} \tag{2.80b}$$

2.21 THERMAL RADIATION

This mode of heat transfer does not require direct contact or a medium. It occurs by electromagnetic waves. A body due to its temperature emits electromagnetic radiation, and it is emitted at all temperatures. It is propagated with the speed of light (3×10^8 m/s) in a straight line in vacuum. Its speed decreases in a medium but it travels in a straight line in a homogeneous medium. The speed of light, c is equal to the product of wavelength λ and frequency ν, that is,

$$c = \lambda \nu$$

The wavelength is expressed in Angstrom (1 Å = 10^{-10} m) or micron (1 μm = 10^{-6} m).

Thermal radiation lies in the range of 0.1 to 100 μm, while visible light lies in the range of 0.35 to 0.75 μm. Most of the thermal radiation problems involve infrared radiation.

Propagation of thermal radiation takes place in the form of discrete quanta, each quantum having energy of

$$E = h\nu \tag{2.81}$$

where, h is Planck's constant, $h = 6.625 \times 10^{-34}$ J-s

The radiation energy is converted into heat when it strikes a body.

2.21.1 Blackbody

The concept of blackbody is very important, as it indicates an ideal radiator and absorber. A blackbody is a hypothetical body that absorbs all the incident (all wavelengths) radiation. The term black has nothing to do with the black colour. A white-coloured body can also absorb infrared radiation as much as a black-coloured surface. A hollow enclosure with a small hole is an approximation to a blackbody. Any radiation that enters through the hole is absorbed by multiple reflections within the cavity. The hole being small, only a very small quantity of radiation is able to escape through the hole.

There are three important laws for emission of radiation from a blackbody.These are Planck's law, Stefan–Boltzmann's law and Wien's Displacement law.

The *emissive power E* of a surface is the amount of energy radiated by the surface per unit time per unit area. The emissive power of a blackbody is the maximum. The energy density of the emitted radiation varies with the wavelength.

2.21.2 Planck's Law

According to Planck's law, monochromatic emissive power of a blackbody is given by

$$E_{b\lambda} = \frac{8\pi hc\lambda^{-5}}{\exp(hc/\lambda kT) - 1} \tag{2.82}$$

where, k is Boltzmann's constant, $k = 1.38066 \times 10^{-23}$ J/mole-K. This is the energy radiated between the wavelengths λ and $\lambda + d\lambda$ per unit area per unit time.

2.21.3 Wien's Displacement Law

The wavelength for maximum emissive power of a blackbody may be obtained by equating the differential of Eq. (2.82) with respect to λ to zero. If λ_{max} is the wavelength at which the maximum occurs, then according to Wien's displacement law, the product of λ_{max} and the absolute temperature T of the body is constant, that is,

$$\lambda_{\max} T = 2.897.6 \ \mu\text{m-K} \tag{2.83}$$

2.21.4 Stefan–Boltzmann's Law

The emissive power of a blackbody is obtained by integrating Eq. (2.82) over all the wavelengths, that is,

$$E_b = \int_0^\infty E_{b\lambda}\, d\lambda = \sigma T^4 \tag{2.84}$$

This is known as Stefan–Boltzmann's law. According to this law, the energy radiated by a black body per unit area per unit time is proportional to the fourth power of the absolute temperature, that is,

$$E_b = \sigma T^4 \tag{2.85}$$

The constant σ is called the Stefan–Boltzmann's constant and is equal to $\sigma = 5.669 \times 10^{-8}$ W/m^2-K^4.

Figure 2.12 schematically illustrates the blackbody radiation as a function of wavelength for three temperatures. Various points of the curves may be calculated from Eq. (2.82). As the temperature increases, the maximum monochromatic emissive power increases and shifts to shorter wavelengths. Wien's displacement law indicates this.

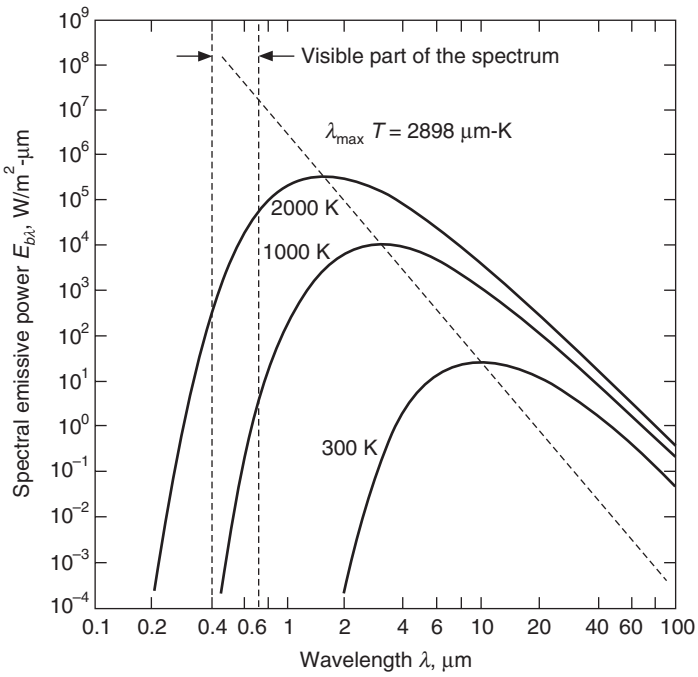

Figure 2.12 Spectral emissive power of a blackbody.

2.21.5 Emissivity

The emissivity ε of a real surface is the ratio of the emissive power of a body to that of a blackbody, that is,

$$\varepsilon = \frac{E}{E_b} \tag{2.86}$$

where, E is the energy radiated by the body per unit area per unit time over all the wavelengths and E_b is same for a blackbody as given by Eq. (2.84).

2.21.6 Monochromatic Emissivity

The monochromatic emissivity ε_λ of a surface is the ratio of the monochromatic emissive power of the surface to that of blackbody, that is

$$\varepsilon_\lambda = \frac{E_\lambda}{E_{b\lambda}} \tag{2.87}$$

where E_λ is the energy radiated by a non-blackbody between the wavelengths λ and $\lambda + d\lambda$ per unit surface area per unit time and $E_{b\lambda}$ is same for a blackbody.

2.21.7 Gray Body

This is a body for which the monochromatic emissivity ε_λ is independent of wavelength, that is, $\varepsilon_\lambda = \varepsilon = a$ constant less than one.

For this hypothetical body the radiation emitted at all wavelengths has the same proportion to that for a blackbody as given by Eq. (2.82).

2.21.8 Absorptivity

The blackbody is an ideal radiator. Likewise, it is an ideal absorber too. That is, it absorbs all the incident radiation whereas non-black surfaces do not absorb all the radiation. If I is the incident radiation intensity (W/m^2) on a surface and I_a the part of this intensity which is absorbed, then we define absorptivity, α, for a real (non-black) surface as follows.

$$\alpha = \frac{I_a}{I} \tag{2.88}$$

The absorptivity for a black surface is unity at all wavelengths, for other surfaces it is less than one. This also depends upon the wavelength λ. Incident radiation may have distribution of intensity similar to that given by Eq. (2.82). The absorptivity, in general, depends upon the source of incident radiation and the surface characteristics of the surface.

2.21.9 Kirchhoff's Law

According to Kirchhoff's law the emissivity ε of a surface is equal to its absorptivity α at thermal equilibrium, that is,

$$\varepsilon = \alpha$$

or, in general

$$\varepsilon_\lambda = \alpha_\lambda \tag{2.89}$$

Thermal equilibrium implies that the temperatures of radiation emitting and absorbing surfaces are the same. The emitted radiation depends upon the temperature and surface characteristics of the emitting surface, while the absorbed radiation depends upon the temperature of the source that emitted it, and the surface characteristics of the surface receiving it.

This law is not valid when a surface emits radiation in the long wavelength range (room temperature) while it receives solar radiation in the short wavelength range.

2.21.10 Reflectivity and Transmissivity

Figure 2.13 shows the changes that occur when a ray of radiation intensity I (W/m^2) strikes a surface at point P at an angle θ with respect to normal PQ to it. Part of radiation, I_r, is reflected, I_a is absorbed and a part I_t is transmitted.

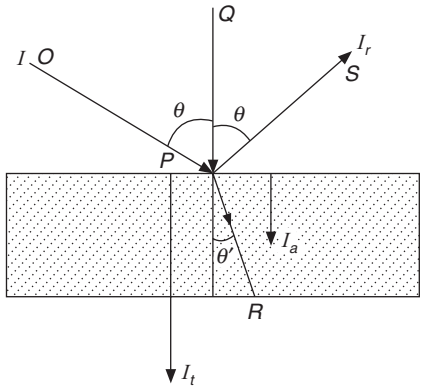

Figure 2.13 Reflection, absorption and transmission of incident radiation.

We define reflectivity ρ, absorptivity α, and transmissivity τ as follows:

$$\rho = \frac{I_r}{I}, \quad \alpha = \frac{I_a}{I} \quad \text{and} \quad \tau = \frac{I_t}{I} \tag{2.90}$$

It is obvious that,

$$I_r + I_a + I_t = I$$

hence,

$$\rho + \alpha + \tau = 1 \tag{2.91}$$

Equation (2.91) is applicable to diathermanous materials such as glass and some plastic materials, which are transparent and hence transmit radiation. Materials that do not transmit radiation are called opaque materials. The transmissivity τ is equal to zero for opaque substances, hence

$$\rho + \alpha = 1 \tag{2.92}$$

Actually, a very thin layer of the material near the surface of the material absorbs the incident radiation. Hence to some extent, radiation is transmitted in all materials. If the thickness is large, no radiation will be transmitted. If a thin wafer is made of any material, it will transmit radiation.

The reflection depends upon the surface characteristics of the material. For a highly smooth surface like mirror and highly polished metal surface, the reflection is *specular*. Specular reflection means that the reflection angle θ'' is equal to the incidence angle θ of the incident radiation. The angles are measured with respect to normal PQ to the surface. The incident beam OP , the reflected beam PS and normal PQ are in the same plane. In case the surface is rough, the reflection occurs in all the directions, and is called *diffuse* reflection.

The refracted beam PR bends as it enters the second medium, that is, the angle θ' with respect to the normal is different from the incident angle θ. The *index of refraction n* is defined as follows:

$$n = \sin \theta / \sin \theta' \tag{2.93}$$

Actually, the speed of light is different in the two media. If one of the media is used as the reference, the reference being either air or vacuum, the index of refraction also is the ratio of speed of light in the two media.

2.21.11 Exchange of Radiation between Bodies

We may assume for simplicity that two bodies are in visible range, and are separated by a medium that does not absorb radiation. In such a case both the bodies exchange energy by a reciprocal process of emitting and absorbing radiation. This is called *radiation heat transfer*. If the bodies are at the same temperature, the net heat exchange is zero. There will be a net heat transfer from the warmer body to the colder body by radiation.

All the energy emitted by a body is not incident upon the other body because of the relative orientation, distance and shape of the bodies. A shape factor F is defined to account for this ratio. If body number 1, the inner cylinder in Figure 2.14 is totally enclosed by body number 2, the outer cylinder, then all the radiation emitted by the inner cylinder is incident upon the outer cylinder and it is said to have a shape factor $F_{12} = 1$. The inner cylinder has a convex surface; it cannot see any of its own part, hence its view factor with respect to itself $F_{11} = 0$. However, a part of the radiation emitted by the inner surface of the outer cylinder is incident upon itself, hence its shape factor with respect to itself $F_{22} \neq 0$ and therefore its shape factor with respect to surface 1, $F_{21} < 1$.

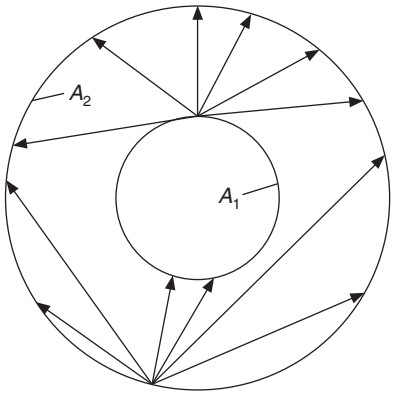

Figure 2.14 Radiation exchange in an enclosure formed by two concentric black spherical surfaces.

It can be shown that $F_{21} = A_1/A_2$ or in general

$$A_1F_{12} = A_2F_{21} \tag{2.94}$$

where, A_1 and A_2 are the areas of the inner and outer surface cylinders respectively.

The absorptivity and emissivity of the surfaces are also not equal to unity unless they are blackbodies. As a result, only a part of the incident radiation is absorbed and the remaining is reflected back. A part of the reflected radiation will be incident on the body that emitted it in the first place. A factor F_E is defined to account for the emission and absorption characteristics of the two surfaces.

If the bodies are at absolute temperatures of T_1(K) and T_2(K) respectively, then the net radiation heat transfer between the two bodies is expressed as

$$Q_{12} = \sigma A_1 F_{12} F_E (T_1^4 - T_2^4) \tag{2.95}$$

where, $\sigma = 5.669 \times 10^{-8}$ W/m^2-K^4 is the Stefan–Boltzmann constant and A is the area in m^2. For the purpose of calculation, Eq. (2.95) may be more conveniently written as

$$Q_{12} = 5.699\, A_1F_{12}F_E \left[\left(\frac{T_1}{100}\right)^4 - \left(\frac{T_2}{100}\right)^4\right] \tag{2.96}$$

For the case of a small body 1 of emissivity ε_1, which is completely enclosed by a much larger body 2, the shape factor $F_{12} = 1$ and Eq. (2.96) reduces to

$$Q_{12} = 5.699\, A_1\varepsilon_1 \left[\left(\frac{T_1}{100}\right)^4 - \left(\frac{T_2}{100}\right)^4\right] \tag{2.97}$$

In many situations involving small temperature differences, it is convenient to express the rate of radiation heat transfer by

$$Q_{12} = h_R A_1 (t_1 - t_2) \tag{2.98}$$

where, h_R is a radiation heat transfer coefficient in W/m^2-K, and t_1 and t_2 are temperatures expressed in degree Celsius. From Eqs. (2.97) and (2.98), we have

$$h_R = \frac{5.669\, F_{12}F_E \left[\left(\frac{T_1}{100}\right)^4 - \left(\frac{T_2}{100}\right)^4\right]}{t_1 - t_2} \tag{2.99}$$

2.22 CONVECTION

Thermal convection is the transfer of heat from one part of a fluid to another part at a lower temperature by bulk motion. In contrast to radiation, it requires a medium and in contrast to conduction, it requires bulk motion of the medium. Two types of convection heat transfer may exist, namely *forced convection* and *free* or *natural convection*. Forced convection occurs, when the fluid is forced to flow by a pump or fan. The examples are flow of cold water by a pump from a cooling tower to a shell-and-tube type heat exchanger where condensation of refrigerant occurs

or where flow of brine by a pump to the shell-and-tube heat exchanger occurs for chilling the refrigerant. Similarly, air is made to flow by a blower through the cooling coil of an air-conditioning system or over the air-cooled condenser.

Free or natural convection occurs when the fluid motion is caused by density difference arising as a result of temperature difference. The density of a fluid particle decreases when it is heated, it becomes lighter and rises up in gravitational field. Similarly, the density of a cooled fluid particle increases and it moves down in a gravitational field. The household refrigerator has its cooling coil at the top part where air is cooled. This air moves down by natural convection and gets heated up by food items and then rises up, thus setting up air circulation by natural convection. The outer shell of the refrigerator is heated by rejection of heat from refrigerant. The room air rises up along the refrigerator walls by natural convection.

All practical problems in convection deal with heat transfer between a fluid and a solid surface. The heat transfer from the solid surface is by molecular conduction by fluid particles in the immediate vicinity of the surface. The actual heat transfer problems involve conduction as well as convection and sometime radiation too.

The flow of fluid can be either laminar or turbulent. One defines a non-dimensional number called Reynolds number as the ratio of inertia to viscous terms to characterize the nature of flow.

At low Reynolds numbers, the viscous forces damp out the disturbances and the flow remains laminar. In laminar flow the fluid particles follow a smooth trajectory; fluid layers kind of glide over each other. The heat and mass transfer occur by laminar convection and molecular diffusion.

At higher Reynolds numbers, the fluid inertia becomes very large compared to viscous terms, as a result the disturbances once initiated start to grow and the flow becomes completely random in space and time. Such a flow is called *turbulent* flow. The turbulence increases the rates of heat and mass transfer by orders of magnitude due to random mixing and stirring. This brings the fluid particles of different temperatures and concentrations into contact and increases the rates of heat and mass transfer. The diffusion due to turbulent mixing is referred to as turbulent diffusion.

When a fluid flows over a surface, its velocity and temperature adjacent to the surface are same as that of the surface. The velocity and temperature far away from the surface may remain unaffected. Figures 2.15(a) and (b) show that a fluid with a free stream velocity U_∞ and free stream temperature T_∞ flows over a flat plate maintained at temperature of $T_w > T_\infty$. In the vicinity of the surface as shown in Figure 2.15(a), the velocity tends to zero from its free stream value U_∞. This happens in a very narrow region of thickness δ of the order of $\mathrm{Re}^{-0.5}$ where there is a sharp velocity gradient, hence the viscous forces are important in this region. Reynolds number, $\mathrm{Re} = U_\infty L/\nu$, has to be large for the boundary layers to exist. This narrow region is called the *hydrodynamic boundary layer* in which the inertia terms are of same order of magnitude as the viscous terms. Similarly, there is a sharp temperature gradient in this vicinity of the plate as shown in Figure 2.15(b). The conduction terms are of the same order of magnitude as the convection terms in this region. This region is called the *thermal boundary layer,* $\delta(t)$, whose thickness is of the order of $(\mathrm{RePr})^{-0.5}$. The ratio of thermal boundary layer thickness to the viscous boundary layer thickness depends upon Prandtl number, Pr ($c_p\ \mu/k = \nu/\alpha$). For large Prandtl numbers, $\delta(t) < \delta(x)$, and for small Prandtl numbers, $\delta(t) > \delta(x)$.

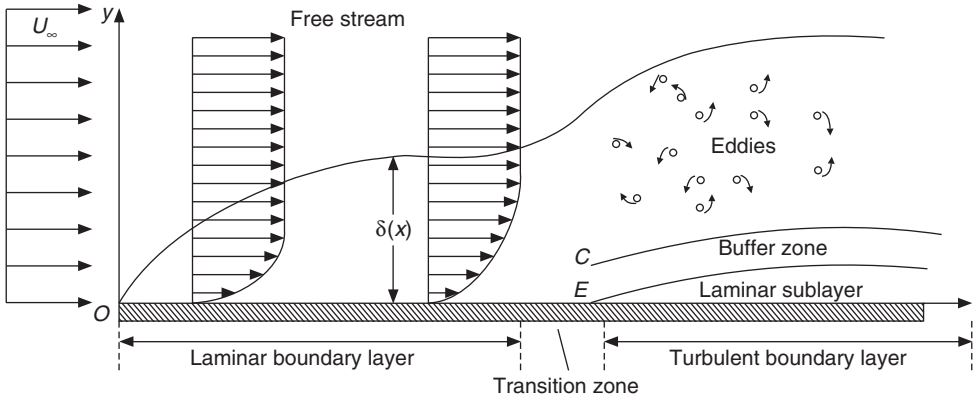

Figure 2.15(a) Velocity boundary layer over a flat plate.

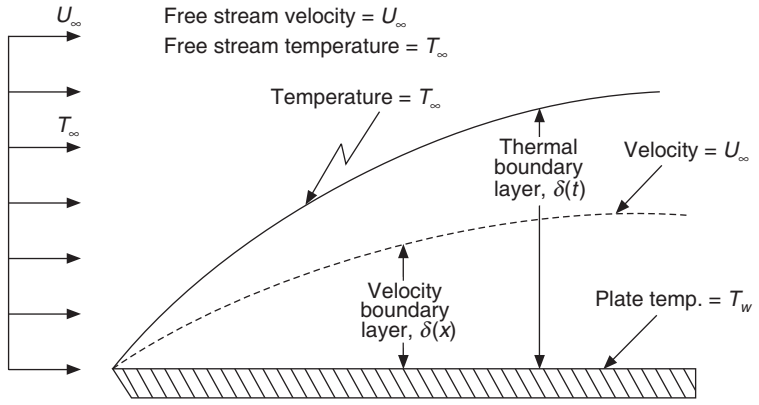

Figure 2.15(b) Temperature boundary layer other a heated plate.

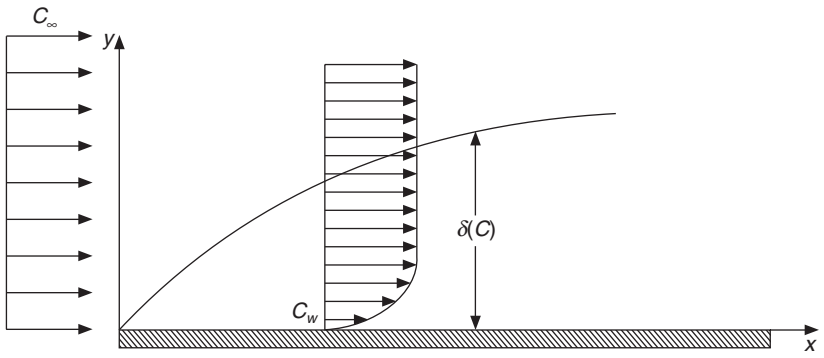

Figure 2.15(c) Mass transfer boundary layer over the free surface of a plate.

In addition, if there is diffusion of some species near the surface, then there will exist mass transfer boundary layer in which the concentration will vary from C_w near the plate to C_∞ far away from the plate in the free stream as shown in Figure 2.15(c).

As the Reynolds number increases, this region becomes narrow, the temperature gradient becomes large and the heat transfer rate increases. The momentum transfer is related to kinematic viscosity ν while the diffusion of heat is related to thermal diffusivity α. Hence the ratio of thermal boundary layer to viscous boundary layer is related to the ratio ν/α, called the Prandtl number. The thermal boundary layer thickness is smaller than that of the viscous boundary layer for large Prandtl numbers.

Since the heat transfer from the surface is by molecular conduction, it depends upon the temperature gradient in the fluid in the immediate vicinity of the surface, i.e.

$$Q = -kA\left(\frac{dt}{dy}\right)_{y=0} \tag{2.100}$$

Since the temperature difference has been recognized as the potential for heat transfer, it is convenient to express convective heat transfer rate as proportional to it, i.e.

$$Q = h_c A\,(t_w - t_\infty) \tag{2.101}$$

This equation defines the heat transfer coefficient h_c. This equation is also referred to as Newton's law of cooling in some elementary textbooks which states that the heat transfer rate is proportional to the temperature difference $(t_w - t_\infty)$.

In analogy with convective heat transfer, we can define the mass transfer coefficient h_M as follows:

$$\dot{m} = h_M A(C_w - C_\infty)$$

or

$$\dot{m} = \rho_a h_D A(W_w - W_\infty) \tag{2.102}$$

where, h_M and h_D are the *mass transfer coefficients, C* is concentration in kg/m^3, and W is the humidity ratio in kg of water vapour per kg of dry air, while ρ_a is the density of dry air.

It is convenient to consider dimensional similarity and express heat transfer rate in terms of Nusselt number, Nu, and mass transfer rate in terms of Sherwood number, Sh, as follows:

$$\text{Nu} = \frac{h_c L}{k} \quad \text{and} \quad \text{Sh} = \frac{\rho_a h_D L}{D} \tag{2.103}$$

The heat transfer and mass transfer, based upon similarity and conservation laws, depend upon the following non-dimensional numbers, which are related to fluid properties, geometry and physical dimensions of the flow.

$$\text{Reynolds Number, Re} = \frac{\rho V L}{\mu} \qquad \text{Prandtl Number, Pr} = \frac{c_p \mu}{k}$$

$$\text{Lewis Number, Le} = \frac{\alpha}{D} \qquad \text{Schimidt Number, Sc} = \frac{\nu}{D}$$

$$\text{Grashof Number, Gr} = \frac{g\beta\Delta T L^3}{\nu^2} \qquad \text{Rayleigh Number, Ra} = \frac{g\beta\Delta t L^3}{\nu a} \tag{2.104}$$

$$\text{Stanton Number} = \frac{\text{Nu}}{\text{Re.Pr}} \qquad \text{Peclet Number, Pe} = \text{Re.Pr}$$

Correlations have been proposed based upon experimental results and the solution of Navier–Stokes equations and energy equations for simple geometries like flat plate, tubes, annulus and ducts of various shapes. This information is available in many textbooks on heat transfer including *Heat Transfer* by J.P. Holman (1989). Some of these correlations are as follows.

2.22.1 Heat Transfer Coefficient Inside Tubes

Laminar flow

1. Nusselt–Graetz correlation

   This is valid for thermal entrance length with parabolic velocity profile and constant wall temperature.

$$\begin{aligned} \mathrm{Nu}_x &= 1.077\ (\mathrm{Pe}.D_i/x)^{1/3} \quad : \quad \mathrm{Pe}.D_i/x > 10^2 \\ &= 3.66 \quad : \quad \mathrm{Pe}.D_i/x < 10^2 \end{aligned} \tag{2.105}$$

$$\begin{aligned} \overline{\mathrm{Nu}} &= 1.61\ (\mathrm{Pe}.D_i/L)^{1/3} \quad : \quad \mathrm{Pe}.D_i/L > 10^2 \\ \overline{\mathrm{Nu}} &= 3.66 \quad : \quad \mathrm{Pe}.D_i/L < 10^2 \end{aligned} \tag{2.106}$$

   where, Pe is Peclet number: $\mathrm{Pe} = \mathrm{Re}.\mathrm{Pr} = \left(\frac{\rho V D_i}{\mu}\right).\left(\frac{c_p \mu}{k}\right)$

2. Hausen's correlation

   This is valid for developing hydrodynamic and thermal boundary layer and for constant wall temperature. All the physical properties are evaluated at average bulk temperature.

$$\overline{\mathrm{Nu}}_d = 3.66 + \frac{0.0668(D_i/L)\mathrm{Pe}}{1 + 0.04\,[(D_i/L)\mathrm{Pe}]^{2/3}} \tag{2.107}$$

   Also,
$$\overline{\mathrm{Nu}} = 3.66 + \frac{0.19(\mathrm{Pe}.D_i/L)^{0.8}}{1 + 0.117[(D_i/L)\,\mathrm{Pe}]^{0.467}} \tag{2.108}$$

3. Sider and Tate correlation

$$\mathrm{Nu}_D = 1.86(\mathrm{Pe}^{1/3}\ (D_i/L)^{1/3}\ (\mu/\mu_w)^{0.14} \tag{2.109}$$

   For constant wall temperature, μ_w is the viscosity at the wall temperature.

4. Schlunder's correlation

   $\overline{\mathrm{Nu}} = [(3.66)^3 + (1.61)^3\ \mathrm{Pe}.D_i/L]^{1/3}$ for constant wall temperature

   For constant heat flux, the following correlation may be used.

$$\begin{aligned} \mathrm{Nu}_x &= 1.302\ (\mathrm{Pe}.D_i/x)^{1/3} \quad : \quad \mathrm{Pe}.D_i/x > 10^4 \\ \mathrm{Nu}_D &= 4.36 \quad : \quad \mathrm{Pe}.D_i/x < 10^3 \end{aligned} \tag{2.110}$$

$$\begin{aligned} \overline{\mathrm{Nu}} &= 1.953\ (\mathrm{Pe}.D_i/L)^{1/3} \quad : \quad \mathrm{Pe}.D_i/x > 10^2 \\ \overline{\mathrm{Nu}} &= 4.36 \quad : \quad \mathrm{Pe}.D_i/x < 10^3 \end{aligned} \tag{2.111}$$

Annular Passage

Stefan's correlation based upon the results of Hausen is

$$D_h = D_o - D_i, \text{Re} = UD_h/\nu \text{ and Nu} = hD_h/k$$

and
$$\text{Nu} = \text{Nu}_\infty f(D_i/D_o)\frac{0.19(\text{Pe}.D_h/L)^{0.8}}{1.0 + 0.117(\text{Pe}.D_h/L)^{0.467}} \quad (2.112)$$

$$0.1 < \text{Pr} < 10^3,\ 0 < D_i/D_o < 1,\ \text{Re} < 2300$$

$\text{Nu}_\infty = 3.66 + 1.2(D_i/D_o)^{-0.8}$: Case I : Outer wall of annulus is insulated.

$\text{Nu}_\infty = 3.66 + 1.2(D_i/D_o)^{0.5}$: Case II : Inner wall of annulus is insulated.

$\text{Nu}_\infty = 3.66 + \left[4 - \frac{0.102}{(D_i/D_o) + 0.2}\right]$: Case III : None of the walls is insulated

The function $f(D_i/D_o)$ is as follows for the three cases:

Case I : $f(D_i/D_o) = 1 + 0.14(D_i/D_o)^{-0.5}$

Case II : $f(D_i/D_o) = 1 + 0.14(D_i/D_o)^{1/3}$

Case III : $f(D_i/D_o) = 1 + 0.14(D_i/D_o)^{0.1}$

Turbulent flow

1. Dittus–Boelter equation

   This is valid for fully developed turbulent flow. Properties are evaluated at bulk temperature

   $$\text{Nu} = 0.023\ \text{Re}^{0.8}\ \text{Pr}^n \quad (2.113)$$

   This is valid for Pr = 0.6 to 100

   $n = 0.4$ for heating

   $n = 0.3$ for cooling

   $\text{Nu} = hD_i/k, \text{Re} = \rho\bar{V}D_i/\mu$

2. Sider and Tate correlation

   This includes the variation of viscosity with temperature.

   $$\text{Nu} = 0.036\ \text{Re}^{0.8}\ \text{Pr}^{1/3}\ (\mu/\mu_w)^{0.14} \quad (2.114)$$

   where, μ_w is viscosity at wall temperature.

3. Nusselt's corelation

   This is valid in the entrance region.

   $$\text{Nu} = 0.036\ \text{Re}^{0.8}\ \text{Pr}^{1/3}\ (\mu/\mu_w)^{0.14}\ (D_i/L)^{0.055} : 10 < D_i/L < 400 \quad (2.115)$$

   where, μ_w is viscosity at wall temperature and all other properties are evaluated at bulk temperature.

4. Petukhov's correlation

This is valid for fully developed turbulent flow.

$$\mathrm{Nu} = \frac{(f/8)\,\mathrm{Re}\,\mathrm{Pr}}{1.07 + 12.7\,(f/8)^{0.5}\,(\mathrm{Pr}^{2/3} - 1)} \left(\frac{\mu_b}{\mu_w}\right)^n \tag{2.116}$$

$0.5 < \mathrm{Pr} < 2000$, $10^4 < \mathrm{Re} < 5 \times 10^6$, $0.8 < \mu_b/\mu_w < 40$

$n = 0.11$ for $T_w > T_b$, $n = 0.25$ for $T_w < T_b$ and $n = 0$ for constant heat flux

$f = (1.82 \log_{10} \mathrm{Re} - 1.64)^{-2}$

Properties are evaluated at $T_f = (T_w + T_b)/2$

Accuracy *:* $0.5 < \mathrm{Pr} < 200$: 6% and $200 << 2000$: 10%

2.22.2 Heat Transfer Coefficient from Flow over a Horizontal Flat Plate

Laminar flow

$$\mathrm{Nu}_x = 0.332\,\mathrm{Re}_x^{0.5}\,\mathrm{Pr}^{1/3} : \text{Isothermal plate} \tag{2.117a}$$

$$\mathrm{Nu}_x = 0.453\,\mathrm{Re}_x^{0.5}\,\mathrm{Pr}^{1/3} : \text{Constant heat flux} \tag{2.117b}$$

Turbulent flow

$$\bar{\mathrm{Nu}}_L = \bar{h}L/k = \mathrm{Pr}^{1/3}\,(0.037\,\mathrm{Re}_L^{0.8} - 850) \ : \text{Isothermal} \tag{2.118}$$

Critical Reynolds number has been taken to be 500,000

For constant heat flux case $\bar{\mathrm{Nu}}_L$ is 4% more than the isothermal case.

2.22.3 Free Convection Heat Transfer Coefficient

Isothermal case

Vertical flat plate and cylinder

$$\mathrm{Nu} = 0.55(\mathrm{Gr}\,\mathrm{Pr})^{1/4} \quad : \quad 10^4 < \mathrm{Ra} < 10^9 \tag{2.119a}$$

$$= 0.1(\mathrm{Gr}\,\mathrm{Pr})^{1/3} \quad : \quad 10^9 < \mathrm{Ra} < 10^{13} \tag{2.119b}$$

For air: $\mathrm{Nu} = 1.42(\Delta t/L)^{1/4} \quad : \quad 10^4 < \mathrm{Ra} < 10^9$ (2.120a)

$= 1.31(\Delta t)^{1/3} \quad : \quad 10^9 < \mathrm{Ra} < 10^{13}$ (2.120b)

Horizontal cylinder

$$\mathrm{Nu} = 0.53(\mathrm{Gr}\,\mathrm{Pr})^{1/4} \quad : \quad 10^4 < \mathrm{Ra} < 10^9 \tag{2.121a}$$

$$= 0.13(\mathrm{Gr}\,\mathrm{Pr})^{1/3} \quad : \quad 10^9 < \mathrm{Ra} < 10^{12} \tag{2.121b}$$

For air: $\mathrm{Nu} = 1.32(\Delta t/d)^{1/4} \quad : \quad 10^4 < \mathrm{Ra} < 10^9$

$= 1.24(\Delta t)^{1/3} \quad : \quad 10^9 < \mathrm{Ra} < 10^{12}$

Upper surface of heated plate or lower surface of cooled plate

$$\mathrm{Nu} = 0.54(\mathrm{Gr}\,\mathrm{Pr})^{1/4} \quad : \quad 2 \times 10^4 < \mathrm{Ra} < 8 \times 10^6 \tag{2.122a}$$

$$= 0.15(\mathrm{Gr}\,\mathrm{Pr})^{1/3} \quad : \quad 8 \times 10^6 < \mathrm{Ra} < 10^{11} \tag{2.122b}$$

For air: $\text{Nu} = 1.32(\Delta t/L)^{1/4}$: $2 \times 10^4 < \text{Ra} < 8 \times 10^6$

$= 1.52\ (\Delta t)^{1/3}$: $8 \times 10^6 < \text{Ra} < 10^{11}$

Lower surface of heated plate or upper surface of cooled plate

$\text{Nu} = 0.27(\text{Gr Pr})^{1/4}$: $10^5 < \text{Ra} < 10^{11}$ (2.123)

For air: $\text{Nu} = 0.59(\Delta t/L)^{1/4}$: $10^5 < \text{Ra} < 10^{11}$

Constant heat flux

Vertical plate: $\text{Nu}_x = 0.6(\text{Gr}^* \text{Pr})^{1/5}$: $10^5 < \text{Gr}^* < 10^{11}$ (2.124)

Horizontal cylinder: $\text{Nu}_d = 0.17(\text{Gr}^* \text{Pr})^{1/4}$: $10^6 < \text{Gr}^* < 10^{13}$

where, $\text{Gr}^* = g\beta q_w x^4/(k\nu^2)$ (2.125)

2.23 CONDENSATION HEAT TRANSFER

The refrigerant condenses inside the tubes of air-cooled condensers and outside the tubes of shell-and-tube condensers. In steam coils, the steam condenses inside the tubes. Water vapour condenses outside the cooling coil of air-conditioning systems. The heat transfer rate can be expressed in this case also in terms of a heat transfer coefficient multiplied by a temperature difference as done in Eq. (2.101).

Figure 2.16 shows a horizontal tube on which vapour condenses. A continuous film of liquid refrigerant is formed over the tube. The film thickness is zero at top of the tube and increases downwards as the liquid flows downwards by gravity. The film thickness offers conduction thermal resistance to heat transfer to the coolant (water) inside the tube. The film thickness should be as small as possible for maximum heat transfer. This phenomenon is known as *film condensation* and it occurs in most practical situations. If the tube surface is clean or a non-wetting agent is used on the surface then it is possible to have *dropwise condensation*. The heat transfer coefficient is very large for dropwise condensation since the film resistance does not occur.

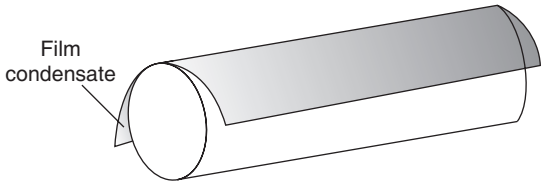

Figure 2.16 Condensate flow in a horizontal tube.

The heat transfer coefficient for film condensation is given by Nusselt's theory that assumes the vapour to be still and at saturation temperature. The heat transfer coefficient is given by

$$h_o = 0.725\left[\frac{k_f^3\,\rho_f^2\,g h_{fg}}{N D_o \mu_f \Delta t}\right]^{1/4} \tag{2.126}$$

where the subscript *f* refers to the saturated liquid state, *N* refers to the number of tubes above each other in a column (Figure 2.17) and $\Delta t = t_r - t_{wo}$, t_r and t_{wo} being the refrigerant and the outside wall temperatures respectively.

The values of condensation heat transfer coefficient are very large compared to free and forced convection heat transfer coefficient, hence these convective and conduction resistances dominate in overall heat transfer coefficient. As a result, sufficiently accurate results may be obtained by using approximate values for condensation heat transfer coefficient. During condensation inside tubes, the area of the tube covered by condensed liquid is not available for condensation heat transfer. Its drainage affects the heat transfer rate. However, decrease in area of cross section increases the vapour velocity, and increases the convective part of heat transfer.

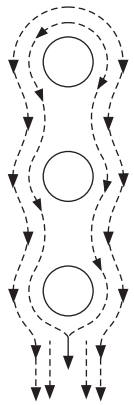

Figure 2.17 Film condensation on a column of three horizontal tubes.

The heat transfer coefficient is dependent upon the enthalpy of evaporation h_{fg}. The value of enthalpy is largest for water, and ammonia has nine times as high a value as those for most of the CFC refrigerants. A larger value of h_{fg} reduces the condensate rate and the film thickness, decreasing the thermal conduction resistance offered by the condensate film, thereby increasing the heat transfer coefficient. For steam condensing inside the tubes of an air-heating coil, $h_c \approx 7000$ W/m^2-K. For refrigerant condensing outside the tubes of shell-and-tube condensers, $h_c \approx 1200$ to 2400 W/m^2-K for halocarbons, whereas for ammonia it is of the order of 6000 W/m^2-K. The empirical correlations are presented in the chapter on condensers.

2.24 BOILING HEAT TRANSFER

Boiling is an essential heat transfer process in refrigeration systems. The refrigerant boils in the evaporator and absorbs its enthalpy of evaporation (latent heat) from the surface or the fluid to be cooled. This is a special case of convective heat transfer, where heat is transferred from a surface to the boiling liquid. There are two essential classes of boiling, namely, nucleate pool boiling and forced convection boiling. Nucleate pool boiling occurs when a relatively stagnant liquid at saturation temperature t_s is heated by a submerged surface from below. A typical plot of the heat transfer rate $q(Q/A)$ versus temperature difference $\Delta t = (t_w - t_s)$ is given in Figure 2.18. If the temperature of the liquid is less than the saturation temperature, then it is called subcooled pool boiling.

For small temperature differences, liquid movement occurs by *natural convection*, there is no bubble formation and the evaporation occurs at the free surface of the pool. As the temperature difference is increased, bubbles start to form at nucleation sites. The bubbles grow up to some critical size as heat is transferred by the surface, then they separate from the surface and move upwards. The upward movement causes stirring of the liquid in the pool. Near the surface, as the bubble leaves, the surrounding liquid rushes to the spot vacated by the bubble causing more stirring and mixing. The bubbles, during their passage transfer heat to the surrounding liquid at lower temperature. At the free surface, the vapour of the bubbles escapes. This regime is known as *individual bubble regime.* The heat transfer rate increases in this regime.

As the temperature difference increases further, more and more bubbles are formed, and columns of bubbles rise to the free surface. The heat transfer rate increases drastically. As the bubble columns move upwards, they also entrain some liquid that rises upwards to the free surface.

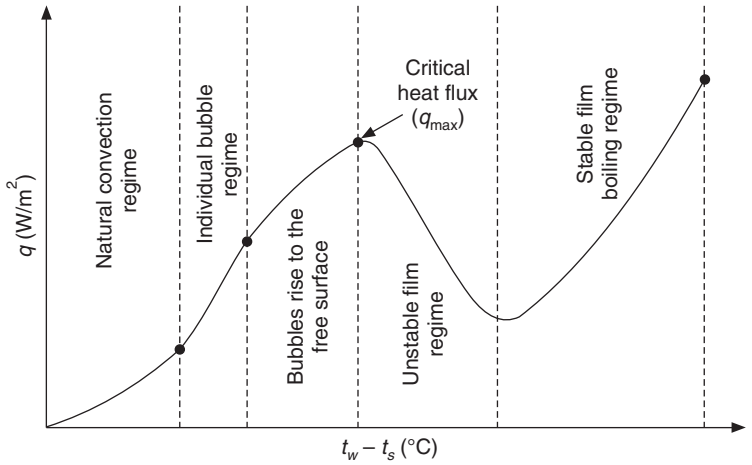

Figure 2.18 A typical plot of heat transfer rate versus temperature gradient.

The vapour in the bubbles escapes at the free surface but the liquid returns to the bottom because of its lower temperature (and higher density) and to satisfy the mass conservation. A given surface can accommodate only a few such rising columns of bubbles and descending columns of relatively colder liquid. Hence, the heat transfer rate cannot increase beyond a certain value. It becomes maximum at some temperature difference. The maximum heat transfer rate $(\dot{q}_{\max})$ is called the *critical heat transfer rate*.

If the temperature difference is increased beyond this value, then a blanket of film forms around the heat transfer surface. This vapour film offers conduction thermal resistance; as a result the heat transfer rate decreases. The film however is unstable and may break at times. This regime is called the *unstable film regime*.

If the temperature difference is increased further, it becomes so high that radiation heat transfer becomes very important and heat transfer rate increases because of radiation component. This regime is called the *stable film boiling regime*.

As the temperature difference is increased, the temperature of the surface t_w continues to increase since the conduction thermal resistance of the film becomes larger as the film thickness increases. All the heat from the surface cannot be transferred across the film and the surface temperature increases. Ultimately the temperature may approach the melting point of the metal and a severe accident may occur (if these are the tubes of nuclear power plant). This point is referred to as the *burnout point*.

Boiling inside tubes consists of nucleate boiling as well as convective heat transfer. As the liquid evaporates, more vapour is formed which increases the average velocity and the convective heat transfer rate. Various regimes like bubbly regime, slug regime, annular regime and mist regime are observed as shown in Figure 2.19. The trend of heat transfer is also shown in the various regimes. The heat transfer coefficient depends upon the fraction of vapour present and the parameters of forced convection heat transfer. Various empirical correlations for the heat transfer coefficients are given in the chapter on evaporators.

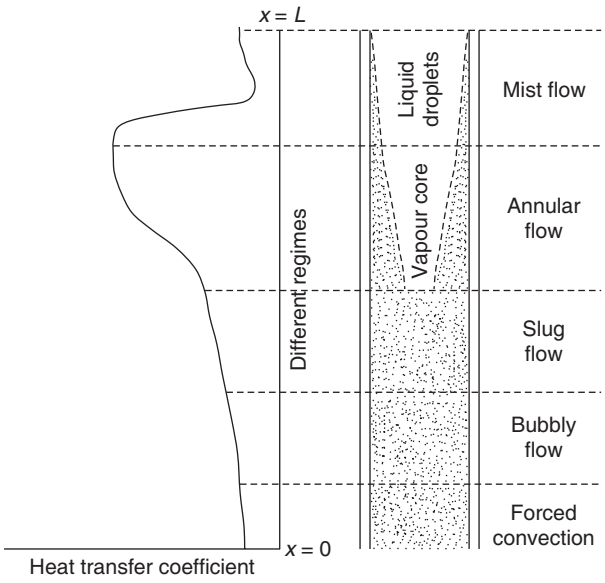

Figure 2.19 Different flow regimes encountered in boiling inside a tube.

2.25 REYNOLDS ANALOGY

The boundary layer equations for momentum for a flat plate are exactly the same as those for energy equation if Prandtl number, Pr = 1, the pressure gradient is zero and viscous dissipation is negligible and there are no heat sources. The boundary conditions are also the same. Hence, the solution for non-dimensional velocity and temperature are the same. It will be shown in Chapter 18 that for such a case,

$$\mathrm{St} = \frac{f}{2} \tag{2.127}$$

where f is the friction factor and St the Stanton number.

This is known as Reynolds analogy. Stanton number is given by

$$\mathrm{St} = \frac{\mathrm{Nu}}{\mathrm{Re\,Pr}} = \frac{h_c L}{k}\frac{\mu}{\rho V L}\frac{k}{c_p \mu} = \frac{h_c}{\rho V c_p} = \frac{f}{2} \tag{2.128}$$

To account for the variation in Prandtl number, this is modified and called Colburn analogy, which is also valid for turbulent flows and is stated as follows.

$$\mathrm{St}\,.\,\mathrm{Pr}^{2/3} = \frac{f}{2} \tag{2.129}$$

2.26 ANALOGY BETWEEN HEAT, MASS AND MOMENTUM TRANSFER

The role that thermal diffusivity plays in the energy equation is played by diffusivity D in the mass transfer equation. Therefore, Sherwood number will depend upon Reynolds number and Schmidt number, and the analogy between momentum transfer and mass transfer for a flat plate will yield

$$\frac{\text{Sh}}{\text{Re Sc}} = \frac{h_D L}{\rho_a} \frac{\mu}{\rho V L} \frac{\rho_a D}{\mu} = \frac{h_D}{\rho V} = \frac{f}{2} \tag{2.130}$$

Similarly, to account for values of Schmidt number different from one, the following correlation is introduced.

$$\frac{\text{Sh}}{\text{Re Sc}} \text{Sc}^{2/3} = \frac{f}{2} \tag{2.131}$$

Comparing Eqs. (2.129) and (2.131), it can be shown that

$$\frac{h_c}{h_D} = c_p \text{Le}^{2/3} \tag{2.132}$$

This analogy is followed in most of the chemical engineering literature and α/D is referred to as Lewis number. In air-conditioning calculations, for convenience the Lewis number is defined as

$$\text{Le} = (\alpha/D)^{2/3} \tag{2.133}$$

And further, it is found to be of the order of unity for moist air. Equation (2.132) is rewritten as

$$h_c = \text{Le}\ c_p\ h_D$$

2.27 HEAT TRANSFER THROUGH COMPOSITE WALLS AND CYLINDER

Most practical problems in heat transfer involve two or more heat transfer modes. Such problems are analyzed from a total or overall aspect. Two important overall parameters that are required are the overall heat transfer coefficient U_o and the mean temperature difference Δt_m. The analysis becomes relatively easy if the surface temperatures are constant. This is considered in the following. The case when the surface temperature varies will be taken up later in case of heat exchangers.

The walls and roofs of buildings are made of layers of homogeneous materials, like brick, plaster, concrete, RCC slabs, air cavities, etc. The heat is transferred by convection from outdoor air and by radiation from outdoor surfaces to the outer surface of the wall; then it is transferred by conduction through various layers of materials and ultimately by convection from inner surface of the wall to the indoor air and by radiation to the inside surfaces. As a first step the heat transfer by radiation and convection are combined together and a single heat transfer coefficient is introduced to represent these.

2.27.1 Combined Convection and Radiation

Radiation heat transfer will be significant if the surface temperature of the surroundings is large. Let t_{si} be the temperature of the indoor surrounding surfaces and t_{so} be the temperature of the outside surrounding surfaces. These may be significantly different from the inside air temperature t_i and outside air temperature t_o respectively. In such a case, radiation heat transfer also has to be considered. The convective heat transfer coefficients for the outside and the inside surfaces are h_{co} and h_{ci} respectively while the radiative heat transfer coefficients are h_{Ro} and h_{Ri} respectively. Hence, the total heat transfer by convection and radiation to the outer surface of the wall, by using Eqs. (2.98) and (2.101) is given by

$$Q/A = q = h_{co}(t_o - t_{w1}) + h_{Ro}(t_{so} - t_{w1}) = h_o(t_o - t_{w1})$$

$$\therefore \quad h_o = h_{co} + h_{Ro}\frac{t_{so} - t_{w1}}{t_o - t_{w1}} \quad \text{with} \quad h_{Ro} = \sigma\varepsilon\frac{t_{so}^4 - t_{w1}^4}{t_{so} - t_{w1}} \tag{2.134}$$

where, in the expression for h_{Ro} given by Eq. (2.99), F_{12}= 1 and $F_E = \varepsilon$ has been taken for simplicity. In air-conditioning calculations, combined radiative and convective heat transfer coefficients are used to simplify the analysis. These combined heat transfer coefficients h_o and h_i are called *outside and inside surface heat transfer coefficients*.

2.27.2 Heat Transfer through a Composite Wall

Figure 2.20(a) shows a composite wall made up of three materials of thermal conductivities k_1, k_2 and k_3 and of thicknesses L_1, L_2 and L_3 respectively. Typical temperature distribution is also shown in the figure. The wall temperatures t_{w1}, t_{w2}, t_{w3}, and t_{w4} are assumed to be uniform over the whole surface. The temperature of the outdoor and indoor air are t_o and t_i respectively.

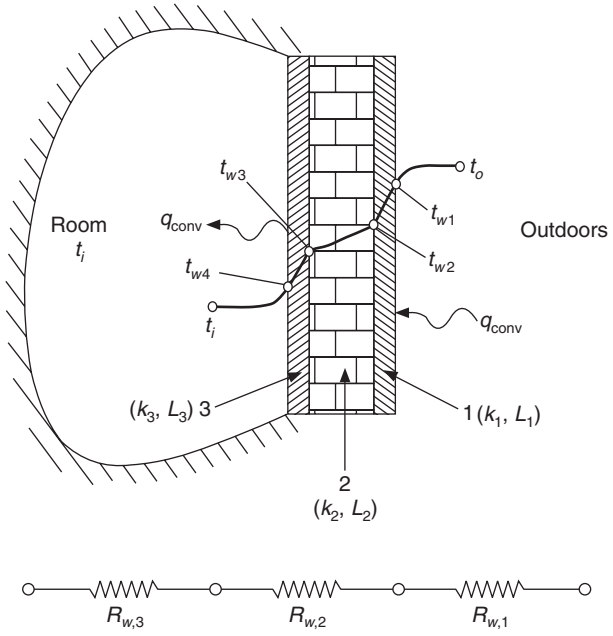

Figure 2.20(a) Multimode heat transfer through a composite wall subjected to convection on both sides.

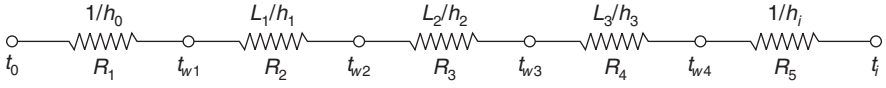

Figure 2.20(b) Electrical analogy of heat transfer through the composite wall of Figure 2.20(a).

In steady state, there is no accumulation of energy; as a result the heat transfer rate by convection from outdoors is equal to the conduction through the materials. If A is the area under consideration and Q is the heat transfer rate, then

$$\frac{Q}{A} = q = h_o(t_o - t_{w1}) = k_1 \frac{t_{w1} - t_{w2}}{L_1} = k_2 \frac{t_{w2} - t_{w3}}{L_2} = k_3 \frac{t_{w3} - t_{w4}}{L_3} = h_i(t_{w4} - t_i) \qquad (2.135)$$

This leads to

$$t_o - t_{w1} = q/h_o$$
$$t_{w1} - t_{w2} = qL_1/k_1$$
$$t_{w2} - t_{w3} = qL_2/k_2$$
$$t_{w3} - t_{w4} = qL_3/k_3$$
$$t_{w4} - t_i = q/h_i$$

Adding these equations, we get

$$t_o - t_i = q\left[\frac{1}{h_o} + \frac{L_1}{k_1} + \frac{L_2}{k_2} + \frac{L_3}{k_3} + \frac{1}{h_i}\right] = \frac{1}{U_o} q$$

$$\therefore \qquad q = U_o\,(t_o - t_i) \qquad (2.136)$$

where, U_o is called the overall heat transfer coefficient, such that

$$\frac{1}{U_o} = \frac{1}{h_o} + \frac{L_1}{k_1} + \frac{L_2}{k_2} + \frac{L_3}{k_3} + \frac{1}{h_i} \qquad (2.137)$$

The same result could have been obtained by electrical analogy described in Eqs. 2.78(a) and 2.78(b). Similar to conduction thermal resistance, a convective thermal resistance can also be defined, that is,

$$q = h_o\,(t_o - t_{w1}) = (t_o - t_{w1})/R \qquad \text{where } R_1 = 1/h_o \qquad (2.138)$$

Similarly, for the inner surface, $R_5 = 1/h_i$.

The conduction thermal resistances for the three wall materials are:

$$R_2 = L_1/k_1\ ;\ R_3 = L_2/k_2 \text{ and } R_3 = L_3/k_3 \qquad (2.139)$$

All these resistances are in series as shown in Figure 2.20(b), hence the total thermal resistance R will be the sum of these.

$$R = \Sigma R_i = 1/h_o + L_1/k_1 + L_2/k_2 + L_3/k_3 + 1/h_i \qquad (2.140)$$

$$\therefore \qquad q = (T_o - T_i)/\,\Sigma R_i = U_o(t_o - t_i) \qquad (2.141)$$

where $$1/U_o = \Sigma R_i \qquad (2.142)$$

Figure 2.21(a) shows the case of a composite wall where the first layer consists of two materials of different conductivities k_1 and k_2 and breadth c_1 and c_2 stacked on each other. This case is in effect the same as shown in Figure 2.20(a) where the materials of conductivity k_1 and k_2 have been

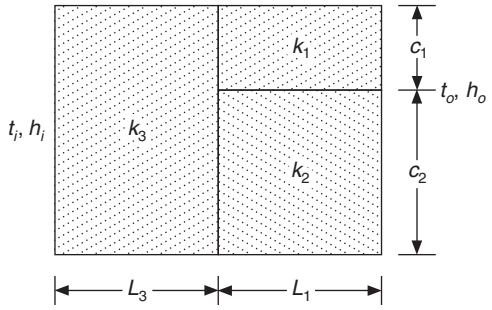

Figure 2.21(a) Composite wall where the first layer consists of two materials of different conductivities and breadths, stacked on each other.

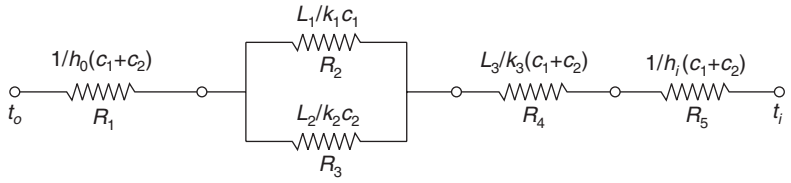

Figure 2.21(b) Equivalent electrical analogue of Figure 2.21(a).

stacked one above the other. In this case, we consider the face width of $(c_1 + c_2)$ and a unit depth perpendicular to the plane of paper so that the area of heat transfer is $(c_1 + c_2)$ m^2. In the previous example of composite wall, heat transfer rate per unit area was considered. In this case the total heat transfer rate is considered. The convection and conduction thermal resistances will also include the area $(c_1 + c_2)$ in this case. Hence,

$$R_1 = 1/\{h_o(c_1 + c_2)\} \text{ and } R_5 = 1/\{h_i(c_1 + c_2)\} \tag{2.143}$$

$$R_2 = L_1/k_1c_1,\ R_3 = L_1/k_2c_2 \text{ and } R_4 = L_3/k_3(c_1 + c_2) \tag{2.144}$$

In this case the thermal conduction resistance due to materials of thickness c_1 and c_2 are in parallel. The equivalent electrical analog is shown in Figure 2.21(b). The equivalent resistance of R_2 and R_3 is

$$R_{23} = R_2R_3/(R_2 + R_3) = L_1/(k_1c_1 + k_2c_2)$$

and total resistance

$$R = \Sigma R_i = R_1 + R_{23} + R_4 + R_5$$

$$R = 1/\{h_o(c_1 + c_2)\} + L_1/(k_1c_1 + k_2c_2) + L_3/k_3(c_1 + c_2) + 1/h_i(c_1 + c_2)\} \tag{3.143}$$

In this case,

$$Q = U_o\,(c_1 + c_2)\,(t_o - t_i) \tag{2.146}$$

where

$$\frac{1}{U_o} = \frac{1}{h_o} + \frac{L_1(c_1 + c_2)}{k_1c_1 + k_2c_1} + \frac{L_3}{k_3} + \frac{1}{h_i} \tag{2.147}$$

2.27.3 Composite Cylinder

Figure 2.22 shows a composite metallic cylinder with insulation at the outer radius. The convective heat transfer coefficient on the inside surface is h_i and the surface heat transfer coefficient on the outside surface is h_o. The metal wall thickness is $(r_2 - r_1)$ and its thermal conductivity is k_{m}. The insulation thickness is $(r_3 - r_2)$ and its thermal conductivity is k_{in}. The heat transfer rate through an annulus of inner and outer radii r_1 and r_2 at temperatures $T_1$and T_2 respectively is given by Eq. (2.77), that is,

$$Q = -2kL\pi \frac{T_1 - T_2}{\ln (r_2 / r_1)}$$

where L is the length of the pipe.

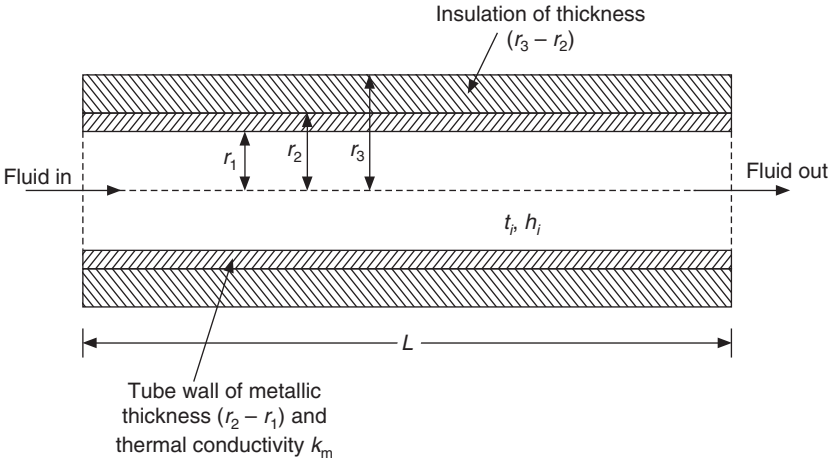

Figure 2.22 Composite metallic cylinder with insulation at the outer surface.

Considering electrical analogy, the thermal conduction resistance for metal wall and insulation are respectively,

$$R_{\text{metal}} = \frac{\ln (r_2 / r_1)}{2\pi L k_{\text{m}}} \quad \text{and} \quad R_{\text{in}} = \frac{\ln (r_3 / r_2)}{2\pi L k_{\text{in}}}$$

Therefore

$$\sum R = \frac{1}{h_i A_i} + \frac{\ln (r_2 / r_1)}{2\pi L k_{\text{m}}} + \frac{\ln (r_3 / r_2)}{2\pi L k_{\text{in}}} + \frac{1}{h_o A_o} \tag{2.148}$$

The total heat transfer rate is given by

$Q = U_o A_o (t_i - t_o)$ where U_o is the overall heat transfer coefficient and it is given by

$$\frac{1}{U_o} + \frac{1}{h_1 A_i} + \frac{\ln (r_2 / r_1)}{2\pi L k_{\text{m}}} + \frac{\ln (r_3 / r_2)}{2\pi L k_{\text{in}}} + \frac{1}{h_o A_o} \tag{2.149}$$

where, $A_i = 2\pi L r_1$ and $A_o = 2\pi L r_3$.

Equations (2.148) and (2.149) assume that the heat transfer surface is clean and do not take into account the fouling of the surface due to deposits of scale by hard water, oil or other foreign matter. Such deposits are thin but offer thermal conduction resistance to heat transfer. Conventionally, the deposit resistance is expressed in terms of a fouling coefficient or deposit factor h_d, which behaves like the heat transfer coefficient. That is, if the temperature on the inside surface of deposit is t_I and the inside wall temperature is t_{wi}, then $Q = h_d A_i (t_I - t_{wi})$. This will add another thermal resistance of $1/(h_d A_i)$ to Eq. (2.148). The inside surface area A_i is used for the deposit radius too, since the deposit thickness is very small. Hence, the expression for the overall heat transfer coefficient reduces to

$$\frac{1}{U_o} = \frac{1}{h_1 A_i} + \frac{1}{h_d A_i} + \frac{\ln (r_2 / r_1)}{2\pi L k_{\text{m}}} + \frac{\ln (r_3 / r_2)}{2\pi L k_{\text{in}}} + \frac{1}{h_o A_o} \tag{2.150}$$

The values of h_d are determined experimentally.

2.28 HEAT EXCHANGERS

We have assumed in the above analysis that the fluid temperature and the surface temperatures do not vary along the length of the surface. In a heat exchanger, both of these temperatures vary along the length of the heat exchanger. Figure 2.23 shows a schematic diagram of a counterflow heat exchanger. The expression for mean temperature difference Δt_m or Log Mean Temperature Difference is therefore derived to take care of such temperature variations along the length of the heat exchanger. This allows us to represent the total heat transfer rate from a heat exchanger as

$$Q = U_o A_o \,(\text{LMTD}) = U_o A_o \Delta t_m \tag{2.151}$$

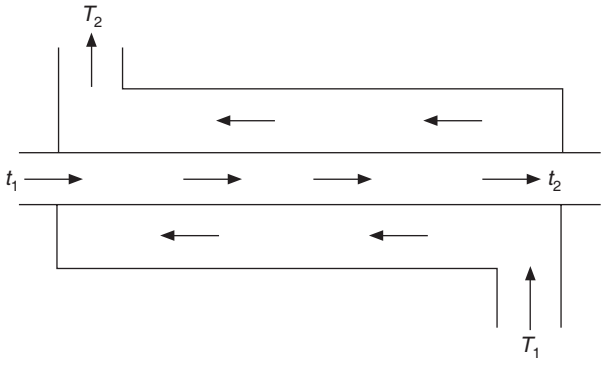

Figure 2.23 Counterflow heat exchanger.

It is assumed that:

- The overall heat transfer coefficient is constant.
- The mass flow rates of both the fluids are constant.
- The specific heats of fluids are constant.
- Fluids do not undergo phase change.
- The heat loss from the outer casing of heat exchanger is negligible and thermal conduction along the walls from left to right side is negligible.

In the derivations below in this section the capital letters denote the temperature, the mass flow rate and the specific heat of the hot fluid and lower case letters denote those quantities for the cold fluid. At the infinitesimal section of area dA_o of the heat exchanger, the temperature of the cold and hot fluids change by dt and dT respectively. Hence, for the elemental area considered,

$$U_o\, dA_o\, (T - t) = \dot{m}c_p\, dt = \dot{M}C_p\, dT \tag{2.152}$$

$$\therefore \qquad dt = U_o\, dA_o\, (T - t) / \dot{m}c_p \quad \text{and} \quad dT = U_o dA_o\, (T - t) / \dot{M}C_p$$

Subtracting one from the other, we get

$$d(T - t) = U_o dA_o\, (T - t)\left[\frac{1}{\dot{M}C_p} - \frac{1}{\dot{m}c_p}\right] \tag{2.153}$$

Defining $\Delta t = (T - t)$ and $\Delta t_1 = (T_2 - t_1)$ and $\Delta t_2 = (T_1 - t_2)$, where, Δt is the temperature difference between the hot and cold fluids at any section, its values are Δt_1 and Δt_2 at the inlet (left) and outlet (right) sections, respectively.

Integrating Eq. (2.153) between the inlet and outlet sections, we get

$$\int_{\Delta t_1}^{\Delta t_2} \frac{d\Delta t}{\Delta t} = U_o\left[\frac{1}{\dot{M}C_p} - \frac{1}{\dot{m}c_p}\right]\int_0^{A_o} dA_o \tag{2.154}$$

$$\ln\left(\frac{\Delta t_2}{\Delta t_1}\right) = \left[\frac{1}{\dot{M}C_p} - \frac{1}{\dot{m}c_p}\right] U_o A_o \tag{2.155}$$

Total heat transfer rate is given by

$$Q = \dot{M}C_p\,(T_1 - T_2) \quad \text{and} \quad Q = \dot{m}c_p\,(t_1 - t_2)$$

$$\therefore \qquad Q\left[\frac{1}{\dot{M}C_p} - \frac{1}{\dot{m}c_p}\right] = [(T_1 - T_2) - (t_2 - t_1)] \tag{2.156}$$

Substituting in Eq. (2.155), we get

$$\ln\left(\frac{\Delta t_2}{\Delta t_1}\right) = \frac{U_o A_o}{Q}[(T_1 - T_2) - (t_2 - t_1)] = \frac{U_o A_o}{Q}[(T_1 - t_2) - (T_2 - t_1)] = \frac{U_o A_o}{Q}(\Delta t_2 - \Delta t_1)$$

Now,
$$Q = U_o A_o\, \Delta t_m = U_o A_o\, \frac{\Delta t_2 - \Delta t_1}{\ln\,(\Delta t_2 / \Delta t_1)}$$

Hence,
$$\text{LMTD} = \Delta t_m = \frac{\Delta t_2 - \Delta t_1}{\ln\,(\Delta t_2 / \Delta t_1)} \tag{2.157}$$

Note that Δt_1 (= $T_2 - t_1$) and Δt_2 (= $T_1 - t_2$) are the temperature differences between the hot and cold fluid streams at the inlet and outlet of the heat exchanger.

Equation (2.157) shows that, for pure counterflow heat exchanger the true mean temperature difference is *logarithmic mean temperature difference* abbreviated LMTD. This expression is

applicable to pure parallel flow heat exchanger and also to any heat exchanger where one fluid temperature remains constant. For other cases, such as crossflow and mixed crosscounter flow with many passes, Eq. (2.157) must be modified. Kern and Bowman et al. (1950) have given solutions for a number of cases. One such expression will be derived in the chapter on condensers for crossflow heat exchangers, typically used in air-cooled condensers.

In general, it is desirable to have large values of overall heat transfer coefficient U_o so that the area A_o required may be made smaller. High values of U_o are obtained at higher velocities but the fluid pressure drops may become excessively high at high velocities causing the pump power to increase. The optimum design is one in which the sum of fixed charges and operating costs are minimum.

2.29 FLUID FLOW

In refrigeration and air conditioning systems, air, vapour, liquids and mixtures of liquids and vapours flow through pipes and ducts for circulation and distribution. In general, the flow can be compressible (i.e. the density of the fluid may vary along the direction of flow), however, in most of the applications dealt with in this book it may be assumed to be incompressible (i.e. the density variations along the direction of flow may be assumed to be negligible). A few basic concepts of incompressible flow are presented here. For details the reader is referred to standard textbooks on Fluid Mechanics.

The first law of thermodynamics dealt with energy conservation. While dealing with fluid flow, we have to consider in addition the mass and momentum conservation.

2.29.1 Mass Conservation

The flow in air conditioning ducts and refrigerant pipes is usually steady. The pressure and the temperature changes are usually small; as a result the density is almost constant. The velocities are usually very small compared to the velocity of sound; as a result the flow may be considered to be incompressible. Consider a duct whose area of cross section increases in the flow direction as shown in Figure 2.24. Since mass cannot be generated or destroyed, it also cannot be stored in the duct for steady flow, hence the mass flow rate at the inlet and the outlet of the duct must be the same. The mass flow rate is the product of area, velocity and density. Hence,

$$\dot{m} = \rho_1 V_1 A_1 = \rho_2 V_2 A_2 \tag{2.158}$$

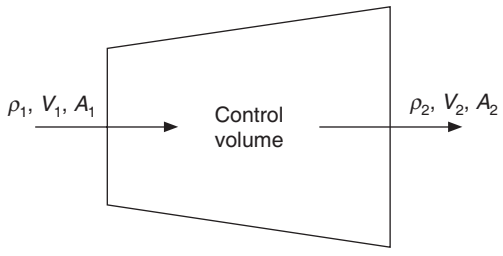

Figure 2.24 Steady flow through a duct.

If the area of cross section increases in the flow direction as shown in Figure 2.25, the velocity will decrease, that is, if $A_2 > A_1$ then $V_2 < V_1$ since density $\rho_1 = \rho_2$. Such a section is called a *diffuser*. On the other hand, if the flow area decreases in the flow direction, the velocity will increase and such a section is called a *nozzle*.

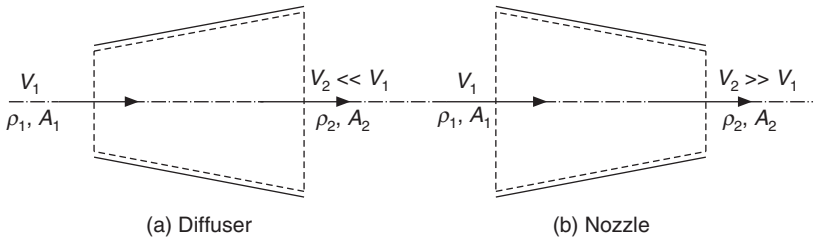

Figure 2.25 Diffuser and nozzle are shaped to cause changes in fluid velocity.

2.29.2 Bernoulli's Equation

The textbooks on fluid mechanics give the derivation of this theorem from momentum conservation. Application of momentum conservation will require the introduction of some more concepts.

Here we derive the Bernoulli's equation, which is the momentum equation for frictionless, incompressible and steady flow, by applying the first law of thermodynamics, which has already been introduced.

Applying the first law of thermodynamics to the duct of Figure 2.26, assuming steady state with constant mass flow rate and no change in the energy of the system, we get

$$(h_2 + V_2^2/2 + gz_2) - (h_1 + V_1^2/2 + gz_1) = q_{12} - w_{12} \tag{2.159}$$

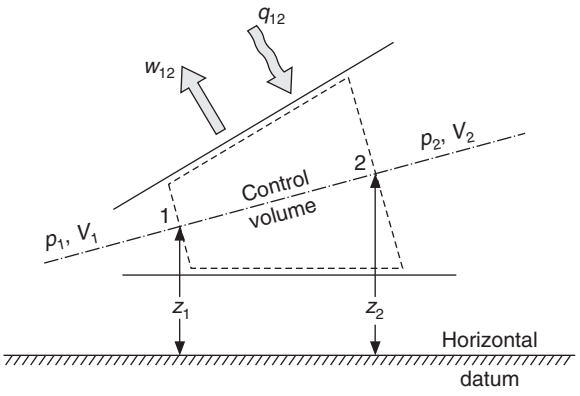

Figure 2.26 Thermodynamic analysis for Bernoulli's equation.

where q_{12} is the heat transfer rate to the system per unit mass flow rate and w_{12} is the work done by the system per unit mass flow rate. Assuming that heat transfer and work done are negligible, we get

$$(h_2 + V_2^2/2 + gz_2) - (h_1 + V_1^2/2 + gz_1) = 0 \tag{2.160}$$

In differential form, Eq. (2.160) may be written as

$$dh + d(V^2/2) + g\,dz = 0 \tag{2.161}$$

Further, from the second fundamental equation of thermodynamics,

$$Tds = dh - v\,dp \tag{2.162}$$

If the process is assumed to be reversible, that is in the absence of friction and heat transfer through temperature difference, then

$$ds = 0 \quad \text{and hence} \quad dh = v\,dp \tag{2.163}$$

Therefore, Eq. (2.161) reduces to

$$d(v\,dp) + d(V^2/2) + g\,dz = 0$$

Integrating this equation, we get

$$\int \frac{dp}{\rho} + \frac{V^2}{2} + gz = \text{constant} \tag{2.164}$$

The first term in Eq. (2.164) is called *flow work* or *flow energy* or loosely called *pressure energy*. If a relation between p and ρ is known (like pv^γ = constant) then it can be integrated. We assume that the density is constant so that the first term can be integrated straightaway and the resulting equation is called the Bernoulli's equation. This equation is as follows:

$$\underset{\substack{\downarrow\\ \text{pressure}\\ \text{head}}}{\frac{p}{\rho g}} + \underset{\substack{\downarrow\\ \text{velocity}\\ \text{head}}}{\frac{V^2}{2g}} + \underset{\substack{\downarrow\\ \text{static}\\ \text{head}}}{z} = \underset{\substack{\downarrow\\ \text{total}\\ \text{head}}}{H} = \text{constant} \tag{2.165}$$

The dimensions of both $p/(\rho g)$ and V^2/g are in metre. According to this equation, water with pressure p_1, velocity V_1 at elevation z_1 metre has a total head of H_1 metre. If p_1 is at atmospheric pressure and if the water were to flow through a vertical pipe, it will rise to a height $z_2 = z_1 + V_1^2/2g$ metre, where its velocity will become zero, pressure remaining the same as $p_1 = p_{atm}$, that is, the kinetic energy is converted to static head. If the pressure p_1 is more than the atmospheric pressure p_{atm}, and the final pressure is atmospheric then water will rise to a greater height, since $(p_1 - p_{atm})$ will also be converted into static head.

Bernoulli's equation is also written in the form

$$\underset{\substack{\downarrow\\ \text{static}\\ \text{pressure}}}{p} + \underset{\substack{\downarrow\\ \text{velocity}\\ \text{pressure}}}{\rho\frac{V^2}{2}} + \underset{\substack{\downarrow\\ \text{pressure due}\\ \text{to datum}}}{\rho g z} = \underset{\substack{\downarrow\\ \text{total}\\ \text{pressure}}}{p_T} \tag{2.166a}$$

or
$$p_S + p_V + \rho g z = p_T \tag{2.166b}$$

where, p_S is the static pressure with units of Pa and $p_V = \rho V^2/2$ is the velocity pressure with units of Pa.

Equations (2.165) and (2.166) are the two forms of Bernoulli's equation. The flow has been assumed to be reversible here, which is equivalent to saying that there is no friction or the irrotationality is synonymous with isentropic condition. This equation is conventionally derived from momentum considerations. This equation is valid in the absence of friction between any two points 1 and 2 for irrotational flow or along a streamline if the flow is rotational. The momentum equation between two points of a stream tube confined by streamlines is given by

$$\frac{p_2}{\rho g} + \frac{V_2^2}{2g} + z_2 = \frac{p_1}{\rho g} + \frac{V_1^2}{2g} + z_1 \tag{2.167}$$

In general, some energy will be lost in overcoming friction. This is referred to as *head loss*, that is, if the fluid were to rise in a vertical pipe, it will rise to a lower height than predicted by this equation. The head loss will cause the pressure to decrease in the flow direction, that is, $p_2 < p_1$ or if the fluid flows downwards, that is, $z_2 < z_1$, it will take care of this head loss. If the head loss is denoted by H_l, then Eq. (2.167) may be modified to

$$\frac{p_1}{\rho g} + \frac{V_1^2}{2g} + z_1 = \frac{p_2}{\rho g} + \frac{V_2^2}{2g} + z_2 + H_l \tag{2.168a}$$

In all real flows, friction will be present. The fluid velocity at the duct walls reduces to zero due to friction. The velocity in the interior of the duct increases so that the mass flow rate remains the same in the duct. In fact, the velocity in the centre of the duct is maximum. This velocity gradient gives rise to shear stress at the wall.

Figure 2.27 shows a duct whose walls offer frictional resistance and there is a fan or a pump in the duct, which adds energy H_p to the fluid. Equation (2.168a) is now modified to

$$\frac{p_1}{\rho g} + \frac{V_1^2}{2g} + z_1 + H_p = \frac{p_2}{\rho g} + \frac{V_2^2}{2g} + z_2 + H_l \tag{2.168b}$$

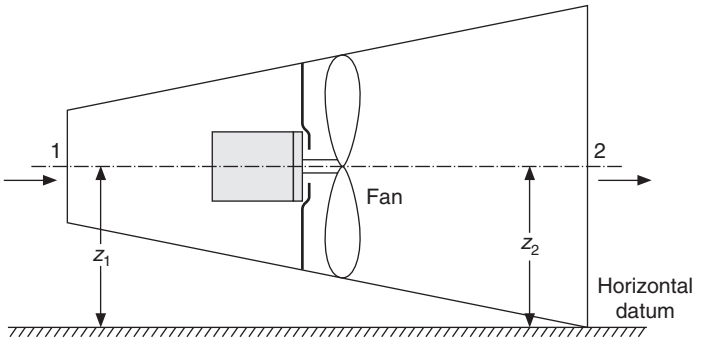

Figure 2.27 Fluid flow through a duct with a fan installed in it.

where H_p and H_l are the gain in head (due to fan or pump) and the loss in head (due to friction), respectively, and the unit of both is m or mm.

2.29.3 Velocity Pressure

The expression for the velocity pressure can be simplified if one considers air of standard density of 1.2 kg/m^3. We then have

$$p_V = (1.2/2)V^2 = 0.6V^2 \text{ Pa} \quad \text{and} \quad V = 1.291\sqrt{p_V} \text{ m/s} \tag{2.169}$$

Also, $1 \text{ bar} = 10^5 \text{ Pa} = 10.2 \text{ m of } H_2O$

$\therefore$ $1 \text{ Pa} = 1.02 \times 10^{-4} \text{ m of } H_2O = 0.102 \text{ mm of } H_2O$

$\therefore$ $1 \text{ mm of } H_2O = 9.81 \text{ Pa}$

$\therefore$ $p_V = 0.6V^2 \text{ Pa} = 0.6/(9.81)V^2 \text{ mm of } H_2O$

$$= 0.0612V^2 = \left(\frac{V}{4.04}\right)^2 \text{ mm of } H_2O$$

Now, $$p_V = \left(\frac{V}{4.04}\right)^2 \text{ mm of } H_2O \quad \text{and} \quad V = 4.04\sqrt{p_V} \text{ m/s} \tag{2.170}$$

In the absence of friction and change in elevation, the sum of static pressure p_S and velocity pressure p_V is constant and this sum is called the total pressure p_T, that is, if height $z_1 = z_2$, then

$$p_{S1} + p_{V1} = p_{S2} + p_{V2} = p_T$$

2.29.4 Pressure Drop

The pressure of a fluid decreases due to three main reasons:

(i) Friction and turbulence
(ii) Change in area
(iii) Sudden change in the flow direction.

The pressure drop is grouped into two categories, *frictional pressure drop* and the *minor loss*. The minor loss is due to area change and change in the direction of flow. In the presence of friction, there will be some pressure drop to overcome the frictional resistance, this pressure drop is denoted by Δp_f. The pressure drop due to change in flow direction is termed minor loss and may be denoted by Δp_m. The total pressure drop may be denoted by $\Delta p_L = \Delta p_f + \Delta p_m$. Hence, the total pressure will decrease in the direction of flow by Δp_L.

Now $$p_{T1} = p_{T2} + \Delta p_L$$

or $$p_{S1} + p_{V1} = p_{S2} + p_{V2} + \Delta p_L \tag{2.171}$$

Turbulence and friction dissipate kinetic energy and cause an increase in internal energy and temperature. The drop in pressure causes adiabatic expansion, which leads to a drop in temperature. Hence, the temperature does not change appreciably due to these two factors.

If there is a fan between the two sections as shown in Figure 2.27, then the fan will add energy to the fluid and the total pressure will increase. If $z_1 = z_2$ as in Figure 2.27, then

$$p_{S1} + p_{V1} + \text{FTP} = p_{S2} + p_{V2} + \Delta p_L \tag{2.172}$$

where FTP is the fan total pressure.

Conversion of velocity pressure into static pressure

The static pressure in a duct may increase in the flow direction if the velocity decreases. This occurs because of conversion of kinetic energy into pressure head. This pressure rise is called *Static Regain*. This occurs if the area increases in the flow direction as in a diffuser. All of us have experienced this phenomenon while holding a hand in front of a stream of water from a hose, we feel the velocity pressure as the kinetic energy is converted to pressure.

2.29.5 Frictional Pressure Drop and Friction Factor

In the presence of friction the velocity near the tube walls is retarded by viscous shear stresses set up between the air and the rough surface of the wall. The velocity near the centre of the duct is larger. The energy of the air is kinetic energy due to velocity and potential energy due to static pressure. If the duct area of cross-section is constant and the density is constant, then the velocity remains constant. The energy lost due to shear stresses is at the expense of drop in static pressure. This is an irreversible energy loss and it tends to increase the temperature of air. The decrease in pressure causes expansion, which tends to reduce the temperature. The net effect of the two processes is that temperature remains almost constant.

One of the simplest solutions of Navier–Stokes equations is for steady, fully developed, laminar incompressible flow in a circular duct of radius R. This is known as Hagen–Poiseuille flow. Fully developed flow implies that the velocity profile does not change in the flow direction and hence the momentum also does not change in the flow direction. In such a case, for an elemental volume for the flow in a circular tube of radius R shown in Figure 2.28, the pressure in the flow direction will balance the shear stress on its radial face. The Navier–Stokes equation will reduce to:

$$\frac{d(2\pi r\tau)}{dr}\,dr\,\Delta x = -2\pi r\,dr\,\frac{dp}{dx}\,\Delta x$$

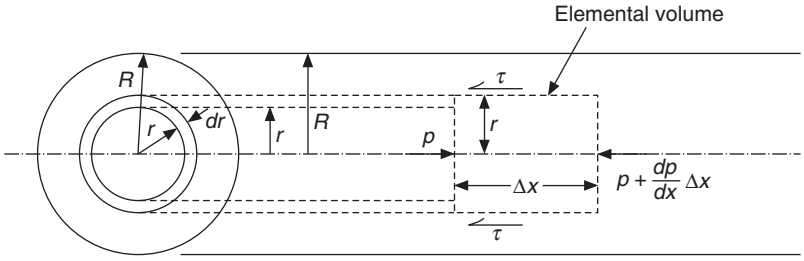

Figure 2.28 Control volume analysis of a fully developed pipe flow.

Substituting $\tau = \mu \dfrac{du}{dr}$ in this equation, we get

$$\frac{d}{dr}\left(r\frac{du}{dr}\right) = -\frac{1}{\mu}\frac{dp}{dx} \tag{2.173}$$

Integrating Eq. (2.173) and applying the boundary condition that the fluid at the wall will not slip, that is, its velocity, u is zero at $R = 0$, we get

$$u = \left(\frac{-1}{4\mu}\frac{dp}{dx}\right)(R^2 - r^2)$$

This equation can be integrated from $r = 0$ to $r = R$ to find the volume flow rate Q. Defining average velocity $= \bar{U} = Q/(\pi R^2)$, we get

$$\bar{U} = (dp/dx)\, R^2/(8u) \tag{2.174}$$

Hence the velocity profile is reduced to

$$u = 2\bar{U}[1 - (r/R)^2] = U_{\max}[1 - (r/R)^2] \tag{2.175}$$

This velocity profile is parabolic in radius. The maximum velocity $U_{\max}$ occurs at the duct centre and is twice the average velocity $\bar{U}$.

The wall shear stress is given by

$$\tau_w = \mu(du/dr)_{r=R} = 4\mu\bar{U}/R \tag{2.176}$$

There are two ways of defining the friction factor, namely the Fanning friction factor and the Darcy–Weisbach friction factor. These are defined as follows. The Fanning friction factor is essentially the skin friction coefficient and is non-dimensional wall shear stress.

$$\text{Fanning friction factor } f' = \tau_w/(0.5\rho\bar{U}^2) \tag{2.177}$$

Substituting for τ_w from Eq. (2.176), we get

$$f' = \frac{4\mu\bar{U}}{R(0.5\rho\bar{U}^2)} = \frac{16\mu}{\rho\bar{U}d} = \frac{16}{\text{Re}} \tag{2.178}$$

The Darcy–Weisbach friction factor f is defined to evaluate the frictional pressure drop Δp_f in a length L of a duct of diameter d, that is,

$$f = \frac{\Delta p_f}{(\rho\bar{U}^2/2)(L/d)}$$

or

$$\Delta p_f = f\frac{L}{d}\frac{\rho\bar{U}^2}{2} \tag{2.179}$$

Substituting for Δp_f from Eq. (2.174) by taking $dx = L$ and $dp = \Delta p_f$, we get

$$f = \frac{8\mu\bar{U}L}{R^2}\frac{d}{L}\frac{2}{\rho\bar{U}^2} = \frac{64}{\text{Re}} \tag{2.180a}$$

It is observed that the Darcy–Weisbach friction factor is four times the Fanning friction factor, i.e.

$$f = 4f' \tag{2.180b}$$

Several textbooks give different explanations for this. One of the common methods is to define d as the hydraulic diameter $d_h = A/P$ instead of $d_h = 4A/P$. The readers are referred to textbooks by Streeter (1981) and White (1986) for details regarding this and for correlations for friction factor.

Equation (2.180a) applies to only laminar flow where the Reynolds number is less than 2300. For turbulent flow, the expression given by Colebrook and White is used, namely,

$$\frac{1}{\sqrt{f}} = -2\log_{10}\left[\frac{k_s}{3.7d} + \frac{2.51}{(\mathrm{Re})\sqrt{f}}\right] \tag{2.181}$$

where k_s is the average roughness of the inner pipe wall expressed in same units as the diameter d. Evaluation of f from this equation requires iteration since f occurs on both the sides of it.

ASHRAE (1997) gives the following form for the determination of friction factor,

$$f_1 = 0.11\left(\frac{k_s}{D_h} + \frac{0.68}{\mathrm{Re}}\right)^{0.25} \tag{2.182a}$$

If $f_1$determined from the above equation equals or exceeds 0.018, then f is taken to be the same as f_1. If it is less than 0.018, then f is given as follows:

$$f = 0.85\,f_1 + 0.0028 \tag{2.182b}$$

Another straightforward equation suggested by Haaland (1983) is as follows:

$$\frac{1}{f^{1/2}} \approx -1.81\log_{10}\left[\frac{6.9}{\mathrm{Re}} + \left(\frac{k_s/d}{3.7}\right)^{1.11}\right] \tag{2.183}$$

These equations can be simplified for sheet-metal ducts, which have $k_s \approx 0.00015$ m.

Further, properties of moist air at standard atmospheric pressure of 101.325 Pa, 20°C, 43% relative humidity, were taken by Fritzsche as $\rho = 1.2$ kg/m^3 and $\mu = 1.8 \times 10^{-5}$ Pa-s to yield the following relation.

$$\Delta p_f = \frac{0.01422V^{1.852}L}{D^{1.269}} \quad \text{[Pa]} \tag{2.184a}$$

This equation can be rearranged by using volume flow rate $Q_v = \pi D^2 V/4$, to give

$$\Delta p_f = \frac{0.022243Q_v^{1.852}L}{D^{4.973}} \quad \text{[Pa]} \tag{2.184b}$$

$$\Delta p_f = \frac{0.02267Q_v^{1.852}L}{D^{4.973}} \quad \text{[mm of } H_2O\text{]} \tag{2.184c}$$

Or in terms of V and Q_v

$$\Delta p_f = \frac{0.0012199 V^{2.4865} L}{Q_v^{0.6343}} \quad \text{[Pa]} \tag{2.184d}$$

Friction factor chart is also available which has flow rate in m^3/s on the ordinate and friction loss in Pa/m of the duct on the abscissa. The velocity and the duct diameter are the parameters. It should be kept in mind that this chart and the Fritzsche's equations given above are valid for standard air and duct roughness of 0.00015 m. If the duct has an acoustic lining or is made of fibre glass, concrete or plastic then it may have a different roughness. In such a case with little effort, Eq. (2.181) may be solved on PC numerically. The values given by Fritzsche's equations may be corrected for actual temperature and other environmental conditions by using the following correction factor.

$$\text{Correction factor } C = \left(\frac{\rho}{1.2}\right)^{0.9} \left(\frac{\mu}{1.8 \times 10^{-5}}\right)^{0.1} \tag{2.185}$$

2.29.6 Minor Losses

The process of converting pressure into kinetic energy is quite efficient. The process of converting kinetic energy into pressure head involves a lot of losses. The losses in energy, which occur in ducts because of bends, elbows, joints, valves, etc. are called minor losses. This is a misnomer, since in many cases minor losses are more significant than the losses due to pipe friction. In all the cases, minor losses are determined by correlations from experimental data. Only for sudden expansion, a theoretical expression is available for minor losses. In turbulent flows, minor losses are proportional to the square of velocity. Hence these are expressed as

$$\Delta p_m = KV^2/2 \tag{2.186}$$

Experimental values for the constant K are available for various valves, elbows, diffusers and nozzles and other fittings. These are discussed in the chapter on distribution of air where these find application.

2.30 COOLING PROCESSES

There is a subtle difference between the cooling processes and the refrigeration systems. The cooling process involves reduction of temperature by heat transfer, heat of solution, change of phase, expansion or some other means. This is not a continuous or cyclic process. This is the part of refrigeration system where cooling is produced.

The cooling processes can be classified as follows:

1. Sensible cooling by a cold medium
2. Heat of solution
3. Change of phase
4. Expansion of liquid and vapours either by throttling or through an expander or turbine
5. Electrical methods

2.30.1 Sensible Cooling by a Cold Medium

If a substance is available at low temperature, it can be used for sensible cooling of a warm substance by contact. Introducing cold air into the building, cools it. Cold water or brine is used for cooling brewages, dairy products and in other industrial processes by absorbing heat from them. The temperature of the cold fluid increases from say t_1 to t_2. The energy absorbed by the fluid, which is also the cooling produced, is given by

$$Q_{12} = \dot{m} c_p (t_2 - t_1) \quad \text{[kW]} \tag{2.187}$$

where $\dot{m}$ is the mass flow rate of fluid in kg/s and c_p is its specific heat in kJ/kg-K.

The outlet warm air or water is recycled by cooling it in a refrigeration system.

2.30.2 Heat of Solution

Cooling to some extent can be obtained by dissolving salt in water. The salt absorbs its heat of solution from water and cools it. Under ideal conditions NaCl can yield temperatures up to –20°C and $CaCl_2$ up to –50°C in properly insulated containers. The salt, however, has to be recovered if the process is to be cyclic. The recovery of salt requires evaporation of water from the solution that requires enormous amount of energy compared to heat of solution.

2.30.3 Change of Phase

Liquids absorb very large amounts of energy during evaporation. This energy is called latent heat of vaporization since the temperature of pure liquid remains constant until all of it evaporates. The process being isothermal involves minimum of irreversibilities and hence is used in modern refrigeration systems. It is possible to recycle the vapours back to liquid state by condensation. The cycle based upon this is called the *vapour compression refrigeration cycle*.

The change of phase from solid to liquid involves absorption of heat of fusion or melting, which can also be used to cool the products. Ice is the most common substance used for this purpose in homes, restaurants, stores, refrigerated transport and for industrial purposes. It provides cooling and is edible too. Water disposal is a problem sometimes. Also, ice cannot produce temperatures below 0°C . Salt solutions with ice can be used to obtain temperatures below 0°C.

Change of phase from solid directly to vapour phase is called *sublimation*. In this process too, latent heat of sublimation is absorbed and the product can be cooled. This normally occurs at lower temperatures and pressures than the vapourization from liquid to vapour phase. Dry ice (solid CO_2) is a substance frequently used for this process. It sublimes at –78°C. Like ice it is also used for industrial cooling processes and refrigerated transport etc. It does not pose any liquid disposal problem like water. The heat transfer rate Q is related to melting rate, $\dot{m}$ kg/s and the latent heat L kJ/kg, that is,

$$Q = \dot{m} L \quad \text{[kW]} \tag{2.188}$$

2.30.4 Expansion of Liquids

Figure 2.29 shows isentropic expansion through a turbine and irreversible adiabatic expansion through a porous plug. The temperature–entropy diagram for a pure substance for these processes is shown in Figure 2.30(a).

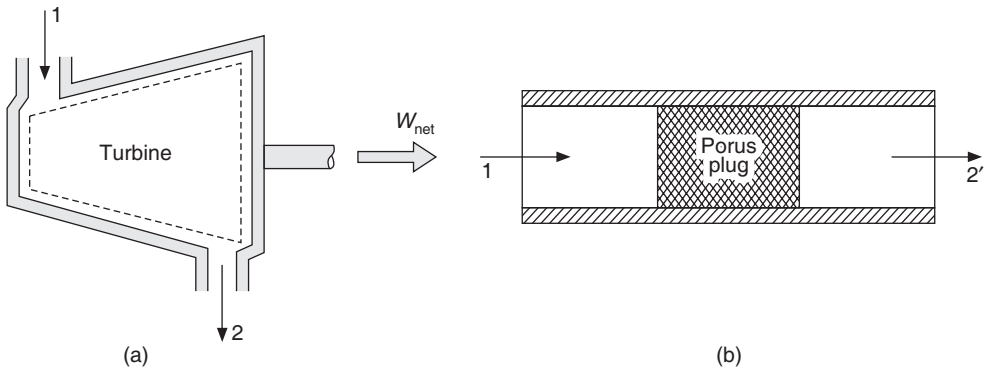

Figure 2.29 (a) Isentropic expansion through a turbine and (b) isentropic expansion through a porus plug.

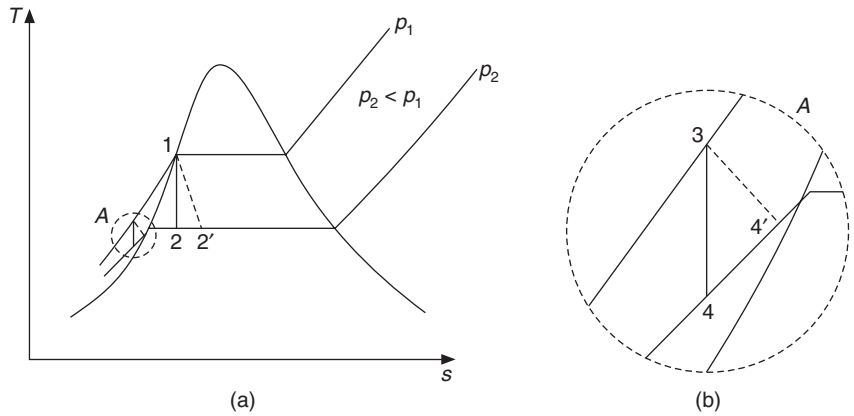

Figure 2.30 (a) Expansion of saturated liquid 1–2: Isentropic; 1–2′: Isenthalpic, and (b) expansion of subcooled liquid 3–4: Isentropic; 3–4′ isenthalpic.

State 1 is saturated liquid state at pressure p_1 in both the cases. During isentropic expansion through the turbine the outlet state lies on a vertical constant entropy line at a lower pressure p_2. In this process, net work is obtained and the enthalpy of the substance decreases. In case of adiabatic irreversible expansion through a porous plug or flow through a resistance, the pressure decreases, but the entropy increases and the end state is 2′ at a lower pressure p_2. This process is called throttling process in which the enthalpy remains constant. In both these adiabatic processes, the states 2 and 2′ are mixture states where some liquid flashes to vapour. The enthalpy of vaporization being absorbed from the mixture, the mixture temperature at state 2 decreases significantly.

On the contrary, as shown in Figure 2.30(b) if the subcooled liquid from state 3 expands isentropically to state 4, which is still a liquid state, the temperature drop is not very significant. In this process some work output is obtained, as a result the enthalpy and the temperature of the liquid decrease. If the expansion occurs by the throttling process 3–4′, the temperature drop is even smaller since no work output is obtained in the throttling process. Hence, it is recommended

that a liquid should be expanded to mixture phase if a significantly lower temperature is to be obtained.

2.30.5 Expansion of Vapours

Irreversible expansion—throttling

The pressure of vapour can be decreased by making it flow through a restriction (reduction in area) such as a throttling valve or through a porous plug as shown in Figures 2.31. The pressure decreases due to frictional resistance. The process is irreversible and is called throttling.

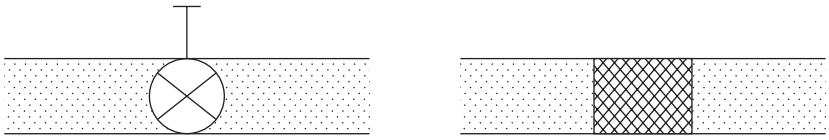

(a) A throttling valve (b) A porus plug

Figure 2.31 Pressure reducing devices.

In the steady state, the first law of thermodynamics for the open system on per unit mass flow rate basis gives

$$(h_2 - h_1) + (V_2^2 - V_1^2)/2 + g(z_2 - z_1) = q - w \tag{2.189}$$

For an adiabatic process without any work output and without any change in potential and kinetic energy, that is, $q = w = 0$, $z_2 = z_1$, and $V_2 = V_1$, the first law reduces to

$$h_1 = h_2 \tag{2.190}$$

The enthalpy remains constant in the throttling process. The enthalpy of perfect gas is function of temperature only; hence the temperature of perfect gas will remain constant during the throttling process. For a real gas the temperature may decrease or increase during throttling depending upon the value of Joule–Thomson coefficient, μ, defined by

$$\mu_{JT} = \left(\frac{\partial T}{\partial p}\right)_h \tag{2.191}$$

The Joule–Thomson coefficient indicates the change in temperature corresponding to a change in pressure along a constant enthalpy line. It can be shown by thermodynamic relations that

$$\mu_{JT} = \frac{T\left(\frac{\partial v}{\partial T}\right) - v}{c_p} \tag{2.192}$$

For a perfect gas,

$$\left(\frac{\partial v}{\partial T}\right)_p = \frac{R}{p} = \frac{v}{T}, \text{ hence } \mu_{JT} = 0$$

Joule–Thomson coefficient is zero for a perfect gas. The magnitude of the Joule–Thompson coefficient is a measure of imperfection of a gas, that is, a deviation from ideal gas behaviour. For a real gas μ may be positive, zero or negative. Figure 2.32 shows constant pressure lines on *T–s* diagram for a real gas. Dashed lines show the constant enthalpy lines. The pressure decreases during the throttling process. Therefore one proceeds from left to right along constant enthalpy lines shown in this figure. A typical process is 1–2–3–4–5. It is observed that during 1–2 along a constant enthalpy line, the temperature increases as the pressure decreases; hence μ_{JT} is negative. At point 2 on this line, the slope of the constant enthalpy line is zero, that is, the behaviour of μ will change; hence $\mu = 0$ at this point and the temperature is maximum at this point. This point is called the *inversion point* and the temperature at this point is called the *inversion temperature*. If the throttling process proceeds along 2–3–4–5, the slope of the constant enthalpy line changes, and the temperature decreases as the pressure decreases. The Joule–Thomson coefficient μ is positive along this part of the line. In this part of the curve the temperature of the gas will decrease during throttling. The figure shows the inversion points for a few constant enthalpy lines and all these are joined by a curve called *inversion curve*.

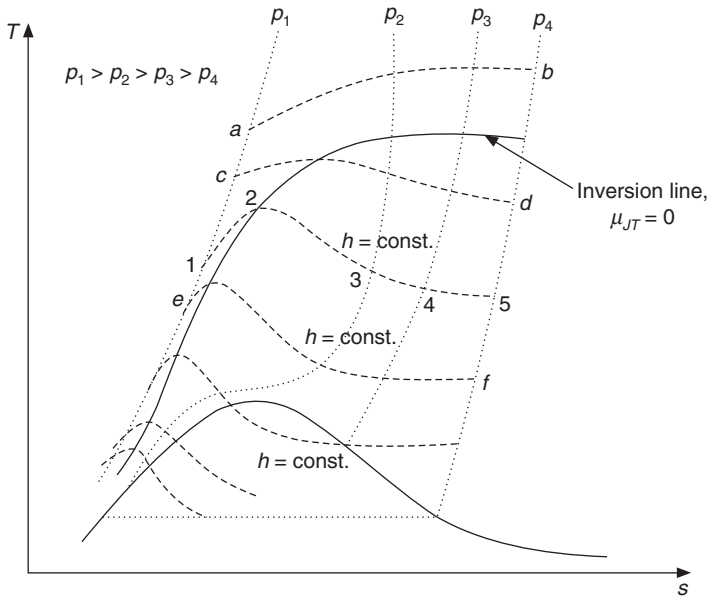

Figure 2.32 Inversion temperature line on *T–s* diagram.

It is observed that at higher temperatures, the constant enthalpy line, for example *a–b* does not show inversion and the temperature continues to increase as the pressure decreases during the throttling process. This is very important for liquefaction of gases by throttling process. First a gas cannot be cooled by throttling unless its temperature is below the inversion temperature corresponding to given conditions of pressure or enthalpy. Processes *c–d* and *e–f* shown in the figure will result in cooling of gas by throttling. Secondly, for liquefaction to occur, the throttling process must continue into the two-phase region. This is achieved by first compressing the gas to

a high pressure and then cooling it isobarically by some efficient method to a low temperature so that it reaches a mixture of liquid and vapour before throttling can be applied.

Expansion with work output

Steady flow expansion of compressed gas through a turbine or an expansion engine results in some work output with a resulting decrease in enthalpy. This decrease in enthalpy leads to a decrease in temperature. The irreversibility due to friction still exists as the fluid flows over the blades of the turbine and heats up the fluid to some extent. Small turbines and expansion engines are not very efficient. Again, if the changes in potential and kinetic energy are negligible and there is no heat transfer, then Eq. (2.189) reduces to

$$w = (h_1 - h_2) \tag{2.193}$$

The outlet enthalpy h_2 is less than the inlet enthalpy h_1; hence the outlet temperature T_2 is less than the inlet temperature T_1. This process is used in liquefaction of gases to initially cool the gas below the inversion temperature so that throttling can do the rest of the cooling. In refrigeration systems involving expansion of a liquid, it is not practical to use expansion engine or turbine since a two-phase mixture results during expansion. Turbines can be used efficiently either for gas or for pure liquids. Cavitation occurs in liquid turbines if a two-phase mixture is encountered leading to damage of blades. Similarly, erosion and pitting of blades occurs if a wet mixture is encountered in vapour turbines. Refrigeration systems invariably use throttling for this reason.

Expansion due to change in kinetic energy

If the flow area changes in the direction of flow as shown in Figure 2.24, the change in kinetic energy may not be negligible. Mass conservation yields

$$V_1 A_1 / v_1 = V_2 A_2 / v_2 \tag{2.194}$$

Therefore,

$$V_2 = V_1 (A_1 / A_2)(v_2 / v_1) \tag{2.195}$$

The ideal gas equation yields

$$v_2 / v_1 = (p_1 / p_2)(T_2 / T_1) \tag{2.196}$$

The specific volume v_2 is greater than v_1 since temperature does not change as significantly as the pressure and pressure $p_1 > p_2$. Therefore, from Eq. (2.194) it can be concluded that the velocity increases if the flow area decreases in the direction of flow. Again, if the change in potential is negligible and there is no heat transfer and work done, then Eq. (2.189) reduces to

$$(h_1 - h_2) = (V_2^2 - V_1^2) / 2 \tag{2.197}$$

Therefore the enthalpy decreases. A relation for temperature can be obtained as follows:

$$T_2 = T_1 - (V_2^2 - V_1^2) / 2c_p \tag{2.198}$$

The velocity can at the most become sonic velocity if the geometry shown is a nozzle and it may become supersonic if the geometry is a convergent-divergent nozzle.

The flow in a pipe of constant diameter has $A_1 = A_2$; hence the pressure drop will be due to friction alone, which may not be significant. If a saturated liquid enters a tube of constant diameter; then a pressure drop due to friction will cause flashing of liquid into vapour as shown by line 1–2 in Figure 2.30(a). The appearance of vapour will reduce the density. The mass flow rate being constant, the velocity will increase in the flow direction, that is, the fluid will accelerate. This acceleration of fluid will require further pressure drop. Hence there will be sufficient pressure in this case and ultimately the velocity may become sonic at the exit of the constant diameter pipe. This is called choked flow condition since sonic velocity is the maximum velocity that can occur in this case. To obtain a larger mass flow rate, one has to use a tube of larger diameter. This is the principle of pressure drop in the capillary tube, commonly used in small refrigeration systems.

2.30.6 Electrical and Magnetic Processes

Thermoelectric cooling

Electrical or magnetic effects can also be used to produce cooling. A thermocouple consists of two junctions of dissimilar materials. When the junctions are placed at two different temperatures, an emf is generated. This effect is called *Seebeck effect*. By utilizing the reverse principle of thermocouple, a temperature difference may be established between two junctions through which a direct current flows. This is called *Peltier effect* (see Figure 2.33).

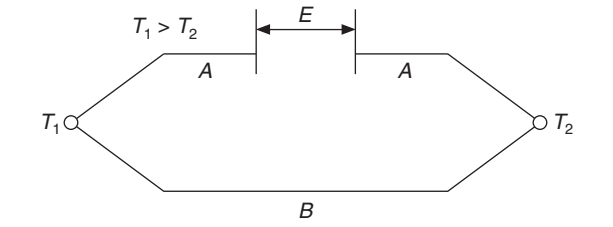

(a) Seebeck effect

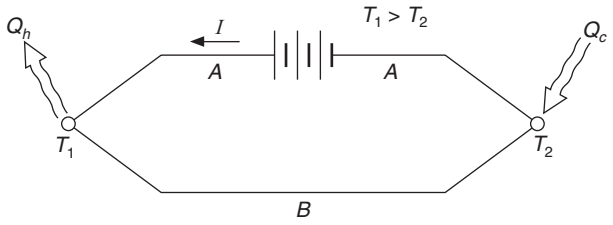

(b) Peltier effect

Figure 2.33 Illustration of Seebeck and Peltier effects.

As the current flows through the thermoelectric material, it gets heated due to its electrical resistance. This is called *Joulean effect*. Further, conduction heat transfer from the hot junction to the cold junction transfers heat. Both these heat transfer rates have to be compensated by the Peltier effect for some cooling to be produced.

Insulating materials give poor thermoelectric performance because of their small electrical conductivity, while metals fail because of their large thermal conductivity. Best thermoelectric effects are obtained with semiconductors. A pile of junctions is used in actual practice with the cold junction kept indoors to absorb heat and warm junction kept outdoors to reject heat. Direct current of high capacity is used to run this system (see Figure 2.34).

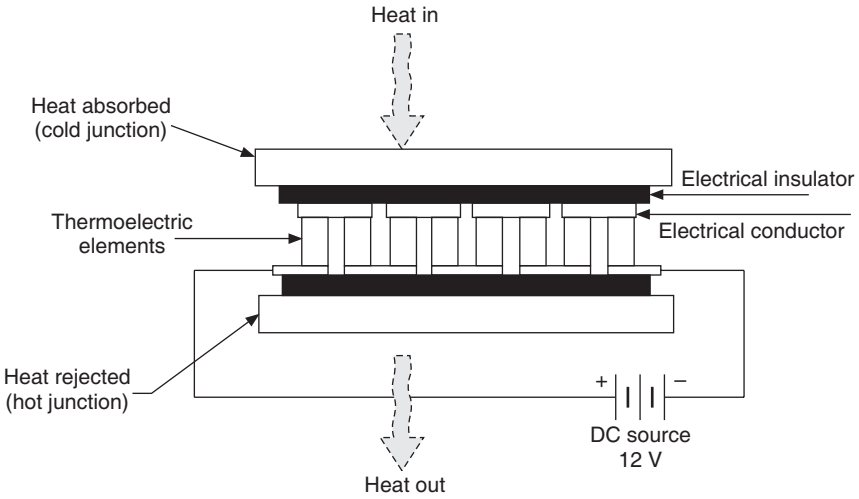

Figure 2.34 Schematic representation of a thermoelectric refrigeration system.

Adiabatic demagnetization

Temperatures very near the absolute zero may be obtained by adiabatic demagnetization of certain paramagnetic salts. Each atom of the paramagnetic salt may be considered to be a tiny magnet. If the salt is not magnetized then all its atoms or the magnets are randomly oriented such that the net magnetic force is zero. If the salt is exposed to a strong magnetic field, the atoms will align themselves to the direction of magnetic field. This requires work and the temperature increases during this process. If the salt is kept in a container surrounded by liquid helium, the heat will be absorbed by helium. There is an outer container, which contains liquid hydrogen. A layer of vacuum separates these liquids. The schematic diagram is shown in Figure 2.35. Now if the magnetic field is suddenly removed, the atoms will come back to their original random orientations. This requires work to be done by the atoms. If there is no heat transfer from surroundings, the internal energy of the salt will decrease as it does work. Consequently the salt will be cooled. This process is used to achieve a temperature near absolute zero. Paramagnetic salts like gadolinium sulphate are used. Magnetization involves alignment of electronic spin. Protons and neutrons also have spins called nuclear spins, which can be aligned by a magnetic field. This gives lower temperatures for a brief instant of time. This is, however, not a macroscopic temperature but the temperature associated with nuclear spin.

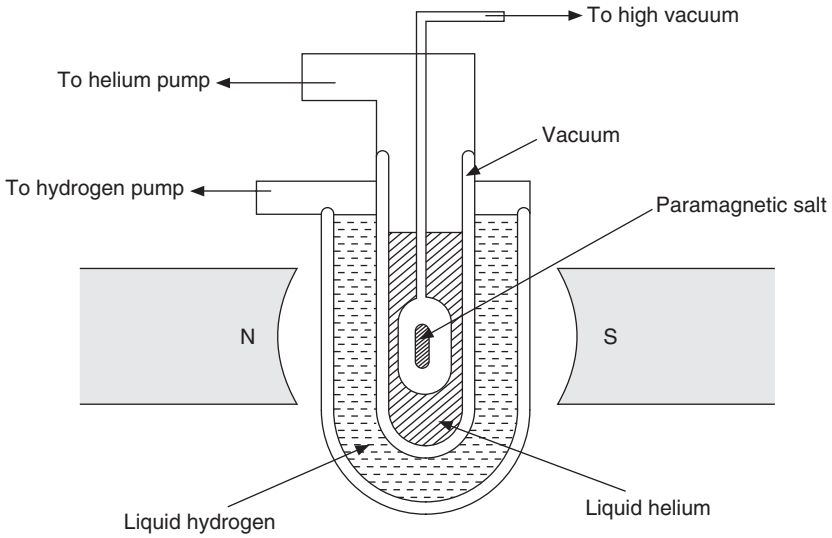

Figure 2.35 Schematic of a set-up depicting magnetic refrigeration.

2.30.7 Vortex Tube

In 1931, George Ranque a French Engineer, based upon his observation of low temperature in cyclone separators, devised a Vortex tube to yield low temperature air. Air at a high pressure is fed tangentially into a cylindrical tube at point 1 as shown in Figure 2.35(a), creating a vortex with low velocity near the core and high velocity at the periphery. A valve is provided at the opposite end 3 of the tube to create some backpressure. Warm air leaves from this end 3. In a *counterflow* arrangement (Figure 2.36(b)), an outlet is provided near the core of the tube at point 2. The cold air leaves from this end. The air expands upon entry into the tube and its velocity increases and the static temperature decreases. The stagnation temperature is the same throughout, that is, $T_0 = T + V^2/2$. A thermometer placed in this stream will indicate temperature very near the stagnation temperature since the fluid will come to rest on the thermometer bulb. If the kinetic energy can be removed from the stream, its temperature will decrease just like what happens in a turbine. Vortex tube is a device that separates the stream into two parts, a high kinetic energy stream and a low kinetic energy stream. The low kinetic energy stream is removed from end 2 and the high kinetic energy stream moves to the other end 3. During its passage to the long end, the wall friction and the dissipation of kinetic energy raise it temperature further. Hence, a warm stream comes out from the long end 3.

If the valve at the long end 3 is closed, all the air will come out through the other end 2 and no cooling will occur since the high and low kinetic energy streams are not separated. As the valve is partially opened, some warm air goes out from the long end 3 and a cold stream starts to come out of the other end 2.

The tube can be arranged such that both the cold and warm streams come out from the same end. Then it is called *uniflow* arrangement as depicted in Figure 2.37. The compressed air is fed tangentially into the tube. This creates a free vortex inside the tube. The fluid in the outer periphery

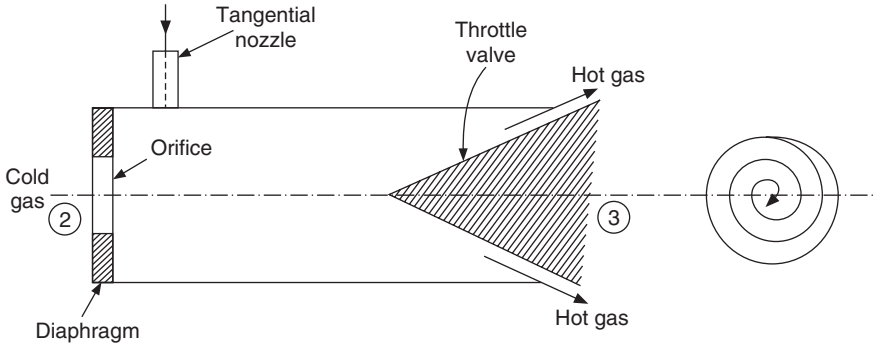

Figure 2.36(a) Vortex tube.

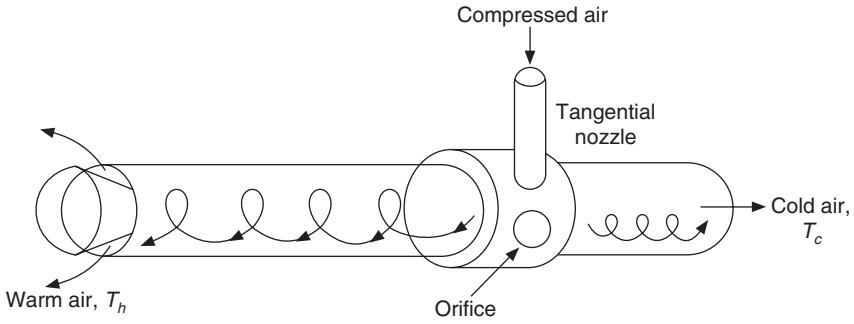

Figure 2.36(b) Counterflow type vortex tube.

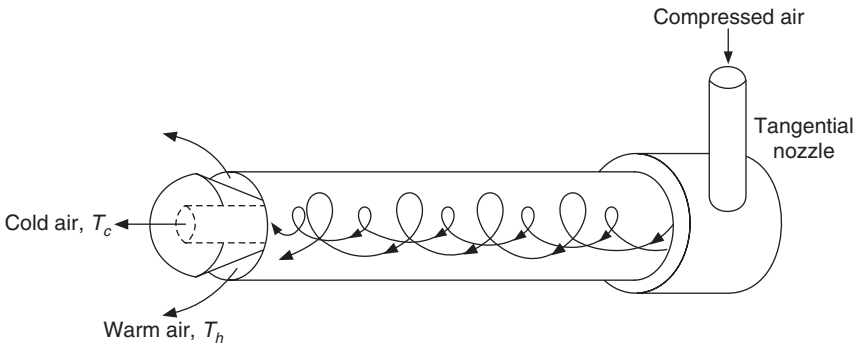

Figure 2.37 Uniflow type vortex tube.

rotates with a higher velocity than the fluid near the tube centreline. In fact the flow is decelerated near the core by the shear stress acting from the high velocity flow in the outer annulus. There is momentum transfer from the core towards the outer annulus. This causes cooling of the inner core. At the same time the viscous dissipation and friction at the wall cause the heating of the fluid in the outer annulus. The warm fluid from the outer annulus comes out around the periphery while the cold fluid comes out from the core of the valve.

In 1946, Rudoph Hilsch, a German Physicist, studied the vortex tube further and recommended optimum dimensions for it performance. Since then many improvements have been reported.

REFERENCES

Haaland, S.E. (1983): Simple and explicit formulas for friction factor in turbulent pipe flow, *J. Fluids Eng.*, pp. 85–90.

Holman, J.P. (1989): *Heat Transfer*, McGraw Hill Book Company, Singapore.

Lay, J.E. (1963): *Thermodynamics*, Charles E Merril Book Inc. Columbus USA.

Streeter, V.L. and E.B., Wilie (1981): *Fluid Mechanics*, McGraw Hill Book Company, Singapore.

White, F.M. (1986): *Fluid Mechanics*, McGraw Hill Book Company, Singapore.

REVIEW QUESTIONS

1. Why does thermodynamics deal with equilibrium states only?
2. Why are properties defined in thermodynamic equilibrium?
3. What is the difference between the closed system and the open system?
4. What are the assumptions in the expressions $dW = p\,d\mathbb{V}$ and $dQ = TdS$?
5. Is it possible to define temperature without using the zeroth law of thermodynamics?
6. Is it possible to create energy out of nothing?
7. What is meant by heat? Can it be stored in a system?
8. How is *pdv* work different from *vdp* work?
9. For which process is the *vdp* work minimum and why?
10. Show that the violation of Clausius statement is a violation of Kelvin–Planck statement of second law of thermodynamics.
11. Prove that all irreversible engines working between high temperature T_H and low temperature T_C have an efficiency lower than the Carnot cycle efficiency by assuming that it is possible and then show that it leads to PMMSK.
12. Define entropy?
13. The first law of thermodynamic does the bookkeeping of energy, then why do we need the second law of thermodynamics?
14. Show that the entropy of an isolated system will always increase?
15. Show that the entropy of world will always increase?
16. Define availability of a system with respect to reference state.
17. Find an expression for the entropy of isothermal mixing of two gases in terms of their partial pressures.
18. How can heat be transferred from a low temperature to a high temperature?
19. What is pure substance?
20. What is simple compressible substance?

21. Define thermal conductivity and explain its significance in heat transfer.

22. Explain the physical laws that govern each mode of heat transfer, and identify the variables involved in each relation.

23. Define absorptivity and emissivity. What is Kirchhoff's law of radiation?

24. What is a blackbody? How do real bodies differ from blackbodies?

25. How does heat conduction differ from convection?

26. How does forced convection differ from natural convection?

27. Draw a typical boiling curve and identify the different boiling regimes. Also, explain the characteristics of each regime.

28. Explain the difference between film condensation and dropwise condensation. Which is a more effective mechanism for heat transfer?

29. Derive the expression for fully developed laminar flow in a circular duct using control volume approach.

30. How do cooling processes differ from refrigeration systems? How are cooling processes classified?

31. Explain the phenomenon of isentropic expansion of liquids through a turbine.

32. Explain the phenomenon of throttling of vapours using (i) a throttling valve and (ii) a porus plug.

33. How does thermoelectric cooling take place? Explain the principle of operation of a thermoelectric refrigeration system.

34. Explain the principle of operation of magnetic refrigeration.

35. Explain the principle of operation of vortex tube.

3

Mechanical Vapour Compression Cycles

LEARNING OBJECTIVES

After studying this chapter the student should be able to:

1. Classify the methods of refrigeration.
2. Explain the basic difference between the mechanical vapour compression refrigeration system and the absorption refrigeration system.
3. Explain the meaning of the terms : refrigeration capacity and coefficient of performance.
4. Explain the concept of reversible heat engine and reversible refrigeration system.
5. Analyse the operation of Reversed Carnot cycle and Reversed Brayton cycle, and saturated Reversed Carnot cycle.
6. Analyse the operation of standard vapour compression refrigeration cycle, i.e. single stage saturation (SSS) cycle.
7. Explain the performance of standard refrigeration cycle vis-a-vis Reversed Carnot cycle using the *T–s* diagram.
8. Perform thermodynamic cyclic calculations for the standard vapour compression refrigeration system.
9. Evaluate the performance of the standard vapour compression system with subcooling from given inputs and known refrigerant property data.
10. Discuss and evaluate the performance of the standard vapour compression system with subcooling and superheating.
11. Evaluate the performance aspects of single stage saturation (SSS) cycle and the effects of evaporator and condensing temperatures on system performance.
12. Discuss the performance of an actual vapour compression refrigeration system with reference to *T–s* and *p–h* diagrams and explain the effects of various irreversibilities due to pressure drops, heat transfer and non-ideal compression.

3.1 INTRODUCTION

Refrigeration in general, can be produced by the following four methods:

1. Vapour Compression Refrigeration Systems
2. Gas Compression followed by expansion to yield work and low temperature
3. Gas Compression followed by throttling or unrestrained expansion
4. Thermoelectric Method

The first three methods involve compression of vapour. In a vapour compression refrigeration system, a working fluid (refrigerant) evaporates at low temperature and pressure. The temperature remains constant while the enthalpy of evaporation or latent heat is absorbed from the space or product to be cooled. The vapour is compressed to a high pressure so that heat can be rejected to the surroundings and the vapour condensed and cycled back to absorb heat. The vapour compression refrigeration system is used in majority of the applications ranging from household refrigerators to large industrial systems. The compression of vapour is achieved either mechanically or by the absorption method. The second method involving gas compression was used with CO_2 for refrigeration in marine applications because of its inherent safety. Now it finds application mainly in aircraft air-conditioning systems. It was used to a limited extent in dense air cycle as well. Both the gas compression methods are used for liquefaction of gases. Irreversible (unrestrained) expansion or the throttling process may not always lead to a drop in temperature, since the irreversibility may lead to heating effect. The enthalpy remains constant during this process. Joule–Thompson coefficient $(\partial T/\partial p)_h$ is a measure of drop in temperature with drop in pressure during the throttling process. This coefficient should be positive to achieve cooling by throttling process. This occurs for most of the real gases at high pressures and low temperature near the inversion temperature.

Peltier effect may be used for producing refrigeration. If direct current is passed through two interconnected junctions of dissimilar metals, one junction gets heated up while the other is cooled. This is called Peltier effect. The heat is absorbed at one junction and rejected at the other junction, which is usually kept outdoors. The Peltier effect is masked by Joulean effect (heating by electrical resistance of the metal) in most of the metals. Semiconductors are good candidates for Peltier effect since they have low electrical resistance and reasonably a large value of Peltier coefficient. The efficiency of thermoelectric methods is rather low. Hence, they are used in applications where efficiency does not matter, for example, in small refrigerators for specimen cooling on microscope stages and instrument for measuring the dew point temperature, etc.

3.2 VAPOUR COMPRESSION CYCLE

In this cycle, the cooling rate Q_e is produced by evaporation of a refrigerant at a reduced temperature called the evaporator temperature T_e. The pressure of the refrigerant, p_e, is the saturation pressure of the refrigerant at T_e. The vapour resulting from evaporation is condensed to liquid state by heat rejection, so that the liquid can absorb heat again and the cycle is made continuous. The heat is rejected to the surroundings, hence the refrigerant temperature, T_c, during condensation is greater than the temperature of the surroundings, T_∞. The saturation pressure of the refrigerant p_c for condensation at T_c is higher than the evaporator pressure p_e. The pressure of the vapour is increased from p_e to p_c either mechanically in a vapour compressor by doing work W, or by absorbing the vapour in a liquid and compressing the liquid dynamically. The energy is conserved as per the first law of thermodynamics, hence the sum of cooling rate, Q_e, and the work done, W, on the system is

rejected to the surroundings during condensation. This method of refrigeration is called the *mechanical vapour compression refrigeration system* if a vapour compressor is used. It is also called the work-driven refrigeration system. It uses high-grade electrical energy to run it. It is called the *absorption refrigeration system* if the vapour is absorbed in an auxiliary liquid called absorbent and the pressure of the solution is increased by a liquid pump; subsequently the high pressure refrigerant is released from the solvent by heat transfer. This is also the vapour compression system, however, it is the heat-driven refrigeration system. It runs on low grade energy. In both these systems, the condensed liquid at high temperature and pressure is expanded to low pressure by a throttle valve to complete the cycle. *This is a closed thermodynamic cycle in which the refrigerant alternately evaporates and condenses with compression of vapour and expansion of liquid.*

3.3 REFRIGERATION CAPACITY

The refrigeration capacity of a refrigeration system is its cooling capacity or the heat transfer rate that it can provide for cooling. The SI unit for heat transfer rate is kW. However, the refrigeration capacity is still measured in Ton of Refrigeration (TR), which is a carry over of the era when the purpose of refrigeration was mainly to produce ice. This is in a way a historical unit. It was defined in such a way as to get a round integer number.

One TR is the rate of heat transfer rate required to produce one US ton (2000 lb) of ice at 0°C from water at 0°C in 24 hours. It involves only the removal of latent heat of fusion of water. The latent heat of fusion of water in the FPS system of units is 144 Btu/lb. Hence

$$\text{I TR} = \frac{144 \times 2000}{24 \times 60} = 200 \text{ Btu/min} \tag{3.1}$$

Some textbooks use an approximate conversion of 1 W = 3.413 Btu/h as done in Section 2.4.12. The exact conversion is as follows:

$$1 \text{ W} = 3.41214 \text{ Btu/h}$$

Therefore, in SI system of units

$$1 \text{ TR} = 3516.85 \text{ W} = 211.01127 \text{ kJ/min} \approx 211 \text{ kJ/min} \tag{3.2}$$

It is convenient to use 1 TR = 211 kJ/min. Some authors also round it off to 210 kJ/min = 3.5 kW. In the metric system of units, this is rounded off to 50 kcal/min, which is a rather crude approximation.

3.4 COEFFICIENT OF PERFORMANCE

The performance index of any device is the ratio of *useful desired effect* to the *amount of expenditure*. The desired effect for a refrigeration system is the cooling capacity or the refrigeration capacity, and the expenditure is expressed in terms of energy input. Hence, the *coefficient of performance*, abbreviated COP, is expressed as

$$\text{COP} = \frac{\text{useful refrigeration effect}}{\text{net energy supplied from external sources}} = \frac{Q_e}{W} \tag{3.3}$$

The term efficiency also has the same meaning; however it refers to the ratio of output to input. This ratio is misleading here, since the output is the heat rejection that is wasted in this case.

In the case of heat pump, this ratio has relevance since the desired effect for heat pump is the heat rejection. The mindset about efficiency is that it is always less than one. The COP, on the other hand, is greater than one for a refrigeration system as well as for the heat pump. Hence, the use of efficiency to indicate performance in the case of refrigerators and heat pumps will be misleading.

The work input usually refers to the shaft power to the compressor. Electric power of the motor is used for this purpose. Absorption refrigeration systems and steam jet refrigeration systems run on low-grade energy, that is, heat transfer to the generator or boiler. The former involves a negligible amount of pump work too. The expenditure for these systems is the heat transfer rate, Q_g, to the generator or boiler. The COP of the heat-driven refrigeration systems is expressed as

$$\text{COP} = \frac{Q_e}{Q_g} \tag{3.4}$$

The COP of these systems is usually less than one since all the heat transfer Q_g cannot be converted into useful work, and the efficiency of this conversion is included in the COP.

It is a common practice to express the performance of mechanical vapour compression refrigeration systems in terms of horsepower required per ton of refrigeration. Hence, from Eq. (3.3), we have

$$W = \frac{Q_e}{\text{COP}}$$

Substituting 1 TR = 3.51685 kW and 1 HP (Imp) = 0.746 kW or HP (metric) = 0.736 kW

$$\text{HP (Imp) / TR} = (3.51685/0.746)/\text{COP} = 4.72 / \text{COP} \tag{3.5}$$

$$\text{HP (metric) / TR} = 4.78 / \text{COP} \tag{3.6}$$

3.5 REVERSED CARNOT CYCLE OR CARNOT REFRIGERATION CYCLE

3.5.1 Reversible Heat Engine

The concept of a heat engine working in a cycle between two heat sources is a very familiar concept in thermodynamics. This is described here for the sake of familiarity and then this concept is extended to the refrigeration system. Treating this system as a block box or a control volume and considering only the heat transfer and work transfer, we may describe its operation across its boundaries. It receives energy, Q_H, as heat transfer from a high-temperature heat source at T_H, converts a part of it into work W, and rejects the remaining energy as heat transfer Q_L to a low-temperature reservoir (heat sink) at temperature T_L. This is schematically shown in Figure 3.1(a). T_L is the temperature of the environment, that is, cooling air or water to which the heat is rejected. According to Kelvin–Planck statement of second law, all the heat transfer Q_H cannot be converted into work, a part of it has to be rejected if it is a cyclic process.

According to Kelvin–Planck statement of second law of thermodynamics: *It is impossible for a device to work in a cycle and convert all the heat transferred to it into work.*

From the first law of thermodynamics,

$$W = Q_H - Q_L \tag{3.7}$$

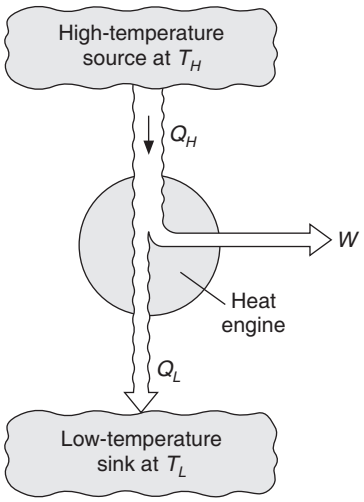

Figure 3.1(a) Schematic diagram of a heat engine receiving heat Q_H from a high temperature zone.

The efficiency of heat engine is defined as

$$\eta = \frac{W}{Q_H} \tag{3.8}$$

Amongst the various cycles for heat engines, the Carnot cycle is a model of perfection and acts as a standard with which the efficiencies of other cycles are compared. This cycle is shown on temperature vs. entropy diagram in Figure 3.1(b). It is a closed cycle that consists of two isentropic and two isothermal processes as follows:

1–2: Isothermal heat addition Q_H from a source at high temperature T_H

2–3: Isentropic work output W_T in a turbine

3–4: Isothermal heat rejection Q_L to a heat sink at low temperature T_L

4–1: Isentropic work input W_C in a compressor or pump

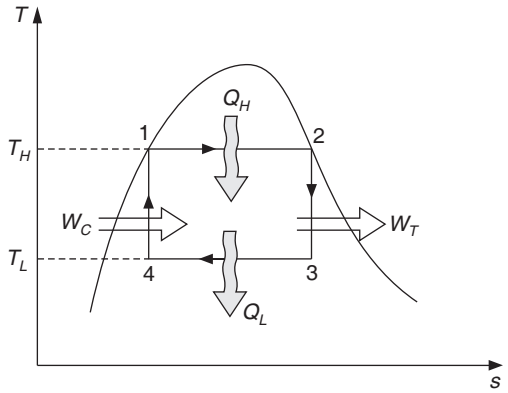

Figure 3.1(b) *T–s* diagram of the Carnot vapour cycle.

All the four processes of this cycle are reversible and this is considered to be a role model for other cycles. There are two Carnot theorems for heat engines, which are as follows:

(i) No heat engine working in a cycle can have efficiency greater than that for a reversible heat engine working in a cycle between the same two temperatures of source T_H and sink T_L.

(ii) All reversible cycles working between the same two temperatures of source and sink, have the same efficiency; or the efficiency of a reversible cycle is independent of the working substance used.

A brief proof of these theorems is given below using the first and the second laws of thermodynamics. Applying the first law of thermodynamics to Figure 3.1(a),

$$W = Q_H - Q_L \tag{3.9}$$

The second law of thermodynamics is applied in the form of Clausius inequality, that is,

$$\oint \frac{dQ}{T} \leq 0 \tag{3.10}$$

The cyclic integral is zero for the reversible cycle and less than zero for the irreversible cycle. Heat transfer to the system is considered positive, that is, Q_H is positive while Q_L is negative. Therefore,

$$\frac{Q_H}{T_H} - \frac{Q_L}{T_L} \leq 0 \tag{3.11}$$

Substituting for Q_L from Eq. (3.9), we get

$$\frac{Q_H}{T_H} - \frac{Q_H - W}{T_L} \leq 0$$

or
$$\frac{W}{T_L} - \frac{Q_H(T_H - T_L)}{T_H T_L} \leq 0$$

$\therefore$
$$\eta = \frac{W}{Q_H} \leq \frac{T_H - T_L}{T_H} \tag{3.12}$$

The equality sign in this equation is for the reversible process, while the inequality sign is for the irreversible process. Equation (3.12) states that the efficiency of a reversible cycle, viz. Carnot cycle, is the maximum; which is a proof of the first Carnot theorem. The Carnot efficiency is equal to

$$\eta_C = \frac{T_H - T_L}{T_H} \tag{3.13}$$

This is the maximum possible efficiency that can be achieved with source temperature of T_H and sink temperature of T_L. Further, it is observed that efficiency is dependent upon temperature only; hence it is independent of the working substance, which is a proof of the second Carnot theorem.

If Q_H is the heat transfer available at temperature T_H, then a maximum of $Q_H\ (T_H - T_L)/T_H$ can be converted into work while $Q_H\ T_L/T_H$ has to be rejected to the low temperature reservoir T_L.

3.5.2 Reversible Refrigeration System

The refrigeration system can also be described by a similar black box disregarding the details of how it works and considering only heat and work transfer across its boundaries. This is shown in Figure 3.2(a). The refrigeration cycle absorbs energy as heat transfer Q_L at a low temperature T_L and rejects energy as heat transfer Q_H to sink at a high temperature T_H.

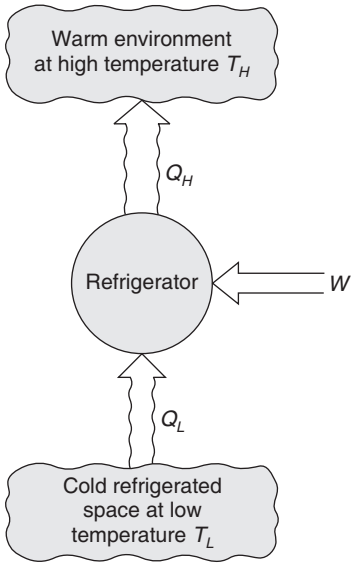

Figure 3.2(a) Schematic diagram of a refrigerator removing heat Q_L from a cold space.

According to Clausius statement of second law of thermodynamics: *It is impossible for a device to work in a cycle and transfer heat from a low temperature to a high temperature without any external work input*. Hence the refrigeration system requires work input W to run the system.

From the first law of thermodynamics

$$Q_H = Q_L + W \tag{3.14}$$

The coefficient of performance of refrigeration system is given by

$$(\text{COP})_\text{R} = \frac{Q_L}{W} \tag{3.15}$$

The heat rejected to the surroundings Q_H is the sum of heat absorbed and work done. The cycle is, therefore, more efficient if the heat rejection is the desired effect. This is the case for heat pump. A heat pump is useful in cold climate where heat is absorbed from the environment, that is, air or water at a low temperature (say around 0°C) and rejected at 40–50°C room temperature or at even higher temperatures for industrial applications.

The coefficient of performance of heat pump is, therefore, given by

$$(\text{COP})_{\text{H}} = \frac{Q_H}{W} \tag{3.16}$$

Comparing the COP of refrigeration system with that of the heat pump as defined in Eqs. (3.15) and (3.16) respectively, we get

$$(\text{COP})_{\text{H}} = (\text{COP})_{\text{R}} + 1 \tag{3.17}$$

Some industries may require cooling in one part and heating in another. Both these requirements can be met by a heat pump. The physical system required for heat pump is the same as that for refrigeration system with flow in the reverse direction. In fact, a year-round air-conditioning system works in refrigeration mode during summer and in heat pump mode during winter.

The *T–s* diagram of Reversed Carnot cycle or Carnot refrigeration cycle is shown in Figure 3.2(b). It is observed that the order of arrows in Figure 3.2(b) is reverse of that in Figure 3.1(b) for the Carnot cycle. This is the reason of calling it the Reversed Carnot cycle. The temperature to which the heat is rejected is the same in both the cycles. This cycle consists of the following reversible processes:

1–2: Isentropic work input W_C in a compressor
2–3: Isothermal heat rejection Q_H to a heat sink at temperature T_H
3–4: Isentropic work output W_T in a turbine
4–1: Isothermal heat absorption Q_L at temperature T_L

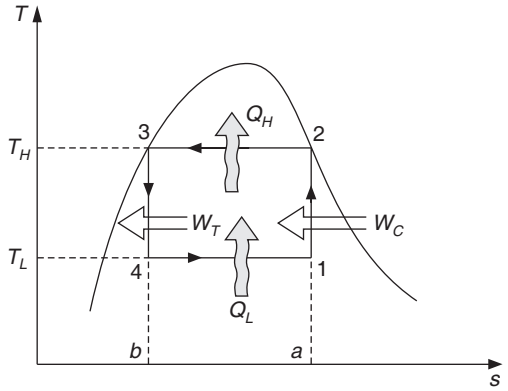

Figure 3.2(b) *T–s* diagram of the Reversed Carnot cycle.

The two theorems similar to Carnot theorems for the refrigeration cycles, called Reversed Carnot theorems, are as follows:

(i) No refrigeration system can have a COP greater than that for a reversible cycle working between the same two temperatures of sink T_H and receiver T_L.
(ii) All reversible cycles operating between the same two temperatures of receiver and sink have the same COP; or the COP of reversible cycle is independent of the working substance.

A brief proof of these theorems is given below using the first and the second laws of thermodynamics. Applying the first law of thermodynamics to Figure 3.2(a), we obtain

$$W = Q_H - Q_L \tag{3.18}$$

The second law of thermodynamics is applied in the form of Clausius inequality, that is,

$$\oint \frac{dQ}{T} \leq 0 \tag{3.19}$$

The cyclic integral is zero for the reversible cycle and less than zero for the irreversible cycle. Heat transfer to the system is considered positive, that is, Q_L is positive while Q_H is negative. Therefore,

$$\frac{Q_L}{T_L} - \frac{Q_H}{T_H} \leq 0 \tag{3.20}$$

Substituting for Q_H from Eq. (3.18), we get

$$\frac{Q_L}{T_L} - \frac{Q_L + W}{T_H} \leq 0$$

or

$$\frac{Q_L(T_H - T_L)}{T_L T_H} - \frac{W}{T_H} \leq 0$$

$\therefore$

$$\text{COP} = \frac{Q_L}{W} \leq \frac{T_L}{T_H - T_L} \tag{3.21}$$

Equation (3.21) states that the COP of the reversible cycle, that is, the Reversed Carnot cycle is the maximum, which is a proof of the first Reversed Carnot theorem. The maximum COP is equal to

$$(\text{COP})_{\text{RC}} = \frac{T_L}{T_H - T_L} \tag{3.22}$$

This is the maximum possible COP that can be achieved with a receiver temperature of T_L and sink temperature of T_H. Further, it is observed that COP is dependent upon the temperature only; hence it is independent of the working substance. This is a proof of the second Reversed Carnot theorem.

It should be noted that the temperatures in the preceding expressions are the absolute temperatures in Kelvin scale. The conventional Celsius temperatures should be converted to absolute temperature in Kelvin scale by using

$$0^{\circ}\text{C} = 273.15 \text{ K} \tag{3.23}$$

It is further known from thermodynamics that for reversible heat transfer,

$$dQ_{\text{rev}} = T\, ds$$

Therefore,

$$Q_L = T_L (s_1 - s_4) = \text{area under line 4–1 in Figure 3.2(b)}$$
$$= \text{Area } b\text{–}4\text{–}1\text{–}a\text{–}b \tag{3.24}$$

$$Q_H = T_H\,(s_2 - s_3) = \text{area under line 2–3 in Figure 3.2(b)}$$
$$= \text{Area } a\text{–}2\text{–}3\text{–}b\text{–}a \tag{3.25}$$
$$W = Q_H - Q_L = \text{area under line 2–3 – area under line 4–1}$$
$$= (T_H - T_L)(s_1 - s_4) \text{ since } s_1 = s_2 \text{ and } s_3 = s_4$$
$$= \text{Area } 1\text{–}2\text{–}3\text{–}4 \tag{3.26}$$

On a T–s diagram, therefore, the area enclosed by the rectangle is the work requirement of the Reversed Carnot cycle. Areas on the T–s diagram also show the heat transfer rates.

To study the relative influence of the two temperatures, T_H and T_L, on COP, Eq. (3.22) is differentiated with respect to both the temperatures T_H and T_L as follows:

$$\frac{d(\text{COP}_{\text{RC}})}{dT_H} = \frac{T_L}{(T_H - T_L)^2} \tag{3.27a}$$

$$\frac{d(\text{COP}_{\text{RC}})}{dT_L} = \frac{T_H}{(T_H - T_L)^2} \tag{3.27b}$$

It is observed that the COP of the Reversed Carnot cycle is more strongly dependent on the low temperature at which the heat is absorbed than on the temperature at which the heat is rejected. Further, the $(\text{COP})_{\text{RC}}$ decreases as T_H increases or as T_L decreases. The work requirement $W = Q_L/(\text{COP})_{\text{RC}}$, hence the work requirement for the same refrigeration capacity increases as T_H increases or as T_L decreases. For example:

At $T_H = 40^{\circ}$ C and $T_L = -20^{\circ}$C $\quad (\text{COP})_{\text{RC}} = 253/(313 - 253) = 4.217$, $W = 0.237\ Q_L$

At $T_H = 50^{\circ}$ C and $T_L = -20^{\circ}$C $\quad (\text{COP})_{\text{RC}} = 253/(323 - 253) = 3.614$, $W = 0.276\ Q_L$

At $T_H = 40^{\circ}$ C and $T_L = -30^{\circ}$C $\quad (\text{COP})_{\text{RC}} = 243/(313 - 243) = 3.471$, $W = 0.288\ Q_L$

T_H fixed as $T_L \to 0$: $(\text{COP})_{\text{RC}} \to 0$ and $W \to \infty$

A decrease of 10°C in low temperature source decreases the $(\text{COP})_{\text{RC}}$ by 17.7% while an increase of 10°C in high temperature source decreases the $(\text{COP})_{\text{RC}}$ by 14.3%. Hence the low temperature source has a more dominant effect on COP.

3.6 EXTERNAL REGIME AND INTERNAL REGIME

The coefficient of performance (COP), as seen from Eq. (3.22), is maximum when the temperatures of the low and the high temperature sources are the same. It should, however, be the kept in mind that the low temperature is the requirement of the cold storage or air-conditioning, etc. while the high temperature depends upon the temperature of the surrounding air or water to which the heat is rejected. The heat transfers in the Reversed Carnot cycle have been assumed to be isothermal which is an ideal condition. A finite temperature difference is always required between the two mediums for heat transfer to take place. The smaller the temperature difference for heat transfer, the smaller is the irreversibility since a temperature difference is essentially a potential for work output which is lost when heat is transferred to a lower temperature. In fact, the energy is said to be degraded if it is transferred to a lower temperature.

The heat transfer is usually by convection that can be expressed as

$$Q = U\,A\,\Delta T$$

where, U is the convective heat transfer coefficient, A is the heat transfer area and ΔT is the temperature difference, which is the driving force for heat transfer rate. The temperature difference can be minimized by increasing U and/or A. An increase in heat transfer coefficient U, requires increase in fluid velocity requiring more pump power or fan power while an increase in the heat transfer area A requires a higher initial cost of the heat exchanger. Also, a larger area will involve more pressure drop requiring more pump or fan power to overcome it. It is obvious that ΔT cannot be made zero. A compromise has to be made and a reasonable ΔT has to be accepted based upon the economic and practical considerations. In general, ΔT varies from 5 to 15 K depending upon whether heat is rejected to water or to air. Hence the temperature of the working substance called the refrigerant will be 5 to 15 K more than the temperature of the surroundings during heat rejection and 5 to 15 K lower than that of the cold space during heat absorption. The temperature of the refrigerant is known as the *Internal Regime*, and the design conditions of cold space and the temperature of the surroundings is called *External Regime.* These two regimes are shown in Figure 3.3.

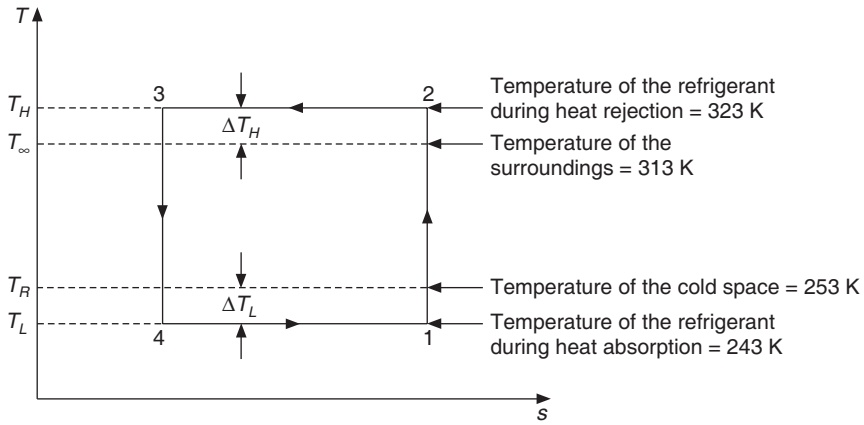

Figure 3.3 Internal and external temperature regimes.

External Regime: Temperature of surroundings, $T_\infty = 40^oC = 313$ K

Temperature of the cold space, $T_R = -20^oC = 253$ K

Assuming a temperature difference of 10^o C, the refrigerant temperatures, called *Internal Regime*, for this case are as follows:

Internal Regime: Temperature during heat rejection, $T_H = 50^oC = 323$ K

Temperature during heat absorption, $T_L = -30^oC = 243$ K

For an efficient cycle, T_H should be kept as low as possible but obviously it cannot be reduced below T_∞ (313 K in above example). Similarly, T_L should be kept as high as possible, the upper

limit being T_R. The area enclosed by the rectangle was shown to represent the work requirement and the area below the rectangle up to the x-axis represents the heat absorbed. It is observed that the work requirement at the internal regime temperatures is more than that of the external regime temperatures. The larger the value of ΔT, the larger will be the irreversibility and the lower will be the COP. It is obvious that the COP based upon external regimes is larger than that based upon the internal regimes. Truly speaking, the cycle shown in Figure 3.2(b) is not reversible since the heat transfers take place through temperature differences. It is a coincidence that the T–s diagram is a rectangle.

The temperature of the refrigerant has been assumed to be constant during heat absorption and during heat rejection, that is what makes the diagram a rectangle. This is possible if the refrigerant is a pure substance that condenses during heat rejection and boils during heat absorption. This is a very important feature for lower irreversibility.

Also, the temperatures of the external regimes have been assumed to remain constant during heat transfers which is not possible if heat is rejected to water, air or any other substance whose specific heat and mass flow rates are finite since $\dot{Q} = (\dot{m}c_p\Delta T)_{\text{air}}$. The temperature will increase when heat is rejected to it. Likewise, the temperature of the food items or the product being cooled will decrease during the cooling process.

3.7 GAS AS REFRIGERANT

3.7.1 Reversed Carnot Cycle

If gas, for example, is used as the refrigerant, the Reversed Carnot cycle would be as shown in Figure 3.2(b). It is a rectangle on T–s diagram. Processes 1–2 and 3–4 are isentropic compression and expansion respectively. Processes 2–3 and 4–1 are isothermal heat rejection and heat absorption respectively. The most important feature to observe is that pressure $p_3 > p_2$. This means that the isothermal heat rejection for a gas also requires a compressor (otherwise, the temperature of the gas will decrease during heat rejection, which is compensated by pressure rise). Similarly, $p_4 > p_1$, implies that a turbine has to be used for isothermal heat absorption. Hence, the Reversed Carnot cycle is not practical with gas as the refrigerant, since it will require two sets of compressors and turbines—one isentropic and the other isothermal. This will involve a higher initial cost and subsequently a higher maintenance cost.

Analysis of Reversed Carnot cycle for perfect gas

To carry out the cycle calculations, the first law of thermodynamics is applied to each component so as to express the work and heat transfer rates in terms of enthalpy of the refrigerant that is found from the refrigerant tables. The first law of thermodynamics for an open system in steady state with 1as inlet and 2 as outlet state is

$$\dot{m}\left(h_2 + \frac{V_2^2}{2} + gz_2\right) - \dot{m}\left(h_1 + \frac{V_1^2}{2} + gz_1\right) = \dot{Q} - \dot{W} \tag{3.28}$$

As a convention, the heat transfer to the system is considered to be positive and the work done by the system is also considered to be positive. In applying the first law to the components, the

specific potential energy change $\Delta PE = g(z_2 - z_1)$ is usually negligible since the height of the inlet is usually not much different from the height of the outlet. It may not be negligible for the pipe work connecting the components. The change in specific kinetic energy $\Delta KE = (V_2^2 - V_1^2)/2$ is also usually negligible. The first law of thermodynamics is applied to all the components.

1–2 Isentropic compression

For this process $s_1 = s_2$ and $q_{12} = 0$. If in addition, the changes in kinetic energy and potential energy, ΔKE and ΔPE, are zero, the first law of thermodynamics for steady flow gives

$$-w_{12} = h_2 - h_1 = c_p\,(t_2 - t_1) \tag{3.29}$$

The negative sign indicates that the work is done on the system. The same result can be obtained for flow work in the open system for the isentropic process $p_1 v_1^{\gamma} = p_2 v_2^{\gamma}$.

i.e.
$$-w_{12} = \int_1^2 v\,dp = \frac{\gamma}{\gamma - 1}(p_2 v_2 - p_1 v_1) = \frac{\gamma}{\gamma - 1} R(T_2 - T_1)$$

or
$$-w_{12} = \frac{\gamma}{\gamma - 1} RT_1 \left(\left(\frac{p_2}{p_1} \right)^{(\gamma-1)/\gamma} - 1 \right) \tag{3.30}$$

2–3 Isothermal heat rejection

The pressure increases during this process, hence work has to be done on the system. For the isothermal process $p_1 v_1 = p_2 v_2 = RT_2$, flow work for the open system is given by

$$-w_{23} = \int_2^3 v\,dp = -RT_2 \int_2^3 \frac{dp}{p} = RT_2 \ln(p_3 / p_2) \tag{3.31}$$

Also, $T_2 = T_3$, hence for a perfect gas, $h_2 = h_3$. From the first law of thermodynamics for a steady flow system with ΔKE = 0 and ΔPE = 0, we get, $q_{23} = w_{23}$ and substituting from (3.31),

$$q_{23} = w_{23} = -RT_2 \ln(p_3/p_2) \tag{3.32}$$

The negative sign indicates that work is done on the system and heat is rejected by the system.

3–4 Isentropic expansion

By analogy with process 1–2, we have $s_3 = s_4$ and $q_{34} = 0$. The first law of thermodynamics for steady flow gives

$$-w_{34} = h_4 - h_3 \quad \text{or} \quad w_{34} = h_3 - h_4 = c_p(t_3 - t_4) \tag{3.33}$$

The same result can be obtained for flow work in the open system for the isentropic process $p_3 v_3^{\gamma} = p_4 v_4^{\gamma}$.

i.e.
$$-w_{34} = \int_3^4 v\,dp = \frac{\gamma}{\gamma - 1}(p_4 v_4 - p_3 v_3) = \frac{\gamma}{\gamma - 1} R(T_4 - T_3)$$

or
$$w_{34} = \frac{\gamma}{\gamma - 1} RT_4 \left(\left(\frac{p_3}{p_4} \right)^{(\gamma-1)/\gamma} - 1 \right) \tag{3.34}$$

It is observed that w_{12} is equal and opposite to w_{34}.

4–1 Isothermal heat absorption

The pressure decreases during this process; hence work has is done by the system. For the isothermal process $p_4v_4 = p_1v_1 = RT_1$, flow work for the open system is given by

$$-w_{41} = \int_4^1 v\,dp = -RT_1 \int_4^1 \frac{dp}{p} = -RT_1 \ln (p_1/p_4) \tag{3.35}$$

or
$$w_{41} = RT_1 \ln (p_4/p_1)$$

Also, $T_1 = T_4$, hence for perfect gas $h_1 = h_4$. From the first law of thermodynamics for steady flow system with $\Delta KE = 0$ and $\Delta PE = 0$, we get, $q_{41} = w_{41}$ and substituting from Eq. (3.35),

$$q_{41} = w_{41} = -RT_1 \ln (p_1/p_4) = RT_1 \ln (p_4/p_1) \tag{3.36}$$

For isentropic processes,

$$\frac{T_2}{T_1} = \left(\frac{p_2}{p_1} \right)^{(\gamma-1)/\gamma} = \frac{T_3}{T_4} = \left(\frac{p_3}{p_4} \right)^{(\gamma-1)/\gamma} \quad \text{Hence,} \quad \frac{p_2}{p_1} = \frac{p_3}{p_4} \tag{3.37}$$

There are two ways to find the net work and the COP.

First method

Applying the first law of thermodynamics to the whole system,

$$|w_{net}| = |q_{23}| - |q_{41}| = RT_2 \ln (p_3/p_2) - RT_1 \ln (p_4/p_1) \tag{3.38}$$

Also from Eq. (3.37), we have $p_3/p_2 = p_4/p_1$. Hence, Eq. (3.38) reduces to

$$|w_{net}| = R(T_2 - T_1) \ln (p_4/p_1)$$

$\therefore$
$$\text{COP} = \frac{q_{41}}{|w_{net}|} = \frac{RT_1 \ln (p_4/p_1)}{R(T_2 - T_1) \ln (p_4/p_1)} = \frac{T_1}{T_2 - T_1} \tag{3.39}$$

This is same as Eq. (3.22).

Second method

The net work can be found by adding the work for the four processes as follows:

$$w_{net} = w_{12} + w_{23} + w_{34} + w_{41} = w_{23} + w_{41} \text{ since } w_{12} = -w_{34}$$

$\therefore$
$$|w_{net}| = |w_{23}| - |w_{41}| = RT_2 \ln (p_3/p_2) - RT_1 \ln (p_4/p_1)$$

which is same as that given by Eq. (3.38).

EXAMPLE 3.1 In a Reversed Carnot refrigeration system of 1 TR cooling capacity running on perfect gas, heat is absorbed at –10°C and rejected at 50°C. Find the states at all the points of the cycle, heat transfer and work done in all the processes, mass flow rate, volume flow rates and the COP. The maximum pressure ratio is 5 and the pressure at inlet to the isentropic compressor is standard atmospheric pressure. Take c_p = 1.005 kJ/kg-K, R = 0.287 kJ/kg-K and γ = 1.4.

Solution:

We have p_1 = 1.01325 bar, t_1 = –10°C (T_1 = 263 K) and t_2 = 50°C (T_2 = 323 K)

$$\frac{p_2}{p_1} = \left(\frac{T_2}{T_1}\right)^{\gamma/(\gamma-1)} = \left(\frac{323}{263}\right)^{1.4/(1.4-1)} = 2.05288$$

Given that $p_3/p_1 = 5$, Therefore, $p_3/p_2 = \dfrac{p_3/p_1}{p_2/p_1} = \dfrac{5}{2.05288} = 2.4356 = p_4/p_1$

Hence,

$p_2 = 2.05288 \times 1.01325 = 2.08$ bar and $p_3 = 5 \times 1.01325 = 5.06625$ bar and

$p_4 = 2.4356 \times 1.01325$ bar

$q_{12} = 0$

$-w_{12} = h_2 - h_1 = c_p(t_2 - t_1) = 1.005\{50 - (-10)\} = 60.3$ kJ/kg

$q_{23} = w_{23} = -RT_2 \ln (p_3/p_2) = -0.287\ (323) \ln (2.4356) = 82.522$ kJ/kg

$w_{34} = h_3 - h_4 = c_p(t_3 - t_4) = 60.3$ kJ/kg

$q_{34} = 0$

$q_{41} = w_{41} = RT_1 \ln (p_4/p_1) = 0.287(263) \ln (2.4356) = 67.1927$ kJ/kg

$|w_{net}| = |w_{23}| - |w_{41}| = 82.522 - 67.1927 = 15.3343$ kJ/kg

COP = $q_{41}/|w_{net}| = 67.1927/15.3343 = 4.382$

Also, COP = $T_1/(T_2 - T_1) = 263/60 = 4.383$

For a system of 1 TR cooling capacity, $\dot{m}q_{41}$ = 1 TR = 3.5167 kW. Therefore

$$\dot{m} = 3.5167/67.1927 = 0.05233 \text{ kg/s}$$

Volume flow rate at state 1 = $\dot{m}\ RT_1/p_1 = 0.05233 \times 0.287 \times 263/101.325 = 0.039$ m^3/s

Volume flow rate at state 4 = $\dot{m}\ RT_4/p_4 = 0.05233 \times 0.287 \times 263/243.56 = 0.0162$ m^3/s

The specific volumes at various points are as follows:

$v_1 = RT_1/p_1 = 0.287(263)/101.325 = 0.745$ m^3/kg

$v_2 = RT_2/p_2 = 0.287(323)/(101.325 \times 2.05288) = 0.4457$ m^3/kg

$v_3 = RT_3/p_3 = 0.287(323)/506.625 = 0.183$ m^3/kg

$v_4 = RT_4/p_4 = 0.287(263)/(2.4356 \times 101.325) = 0.3058$ m^3/kg

This Reversed Carnot cycle is illustrated in Figure 3.4 along with its *T–s* and *p–v* diagrams. It may be observed that the *p–v* of the cycle is a very narrow diagram.

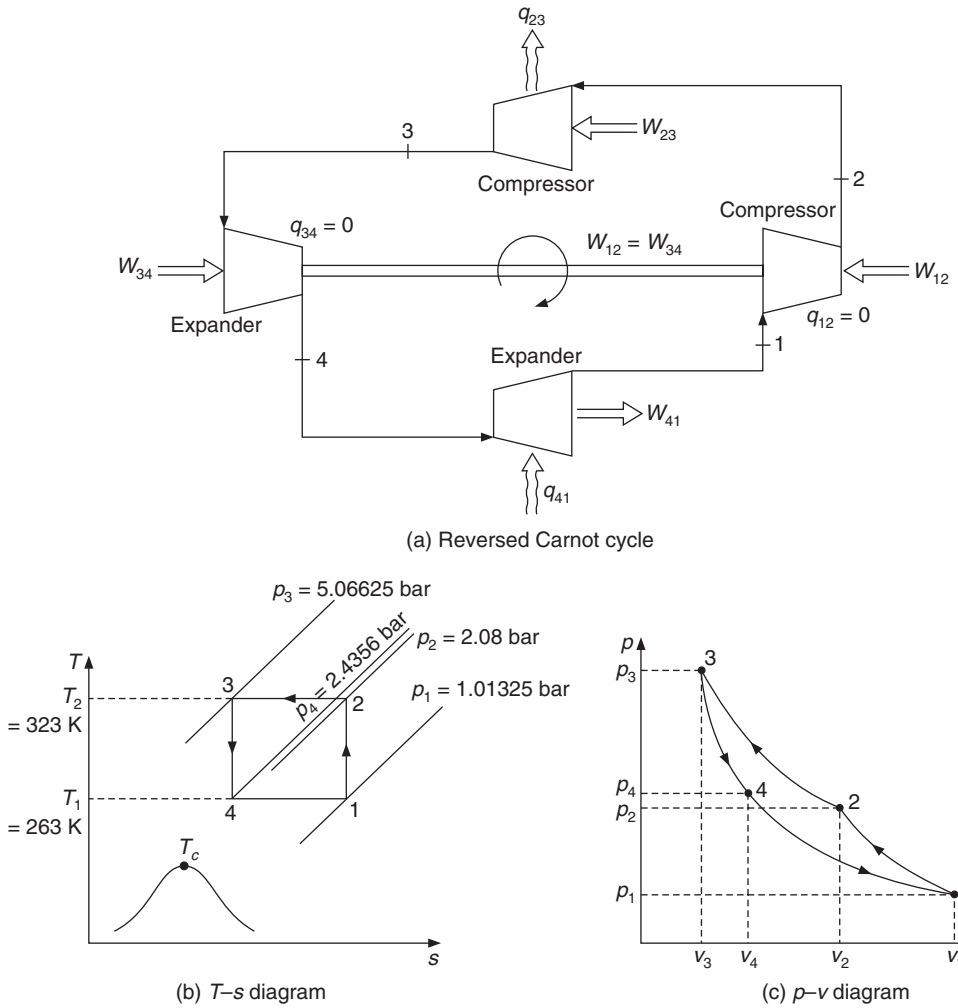

Figure 3.4 Example 3.1.

3.7.2 Joule Cycle or Bell-Coleman Cycle or Reversed Brayton Cycle

It is observed that the Reversed Carnot cycle is not a practical cycle since it requires two compressors and two expanders. Hence, in a practical cycle the isothermal heat rejection is replaced by isobaric heat rejection, which is carried out in heat exchangers with little bit of pressure drop to overcome the frictional resistance of tubes. The gas in this cycle will still have to be isentropically compressed to a maximum pressure ratio p_3/p_1. This cycle is called the Joule cycle or Bell Coleman cycle or Reversed Brayton cycle. It is shown in Figure 3.5.

The pressure ratio for isentropic compression in the process 1–2′ is more than that in the Reversed Carnot cycle. The isentropic expansion is also carried out through a larger pressure ratio. The temperature of gas decreases during heat rejection process 2′–3. Hence for heat rejection right up to point 3, temperature T_3 must be higher than the atmospheric temperature T_∞. Obviously

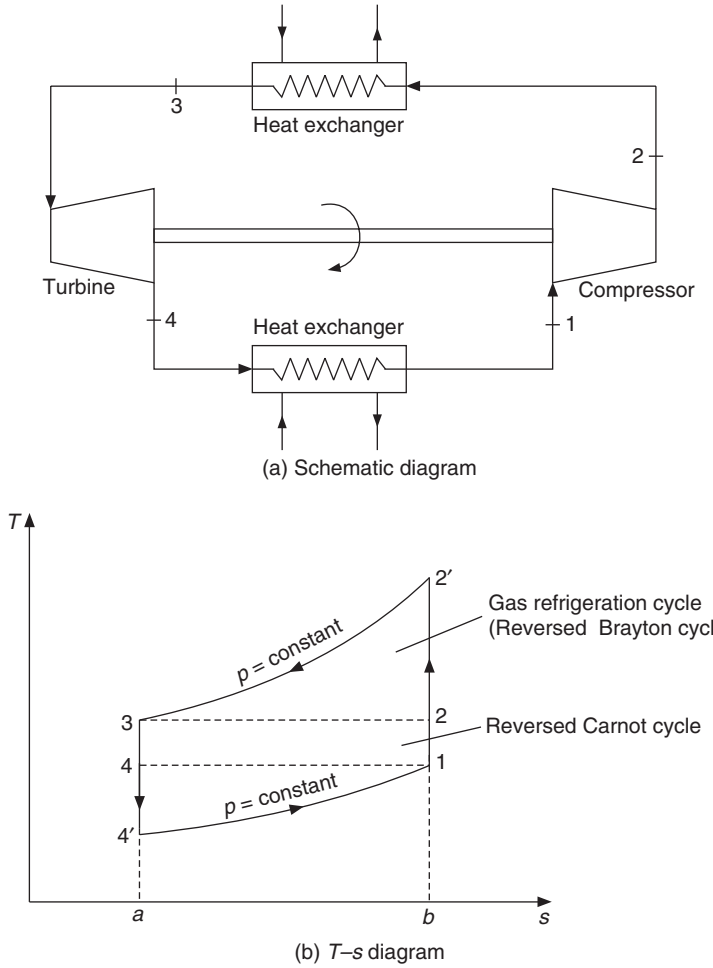

Figure 3.5 Reversed Brayton cycle.

$T_{2'}$ is much higher than T_∞ and there will be a significant temperature drop during heat rejection leading to irreversibility. Heat is absorbed during 4′–1, hence the temperature T_1 must be higher than the cold room temperature T_R, and $T_{4'}$ must be significantly smaller than T_R leading to a large irreversibility. It will be shown later that if the temperatures of the external regime also vary in the similar manner as those of the internal regime so that the temperature difference between the two regimes is small throughout, this cycle may be more efficient than the Reversed Carnot cycle.

The work requirement of Reversed Brayton cycle is = Area 1–2′–3–4′–1

The work requirement of Reversed Carnot cycle is = Area 1–2–3–4–1

Hence the work requirement compared to Reversed Carnot cycle increases by the sum of areas 2–2′–3–2 and 4–4′–1–4.

The heat absorbed in Reversed Brayton cycle is = Area 4′–*a*–*b*–1–4′

The heat absorbed in Reversed Carnot cycle is = Area 4–*a*–*b*–1–4

The heat absorbed compared to Reversed Carnot cycle decreases by area 4–4′–1–4 and the COP is far less compared to Reversed Carnot cycle. Hence. the Reversed Brayton is not a desirable cycle, however this cycle finds limited applications in aircraft refrigeration.

Analysis of Joule cycle for perfect gas

1–2′ isentropic compression: For this process $s_1 = s_{2'}$ and $q_{12'} = 0$. Following Eq. (3.29) for this process, we get

$$-w_{12'} = h_{2'} - h_1 = c_p(t_{2'} - t_1) = \frac{\gamma}{\gamma - 1} RT_1 \left(\left(\frac{p_{2'}}{p_1} \right)^{(\gamma-1)/\gamma} - 1 \right) \tag{3.40}$$

2′–3 isobaric heat rejection: The work done in this process is zero and heat is transferred at constant pressure. Hence,

$$w_{2'3} = 0$$

$$q_{2'3} = h_{2'} - h_3 = c_p\,(t_{2'} - t_3) \tag{3.41}$$

3–4′ isentropic expansion: For this process $s_3 = s_{4'}$ and $q_{34'} = 0$. Following Eq. (3.33) for this process, we get

$$-w_{34'} = h_{4'} - h_3$$

or

$$w_{34'} = h_3 - h_{4'} = c_p(t_3 - t_{4'}) = \frac{\gamma}{\gamma - 1} RT_{4'} \left(\left(\frac{p_3}{p_{4'}} \right)^{(\gamma-1)/\gamma} - 1 \right) \tag{3.42}$$

4′–1 isobaric heat absorption: The work done in this process is zero and heat is transferred at constant pressure, hence

$$w_{4'1} = 0$$

and

$$q_{4'1} = h_1 - h_{4'} = c_p(t_1 - t_{4'}) \tag{3.43}$$

For isentropic compression 1–2′ and isentropic expansion 3–4′,

$$\frac{T_{2'}}{T_1} = \left(\frac{p_{2'}}{p_1} \right)^{(\gamma-1)/\gamma} = \frac{T_3}{T_{4'}} = \left(\frac{p_3}{p_{4'}} \right)^{(\gamma-1)/\gamma} \text{ Hence, } \frac{T_{2'}}{T_1} = \frac{T_3}{T_{4'}} \text{ since } \frac{p_{2'}}{p_1} = \frac{p_3}{p_{4'}} \tag{3.44}$$

Applying the first law of thermodynamics to the whole system, we get

$$|\,w_{\text{net}}\,| = |\,w_{12'}\,| - |\,w_{34'}\,| = |\,q_{2'3}\,| - |\,q_{4'1}\,| = c_p\,(T_{2'} - T_3) - c_p(T_1 - T_{4'})$$

$$\text{COP} = \frac{q_{4'1}}{|\,w_{\text{net}}\,|} = \frac{T_1 - T_{4'}}{(T_{2'} - T_3) - (T_1 - T_{4'})} = \frac{1}{[(T_{2'} - T_3)/(T_1 - T_{4'})] - 1}$$

$\therefore$

$$\text{COP} = \frac{1}{\dfrac{T_{2'}}{T_1}\dfrac{(1 - T_3/T_{2'})}{(1 - T_{4'}/T_1)} - 1} = \frac{1}{(T_{2'}/T_1) - 1} = \frac{1}{\left(\dfrac{p_{2'}}{p_1} \right)^{(\gamma-1)/\gamma} - 1} \tag{3.45}$$

EXAMPLE 3.2 In a Reversed Brayton cycle running on air, the temperature at the exit of refrigerator is –10°C and that at the exit of heat rejection is 50°C. The cooling capacity is one TR. Find the states at all the points of the cycle, heat transfer and work done in all the processes, mass flow rate, volume flow rates and COP. The maximum pressure ratio is 5 and the pressure at inlet to isentropic compressor is standard atmospheric pressure. Take c_p= 1.005 kJ/kg-K, R = 0.287 kJ/kg-K and γ= 1.4.

Solution:

We have $p_1 = 1.01325$ bar, $t_1 = -10°C$ ($T_1 = 263$ K) and $t_3 = 50°C$ ($T_3 = 323$ K)

$v_1 = RT_1/p_1 = 0.287(263)/101.325 = 0.745$ m^3/kg

$p_{2'} = 5p_1 = 5 \times 101.325 = 506.625$ kPa

$T_{2'} = T_1(p_{2'}/p_1)^{(\gamma-1)/\gamma} = 263(5)^{0.4/1.4} = 416.544$ K

$v_{2'} = RT_{2'}/p_{2'} = 0.287(416.544)/506.625 = 0.236$ m^3/kg

$v_3 = RT_3/p_3 = 0.287(323)/506.625 = 0.183$ m^3/kg

$T_{4'} = T_3/(p_3/p_{4'})^{(\gamma-1)/\gamma} = 323/\ (5)^{0.4/1.4} = 203.937$ K

$v_{4'} = RT_{4'}/p_{4'} = 0.287(203.937)/101.325 = 0.5776$ m^3/kg

$w_{12'} = 1.005(T_{2'} - T_1) = 1.005(416.544 - 263) = 154.31$ kJ/kg

$q_{2'3} = 1.005(T_{2'} - T_3) = 1.005(416.544 - 323) = 94.012$ kJ/kg

$w_{34'} = 1.005(T_3 - T_{4'}) = 1.005(323 - 203.937) = 119.658$ kJ/kg

$q_{4'1} = 1.005(T_1 - T_{4'}) = 1.005(263 - 203.937) = 59.358$ kJ/kg

$|w_{net}| = |w_{12'}| - |w_{34'}| = 154.31 - 119.658 = 34.652$ kJ/kg

$$\text{COP} = \frac{q_{4'1}}{|w_{net}|} = \frac{59.358}{34.625} = 1.713$$

Also, from Eq. (3.45),

$$\text{COP} = 1/[(p_{2'}/p_1)^{(\gamma-1)/\gamma} - 1\ ] = 1/(5^{(1.4-1)/1.4} - 1) = 1.713$$

For a system of 1 TR cooling capacity, $\dot{m}q_{4'1}$ = 1 TR = 3.5167 kW. Therefore,

$$\dot{m} = 3.5167/59.358 = 0.05924 \text{ kg/s}$$

Volume flow rate at state 1 = $\dot{m}v_1 = 0.05924 \times 0.745 = 0.04413$ m^3/s

Volume flow rate at state 4 = $\dot{m}v_{4'} = 0.05924 \times 0.5776 = 0.0342$ m^3/s

Comparing these results with those of the Reversed Carnot cycle, it is observed that the COP reduces drastically. The highest and the lowest temperatures are 416.544 K and 203.937 K respectively. The maximum COP based upon these temperatures is (203.937/212.607) = 0.96. This is rather low, since we have taken the lowest and highest temperatures at which heat transfers take place. If the average values of temperature were taken, the result may be better. The average temperature for heat rejection is (416.544 + 323)/2 = 369.772 K; and the average temperature for heat absorption is (203.937 + 263)/2 = 233.4685 K. The maximum COP based upon these two temperatures is 1.713. This is good but the prevalent practice is to define entropic average temperature based upon $q_{rev} = T\,\Delta s$ as follows and define a COP.

The entropy changes during heat transfers 2′–3 and 4′–1 are

$$s_{2'3} = c_p \ln (T_{2'}/T_3) = 1.005 \ln (416.544/323) = 0.2556$$

$$s_{4'1} = c_p \ln (T_1/T_{4'}) = 1.005 \ln(263/203.937) = 0.2556$$

If we define entropic average temperatures

$$\bar{T}_h = \frac{q_{2'3}}{s_{2'3}} = \frac{94.012}{0.2556} = 367.792$$

$$\bar{T}_c = \frac{q_{4'1}}{s_{4'1}} = \frac{59.358}{0.2556} = 232.219$$

then, we have, based upon these temperatures,

$$\text{COP} = 232.219/(367.792 - 232.219) = 1.712$$

which is same as that for the actual cycle. The temperature varies during the heat transfer processes in the Joule cycle. It appears that entropic average temperature may be used to find the COP, based upon the Reversed Carnot COP. In this case the result is same since the entropy change is same for heat rejection and absorption and these terms cancel out.

3.8 PURE SUBSTANCE AS REFRIGERANT

3.8.1 Wet Compression Cycle

It has been observed that with gas as a working substance, isothermal heat transfers are not possible without a compressor or an expander. If the refrigerant condenses during heat rejection and boils during heat absorption, that is, if both the heat transfer processes involve latent heat transfer, then the processes will be isothermal and reversible. Such a Reversed Carnot cycle with wet compression is shown in Figure 3.6(a). It consists of:

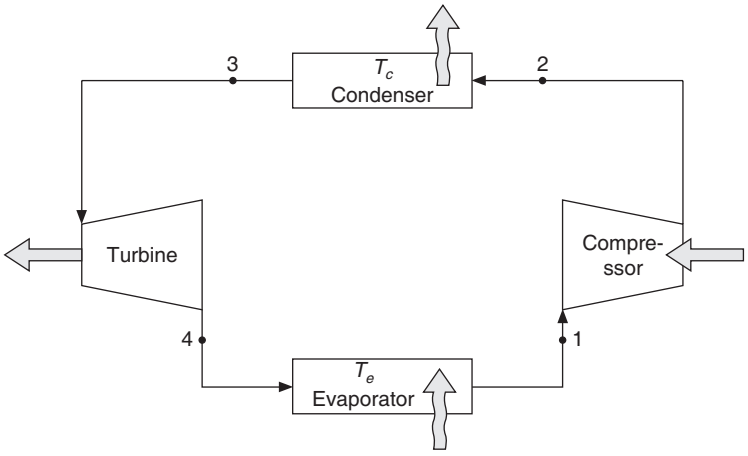

Figure 3.6(a) Schematic of the Reversed Carnot refrigeration system with wet vapour.

(i) **1–2:** Isentropic compression carried out in an isentropic compressor.

(ii) **2–3:** Isothermal heat rejection by condensation carried out in an *heat exchanger* called condenser. Subscript *c* has been used for temperature and heat transfer in this component to denote condenser.

(iii) **3–4:** Isentropic expansion carried out in a turbine or an expansion engine.

(iv) **4–1:** Isothermal heat absorption by boiling carried out in an *heat exchanger* called evaporator. Subscript *e* has been used for temperature and heat transfer in this component to denote evaporator.

The states 2 and 3 at inlet and exit of the condenser are saturated vapour and liquid states respectively.

The *T–s* diagram of the Reversed Carnot cycle with wet vapour is shown in Figure 3.6(b). It involves wet compression and expansion, both of which have practical disadvantages. Compression 1–2 is called wet compression since whole of the process occurs in the mixture region where liquid droplets of refrigerant are present. In a typical high speed reciprocating compressor the rpm is around 1440, therefore, the compression stroke takes less than 0.02 second (less than half of one cycle). This time is not sufficient for all liquid droplets to evaporate. The end state is shown to be saturated state, which may be on the average a mixture of some superheated vapour and some left over liquid droplets. The average piston velocity is 2–3 m/s. The outlet valve passage area may be 1/6 of the cross section area of cylinder; hence the refrigerant outlet velocity will be around 12–18 m/s. *The liquid refrigerant droplets coming out with such a high velocity hit the compressor valves like bullets and damage them.*

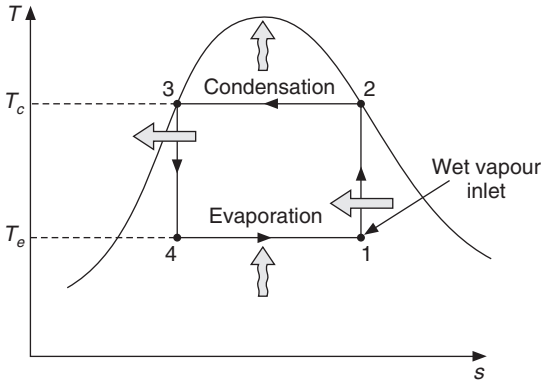

Figure 3.6(b) The *T–s* diagram of the Reversed Carnot refrigeration cycle with wet vapour.

Further, the liquid refrigerant has more solubility for the lubricant oil than the vapour refrigerant. Hence, the liquid refrigerant droplets will dissolve more lubricating oil present on the walls of the cylinder. *This will increase the wear and tear of the compressor.* In the older models of compressors the rpm used to be around 100–400; this speed usually gave sufficient time for heat transfer to evaporate the liquid refrigerant present at the inlet.

The wet compression cycle is of academic interest and is described in most of the textbooks, since for illustration purpose calculations it can be conveniently carried out using only the saturated

properties of refrigerants. This will be shown by solved examples. It is therefore advised that dry compression be carried out in high speed reciprocating compressors.

3.8.2 Saturated Reversed Carnot Cycle

The practical Reversed Carnot cycle that is considered a standard for comparison with other cycles is shown in Figure 3.7.

The description of this cycle in Figure 3.7 is as follows:

(i) Compressor inlet state 1 is saturated vapour state.

(ii) 1–2 is isentropic compression process that occurs in superheated state.

(iii) 2–*a* is isothermal heat rejection. However, just like the gas cycle the pressure during the part 2–*a* increases, that is $p_a = p_c > p_2$. Therefore this requires an isothermal compressor.

(iv) *a*–3 is isothermal heat rejection.

(v) 3–4: Isentropic expansion carried out in a turbine or an expansion engine.

(vi) 4–1: Isothermal heat absorption by evaporation carried out in on evaporator.

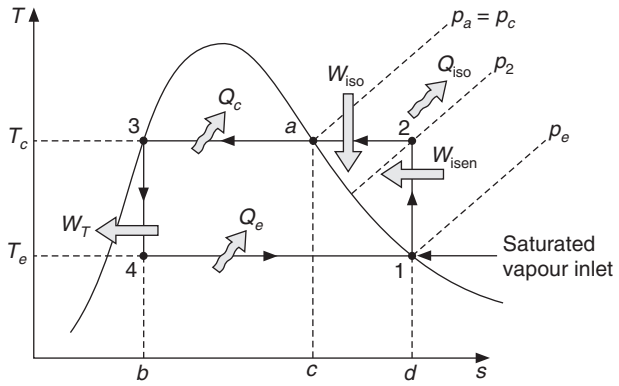

Figure 3.7 The *T*–*s* diagram of Reversed Carnot refrigeration cycle with saturated vapour.

The schematic diagram of this cycle is shown in Figure 3.8. This cycle is also not a practical one since it requires two compressors apart from a turbine that works in the two-phase region. This cycle, however, is considered a standard one with which we compare the performance of other vapour compression cycles.

Analysis of the cycle

The first law of thermodynamics, i.e. Eq. (3.28), is applied to all the components.

Isentropic compression 1–2

Assume that the changes in kinetic and potential energy are negligible, that is, ΔKE = 0 and ΔPE = 0. Isentropic process means adiabatic and reversible, hence $q = 0$. If W_{isen} is the work input to the isentropic compressor, the first law of thermodynamics reduces to

$$-W_{isen} = \dot{m}(h_2 - h_1) \tag{3.46}$$

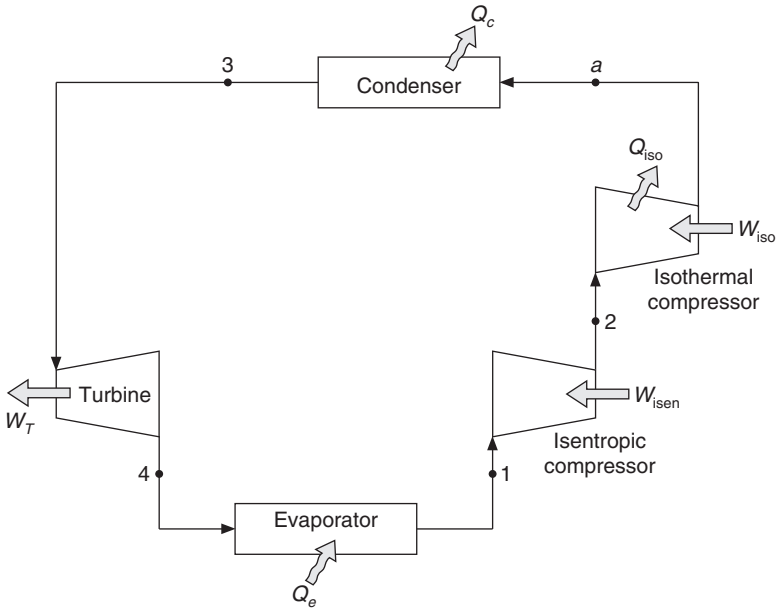

Figure 3.8 Schematic of saturated Reversed Carnot system.

On per unit mass flow rate basis, the specific work input is

$$-w_{\text{isen}} = h_2 - h_1 \tag{3.47}$$

The negative sign indicates that the work is done on the system. The right hand side is positive, hence, $|\, w_{\text{isen}} \,| = h_2 - h_1$.

Expansion turbine 3–4

Again for isentropic process $q = 0$, and we assume changes in kinetic and potential energy to be negligible. If w_T is specific turbine work output, the first law of thermodynamics reduces to:

$$w_T = h_3 - h_4 \tag{3.48}$$

Isothermal compression 2–a

W_{iso} is the work done on the isothermal compressor and Q_{iso} is the heat rejected by the compressor. Both of these are negative. The first law of thermodynamics reduces to

$$Q_{\text{iso}} - W_{\text{iso}} = \dot{m}(h_a - h_2)$$

The process is considered to be reversible, hence using $Q_{\text{rev}} = Tds$,

$$-Q_{\text{iso}} = \dot{m}T_c\,(s_2 - s_a) = \dot{m}\,(\text{area } 2\text{–}a\text{–}c\text{–}d\text{–}2 \text{ on the } T\text{–}s \text{ diagram}).\ \text{Therefore,}$$

$$-W_{\text{iso}} = \dot{m}\,(h_a - h_2) + \dot{m}T_c\,(s_2 - s_a)$$

or
$$-w_{\text{iso}} = T_c(s_2 - s_a) - (h_2 - h_a) \tag{3.49}$$

This result can also be obtained by integrating $Tds = dh - v\,dp$ along the process 2–a and using the fact that for an open system, by definition, $w = -v\,dp$. Therefore,

$$w_{\text{iso}} = -\int_2^a v\,dp = \int_2^a T\,ds - \int_2^a dh = T_c\,(s_a - s_2) - (h_a - h_2)$$

This is the work done on the system, hence it is negative and $|\,w_{\text{iso}}\,| = T_c(s_2 - s_a) - (h_2 - h_a)$.

Condensation a–3

In this case too, steady state is assumed and the changes in kinetic and potential energy are assumed to be negligible. There is no work involved in this process, that is, $W = 0$.

Hence, the first law of thermodynamics reduces to

$$-Q_c = \dot{m}(h_a - h_3) - \dot{m}T_c\,(s_a - s_3) \tag{3.50}$$

In fact, considering *a*–3 to be isothermal and isobaric process and using $Tds = dh - v\,dp$, we get $dh = Tds$ since $dp = 0$ for isobaric process. Integrating it along *a*–3, we get

$$h_a - h_3 = \int_3^a T_c\,ds = T_c\,(s_a - s_3) \;= \text{area } 3\text{–}b\text{–}c\text{–}a\text{–}3 \text{ on the } T\text{–}s \text{ diagram}$$

Evaporation 4–1

In this case too, steady state is assumed and the changes in kinetic energy ΔKE and potential energy ΔPE are assumed to be negligible. There is no work involved in this process, hence the first law of thermodynamics reduces to

$$Q_e = \dot{m}(h_1 - h_4)$$

or

$$q_e = (h_1 - h_4) \tag{3.51}$$

This process is also isobaric and isothermal, hence from $Tds = dh - v\,dp$

$$q_e = (h_1 - h_4) = T_e\,(s_1 - s_4) = \text{area } 4\text{–}1\text{–}d\text{–}b\text{–}4 \text{ on the } T\text{–}s \text{ diagram} \tag{3.52}$$

In fact, this relation could have been written from $dQ_{\text{rev}} = T\Delta s$ as well.

Net work

The net work for the cycle is the difference between the total work input to the compressors and the work output of the turbine. This will be negative.

$$|\,w\,| = |\,w_{\text{isen}}\,| + |\,w_{\text{iso}}\,| - w_T = (h_2 - h_1) + T_c(s_2 - s_a) - (h_2 - h_a) - (h_3 - h_4)$$
$$= T_c\,(s_2 - s_a) + (h_a - h_3) - (h_1 - h_4)$$

Processes *a*–3 and 1–4 are isobaric and isothermal processes; hence, $(h_a - h_3) = T_c\,(s_a - s_3)$ and $(h_1 - h_4) = T_e\,(s_1 - s_4)$. Therefore,

$$w = T_c\,(s_2 - s_a) + T_c\,(s_a - s_3) - T_e\,(s_1 - s_4)$$
$$= T_c\,(s_2 - s_3) - T_e\,(s_1 - s_4) = T_c\,(s_1 - s_4) - T_e\,(s_1 - s_4)$$
$$= \text{area under line 2–3} - \text{area under line 1–4}$$

Also since $s_1 = s_2$ and $s_3 = s_4$,

$$w = (T_c - T_e)(s_1 - s_4) = \text{area } 1\text{–}2\text{–}3\text{–}4\text{–}1 \tag{3.53}$$

By Eqs. (3.52) and (3.53) the COP may be expressed as

$$COP = \frac{q_e}{w} = \frac{T_e (s_1 - s_4)}{(T_c - T_e)(s_1 - s_4)} = \frac{T_e}{T_c - T_e} \tag{3.54}$$

This agrees with the result derived earlier from the first and the second law of thermodynamics.

3.9 STANDARD VAPOUR COMPRESSION CYCLE OR VAPOUR COMPRESSION CYCLE OR SINGLE STAGE SATURATION (SSS) CYCLE

It is desirable for the refrigeration cycle to approach the Reversed Carnot cycle since this cycle has the highest possible COP. As already observed, this cycle, however, is not a practical cycle for the following reasons:

1. It uses two compressors, an isentropic compressor and an isothermal compressor. Use of two compressors involves more capital cost and more maintenance and running cost, hence it is not desirable.
2. The expansion engine cannot be used in the two-phase region due to practical considerations.

The work output of this engine is a small fraction of the work input to the compressors, which may be lost in overcoming friction and in transmission to the compressor shaft. The lubrication of an expansion engine using a mixture of liquid and vapour poses a big problem since the liquid refrigerant dissolves the lubricating oil. Turbines are conventionally designed either for liquid or for vapour. Hydraulic turbines face problems when cavitation occurs and steam turbines face problems when wet steam is encountered. The smooth surfaces of the turbine blades become eroded and the skin friction increases during operation under the two-phase region. The economics of power recovery does not justify the cost of an expansion engine or turbine. Hence, in a practical cycle the expansion turbine is replaced by a throttling device. The throttling process is an irreversible process and entropy increases during this process.

Further, it is not economical to use two compressors. Therefore, a single isentropic compressor is used right up to the condenser pressure, which requires a rather higher compression ratio. This cycle is called *standard vapour compression cycle* or *vapour compression cycle* or *single stage saturation cycle* (SSS cycle). The saturation refers to the saturated states at the inlet of compressor and at the outlet of condenser. This cycle is used as model for actual cycles since it is closer to them than the Reversed Carnot cycle. The schematic diagram of this cycle is shown in Figure 3.9. The *T–s* and *p–h* diagrams of the cycle are shown in Figures 3.10 and 3.11, respectively.

The assumptions of the standard vapour compression cycle are:

1. State at compressor inlet or evaporator outlet is saturated vapour state.
2. Compression is isentropic.
3. Heat rejection is isobaric.
4. State at condenser exit is saturated liquid.
5. Expansion is by throttling process with constant enthalpy.
6. Heat absorption is by evaporation and is isobaric.

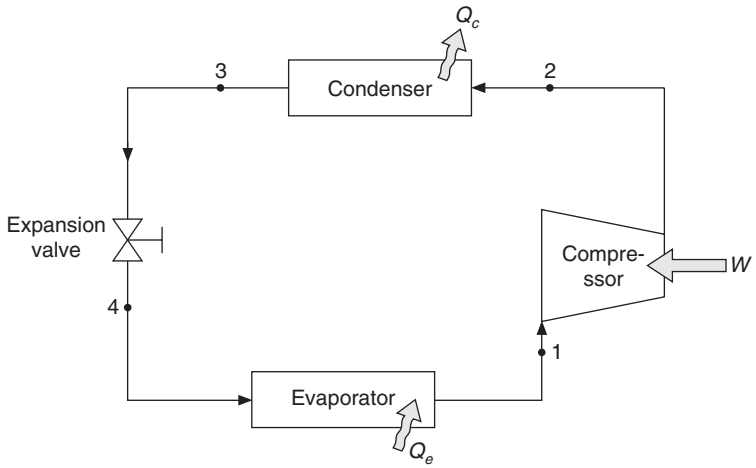

Figure 3.9 Schematic of the standard vapour compression refrigeration system.

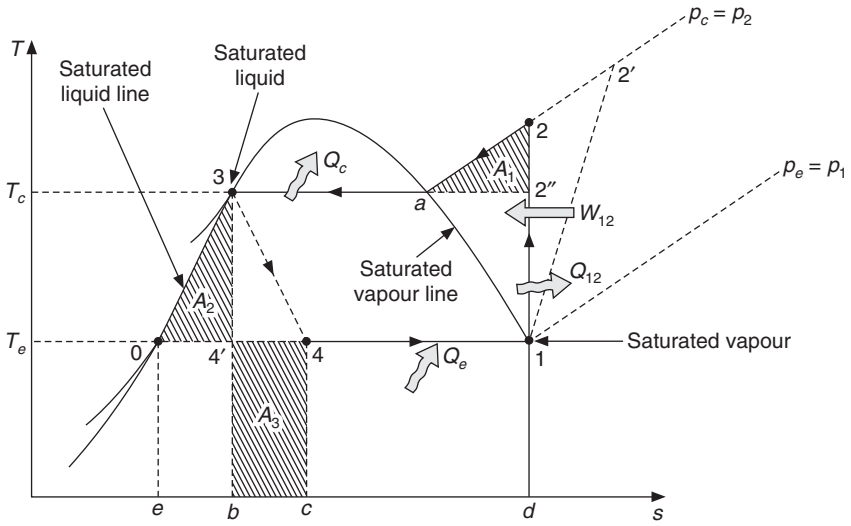

Figure 3.10 Standard vapour compression refrigeration cycle on *T–s* diagram.

Compressor

Assuming steady state and the compression to be isentropic with ΔPE = ΔKE = 0, the first law of thermodynamics yields

$$W = \dot{m}(h_2 - h_1)\ \text{kW},\ \ w = (h_2 - h_1)\ \text{kJ/kg}\ \ \text{and}\ \ s_2 = s_1 \tag{3.55}$$

Condenser

Assuming steady state, ΔPE = ΔKE = 0 and no work done during heat rejection, the first law of thermodynamics for the condenser yields

$$Q_c = \dot{m}(h_2 - h_3)\ \text{kW},\ \ q_c = (h_2 - h_3)\ \text{kJ/kg} \tag{3.56}$$

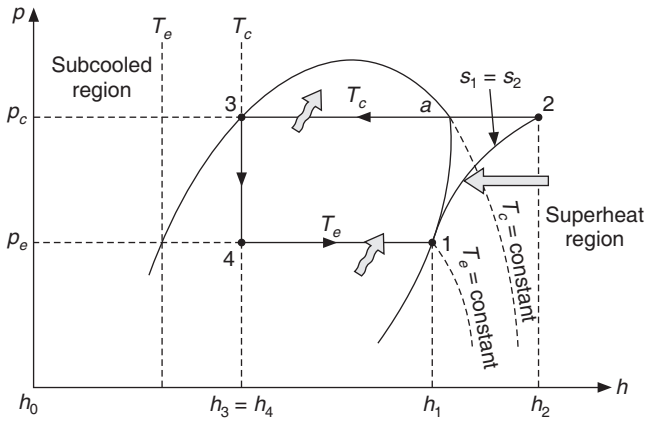

Figure 3.11 Standard vapour compression refrigeration cycle on *p–h* diagram.

Evaporator

Again, assuming steady state, ΔPE = ΔKE = 0 and no work done during heat absorption, the first law of thermodynamics for the evaporator yields

$$Q_e = \dot{m}(h_1 - h_4) \text{ kW}, \quad q_e = (h_1 - h_4) \text{ kJ/kg} \tag{3.57}$$

Expansion valve

The expansion through a throttling device is an irreversible process in which the pressure decreases while no work output is obtained. The dimensions of the valve being small, the heat transfer from expansion valve is negligible. Assuming steady state, ΔPE = ΔKE = 0 and no shaft work done, the first law of thermodynamics for the expansion valve yields

$$Q = W = 0 = \dot{m}(h_3 - h_4)$$

or

$$h_4 = h_3 \tag{3.58}$$

This is an irreversible process and hence sometimes it is shown by a dashed line on the *T–s* diagram. Obviously $s_4 > s_3$. On the *p–h* diagram, this is shown by a vertical line.

Refrigeration effect

The difference in specific enthalpy across the evaporator is called the refrigeration effect, i.e.

$$q_e = (h_1 - h_4) \text{ kJ/kg} \tag{3.59}$$

The refrigeration effect depends upon the latent heat of the refrigerant. This value is very large for NH_3 compared to that for CFCs. It varies slightly with T_c and T_e. The mass flow rate is related to actual swept flow rate V_s at entry to the compressor, which in turn is related to the physical size, rpm and volumetric efficiency of the compressor. If v_1 is the specific volume at the compressor inlet, then

$$\dot{m} = \mathbb{V}_s / v_1 \tag{3.60}$$

$$Q_e = \mathbb{V}_s(h_1 - h_4)/v_1 \text{ kW} \tag{3.61}$$

The term $(h_1 - h_4)/v_1$ has the units of kJ/m^3. This indicates the cooling capacity per unit volume flow rate. It depends upon the refrigerant, T_c and T_e and is called the volumic refrigeration effect.

Coefficient of performance

This is defined as the ratio of the measure of desired output to the measure of work input, that is, the ratio of refrigeration effect to the work input and it is expressed as

$$\text{COP} = \frac{q_e}{W} = \frac{h_1 - h_4}{h_2 - h_1} \tag{3.62}$$

The COP thus depends upon the enthalpies at the four state points of the cycle, which in turn depend upon the temperatures T_e, T_c and the properties of the refrigerant used in the system.

The compression in this cycle is assumed to be isentropic, that is, reversible and adiabatic. Reversible implies that the process is carried out in a slow manner through a large number of equilibrium states and the process is allowed to come to equilibrium at each state, such that the process can be reversed if the sign of work input and heat transfer are reversed. In reality the compression will occur in finite time and will be irreversible. The idealization is done so that the work requirement can be calculated easily. An isentropic process is adiabatic. Hence, if this is taken as a standard of minimum work, it would imply that there is no heat transfer during compression. In an actual process, there is heat rejection during compression. Considering heat rejection Q_{12} during compression as shown in Figure 3.10, then

$W = -W_{12}$: work is done on the system hence it is negative

$Q = -Q_{12}$: heat is rejected from the system, hence it is negative

The first law of thermodynamics yields

$$-Q_{12} + W_{12} = \dot{m}(h_2 - h_1)$$

$$\therefore \quad W_{12} = \dot{m}(h_2 - h_1) + Q_{12} \tag{3.63}$$

In such a case the work is required to increase the enthalpy of the refrigerant and to make up for the heat rejection The work requirement will reduce, if Q_{12} is zero, that is, if the process is adiabatic. In addition, if the process is reversible, then no work is required to overcome the friction. Hence the work requirement is minimum for the isentropic process.

For air compressors, isothermal compression is adopted as a standard. The air usually enters the compressor at room temperature and as compression occurs, the temperature of compressed air rises so that heat can be rejected to the surroundings. For the isentropic process $v \propto p^{-1/\gamma}$ while for the isothermal process $v \propto 1/p$. Therefore, the specific volume decreases at a faster rate for the isothermal process and the requirement $\int v\, dp$ is smaller than that for the isentropic compression.

If air is assumed to be perfect gas, its enthalpy is a function of temperature alone. As a result, for isothermal compression $T_2 = T_1$ and $h_2 = h_1$, therefore Eq. (3.63) for the work requirement reduces to $W = Q$. Hence, for isothermal compression of perfect gas the work done is equal to the heat rejection. That is , the work is done to maintain the perfect gas at constant temperature while its pressure increases.

In the case of refrigeration system, the refrigerant enters the compressor at very low temperature compared to the temperature of the surroundings, hence heat cannot be rejected to the surroundings.

Towards the end of the compression, vapour temperature may become larger than the room temperature and some heat may be rejected to the surroundings. However, the time available for heat transfer is small in modern high speed compressors. The saturation temperature also increases with increase in pressure. Hence during compression of vapour, a rise in temperature is inevitable and isothermal compression is not feasible. The actual compression will require more work than isentropic compression because of irreversibilities associated with friction and heat transfer through temperature difference. The entropy will not remain constant during compression. This is shown by dashed line 1–2′ in Figure 3.10. The dashed line is used to indicate that it is an irreversible process. The actual process is very difficult to trace and define; hence an isentropic efficiency is defined for a compressor. The ratio of the isentropic specific work ($h_2 - h_1$) to the actual specific work ($h_{2'} - h_1$) is called the *isentropic efficiency* of the compressor and is given by

$$\eta_{\text{isen}} = \frac{\text{isentropic work}}{\text{actual work}} = \frac{h_2 - h_1}{h_{2'} - h_1} \tag{3.64}$$

The isentropic efficiency varies with condenser and evaporator pressures. It is typically 0.5 for hermetic compressors and about 0.8 for larger compressors. At a given T_e and T_c the COP of the Reversed Carnot cycle is maximum. The concept of refrigerating efficiency is introduced to judge the relative performance of a cycle. The *refrigerating efficiency* is defined as

$$\eta_R = \frac{\text{COP}}{\text{COP}_{\text{RC}}} \tag{3.65}$$

This indicates how closely the cycle or the refrigeration system approaches the ideal reversible cycle.

3.10 REPRESENTATION OF WORK AS AREAS ON THE *T–s* DIAGRAM

The work requirement of Reversed Carnot cycle was shown to be the area of the rectangle enclosing the cycle state points on the *T–s* diagram. The work requirement of the *standard refrigeration cycle* can also be represented as an area on the *T–s* diagram by writing it as the difference between the condenser heat rejection and the evaporator refrigeration effect. Applying energy balance to Figure 3.9, we get

$$W = Q_c - Q_e$$

or

$$w = q_c - q_e \tag{3.66}$$

From Eqs. (3.56) and (3.57),

$$q_c = h_2 - h_3 \quad \text{and} \quad q_e = h_1 - h_4$$

The heat rejection 2–3 is an isobaric process. Considering the fundamental relationship of thermodynamics, $T\,ds = dh - v\,dp$ with dp equal to zero and integrating it from 3 to 2, we have

$$\int_3^2 T\,ds = \int_3^2 dh = h_2 - h_3 = q_c = \text{area } 2\text{–}a\text{–}3\text{–}b\text{–}d\text{–}1\text{–}2 \tag{3.67}$$

= area under the line 2–3 by definition of integral of $T\,ds$ in *T–s* coordinates.

Therefore, specific condenser heat rejection is equal to the area under the line 2–3. Similarly,

$$\int_4^1 T\,ds = h_1 - h_4 = q_e = \text{area } 4\text{–}c\text{–}d\text{–}1\text{–}4 \tag{3.68}$$

That is, the refrigeration effect is equal to the area under the line 1–4 on the *T*–*s* diagram. Therefore, from Eq. (3.66),

$$w = q_c - q_e = \text{area under } 2\text{–}3 - \text{area under } 1\text{–}4 = \text{area } 1\text{–}2\text{–}a\text{–}3\text{–}b\text{–}c\text{–}4\text{–}1 \tag{3.69}$$

In Figure 3.10 the characteristic areas are as follows:

Area A_1 = area 2″–2–*a*–2″ is called the area of superheat horn.

Area A_3 = area 4′–*b*–*c*–4–4′ is called the area of loss in refrigeration effect.

Area 1–2″–3–4′–1 is the work requirement of the Reversed Carnot cycle.

The work requirement of the SSS cycle by area, however, does not look very neat with superheat horn 2″–2–*a*–2″ (shown by area A_1) at the top and a leg 4′–*b*–*c*–4–4′ (shown by area A_3) at the bottom. To simplify it, a far-reaching assumption based upon refrigeration property data is made. Figure 3.10 shows on *T*–*s* diagram, the constant pressure lines for two pressures p_e and p_c. It is observed that in the subcooled region the constant pressure lines are very close to the saturated liquid line. In fact, these are so close that one may *assume that all constant pressure lines in the subcooled region are coincident with the saturated liquid line*. Having made this assumption, it is observed that the line 2–*a*–3–0 may be considered a constant pressure line, hence

$$\int_0^2 T\,ds = h_2 - h_0$$

Therefore, the specific work requirement of the compressor may be expressed as

$$w = h_2 - h_1 = (h_2 - h_0) - (h_1 - h_0)$$

or

$$w = \int_0^2 T\,ds - \int_0^1 T\,ds = \text{area under the line } 2\text{–}3\text{–}0 - \text{area under the line } 0\text{–}1$$

$$= \text{area } 2\text{–}a\text{–}3\text{–}0\text{–}e\text{–}d\text{–}1\text{–}2 - \text{area } 0\text{–}e\text{–}d\text{–}1\text{–}0$$

$$= \text{area } 1\text{–}2\text{–}a\text{–}3\text{–}0\text{–}1 \tag{3.70}$$

Hence, we have two areas representing the work requirement for SSS cycle, namely the area 1–2–*a*–3–*b*–*c*–4–1and area 1–2–*a*–3–0–1. These two areas will be equal if the areas 4′–*b*–*c*–4–4′ (area A_3) and 3–0–4′–3 are equal. Area 3–0–4′–3 is referred to as area A_2 in Figure 3.10. This is essentially due to the loss in work because of the throttling process.

3.11 COMPARISON OF STANDARD REFRIGERATION CYCLE WITH REVERSED CARNOT CYCLE

It is interesting and informative to compare the performance of these two cycles on the *T*–*s* diagram. Figure 3.10 shows the single stage saturation (SSS) cycle and the Reversed Carnot cycle together for the same condenser and evaporator temperatures. States (1) and (3) are common to both the cycles. There are basically two differences between the two cycles. The first difference is the appearance of a superheat horn 2″–2–*a*–2″ in the SSS cycle. This is due to dispensing with the

isothermal compressor during 2″–*a* in the Reversed Carnot cycle and continuing the compression up to $p_2 = p_c$, the saturation pressure at condenser temperature. The extra work required for this purpose is shown by the area A_1 called the area of the superheat horn.

Area A_1 = area under line 2–*a* – area under line 2″–*a*.

Line 2–*a* is a constant pressure process, hence $T\,ds = dh - v\,dp$ reduces to $T\,ds = dh$ and since $\int T\,ds$ on *T*–*s* diagram represents an area,

$$\int_a^2 T\,ds = h_2 - h_a = \text{area under line } 2\text{–}a$$

Similarly, line 2″–*a* is an isothermal process and for this process,

$$\int_a^{2''} T\,ds = T_c\,(s_{2''} - s_a) = T_c\,(s_1 - s_a) = \text{area under line } 2''\text{–}a \text{ since } s_{2''} = s_1$$

$$\therefore \qquad A_1 = (h_2 - h_a) - T_c(s_1 - s_a) \text{ kJ/kg} \tag{3.71}$$

The second difference is due to irreversible expansion 3–4 (throttling) replacing the reversible expansion 3–4′ (isentropic turbine or expander) of the Reversed Carnot cycle. This causes an increase in entropy from $s_{4'}$ to s_4. During reversible expansion in the turbine, work output of $h_3 - h_{4'}$ is obtained whereas in irreversible expansion, $h_4 = h_3$ (Figure 3.11) and hence no work output is obtained. It is further observed that due to this irreversible expansion, the refrigeration effect or the cooling starts from point 4 instead of point 4′, that is, the refrigeration effect is reduced by $h_4 - h_{4'}$. This is shown by area A_3 called the *Loss in Refrigeration Effect*.

$$A_3 = T_e\,(s_4 - s_{4'}) = h_4 - h_{4'} = h_3 - h_{4'} = T_e\,(s_4 - s_3) \tag{3.72}$$

The area A_2 is called the *Area of Throttling Loss*. It may be considered as the difference between the area under line 3–0 – area under line 0–4′. Considering 3–0 to be a constant pressure line (coincident with the saturated liquid line)

$$\text{Area under line } 3\text{–}0 = \int_0^3 T\,ds = h_3 - h_0$$

$$\text{Area under line } 0\text{–}4' = h_{4'} - h_0$$

$$\therefore \qquad \text{Area } A_2 = (h_3 - h_0) - (h_{4'} - h_0) = h_3 - h_{4'} = h_4 - h_{4'} = \text{Area } A_3 \tag{3.73}$$

This was observed during the comparison of the two areas, namely 1–2–*a*–3–*b*–*c*–4–1and 1–2–*a*–3–0–1 obtained for the work requirement of SSS cycle. Therefore, we get

$$W_{SSS} = W_{RC} + A_1 + A_2 \tag{3.74}$$

$$Q_{e,SSS} = Q_{e,RC} - A_2 \tag{3.75}$$

The refrigerating efficiency is defined as the ratio of the COP of SSS cycle and RC cycle, that is,

$$\eta_R = \frac{\text{COP}_{SSS}}{\text{COP}_{RC}} = \frac{1 - \dfrac{A_2}{Q_{RC}}}{1 + \dfrac{(A_1 - A_2)}{W_{RC}}} \tag{3.76}$$

The areas A_1 and A_2 account for the deviation of the SSS cycle from the RC cycle. These areas are dependent upon the shape of the saturation lines on the *T–s* diagram. The area A_2 would disappear if the saturated liquid line were vertical as shown in Figure 3.12. This, however, implies that the specific heat of the liquid is zero, which is not possible. But it does indicate that the area of throttling loss will be small if the liquid specific heat is small. Similarly, the area of superheat horn A_1 would also be zero if the saturated vapour line were vertical or if it had a positive slope as shown in Figure 3.13. The naturally occurring substances with simple molecules like H_2O, NH_3 and CO_2 have symmetrical saturated vapour and saturated liquid lines. As a result, both the areas A_1 and A_2 are large for these substances as shown in Figure 3.14 for NH_3. For the complicated molecules, the saturated liquid and saturated vapour lines are unsymmetrical. Refrigerants R12 (Dichlorodifluoromethane, CCl_2F_2) and R134a (Tetrafluoroethane, CH_2FCF_3) have very small areas of superheat horn while the area of throttling loss is quite significant as shown in Figure 3.15.

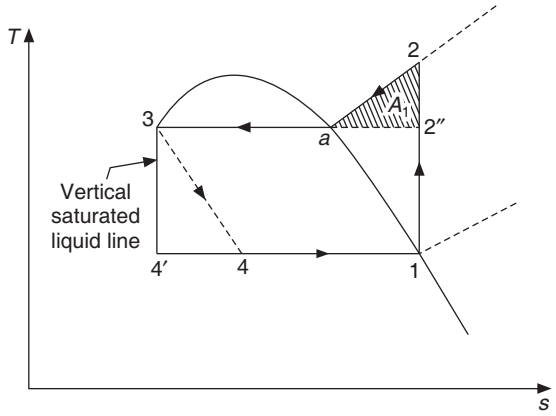

Figure 3.12 *T–s* diagram of the SSS cycle with vertical saturated liquid line, making the area A_2 disappear.

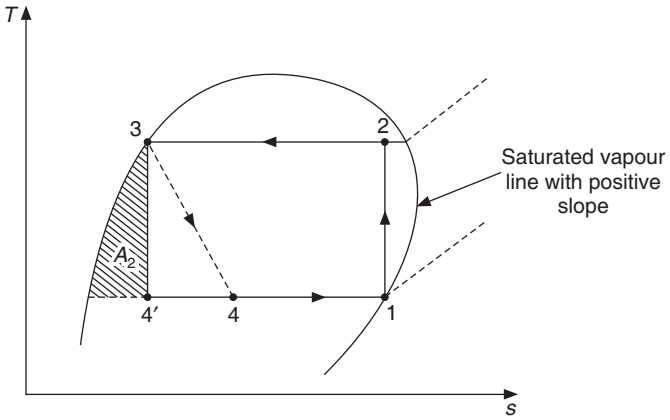

Figure 3.13 *T–s* diagram of the SSS cycle with positive slope of the saturated vapour line, making the area A_1 disappear.

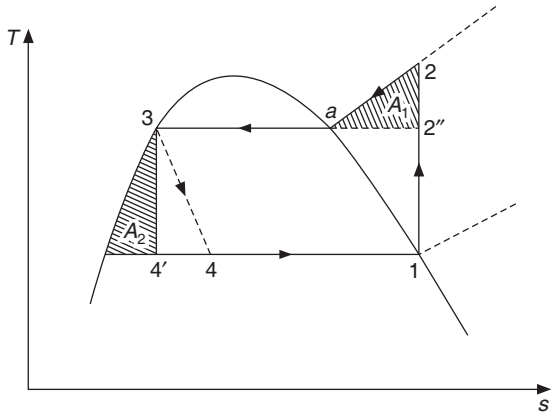

Figure 3.14 *T–s* diagram of the SSS cycle with symmetrical saturated vapour and saturated liquid lines, making both the areas A_1 and A_2 large.

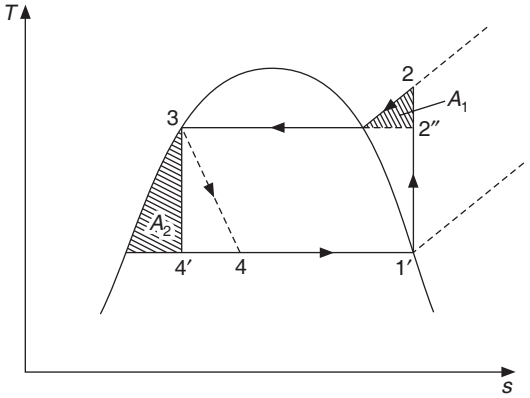

Figure 3.15 *T–s* diagram of the SSS cycle with unsymmetrical saturated vapour and saturated liquid lines, making the area A_1 small while the area A_2 remains large.

R22 (Monochlorodifluoromethane, $CHClF_2$) has a slightly larger area of superheat horn than R12. Ethane derivatives like CCl_3CF_3, CCl_2FCF_3 and $CClF_2CF_3$ and R502 have a positive slope of saturated vapour line, as a result isentropic compression starting from saturated vapour line will end up in the wet region as shown in Figure 3.13 by line 1–2. This is not desirable since it can lead to damage of the compressor. Hence the compression is usually started from a superheated state 1′ for these refrigerants as shown by line 1′–2″ in Figure 3.15.

Many of the early slow speed compressors (including NH_3 compressors) were operated in the wet region as shown in Figure 3.13. However, due to poor performance of reciprocating compressors this cycle is not used any more. The refrigeration effect in this case is $(h_1 - h_4)$ that is less than that for saturation cycle, namely $(h_{1'} - h_4)$. The COP, refrigerating efficiency and other characteristics of the saturation cycle depend upon these characteristics of the refrigerant apart from the evaporator and condenser temperatures.

In the following section the calculation procedure for the refrigeration cycles by using the properties of the refrigerants is illustrated.

3.12 REFRIGERANT TABLES—THERMODYNAMIC PROPERTIES

The cycle calculations outlined above require tables of thermodynamic properties of refrigerant at saturated and superheated states or the pressure–enthalpy chart for the refrigerant. Empirical equations have also been proposed for the calculation of properties. The tabular data is based upon temperature as an argument and is presented in a set of two tables, namely, Properties at Saturation and Properties for Superheated Vapour. The table of Properties at Saturation gives for each temperature, a list of saturation pressure, specific volumes of saturated liquid and vapour, specific enthalpy of saturated liquid and vapour, latent heat or the specific enthalpy of evaporation, and the specific entropy of saturated liquid and vapour. These are in SI units, that is, pressure p in kPa or bar, specific volume of vapour v_g in m^3/kg, specific volume of liquid v_f in litre/kg, enthalpy in kJ/kg and entropy in kJ/kg-K. The saturated liquid and vapour are indicated by subscripts f and g respectively. The enthalpy of evaporation is denoted by h_{fg}. A sample of the table for R22 is as follows:

t (°C)	p (bar)	v_f (L/kg)	v_g (m^3/kg)	h_f (kJ/kg)	h_g (kJ/kg)	h_{fg} (kJ/kg)	s_f (kJ/kg-K)	s_g (kJ/kg-K)
–10	3.550	0.758	0.0654	34.25	247.37	213.12	0.1374	0.9473
–9	3.667	0.76	0.0632	35.42	247.76	212.33	0.1418	0.9457

The datum is either ASHRAE standard or the IIR standard. In ASHRAE standard the enthalpy of saturated liquid $h_f = 0.0$ and entropy of saturated liquid is $s_f = 1.0$ at -40^oC, while in IIR standard, $h_f = 200.0$ kJ/kg and $s_f = 1.0$ kJ/kg-K at 0^oC. These tables are given in Appendix B for R12, R22, R134a and NH_3. The idea of choosing a datum at -40^oC in ASHRAE standard was to keep the value of enthalpy positive in most of the region of calculation. In IIR standard it is kept positive by choosing a datum value of 200.0 for enthalpy.

The superheat tables give specific volume, enthalpy and entropy for various degrees of superheat starting from saturated state at constant pressure. Typically, these are the properties along the constant pressure line like a–2 on T–s diagram in Figure 3.10, starting from the saturated vapour state a. There is one superheat table for each saturation pressure corresponding to saturation temperature say -40^oC, -39^oC, -38^oC, etc. The argument in these tables is the degree of superheat, which is the difference between temperature t of vapour and the saturation temperature t_s at the same pressure. A sample of the table for R22 is as follows:

t (°C) p_s (bar)	Superheat (°C)	5	10	15	20	30	40
40	v	0.0157	0.0162	0.0167	0.0172	0.0182	0.0191
15.267	h	266.09	270.69	275.19	279.61	288.31	296.84
	s	0.8917	0.9062	0.9202	0.9332	0.9592	0.9832

Superheat tables are used for finding the specific enthalpy and specific volume after isentropic compression at condenser pressure using $s_1 = s_2$. This requires interpolation in the table for the given value of s_1. As a caution, the values given in the table should not be rounded off since datum for entropy and enthalpy are arbitrary and accuracy and consistency may be lost during round-off. Linear interpolation is good enough if the values of v, h and s are given at sufficiently close intervals.

EXAMPLE 3.3 Find the end states of isentopic compression between the saturation pressure at –10°C evaporator temperature, state 1, to saturation pressure at 40°C condenser temperature, state 2 for refrigerant $CHClF_2$.

Solution:

From the saturation table given above, we find that at –10°C , $s_1 = s_g$ (–10°C) = 0.9473 kJ/kg-K. We have to find the end state 2 in the superheat table for 40°C such that $s_1 = s_2$. We observe that this state lies between 20°C and 30°C superheat. A linear interpolation gives

$$\frac{0.9473 - 0.9332}{0.9592 - 0.9332} = \frac{0.014}{0.026} = \frac{h_2 - 279.61}{288.31 - 279.61} = \frac{v_2 - 0.0172}{0.0182 - 0.0172}$$

The calculation gives $h_2 = 284.328$, $v_2 = 0.01774$ and $t_2 = 40 + 20 + 5.423 = 65.423$°C.

The variation of vapour pressure with temperature is not linear, hence a linear interpolation will yield incorrect results. This variation may be expressed as

$$\ln p = A - B/T$$

By using this equation, interpolation between (p_1, T_1) and (p_2, T_2) gives

$$\ln (p / p_1) = \frac{(1/T_1) - (1/T)}{(1/T_1) - (1/T_2)} \ln (p_2 / p_1) \tag{3.77}$$

If the enthalpy of superheated vapour after isentropic compression has to be found at a pressure not listed in the table, then the value h_i at the nearest pressure $p_i < p_2$ is found from the table. This is corrected by using $T\,ds = dh - v\,dp$ which reduces to $dh = v\,dp$ for constant entropy. Integrating it, we get

$$\int_i^2 dh = \int_i^2 v\,dp \approx v_i\,(p_2 - p_i)$$

That is, $h_2 = h_i + v_i\,(p_2 - p_i)$.

EXAMPLE 3.4 Find the end states of isentopic compression between 0°C evaporator temperature, state 1, and condenser pressure of 15.5 bar at state 2 for refrigerant $CHClF_2$.

Solution:

It is observed that the tabulated values are for pressure of 15.267 bar (40°C) and for 16.024 bar (42°C). Hence, we use the value of enthalpy found in Example 3.3 along the constant entropy line as h_i at 15.267 bar and add v_i (15.5 – 15.267) × 100 to it. Multiplication by 100 is required since bar has to be converted to kPa. We had $h_i = 284.328$ kJ/kg and $v_i = 0.01774$ m^3/kg.

$\therefore$ $h_2 = 284.328 + 0.01774(15.5 - 15.267) \times 100 = 288.461$ kJ/kg

The other method will be to prepare a superheat table at the given pressure by interpolating between two consecutive pressures and then interpolating in the prepared table for constant entropy of 0.9473 kJ/kg-K.

In some cases a two-way interpolation is required in the superheat tables. This illustrated by the following example.

EXAMPLE 3.5 Determine the enthalpy and specific volume for isentropic compression from saturation pressure corresponding to evaporator temperature of –10°C, state 1, to 40°C temperature at state 2 for refrigerant $CHClF_2$.

Solution:

This is the typical isentropic compression process 1–2 shown in Figure 3.7 for saturated RC cycle. The pressure at point 2 is not known in this case, hence interpolation in any superheat table is not possible. This requires a two-way interpolation.

The entropy at state 1 is $s_1 = 0.9473$ kJ/kg-K.

We first interpolate in the superheat tables at 9.59 bar (22°C) and 10.13 bar (24°C) and find that at 40°C the values of v, h and s are as follows:

Pressure (bar)	9.59	10.13
Specific volume	0.02722	0.02546
Enthalpy	272.79	271.0954
Entropy	0.94894	0.9399

Next we interpolate in this table for $s_1 = s_2 = 0.9473$. We get

$$p_2 = 10.032 \text{ bar}, h_2 = 272.485 \text{ kJ/kg and } v_2 = 0.0269 \text{ m}^3/\text{kg}.$$

Pressure–enthalpy chart

An accurate pressure–enthalpy chart is very convenient to use for thermodynamic cycle calculations. This is particularly useful for finding the value of specific enthalpy for isentropic compression. Richard Mollier proposed this chart. The pressure scale in this chart is lograthmic. The lograthmic scale gives better accuracy at lower pressures. Near the critical pressure the chart is very flat. Constant entropy lines concave downwards because of this choice of pressure scale. The p–h diagram of Figure 3.11 has a linear pressure scale. The isotherms in this chart are lines running downwards from the saturated vapour line. These lines become same as lines of constant enthalpy (vertical) at low pressures indicating that enthalpy does not vary significantly with pressure at low pressures. Vapour compression cycle (SSS cycle) is very conveniently shown on this chart. State 2 after isentropic compression is located at condenser pressure, along the constant entropy line starting from evaporator temperature at state 1. The throttling process 3–4 is a vertical line between the two pressures. Such a chart can be used with some loss in accuracy.

3.13 SUBCOOLING AND SUPERHEATING

3.13.1 Subcooling

Frequently the liquid refrigerant leaving the condenser may be subcooled which implies that its temperature is less than the saturation temperature at condenser pressure. The subcooling may

occur, say, within the condenser or the liquid may be subcooled after leaving the condenser. If a shell-and-tube heat exchanger with water on the tube side is used as a condenser, then subcooling can be obtained if the cold water first comes into contact with the liquid refrigerant which collects at the bottom of the shell. Subcooling is usually obtained by cold water in a separate subcooling heat exchanger (HEX). The cold water may be fed independently to the subcooling HEX and the condenser as shown in Figure 3.16, or the outlet water from subcooing HEX may be fed to the condenser as shown by the dotted rule in Figure 3.16. In air-cooled condensers too, subcooling may be obtained if the liquid comes into contact with the coldest air entering the condenser since the saturated liquid temperature is 10 to 15°C more than the air inlet temperature.

The expansion valve usually has a narrow orifice, which is calibrated for flow of liquid. If a mixture of liquid and vapour enters the orifice, mass flow rate will decrease drastically since the density of mixture of liquid and vapour is much less than that of the liquid. Hence, all attempts should be made to ensure that only the liquid or the subcooled liquid enters the expansion valve. The expansion valve is connected to the condenser by a tube in which some pressure drop will occur due to friction. Some additional pressure drop will occur due to gravity if the expansion valve is located at a higher elevation than the condenser. Hence, if the saturated liquid enters the tube, then by the time it reaches the expansion valve the pressure would have decreased from 3 to 3*a* and the liquid will flash into a mixture of liquid and vapour, thereby upsetting the flow rate through the expansion valve. For the subcooled liquid, the same pressure drop changes the state from 3′ to 3′*a* with the liquid still in subcooled state or at the most in saturated state as shown in Figure 3.17. *Therefore it is always desirable to subcool the liquid refrigerant before the expansion valve.*

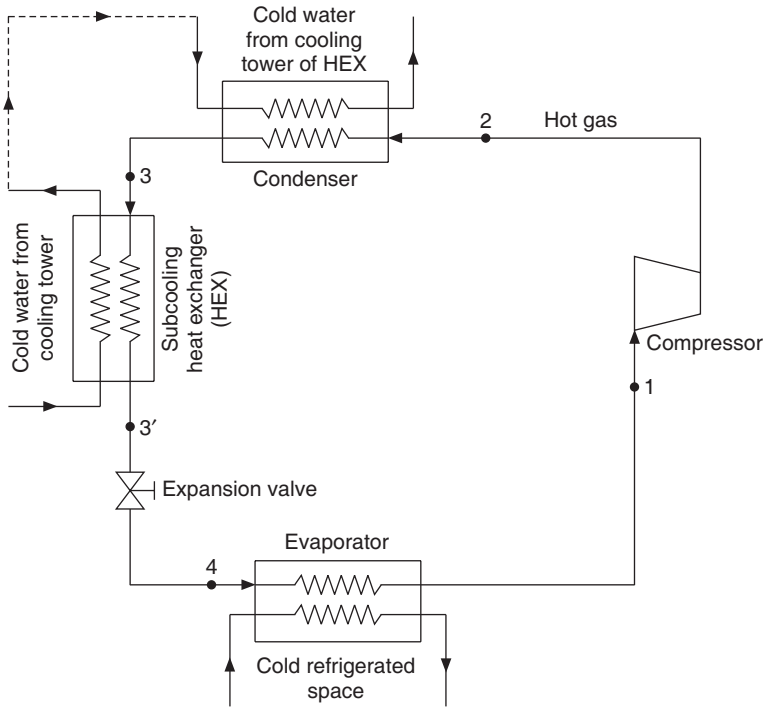

Figure 3.16 Vapour compression refrigeration cycle with subcooling.

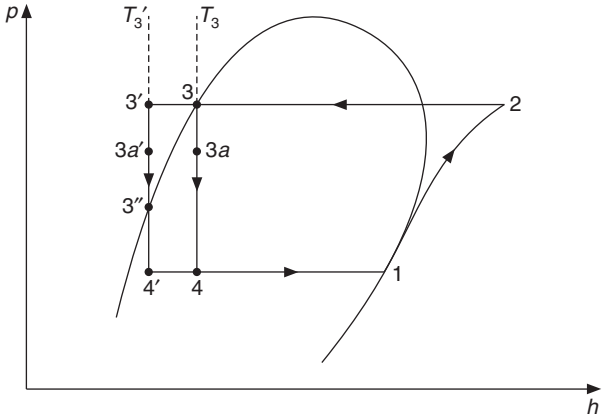

Figure 3.17 *p–h* diagram showing the subcooling effect, i.e. cooling the liquid from point 3 to point 3′.

Another advantage of subcooling is that the refrigeration effect increases. For a given subcooling in °C the increase in refrigeration effect is proportional to the specific heat of the liquid which is the largest for NH_3.

The enthalpy of the subcooled liquid is not available in the property table. It has to be calculated. Figures 3.17 and 3.18 show the subcooled state on *T–s* and *p–h* diagrams.

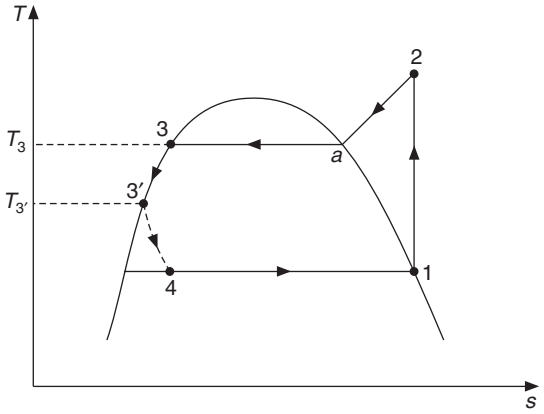

Figure 3.18 *T–s* diagram showing the subcooling effect, i.e. cooling the liquid from point 3 to point 3′.

There are two methods to find out the enthalpy of the subcooled state.

(i) If the specific heat c_{pf} of the liquid is known, then $h_{3'} = h_3 - c_{pf}(t_3 - t_{3'})$. This is not of much use since the specific heat of liquid is not given in the tables.

(ii) Consider the saturated liquid at temperature $t_{3'}$, its enthalpy $h_{3''} = h_f(t_{3'})$ is available in the table. However, the pressure at 3″, $p_{3''}$ is less than the condenser pressure p_c. Hence if the saturated liquid at state 3″ is compressed from pressure $p_{3''}$ to p_c, we will obtain state 3′. Therefore,

$$h_{3'} = h_f(t_{3'}) + v_f(p_c - p_{3''})$$

In this expression the liquid is assumed to be incompressible and its enthalpy is assumed to be a function of temperature only. The work term in this expression is usually negligible since $v_f \approx 10^{-3}$. In fact, it was stated that the constant pressure lines in the subcooled region are coincident with the saturated liquid line, hence for all practical purposes,

$$h_{3'} = h_f\,(t_{3'})$$

EXAMPLE 3.6 Show that for subcooling from condenser temperature of 40°C to 30°C the enthalpy of subcooled liquid may be approximated by the enthalpy of saturated liquid at 30°C for R22 and NH_3.

Solution:

For R22 :

At 30°C : $p_{3''} = 11.889$ bar, $v_f = 0.852 \times 10^{-3}$ m^3/kg and $h_f = 82.88$ kJ/kg

At 40°C : $p_c = 15.267$ bar, $v_f = 0.884 \times 10^{-3}$ m^3/kg and $h_f = 95.4$ kJ/kg

$$v_{f,\,\text{avg}} = \frac{1}{2}(0.852 + 0.884) \times 10^{-3} = 0.868 \times 10^{-3}\ \text{m}^3/\text{kg}$$

Therefore, $v_{f,\,\text{avg}}\,(p_c - p_{3''}) = 0.868 \times 10^{-3}(15.267 - 11.889\ ) \times 100 = 0.29$ kJ/kg

Hence this difference is negligible and enthalpy $h_{3'} = 82.88 + 0.29 = 83.17$ kJ/kg.

For NH_3 :

At 30°C : $p_{3''} = 11.67$ bar, $v_f = 1.68 \times 10^{-3}$ m^3/kg and $h_f = 322.57$ kJ/kg

At 40°C : $p_c = 15.55$ bar, $v_f = 1.726 \times 10^{-3}$ m^3/kg and $h_f = 371.47$ kJ/kg

$$v_{f,\,\text{avg}} = \frac{1}{2}(1.68 + 1.726) \times 10^{-3} = 1.703 \times 10^{-3}$$

Therefore, $v_{f,\,\text{avg}}\,(p_c - p_{3''}) = 1.703 \times 10^{-3}(15.55 - 11.67\ ) \times 100 = 0.661$ kJ/kg

Hence this difference is negligible and enthalpy $h_{3'} = 322.57 + 0.661 = 323.231$ kJ/kg

It is observed that to a good approximation the enthalpy of the subcooled liquid may be approximated by that of the saturated liquid at the given temperature.

3.13.2 Superheating

The vapour leaving the evaporator is usually at a temperature lower than the temperature of the surrounding air. The tube connecting the evaporator to the compressor is usually insulated. Even then some leakage heat transfer occurs to the refrigerant and it gets superheated by the time it leaves the tube and enters the compressor. Some pressure drop also occurs in this tube due to frictional resistance offered by the tube wall. It was pointed out that superheating is desirable as it ensures that liquid refrigerant does not enter the compressor and therefore dry compression only occurs. The disadvantages of wet compression are:

1. In wet compression some liquid refrigerant droplets may leave the compressor with very high velocity and hit the valves like bullets and damage them.
2. Further, the liquid droplets dissolve more lubricating oil than vapour refrigerant and thereby increase the wear and tear of the reciprocating compressor.

3. The formation of bubbles and bursting of bubbles during evaporation may damage the surface of the blades of centrifugal compressor and thereby increase the frictional resistance.

Hence, it is desirable to superheat the vapour before its entry into the compressor. It is sometimes done by superheating the vapour in the evaporator itself, which results in some additional refrigeration effect also being obtained. This is usually achieved by using a thermostatic expansion valve. It is unreliable to try to achieve superheating by leakage heat transfer in the tube that connects evaporator to the compressor. This is a loss of energy and it reduces the COP. Hence, it is recommended that vapour may be superheated in a regenerative process, that is, in a heat exchanger between the liquid refrigerant and the vapour refrigerant. In this heat exchanger the low temperature vapour leaving the evaporator gets superheated by heat transfer from the liquid leaving the condenser, which in turn gets subcooled. Hence, this heat exchanger serves both the purposes — subcooling the liquid and superheating the vapour. Also, the leakage heat transfer to the tube connecting the evaporator to the compressor will reduce since the vapour will enter the tube at higher temperature. The schematic diagram of such a cycle is shown in Figure 3.19(a) and its *T–s* and *p–h* cycle diagrams are shown in Figures 3.19(b) and 3.19(c), respectively. The refrigeration effect increases by $h_3 - h_{3'}$. Assuming the HEX to be perfectly insulated so that there is no leakage heat transfer to the surroundings, the energy balance for the heat exchanger yields

$$h_3 - h_{3'} = h_{1'} - h_1 \tag{3.78}$$

$$\therefore \quad q_{e'} = h_1 - h_{3'} = h_{1'} - h_3 \tag{3.79}$$

$$h_3 - h_{3'} = c_{pf}\,(t_3 - t_{3'}) = c_{pg}(t_{1'} - t_1)$$

$$(t_{1'} - t_1) > (t_3 - t_{3'}) \text{ since } c_{pf} > c_{pg}$$

The degree of superheating is always greater than the degree of subcooling, since the liquid specific heat is always greater than the vapour specific heat.

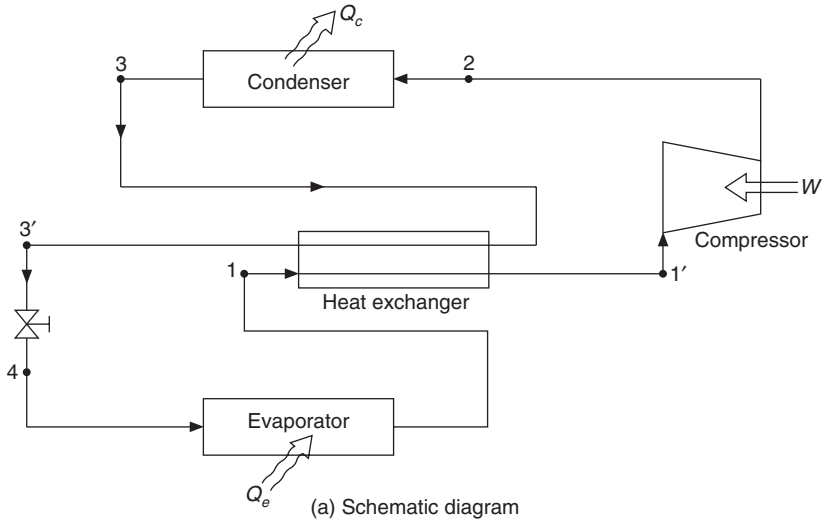

(a) Schematic diagram

Figure 3.19 Contd.

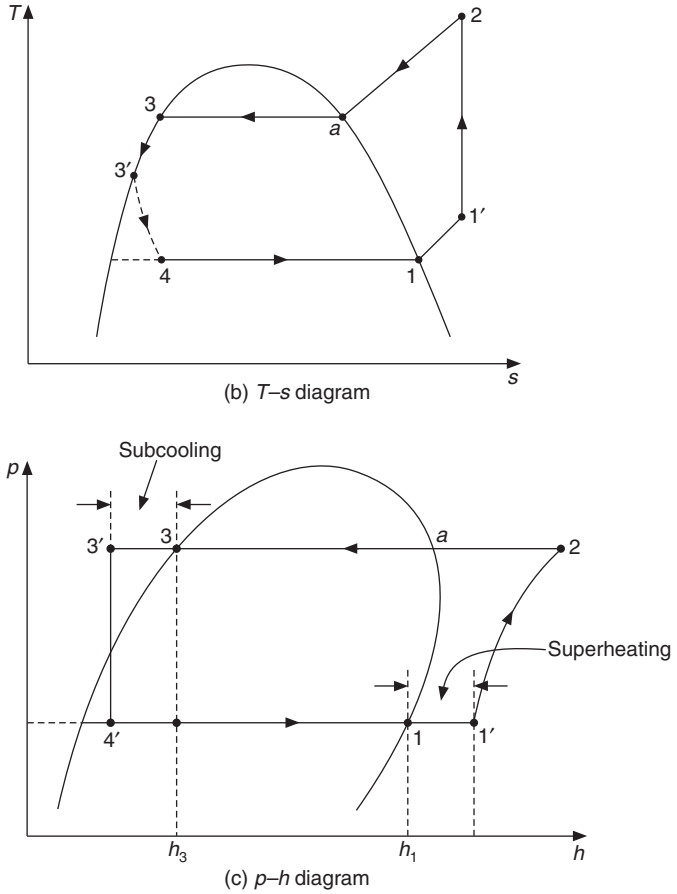

Figure 3.19 Standard vapour compression refrigeration system with a heat exchanger between the liquid refrigerant and the vapour refrigerant.

It must be observed that superheating and subcooling are done for practical reasons. This does not lead to increase in COP all the time. Although the refrigeration effect increases, the work requirement also increases because of the area of superheat horn. For refrigerants R12 and R134a and R22 (in some cases) it will lead to increase in COP as well, whereas for NH_3 it leads to decrease in COP since its area of superheat is very large. However, for NH_3 too, superheating to some extent is carried out since superheating always leads to increase in volumetric efficiency.

3.14 PERFORMANCE OF SINGLE STAGE SATURATION CYCLE

The performance of this refrigeration cycle depends upon the evaporator and condenser temperatures and the characteristics of the refrigerant.

3.14.1 Refrigeration Effect

At fixed condenser temperature, the enthalpy of saturated liquid $h_3 = h_f(t_c)$ is fixed. It is observed from the *p–h* diagram in Figure 3.20 that saturated vapour line has a positive slope. Therefore, as

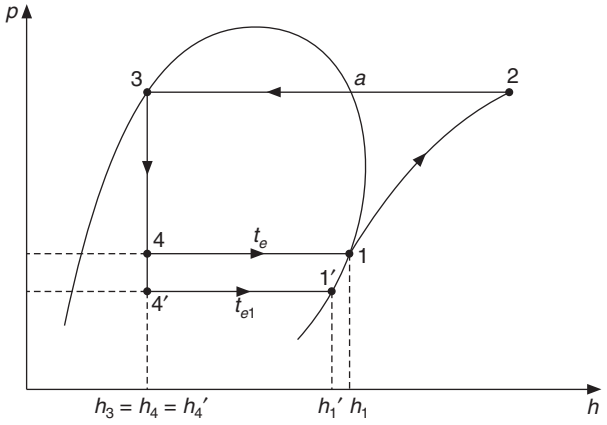

Figure 3.20 Saturation cycle with decrease in evaporator temperature.

the evaporator temperature decreases from t_e to t_{e1}, the enthalpy of saturated vapour decreases, as a result the refrigeration effect decreases from $(h_1 - h_3)$ to $(h_{1'} - h_3)$.

At fixed evaporator temperature, the enthalpy of saturated vapour $h_1 = h_g(t_e)$ is fixed. It is observed from *p–h* diagram in Figure 3.21 that as the condenser temperature increases from t_c to t_{c1}, the enthalpy of saturated liquid increases from h_3 to $h_{3'}$ as seen in Figure 3.21. The refrigeration effect $(h_1 - h_3)$ decreases to $(h_1 - h_{3'})$ with increase in condenser temperature. The difference $(h_{3'} - h_3) \approx c_{pf}\,(t_{c'} - t_c)$. Hence, the decrease in refrigeration effect with condenser temperature depends upon the specific heat of liquid refrigerant. Refrigeration effect $(h_1 - h_3)$ is proportional to enthalpy of evaporation or the latent heat. For NH_3, this is very large and hence the effect of condenser temperature on the decrease in refrigeration effect is relatively small compared to other refrigerants like R12 and R22, etc.

The variation of refrigeration effect (also called specific refrigeration effect) with evaporator temperature for fixed condenser temperatures, is not very significant.

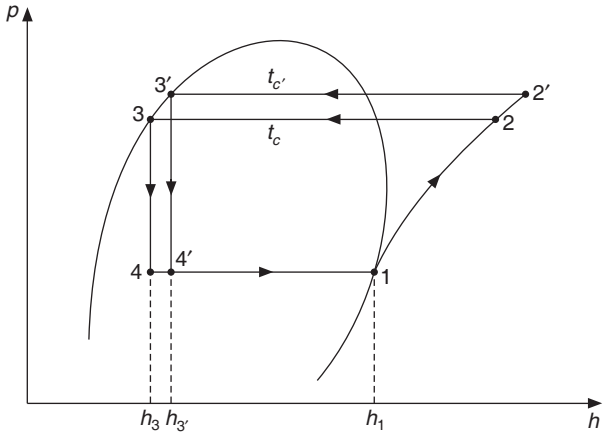

Figure 3.21 Saturation cycle with increase in condenser temperature.

The specific volume of the saturated vapour at evaporator exit increases as the evaporator temperature decreases (since the corresponding evaporator pressure decreases at a fast rate). The vapour density drastically decreases with decrease in pressure. For a given compressor of fixed dimensions and running at constant rpm, the swept volume flow rate (swept volume rate) at its inlet, V_s m^3/s is fixed, hence the mass flow rate V_s/v_1 decreases as the evaporator temperature decreases. This decrease is rather drastic. The refrigeration capacity corresponding to this, $V_s(h_1 - h_3)/3.5167v_1$ TR, decreases drastically as the evaporator temperature decreases, where $(h_1 - h_3)/v_1$ is called *volumic refrigeration effect*. This is a direct measure of the refrigeration capacity. The volumic refrigeration effect decreases very drastically with decrease in evaporator temperature although its decrease with increase in condenser temperature is not very drastic.

For reciprocating compressors, the volumetric efficiency decreases with increase in condenser temperature and decrease in evaporator temperature. The mass flow rate for a fixed compressor swept volume flow rate V_s m^3/s is $V_s\eta_{vol}/v_1$ kg/s, where

$$V_s = \frac{\pi d^2}{4} L \frac{N}{60} no \ \text{m}^3/\text{s} \tag{3.79}$$

where, d and L are cylinder bore and stroke respectively, N is rpm and no is number of cylinders

$$\dot{m} = \frac{V_s \eta_{vol}}{v_1} \ \text{kg/s} \tag{3.80}$$

and

$$q_e = \frac{V_s (h_1 - h_3) \eta_{vol}}{3.5167 v_1} \ \text{TR} \tag{3.81}$$

The refrigeration capacity decreases drastically with decrease in evaporator temperature and increase in condenser temperature.

3.14.2 Isentropic Compression Work

It is observed that the constant entropy lines are divergent on the p–h diagram. This divergence is more for NH_3 than that for CFCs.The specific isentropic compression work, w_c, increases as the evaporator temperature decreases on two counts—firstly because the pressure ratio increases and secondly because the divergence between the constant entropy lines increases. Similarly, as the condenser temperature increases, the specific isentropic work increases. The divergence of constant entropy lines is large if the vapour specific is large. Hence the divergence of constant entropy lines is more for NH_3 than that for CFCs. The variation of specific isentropic compression work with evaporator temperature is shown in Figure 3.22 for condenser temperatures of 30°C, 40°C and 50°C. For a fixed swept volume flow rate of V_s m^3/s and specific volume v_1 at inlet, the isentropic work requirement is $\dot{m}(h_2 - h_1) = V_s(h_2 - h_1)/v_1$.

$$\therefore \quad W = \dot{m}(h_2 - h_1) = V_s(h_2 - h_1)/v_1 \tag{3.82}$$

The swept volume rate being fixed, $(h_2 - h_1)/v_1$ becomes a significant parameter. It is also called volumic work of isentropic compression, w_u.

It was observed that the specific volume v_1 increases significantly as the evaporator temperature decreases. The variation of $(h_2 - h_1)/v_1$ with evaporator temperature is shown in Figure 3.22. It is observed that to start with, it increases as the evaporator temperature decreases, passes through a

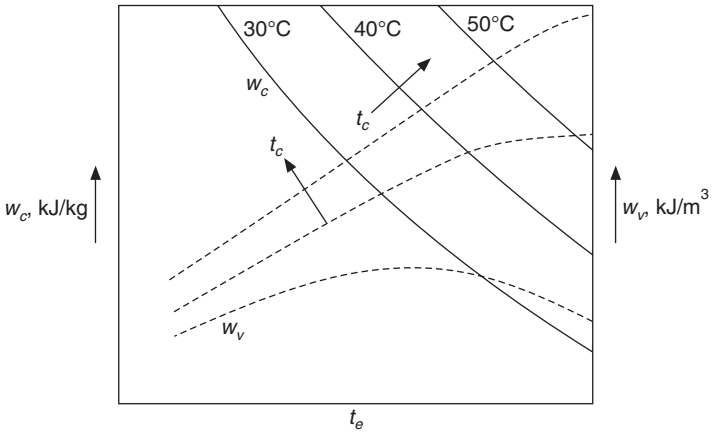

Figure 3.22 Effect of evaporator and condenser temperatures on specific and volumic works of compression of a standard vapour compression refrigeration cycle.

maximum and then decreases. Initially the increase in numerator, i.e. the specific isentropic compression work $(h_2 - h_1)$ dominates as t_e decreases and later on the increase in denominator, i.e. the specific volume v_1 dominates which makes w_v pass through a maximum and then decreases its value. The compressor power input divided by the swept volume flow rate is called the *mean effective pressure,* p_{em}, for a reciprocating compressor. That is, $\dot{m}(h_2 - h_1) / \mathbb{V}_s = (h_2 - h_1)/v_1$, the volumic isentropic work requirement, is the mean effective pressure.

$$\therefore \qquad p_{\text{em}} = \dot{m}(h_2 - h_1) / \mathbb{V}_s = (h_2 - h_1)/v_1 \tag{3.83}$$

The fact that the volumic isentropic work goes through a maximum as the evaporator temperature decreases, is very important during *pull-down* of a refrigeration system. Under idle conditions or during off-cycle, the evaporator is at room temperature. When the refrigeration plant is started, the evaporator temperature decreases from room temperature to the design temperature. The period during which this occurs is called *pull-down period* indicating the period when t_e is pulled down. During this period, the power requirement passes through a peak before settling to its design value. This phenomenon is very important from the point of view of selection of the motor capacity. If a motor is selected according to the power requirement at design value, this value being lower than the power peak, the motor may burn down during *pull-down* when the power requirement passes through a peak. Hence, the motor should be rated for the power peak. This, however, makes the system more expensive. Hence to keep the motor size small, a motor corresponding to design value is chosen and the mass flow rate through the compressor is reduced by a hand valve which simultaneously throttles the gas and reduces the suction pressure for a rapid pull-down. As the desired temperature is reached, the operator opens the valve to full its opening position. A thermostatic expansion valve with fade-out point set near the design point temperature will limit the pressure, and help in reducing the mass flow rate through compressor and cause a rapid pull-down. In both these methods, the evaporator is starved of refrigerant during pull-down, hence if rapid cooling is desired these methods are not recommended. This has been described in detail in the section on power requirement of compressors.

3.14.3 Coefficient of Performance (COP)

The COP is the ratio of refrigeration effect to the isentropic work. The refrigeration effect as was seen from the *p–h* diagram (Figure 3.20), decreases very slowly while the isentropic work increases significantly with decrease in evaporator temperature. Hence, the COP as shown in Figure 3.23 decreases with decrease in evaporator temperature. It decreases with increase in condenser temperature as well, since the refrigeration effect decreases and simultaneously the work requirement increases. This is the COP of the SSS cycle. The COP of the actual cycle will be less than that of the SSS cycle. The trend, however, remains the same, that is, more power is required at lower evaporator temperatures and high condenser temperatures.

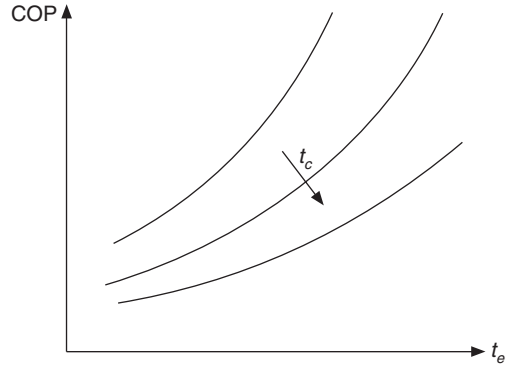

Figure 3.23 Effect of evaporator and condenser temperatures on COP of a standard vapour compression refrigeration cycle.

3.15 EFFECT OF REFRIGERANT PROPERTIES

The values of parameters discussed above for condenser and evaporator temperatures of 30°C and –15°C, respectively, are listed in Table 3.1 for refrigerants commonly used. These results are discussed here.

Table 3.1 Performance of various refrigerants at evaporator temperature of –15°C and condenser temperature of 30°C.

Parameter	NH_3	CO_2	CCl_3F R11	CCl_2F R12	$CHClF_2$ R22	R502	*Propane*
M	17	4	137.4	120.9	86.5	111.6	44.1
p_c	11.66	72.1	1.25	7.45	11.92	13.19	10.85
p_e	2.36	22.9	0.202	1.83	2.96	3.48	2.92
p_c/p_e	4.94	3.15	6.19	4.08	4.03	3.78	3.72
$h_1 - h_4$	1102	132	155.4	116.4	162.9	104.4	285
v_1	0.509	0.0166	0.762	0.091	0.0776	0.05	0.153
$(h_1 - h_3)/v_1$	2170	7940	204	1280	2100	2090	1860
$h_2 - h_1$	231.0	48.6	30.9	24.7	34.9	24.0	60.5
COP	4.77	2.72	5.03	4.7	4.66	4.35	4.71

3.15.1 Specific Refrigeration Effect ($h_1 - h_3$)

Latent heat and vapour density of refrigerant are the two most important properties apart from pressure ratio, which affect the performance of the SSS cycle. The specific refrigeration effect is related to latent heat. For a given cooling capacity, the specific refrigeration effect fixes the mass flow rate and when the vapour specific volume multiplies it, it determines the swept volume flow rate and the physical size of the compressor. The latent heat is the largest for the lighter molecules like water and ammonia while it has a low value for large CFC molecules. This correlation of latent heat with molecular weight for similar substances is known as *Trouton's rule* and is stated as follows.

Trouton's rule

$$\frac{Mh_{fg}}{T_{\text{nb}}} = 85 \text{ kJ/kmol-K} \tag{3.84}$$

where M is the molecular weight in kg/ kmol and T_{nb} is the normal boiling point, that is, the boiling point at atmospheric pressure. There are two ways of stating this rule:

1. The molal entropy of evaporation at normal atmospheric pressure is same for all similar substances.
2. The molal specific latent heat of similar substances is same, where substances which have similar normal boiling points are called similar.

The refrigeration effect is intimately related to the latent heat. The specific refrigeration effect is given by

$$q_e = h_1 - h_4 = h_g(t_e) - h_f(t_c) = h_{fg}(t_e) - [h_f(t_c) - h_f(t_e)]$$

or

$$q_e = h_{fg}(t_e) - c_{pf}(t_c - t_e) \tag{3.85}$$

The liquid specific heat is larger for lighter molecules like NH_3. The refrigeration effect, work requirement, COP, and some other information about a few commonly used refrigerants are given in Table 3.1

3.15.2 Volumic Refrigeration Effect ($h_1 - h_3$)/v_1

It was shown that the volumic refrigeration effect determines the swept volume flow rate of a reciprocating compressor and hence the physical size of the compressor. R11 has a value of 204 kJ/m^3, which is the lowest value in Table 3.1. All other refrigerants have large values. R11 requires a very large swept volume flow rate, hence the centrifugal compressor is used for it. R22 has a higher value than R12. This gives another flexibility to the manufacturer that a given compressor running at same rpm will give a higher cooling capacity if R22 is used in place of R12. If perfect gas relation is used and T_{nb} is replaced by $p_{\text{atm}}v_g/R$ in Eq. (3.84), we get

$$h_{fg} / v_g = 85\, p_{\text{atm}} / \bar{R} = 1022 \text{ kJ/m}^3 \tag{3.86}$$

This is true for all similar refrigerants compared at one atmospheric pressure. It is observed that NH_3, R12, R22 and propane have similar values of volumic refrigeration effect, values being higher for refrigerants with higher evaporator pressures.

3.15.3 Specific Work ($h_2 - h_1$)

The specific work determines the horsepower requirement of the compressor motor for SSS cycle. However, it has a special significance for centrifugal compressors whose square of tip speed is proportional to specific work. Smaller specific work will require lower tip speed or low impeller diameter for a fixed rpm. Ammonia is rather unusual from this point of view; it requires a very high tip speed.

3.15.4 COP

It is observed from Table 3.1 that COP of all the refrigerants considered, is almost the same except CO_2 which has a low COP since its critical temperature, 31°C, is very near the condenser temperature.

3.15.5 Adiabatic Discharge Temperature

Ammonia has the largest value of specific heat ratio, therefore it leads to the highest adiabatic discharge temperature. Ammonia has a large area of superheat horn for this reason. The ammonia compressors have to be cooled by water since at temperatures above 150°C carbonization and fuming of lubricating oil take place. This is not desirable because it makes the valves sticky. The viscosity of lubricating oil decreases with increase in temperature, hence wear and tear may increase.

R12 and R502 have a small area of superheat horn, therefore the adiabatic discharge temperature is very small and air-cooling of the compressor is sufficient. This is very important for semi-hermetic and hermetic compressors. The windings and the compressor in this case are cooled by the refrigerant itself. If the adiabatic discharge temperature is high, more refrigerant will be used up in cooling the winding rather than producing refrigeration. R12 is used in hermetic compressors since its c_p/c_v ratio is small. Ammonia has c_p/c_v ratio of 1.3, hence it cannot be used in hermetic compressors. Many of the refrigerants, which are ethane derivatives, have a negative slope of the saturated vapour line, hence isentropic compression ends up in wet region. These refrigerants also have low value of adiabatic discharge temperature.

3.15.6 Pressure Ratio and Pressures

Carbon dioxide has the highest condenser pressure as seen in Table 3.1. This demands a very heavy construction. At the same time, it has a very high volumic refrigeration effect which requires a smaller bore and stroke compared to other compressors. Ammonia and R11 have larger pressure ratios compared to R12, R22 and R502. The pressure ratio of ammonia actually becomes greater than that of R22 at higher condenser temperatures ($t_c > 36$°C).

3.16 SUCTION STATE FOR OPTIMUM COP, EWING'S CONSTRUCTION

Although it has been stated that it is not practical to have suction state in the wet region, in slow speed NH_3 compressors, it was a usual practice to have wet suction state since it gave better COP. In case of NH_3, COP of the refrigeration cycle actually increases as the suction state approaches the saturated state. It starts to decrease during approach to saturated state when the superheat horn is encountered. For refrigerants that have small area of superheat horn the COP may continue to increase with suction state even in the superheated state.

Figure 3.24 shows the refrigeration cycles at fixed evaporator and condenser temperatures for various suction states. The state 3 at the exit of condenser is saturated liquid state and state 4 is the state after throttling. These two states are the same for all cycles considered.

In cycle 3–4–2′–3 there is no refrigeration effect since the refrigerant is immediately compressed after expansion. Hence the COP is zero.

In cycle 3–4–1*a*–2*a*–3, there is some refrigeration effect of $(h_1 - h_3)$ and the COP increases from 0 to some finite value.

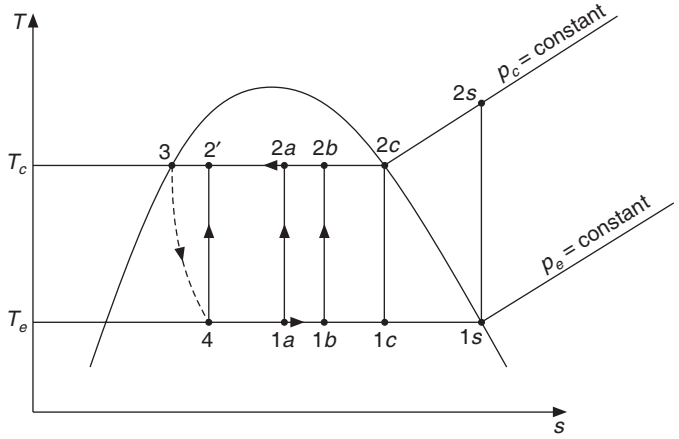

Figure 3.24 Effect of variable suction state.

In cycle 3–4–1*b*–2*b*–3, the refrigeration effect increases further while the isentropic compression work does not increase significantly, hence the COP increases.

This trend of increase in COP continues till about 3–4–1*c*–2*c*–3. After this, as the suction state moves towards 1*s*, area of superheat horn is encountered, as a result the isentropic work may suddenly increase and COP may decrease.

This aspect is more lucidly seen on the *h*–*s* diagram as proposed by Ewing. Figure 3.25 shows one such diagram. The constant temperature lines in the mixture region in this diagram are inclined lines with constant slope. Starting from $Tds = dh - vdp$, for condensation process at constant temperature and pressure, we get $T_c\, ds = dh$

$$\left(\frac{dh}{ds}\right)_p = T_c \text{ is the slope of line 3–2}c \tag{3.87}$$

and

$$\left(\frac{dh}{ds}\right)_p = T_e \text{ is the slope of line 4–1}s \tag{3.88}$$

Also

$$T_e(s_1 - s_4) = (h_1 - h_4) \quad \therefore \quad T_e = \frac{h_1 - h_4}{s_1 - s_4} \tag{3.89}$$

$$\text{COP} = \xi = \frac{h_1 - h_4}{h_2 - h_1} = \frac{h_1 - h_4}{h_2 - h_4 - h_1 + h_4} = \frac{\dfrac{h_1 - h_4}{s_1 - s_4}}{\dfrac{h_2 - h_4}{s_1 - s_4} - \dfrac{h_1 - h_4}{s_1 - s_4}} \tag{3.90}$$

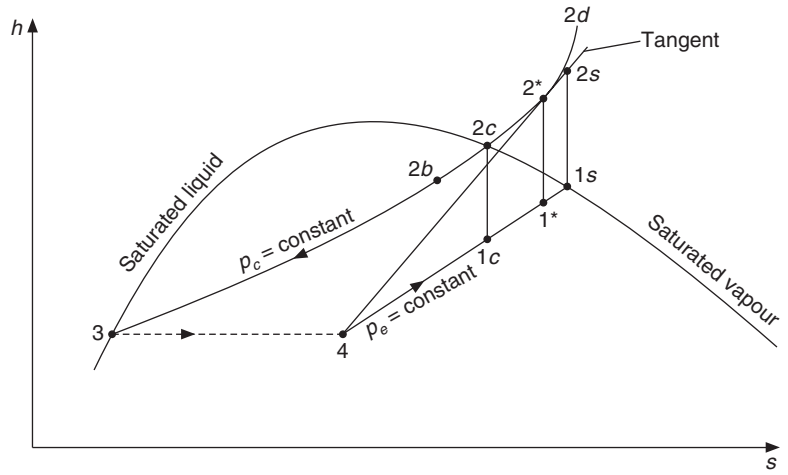

Figure 3.25 Ewing's construction.

$$\therefore \qquad \xi = \frac{T_e}{\dfrac{h_2 - h_4}{s_2 - s_4} - T_e}$$

Equation (3.90) is valid as long as the suction state is in the wet region since the relation (3.89) used in this equation is valid only in the wet region. For constant T_e the COP will be maximum if the first term in the denominator is minimum, that is,

$$\text{For COP to be maximum, } \frac{h_2 - h_4}{s_2 - s_4} \text{ should be minimum.}$$

This is seen to be the slope of the line joining point 4 to point 2. It is seen that as point 1 moves up along the straight line 4–1s (constant evaporator temperature), the corresponding point 2 for isentropic compression moves along the line 3–2s (constant condenser temperature). As point 2 moves along 3–2s, the slope of line 4–2 continues to decrease, that is,

$$\text{slope of line } 4\text{–}2' > \text{slope of line } 4\text{–}2a > \text{slope of line } 4\text{–}2b > \text{slope of line } 4\text{–}2c$$

Since the slope of this line continues to decrease as state 1 moves towards the saturation state 1s, the COP given by Eq. (3.90) continues to increase. This trend of increasing COP continues until state 2 becomes saturated at 2c. Beyond 2c, the temperature is not constant hence the constant pressure line 2c–2s–2d is not a straight line. In fact, at any point along the constant pressure line $(dh/ds)_p = T$, that is, the slope of the tangent to line 2c–2d at any point is equal to the temperature at that point. Beyond 2c, the area of superheat horn occurs. The trend of increasing COP continues for a short distance beyond 2c. Eventually, the slope of constant pressure line increases and the specific work increases faster than the specific refrigeration effect and COP reaches a maximum and then decreases. In terms of slope of line 4–2 the following picture emerges.

The slope of the line 4–2 continues to decrease as point 2 moves along 2′ to 2c. Eventually, at some point 2* it may so happen that the line 4–2* becomes tangent to constant pressure line. At this point the slope of the line 4–2* is minimum since it is a fundamental theorem in geometry that

a line drawn from a point and touching a curve, has minimum slope when it is tangent to a curve. At this point, the first term in the denominator of Eq. (3.90) will be minimum and the COP will be maximum. In addition, since the line 4–2* is tangent to constant pressure line the slope at this point is equal to the temperature at 2*, that is

$$\left[\frac{h_{2^*} - h_4}{s_{2^*} - s_4}\right]_{\min} = T_{2^*} \tag{3.91}$$

Substituting this in the last part of Eq. (3.90), we get

$$(\text{COP})_{\max} = \frac{T_e}{T_{2^*} - T_e} \tag{3.92}$$

The temperature T_{2^*} is a function refrigerant, T_e and T_c. It is not possible to determine it in a straightforward manner; it has to be found by iteration. An expression for it can be obtained by assuming the vapour to be perfect gas and specific heat to be constant along the line $2c$–$2s$.

$$h_2 = h_{2c} + c_p\,(T_2 - T_c) \qquad \text{and} \qquad s_2 = s_{2c} + c_p \ln (T_2/T_c) \tag{3.93}$$

or

$$\frac{h_{2c} - h_4}{s_{2c} - s_4} = \frac{h_{2c} - h_4 + c_p(T_2 / T_4)}{s_{2c} - s_4 + c_p \ln (T_2 / T_4)} \tag{3.94}$$

The COP is maximum when the denominator term in Eq. (3.94) is minimum. In Eq. (3.94), states 4 and $2c$ are fixed. The only variable is T_2 corresponding to the suction state 1. Hence, it can be differentiated w.r.t. T_2 and the derivative equated to zero to obtain the condition for minimum slope. This process yields the following equation, where we have replaced T_2 by T_{2^*}, which is the temperature at optimum condition.

$$T_{2^*} = \frac{h_{2c} - h_4 + c_p(T_{2^*} / T_4)}{s_{2c} - s_4 + c_p \ln (T_{2^*} / T_4)} = \frac{h_{2^*} - h_4}{s_{2^*} - s_4} \tag{3.95}$$

This when substituted in last part of Eq. (3.90) yields

$$(\text{COP})_{\max} = \frac{T_e}{T_{2^*} - T_e}$$

This expression is similar to Reversed Carnot COP, that is, $T_e/(T_c - T_e)$, but is less than it since temperature T_{2^*} is greater than T_c, the condenser temperature. The above analysis is valid as long as state 1 is in the wet region since Eq. (3.90) is valid only for this condition.

Refrigerants such as R12 and R134*a* have a very small area of superheat horn. As a result, the trend of increasing COP continues even beyond $2s$, that is, with suction state in the superheated region. If the maximum COP occurs at 2* with suction state 1* in the wet region, it is observed from Figure 3.25 that

$$\text{Slope of tangent at } 2s > \text{Slope of line } 4\text{–}2s > \text{Slope of line } 4\text{–}2^* \tag{3.96}$$

The slope of tangent at $2s = T_{2s}$ since it is tangent to the constant pressure line. Similarly, slope of 4–2* = slope of tangent at 2* = T_{2^*}. Hence, Eq. (3.96) may be written as follows:

$$T_{2s} > \frac{h_{2s} - h_4}{s_{2s} - s_4} > T_{2^*} \tag{3.97}$$

The slopes of tangent and lines are the first term in the denominator of Eq. (3.90). Substituting these for the first term in the denominator, we get

$$\frac{T_e}{\dfrac{h_{2*} - h_4}{s_{2*} - s_4} - T_e} = \frac{T_e}{T_{2s} - T_e}$$

and

$$\frac{T_e}{\dfrac{h_{2s} - h_4}{s_{2s} - s_4} - T_e} = \frac{T_e}{T_{2s} - T_e}$$

$\therefore$

$$\xi = (\text{COP})_s = \frac{T_e}{\dfrac{h_{2s} - h_4}{s_{2s} - s_4} - T_e}$$

The inequality in Eq. (3.97) in combination with these terms gives:

$$\frac{T_e}{T_{2*} - T_e} > \xi_s > \frac{T_e}{T_{2s} - T_e} \tag{3.98}$$

Since this derivation is valid for suction state in the wet region, hence the last part of this expression is used as the condition for optimum COP to occur with the suction state in the wet region. The opposite of will be true for optimum COP to occur with suction state in the superheated region.

For optimum COP to occur with suction state in wet region

$$\xi_s > \frac{T_e}{T_{2s} - T_e} \tag{3.99}$$

For optimum COP to occur with suction state in superheated region

$$\xi_s < \frac{T_e}{T_{2s} - T_e} \tag{3.100}$$

It may be noted that one can find out the region in which the optimum occurs without finding out the temperature for optimum COP. The procedure is to carry out the calculations for SSS cycle, that is, saturated cycle and find out the temperature at the end of isentropic compression, T_{2s} and the COP for the cycle, that is, ξ_s, and then check the inequalities (3.99) and (3.100). Table 3.2 gives the results for some refrigerants at $T_e = -15^oC$ and $T_c = 30^oC$.

Table 3.2 Conditions for suction state for the optimum COP to occur

Refrigerant	ξ_s	t_{2s} (°C)	$T_e/(T_{2s} - T_e)$	*Wet region*	*Superheated*
NH_3	4.77	99	2.26	Yes	
CO_2	2.72	68	3.11		Yes
C_3H_8	4.71	37	4.96		Yes
R11	5.03	44	4.38	Yes	
R12	4.7	38	4.87		Yes
R22	4.66	53	3.8	Yes	
R502	4.35	37	4.96		Yes

It is observed that ammonia, R11 and R22 have optimum COP with suction state in the wet region for the evaporator and condenser temperatures considered. The other refrigerants actually show no maximum. For these refrigerants the COP continues to increase as the suction state moves in superheated region. The heat transfer coefficient in the vapour region is very small compared to the boiling heat transfer coefficient. Hence, in practical cycles it is not possible to obtain large superheat in the evaporator since this requires a very large evaporator area with accompanying large pressure drop requiring more compressor work. Hence, the degree of superheat for these refrigerants gives higher COP but it is limited for practical reasons.

3.16 ACTUAL CYCLE DIAGRAM

The actual cycle deviates in many aspects from the ideal cycles considered so far. In the following discussion we consider these deviations and suggest methods to account for them.

3.16.1 Isentropic Efficiency

The compression has been assumed to be isentropic, that is, reversible and adiabatic. Reversible process is possible if it is carried out in a very slow manner so that the system passes through a set of infinitesimal equilibrium states. The presence of friction between piston and cylinder and the heat transfer through temperature difference make this process irreversible. On the *T*–*s* diagram in Figure 3.10 and *p*–*h* diagram in Figure 3.11, the entropy remains unchanged for isentropic compression 1–2, that is, $s_1 = s_2$, while entropy increases for the actual compression 1–2′, that is, $s_{2'} > s_1$. The deviation from isentropic compression is conveniently specified in terms of isentropic compressor efficiency, which is the ratio of specific isentropic work to the specific actual work, that is

$$\eta_{c,\,\text{isen}} = \frac{\text{specific isentropic work}}{\text{specific actual work}} = \frac{(h_2 - h_1)_s}{h_{2'} - h_1}$$

This is not "something out" divided by "something in", which is the usual meaning of efficiency. This just indicates the deviation from ideal behaviour. Isentropic efficiency varies from 0.5 for small compressors to around 0.8 for large compressors and screw compressors. Actual work is more than isentropic work since work has to be done to overcome friction and to make up for the heat loss to the surroundings. This is determined from experimental results.

In a similar manner, isentropic efficiency is defined for a turbine too. In Figure 3.10 the process 3–4′ represents isentropic expansion with $s_3 = s_{4'}$, while 3–4 represents the actual expansion with $s_4 > s_3$. The expression for isentropic efficiency of turbine, $h_{t,\,\text{isen}}$ is defined as follows:

$$\eta_{t,\,\text{isen}} = \frac{\text{actual specific work}}{\text{isentropic specific work}} = \frac{h_3 - h_4}{(h_3 - h_{4'})_s}$$

In this case the actual work output is less than the isentropic work since some output is lost in overcoming friction and some is lost as heat transfer to the surroundings.

3.16.2 Heat Transfer and Pressure Drops

It was assumed in thermodynamics analysis that the heat transfer and the pressure drops in the tubes connecting various components are negligible. In the following discussion, the change in thermodynamic state of refrigerant in the tubes connecting various components is presented.

Tube connecting evaporator and compressor

This tube is called the suction line. This tube is usually insulated since vapour leaving the evaporator is at low temperature. The temperature of the vapour will rise due to heat transfer, the density will decrease, and as a result the mass flow rate of refrigerant will decrease. This will decrease the cooling capacity. However, in most of the compressors, the volumetric efficiency increases to some extent with increase in the degree of superheat. This may compensate for decrease in density.

Another advantage of superheating is that it prevents the liquid refrigerant from entering the compressor, thus avoiding the classical problem of slugging of compressor, which causes valve damage.

A subcooling heat exchanger as shown in Figure 3.19(a) will subcool the liquid refrigerant and heat the vapour to a temperature around 15°C to 25°C, which is very close to the temperature of the surroundings. Therefore, the leakage heat transfer from the surroundings to the tube will be small, and tube insulation will further reduce it. The superheating in the subcooling heat exchanger shifts the state 1 at evaporator exit to state 1′ as shown in Figures 3.26(a) and 3.26(b). Further superheat in the suction line due to heat absorbed from the surroundings is represented by 1′–1a′.

There will always be some drop in pressure to overcome the frictional resistance offered by tube wall. The bends in the tube and valves will also lead to pressure drop (1a′–1″). The vapour density decreases as the pressure decreases, which in turn may decrease the mass flow rate and the cooling capacity. The compressor pressure ratio will increase, requiring more power for compression and thus giving less cooling capacity. The state at inlet to compressor accounting for this pressure drop is shown by 1″ in Figures 3.26(a) and 3.26(b) where the inlet pressure is p_1. Some drop in pressure will occur due to frictional resistance offered by the suction valve of the compressor. The pressure in the cylinder due to this will reduce to p_s as shown by state 1‴ in Figure 3.26(a) and 3.26(b).

The effect of pressure drop is equivalent to a drop in evaporator temperature. A pressure drop of 0.1 bar for R22 is equivalent to 1.1 K drop in evaporator temperature. That is, if the evaporator temperature is –10°C, then due to pressure drop of 0.1 bar, the compressor performance is as if the evaporator temperature was –11.1°C.

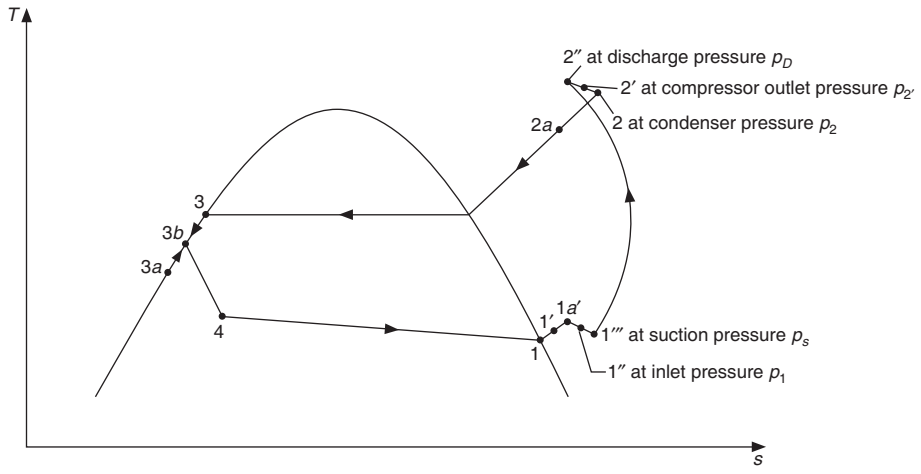

Figure 3.26(a) Actual vapour compression refrigeration cycle on *T–s* diagram.

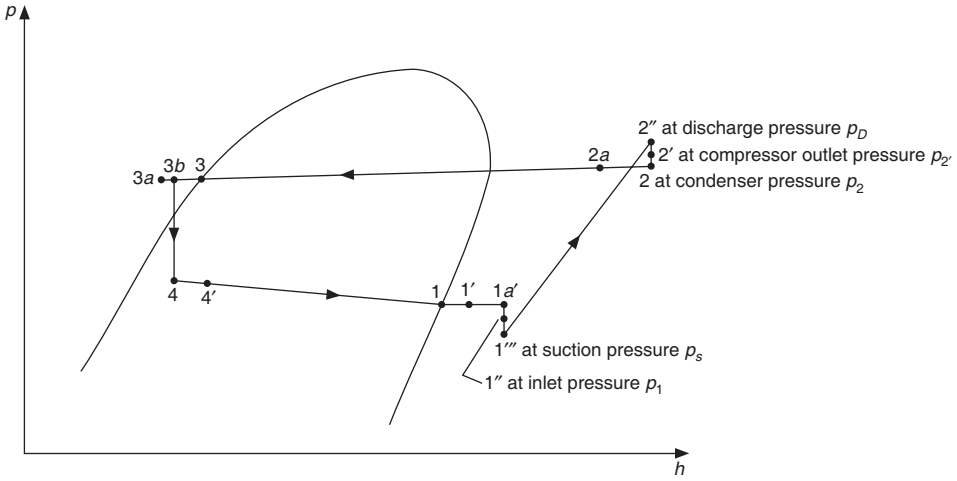

Figure 3.26(b) Actual vapour compression refrigeration cycle an *p–h* diagram.

Process	*State* Figures 3.26(a) and 3.26(b)
Pressure drop in evaporator	4–1
Superheat of vapour in evaporator	1–1′
Useless superheat in suction line	1′–1*a*′
Suction line pressure drop	1*a*′–1″
Pressure drop across suction valve	1″–1‴
Non-isentropic compression	1‴–2″
Pressure drop across discharge valve	2″–2′
Pressure drop in the delivery line	2′–2
Desuperheating of vapour in delivery pipe	2–2*a*
Pressure drop in the condenser	2–3
Subcooling of liquid refrigerant	3–3*a*
Heat gain in liquid line	3*a*–3*b*

Sometimes, pressure is intentionally decreased by throttle valve at compressor inlet to reduce the cooling capacity. At lower pressure, the mass flow rate through compressor will decrease, evaporator pressure and temperature remaining the same.

Choosing a larger diameter tube, which will give a lower vapour velocity, can reduce the pressure drop. R12, R22, R134a and R502 refrigeration systems require sufficiently large vapour velocity, so that the lubricating oil picked up by the vapour travels throughout the system without accumulating anywhere, and returns to the compressor. The velocity may be of the order of 6 m/s in vertical tubes. *ASHRAE Handbook* has given recommendations for diameter selection in suction as well liquid lines depending upon the cooling capacity and refrigerant used so that accumulation of lubricant does not occur in the system.

Tube connecting compressor to condenser

This tube is called the discharge line. The vapour temperature at compressor exit is more than the temperature of ambient air and the surroundings. Heat rejection from this tube is welcome since it will reduce of the load on the condenser. However, this tube is kept small by locating the condenser close to the compressor to avoid excessive pressure drop. The drop in pressure in this tube has to be made up by the compressor; otherwise the pressure ratio will increase, reducing the mass flow rate and increasing the power input. The compressor cylinder discharge pressure at point 2″ is p_D. There will be some pressure drop across the discharge valve giving a compressor outlet pressure of $p_{2'}$ at state 2′. Finally, there will be pressure drop in the discharge line and the condenser pressure will be p_2 as shown at state 2 in Figures 3.26(a) and 3.26(b).

Tube connecting condenser to expansion valve

This tube is called the liquid line. The temperature of the condensed liquid is more than the ambient temperature in case of air-cooled condensers. In that case, the heat rejection from refrigerant will give rise to useful subcooling, resulting in a rise in cooling capacity. In water-cooled condensers, the condensed liquid temperature may be less than the ambient temperature. The leakage heat transfer may cause vapourization of refrigerant, which is not desirable. The expansion valve has a narrow orifice, which is calibrated for liquid flow. The presence of vapour decreases the mixture density and hence the mass flow rate through the orifice resulting in a lower cooling capacity.

The pressure drop in liquid line may occur due to friction. This is, however, very small. If the expansion valve is located at a higher elevation than that of the condenser, then significant pressure drop occurs as the liquid rises against gravity. From Bernoulli's equation for flow in absence of friction, the pressure drop is given by the following equation:

$$p_{ev} = p_c - g(z_{ev} - z_c)/v_c$$

where the subscripts *ev* and *c* refer to expansion valve inlet and condenser outlet, and *z* is the elevation.

The pressure drop during constant enthalpy throttling process, will take it from saturated liquid to a mixture state. That is, some liquid will flash into vapour. This will reduce the mass flow rate through the expansion valve. Subcooling of liquid refrigerant provides protection against this phenomenon. Hence in all the practical refrigeration systems, subcooling (see 3–3*a* in Figures 3.26(a) and 3.26(b)) is done either in the condenser or in a subcooling heat exchanger.

Tube connecting expansion valve to evaporator

The expansion valve is usually located very close to the evaporator, which prevents the pressure drop in this line. Further, the expansion valve is always located inside the refrigerated space; hence the leakage heat transfer is a part of the cooling capacity.

Expansion valve

It has been assumed that there is no heat transfer, and the change in KE is negligible during throttling, as a result $h_4 = h_{3b.}$ In actual practice there will some heat transfer to the expansion valve and the enthalpy $h_{4'} > h_{3b}$ as shown in Figure 3.26(b). This will reduce the refrigeration effect.

Pressure drop in the evaporator

The pressure in the evaporator will reduce to overcome the frictional resistance from $p_{4'}$ to p_1 as shown in Figure 3.26(b). Pressure drop in the evaporator reduces the saturation temperature at which the boiling will occur. In effect due to this the evaporator temperature will be higher at evaporator inlet than at the outlet. Large pressure drop may occur due to poor design of a single long tube as evaporator, compared to a large number of tubes arranged in parallel that will require small pressure drop. A large velocity results in large pressure drop, but it makes the evaporator more compact due to larger heat transfer coefficient. In such a situation, one has to make a compromise from initial cost vs. running cost point of view. In general, a reduction in pressure at evaporator exit decreases the vapour density and increases the pressure ratio, which decreases the volumetric efficiency and increases the power input to the compressor.

Flooded evaporators have pressure variation due to depth of liquid inside the evaporator. The pressure at the bottom of a flooded evaporator would be more due to larger hydrostatic pressure of gz/v_f, z being the depth. This would cause boiling to occur at higher saturation temperature at the bottom compared to boiling at lower saturation temperature at lower pressure at the top. For ammonia at –50°C, $v_f = 1.425 \times 10^{-3}$ m^3/kg. A depth of 0.5 m will lead to a pressure difference of $gz/v_f = 9.81(0.5) \times 1000/1.425 = 3.442$ kPa. The saturation pressures of NH_3 at –50°C and –52°C are 40.8 kPa and 36.2 kPa respectively. This pressure difference will cause a temperature difference of 1.5°C between the top the and the bottom. R22 has $v_f = 0.695$ m^3/kg at –50°C. This will give rise to a pressure difference of 7 kPa and a temperature difference of 2°C. This phenomenon is referred to as *static head penalty*. Sometimes, in shell-and-tube or flooded evaporators forced recirculation by a liquid pump is used to reduce the static head penalty.

Effect of noncondensable gases and moisture

All refrigeration systems are adequately evacuated after assembly. Thereafter, the refrigerant is charged into the system. Some air and moisture may be left behind in the system since perfect vacuum cannot be obtained. The moisture sticks to the surfaces, hence the system is heated by radiation heat transfer from a heater. If the evaporator pressure is less than the atmospheric pressure, then air and moisture may leak into the system. Moisture causes corrosion problems. If it is not dissolved in the refrigerant, then it remains as free water, which is liable to freeze below 0°C. The first opportunity of freezing occurs in the narrow orifice of the expansion valve causing choking of flow.

If the air leaks into the system, it gets trapped in the condenser since it cannot pass through the liquid seal at the exit of the condenser. The heat transfer in the condenser may be expressed as

$$Q_c = U_c A_c \Delta t$$

The presence of air may reduce the heat transfer area available to refrigerant for condensation. This will increase the temperature difference for a given amount of heat transfer rate, thus increasing the condenser temperature and pressure. If liberal area were provided in the condenser, even then this would occur. The total pressure in condenser is the sum of partial pressures of refrigerant and air. The refrigerant for a given coolant temperature will condense at its saturation pressure which would occur at a higher total pressure. As a result, the compressor has to work against a higher-pressure ratio. This will increase the compressor work and decrease the COP. A high pressure may sometime cause rupture of copper tubes or some joints may start leaking. Hence all the refrigeration systems are provided with a high pressure cutout which cuts off the power supply to the compressor

if the condenser pressure exceeds an upper limit. Similarly, a safety is provided against low pressure too. In fact, both these features are provided in a single switch called LP/HP cutout switch.

Ten point cycle

According to ISI Code No. 1476-1979 for testing refrigerators, the test conditions are as follows:

Condenser temperature	55°C
Evaporator temperature	–25°C
Subcooling in condenser	12°C
Temperature at condenser outlet	43°C
Subcooing in HEX	11°C
Temperature of liquid at HEX outlet	32°C
Pressure drop in evaporator	0.1 bar
Pressure drop on suction side of compressor	0.1 bar
Pressure drop on discharge side of compressor	0.25 bar

This ten-point cycle is shown in Figure 3.27.

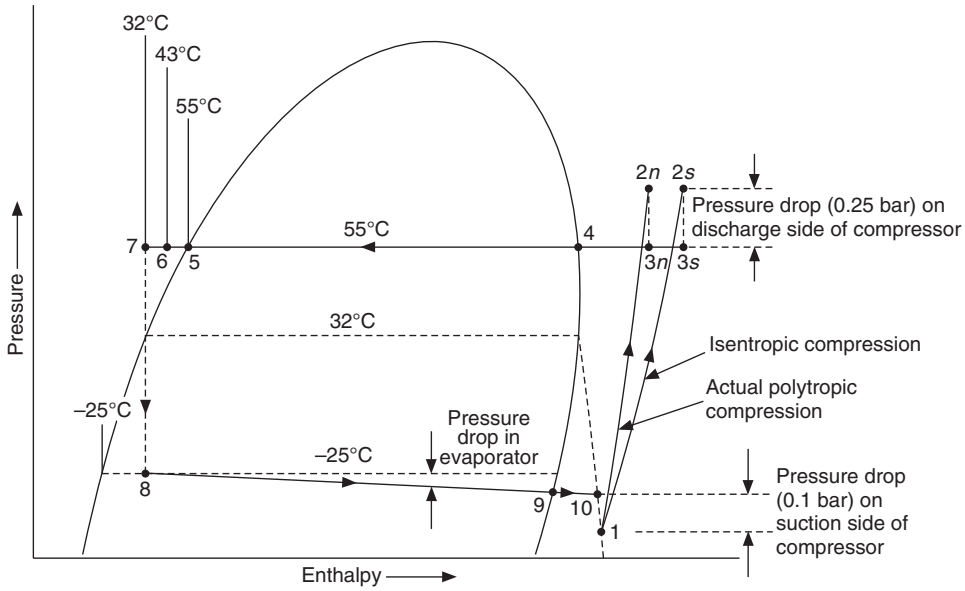

Figure 3.27 Standard ten state point cycle.

EXAMPLE 3.7 The condenser and evaporator temperatures are 40°C and –20°C respectively. Assuming that wet compression and wet expansion are feasible in Reversed Carnot cycle as shown in Figure 3.6(b), determine on per TR basis the mass flow rate, compressor work, turbine work, net work, condenser heat rejection and COP for three refrigerants namely, R12, R22 and NH_3. The properties at saturation for the three refrigerants are as follows.

R12:

Temperature (°C)	*Pressure* (bar)	h_f (kJ/kg)	h_g (kJ/kg)	s_f (kJ/kg-K)	s_g (kJ/kg-K)
–20	1.51	17.85	179.63	0.0732	0.7123
40	9.634	74.77	204.75	0.2725	0.6876

R22:

Temperature (°C)	*Pressure* (bar)	h_f (kJ/kg)	h_g (kJ/kg)	s_f (kJ/kg-K)	s_g (kJ/kg-K)
–20	2.455	22.53	243.26	0.0923	0.9642
40	15.267	95.4	261.38	0.3466	0.8767

NH_3:

Temperature (°C)	*Pressure* (bar)	h_f (kJ/kg)	h_g (kJ/kg)	s_f (kJ/kg-K)	s_g (kJ/kg-K)
–20	1.901	89.48	1417.97	0.3685	5.6169
40	15.55	371.47	1472.02	1.3579	4.8728

Solution:

R12:

The compression is isentropic hence, we have $s_1 = s_2 = s_g\,(40^oC) = 0.6876$ since state 2 is a saturated vapour state. If x_1 is the quality or the dryness fraction at point 1, then

$$s_1 = x_1\, s_g\,(-20^oC) + (1 - x_1)\, s_f\,(-20^oC) = 0.6876$$

or $$0.6876 = x_1\,(0.7123) + (1 - x_1)\,0.0732$$

$$\therefore \quad x_1 = \frac{0.6876 - 0.0732}{0.7123 - 0.0732} = 0.9613 \text{ and } h_1 = x_1\, h_g(-20^oC) + (1 - x_1)\, h_f\,(-20^oC)$$

$$\therefore \quad h_1 = 0.9613(179.63) + 0.0387(17.85) = 173.3775 \text{ kJ/kg}$$

Similarly, state 3 is a saturated liquid state hence $s_3 = s_f(40^oC) = 0.2775$
Process 3–4 is isentropic expansion, hence $s_3 = s_4$. If x_4 is the quality at point 4, then

$$s_4 = x_4\, s_g\,(-20^oC) + (1 - x_4)\, s_f\,(-20^oC)$$

$$\therefore \quad x_4 = \frac{0.2725 - 0.0732}{0.7123 - 0.0732} = 0.33384 \text{ and } h_4 = x_4\, h_g(40^oC) + (1 - x_4)\, h_f\,(40^oC)$$

$$\therefore \quad h_4 = 0.31184(179.63) + 0.68816(17.85) = 68.3 \text{ kJ/kg}$$

Refrigeration effect = $h_1 - h_4 = 173.3775 - 68.3 = 105.0772$ kJ/kg

This may also be expressed as: $h_1 - h_4 = T_e\,(s_1 - s_4)$

Using $s_1 = s_2$ and $s_3 = s_4$, we get $h_1 - h_4 = (273.15 - 20)(0.6876 - 0.2725)$

$= 105.082$ kJ/kg

The two results are slightly different because of some inconsistency in the table of properties at saturation.

For 1 TR plant, the refrigeration capacity Q_e is 3.51667 kW $\quad \therefore \quad \dot{m}(h_1 - h_4) = 3.51667$ kW

$$\dot{m} = 3.51667/105.0772 = 0.03346 \text{ kg/s}$$

The work is done on the compressor hence according to our sign convention it is negative. The work output of the turbine is positive. The net work is negative. In the following we consider modulus of compressor work.

Compressor work $|W_c| = \dot{m}(h_2 - h_1) = 0.03346(204.75 - 173.3775) = 1.05$ kW

Turbine work, $W_t = \dot{m}(h_3 - h_4) = 0.03346(74.77 - 68.3) = 0.2165$ kW

Net work $= |W_{net}| = |W_c| - W_t = 0.83334$ kW

This may also be expressed as

$$\dot{m}(T_c - T_e)(s_2 - s_3) = 0.03346(60)(0.6876 - 0.2725) = 0.8335 \text{ kW}$$

which is very close to the previous result.

Condenser heat rejection, $Q_c = \dot{m}(h_2 - h_3) = T_c(s_2 - s_3)$:

$$Q_c = \dot{m}(h_2 - h_3) = 0.03346(204.75 - 74.77) = 4.3499$$

and $\quad Q_c = 0.03346(273.15 + 40)(0.6876 - 0.2725) = 4.35$ kW.

Again the two results are same.

$$\text{COP} = \frac{Q_e}{|W_{net}|} = \frac{3.51167}{0.83334} = 4.22$$

Alternately for Reversed Carnot cycle COP $= T_e/(T_c - T_e) = 263.15/60 = 4.219$

R22: Following the above procedure, the results for R22 are as follows:

$$x_1 = \frac{0.87676 - 0.0923}{0.9642 - 0.0923} = 0.89965$$

$$h_1 = 0.89965\ (243.26) + 0.10035(22.53) = 221.1085 \text{ kJ/kg}$$

$$x_4 = \frac{0.3466 - 0.0923}{0.9642 - 0.0923} = 0.29166$$

$$h_4 = 0.29166(243.26) + 0.70834(22.53) = 86.9085 \text{ kJ/kg}$$

Refrigeration effect $= h_1 - h_4 = 221.1085 - 86.9085 = 134.2$ kJ/kg

Also, $\quad h_1 - h_4 = T_e(s_1 - s_4) = (273.15 - 20)(0.8767 - 0.3466) = 134.1948$ kJ/kg

$$\dot{m} = 3.51667/134.2 = 0.0262 \text{ kg/s}$$

Compressor work $|W_c| = \dot{m}(h_2 - h_1) = 0.0262(261.38 - 221.1085) = 1.05553$ kW

Turbine work $W_t = \dot{m}(h_3 - h_4) = 0.0262(95.4 - 86.9085) = 0.2225$ kW

Net work = $|W_{net}| = |W_c| - W_t = 0.83278$ kW

Also $|W_{net}| = \dot{m}(T_c - T_e)(s_2 - s_3) = 0.0262(60)(0.8767 - 0.3466) = 0.83346$ kW

$Q_c = \dot{m}(h_2 - h_3) = 0.0262(261.38 - 95.4) = 4.3495$ kW

and $Q_c = 0.0262(273.15 + 40)(0.8767 - 0.3466) = 4.35$ kW.

Again the two results are same.

$$\text{COP} = \frac{Q_e}{|W_{net}|} = \frac{3.51167}{0.83278} = 4.223$$

NH_3: Following the above procedure, the results for NH_3 are as follows:

$$x_1 = \frac{4.8728 - 0.3685}{5.6169 - 0.3685} = 0.8582$$

$$h_1 = 0.8582(1417.97) + 0.1418(89.48) = 1229.621 \text{ kJ/kg}$$

$$x_4 = \frac{1.3579 - 0.3685}{5.6169 - 0.3685} = 0.1885$$

$$h_4 = 0.1885(1417.97) + 0.8115(89.48) = 339.9197 \text{ kJ/kg}$$

Refrigeration effect = $h_1 - h_4 = 1229.621 - 331.9197 = 889.7$ kJ/kg

Also $h_1 - h_4 = T_e(s_1 - s_4) = (273.15 - 20)(4.8728 - 013579) = 889.797$ kJ/kg

$\dot{m} = 3.51667/889.7 = 0.003952$ kg/s

Compressor work $|W_c| = \dot{m}(h_2 - h_1) = 0.003952(1472.02 - 1229.621) = 9581$ kW

Turbine work $W_t = \dot{m}(h_3 - h_4) = 0.003952\ (371.47 - 339.9197) = 0.1247$ kW

Net work = $|W_{net}| = |W_c| - W_t = 0.8334$ kW

Also $|W_{net}| = \dot{m}(T_c - T_e)(s_2 - s_3) = 0.003952\ (60)(4.8728 - 013579) = 0.8336$ kW

$Q_c = \dot{m}(h_2 - h_3) = 0.003952(1472.02 - 371.47) = 4.35$ kW

and $Q_c = 0.003952(273.15 + 40)(4.8728 - 013579) = 4.3506$ kW

Again the two results are same.

$\therefore$ $$\text{COP} = \frac{Q_e}{|W_{net}|} = \frac{3.51167}{0.8334} = 4.2196$$

EXAMPLE 3.8 (a) The condenser and evaporator temperatures are 40°C and –20°C respectively for an ammonia refrigeration system of 1TR cooling capacity. Find the mass flow rate, swept volume rate and work requirement of the compressor, condenser heat rejection and COP considering SSS cycle. The volumetric efficiency may be expressed as $\eta_{vol} = 1 + \varepsilon - \varepsilon\,(v_1/v_2)$ where, ε is the clearance volume ratio for the compressor and it is equal to 0.04.

(b) Consider the saturated RC cycle and find the work requirements of isentropic compressor, isothermal compressor and isentropic turbine. Find the net work and compare the result with that found from the area of diagram on *T*–*s* plot.

The required thermodynamic properties of NH_3 at saturation are as follows:

Temperature (°C)	*Pressure* (bar)	v_g (m^3/kg)	h_f (kJ/kg)	h_g (kJ/kg)	s_f (kJ/kg-K)	s_g (kJ/kg-K)
–20	1.901	0.624	89.48	1417.97	0.3685	5.6169
40	15.55	0.0833	371.47	1472.02	1.3579	4.8728

The properties of superheated vapour at 15.55 bar (40°C) are as follows:

Degree of superheat	80°C	100°C
v	0.116	0.123
h	1700.3	1751.7
s	5.5253	5.65283

Solution:

Referring to Figure 3.11 state 1 is saturated vapour state, therefore

$$h_1 = h_g\ (-20^oC) \quad \text{and} \quad s_1 = s_g\ (-20^oC)$$

Similarly state 3 is a saturated liquid state, hence

$$h_3 = h_f\ (40^oC) \quad \text{and} \quad s_3 = s_f\ (40^oC)$$

Referring to Figure 3.11 and from the properties given in the table, we get

$$h_1 = 1417.97,\ v_1 = 0.624 \text{ and } s_1 = 5.6169$$

$$h_a = 1472.02,\ v_a = 0.0833 \text{ and } s_a = 4.8728$$

$$h_3 = 371.47 \text{ and } s_3 = 1.3579$$

(a) *SSS cycle*

State 2 is a superheated state at 15.55 bar pressure such that $s_1 = s_2 = 5.6169$

It is observed from the superheat table that $s_2 = 5.6179$ lies between 80°C and 100°C

By interpolating in the superheat table for pressure of 15.55 bar (40°C) between 80°C and 100°C superheat for $s_1 = s_2 = 5.6169$, we get

$$\Delta t = (5.6169 - 5.5253)/(5.65283 - 5.5253) \times 20 = 0.71826 \times 20 = 14.365^oC$$

$$\therefore \quad t_2 = 40 + 80 + 14.365 = 134.365^oC$$

$$h_2 = 1700.3 + 0.71826(1751.7 - 1700.3) = 1737.219$$

and $$v_2 = 0.116 + 0.71826(0.123 - 0.116) = 0.121$$

Process 3-4 is a throttling process, hence

$$h_4 = h_3 = 371.47$$

Cooling capacity is given by $Q_e = \dot{m}(h_1 - h_4)$, Therefore for 1 TR = 3.5167 kW, we get

$$\dot{m} = \frac{3.5167 \times \text{TR}}{h_1 - h_4} = \frac{3.5167}{1417.97 - 371.47} = 0.00336 \text{ kg/s}$$

$$W = \dot{m}(h_2 - h_1) = 0.00336(1739.219 - 1417.97) = 1.0728 \text{ kW}$$

$$Q_c = \dot{m}(h_2 - h_3) = 0.00336(1739.219 - 371.47) = 4.589 \text{ kW}$$

From Eq. (3.71) the area of superheat horn, A_1, is given by

$$A_1 = (h_2 - h_a) - T_c(s_1 - s_a)$$
$$= (1739.219 - 1472.02) - 313(5.6169 - 4.8728)$$
$$= 32.2957 \text{ kJ/kg} \quad \text{and} \quad \dot{m}A_1 = 0.00336 \times 32.2957 = 0.10426 \text{ kW}$$

The area A_2 (Figure 3.10) is the loss in refrigeration effect compared to RC cycle. It may be written as

$$A_2 = (q_e)_{\text{RC}} - (q_e)_{\text{SSS}} = T_e(s_1 - s_{4'}) - (h_1 - h_4) = T_e(s_1 - s_3) - (h_1 - h_4)$$

$$A_2 = 253(5.6169 - 1.3579) - (1417.97 - 371.47) = 31.027 \text{ kJ/kg}$$

and $\dot{m}A_2 = 0.00336 \times 31.027 = 0.10426$ kW

Alternatively, can find quality $x_{4'}$ at 4′ by considering $s_3 = s_{4'}$, then find enthalpy $h_{4'}$ and write $A_2 = h_3 - h_{4'}$

$$x_{4'} = \frac{1.3579 - 0.3685}{5.6169 - 0.3685} = 0.1885 \quad \therefore \quad h_{4'} = 0.1885(1417.97) + (1.0 - 0.1885)89.48$$

or $h_{4'} = 339.91975 \quad \therefore \quad A_2 = h_3 - h_{4'} = 371.47 - 339.91975 = 31.55024$

which, is luckily the same as that found by the other method.

$$\text{COP} = 3.5167/W = 3.5167/1.0728 = 3.278$$

$$(\text{COP})_{\text{RC}} = T_e/(T_c - T_e) = 253/60 = 4.216$$

$$\eta_{\text{R}} = \text{COP}/\text{COP}_{\text{RC}} = 3.278/4.216 = 0.777$$

$\eta_{\text{vol}} = 1 - \varepsilon(v_1/v_2 - 1)$, where $\varepsilon = \mathbb{V}_{cl}/\mathbb{V}_D$ is the clearance ratio and

$(p_2/p_1)^{1/m} = v_1/v_2$ for polytropic process $p_1 v_1^m = p_2 v_2^m$

$\therefore \quad \eta_{\text{vol}} = 1 - 0.04[(0.624/0.116) - 1] = 0.825$

$$\mathbb{V}_S = \dot{m}v_1/\eta_{\text{vol}} = 0.00336(0.624)/0.825 = 0.00254 \text{ m}^3/\text{s}$$

(b) Figures 3.7 and 3.10 show the RC cycle and SSS cycle for comparison. Referring to these figures, we locate the state points for the RC cycle.

The solution of RC cycle requires the evaluation of enthalpy at point 2″ where $s_{2''} = s_1 = 5.6169$ and temperature is T_c (40°C). The superheat tables are for constant pressure lines, hence evaluation of $h_{2''}$ requires interpolation between two such isobars. It is observed that this point will lie between 4.625 and 4.975 bar pressures (the saturation temperatures for these temperatures are (2°C and 4°C). We first find the values of h and s at 40°C along the isobars 4.625 bar and 4.975 bar.

Superheat table for 4.625 bar (2°C)			Superheat table for 4.975 bar (4°C)		
Degree of superheat	30°C	40°C	*Degree of superheat*	30°C	40°C
Actual temperature	32°C	42°C	*Actual temperature*	34°C	44°C
v	0.307	0.319	v	0.288	0.299
h	1522.2	1546.5	h	1525.0	1545.9
s	5.5756	5.6536	s	5.5510	5.6295
At 40°C : s = 5.63824 , h = 1536.78			At 40°C : s = 5.5981, h = 1537.54		

Next we interpolate at 40°C between s = 5.63824 and s = 5.5981

Interpolating between s = 5.63824 and s = 5.5981, we find the enthalpy for $s_1 = s_{2''} = 5.6169$

$$h_{2''} = 1537.54 - \frac{5.6169 - 5.5981}{5.63824 - 5.5981}(1537.54 - 1536.78) = 1537.182 \text{ kJ/kg}$$

Similar process gives $v_{2''} = 0.3044$ and $p_{2''} = 4.79$ bar

Refrigeration effect $q_e = T_e\,(s_1 - s_3) = 253(5.6169 - 1.3579) = 1077.527$ kJ/kg

Also from the calculated value of $h_{4'}$, $q_e = h_1 - h_{4'} = 1417.97 - 339.91975 = 1078.05$ which is slighty larger than the first value due to inconsistency in property table.

$$\dot{m}_{RC} = 3.5167/q_e = 3.5167/1077.527 = 0.0032636$$

$$W_{isen} = \dot{m}(h_{2''} - h_1) = 0.0032636(1537.182 - 1417.97) = 0.389 \text{ kW}$$

The heat rejected from isothermal compressor = $\dot{m}T_c(s_1 - s_a)$. Hence, energy balance for the compressor gives the work input to compressor.

$$W_{isoth} = \dot{m}[(h_a - h_{2''}) + T_c(s_1 - s_a)]$$

$$= 0.0032636[(1472.02 - 1537.182) + 313(5.6169 - 4.8728)] = 0.5475 \text{ kW}$$

$$W_{turbine} = \dot{m}(h_3 - h_{4'}) = 0.0032636(371.47 - 339.91975) = 0.0032636 \times 31.55025$$

$$= 0.10297 \text{ kW}$$

$$W_{net} = 0.389 + 0.5475 - 0.10297 = 0.83353 \text{ kW}$$

COP = 3.5167/0.83353 = 4.219, whereas, $T_e/(T_c - T_e) = 253/60 = 4.216$

From the area on T–s diagram, $W_{net} = \dot{m}(T_c - T_e)(s_1 - s_3)$

$$= 0.0032636 \times 60(5.6169 - 1.3579) = 0.834 \text{ kW}$$

This checks with the value calculated from the various components.

EXAMPLE 3.9(a) The condenser and evaporator temperatures are 40°C and 0°C respectively for $CHClF_2$ refrigeration system of 1TR cooling capacity. Consider the saturated RC cycle as was done in Example 3.5 to find the state after isentropic compression and find the work requirements of isentropic compressor, isothermal compressor and isentropic turbine. Find the net work and compare the result with that found from the area of diagram on T–s plot.

The properties from the saturation table for refrigerant $CHClF_2$ (R22) are as follows:

Temperature (°C)	*Pressure* (bar)	v_g (m^3/kg)	h_f (kJ/kg)	h_g (kJ/kg)	s_f (kJ/kg-K)	s_g (kJ/kg-K)
0	4.98	0.0472	46.19	251.12	0.1815	0.9317
40	15.267	0.0152	95.4	261.38	0.3466	0.8767

Solution:

Figures 3.7 and 3.10 show the RC cycle and the SSS cycle for comparison. Referring to these figures, we locate the state points for the RC cycle.

In Example 3.5 the state at the end of isentropic compression was found to be

$$h_2 = 272.485,\ v_2 = 0.0269 \text{ and } p_2 = 10.032 \text{ bar}$$

$$h_1 = 251.12,\ v_1 = 0.0472 \text{ and } s_1 = 0.9317$$

$$h_a = 261.38,\ v_a = 0.0152 \text{ and } s_a = 0.8767$$

$$h_3 = 95.4 \text{ and } s_3 = 0.3466$$

Refrigeration effect $q_e = T_e\,(s_1 - s_3) = 273(0.9317 - 0.3466) = 159.7273$ kJ/kg

Alternately, h_4 can be found by putting $s_3 = s_4$

$$x_4 = \frac{0.3466 - 0.1815}{0.9317 - 0.1815} = 0.2201 \quad \therefore \quad h_4 = 0.2201(251.12) + (1.0 - 0.2201)46.19$$

$$h_4 = 91.29$$

Therefore $q_e = h_1 - h_4 = 251.12 - 91.29 = 159.83$

which is slighty larger than the first value due to inconsistency in property table.

$$\dot{m}_{RC} = 3.5167/q_e = 3.5167/159.825 = 0.022 \text{ kg/s}$$

$$W_{isen} = \dot{m}(h_{2'} - h_1) = 0.022(272.485 - 251.12) = 0.47 \text{ kW}$$

The heat rejected from isothermal compressor = $\dot{m}T_c(s_1 - s_a)$. Hence, energy balance for the compressor gives the work input to compressor.

$$W_{isoth} = \dot{m}[(h_a - h_2) + T_c(s_1 - s_a)]$$

$$= 0.022[(261.38 - 272.485) + 313(0.9317 - 0.8767)] = 0.1344 \text{ kW}$$

$$W_{turbine} = \dot{m}(h_3 - h_4) = 0.022(95.4 - 91.2951) = 4.105 \times 0.022 = 0.0903 \text{ kW}$$

$$W_{net} = 0.47 + 0.1344 - 0.0903 = 0.5141 \text{ kW}$$

COP = 3.5167/0.5141 = 6.84, whereas, $T_e/(T_c - T_e) = 273/40 = 6.825$

From the area on T–s diagram $W_{net} = \dot{m}(T_c - T_e)(s_1 - s_3)$

$$= 0.22 \times 40(0.9317 - 0.3466) = 0.515 \text{ kW}$$

This checks with the value calculated from the various components.

EXAMPLE 3.9(b) The condenser and evaporator temperatures are 40°C and –20°C respectively for a $CHClF_2$ refrigeration system of 1TR cooling capacity. Find the mass flow rate, swept volume rate and work requirement of the compressor, condenser heat rejection and COP considering SSS

cycle. The volumetric efficiency may be expressed as $\eta_{vol} = 1 + \varepsilon - \varepsilon\,(v_1/v_2)$ where, ε is the clearance volume ratio for the compressor and it is equal to 0.04.

The properties of superheated vapour at 15.267 bar (40°C) are as follows:

Degree of superheat	15°C	20°C
v	0.0167	0.0172
h	275.19	279.61
s	0.9202	0.9332

Solution:

Referring to Figure 3.7, states 1, a and 3 are saturated states.

From the last example the properties at saturated states are as follows:

$$h_1 = 251.12,\ v_1 = 0.0472 \text{ and } s_1 = 0.9317$$

$$h_a = 261.38,\ v_a = 0.0152 \text{ and } s_a = 0.8767$$

$$h_3 = 95.4 \text{ and } s_3 = 0.3466$$

State 2 is a superheated state at 15.267 bar pressure such that $s_1 = s_2 = 0.9317$.

It is observed from the superheat table that $s_2 = 0.9317$ lies between 15°C and 20°C.

By interpolating in the superheat table for pressure of 15.267 bar (40°C) between 15°C and 20°C superheat for $s_1 = s_2 = 0.9317$, we get

$$\Delta t = (0.9317 - 0.9202)/(0.9332 - 0.9202) \times 5 = 0.8846 \times 5 = 4.423^{\circ}\text{C}$$

$$\therefore \quad t_2 = 40 + 15 + 4.23 = 59.23^{\circ}\text{C}$$

$$h_2 = 275.19 + 08846\ (279.61 - 275.19) = 279.1$$

and $$v_2 = 0.0167 + 0.8846\ (0.172 - 0.0167) = 0.01714$$

Process 3–4 is a throttling process, hence

$$h_4 = h_3 = 95.4$$

Cooling capacity is given by $Q_e = \dot{m}(h_1 - h_4)$, Therefore for 1 TR = 3.5167 kW, we get

$$\dot{m} = \frac{3.5167 \times \text{TR}}{h_1 - h_4} = \frac{3.5167}{251.12 - 95.4} = 0.022583 \text{ kg/s}$$

$$W = \dot{m}(h_2 - h_1) = 0.022583(279.1 - 251.12) = 0.632 \text{ kW}$$

$$Q_c = (h_2 - h_3) = 0.022583(279.1 - 95.4) = 4.148 \text{ kW}$$

From Eq. (3.71) the area of superheat horn, A_1, is given by

$$A_1 = (h_2 - h_a) - T_c(s_1 - s_a)$$

$$= (279.1 - 261.38) - 313(0.9317 - 0.8767)$$

$$= 0.505 \text{ kJ/kg} \text{ and } \dot{m}A_1 = 0.022583 \times 0.505 = 0.0114 \text{ kW}$$

The area A_2 is the loss in refrigeration effect compared to RC cycle. It may be written as

$$A_2 = (q_e)_{RC} - (q_e)_{SSS} = T_e(s_1 - s_{4'}) - (h_1 - h_4) = T_e(s_1 - s_3) - (h_1 - h_3)$$

$\therefore \quad A_2 = 273(0.9317 - 0.3466) - (251.12 - 95.4) = 4.0123$ k J/kg

and $\dot{m}A_2 = 0.022583 \times 4.0123 = 0.0906$ kW

Alternatively, one can find the quality $x_{4'}$ at 4′ by considering $s_3 = s_{4'}$, then find enthalpy $h_{4'}$ and write $A_2 = h_3 - h_{4'}$. The enthalpy $h_{4'}$ has already been found in part (a) of this example.

$$h_{4'} = 91.29$$

$\therefore \quad A_2 = h_3 - h_{4'} = 95.4 - 91.29 = 4.11$

which is slightly different from that found by the other method due to inconsistency in property table.

$$\text{COP} = 3.5167/W = 3.5167/0.632 = 5.564$$

$$(\text{COP})_{\text{RC}} = T_e/(T_c - T_e) = 273/40 = 6.825$$

$$\eta_{\text{R}} = \text{COP}/\text{COP}_{\text{RC}} = 5.564/6.825 = 0.815$$

$\eta_{\text{vol}} = 1 - \varepsilon\,(v_1/v_2 - 1)$, where $\varepsilon = \mathbb{V}_{cl}/\mathbb{V}_D$ is the clearance ratio and $(p_2/p_1)^{1/m} = v_1/v_2$. For polytropic process $p_1 v_1^{\,m} = p_2 v_2^{\,m}$

$$\eta_{\text{vol}} = 1 - 0.04[(0.0472/0.01714) - 1] = 0.93$$

$$\mathbb{V}_S = \dot{m} v_1/\eta_{\text{vol}} = 0.022583(0.0472)/0.93 = 0.00211 \text{ m}^3/\text{s}$$

EXAMPLE 3.10 The condenser and evaporator temperatures in a refrigeration system are 45°C and –10°C respectively. Determine the mass flow rate, compressor work, condenser heat rejection and COP for a single stage saturation cycle and Reversed Carnot cycle for a plant of 1 TR capacity for three refrigerants, R12, R22 and R717. Determine the areas of superheat horn and throttling loss and the refrigerating efficiency. The required data for the three refrigerants from the superheat tables is as follows.

	R12, 45°C (10.88 bar)		R22, 45°C (17.209 bar)		R717, 45°C (17.82 bar)	
ΔT_s	5	10	20	30	60	80
v	0.0165	0.0170	0.0152	0.0161	0.096	0.102
h	210.40	214.49	280.95	289.87	1653.4	1706.7
s	0.6985	0.7109	0.9270	0.9530	5.3412	5.4787

Solution:

R12:

The SSS cycle 1–2–3–4–1 and the saturated RC cycle 1–2″–3–4′ are shown in Figures 3.10. The properties from the saturation table for R12 at $t_c = 45$°C and $t_e = -10$°C :

$h_1 = 184.22$ kJ/kg, $s_1 = 0.7060$ kJ/kg-K, $v_1 = 0.077$ m^3/kg, $h_a = 206.46$, $s_a = 0.6863$,

$v_a = 0.0161$, $h_3 = 79.9$, $s_3 = 0.2884$, $h_0 = 26.94$ and $s_0 = 0.1083$.

The state 2 after isentropic compression is a superheated state at condenser pressure of 10.88 bar. State 2 is located by interpolating in the superheat table at 10.88 bar such that

$s_2 = s_1 = 0.7060$. Interpolating in the table, we get

$$h_2 = 210.4 + \frac{0.7060 - 0.6985}{0.7109 - 0.6985}(214.49 - 210.4) = 210.4 + 0.6048387\,(4.09)$$

$h_2 = 212.874$ kJ/kg

$t_2 = 45 + 5 + 5 \times 0.6048387 = 53.024^{\circ}\text{C}$

$v_2 = 0.0165 + 0.60484(0.0175 - 0.0165) = 0.0171\ \text{m}^3/\text{kg}$

State 4′: This would be the state if the expansion was carried out isentropically.

$$s_3 = s_{4'} \quad \therefore \quad 0.2884 = x_{4'}\, s_g\,(-10\,^{\circ}\text{C}) + (1.0 - x_{4'})\, s_f\,(-10^{\circ}\text{C})$$

$$\therefore \qquad x_{4'} = \frac{0.2882 - 0.1083}{0.7060 - 0.1083} = 0.3013217$$

$$h_{4'} = x_{4'}\, h_g\,(-10^{\circ}\text{C}) + (1 - x_{4'})\, h_f\,(-10^{\circ}\text{C}) = 0.3013217(184.22) + 0.6986788(26.94)$$

$h_{4'} = 74.331883$ kJ/kg

Reversed Carnot cycle

Refrigeration effect $= h_1 - h_{4'} = 109.88812$ kJ/kJ

A shortcut for finding the refrigeration effect without calculating $h_{4'}$ is to use the relation

$$h_1 - h_{4'} = T_e\,(s_1 - s_{4'}) = T_e\,(s_1 - s_3) \text{ since } s_3 = s_{4'}$$

$$\therefore \qquad \text{Refrigeration effect} = T_e\,(s_1 - s_3) = 263(0.7060 - 0.2884) = 109.8288$$

This is slightly different from $h_1 - h_{4'} = 109.88812$ because of inconsistency in the tabulated properties of the refrigerant.

For 1 TR system the mass flow rate $\dot{m} = 3.51667/(h_1 - h_{4'})$

$$\therefore \qquad \dot{m} = \frac{3.51667}{109.88812} = 0.0320022\ \text{kg/s}$$

Condenser heat rejection $Q_c = \dot{m} T_c\,(s_1 - s_3) = 0.032\,(318)(0.7060 - 0.2884) = 4.2495$ kW

$$\text{Work done} = Q_c - Q_e = 4.2495 - 3.51667 = 0.73283\ \text{kW}$$

Also $W = \dot{m}(T_c - T_e)(s_1 - s_3) = 0.032(55)(0.7060 - 0.2884) = 0.734976$ kW

$$\text{COP} = \frac{T_e}{T_c - T_e} = \frac{263}{318 - 263} = 4.78182$$

In the Reversed Carnot cycle, de-superheating 2″–*a* occurs in an isothermal compressor and some heat q_{iso} is rejected ending up in saturated state *a* (see Figure 3.7). Thereafter q_c' heat is rejected in condenser during condensation from vapour state *a* to saturated liquid state 3. In the above calculation total heat rejection $q_{\text{iso}} + q_c' = T_c(s_1 - s_3)$ has been calculated. The state at point 2″ is required for the calculation of q_{iso}. It is known that entropy at 2″ is 0.7060 and temperature is 45°C. The superheat tables are pressure based and the pressure is not known at point 2″. Hence a two-way interpolation has to be done to locate point 2″. The values of *s* from superheat tables at two neighbouring pressure are:

	36°C (8.717 bar)		38°C (9.167 bar)	
ΔT_s	5	10	5	10
v	0.021	0.021	0.020	0.020
h	207.15	210.93	207.9	211.72
s	0.7012	0.7130	0.7004	0.7124

Interpolating at 8.717 bar for $s = 0.7060$, $t = 36 + 5 + \dfrac{0.7060 - 0.7012}{0.7130 - 0.7012}(5) = 43.3°C$

Interpolating at 9.167 bar for $s = 0.7060$, $t = 38 + 5 + \dfrac{0.7060 - 0.7004}{0.7124 - 0.7004}(5) = 45.33°C$

The point 2″ will lie very near 9.167 bar along $s_1 = s_{2''} = 0.7060$

Single Stage Saturation cycle

Refrigeration effect = $h_1 - h_4 = h_1 - h_3 = 184.22 - 79.9 = 104.32$ kJ/kg

The refrigeration effect for the Reversed Carnot cycle was 109.8288 which is larger than the SSS cycle refrigeration effect, since some work is lost in the throttling process.

$$\dot{m} = \frac{3.51667}{104.32} = 0.0337103 \text{ kg/s}$$

$$W = \dot{m}(h_2 - h_1) = 0.0337103(212.874 - 184.22) = 0.9659 \text{ kW}$$

This is larger than the RC work since the area of superheat is involved in the SSS cycle.

$$Q_c = \dot{m}(h_2 - h_3) = 0.0337103(212.874 - 79.9) = 4.4826 \text{ kW}$$

It is larger than RC cycle heat rejection by the same amount as the work requirement.

$$\text{COP} = \frac{3.51667}{\dot{m}(h_2 - h_1)} = \frac{3.51667}{0.9659} = 3.6408$$

Area of superheat horn $A_1 = h_2 - h_a - T_c(s_1 - s_a) = 212.874 - 206.46 - 318(0.706 - 0.6863)$

$= 0.1494$ kJ/kg

Throttling loss, $A_2 = h_4 - h_{4'} = h_3 - h_{4'} = 79.9 - 74.332 = 5.568$ kJ/kg

Alternatively, loss in refrigeration effect = $(q_E)_{RC} - (q_E)_{sss} = T_e(s_1 - s_{4'}) - (h_1 - h_4)$

or $A_2 = T_e\,(s_1 - s_3) - (h_1 - h_3) = 263\,(0.706 - 0.2884) - (184.22 - 79.9) = 5.535$ kJ/kg

The error in the second place of decimal is due to inconsistency in tabulated data.

$$\text{Refrigerating efficiency} = \eta = \frac{(\text{COP})_{SSS}}{\text{COP}_{RC}} = \frac{3.6408}{4.78182} = 0.7614$$

R22:

The properties from the saturation table for R22 at $T_c = 45^oC$ and $T_e = -10^oC$ are:

h_1= 247.37 kJ/kg, s_1 = 0.9473 kJ/kg-K, v_1 = 0.0654 m^3/kg, h_a = 261.95,

s_a = 0.8697, v_a = 0.0152, h_3 = 101.76 s_3 = 0.3662, h_0 = 34.25 and s_0 = 0.1374.

The state 2 after isentropic compression is a superheated state at condenser pressure of 17.209 bar. State 2 is located by interpolating in the superheat table at 17.209 bar such that $s_2 = s_1 = 0.9473$. Interpolating in the table, we get

$$h_2 = 280.95 + \frac{0.9473 - 0.9270}{0.953 = 0.927}(287.87 - 280.95) = 280.95 + 0.78077(289.7 - 280.95)$$

h_2 = 287.914 kJ/kg

$t_2 = 45 + 20 + 0.780077 \times 10 = 72.808°C$

$v_2 = 0.0152 + 0.780077(0.0161 - 0.0152) = 0.0159$ m^3/kg

Reversed Carnot cycle

Refrigeration effect = $h_1 - h_{4'} = T_e\,(s_1 - s_{4'}) = T_e\,(s_1 - s_3)$

$= 263(0.9473 - 0.3662) = 152.8293$ kJ/kg

For 1 TR system the mass flow rate $\dot{m} = 3.51667/(h_1 - h_{4'})$

$$\dot{m} = \frac{3.51667}{152.8293} = 0.0230104 \text{ kg/s}$$

$$Q_c = \dot{m}T_c\,(s_1 - s_3) = 0.0230104\ (318)(0.9473 - 0.3662) = 4.2521 \text{ kW}$$

$$W = \dot{m}(T_c - T_e)(s_1 - s_3) = 0.7354 \text{ kW}$$

$$\text{COP} = \frac{T_e}{T_c - T_e} = \frac{263}{318 - 263} = 4.78182$$

Single Stage Saturation cycle

Refrigeration effect = $h_1 - h_4 = h_1 - h_3 = 247.37 - 101.76 = 145.61$

$\dot{m} = 3.51667/145.61 = 0.0241512$ kg/s

$W = \dot{m}(h_2 - h_1) = 0.0241512(287.914 - 247.37) = 0.9792$ kW

This is larger than the RC work since the area of superheat is involved in SSS cycle.

$Q_c = \dot{m}(h_2 - h_3) = 0.0241512(287.914 - 101.76) = 4.4958$ kW

It is larger than RC cycle heat rejection by the same amount as the work requirement.

$$\text{COP} = \frac{3.51667}{\dot{m}(h_2 - h_1)} = \frac{3.51667}{0.9792} = 3.5914$$

Area of superheat horn, $A_1 = h_2 - h_a - T_c(s_1 - s_a) = 287.914 - 261.95 - 318(0.9473 - 0.8697)$

$= 1.2872$ kJ/kg

$A_2 = (q_e)_{RC} - (q_e)_{sss} = T_e\,(s_1 - s_{4'}) - (h_1 - h_4)$

$A_2 = T_e\,(s_1 - s_3) - (h_1 - h_3) = 263\,(0.9473 - 0.3662) - (247.37 - 101.76) = 7.2193$ kJ/kg

Refrigerating efficiency, $\eta = \dfrac{(\text{COP})_{sss}}{\text{COP}_{RC}} = \dfrac{3.5914}{4.78182} = 0.751$

NH_3:

The properties from the saturation table for NH_3 at $t_c = 45^oC$ and $t_e = -10^oC$ are:

$h_1 = 1431.409$ kJ/kg, $s_1 = 5.4712$ kJ/kg-K, $v_1 = 0.418$, $h_a = 1473.03$, $s_a = 4.8201$,

$v_a = 0.0726$, $h_3 = 396.22$ and $s_3 = 1.4349$, $s_0 = 0.5435$ and $h_0 = 134.95$

The state 2 after isentropic compression is a superheated state at condenser pressure of 17.82 bar. State 2 is located by interpolating in the superheat table at 17.82 bar such that $s_2 = s_1 = 5.4712$. Interpolating in the table, we get

$$h_2 = 1653.4 + \frac{5.4712 - 5.3412}{5.4787 - 5.3412}(1706.7 - 1653.4) = 1653.4 + 0.94545(1706.7 - 1653.4)$$

$h_2 = 1703.793$ kJ/kg

$t_2 = 45 + 60 + 0.94545 \times 20 = 123.91^oC$

$v_2 = 0.096 + 0.94545(0.102 - 0.096) = 0.1017$ m^3/kg

Reversed Carnot cycle

Refrigeration effect $= h_1 - h_{4'} = T_e(s_1 - s_{4'}) = T_e(s_1 - s_3)$

$= 263(5.4712 - 1.4349) = 1061.547$ kJ/kg

For 1 TR system the mass flow rate $\dot{m} = 3.51667/(h_1 - h_{4'})$

$$\dot{m} = \frac{3.51667}{1061.547} = 0.003313 \text{ kg/s}$$

$Q_c = \dot{m}T_c\,(s_1 - s_3) = 0.003313\,(318)(5.4712 - 1.4349) = 4.2521$ kW

$W = \dot{m}(T_c - T_e)(s_1 - s_3) = 0.7354$ kW

$$\text{COP} = \frac{T_e}{T_c - T_e} = \frac{263}{318 - 263} = 4.78182$$

Single Stage Saturation cycle

Refrigeration effect $= h_1 - h_4 = h_1 - h_3 = 1431.409 - 396.22 = 1035.189$

$\dot{m} = 3.51667/1035.189 = 3.39712 \times 10^{-3}$ kg/s

$W = \dot{m}(h_2 - h_1) = 0.003397(1703.793 - 1431.409) = 0.9253$ kW

This is larger than the RC work since the area of superheat is involved in SSS cycle.

$Q_c = \dot{m}(h_2 - h_3) = 0.003397(1703.793 - 396.22) = 4.442$ kW

It is larger than RC cycle heat rejection by the same amount as the work requirement.

$$\text{COP} = \frac{3.51667}{\dot{m}(h_2 - h_1)} = \frac{3.51667}{0.9253} = 3.8006$$

Area of superheat horn $A_1 = h_2 - h_a - T_c(s_1 - s_a) = 1703.793 - 1473.03 - 318(5.4712 - 4.8201)$

$= 23.713$ kJ/kg

$A_2 = (q_e)_{\text{RC}} - (q_e)_{\text{sss}} = T_e\,(s_1 - s_{4'}) - (h_1 - h_4)$

$A_2 = T_e\,(s_1 - s_3) - (h_1 - h_3) = 263(5.4712 - 1.4349) - (1431.409 - 396.22) = 26.3579$ kJ/kg

Refrigerating efficiency, $\eta = \dfrac{(\text{COP})_{\text{SSS}}}{\text{COP}_{\text{RC}}} = \dfrac{3.8006}{4.78182} = 0.795$

EXAMPLE 3.11 The average specific heats of R12, R22 and R717 at condenser pressures are 0.793 kJ/kg-K, 0.9335 kJ/kg-K and 2.963 kJ/kg-K respectively. Determine the parameters of Example 3.10 for 1 TR cooling capacity and compare the results with those of Example 3.10.

Solution:

The temperature at point 2 is determined by assuming the vapour along process 2–*a* to behave like a perfect gas with constant specific heat. We have $Tds = dh - v\,dp$. Along line 2–1 the pressure is constant hence, $dp = 0$. Therefore, $ds = dh/T = c_p\,dT/T$. Integrating it along *a*–2, we get

$$\int_a^2 ds = c_p \int_a^2 \frac{dT}{T} \qquad \therefore \quad s_2 - s_a = c_p \ln \frac{T_2}{T_a}$$

$$\therefore \qquad T_2 = T_a \exp\left\{\frac{s_2 - s_a}{c_p}\right\} = T_c \exp\left\{\frac{s_1 - s_a}{c_p}\right\}$$

and $$h_2 = h_a + c_p(T_2 - T_c)$$

R12:

$h_1 = 184.22$ kJ/kg, $s_1 = 0.7060$ kJ/kg-K, $v_1 = 0.077$ m^3/kg, $h_a = 206.46$,

$s_a = 0.6863$, $v_a = 0.0161$, $h_3 = 79.9$, $s_3 = 0.2884$ and $c_p = 0.793$ kJ/kg-K

$$T_2 = T_c \exp\left\{\frac{s_1 - s_a}{c_p}\right\} = 318 \exp\left\{\frac{0.7060 - 0.6863}{0.793}\right\} = 326 \text{ K}$$

In Example 3.10, it was 326.024 K.

$$h_2 = 206.46 + 0.793(326 - 318) = 212.804 \text{ kJ/kg}$$

In Example 3.10 it was 212.874 kJ/kg.

Refrigeration effect = $h_1 - h_4 = h_1 - h_3 = 184.22 - 79.9 = 104.32$

$$\dot{m} = \frac{3.51667}{104.32} = 0.0337103 \text{ kg/s}$$

$W = (h_2 - h_1) = 0.0337103(212.804 - 184.22) = 0.9636$ kW

$Q_c = (h_2 - h_3) = 0.0337103(212.804 - 79.9) = 4.48$ kW

$$\text{COP} = \frac{3.51667}{0.9636} = 3.65$$

$$A_1 = h_2 - h_a - T_c(s_1 - s_a) = 212.804 - 206.46 - 318(0.706 - 0.6863)$$
$$= 0.0794 \text{ kJ/kg}$$

In Example 3.10, it was 0.1494 kJ/kg

Throttling loss remains the same as in Example 3.10. $A_2 = 79.9 - 74.332 = 5.568$ kJ/kg

Refrigerating efficiency = $\eta = \dfrac{(\text{COP})_{\text{SSS}}}{\text{COP}_{\text{RC}}} = \dfrac{3.65}{4.78182} = 0.7614$

R22:

The properties from the saturation table for R22 at $T_c = 45^{\circ}$C and $T_e = -10^{\circ}$C are:

$h_1 = 247.37$ kJ/kg, $s_1 = 0.9473$ kJ/kg-K, $v_1 = 0.0654$ m^3/kg, $h_a = 261.95$,
$s_a = 0.8697$, $v_a = 0.0152$, $h_3 = 101.76$, $s_3 = 0.3662$, $h_0 = 34.25$ and
$s_0 = 0.1374$ and $c_p = 0.935$ kJ/kg-K

$$T_2 = T_c \exp\left\{\frac{s_1 - s_a}{c_p}\right\} = 318 \exp\left\{\frac{0.9473 - 0.8697}{0.9335}\right\} = 345.56 \text{ K}$$

In Example 3.10, it was 345.808 K.

$$h_2 = 261.95 + 0.9335(345.56 - 318) = 287.68 \text{ kJ/kg}$$

In Example 3.10, it was 287.914 kJ/kg.

Refrigeration effect = $h_1 - h_4 = h_1 - h_3 = 247.37 - 101.76 = 145.61$

$$\dot{m} = 3.51667/145.61 = 0.0241512 \text{ kg/s}$$
$$W = \dot{m}(h_2 - h_1) = 0.0241512\ (287.68 - 247.37) = 0.9735 \text{ kW}$$
$$Q_c = \dot{m}(h_2 - h_3) = 0.0241512\ (287.68 - 101.76) = 4.49 \text{ kW}$$

$$\text{COP} = \frac{3.51667}{0.9735} = 3.612$$

$$A_1 = h_2 - h_a - T_c(s_1 - s_4)$$
$$= 287.68 - 261.95 - 318(0.9473 - 0.8697) = 1.0532 \text{ kJ/kg}$$

In Example 3.10, it was 1.2872 kJ/kg.

Throttling loss remains the same as in Example 3.10.

$$A_2 = (q_e)_{\text{RC}} - (q_e)_{\text{sss}} = T_e(s_1 - s_{4'}) - (h_1 - h_4)$$

Refrigerating efficiency, $\eta = \dfrac{(\text{COP})_{\text{SSS}}}{\text{COP}_{\text{RC}}} = \dfrac{3.612}{4.78182} = 0.751$

NH_3:

The properties from the saturation table for NH_3 at $t_c = 45^{\circ}$C and $t_e = -10^{\circ}$C are:

$h_1 = 1431.409$ kJ/kg, $s_1 = 5.4712$ kJ/kg-K, $h_a = 1473.03$, $s_a = 4.8201$,
$h_3 = 396.22$ and $c_p = 2.963$ kJ/kg-K, $s_3 = 1.4349$, $s_0 = 0.5435$ and $h_0 = 134.95$

$$T_2 = T_c \exp\left\{\frac{s_1 - s_a}{c_p}\right\} = 318 \exp\left\{\frac{5.4712 - 4.8201}{2.963}\right\} = 396.15 \text{ K}$$

In Example 3.10 it was 396.9 K

$$h_2 = 1473.03 + 2.963(396.15 - 318) = 1704.6 \text{ kJ/kg}$$

In Example 3.10 it was 1703.79 kJ/kg.

Refrigeration effect = $h_1 - h_4 = h_1 - h_3 = 1035.189$

$$\dot{m} = 3.51667/1035.189 = 3.39712 \times 10^{-3} \text{ kg/s}$$

$$W = \dot{m}(h_2 - h_1) = 0.00339712(1704.6 - 1431.409) = 0.928 \text{ kW}$$

$$Q_c = \dot{m}(h_2 - h_3) = 0.00339712(1704.6 - 396.22) = 4.4447 \text{ kW}$$

$$\text{COP} = \frac{3.51667}{0.928} = 3.789$$

$$A_1 = h_2 - h_a - T_c(s_1 - s_4) = 1704.6 - 1473.03 - 318(5.4712 - 4.8201) = 24.52 \text{ kJ/kg}$$

In Example 3.10, it was 23.71 kJ/kg.

Throttling loss remains the same as in Example 3.10.

$$A_2 = (q_e)_{\text{RC}} - (q_e)_{\text{sss}} = T_e(s_1 - s_{4'}) - (h_1 - h_4) = 26.3579 \text{ kJ/kg}$$

Refrigerating efficiency, $\eta = \dfrac{(\text{COP})_{\text{SSS}}}{\text{COP}_{\text{RC}}} = \dfrac{3.789}{4.78182} = 0.792$

REVIEW QUESTIONS

1. Name the various methods of classifying the refrigeration systems.
2. Define the terms ‘refrigeration capacity’ and ‘coefficient of performance’ in relation to a refrigeration system. Why is the term ‘efficiency’ not used to indicate the performance in the case of refrigerators and heat pumps?
3. Differentiate between a heat engine and a refrigerator, using the appropriate schematic and cycle diagrams.
4. Discuss the working of the Reversed Carnot cycle on *T*–*s* diagram, employing perfect gas as the refrigerant.
5. Why is Reversed Carnot cycle not a practical cycle? Explain the modifications done to Reversed Carnot cycle in the Reversed Brayton cycle.
6. In a Reversed Brayton cycle operating on air, the temperature at the exit of refrigerator is –12°C and that at the exit of heat rejection is 25°C. The air at the inlet to the compressor is 1 bar and is compressed to 5 bar. The cooling capacity is 1 TR. Polytropic law $pv^{1.3}$ = constant is followed during compression and expansion.
   Find the states at all points of the cycle, heat transfer and work done in all the processes, mass flow rate, volume flow rates and the COP. Take c_p = 1.005 kJ/kg-K and R = 0.287 kJ/kg-K.

7. Explain the working of the saturated Reversed Carnot refrigeration cycle on *T*–*s* diagram.
8. Compare the performance of standard, saturated, single stage (SSS) vapour compression refrigeration system, using the same *T*–*s* diagram, with that of the Reversed Carnot cycle.
9. Find the end states of isentropic compression between the saturation pressure at –20°C evaporator temperature, state 1, to saturation pressure at 35°C condenser temperature, state 2 for refrigerant $CHClF_2$.
10. Explain the effect of variable suction and discharge pressures on the performance of the standard vapour compression refrigeration system.
11. Discuss the effects of subcooling and superheating on the performance of standard vapour compression system.
12. Describe the actual vapour compression refrigeration cycle on *T*–*s* and *p*–*h* diagrams.
13. The condensing and evaporating pressures in a 10 TR refrigeration system are 11.82 bar and 1.64 bar, respectively. The refrigerant enters the compressor at dry and saturated state and leaves the condenser subcooled by 10°C. The actual COP is 70% of its theoretical value. Determine the mass flow rate, theoretical and actual COPs and the compressor power for a single stage saturation cycle. The properties of R22 are:

p (bar)	t (°C)	h_f (kJ/kg)	s_f (kJ/kg-K)	h_g (kJ/kg)	s_g (kJ/kg-K)
1.64	–30	166.1	0.8698	393.1	1.803
11.82	+30	236.7	1.125	414.5	1.712

14. The condensing and evaporating temperatures in a refrigeration system of 100 TR capacity are –30°C and 30°C. The refrigerant at the suction of compressor is dry and saturated and at the exit of the condenser it is subcooled by 10°C. The actual COP is 80% of the theoretical value. Determine the mass flow rate, actual and theoretical COP and compressor power. The properties of the refrigerant are:

t (°C)	p (bar)	v_g (m^3/kg)	h_f (kJ/kg)	h_g (kJ/kg)	s_f (kJ/kg-K)	s_g (kJ/kg-K)
–30	1.6	0.136	166.2	393	0.87	1.803
30	1.2	0.020	236.8	415	1.13	1.712

15. The condensing and evaporating temperatures in a refrigerating plant of 5 TR capacity working on ammonia, are 40°C and 0°C respectively. Assume the refrigerant to be dry and saturated at the entry to the compressor and the compression to be isentropic. Find the power required to drive the plant and the COP of the unit. What will be the effect on these values if the suction vapour is superheated to 10°C?
16. The condenser and evaporator temperatures are 40°C and –5°C respectively. The liquid is subcooled from 40°C to 30°C in the condenser. The refrigerant used is R134a and the refrigerating effect is 10 TR. Considering SSS cycle, calculate the mass flow rate, volume of vapour handled by the compressor, power requirement and the COP, all for the subcooled cycle.

4

Compressors

LEARNING OBJECTIVES

After studying this chapter the student should be able to:

1. Describe the types of compressors used in refrigeration systems.
2. Understand the thermodynamics of compression.
3. Describe the working principle of the reciprocating compressor.
4. Calculate the volumetric efficiency of an ideal reciprocating compressor with clearance.
5. Discuss the effects of pressure drop, heat transfer, superheating, and leakage on the volumetric efficiency of a reciprocating compressor with clearance.
6. Calculate the power input of an ideal reciprocating compressor and the actual compressor with clearance.
7. Discuss the effects of blowby, kinetic energy, heat transfer, superheat, leakages, speed, etc. on the performance of a real reciprocating compressor.
8. Understand the working principle of hermetic compressors.
9. Describe the types of rotary compressors used in refrigeration systems and discuss their respective working principles.
10. Describe the working principle and characteristics of screw compressors.
11. Explain the working principle of the centrifugal compressor.
12. Analyse the performance of centrifugal compressors using velocity diagrams.
13. Explain the phenomenon of surging in centrifugal compressors.
14. Explain the methods of capacity control of centrifugal compressor.
15. Compare the performance aspects of centrifugal and reciprocating compressors.

4.1 INTRODUCTION

The compressor is said to be the heart of the refrigeration system. It circulates the refrigerant in the system and it raises the pressure of the refrigerant from evaporator pressure p_e to condenser pressure p_c so that vapour can be condensed at the corresponding saturation temperature t_c (high temperature) by rejecting heat to the surroundings, that is, either cold water or air. The compressors can be classified into two types based upon the principle of operation.

1. Positive displacement type
2. Dynamic type.

In a positive displacement type of compressor, a certain volume of vapour is drawn into it and trapped by closing the inlet and outlet valves. The rise in pressure is obtained by mechanically decreasing the volume. The compressed vapour is pushed out when the desired pressure is reached. This type of compressor aspirates the vapour in a certain part of the cycle, compresses it and discharges the vapour in pulses and not in steady flow. This process is used mainly for vapours. These compressors are called positive displacement type since almost all the fluid aspirated is discharged without any leakage to suction side. These compressors typically have low volume flow rates and large pressure ratios.

In a dynamic type of compressor, kinetic energy is imparted by the rotating blades to the fluid in the steady flow process. The kinetic energy is converted into pressure head when the fluid flows through a passage of diverging (increasing) area in flow direction. The passage between blades is also diverging, as a result a part of pressure rise is obtained during flow through blades as well. These compressors can be used for gases as well as liquids. The liquids being almost incompressible, the rise in pressure is usually obtained by this principle in pumps. This can be done in both axial and radial flow, however in all refrigeration applications the dynamic compressors are of the centrifugal type. Axial compressors are used mainly in liquefaction plants for natural gas.

The following three types of positive displacement compressors are commonly used in refrigeration systems.

1. Reciprocating compressor
2. Sliding vane type or fixed vane type rotary compressor
3. Rotary screw type compressor.

4.2 THERMODYNAMICS OF COMPRESSION

The vapour in refrigeration systems is in near saturated state and hence it does not behave like perfect gas and the specific heat ratio c_p/c_v is not constant during the compression process. For gases, c_p/c_v has a fixed value usually denoted by γ which is 1.4 for air. For vapours the specific heat ratio will have different values at evaporator and condenser pressures. The compression of vapour, for this reason is usually described by change in enthalpy and is shown on p–h diagram. However to understand the underlying thermodynamic principle, compression may be assumed to follow polytropic process described by

$$pv^n = \text{constant} = c \tag{4.1}$$

The index of compression n is different from γ. The index n is equal to γ for an adiabatic (no heat transfer) and reversible process, that is, isentropic process. It should be noted that $n \neq \gamma$ for adiabatic process alone, it has to be reversible process as well for $n = \gamma$.

The index n is equal to one for isothermal process. The temperature of gas usually increases during compression; hence for temperature to remain constant during isothermal compression, heat has to be rejected to the surroundings.

The index n lies in the range $1 \leq n \leq \gamma$ for compression with heat rejection. The index n is greater than γ ($n > \gamma$) if heat is added to the gas during compression. In Figure 4.1(a), lines 1–2 and 1–4 show isentropic and isothermal processes respectively. Process 1–3 is for polytropic compression with $n < \gamma$. The process $n = \gamma$ is border line from heat transfer point of view. If the compression process lies to the right of it, then it involves addition of heat during compression. For constant volume compression, the index n approaches ∞. On the other hand, if the compression process lies to the left of $n = \gamma$, then it involves heat rejection during compression.

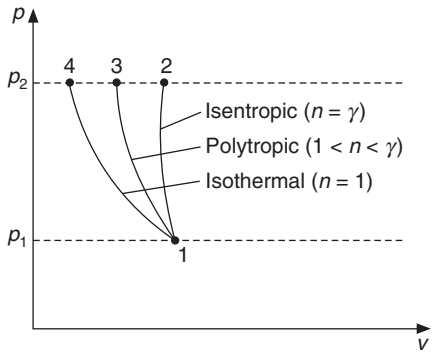

Figure 4.1(a) Pressure–volume diagrams of isentropic, polytropic and isothermal compression processes between the same pressure limits.

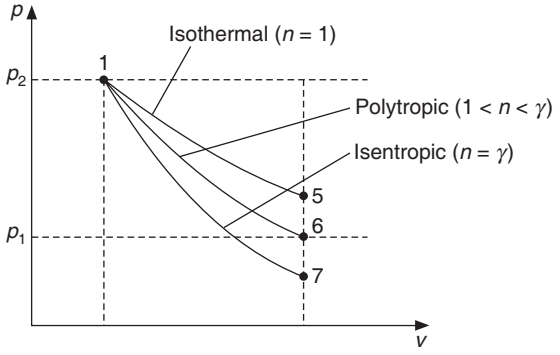

Figure 4.1(b) Pressure–volume diagram of isentropic, polytropic and isothermal expansion processes between the same volume limits.

The situation during expansion as shown in Figure 4.1(b) is directly opposite to that shown in Figure 4.1(a). For gases, the temperature decreases during expansion; hence isothermal expansion would require addition of heat to keep the temperature constant—this is shown by line 1–5 whereas isentropic expansion is shown by line 1–7. The isothermal expansion line lies to the right of isentropic line since it involves heat addition.

The specific compression work for an open system is given by

$$w = -\int_1^2 v\, dp \tag{4.2}$$

This is shown by the shaded area 1–2–*a*–*b*–1 in Figure 4.2(a). The minus sign would give a positive number if expansion occurs. In the present case, compression occurs, that is, work is done on the system and it is negative. For a closed system the specific work is given by

$$w = \int_1^2 p\, dv \tag{4.3}$$

This is shown by the shaded area1–2–*c*–*d*–1 in Figure 4.2(b).

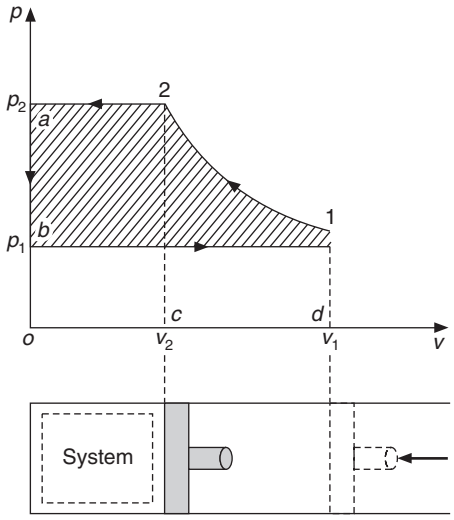

Figure 4.2(a) Pressure–volume diagram of a compression process—work done in an open system.

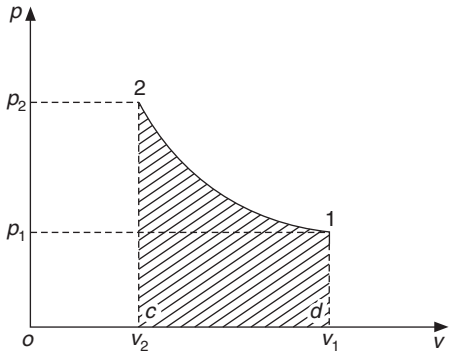

Figure 4.2(b) Work done in a closed system.

The open system such as a compressor requires some work to be done on the system in pushing the vapour into the compressor, that is $-p_1v_1$, and some work is required to push it out, that is p_2v_2,

after it has been compressed. These work requirements are called flow work. When these are included with *pdv* work, we get the expression for an open system as follows:

$$\int_1^2 p\,dv + p_2v_2 - p_1v_1 = \text{Area } 1\text{–}2\text{–}c\text{–}d\text{–}1 + \text{Area } o\text{–}a\text{–}2\text{–}c\text{–}o - \text{Area } o\text{–}d\text{–}1\text{–}b$$

$$= \text{Area } 1\text{–}2\text{–}a\text{–}b\text{–}1 = -\int_1^2 v\,dp$$

The expression for polytropic compression work can be obtained by integrating Eq. (4.2) by substituting for v from Eq. (4.1) as follows:

$$-w_{12} = \int_1^2 v\,dp = c^{1/n}\int_{p_1}^{p_2} p^{-1/n}\,dp = \frac{n}{n-1}c^{1/n}\,[p_2^{(n-1)/n} - p_1^{(n-1)/n}]$$

Substituting $c^{1/n} = p_2^{1/n}v_2 = p_1^{1/n}v_1$ from Eq. (4.1), we get

$$-w_{12} = \frac{n}{n-1}(p_2v_2 - p_1v_1) \tag{4.4a}$$

Again by using Eq. (4.1), Eq. (4.4a) may be reduced to

$$-w_{12} = \frac{n}{n-1}\,p_1v_1\left[\left(\frac{p_2}{p_1}\right)^{(n-1)/n} - 1\right] \tag{4.4b}$$

It can be shown that the work requirement for a closed system is as follows:

$$\int_1^2 p\,dv = -\frac{1}{n-1}\,p_1v_1\left[\left(\frac{p_2}{p_1}\right)^{(n-1)/n} - 1\right] \tag{4.4c}$$

For isothermal compression, substitution of pv = constant in Eq. (4.2) yields

$$-w_{12} = \int_1^2 v\,dp = \int_1^2 \frac{mRT_1}{p}\,dp = p_1v_1\,\ln\left(\frac{p_2}{p_1}\right) \tag{4.5a}$$

The work requirement for a closed system for isothermal compression is as follows:

$$w_{12} = \int_1^2 p\,dv = \int_1^2 \frac{mRT_1}{v}\,dv = -p_1v_1\,\ln\left(\frac{v_1}{v_2}\right) = -p_1v_1\,\ln\left(\frac{p_2}{p_1}\right) \tag{4.5b}$$

It is therefore observed that the isothermal work is same for closed and open systems.

The work done can be represented by the area projected on the *y*-axis, for example, areas 1–2–*b*–*a*–1 and 1–4–*b*–*a*–1 are the work requirements for isentropic and isothermal processes respectively in Figure 4.1. Isothermal compression requires minimum work. Isentropic compression would require more work than isothermal work by an amount equal to area 1–2–4–1, as seen in Figure 4.1. The reciprocating compressor runs at low speed; hence the vapour gets sufficient time for heat rejection to take place, therefore $n < \gamma$ for this class. For some reciprocating compressors cooled by water jacket or air, heat is rejected to the surroundings but some heat is added by friction

between piston and cylinder; as a result the net process may be close to adiabatic (not isentropic since it is not reversible) and $n \approx \gamma$. The centrifugal compressors run at very high speed. The vapour does not get sufficient time for heat rejection. The frictional heating is significant because of high speed; hence this class consists of heating during compression and $n > \gamma$ in this case.

EXAMPLE 4.1 Air is compressed from 300 K and 1.0 bar pressure to a pressure of 5.0 bar. Determine the work requirement for open and closed systems for isentropic compression and for polytropic compression with $n = 1.35$ and $n = 1.1$.

Solution:

We have for perfect gas: $p_1v_1 = RT_1$ and for air $R = 0.2871$ kJ/kg-K and $\gamma = 1.4$

Polytropic compression with $n = 1.35$

$$T_2 = T_1\left(\frac{p_2}{p_1}\right)^{(n-1)/n} = 300(5)^{0.35/1.35} = 455.34 \text{ K}$$

From Eqs. (4.4b) and (4.4c) for open and closed systems, we get

$$\text{Open system: } (w_{12})_{\text{open}} = \left(\frac{1.35}{0.35}\right)0.2871(300)[(5)^{(0.35)/1/35} - 1] = 172.021 \text{ kJ/kg}$$

$$\text{Closed system: } (w_{12})_{\text{closed}} = \frac{172.021}{1.35} = 127.4231 \text{ kJ/kg}$$

$$\text{Total flow work} = p_2v_2 - p_1v_1 = R(T_2 - T_1) = 0.2871(455.34 - 300) = 44.6 \text{ kJ/kg}$$

$$\therefore \quad (w_{12})_{\text{open}} = (w_{12})_{\text{closed}} + \text{flow work} = 127.4231 + 44.6 = 172.0231 \text{ kJ/kg}$$

Polytropic compression with $n = 1.1$

$$T_2 = 300(5)^{0.1/1.1} = 347.267 \text{ K}$$

From Eqs. (4.4b) and (4.4c) for open and closed systems, we get

$$\text{Open system: } (w_{12})_{\text{open}} = \left(\frac{1.1}{0.1}\right)0.2871(300)[(5)^{0.1/1.1} - 1] = 149.275 \text{ kJ/kg}$$

$$\text{Closed system: } (w_{12})_{\text{closed}} = \frac{149.275}{1.1} = 135.705 \text{ kJ/kg}$$

$$\text{Total flow work} = p_2v_2 - p_1v_1 = R(T_2 - T_1) = 0.2871(347.267 - 300) = 13.57 \text{ kJ/kg}$$

$$\therefore \quad (w_{12})_{\text{open}} = (w_{12})_{\text{closed}} + \text{flow work} = 135.705 + 13.57 = 149.275 \text{ kJ/kg}$$

Isentropic compression with $\gamma = 1.4$

$$T_2 = 300(5)^{0.4/1.4} = 475.146 \text{ K}$$

$$\text{Open system: } (w_{12})_{\text{open}} = \left(\frac{1.4}{0.4}\right)0.2871(300)[(5)^{(0.4)/1.4} - 1] = 176.0 \text{ kJ/kg}$$

$$\text{Closed system: } (w_{12})_{\text{closed}} = \frac{176.0}{1.4} = 125.711 \text{ kJ/kg}$$

Isothermal compression:

$$w_{12} = RT_1 \ln (p_2/p_1) = 0.2871(300) \ln (5) = 138.\ 621 \text{ kJ/kg}$$

Observations: The compression discharge temperature T_2 increases as the index n increases.
vdp work increases as the index n increases.
pdv work decreases as the index n increases.
Isothermal work is minimum compared to *vdp* work but not *pdv* work.

4.3 RECIPROCATING COMPRESSORS

A reciprocating compressor is like an IC engine consisting of a piston, a cylinder, a crankshaft, a connecting rod, and suction and discharge valves. Most of the modern compressors are of vertical configuration. The rotating crankshaft moves the piston between two limits in the vertical direction. These are called dead centres, since the piston comes to rest at these locations and reverses its direction once in each revolution. These locations are called top dead centre (TDC) and bottom dead centre (BDC).

The suction and the discharge valves in the compressor, unlike IC engine, are not operated by camshaft. These are actuated by the pressure difference across them. The valves are usually located on a valve plate; on one side of which is the cylinder and on the other side are the suction and discharge manifolds in the cylinder head. In some compressors the suction valve is located on the piston, allowing a larger area for the passage of refrigerant. A larger area results in smaller velocity and lower pressure drop. The flow is also towards the TDC during suction stroke in contrast to reverse flow when the valve is located on the valve plate where the refrigerant flows downwards upon entry. In such a case, only the discharge valve is located on the valve plate.

In reciprocating compressors the cylinder is cooled so that heat is rejected to the surroundings but friction adds heat to the vapour being compressed and hence in some cases the process may be close to adiabatic. All reciprocating compressors are provided with some clearance between the valve plate and the TDC for the following reasons :

1. So that the piston does not hit and damage the valves (the inlet valve is usually mounted towards the cylinder side of the valve plate).
2. To take care of the differential thermal expansion of the piston and cylinder since these are made of different materials.
3. To provide machining tolerances.

The outlet valve is on the manifold side of the valve plate and there are valve passages in the valve plate connecting the discharge valve to the cylinder. The volume of the space between the TDC and the valve plate along with the volume of valve passage is called *clearance volume*. In some compressors, a filler plate is provided between the cylinder head and the valve plate to provide clearance or to increase the clearance volume. At the end of the discharge stroke, some high-pressure refrigerant vapour is trapped in the clearance volume—which is usually a waste. The clearance volume is usually between 4% and 9% of the displacement volume.

The cylinder has suction and discharge manifolds. The condenser pressure, which is the saturation pressure at condenser temperature, depends upon heat transfer characteristics of the condenser. This is the pressure in the discharge manifold. Similarly, the evaporator pressure, which is saturation pressure at evaporator temperature, depends upon heat transfer characteristics of the

evaporator. This is the pressure in the suction manifold. The manifolds are provided so that the valves can open and close against a stable pressure. If the discharge valve is connected to a tube (instead of opening in a manifold) there may be premature opening and closing of the valve.

If the cylinder pressure exceeds the sum of the condenser pressure and the effect of valve springs, the outlet valve will open up, otherwise it will remain closed. Similarly, when the cylinder pressure becomes less than the evaporator pressure, the inlet valve opens up, otherwise the higher pressure on the cylinder side holds the inlet valve tightly against the valve plate keeping it closed. The valves have some inertia, hence opening and closing of a valve takes some time. The pressure of the vapour decreases when it flows through the valve passage and over the valves, to overcome the frictional resistance offered by these. That is, the cylinder pressure will be lower than the suction manifold pressure during the suction stroke. The cylinder pressure will be larger than the discharge manifold pressure during discharge. If we neglect these pressure drops and valve inertia, the p–$\mathbb{V}$ diagram and the working principle of reciprocating compressor may be described as follows.

For illustration purpose the cylinder is taken in horizontal position, actually it is vertically up in most of the compressors. The volume of vapour at TDC is called *clearance volume* $\mathbb{V}_{cl}$ as shown in Figure 4.3. At this position, the discharge valve is open since vapour has been discharged. The suction valve is closed, since the cylinder pressure is greater than p_1. As the crankshaft revolves, the piston moves to the right, the volume available to the vapour increases, vapour expands and the cylinder pressure reduces. The discharge valve closes very near c as the cylinder pressure becomes less than p_2. Both the valves are closed during the process c–d. The vapour trapped in the clearance volume expands and the pressure reduces. The process c–d is called *re-expansion stroke.*

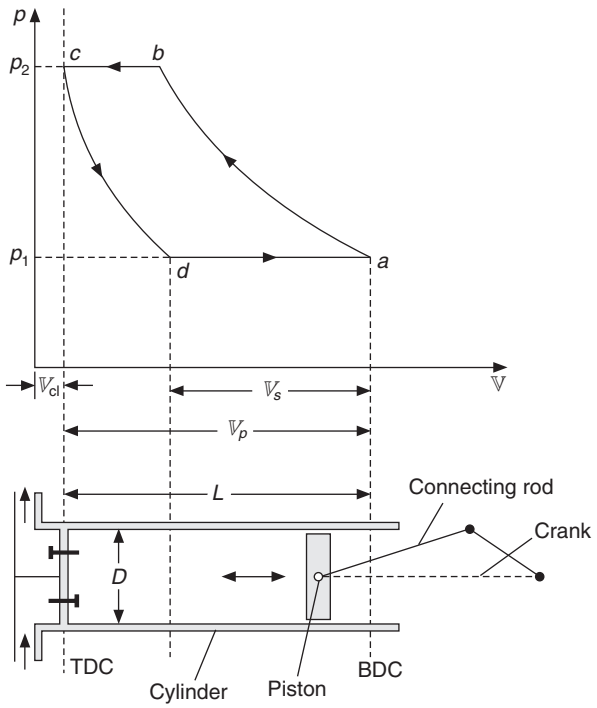

Figure 4.3 Pressure–volume diagram of a reciprocating compressor and its cylinder and piston mechanism.

The expansion continues until at point *d*, the cylinder pressure becomes slightly less than the suction pressure p_1. The suction valve opens, and the refrigerant vapour enters the cylinder. The refrigerant continues to enter the cylinder until the piston reaches the bottom dead center at point *a*. The process *d–a* is called *suction stroke*.

The volume of refrigerant aspirated per cycle is $\mathbb{V}_s = \mathbb{V}_a - \mathbb{V}_d$. This is less than $\mathbb{V}_p$, the volume swept by the piston from TDC to BDC.

The swept volume, $\mathbb{V}_p = \mathbb{V}_a - \mathbb{V}_{cl} = \pi D^2 L/4$, where, *D* and *L* are, bore of piston and stroke length respectively.

It is observed that if the clearance volume is zero, than re-expansion would occur along the *y*–axis at zero volume and the aspirated volume will be same as the swept volume as seen in Figure 4.4 for the ideal compression.

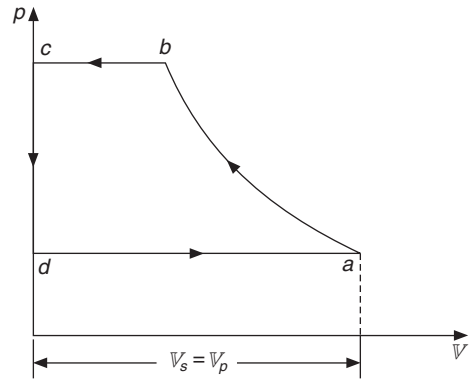

Figure 4.4 Ideal pressure–volume diagram of a reciprocating compressor.

The aspirated volume will be smaller, if the clearance volume is large since the point *d* will shift to the right. The aspirated volume will also decrease if the evaporator pressure is decreased from p_1 to $p_{1'}$ as shown in Figure 4.5.

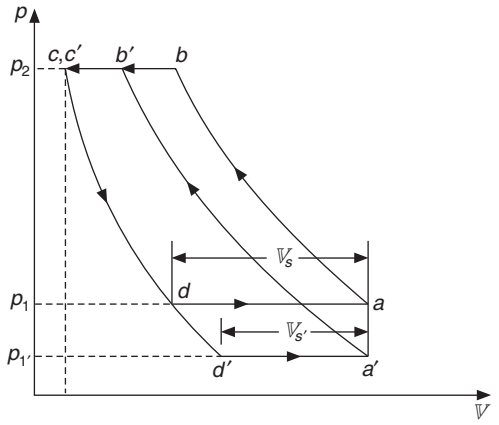

Figure 4.5 Decrease in aspirated volume of a reciprocating compressor with decreasing evaporating (suction) pressure.

Figure 4.6 shows that aspirated volume $\mathbb{V}_s$ decreases as the discharge pressure p_2 is increased to $p_{2'}$ since the point d at which the suction valve opens is shifted to the right at d' thereby decreasing the aspirated volume $\mathbb{V}_{s'} = \mathbb{V}_a - \mathbb{V}_{d'}$.

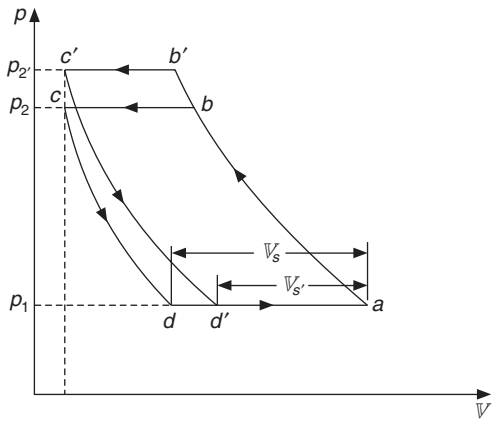

Figure 4.6 Decrease in aspirated volume of a reciprocating compressor with increasing condensing (discharge) pressure.

As the piston moves to the left from BDC at a, the cylinder volume starts to decrease and the pressure increases. The cylinder pressure becomes slightly greater than the suction pressure p_1 very near the point a and the inlet valve closes. Hence, both the valves are closed near a. The motion of the piston from a to b will decrease the volume, and thereby increase the pressure. Thus, the process a–b is called the *compression stroke*.

The cylinder pressure becomes greater than the discharge pressure p_2 very close to the b; hence the discharge valve opens at b. The compressed vapour is discharged to the discharge manifold during b–c. The process b–c is called the *discharge stroke*. Ultimately, at point c, we are left with high-pressure vapour trapped in clearance volume $\mathbb{V}_{cl}$, which re-expands along c–d and the cycle repeats for each revolution. The cycle therefore consists of four strokes as follows:

1. Suction stroke d–a ,
2. Compression stroke a–b,
3. Discharge stroke b–c and
4. Re-expansion stroke c–d.

4.3.1 Volumetric Efficiency

It has been observed that the volume of vapour aspirated $\mathbb{V}_s$, is less than the swept volume $\mathbb{V}_p$, since the vapour trapped in clearance volume expands to $\mathbb{V}_d$ at pressure p_1 before the vapour can enter the cylinder. This is due to the presence of clearance volume; hence this is referred to as *clearance volumetric efficiency*, $\eta_{vol,cl}$.

$\therefore$ $\eta_{vol,cl} = \mathbb{V}_s / \mathbb{V}_p$

We have $\mathbb{V}_s = (\mathbb{V}_a - \mathbb{V}_d)$ and $\mathbb{V}_a = \mathbb{V}_{cl} + \mathbb{V}_p$

$$\therefore \quad \eta_{\text{vol,cl}} = (\mathbb{V}_{\text{cl}} + \mathbb{V}_p - \mathbb{V}_d) / \mathbb{V}_p$$

$$= 1 + \varepsilon - \varepsilon \mathbb{V}_d / \mathbb{V}_{\text{cl}} \tag{4.6a}$$

where, $\varepsilon = \mathbb{V}_{\text{cl}} / \mathbb{V}_p$ is the clearance volume ratio.

Approximate expression for $\eta_{\text{vol,cl}}$

It is observed that during the re-expansion process *c–d* the mass of the vapour remains the same, hence $\mathbb{V}_d / \mathbb{V}_c = \mathbb{V}_d / \mathbb{V}_{\text{cl}} = v_d / v_c$. Therefore,

$$\eta_{\text{vol,cl}} = 1 + \varepsilon - \varepsilon v_d / v_c \tag{4.6b}$$

where, v_d and v_c are the specific volumes of the saturated vapour at evaporator pressure and condenser pressure respectively. This is an approximate expression but it is very useful, since $\eta_{\text{vol,cl}}$ can be calculated from the known values of $v_1 = v_d$ and $v_2 = v_c$ during SSS cycle calculation.

Assuming re-expansion to be polytropic process with polytropic index *m*, we have

$$p_2 \mathbb{V}_{\text{c}}^{\,m} = p_1 \mathbb{V}_d^{\,m} \quad \text{or} \quad p_2 \mathbb{V}_{\text{cl}}^{\,m} = p_1 \mathbb{V}_d^{\,m}$$

$$\therefore \quad (\mathbb{V}_d / \mathbb{V}_{\text{cl}}) = (p_2 / p_1)^{1/m} \tag{4.7}$$

Substitution of Eq. (4.7) in Eq. (4.6a) reduces it to

$$\eta_{\text{vol,cl}} = 1 - \varepsilon \left[(p_2 / p_1)^{1/m} - 1 \right] \tag{4.8}$$

The clearance volumetric efficiency therefore decreases,

(i) as the clearance volume ratio ε increases or
(ii) the pressure ratio p_2/p_1 increases or
(iii) the index *m* increases.

It was observed in Figures 4.5 and 4.6 that the aspirated volume decreases as the evaporator pressure decreases or the discharge (condenser) pressure increases. The same result is observed from Eq. (4.8).

Figure 4.7 shows the limiting case of low pressure $p_{1'}$ at which the volumetric efficiency becomes zero. The vapour trapped in the clearance volume expands and occupies the whole of

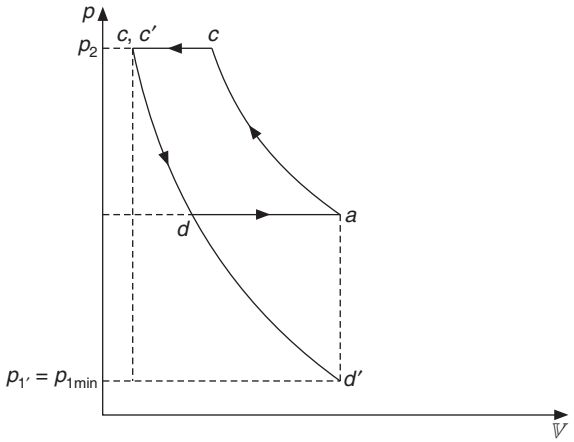

Figure 4.7 Decrease in volumetric efficiency of a reciprocating compressor with decreasing suction pressure.

swept volume leaving no scope for the fresh vapour to enter the compressor. The pressure ratio corresponding to zero volumetric efficiency is given by

$$\eta_{vol,cl} = 0.0 : \text{at } (p_2/p_1)_{max} = (1 + 1/\varepsilon)^m \tag{4.9}$$

When a refrigeration system is assembled or after repairs the air and moisture has to be removed from the system by evacuating the system, the service valve on the discharge side of the compressor is opened to the atmosphere and the compressor is run. The compressor removes the water vapour and air from the system, and in this process the suction pressure decreases, while the discharge pressure remains constant at atmospheric pressure. The suction pressure continues to decrease until the volumetric efficiency reduces to zero. The limiting value of the suction pressure is given by

$$p_{1\ min} = p_{atm} / (1 + 1/\varepsilon)^m \tag{4.10}$$

Hence, the minimum pressure that can be achieved if a reciprocating compressor is used as a vacuum pump is also obtained from this expression. After the compressor has achieved this vacuum, a vacuum pump is connected to the refrigeration system to further evacuate it before charging it with the refrigerant.

EXAMPLE 4.2 Determine the variation in clearance volumetric efficiency with pressure ratio and polytropic index of a reciprocating compressor with a clearance ratio of 0.04, taking pressure ratios of 4, 6 and 8, and m = 1.0, 1.1, 1.3 and 1.4. Also find the pressure ratios at which the volumetric efficiency reduces to zero.

Solution:

Equation (4.8) will be used for calculations.

m = 1.0:

$$p_2 / p_1 = 4,\ \eta_{vol,cl} = 1.04 - 0.04(4) = 0.88$$

$$p_2 / p_1 = 6,\ \eta_{vol,cl} = 1.04 - 0.04(6) = 0.8$$

$$p_2 / p_1 = 8,\ \eta_{vol,cl} = 1.04 - 0.04(8) = 0.72$$

From Eq. (4.9), $\eta_{vol,cl} = 0.0$ at $p_2 / p_1 = (1 + 1/\varepsilon)^m$

$$\therefore \quad p_2 / p_1 = (1.0 + 1.0/0.04)^1 = 26$$

m = 1.1:

$$p_2 / p_1 = 4\ ,\ \eta_{vol,cl} = 1.04 - 0.04(4)^{1/1.1} = 0.899$$

$$p_2 / p_1 = 6\ ,\ \eta_{vol,cl} = 1.04 - 0.04(6)^{1/1.1} = 0.836$$

$$p_2 / p_1 = 8\ ,\ \eta_{vol,cl} = 1.04 - 0.04(8)^{1/1.1} = 0.775$$

$$\eta_{vol,cl} = 0.0 \text{ at } p_2 / p_1 = (1 + 1/\varepsilon)^m$$

$$\therefore \quad p_2 / p_1 = (1.0 + 1.0/0.04)^{1.1} = (26)^{1.1} = 36.01$$

The values of volumetric efficiency for other values of m are summarized in Table 4.1.

Table 4.1 Variation in clearance volumetric efficiency with pressure ratio and polytropic index of a reciprocating compressor

Polytropic index, m	*Clearance volumetric efficiency,* $\eta_{vol,cl}$			*Pressure ratio,* $(p_2/p_1)_{max}$ *for* $\eta_{vol,cl} = 0$
	$(p_2/p_1) = 4$	$(p_2/p_1) = 6$	$(p_2/p_1) = 8$	
1.0	0.88	0.8	0.72	26
1.1	0.899	0.836	0.775	36.01
1.3	0.9238	0.8813	0.842	69.1
1.4	0.932	0.896	0.863	95.7

It is observed that isothermal compression ($m = 1$) has the lowest volumetric efficiency and volumetric efficiency is maximum for $m = 1.4$. Ammonia compressors have $m \approx 1.3$ whereas for CFCs $m \approx 1.1$, hence ammonia compressors will have better clearance volumetric efficiency compared to compressors using CFCs.

4.3.2 Effect of Pressure Drops on Volumetric Efficiency

In actual compressors there is some pressure drop as the vapour flows through the valve passage and over the valves as shown in Figure 4.8. As a consequence of this, the cylinder pressure p_D is more than the discharge manifold pressure p_2 during the discharge stroke. Similarly, during the suction stroke the cylinder pressure p_S is less than the suction manifold pressure p_1, otherwise the vapour cannot flow into the compressor. Apart from this, the suction and discharge valves have some inertia due to which these take some time to open and close. The suction valve begins to open at point d and by the time it is fully open at d' the cylinder pressure decreases to a value even lower than p_S due to expansion. After this, pressure recovery takes place and the pressure returns to the value p_S. The hump d–d'–d'' is due the suction valve inertia. Similarly the discharge valve

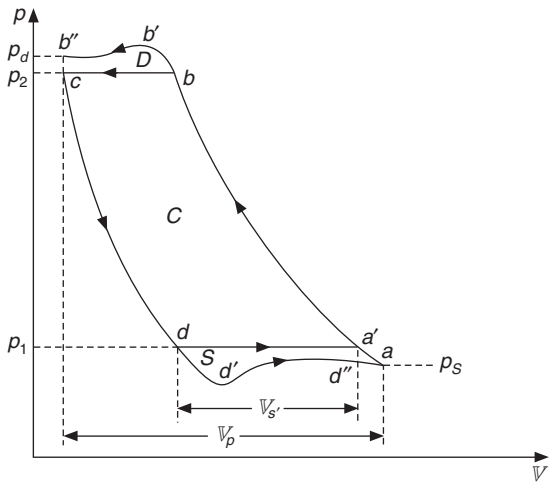

Figure 4.8 Effect of valve pressure drops on volumetric efficiency of reciprocating compressor.

begins to open at b and by the time it is fully open at b' the pressure has increased beyond p_D. This is followed by the pressure dropping to the steady value p_D during the discharge stroke. This results in hump b–b'–b'' due to valve inertia. The most adverse effect of suction side pressure drop is the delay in closing of the suction valve. The suction valve closes when the cylinder pressure becomes larger than the suction manifold pressure and this occurs near the point a'. Ideally the suction valve should have closed at point a, that is the beginning of the compression stroke. During the process a–a', as the piston moves forward, some refrigerant vapour is pushed out of the cylinder since the suction valve closes at point a' only. Hence, the aspirated or induced volume per cycle reduces to $\mathbb{V}_{a'} - \mathbb{V}_d$. The aspirated volume is shown by $\mathbb{V}_{s'}$ in Figure 4.8. The volumetric efficiency due to combined effects of pressure drop and clearance volume is derived as follows:

$$\eta_{\text{vol,cl},\Delta p} = \mathbb{V}_{s'} / \mathbb{V}_p \tag{4.11a}$$

We have $$\mathbb{V}_{s'} = \mathbb{V}_{a'} - \mathbb{V}_d ; \; \mathbb{V}_{a'}\mathbb{V}_d = (\mathbb{V}_{a'} / \mathbb{V}_a)/(\mathbb{V}_a / \mathbb{V}_p)$$

$$\eta_{\text{vol,cl},\Delta p} = (\mathbb{V}_{a'} - \mathbb{V}_d)/\mathbb{V}_p = (\mathbb{V}_{a'} / \mathbb{V}_a)/(\mathbb{V}_a / \mathbb{V}_p) - (\mathbb{V}_d / \mathbb{V}_{\text{cl}})\,(\mathbb{V}_{\text{cl}} / \mathbb{V}_p) \tag{4.11b}$$

$$\mathbb{V}_a / \mathbb{V}_p = (\mathbb{V}_p + \mathbb{V}_{\text{cl}})/\mathbb{V}_p = 1 + \varepsilon \tag{4.12a}$$

The polytropic index of compression is assumed to be n, which is different from the polytropic index of re-expansion m .

Hence, $$p_a \mathbb{V}_a^n = p_{a'} \mathbb{V}_{a'}^n \quad \text{or} \quad p_S \mathbb{V}_a^n = p_1 \mathbb{V}_{a'}^n \quad \text{or} \quad \mathbb{V}_{a'} / \mathbb{V}_a = (p_S / p_1)^{1/n} \tag{4.12b}$$

Similarly, $$p_D \mathbb{V}_a^m = p_D \mathbb{V}_{\text{cl}}^m = p_1 \mathbb{V}_d^m \quad \therefore \quad (\mathbb{V}_d / \mathbb{V}_{\text{cl}}) = (p_P / p_1)^{1/m} \tag{4.12c}$$

Substituting Eqs. (4.12a), (4.12b) and (4.12c) in Eq. (4.11b), we get

$$\eta_{\text{vol,cl},\Delta p} = (1 + \varepsilon)\,(p_S/p_1)^{1/n} - \varepsilon\,(p_D/p_1)^{1/m} \tag{4.13}$$

It is observed that in the limit of zero pressure drops $p_S \to p_1$ and $p_D \to p_2$ and the above expression reduces to the clearance volumetric efficiency given by Eq. (4.8).

4.3.3 Effect of Heat Transfer

The re-expansion processes are shown in Figure 4.9. The temperature decreases during expansion, hence if the temperature is to be kept constant during expansion then heat has to be added during this process. The index m is equal to unity along this process. This isothermal expansion is shown by line 1–2 in Figure 4.9. Isothermal expansion lies to the right of the isentropic expansion process 1–3 during which the heat transfer is zero. The index $m = \gamma$ along the isentropic expansion process. The processes to the right of the line 1–3, involve heat addition and the processes to the left of this line involve heat rejection. A typical polytropic process with $\gamma > m > 1$ is shown by line 1–4 while a process with $m > \gamma$ is shown by line 1–5 in Figure 4.9.

It is observed that the volume at the end of isothermal expansion is maximum and minimum for cooling of gas during expansion, that is, process 1–5. The aspirated volume will be minimum for the isothermal process and maximum for a process like 1–5. The volumetric efficiency will also exhibit the same trend.

As the vapour is compressed its temperature increases along the compression stroke a–b, the cylinder walls also get heated up (see Figure 4.3). The cylinder walls are therefore cooled by water flowing through a jacket around cylinder walls in case of NH_3 compressor and by forced/free

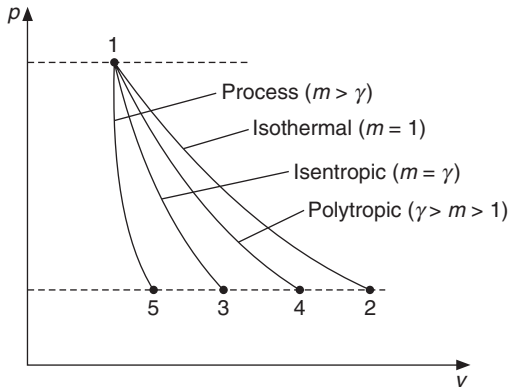

Figure 4.9 Effect of heat transfer on re-expansion curves of a reciprocating compressor.

convection by air in case of freon compressors. Fins are provided on the outer surface of the compressor in case it is air-cooled. The viscosity of lubricating oil decreases at higher temperatures, and at very high temperatures it may start fuming which causes de-carbonization that makes the valves sticky. Therefore, the cooling of the cylinder improves lubrication and at the same time reduces the cylinder wall temperature.

During the compression stroke, the vapour is usually at a higher temperature than the walls; hence heat is rejected during compression. The adiabatic temperature rise is more for NH_3 than that for freons, since specific heat ratio is larger ($\gamma \approx 1.3$) for NH_3 than for freons ($\gamma \approx 1.1$). On the other hand, some heat is added to the vapour due to friction. It might so happen that for freons the heat added by friction may be almost equal to heat rejected by convection, as a result the process may be approximated by adiabatic process (not isentropic process?) The polytropic index of compression n in such a case will be around γ. For NH_3 compressors there is always heat rejection from the cylinder walls hence the polytropic index of compression $m < \gamma$.

At the end of the discharge stroke, point c in Figure 4.3, the vapour is still at a temperature higher than that of the walls, so that when the re-expansion c–d starts, heat is rejected from vapour to the walls. As a result, the index $m > \gamma$ and the line is steeper than the isentropic line, that is, it lies to the left of the isentropic line. As the expansion proceeds, the vapour temperature decreases and approximately half way through the expansion process, it becomes less than the cylinder wall temperature. From this point onwards, heat is transferred from cylinder walls to the vapour. The expansion process will lie to the right of the isentropic process, that is, it is less steeper than isentropic process and $m < \gamma$. As a result of this reversal in heat transfer rate, the net heat transfer may be zero for the total re-expansion process and the end points may be approximated by an adiabatic process with $m = \gamma$. The reader is referred to Chlumsky [1965] for further details of the effect of heat transfer on volumetric efficency.

The value of $\gamma \approx 1.3$ for NH_3 and 1.1 for freons, hence freons will occupy larger volume $\mathbb{V}_d$ at the end of re-expansion stroke leading to a lower volumetric efficiency compared to that of NH_3 compressors. As a design criterion, the clearance volume is therefore kept very small for freon compressors due to this reason.

4.3.4 Effect of Superheating and Leakage on Volumetric Efficiency

Superheating effect

The vapour leaving the evaporator and entering the suction flange of the compressor is at low temperature. The cylinder head, walls and valves all are at higher temperature, hence the vapour gets heated up as it enters the manifolds, flows over the valves and enters the cylinder. The mass of the vapour in the aspirated volume $\mathbb{V}_s$ will be smaller at higher temperatures because of the lower density compared to that at lower temperatures. A well cooled-cylinder will aspirate more mass of vapour than a heated cylinder. Maximum possible mass will be aspirated if the density of suction vapour is same as that at suction flange of compressor. The vapour entering the cylinder gets superheated, hence this reduction in aspirated mass is called the *superheating effect.* To account for this effect, the *overall volumetric efficiency* is defined in terms of mass flow rate as follows:

$$\eta_{\text{vol,o}} = \frac{\text{mass delivered by the compressor per cycle}}{\text{mass of the vapour in swept volume at the suction flange condition}} \tag{4.14}$$

If v_1 and v_a are the specific volumes at the suction flange and at the end of suction stroke, the aspirated mass is equal to $\mathbb{V}_{s'}/v_a$ and the overall volumetric efficiency is

$$\eta_{\text{vol,o}} = \frac{\mathbb{V}_{s'}}{v_a} \Big/ \frac{\mathbb{V}_p}{v_1} = \frac{\mathbb{V}_{s'}}{\mathbb{V}_p} \Big/ \frac{v_1}{v_a} \tag{4.15}$$

The leakage past the valves and piston rings is directly proportional to the pressure ratio, that is, the higher the pressure ratio the more will be the leakage. It has been observed that as a thumb rule, that the leakage reduces the volumetric efficiency by the same percentage as does the pressure ratio. Hence, the expression for volumetric efficiency reduces to

$$\eta_{\text{vol,o}} = \left(\frac{\mathbb{V}_{s'}}{\mathbb{V}_p}\right)\left(\frac{v_1}{v_a}\right) - 0.01\, p_D/p_S$$

Substituting for $\mathbb{V}_{s'}/\mathbb{V}_p$ from Eq. (4.13), we get

$$\eta_{\text{vol,o}} = \left[(1+\varepsilon)\left(\frac{p_S}{p_1}\right)^{1/n} - \varepsilon\left(\frac{p_D}{p_1}\right)^{1/m}\right]\left(\frac{v_1}{v_a}\right) - 0.01\,\frac{p_D}{p_S} \tag{4.16}$$

Evaluation of volumetric efficiency from this expression requires the values of specific volumes v_1 and v_a which can be obtained only from experimental data. Hence one resorts to experimental data to specify volumetric efficiency. Equation (4.16) is, however, useful in indicating the characteristic trends of its dependence on various parameters.

Hence, the volumetric efficiency of a reciprocating compressor is less than 100% due to the following reasons:

1. Clearance volume
2. Pressure drops
3. Superheating effect
4. Leakages.

A few empirical expressions have been developed for the volumetric efficiency. Pierre (1958) has reported that for R12 compressors the refrigeration capacity within ±10% is given by

$$Q_e = [(890 - 6.6t_c)\, p_1 - 180]\, \mathbb{V}_S \ \text{kW/m}^3 \tag{4.17}$$

where, t_c is the condenser temperature in °C and p_1 is the evaporator pressure in bar.

This correlation is based upon experimental results of about 150 compressors in the cooling range of 1–60 kW with no subcooling and a temperature of 18°C at suction. An expression for volumetric efficiency deduced from this correlation is as follows:

$$\eta_{\text{vol,o}} = 0.948 - 0.0285(p_2/p_1) \tag{4.18}$$

Löffler (1941) observed from experimental data on NH_3 compressors that the average value of m is 1.15 provided that the vapour at entry is superheated by 5 K, and water from condenser outlet enters the compressor jacket. If colder water is used, then $m = 1.15$ for superheat of 10–15 K. The correlation for volumetric efficiency is as follows:

$$\eta_{\text{vol,o}} = 1 + \varepsilon - \varepsilon\left(\frac{p_2}{p_1}\right)^{1/1.15} - K\left[\left(\frac{p_2}{p_1}\right)^{0.17} - 1.0\right] \tag{4.19}$$

$$K = \frac{6.95}{(D)^{0.36}\,(L)^{0.168}\,(N)^{0.24}}$$

where, D and L are in cm and N is in rpm.

4.3.5 Power Requirement

The area of humps (Figure 4.8) due to valve inertia is very small, hence the work required for these may be neglected and a simple p–$\mathbb{V}$ diagram shown in Figure 4.3 between the suction and discharge pressures $p_S(p_1)$ and $p_D(p_2)$ may be considered for evaluation of work requirement.

The work requirement for an open system is given by $W = -\int \mathbb{V}\, dp$, the work done by the system is considered to be positive and the work done on the system is considered to be negative. Hence for the cycle, the net work is the algebraic sum of the work done in compression stroke and that in re-expansion stroke. Therefore,

$$-W = \int_a^b \mathbb{V}\, dp + \int_c^d \mathbb{V}\, dp \tag{4.20}$$

Substituting for the integrals from Eq. (4.4b) with n and m as polytropic indicies of compression and expansion respectively,

$$-W = \frac{n}{n-1}(p_b \mathbb{V}_b - p_a \mathbb{V}_a) + \frac{m}{m-1}(p_d \mathbb{V}_d - p_c \mathbb{V}_c) \tag{4.21}$$

$$-W = \frac{n}{n-1} p_S \mathbb{V}_a \left[\left(\frac{p_D}{p_S}\right)^{(n-1)/n} - 1\right] - \frac{m}{m-1} p_S \mathbb{V}_d \left[\left(\frac{p_D}{p_S}\right)^{(m-1)/m} - 1\right] \tag{4.22}$$

In case, the polytropic index of compression is equal to the polytropic index of expansion, that is, $m = n$, Eq. (4.22) reduces to

$$-W = \frac{n}{n-1} p_S (\mathbb{V}_a - \mathbb{V}_d) \left[\left(\frac{p_D}{p_S} \right)^{(n-1)/n} - 1 \right] \text{ kJ/cycle} \tag{4.23}$$

where the pressure is in kPa.

The negative sign indicates that the net work is done on the system. If the reader is familiar with the sign convention then the negative sign can be omitted too.

Equation (4.23) gives the appearance that the net work is done during the compression stroke on only the aspirated volume. On the other hand, the first term in Eq. (4.22) is the work done on volume $\mathbb{V}_a$ (sum of clearance volume and the aspirated vapour) during compression stroke, while the second term is the work recovered from the clearance vapour during the re-expansion stroke. Therefore, the assumption $m = n$ implies that the work done on the clearance vapour during the compression stroke, is exactly recovered during the re-expansion stroke.

The aspirated volume $\mathbb{V}_s = \mathbb{V}_a - \mathbb{V}_d = \eta_{\text{vol,cl}} \mathbb{V}_p$. Hence, the expression (4.23) for work requirement reduces to

$$-W = \frac{n}{n-1} p_S \mathbb{V}_p \eta_{\text{vol,cl}} \left[\left(\frac{p_D}{p_S} \right)^{(n-1)/n} - 1 \right] \text{ kJ/cycle} \tag{4.24}$$

If we substitute the simplest expression for volumetric efficiency that is, the clearance volumetric efficiency given by Eq. (4.6), we get

$$-W = \frac{n}{n-1} p_S \mathbb{V}_p \left[1 - \varepsilon \left[\left(\frac{p_2}{p_1} \right)^{1/m} - 1 \right] \right] \left[\left(\frac{p_D}{p_S} \right)^{(n-1)/n} - 1 \right] \text{ kJ/cycle} \tag{4.25}$$

Mass of refrigerant aspirated per cycle

The mass at the beginning of the suction stroke is the vapour which was trapped in the clearance volume and is equal to $\mathbb{V}_d/v_d$, v_d being the specific volume at the end of the re-expansion stroke. The mass at the end of the suction stroke is $\mathbb{V}_a/v_a$. Hence, the mass of refrigerant aspirated or induced per cycle, m_{cycle} is the difference between these two amounts, that is,

$$m_{\text{cycle}} = (\mathbb{V}_a/v_a - \mathbb{V}_d/v_d)$$

If the suction stroke is assumed to be isothermal apart from being isobaric, then

$$v_a = v_d$$

$$\therefore \quad m_{\text{cycle}} = (\mathbb{V}_a - \mathbb{V}_d)/v_a \quad \text{kg/cycle} \tag{4.26}$$

If N is the rpm of the compressor crankshaft, then the mass flow rate of refrigerant is given by

$$\dot{m} = \frac{m_{\text{cycle}} N}{60} = \frac{(\mathbb{V}_a - \mathbb{V}_d) N}{60 v_a} \text{ kg/s} \tag{4.27}$$

Substituting for ($\mathbb{V}_a - \mathbb{V}_d$) from Eq. (4.26) in Eq. (4.23), we get

$$-W = m_{\text{cycle}} \frac{n}{n-1} p_S v_a \left[\left(\frac{p_D}{p_S} \right)^{(n-1)/n} - 1 \right] \text{ kJ/cycle} \tag{4.28}$$

or

$$-W = \dot{m} \frac{n}{n-1} p_S v_a \left[\left(\frac{p_D}{p_S} \right)^{(n-1)/n} - 1 \right] \text{ kW} \tag{4.29}$$

Isentropic compression

For single stage saturation cycle with isentropic compression the work requirement was shown to be

$$-W = \dot{m}(h_2 - h_1)_s$$

It may be noted that the index of polytropic compression n is different from specific heat ratio γ. Further, the specific heat ratio for vapours varies with evaporator and condenser temperatures. It does not remain constant along the isentropic process 1–2. However, we seek a simple algebraic relation here, which can be used to understand the basics of the process for manipulation and calculation. It is the isentropic process we are looking at, hence we introduce another index k, which will approximate the isentropic compression. Hence, k may be thought of as an average value of γ for the process. We assume that isentropic process is represented by

$$pv^k = \text{constant}$$

In the integral $\int vdp$ of Eq. (4.29), we replace n by k and put the expression equal to $(h_2 - h_1)_s$, i.e.

$$\frac{k}{k-1} p_S v_a \left[\left(\frac{p_D}{p_S} \right)^{(k-1)/k} - 1 \right] = (h_2 - h_1)_s \tag{4.30}$$

Hence, Eq. (4.30) presents an equation for finding the values of k dependent upon the refrigerant and the evaporator and condenser temperatures. The values of k are usually presented in plots separately for each refrigerant. Alternatively, if the end states p_1, v_1 and p_2, v_2 are known from the SSS cycle calculations, then the value of k can be found from the following relation,

$$k = \frac{\ln (p_2 / p_1)}{\ln (v_1 / v_2)} \tag{4.31}$$

If the value of k is known, it becomes easy to find the isentropic work without looking into superheat tables. Hence the plots of k have been made for different refrigerants at various condenser and evaporator temperatures. The left hand side of Eq. (4.30) has also been plotted for various values of k so that if the value of k is known, then the work requirement can be read from the plot.

Mean effective pressure

The mass flow rate can also be expressed in terms of volumetric efficiency, swept flow rate and specific volume. The specific volume was assumed to remain constant during the suction stroke. If in addition it is assumed to be equal to specific volume at evaporator exit, that is,

$$v_d = v_a = v_1 \quad \text{then} \quad \dot{m} = \eta_{\text{vol}}\, \mathbb{V}_D / v_1$$

The mean effective pressure p_{em} of compressor is defined as the ratio of power required to the swept volume flow rate of compressor. The swept volume and the swept flow rate for the compressor are $\mathbb{V}_D$ and $\mathbb{V}_D N/60$ respectively. Hence,

$$p_{\text{em}} = \frac{k}{k-1} p_S \left[\left(\frac{p_D}{p_S} \right)^{(k-1)/k} - 1 \right] \eta_{\text{vol}} = \eta_{\text{vol}} (h_2 - h_1)_s / v_1 \tag{4.32}$$

To get some idea about the increase in work requirement due to deviations from the ideal cycle, the work requirement of ideal cycle is discussed first, then the implications of the above equation will be discussed.

4.3.6 Power Requirement of Ideal Cycle

The ideal compression cycle has been shown in Figure 4.4 as the one in which the clearance volume is zero and the clearance volumetric efficiency is 100%. The re-expansion work for this cycle is zero. Hence,

$$-W = \frac{n}{n-1} p_S \mathbb{V}_a \left[\left(\frac{p_D}{p_S} \right)^{(n-1)/n} - 1 \right] \text{ kJ/cycle} \tag{4.33}$$

If the rps of the compressor motor is $N/60$, then $N/60$ cycles will occur per second. Multiplication of the above expression by $N/60$ (rps) yields the power requirement in kW, i.e.

$$-W = \frac{n}{n-1} p_S \mathbb{V}_a \left[\left(\frac{p_D}{p_S} \right)^{(n-1)/n} - 1 \right] \frac{N}{60} \text{ kW} \tag{4.34}$$

The mean effective pressure p_{em} of ideal compressor is given by

$$p_{\text{em}} = \frac{n}{n-1} p_S \left[\left(\frac{p_D}{p_S} \right)^{(n-1)/n} - 1 \right] \tag{4.35}$$

The mass flow rate of ideal compressor is given by

$$\dot{m} = \frac{\mathbb{V}_p}{v_1} = \frac{\mathbb{V}_a}{v_1} = \frac{\mathbb{V}_D}{v_1}$$

Another expression for work requirement in terms of enthalpy rise is

$$W = \dot{m} (h_2 - h_1)_s = \frac{\mathbb{V}_p}{v_1} (h_2 - h_1)_s \tag{4.36}$$

Hence another expression for mean effective pressure is

$$p_{\text{em}} = \frac{(h_2 - h_1)_s}{v_1} \tag{4.37}$$

Equating the two expressions,

$$\frac{n}{n-1} p_S \left[\left(\frac{p_D}{p_S} \right)^{(n-1)/n} - 1 \right] = \frac{(h_2 - h_1)_s}{v_1} \tag{4.38}$$

The right hand side is volumic isentropic work requirement, and its trend was discussed in the section on performance of SSS cycle. Likewise, the left hand side of this expression has similar implications. The work requirement of ideal compressor exhibits a maximum as the evaporator pressure (or the suction p_S) decreases. Differentiating Eq. (4.34) w.r.t. p_S and equating it to zero to obtain the conditions for maximum, we get

$$\left(\frac{p_D}{p_S} \right)^{(n-1)/n} = n$$

or

$$\frac{p_D}{p_S} = (n)^{n/(n-1)} \tag{4.39}$$

This is the pressure ratio at which ideal compressor requires maximum power. Differentiation of Eq. (4.34) with respect to p_D does not yield any optimum condition.

4.3.7 Power Requirement of Actual Compressor

The variation of power requirement of an actual reciprocating compressor with evaporator temperature (or the suction pressure) at fixed condenser or discharge pressure as expressed by Eq. (4.25) is shown in Figure 4.10. It is observed that the power requirement is the product of mass flow rate through the compressor and the specific polytropic compression work. The compression work involves the term $[\{p_D/p_S\}^{(n-1)/n} - 1]$, which is zero at $p_S = p_D$ and increases as the suction pressure decreases.

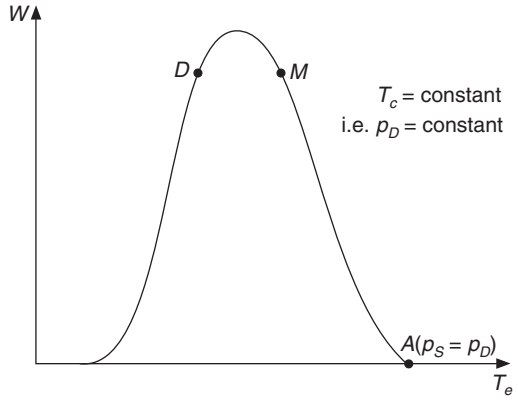

Figure 4.10 Effect of evaporator temperature (or the suction pressure) on the power requirement of an actual reciprocating compressor.

The mass flow rate is dependent upon the volumetric efficiency term which is equal to 1.0 when $p_S = p_D$ and decreases as the suction pressure decreases. The volumetric efficiency becomes zero at $p_S = p_D/(1.0/\varepsilon + 1.0)^n$. Since the power input to the compressor is a product of mass flow

rate and work of compression, it has two zeros and a maximum in between the two zeros. The maximum of this curve occurs at suction pressures corresponding to the evaporator temperature of 0 to 5°C, which is the air-conditioning range of temperatures. The compressors of most of the other refrigeration systems involving lower evaporator temperatures, operate below the peak power requirement of the compressor. That is, the design point *D* lies on the left leg of the curve of Figure 4.10. When the compressor is started with warm evaporator or after pressure balancing ($p_S = p_D$), the compressor starts at point *A* on the right leg of the figure. As the evaporator temperature decreases the power requirement of the compressor increases from *A* to *M* and reaches the peak and then decreases to the design value *D*. The period from starting at *A* and arriving at *D* is called the *pull-down period* and the process is called the *pull-down process*. The passage through the power peak requires a motor of capacity higher than the design value corresponding to *D*. This motor will run most of the time at or near the design power and a few times during pull down it will run at peak power. Hence, it is not economical to use a large motor. The recommended practice is to use a motor corresponding to design power with a thermostatic expansion valve with limit charge which is set to starve the evaporator (reduces the mass flow rate at a pressure larger than that at the design point) temporarily until the system is pulled down through the power peak at a lower mass flow rate thereby drawing less power.

This can also be done by reducing the suction pressure artificially by throttling the suction gas through a hand valve until the evaporator pressure drops below the peak to the design point. This reduces the mass flow rate through the compressor. Once the design temperature is achieved the hand valve is fully opened. Some cylinders of the multiple cylinder compressor may also be cut out by lifting suction valves to achieve this condition at lower power.

Once the design condition has been achieved, there is a possibility that due to variation in refrigeration load, the evaporator temperature and pressure may rise leading to a tendency towards the power peak from *D* to *M* in Figure 4.10. This is avoided by setting the fade-out point of the Thermostatic Expansion Valve (TEV) to occur around *D* so that all the liquid in the feeler bulb evaporates and TEV loses its sensitivity, that is, changes in temperature do not bring about significant changes in pressure. The evaporator pressure is thus controlled to a narrow range around *D*.

It may be remarked that the volumic isentropic work $(h_2 - h_1)_s / v_1$ was also observed to exhibit similar characteristics as discussed in Chapter 3. This was attributed to the significant increase in specific volume v_1 at low evaporator temperatures compared to increase in specific isentropic work $(h_2 - h_1)_s$. For a reciprocating compressor, the power peak is observed due to the fact that volumetric efficiency decreases at a very fast rate at lower evaporator temperatures.

Suction pressure at peak power

For a fixed condenser pressure, differentiating the expression for work and putting it equal to zero, we can find the suction pressure for peak power. We have from Eq. (4.25),

$$W = \frac{n}{n-1} p_S \mathbb{V}_D \left[1 + \varepsilon - \varepsilon \left(\frac{p_D}{p_S} \right)^{1/m} \right] \left[\left(\frac{p_D}{p_S} \right)^{(n-1)/n} - 1 \right] \tag{4.40}$$

We assume $m = n$ and, define $r = p_D / p_S$ and $s = 1/n$, so that

$$\frac{dr}{dp_S} = -\frac{s}{p_S} r^s \tag{4.41}$$

Differentiation of Eq. (4.40) yields

$$s(1+\varepsilon)\, r^{1-s} + \varepsilon\,(1-s)r^{s} - (1+\varepsilon) = 0 \tag{4.42}$$

Rearranging it, we get

$$r^{(n-1)/n} + \frac{\varepsilon}{1+\varepsilon}(n-1)\, r^{1/n} - n = 0 \tag{4.43}$$

The term $\varepsilon/(1+\varepsilon)$ may be neglected for small values of ε. This leads to

$$r = (n)^{n/(n-1)} \tag{4.44}$$

For isothermal process, n =1 and the work requirement is given by

$$-W = p_S \mathbb{V}_D\,(1+\varepsilon-\varepsilon r)\ln r \tag{4.45}$$

Differentiation of Eq. (4.45) w.r.t. to p_S yields

$$\ln r + \varepsilon\, r/(1+\varepsilon) - 1 = 0 \tag{4.46}$$

Discharge pressure at peak power

In a similar manner the power requirement becomes maximum, if the discharge pressure varies for fixed evaporator pressure. This is obtained by differentiating Eqs. (4.40) and (4.45) respectively for polytropic and isothermal processes.

$$\frac{d}{dp_D}\left[(1+\varepsilon)\, r^{1-s} - (1+\varepsilon) - \varepsilon r + \varepsilon r^{s}\right] = 0 \tag{4.47}$$

or $$(1+\varepsilon)(1 - s r^{-s} - \varepsilon + \varepsilon\, s\, r^{s-1} = 0$$

or $$n\left(\frac{\varepsilon}{1+\varepsilon}\right) r^{1/n} - \left(\frac{\varepsilon}{1+\varepsilon}\right) r^{(2-n)/n} - (n-1) = 0 \tag{4.48}$$

Similarly for the isothermal process,

$$\frac{\varepsilon}{1+\varepsilon}\ln r + \frac{\varepsilon}{1+\varepsilon} - \frac{1}{r} = 0 \tag{4.49}$$

Equations (4.48) and (4.49) may be solved by iteration for a given value of clearance volume ratio ε. The optimum values of r are found for different values of n that satisfy these equations. Some solutions for $\varepsilon = 0.4$ and 0.5 are given Table 4.2.

Table 4.2 Pressure ratios for maximum power for four values of index n and two values of clearance volume ratio

	ε	*Optimum* p_D/p_S	n = 1.0	n = 1.1	n = 1.2	n = 1.3
p_D fixed	0.4	p_D/p_S	2.472	2.602	2.731	2.857
p_S fixed	0.4	p_D/p_S	8.333	10.94	14.51	19.44
p_D fixed	0.5	p_D/p_S	2.422	2.55	2.677	2.902
p_S fixed	0.5	p_D/p_S	7.095	9.1	1.8	15.42

It is observed that for fixed discharge pressure, the pressure ratio for peak power occurs in the range of 2.5 to 3.0, occurring at larger values for larger n and at smaller values for larger ε. For fixed suction pressure, the pressure ratio for peak power increases drastically with increase in the value of n, that is, for ammonia it will have a value in the range of 15–20 whereas for R22 it will be around 10.

4.3.8 Real Compressor

Blowby and effect of kinetic energy

The indicator diagram of real compressor is shown in Figure 4.8. This was approximated in Figure 4.3 by neglecting the inertia humps since these do not affect the volumetric efficiency. However, these must be included when the work requirement is considered. It was observed that the point a' does not coincide with the BDC, as a result some vapour between a to a' leaks to the inlet manifold before the inlet valve closes at a'. This is called *blowby*. Further in high speed compressors as the piston comes to rest at BDC the kinetic energy of the vapour will become zero and increase the pressure slightly by $\rho c^2/2$, c being the average piston velocity. This will shift the point a slightly upwards counteracting the effect of a'.

Effect of heat transfer

An examination of the lines of compression and re-expansion strokes in indicator diagram shows that these lines are less steep than the isentopic lines, that is, the values of n for compression stroke and m for re-expansion stroke are both less than k. This is due to heat transfer during these strokes. For CFCs, the difference is not very large but it is significant for NH_3. The value of m is important for volumetric efficiency. Since the indicator diagram shows that the re-expansion line is less steeper than the isentropic line, the suction valve opens later than predicted and the actual volumetric efficiency is less than the predicted.

The effects of heat transfer have already been discussed. In a uniflow compressor the inlet valve is located on the piston. The cold vapour enters through the top of the piston and contacts the lower part of the cylinder walls which have not immediately before been subjected to hot delivery gas. In return flow compressors, the inlet valve is located on the valve plate. The cold vapour enters from the cylinder head and comes into contact with the top part of the cylinder wall which has just been heated by discharge vapour. At one time it was thought that this makes a lot of difference in volumetric efficiency. However, the test results of Bendixen [2] indicate otherwise.

Superheat before entry into compressor

There is some heat transfer from surroundings to the cold vapour in the tube connecting the evaporator to the compressor. Then some heat transfer occurs in the suction manifold as well.

If the suction manifold is separate and bolted to the compressor, then the heat transfer is less. These heat transfer rates decrease the density of the vapour and thereby the volumetric efficiency of the compressor.

The point at which the specific volume v_1 used in Eq. (4.15) is defined, is quite important; for example, is at the suction flange of the compressor or is it at the entry to the cylinder just before the suction valve. This difference is important for hermetic compressor where the vapour is heated after entry into the shell by heat rejection from the compressor and the motor.

Effect of superheat

Experimental results of Giffen et al. [1940] for NH_3 and Gosney [1953] for R12 indicate that the volumetric efficiency continues to increase with superheat. Wirth [1933] suggested that condensation takes place on the cylinder walls towards the end of compression stroke. Figure 4.11 shows the *T–s* diagram for compression with average wall temperature t_w. The vapour enters the cylinder in superheated state 1′ and leaves in state 2′ . The cylinder wall temperature t_w is shown to be less than the outlet temperature $t_{2'}$ and also less than the condenser temperature t_c. This is typically the case of a compressor with water-cooled jacket. The inside wall temperature undergoes cyclic variation but for the metal wall, the fluctuations may not be large. Figure 4.11 also shows the constant pressure line *X–Y* for saturation pressure at temperature t_w. At inlet 1′, the vapour temperature is less than the wall temperature, hence heat is transferred to vapour, therefore its entropy increases near 1′. Beyond point *B*, the vapour temperature is more than the wall temperature, therefore heat is rejected and the entropy decreases. At any point above *X*, the vapour can be cooled along the constant pressure line *X–Y* to its dew point at *Y* and some vapour can condense into liquid state. Hence, although the compression started with superheated state, some liquid refrigerant droplets will appear due to this phenomenon.

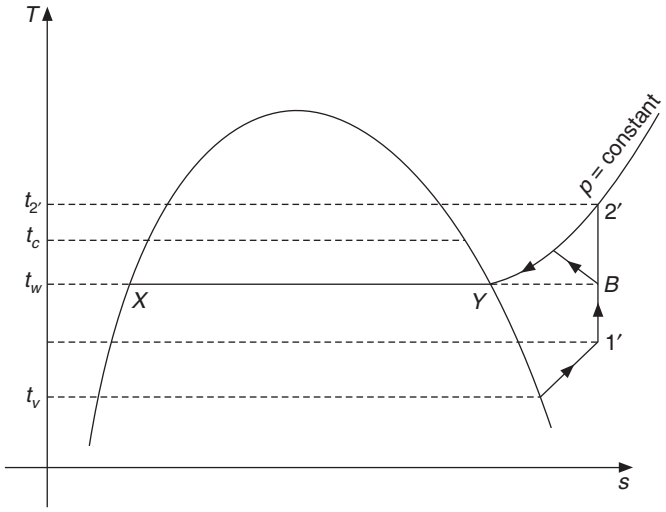

Figure 4.11 Compression of superheated vapour in a compressor with a water-cooled jacket.

The liquid droplets may be dissolved by the lubricating oil for R12 or propane which have very high solubility for the lubricating oil; drain to crankcase and come back to suction side. Or, these may be swept to the clearance volume and left there at the end of the discharge stroke. The liquid droplets will evaporate during the re-expansion stroke occupying more volume at the end of re-expansion stroke, thereby reducing the aspirated volume and reducing the volumetric efficiency. The cooling of vapour produced by evaporation depresses the polytropic index *m*, thus reducing the volumetric efficiency further. This is where the effect of superheat comes in. If the degree of superheat increases at inlet 1′, the wall temperature as well as the temperature at *X* will be large to such an extent that condensation will not occur on the cylinder wall. Hence, the volumetric efficiency

improves with increase in superheat, since less and less of condensation occurs as the degree of superheat increases. In fact, this trend of increase in volumetric efficiency starts with wet vapour as it becomes saturated.

It was pointed out earlier that wet compression should be avoided, since it washes away the lubricant, increasing the wear and tear of compressor and also the liquid refrigerant droplets come out of the cylinder with high velocity like bullets and damage the valves. This was particularly so for high speed compressors where the liquid droplets do not get sufficient time to evaporate. All modern compressors operate with superheat at inlet.

Cheglikov and Brown and Kennedy [1971] have reported the evidence of condensation on cylinder walls.

Effect of leakages

In small compressors, there is no piston ring and clearance of the order of 0.05 mm is kept between the piston and the cylinder with a good supply of oil to prevent leakage. Leakage can also occur across piston rings when the cylinder becomes oval after some use. The refrigerant leaking past piston rings to the crankcase, goes back to the suction side since the crankcase is connected to it via an equalizing port. Some refrigerant dissolved in lubricating oil is also drained to the crankcase. Leakage to suction side occurs when the cylinder pressure is more than the suction pressure. This occurs during compression, discharge and re-expansion strokes. This increases the index of compression n and decreases the index of re-expansion m, and reduces the volumetric efficiency. If the valve surfaces are not good, leakage may occur across the valves.

Effect of speed

As the rpm of the compressor increases, the gas gets less time for heat transfer; the index of re-expansion remains large. The leakages are also small since less time is available. Therefore, the volumetric efficiency increases with increase in speed. However, with increase in speed the mean piston velocity and the average gas velocity increase causing an increase in pressure drops across the valves, which decreases the volumetric efficiency. The leakages also increase due to dynamic effect.

Hence, volumetric efficiency increases and then decreases showing a maximum at a particular speed. Gosney [1982] quotes that higher the molar mass, the lower is the vapour velocity c_{opt} for the optimum speed, that is, $c_{opt}\sqrt{(M \text{ in kg/kmole})} = 420$ m/s.

Deviations from indicated work

In the indicator diagram of Figure 4.8 the area indicated by C (a'–b–c–d–a') has been shown to be given by Eq. (4.25). The areas S (d–d'–a–a'–d) and D (c–b–b'–b''–c) are known to be the *wiredrawing* effects in steam engines. The same terminology is used in compressors too. The area S is the work done in pushing the refrigerant into the compressor and D is the work required to push it out of the compressor with accompanying

(i) pressure drops across the valves, valve passages and in the cylinder and

(ii) valve inertia humps.

Gosney [1982] quotes that the sum of these two areas ($S + D$) divided by the swept flow rate is of the order of 0.05–0.1 bar for ammonia and 0.1–0.15 bar for CFCs, the values being strongly dependent upon speed and valve design.

The work required to overcome the bearing friction, the sliding piston friction, the shaft seal friction and the work for internal oil pump may be represented by w_f. Gosney [1982] quotes that $w_f / \mathbb{V}_S$ is of the order of 0.5–1.0 bar for modern compressors.

Compressor dimensions

It has been a design practice to make the IC engine and the compressor as compact as possible by increasing the speed. For the same refrigeration capacity, that is the swept flow rate, the displacement volume of the compressor can be reduced with increase in speed. This will reduce the cost of manufacture, give a savings in handling, transport, floor space, etc. The areas S and D and other dynamic losses increase with speed, hence it is not possible to increase the speed beyond a certain limit. The mean piston speed is defined by

$$V_p = 2NL/60$$

where L is the stroke and N is the rpm.

V_p used to be approximately 2 m/s, for slow speed large compressors. The compressors with improved designs had 3 m/s and the modern compressor have around 4 m/s.

Since the swept volume is to be kept high, one way to reduce the speed is to reduce the stroke length L or the stroke/bore ratio. The stroke is nowadays less than the bore of the cylinder. Another way is to provide more number of cylinders, however, this number also cannot be increased beyond 12 or 16. It means that it is not possible to have a single compressor beyond a certain cooling capacity. Some of the commonly used values of L/D are as follows:

Vacuum pumps and high speed compressors	$L/D \leq 0.5$
CFC compressors	$L/D \approx 0.8$
Ammonia compressors	$L/D \approx 1.0$

4.4 HERMETIC COMPRESSORS

In hermetic compressors there is direct drive; hence the shaft is shorter and more rigid, the bearing arrangement is simple and the motor is quieter. The motor and the compressor combination are put inside a welded steel shell. All the tubes in the system are either welded or brazed to avoid leakage of refrigerant. The electrical connections to the motor are through sealed terminals. With this arrangement and the use of shaft seal, the accompanying leakage is avoided. The cooling of motor is a problem in these sealed units. In the earlier designs, the stator was pressed onto the steel shell so that it could lose heat to the surroundings. However, the rotor and the compressor cannot reject heat to the surroundings. Cold suction gas flows over the motor winding and the compressor before entering the compressor.

Obviously, some refrigeration effect is lost and vapour enters the compressor with a large superheat. As the evaporator temperature decreases, the volumetric efficiency decreases and the mass flow of refrigerant rate decreases. This means that it will have lesser capacity to cool the motor and the compressor and there is a possibility of motor burnout. For this reason, a hermetic compressor designed for air-conditioning application and cannot be used for freezing food.

If the temperature control system is poorly designed or ineptly applied or if the compressor is allowed to start too frequently, there is a risk of motor burnout. Once the motor burnout occurs, the whole system gets contaminated requiring thorough cleaning.

Semi-hermetic compressors have bolted cylinder heads to make them accessible for periodic maintenance. Hermetic compressors are available up to 20 TR and semi-hermetic compressors are available in larger capacities. CFCs have affinity to lubricating oil.

During off-cycle, pressure balancing occurs in hermetic compressors; as a result the crankcase pressure is high and the oil is cold. Under these conditions, the refrigerant gets adsorbed on oil surface or dissolves in the lubricating oil, since in hermetic compressors there is direct contact between the two. In open compressors, the refrigerant is above the piston and the oil is below it, hence there is no direct contact. When the compressor is started, a low pressure develops in the crankcase, the adsorbed refrigerant may boil at low pressure and carry away a mixture of oil and refrigerant called *froth* to the compressor and the rest of the system. This phenomenon is called *frothing*. It reduces the volumetric efficiency and the cooling capacity. Frothing can be avoided if a crankcase heater is provided around the casing of an hermetic compressor during off-cycle.

EXAMPLE 4.3 R22 is compressed in a reciprocating compressor from saturation pressure at –15°C to saturation pressure at 45°C. The compressor has four cylinders, each with a bore of 10.0 cm and a stroke of 11.5 cm, clearance volume ratio is 0.04 and it runs at 750 rpm. Find (i) the clearance volumetric efficiency assuming isentropic compression using Eq. (4.6b), (ii) the swept flow rate, (iii) the mass flow rate and (iv) the refrigeration capacity.

Solution:

We have from the saturation table for R22:

t, °C	p, bar	v_g, m^3/kg	h_f, kJ/kg	h_g, kJ/kg	s_g, kJ/kg-K
–15	2.964	0.0777	28.36	245.36	0.9555
45	17.209	0.0133	101.76	261.95	0.8697

We have from the superheat table at 17.209 bar:

Superheat, K	30°C	40°C
v, m^3/kg	0.0161	0.0169
h, kJ/kg	289.87	298.66
s, kJ/kg-K	0.9530	0.9781

The state at inlet to compressor is: $p_1 = 2.964$, $v_1 = 0.0777$, $h_1 = 245.36$ and $s_1 = 0.9555$
Referring to SSS cycle, $p_2 = 17.209$ and $h_3 = 101.76$
For isentropic compression, we interpolate in the superheat table for $s_2 = s_1 = 0.9555$, to obtain

$$t_2 = 45 + 30 + 10(0.9555 - 0.9530)/(0.9781 - 0.9530) = 75 + 10(0.1) = 76°C$$

$$h_2 = 289.87 + 0.1(298.66 - 289.87) = 290.745$$

$$v_2 = 0.0161 + 0.1(0.0169 - 0.0161) = 0.01618$$

We have from Eq. (4.8),

$$\eta_{vol,cl} = 1 + \varepsilon - \varepsilon\,(p_2/p_1)^{1/m}$$

For the re-expansion process $(p_2/p_1)^{1/m} = v_1/v_2 = 0.0777/0.01618$

Hence, $\eta_{vol,cl} = 1.04 - 0.04(0.0777/0.01618) = 0.8479$

We have $d = 10.0$ cm $= 0.1$ m and $L = 11.5$ cm $= 0.115$ m

We have displacement volume = $\mathbb{V}_D = \pi L d^2/4$

Swept flow rate, $\mathbb{V}_S = \mathbb{V}_D \times$ number of cylinders $\times N/60 = 4\pi (0.115)(0.1)^2 (750/60)/4$

$= 0.04516$ m^3/s

Mass flow rate, $\dot{m} = \mathbb{V}_S \eta_{\text{vol,cl}}/v_1 = 0.04516\ (0.8479)/0.0777 = 0.516$ kg/s

Refrigeration effect = $h_1 - h_3 = 245.36 - 101.76 = 143.6$ kJ/kg

Refrigeration capacity = $Q_e = \dot{m}(h_1 - h_3) = 0.516(143.6) = 74.106$ kW = 21.07 TR

EXAMPLE 4.4 In Example 4.3, determine the isentropic index of compression k from the end states of compression and determine the work requirement and volumetric efficiency based upon it and compare the values obtained with the isentropic values. Find the total work and the mean effective pressure as well.

Solution:

We have from Eq. (4.31), $k = \dfrac{\ln (p_2 / p_1)}{\ln (v_1 / v_2)} = \dfrac{\ln (17.209/2.964)}{\ln (0.0777/0.01618)} = 1.121$

From Eq. (4.29) we have for specific work, $w_{12} = \dfrac{k}{k-1} p_S v_a \left[\left(\dfrac{p_D}{p_S} \right)^{(k-1)/k} - 1 \right]$

The pressure is given in bar. We convert it to kPa by multiplying by 100. Therefore,

$$w_{12} = \frac{1.121}{1.121 - 1} 2.964\ (100)(0.0777) \left[\left(\frac{17.209}{2.964} \right)^{(1.121-1)/1.121} - 1 \right] = 44.607 \text{ kJ/kg}$$

The enthalpy after isentropic compression in Example 4.3 was $h_2 = 290.745$ kJ/kg and $h_1 = 245.36$ kJ/kg.

Hence, $w_{12} = (h_2 - h_1)_s = 290.745 - 245.36 = 45.385$ kJ/kg

It is observed that the two values are very close to each other.

$$\eta_{\text{vol,cl}} = 1 + \varepsilon - \varepsilon (p_2 / p_1)^{1/k} = 1.04 - 0.04(17.209/2.964)^{1/1.121} = 0.8479$$

which is exactly the same as in Example 4.3 since we have used $v_1/v_2 = (p_2/p_1)^{1/k}$.
Hence the mass flow rate will remain unchanged.
The empirical expression Eq. (4.18) gives

$$\eta_{\text{vol,o}} = 0.948 - 0.0285(p_2/p_1) = 0.948 - 0.0285(17.209/2.964) = 0.7825$$

This is lower than the other values. This expression is valid for superheat of 18°C, which results in lower value for it.

Work requirement is $W = \dot{m}(h_2 - h_1)_s = 0.516(45.385) = 23.42$ kW

The mean effective pressure is given by Eq. (4.32),

$$p_{\text{em}} = \eta_{\text{vol}}(h_2 - h_1)_s / v_1 = 0.8479(45.385)/0.0777 = 495.26 \text{ kPa}$$

EXAMPLE 4.5 R22 is compressed in a reciprocating compressor from saturation pressure at –15°C to saturation pressure at 45°C. The compressor has four cylinders each with a bore of 10.0 cm and a stroke of 11.5 cm, clearance volume ratio is 0.04 and it runs at 750 rpm. The vapour entering the compressor gets superheated to 15°C outside the evaporator. The pressure drops across the suction and discharge valves are 0.1 bar and 0.15 bar respectively. Find (i) the clearance volumetric efficiency by using the isentropic index, (ii) the swept flow rate, (iii) the mass flow rate, and (iv) the refrigeration capacity and work requirement.

Solution:

The evaporator pressure $p_1 = 2.964$ bar and the condenser pressure $p_2 = 17.209$ bar
From superheat table at 2.964 bar and 15°C: $v_{1'} = 0.0886$, $h_{1'} = 265.54$ and $s_{1'} = 1.0243$
We have from superheat table at 17.209 bar :

Superheat, K	50°C	60°C
v, m^3/kg	0.0177	0.0184
h, kJ/kg	307.31	315.71
s, kJ/kg-K	1.0022	1.0254

For isentropic compression we interpolate in the superheat table for $s_2 = s_{1'} = 1.0243$. Thus, we get

$$t_2 = 45 + 50 + 10(1.0243 - 1.0022)/(1.0254 - 1.0022) = 95 + 10(0.957) = 104.57°C$$

$$h_2 = 307.31 + 0.957(315.71 - 307.31) = 315.31$$

$$v_2 = 0.0177 + 0.1(0.0184 - 0.0177) = 0.01837$$

We have from Eq. (4.31),

$$k = \frac{\ln (p_2 / p_1)}{\ln (v_1 / v_2)} = \frac{\ln (17.209 / 2.964)}{\ln (0.0886 / 0.01837)} = 1.1179$$

From Eq. (4.13),

$$\eta_{\text{vol,cl},\Delta p} = (1 + \varepsilon)\,(p_S/p_1)^{1/n} - \varepsilon\,(p_D/p_1)^{1/m}$$

We have $p_S = 2.964 - 0.1 = 2.864$ bar and $p_D = 17.209 + 0.15 = 17.359$ bar, and we assume $m = n$. Therefore,

$$\eta_{\text{vol,cl},\Delta p} = 1.04(2.864/2.964)^{1/1.1179} - 0.04(17.359/2.964)^{1/1.1179} = 0.81413$$

Neglecting the pressure drops, $\eta_{\text{vol,cl}} = 1.04 - 0.04(0.0886/0.01837) = 0.847$
Empirical expression for η_{vol} in Example 4.4 gave $\eta_{\text{vol.o}} = 0.7825$
From Example 4.3: $\mathbb{V}_S = 0.04516$ m^3/s
Mass flow rate = $\dot{m} = \mathbb{V}_S\, \eta_{\text{vol,cl},\Delta p} / v_{1'} = 0.04516\,(0.81413)/0.0886 = 0.415$ kg/s
Refrigeration effect = $h_1 - h_3 = 245.36 - 101.76 = 143.6$ kJ/kg
Refrigeration capacity = $Q_e = \dot{m}(h_1 - h_3) = 0.415(143.6) = 59.59$ kW = 16.94 TR
Work requirement = $W = \dot{m}(h_2 - h_{1'})_s = 0.415(315.31 - 265.54) = 20.65$ kW
Mean effective pressure = $p_{\text{em}} = \eta_{\text{vol}}\,(h_2 - h_{1'})_s / v_{1'} = 0.81413\,(49.77)/\,0.0886 = 457.33$ kPa

EXAMPLE 4.6 Suppose the evaporator and condenser temperatures are 0°C and 40°C respectively and in case (a) vapour enters the compressor as saturated vapour while in case (b) the vapour enters the compressor at 15°C. All other parameters being the same as in Example 4.4, find all the results as in that example.

Solution:

We have from the saturation table for R22:

t, °C	p, bar	v_g, m³/kg	h_f, kJ/kg	h_g, kJ/kg	s_g, kJ/kg-K
0	4.98	0.0472	46.19	251.12	0.9317
40	15.267	0.0152	95.4	261.38	0.8767

We have from superheat table at 15.267 bar:

Superheat, K	15°C	20°C
v, m³/kg	0.0167	0.0172
h, kJ/kg	275.19	279.61
s, kJ/kg-K	0.9202	0.9332

Case (a):

For isentropic compression we interpolate in the superheat table for $s_2 = s_1 = 0.9317$. Thus, we get

$$t_2 = 40 + 15 + 5(0.9317 - 0.9202)/(0.9332 - 0.9292) = 55 + 5(0.8846)$$

$$h_2 = 275.19 + 0.8846(279.61 - 275.19) = 279.1$$

$$v_2 = 0.0167 + 0.8846(0.0171 - 0.0167) = 0.0171$$

We have from Eq. (4.31),

$$k = \frac{\ln (p_2 / p_1)}{\ln (v_1 / v_2)} = \frac{\ln (15.267/4.98)}{\ln (0.0472/0.0171)} = 1.10336$$

$$\eta_{\text{vol,cl}} = 1.04 - 0.04(0.0472/0.0171) = 0.9296$$

From Example 4.3: $\mathbb{V}_S = 0.04516$ m³/s

Mass flow rate = $\dot{m} = \mathbb{V}_S \, \eta_{\text{vol,cl, }\Delta p} / v_1 = 0.04516\,(0.9296)/0.0472 = 0.8896$ kg/s

Refrigeration effect = $h_1 - h_3 = 251.12 - 95.4 = 155.72$ kJ/kg

Refrigeration capacity = $Q_e = \dot{m}(h_1 - h_3) = 0.8896\,(155.72) = 138.5$ kW = 39.38 TR

Work requirement = $W = \dot{m}(h_2 - h_1)_s = 0.8896(279.1 - 251.12) = 24.89$ kW

Mean effective pressure = $p_{\text{em}} = \eta_{\text{vol}}(h_2 - h_1)_s / v_1 = 0.9296(27.98)/\ 0.0472 = 551.06$ kPa

Also from Eq. (4.29),

$$w_{12} = \frac{1.10336}{1.10336 - 1} 4.98\,(100)(0.0472)\left[\left(\frac{15.267}{4.98}\right)^{(1.10336-1)/1.10336} - 1\right] = 27.76$$

and $(h_2 - h_1)_s = 27.98$. The two results are close to each other.

Case (b):

Next we consider superheat up to 15°C at inlet to compressor.

From superheat table at 4.98 bar and 15°C: $v_{1'} = 0.0508$, $h_{1'} = 261.921$ and $s_{1'} = 0.96985$

We have from superheat table at 15.267 bar:

Superheat, K	30°C	40°C
v, m^3/kg	0.0182	0.0191
h, kJ/kg	288.31	296.84
s, kJ/kg-K	0.9592	0.9832

For isentropic compression we interpolate in the superheat table for $s_2 = s_{1'} = 0.96985$. Thus, we get

$$t_2 = 40 + 30 + 10(0.96985 - 0.9592)/(0.9832 - 0.9592) = 70 + 10(0.4438) = 74.438$$

$$h_2 = 288.31 + 0.4438(296.84 - 288.31) = 292.095$$

$$v_2 = 0.0182 + 0.4438(0.0191 - 0.0182) = 0.0186$$

We have from Eq. (4.31),

$$k = \frac{\ln (p_1 / p_1)}{\ln (v_1 / v_2)} = \frac{\ln (15.267/4.98)}{\ln (0.0508/0.0186)} = 1.11498$$

$$\eta_{\text{vol,cl}} = 1.04 - 0.04(0.0508/0.0186) = 0.93$$

From Example 4.3: $\mathbb{V}_S = 0.04516$ m^3/s

Mass flow rate = $\dot{m} = \mathbb{V}_S \, \eta_{\text{vol,cl, }\Delta p} / v_{1'} = 0.04516\,(0.93)/0.0508 = 0.8267$ kg/s

Refrigeration effect = $h_1 - h_3 = 251.12 - 95.4 = 155.72$ kJ/kg

Refrigeration capacity = $Q_e = \dot{m}(h_1 - h_3) = 0.8267(155.72) = 128.74$ kW = 136.6 TR

Work requirement = $W = \dot{m}(h_2 - h_{1'})_s = 0.8267(292.095 - 261.921) = 24.95$ kW

Mean effective pressure = $p_{\text{em}} = \eta_{\text{vol}}\,(h_2 - h_{1'})_s / v_{1'} = 0.93(30.174)/\,0.0508 = 552.4$ kPa

$$w_{12} = \frac{1.11498}{1.11498 - 1}\, 4.98\,(100)\,(0.0508)\left[\left(\frac{15.267}{4.98}\right)^{(1.11498-1)/1.11498} - 1\right] = 30.04 \text{ kJ/kg}$$

$$(h_2 - h_{1'})_s = 292.095 - 261.921 = 30.174 \text{ kJ/kg}$$

EXAMPLE 4.7 NH_3 is compressed in a reciprocating compressor from saturation pressure at –10°C to saturation pressure at 40°C. The compressor has four cylinders, each with a bore of 10 cm and a stroke of 8 cm, clearance volume ratio is 0.04 and it runs at 750 rpm. Find (i) the clearance volumetric efficiency assuming isentropic compression using Eq. (4.6b), (ii) the swept flow rate, (iii) the mass flow rate and refrigeration capacity.

Solution:

We have from the saturation table for NH_3:

t, °C	p, bar	v_g, m³/kg	h_f, kJ/kg	h_g, kJ/kg	s_g, kJ/kg-K
–10	2.908	0.418	134.95	1431.409	5.4712
40	15.55	0.0832	371.47	1472.02	4.8728

We have from superheat table at 15.55 bar

Superheat, K	60°C	80°C
v, m³/kg	0.108	0.116
h, kJ/kg	1647.9	1700.3
s, kJ/kg-K	5.3883	5.5253

The state at inlet to compressor is: $p_1 = 2.908$, $v_1 = 0.418$, $h_1 = 1431.409$ and $s_1 = 5.4712$

Referring to SSS cycle, $p_2 = 15.55$ and $h_3 = 371.47$

For isentropic compression we interpolate in the superheat table for $s_2 = s_1 = 5.4712$. Thus, we get

$$t_2 = 40 + 60 + 20(5.4712 - 5.3883)/(5.5253 - 5.3883) = 100 + 20(0.605) = 112.1^{\circ}\text{C}$$

$$h_2 = 1647.9 + 0.605(1700.3 - 1647.9) = 1679.61$$

$$v_2 = 0.108 + 0.605(0.116 - 0.108) = 0.11284$$

We have from Eq. (4.8),

$$\eta_{\text{vol,cl}} = 1.04 - 0.04(0.418/0.11284) = 0.892$$

We have $d = 10$ cm $= 0.1$ m and $L = 8$ cm $= 0.08$ m

The empirical expression for volumetric efficiency Eq. (4.19) may also be used. Therefore,

$$K = \frac{6.95}{(10)^{0.36}(8)^{0.168}(850)^{0.24}} = 0.437$$

and

$$\eta_{\text{vol,o}} = 1 + 0.04 - 0.04\left(\frac{15.55}{2.908}\right)^{1/1.15} - 0.437\left[\left(\frac{15.55}{2.908}\right)^{0.17} - 1.0\right] = 0.724$$

The empirical expression gives a lower value than the value given by ideal case.

We have displacement volume = $\mathbb{V}_D = \pi L d^2/4$

Swept flow rate, $\mathbb{V}_S = \mathbb{V}_D \times$ number of cylinders $\times N/60 = 4\pi(0.08)(0.1)^2(750/60)/4 = 0.031416$ m³/s

Mass flow rate, $\dot{m} = \mathbb{V}_S \eta_{\text{vol,cl}} / v_1 = 0.031416\ (0.892)/0.418 = 0.06704$ kg/s

Refrigeration capacity = $Q_e = \dot{m}(h_1 - h_3) = 0.06704(1431.409 - 371.47) = 71.06$ kW

$= 20.2$ TR

Work requirement = $W = \dot{m}(h_2 - h_1)_s = 0.0674(1679.61 - 1431.409) = 16.639$ kW

Mean effective pressure = $p_{\text{em}} = \eta_{\text{vol}}\ (h_2 - h_1)_s / v_1 = 0.892(27.98)/\ 0.418 = 529.65$ kPa

We have from Eq. (4.31),

$$k = \frac{\ln(p_2/p_1)}{\ln(v_1/v_2)} = \frac{\ln(15.55/2.908)}{\ln(0.418/0.11284)} = 1.28033$$

Also from Eq. (4.29),

$$w_{12} = \frac{1.28033}{1.28033 - 1} 4.98\,(100)\,(0.0472)\left[\left(\frac{15.55}{2.908}\right)^{(1.28033-1)/1.28033} - 1\right] = 246.234$$

and $(h_2 - h_1)_s = 248.2$.
The two results are close to each other.

EXAMPLE 4.8 For a four-cylinder ammonia compressor with 10 cm bore and 8 cm stroke running at 750 rpm, the condenser temperature is 40°C. Find the volumetric efficiency, the mass flow rate, the refrigeration capacity and the work requirement for evaporator temperatures of –40, –30, –20, –10, 10 and 20°C and show that the power requirement has a maximum with respect to evaporator temperature.

Solution:

The solution procedure is very similar to that of Example 4.7. As a first step, the values of specific volume, enthalpy and temperature at state 2 are calculated by interpolation in the superheat table. These results are presented in Table 4.3.

Table 4.3 The values of parameters at the end points of isentropic compression in Example 4.8

t_e, °C	p_e, bar	v_1	h_1	s_1	t_2	h_2	v_2
–40	0.717	1.55	1387.15	5.9518	191.17	1881.77	0.1409
–30	1.195	0.963	1403.11	5.776	160.5	1803.84	0.13
–20	1.901	0.624	1417.97	5.6169	134.36	1737.219	0.121
–10	2.908	0.418	1431.409	5.4712	112.1	1679.61	0.11284
0	4.294	0.29	1443.34	5.3368	92.945	1628.922	0.1059
10	6.15	0.206	1453.52	5.2112	73.358	1574.7	0.0983
20	8.574	0.149	1461.81	5.0391	62.63	1543.365	0.09405

Following Example 4.7, the values of various parameters are given in Table 4.4.

Table 4.4 The results for Example 4.8

t_e, °C	$\eta_{vol,cl}$	$\dot{m}$	Q_e, kW	Q_e, TR	W	$\eta_{vol,o}$	$(h_2 - h_1)_s$
–40	0.6	0.01216	12.35	3.51	6.015	0.159	494.62
–30	0.7437	0.02426	25.03	7.12	9.722	0.4286	400.73
–20	0.8337	0.04197	43.92	12.49	13.4	0.6036	319.249
–10	0.892	0.06704	71.06	20.2	16.639	0.724	248.2
0	0.9305	0.1008	108.04	30.72	18.706	0.8107	185.582
10	0.956	0.1458	157.78	44.87	17.67	0.8757	121.18
20	0.977	0.2059	224.52	63.84	16.81	0.9263	81.655

It is observed that the power requirement W is maximum around the evaporator temperature of 0°C. The overall volumetric efficiency given by the empirical expression reduces drastically at –40°C. The mass flow rate and the refrigeration capacity reduce drastically as the evaporator temperature decreases.

EXAMPLE 4.9 Assuming an average piston speed of 4 m/s, stroke-to-bore ratio of 0.8 and rpm of 1440, find the maximum cooling capacity of an eight-cylinder NH_3 compressor operating at evaporator and condenser temperatures of –20°C and 40°C respectively. The volumetric efficiency may be taken to be 0.6.

Solution:

We have from the tabulated data in Example 4.8 at evaporator temperature of –20°C,

$$v_1 = 0.624 \text{ m}^3/\text{kg}, \; h_1 = 1417.97 \text{ kJ/kg}$$

At 40°C, $h_3 = 371.47$ kJ/kg

Average piston speed, $V_p = 2NL \quad \therefore \quad 4 = 2(1400/60)L \quad \therefore \quad L = 0.0833$ m

Given that $L/d = 0.8, \quad \therefore \quad d = 0.0833/0.8 = 0.104$ m

Swept flow rate, $\mathbb{V}_S = \mathbb{V}_D \times$ number of cylinders $\times N/60$

$$= 4\pi\,(0.0833)\,(0.104)^2\,(1440/60)/4 = 0.136 \text{ m}^3/\text{s}$$

Mass flow rate = $\dot{m} = \mathbb{V}_S\, \eta_{\text{vol,cl}} / v_1 = 0.136(0.6)/0.624 = 0.13064$ kg/s

Refrigeration effect = $h_1 - h_3 = 1417.97 - 371.47 = 1046.5$ kJ/kg

Refrigeration capacity = $Q_e = \dot{m}(h_1 - h_3) = 0.13064(1046.5) = 136.7 \text{ kW} = 38.87$ TR

4.5 ROTARY COMPRESSORS

The rotary compressors in common use are of the following three types:

1. Rolling piston or single vane compressor
2. Rotating vane or multiple vane compressor
3. Screw compressors

4.5.1 Rolling Piston Compressor

The rolling piston type compressor consists of a cylinder and a cylindrical steel roller that acts like a piston. The roller is mounted on an eccentric shaft as shown in Figure 4.12. The shaft and the cylinder have the same axis. The roller because of its eccentric shaft makes contact with the cylinder wall at its point of minimum clearance and creates an eccentric cavity between the roller and the cylinder. As the shaft revolves, the roller rolls around the cylinder wall in the direction of shaft rotation, the point of contact *A* moving on the cylinder surface as shown in Figure 4.12(a), (b) and (c) and (d). A spring-loaded blade is mounted in a slot in the cylinder. It makes a firm contact with the roller at all times and divides the eccentric cavity into suction side (left side in the figure) and discharge side. The blade moves in and out of the slot as the roller comes closer or moves away from it. The rotating motion of the roller thus causes a reciprocating motion of the single vane. Since there is only one blade, this compressor is also called the single vane compressor. The suction and discharge ports in the cylinder wall are located on the opposite side of the blade. In Figure 4.12, the suction port is below the blade and the discharge port is above it. It may be observed that suction and discharge vapours are separated by the point of contact of roller with blade at *A*, and the point of contact of roller with cylinder at *B*. Clockwise from *B* to *A* is the suction side and from *A* to *B* is the discharge side. The flow of vapour through the suction and discharge ports is continuous except when the roller itself interrupts the flow at the time when it covers either of the ports.

In Figure 4.12(a) the roller is covering the discharge port, hence there is only low-pressure vapour in the cavity. This is the aspirated volume of refrigerant per cycle. As the roller revolves eccentrically counterclockwise, the point of contact *B* moves to location *C* in Figure 4.12(c) which reduces the volume of vapour and compresses it. In Figure 4.12(b), fresh vapour starts filling the suction side while compression occurs in the space at top. As the revolution of the roller continues the aspirated volume decreases and finally in Figure 4.12(d), it is discharged through the discharge port. It may be noted that the whole cylinder assembly is enclosed in a housing and submerged in a bath of oil. The high-pressure vapour is discharged in the space between the housing and the oil level. It is then taken to the condenser from this place. There is a flapper valve in the discharge passage to prevent back flow. All rubbing surfaces are highly polished and fitted with close tolerances.

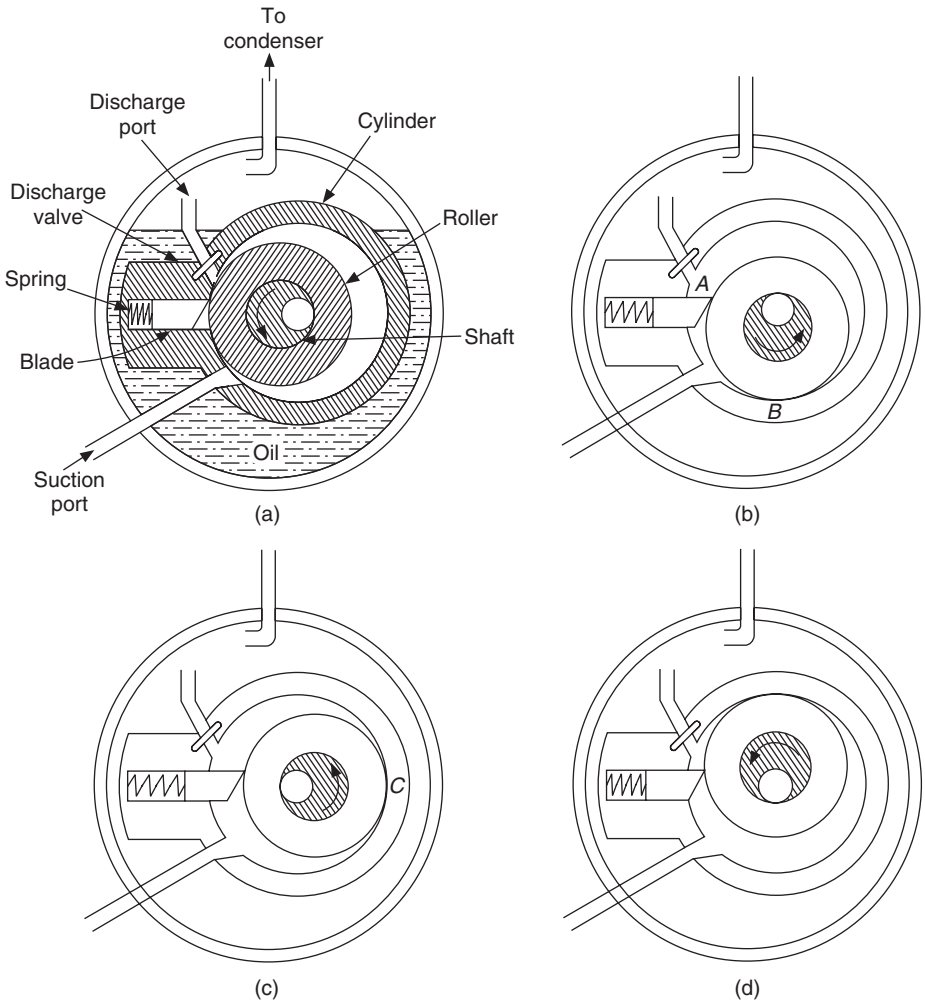

Figure 4.12 Working principle of a rolling piston type rotary compressor.

There will be an oil seal formed (due to an oil film) at the point of contact between the roller and the cylinder, which prevents the leakage of vapour being compressed to the low-pressure side. This seal will not be there during off-cycle when the compressor is not operating. Hence, balancing of pressure will occur between the condenser and evaporator sides during the off-cycle. At the end of delivery some vapour is left in the clearance space, which is at topside of the blade. The suction space is below the blade and it is in the process of being filled when the high-pressure vapour is being discharged, hence the high-pressure clearance volume vapour does not stop the suction vapour from entering the cylinder. This is unlike a reciprocating compressor, where the clearance gas retards the opening of the suction valve.

The high-pressure clearance vapour just mixes with the suction vapour. Further, the volumetric efficiency is not a function of pressure ratio. For this reason, a rotary compressor acts as a better vacuum pump than a reciprocating compressor does.

If d_C and d_R are the cylinder and roller diameters respectively in metre, L the length of the cylinder in metre and N the rotation speed in rpm, then the displacement volume and swept flow rate are given by

$$\mathbb{V}_D = \frac{\pi}{4}(d_C^2 - d_D^2)\, L \ \text{m}^3/\text{s} \tag{4.50}$$

$$\mathbb{V}_S = \frac{\pi}{4}(d_C^2 - d_D^2)\, L \frac{N}{60} \ \text{m}^3/\text{s} \tag{4.51}$$

The rolling piston type compressors have a fixed volume ratio, hence for a given refrigerant these compressors have a fixed pressure ratio depending upon the index of compression.

The rolling piston type compressors are used in small refrigeration systems, refrigerators and freezers up to 5 TR cooling capacity with R12 and R114 with a compression ratio up to 7. As observed there is negligible clearance space, hence the volumetric efficiencies of these compressors are very high.

4.5.2 Rotating Vane or Multiple Vane Compressor

The rotating vane type of rotary compressor consists of a cylinder and an eccentrically mounted slotted rotor. The slotted rotor has two or more sliding vanes, which are held against the cylinder by the action of the centrifugal force developed by the rotating rotor. The eccentric rotor touches the cylinder wall at point *A*. An oil film between the two prevents the leakage. The clearance between the two is maximum at point *B*. In the four-vane compressor shown in Figure 4.13 the volume between the two adjoining vanes is optimum at location when one of the vanes just leaves the suction port. This volume is shown cross hatched in the figure. As the rotor revolves, this hatched volume reduces because of eccentricity of the rotor, and hence the pressure increases. The pressure difference across the vanes is not the total pressure difference but only a part of it, since the pressure increases progressively in the vane spaces. Therefore, the driving force for the leakage past the vanes is small. The contact between the rotor and the cylinder should be good to reduce the clearance volume.

In the two-vane compressor the displacement per revolution is proportional to twice the cross-hatched area and in the four-vane compressor it is proportional to four times the cross-hatched area. The displacement volume increases with the number of vanes.

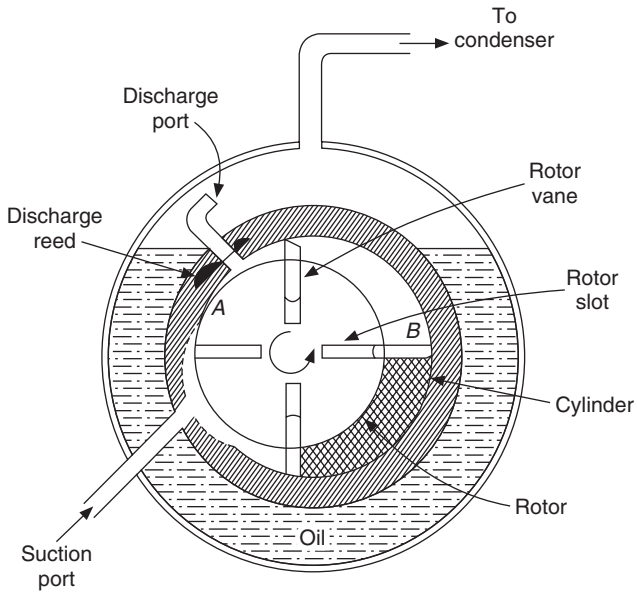

Figure 4.13 Working principle of a multiple vane type compressor.

The vanes are free to move radially inwards and outwards in the slots. They are held firmly against the wall by centrifugal force. The vanes may be spring loaded as well, to obtain a better seal against the cylinder wall.

Rotary compressors, because of rotary motion result in a more uniform flow, have much less vibrations and discharge pulsations that are pronounced in reciprocating compressors. As in the case of reciprocating compressors, rotary compressors also have some volumetric and compression losses. These are due to some back leakages across the vanes and blow-by around the compressing element, cylinder heating, clearance and wire-drawing. However, the clearance volume and its associated re-expansion effects are very small, as a result the volumetric efficiency is very high.

Large multi-vane rotary compressors are widely used with R12, R22 and NH_3 as the low stage or booster compressor in multistage refrigeration systems with suction temperatures ranging from –90°C. These compressors are equipped with water/glycol-cooled jacket or oil cooling to prevent excessive heating. Large compressors have forced lubrication using gear pumps. Although in some cases, oil is cooled by water/glycol oil-coolers in conjunction with evaporative condenser, oil is usually chilled in direct expansion chiller. The capacity of a rotary compressor varies directly with speed. The capacity reduction is also done in some cases by relieving the partly compressed gas from blade pocket to the suction port.

These compressors can provide very large volume flow rates compared to reciprocating compressors for the same physical size since higher speeds are possible. Screw compressors supersede the largest of these compressors.

4.5.3 Screw Compressors

Screw compressors come in two types, namely, the twin-screw compressor and the single-screw compressor. The twin-screw compressor is more popular and is described below.

The twin-screw compressor was developed in 1930 by Lysholm [1943] and became popular in Europe in the 1950s and 1960s. In the early designs, two rotors were geared to each other and no lubrication was provided. These used to run at extremely high speeds. The current practice is to inject oil for cooling and sealing and also, the gears are no longer symmetrical. The working principle is explained below.

These compressors essentially comprise a pair of helical gears with a special tooth profile and a large wrap angle. Wrap angle is the angle through which the radius vector generating the helix rotates from one end to the other end. A large wrap angle gives a large volume ratio.

When two spur gears mesh with each other and rotate in tendon, the contact between their teeth is along a straight line covering the whole length of the teeth.

On the other hand, when two helical gears mesh with each other and rotate, the meshing occurs over a small curved line and the contact area moves along a helix from one end to the other end. If the helical gears are enclosed in a casing and end plates are provided, then it becomes a screw compressor. Suppose some of the flutes of the helical gears are filled with gas. As the gears mesh and rotate, the point of contact moves downwards and the gas filled in the flutes also moves downwards. If there is an end plate at the bottom, then the gas volume between the moving contact point and the bottom end plate decreases, giving rise to an increasing pressure with further movement of the gears. This happens simultaneously in all the flutes with the point of contact at progressively downwards position.

The screw compressor consists of two rotors, a driver called male rotor and a driven rotor called female rotor. These are a pair of helical gears with a special tooth profile and large wrap angle. The male rotor usually has four lobes and the female rotor has six flutes or gullies. This choice gives equal stiffness of rotors in bending and high swept volume. The rotors mesh together in an outer casing, a top plate and a bottom plate where suction and discharge respectively are provided. In Figure 4.14 the male and female rotors are on the left and right side respectively. The lobes are marked I, II ,III and IV. The interlobe spaces are shown by *a*, *b*, *c* and *d* while the flutes on the female rotor are shown by *A*, *B*, *C, D, E* and *F*. The flute *F* is meshed with a lobe in the figure in the front part of the gears and the gas in this space is being compressed. The dashed line

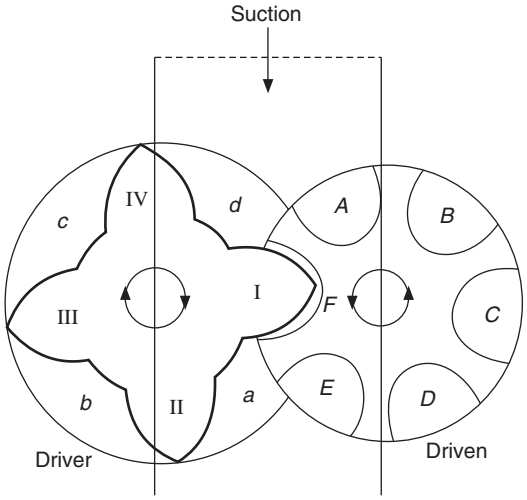

Figure 4.14 Twin-screw compressor with 4 male lobes and 6 female flutes or gullies.

on the top shows the inlet port. The flutes *A, B, C* and *D* and interlobe spaces *a, b* and *c* are being filled with gas in the position shown in the figure. As the gears rotate in the direction indicated in the figure, the flute *A* is cut off from inlet port and comes to the position *E.* The interlobe space *c* moves to the location of *d*. The gas in these spaces in this position is trapped between the two ends plates—a requirement of positive displacement compressor. Further rotation will bring the lobe IV to mesh with flute *E* and compression will begin. In the position shown, the gas in flute *F* is being compressed by lobe I, since it cannot escape above the contact line of helical gears and is restrained at the bottom. The sealing line moves downwards, causing compression by direct volume reduction. The gas moves axially as well as azimuthally along the helix as the enmeshing of lobes progressively reduces the space occupied by the gas. The compression continues until the interlobe space comes across the discharge port. Screw compressor is also a fixed volume ratio and pressure ratio compressor, the volume ratio being a function of compressor design. This fixed pressure ratio is a function of polytropic index of compression and it is called the internal pressure ratio.

These machines operate efficiently when the internal pressure ratio is equal to the system pressure ratio decided by evaporator and condenser temperatures. In practice, it is not possible since the compressor has to work at different condenser and evaporator temperatures during summer and winter. In contrast, in reciprocating compressors, the condenser and evaporator pressures are fed to discharge and suction manifolds and the compressor has the same pressure ratio except for some pressure drops.

If the pressure in the flutes and interlobe spaces has not reached the delivery pipe pressure when the discharge port is opened, the gas from the delivery pipe flows back into the flutes and spaces until the pressure builds up.

Similarly, if the inside pressure is more than the delivery pipe pressure, the gas undergoes a sudden expansion when the discharge port is encountered. Manufacturers usually offer three built-in pressure ratios, for example, a low one for air conditioning, the medium one for ice freezing and refrigeration and the high one for food freezing.

In the axial direction, there is high pressure at the discharge end. Hence the bearing on that side is overloaded. The high pressure may also cause bending of the rotors. Also, the different flutes and interlobe spaces are at different stage of compression. In the figure, the side facing the viewer is under compression whereas the side away from the viewer is not under compression. This causes further unbalanced forces. A slide valve on the casing is provided for capacity reduction.

The earlier versions of screw compressors had dry operation with minimal or no lubrication at all of the rotors. The gears were designed and accurately cut *timing gears*, manufactured in such a way that these did not touch each other. The leakages were very high in these compressors; hence these were run at 5000 to 8000 rpm to obtain sizable flow rates. The gas was effectively cooled during compression because of high velocity. Large pressure ratios could not be achieved. Oil injection in modern compressors has reduced the leakages and now pressure ratios up to 20 can be achieved with NH_3 without exceeding discharge temperature of 100°C, and with satisfactory volumetric efficiency when running at rotor tip speeds of 50–60 m/s. Oil is injected through holes in the slide valve. The bearings are also cooled. At evaporator temperature of –15°C the mass flow rate of oil is about the same as that of ammonia. Hence, an efficient oil separator is required to avoid oil logging of condenser.

In the first twin-screw compressor, the flutes and the lobes were symmetrical. In modern designs, an unsymmetrical profile is used which improves the sealing between flutes and lobes and gives a better volumetric efficiency.

If the male rotor with four lobes rotates at N rpm, then the female rotor with six flutes will rotate with $2N/3$ rpm. Let A_l and A_f be the cross-section areas of each lobe and flute respectively. Let L be the length of the flutes and interlobe passages. Assuming that all the flutes and the lobes are filled with vapour when the compressor is cut-off from the suction port, the swept flow rate is given by

$$\mathbb{V}_S = N(4A_l)L + 6A_f(2N/3)L = 4N(A_l + A_f)L \ \text{m}^3/\text{s} \tag{4.52}$$

Let
$$S = (A_l + A_f)/(\pi D^2/4) \tag{4.53}$$

$\therefore$
$$\mathbb{V}_s = SN\pi D^2 L \tag{4.54}$$

where, D is the diameter of the rotors.

The value of S is usually around 0.155 with asymmetric rotors. The clearance volume at the end of discharge is very small and does not affect the aspirated volume. Hence, the volumetric efficiency is almost constant and we can achieve a higher pressure ratio without loss in volumetric efficiency. In the dry compressor, there is significant leakage which makes the volumetric efficiency depend upon the rotational Mach number. Oil injection gives very good volumetric efficiency, almost independent of the pressure ratio as for other rotary compressors.

Like other rotary compressors, screw compressors also have a fixed built-in volume ratio, say φ. If the index of compression is n, then the built-in pressure ratio is given by

$$R_b = \varphi^n \tag{4.55}$$

The index n depends upon the gas, the inlet conditions and the extent of cooling. If the system pressure ratio is r and the inlet pressure is p_1, then the pressure in the delivery pipe is $p_2 = rp_1$. If the system pressure ratio is less than R_b, then the vapour compressed to rp_1 rushes out in an unrestrained expansion as soon as the outlet port opens. The pressure falls rapidly to p_2 ($r < R_b$).

If the system pressure is more ($r > R_b$) than the built-in pressure ratio, then the system would not reach the pressure p_2 in the delivery pipe when the discharge valve opens. As a result, the gas from the delivery pipe rushes onto the compressor, increasing the pressure in the compressor from $R_b p_1$ to p_2.

The work done from p_1 to p_2 for a pressure ratio R_b, initial pressure p_1 and swept volume $\mathbb{V}_S$ is obtained by using Eq. (4.4b).

$$W' = p_1 \mathbb{V}_S \frac{n}{n-1}[(R_b)^{(n-1)/n} - 1] = p_1 \mathbb{V}_S \frac{n}{n-1}(\varphi^{n-1} - 1) \tag{4.56}$$

The work required to increase the pressure ratio of compressed volume $\mathbb{V}_S/\varphi$ from pressure $R_b p_1$ to p_2 is given by

$$W'' = (p_2 - R_b p_1)\mathbb{V}_S/\varphi = p_1(r - R_b)\mathbb{V}_S/\varphi \tag{4.57}$$

The total work is

$$W' + W'' = p_1 \mathbb{V}_S \left[\frac{n}{n-1}(\varphi^{n-1} - 1) + \frac{r - R_b}{\varphi}\right] \tag{4.58}$$

The work done for the system pressure ratio r is given by

$$W_{\text{ideal}} = p_1 \mathbb{V}_S \frac{n}{n-1}[(r)^{(n-1)/n} - 1] \tag{4.59}$$

Therefore the built-in efficiency is given by the ratio of W_{ideal} to the total work, that is,

$$\eta_\varphi = \frac{[n/(n-1)][r^{(n-1)/n} - 1]}{[n/(n-1)][\varphi^{n-1} - 1] + (r - \varphi^n)/\varphi} \tag{4.60}$$

In case of n =1, that is, isothermal compression, it can be easily shown that

$$\eta_\varphi = \frac{\ln r}{\ln \varphi + (r - \varphi)/\varphi}$$

The case of $\varphi = 1$ refers to a machine for which there is no internal compression since $R_b = 1$. This is the case of roots blower or a liquid pump used on gas. It is very inefficient for pressure ratios greater than 1.5.

It is obvious that the built-in efficiency will be optimum when the system pressure ratio is the same as the built-in pressure ratio. Figure 4.15 shows the variation of built-in efficiency with pressure ratio for increasing values of the built-in volume ratio, namely, 5, 4 and 3. The value of n is taken to be 1.15. Hence, the value of R_b for these volume ratios is 3.54, 4.92, 6.32 respectively (see Eq. (4.55)). The figure shows that the efficiency is optimum at these pressure ratios. The efficiency drops very rapidly for pressure ratios less than R_b, hence, it is advisable to choose a compressor of built-in pressure ratio less than the normal system operating pressure ratio. It has been observed that under part load operation the built-in volume ratio decreases and the corresponding built-in pressure ratio also decreases. Hence, if the compressor is to run on part load for considerable period of time, then it should be chosen accordingly. This efficiency takes

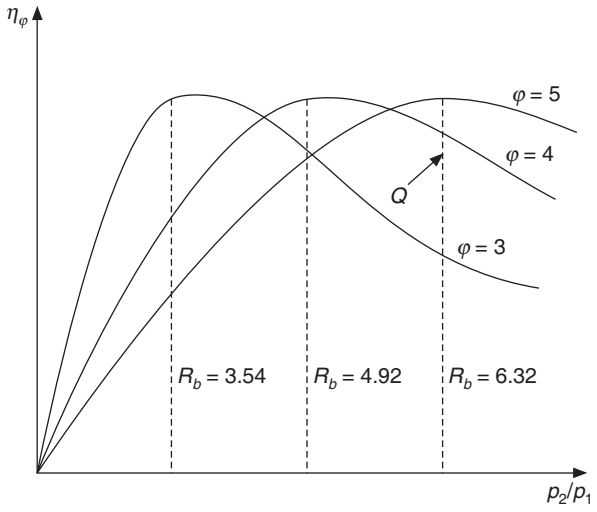

Figure 4.15 Variation of built-in efficiency of a twin-screw compressor with pressure ratio and built-in volume ratio.

care of only the mismatch between the system pressure ratio and the built-in pressure ratio. The other losses like pressure drops in the ports and friction have to be taken into account to define the isentropic efficiency. These losses increase with increase in load and pressure ratio. The peak isentropic efficiency of twin-screw compressor with oil injection is around 75%.

EXAMPLE 4.10 In a twin-screw R22 compressor, the rotor diameter and length are 0.2 m and 0.4 m respectively and it runs at 1432 rpm. The ratio of flute area to cross-section area of rotor is 0.15. This fixes the volume ratio to be 2.85. The compressor is designed for evaporator and condenser temperatures of –5°C and 35°C respectively.

(a) Find the swept flow rate and the built-in pressure ratio if $n = 1.11$.

(b) Find the work required for built-in pressure ratio. Is this work the same as that for the design pressure ratio? Find the cooling capacity.

(c) If the evaporator temperature remains constant while the condenser temperature is 30°C in winter and 40°C in summer, find the difference in work requirement and the built-in efficiencies.

Solution:

Given $S = 0.15$, $D = 0.2$ m, $L = 0.4$ m, $N = 1432$ rpm, $\varphi = 2.85$ and $n = 1.11$
From Eqs. (4.54) and (4.55), we get

Swept flow rate = $\mathbb{V}_S = SN\pi D^2 L = 0.15(1432/60)\ \pi\ (0.2)^2\ (0.4) = 0.18$ m^3/s

Built-in pressure ratio = $R_b = \varphi^n = (2.85)^{1.11} = 3.198$

Properties of R22 from the saturation table are as follows:

t, °C	p, bar	v_g, m^3/kg	h_f, kJ/kg	h_g, kJ/kg	s_g, kJ/kg-K
–5	4.219	0.0554		249.29	0.9393
30	11.885	82.88			
35	13.496		89.12		
40	15.267		95.4		

At the design condition of evaporator and condenser temperatures of –5°C and 35°C, we have

$$r = p_2/p_1 = 13.496/4.219 = 3.1988$$

This is same as the built-in pressure ratio.
Referring to Eqs. (4.56), (4.57), (4.58) and (4.59),

$$W' = p_1 \mathbb{V}_S \frac{n}{n-1}[(R_b)^{(n-1)/n} - 1] = p_1 \mathbb{V}_S \frac{n}{n-1}(\varphi^{n-1} - 1)$$

or $$W' = 4.219(100)(0.18)(1.11/0.11)[\ (2.85)^{0.11} - 1] = 93.571 \text{ kW}$$

$$W_{\text{ideal}} = p_1 \mathbb{V}_S \frac{n}{n-1}[(r)^{(n-1)/n} - 1]$$

or $$W_{\text{ideal}} = 4.219(100)(0.18)(1.11/0.11)[\ (3.198)^{0.11/1.11} - 1] = 93.59 \text{ kW}$$

It was expected since the built-in pressure ratio is same as the actual pressure ratio.

The pressure ratio at 30°C condenser temperature is $r = 11.885/4.219 = 2.818$

$$W_{\text{ideal}} = 4.219(100)(0.18)(1.11/0.11)[\ (2.818)^{0.11/1.11} - 1] = 82.859 \text{ kW}$$

The difference in work required = $W'' = (p_2 - R_b p_1)\, \mathbb{V}_S/\varphi = p_1(r - R_b)\, \mathbb{V}_S/\varphi$

$$W'' = 4.219(100)0.15(2.818 - 3.198)/2.85 = -10.126 \text{ kW}$$

The pressure ratio at 40°C condenser temperature is $r = 15.267/4.219 = 3.619$

$$W_{\text{ideal}} = 4.219(100)(0.18)(1.11/0.11)[\ (3.619)^{0.11/1.11} - 1] = 104.789 \text{ kW}$$

$$W'' = p_1(r - R_b)\, \mathbb{V}_S/\varphi = 4.219(100)0.15(3.619 - 3.198)/2.85 = 11.218 \text{ kW}$$

The built-in efficiency at 30°C condenser temperature,

$$\eta_b = W_{\text{ideal}}/(W' + W'') = 82.859/(93.571 - 10.126) = 99.3\%$$

Built-in efficiency at 40°C condenser temperature,

$$\eta_b = W_{\text{ideal}}/(W' + W'') = 93.59/(93.571 + 11.218) = 99.4\%$$

Cooling capacities:

At 30°, $Q_e = (\mathbb{V}_S/v_1)\,(h_1 - h_3) = (0.18/\ 0.0554)(249.29 - 82.88) = 542.63 \text{ kW} = 154.3 \text{ TR}$
At 35°, $Q_e = (\mathbb{V}_S/v_1)\,(h_1 - h_3) = (0.18/\ 0.0554)(249.29 - 89.12) = 520.41 \text{ kW} = 148 \text{ TR}$
At 40°, $Q_e = (\mathbb{V}_S/v_1)\,(h_1 - h_3) = (0.18/\ 0.0554)(249.29 - 95.4) \ = 500 \text{ kW} \quad = 142.2 \text{ TR}$

4.6 CENTRIFUGAL COMPRESSORS

Reciprocating compressors usually run at 1440 rpm. Each cylinder may be of 10 TR (maximum 25 TR) capacity with up to 16 cylinders in a single machine giving a capacity of 160 TR. Unloading the cylinders regulates the capacity of reciprocating compressor. The suction valve is held open mechanically in response to fall in evaporator pressure (less cooling capacity required) or thermostat setting. This actuates a solenoid valve in the cylinder unloading mechanism. If the suction valve is held open, the vapour enters and leaves it without compression. By opening the valves on one or more cylinders, the mass flow rate can be decreased. The complication of part load operation makes the reciprocating compressor an unfavourable option compared to centrifugal compressors in which the capacity control is done in a simple manner by change of speed. Also, centrifugal compressors are available in single units of very large capacity. The economic designs start from 200 TR onwards, but smaller units of up to 80 TR are also available.

In reciprocating compressors, a finite volume of vapour refrigerant is aspirated, valves are closed and the volume of vapour is mechanically decreased to obtain a rise in pressure; subsequently the vapour is discharged to the condenser. This cycle is repeated in each revolution and the refrigerant is discharged in spurts. In contrast, the compression in a centrifugal compressor is a continuous process. It has an impeller that has fixed vanes, which makes diverging passages in which the refrigerant vapour is decelerated with a consequent rise in pressure. The vapour enters the eye of the impeller and is whirled around at high speed by the vanes. At any point of flow, centripetal acceleration ($v^2/r = \partial p/\partial r$) is balanced by pressure gradient, that is, the static pressure increases from the eye to the tip of the impeller. The impeller imparts kinetic energy to the vapour, which is converted to pressure rise in the casing or the volute with as much efficiency as possible. The area

of the volute casing increases in the flow direction like that in a diffuser where the velocity decreases and the pressure increases. It is an accepted design procedure to design centrifugal compressors such that 50% of the pressure rise is obtained in the vane passages and the remaining 50% in the volute casing.

Normally, the vapour moves in a radial direction in the impeller from low pressure in the inlet eye to the periphery. The higher pressure on the leading side of the blade compared to that on the trailing side of the blade and the Corriolis force between the flow passages, cause a re-circulation which reduces the velocity on the trailing side of the blade. There is also slip in the passage. More number of blades will reduce it, however, there is a limitation to the number of blades since these occupy some flow area and increase the flow friction. There is an optimum number of blades for a given blade angle. This is very crucial at the inlet eye where the flow area decreases with increase in the number of blades. The inlet has to accommodate the flow rate. Hence there is a limitation on the size of impeller. It cannot be made very small. Therefore there is a limitation of 200 TR on the economic size of a centrifugal compressor for the refrigeration purpose.

Since there is a slightly higher static pressure on the leading side of the vane than that on the trailing side, it leads to leakage around the edges of the vanes in the clearance space between the casing and the vanes. Leakage is avoided by keeping the clearance to a minimum value. A shroud attached on the vanes side will reduce leakage, however it will increase the disc friction drastically. Hence, a shroud is not used in centrifugal compressors.

The phenomenon of surging is unique to centrifugal compressors. There is no analogue of it in reciprocating compressors. If the difference between the condenser pressure and the evaporator pressure exceeds the design value, the capacity of the centrifugal compressor falls rapidly. This leads to the phenomenon of surging. When the pressure rise becomes very large, the flow ceases and its direction reverses since high condenser pressure drives the vapour back to the lower suction pressure side. The evaporator pressure rises in response to this, and when the pressure difference becomes equal to the capability of the impeller, the flow resumes its normal direction—only to reverse after some time. This oscillation of flow and the rapid variation in pressure that it produces, is called *surging*. It produces noise and large stresses that can damage the bearings and other components of motor and impeller. High head can be developed by running the compressor at high tip speed or by using multistage compression. A large diameter impeller will also give high tip speed but the structural and material restrictions limit the maximum tip speed. The two-pole motor gives 48 revolutions per second. The frequency of electrical supply may be changed by the inverter and controlled in the range of 30 to 1500 Hz giving a range of pressures.

In reciprocating compressors heat is invariably rejected to the surroundings during compression. Normal pressure acts on the piston and the piston does work against it. In centrifugal compressors, the heat rejection is negligible since the area available for heat rejection per unit volume flow rate is very small. However, the velocities are very large which lead to high shear stresses, as a result the work is done against shear stresses as well as the normal pressure. The work done against shear stresses leads to viscous dissipation that causes heating of the vapour during compression in contrast to cooling of the vapour during compression in reciprocating compressors. Figure 4.16 shows the process 1–2 for the reciprocating compressor and process 1–2c for the centrifugal compressor. It is observed that these are on the opposite sides of isentropic compression shown by line 1–2s . If the changes in kinetic and potential energy are neglected, the first law of thermodynamics for the compressor reduces to

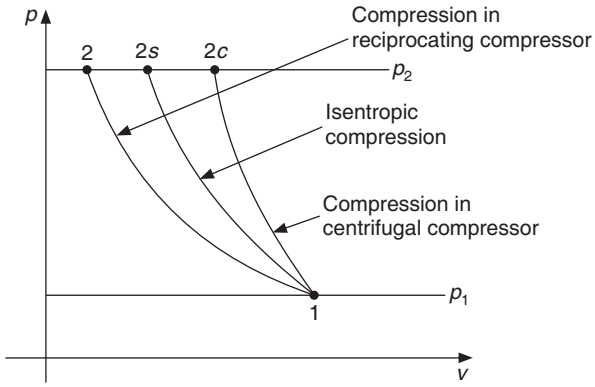

Figure 4.16 Compression processes in reciprocating and centrifugal compressors vis-a-vis the isentropic compression process.

$$Q - W = \dot{m}(h_2 - h_1) \tag{4.61}$$

where the work done as well the heat transfer are both negative for the reciprocating compressor. In the centrifugal compressor, heat transfer Q is zero. Hence

$$W = \dot{m}(h_2 - h_1) \tag{4.62}$$

If internal friction is also negligible then the process may be considered to be isentropic, that is,

$$W_{\text{isen}} = \dot{m}(h_2 - h_1)_s = \dot{m}\int_{p_1}^{p_2} (v\,dp)_s \tag{4.63}$$

4.6.1 Small-stage Efficiency

In reciprocating compressors, the work is done by the piston against the normal pressure acting on it. In centrifugal compressor the work is done against viscous shear stresses as well as the normal pressure. Therefore, the elemental work dw cannot be related to pressure changes alone and at each stage of compression, it is greater than $v\,dp$. Hence for centrifugal compressor even at elemental stage one defines an efficiency called small-stage efficiency η_{ss} to account for this deviation, that is,

$$\eta_{ss} = \frac{v\,dp}{dw} \tag{4.64}$$

The work done dw is equal to dh for the adiabatic process, hence the small-stage efficiency expression reduces to

$$\eta_{ss} = \frac{v\,dp}{dh} \tag{4.65}$$

4.6.2 Polytropic Efficiency

It may be mentioned here that due to internal frictional heating, the specific volume v will be larger than that for the isentropic process 1–2s, hence the work requirement as area to the left of

line 1–2c will be more than that for isentropic process. Further, the area to the left of line 1–2c does not represent dw at elemental level. In the cylinder–piston arrangement, one defines a quasi-static process that is carried out in a slow manner such that at each stage the piston is in equilibrium and the pressure is thermodynamic pressure. One moves from one equilibrium state to another equilibrium state. Such a work is called reversible work and is equal to $\int (v\,dp)$. In the presence of shear stresses, there will be irreversibility and the equilibrium state is not achieved, and the work is not equal to $\int (v\,dp)$. This deviation cannot be seen in the diagram. It has been explained above. The work done $h_2 - h_1$ will be greater than the integral $\int (v\,dp)$. This deviation is represented by polytropic efficiency defined as

$$\eta_p = \frac{\int_{p_1}^{p_2} (v\,dp)_s}{h_2 - h_1} \tag{4.66}$$

This equation represents the cumulative effect of deviation of $v\,dp$ from dw. Increase in specific volume at each elemental level increases the work requirement not only in that elemental level but in subsequent level as well, since starting from a larger specific volume the specific volume will be even more in the next level. If the variation of specific volume with pressure is known during compression, then the above integral can be evaluated. However this is never the case. For ideal gas with constant specific heat, it is possible to evaluate this integral but not so for vapours due to lack of simple equation of state. One has to therefore use experimental test results for vapours.

4.6.3 Relation between Small-stage Efficiency and Polytropic Efficiency

For ideal gas,

$$dh = c_p\,dT = c_p\,d(p\,v)/R = c_p\,(p\,dv + v\,dp)/R$$

Substituting this in Eq. (4.65) for small-stage efficiency, we get

$$\eta_{ss} = \frac{Rv\,dp}{c_p\,(v\,dp + p\,dv)}$$

or
$$v\,dp\,(R - c_p\eta_{ss}) = \eta_{ss}c_p\,p\,dv$$

$\therefore$
$$\frac{c_p\,\eta_{ss}}{c_p\,\eta_{ss} - R}\frac{dv}{v} - \frac{dp}{p} = 0 \tag{4.67}$$

If one assumes that the small-stage efficiency and the specific heat are constant, then the first term in this expression is constant which can be denoted by n as follows:

$$n = \frac{c_p\eta_{ss}}{c_p\eta_{ss} - R} \tag{4.68}$$

Equation (4.67) now reduces to

$$p\,v^{\,n} = \text{constant} \tag{4.69}$$

Substituting $R = c_p\,(\gamma - 1)/\gamma$, we get from Eq. (4.68),

$$n = \frac{\gamma\,\eta_{ss}}{\gamma\,\eta_{ss} - \gamma + 1}$$

Solving this for η_{ss} and assuming $\eta_p = \eta_{ss}$,

$$\eta_{ss} = \eta_p = \frac{n}{n-1}\,\frac{\gamma - 1}{\gamma} \tag{4.70}$$

If the inlet conditions p_1, T_1 and the outlet conditions p_2, T_2 are known, then the index n is evaluated from

$$\frac{T_2}{T_1} = \left(\frac{p_2}{p_1}\right)^{(n-1)/n} \tag{4.71}$$

Subsequently η_{ss} and η_p are evaluated from Eq. (4.70) for the known value of γ.

If the polytropic efficiency is known, then n is calculated from Eq. (4.70) and T_2 is found from Eq. (4.71). Subsequently, specific work and power requirement are found from

$$w = c_p(T_2 - T_1) \quad \text{and} \quad P = \dot{m}w \tag{4.72}$$

respectively.

EXAMPLE 4.11 Air is compressed at the rate of 1.5 kg/s in a centrifugal compressor from 30°C and 1.01325 bar pressure to a pressure of 4.5 bar. The small-stage efficiency is given to be 0.8, c_p = 1.005 kJ/kg-K and γ = 1.4. Find the specific work and the shaft power.

Solution:

We have from Eq. (4.70) for small-stage efficiency,

$$0.8 = [n/(n-1)]\ 0.4/1.4 \qquad \therefore \quad [n/(n-1)] = 2.8$$

From Eq. (4.71), $\quad T_2 = 303[4.5/1.01325]^{1/2.8} = 516.05$

From Eq. (4.72), $\quad w = c_p\,(T_2 - T_1) = 1.005(516.05 - 303) = 214.11$ kJ/kg

and $\quad P = \dot{m}w = 1.5(214.11) = 3212.7$ kW

EXAMPLE 4.12 R22 is compressed in a centrifugal compressor from a pressure of 4.98 bar to 15.267 bar corresponding to evaporator and condenser temperatures of 0°C and 40°C respectively. The small-stage efficiency is 0.8. Determine the specific work, the adiabatic discharge temperature and the polytropic efficiency.

Solution:

Isentropic compression:

In Example 4.6(a), isentropic compression was considered and the values of v_2 and h_2 were determined by interpolation in superheat table.

$$p_1 = 4.98,\ v_1 = 0.0472 \text{ and } h_1 = 251.12 \text{ and } p_2 = 15.267,\ h_2 = 279.1 \text{ and } v_2 = 0.0171$$

Subsequently considering,

$$p_1\,v_1^{\,k} = p_2\,v_2^{\,k}$$

the value of isentropic index for vapour, k, was found to be

$$k = 1.10334 \quad \text{and} \quad (h_2 - h_1)_s = 279.1 - 251.12 = 27.98 \text{ kJ/kg}$$

Polytropic compression:

From Eq. (4.70) assuming that the small-stage and polytropic efficiencies are the same

$$\eta_p = \frac{n}{n-1}\frac{k-1}{k} \quad \text{or} \quad 0.8 = \frac{n}{n-1}\frac{1.10334-1}{1.10334} \qquad \therefore \quad n = 1.1327$$

We may now find the value of v_2 for polytropic compression by considering $p_1 v_1^{\,n} = p_2 v_2^{\,n}$, i.e.

$$v_2 = v_1 (p_1/p_2)^{1/n} \quad \text{or} \quad v_2 = 0.0472(4.98/15.267)^{1/1.1327} = 0.01755 \text{ m}^3/\text{kg}$$

Now we interpolate in the superheat table to find the temperature, enthalpy and entropy at the end of polytropic compression corresponding to $v_2 = 0.01755$ m^3/kg. The superheat table is:

Superheat K	20°C	30°C
v	0.0172	0.0182
h	279.61	288.31
s	0.9332	0.9592

Interpolation gives:

$T_2 = 63.5^{\circ}\text{C}$, $h_2 = 282.655$ and $s_2 = 0.9423$ and $(h_2 - h_1)_{\text{poly}} = 282.655 - 251.12 = 31.535$

Now,

$$\int_1^2 v\,dp = p_1 v_1 \frac{n}{n-1}\left[\left(\frac{p_2}{p_1}\right)^{(n-1)/n} - 1\right]$$

$$= 4.98 \times 100 \times 0.0472 \frac{1.1327}{1.1327-1}\left[\left(\frac{15.267}{4.98}\right)^{(1.1327-1)/1.1327} - 1\right]$$

$$= 28.138 \text{ kJ/kg}$$

i.e. the specific work = 28.138 kJ/kg

This gives a polytropic efficiency of $\eta_{\text{poly}} = \dfrac{\int v\,dp}{(h_2 - h_1)_{\text{poly}}} = \dfrac{28.138}{31.535} = 0.892$

It is observed that in this case the small-stage efficiency and polytropic efficiency are different.

4.6.4 Work Done and Pressure Rise in Centrifugal Compressor

It has been observed that the compressors are designed such that 50% of the pressure rise usually occurs during the flow through the passage between the vanes, and the remaining 50% occurs in the diffuser. There is no work done on the refrigerant in the diffuser of the compressor. Similarly, no external work is done from suction flange to the inlet of the impeller. A decrease in flow area at the inlet may cause some acceleration of flow and raise the static pressure but the stagnation enthalpy remains constant at the inlet.

Therefore, the energy absorbed by the compressor is determined by the conditions of refrigerant at inlet and outlet of the impeller. Figure 4.17 shows the velocity diagrams at the inlet and outlet of the compressor for backward swept blades. Figure 4.18 shows the velocity diagrams at the inlet and outlet of the compressor for radial blades. Subscripts 1 and 2 are used for the inlet and outlet, respectively, to the compressor. Various velocity components are denoted by the following symbols.

C : absolute velocity of the refrigerant
C_r : relative velocity which is usually parallel to the blade angle
C_u : whirl component, i.e. the component in the tangential direction
C_m : meridonial component, i.e. the velocity in the radial direction
U : the tangential component of velocity

Velocity triangles

The vapour enters the impeller eye in the axial direction (perpendicular to the plane of paper or impeller) and turns by 90° into the passage between the vanes of the impeller. There is no rotational or whirl component of velocity at inlet under ideal conditions. The axial portion of the vane is curved as shown in Figures 4.17 and 4.18 so that the vapour smoothly enters the eye. The leading edge of the vane makes an angle β_1 with the tangential direction. This is the direction of the relative velocity C_{r1} at inlet. The velocity diagrams also show the absolute velocity C_1 and the rotational velocity U_1 (= $r_1\omega$) for the general case (Figure 4.19) and the ideal case (Figures 4.17 and 4.18). The meridonial component C_{m1} is same as C_1 in the ideal case where the whirl component of velocity is zero. In the general case C_1 makes an angle α_1 with the tangential direction.

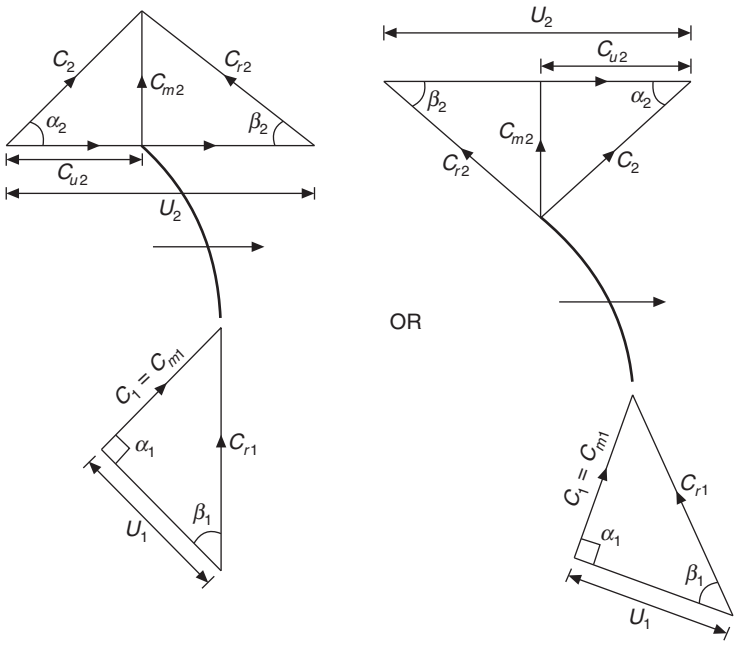

Figure 4.17 Velocity triangles for backward curved vanes: $\beta_2 < 90°$, $\alpha_1 = 90°$, $C_{u1} = 0$, $C_{m1} = C_1$.

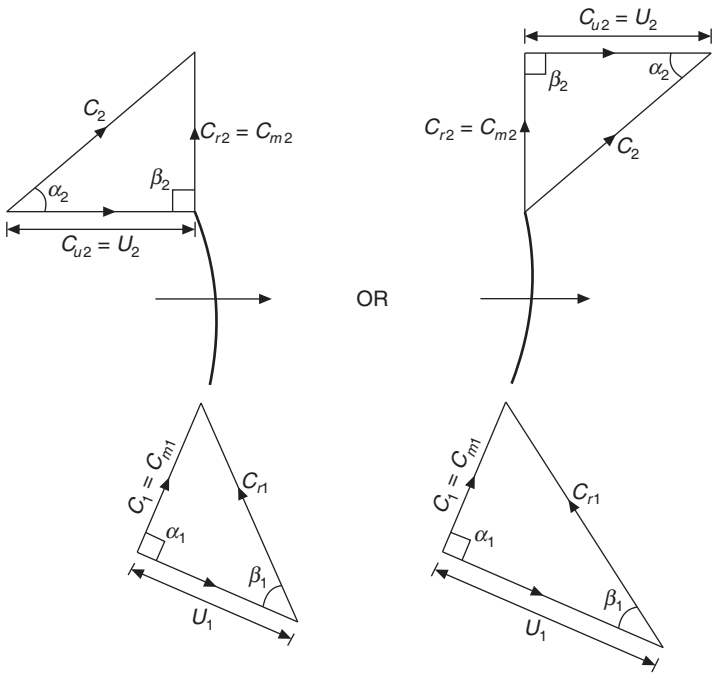

Figure 4.18 Velocity triangles for radial curved vanes: $\beta_2 = 90°$, $\alpha_1 = 90°$, $C_{u1} = 0$, $C_{r2} = C_{m2}$, $C_{u2} = U_2$, $C_1 = C_{m1}$.

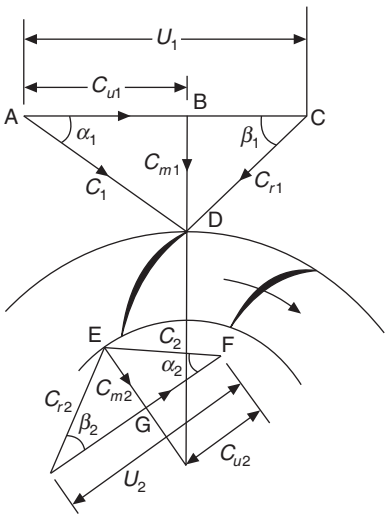

Figure 4.19 Generalized velocity triangles.

The vapour flows outwards through impeller passages where work is done on it. The static pressure, the absolute velocity and the stagnation enthalpy increase. The relative velocity decreases due to friction. The velocity diagrams at the tip are shown in Figures 4.17 and 4.18. The relative

velocity at the tip of vanes, C_{r2} (at exit of impeller) conforms to the vane tip angle β_2 under ideal conditions. The absolute velocity C_2, its tangential or whirl component C_{u2}, the tangential velocity U_2 and meridional component C_{m2} are also shown in the velocity diagram. In case of radial blades, under ideal conditions C_2 would be such that $C_{u2} = U_2$ and the relative velocity is exactly radial or meridional. For backward curved blades, under ideal conditions, the relative velocity would make an angle β_2 with the tangential direction. In general, there will be some slip and the true angle of vapour will be less than β_2. This is discussed later. For the time being, ideal conditions are assumed.

Moment of momentum

The torque required to turn the impeller is determined by taking a control volume around the impeller and applying moment of momentum to it. The torque is equal to the difference of moment of momentum at the outlet and inlet.

For axial approach at the impeller eye, the whirl component of velocity C_{u1} is zero, hence there is no moment of momentum at the inlet, otherwise it is r_1C_{u1}. At the outlet, the specific moment of momentum is r_2C_{u2}. For a mass flow rate of $\dot{m}$, the torque is given by

$$T = \dot{m}(r_2C_{u2} - r_1C_{u1}) \tag{4.73}$$

Work done is given by the following expression for a rotational speed ω rad/s and peripheral velocities $U_1 = r_1\omega$ and $U_2 = r_2\omega$ at the inlet and outlet respectively.

$$W = T\omega = \dot{m}(r_2C_{u2}\omega - r_1C_{u1}\omega) = \dot{m}(C_{u2}U_2 - C_{u1}U_1) \tag{4.74}$$

The specific work is given by

$$w = C_{u2}U_2 - C_{u1}U_1 \tag{4.75}$$

It is observed from the velocity triangles that

$$(C_{r2})^2 = (U_2 - C_{u2})^2 + (C_{m2})^2 = (U_2 - C_{u2})^2 + (C_2^2 - C_{u2}^2)$$

$$\therefore \quad (C_{r2})^2 = U_2^2 + C_2^2 - 2U_2C_{u2}$$

and $$(C_{r1})^2 = U_1^2 + C_1^2 - 2U_1C_{u1}$$

$\therefore$ The specific work, $w = C_{u2}U_2 - C_{u1}U_1 = (U_2^2 - U_1^2)/2 + (C_2^2 - C_1^2)/2 + (C_{r2}^2 - C_{r1}^2)/2$ (4.76)

The term $(C_2^2 - C_1^2)/2$ is the increase in specific kinetic energy in the impeller and is sometimes called the *dynamic head*. There are two parts of the static head, namely, $(U_2^2 - U_1^2)/2$ called the *centrifugal head* and $(C_{r2}^2 - C_{r1}^2)/2$ called the *relative head* which is due to change in the area of flow.

Compressor with axial entry

It is observed that the work requirement is smaller and the corresponding head developed is also smaller because of the pre-whirl component C_{u1} at the inlet to the compressor. The inlet is usually designed such that $C_{u1} = 0$. In multistage compressors, it is not zero since the vapour from the preceding stage is still rotating, and also with the method of capacity control by inlet guide vanes some whirl may be generated at inlet.

Referring to the velocity diagram for backward curved blades (Figure 4.17), it is observed that the whirl velocity at the outlet C_{u2} is the projection of absolute velocity C_2 in the direction of peripheral velocity U_2, that is,

$$C_{u2} = U_2 - C_{m2} \cot \beta_2$$

Equation (4.75) for specific work reduces to

$$w = U_2(U_2 - C_{m2} \cot \beta_2) \tag{4.77}$$

and

$$W = \dot{m}U_2^2 \left[1 - \frac{C_{m2}}{U_2} \cot \beta_2\right] \tag{4.78}$$

For the case of radial blades the angle β_2 is 90°, hence

$$W = \dot{m}U_2^2 \tag{4.79}$$

For forward curved blades the work requirement will be

$$W = \dot{m}U_2^2 \left[1 + \frac{C_{m2}}{U_2} \cot \beta_2\right] \tag{4.80}$$

This is greater than $\dot{m}U_2^2$. The work is non-dimensionalized w.r.t U_2^2 and called *work coefficient* μ. Similarly, the non-dimensional velocity ratio $\varphi = C_{m2}/U_2$ is indicative of the mass flow rate.

$$\mu = \frac{W}{\dot{m}U_2^2} = \frac{w}{U_2^2} = \frac{C_{u2}U_2 - C_{u1}U_1}{U_2^2} \approx \frac{C_{u2}U_2}{U_2^2} \approx C_{u2}U_2 \text{ (with no prewhirl) and } \varphi = \frac{C_{m2}}{U_2} \tag{4.81}$$

The expression for work reduces to

$$\mu = (1 - \varphi \cot \beta_2) \tag{4.82}$$

For backward curved blades with $\beta_2 = 45°$, $\mu = 1 - \varphi$ and for forward curved blades with say, $\beta_2 = 135^o$, $\mu = 1 + \varphi$. For radial blades with $\beta_2 = 90^o$, $\mu = 1$.

For fixed r_2 and rotational speed ω, the specific work is proportional to work coefficient μ and flow rate is proportional to flow coefficient φ. The work absorbed by compressor with forward curved blades is more than that for the backward blades. Hence, forward curved blades will produce a higher pressure ratio than the backward blades for the same r_2 and ω. The mass flow rate is proportional to the meridional velocity C_{m2}. Hence the total power requirement will be proportional to $\mu\varphi$, that is,

$$W \approx \varphi (1 - \varphi \cot \beta_2) \tag{4.83}$$

The variation of power requirement with flow rate φ is shown in Figure 4.20 The power requirement for forward curved blades rises rapidly whereas it decreases for backward blades. The kinetic energy of the vapour leaving the impeller is given by

$$C_2^2/2 = (C_{m2}^2 + C_{u2}^2)/2 = U_2^2(\varphi^2 + \mu^2)/2 \tag{4.84}$$

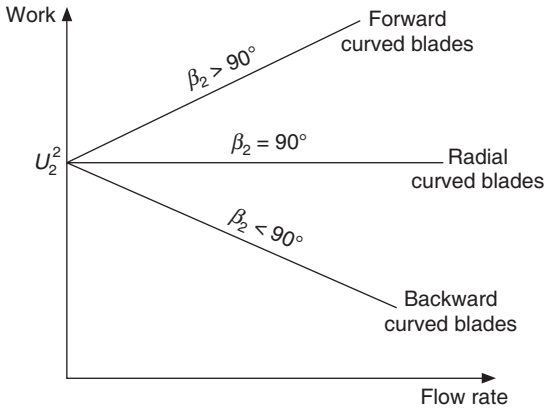

Figure 4.20 Power requirement vs. flow rate.

The kinetic energy of the vapour leaving the impeller is very large for forward curved blades. Hence, a larger pressure recovery is required in the diffuser of forward curved compressor than for backward curved compressor. The diffuser is the most inefficient part of centrifugal compressor; hence the backward curved impeller is preferred. The tip speed is usually limited (100 – 150 m/s for CFCs) for efficient diffuser performance.

The whirl component of velocity is inferred from the blade angle β_2. The actual blade angle or the flow angle is different from the blade angle β_2. Because of the viscous boundary layer, the velocity is different from relative velocity away from the blade and so is the angle. There is high static pressure on the leading edge of the blades than that on the trailing side. This may be attributed to Coriolis force, which occurs when the fluid moves in the radial direction while undergoing rotation. This pressure gradient causes an eddy, which rotates in opposite direction to that of impeller. This retards the flow on the forward face of the blade angle and the true blade angle is less than the blade angle β_2. Also the bulk of the vapour at exit of blade has a lower whirl velocity than C_{u2}. This effect is known as *slip* and it largely depends upon the number of vanes on the impeller. A slip factor, σ, is defined as the ratio of actual whirl velocity to the assumed whirl velocity $C_{u2'}$, that is,

$$\sigma = C_{u2}/C_{u2'} \tag{4.85}$$

An approximate formula based upon simple approximate studies, and based upon experimental results has been proposed for the slip factor. One such formula due to Stanitz [1952] is

$$\sigma = 1.0 - 0.63\ \pi/n \tag{4.86}$$

where n is the number of blades. Impellers for the refrigerants are currently using between $n = \beta_2/3$ and $\beta_2/4$ blades where β_2 is in degrees . The meridional component of velocity C_{m2} is also non-uniform at the tip of impeller. A correction factor λ is introduced to account for this. Hence, for the case of axial entry Eq. (4.82) becomes

$$\mu = \sigma\,(1 - \lambda\ \varphi \cot \beta_2) \tag{4.87}$$

EXAMPLE 4.13 The impeller of a centrifugal compressor is of 300 mm diameter and it has backward curved blades with blade angle of 35°. It rotates at 12,000 rpm. The flow coefficient for maximum efficiency is given by $\varphi = (1 - \sin \beta_2) \tan \beta_2$. The slip factor of $\sigma = 0.8$ may be assumed. The flow area at the impeller outlet is 0.005 m^2, and the specific volume of refrigerant is 0.025 m^3/kg. Determine the specific work and the power requirement of compressor.

Solution:

It is assumed that the flow enters the compressor in axial direction, hence $C_{u1} = 0$

We have from the relation provided in example

$$\varphi = (1 - \sin 35^o) \tan 35^o = 0.298$$

The correction factor λ to C_{m2} is assumed to be 1.0.

Therefore from Eq. (4.87),

$$\mu = \sigma (1 - \varphi \cot \beta_2), \text{ that is, } \mu = 0.8(1.0 - 0.298 \cot 35^o) = 0.459$$

Tip speed $U_2 = \pi(0.3)12000/60 = 188.5$ m/s and $U_2^2 = 35.53$ kJ/kg

$C_{m2} = 0.298U_2 = 0.298 \times 188.5 = 56.173$ m/s

Mass flow rate $\dot{m} = A_2.C_{m2}/v_2 = 0.005 \times 56.173/0.025 = 11.2346$ kg/s

Specific work $w = \mu U_2^2 = 0.459 \times 35.53 = 16.308$ kJ/kg

Power $W = \dot{m}w = 11.2346 \times 16.308 = 183.2$ kW

EXAMPLE 4.14 R22 is compressed in a centrifugal compressor from a pressure of 4.98 bar to 15.267 bar corresponding to evaporator and condenser temperatures of 0° and 40°C respectively. Polytropic efficiency is 0.85, isentropic head coefficient is 0.55, outlet blade angle is 32°, flow coefficient is given by $\varphi = (1 - \sin \beta_2) \tan \beta_2$, compressor rpm is 2880 and the cooling capacity is 600 TR. Determine the isentropic work, actual work, adiabatic discharge temperature, impeller diameter, outlet width and outlet Mach number.

Solution:

In Example 4.12, for isentropic compression the end states for $p_1 = 4.98$ bar and $p_2 = 15.267$ bar were found to be:

$$p_1 = 4.98,\ v_1 = 0.0472 \text{ and } h_1 = 251.12 \text{ and } p_2 = 15.267,\ h_2 = 279.1 \text{ and } v_2 = 0.0171$$

Also at 40°C : $h_3 = h_4 = h_f = 95.4$ kJ.kg

Therefore $(h_2 - h_1)_s = 279.1 - 251.12 = 27.98$ kJ/kg

Ploytropic efficiency is given to be 0.85, hence, $(h_2 - h_1)_{\text{actual}} = (h_2 - h_1)_s/0.85$

$(h_2 - h_1)_{\text{actual}} = 27.98/0.85 = 32.918$, Therefore $h_2 = 251.12 + 32.918 = 284.038$ kJ/kg

We interpolate in the superheat table for R22 at 15.267 bar for $h_2 = 284.038$ kJ/kg

Superheat K	20°C	30°C
v	0.0172	0.0182
h	279.61	288.31
s	0.9332	0.9592

Interpolation gives $T_2 = 65.09$ °C and $v_2 = 0.01771$

Head coefficient is given to be 0.55. Therefore $U_2^2 = (h_2 - h_1)_s / 0.55$

$$U_2^2 = 27.98 \times 1000/0.55 \text{ or } U_2 = 244.64 \text{ m/s}$$

$$D_2 = 60U_2/(\pi N) = 60 \times 244.64/(\pi \times 2880) = 1.662 \text{ m}$$

Flow coefficient $\varphi = (1 - \sin 32°) \tan 32° = 0.2937$

$$C_{m2} = \varphi U_2 = 0.2937(244.64) = 71.85 \text{ m/s}$$

For 600 TR cooling capacity, $600 \times 3.5167 = (h_1 - h_4) = (251.12 - 95.4)$

$$\dot{m} = 600 \times 3.5167/(251.12 - 95.4) = 13.55 \text{ kg/s}$$

Also $\dot{m} = \pi D_2 b_2 C_{m2} / v_2$

$\therefore$ $b_2 = 13.55\ (0.0171)/(\pi \times 1.622 \times 71.85) = 0.655$ mm

This is rather small. In fact the rotational speed is much larger in an actual compressor, which will make the diameter small and this to be reasonable.

With $U_2 = 244.64$, $C_{m2} = 71.85$ and $\beta = 32°$, we get from the velocity triangle

$$C_2 = 148.23 \text{ m/s}$$

Speed of sound, $C_{\text{sonic}} = \sqrt{kRT_2} = \sqrt{1.034\ (96.13)(273 + 65.09)} = 183.28$ m/s

Mach number, $M = C_2/C_{\text{sonic}} = 148.23/183.28 = 0.81$

Enthalpy vs. entropy diagram for the compressor

Figure 4.21 shows the schematic diagram of a centrifugal compressor. In this diagram the inlet to the eye of the impeller is represented by *i*, state 1 refers to the inlet of the impeller, 2 refers to the outlet of impeller, 3 refers to outlet of diffuser and 4 refers to the outlet of the volute casing of compressor.

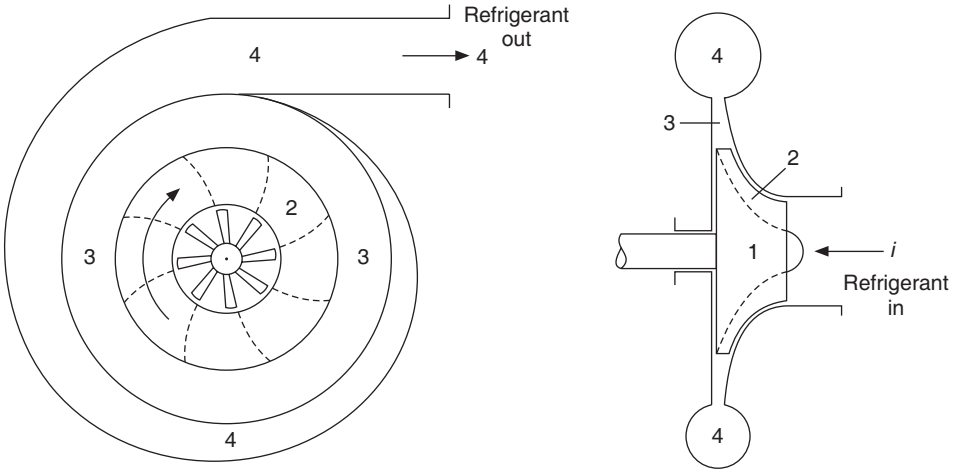

Figure 4.21 Schematic diagram of a centrifugal compressor.

The compression being irreversible, the entropy will increase along it. The enthalpy at various points may be obtained by neglecting the heat transfer from the compressor and applying the first law of thermodynamics to the vapour. Its state from inlet to the outlet is shown in Figure 4.22. This is in superheated state, hence the saturation curve is not shown. State 0 refers to stagnation state. This state is obtained when vapour moving with velocity C is brought to rest ($C = 0$) adiabatically. Stagnation enthalpy is the sum of specific enthalpy h and specific kinetic energy $C^2/2$, that is,

$$h_{i0} = h_i + C_i^2/2 \tag{4.88}$$

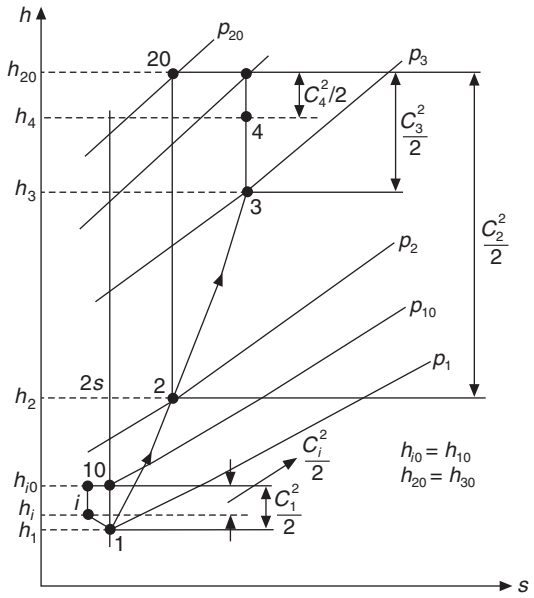

Figure 4.22 Enthalpy–entropy diagram for a centrifugal compressor.

The stagnation pressure or total pressure is the pressure developed when a stream with velocity C_i is decelerated isentropically and brought to rest , that is, zero velocity.

$$\int_{p_1}^{p_0} v\,dp = C_i^2/2 \tag{4.89}$$

For incompressible flow this reduces to

$$p_0 = p_i + \rho\, C_i^2/2 \tag{4.90}$$

where p_i is the static pressure and p_0 is the total pressure or the stagnation pressure.

Inlet to the compressor (process i–1):

In the absence of work done and heat transfer, according to the first law of thermodynamics the stagnation enthalpy remains constant, that is,

$$h_{i0} = h_i + C_i^2/2 = h_{10} = h_1 + C_1^2/2 \tag{4.91}$$

Assuming that the vapour accelerates upon entry to the compressor eye, i.e. $C_1 > C_i$

$$h_i > h_1 \quad \text{and} \quad p_i > p_1$$

It is seen from Figure 4.22 that the static pressure and enthalpy decrease and the velocity increases from i to 1 while stagnation enthalpy remains constant. There is some irreversibility associated with the process hence the entropy increases from i to 1.

Impeller (process 1–2):

The work done by the impeller increases the enthalpy, pressure and the kinetic energy. The specific work done is given by

$$w = h_2 - h_1 + (C_2^2 - C_1^2)/2 = h_{20} - h_{10} \tag{4.92}$$

Therefore, using Eqs. (4.75) and (4.76),

$$h_2 - h_1 + (C_2^2 - C_1^2)/2 = w = C_{u2}U_2 - C_{u1}U_1 \tag{4.93}$$

$$\therefore \qquad h_2 - h_1 = C_{u2}U_2 - C_{u1}U_1 - (C_2^2 - C_1^2)/2 = (U_2^2 - U_1^2)/2 + (C_{r1}^2 - C_{r2}^2)/2 \tag{5.95}$$

This process also has irreversibility. Hence the entropy increases along this process. If the process were reversible it would end at state 2s.

Diffuser and volute casing (processes 2–3 and 3–4):

There is no external work done during these processes. A part of kinetic energy is converted into internal energy or enthalpy, which results in a rise in pressure.

$$h_{20} = h_2 + C_2^2/2 = h_{30} = h_3 + C_3^2/2 \tag{4.95}$$

$$h_{30} = h_{40} = h_4 + C_4^2/2 \tag{4.96}$$

There are irreversibilities in these processes as well. Equations (4.92), (4.95) and (4.96) yield

$$w = h_{20} - h_{10} = h_4 - h_1 + (C_4^2 - C_1^2)/2$$

Since $$w = C_{u2}U_2 - C_{u1}U_1$$

$$\therefore \qquad h_4 - h_1 = C_{u2}U_2 - C_{u1}U_1 - (C_4^2 - C_1^2)/2 \tag{4.97}$$

If the kinetic energy at the inlet and outlet is negligible then

$$w = h_4 - h_1$$

$$\mu = w/U_2^2 \qquad \therefore \qquad h_4 = h_1 + \mu U_2^2$$

Pressure ratio developed:

As mentioned earlier, the heat transfer to the surroundings is negligible in an actual compressor but there is internal irreversibility, that is, the process may be considered to be adiabatic.

For a reversible process

$$T\,ds = 0 = dh - v\,dp$$

Therefore for the whole compressor, considering isentropic compression from state 1 to 4, we get

$$(h_4 - h_1)_s = \int (v\,dp)_s \tag{4.98}$$

If polytropic efficiency is denoted by η_{pol}, then the actual enthalpy rise is given by

$$(h_4 - h_1) = \frac{1}{\eta_{\text{pol}}} \int (v\,dp) \tag{4.99}$$

It is clear that the momentum equation considering the velocity diagrams is not sufficient to give the pressure rise. This depends upon the irreversibility in the process. For a perfect gas, the integral in Eq. (4.98) can be evaluated using pv^{γ} = constant where γ is the specific heat ratio. For a vapour it may be evaluated by using pv^{k} = constant where the value of k is obtained from isentropic end states. The integral in Eq. (4.99) may be evaluated by assuming that vapour follows pv^{n} = constant with value of n given by the initial and final states that is p_1, v_1, p_2 and v_2.

For the isentropic case,

$$(h_4 - h_1)_s = \frac{k}{k-1} p_1 v_1 \left[\left(\frac{p_4}{p_1} \right)^{(k-1)/k} - 1 \right] \tag{4.100}$$

For the actual case, k is replaced by n and combined with Eq. (4.97),

$$(h_4 - h_1) = \frac{n}{n-1} p_1 v_1 \left[\left(\frac{p_4}{p_1} \right)^{(n-1)/n} - 1 \right] = C_{u2}U_2 - C_{u1}U_1 - (C_4^2 - C_1^2)/2 \tag{4.101}$$

The expression for pressure ratio reduces to

$$\frac{p_4}{p_1} = \left[\frac{n-1}{n} \frac{1}{p_1 v_1} \left(C_{u2}U_2 - C_{u1}U_1 - \frac{C_4^2 - C_1^2}{2} \right) + 1 \right]^{n/(n-1)} \tag{4.102}$$

For the compressor with radial blades and axial entry, $C_{u2} = U_2$ and $C_{u1} = 0$, hence

$$\frac{p_4}{p_1} = \left[\frac{n-1}{n} \frac{1}{p_1 v_1} \left(U_2^2 - \frac{C_4^2 - C_1^2}{2} \right) + 1 \right]^{n/(n-1)} \tag{4.103}$$

In addition, if the change in kinetic energy at inlet and outlet is negligible then

$$\frac{p_4}{p_1} = \left[\frac{n-1}{n} \frac{U_2^2}{p_1 v_1} + 1 \right]^{n/(n-1)} \tag{4.104}$$

To find expressions for individual pressure rise in impeller and diffuser, we have from Eqs. (4.94), (4.95) and (4.96),

$$h_2 - h_1 = C_{u2}U_2 - C_{u1}U_1 - (C_2^2 - C_1^2)/2$$

$$h_4 - h_2 = (C_2^2 - C_4^2)/2$$

$\therefore$

$$\frac{p_2}{p_1} = \left[\frac{n-1}{n} \frac{1}{p_1 v_1} \left(C_{u2}U_2 - C_{u1}U_1 - \frac{C_2^2 - C_1^2}{2} \right) + 1 \right]^{n/(n-1)} \tag{4.105}$$

or

$$\frac{p_2}{p_1} = \left[\frac{n-1}{n} \frac{1}{p_1 v_1} \left(\frac{U_2^2 - U_1^2}{2} - \frac{C_{r2}^2 - C_{r1}^2}{2} \right) + 1 \right]^{n/(n-1)} \tag{4.106}$$

and

$$\frac{p_4}{p_2} = \left[\frac{n-1}{n} \frac{1}{p_2 v_2} \left(\frac{C_2^2 - C_4^2}{2} \right) + 1 \right]^{n/(n-1)} \tag{4.107}$$

EXAMPLE 5.15 The specific work of an impeller is 20 kJ/kg when R134 vapour enters at 2.93 bar (0°C). Determine the discharge pressure if (a) compression is isentropic, (b) polytropic with η_{pol} of 0.75. Given that the average value of k is 1.11 and $v_1 = 0.0694$ m^3/kg.

Solution:

(a) If the change in kinetic energy is neglected then for isentropic case,

$$w = (h_4 - h_1) = \frac{k}{k-1} p_1 v_1 \left[\left(\frac{p_4}{p_1} \right)^{(k-1)/k} - 1 \right]$$

$$20000 = \frac{1.11}{0.11} 2.93 \times 10^5 \, (0.0694) \left[\left(\frac{p_4}{p_1} \right)^{0.11/1.11} - 1 \right]$$

or $$\left(\frac{p_4}{p_1} \right)^{0.11/1.11} = 1.097 \quad \therefore \quad \left(\frac{p_4}{p_1} \right) = 0.556 \text{ and } p_4 = 2.93 \times 2.556 = 7.4897 \text{ bar}$$

(b) For polytropic case

$$(h_4 - h_1) = \frac{1}{\eta_{pol}} \int (v \, dp) \qquad \therefore \quad \int v \, dp = 0.75(20) = 15 \text{ kJ/kg}$$

Assuming the small-scale efficiency to be the same as the polytropic efficiency, from Eq. (4.70) we get

$$\frac{n}{n-1} \frac{\gamma - 1}{\gamma} = 0.75 \qquad \therefore \qquad \frac{n}{n-1} = 0.75 \frac{1.11}{0.11} = 7.5682$$

$\therefore$ $$15000 = 7.5682 \times 2.93 \times 0.0694 \left[\left(\frac{p_4}{p_1} \right)^{1/7.5682} - 1 \right]$$

$\therefore$ $$\left(\frac{p_4}{p_1} \right) = 2.021 \qquad \therefore \quad p_4 = 2.93 \times 2.021 = 5.923 \text{ bar}$$

4.6.5 Performance Characteristics

The work coefficient μ and efficiency η are the characteristic parameters for a compressor. If these are known then the work requirement and pressure ratio developed can be found. These depend upon compressor dimensions, refrigerant used, flow rate and speed, etc. Correlations or characteristics plots are usually given in terms of the following parameters.

Flow coefficient $\varphi = C_{m2}/U_2$

Rotational Reynolds number $\text{Re} = 2U_2 r_2/\nu_2$

Rotational Mach number $M = U_2/C_{\text{sonic},1}$

where ν_2 is the kinematic viscosity of the fluid at the rotor exit and $C_{\text{sonic},1}$ is the velocity of the vapour at the inlet to the compressor.

For a compressor running at constant speed and using the same refrigerant, the variation of Re and M are negligible. However, these have little effect on the characteristics. The Mach number is limited to 0.9. If it is greater than one, then it may lead to shock waves. A shock at the inlet to the compressor will adversely affect the flow through the compressor.

It has been shown by Gosney [1982] that the relative velocity at the inlet is maximum when it makes an angle of 34° with the tangential direction. At a given flow rate and rotational speed the eye radius may be chosen based upon this. The relative velocity and hence the Mach number reduces as the fluid passes through the impeller. Absolute velocity increases through the impeller and it may become supersonic. Some of the compressors running at high speeds operate with shock in the diffuser section. In some designs, the diffusion from supersonic to subsonic occurs in the vane-less space between the impeller and diffuser.

The flow coefficient φ is of primary importance in deciding the characteristics of centrifugal compressor. The volume flow rate through the compressor is also directly related to the flow coefficient. A general plot of variation of work coefficient $\mu = w/U_2^2$ and polytropic efficiency η_{pol} with flow coefficient φ is given in Figure 4.23. It is observed that work coefficient continuously decreases as the flow rate or the flow coefficient increases. Polytropic efficiency increases and reaches an optimum value and then decreases for larger values of φ. An approximate expression for the optimum value of φ is

$$\varphi_{opt} = (1 - \sin \beta_2) \tan \beta_2$$

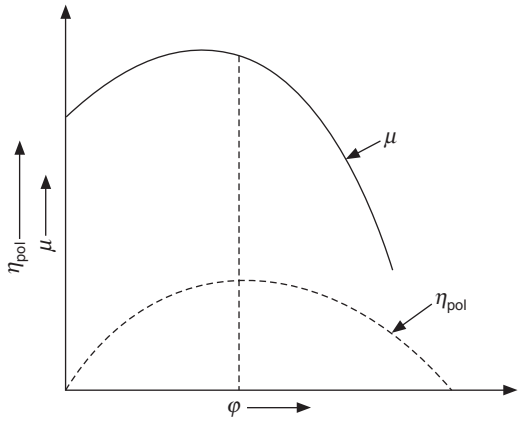

Figure 4.23 Variation of work coefficient μ and polytropic efficiency η_{pol} with flow coefficient φ.

Stepanoff [1955] has shown that the following relation holds for flow coefficient at maximum efficiency.

$$\int_{p_1}^{p_4} v\,dp = 0.69\,(1.0 - \varphi_2 \cot \beta_2) U_2^2$$

Wiesener and Caswell [1959] and Weisner [1960] have extensively tested this relation.

The value of φ_2 is in the range of 0.3 to 0.35 for optimum polytropic efficiency.

The load is proportional to the flow coefficient, while the pressure ratio developed is proportional to the work coefficient. Hence, it can be seen that the pressure ratio decreases as the flow rate increases. Higher pressure can be developed at smaller flow rates. The flow coefficient is not very convenient to work with, hence a modified flow coefficient is also defined in some textbooks. This is given by

$$\varphi_{\text{mod}} = Q_v/(ND^3)$$

where Q_v is the volume flow rate in m^3/s.

It has been observed that the value of modified flow coefficient should be more than 0.05 to obtain good efficiency out of a centrifugal compressor. Also, the isentropic head coefficient is around 0.55 for good efficiency. Actually, based upon these results, the minimum cooling capacity of a centrifugal compressor for various refrigerants can be determined. The compressors of cooling capacity lower than this will not give good efficiency. This is illustrated by the following example.

EXAMPLE 4.16 Find the minimum cooling capacity for a centrifugal compressor to run between the evaporator and condenser temperatures of 0°C and 40°C respectively for R12, R22 and NH_3 as refrigerants. The modified flow coefficient is 0.15 and the isentropic head coefficient is 0.55. Find the volume flow rate, the mass flow rate and the impeller diameter as well.

Solution:

R22:

In Example 4.6(a), isentropic compression was considered and the values of v_2 and h_2 were determined by interpolation in superheat table. These are as follows:

$p_1 = 4.98$, $v_1 = 0.0472$ and $h_1 = 251.12$ and $p_2 = 15.267$, $h_2 = 279.1$and $v_2 = 0.0171$

$\therefore \quad (h_2 - h_1)_s = 279.1 - 251.12 = 27.98$ kJ/kg

Given that the isentropic head coefficient $= (h_2 - h_1)_s/U_2^2 = 0.55$, hence

$$U_2^2 = 27.98 \times 1000/0.55 \text{ and } U_2 = 225.55 \text{ m/s}$$

Also $\quad U_2 = \pi D_2 N/60. \quad \therefore \quad D_2 = 60U_2/(\pi N)$

or $\quad D_2 = 225.55 \times 60/24000\pi = 225.55/400\pi = 0.1795$ m

$\therefore \quad Q_v = \varphi_{\text{mod}} (ND^3) = 0.15(24000/60)\ (0.1795)^3 = 0.1156\ m^3/s$

and $\quad \dot{m} = Q_v/v_1 = 0.1156/0.0472 = 2.449$ kg/s

Now $\quad (h_1 - h_3) = 251.12 - 95.4 = 155.72$ kJ/kg

$\therefore \quad Q_e = \dot{m}(h_1 - h_3) = 2.449(155.72) = 381.36$ kW

R12:

We have from the saturation table for R12

t, °C	p, bar	v_g, m^3/kg	h_f, kJ/kg	h_g, kJ/kg	s_g, kJ/kg-K
0	3.088	0.0557	36.15	188.69	0.7008
40	9.167	0.0183	74.77	204.75	0.6876

Superheat, K	5°C	10°C
v, m^3/kg	0.019	0.019
h, kJ/kg	208.65	212.5
s, kJ/kg-K	0.70	0.712

Interpolating in the superheat table for $s_1 = s_2 = 0.7008$, we get

$$t_2 = 45.33^oC\ ,\ h_2 = 208.9067 \text{ and } v_2 = 0.019$$

$$\therefore \quad (h_2 - h_1)_s = 208.9067 - 188.69 = 20.2167 \text{ kJ/kg}$$

$$U_2^2 = 20.2167 \times 1000 / 0.55 \text{ and } U_2 = 191.7 \text{ m/s}$$

$$D_2 = 191.7/400\pi = 0.153 \text{ m}$$

$$Q_v = \varphi_{\text{mod}} (ND^3) = 0.15(24000/60)\ (0.153)^3 = 0.071 \text{ m}^3/\text{s}$$

$$\dot{m} = Q_v / v_1 = 0.1156/0.0557 = 1.2747 \text{ kg/s}$$

$$(h_1 - h_3) = 188.69 - 74.77 = 113.92 \text{ kJ/kg}$$

$$Q_e = \dot{m}(h_1 - h_3) = 1.2747\ (113.92) = 145.2 \text{ kW}$$

NH_3 :

We have from the saturation table for NH_3,

T, °C	p, bar	v_g, m^3/kg	h_f, kJ/kg	h_g, kJ/kg	s_g, kJ/kg-K
0	4.294	0.29	180.88	1443.34	5.3368
40	15.55	0.0833	371.47	1472.02	4.8728

Superheat, K	5°C	10°C
v, m^3/kg	0.105	0.108
h, kJ/kg	1621.0	1647.9
s, kJ/kg-K	5.3153	5.3883

Interpolating in the superheat table for $s_1 = s_2 = 5.3368$, we get

$$t_2 = 92.945^oC,\ h_2 = 1628.922 \text{ and } v_2 = 0.10588$$

$$(h_2 - h_1)_s = 1628.922 - 1443.34 = 185.58 \text{ kJ/kg}$$

$$U_2^2 = 185.58 \times 1000 / 0.55 \text{ and } U_2 = 580.9 \text{ m/s}$$

$$D_2 = 580.9/400\pi = 0.46228 \text{ m}$$

$$Q_v = \varphi_{\text{mod}} (ND^3) = 0.15(24000/60)\ (0.46228)^3 = 1.9756 \text{ m}^3/\text{s}$$

$$\dot{m} = Q_v / v_1 = 1.9756/0.29 = 6.8125 \text{ kg/s}$$

$$h_1 - h_3 = 1443.34 - 371.47 = 1071.07 \text{ kJ/kg}$$

$$Q_e = \dot{m}(h_1 - h_3) = 1.2747\ (113.92) = 7302 \text{ kW}$$

The results are summarized in the following table.

Refrigerant	$(h_2 - h_1)_s$	U_2	D_2	Q_v	v_1	$h_1 - h_3$	Q_e
R12	20.217	191.7	0.153	0.071	0.0557	113.92	145.2
R22	27.98	225.55	0.1795	0.1156	0.0472	155.72	381.36
NH_3	185.58	580.9	0.46228	1.9756	0.29	1071.07	7302

These are the typical ranges of centrifugal compressors if good efficiency is to be obtained since the values of modified flow coefficient of 0.15 and isentropic head coefficient of 0.55 have been taken for best possible efficiency. If a plant of given capacity is to be chosen, then choice cannot be arbitrary. For example, a plant of 145 kW cooling capacity at 24,000 rpm should be the R12 plant.

The variation of characteristics with speed is shown in Figure 4.24. There is a surge envelope on the left hand side of the figure at low volume flow rates. The % values indicated in this figure are the % of rated speed. The rated condition is denoted by subscript n at which the volume flow ratio is φ_n and the work done is w_n. The ordinate may also denote the ratio of actual power to the rated power and abscissa the ratio of actual flow rate to the rated flow rate. It is observed that efficiency is optimum at the rated design condition and decreases at higher and lower speeds that are adopted for load variation. The load is proportional to the flow rate while the pressure ratio developed is proportional to the specific work input.

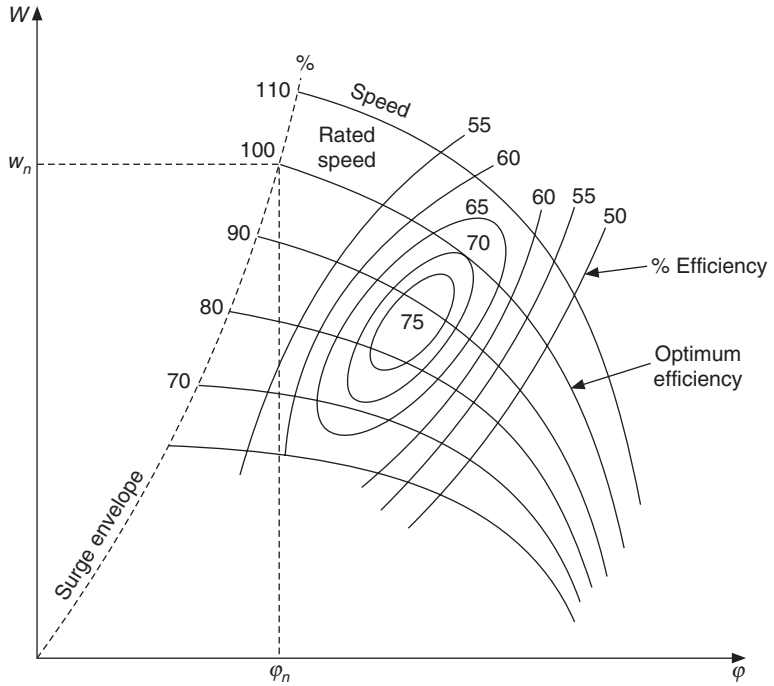

Figure 4.24 Efficiency curves of a centrifugal compressor at different percentages of rated speed and capacity.

Surge characteristics

The variation of pressure ratio with flow rate is shown in Figure 4.25. As the load decreases from the design point *A*, the performance of the backward curved compressor improves and shifts to point *B*. The pressure ratio developed at point *B* is optimum. A further decrease in flow rate will decrease the pressure ratio to point *C*. This is due to inherent characteristics of backward curved blades and the fact that flow separation starts to occur on the blades if the pressure ratio is large. The pressure ratio of the compressor decreases but the refrigerant continues to boil in the evaporator, building the evaporator pressure and thereby decreasing the pressure ratio. When the pressure ratio becomes equal to that at *A*, the compressor then momentarily shifts back to the design point *A*. The cycle however repeats itself giving rise to a transient condition called *surging*. This is characterized by loud noise and fluctuating load on compressor and motor with a period of approximately 2–5 seconds depending upon the size of compressor. At the higher speed of the compressor the pressure peak occurs at higher flow rate and at smaller flow rate at lower speed. The envelope of the peaks is also shown in Figure 4.24, labelled *surge envelope*. Surging is instability of operation caused by mismatch between the impeller and the diffuser at low flow rates.

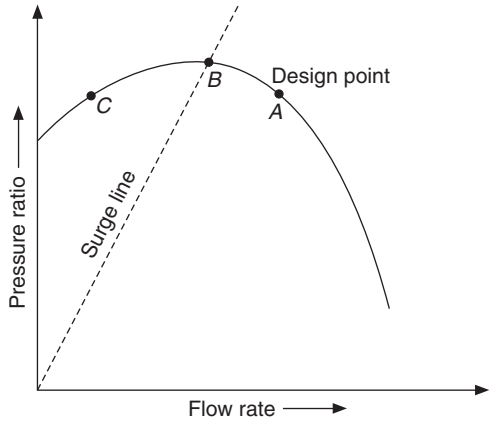

Figure 4.25 Surging phenomenon of centrifugal compressor.

4.7 COMPARISON WITH RECIPROCATING COMPRESSOR

The centrifugal compressor is very sensitive to evaporator and condenser temperatures. Figure 4.26 shows the variation of cooling capacity at fixed condenser temperature of 38°C and constant speed for both reciprocating and centrifugal compressors. It is observed that reduction in capacity from 240 TR to 100 TR is obtained by a change in evaporator temperature of 5.5°C (2 to 7.5°C) in centrifugal compressor whereas in the reciprocating compressor the same capacity occurs by 17°C (–11 to 6°C) temperature difference. This means that the centrifugal compressor will maintain a more uniform evaporator temperature over a much wider range of load when compared to reciprocating compressor. Since a small change in evaporator temperature brings a large change in capacity, the suction gas throttling (leading to lower suction pressure at compressor inlet) becomes an effective method of capacity control. The operating range is limited by surging limit or hunting limit of the compressor (in the figure it is 100 TR and 2°C evaporator temperature). Unsteady operation will occur below this evaporator temperature irrespective of evaporator load.

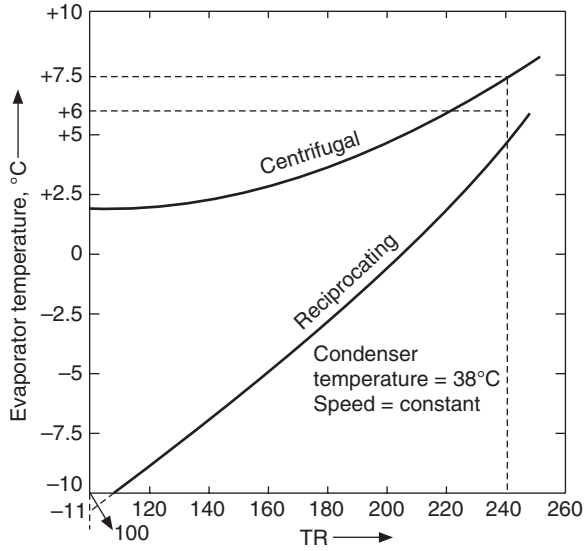

Figure 4.26 Effect of evaporator temperature on the cooling capacity of centrifugal and recriprocating compressors.

Figure 4.27 shows the variation of cooling capacity with condenser temperature at fixed evaporator temperature of 4.4ºC and constant speed. As the condenser temperature increases the

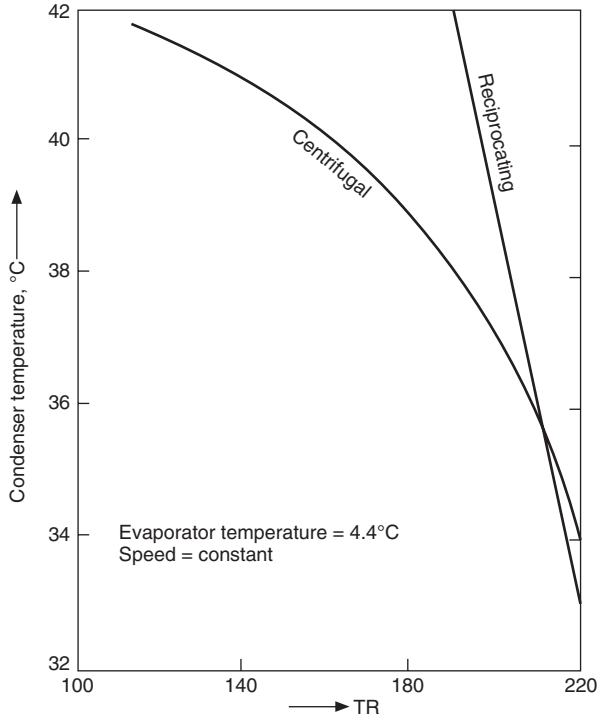

Figure 4.27 Effect of condenser temperature on the cooling capacity of centrfigual and reciprocating compressors.

decrease in capacity of the reciprocating compressor is rather small compared to centrifugal compressor for which there is a drastic decrease. If the condenser temperature is very high, the system pressure ratio becomes so large that the compressor cannot match this pressure ratio. That is, the compressor cannot develop the head required by the system and hunting will occur. Decreasing the mass flow rate of cold water to the condenser can increase the condenser temperature. This then becomes a very effective method of capacity control of centrifugal compressors. The reduction in capacity of reciprocating compressor is rather small and the compressor continues to have positive displacement and produce refrigeration until its volumetric efficiency becomes zero. However it does not face the surge instability.

The power requirement of the centrifugal compressor decreases as the condenser temperature increases, since the capacity reduces drastically, as shown in Figure 4.28. However, the power required per TR increases. Therefore, in summer the capacity will decrease and hence the motor will not be overloaded. This is called *non-overloading characteristic* of the centrifugal compressor. The power requirement of the reciprocating compressor increases as the condenser temperature increases. This causes overloading of the motor during peak summer.

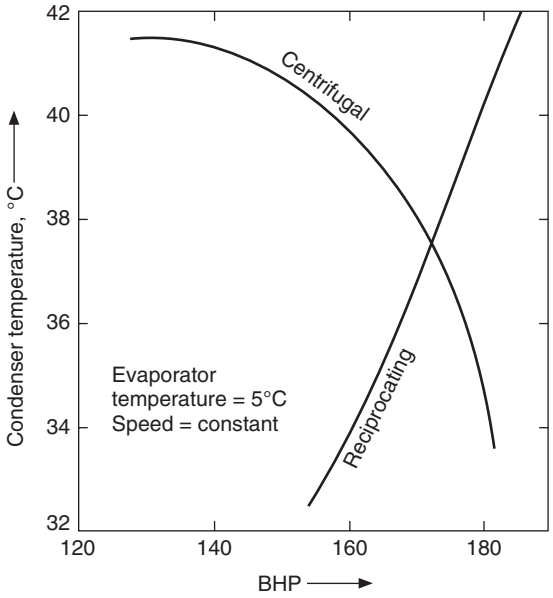

Figure 4.28 Effect of condenser temperature on the power requirement of centrifugal and reciprocating compressors.

Figure 4.29 shows that the centrifugal compressor is more sensitive to speed changes than the reciprocating type of compressor. In the reciprocating compressor the change in capacity is proportional to the speed, for example, a change in speed of 12.5% can bring about a change of 50% in cooling capacity.

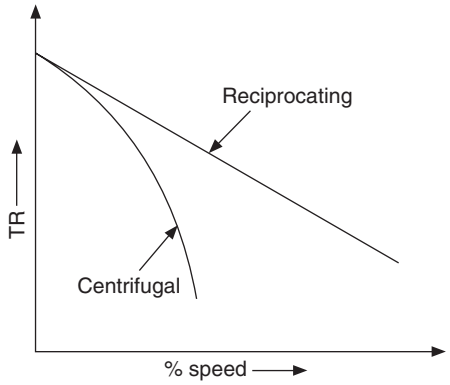

Figure 4.29 Effect of compressor speed on the performance of reciprocating and centrifugal compressors at the given condensing and evaporator temperatures.

4.8 CAPACITY CONTROL

One of the main advantages of centrifugal compressors is its capability to achieve smooth reduction in flow rate and thereby a reduction in cooling capacity. There are four methods of achieving this, namely:

1. Adjusting pre-rotation blades at the impeller inlet.
2. Speed variation
3. Increase in condenser pressure by controlling the water flow rate to the condenser.
4. Hot gas bypass

The first two methods are the popular methods and the first method is the most commonly used method.

A set of adjustable guide vanes in the inlet duct deflect the inlet stream towards the direction of rotation of impeller. It may be seen from Figure 4.30 that this introduces a prewhirl component and reduces the relative velocity C_{r1} at the same time, thereby resulting in decreased flow rate. The

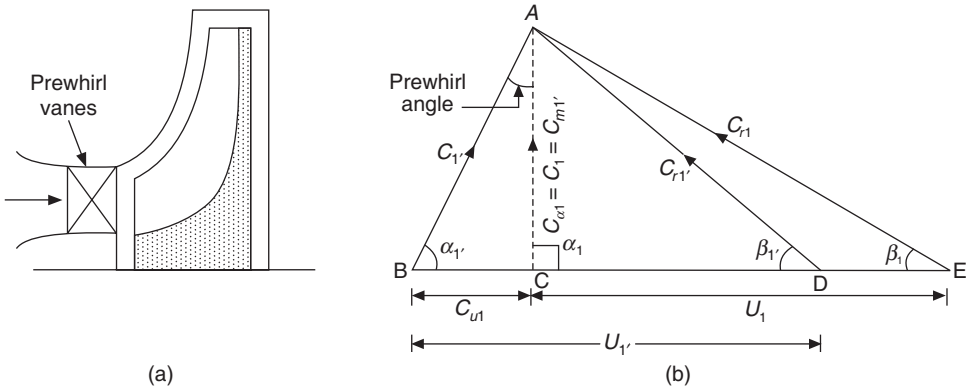

Figure 4.30 (a) Inlet guide vanes (prewhirl vanes) and (b) inlet velocity triangle with and without prewhirl.

introduction of prewhirl reduces the power input and the associated pressure ratio. At small flow rates the diffuser is not matched to the impeller, and it may be necessary to also adjust the width of the diffuser passages for smooth flow.

The vanes of the diffuser may be used to decrease the flow area. This will give rise to higher static pressure, which will reduce the flow rate. Figure 4.31 shows the effect of pre-rotation on the capacity of a centrifugal compressor. The position indicated by 90° is the full open position whereas 0° is the fully closed position. This is an efficient method when the vanes are in the near fully open position.

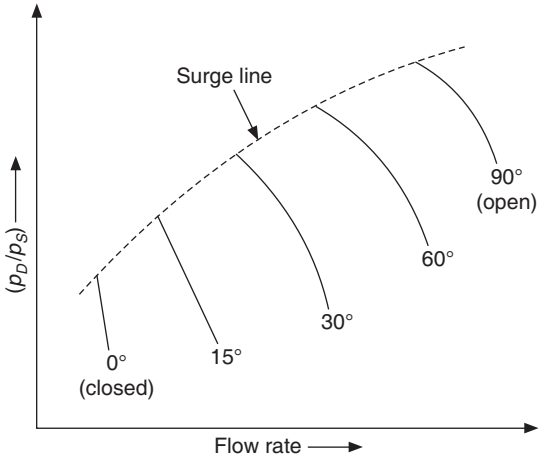

Figure 4.31 Effect of the angle of pre-rotation vanes on the capacity of a centrifugal compressor.

The capacity variation by speed control is the most common method used for centrifugal compressors. The typical variation has been shown in Figure 4.24 where at each speed, as the flow rate decreases, the work requirement and the corresponding pressure ratio increases. When the centrifugal compressor is driven by a steam or gas turbine, the variation of speed can be achieved very easily. These days, frequency controlled motors are used to achieve variation of speed efficiently.

4.9 SELECTION OF COMPRESSORS

Reciprocating compressor are normally used up to 350 kW or 100 TR cooling capacity. Very large numbers of these are manufactured since all small refrigeration and air-conditioning systems use the reciprocating compressor.

Centrifugal compressors are usually suitable for systems of 500 kW and higher cooling capacities.

Screw compressors fill the gap between the reciprocating compressors and the centrifugal compressors in the range of 300 to 500 kW. Screw compressors are more efficient at full load. Screw compressors have less number of moving parts than the reciprocating compressor, thus affording longer gaps between successive overhauls. This feature competes well with large reciprocating compressors and small centrifugal compressors.

Reciprocating compressors have better efficiency at part load and longer operating life than the screw compressors.

A good practice is to use the screw compressor for base load and the reciprocating compressor for variation above the base load. This will give the advantage of efficient operation of screw compressor at full load and good performance of reciprocating compressor at variable load.

For large capacities there is no alternative to centrifugal compressors. These have high efficiency over a wide load range with speed control. Hence, speed control by a frequency-controlled motor is essential, without which it gives poor performance at reduced loads. It has high volume flow rate per unit size. It has flat head vs. capacity characteristics compared to the reciprocating compressor.

REFERENCES

Bendixen ,I. (1959): The volumetric efficiency of reciprocating compressors, *Proc. 10th Int. Congr. Refrig.*, Copenhagen, Vol. 2 pp. 190–198.

Brown, J. and Kennedy, W.K. (1971): Cylinder heat transfer in the cylinder of a refrigeration compressor, *Proc. 13th Int. Congr. Refrig*., Washington, Vol. 2, pp. 545– 549.

Cheglikov, A.G., Effect of suction vapour superheat on the volumetric efficiency of a propane compressor, Abstract in *J. Refrig*. Vol. 6, pp. 112–114, 1063.

Chlumsky, V. (1965): *Reciprocating and Rotary Compressors*, E and FN Spon, London.

Cohen, H., Rogers, G.F.C. and Saravanamuttoo, H.I.H. (1987): *Gas Turbine Theory*, Longman Scientific and Technical, London.

Fergusen, T.B. (1963): *The Centrifugal Compressor Stage*, Butterworth, London.

Giffen, E. and Newly, E.F. (1940): Refrigerator performance: An investigation into volumetric efficiency, *Proc. Inst. Mech. Eng*., Vol. 143, pp. 227–236.

Gosney, W.B. (1953): An analysis of the factors affecting performance of small compressors, *Proc. Inst. Refrig*. Vol. 49, pp. 185–216.

Gosney, W.B. (1982): *Principles of Refrigeration*, Cambridge University Press, London.

Löffer, G. (1943): Die rechnerische Erfassung des Ausnutzungsgrades (Liefergrades) von Ammoniak Kolbenverdichtern, *Z. ges. Kalte-Industrie*, Vol. 48, pp. 169–173.

Lysholm, A.J.R. (1943): New Rotary Compressor, *Proc. Inst. Mech. Eng*., Vol. 150, pp. 11–16, 151, 179–184.

Pierre, Bo. (1958): *Eigenschaften moderner amerikaner Freonverdichter, Kaltetexhnik*, Vol. 4, pp. 83–87.

Stanitz, J.D. (1952): Some theoretical aerodynamic investigations of impellers in radial and mixed-flow centrifugal compressors, *TRANS. ASME*, Vol. 74, pp. 473–97.

Stepanoff, A.J. (1955): *Turboblowers*, Wiley, New York.

Wiesner, F.J. and Caswell, H.E. (1959): How Refrigerant Properties Effect Impeller Dimensions, *ASHRAE J*. 1, no.10, pp. 31–37, 104–106.

Wiesner, F.J. (1970): Practical Stage Performance Correlations for Centrifugal Compressors, *ASME Paper*, 60-Hyd-17.

Wirth, G. (1933): Uber den Einfluss der Wandtemperatur auf den Arbeitsprozess des Kaltekolbenmaschinen, *Z. ges. Kalte-Industrie*, Vol. 40, pp. 138.

REVIEW QUESTIONS

1. Derive expressions for the work requirement for open and closed systems for polytropic compression.
2. Derive an expression for the clearance volumetric efficiency of reciprocating compressor. Also, find the pressure ratio at which the volumetric efficiency reduces to zero.
3. Discuss the effect of valve pressure drops on volumetric efficiency of reciprocating compressor.
4. Discuss all the factors that affect the volumetic efficiency of reciprocating compressor.
5. Discuss all the factors that affect the performance of a real compressor.
6. Discuss the features of hermetic compressors.
7. What are the different types of rotary compressors? Explain the working principle of each one of them.
8. Explain the surging phenomenon in centrifugal compressors.
9. Differentiate between the centrifugal compressor and the reciprocating compressor from the point of view of effect of evaporator temperature and condenser temperature on their cooling capacity and power requirement.
10. Enumerate the factors governing the selection of compressors for different applications.
11. R22 is compressed in a reciprocating compressor from saturation pressure at –18°C to saturation pressure at 40°C. The compressor has four cylinders each with a bore/stroke ratio of 1, and runs at 1420 rpm. Assume a pressure drop of 5% of the value of pressure at the compressor valves. The clearance volume ratio is 0.04. The vapour entering the compressor gets superheated to 15°C outside the evaporator. Find the clearance volumetric efficiency by using the isentropic index, (ii) the swept flow rate, (iii) the mass flow rate, and (iv) the refrigeration capacity and work requirement.
12. R22 is compressed in a centrifugal compressor between a condenser temperature of 35°C and an evaporator temperature of –15°C. The small-stage efficiency is 0.8. Determine the specific work, the adiabatic discharge temperature and the polytropic efficiency.
13. R134a is compressed in a backward-curved centrifugal compressor to a pressure of 7.702 bar and 40°C at the exit of the impeller. The diameter of the impeller is 0.6 m and the blade angle is 60°. The peripheral area is 0.02 m^2 and the flow coefficient (ratio of normal component of velocity to the tip speed) is 0.5. The impeller rotates at 900 rpm. The tangential component of velocity at the inlet to the compressor may be assumed to be negligible. Find the specific work and the power input to the compressor.

5

Performance of Single Stage Saturation Cycle with Reciprocating Compressor

LEARNING OBJECTIVES

After studying this chapter the student should be able to:

1. Derive expressions for the work requirement of the reciprocating compressor in a refrigeration system using single stage saturation (SSS) cycle.
2. Explain how the volumetric efficiency and mass flow rate of the reciprocating compressor vary with the evaporator temperature for a fixed condenser temperature.
3. Explain the effect of evaporator temperature on the work requirement of the reciprocating compressor for a fixed value of condenser temperature.
4. Analyze the effect of suction pressure on the horsepower per TR of the reciprocating compressor for a fixed value of condenser temperature.
5. Discuss the effect of evaporator temperature on refrigeration effect and refrigeration capacity of the SSS cycle with reciprocating compressor.
6. Explain the effect of evaporator temperature on the capacity of the reciprocating compressor.
7. Explain how the compressor discharge temperature varies with the pressure ratio for different refrigerants keeping the condenser temperature fixed.
8. Show why the SSS cycle with reciprocating compressor is not suitable for low evaporator temperatures.
9. Show how reduction in isentropic compressor work and increase in refrigeration effect can be achieved by multistage compression.
10. Explain the factors governing the choice of intermediate pressure in a two-stage SSS cycle.
11. Derive the expression for optimum intermediate pressure for ideal gas reciprocating compressor with ideal intercooling.

12. Derive the expression for optimum intermediate pressure for nonideal intercooling.
13. Write the expressions for optimum intermediate pressures for three-stage and four-stage compression.

5.1 INTRODUCTION

The general performance characteristics of SSS cycle have been discussed in Chapter 3 while the performance of the reciprocating compressor has been discussed in Chapter 4. The refrigeration system has to work at varying condenser temperatures, which is high during summer months and relatively low during winter months. The load on the system is also variable, being high during pull-down period and low during steady state. Then there can be seasonal variations in load as well. The most important parameter from the performance point of view is the evaporator temperature. It is dependent upon the requirement, for example a food freezing application may require –30°C and air-conditioning may require around 0°C. Chemical processing plants may require the evaporator to be as low as –60°C.

In this chapter, the results of Chapters 3 and 4 are combined together for a reciprocating compressor and discussed for varying condenser and evaporator temperature. For a given reciprocating compressor of bore d, stroke L and running at constant rpm of N, the swept or displaced volume and the swept flow rate are respectively given by

$$\mathbb{V}_D = (\pi d^2/4)L \times nu \tag{5.1}$$

$$\mathbb{V}_S = \mathbb{V}_D N/60 \tag{5.2}$$

where, nu is the number of cylinders.

If v_1 is the specific volume at suction flange of the compressor and η_{vol} is the volumetric efficiency, the mass flow rate of refrigerant is given by

$$\dot{m} = \mathbb{V}_S \eta_{vol}/v_1 \tag{5.3}$$

The volumetric efficiency in its simplest form is given by

$$\eta_{vol} = 1 + \varepsilon - \varepsilon\left(\frac{p_D}{p_S}\right)^{1/n} \tag{5.4}$$

where, ε is the clearance volume ratio $\mathbb{V}_{cl}/\mathbb{V}_D$, p_S and p_D are the suction and discharge pressures of compressor respectively as shown in Figure 5.1.

The work requirement for the reciprocating compressor as given by Eq. (4.29) is

$$W = \dot{m}\left(\frac{n}{n-1}\right)p_S v_S\left[\left(\frac{p_D}{p_S}\right)^{(n-1)/n} - 1\right]\frac{1}{\eta_{mech}} \tag{5.5}$$

where, η_{mech} is the mechanical efficiency of the compressor and v_S is the specific volume at the end of the suction stroke.

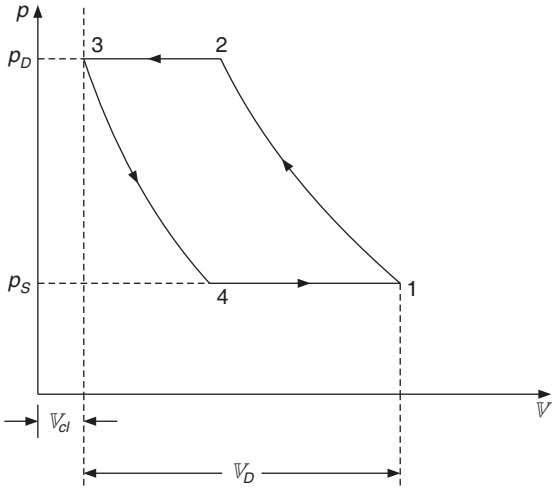

Figure 5.1 Pressure–volume diagram of a reciprocating compressor.

Substituting for $\dot{m}$ from Eq. (5.3) and assuming that specific volume during suction stroke v_S is same as v_1, we get

$$W = \left(\frac{n}{n-1}\right) p_S \mathbb{V}_S \eta_{\text{vol}} \left[\left(\frac{p_D}{p_S}\right)^{(n-1)/n} - 1\right] \frac{100}{\eta_{\text{mech}}} \text{ kW, where } p_S \text{ is in bar} \tag{5.6}$$

Another way of expressing these relations is to find the compressor swept flow rate and specific work requirement for a given cooling capacity in TR. It was shown in Chapter 3 that

$$\text{Specific refrigeration effect} = (h_1 - h_3) \text{ kJ/kg} \tag{5.7}$$

$$\text{Hence, mass flow rate of refrigerant,} \quad \dot{m} = \frac{3.5167 \text{ TR}}{(h_1 - h_3)} \text{ kg/s} \tag{5.8}$$

$$\text{Therefore, from Eq. (5.3),} \quad \mathbb{V}_S = \dot{m} v_1 / \eta_{\text{vol}} = \frac{3.5167 \text{ TR } v_1}{(h_1 - h_3)\eta_{\text{vol}}}$$

$$\therefore \quad \mathbb{V}_S / \text{TR} = \frac{3.5167 v_S}{(h_1 - h_3)\eta_{\text{vol}}} \qquad (\because \ v_1 = v_S) \tag{5.9}$$

Substituting for $\mathbb{V}_S$ from Eq. (5.9) into Eq. (5.6) for work requirement,

$$W = \left(\frac{n}{n-1}\right) \frac{3.5167 \text{ TR}}{(h_1 - h_3)} p_S v_S \left[\left(\frac{P_D}{P_S}\right)^{(n-1)/n} - 1\right] \frac{100}{0.736 \eta_{\text{mech}}} \text{ HP}$$

$$\therefore \quad \frac{\text{HP}}{\text{TR}} = 477.81 \left(\frac{n}{n-1}\right) \frac{p_S v_S}{(h_1 - h_3)} \left[\left(\frac{p_D}{p_S}\right)^{(n-1)/n} - 1\right] \frac{1}{\eta_{\text{mech}}} \tag{5.10}$$

where, p_S is in pascal.

The expression for isentropic work is given by

$$W = \dot{m}(h_2 - h_1) \tag{5.11}$$

If isentropic compression efficiency is η_{isen}, then the actual work requirement is

$$W = \frac{\dot{m}\,(h_2 - h_1)_{\text{isen}}}{0.736\,\eta_{\text{mech}}\,\eta_{\text{isen}}}\ \text{HP} \tag{5.12}$$

Substituting for $\dot{m}$ from Eq. (5.8), we get

$$W = \frac{3.5167\ \text{TR}\ (h_2 - h_1)_{\text{isen}}}{0.736\,(h_1 - h_3)\,\eta_{\text{mech}}\,\eta_{\text{isen}}}\ \text{HP}$$

$$\therefore \quad \frac{\text{HP}}{\text{TR}} = 4.7781\,\frac{(h_2 - h_1)_{\text{isen}}}{(h_1 - h_3)\,\eta_{\text{mech}}\,\eta_{\text{isen}}} \tag{5.13}$$

or

$$\frac{\text{kW}}{\text{TR}} = 3.5167\,\frac{(h_2 - h_1)_{\text{isen}}}{(h_1 - h_3)\,\eta_{\text{mech}}\,\eta_{\text{isen}}}$$

5.2 VOLUMETRIC EFFICIENCY AND MASS FLOW RATE

The volumetric efficiency as given by Eq. (5.4) depends upon compressor suction and discharge pressures p_S and p_D respectively. The evaporator and condenser pressures are p_1 and p_2 respectively. In the following we assume that the pressure drops are negligible, hence $p_S = p_1$ and $p_D = p_2$. The evaporator and condenser temperatures are the saturation temperatures t_e and t_c at pressures p_1 and p_2 respectively for the given refrigerant. The variation of volumetric efficiency can, therefore, be plotted with t_c and t_e as variables. The variation of volumetric efficiency and the variation of mass flow rate with the evaporator temperature (or pressure) are shown in Figure 5.2 for a fixed value of condenser temperature. For a fixed condenser temperature, η_{vol} decreases with decrease in evaporator temperature since the pressure ratio increases.

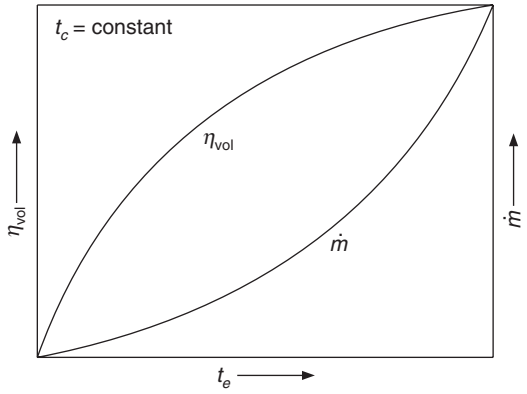

Figure 5.2 Effect of evaporator temperature on volumetric efficiency and refrigerant mass flow rate.

$$\eta_{vol} = 1 \quad \text{for} \quad p_1 = p_2$$

and $$\eta_{vol} = 0 \quad \text{for} \quad p_1 = p_2/(1 + 1/\varepsilon)^n$$

These two results can easily be derived from Eq. (5.4). For ammonia and R22, the value of n may be taken as 1.3 and 1.1 respectively. The volumetric efficiency is zero at pressure ratio of 69 for NH3 and 36 for R22.

As the condenser temperature increases, the volumetric efficiency decreases for all evaporator temperatures since the pressure ratio increases.

The mass flow rate decreases at a faster rate with decrease in suction pressure as compared to η_{vol} since the specific volume v_1 of the refrigerant in Eq. (5.3) increases as the pressure decreases. The mass flow rate is maximum when $p_1 = p_2$ and zero when the volumetric efficiency is zero. As the condenser temperature increases, the mass flow rate decreases as a direct result of decrease in volumetric efficiency.

5.3 WORK REQUIREMENT AND HP/TR

5.3.1 Work Requirement

The variation of work requirement with evaporator temperature (or pressure) as given by Eq. (5.5) is shown in Figure 5.3 for a fixed value of condenser temperature.

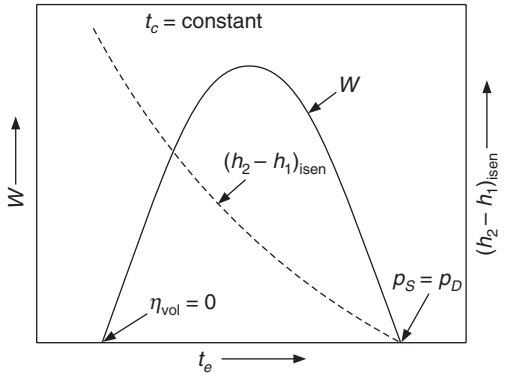

Figure 5.3 Effect of evaporator temperature on the work requirement for the reciprocating compressor.

In Eq. (5.5) at fixed discharge pressure (or temperature), as the suction pressure (or temperature) decreases, the specific volume v_S and pressure ratio increase, while suction pressure and mass flow rate both decrease. When suction pressure is equal to discharge pressure, that is, $p_D/p_S = 1$, the power requirement is zero. As the suction pressure starts decreasing, the effect of rise in pressure ratio and specific volume will dominate and the work requirement will increase.

This trend in rise in work requirement continues until the decrease in suction pressure and mass flow rate counterbalance and start to dominate. Then the power requirement decreases with decrease in suction pressure and becomes zero at the pressure where the volumetric efficiency is zero. The variation of work requirement with suction pressure exhibits a maxima. The location of the maxima has been discussed in Section 4.3.7.

As the condenser temperature increases the curve in Figure 5.3 shifts to the right, $p_D/p_S = 1$ where $W = 0$ occurs at a higher suction pressure (equal to condenser pressure). The location of maximum also shifts to a higher evaporator temperature.

Alternatively, the compressor work = $\dot{m}(h_2 - h_1)_{\text{isen.}}$ The specific isentropic work as seen in Figure 5.3 continuously increases as the suction pressure (or temperature) deceases. While the mass flow rate as seen in Figure 5.2 continuously decreases, these two counteracting terms give rise to a maximum.

5.3.2 HP/TR

Horsepower per TR is given by Eqs. (5.10) and (5.13). An inspection of Eq. (5.10) reveals that as the suction pressure decreases, the pressure ratio and the specific volume increase. Their combined effect dominates over the decrease in p_S. As a result, as shown in Figure 5.4, the HP/TR increases as p_S decreases. As the condenser temperature increases, HP/TR becomes larger since the pressure ratio is larger.

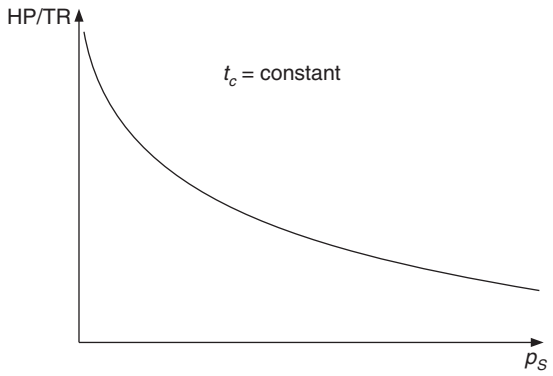

Figure 5.4 Effect of suction pressure (or temperature) on the horsepower per ton of reciprocating compressor.

5.4 SPECIFIC REFRIGERATION EFFECT AND REFRIGERATION CAPACITY

We know that:

$$\text{Specific refrigeration effect} = (h_1 - h_3) \tag{5.14}$$

$$\text{Refrigeration capacity} = \frac{\dot{m}(h_1 - h_3)}{3.5167} = \frac{\mathbb{V}_S \eta_{\text{vol}}}{v_1} \frac{(h_1 - h_3)}{3.5167} \tag{5.15}$$

It is observed that specific refrigeration effect decreases slightly with decrease in suction pressure (or temperature) as shown in Figure 5.5. As the condenser temperature increases, the specific refrigeration effect further decreases for all evaporator temperatures. In Eq. (5.15) for refrigeration capacity, it is observed that as the evaporator temperature decreases, η_{vol} and $(h_1 - h_3)$ (seen from Figures 5.2 and 5.4 respectively) decrease while the specific volume in the denominator increases. Hence, all of these contribute towards the decrease in refrigeration capacity. As a result,

the refrigeration capacity decreases at a very fast rate with decrease in evaporator pressure as shown in Figure 5.5. Refrigeration capacity is zero at the pressure where the volumetric efficiency is zero.

An increase in condenser temperature decreases both the refrigeration effect and the volumetric efficiency, hence the refrigeration capacity decreases with increase in condenser temperature.

A given refrigeration system will give lower refrigeration capacity at lower t_e and at higher condenser temperature t_c.

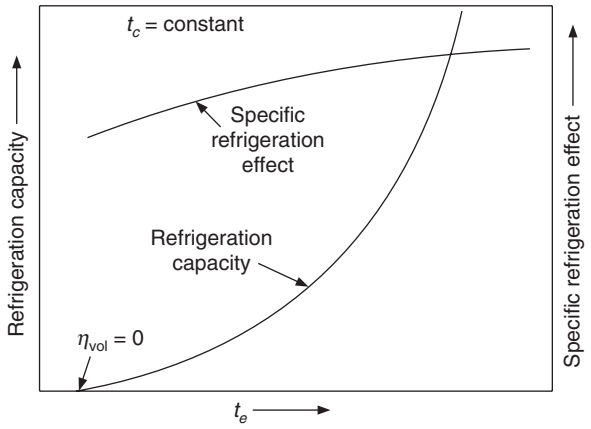

Figure 5.5 Effect of evaporator temperature on specific refrigeration effect and refrigeration capacity.

5.5 SWEPT FLOW RATE PER TR

It is observed from Eq. (5.9) that specific volume v_1 increases while volumetric efficiency η_{vol} and specific refrigeration effect both decrease (in denominator) as the suction pressure decreases, thus contributing towards drastic increase in swept flow rate per TR. $\mathbb{V}_S$/TR becomes infinitely large at suction pressure for which η_{vol} is zero. This is shown in Figure 5.6.

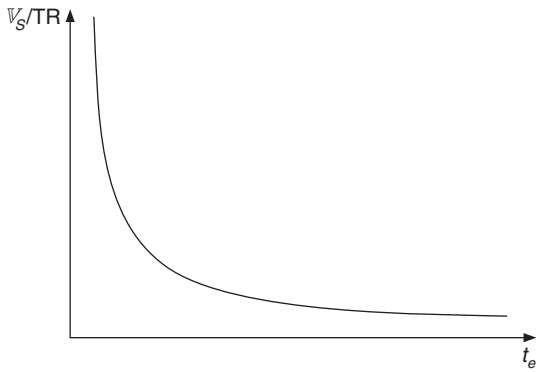

Figure 5.6 Effect of evaporator temperature on swept flow rate per TR.

This implies that lower the evaporator temperature the larger will be the compressor required to produce the given refrigeration capacity.

OR

A given compressor will give lower refrigeration capacity at lower evaporator temperature.

At larger condenser temperature both the η_{vol} *and the specific refrigeration effect decrease and hence* $\mathbb{V}_S$ / TR *increases with increase in* t_c.

5.6 ADIABATIC DISCHARGE TEMPERATURE

An approximate expression for adiabatic discharge temperature is

$$T_2 = T_e \left(\frac{p_D}{p_S} \right)^{(k-1)/k}$$

The index of compression k depends upon t_c, t_e and the extent of superheating since refrigerant is vapour and not a gas, still it is very close to specific heat ratio γ. The index k is the average index for isentropic compression. The state 2 at the end of isentropic compression is found by looking into superheat tables for $s_1 = s_2$ and then v_2 is found. Finally, index k is found from $p_2 v_2^{\,k} = p_1 v_1^{\,k}$. The procedure for this was outlined in Section 4.3.5, Eq. (4.31).

The value of k is around 1.3 for NH_3 and around 1.1 for R22 and the value is still lower for R12. For a fixed condenser temperature (and pressure), as the suction pressure decreases, the pressure ratio increases and hence the adiabatic discharge temperature increases. Figure 5.7 shows the variation of adiabatic discharge temperature with pressure ratio for three refrigerants at a condenser temperature of 32°C. NH_3 has the highest value of t_2. R22 also has a significantly high value of t_2 at low suction pressures (i.e. high pressure ratios) while R12 has low value of t_2. R134a also has a value similar to that for R12. The lubricant in contact with vapour also gets heated to a high temperature and may start to fume at temperature around 175°C. The fuming will cause carbonization of lubricant; this carbon will adversely affect the viscosity of lubricant and the sticky mixture of carbon and lubricant may deposit on the valves and make their operation sluggish. Ammonia compressors for this reason are provided with water jackets around the cylinder and cold water is circulated in the jacket to keep the vapour temperature low.

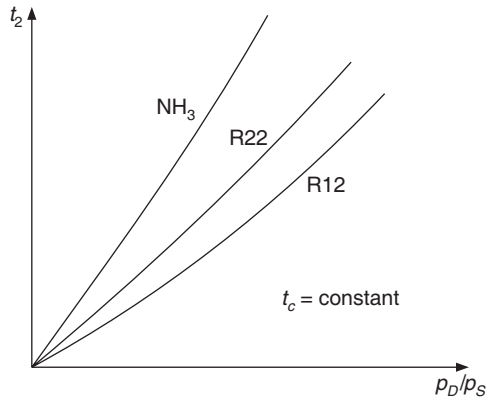

Figure 5.7 Variation of compressor discharge temperature with pressure ratio for different refrigerants for a fixed condenser temperature.

5.7 COEFFICIENT OF PERFORMANCE

Figure 5.8 shows the variation of COP with suction pressure (or evaporator temperature). The COP of the refrigerants NH_3, R22 and R12 are about the same, NH_3 having a slightly larger value and R22 having the lowest value. The COP decreases drastically with decrease in suction pressure. This trend has already been discussed in Section 3.14.3 .

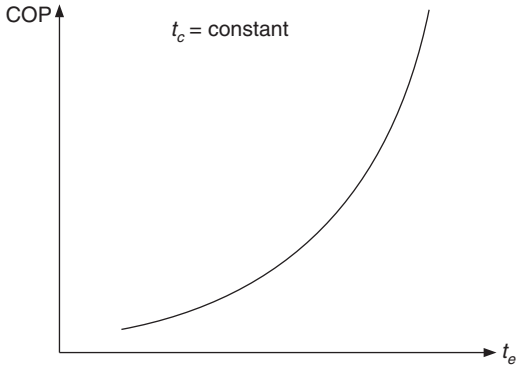

Figure 5.8 Effect of evaporator temperature on COP of SSS cycle with reciprocating compressor.

It is evident from the preceding discussion that the Single Stage Saturation (SSS) cycle with reciprocating compressor is not suitable for low evaporator temperatures mainly because of the following reasons.

1. The swept flow rate per TR is very high as shown in Figure 5.6, thereby requiring a large compressor.
2. Refrigerating efficiency is very low, that is, the COP is very low. Hence the cycle is not energy efficient at low evaporator temperatures (see Figure 5.8).
3. Adiabatic discharge temperature is very high which may cause fuming of lubricating oil (see Figure 5.7).

5.8 METHODS OF IMPROVING COP

COP being the ratio of specific refrigerating effect and specific isentropic compression work, can be improved by either reducing the specific isentropic compression work or by increasing the specific refrigeration effect.

5.8.1 Reduction in Isentropic Compression Work

Carrying the work in a number of stages can reduce the isentropic compression work. This is illustrated below. Figure 5.9(a) shows isentropic work from pressure p_1 to p_2 in single stage compression along process 1–2. An alternative way to decrease the work requirement is to carry the compression in two stages, as follows:

- First stage isentropic compression 1–3 up to an intermediate pressure $p_{i1} < p_2$.

- Intercooling from temperature t_3 along the constant pressure line up to the saturated state 4.
- Followed by second stage isentropic compression 4–5 up to the final pressure p_2.

Single-stage compression work (Figure 5.9(a)) = $h_2 - h_1$

Two-stage work (Figure 5.9(b)) = $(h_3 - h_1) + (h_5 - h_4)$

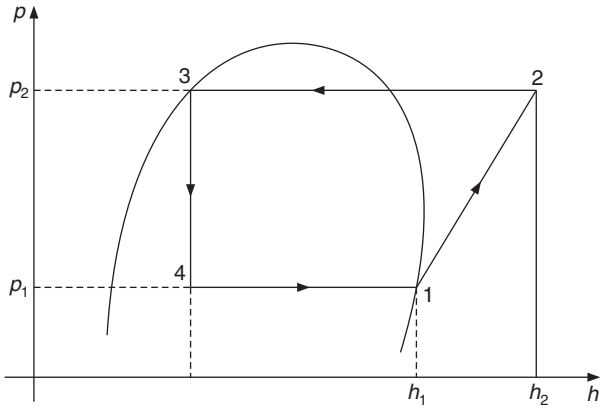

Figure 5.9(a) Single-stage compression along process 1–2.

Two-stage compression will result in a saving of work if

$$(h_3 - h_1) + (h_5 - h_4) < h_2 - h_1$$

or $$(h_3 - h_1) + (h_5 - h_4) < (h_2 - h_3) + (h_3 - h_1)$$

or $$(h_5 - h_4) < (h_2 - h_3)$$

This is possible only when the constant entropy lines 1–2 and 4–5 on p–h diagram 5.9(b) are divergent. If lines 1–2 and 4–5 are parallel, then $(h_5 - h_4) = (h_2 - h_3)$ and there will be no saving in work.

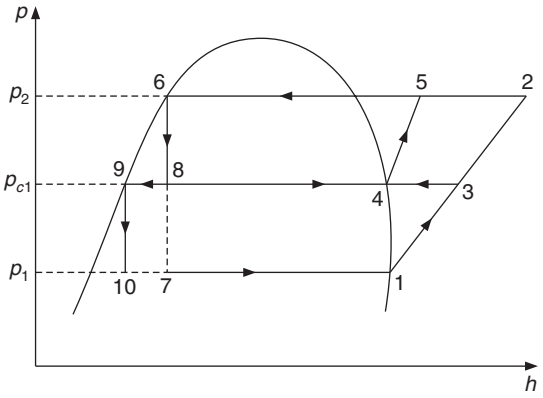

Figure 5.9(b) Two-stage compression.

Figures 5.10(a) and (b) show three-stage compression on *p–h* and *T–s* diagrams respectively with intercooling between the stages. Process 1–3 is the first stage isentropic compression to pressure p_{i1} followed by isobaric intercooling 3–4. Process 4–5 is the second stage isentropic compression from pressure p_{i1} to pressure p_{i2} followed by isobaric intercooling 5–6. Finally, process 6–7 is the third stage isentropic compression from pressure p_{i2} to pressure p_2. Following the reasoning given above, the saving in work will be the crosshatched area 3–4–5–6–7–2–3 in Figure 5.10. The saving in work for three-stage compression is more than that for a two-stage cycle. Therefore, the saving in work increases as the number of stages is increased, i.e. the work requirement continues to decrease as long as the constant entropy lines are divergent. In other words, *the work requirement is minimum if it is carried close to the saturated vapour line, and theoretically minimum work will be required if the compression can be carried along the saturated vapour line.* However, this is not possible since entropy decreases along the saturated vapour line for most of the refrigerants.

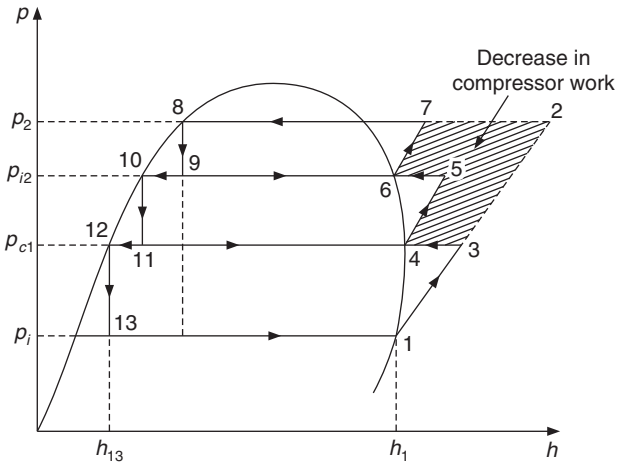

(a) *p–h* cycle

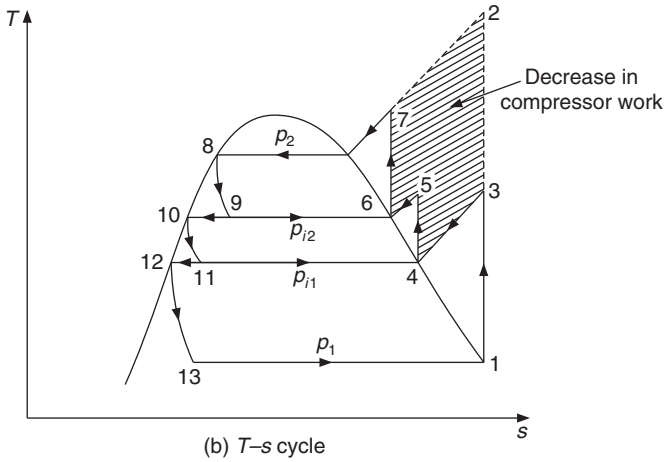

(b) *T–s* cycle

Figure 5.10 Three-stage compression.

There are two more advantages of multistage compression:

(i) In Figure 5.9(b), temperature $t_2 > t_5$ and in Figure 5.10, temperature $t_2 > t_7$. This implies that the adiabatic discharge temperature decreases as the number of stages increase.

(ii) The volumetric efficiency in each stage will also increase, since the pressure ratio is smaller in all the stages compared to that in single stage.

These two aspects were the other two disadvantages of the SSS cycle at low evaporator temperatures.

More number of stages will require more compressors and intercoolers, requiring more capital, maintenance and running cost. Therefore, the number of stages in a practical system are decided by economic as well as thermodynamic considerations.

5.8.2 Increase in Specific Refrigeration Effect

Figure 5.9(a) shows that throttling process along 3–4 from condenser pressure p_2 to evaporator pressure p_1 gives specific refrigeration effect of $h_1 - h_4$. Carrying out the expansion in two stages (Figure 5.9(b)) as follows can increase this specific refrigerating effect.

- Carry out first stage throttling along 6–8 up to intermediate pressure p_{i1}.
- Separate out the liquid at state 9 and vapour at state 4 in a surge chamber at pressure p_{i1}.
- Throttle the liquid at state 9 in second stage throttling along 9–10 from pressure p_{i1} to pressure p_2.

The specific refrigeration effect of two-stage throttling is $(h_1 - h_{10})$, which is greater than the refrigeration effect of single-stage throttling $(h_1 - h_7)$. See Figure 5.9(b).

Similarly, in a three-stage system shown in Figure 5.10(a), the specific refrigeration effect $(h_1 - h_{13})$ is greater than that of the two-stage system $(h_1 - h_{10})$ in Figure 5.9(b) and single-stage system $(h_1 - h_4)$ in Figure 5.9(a). Similarly, the specific refrigeration effect continues to increase with the number of stages, that is, it continues to increase as the process becomes closer and closer to the saturated liquid line. *The refrigeration effect shall be maximum if the expansion can be carried out along the saturated liquid line with continuous removal of vapour as it is formed by flashibg*.

There is another subtle practical advantage that cannot be seen in the diagrams. The refrigeration effect is produced by evaporation of liquid, the vapour present at point 7 in Figure 5.9(b) remains at constant temperature t_e throughout the evaporation process in the evaporator. It unnecessarily occupies some volume and precious heat transfer area in the evaporator. If this vapour is removed before entry into the evaporator, then the evaporator can be made more compact. During the expansion in two stages the vapour formed during the first stage expansion at state 8 is removed and fed to the high-pressure compressor at state 4. Thus, this vapour is not unnecessarily expanded to low pressure compressor p_1 and compressed again to intermediate pressure p_{1i}. Similarly, in three-stage expansion, the vapour formed during expansions 8–9, and 10–11 is fed to the intermediate compressors. The best possible expansion process will be the one in which the vapour is removed as soon as it is formed. Such a process will however require a large number of compressors as well. *Maximum specific refrigeration effect will occur if the expansion is carried out along the saturated liquid line with continuous removal of flash vapour.*

5.9 CHOICE OF INTERMEDIATE PRESSURE

In Figure 5.11, two possible choices of intermediate pressure are shown on the *T–s* diagram for a two-stage cycle. The corresponding saving in work requirement and the increase in refrigeration effect are also shown for a two-stage system. Single-stage saturation cycle (SSS cycle) is shown by 1–2–6–7–1. It is observed that at intermediate pressure p_{i1}, the cycle is 1–3–4–5–6–8–9–10–1. The saving in work is the area 3–2–5–4–3 and the increase in refrigeration effect is the area 7–10–*b*–*d*–7. As the intermediate pressure is increased to p_{i2}, the cycle is 1–3′–4′–5′–6–8′–9′–10′–1. Compared to SSS cycle the saving in work is the area 3′–2–5′–4′–3′ and the increase in refrigeration effect is the area 7–10′–*c*–*d*–7. The increment in refrigeration effect decreases with increase in intermediate pressure, while the area of saving in work increases in horizontal extent and decreases in vertical extent. The saving in work is strongly dependent upon the slopes of the saturated vapour lines and the slope of the constant pressure lines on the *T–s* diagram. Similarly, the increase in refrigeration effect is dependent upon the slope of the saturated liquid line on the *T–s* diagram.

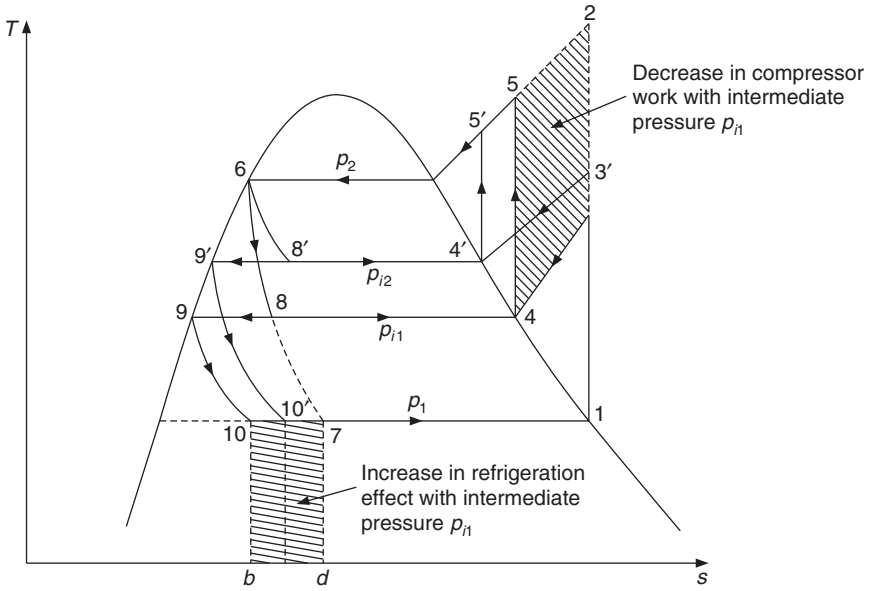

Figure 5.11 A two-stage SSS cycle at intermediate pressures p_{i1} and p_{i2}.

It can be shown that the mass flow rate of flash vapour after the first stage expansion is $\dot{m}_4 = x_8 \dot{m}_6$ and that of liquid $\dot{m}_9 = (1 - x_8)\dot{m}_6$. The mass flow rate $\dot{m}_9$ in the evaporator and through the first stage low-pressure compressor is less than the mass flow rate through the evaporator and compressor of the SSS cycle since the refrigeration effect of the SSS cycle is less than that of the two-stage cycle. On the other hand, the mass flow rate through the second stage, the high-pressure compressor, is more than that in the first stage. It is further observed that $x_{8'} < x_8$. That is, as the intermediate pressure increases the proportion of mass flow rate through the evaporator increases. The saving in refrigeration effect decreases (as discussed above), but the mass flow rate may be the same. The total work input $\dot{m}_{LP}(h_3 - h_1) + \dot{m}_{HP}(h_5 - h_4)$ depends upon mass flow rates too, apart from enthalpy differences. It appears that as the intermediate pressure increases (from

say evaporator pressure) the saving in work increases at first and then decreases. The combined effect of these two is that the COP will be optimum at some intermediate pressure.

The saving of work requirement in the two-stage system, further depends upon the effectiveness of intercooling. The adiabatic discharge temperature after the LP compressor may be less than 25°C. In such a case, intercooling cannot be done by water which may be available typically at 30°C or above during summer months. Therefore, in this case the intercooling has to be done by the refrigerant in a regenerative manner. The refrigerant that is used for intercooling would have given some refrigeration capacity that will be lost in this process. The crucial question is—will such a system still give improvement in COP. It so happens that this system still gives higher COP, hence it is used for multistage systems. This method of intercooling will also affect the choice of optimum intermediate pressure.

The optimum intermediate pressure can be obtained for a pair of evaporator and condenser pressures by carrying out thermodynamic cycle calculations for various intermediate pressures and plotting the COP vs. p_i. This, however, is a time consuming process and usually a first estimate or the range in which the optimum pressure occurs, will be required to start the calculations.

5.10 OPTIMUM INTERMEDIATE PRESSURE FOR IDEAL GAS COMPRESSOR WITH IDEAL INTERCOOLING

An estimate for optimum intermediate pressure may be obtained by considering the work requirement of a two-stage reciprocating ideal compressor with ideal intercooling with perfect gas as working substance. Ideal reciprocating compressor is a hypothetical compressor, which has zero clearance volume and ideal intercooling means that the gas after the first stage compression is intercooled to the initial temperature.

Figure 5.12 shows the pressure vs. volume diagram for the compression stroke for isentropic, polytropic and isothermal processes. Line 1–2*s* indicates the isentropic process with $n = \gamma$. Line 1–2*p* indicates the polytropic process with compression index n while line $1–2_{is}$ indicates the isothermal process with $n = 1$. In a flow process the work requirement is $\int \mathbb{V}\, dp$, hence the work requirement is the area projected on the pressure axis, i.e. area $1–2_{is}–b–a–1$ is the work requirement for isothermal compression, which is observed to be minimum amongst the processes shown. The

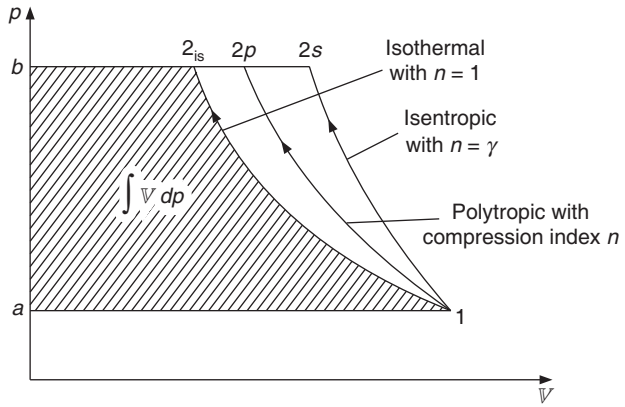

Figure 5.12 The ideal compression process on p–$\mathbb{V}$ diagram.

work requirement for isentropic process is the area 1–2*s*–*b*–*a*–1,which is larger than that for the isothermal process. Isothermal compression requires large heat rejection rate, which is rather difficult to achieve since (i) in high speed compressors the time available for heat rejection is small, (ii) the average piston velocity is small and hence the convective heat transfer coefficient on the gas side is small, (iii) the area available for heat rejection outside the cylinder block is small and (iv) heat transfer coefficient for heat rejection to outside air is also limited. Water cooling by a jacket around the cylinder and providing fins outside the cylinder block for air-cooling help to some extent. But isothermal compression is the theoretical and practical limit, which can be approached by multistage compression with intercooling between the stages.

In general, the compression process in reciprocating compressors is polytropic with $1 < n < \gamma$, while for centrifugal compressors $n > \gamma$. In reciprocating compressors, as the pressure ratio increases the volumetric efficiency decreases and the adiabatic discharge temperature increases. Both of these can be improved if the compression is carried in more than one stage with intercooling between the stages as shown in Figure 5.13 for a two-stage process. This process consists of

Process 1–3 : First stage polytropic compression
Process 3–3′ : Intercooling
Process 3′–2 : Second stage polytropic compression

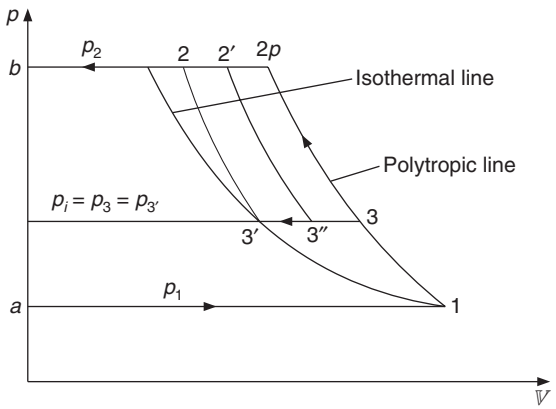

Figure 5.13 Two-stage reciprocating compressor with intercooling.

The intercooling is carried in a heat exchanger with heat rejection to either air or water.
An ideal intercooler is one in which

(i) there is no pressure drop, that is, $p_{3'} = p_3$ and
(ii) the temperature at 3′ is same as the inlet temperature to the first stage, that is, $t_{3'} = t_1$

The work requirement for single-stage compression is equal to the area 1–2*p*–*b*–*a*–1 while the work requirement for two-stage compression is the area 1–3–3′–2–*b*–*a*–1. It is observed from Figure 5.13 that two-stage compression leads to saving in work equivalent to area 3–3′–2–2*p*–3.

The work requirements of the first-stage compression 1–3 and the second stage compression 3′–2 are:

$$W_{13} = \frac{n}{n-1} p_1 \mathbb{V}_1 \left[\left(\frac{p_3}{p_1} \right)^{(n-1)/n} - 1 \right] \tag{5.16}$$

and

$$W_{3'2} = \frac{n}{n-1} p_{3'} \mathbb{V}_{3'} \left[\left(\frac{p_2}{p_{3'}} \right)^{(n-1)/n} - 1 \right] \tag{5.17}$$

From the ideal gas relation $p_1 \mathbb{V}_1 = m_1 R T_1$ and for ideal intercooling $T_{3'} = T_1$, therefore, $p_{3'} \mathbb{V}_{3'} = m_1 R T_1$ and Eqs. (5.16) and (5.17) reduce to

$$W_{13} = \frac{n}{n-1} m_1 R T_1 \left[\left(\frac{p_3}{p_1} \right)^{(n-1)/n} - 1 \right]$$

and

$$W_{3'2} = \frac{n}{n-1} m_1 R T_1 \left[\left(\frac{p_2}{p_{3'}} \right)^{(n-1)/n} - 1 \right] \tag{5.18}$$

Combining these two equations and denoting the intermediate pressure $p_{3'} = p_3$ by p_i, the net work requirement is given by

$$W_{\text{net}} = \frac{n}{n-1} m_1 R T_1 \left[\left(\frac{p_i}{p_1} \right)^{(n-1)/n} + \left(\frac{p_2}{p_i} \right)^{(n-1)/n} - 2 \right] \tag{5.19}$$

The optimum intermediate pressure for minimum work requirement is obtained by differentiating Eq. (5.19) with respect to p_i and equating it to zero. The terms outside the parenthesis in Eq. (5.19) are constants and hence only the terms inside are considered for differentiation. This differentiation yields

$$\frac{p_i^{-1/n}}{p_1^{(n-1)/n}} - \frac{p_2^{(n-1)/n}}{p_i^{(2n-1)/n}} = 0$$

or

$$p_i^{(2n-2)/n} = (p_1 p_2)^{(n-1)/n} \quad \text{or} \quad p_i^2 = p_1 p_2 \tag{5.20}$$

Therefore,

$$p_i = \sqrt{p_1 p_2}$$

or

$$\frac{p_i}{p_1} = \frac{p_2}{p_i} = \left(\frac{p_2}{p_1} \right)^{1/2} \tag{5.21}$$

Hence, the pressure ratio for the two stages of compression must be same for the work requirement to be minimum. In fact, it is observed from Eq. (5.18) that the work requirement will be same for the two stages if the pressure ratio is same and the polytropic index n is same. As a result, the above expression for optimum intermediate pressure could have been obtained by equating the work requirement of the two stages. Following this process, Eq. (5.18) yields

$$W_{13} = \frac{n}{n-1} m_1 RT_1 \left[\left(\frac{p_i}{p_1} \right)^{(n-1)/n} - 1 \right] = W_{3'2} = \frac{n}{n-1} m_1 RT_1 \left[\left(\frac{p_2}{p_i} \right)^{(n-1)/n} - 1 \right]$$

$\therefore$ $$\frac{p_i}{p_1} = \frac{p_2}{p_i} \quad \text{or} \quad p_i = \sqrt{p_1 p_2}$$

5.11 OPTIMUM INTERMEDIATE PRESSURE IF INTERCOOLING IS DONE UP TO TEMPERATURE T_w

The intercooling is done either by air or water made available from a cooling tower. Hence in either case the temperature at the exit of the intercooler cannot be below the temperature of air or water since some temperature difference is required for heat transfer to take place. Therefore, in Figure 5.13 point 3′ may not lie on isothermal line but it may be at 3″ where the temperature is $T_w > T_1$. In the case of refrigerant vapour, the refrigerant temperature at 3 may be less than the air temperature or water temperature and the intercooling may have to be done by the refrigerant itself.

The saving in work in this case is the area 3–3″–2′–2*p*–3 which is less than the saving in area 3–3′–2–2*p*–3 for the case of ideal intercooling.

In this case $p_{3''} \mathbb{V}_{3''} = m_1 RT_w$, hence Eq. (5.18) reduces to

$$W_{13} = \frac{n}{n-1} m_1 RT_1 \left[\left(\frac{p_3}{p_1} \right)^{(n-1)/n} - 1 \right] \tag{5.22a}$$

and $$W_{3''2'} = \frac{n}{n-1} m_1 RT_w \left[\left(\frac{p_2}{p_{3''}} \right)^{(n-1)/n} - 1 \right] \tag{5.22b}$$

The net work becomes

$$W_{\text{net}} = \frac{n}{n-1} m_1 R \left[T_1 \left\{ \left(\frac{p_i}{p_1} \right)^{(n-1)/n} - 1 \right\} + T_w \left\{ \left(\frac{p_2}{p_i} \right)^{(n-1)/n} - 1 \right\} \right] \tag{5.23}$$

Equating the derivative of this with respect to p_i to zero as done in Eq. (5.20), we get

$$T_1 \frac{p_i^{-1/n}}{p_1^{(n-1)/n}} - T_w \frac{p_2^{(n-1)/n}}{p_i^{(2n-1)/n}} = 0$$

or $$p_i^{(2n-2)/n} = (p_1 p_2)^{(n-1)/n} \frac{T_w}{T_1}$$

or $$p_i = \sqrt{p_1 p_2} \left(\frac{T_w}{T_1} \right)^{n/2(n-1)} \tag{5.24}$$

5.12 OPTIMUM INTERMEDIATE PRESSURES FOR THREE-STAGE COMPRESSION

Three-stage compression requires two intercoolers and thereby the optimization process requires determination of two interstage *pressures, namely* p_{i1} *and* p_{i2} *as shown in Figure 5.14. In case of ideal intercooling* $p_{3'}\mathbb{V}_{3'} = p_{4'}\mathbb{V}_{4'} = mRT_1$ and the net work is given by

$$W_{\text{net}} = \frac{n}{n-1} m_1 RT_1 \left[\left(\frac{p_{i1}}{p_1} \right)^{(n-1)/n} + \left(\frac{p_{i2}}{p_{i1}} \right)^{(n-1)/n} + \left(\frac{p_2}{p_{i2}} \right)^{(n-1)/n} - 3 \right] \tag{5.25}$$

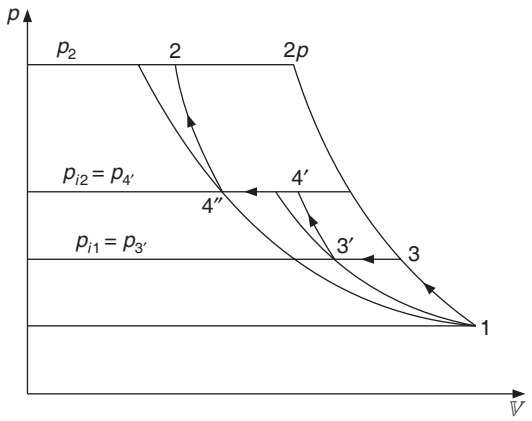

Figure 5.14 Three-stage reciprocating compressor with ideal two intercoolers.

The derivatives of W_{net} with respect to p_{i1} and p_{i2} are put equal to zero resulting in two equations for p_{i1} and p_{i2} for the determination of optimum intermediate pressures. It can be shown that these are:

$$\frac{p_{i1}}{p_1} = \frac{p_{i2}}{p_{i1}} = \frac{p_2}{p_{i2}} = \left(\frac{p_2}{p_1} \right)^{1/3} \tag{5.26}$$

For a four-stage compression with ideal intercooling, the derivation for optimum intermediate pressures is rather simple. At first we consider the two-stage system and then divide each of the two stages into two sub-stages each, resulting in a total of four stages. The result for optimum pressure ratio for each stage will be

$$\frac{p_{i1}}{p_1} = \frac{p_{i2}}{p_{i1}} = \frac{p_{i3}}{p_{i2}} = \frac{p_2}{p_{i3}} = \left(\frac{p_2}{p_1} \right)^{1/4} \tag{5.27}$$

In refrigeration applications more than three stages is very rare. In fact, it is economical to use liquid nitrogen rather than using a three-stage refrigeration system. The optimum pressure ratios given by Eqs. (5.26) and (5.27) are first estimates only for three-stage and four-stage refrigeration systems since there are some major differences between multistage gas compression and multistage refrigeration systems. Some of these differences are:

(i) The refrigerant vapour is not an ideal gas and the c_p/c_v ratio is not constant.

(ii) The refrigerant vapour can be intercooled only up to saturation temperature at the intermediate pressure and not up to the initial temperature of the evaporator.

(iii) In the first stage the adiabatic discharge temperature may be less than the available cooling water temperature or air temperature. As a result the intercooling has to be done by the liquid refrigerant itself, thereby losing some refrigeration capacity.

In such a case the optimization of the cycle is altogether different from optimization of the compressor work alone. R. Plank in 1928 has shown that the two-stage cycle for NH_3 always has a larger COP than that of a single-stage cycle. It is also observed that the optimum pressure for the actual cycle is larger than that predicted by Eq. (5.21). The following empirical expression is sometimes used to estimate the optimum intermediate pressure for a two-stage system.

$$p_i = \sqrt{\frac{T_c}{T_e}\, p_c p_e} \tag{5.28}$$

where, T_c and T_e are condenser and evaporator temperatures in kelvin.

Another empirical expression is for the saturation temperature T_i at the intermediate pressure. If T_i^* is the saturation temperature at pressure $p_i^* = \sqrt{p_c p_e}$, then the intermediate temperature t_i for the actual case is given by

$$T_i = T_i^* + 5 \text{ K} \tag{5.29}$$

EXAMPLE 5.1 A R22 compressor with bore of 0.1 m and stroke of 0.08 m runs at 750 rpm. The clearance volume is 0.04. It runs between the evaporator and condenser temperatures of –10°C and 45°C respectively. The isentropic index k of compression is 1.1163. (a) Determine the mass flow rate, refrigeration capacity and the work requirement if the mechanical efficiency is 90%. Compare the results of isentropic work requirement determined using the superheat table. (b) If the isentropic efficiency of the compressor is 80%, determine the index of compression and compare the results for work requirement and discharge temperature.

Solution:

(a) From the saturation table for R22, we have

t	p_s	v_g	h_f	h_g	s_g
–10	3.55	0.0654	34.25	247.37	0.9473
45	17.209	0.0133	101.76	261.95	0.8697

From superheat table for 17.209 bar, we have

Superheat	20°C	30°C	40°C
v	0.0152	0.0161	0.0169
h	280.95	289.87	298.66
s	0.9270	0.9530	0.9781

Interpolating in the superheat table for $s_1 = s_2 = 0.9473$ between 20°C and 30°C, we get

$$t_2 = 72.8077\ ^{o}\text{C}\ ,\ h_2 = 287.914 \text{ and } v_2 = 0.0159$$

Specific isentropic work,

$$w = h_2 - h_1 = 287.914 - 247.37 = 40.544 \text{ kJ/kg}$$

The isentropic index of compression given in the question is actually determined from this data as follows. As a check, we determine it again as follows

$$k = \frac{\ln (p_2 / p_1)}{\ln (v_1 / v_2)} = \frac{\ln (17.209/3.55)}{\ln (0.0654/0.0159)} = 1.1163$$

From Eq. (5.5) with some modification the specific work is given by

$$w = \left(\frac{n}{n-1}\right) p_S v_S \left[\left(\frac{p_D}{p_S}\right)^{(k-1)/k} - 1\right]$$

$$= \frac{1.1163}{0.1163} 3.55 \times 100 \times 0.0654 \left[\left(\frac{17.209}{3.55}\right)^{(0.1163)/1.1163} - 1\right] = 39.83 \text{ kJ/kg}$$

Swept flow rate $\mathbb{V}_S = (\pi/4)(0.1)^2\ (0.08)\ 4 \times 750/60 = 0.031416\ \text{m}^3/\text{s}$

$$\eta_{\text{vol}} = 1.0 + 0.04 - \varepsilon 0.04 \left(\frac{0.0654}{0.0159} - 1\right) = 0.9155$$

$$\dot{m} = \mathbb{V}_S \eta_{\text{vol}} / v_1 = 0.031416 \times 0.9155 / 0.0654 = 0.43976 \text{ kg/s}$$

$$W = \dot{m} w / \eta_{\text{mech}} = 0.43976 \times 40.544/0.9 = 19.811 \text{ kW}$$

$$Q_e = \dot{m}(h_1 - h_4) = 0.43976(247.37 - 101.76) = 64.034 \text{ kW} = 18.21 \text{ TR}$$

$$\text{COP} = Q_e / W = 3.232$$

If the value of k obtained is used to find the discharge temperature, it gives a drastically different result.

$$T_2 = T_1 \left(\frac{p_2}{p_1}\right)^{(k-1)/k} = 374.8415 \text{ K or } t_2 = 101.84°\text{C}$$

This is very much different from 72.8072°C obtained from the superheat table.

(b) If isentropic efficiency is 80%, then the actual work requirement will be more.

Specific isentropic work = 40.544 kJ/kg

$$\eta_{\text{isen}} = (h_2 - h_1)_{\text{isen}} / (h_{2'} - h_1)_{\text{actual}} = 0.80$$

$$w_{\text{actual}} = 40.544/0.8 = 50.68 \text{ k/kg}$$

If it is assumed that the volumetric efficiency is the same, then the mass flow rate will remain unchanged. Hence, the refrigeration capacity remains unchanged while the work is

$$W = \dot{m} w_{\text{actual}} / \eta_{\text{mech}} = 24.7635 \text{ kW}$$

$$\text{COP} = 2.586$$

For illustration purpose, we calculate the polytropic index of compression for the process. The enthalpy at compressor exit for the actual compression is given by

$$h_{2'} = h_1 + w_{\text{actual}} = 247.37 + 50.68 = 298.05$$

Interpolating in the superheat table between 30°C and 40°C for this value of enthalpy, we get

$$t_{2'} = 84.306^{\circ}\text{C},\ v_{2'} = 0.168445 \text{ and } s_{2'} = 0.97636$$

If we calculate the polytropic index of compression with this data, we get

$$n = \frac{\ln (p_2 / p_1)}{\ln (v_1 / v_2)} = \frac{\ln (17.209 / 3.55)}{\ln (0.0654 / 0.0168445)} = 1.163647$$

The modified form of Eq. (5.5) used above gives

$$w = 41.033 \text{ kJ/kg}$$

This is very much different from 50.68 obtained above.

$$T_{2'} = T_1 \left(\frac{p_2}{p_1} \right)^{(n-1)/n} = 397.04 \text{ K} = 124.04^{\circ}\text{C}$$

This is also very different from 84.306°C obtained from the superheat table.

EXAMPLE 5.2 Show that the work requirement for two-stage isentropic compression with intercooling up to saturated stage is less than the single-stage compression for R22 between the evaporator and condenser temperatures of –40°C and 40°C respectively. Consider the intermediate temperature of –8°C.

Solution:

From the saturation table for R22, we have

t	p_s	v_g	h_f	h_g	s_g
–70	0.2062	0.94	–30.78	219.17	1.0896
–45	0.83	0.257	–5.4	231.75	1.0161
–40	1.053	0.206	0.0	234.17	1.0044
–28	1.783	0.126	13.35	239.75	0.9792
–10	3.55	0.0654	34.25	247.37	0.9473
–8	3.807	0.0612	36.62	248.15	0.9441
0	4.98	0.0472	46.19	251.12	0.9317
40	15.267	0.0152	95.4	261.38	0.8767

From superheat table for 15.267 bar (40°C), we have

Superheat	20°C	30°C	40°C	50°C	80°C	100°C
v	0.0172	0.0182	0.0191	0.0199	0.0224	0.0239
h	279.61	288.31	296.84	305.26	330.24	346.91
s	0.9332	0.9592	0.9832	1.007	1.0224	1.1143

From superheat table for 3.807 bar (–8°C), we have

Superheat	20°C	30°C
v	0.0673	0.072
h	262.7	269.74
s	0.9941	1.0186

Referring to Figure 5.9(b), we have

$$h_1 = 234.17,\ s_1 = 1.0044,\ v_1 = 0.206,\ s_4 = 0.9441 \text{ and } h_4 = 248.15$$

Interpolating for $s_1 = s_3 = 1.0044$ for 3.807 bar, we get

$$t_3 = 16.204,\ h_3 = 265.66 \text{ and } v_3 = 0.06852$$

Next, interpolating in the superheat table for 15.267 bar for $s_4 = s_5 = 0.9441$, we get

$$t_5 = 64.192\ ,\ h_5 = 283.2573 \text{ and } v_5 = 0.01762$$

If the compression is carried out in single-stage, then interpolating in superheat table for 15.267 bar for $s_1 = s_2 = 1.0044$ between 0 and 50°C, we get

$$t_2 = 88.907,\ h_2 = 304.34 \text{ and } v_2 = 0.01981$$

Single-stage specific work, $w_{12} = h_2 - h_1 = 304.34 - 234.17 = 70.17$ kJ/kg

First-stage specific work, $w_{13} = h_3 - h_1 = 265.66 - 234.17 = 31.49$ kJ/kg

Second-stage specific work = $w_{45} = h_5 - h_4 = 283.2573 - 248.15 = 35.1073$ kJ/kg

Total specific work of two stages = $w_{13} + w_{45} = 31.49 + 35.1073 = 66.5973$ kJ/kg

Saving in work by the two-stage system = $70.17 - 66.5973 = 3.573$ kJ/kg

EXAMPLE 5.3 Show that the work requirement for three-stage isentropic compression with intercooling up to saturated stage is less than that for a two-stage and single-stage compressions for R22 between the evaporator and condenser temperatures of –70°C and 40°C respectively. Consider intermediate temperatures of – 45°C and –10°C respectively, while for two-stage consider an intermediate temperature of –28°C.

Solution:

From superheat table for 0.83 bar (–45°C), we have

Superheat	20°C	30°C
v	0.282	0.295
h	243.69	249.8
s	1.0063	1.0904

From superheat table for 3.55 bar (–10°C), we have

Superheat	20°C	30°C
v	0.0719	0.0751
h	261.1	268.65
s	0.9976	1.0206

Three-stage system:

Referring to Figure 5.10 for the three-stage system and the saturation table for R22 as reproduced in Example 5.2,

$$h_1 = 219.17,\ s_1 = 1.0896,\ v_1 = 0.94,\ s_4 = 1.0161,\ h_4 = 231.75,$$

$$s_6 = 0.9473 \text{ and } h_6 = 247.37$$

Interpolating for first-stage isentropic compression with $s_1 = s_3 = 1.0896$ for 0.83 bar pressure, we get

$$t_3 = -15.332,\ h_3 = 249.4 \text{ and } v_3 = 0.29457$$

Interpolating for second-stage isentropic compression with $s_4 = s_5 = 1.0161$ for 3.55 bar pressure, we get

$$t_5 = 18.0435,\ h_5 = 267.177 \text{ and } v_5 = 0.07447$$

Interpolating for third-stage isentropic compression with $s_6 = s_7 = 0.9473$ for 15.267 bar condenser pressure, we get

$$t_7 = 65.423,\ h_7 = 284.328 \text{ and } v_7 = 0.017742$$

For single-stage isentropic compression with $s_1 = s_2 = 1.0896$ between superheat of 80°C to 100°C, we get

$$t_2 = 134.624°\text{C},\ h_2 = 342.4296.34 \text{ and } v_2 = 0.0235$$

Single-stage specific work $w_{12} = h_2 - h_1 = 342.4296 - 219.17 = 123.26$ kJ/kg

First-stage specific work, $w_{13} = h_3 - h_1 = 249.4 - 219.17 = 30.23$ kJ/kg

Second-stage specific work, $w_{45} = h_5 - h_4 = 267.177 - 231.75 = 35.427$ kJ/kg

Third-stage specific work, $w_{67} = h_7 - h_6 = 284.328 - 247.37 = 36.958$ kJ/kg

Total specific work of three stages = $w_{13} + w_{45} + w_{67} = 30.23 + 35.427 + 36.958$
$= 102.6151$ kJ/kg

Saving in work by the three-stage system = 123.26 – 102.6151 = 20.645 kJ/kg

Two-stage system:

Next we consider a two-stage system between –70°C and 40°C with intermediate temperature of –28°C.

$$h_1 = 219.17,\ s_1 = 1.0896,\ h_4 = 239.75 \text{ and } s_4 = 0.9792$$

From superheat table for 1.783 bar (–28°C), we have

Superheat	20°C	30°C
v	0.15	0.155
h	265.47	272.09
s	1.0764	1.0992

Interpolating for first-stage isentropic compression with $s_1 = s_3 = 1.0896$ for 1.783 bar pressure, we get

$$t_3 = 17.789,\ h_3 = 269.302 \text{ and } v_3 = 0.1529$$

Interpolating for second-stage isentropic compression with $s_4 = s_5 = 0.9792$ for 15.267 bar condenser pressure between 30°C and 40°C, we get

$$t_5 = 78.33,\ h_5 = 295.418 \text{ and } v_5 = 0.01895$$

Single-stage specific work, $w_{12} = h_2 - h_1 = 342.4296 - 219.17 = 123.26$ kJ/kg

First stage specific work, $w_{13} = h_3 - h_1 = 269.302 - 219.17 = 50.132$ kJ/kg

Second-stage specific work, $w_{45} = h_5 - h_4 = 295.418 - 239.75 = 55.668$ kJ/kg

Total specific work of two stages = $w_{13} + w_{45} = 50.132 + 55.668 = 105.8$ kJ/kg

Saving in work by the two-stage system =123.26 – 105.8 = 17.46 kJ/kg

Obviously the three-stage system gives more saving in work compared to a two-stage system. At the same time, the adiabatic discharge temperatures are low for each stage, which ensures proper lubrication. Also the pressure ratios being small for each stage the volumetric efficiency improves for each stage.

EXAMPLE 5.4 An air compressor with bore of 10 cm and stroke of 10 cm runs at 750 rpm. The inlet air conditions are 300 K and 1.01325 bar pressure. The total pressure ratio is 16 and polytropic index of compression is 1.35 for both the stages. Neglect the clearance volume and determine the total work requirement if the

(a) pressure ratio for the first stage is 5
(b) pressure ratio for the first stage is 3
(c) pressure ratio is same for both the stages.

Solution:

(a) The displacement volume, $\mathbb{V}_1 = \pi(0.1)^2 \times 0.1/4 = 7.85398 \times 10^{-4}$ m^3

$$p_1 = 101.325 \text{ kPa and } T_1 = 300 \text{ K}$$

For air, $R = 0.2871$ kJ/kg-K $\quad \therefore \quad m_1 = p_1 \mathbb{V}_1 / RT_1 = 9.23958 \times 10^{-4}$ kg

$$p_1 \mathbb{V}_1 = m_1 RT_1 = 0.07958$$

From Eq. (5.18),

$$W_{13} = \frac{1.35}{1.35 - 1} 0.07958 \left[(5)^{0.35/1.35} - 1\right] = 0.15894 \text{ kJ}$$

$$W_{3'2} = \frac{1.35}{1.35-1} 0.07958 \left[\left(\frac{16}{5} \right)^{0.35/1.35} - 1 \right] = 0.108036 \text{ kJ}$$

Total work = 0.15894 + 0.108036 = 0.266976 kJ

(b) $p_1 \mathbb{V}_1$ remains the same, the pressure ratio changes in this case, therefore,

$$W_{13} = \frac{1.35}{1.35-1} 0.07958 [(3)^{0.35/1.35} - 1] = 0.10115 \text{ kJ}$$

$$W_{3'2} = \frac{1.35}{1.35-1} 0.07958 \left[\left(\frac{16}{3} \right)^{0.35/1.35} - 1 \right] = 0.1668 \text{ kJ}$$

Total work = 0.10115 + 0.1668 = 0.26795 kJ

(c) The pressure ratio is 4 for both the stages hence the work is given by

$$W_{12} = 2W_{13} = 2 \times \frac{1.35}{1.35-1} 0.07958 [(4)^{0.35/1.35} - 1] = 2 \times 0.13275 = 0.2655 \text{ kJ}$$

Hence the work requirement is minimum when the pressure ratio is same across both the stages and is equal to square root of the total pressure ratio.

EXAMPLE 5.5 An air compressor with bore of 10 cm and stroke of 10 cm runs at 750 rpm. The inlet air conditions are 300 K and 1.01325 bar pressure. The total pressure ratio is 16 and the polytropic index of compression is 1.35 for both the stages. However, it is not possible to obtain ideal intercooling since the water temperature available from the cooling tower is high. Intercooling can be done up to 320 K only. Neglect the clearance volume and determine the total work requirement if the

(a) pressure ratio for the first stage is 5
(b) pressure ratio for the first stage is 3
(c) pressure ratio is optimum as given by Eq. (5.24).

Solution:

For the second-stage compression the inlet temperature is 320 K. Hence,

$$m_1 RT_3 = 9.23958 \times 10^{-4} \times 0.2871 \times 320 = 0.084885$$

(a) From Eqs. (5.22a) and (5.22b) for $p_3/p_1 = 5$, we get

$$W_{13} = \frac{n}{n-1} m_1 RT_1 \left[\left(\frac{p_3}{p_1} \right)^{(n-1)/n} - 1 \right] = \frac{1.35}{0.35} 0.079581 [(5)^{0.35/1.35} - 1] = 0.15894 \text{ kJ}$$

$$W_{3''2'} = \frac{n}{n-1} m_1 RT_w \left[\left(\frac{p_2}{p_{3''}} \right)^{(n-1)/n} - 1 \right]$$

$$= \frac{1.35}{0.35} 0.084885 \left[\left(\frac{16}{5} \right)^{0.35/1.35} 1 \right] = 0.115238 \text{ kJ}$$

Total work = 0.15894 + 0.115238 = 0.274178 kJ

(b) From Eqs. (5.22a) and (5.22b) for $p_3/p_1 = 3$, we get

$$W_{13} = \frac{1.35}{0.35} 0.07958 \left[(3)^{0.35/1.35} - 1 \right] = 0.10115 \text{ kJ}$$

$$W_{3''2'} = \frac{1.35}{0.35} 0.084885 \left[\left(\frac{16}{3} \right)^{0.35/1.35} 1 \right] = 0.17792 \text{ kJ}$$

Total work = 0.10115 + 0.17792 = 0.27907 kJ

The optimum intermediate pressure is given by, $p_i = \sqrt{p_1 p_2 (T_w / T_1)^{n/(n-1)}}$

or $$p_i = \sqrt{1 \times 16 (329/300)^{1.35/0.35}} = 4.53 \text{ bar}$$

Hence the optimum pressure ratio is $p_i/p_1 = 4.53$ ($\because$ $p_1 = 1$ bar)

For this pressure ratio, we get, $W_{12} = 0.147172$ and $W_{3''2'} = 0.1267$

Total work = 0.27388 kJ

REFERENCE

R. Plank (Feb. 1928): Üeber den ideal Prozess von Kältemaschinen bei Vernbund-Kompression, *Zeitschrift für die gesamte Kälte-Industrie*, pp. 17–24, vol. 35.

REVIEW QUESTIONS

1. Discuss why the SSS cycle with reciprocating compressor is not suitable for low evaporator temperatures.
2. Show how reduction in isentropic work and increase in refrigeration effect can be achieved by multistage compression in a reciprocating compressor.
3. Discuss the factors governing the choice of intermediate compression pressure in a two-stage SSS cycle.
4. Derive the expression for optimum intermediate pressure for ideal gas reciprocating compressor with ideal intercooling.
5. Derive the expression for optimum intermediate pressure for ideal gas reciprocating compressor with non-ideal intercooling.

6. An air compressor with a bore of 0.1 m and stroke of 0.08 m runs at 750 rpm. The inlet air conditions are 303 K and 1.01325 bar pressure. The total pressure ratio is 18 and the polytropic index of compression is 1.30 for both the stages. Neglect the clearance volume and determine the total work requirement if the
   (a) pressure ratio for the first stage is 6
   (b) pressure ratio for the first stage is 3
   (c) pressure ratio is same for both the stages.
7. Workout the parameters at (a), (b) and (c) of Question No. 6 if intercooling is done up to 320 K.
8. An R22 compressor with bore of 10 cm and stroke of 10 cm runs at 750 rpm. The clearance volume is 0.04. It runs between the evaporator and condenser temperatures of –5°C and 40°C respectively. The isentropic index of compression is 1.35. The mechanical efficiency of the compressor is 85%. (a) Determine the mass flow rate, refrigeration capacity and the work requirement. Compare the results of isentropic work requirement determined using the superheat table. (b) If the isentropic efficiency of the compressor is 80%, determine the index of compression and compare the results for work requirement and discharge temperature.

6

Multistage Refrigeration Systems

LEARNING OBJECTIVES

After studying this chapter the student should be able to:

1. Understand the disadvantages of the single-stage refrigeration cycle for operation at low evaporator temperatures.
2. Explain as to how the disadvantages of the single-stage refrigeration system can be overcome by using the multistage system.
3. Discuss the concepts of intercooling and flash gas removal in multistage vapour compression refrigeration systems.
4. Determine the intermediate pressure that a two-stage vapour compression refrigeration system would seek, given the condenser and evaporator temperatures and swept volume flow rates of LP and HP compressors.
5. Describe the practical disadvantages of flash chamber and how they are overcome by subcooling the refrigerant before feeding to the evaporator.
6. Explain the differences between a two-stage NH_3 cycle and a two-stage R12 cycle.
7. Explain the temperature ranges for multistage systems.
8. Understand the necessity of multi-evaporator systems and evalute the performance of two-evaporator, single-compressor system with individual expansion valves and a pressure reduction valve.
9. Evalute the performance of multi-evaporator systems with multi-compression, intercooling, flash gas removal and subcooling.
10. Understand the limitations of the multistage system. Describe the working principle of the cascade system.
11. Derive the expression for optimum intermediate temperature of the cascade system.
12. Evalute the performance of the cascade systems. Describe the measures needed to undertake the performance improvements to cascade refrigeration systems.
13. Explain the process of dry ice manufacture with the help of a schematic diagram.
14. Describe the working principle of the auto-cascade system.

6.1 INTRODUCTION

It has been observed that the single-stage refrigeration cycle essentially has three disadvantages for operation at low evaporator temperatures, namely:

(i) Low volumetric efficiency due to large pressure ratio, requiring large displacement volume per TR

(ii) Low coefficient of performance and refrigerating efficiency, requiring large HP per TR

(iii) High adiabatic discharge temperature particularly in case of ammonia. This may lead to fuming and carbonization of lubricating oil resulting in sticky valve operation and lubrication problems due to lower viscosity of oil at higher temperatures.

It has been shown in Chapter 5 that by using multiple compressors with intercooling of vapour and multistage expansion with separation of liquid, these disadvantages may be overcome.

Multistaging reduces the pressure ratio across each stage, thus resulting in higher volumetric efficiency in each stage. Intercooling increases the density at inlet to the next stage compressor, which further improves volumetric efficiency. In addition, lower pressure ratio decreases the wear and tear of each stage compressor.

Multistaging with intercooling reduces the work requirement and multistage expansion with flash gas removal increases the refrigeration effect, thereby increasing the COP. This will be shown to be true even when intercooling is done with the liquid refrigerant as long as the operation is not near the critical temperature. The removal of flash vapour at intermediate pressure also leads to saving in work since if it is expanded to evaporator pressure then it has to be compressed to a higher-pressure ratio. Only the liquid refrigerant gives refrigeration effect by evaporating and absorbing its latent heat. The flash vapour remains vapour at constant temperature and does not give refrigeration effect. Its removal makes the evaporator more compact.

Adiabatic discharge temperature decreases since the temperature rise across each stage decreases and intercooling further reduces it.

Apart from this, the load on condenser decreases since the inlet temperature to it (the adiabatic discharge temperature) decreases. The evaporator size decreases since some of the vapour formed during expansion is passed straightaway to the high-pressure compressor. Also the area of throttling loss decreases.

In this chapter, we deal with multistage systems where NH_3 and R12, R22 and R134a are used as refrigerants. NH_3 has a large area of superheat horn and its constant entropy lines are very divergent, hence multistaging will result in significant saving in work. Also, it has a large latent heat hence only a small mass flow rate of refrigerant will be sufficient for intercooling. On the other hand for R12 and R22 or for that matter R134a, the area of superheat horn is small and constant entropy lines are not very divergent. It was also observed that maximum COP for these refrigerants occurs with the suction state in superheated region, hence, intercooilng is not required to such a large extent for these refrigerants. It will be further observed that subcooling of liquid refrigerant is required in all the cases for practical reasons.

6.2 TWO-STAGE NH_3 CYCLE

Figures 6.1(a) and (b) show the schematic and *p–h* cycle diagram of a two-stage system commonly used for ammonia. It consists of two compressors, a low-pressure (LP) compressor and a high-

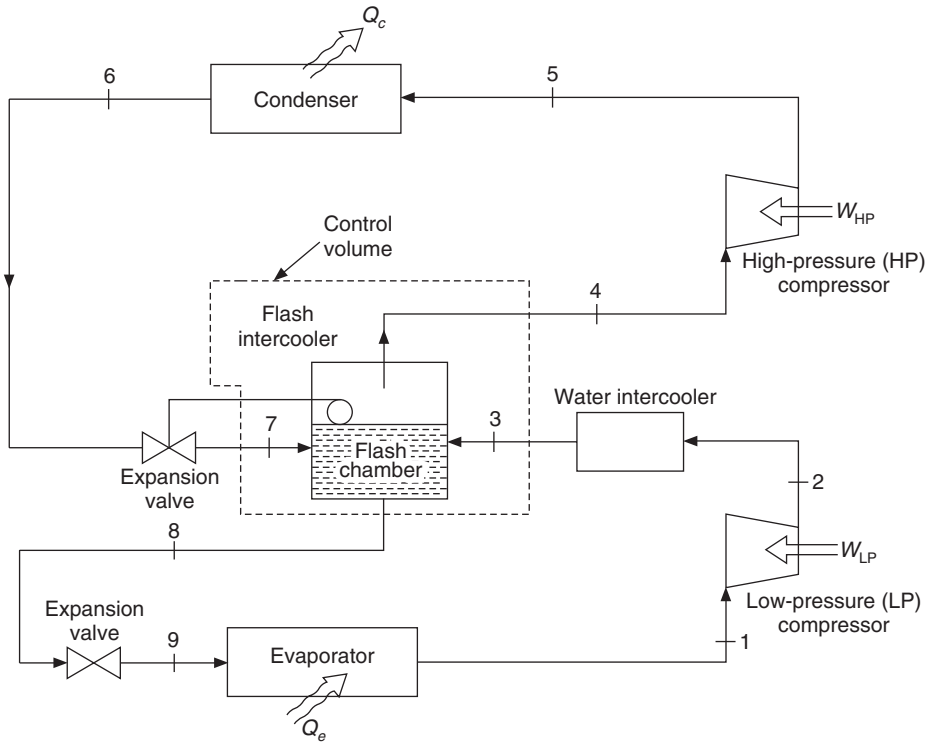

Figure 6.1(a) Schematic diagram of a two-stage compression system with water intercooler and flash intercooler.

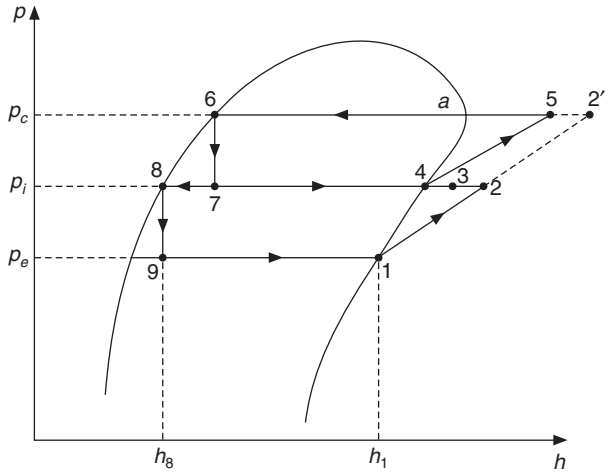

Figure 6.1(b) *p–h* diagram for the system shown in Figure 6.1(a).

pressure (HP) compressor, a water intercooler, a flash intercooler, two expansion valves, evaporator and condenser. The vapour leaving the low-pressure (LP) compressor at state 2 may be first intercooled in the water intercooler, which may be a double tube heat exchanger. However, if

water is not available at temperature lower than the adiabatic discharge temperature of low-pressure compressor, this heat exchanger may not be feasible. After leaving the water intercooler, the vapour enters the flash intercooler at state 3 where it is cooled by direct contact (without any separating walls with conduction thermal resistance) with the cold liquid refrigerant.

The flash intercooler is a pressure vessel in which a constant level of liquid refrigerant is maintained by a float type expansion valve 6–7. The pressure in this vessel is intermediate pressure p_i and the temperature is T_i being the corresponding saturation value. The LP vapour at state 3 is admitted through a slotted pipe or through orifices, and bubbles through the liquid rising up and being cooled in this process. The cooling of LP vapour (desuperheating of vapour) is done by evaporation of liquid refrigerant in the flash chamber. The extent of desuperheating of LP vapour depends upon the direct contact heat transfer coefficient. Complete desuperheating to saturated state 4 (temperature of liquid refrigerant in the flash chamber) is not possible. However, for simplicity of calculation it is assumed in the cycle shown in Figure 6.1(b).

The vapour entering the high pressure (HP) compressor at state 4 consists of

(i) Flash vapour formed during expansion, 6–7 in the float valve.

(ii) Intercooled refrigerant vapour from LP compressor

(iii) Vapour formed in flash chamber by evaporation of liquid refrigerant to produce intercooilng.

The calculation procedure is very similar to that followed for SSS cycle. Compression in both the stages is assumed to be isentropic and expansions are assumed to occur at constant enthalpy. States 2 and 5 at the end of isentropic compression are found either by (i) interpolation in the superheat tables or by (ii) assuming constant average specific heat along 2–4 and 5–a as outlined in the calculations for SSS cycle. If T_e and T_c are evaporator and condenser temperatures respectively and p_i is the intermediate pressure or T_i is the intermediate temperature, then the properties at states 1, 4, a, 6 and 8 can be found from the saturation table for the refrigerant. State at 3 has to be specified in terms of effectiveness of the water intercooler or by temperature at point 3. Say, TR is the cooling capacity of the system. Let $\dot{m}_{LP}$ and $\dot{m}_{HP}$ be the mass flow rates of refrigerant through the low-pressure and high-pressure compressors respectively. Then,

$$\dot{m}_{LP} = \frac{3.51667\,TR}{h_1 - h_8} \tag{6.1}$$

Figure 6.1(a) shows a control volume around the flash intercooler. The mass conservation is satisfied for this control volume. Assuming it to be insulated, the energy conservation for this control volume yields

$$\dot{m}_{LP}h_3 + \dot{m}_{HP}h_7 = \dot{m}_{LP}h_8 + \dot{m}_{HP}h_4 \tag{6.2}$$

i.e. $$\dot{m}_{HP}(h_4 - h_7) = \dot{m}_{LP}(h_3 - h_8)$$

$\therefore$ $$\dot{m}_{HP} = \dot{m}_{LP}\frac{h_3 - h_8}{h_4 - h_7} \tag{6.3}$$

Now, $$W_{LP} = \dot{m}_{LP}(h_2 - h_1) \quad \text{and} \quad W_{HP} = \dot{m}_{HP}(h_5 - h_4) \tag{6.4}$$

$$\therefore \quad W_{net} = W_{LP} + W_{HP} = \dot{m}_{LP}\left\{(h_2 - h_1) + \frac{h_3 - h_8}{h_4 - h_7}(h_5 - h_4)\right\} \tag{6.5}$$

and
$$\text{COP} = \frac{\dot{m}_{LP}(h_1 - h_8)}{W_{LP} + W_{HP}} = \frac{h_1 - h_8}{(h_2 - h_1) + \dfrac{h_3 - h_8}{h_4 - h_7}(h_5 - h_4)} \tag{6.6}$$

Volumetric efficiencies of the LP and HP compressors may be determined from

$$\eta_{vol,LP} = 1.0 + \varepsilon - \varepsilon\,(v_1/v_2) \quad \text{and} \quad \eta_{vol,HP} = 1.0 + \varepsilon - \varepsilon\,(v_4/v_5) \tag{6.7}$$

The swept flow rates of the two compressors are as follows

$$(\mathbb{V}_s)_{LP} = \dot{m}_{LP}\, v_1/\eta_{vol,LP} \quad \text{and} \quad (\mathbb{V}_s)_{HP} = \dot{m}_{HP}\, v_4/\eta_{vol,HP} \tag{6.8}$$

EXAMPLE 6.1(a) The condenser and evaporator temperatures are 40°C and –40°C respectively for a two-stage NH_3 refrigeration system of 10 TR cooling capacity. A water intercooler intercools the LP vapour to 40°C and further intercooling up to saturated state is done in a flash chamber. Find the mass flow rates, swept volume rates and work requirements of the compressors, condenser heat rejection and COP. Compare the results with the SSS cycle. The clearance volume ratio for both the compressors is 0.04.

Solution:

The evaporator temperature is less than –30°C, therefore, a two-stage system is recommended. The evaporator and condenser pressures are:

$$p_e = 0.717 \text{ bar} \quad \text{and} \quad p_c = 15.55 \text{ bar}$$

$\therefore$ Ideal Intermediate pressure $p_i^* = \sqrt{p_c p_e} = 3.339$ bar

Corresponding saturation temperature $t_i^* = -6.5$°C (by interpolating in the NH_3 table)

As a thumb rule the recommended intermediate temperature should be 5°C more than t_i^*. Therefore, intermediate temperature $t_i = -6.5$°C + 5°C = –1.5°C ≈ –2°C for convenience since saturation and superheated properties are available for it.

The required thermodynamic properties of NH_3 at saturation are as follows:

Temperature (°C)	*Pressure* (bar)	v_g (m^3/kg)	h_f (kJ/kg)	h_g (kJ/kg)	s_f (kJ/kg-K)	s_g (kJ/kg-K)
–40	0.717	1.55	0.0	1387.15	0.0	5.9518
–2	3.982	0.317	171.63	1441.08	0.6894	5.3627
40	15.55	0.0833	371.47	1472.02	1.3579	4.8728

The properties of superheated vapour at – 2°C are as follows:

Degree of superheat	5°C	40°C	50°C	60°C	80°C	100°C
v	0.325	0.374	0.388	0.401	0.428	0.454
h	1454.11	1540.4	1564.1	1587.5	1634.1	1680.4
s	5.4105	5.7048	5.7797	5.8516	5.988	6.1165

The properties of superheated vapour at 40°C are as follows:

Degree of superheat	50°C	60°C	80°C	100°C	120°C	140°C	160°C
v	0.105	0.108	0.116	0.123	0.130	0.137	0.142
h	1621.0	1647.9	1700.3	1751.7	1802.6	1853.4	1904.2
s	5.3153	5.3883	5.5253	5.65283	5.7732	5.8878	5.99802

Referring to Figure 6.1, we have

$h_1 = 1387.15$, $s_1 = 5.9518$ and $v_1 = 1.55$;

$h_4 = 1441.08$, $h_8 = h_9 = 171.63$, $v_4 = 0.317$ and $s_4 = 5.3627$

$h_a = 1472.02$, $v_a = 0.0833$, $s_a = 4.8728$, $h_6 = h_7 = 371.47$ and $s_6 = 1.3579$

State 3:

The pressure and temperature at state 3 are 3.982 bar and 40°C respectively. The enthalpy is obtained from superheat table for 3.982 bar (–2°C) at 40°C implies at a superheat of 42°C. Interpolating between 40°C superheat and 50°C superheat, we get

$$h_3 = 1540.4 + (1564.1 - 1540.4) \times 2/10 = 1545.14 \text{ kJ/kg}$$

State 2:

This is obtained by interpolating in the superheat table for intermediate pressure of 3.982 bar (–2°C) between 60°C and 80°C superheat for $s_1 = s_2 = 5.9518$, which yields

$$\Delta t = 20 \times (5.9518 - 5.8516)/(5.988 - 5.8516) = 0.734604 \times 20 = 14.6921^\circ\text{C}$$

$$\therefore \quad t_2 = -2 + 60 + 14.6921 = 72.6921^\circ\text{C}$$

$h_2 = 1587.5 + (1634.1 - 1567.5) \times 0.734604 = 1621.733$. Similarly, $v_2 = 0.42083$

State 5:

Similarly, by interpolating in the superheat table for condenser pressure of 15.55 bar (40°C) between superheat of 50°C and 60°C for $s_4 = s_5 = 5.3627$

$$\Delta t = 10 \times (5.3627 - 5.3153)/(5.3883 - 5.3153) = 0.6493 \times 10 = 6.493^\circ\text{C}$$

$$\therefore \quad t_5 = 40 + 50 + 6.493 = 96.493^\circ\text{C}$$

$h_5 = 1621.0 + (1647.9 - 1621.0) \times 0.6493 = 1639.366$. Similarly, $v_5 = 0.105$

State 2′ for SSS cycle:

For SSS cycle, interpolating in the superheat table for 15.55 bar (40°C) for $s_1 = s_{2'} = 5.9518$ between 140°C and 160°C, we get

$$t_{2'} = 40 + 140 + 11.613 = 191.613^\circ\text{C}, \quad h_{2'} = 1882.897 \quad \text{and} \quad v_{2'} = 0.13406$$

Two-stage system:

$$\dot{m}_{\text{LP}} = \frac{3.51667\,\text{TR}}{(h_1 - h_8)} = \frac{3.51667 \times 10}{1387.15 - 171.63} = 0.02893 \text{ kg/s}$$

$$\dot{m}_{HP} = \dot{m}_{LP}\frac{(h_3 - h_8)}{(h_4 - h_7)} = 0.02893\,\frac{1545.14 - 171.63}{1441.08 - 371.47} = 0.0371514 \text{ kg/s}$$

$$W_{LP} = \dot{m}_{LP}(h_2 - h_1) = 0.02897(1621.733 - 1387.15) = 6.7868 \text{ kW}$$

$$W_{HP} = \dot{m}_{HP}(h_5 - h_4) = 0.0371514(1639.3666 - 1441.08) = 7.3663 \text{ kW}$$

$$W_{net} = W_{LP} + W_{HP} = 14.1531 \text{ kW}$$

$$Q_c = \dot{m}_{HP}(h_5 - h_6) = 0.0371514(1639.3666 - 371.47) = 47.104 \text{ kW}$$

Heat rejection ratio = $Q_c/Q_e = 47.104/35.1667 = 1.339$

$$\text{COP} = Q_e/W_{net} = 35.1667/14.1531 = 2.4847$$

$$\eta_{vol,LP} = 1.0 + \varepsilon - \varepsilon\,(v_1/v_2) = 1.04 - 0.04(1.55/0.42083) = 0.8927$$

$$\eta_{vol,HP} = 1.0 + \varepsilon - \varepsilon\,(v_4/v_5) = 1.04 - 0.04(0.317/0.105) = 0.9192$$

$$(\mathbb{V}_S)_{LP} = \dot{m}_{LP}v_1/\eta_{vol,LP} = 0.02893 \times 1.55/0.8927 = 0.0502 \text{ m}^3/\text{s}$$

$$(\mathbb{V}_S)_{HP} = \dot{m}_{HP}v_4/\eta_{vol,HP} = 0.0371514 \times 0.317/0.9192 = 0.0128 \text{ m}^3/\text{s}$$

$$(\mathbb{V}_S)_{LP}/(\mathbb{V}_S)_{HP} = 3.918$$

SSS cycle:

This cycle is shown by 1–2′–*a*–6–10–1 in Figure 6.2.

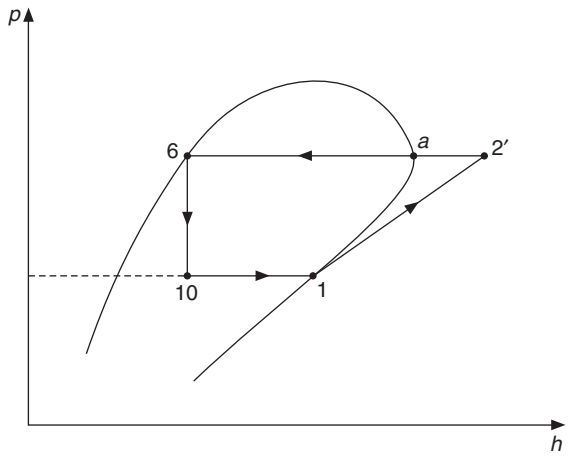

Figure 6.2 SSS cycle—Example 6.1(a).

$$\dot{m} = \frac{3.51667 \text{ TR}}{h_1 - h_6} = \frac{3.51667 \times 10}{1387.15 - 371.47} = 0.03462 \text{ kg/s}$$

$$W = \dot{m}(h_{2'} - h_1) = 0.03462(1882.897 - 1387.15) = 17.1646 \text{ kW}$$

$$Q_c = \dot{m}(h_{2'} - h_6) = 0.03462(1882.897 - 371.47) = 52.3313 \text{ kW}$$

$$\text{COP} = 35.1667/W = 35.16661/17.1646 = 2.0488$$

$$\eta_{\text{vol,}} = 1.0 + \varepsilon - \varepsilon\,(v_1/v_{2'}) = 1.04 - 0.04(1.55/0.13406) = 0.5775$$

$$\mathbb{V}_S = \dot{m} v_1/\eta_{\text{vol}} = 0.03462 \times 1.55/0.5775 = 0.093 \text{ m}^3\text{/s}$$

It is obvious that the adiabatic discharge temperature is very high for the SSS cycle and it will cause fuming of lubricating oil. The coefficient of performance is very low and the swept volume rate is very high. A very approximate expression has been used for evaluation of volumetric efficiency; if a better expression is used then the volumetric efficiency will be very low and the swept volume rate will be very high in actual practice.

EXAMPLE 6.1(b) If in Example 6.1(a) suppose the superheat table is not provided, instead the specific heats at intermediate pressure and condenser pressure are given to be 2.354 kJ/kg-K and 2.931 kJ/kg-K respectively for the two-stage system. For the SSS cycle the adiabatic discharge temperature is very high, hence the average specific heat is 2.701, which is different from the two-stage system. All other conditions being the same as in Example 6.1(a), determine all the parameters of Example 6.1(a).

Solution:

$$c_{pi} = 2.354 \text{ kJ/kg-K} \quad \text{and} \quad c_{pc} = 2.931 \text{ kJ/kg-K}$$

State 2:

This is determined by using $T\,ds = dh = c_p\,dt$ along the constant pressure line 4–2.

$$T_2 = T_4 \exp\left(\frac{s_2 - s_4}{c_{pi}}\right) = T_4 \exp\left(\frac{s_1 - s_4}{c_{pi}}\right) = 271 \exp\left(\frac{5.9518 - 5.3647}{2.354}\right) = 348.06 \text{ K}$$

$$t_2 = 348.06 - 273 = 75.06°\text{C}, \; h_2 = h_4 + c_{pi}\,(t_2 - t_4) = 1441.08 + 2.354(75.06 - (-2)) = 1622.48$$

$$v_2 = v_4 T_2/T_4 = 0.3117(348.06)/271 = 0.407$$

Similarly, along the constant pressure line a–5, using $T\,ds = dh = c_p\,dt$

$$T_5 = T_c \exp\left(\frac{s_5 - s_a}{c_{pc}}\right) = 313 \exp\left(\frac{5.3627 - 4.8728}{2.931}\right) = 369.94 \text{ K} = 96.94°\text{C}$$

$$h_5 = h_a + c_{pc}\,(t_5 - t_c) = 1472.62 + 2.9311(96.94 - 40) = 1638.91$$

and $$v_5 = v_a\,T_5/T_a = 0.0833(369.94)/313 = 0.984$$

The mass flow rates remain the same as in Example 6.1(a) since h_1, h_3, h_4, h_7 and h_8 are the same.

Two-stage system

$$\dot{m}_{\text{LP}} = 0.02893 \text{ kg/s}$$

$$\dot{m}_{\text{HP}} = 0.0371514 \text{ kg/s}$$

$$W_{\text{LP}} = \dot{m}_{\text{LP}}\,(h_2 - h_1) = 0.02897(1622.48 - 1387.15) = 6.808 \text{ kW}$$

$$W_{\text{HP}} = \dot{m}_{\text{HP}}\,(h_5 - h_4) = 0.0371514(1638.91 - 1441.08) = 7.349 \text{ kW}$$

$$W_{\text{net}} = W_{\text{LP}} + W_{\text{HP}} = 14.157 \text{ kW}$$

$$Q_c = \dot{m}_{\text{HP}}\,(h_5 - h_6) = 0.0371514(1638.91 - 371.47) = 47.085 \text{ kW}$$

Heat rejection ratio = $Q_c/Q_e = 1.339$

$$\text{COP} = Q_e/W_{\text{net}} = 35.16667/14.157 = 2.484$$

$$\eta_{\text{vol,LP}} = 1.0 + \varepsilon - \varepsilon\,(v_1/v_2) = 1.04 - 0.04(1.55/0.407) = 0.8877$$

$$\eta_{\text{vol,HP}} = 1.0 + \varepsilon - \varepsilon\,(v_4/v_5) = 1.04 - 0.04(0.317/0.0984) = 0.911$$

$$(\mathbb{V}_S)_{\text{LP}} = \dot{m}_{\text{LP}}\, v_1/\eta_{\text{vol,LP}} = 0.02893 \times 1.55/0.8877 = 0.0505 \text{ m}^3/\text{s}$$

$$(\mathbb{V}_S)_{\text{HP}} = \dot{m}_{\text{HP}}\, v_4/\eta_{\text{vol,HP}} = 0.0371514 \times 0.317/0.911 = 0.0129 \text{ m}^3/\text{s}$$

$$(\mathbb{V}_S)_{\text{LP}}/(\mathbb{V}_S)_{\text{HP}} = 3.918$$

SSS cycle:

For this case, $c_{pc} = 2.701$

This cycle is shown by 1–2′–*a*–6–10–1 in Figure 6.2. The mass flow rate remains unchanged since h_1 and h_6 are the same.

$$\dot{m} = 0.03462 \text{ kg/s}$$

Temperature $t_{2'}$ is determined by using $T\,ds = dh = c_p\,dt$ along *a*–2′

$$T_{2'} = T_c \exp\left(\frac{s_1 - s_a}{c_{pc}}\right) = 313 \exp\left(\frac{5.9518 - 4.8728}{2.701}\right) = 466.7 \text{ K} = 193.7°\text{C}$$

$$h_{2'} = h_a + c_{pc}\,(t_{2'} - t_c) = 1472.02 + 2.701(193.2 - 40) = 1887.164$$

$$v_{2'} = v_a T_{2'}/T_a = 0.833(466.7)/313 = 0.1242$$

$$W = \dot{m}(h_{2'} - h_1) = 0.03462(1887.164 - 1387.15) = 17.31 \text{ kW}$$

$$Q_c = \dot{m}(h_{2'} - h_6) = 0.03462(1887.164 - 371.47) = 52.473 \text{ kW}$$

$$\text{COP} = 35.16667/W = 35.16661/17.31 = 2.0316$$

$$\eta_{\text{vol}} = 1.0 + \varepsilon - \varepsilon\,(v_1/v_2) = 1.04 - 0.04(1.55/0.1242) = 0.541$$

$$\mathbb{V}_S = \dot{m} v_1/\eta_{\text{vol}} = 0.03462 \times 1.55/0.541 = 0.099 \text{ m}^3/\text{s}$$

The results obtained by using average specific heat are very similar to those obtained by interpolation in the superheat tables. In fact the results are as good as the values of average specific heats. The specific heat varies with temperature at constant pressure. It may be noted that for this reason we had to take two values for it at the condenser pressure. A smaller value was taken for the SSS cycle, which involved larger temperature.

EXAMPLE 6.2 If the water intercooler is not used and the remaining data is same as that in Example 6.1, determine the parameters of Example 6.1.

Solution:

In many installations the water intercooler is not used in two-stage systems although it has been observed that it can cool the refrigerant from $t_2 = 72.69°\text{C}$ to 40°C. This cooling is done by cold water made available from the cooling tower, hence the vapour can be cooled to approximately the condenser temperature.

In the absence of water intercooler the schematic diagram and *p–h* diagram of the cycle are as shown in Figures 6.3(a) and (b), respectively.

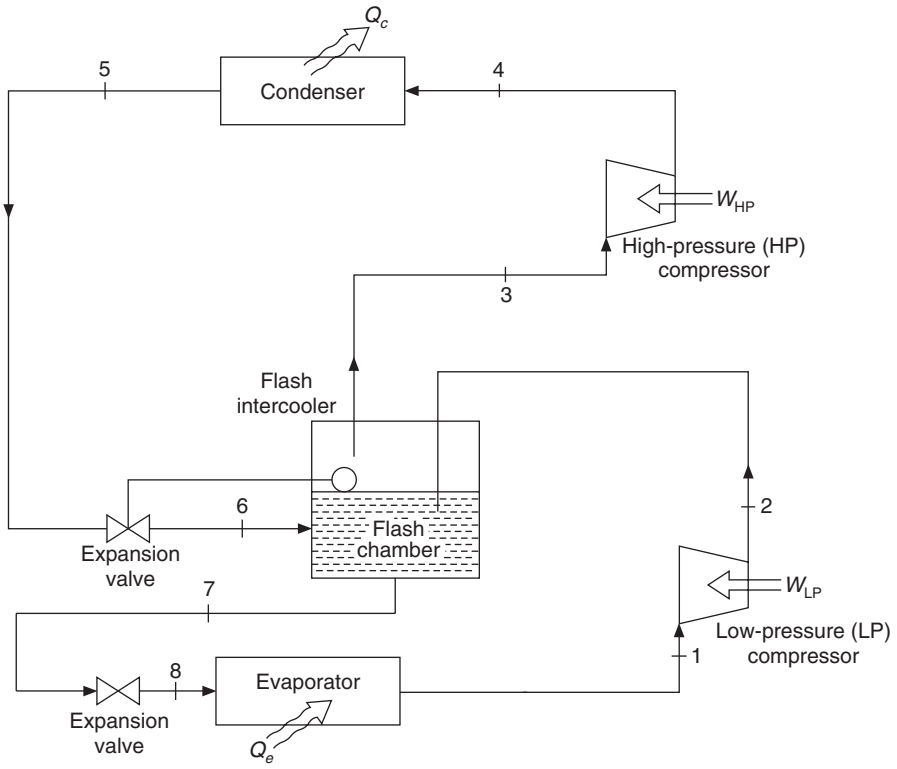

Figure 6.3(a) Schematic diagram of a two-stage compression system with flash intercooling.

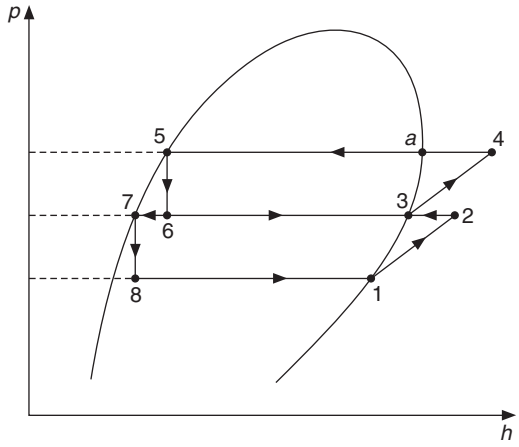

Figure 6.3(b) *p–h* diagram for the system shown in Figure 6.3(a).

The mass flow rate and work requirement of the LP compressor will remain the same as in Example 6.1, that is,

$$\dot{m}_{LP} = 0.02893 \text{ kg/s} \quad \text{and} \quad W_{LP} = 6.7868 \text{ kW}$$

All other enthalpies, entropies and specific volumes are the same as in the last example; only the subscripts have changed. Hence, from the last example, we have

$h_1 = 1387.15$, $s_1 = 5.9518$ and $v_1 = 1.55$

$t_2 = 72.6921^{o}C$, $h_2 = 1621.733$ and $v_2 = 0.42083$

$h_3 = 1441.08$, $h_7 = h_8 = 171.63$, $v_3 = 0.317$ and $s_3 = 5.3627$

$h_a = 1472.02$, $v_a = 0.0833$, $s_a = 4.8728$, $h_5 = h_6 = 371.47$ and $s_5 = 1.3579$

$t_4 = 96.493^{o}C$, $h_4 = 1639.366$ and $v_4 = 0.105$

The mass flow rate in the HP compressor will be different from that of Example 6.1. Energy balance across the heat exchangers gives

$$\dot{m}_{HP}(h_3 - h_6) = \dot{m}_{LP}(h_2 - h_7)$$

$$\therefore \quad \dot{m}_{HP} = \dot{m}_{LP}\frac{(h_2 - h_7)}{(h_3 - h_5)} = 0.02893\,\frac{1621.733 - 171.63}{1441.08 - 371.47} = 0.03922 \text{ kg/s}$$

$$W_{HP} = \dot{m}_{HP}(h_4 - h_3) = 0.03922(1639.3666 - 1441.08) = 7.777 \text{ kW}$$

$$W_{net} = W_{LP} + W_{HP} = 14.5638 \text{ kW} \qquad (\because \ W_{LP} = 6.7868 \text{ kW})$$

$$Q_c = \dot{m}_{HP}(h_4 - h_5) = 0.03922(1639.3666 - 371.47) = 49.731 \text{ kW}$$

Heat rejection ratio = $Q_c/Q_e = 1.414$

$$\text{COP} = Q_e/W_{net} = 35.1667/14.5638 = 2.4146$$

$$\eta_{vol,LP} = 1.0 + \varepsilon - \varepsilon(v_1/v_2) = 1.04 - 0.04(1.55/0.42083) = 0.8927$$

$$\eta_{vol,HP} = 1.0 + \varepsilon - \varepsilon(v_4/v_5) = 1.04 - 0.04(0.317/0.105) = 0.9192$$

$$(\mathbb{V}_S)_{LP} = \dot{m}_{LP}.\ v_1/\eta_{vol,LP} = 0.02893 \times 1.55/0.8927 = 0.0502 \text{ m}^3/\text{s}$$

$$(\mathbb{V}_S)_{HP} = \dot{m}_{HP}.\ v_4/h_{vol,HP} = 0.03922 \times 0.317/0.9192 = 0.0135 \text{ m}^3/\text{s}$$

$$(\mathbb{V}_S)_{LP}/(\mathbb{V}_S)_{HP} = 3.711$$

The water intercooler reduces the load on the flash intercooler, as a result a smaller flow rate of refrigerant evaporates to intercool the refrigerant thereby reducing the mass flow rate of refrigerant in the high-pressure compressor. This reduces the work requirement of the high-pressure compressor and improves the COP as well.

6.2.1 Intermediate Pressure Achieved for the Chosen Compressors

A question that is sometimes asked is that if LP and HP compressors of specified swept flow rates $(\mathbb{V}_S)_{LP}$ and $(\mathbb{V}_S)_{HP}$, respectively, have been chosen, then the evaporator and the condenser temperatures being specified what will be the intermediate pressure? For a simple analysis, it is assumed that there is no water intercooler so that the schematic and *p–h* diagram are as shown in Figures 6.3(a) and (b), respectively.

The energy balance across the heat exchangers by analogy with Eq. (6.2) yields

$$\dot{m}_{LP}\,(h_2 - h_7) = \dot{m}_{HP}\,(h_3 - h_6) \tag{6.9}$$

The left hand side of this equation represents the condenser heat rejection of a SSS cycle operating between T_e and T_i with the LP compressor and the right hand side of this equation represents the refrigeration capacity of an SSS cycle operating between T_i and T_c with the HP compressor. Substituting for the swept flow rates by analogy with Eq. (6.8), we get

$$(\mathbb{V}s)_{LP}\,(\eta_{vol,LP}/v_1)\,(h_2 - h_7) = (\mathbb{V}_S)_{HP}\,(\eta_{vol,HP}/v_3)\,(h_3 - h_6) \tag{6.10}$$

The intermediate pressure can be determined by plotting the left hand and right hand sides of this equation for various intermediate pressures. The point of intersection of these two curves determines the intermediate pressure that the system will arrive at or seek. This is illustrated in the following Example 6.3, where Eq. (6.10) is solved by trial and error calculations. An intermediate temperature T_i is assumed and the two sides of Eq. (6.10) are evaluated, and T_i is corrected until the two sides become equal.

One of the problems faced by multistage refrigeration systems is that of *Oil Wandering*, that is, the lubricating oil may accumulate in either the LP stage compressor or the HP stage compressor, making one of the compressors devoid of lubricating oil and increasing its wear and tear. The oil equalization system requires float valves, solenoid valves, pressure reduction valve and an oil pump so that lubricating oil level is sensed in both the compressors and oil is transferred to the compressor with a lower level of it. This system is expensive and not very reliable. The *Oil Wandering* problem is avoided by using a multi-cylinder compressor with a few cylinders used as LP stage and the remaining cylinders as HP stage. The crankcase is common to LP and HP stages, hence the oil wandering problem does not occur. The ratio of swept flow rates will be a proper fraction or an integer for this choice.

The swept volume flow rates in Example 6.2 are 0.0502 and 0.0135 m^3/s respectively for high and low-pressure compressors with their ratio being 3.711. If a multi-cylinder compressor is used then, 3.711 cylinders have to be used as LP stage and one cylinder as HP stage if all the cylinders have identical bore and stroke. It is a common practice to have identical cylinders in a multistage compressor. Therefore, a practical system that will be closest to the above example will be one with four cylinders as LP stage and one cylinder as HP stage. (Although it is common practice to have even number of cylinders.) Obviously such a system will not achieve the optimum intermediate pressure of Example 6.2. In the following example the intermediate pressure is determined with swept volume rates of LP and HP stages as 0.05 m^3/s and 0.0125 m^3/s respectively so that their ratio is 4.0.

EXAMPLE 6.3 The condenser and evaporator temperatures are 40°C and –50°C respectively for a two-stage NH_3 refrigeration system. The water intercooler is not used. The LP vapour is intercooled up to saturated state in a flash chamber. The swept volume rates of LP and HP compressors are 0.05 m^3/s and 0.0125 m^3/s respectively. Find the intermediate pressure and the cooling capacity that the system of Figure 6.3 will achieve.

Solution:

At –50°C, we have $v_1 = 2.623$, $h_1 = 1370.41$ and $s_1 = 6.1478$

At 40°C: $h_a = 1472.02$, $v_a = 0.0833$, $s_a = 4.8728$, $h_5 = h_6 = 371.47$ and $s_5 = 1.3579$

Assume an intermediate temperature of $T_i = -4^oC$

At -4^oC : $v_3 = 0.334$, $h_3 = 1438.74$, $s_3 = 5.3895$, $h_7 = 162.41$

At 100^oC superheat : $v = 0.480$, $h = 1676.6$ and $s = 6.1433$

At 120^oC superheat : $v = 0.50$, $h = 1723.0$ and $s = 6.2665$

Interpolating for $s_1 = s_2 = 6.1478$, $\Delta t = 20(6.1478 - 6.1433)/(6.2665 - 6.1433)$

$= 0.03652 \times 20 = 0.7305$

$\therefore \quad t_2 = -4 + 100 + 0.7305 = 96.7305°C$

$h_2 = 1676.6 + 0.03652\ (1723.0 - 1676.6) = 1678.295$ and similarly, $v_2 = 0.48073$

For $s_3 = s_4 = 5.3895$, interpolating in the superheat table given in Example 6.1 for condenser temperature of 40^oC between superheat of $60°C$ and 80^oC

$\Delta t = 20(5.3895 - 5.3883)/(5.5253 - 5.\ 3883) = 0.00826 \times 20 = 0.175$

$\therefore \quad t_4 = 40 + 60 + 0.175 = 100.175^oC$

$h_4 = 1647.9 + 0.00876(1700.3 - 1647.9) = 1648.359$ and similarly, $v_4 = 0.10807$

$\eta_{vol,LP} = 1.0 + \varepsilon - \varepsilon\ (v_1/v_2) = 1.04 - 0.04(2.623/0.48073) = 0.82175$

$\eta_{vol,HP} = 1.0 + \varepsilon - \varepsilon\ (v_3/v_4) = 1.04 - 0.04(0.334/0.10807) = 0.916376$

The left hand and right hand sides of Eq. (6.10) are:

$(\mathbb{V}_S)_{LP}\ (\eta_{vol,LP})(h_2 - h_7)/v_1 = 0.05(0.82175)(1678.295 - 162.41)/2.623 = 23.7453$

$(\mathbb{V}_S)_{HP}\ (\eta_{vol,HP})(h_3 - h_6)/v_3 = 0.0125(0.916376)(1438.74 - 371.47)/0.334 = 36.60258$

Obviously the left and right hand sides of Eq. (6.10) are not the same, hence this is not the correct intermediate temperature.

Assume intermediate temperature $T_i = -10^oC$

At -10^oC : $v_3 = 0.418$, $h_3 = 1431.409$, $s_3 = 5.4712$, $h_7 = 134.95$

At 80^oC superheat: $v = 0.566$, $h = 1619.4$ and $s = 6.0964$

At 100^oC superheat: $v = 0.601$, $h = 1665.0$ and $s = 6.2256$

Interpolating for $s_1 = s_2 = 6.1468$, $\Delta t = 20(6.1478 - 6.0964)/(6.2256 - 6.0964)$

$= 0.3978 \times 20 = 7.95666$

$\therefore \quad t_2 = -10 + 80 + 7.95666 = 77.95666°C$

$h_2 = 1619.4 + 0.3978(1665.0 - 1619.4) = 1637.5412$ and $v_2 = 0.47992$

For $s_3 = s_4 = 5.4712$, interpolating in the superheat table given in Example 6.1 for condenser temperature of 40^oC between superheat of $60°C$ and 80^oC,

$\Delta t = 20(5.4712 - 5.3883)/(5.5253 - 5.3883) = 12.102$

$\therefore \quad t_4 = 40 + 60 + 12.102 = 112.102^oC$, $h_4 = 1679.6077$ and $v_4 = 0.112841$

$\eta_{vol,LP} = 1.0 + \varepsilon - \varepsilon\ (v_1/v_2) = 1.04 - 0.04(2.623/0.57992) \quad = 0.8591$

$\eta_{vol,HP} = 1.0 + \varepsilon - \varepsilon\ (v_3/v_4) = 1.04 - 0.04(0.418/0.112841) = 0.8918$

The left hand and right hand sides of Eq. (6.10) are:

$$(\mathbb{V}_S)_{LP}(\eta_{vol,LP})(h_2 - h_7)/v_1 = 0.05(0.8591)(1637.5412 - 134.95)/2.623 \quad = 24.607$$

$$(\mathbb{V}_S)_{HP}(\eta_{vol,HP})(h_3 - h_6)/v_3 = 0.0125(0.8918)(1431.409 - 371.47)/0.418 = 28.267$$

Again it is observed that the left and right hand sides of Eq. (6.10) are not the same, hence this is not the correct intermediate temperature.

Assume intermediate temperature $T_i = -15^oC$

At -15^oC : $v_3 = 0.509$, $h_3 = 1424.919$, $s_3 = 5.5423$, $h_7 = 112.17$

At 60^oC superheat : $v = 0.6422$, $h = 1564.9$ and $s = 6.0304$

At 80^oC superheat : $v = 0.6875$, $h = 1610.1$ and $s = 6.16814$

Interpolating for $s_1 = s_2 = 6.1468$, $\Delta t = (6.1478 - 6.0304)/(6.16814 - 6.0304) \times 20 = 17.0466°C$

$\therefore$ $t_2 = -15 + 60 + 17.0466 = 62.90466$, $h_2 = 1603.42534$ and $v_2 = 0.68081$

For $s_3 = s_4 = 5.5423$, interpolating in the superheat table given in Example 6.1 for condenser temperature of 40^oC between superheat of $80°C$ and 100^oC,

$$\Delta t = 20(5.5423 - 5.5253)/(5.65283 - 5.5253) = 2.666°C$$

$\therefore$ $t_4 = 40 + 80 + 2.666 = 122.666^oC$, $h_4 = 1707.1517$ and $v_4 = 0.116933$

$$\eta_{vol,LP} = 1.0 + \varepsilon - \varepsilon\,(v_1/v_2) = 1.04 - 0.04(2.623/0.68081) \quad = 0.8859$$

$$\eta_{vol,HP} = 1.0 + \varepsilon - \varepsilon\,(v_3/v_4) = 1.04 - 0.04(0.509/0.116933) = 0.8659$$

The left hand and right hand sides of Eq. (6.10) are:

$$(\mathbb{V}_S)_{LP}(\eta_{vol,LP})(h_2 - h_7)/v_1 = 0.05(0.8859)(1603.42534 - 112.17)/2.623 = 25.18305$$

$$(\mathbb{V}_S)_{HP}(\eta_{vol,HP})(h_3 - h_6)/v_3 = 0.0125(0.8659)(1424.919 - 371.47)/0.509 = 22.4013$$

A comparison of the results for intermediate temperature of $-10°C$ and -15^oC indicates that the left hand side and right hand side of Eq. (6.10) would become equal at some temperature between these two values.

Assume intermediate temperature $T_i = -12^oC$

At $T_i = -12^oC$: $v_3 = 0.452$, $h_3 = 1428.855$ and $s_3 = 5.4996$, $h_7 = 125.82$

At 80^oC superheat : $v = 0.612$, $h = 1615.7$ and $s = 6.125$

At 100^oC superheat : $v = 0.650$, $h = 1661.1$ and $s = 6.2545$

Interpolating in the superheat table for intermediate temperature of -12^oC for $s_1 = s_2 = 6.1468$, $\Delta t = 20(6.1478 - 6.125)/(6.2545 - 6.125) = 3.5212$

$\therefore$ $t_2 = -12 + 80 + 3.5212 = 71.5212$, $h_2 = 1623.6932$ and $v_2 = 0.6187$

For $s_3 = s_4 = 5.4996$, interpolating in the superheat table given in Example 6.1 for condenser temperature of 40^oC between superheat of $60°C$ and 80^oC

$$\Delta t = 20(5.4996 - 5.3883)/(5.5253 - 5.3883) = 16.2482°C$$

$\therefore$ $t_4 = 40 + 60 + 16.248 = 116.248^oC$, $h_4 = 1690.4702$ and $v_4 = 0.1145$

$$\eta_{vol,LP} = 1.0 + \varepsilon - \varepsilon\,(v_1/v_2) = 1.04 - 0.04(2.623/0.6187) = 0.87042$$

$$\eta_{vol,HP} = 1.0 + \varepsilon - \varepsilon\,(v_3/v_4) = 1.04 - 0.04(0.452/0.1145) = 0.8821$$

The left hand and right hand sides of Eq. (6.10) are:

$$(\mathbb{V}_S)_{LP}(\eta_{vol,LP})(h_2 - h_7)/v_1 = 0.05(0.87042)(1623.6932 - 125.82)/2.623 = 24.8528$$

$$(\mathbb{V}_S)_{HP}(\eta_{vol,HP})(h_3 - h_6)/v_3 = 0.0125(0.8821)(1428.855 - 371.47)/0.452 = 25.794$$

The left hand and the right hand side of Eq. (6.10) are almost the same for $T_i = -12^oC$. It appears that these will be the same for $T_i = -13^oC$.

Assume intermediate temperature $T_i = -13^oC$:

At $T_i = -13^oC$: $v_3 = 0.47$, $h_3 = 1427.557$ and $s_3 = 5.5139$, $h_7 = 121.26$

At 80^oC superheat : $v = 0.637$, $h = 1613.8$ and $s = 6.1394$

At 100^oC superheat : $v = 0.6768$, $h = 1659.15$ and $s = 6.269$

Interpolating in the superheat table for intermediate temperature of -12^oC

for $s_1 = s_2 = 6.1468$, $\Delta t = 20(6.1478 - 6.1394)/(6.269 - 6.1394) = 1.2963°C$

$\therefore$ $t_2 = -13 + 80 + 1.2963 = 68.2963$, $h_2 = 1616.7393$ and $v_2 = 0.63958$

For $s_3 = s_4 = 5.5139$, interpolating in the superheat table given in Example 6.1 for condenser temperature of 40^oC between superheat of 60°C and 80^oC.

$$\Delta t = (5.5139 - 5.3883)/(5.5253 - 5.3883) \times 20 = 0.9168 \times 20 = 18.336°C$$

$\therefore$ $t_4 = 40 + 60 + 18.336 = 118.336^oC$, $h_4 = 1695.94$ and $v_4 = 0.11533$

$$\eta_{vol,LP} = 1.0 + \varepsilon - \varepsilon\,(v_1/v_2) = 1.04 - 0.04(2.623/0.63958) = 0.87595$$

$$\eta_{vol,HP} = 1.0 + \varepsilon - \varepsilon\,(v_3/v_4) = 1.04 - 0.04(0.47/0.11533) = 0.87699$$

The left hand and right hand sides of Eq. (6.10) are:

$$(\mathbb{V}_S)_{LP}(\eta_{vol,LP})(h_2 - h_7)/v_1 = 0.05(0.87595)(1616.7393 - 121.26)/2.623 = 24.9707$$

$$(\mathbb{V}_S)_{HP}(\eta_{vol,HP})(h_3 - h_6)/v_3 = 0.0125(0.87699)(1427.557 - 371.47)/0.47 = 24.632$$

The two sides of Eq. (6.10) are same to a very good accuracy. Hence it is presumed that the intermediate temperature achieved by the two compressors will be -13^oC.

$$\dot{m}_{LP} = (\mathbb{V}_S)_{LP}(\eta_{vol,LP})/v_1 = 0.05 \times 0.87595/2.623 = 0.0166975 \text{ kg/s}$$

$$\dot{m}_{HP} = (\mathbb{V}_S)_{HP}(\eta_{vol,HP})/v_3 = 0.0125 \times 0.87699/0.47 = 0.023324 \text{ kg/s}$$

$$Q_e = \dot{m}_{LP}\,(h_1 - h_7) = 0.0166975\ (1370.41 - 121.26) = 20.858 \text{ kW} = 5.93 \text{ TR}$$

$$W_{LP} = \dot{m}_{LP}\,(h_2 - h_1) = 0.0166975(1616.7393 - 1370.41) = 4.113 \text{ kW}$$

$$W_{HP} = \dot{m}_{HP}\,(h_4 - h_3) = 0.023324\ (1695.94 - 1427.557) = 6.25982\text{kW}$$

$$\text{COP} = Q_e/(W_{LP} + W_{HP}) = 20.858/(4.113 + 6.25982) = 2.011$$

$$Q_c = \dot{m}_{HP}\,(h_4 - h_5) = 0.023324(1616.7393 - 371.47) = 29.045 \text{ kW}$$

If the following tabulated values of the two sides of Eq. (6.10) are plotted against the intermediate temperature, the point of intersection of the two sides would seen to be at $T_i = 13°C$.

T_i (°C)	−4	−10	−15	−12	−13
$(\mathbb{V}_S)_{LP}(\eta_{vol,LP})(h_2 - h_7)/v_1$	23.7453	24.607	25.18305	24.8528	24.9707
$(\mathbb{V}_S)_{HP}(\eta_{vol,HP})(h_3 - h_6)/v_1$	36.60258	28.267	22.4013	25.794	24.632

6.2.2 Practical Disadvantages of Flash Chamber

The liquid refrigerant in the flash chamber is saturated liquid at state 8 (see Figure 6.1) at the intermediate pressure p_i, hence there is a possibility that some of it may evaporate ahead of the expansion valve due to the following reasons:

(i) If the evaporator is located at a higher elevation than the flash chamber, then there will be pressure drop in rising against gravity.

(ii) There is pressure drop due to friction in the line connecting the flash chamber to the expansion valve.

The expansion valve is calibrated for flow of liquid through its narrow orifice. If a mixture of liquid and vapour (of lower density than that of the liquid) flows through the orifice the mass flow rate of refrigerant will decrease drastically. In addition, the operation of expansion valves will become sluggish since the pressure difference across both the valves is small. Hence, if the flash chamber cannot be placed very close to the evaporator, it is recommended that the liquid refrigerant be subcooled ahead of the expansion valve inlet.

6.2.3 Improved Two-stage Cycle

Figures 6.4(a) and (b) show the schematic and *p–h* cycle diagram of a two-stage system frequently used with NH_3, which does not suffer from the above mentioned disadvantages. In this system, the flash chamber is replaced by a flooded type shell-and-coil heat exchanger. The refrigerant that is fed to evaporator passes through this HEX and is effectively subcooled to state 8 that eliminates the possibility of flashing ahead of expansion valve. The float type expansion valve 6–7 is an auxiliary valve through which flows only a small quantity of refrigerant required for subcooling and intercooling. The pressure drop across the main expansion valve 8–9 is large since the liquid refrigerant is at condenser pressure.

The subcooling is done by liquid refrigerant at intermediate pressure, which evaporates and the resulting vapour acts as an additional load on the HP compressor instead of going to LP compressor. An energy balance across the heat exchanger yields

$$\dot{m}_{LP}\, h_8 + (\dot{m}_{LP} + \dot{m}')\, h_4 = (\dot{m}_{LP} + \dot{m}')\, h_6 + \dot{m}_{LP}\, h_3 \tag{6.11}$$

or

$$\dot{m}'(h_4 - h_6) = \underbrace{\dot{m}_{LP}\,(h_3 - h_4)}_{\text{Intercooling}} + \underbrace{\dot{m}_{LP}\,(h_6 - h_8)}_{\text{Subcooling}}$$

$$\dot{m}_{HP} = \dot{m}_{LP} + \dot{m}' \quad \text{and} \quad \dot{m}' = m_{LP}\,\frac{(h_3 - h_4) + (h_6 - h_8)}{(h_4 - h_6)} \tag{6.12}$$

Also

$$\dot{m}_{LP}\,(h_3 - h_8) = \dot{m}_{HP}\,(h_4 - h_6) \quad \text{and} \quad \dot{m}_{HP} = \dot{m}_{LP}\,\frac{(h_3 - h_8)}{(h_4 - h_6)} \tag{6.13}$$

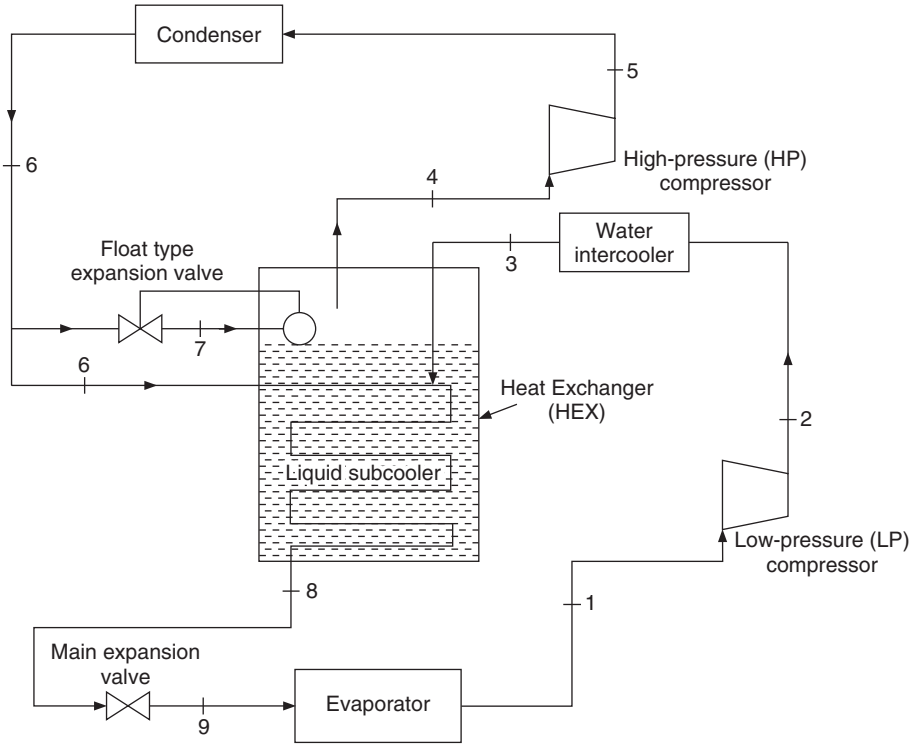

Figure 6.4(a) Schematic diagram of an NH_3 two-stage compression system with water intercooler and liquid subcooler.

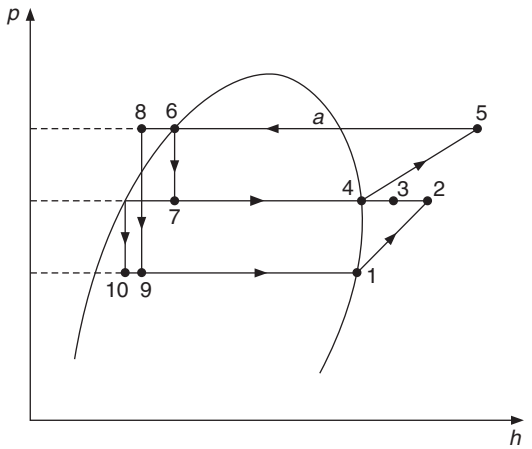

Figure 6.4(b) *p–h* cycle diagram of system of Figure 6.4(a).

$$W_{\text{net}} = W_{\text{LP}} + W_{\text{HP}} = \dot{m}_{\text{LP}} \left\{ (h_2 - h_1) + \frac{(h_3 - h_8)}{(h_4 - h_6)} (h_5 - h_4) \right\} \tag{6.14}$$

Equation (6.14) is same as Eq. (6.4). Since $h_6 = h_7$, hence the expression for COP will also be the same as Eq. (6.6). The value of enthalpy h_8 in these expressions is more than that in Eqs. (6.5) and (6.6), hence the refrigeration effect is less and the work requirement is more. Further, the temperature of the subcooled refrigerant at state 8 is more than the temperature of the liquid at 4,which subcools it since some temperature drop is required for heat transfer. In the last case the liquid refrigerant was fed to evaporator at state 10 as shown in Figure 6.4(b) and $h_9 > h_{10}$, therefore, the refrigeration effect reduces in this system. Moreover the heat exchanger is more expensive than the flash chamber.

EXAMPLE 6.4(a) The condenser and evaporator temperatures are 40°C and –40°C respectively for a two-stage NH_3 refrigeration system of 10 TR cooling capacity. The intermediate temperature is –2°C. A water intercooler cools the LP vapour to 40°C. LP vapour is subsequently intercooled up to saturated state in a shell-and-coil heat exchanger. The liquid is subcooled in the same HEX from 40°C to a temperature of 5°C. Find the mass flow rates and the swept volume rates and work requirements of both the compressors, condenser heat rejection and COP. Compare the results with those in Example 6.1. The clearance volume ratio for both the compressors is 0.04.

Solution:

A comparison of cycle diagrams in Figures 6.1(b) and Figure 6.4(b) indicates that the temperatures, enthalpies and specific volumes at state points 1, 2, 3, 4 and 5 are the same as in Example 6.1.

The only difference is in enthalpy at state point 8, which is subcooled liquid state at 5°C. From saturation table the enthalpy of saturated liquid h_f at 5°C = h_8 = 204.07 kJ/kg.

$$\dot{m}_{LP} = \frac{3.51667 \text{ TR}}{(h_1 - h_8)} = \frac{3.51667 \times 10}{1387.15 - 204.07} = 0.02972 \text{ kg/s}$$

$$\dot{m}' = \dot{m}_{LP} \frac{(h_3 - h_4) + (h_6 - h_8)}{(h_4 - h_6)} = 0.02972 \frac{(1545.14 - 1441.08) + (371.47 - 204.07)}{1441.08 - 371.47}$$

$$= 0.0075427$$

$$\dot{m}_{HP} = \dot{m}_{LP} + \dot{m}' = 0.02972 + 0.0075427 = 0.037263 \text{ kg/s}$$

$$W_{LP} = \dot{m}_{LP} (h_2 - h_1) = 0.02972(1621.733 - 1387.15) = 6.9729 \text{ kW}$$

$$W_{HP} = \dot{m}_{HP} (h_5 - h_4) = 0.037263(1639.3666 - 1441.08) = 7.3887 \text{ kW}$$

$$W_{net} = W_{LP} + W_{HP} = 14.3616 \text{ kW}$$

$$Q_c = \dot{m}_{HP} (h_5 - h_6) = 0.037263(1639.3666 - 371.47) = 47.2453 \text{ kW}$$

Heat rejection ratio = Q_c/Q_e = 1.3435

$$\text{COP} = Q_e/W_{net} = 35.1667/14.78482 = 2.44866$$

$$h_{vol,LP} = 1.0 + \varepsilon - \varepsilon (v_1/v_2) = 1.04 - 0.04(1.55/0.42083) = 0.8927$$

$$h_{vol,HP} = 1.0 + \varepsilon - \varepsilon (v_4/v_5) = 1.04 - 0.04(0.317/0.105) = 0.9192$$

$$(\mathbb{V}_S)_{LP} = \dot{m}_{LP} v_1/\eta_{vol,LP} = 0.02972 \times 1.55/0.8927 = 0.05164 \text{m}^3/\text{s}$$

$$(\mathbb{V}_S)_{HP} = \dot{m}_{HP} v_4/\eta_{vol,HP} = 0.037263 \times 0.317/0.9192 = 0.01285 \text{ m}^3/\text{s}$$

$$(\mathbb{V}_S)_{LP}/(\mathbb{V}_S)_{HP} = 4.0187$$

When these results are compared with the results of Example 6.1, it is observed that the mass flow rate of LP compressor increases since the specific refrigeration effect decreases ($h_9 > h_{10}$ in Figure 6.4(b)). W_{LP} increases on account of increase in $\dot{m}_{LP}$. The mass flow rate of HP compressor also increases, as a result W_{HP} also increases. The increase in $\dot{m}_{HP}$ is not very pronounced since in Example 6.1 the flash vapour generated out of the total mass flow rate is very large, whereas in this example the flash vapour is generated from only the refrigerant passing through the auxiliary expansion valve, since the main refrigerant flow is subcooled. The mass flow rate $\dot{m}_{HP}$ increases since subcooling is also done by the liquid refrigerant. The COP decreases. The swept flow rates for both the compressors are large compared to the previous case. However, this system is used for its practical advantages.

EXAMPLE 6.4(b) If water intercooler is not used in Example 6.4(a), find all the parameters for the same condenser, evaporator and intermediate temperatures as in Example 6.4(a).

Solution:

The cycle diagram is same as in Figure 6.4(b) except that entry to the HEX will be at state 2 rather than state 3.

The mass flow rate, the work requirement and the swept volume rates of LP compressor will be the same as in Example 6.4(a). The mass flow rate through the float type expansion valve m' will involve h_2 instead of h_3 and is calculated as follows.

$$\dot{m}' = \dot{m}_{LP} \frac{(h_6 - h_8) + (h_2 - h_4)}{(h_4 - h_6)} = 0.02972 \frac{(371.47 - 204.07) + (1621.73 - 1441.08)}{1441.08 - 371.47}$$

$$= 0.009672$$

$$\dot{m}_{HP} = \dot{m}_{LP} + \dot{m}' = 0.02972 + 0.009672 = 0.039397 \text{ kg/s}$$

By using the property values from Example 6.1, we get

$$W_{LP} = \dot{m}_{LP} (h_2 - h_1) = 0.02972(1621.733 - 1387.15) = 6.9729 \text{ kW}$$

$$W_{HP} = \dot{m}_{HP} (h_5 - h_4) = 0.039397(1639.3666 - 1441.08) = 7.81192 \text{ kW}$$

$$W_{net} = W_{LP} + W_{HP} = 14.78482 \text{ kW}$$

$$Q_c = \dot{m}_{HP} (h_5 - h_6) = 0.039397(1639.3666 - 371.47) = 49.9515 \text{ kW}$$

Heat rejection ratio = $Q_c/Q_e = 1.4204$

$$\text{COP} = Q_e/W_{net} = 35.16667/14.78482 = 2.37856$$

$$\eta_{vol,LP} = 1.0 + \varepsilon - \varepsilon (v_1/v_2) = 1.04 - 0.04(1.55/0.42083) = 0.8927$$

$$\eta_{vol,HP} = 1.0 + \varepsilon - \varepsilon (v_4/v_5) = 1.04 - 0.04(0.317/0.105) = 0.9192$$

$$(\mathbb{V}_S)_{LP} = \dot{m}_{LP} v_1/\eta_{vol,LP} = 0.02972 \times 1.55/0.8927 = 0.05164 \text{m}^3/\text{s}$$

$$(\mathbb{V}_S)_{HP} = \dot{m}_{HP} v_4/\eta_{vol,HP} = 0.039397 \times 0.317/0.9192 = 0.013587 \text{m}^3/\text{s}$$

$$(\mathbb{V}_S)_{LP}/(\mathbb{V}_S)_{HP} = 3.799$$

The systems of Figures 6.1 and 6.4 assume that the vapour at inlet to both the compressors is saturated vapour. It has been observed that the saturated state 1 may consist of some fine liquid droplets (mist) suspended in superheated vapour. Hence state at 1 may be on the average a saturated

state. The liquid refrigerant droplets may not evaporate by the end of compression stroke. Therefore, saturated state at inlet to compressor is prone to slugging of the compressor. Hence, the expansion valve usually ensures that the state at entry to compressors is superheated by at least 5°C. In any case, the HEX used in both the systems cannot be ideal in practice, hence it will not cool the vapour to the liquid temperature and the temperature of vapour will be at least 5°C more than that of liquid inside HEX. This is desirable also from the volumetric efficiency point of view since it has been noted that the volumetric efficiency of NH_3 compressor also improves with some superheat. Example 7.5 considers this with inlet to both the compressors at 5°C superheat.

EXAMPLE 6.5 The condenser and evaporator temperatures are 40°C and −40°C respectively for a two-stage NH_3 refrigeration system of 10 TR cooling capacity. The vapour leaves the evaporator and enters the LP compressor at 5°C superheat. The intermediate temperature is −2°C. A water intercooler intercools the LP vapour to 40°C and further intercooling up to 5°C superheat is done in shell-and-coil heat exchanger that subcools the liquid refrigerant from 40°C to a temperature of 5°C. Find the mass flow rates and swept volume rates and work requirements of both the compressors, condenser heat rejection and COP. Compare the results with those in Example 6.4. The clearance volume ratio for both the compressors is 0.04. The thermodynamic *p–h* cycle diagram is shown in Figure 6.4(c).

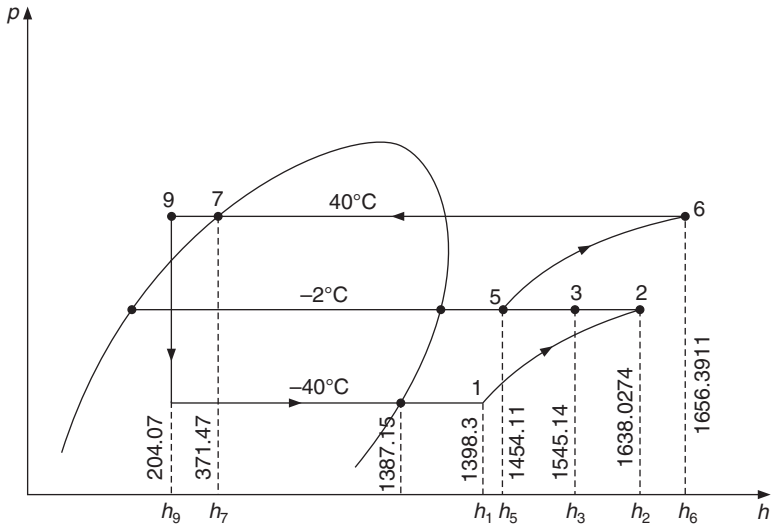

Figure 6.4(c) The *p–h* cycle diagram for Example 6.5.

Solution:

From superheat table for 0.717 bar (– 40°C = T_e) at 5°C superheat

$$v_1 = 1.588\ ,\ h_1 = 1398.3 \text{ and } s_1 = 5.9989$$

Interpolating in the superheat table given in Example 6.1 for 3.982 bar (−2°C) for $s_1 = s_2 = 5.9989$ between 80°C and 100°C superheat, we get

$$\Delta t = 20(5.9989 - 5.988)/(6.1165 - 5.9880) = 0.08482 \times 20 = 1.6965°C$$

$\therefore$ $t_2 = -2 + 80 + 1.6965 = 79.6965$, $h_2 = 1638.0274$, similarly, $v_2 = 0.4302$

Also, from the same superheat table given in Example 6.1 at 5°C superheat, 3.982 bar,

$$v_5 = 0.325,\ h_5 = 1454.11 \text{ and } s_5 = 5.4105$$

Interpolating in the superheat table given in Example 6.1 for 15.55 bar (40°C) for $s_5 = s_6 = 5.4105$ between superheat of 60°C and 80°C, we get

$$\Delta t = 20(5.4105 - 5.3883)/(5.5253 - 5.3883) = 0.16204 \times 20 = 3.241°\text{C}$$

$$t_6 = 40 + 60 + 3.241 = 103.241°\text{C},\ h_6 = 1647.9 + 0.16204(91700.3 - 1647.9) = 1656.3911$$

and similarly, $v_6 = 0.109296$

The exit of water intercooler is at 40°C. From Example 6.1 the enthalpy at point 3 which is at 40°C and 3.982 bar is

$$h_3 = 1545.14$$

The enthalpy at point 9 the subcooled liquid at 5°C, is same as in Example 6.4, that is,

$$h_9 = h_f(5°\text{C}) = 204.07$$

$$\dot{m}_{\text{LP}} = \frac{3.51667 \text{ TR}}{(h_1 - h_9)} = \frac{3.51667 \times 10}{1398.3 - 204.07} = 0.029447 \text{ kg/s}$$

$$\dot{m}' = \dot{m}_{\text{LP}} \frac{(h_7 - h_9) + (h_3 - h_5)}{(h_5 - h_7)}$$

$$= 0.02447 \frac{(371.47 - 204.07) + (1545.14 - 1454.11)}{1454.11 - 371.47} = 0.007029$$

$$\dot{m}_{\text{HP}} = \dot{m}_{\text{LP}} + \dot{m}' = 0.029447 + 0.007029 = 0.036476 \text{ kg/s}$$

$$W_{\text{LP}} = \dot{m}_{\text{LP}}(h_2 - h_1) = 0.029447(1638.0274 - 1398.3) = 7.05929 \text{ kW}$$

$$W_{\text{HP}} = \dot{m}_{\text{HP}}(h_6 - h_5) = 0.036476(1656.3911 - 1454.11) = 7.37846 \text{ kW}$$

$$W_{\text{net}} = W_{\text{LP}} + W_{\text{HP}} = 14.43775 \text{ kW}$$

$$Q_c = \dot{m}_{\text{HP}}(h_6 - h_7) = 0.036476(1656.3911 - 371.47) = 46.869 \text{ kW}$$

Heat rejection ratio = $Q_c/Q_e = 1.4204$

$$\text{COP} = Q_e/W_{\text{net}} = 35.1667/14.43775 = 2.4357$$

$$\eta_{\text{vol,LP}} = 1.0 + \varepsilon - \varepsilon(v_1/v_2) = 1.04 - 0.04(1.588/0.432) = 0.89235$$

$$\eta_{\text{vol,HP}} = 1.0 + \varepsilon - \varepsilon(v_5/v_6) = 1.04 - 0.04(0.325/0.109296) = 0.92106$$

$$(\mathbb{V}_S)_{\text{LP}} = \dot{m}_{\text{LP}} v_1/\eta_{\text{vol,LP}} = 0.029447 \times 1.588/0.89235 = 0.052403 \text{ m}^3/\text{s}$$

$$(\mathbb{V}_S)_{\text{HP}} = \dot{m}_{\text{HP}} v_5/\eta_{\text{vol,HP}} = 0.036476 \times 0.325/0.92106 = 0.012871 \text{ m}^3/\text{s}$$

$$(\mathbb{V}_S)_{\text{LP}}/(\mathbb{V}_S)_{\text{HP}} = 4.0714$$

Two-stage R12 cycle

The latent heat of NH_3 is large, hence only a small quantity of liquid refrigerant is required for intercooling. Further the constant entropy lines are very divergent, whereas for R12 it is not the case. In fact the COP of R12 systems is better if superheated vapour enters the HP compressor. Hence for a two-stage R12 system, intercooling is not done in the heat exchanger. It is possible

that the work requirement for R12 may increase if the intercooling is done up to the saturated state. The schematic diagram and *p–h* cycle diagram of the recommended R12 cycle are shown in Figures 6.5(a) and (b). The subcooling of the liquid refrigerant is done in a flooded type of shell-and-tube heat exchanger. A thermostatic expansion valve (TEV) feeds the refrigerant to the HEX. The feeler bulb of the TEV is attached at inlet of HP compressor. The LP vapour at state 2 is adiabatically mixed with vapour from HEX at state 9. This adiabatic mixing does the intercooling. The TEV controls the mass flow rate to the HEX such that the required subcooling is obtained and also LP vapour is intercooled so as to maintain at least 5 K superheat at inlet to HP compressor. The state 9 may not be saturated state in all the cases, it may contain some liquid refrigerant too, that is, it may lie in the mixture region. This liquid, if present, will also do the intercooling of vapour.

The latent heat of R12 is very small, hence if the vapour of the LP stage is to be intecooled to saturated state, a large quantity of refrigerant will be required that will increase the load on HP compressor. The adiabatic discharge temperature of R12 is small, hence without intercooling also it will be within safe limit.

The mass flow rate through the LP compressor is given by $\dot{m}_{LP} = 3.51667 \text{ TR}/(h_1 - h_8)$. The mass flow rate $\dot{m}'$ through the HEX is determined by considering the energy balance,

$$\dot{m}'(h_3 - h_5) = \underset{\text{Intercooling}}{\dot{m}_{LP}(h_2 - h_3)} + \underset{\text{Subcooling}}{\dot{m}_{LP}(h_5 - h_7)}$$

$$\dot{m}_{HP} = \dot{m}_{LP}\frac{(h_2 - h_7)}{(h_3 - h_5)} \text{ and } W_{net} = \dot{m}_{LP}\left\{(h_2 - h_1) + \frac{(h_2 - h_7)}{(h_3 - h_5)}(h_4 - h_3)\right\} \tag{6.15}$$

and

$$\text{COP} = \frac{(h_1 - h_8)}{(h_2 - h_1) + \dfrac{(h_2 - h_7)}{(h_3 - h_5)}(h_4 - h_3)} \tag{6.16}$$

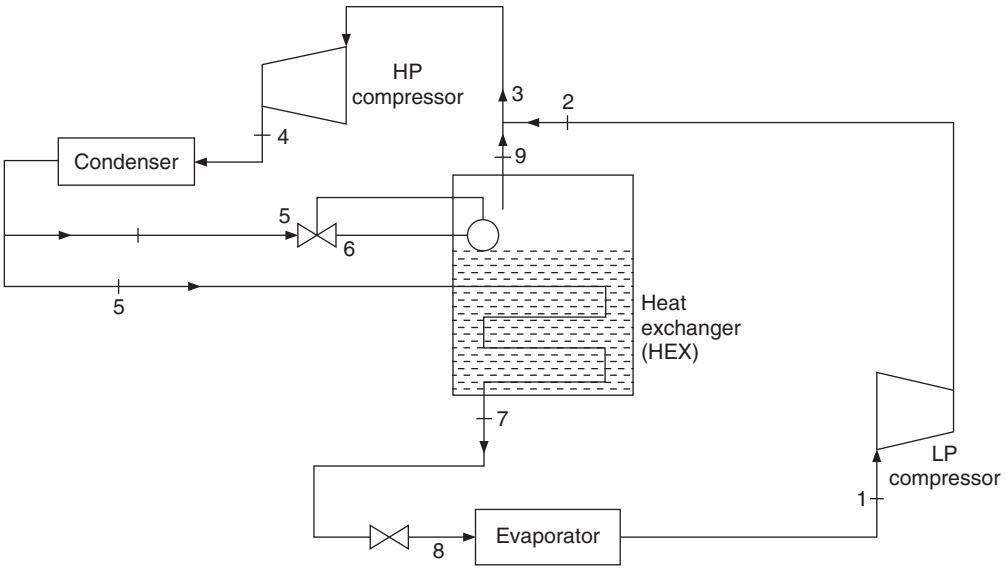

Figure 6.5(a) Schematic diagram of a two-stage compression system for R12 refrigerant.

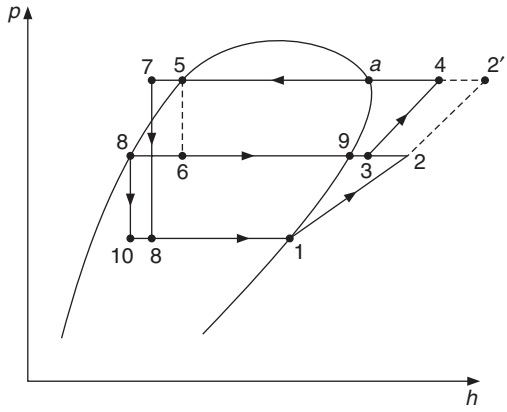

Figure 6.5(b) *p–h* diagram of the system shown in Figure 6.4(a).

6.3 RECOMMENDED TEMPERATURE RANGES FOR MULTISTAGE SYSTEMS

The two-stage systems of Figures 6.1 and 6.3 are very often used with ammonia for ice cream manufacture and holding rooms, food freezing and frozen food storage apart from other industrial and commercial low-temperature applications. Similarly, R12 and R22 are used for low-temperature test rooms and environmental chambers with two-stage systems as shown in Figure 6.5. A three-stage system is used for biotechnology applications and other laboratory applications in the range of –75° C to – 60°C. One rarely uses a refrigeration system with more than three stages.

It is observed that the COP increases as the number of stages increase, thereby the work requirement and the running cost of the refrigeration system decrease. However, the initial cost and the maintenance cost increase as the number of stages increase. Therefore, the number of stages is decided by economic as well as practical considerations rather than thermodynamic considerations.

Single-stage systems may be used above the evaporator temperature of –30°C with R12, R22 and NH_3. Single-stage systems can be more effectively used with R12 and R22 rather than with NH_3 at lower temperatures.

In the evaporator temperature range of –60°C to –30°C, a two-stage system is more economical.

Below the evaporator temperatures of – 60°C, a three-stage system is recommended.

These guidelines are, however, for large systems and may be relaxed for smaller systems or when the system will be occasionally used. For example, a single-stage system may be used below –50°C and a two-stage system may be used up to –75°C if the cooling capacity is small or if the system is used sparingly.

In recent years, large-scale liquid nitrogen production has become very economical. Hence in many applications including food-freezing applications, it is economical to use liquid nitrogen. From thermodynamic point of view the use of liquid nitrogen at –185°C to freeze food products at –30°C through a temperature difference of 155°C is a waste of lot of exergy or availability. One can run a heat engine between –185°C and –30°C and get some work output while transferring heat from –30°C and rejecting it to –185°C. However, economic considerations permit the use of liquid nitrogen. Earlier the dividing line between Cryogenics and Refrigeration was 123 K (–150°C). Nowadays, below –100°C one uses liquid nitrogen only.

The screw compressor has good volumetric efficiency at low evaporator temperature and the adiabatic discharge temperature is also low if oil cooling is used. Hence, this gives satisfactory performance at low temperatures. However, the saving in work can be obtained only by multistage compression with intercooling and increase in specific refrigeration effect is obtained with multistage expansion.

Two-stage systems improve the performance of turbo-compressor based systems as well.

EXAMPLE 6.6(a) The condenser and evaporator temperatures are 40°C and –40°C respectively for a two-stage R12 refrigeration system of 10 TR cooling capacity. Subcooling is done in a flooded type shell-and-coil heat exchanger as shown in Figure 6.5. It subcools the liquid refrigerant from 40°C to a temperature of 5°C. The Thermostatic Expansion Valve feeding the refrigerant to HEX maintains a superheat of 5°C at the inlet to the high-pressure compressor. Find the mass flow rates and the swept volume rates and work requirements of both the compressors, condenser heat rejection and COP. Compare the results with the SSS cycle. The clearance volume ratio for both the compressors is 0.04.

Solution:

The evaporator temperature is less than –30°C, therefore, a two-stage system is recommended. The evaporator and condenser pressures are:

$$p_e = 0.642 \text{ bar} \quad \text{and} \quad p_c = 9.634 \text{ bar}$$

Ideal intermediate pressure, $p_i^* = \sqrt{p_c p_e} = 2.487$ bar

Corresponding saturation temperature $t_i^* = -6.42$°C (by interpolating in R12 table)

Therefore intermediate temperature $t_i = -6.42$°C + 5°C = –1.42°C ≈ –2°C for convenience since saturation and superheated properties are available for it.

The required thermodynamic properties of R12 at saturation are as follows:

Temperature (°C)	*Pressure* (bar)	v_g (m^3/kg)	h_f (kJ/kg)	h_g (kJ/kg)	s_f (kJ/kg-K)	s_g (kJ/kg-K)
–40	0.642	0.2427	0.0	170.23	0.0	0.7301
–2	2.891	0.0593	34.3	187.81	0.1356	0.7018
40	9.634	0.0183	74.77	204.75	0.2725	0.6876

At 5°C, $h_f = 40.81$kJ/kg

The properties of superheated vapour at 2.891 bar (–2°C) are as follows:

Degree of superheat	5°C	10°C	15°C	20°C
v	0.06	0.062	0.063	0.065
h	191.02	194.23	197.45	200.67
s	0.7135	0.7251	0.7364	0.7475

The properties of superheated vapour at 9.634 bar(40°C) are as follows:

Degree of superheat	5°C	10°C	15°C	20°C
v	0.019	0.019	0.020	0.021
h	208.65	212.5	216.3	220.0
s	0.70	0.7120	0.7236	0.7350

Referring to Figure 6.5 the properties at various state points are:

$$h_1 = 170.23,\ v_1 = 0.2427 \text{ and } s_1 = 0.7301$$

$$h_9 = 187.81,\ v_9 = 0.0593 \text{ and } s_9 = 0.7018$$

State 3 is at 2.891 bar and 5 K superheat. Hence from superheat table,

$$h_3 = 191.02,\ v_3 = 0.06 \text{ and } s_3 = 0.7135$$

$$h_a = 204.75,\ v_a = 0.0183 \text{ and } s_a = 0.6876,\ h_5 = 74.77$$

State 7 is subcooled liquid at 9.634 bar and 5°C. It is assumed that its enthalpy is that of saturated liquid at 5°C, that is

$$h_7 = h_f\,(5^\circ\text{C}) = 40.81$$

By interpolating in the superheat table for intermediate pressure of 2.891 bar(−2°C) between 10°C and 15°C superheat for $s_1 = s_2 = 0.7301$, we get

$$\Delta t = 5\ (0.7301 - 0.7251)/(0.7364 - 0.7251) = 0.44248 \times 5 = 2.212^\circ\text{C}$$

$$\therefore \quad t_2 = -2 + 10 + 2.212 = 10.212^\circ\text{C}$$

$h_2 = 194.23 + (197.45 - 194.23) \times 0.44248 = 195.6547$. Similarly $v_2 = 0.06244$

Similarly, by interpolating in the superheat table for condenser pressure of 9.634 bar (40°C) between superheat of 10°C and 15°C for $s_3 = s_4 = 0.7135$

$$\Delta t = 5(0.7135 - 0.7120)/(0.7236 - 0.7120) = 0.1293 \times 5 = 0.646^\circ\text{C}$$

$$\therefore \quad t_4 = 40 + 10 + 0.646 = 50.646^\circ\text{C}$$

$h_4 = 212.5 + (216.3 - 212.5) \times 0.1293 = 212.99$. Similarly, $v_4 = 0.0193$

For SSS cycle, interpolating in the superheat table for 9.634 bar (40°C) for $s_1 = s_2 = 0.7301$, we get

$$\Delta t = 5\ (0.7301 - 0.7236)/(0.7350 - 0.7236) = 5 \times 0.572 = 2.851^\circ\text{C}$$

$t_{2'} = 40 + 15 + 2.851 = 57.851^\circ\text{C}$, $h_{2'} = 218.41$ and $v_{2'} = 0.02057$

Two-stage system:

$$\dot{m}_{\text{LP}} = \frac{3.51667\,TR}{h_1 - h_7} = \frac{3.51667 \times 10}{170.23 - 40.81} = 0.2717 \text{ kg/s}$$

$$\dot{m}' = \dot{m}_{\text{LP}}\,\frac{(h_2 - h_3) + (h_5 - h_7)}{(h_3 - h_5)} = 0.2717\,\frac{(195.6547 - 191.02) + (74.77 - 40.81)}{191.02 - 74.77}$$

$$= 0.09021$$

$$\dot{m}_{HP} = \dot{m}_{LP} + \dot{m}' = 0.2717 + 0.09021 = 0.361937 \text{ kg/s}$$

$$W_{LP} = \dot{m}_{LP}\,(h_2 - h_1) = 0.2717(195.6547 - 170.23) = 6.9085 \text{ kW}$$

$$W_{HP} = \dot{m}_{HP}\,(h_4 - h_3) = 0.361937(212.99 - 191.02) = 7.95226 \text{ kW}$$

$$W_{net} = W_{LP} + W_{HP} = 14.8608 \text{ kW}$$

$$Q_c = \dot{m}_{HP}\,(h_4 - h_5) = 0.361937(212.99 - 74.77) = 50.02748 \text{ kW}$$

Heat rejection ratio = $Q_c/Q_e = 1.4226$

$$\text{COP} = Q_e/W_{net} = 35.16667/14.8608 = 2.3664$$

$$\eta_{vol,LP} = 1.0 + \varepsilon - \varepsilon\,(v_1/v_2) = 1.04 - 0.04(0.2427/0.06244) = 0.88452$$

$$\eta_{vol,HP} = 1.0 + \varepsilon - \varepsilon\,(v_4/v_5) = 1.04 - 0.04(0.06/0.01913) = 0.91454$$

$$(\mathbb{V}_S)_{LP} = \dot{m}_{LP}\,v_1/\eta_{vol,LP} = 0.2717 \times 0.02427/0.8844 = 0.07455 \text{ m}^3\text{/s}$$

$$(\mathbb{V}_S)_{HP} = \dot{m}_{HP}\,v_3/\eta_{vol,HP} = 0.361937 \times 0.06/0.91454 = 0.023745 \text{ m}^3\text{/s}$$

$$(\mathbb{V}_S)_{LP}/(\mathbb{V}_S)_{HP} = 3.14$$

Verification of state 9

It was pointed out that refrigerant at state 9 may be a two-phase mixture, since it has to intercool the LP vapour. The adiabatic mixing of stream 9 and stream 2 results in stream 3. Energy balance for this process yields

$$\dot{m}'\,h_9 + \dot{m}_{LP}\,h_2 = \dot{m}_{HP}\,h_3 \quad \therefore \quad h_9 = (\dot{m}_{HP}\,h_3 - \dot{m}_{LP}\,h_2)/\dot{m}'$$

or $h_9 = (0.361937 \times 191.02 - 0.2717 \times 195.65470)/0.09021 = 177.1181$ kJ/kg

This is less than the enthalpy of saturated vapour at -2°C, which is 187.81. Therefore, state 9 is a mixture state and quality at state 9,

$$x_9 = (177.1181 - 34.3)/(187.81 - 34.3) = 0.93035$$

SSS cycle: This cycle is shown by 1–2′–*a*–5–10–1 in Figure 6.5(c)

$$\dot{m} = 3.51667 \times 10/(170.23 - 74.77) = 0.3684 \text{ kg/s}$$

$$W = \dot{m}(h_{2'} - h_1) = 0.3684(218.41 - 170.23) = 17.7499 \text{ kW}$$

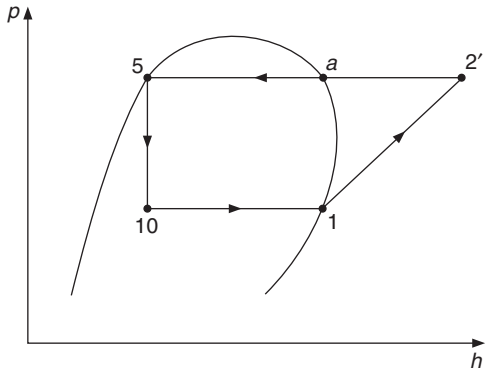

Figure 6.5(c) SSS cycle of the system shown in Figure 6.5(a).

$$Q_c = (h_{2'} - h_5) = 0.3684(218.41 - 74.77) = 52.9156 \text{ kW}$$

$$\text{COP} = 35.1667/W = 35.16661/17.7499 = 1.9813$$

$$\eta_{\text{vol}} = 1.0 + \varepsilon - \varepsilon\,(v_1/v_{2'}) = 1.04 - 0.04(0.2427/0.02057) = 0.558$$

$$\mathbb{V}_S = \dot{m} v_1/\eta_{\text{vol,}} = (0.3684) \times 0.2427/0.558 = 0.1574 \text{ m}^3/\text{s}$$

It is observed that the work requirement of the single stage saturation cycle is very high compared to that for the two-stage cycle, hence as a result the COP is very low. The volumetric efficiency of SSS cycle is very low, as a result the swept volume rate is 1.6 times the combined swept volume rate of the two compressors.

EXAMPLE 6.6(b) Suppose in Example 6.6(a) the superheat table is not provided, instead the average specific heats at intermediate pressure and condenser pressure are given to be c_{pi}= 0.6427 kJ/kg-K and c_{pc} = 0.77 kJ/kg-K respectively. All other conditions being the same as in Example 6.6(a), determine all the parameters of Example 6.6(a).

Solution:

$$c_{pi} = 0.6427 \text{ kJ/kg-K} \quad \text{and} \quad c_{pc} = 0.77 \text{ kJ/kg-K}$$

State 2:

This is determined by using $T\,ds = dh = c_p\,dt$ along the constant pressure line 9–2 and $s_2 = s_1$ = 0.7301

$$T_2 = T_i \exp\left(\frac{s_2 - s_9}{c_{pi}}\right) = T_i \exp\left(\frac{s_1 - s_9}{c_{pi}}\right) = 271 \exp\left(\frac{0.7301 - 0.7018}{0.6427}\right) = 283.2 \text{ K}$$

$$t_2 = 283.2 - 273 = 10.2°\text{C}, \; h_2 = h_9 + c_{pi}\,(t_2 - t_i) = 187.81 + 0.6427(10.2 - (-2)) = 195.65°\text{C}$$

and $$v_2 = v_9\, T_2/T_i = 0.0593\ (283.2)/271 = 0.06179$$

Similarly, along the constant pressure line a–4 using $T\,ds = dh = c_p\,dt$ and $s_4 = s_3 = 0.7135$

$$T_4 = T_c \exp\left(\frac{s_4 - s_a}{c_{pc}}\right) = 313 \exp\left(\frac{0.7135 - 0.6876}{0.77}\right) = 323.71 \text{ K} = 50.71°\text{C}$$

$$h_4 = h_a + c_{pc}\,(t_4 - t_c) = 204.75 + 0.77(50.71 - 40) = 212.997$$

and $$v_4 = v_a T_4/T_a = 0.0183(323.71)/313 = 0.0189$$

Two-stage system:

The mass flow rate $\dot{m}_{\text{LP}}$ remains same as in Example 6.6(a) since h_1 and h_7 are the same. The mass flow rate $\dot{m}'$ will change slightly since h_2 has changed slightly.

$$\dot{m}_{\text{LP}} = 0.2717 \text{ kg/s}$$

$$\dot{m}' = \dot{m}_{\text{LP}} \frac{(h_2 - h_3) + (h_5 - h_7)}{(h_3 - h_5)} = 0.2717 \frac{(195.65 - 191.02) + (74.77 - 40.81)}{191.02 - 74.77}$$

$$= 0.09019$$

$$\dot{m}_{HP} = 0.2717 + 0.09019 = 0.36189 \text{ kg/s}$$

$$W_{LP} = \dot{m}_{LP}(h_2 - h_1) = 0.2717(195.65 - 170.23) = 6.9066 \text{ kW}$$

$$W_{HP} = \dot{m}_{HP}(h_4 - h_3) = 0.36189(212.997 - 191.02) = 7.953 \text{ kW}$$

$$W_{net} = W_{LP} + W_{HP} = 14.8596 \text{ kW}$$

$$Q_c = \dot{m}_{HP}(h_4 - h_5) = 0.36189(212.997 - 74.77) = 50.02 \text{ kW}$$

Heat rejection ratio $= Q_c/Q_e = 1.4226$

$$\text{COP} = Q_e/W_{net} = 35.1667/14.8596 = 2.3666$$

$$\eta_{vol,LP} = 1.0 + \varepsilon - \varepsilon(v_1/v_2) = 1.04 - 0.04(0.2427/0.06197) = 0.8833$$

$$\eta_{vol,HP} = 1.0 + \varepsilon - \varepsilon(v_4/v_5) = 1.04 - 0.04(0.06/0.0189) = 0.913$$

$$(\mathbb{V}_S)_{LP} = \dot{m}_{LP} v_1/\eta_{vol,LP} = 0.2717 \times 0.02427/0.8833 = 0.0746 \text{ m}^3/\text{s}$$

$$(\mathbb{V}_S)_{HP} = \dot{m}_{HP} v_4/\eta_{vol,HP} = 0.36189 \times 0.06/0.913 = 0.02378 \text{ m}^3/\text{s}$$

$$(\mathbb{V}_S)_{LP}/(\mathbb{V}_S)_{HP} = 3.137$$

SSS cycle:

For this case, $c_{pc} = 2.701$

This cycle is shown by 1–2′–*a*–5–10–1 in Figure 6.5(c). The mass flow rate remains unchanged since h_1 and h_5 are the same.

$$\dot{m} = 3.51667 \times 10/(170.23 - 74.77) = 0.3684 \text{ kg/s}$$

Temperature $t_{2'}$ is determined by using $T\,ds = dh = c_p\,dt$ along *a*–2′

$$T_{2'} = T_c \exp\left(\frac{s_1 - s_a}{c_{pc}}\right) = 313 \exp\left(\frac{0.7301 - 0.6876}{0.77}\right) = 330.76 \text{ K} = 57.76°\text{C}$$

$$h_{2'} = h_a + c_{pc}(t_{2'} - t_c) = 204.75 + 0.77(57.76 - 40) = 218.425$$

$$v_{2'} = v_a T_{2'}/T_a = 0.0183\ (330.76)/313 = 0.0193$$

$$W = \dot{m}(h_2' - h_1) = 0.3684(218.425 - 170.23) = 17.755\text{kW}$$

$$Q_c = \dot{m}(h_{2'} - h_5) = 0.3684(218.425 - 74.77) = 52.92 \text{ kW}$$

$$\text{COP} = 35.1667/W = 35.1667/17.755 = 1.9813$$

$$\eta_{vol,} = 1.0 + \varepsilon - \varepsilon(v_1/v_{2'}) = 1.04 - 0.04(0.2427/0.0193) = 0.537$$

$$\mathbb{V}_S = \dot{m} v_1/\eta_{vol,} = (0.3684) \times 0.2427/0.537 = 0.1665 \text{ m}^3/\text{s}$$

The results are similar to those obtained in Example 6.6(a) by using the superheat. The accuracy of the results depends upon the accuracy to which the specific heats are specified. In fact in this problem the specific heats were obtained from Example 6.6(a) by using the calculated value of h_2 and t_2, etc.

EXAMPLE 6.7 The condenser and evaporator temperatures are 40°C and −40°C respectively for a two-stage R12 refrigeration system of 10 TR cooling capacity. Subcooling and intercooling are done in a flooded type shell-and-tube HEX just like that in NH_3 system of Figure 6.4(a) except that the water intercooler is not used. It subcools the liquid refrigerant from 40°C to a temperature

of 5°C. The refrigerant vapour leaves the HEX in saturated state at –2°C. Find the mass flow rates and the swept volume rates and the work requirement of both the compressors, condenser heat rejection and COP. Compare the results with those in Example 6.6(a). The clearance volume ratio for both the compressors is 0.04.

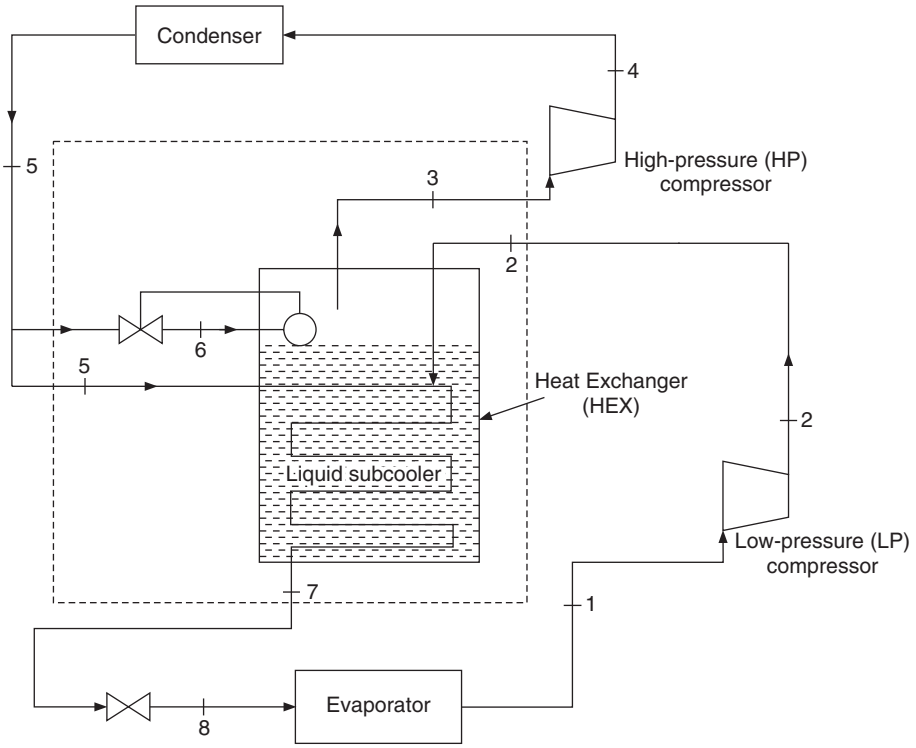

Figure 6.6(a) Schematic diagram of a R12/R22 two-stage compression system with liquid subcooler

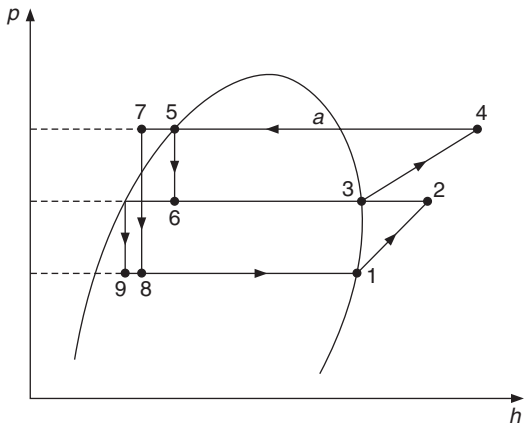

Figure 6.6(b) *p–h* cycle diagram of system of Figure 6.6(a).

Solution:

The schematic diagram and *p–h* cycle diagram of this system are shown in Figures 6.6(a) and (b) respectively. The mass flow rate, the work requirement, the volumetric efficiency and the swept flow rate for the LP compressor of this system are the same as those for Example 6.6(a), that is

$$\dot{m}_{LP} = 0.2717 \text{ kg/s and } W_{LP} = 6.9085 \text{ kW}, \ \eta_{vol,LP} = 0.8833 \text{ and } (\mathbb{V}_s)_{LP} = 0.07455$$

The state 3 is saturated vapour state at intermediate pressure 2.891 bar, therefore

$$s_3 = 0.7018, \ h_3 = 187.81 \text{ and } v_3 = 0.0593$$

Interpolating in the superheat table for 9.634 bar (40°C) between 5°C and 10°C superheat for $s_3 = s_4 = 0.7018$, we get

$$\Delta t = 5(0.7018 - 0.70)/(0.7120 - 0.70) = 5 \times 0.15 = 0.75^{\circ}\text{C}$$

$$t_4 = 40 + 5 + 0.75 = 45.75^{\circ}\text{C}, \ h_4 = 209.227 \text{ and } v_4 = 0.019$$

Considering the control volume around HEX as shown in Figure 6.6(a), we get

$$\dot{m}' = \dot{m}_{LP} \frac{(h_2 - h_3) + (h_5 - h_7)}{(h_3 - h_5)} = 0.2717 \frac{(195.6547 - 187.81) + (74.77 - 40.81)}{187.81 - 74.77}$$

$$= 0.1005$$

$$\dot{m}_{HP} = \dot{m}_{LP} + \dot{m}' = 0.2717 + 0.1005 = 0.3722$$

$$W_{HP} = \dot{m}_{HP} (h_4 - h_3) = 0.3722 \ (209.227 - 187.81) = 7.97192 \text{ kW}$$

$$W_{net} = W_{LP} + W_{HP} = 6.9085 + 7.97192 = 14.8804 \text{ kW}$$

$$\text{COP} = 31.667/14.8804 = 2.3633$$

$$Q_c = \dot{m}_{HP} (h_4 - h_5) = 0.3722(209.227 - 74.77) = 50.047 \text{ kW}$$

$$\eta_{vol,HP} = 1.0 + \varepsilon - \varepsilon (v_3/v_4) = 1.04 - 0.04(0.0593/0.019) \quad = 0.91516$$

$$(\mathbb{V}_S)_{HP} = \dot{m}_{HP} \, v_3 / \eta_{vol,HP} = 0.3722 \times 0.0593/0.91516 = 0.0241 \text{ m}^3/\text{s}$$

$$(\mathbb{V}_S)_{LP}/(\mathbb{V}_S)_{HP} = 3.093$$

It is observed that if the LP vapour of R12 is intercooled to the saturated state, the work requirement increases and the COP decreases compared to the case when the vapour is not intercooled to saturated state as in Example 6.5. The swept volume rate of the HP compressor also increases since some additional refrigerant is required for intercooling to the saturated state. Hence, the system of Figure 6.5 is the recommended two-stage system for R12.

EXAMPLE 6.8(a) If R22 is used in the system of Figure 6.5, find all the parameters of Example 6.6(a) for evaporator and condenser temperatures are –40°C and 40°C respectively. The subcooling of liquid refrigerant is done from 40°C to 5°C and the superheating at inlet to HP compressor is 5°C

Solution:

The evaporator and condenser pressures are:

$$p_e = 1.053 \quad \text{and} \quad p_c = 15.267 \text{ bar},$$

Ideal intermediate pressure $p_i^* = \sqrt{p_c p_e} = 4.005$ bar

Corresponding saturation temperature $t_i^* = -6^oC$ (by interpolating in R22 table)

Therefore intermediate temperature $t_i = -6^oC + 5^oC = -1^oC \approx -2^oC$ for convenience since saturation and superheated properties are available for it.

The required thermodynamic properties of R22 at saturation are as follows:

Temperature (°C)	*Pressure* (bar)	v_g (m^3/kg)	h_f (kJ/kg)	h_g (kJ/kg)	s_f (kJ/kg-K)	s_g (kJ/kg-K)
–40	1.053	0.206	0.0	234.17	0.0	1.0044
–2	4.664	0.0503	43.79	250.4	0.1728	0.9348
40	15.267	0.0152	95.4	261.38	0.3446	0.8767

At 5°C, $h_f = 40.81$kJ/kg

The properties of superheated vapour at 4.664 bar (–2°C)are as follows:

Degree of superheat	5°C	20°C	30°C
v	0.0516	0.0554	0.0578
h	253.97	264.65	271.75
s	0.9479	0.98507	1.00791

The properties of superheated vapour at 15.267 bar (40°C) are as follows:

Degree of superheat	20°C	30°C	40°C	50°C
v	0.0172	0.0182	0.0191	0.0199
h	279.61	288.31	296.84	305.26
s	0.9332	0.9592	0.9832	1.007

Referring to Figure 6.5 the properties at various state points are:

$$h_1 = 234.17,\ v_1 = 0.206 \text{ and } s_1 = 1.0044$$

It is assumed that at the exit of the heat exchanger the vapour is saturated at intermediate temperature, i.e.

$$h_9 = 250.4,\ v_9 = 0.0503 \text{ and } s_9 = 0.9348$$

State 3 is located at intermediate pressure 4.664 bar and 5°C superheat.

$$h_3 = 253.97,\ v_3 = 0.0516 \text{ and } s_3 = 0.9479$$

$$h_a = 261.38,\ v_a = 0.0152 \text{ and } s_a = 0.8767,\ h_5 = 95.4,\ h_7 = 52.23 (\ h_f \text{ at } 5^oC)$$

By interpolating in the superheat table for intermediate pressure of 4.664 bar (–2°C) between 20°C and 30°C superheat for $s_1 = s_2 = 1.0044$, we get

$$\Delta t = 10\ (1.0044 - 0.98507)/(1.00791 - 0.98507) = 0.8463 \times 10 = 8.463^oC$$

$$\therefore \quad t_2 = -2 + 20 + 8.463 = 26.463^oC$$

$$h_2 = 264.65 + (271.75 - 264.65) \times 0.8463 = 270.659 \text{ and } v_2 = 0.05743$$

Similarly, by interpolating in the superheat table for condenser pressure of 15.267 bar (40°C) between superheat of 20°C and 30°C for $s_3 = s_4 = 0.9479$

$$\Delta t = 10\ (0.9479 - 0.9332)/(0.9592 - 0.9332) = 0.56538 \times 10 = 5.654^{\circ}\text{C}$$

$$\therefore \quad t_4 = 40 + 20 + 5.654 = 65.654^{\circ}\text{C}$$

$$h_4 = 279.61 + (288.31 - 279.61) \times 0.56538 = 284.5288 \text{ and } v_4 = 0.017765$$

Two-stage system:

$$\dot{m}_{LP} = \frac{3.51667 \text{ TR}}{h_1 - h_7} = \frac{3.51667 \times 10}{234.17 - 52.23} = 0.19327 \text{ kg/s}$$

$$\dot{m}' = \dot{m}_{LP} \frac{(h_2 - h_3) + (h_5 - h_7)}{(h_3 - h_5)} = 0.19327 \frac{(270.659 - 253.97) + (95.4 - 52.23)}{253.97 - 95.4}$$

$$= 0.072964$$

$$\dot{m}_{HP} = \dot{m}_{LP} + \dot{m}' = 0.19327 + 0.072964 = 0.266234 \text{ kg/s}$$

$$W_{LP} = \dot{m}_{LP}\ (h_2 - h_1) = 0.19327(270.659 - 234.17) = 7.0522 \text{ kW}$$

$$W_{HP} = \dot{m}_{HP}\ (h_4 - h_3) = 0.266234(284.5288 - 253.97) = 8.13579 \text{ kW}$$

$$W_{net} = W_{LP} + W_{HP} = 15.188 \text{ kW}$$

$$Q_c = \dot{m}_{HP}\ (h_4 - h_5) = 0.266234(284.5288 - 95.4) = 50.352 \text{ kW}$$

Heat rejection ratio = $Q_c/Q_e = 1.4318$

$$\text{COP} = Q_e/W_{net} = 35.1667/15.188 = 2.315$$

$$\eta_{vol,LP} = 1.0 + \varepsilon - \varepsilon\ (v_1/v_2) = 1.04 - 0.04(0.206/0.057433) = 0.8965$$

$$\eta_{vol,HP} = 1.0 + \varepsilon - \varepsilon\ (v_3/v_4) = 1.04 - 0.04(0.0516/0.017765) = 0.9238$$

$$(\mathbb{V}_S)_{LP} = \dot{m}_{LP}\ v_1/\eta_{vol,LP} = 0.\ 19327 \times 0.0206/0.8925 = 0.04441 \text{ m}^3\text{/s}$$

$$(\mathbb{V}_S)_{HP} = \dot{m}_{HP}\ v_4/\eta_{vol,HP} = 0.\ 266234 \times 0.0516/0.9238 = 0.01487 \text{ m}^3\text{/s}$$

$$(\mathbb{V}_S)_{LP}/(\mathbb{V}_S)_{HP} = 2.986$$

Verification of state 9:

It was pointed out that refrigerant at state 9 may be a two-phase mixture, since it has to intercool the LP vapour. The adiabatic mixing of stream 9 and stream 2 results in stream 3. Energy balance for this process yields

$$\dot{m}'\ h_9 + \dot{m}_{LP}\ h_2 = \dot{m}_{HP}\ h_3$$

$$\therefore \quad h_9 = (\dot{m}_{HP}\ h_3 - \dot{m}_{LP}\ h_2)/\dot{m}'$$

$$= (0.266234 \times 253.97 - 0.19327 \times 270.659)/0.0674 = 209.765 \text{ kJ/kg}$$

This is less than the enthalpy of saturated vapour at –2°C, which is 250.4. Therefore, state 9 is a mixture state and quality at state 9 is

$$x_9 = (209.765 - 43.79)/(250.4 - 43.79) = 0.803$$

SSS cycle: This cycle is shown by 1–2′–*a*–5–10–1 in Figure 6.5(c).

For SSS cycle, interpolating in the superheat table for 15.267 bar (40°C) for $s_1 = s_{2'} = 1.0044$ between 40°C and 50°C superheat, we get

$$\Delta t = 10(1.0044 - 0.9832)/(1.007 - 0.9832) = 10 \times 0.8908 = 8.908^{\circ}\text{C}$$

$$t_{2'} = 40 + 40 + 8.908 = 88.908^{\circ}\text{C}$$

$$h_{2'} = 296.84 + (305.26 - 296.84) \times 0.8908 = 304.3402 \text{ and } v_{2'} = 0.0198126$$

$$\dot{m} = \frac{3.51667 \text{ TR}}{h_1 - h_{10}} = \frac{3.51667 \times 10}{234.17 - 95.4} = 0.2534 \text{ kg/s}$$

$$W = \dot{m}(h_{2'} - h_1) = 0.2534(304.3402 - 234.17) = 17.7823 \text{ kW}$$

$$Q_c = \dot{m}(h_{2'} - h_5) = 0.2534(304.3402 - 95.4) = 52.949 \text{ kW}$$

$$\text{COP} = 35.1667/W = 35.1667/17.7823 = 1.9776$$

$$\eta_{\text{vol}} = 1.0 + \varepsilon - \varepsilon\,(v_1/v_{2'}) = 1.04 - 0.04(0.206/0.0198126) = 0.6241$$

$$\mathbb{V}_S = \dot{m} v_1/\eta_{\text{vol}} = 0.2534 \times 0.206/0.5241 = 0.08365 \text{ m}^3/\text{s}$$

EXAMPLE 6.8(b) Suppose in Example 6.8(a) the superheat table is not provided, instead of it the average specific heats at intermediate pressure and condenser pressure are given to be $c_{pi} = 0.712$ kJ/kg-K and $c_{pc} = 0.8977$ kJ/kg-K respectively. All other conditions being the same as in Example 6.8(a), determine all the parameters of Example 6.8(a).

Solution:

$$c_{pi} = 0.712 \text{ kJ/kg-K and } c_{pc} = 0.7897 \text{ kJ/kg-K}$$

State 2:

This is determined by using $T\,ds = dh = c_p\,dt$ along the constant pressure line 9–2 and $s_1 = s_2 = 1.0044$

$$T_2 = T_i \exp\left(\frac{s_2 - s_9}{c_{pi}}\right) = T_4 \exp\left(\frac{s_1 - s_9}{c_{pi}}\right) = 271 \exp\left(\frac{1.0044 - 0.9348}{0.712}\right) = 298.829 \text{ K}$$

$$t_2 = 298.829 - 273 = 25.829^{\circ}\text{C}$$

$$h_2 = h_9 + c_{pi}\,(t_2 - t_i) = 250.4 + 0.712(25.829 - (-2)) = 270.213$$

and $$v_2 = v_9\, T_2/T_i = 0.0503(298.84)/271 = 0.05546$$

Similarly, along the constant pressure line a–4 using $T\,ds = dh = c_p\,dt$ and $s_4 = s_3 = 0.9479$

$$T_4 = T_c \exp\left(\frac{s_4 - s_a}{c_{pc}}\right) = 313 \exp\left(\frac{0.9479 - 0.8767}{0.8977}\right) = 338.837 \text{ K} = 65.837^{\circ}\text{C}$$

$$h_4 = h_a + c_{pc}\,(t_4 - t_c) = 261.38 + 0.8977\,(65.837 - 40) = 284.57$$

and $$v_4 = v_a\, T_4/T_a = 0.0152(338.837)/313 = 0.01645$$

For SSS cycle, temperature $t_{2'}$ is determined by using $T\,ds = dh = c_p\,dt$ along a–$2'$

$$T_{2'} = T_c \exp\left(\frac{s_1 - s_a}{c_{pc}}\right) = 313 \exp\left(\frac{1.0044 - 0.8767}{0.8977}\right) = 360.847.76 \text{ K} = 87.847^{\circ}\text{C}$$

$$h_{2'} = h_a + c_{pc}\,(t_{2'} - t_c) = 261.38 + 0.8977\,(87.847 - 40) = 304.332$$

$$v_{2'} = v_a\,T_{2'}/T_a = 0.0152\,(360.847)/313 = 0.01751$$

Two-stage system:

The mass flow rate $\dot{m}_{LP}$ remains same as in Example 6.8(a) since h_1 and h_7 are the same. The mass flow rate $\dot{m}'$ will change slightly since h_2 has changed slightly.

$$\dot{m}_{LP} = 0.19327 \text{ kg/s}$$

$$\dot{m}' = \dot{m}_{LP}\,\frac{(h_2 - h_3) + (h_5 - h_7)}{(h_3 - h_5)} = 0.19327\,\frac{(270.213 - 253.97) + (95.4 - 52.23)}{253.97 - 95.4}$$

$$= 0.07242$$

$$\dot{m}_{HP} = \dot{m}_{LP} + \dot{m}' = 0.19327 + 0.07242 = 0.265708 \text{ kg/s}$$

$$W_{LP} = \dot{m}_{LP}\,(h_2 - h_1) = 0.19327(270.213 - 234.17) = 6.966 \text{ kW}$$

$$W_{HP} = \dot{m}_{HP}\,(h_4 - h_3) = 0.265708(284.57 - 253.97) = 8.1307 \text{ kW}$$

$$W_{net} = W_{LP} + W_{HP} = 15.097 \text{ kW}$$

$$Q_c = \dot{m}_{HP}\,(h_4 - h_5) = 0.265708(284.57 - 95.4) = 50.264 \text{ kW}$$

Heat rejection ratio = $Q_c/Q_e = 1.429$

$$\text{COP} = Q_e/W_{net} = 35.1667/15.097 = 2.329$$

$$\eta_{vol,LP} = 1.0 + \varepsilon - \varepsilon\,(v_1/v_2) = 1.04 - 0.04(0.206/0.05546) = 0.8914$$

$$\eta_{vol,HP} = 1.0 + \varepsilon - \varepsilon\,(v_3/v_4) = 1.04 - 0.04(0.0516/0.01645) = 0.9145$$

$$(\mathbb{V}_S)_{LP} = \dot{m}_{LP}\,v_1/\eta_{vol,LP} = 0.\ 19327 \times 0.0206/0.8914 = 0.04466 \text{ m}^3/\text{s}$$

$$(\mathbb{V}_S)_{HP} = \dot{m}_{HP}\,v_3/\eta_{vol,HP} = 0.26569 \times 0.0516/0.9145 = 0.015 \text{ m}^3/\text{s}$$

$$(\mathbb{V}_S)_{LP}/(\mathbb{V}_S)_{HP} = 2.977$$

$$\dot{m} = \frac{3.51667 \text{ TR}}{h_1 - h_{10}} = \frac{3.51667 \times 10}{234.17 - 95.4} = 0.2534 \text{ kg/s}$$

$$W = \dot{m}(h_{2'} - h_1) = 0.2534(304.332 - 234.17) = 17.779 \text{ kW}$$

$$Q_c = (h_{2'} - h_5) = 0.2534\,(304.332 - 95.4) = 52.943 \text{ kW}$$

$$\text{COP} = 35.1667/W = 35.1667/17.779 = 1.978$$

$$\eta_{vol} = 1.0 + \varepsilon - \varepsilon\,(v_1/v_{2'}) = 1.04 - 0.04(0.206/0.01751) = 0.5694$$

$$\mathbb{V}_s = \dot{m}v_1/\eta_{vol,} = 0.2534 \times 0.206/0.5694 = 0.09167 \text{ m}^3/\text{s}$$

EXAMPLE 6.9 A flooded-type HEX is used and the R22 LP vapour is intercooled up to saturated state by direct contact with liquid refrigerant at intermediate pressure; the liquid refrigerant at condenser pressure is subcooled in the HEX from 40°C to 5°C. Repeat Example 6.7 for R22.

Solution:

The schematic diagram and *p–h* cycle diagram of this system are shown in Figure 6.6(a) and (b) respectively.

The mass flow rate and the work requirement for the LP compressor of this system are the same as those for Example 6.8(a), that is, $\dot{m}_{LP} = 0.19327$ and $W_{LP} = 7.0522$ kW. The state 3 is saturated vapour state at intermediate pressure 4.664 bar, therefore,

$$s_3 = 0.9348,\ h_3 = 250.4 \text{ and } v_3 = 0.0503$$

Interpolating in the superheat table for 15.267 bar (40°C) between 20°C and 30°C superheat for $s_3 = s_4 = 0.9348$, we get

$$\Delta t = 10\ (0.9348 - 0.9334)/(0.9592 - 0.9332) = 0.0615 \times 10 = 0.615^{o}\text{C}$$

$$t_4 = 40 + 20 + 0.615 = 60.615^{o}\text{C},\ h_4 = 280.14538 \text{ and } v_4 = 0.0172615$$

Considering the control volume around the HEX as shown in Figure 6.6(a), we get

$$\dot{m}' = \dot{m}_{LP}\frac{(h_2 - h_3) + (h_5 - h_7)}{(h_3 - h_5)} = 0.193287\frac{(266.1096 - 250.4) + (95.4 - 52.23)}{250.4 - 95.4}$$

$$= 0.07342$$

$$\dot{m}_{HP} = \dot{m}_{LP} + \dot{m}' = 0.19327 + 0.07342 = 0.26669 \text{ kg/s}$$

$$W_{HP} = 0.26669(280.1454 - 250.4) = 7.9328 \text{ kW}$$

$$W_{net} = 7.0522 + 7.9328 = 14.985 \text{ kW}$$

$$\text{COP} = 31.667/14.1069 = 2.347$$

$$Q_c = 0.26669\ (280.1454 - 95.4) = 49.27\text{kW}$$

$$\eta_{vol,HP} = 1.0 + \varepsilon - \varepsilon\ (v_3/v_4) = 1.04 - 0.04(0.0503/0.0172615) = 0.92344$$

$$(\mathbb{V}_S)_{HP} = \dot{m}_{HP}\ v_3/\eta_{vol,HP} = 0.26671 \times 0.0503/0.92344 = 0.014528 \text{ m}^3/\text{s}$$

$$(\mathbb{V}_S)_{LP}/(\mathbb{V}_S)_{HP} = 3.093$$

6.4 MULTI-EVAPORATOR SYSTEMS

In many applications two or even three temperatures have to be maintained in a building. In departmental stores, –30°C to –20°C may be required for frozen storage and –5°C to 0°C for brewages and air-conditioning. A single evaporator operating at –30°C, will freeze the beverages and milk thereby spoiling its quality. If the air is cooled by an evaporator at –30°C the water vapour from the air will freeze on evaporator coils and block its passage. It will also dehumidify the air so much that other products will be dehydrated. Many industries also require very low temperature for process cooling and a temperature of 0–5°C for air-conditioning.

Hence, it is advised that two evaporators operating at two different temperatures with a single compressor be used for these applications. Two independent refrigeration systems can always be used, however, it will be more economical to use one compressor to reduce operation and maintenance cost and to reduce the inventory of spare parts. If the temperature of evaporator is less than –30°C, then two-stage compression is recommended.

6.4.1 One Compressor and Two Evaporators

The schematic diagram and *p–h* cycle of a two-evaporator, single-compressor system, with a pressure reducing valve (PRV), are shown in Figures 6.7(a) and (b) respectively. The evaporator

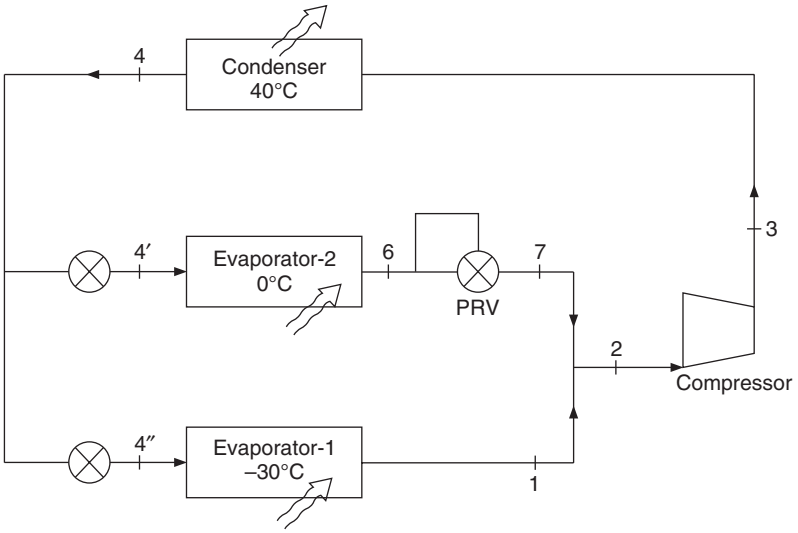

Figure 6.7(a) Two-evaporator system with a single compressor, individual expansion valves and a pressure reducing valve (PRV).

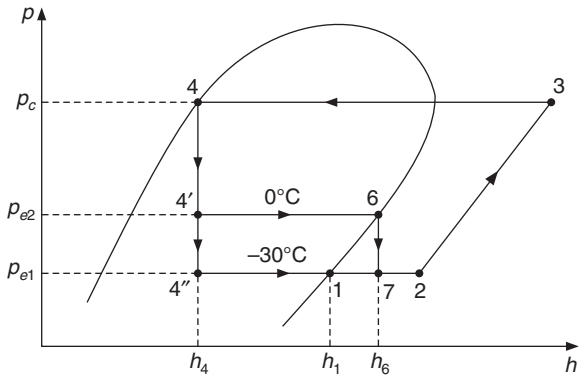

Figure 6.7(b) *p–h* diagram for the system shown in Figure 6.7(a).

pressure p_{e2} in the high temperature evaporator-2 will be higher than the evaporator pressure p_{e1} in the low temperature evaporator-1. The suction pressure of the compressor is equal to the evaporator pressure of low temperature evaporator. Hence, a pressure reduction valve (PRV) is installed after the high temperature evaporator to reduce its pressure from p_{e2} to p_{e1}. Then the vapours from the two evaporators are adiabatically mixed and compressed. This is an efficient system since the vapour from the high temperature evaporator is also compressed through the pressure ratio of low temperature evaporator involving a large amount of work.

A typical application is evaporator-1 at –30°C for frozen storage, and evaporator-2 at –5 to 0°C for air-conditioning and or for storage of beverages and milk.

EXAMPLE 6.10 An ammonia refrigeration system has two evaporators both of 5 TR capacity. Evaporator-1 is kept at –30°C and Evaporator-2 is kept at 0°C. The vapour from Evaporator-2 is throttled to the pressure of Evaporator-1. The two vapours are adiabatically mixed and compressed

in a compressor. The condenser temperature is 40°C. Determine the enthalpies, temperatures and entropies after throttling and adiabatic mixing. Find the mass flow rate, volumetric efficiency, swept volume rate and work requirement of compressor, condenser heat rejection and COP.

Solution:

The properties of NH_3 at the required states are as follows:

Temperature (°C)	*Pressure* (bar)	v_g (m^3/kg)	h_f (kJ/kg)	h_g (kJ/kg)	s_f (kJ/kg-K)	s_g (kJ/kg-K)
–30	1.195	0.963	44.47	1403.11	0.18720	5.776
0	4.294	0.29	180.88	1443.34	0.7139	5.3368
40	15.55	0.083	371.47	1472.02	1.3579	4.8728

The properties of superheated vapour at 1.195 bar (–30°C) are as follows:

Degree of superheat	5°C	10°C	15°C	20°C
v	0.985	1.008	1.03	1.052
h	1414.6	1426.0	1437.3	1448.5
s	5.8229	5.8684	5.9126	5.9556

The properties of superheated vapour at 15.55 bar (40°C) are as follows:

Degree of superheat	50°C	60°C	80°C	100°C	120°C	140°C	160°C
v	0.105	0.108	0.116	0.123	0.130	0.137	0.142
h	1621.0	1647.9	1700.3	1751.7	1802.6	1853.4	1904.2
s	5.3153	5.3883	5.5253	5.65283	5.7732	5.8878	5.99802

The enthalpy remains constant during the throttling process 6–7, that is, $h_6 = h_7$.

Referring to Figure 6.7 the properties at various state points are as follows:

$$h_1 = 1403.11,\ h_6 = h_7 = 1443.34 \text{ and } h_4 = 371.47$$

$$\dot{m}_1 = \frac{3.51667 \times 5}{h_1 - h_4} = \frac{17.58335}{1403.11 - 371.47} = 0.017044 \text{ kg/s}$$

$$\dot{m}_2 = \frac{3.51667 \times 5}{h_6 - h_4} = \frac{17.58335}{1443.34 - 371.47} = 0.016404 \text{ kg/s}$$

and $$\dot{m}_1 + \dot{m}_2 = 0.033448 \text{ kg/s}$$

Considering adiabatic mixing of streams 1 and 7:

$$\dot{m}_1 h_1 + \dot{m}_2 h_7 = (\dot{m}_1 + \dot{m}_2) h_2$$

$$\therefore \quad h_2 = [(0.017044 \times 1403.11 + 0.016404 \times 1443.34)]/0.033448 = 1422.84 \text{ kJ/kg}$$

The entropy and specific volume at state 2 can be found either by interpolation in the superheat table for pressure 1.195 bar (–30°C) or by using the average specific heat and perfect gas relation.

First method: Interpolation in superheat table

Interpolating in the superheat table between superheat of 5°C and 10°C for $h_2 = 1422.84$

$$\Delta t = (1422.84 - 1414.6) \times 5/(1426.0 - 1414.6) = 0.7228 \times 5 = 3.6142^\circ C$$

$$\therefore \quad t_2 = -30 + 5 + 3.6142 = -21.3858^\circ C$$

$$\therefore \quad s_2 = 5.8229 + 0.7228 \times (5.8684 - 5.8229) = 5.85579. \text{ Similarly, } v_2 = 1.001625$$

Second method: Use average specific heat

Average specific heat is determined from the enthalpy values given in the superheat table between saturated state and 10°C . This is as follows:

$$c_p = (1426.0 - 1403.110)/10 = 2.289 \text{ kJ/kg-K}$$

Hence, for $h_2 = 1422.84$,

$$\Delta t \text{ from saturated state} = (h_2 - h_1)/c_p = (1422.84 - 1403.11)/2.289 = 8.6196^\circ C$$

$$\therefore \quad t_2 = -30 + 8.6196 = -21.3804^\circ C$$

$$\therefore \quad T_2 = -21.3804 + 273.16 = 251.7796 \text{ K and } T_1 = -30 + 273.16 = 243.16 \text{ K}$$

$$\therefore \quad s_2 = s_1 + c_p \ln (T_2/T_1) = 5.776 + 2.289 \ln (251.7796/243.16) = 5.85574$$

which is same as found by interpolation.

Third method: Consider throttling to find state 7 and then find s_2

Consider $h_7 = h_6 = 1443.34$ and interpolate to find temperature t_7 from the superheat table between superheat of 15°C and 20°C. Thus, we get

$$\Delta t = 5\ (1443.34 - 1437.3)/(1448.5 - 1437.3) = 0.5389 \times 5 = 2.6964$$

$$t_7 = -30 + 15 + 2.6964 = -12.30357^\circ C \text{ and } s_7 = 5.93579$$

Considering mixing of two streams at constant pressure, we get

$$s_2 = (\dot{m}_1 s_1 + \dot{m}_2 s_7)/(\dot{m}_1 + \dot{m}_2) = 5.85437$$

This is obviously less than the values of last two methods since the entropy of mixing (which is an irreversible process) has to be added to it.

State 3 after compression:

This is obtained by interpolating in the superheat table for 15.55 bar (40°C) between 120°C and 140°C superheat for $s_2 = s_3 = 5.85579$.

$$\Delta t = 20(5.85579 - 5.7732)/(5.8878\text{-}5.7732) = 0.7207 \times 20 = 14.4136$$

$$\therefore \quad t_3 = 40 + 120 + 14.4136 = 174.4136^\circ C$$

$$h_3 = 1802.6 + 0.7207(1853.4 - 1802.6) = 1839.2106. \text{ Similarly, } v_3 = 0.135045$$

$$W = (\dot{m}_1 + \dot{m}_2)(h_3 - h_2) = 13.927 \text{ kW}$$

$$Q_c = (\dot{m}_1 + \dot{m}_2)(h_3 - h_4) = 49.0936 \text{ kW}$$

$$\text{COP} = Q_e/W = 10 \times 3.51667/13.927 = 2.5251$$

$$\eta_{\text{vol}} = 1 + \varepsilon - \varepsilon(v_2/v_3) = 1.04 - 0.04\ (1.001625/0.135045) = 0.74332$$

$$\mathbb{V}_S = (\dot{m}_1 + \dot{m}_2)v_2/\eta_{\text{vol}} = 0.0334484 \times 1.001625/0.74332 = 0.04507\ \text{m}^3/\text{s}$$

EXAMPLE 6.11 Suppose R12 is used instead of NH_3 in the refrigeration system of Example 6.10. Determine the enthalpies, temperatures and entropies after throttling and adiabatic mixing. Find the mass flow rate, volumetric efficiency, swept volume rate and work requirement of compressor, condenser heat rejection and COP.

Solution:

The properties of R12 at the required states are as follows:

$v_1 = 0.16$, $h_1 = 174.96$ and $s_1 = 0.7203$
$v_6 = 0.0557$, $h_6 = 188.69$ and $s_6 = 0.7008$
$h_4 = 74.77$

The properties of superheated vapour at 1.005 bar (– 30°C) are as follows:

Degree of superheat	10°C	15°C
v	0.168	0.171
h	180.74	183.66
s	0.7436	0.755

The properties of superheated vapour at 9.634 bar (40°C) are as follows:

Degree of superheat	20°C	30°C
v	0.021	0.022
h	220.0	227.5
s	0.735	0.7571

$$\dot{m}_1 = \frac{3.51667 \times 5}{h_1 - h_4} = \frac{17.58335}{174.96 - 74.77} = 0.1755\ \text{kg/s}$$

$$\dot{m}_2 = \frac{3.51667 \times 5}{h_6 - h_4} = \frac{17.58335}{188.69 - 74.77} = 0.15435\ \text{kg/s}$$

$$\dot{m}_1 + \dot{m}_2 = 0.32985\ \text{kg/s}$$

Process 6-7 is throttling process, therefore, $h_6 = h_7$

Considering adiabatic mixing of streams 1 and 7:

$$\dot{m}_1 h_1 + \dot{m}_2 h_7 = (\dot{m}_1 + \dot{m}_2)h_2$$

$$\therefore \quad h_2 = (0.1755 \times 174.96 + 0.15435 \times 188.69)/0.32985 = 181.38477\ \text{kJ/kg}$$

The entropy and specific volume at point 2 can be found by interpolation in the superheat table for pressure 1.005 bar (–30°C) for $h_2 = 181.38477$.

Interpolating in superheat table between superheat of 10°C and 15°C for $h_2 = 181.38477$

$$\Delta t = 5\ (181.38477 - 180.74)/(183.66 - 180.74) = 0.22081 \times 5 = 1.1041^{\circ}C$$

$$\therefore \quad t_2 = -30 + 10 + 1.1041 = -18.896^{\circ}C$$

$$\therefore \quad s_2 = 0.7436 + 0.22081 \times (0.755 - 0.7436) = 0.746117.\ \text{Similarly, } v_2 = 0.168661$$

State 3 after compression:

This is obtained by interpolating in the superheat table for 9.634 bar (40°C) between 20°C and 30°C superheat for $s_2 = s_3 = 0.746117$

$$\Delta t = (0.746117 - 0.735) \times 10/(0.7571 - 0.735) = 0.50304 \times 10 = 5.03$$

$$\therefore \quad t_3 = 40 + 20 + 5.03 = 65.03^{\circ}C$$

$$h_3 = 220.0 + 0.50304(227.5 - 220.0) = 223.7728.\ \text{Similarly, } v_3 = 0.021503$$

$$W = (\dot{m}_1 + \dot{m}_2)(h_3 - h_2) = 13.9816 \text{ kW}$$

$$Q_c = (\dot{m}_1 + \dot{m}_2)(h_3 - h_4) = 49.1483 \text{ kW}$$

$$\text{COP} = Q_e/W = 10 \times 3.51667/13.9816 = 2.51521$$

$$\eta_{vol} = 1 + \varepsilon - \varepsilon\ (v_2/v_3) = 1.04 - 0.04\ (0.16866/0.021503) = 0.72626$$

$$\mathbb{V}_S = (\dot{m}_1 + \dot{m}_2)\ v_2/\eta_{vol} = 0.32985 \times 0.16866/0.72626 = 0.0766 \text{ m}^3/\text{s}$$

EXAMPLE 6.12 Suppose R22 is used instead of NH_3 in the refrigeration system of Example 6.10. Determine the enthalpies, temperatures and entropies after throttling and adiabatic mixing. Find the mass flow rate, volumetric efficiency, swept volume rate and work requirement of compressor, condenser heat rejection and COP.

Solution:

The properties of R22 at the required states are as follows.

$v_1 = 0.136$, $h_1 = 238.84$ and $s_1 = 0.9831$ at 1.64 bar (–30°C)
$v_6 = 0.0472$, $h_6 = 251.12$ and $s_6 = 0.9317$ at 4.98 bar (0°C)
$h_4 = 95.4$

The properties of superheated vapour at 1.64 bar (–30°C) are as follows:

Degree of superheat	5°C	10°C
v	0.139	0.143
h	241.98	245.17
s	0.9959	1.0085

The properties of superheated vapour at 15.267 bar (40°C) are as follows:

Degree of superheat	20°C	30°C
v	0.0191	0.0199
h	296.84	305.26
s	0.9832	1.007

$$\dot{m}_1 = \frac{3.51667 \times 5}{h_1 - h_4} = \frac{17.58335}{238.84 - 95.4} = 0.122583 \text{ kg/s}$$

$$\dot{m}_2 = \frac{3.51667 \times 5}{h_6 - h_4} = \frac{17.58335}{251.12 - 95.4} = 0.112916 \text{ kg/s}$$

$$\dot{m}_1 + \dot{m}_2 = 0.2355 \text{ kg/s}$$

Process 6–7 is throttling process, therefore, $h_6 = h_7$
Considering adiabatic mixing of streams 1 and 7

$$\dot{m}_1 h_1 + \dot{m}_2 h_7 = (\dot{m}_1 + \dot{m}_2) h_2$$

$$\therefore \quad h_2 = (0.122583 \times 238.84 + 0.11291 \times 251.12)/0.2355 = 244.728 \text{ kJ/kg}$$

The entropy and specific volume can be found by interpolation in the superheat table for pressure 1.64 bar (–30°C). Interpolating in superheat table between superheat of 5°C and 10°C for h_2 = 244.728, we get

$$\Delta t = (244.728 - 241.98) \times 5/(245.17 - 241.98) = 0.86143 \times 5 = 4.3071^\circ\text{C}$$

$$\therefore \quad t_2 = -30 + 5 + 4.3071 = -20.6928^\circ\text{C}$$

$$\therefore \quad s_2 = 0.9959 + 0.86143 \times (1.0085 - 0.9959) = 1.006754. \text{ Similarly, } v_2 = 0.14245.$$

State 3 after compression:

This is obtained by interpolating in the superheat table for 15.267 bar (40°C) between 40°C and 50°C superheat for $s_2 = s_3 = 1.006754$

$$\Delta t = (1.006754 - 0.9832) \times 10/(1.007 - 0.9832) = 0.989665 \times 10 = 9.897$$

$$\therefore \quad t_3 = 40 + 40 + 9.897 = 89.897^\circ\text{C}$$

$$h_3 = 241.98 + 0.989665(245.17 - 241.98) = 305.173. \text{ Similarly, } v_3 = 0.01989$$

$$W = (\dot{m}_1 + \dot{m}_2)(h_3 - h_2) = 14.2348 \text{ kW}$$

$$Q_c = (\dot{m}_1 + \dot{m}_2)(h_3 - h_4) = 49.4014 \text{ kW}$$

$$\text{COP} = Q_e/W = 10 \times 3.51667/14.2348 = 2.4705$$

$$\eta_{\text{vol}} = 1 + \varepsilon - \varepsilon\,(v_2/v_3) = 1.04 - 0.04\,(0.14245/0.01989) = 0.7535$$

$$\mathbb{V}_S = (\dot{m}_1 + \dot{m}_2) v_2/h_{\text{vol}} = 0.32985 \times 0.14245/0.7535 = 0.04452 \text{ m}^3\text{/s}$$

6.4.1 Two Compressors and Two Evaporators

If the temperature of one of the evaporators is below –30°C, then it is advised to use two compressors with intercooling and subcooling. The evaporator-2 may operate at the intermediate pressure, which may be chosen as the optimum intermediate pressure or slightly different from it depending upon the requirement. The system will be different for NH_3 and R12 since the basic two-stage system is different for the two refrigerants. The schematic diagram and *p–h* cycle for NH_3 are shown in Figures 6.8(a) and (b) respectively. In this case, a separate expansion valve feeds the liquid refrigerant to high temperature evaporator-2. It is possible to avoid this expansion valve and feed the liquid refrigerant to the high temperature evaporator-2 from the flash chamber (heat

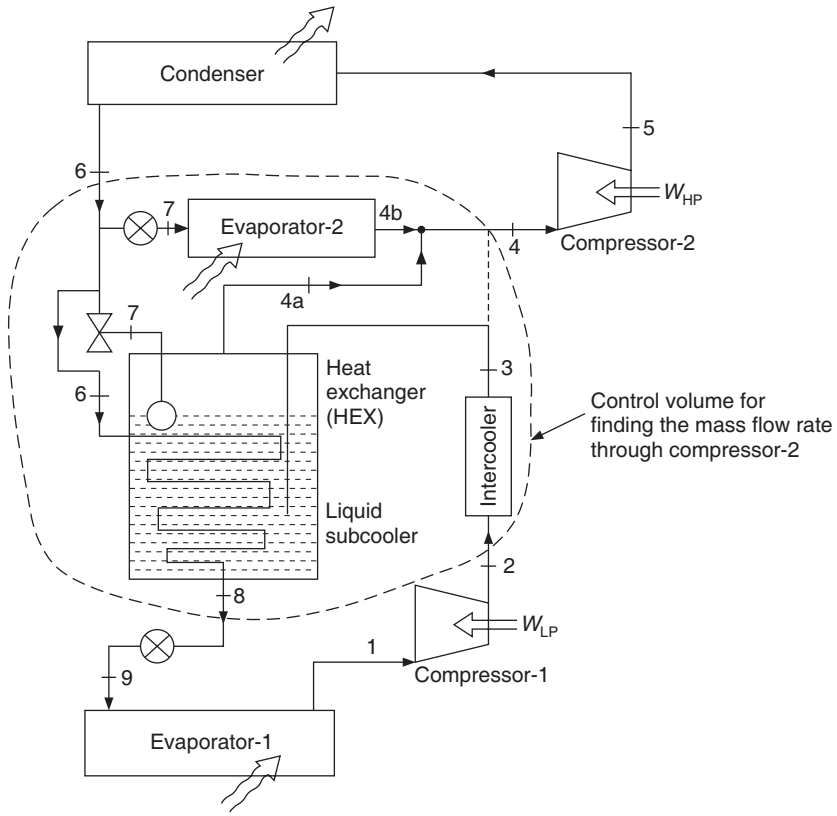

Figure 6.8(a) Multi-evaporator system with multiple compressors with an intercooler and a flooded type shell-and-tube heat exchanger for flash gas removal and subcooling.

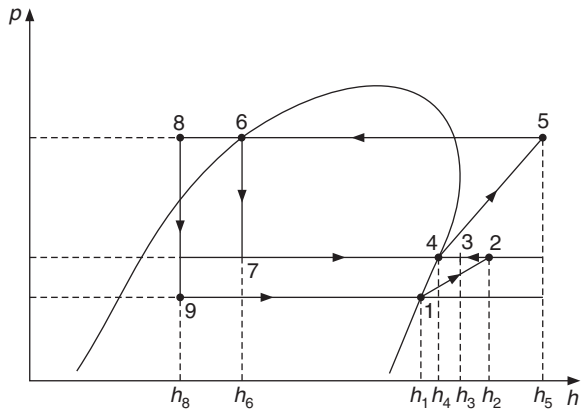

Figure 6.8(b) *p–h* cycle for the system in Figure 6.8(a).

exchanger) by a pump and return the mixture of liquid and vapour from flooded evaporator-2 back to the flash chamber like in a pumped circulation system. The pressure in flash chamber is same as in evaporator-2.

Similarly, Figures 6.9(a) and (b) show these diagrams for the R12 or R22 system. In a practical system the vapour will leave both the evaporators usually at 5°C superheat. The refrigerant coming from the flooded type shell-and-tube heat exchanger usually contains some liquid refrigerant so as to do the intercooling of stream from low temperature evaporator. The calculation procedures are best illustrated by solved examples given below.

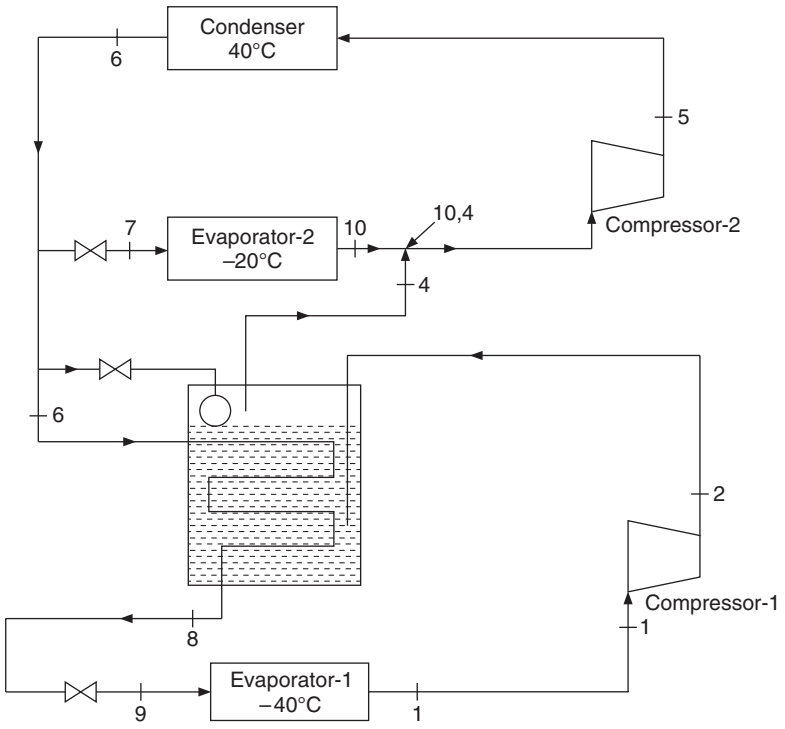

Figure 6.9(a) Schematic diagram of a two-stage R12/R22 refrigeration system with flooded type shell-and-tube type heat exchanger for flash gas removal and intercooling.

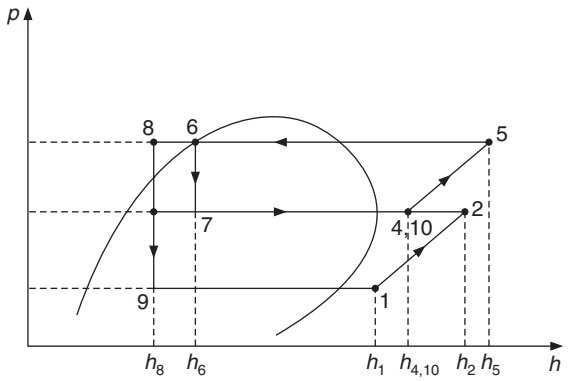

Figure 6.9(b) *p–h* cycle for the system shown in Figure 6.9(a).

EXAMPLE 6.13 A two-stage NH_3 refrigeration system serves Evaporator-1 at -40^oC and Evaporator-2 at -2^oC. Both the evaporators are of 10 TR capacity and the vapour leaves both the evaporators in saturated state. The condenser temperature is 40^oC. A water intercooler cools the LP vapours to 40^oC. The subcooling HEX subcools the liquid refrigerant from 40^oC to 5^oC before it is fed to main expansion valve. Find the mass flow rates, swept volume rates and work requirement of both the compressors, the condenser heat rejection and the COP.

Solution:

The schematic diagram and *p–h* and cycle are shown in Figure 6.8(a) and (b) respectively. The properties at various state points are same as those in Examples 6.1. The properties at state point 8 and mass flow rates through LP compressor and through HEX are same as those in Example 6.4(a).

$$h_1 = 1387.15,\ s_1 = 5.9518 \text{ and } v_1 = 1.55$$

By interpolating in the superheat table for intermediate pressure of 3.982 bar (-2^oC) between 60°C and 80^oC superheat for $s_1 = s_2 = 5.9518$ as done in Example 6.1, we get

$$t_2 = 72.6921^oC,\ h_2 = 1621.733 \text{ and } v_2 = 0.42083$$

At the exit of water intercooler, $p_3 = 3.982$ bar and $t_3 = 40^oC$, hence from Example 6.1,

$$h_3 = 1545.14$$

State 4 is saturated vapour at 3.982 bar, hence from saturation table, we get

$$h_4 = 1441.08,\ v_4 = 0.317 \text{ and } s_4 = 5.3627$$

$$h_6 = h_7 = h_f(40^oC) = 371.47 \text{ and } h_8 = h_f(5^oC) = 204.07 \text{ as in Example 6.4(a)}$$

Interpolating in the superheat table for condenser pressure of 15.55 bar (40^oC) between superheat of 50°C and 60^oC for $s_4 = s_5 = 5.3627$ as in Example 6.1,

$$t_5 = 96.493^oC,\ h_5 = 1639.366 \text{ and } v_5 = 0.105$$

As in Example 6.4(a), $\dot{m}_{LP} = 0.02977$, $W_{LP} = 6.9729$ kW and $(\mathbb{V}_S)_{LP} = 0.05161$ m^3/s

The exit of evaporator-2 and the HEX, we have saturated vapours at the same temperature, hence the mass flow rate through HEX is same as calculated in Example 6.4(a), that is,

$$\dot{m}' = \dot{m}_{LP}\frac{(h_3 - h_4) + (h_6 - h_8)}{h_4 - h_6} = 0.02972\,\frac{(371.47 - 204.07) + (1545.14 - 1441.08)}{1441.08 - 371.47}$$

$$= 0.0075427$$

The mass flow rate m_2 through evaporator-2 is

$$\dot{m}_2 = \frac{3.51667 \text{ TR}}{h_4 - h_7} = \frac{3.51667 \times 10}{1441.08 - 371.47} = 0.032878 \text{ kg/s}$$

$$\therefore \quad \dot{m}_{HP} = \dot{m}_{LP} + \dot{m}' + \dot{m}_2 = 0.02972 + 0.0075427 + 0.032878 = 0.070147 \text{ kg/s}$$

$$W_{HP} = \dot{m}_{HP}(h_5 - h_4) = 0.070147(1639.3666 - 1441.08) = 13.90913 \text{ kW}$$

$$W_{net} = W_{LP} + W_{HP} = 6.9729 + 13.90913 = 20.882$$

$$\text{COP} = 2 \times 35.1667/20.882 = 3.3681$$

$$\eta_{vol,HP} = 1.0 + \varepsilon - \varepsilon\,(v_4/v_5) = 1.04 - 0.04(0.317/0.105) = 0.9192 \text{ m}^3/\text{s}$$

$$(\mathbb{V}_S)_{HP} = \dot{m}_{HP}\, v_4/\eta_{vol,HP} = 0.070147 \times 0.317/0.9192 = 0.02419 \text{ m}^3/\text{s}$$

EXAMPLE 6.14 A two-stage R12 refrigeration system serves Evaporator-1 at –40°C and Evaporator-2 at –2°C. Both the evaporators are of 10 TR capacity. The vapour leaves both the evaporators at 5°C superheat. The condenser temperature is 40°C. The subcooling HEX subcools the liquid refrigerant to 5°C before it is fed to main expansion valve. The TEV of the HEX maintains a superheat of 5°C when the mixture from HEX mixes adiabatically with LP vapour. Find the mass flow rates, swept volume rates and work requirements of both the compressors, the condenser heat rejection and the COP.

Solution:

The schematic diagram and *p–h* cycle are shown in Figures 6.9(a) and (b) respectively. State 1 is superheated by 5°C at 0.642 bar. From superheat table at 0.642 bar, we get

$$v_1 = 0.249,\ h_1 = 173.01 \text{ and } s_1 = 0.7419$$

Interpolating in the superheat table given in Example 6.6 for 2.891 bar (–2°C) between superheat of 15°C and 20°C for $s_1 = s_2 = 0.7419$, we get

$$\Delta t = 5(0.7419 - 0.7364)/(0.7475 - 0.7364) = 0.495 \times 5 = 2.4775^\circ\text{C}$$

$$t_2 = -2 + 15 + 2.4774 = 15.4774^\circ\text{C}$$

$h_2 = 197.5 + 0.495(200.67 - 197.45) = 199.0455$. Similarly, $v_2 = 0.064$

State 4 is superheated by 5°C at 2.891 bar. From superheat table given in Example 6.6,

$$v_4 = 0.06,\ h_4 = 191.02 \text{ and } s_4 = 0.7135$$

State 5 is obtained by interpolating in the superheat table for condenser pressure of 9.634 bar (40°C) between superheat of 10°C and 20°C for $s_4 = s_5 = 0.7135$ as shown in Example 6.6 (where it is state 4)

$$t_5 = 50.646^\circ\text{C},\ h_5 = 212.99 \text{ and } v_5 = 0.01913$$

$$h_6 = h_f\,(40^\circ\text{C}) = 74.77 \text{ and } h_8 = h_f\,(5^\circ\text{C}) = 40.81$$

$$\dot{m}_1 = \frac{3.51667 \times 10}{h_1 - h_9} = \frac{35.1667}{173.01 - 40.81} = 0.2660111 \text{ kg/s}$$

State 10 is at the exit of Evaporator-2. It is at 2.891 bar and 5°C superheat, that is, it is same as state 4.

$$\dot{m}_2 = \frac{3.51667 \times 10}{h_{10} - h_6} = \frac{35.1667}{191.02 - 74.77} = 0.30251 \text{ kg/s}$$

In this case state 10 at the exit of Evaporator-2 and state 4 are the same, hence, stream $\dot{m}_2$ may not be considered in the energy balance to find $\dot{m}'$ required for subcooling and intercooling of LP vapour. Also, stream $\dot{m}_2$ may be combined with the other streams 2 and 3 after adiabatic mixing as shown by dashed line in Figure 6.8(a).

$$\dot{m}' = \dot{m}_{LP}\frac{(h_2 - h_4) + (h_6 - h_9)}{(h_4 - h_6)} = 0.266011\frac{(199.0455 - 191.02) - (74.77 - 40.81)}{191.02 - 74.77}$$

$$= 0.096074$$

$$\therefore \quad \dot{m}_{HP} = \dot{m}_{LP} + \dot{m}_2 + \dot{m}' = 0.6645941 \text{ kg/s}$$

$$W_{LP} = \dot{m}_{LP}(h_2 - h_1) = 0.2660111(199.0455 - 173.01) = 6.92573 \text{ kW}$$

$$W_{HP} = \dot{m}_{HP}(h_5 - h_4) = 0.6645941(212.99138 - 191.02) = 14.602 \text{ kW}$$

$$W_{net} = W_{LP} + W_{HP} = 6.925739 + 14.602 = 21.52778 \text{ kW}$$

$$\text{COP} = 2 \times 35.1667/21.52778 = 3.2671$$

$$Q_c = 0.6645941(212.99138 - 74.77) = 91.861 \text{ kW}$$

$$\eta_{vol,LP} = 1.0 + \varepsilon - \varepsilon(v_1/v_2) = 1.04 - 0.04(0.249/0.064) = 0.844375$$

$$(\mathbb{V}_S)_{LP} = \dot{m}_{LP} v_1/\eta_{vol,LP} = 0.2660111 \times 0.249/0.844375 = 0.07844 \text{ m}^3/\text{s}$$

$$\eta_{vol,HP} = 1.0 + \varepsilon - \varepsilon(v_4/v_5) = 1.04 - 0.04(0.06/0.01913) = 0.9145$$

$$(\mathbb{V}_S)_{HP} = \dot{m}_{HP} v_4/\eta_{vol,HP} = 0.6645941 \times 0.06/0.9145 = 0.0436 \text{ m}^3/\text{s}$$

EXAMPLE 6.15(a) A two-stage R22 refrigeration system serves Evaporator-1 at –40°C and Evaporator-2 at –2°C. Both the evaporators are of 10 TR capacity. The vapour leaves both the evaporators at 5°C superheat. The condenser temperature is 40°C. The subcooling HEX subcools the liquid refrigerant to 5°C, before it is fed to the main expansion valve. The TEV of the HEX maintains a superheat of 5°C when mixture from HEX mixes adiabatically with LP vapour. Find the mass flow rates, swept volume rates and work requirements of both the compressors, the condenser heat rejection and the COP.

Solution:

The schematic diagram and *p–h* cycle are shown in Figures 6.9(a) and (b), respectively. State 1 is superheated by 5°C at 1.053 bar. From superheat table,

$$v_1 = 0.211,\ h_1 = 237.17 \text{ and } s_1 = 1.0172$$

Interpolating in the superheat table given in Example 6.8 for 4.664 bar (–2°C) between superheat of 20°C and 30°C for $s_1 = s_2 = 1.0072$, we get

$$\Delta t = (01.0072 - 0.98507) \times 5/(1.0791 - 0.98507) = 0.3417 \times 10 = 3.417^\circ\text{C}$$

$$t_2 = -2 + 20 + 3.417 = 21.417^\circ\text{C},\ h_2 = 267.0761 \text{ and } v_2 = 0.05622$$

States 4 and 10 are superheated by 5° C at 4.664 bar. From superheat table given in Example 6.8,

$$v_4 = 0.0516,\ h_4 = 253.97 \text{ and } s_4 = 0.9479$$

Similarly, by interpolating in the superheat table for condenser pressure of 15.267 bar (40°C) between superheat of 20°C and 30 °C for $s_4 = s_5 = 0.9479$ as shown in Example 6.8 (where it is state 4)

$$t_5 = 65.654^\circ\text{C},\ h_5 = 284.5288 \text{ and } v_5 = 0.017765$$

$$h_6 = h_f(40^\circ\text{C}) = 95.4 \text{ and } h_8 = h_f(5^\circ\text{C}) = 52.23$$

$$\dot{m}_1 = \dot{m}_{LP} = \frac{3.51667 \times 10}{h_1 - h_9} = \frac{35.1667}{237.17 - 52.23} = 0.190151 \text{ kg/s}$$

$$\dot{m}_2 = \frac{3.51667 \times 10}{h_{10} - h_6} = \frac{35.1667}{253.97 - 95.4} = 0.221774 \text{ kg/s}$$

In this case state 10 at the exit of evaporator-2 and state 4 are the same, hence, stream $\dot{m}_2$ may not be considered in the energy balance to find $\dot{m}'$ required for subcooling and intercooling of LP vapour. Also stream $\dot{m}_2$ may be combined with the other streams after adiabatic mixing instead of what is shown in Figure 6.8(a). It may proceed along the dashed line shown in Figure 6.8(a)

$$\dot{m}' = \dot{m}_{LP} \frac{(h_2 - h_4) + (h_6 - h_9)}{(h_4 - h_6)} = 0.266011 \frac{(267.0761 - 253.97) - (95.4 - 52.23)}{253.97 - 95.4}$$

$$= 0.067484 \text{ kg/s}$$

$\therefore$ $\dot{m}_{HP} = \dot{m}_{LP} + \dot{m}_2 + \dot{m}' = 0.47941$ kg/s

$W_{LP} = \dot{m}_{LP}(h_2 - h_1) = 0.19015(267.0761 - 237.17) = 5.68669$ kW

$W_{HP} = \dot{m}_{HP}(h_5 - h_4) = 0.47941(284.5288 - 253.97) = 14.6502$ kW

$W_{net} = W_{LP} + W_{HP} = 5.68669 + 14.6502 = 20.3369$ kW

COP $= 2 \times 35.1667/20.3369 = 3.45841$

$Q_c = 0.47941(284.5288 - 95.4) = 90.67024$ kW

$\eta_{vol,LP} = 1.0 + \varepsilon - \varepsilon(v_1/v_2) = 1.04 - 0.04(0.211/0.05622) = 0.8899$

$(\mathbb{V}_S)_{LP} = \dot{m}_{LP}.\ v_1/\eta_{vol,LP} = 0.19015 \times 0.211/0.8899 = 0.045087$ m^3/s

$\eta_{vol,HP} = 1.0 + \varepsilon - \varepsilon(v_4/v_5) = 1.04 - 0.04(0.0516/0.017765) = 0.9238$

$(\mathbb{V}_S)_{HP} = \dot{m}_{HP}.\ v_4/\eta_{vol,HP} = 0.47941 \times 0.0516/0.9238 = 0.02678$ m^3/s

EXAMPLE 6.15(b) Repeat Example 6.15(a) if the vapour leaving the evaporator-2 is saturated vapour. In this case the stream from evaporator-2 is at a temperature of –2°C. This will also help in cooling the LP vapour since the stream from evaporator-2 is at a lower temperature than t_2 = 21.417°C. As a result, the mass flow rate of stream $\dot{m}'$ through the heat exchanger will decrease. The energy balance over the control volume including this stream yields

$$(m' + m_{LP})h_6 + m_2 h_8 + m_{LP} h_2 = m_{LP} h_9 + (m_{LP} + m_2 + m')h_4$$

$$\dot{m}' = \dot{m}_{LP} \frac{(h_2 - h_4) + (h_6 - h_9)}{(h_4 - h_6)} - m_2 \frac{h_4 - h_8}{h_4 - h_6} = 0.067484 - 0.221774 \frac{253.97 - 250.4}{253.97 - 95.4}$$

$$= 0.062492 \text{ kg/s}$$

The first term in this expression is the same as in the last example. The second term is contribution to intercooling by vapour of evaporator-2.

$\therefore$ $\dot{m}_{HP} = \dot{m}_{LP} + \dot{m}_2 + \dot{m}' = 0.190151 + 0.221774 + 0.062492 = 0.474417$ kg/s

$W_{LP} = \dot{m}_{LP}(h_2 - h_1) = 0.19015(267.0761 - 237.17) = 5.68669$ kW

$W_{HP} = \dot{m}_{HP}(h_5 - h_4) = 0.474417(284.5288 - 253.97) = 14.4976$ kW

$$W_{net} = W_{LP} + W_{HP} = 5.68669 + 14.4976 = 20.18432 \text{ kW}$$

$$\text{COP} = 2 \times 35.1667/20.18432 = 3.4845$$

$$Q_c = 0.474417(284.5288 - 95.4) = 89.72592 \text{ kW}$$

$$(\mathbb{V}_S)_{HP} = \dot{m}_{HP}\, v_4/\eta_{vol,HP} = 0.474417 \times 0.0516/0.9238 = 0.0265 \text{ m}^3/\text{s}$$

6.5 TWO-STAGE REVERSED CARNOT CYCLE

It has been shown earlier in Chapter 3 (Figure 3.7) that the single-stage Reversed Carnot cycle requires two compressors, namely, one isentropic and another isothermal. A two-stage Reversed Carnot cycle will, therefore, require two compressors for each stage, i.e. a total of four compressors. The *T*–*s* diagram of such a two-stage Reversed Carnot Cycle is shown in Figure 6.10(a). A comparison of this with the actual two-stage cycle is shown in Figure 6.10(b). A single-stage cycle is shown by 1–2″–5–9′–1 in Figure 6.10(c).

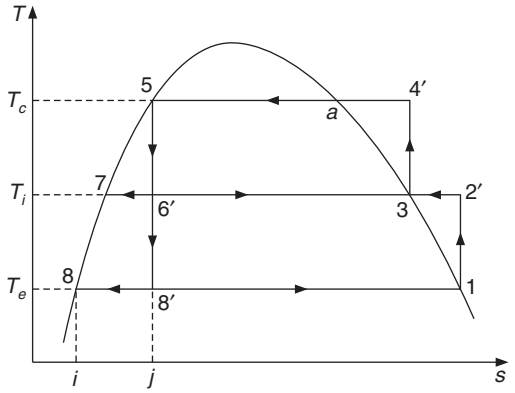

Figure 6.10(a) Two-stage Reversed Carnot cycle.

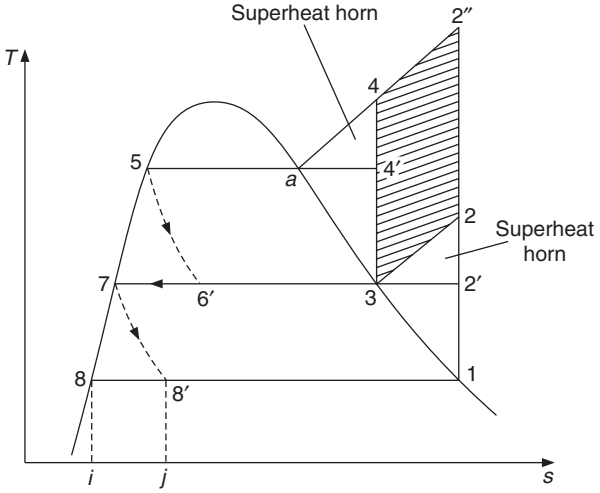

Figure 6.10(b) Two-stage standard vapour compression cycle.

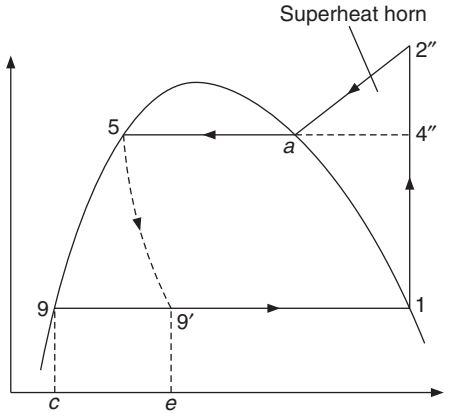

Figure 6.10(c) A single-stage standard vapour compression cycle.

Figure 6.10(b) shows that the two-stage cycle results in a saving of work approximately equal to area 3–2–2″–4–3. This is shown by cross hatching. This is approximate since the mass flow rates for the single-stage cycle and two-stage cycle are different. The area of superheat horn in single stage cycle is 4″–2″–*a*–4″, whereas for the two stage cycle it is the sum of the areas 2′–2–3–2′ and 4′–4–*a*–4′ which is definitely less than that for the single-stage cycle. The throttling loss is rather difficult to estimate since the expansion is carried out in two stages. It may be said that in the final stage the throttling loss is the area 8–*i*–*j*–8′–8 which is small compared to area 9–*c*–*e*–9′–9 for the single-stage cycle.

In the two-stage RC cycle shown in Figure 6.10(a), the quality at point 6′ is given by

$$x_{6'} = (s_{6'} - s_7)/(s_3 - s_7) = (s_5 - s_7)/(s_3 - s_7) \text{ since } s_5 = s_{6'}$$

$$\therefore \quad (1 - x_{6'}) = (s_3 - s_5)/(s_3 - s_7)$$

Hence, if $\dot{m}_{HP}$ is the mass flow rate at point 5, then $x_{6'}\dot{m}_{HP}$ will flash into vapour and it will be taken to high pressure compressor from the flash chamber. The liquid flow rate from the flash chamber to the LP compressor will be $(1 - x_{6'})$

$$\therefore \quad \dot{m}_{LP} = \dot{m}_{HP}(1 - x_{6'}) = \dot{m}_{HP}(s_3 - s_5)/(s_3 - s_7)$$

Hence the COP of the two-stage Reversed Carnot cycle is as follows:

$$\text{COP} = \frac{\dot{m}_{LP} T_e (s_1 - s_7)}{\dot{m}_{LP}(T_i - T_e)(s_1 - s_7) + \dot{m}_{HP}(T_c - T_i)(s_3 - s_5)}$$

$$= \frac{\dot{m}_{LP} T_e (s_1 - s_7)}{\dot{m}_{LP}(T_i - T_e)(s_1 - s_7) + \dot{m}_{LP}\dfrac{(s_3 - s_7)}{(s_3 - s_5)}(T_c - T_i)(s_3 - s_5)}$$

$$= \frac{T_e}{(T_i - T_e) + \dfrac{(s_3 - s_7)}{(s_1 - s_5)}(T_c - T_i)} \tag{6.17}$$

EXAMPLE 6.16 Show that the COP of the two-stage Reversed Carnot cycle is maximum at intermediate temperature very near the value given by the expression $\sqrt{T_c T_e}$.

Solution:

The COP given by Eq. (6.17) exhibits a maxima. For evaporator and condenser temperatures of –40°C and 40°C respectively the values of COP at various intermediate temperatures are given in Table 6.1.

Table 6.1 COP of the two-stage RC cycle for various intermediate temperatures at $t_c = 40°C$ and $t_e = -40°C$

T_i	–4°C	–2°C	–1°C	0°C	1°C	2°C
NH_3 COP	3.0929	3.094	3.0942	3.0941	3.0939	3.0934
R12 COP	2.9871	3.02132	2.987	2.987	2.98676	2.9862
R22 COP	3.04523	3.04635	3.04689	3.0471	3.04697	3.04688

For evaporator and condenser temperatures of –50°C and 40°C respectively, the COP values for various intermediate temperatures are given in Table 6.2.

Table 6.2 COP of two-stage RC cycle for various intermediate temperatures at $t_c = 40°C$ and $t_e = -50°C$

T_i	–10°C	–9°C	–8°C	–7°C	–6°C	–5°C	–4°C	–3°C
NH_3 COP	2.6559	2.6565	2.6569	2.65727	2.6572	2.6573	2.6569	2.6564
R12 COP	2.5594	2.5595	2.5596	2.5594	2.5592	2.5588	2.5588	2.5581
R22 COP	2.6102	2.6108	2.6113	2.6117	2.6119	2.6121	2.612	2.6118

The intermediate temperature for maximum COP is shown in Table 6.3 for condenser temperature of 40°C along with the value of $\sqrt{T_c T_e}$.

Table 6.3 Optimum intermediate temperature for two-stage RC cycle for $t_c = 40°C$ and $t_e = -40°C$ and –50°C

T_e	NH_3	R-22	R-12	$\sqrt{T_c T_e}$
–40°C	–1°C	0°C	–2°C	–2.946°C
–50°C	–5°C	–5°C	–8°C	–8.8°C

The optimum intermediate temperature is observed to be closer to $\sqrt{T_c T_e}$ for R12 whereas for NH_3 and for R22 it is 2°C to 3°C more than $\sqrt{T_c T_e}$.

6.6 LIMITATIONS OF MULTISTAGE SYSTEMS

Conventionally, multistage systems do not use more than three stages and the minimum temperature up to which a multistage system can be used is –100°C. It is not economical to use multistage systems below this temperature.

Low-pressure refrigerants like R134a, R12, R22. R502, R507 and NH_3 are usually used in multistage systems. As a result, the lower-stage compressor works at vacuum pressure since the normal boiling point of all these refrigerants is above –40°C. This makes the system prone to ingress of air and moisture. Hermetic compressors cannot be used as these are not designed to work in vacuum. The mass flow rate reduces at low temperatures since the gas specific volume is larger at lower temperatures, for example it is 9.01 m^3/kg at –70°C while it is 1.55 m^3/kg at –40°C. The motor of the hermetic compressor cannot be effectively cooled at lower mass flow rates, hence the possibility of motor burn-out increases.

The specific volume being large at low temperatures, the swept volume rate and therefore the size of the LP compressor becomes very large.

Multistage systems suffer from the *oil wandering* problem. Some oil is always mechanically carried or dissolved by refrigerant coming out of both the LP and HP compressors. Excess oil may accumulate in either LP or HP compressor making the other compressor devoid of lubricating oil and thereby increasing the wear and tear of the compressor. This is called the *oil wandering problem in multistage systems.* This is avoided as mentioned earlier by using a multi-cylinder compressor with a few cylinders used as LP stage and the remaining cylinders as HP stage. Use of centrifugal or rotary vane compressor also avoids this problem. Oil separator is used in all low temperature refrigeration systems even with R12 in which it makes a homogeneous mixture.

If the evaporator temperature is less than –70°C, the pull-down load is very high; hence the motor is oversized by up to 150 per cent. The condenser is designed for pull-down load, which is maximum. The intermediate temperature is decided by the matching of two stages as shown in Example 6.3.

The oil return from the evaporator is poor since the mass flow rate of the refrigerant is reduced. A direct expansion coil (DX coil) may be used as evaporator since it has better oil return and uses a small refrigerant charge.

The change in specific volume is very large during evaporation at low temperatures. This leads to a high velocity in the evaporator, leading to large pressure drops. A flash cooler or re-circulation type of evaporator is preferred for this reason. Superheating in a subcooling type of heat exchanger also helps. All these efforts reduce the mass flow rate per TR.

The thermostatic expansion valve demands more superheat for the same setting of spring force. The spring force $F_s = A_b(p_p - p_E)$ where A_b is the area of bellows or diaphragm. At –70°C and –65°C the saturation pressures for R22 (p_e and p_p respectively) are 0.2062 bar and 0.2812 bar respectively, a difference of 0.075 bar. At 40°C and 41°C the pressures are 15.267 bar and 15.643 bar respectively. A spring force corresponding to 0.075 bar, that is 5°C superheat will result in 0.075/(15.643 – 15.267) = 0.2°C superheat at 40°C evaporator temperature when compressor is started at ambient condition of 40°C. This might lead to flooding of the evaporator. Hence, a larger degree of superheat has to be maintained at evaporator temperature of –70°C.

In reciprocating compressors, the valve operation is impaired below a pressure of 0.2 bar. The shaft seal also poses problems since the pressure outside is more while it is designed for higher inside pressure.

The multistage system is very expensive and therefore requires special design.

6.7 CASCADE REFRIGERATION SYSTEM

Some of the disadvantages of multistage refrigeration system are specifically due to the use of single refrigerant. A low NBP refrigerant (called high pressure refrigerant) will be most suited at lower evaporator temperatures, but this will result in very high condenser pressures. Further, it will require a smaller swept flow rate since the evaporator pressure is higher. According to Guldberg number, the ratio $T_{nb}/T_{crit} = 0.6$ for most of the refrigerants. This means that the critical temperature of low NBP refrigerants may be lower than the ambient temperature, as a result these cannot be used in the condenser. A high NBP (low pressure) refrigerant can be used in condensers, however, it will be disastrous because of its negative pressure at low evaporator temperatures although it has low condenser pressure.

The best features can be obtained by using two different refrigerants, i.e. a low NBP refrigerant in the evaporator and a high NBP refrigerant in the condenser. Actually these are used in two independent single stage refrigeration systems. A low temperature (LT) side system using the low NBP refrigerant absorbs heat at low temperature and its condenser rejects heat at some intermediate temperature to the evaporator of the high temperature (HT) side refrigeration system that uses a high NBP refrigerant. This is the cascading effect, i.e. one system (LT) absorbs heat at low temperature and rejects it to another system (HT) which ultimately rejects it to the surroundings. Up to two cascade stages have been used for liquefaction of air. Further, each stage, that is, LT or HT can have multistage systems to make them more efficient.

A cascade refrigeration system is shown in Figure 6.11(a). The condenser of the high temperature (HT) side system rejects heat to the surroundings. The heat exchanger which acts as the condenser of the low temperature (LT) side at $T_{c\text{LT}}$ and evaporator of HT side at $T_{e\text{HT}}$ is called *cascade condenser*. Heat is transferred from LT side to HT side hence $T_{c\text{LT}} > T_{e\text{HT}}$.

R13, R14, R23, $R13B_1$ and R508B are usually used on the LT side and R134a, R12, R22, R502, R507 and NH_3 are conventionally used on the HT side.

The system will not have the oil-wandering problem. The compressor sizes will also be reasonable and pressures will be positive everywhere. Hence, from a practical point of view this is a good system. However, in the cascade condenser, for heat transfer to occur the temperature of the LT side has to be greater than the temperature of the HT side. This will give rise to irreversibility and decrease the COP. The cascade refrigeration system does not compete with the multistage system from thermodynamic point of view. It is more convenient and a practical system to use at low temperatures.

The cascade refrigeration system was first used by Picted in 1877 for liquefaction of O_2 employing SO_2 and CO_2 as intermediate refrigerants in a two-stage cascade system. Another system using NH_3, ethylene and CH_4 in three-stage cascade, was also employed for liquefaction of O_2. Dry ice manufacture also uses a cascade system with NH_3 on the HT side.

The *T–s* diagram of the cascade system is shown in Figure 6.11(b) by assuming SSS cycles for both the LT and the HT sides. The evaporator and condenser temperatures are T_e and T_c respectively. In the cascade condenser the temperature of LT side refrigerant is $T_{c\text{LT}}$ and that of HT side refrigerant is $T_{e\text{HT}} < T_{c\text{LT}}$. The temperature difference $DT = T_{c\text{LT}} - T_{e\text{HT}}$ required for heat transfer to take place from LT side to HT side is called the *overlap temperature*.

If the cooling capacity of the system is TR, the evaporator heat transfer rate $Q_e = 3.51667$ TR. The refrigeration effect is $(h_a - h_d)$, hence the mass flow rate of the low temperature side (LT) compressor is given by

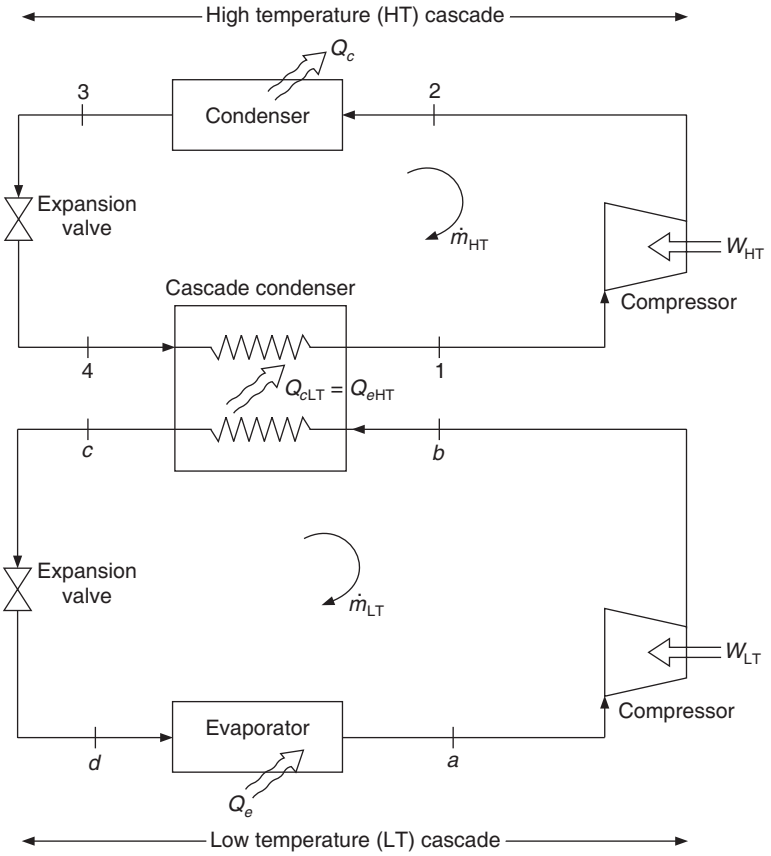

Figure 6.11(a) A two-stage cascade refrigeration system with the different refrigerants.

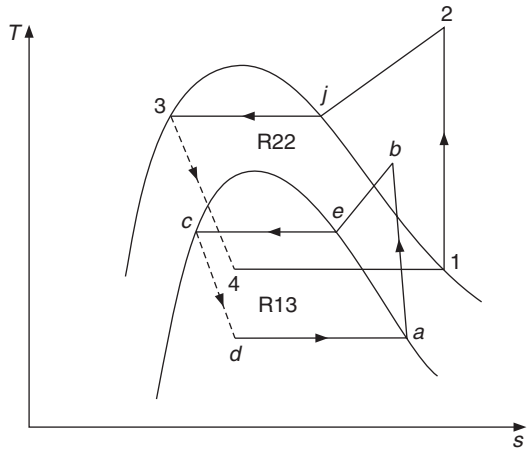

Figure 6.11(b) The *T–s* diagram of the cascade system of Figure 6.11(a).

$$\dot{m}_{\mathrm{LT}} = \frac{3.51667\ \mathrm{TR}}{h_a - h_d}$$

The compressor work and condenser heat rejection rate are given by

$$W_{\mathrm{LT}} = \dot{m}_{\mathrm{LT}}\,(h_b - h_a) \quad \text{and} \quad Q_{c\mathrm{LT}} = \dot{m}_{\mathrm{LT}}\,(h_b - h_c)$$

In steady state the heat rejection of LT side is equal to the evaporator heat transfer of HT side, that is,

$$Q_{c\mathrm{LT}} = Q_{e\mathrm{HT}} \quad \text{or} \quad \dot{m}_{\mathrm{LT}}\,(h_b - h_c) = \dot{m}_{\mathrm{HT}}(h_1 - h_4) \tag{6.18}$$

Therefore, the mass flow rate, the work requirement of HT side, condenser heat rejection and COP of the system are given by

$$\begin{gathered}\dot{m}_{\mathrm{HT}} = \dot{m}_{\mathrm{LT}}\,\frac{h_b - h_c}{h_1 - h_4}, \quad W_{\mathrm{HT}} = \dot{m}_{\mathrm{HT}}\,(h_2 - h_1) \\ Q_c = \dot{m}_{\mathrm{HT}}(h_2 - h_3) \ \text{ and } \ \mathrm{COP} = \frac{3.51667\ \mathrm{TR}}{W_{\mathrm{LT}} + W_{\mathrm{HT}}}\end{gathered} \tag{6.19}$$

The intermediate temperature T_i is defined as the mean of $T_{c\mathrm{LT}}$ and $T_{e\mathrm{HT}}$ so that

$$\begin{aligned} DT &= T_{c\mathrm{LT}} - T_{e\mathrm{HT}} \quad \text{and} \quad T_i = (T_{c\mathrm{LT}} + T_{e\mathrm{HT}})/2 \\ T_{c\mathrm{LT}} &= T_i + DT/2 \quad \text{and} \quad T_{e\mathrm{HT}} = T_i - DT/2 \end{aligned} \tag{6.20}$$

6.7.1 Optimum Intermediate Temperature

The COP may be determined from Eq. (6.19) for the saturation cycle shown in Figure 6.11(a) for different intermediate temperatures. The optimum intermediate temperature may be determined from the plot of COP against intermediate temperature.

Case I: zero overlap temperature

In our attempt to obtain an analytical expression for intermediate temperature we consider the Reversed Carnot cycles for both LT and HT sides as shown in Figure 6.12(a) with overlap temperature *DT*. To obtain a simple result, we consider the overlap temperature to be zero to start with as shown in Figure 6.12(b). In this case, the heat transfer from LT to HT side takes place without any temperature difference, that is, $T_{c\mathrm{LT}} = T_{e\mathrm{HT}} = T_i$ in the cascade condenser. Also, we have $Q = T\,\Delta s$ for reversible heat transfer in the cascade condenser, which gives

$$Q_{c\mathrm{LT}} = \dot{m}_{\mathrm{LT}} T_i\,(s_a - s_d) = \dot{m}_{\mathrm{LT}} T_i\,(s_a - s_c) \quad \text{and} \quad Q_{e\mathrm{HT}} = \dot{m}_{\mathrm{HT}} T_i\,(s_1 - s_3)$$

From Eq. (6.18), $Q_{c\mathrm{LT}} = Q_{e\mathrm{HT}}$. Substituting in this from the above equation, we get

$$\dot{m}_{\mathrm{LT}}(s_a - s_c) = \dot{m}_{\mathrm{HT}}(s_1 - s_3) \tag{6.21}$$

Also, for the Reversed Carnot cycles

$$Q_e = \dot{m}_{\mathrm{LT}}\,T_e\,(s_a - s_c),\ W_{\mathrm{LT}} = \dot{m}_{\mathrm{LT}}\,(T_i - T_e)(s_a - s_c)$$

and $$W_{\mathrm{HT}} = \dot{m}_{\mathrm{HT}}\,(T_c - T_i)(s_1 - s_3)$$

$$\mathrm{COP} = \frac{Q_e}{W_{\mathrm{LT}} + W_{\mathrm{HT}}} = \frac{\dot{m}_{\mathrm{LT}}\,T_e\,(s_a - s_c)}{\dot{m}_{\mathrm{LT}}\,(T_i - T_e)(s_a - s_c) + \dot{m}_{\mathrm{HT}}\,(T_c - T_i)(s_1 - s_3)}$$

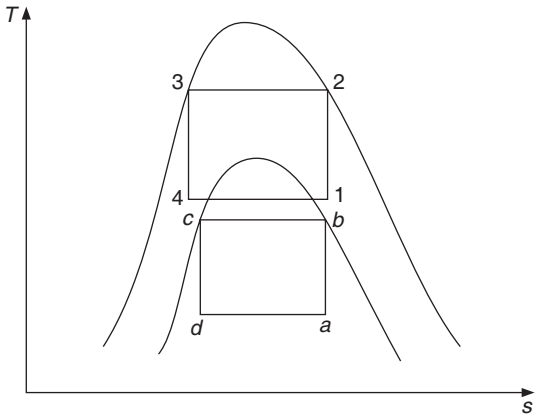

Figure 6.12(a) Reversed Carnot cycles for both LT and HT sides with nonzero overlap temperature difference.

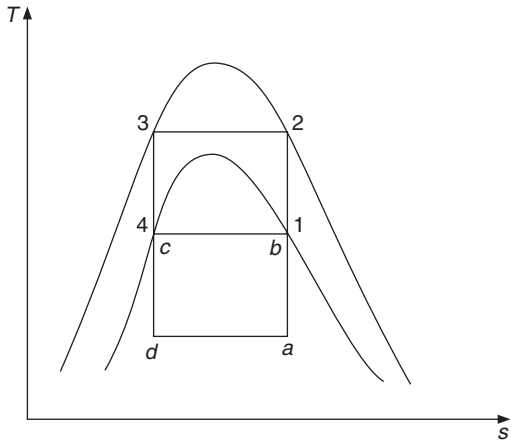

Figure 6.12(b) Reversed Carnot cycles for both LT and HT with zero overlap temperature difference.

Substituting from Eq. (6.21),

$$\text{COP} = \frac{\dot{m}_{\text{LT}}\, T_e\, (s_a - s_c)}{\dot{m}_{\text{LT}}\, (T_i - T_e)(s_a - s_c) + \dot{m}_{\text{LT}}\, (T_c - T_i)(s_a - s_c)} = \frac{T_e}{T_c - T_e} \tag{6.22}$$

This expression is independent of intermediate temperature, hence there is no way of optimizing it. The COPs of the individual HT and LT RC cycles are as follows:

$$(\text{COP})_{\text{RC,LT}} = T_e/(T_i - T_e) \text{ and } (\text{COP})_{\text{RC,HT}} = T_i/(T_c - T_i) \tag{6.23}$$

It is observed that as the intermediate temperature T_i increases, $(\text{COP})_{\text{RC,LT}}$ decreases and $(\text{COP})_{\text{RC,HT}}$ increases, i.e. T_i has opposite effects on these COPs. Therefore, it will be optimum if the two COPs are same. This was proposed by Schmidt (1965). Equating the two COPs, leads to

$$\frac{T_e}{T_i - T_e} = \frac{T_i}{T_c - T_i} \;\therefore\; T_e T_c - T_e T_i = T_i^2 - T_i T_e \;\text{ or }\; T_i^2 = T_e T_c \;\therefore\; T_i = \sqrt{T_e T_c} \tag{6.24}$$

The same result can be obtained if we optimize the product of the LT and HT side COPs, that is, $(\text{COP})_{\text{RC,LT}}\,(\text{COP})_{\text{RC,LT}}$

Let, $$\xi = (\text{COP})_{\text{RT,LT}}\,(\text{COP})_{\text{RC,LT}} = \frac{T_e}{T_i - T_e}\,\frac{T_i}{T_c - T_i}$$

To obtain the optimum T_i, the derivative of ξ w.r.t to T_i is put equal to zero, that is

$$\frac{d\xi}{dT_i} = 0 = \frac{T_e\{(T_i - T_e)(T_c - T_i)\} - T_e T_i\{(T_c - T_i) - (T_i - T_e)\}}{(T_i - T_e)^2 (T_c - T_i)^2} = 0$$

which yields

$$-T_i^2 - T_e T_c + 2T_i^2 = 0 \;\;\therefore\;\; T_i = \sqrt{T_e T_c} \tag{6.25}$$

This result is very similar to the optimum intermediate pressure for the two-stage system where the optimum pressure was obtained instead of temperature and the work requirement of the two sides was equal instead of the COPs being equal.

Case II : nonzero overlap temperature

In case the overlap temperature *DT* is not zero, hence the condenser temperature of LT side is not equal to the evaporator temperature of HT side. These temperatures are now as follows:

$$T_{c\text{LT}} = T_i + DT/2 \;\text{ and }\; T_{e\text{HT}} = T_i - DT/2$$

This cycle is shown in Figure 6.12(a). In this case:

$$(\text{COP})_{\text{RC,LT}} = T_e/(T_{c\text{LT}} - T_e) = T_e/(T_i + DT/2 - T_e)$$

and $$(\text{COP})_{\text{RC,HT}} = T_{e\text{HT}}/(T_c - T_{e\text{HT}}) = (T_i - DT/2)/(T_c - T_i + DT/2)$$

The optimum COP may be obtained by requiring the two COPs to be equal. This yields

$$\frac{T_e}{T_i + DT/2 - T_e} = \frac{T_i - DT/2}{T_c - T_i + DT/2}$$

which is simplified to

$$T_i^2 = T_e T_c + \frac{(DT)^2}{4} \;\text{ or }\; T_i = \sqrt{T_e T_c}\left(1 + \frac{(DT)^2}{4T_e T_c}\right)^{0.5} \approx \sqrt{T_e T_c}\left(1 + \frac{(DT)^2}{8T_e T_c} + \cdots\right)$$

or $$T_i = \sqrt{T_e T_c} + \frac{(DT)^2}{8\sqrt{T_e T_c}} \tag{6.26}$$

Also, taking the product of the two COPs and putting its derivative with respect to T_i equal to zero may yield the expression for optimum intermediate temperature as follows:

$$\xi = \frac{T_e}{T_{c\,\mathrm{LT}} - T_e} \cdot \frac{T_{e\,\mathrm{HT}}}{T_c - T_{e\,\mathrm{HT}}} = \frac{T_e}{T_i + \frac{DT}{2} - T_e} \frac{T_i - \frac{DT}{2}}{T_c - T_i + \frac{DT}{2}} \tag{6.27}$$

$$\frac{d\xi}{dT_i} = 0 \text{ yields}$$

$$T_i^2 - T_i\,DT + T_c\,DT - T_eT_c + \frac{DT^2}{4} = 0$$

The solution of this quadratic equation for T_i yields

$$T_i = \frac{DT}{2} \pm \frac{1}{2}\sqrt{(DT)^2 - 4\{(DT)^2/4 + T_c\,DT - 4T_eT_c\}}$$

A bionomial expansion followed by approximation yields the following expression:

$$T_i = \sqrt{T_eT_c} + \frac{DT}{2}\left[1 - \frac{T_c}{\sqrt{T_eT_c}} + \cdots\right] \tag{6.28}$$

It is observed that Eqs. (6.26) and (6.28) give slightly different results.

EXAMPLE 6.17(a) A cascade refrigeration system uses R13 on the LT side and NH_3 on the HT side. The evaporator and condenser temperatures are –75°C and 40°C respectively. In the cascade condenser, R13 condenses at –20°C and NH_3 evaporates at –25°C. Consider SSS cycles on both the sides and determine the mass flow rates, the work requirement and swept volume rates of the two sides on per TR basis, condenser heat rejection and the COP. The clearance volume ratio is 0.04.

Solution:

The cycle is shown in Figure 6.11(b) in *T–s* coordinates. The thermodynamic properties are as follows:

R13:

Temperature (°C)	*Pressure* (bar)	v_g (m^3/kg)	h_f (kJ/kg)	h_g (kJ/kg)	s_f (kJ/kg-K)	s_g (kJ/kg-K)
–75	1.414	0.1047	154.98	267.3	0.18720	1.407
–20	11.52	0.01316	176.7	283.3	1.1335	5.3368

The properties of superheated vapour at 11.52 bar are as follows:

Temperature	3°C	4°C
v	0.01589	0.01599
h	301.9	302.6
s	1.405	1.408

NH_3:

Temperature (°C)	*Pressure* (bar)	v_g (m^3/kg)	h_f (kJ/kg)	h_g (kJ/kg)	s_g (kJ/kg-K)
–25	1.515	0.771	66.91	1410.68	5.6948
40	15.55	0.0833	371.47	1472.02	4.8728

The properties of superheated vapour at 15.55 bar pressure are as follows:

Tempeature	100°C	120°C
v	0.123	0.130
h	1751.7	1802.6
s	5.65283	5.7732

LT side:

For the SSS cycle shown in Figure 6.11(b),

$$h_a = 267.3,\ s_a = 1.407,\ v_a = 0.1047 \text{ and } h_c = 176.7$$

Properties at point *b* after isentropic compression are found by interpolation in the superheat table for $s_a = s_b = 1.407$ as follows:

$$t_b = 3 + (1.407 - 1.405)/(1.408 - 1.405) = 3 + 0.667 = 3.667^oC$$

$$h_b = 301.9 + 0.667(302.6 - 301.9) = 302.37 \text{ kJ/kg}$$

$$v_b = 0.01589 + 0.667(0.01599 - 0.01589) = 0.01596 \text{ m}^3\text{/kg}$$

The mass flow rate on LT side for 1 TR cooling capacity is given by

$$\dot{m}_{LT} = \frac{3.51667 \text{ TR}}{h_a - h_d} = \frac{3.51667}{267.3 - 176.7} = 0.038815 \text{ kg/s}$$

$$\eta_{vol,LT} = 1.0 + \varepsilon - \varepsilon\,(v_a/v_b) = 1.04 - 0.04(0.1047/0.01596) = 0.7776$$

$$(\mathbb{V}_S)_{LT} = \dot{m}_{LT}\, v_a/\eta_{vol,LT} = 0.038815 \times 0.1047/0.7776 = 0.005226 \text{ m}^3\text{/s}$$

$$W_{LT} = \dot{m}_{LT}(h_b - h_a) = 0.038815(302.37 - 267.3) = 1.3612 \text{ kW}$$

$$Q_{cLT} = \dot{m}_{LT}(h_b - h_c) = 0.038815(302.37 - 176.7) = 4.8779 \text{ kW}$$

HT side:

For the SSS cycle shown in Figure 6.11(b),

$$h_1 = 1410.68,\ s_1 = 5.6948\ ,\ v_1 = 0.771 \text{ and } h_3 = 371.47$$

To find properties at point 2 after isentropic compression, we interpolate in the superheat table for $s_1 = s_2 = 5.6948$. We get

$$t_2 = 140 + 20(5.6948 - 5.6528)/(5.7732 - 5.6528) = 140 + 0.3488 \times 20$$

$$= 146.977^oC$$

$$h_2 = 1751.7 + 0.3488 \times (1802.6 - 1751.7) = 1769.456 \text{ kJ/kg}$$

$$v_2 = 0.123 + 0.3488 \times (0.13 - 0.123) = 0.1254 \text{ m}^3/\text{kg}$$

$$\eta_{\text{vol,HT}} = 1.0 + \varepsilon - \varepsilon\,(v_1/v_2) = 1.04 - 0.04(0.771/0.1254) = 0.794$$

Considering energy balance in cascade condenser

$$Q_{c\text{LT}} = Q_{e\text{HT}} \quad \text{or} \quad \dot{m}_{\text{LT}}\,(h_b - h_c) = \dot{m}_{\text{HT}}\,(h_1 - h_4)$$

$$\dot{m}_{\text{HT}} = \dot{m}_{\text{LT}}\,\frac{h_b - h_c}{h_1 - h_4} = \frac{Q_{c\,\text{LT}}}{h_1 - h_4} = \frac{4.8779}{1410.68 - 371.37} = 0.004697$$

$$(V_s)_{\text{HT}} = \dot{m}_{\text{HT}}\,v_1/\eta_{\text{vol,HT}} = 0.004697(0.771)/0.794 = 0.00455 \text{ m}^3/\text{s}$$

$$W_{\text{HT}} = \dot{m}_{\text{HT}}\,(h_2 - h_1) = 0.004694(1769.456 - 1410.68) = 1.684 \text{ kW}$$

$$Q_c = \dot{m}_{\text{HT}}\,(h_2 - h_3) = 0.004694(1769.456 - 371.47) = 6.562 \text{ kW}$$

$$\text{COP} = \frac{3.51667 \text{ TR}}{W_{\text{LT}} + W_{\text{HT}}} = \frac{3.5167}{1.3612 + 1.684} = 1.155$$

EXAMPLE 6.17(b) In Example 6.17(a) suppose the superheat table is not provided, instead the average specific heat of R13 is given to be 0.8042 kJ/kg-K and that of ammonia to be 2.7739 kJ/kg-K at their condenser pressures. Determine all the parameters of Example 6.17(a).

Solution:

The properties at point *b* of the LT side and point 2 of the HT side are determined by integrating $Tds = c_p\,dT$ along *e*–*b* and *j*–2 respectively.

LT side:

$$T_b = T_{c\,\text{LT}}\,\exp\left(\frac{s_a - s_e}{c_p}\right) = 253\exp\left(\frac{1.407 - 1.335}{0.8042}\right) = 276.696 \text{ K} = 3.696°\text{C}$$

$$h_b = 283.3 + 0.8042\,(3.696 - (-20)) = 302.356$$

$$v_b = 0.01316(276.696/353) = 0.01439$$

The mass flow rate on LT side for 1 TR cooling capacity is given by

$$\dot{m}_{\text{LT}} = \frac{3.51667 \text{ TR}}{h_a - h_d} = \frac{3.51667}{267.3 - 176.7} = 0.038815 \text{ kg/s}$$

$$\eta_{\text{vol,LT}} = 1.0 + \varepsilon - \varepsilon\,(v_a/v_b) = 1.04 - 0.04(0.1047/0.01439) = 0.749$$

$$(\mathbb{V}_S)_{\text{LT}} = \dot{m}_{\text{LT}}\,v_a/\eta_{\text{vol,LT}} = 0.038815 \times 0.1047/0.749 = 0.005425 \text{ m}^3/\text{s}$$

$$W_{\text{LT}} = \dot{m}_{\text{LT}}\,(h_b - h_a) = 0.038815(302.356 - 267.3) = 1.3607 \text{ kW}$$

$$Q_{c\text{LT}} = \dot{m}_{\text{LT}}\,(h_b - h_c) = 0.038815(302.356 - 176.7) = 4.8773 \text{ kW}$$

HT side:

Along the constant pressure line *j*–2, we get

$$T_2 = T_c\,\exp\left(\frac{s_j - s_1}{C_p}\right) = 313\exp\left(\frac{5.6948 - 4.8728}{2.7739}\right) = 420.96 \text{ K} = 147.96°\text{C}$$

$h_2 = 1472.02 + 2.7739\ (147.96 - 40) = 1771.489$

$v_2 = 0.0883\ (420.96/313) = 0.11203$

Considering energy balance in cascade condenser, mass flow rate of HT side is found by equating the condenser heat rejection of LT side to the refrigeration capacity of LT side.

$$\dot{m}_{\text{HT}} = \frac{Q_{c\,\text{LT}}}{h_1 - h_4} = \frac{4.8773}{1410.68 - 371.47} = 0.0056933 \text{ kg/s}$$

$$\eta_{\text{vol,HT}} = 1.0 + \varepsilon - \varepsilon\,(v_1/v_2) = 1.04 - 0.04(0.771/0.11203) = 0.7647$$

$$(\mathbb{V}_S)_{\text{HT}} = \dot{m}_{\text{HT}}.v_1/\eta_{\text{vol,HT}} = 0.0046933(0.771)/0.7647 = 0.00473 \text{ m}^3\text{/s}$$

$$Q_c = \dot{m}_{\text{HT}}(h_2 - h_3) = 0.004694\ (1771.489 - 371.47) = 6.571 \text{ kW}$$

$$\text{COP} = \frac{3.51667 \text{ TR}}{W_{\text{LT}} + W_{\text{HT}}} = \frac{3.5167}{1.3607 + 1.6934} = 1.1514$$

The results are very close to those obtained by interpolation in the superheat table.

EXAMPLE 6.18 Determine the parameters of Example 6.17(a) for the cascade system if (a) R12 and (b) R22 are the refrigerants on the HT side and R13 is the refrigerant on the LT side with all conditions being the same as in Example 6.17(a).

Solution:

(a) *R12:*

The properties of R12 are:

Temperature (°C)	*Pressure* (bar)	v_g (m^3/kg)	h_f (kJ/kg)	h_g (kJ/kg)	s_g (kJ/kg-K)
–25	1.238	0.1318	13.35	177.31	0.7161
40	9.634	0.0183	74.77	204.75	0.6876

The properties of superheated vapour at 9.634 bar pressure are as follow:

Tempeature	50°C	55°C
v	0.019	0.020
h	212.5	216.3
s	0.7120	0.7236

The mass flow rate, condenser heat rejection and compressor work of LT side remain unchanged. The calculations are done with $Q_{c\text{LT}}$ of LT side as the starting point. For the HT side, we have from the saturation table

$$h_1 = 177.31,\ s_1 = 0.7161\ ,\ v_1 = 0.1318 \text{ and } h_3 = 74.77$$

To find the properties at point 2 after isentropic compression, we interpolate in the superheat table for $s_1 = s_2 = 0.7120$ to obtain

$$t_2 = 50 + 5 \times (0.7161 - 0.712)/(0.7236 - 0.712)$$
$$= 50 + 0.3534 \times 5 = 51.767^{o}C$$
$$h_2 = 212.5 + 0.3534 \times (216.3 - 212.5) = 213.8431 \text{ kJ/kg}$$
$$v_2 = 0.019 + 0.3534 \times (0.02 - 0.019) = 0.01935 \text{ m}^3\text{/kg}$$
$$\eta_{vol,HT} = 1.0 + \varepsilon - \varepsilon\,(v_1/v_2) = 1.04 - 0.04(0.1318/0.01935) = 0.7676$$

Considering energy balance in cascade condenser,

$$Q_{c\text{LT}} = Q_{e\text{HT}} \quad \text{or} \quad \dot{m}_{\text{LT}}\,(h_b - h_c) = \dot{m}_{\text{HT}}(h_1 - h_4)$$

$$\therefore \quad \dot{m}_{\text{HT}} = \dot{m}_{\text{LT}}\,\frac{h_b - h_c}{h_1 - h_4} = \frac{Q_{c\,\text{LT}}}{h_1 - h_4} = \frac{4.87792}{177.31 - 74.77} = 0.04757 \text{ kg/s}$$

$$(\mathbb{V}_S)_{\text{HT}} = \dot{m}_{\text{HT}}\,v_1/\eta_{vol,HT} = 0.04757(0.1318)/0.7676 = 0.00817 \text{ m}^3\text{/s}$$
$$W_{\text{HT}} = \dot{m}_{\text{HT}}(h_2 - h_1) = 0.04757(213.8431 - 177.31) = 1.7379 \text{ kW}$$
$$Q_c = \dot{m}_{\text{HT}}(h_2 - h_3) = 0.04757(213.8431 - 74.77) = 6.616 \text{ kW}$$
$$\text{COP} = \frac{3.51667 \text{ TR}}{W_{\text{LT}} + W_{\text{HT}}} = \frac{3.51667}{1.3612 + 1.7379} = 1.1347$$

(b) *R22:*

The properties of R22 are:

Temperature (°C)	*Pressure* (bar)	v_g (m^3/kg)	h_f (kJ/kg)	h_g (kJ/kg)	s_g (kJ/kg-K)
–25	2.016	0.112	16.77	241.09	0.9734
40	15.267	0.0152	95.4	261.38	0.8767

The properties of superheated vapour at 9.634 bar pressure are as follow:

Tempeature	70°C	80°C
v	0.0182	0.0191
h	288.31	296.84
s	0.9592	0.9832

From the saturation table for R22, we get

$$h_1 = 241.09,\ s_1 = 0.9734\ ,\ v_1 = 0.112 \text{ and } h_3 = 95.4$$

To find the properties at point 2 after isentropic compression, we interpolate in the superheat table for $s_1 = s_2 = 0.9734$ to obtain

$$t_2 = 70 + 10 \times (0.9734 - 0.9592)/(0.9832 - 0.9592)$$
$$= 70 + 0.59167 \times 10 = 75.9167^{o}C$$

$$h_2 = 288.31 + 0.59167 \times (296.84 - 288.31) = 293.357 \text{ kJ/kg}$$

$$v_2 = 0.0182 + 0.59167 \times (0.0191 - 0.0182) = 0.018732 \text{ m}^3/\text{kg}$$

$$\eta_{\text{vol,HT}} = 1.0 + \varepsilon - \varepsilon\,(v_1/v_2) = 1.04 - 0.04(0.112/0.018732) = 0.80084$$

Considering energy balance in cascade condenser,

$$Q_{c\text{LT}} = Q_{e\text{HT}} \quad \text{or} \quad \dot{m}_{\text{LT}}\,(h_b - h_c) = \dot{m}_{\text{HT}}\,(h_1 - h_4)$$

$$\dot{m}_{\text{HT}} = \dot{m}_{\text{LT}}\,\frac{h_b - h_c}{h_1 - h_4} = \frac{Q_{c\,\text{LT}}}{h_1 - h_4} = \frac{4.87792}{241.09 - 95.4} = 0.03348 \text{ kg/s}$$

$$(\mathbb{V}_S)_{\text{HT}} = \dot{m}_{\text{HT}}.v_1/\eta_{\text{vol,HT}} = 0.03348(0.112)/0.80084 = 0.00468 \text{ m}^3/\text{s}$$

$$W_{\text{HT}} = \dot{m}_{\text{HT}}(h_2 - h_1) = 0.03348(293.357 - 241.09) = 1.74998 \text{ kW}$$

$$Q_c = \dot{m}_{\text{HT}}(h_2 - h_3) = 0.03348(293.357 - 95.4) = 6.628 \text{ kW}$$

$$\text{COP} = \frac{3.51667 \text{ TR}}{W_{\text{LT}} + W_{\text{HT}}} = \frac{3.51667}{1.3612 + 1.74998} = 1.1303$$

It is observed that the COP for NH_3 is the highest followed by R12, and R22 has the minimum COP, all of them being very close together. The swept volume rate is very similar for NH_3 and R22 while, the swept volume rate for R12 is approximately twice that of R22.

6.7.2 Performance Improvement of Cascade System

The cascade refrigeration system faces some unbalance problems during pull-down. At the time of starting the system, the evaporator, the cascade condenser and the condenser are all at room temperature. During pull-down the power requirement of the LT side passes through a peak and the heat rejection also passes through a peak. The HT side may not be able to take this load since it is designed for steady-state load.

It was observed that the COPs of R12 and R502 increase with increase in suction superheat, whereas those for NH_3 and R22 decrease. The COP decreases with increase in superheat for all the recommended LT side refrigerants, namely, R13, R14, R13B1, CO_2, ethane, and nitrus oxide N_2O.

In any case, the LT compressor is kept under ambient conditions and the suction line is insulated. The insulation cannot be perfect, hence leakage heat transfer through insulation will superheat the LT vapour. This increase in superheat is wasteful, hence it is advisable to subcool the liquid refrigerant by this vapour in a subcooling heat exchanger. This is illustrated in Figures 6.13(a) and 6.13(b) where HEX 1 does this. The temperature at a' is so low that this vapour before entry to LT compressor can subcool even the liquid refrigerant of HT side in HEX 2 . This cycle may not improve the COP of the system but it is a more practical cycle.

It was pointed out in an earlier section that subcooling is desirable and superheating may be done even right up to condenser temperature. If the vapour enters the compressor at higher temperature, then the discharge temperature at b' may be high enough to reject heat to water in a HEX along b'–b'' and save the load on cascade condenser. It is certainly desirable to reject heat directly to surroundings rather than to a medium at low temperature, which in turn rejects it to surroundings.

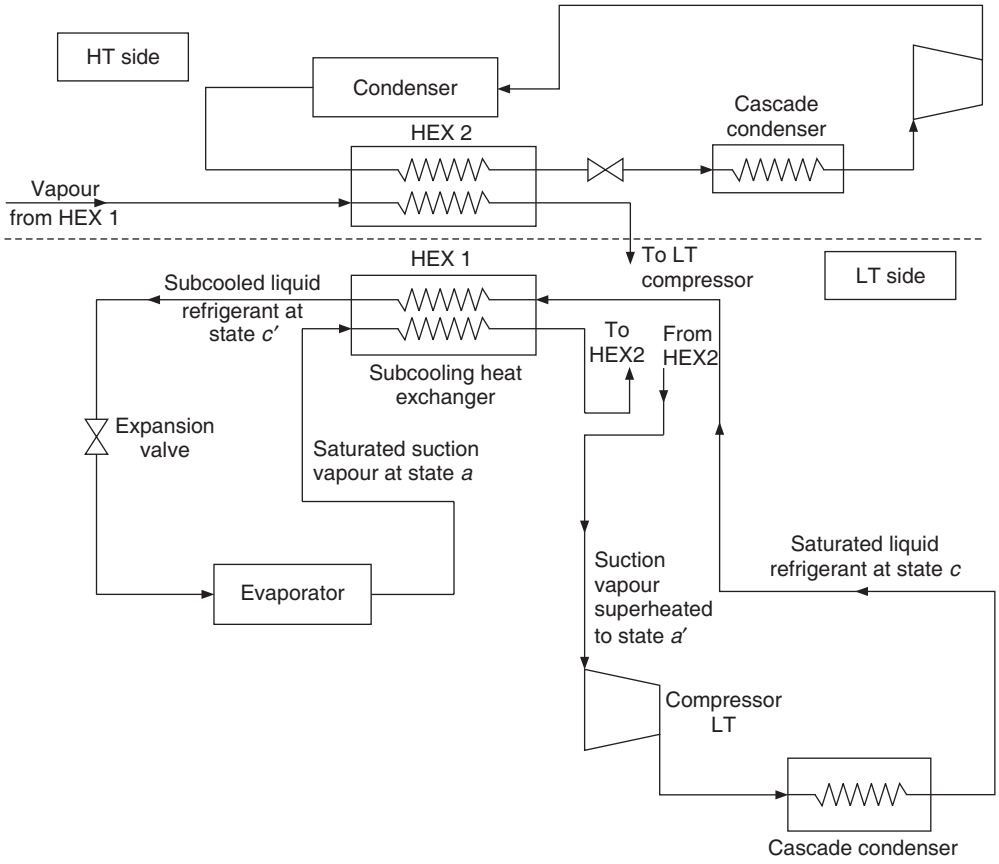

Figure 6.13(a) Flow diagram illustrating the use of subcooling heat exchangers in LT and HT sides of cascade refrigeration system.

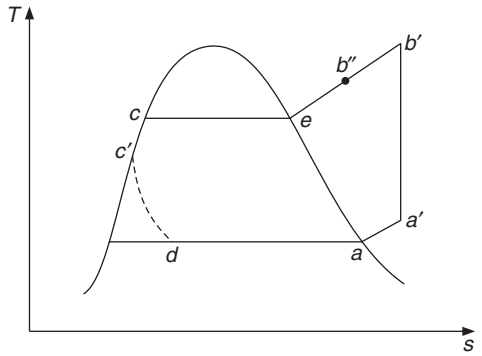

Figure 6.13(b) *T–s* diagram of the LT side of the system in Figure 6.13(a).

EXAMPLE 6.19(a) In a cascade refrigeration system, R13 and NH_3 are used on LT and HT sides respectively. The evaporator and condenser temperatures are –75°C and 40°C respectively. In cascade condenser, R13 condenses at –20°C and NH_3 evaporates at –25°C similar to that in Example 6.17(a). The vapour leaving the evaporator is used to subcool the liquid leaving the cascade condenser in a subcooling heat exchanger. The vapour leaves the heat exchanger at –50°C. Determine the parameters of Example 6.17(a).

Solution:

Superheat data for R13 at pressure of 1.414 bar (–75°C) is as follows.

Tempeature	–50°C	–30°C
v	0.1207	0.1330
h	281.4	293.1
s	1.475	1.525

The properties of superheated R13 vapour at 11.52 bar are as follows:

Temperature	3°C	4°C	30°C	40°C	51°C	52°C
v	0.01589	0.01599	0.01853	0.01942	0.02040	0.02048
h	301.9	302.6	322.0	329.3	337.3	338.0
s	1.405	1.408	1.475	1.4975	1.523	1.526

The schematic diagram of the LT side and *T*–*s* cycle of the LT side are shown in Figures 6.13(a) and 6.13(b) respectively. From the saturation table for R13 (see Example 6.17(a)), we get

$$h_a = 267.3,\ s_a = 1.407,\ v_a = 0.1047 \text{ and } h_c = 176.7$$

From the superheat table for R13 at1.414 bar at –50°C

$$h_{a'} = 281.4,\ s_{a'} = 1.475 \text{ and } v_{a'} = 0.1207$$

Energy balance across the heat exchanger gives: $h_{a'} - h_a = h_c - h_{c'}$

Therefore $h_{c'} = 176.7 - (281.4 - 267.3) = 162.6$ kJ/kg

To locate point b' after isentropic compression we interpolate in superheat table at 11.52 bar at $s_{b'} = s_{a'} = 1.475$.

It is observed that the table luckily has $s = 1.475$ at $t = 30$°C, therefore interpolation is not required. At 30°C, and $p = 11.52$ bar, $h_{b'} = 322.0$ and $v_{b'} = 0.01853$

$$\dot{m}_{LT} = \frac{3.51667 \text{ TR}}{h_a - h_{c'}} = \frac{3.51667}{267.3 - 162.6} = 0.033588 \text{ kg/s}$$

$$\eta_{vol,LT} = 1.0 + \varepsilon - \varepsilon\,(v_{a'}/v_{b'}) = 1.04 - 0.04(0.1207/0.01853) = 0.77945$$

$$(\mathbb{V}_S)_{LT} = \dot{m}_{LT}\, v_{a'}/\eta_{vol,LT} = 0.033588 \times 0.1207/0.77945 = 0.0052 \text{ m}^3\text{/s}$$

$$W_{LT} = \dot{m}_{LT}\,(h_{b'} - h_{a'}) = 0.033588\ (322.0 - 281.4) = 1.3637 \text{ kW}$$

$$Q_{cLT} = \dot{m}_{LT}\,(h_{b'} - h_c) = 0.033588\ (322.0 - 176.7) = 4.88034 \text{ kW}$$

$$\dot{m}_{HT} = \dot{m}_{LT}\frac{h_{b'} - h_c}{h_1 - h_4} = \frac{Q_{c\,LT}}{h_1 - h_4} = \frac{4.88034}{1410.68 - 371.47} = 0.0046962$$

$$(\mathbb{V}_s)_{HT} = \dot{m}_{HT}\, v_1/\eta_{vol,HT} = 0.0046962(0.771)/0.794 = 0.00456 \text{ m}^3/\text{s}$$

$$W_{HT} = \dot{m}_{HT}\,(h_2 - h_1) = 0.0046962(1769.456 - 1410.68) = 1.68488 \text{ kW}$$

$$Q_c = \dot{m}_{HT}\,(h_2 - h_3) = 0.0046962(1769.456 - 361.47) = 6.565 \text{ kW}$$

$$\text{COP} = \frac{3.51667 \text{ TR}}{W_{LT} + W_{HT}} = \frac{3.5167}{1.3612 + 1.68488} = 1.1535$$

It is observed that the COP decreases marginally. However, for practical reasons the inclusion of the subcooling heat exchanger is recommended. In the next example the extent of subcooling is increased to see its effect on COP.

EXAMPLE 6.19(b) Superheat tables are not provided as given in Example 6.19(a), but it is given that the average specific heat of R13 at its evaporator pressure is 0.564 kJ/kg-K and the average specific heat at condenser pressure is 0.774 kJ/kg-K. The average specific heat of ammonia is 2.739 as in Example 6.17(b). Using these specific heats, determine all the parameters of Example 6.17(b).

Solution:

We have

$$T_a = 273 - 75 = 198 \text{ K and } T_{a'} = 273 - 50 = 223 \text{ K}$$

From the saturation table for R13, we get

$h_a = 267.3$, $s_a = 1.407$, $v_a = 0.1047$ and $h_c = 176.7$

$h_e = 283.3$, $s_e = 1.335$, $v_e = 0.01316$

$h_{a'} = 267.3 + 0.564\,(25) = 281.4$ and $v_{a'} = v_a T_{a'}/T_a = 0.1047(223/198) = 0.11792$

$s_{a'} = s_a + c_{pa} \ln (T_{a'}/T_a) = 1.407 + 0.564 \ln (223/198) = 1.47406$

Energy balance for the heat exchanger gives : $h_{a'} - h_a = h_c - h_{c'}$. Actually $h_{a'}$ is the same as in Example 6.19(a), therefore $h_{c'}$ will also remain the same, that is $h_{c'} = 162.6$.

We determine temperature $T_{b'}$ by using specific heat of 0.774 kJ/kg-K along e–b'

$$T_{b'} = T_e \exp\left(\frac{s_{a'} - s_e}{c_p}\right) = 253 \exp\left(\frac{1.47406 - 1.335}{0.774}\right) = 302.794 \text{ K} = 29.794°\text{C}$$

$h_{b'} = 283.3 + 0.774\,(29.794 - (-20)) = 321.84$

$v_{b'} = 0.01316(302.794/253) = 0.01575$

The mass flow rate through LT side remains the same, that is, $\dot{m}_{LT} = 0.033588$ kg/s

$$\eta_{vol,LT} = 1.0 + \varepsilon - \varepsilon\,(v_{a'}/v_{b'}) = 1.04 - 0.04(0.11792/0.01575) = 0.7405$$

$$(\mathbb{V}_S)_{LT} = \dot{m}_{LT}\, v_a/\eta_{vol,LT} = 0.033588 \times 0.11792/0.7405 = 0.00535 \text{ m}^3/\text{s}$$

$$W_{LT} = \dot{m}_{LT}\,(h_{b'} - h_{a'}) = 0.033588\,(321.84 - 281.4) = 1.3483 \text{ kW}$$

$$Q_{cLT} = \dot{m}_{LT}\,(h_{b'} - h_c) = 0.033588\,(321.84 - 176.7) = 4.875 \text{ kW}$$

$$\dot{m}_{HT} = \dot{m}_{LT}\frac{h_{b'} - h_c}{h_1 - h_4} = \frac{Q_{c\,LT}}{h_1 - h_4} = \frac{4.875}{1410.68 - 371.47} = 0.004691$$

The enthalpy after isentropic compression on HT side is same as determined in Example 6.16(b), that is,

$$h_2 = 1771.489\ ,\ v_2 = 0.11203 \text{ and } \eta_{vol,HT} = 0.7647$$

$$(\mathbb{V}_S)_{HT} = \dot{m}_{HT}\, v_1/\eta_{vol,HT} = 0.004691(0.771)/0.7647 = 0.00473 \text{ m}^3/\text{s}$$

$$W_{HT} = \dot{m}_{HT}\,(h_2 - h_1) = 0.004691\ (1771.489 - 1410.68) = 1.6925 \text{ kW}$$

$$Q_c = \dot{m}_{HT}\,(h_2 - h_3) = 0.004691\ (1771.489 - 371.47) = 6.567 \text{ kW}$$

$$\text{COP} = \frac{3.51667 \text{ TR}}{W_{LT} + W_{HT}} = \frac{3.51667}{1.3583 + 1.6925} = 1.1527$$

EXAMPLE 6.20(a) If the vapour in Example 6.19 leaves the subcooling heat exchanger at –30°C, all other parameters remaining the same, determine the mass flow rates, swept flow rates and COP.

Solution:

The cycle is the same as shown in Figures 6.13(a) and (b). The superheat table of R13 in Example 6.19 gives the data for –30°C, 1.414 bar as well.

$$v_{a'} = 0.133,\ h_{a'} = 293.1,\ s_{a'} = 1.525 \text{ also } h_a = 267.3 \text{ and } h_c = 176.7$$

An energy balance for the heat exchanger gives, $h_{c'} = 176.7 - (293.1 - 267.3) = 150.9$
To find the properties at point b' we interpolate in the R13 superheat table for 11.52 bar
For $s_{b'} = s_{a'} = 1.525$, we get

$$t_{b'} = 51 + (1.525 - 1.523)/(1.526 - 1.523) = 51 + 0.6667 = 51.6667\ ^{o}\text{C}.$$

$$h_{b'} = 337.3 + 0.6667(338 - 337.3) = 337.767 \text{ and } v_{b'} = 0.020453$$

$$\dot{m}_{LT} = \frac{3.51667 \text{ TR}}{h_a - h_{c'}} = \frac{3.5167}{267.3 - 150.9} = 0.03021 \text{ kg/s}$$

$$\eta_{vol,LT} = 1.0 + \varepsilon - \varepsilon\,(v_{a'}/v_{b'}) = 1.04 - 0.04(0.133/0.020453) = 0.77989$$

$$(\mathbb{V}_S)_{LT} = \dot{m}_{LT}\, v_a/\eta_{vol,LT} = 0.03021 \times 0.133/0.77945 = 0.002576 \text{ m}^3/\text{s}$$

$$W_{LT} = \dot{m}_{LT}\,(h_{b'} - h_{a'}) = 0.03201(337.767 - 293.1) = 1.34947 \text{ kW}$$

$$Q_{cLT} = \dot{m}_{LT}\,(h_{b'} - h_c) = 0.03021(337.767.0 - 176.7) = 4.866142 \text{ kW}$$

$$\dot{m}_{HT} = \dot{m}_{LT}\frac{h_{b'} - h_c}{h_1 - h_4} = \frac{Q_{c\,LT}}{h_1 - h_4} = \frac{4.866142}{1410.68 - 371.37} = 0.0046825 \text{ kg/s}$$

$$(\mathbb{V}_S)_{HT} = \dot{m}_{HT}\, v_1/\eta_{vol,HT} = 0.0046825(0.771)/0.794 = 0.004547 \text{ m}^3/\text{s}$$

$$W_{HT} = \dot{m}_{HT}\,(h_2 - h_1) = 0.0046825(1769.456 - 371.47) = 1.67998 \text{ kW}$$

$$Q_c = \dot{m}_{HT}\,(h_2 - h_3) = 0.0046825(1769.456 - 371.47) = 6.546 \text{ kW}$$

$$\text{COP} = \frac{3.51667 \text{ TR}}{W_{LT} + W_{HT}} = \frac{3.51667}{1.34947 + 1.67998} = 1.1608$$

EXAMPLE 6.20(b) The vapour leaves the subcooling heat exchanger at –30°C. All other parameters are the same except that a water intercooler is used to cool the compressed LT vapour from 51.6667°C (in Example 6.20(a)) to 40°C, that is from state b' to state b'' as shown in Figure 6.13(b). Determine the mass flow rates, swept flow rates and the COP.

Solution:

The enthalpy of R13 vapour at 40°C, 11.52 bar from Table in Example 6.19(a) is

$$h_{b''} = 329.3 \text{ kJ/kg}$$

This does not change the mass flow rate through the LT compressor, however, it reduces the load on the cascade condenser and consequently it reduces the mass flow rate on the HT side.

$$Q_{c\text{LT}} = \dot{m}_{\text{LT}} (h_{b''} - h_c) = 0.03021(329.3 - 176.7) = 4.61033 \text{ kW}$$

$$\dot{m}_{\text{HT}} = \frac{Q_{c\,\text{LT}}}{h_1 - h_4} = \frac{4.61033}{1410.68 - 371.37} = 0.0044364 \text{ kg/s}$$

$$(\mathbb{V}_S)_{\text{HT}} = \dot{m}_{\text{HT}} v_1/\eta_{\text{vol,HT}} = 0.0044364(0.771)/0.794 = 0.004308 \text{ m}^3\text{/s}$$

$$W_{\text{HT}} = \dot{m}_{\text{HT}} (h_2 - h_1) = 0.0044364(1769.456 - 1410.68) = 1.59166 \text{ kW}$$

$$Q_c = \dot{m}_{\text{HT}} (h_2 - h_3) = 0.0044364(1769.456 - 371.47) = 6.202 \text{ kW}$$

$$\text{COP} = \frac{3.51667 \text{ TR}}{W_{\text{LT}} + W_{\text{HT}}} = \frac{3.5167}{1.34947 + 1.59166} = 1.19568$$

It is observed that the COP improves by reducing the load on the cascade condenser. The vapour entering the LT compressor at –30°C has the potential to do further subcooling. In fact, the subcooling of the HT stage liquid is also done by the LP vapour. The following example illustrates this.

EXAMPLE 6.21 In a cascade Refrigeration system R13 and NH_3 are used on LT and HT side respectively. The evaporator and condenser temperatures are –75°C and 40°C respectively. In cascade condenser, R13 condenses at –20°C and NH_3 evaporates at –25°C similar to that in Example 6.17. The vapour leaving the evaporator is used to subcool the liquid leaving the cascade condenser in a subcooling heat exchanger. The vapour leaves this heat exchanger (HEX1) at –50°C. This vapour then subcools the liquid of the HT side from 3 to 3′ as shown in Figure 6.14 and its vapour leaves the second heat exchanger at –30°C as shown in Figure 6.13(a). The compressed vapour of the LT side is cooled to 40°C in a water cooled HEX. The *T*–*s* diagram of the LT side of this example is shown in Figure 6.15. Determine the parameters of Example 6.17.

Solution:

The enthalpy values for R13 are same as in Example 6.19(b), that is,

$$h_{a'} = 281.4, \text{ at } -50^\circ\text{C}$$

From energy balance across HEX1 just like in Example 6.19(a), we get $h_{c'} = 162.6$
From superheat table at 1.414 bar –30°C for R13, we have

$$v_{a''} = 0.133,\ h_{a''} = 293.1,\ s_{a''} = 1.525, \text{ also } h_a = 267.3 \text{ and } h_c = 176.7$$

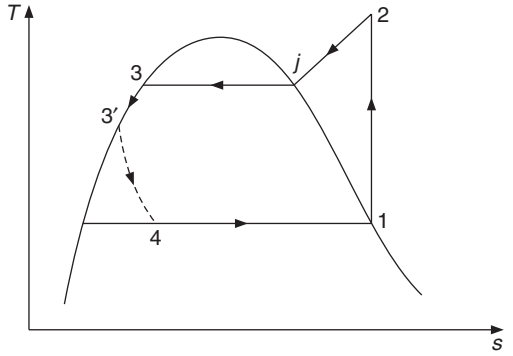

Figure 6.14 *T–s* diagram of the HT side of the system in Figure 6.13(a).

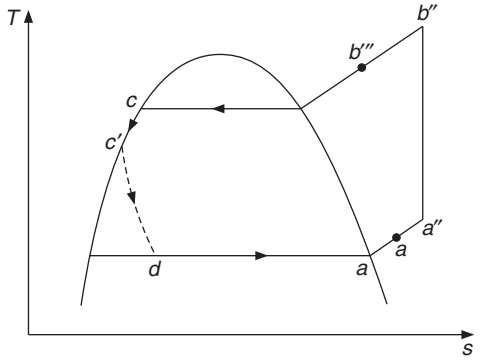

Figure 6.15 *T–s* diagram of LT side of the cascade system of Example 6.21.

For $s_{b''} = s_{a''} = 1.525$, we have from Example 6.20(a),

$$t_{b''} = 51.6667^{o}\text{C},\ h_{b''} = 337.767 \text{ and } v_{b'''} = 0.020453$$

At the exit of the water cooled HEX, $h_{b'''} = 329.3$

$$\dot{m}_{LT} = \frac{3.5167}{267.3 - 162.6} = 0.033588 \text{ kg/s}$$

$$W_{LT} = \dot{m}_{LT}\,(h_{b''} - h_{a''}) = 0.033588(337.767 - 293.1) = 1.500276 \text{ kW}$$

The mass flow rate of the HT side cannot be determined just by energy balance across the cascade condenser. This is coupled with the energy balance of HEX2 which determines the enthalpy of HT side at inlet to cascade condenser. We have for HEX2,

$$\dot{m}_{LT}\,(h_{a''} - h_{a'}) = \dot{m}_{HT}\,(h_3 - h_{3'})$$

We have for the cascade condenser,

$$\dot{m}_{LT}\,(h_{b'''} - h_c) = \dot{m}_{HT}\,(h_1 - h_{3'}) = \dot{m}_{HT}\,(h_1 - h_{3'} + h_3 - h_3) = \dot{m}_{HT}\,(h_1 - h_3) + \dot{m}_{HT}\,(h_3 - h_{3'})$$

Substituting for $\dot{m}_{HT}\,(h_3 - h_{3'})$ from the last equation, we get

$$\dot{m}_{LT}\,(h_{b'''} - h_c) = \dot{m}_{HT}\,(h_1 - h_3) + \dot{m}_{LT}\,(h_{a''} - h_{a'})$$

$$\therefore \quad \dot{m}_{LT}(h_{b'''} - h_c - (h_{a''} - h_{a'}) = \dot{m}_{HT}(h_1 - h_3)$$

or
$$\dot{m}_{HT} = \frac{329.3 - 176.7 - (293.1 - 281.4)}{1410.68 - 371.37} = 0.00455391 \text{ kg/s}$$

$$W_{HT} = \dot{m}_{HT}(h_2 - h_1) = 0.00455391(1769.456 - 371.47) = 1.63386 \text{ kW}$$

$$Q_c = \dot{m}_{HT}(h_2 - h_3) = 0.00455391(1769.456 - 371.47) = 6.3664 \text{ kW}$$

$$\text{COP} = \frac{3.51667 \text{ TR}}{W_{LT} + W_{HT}} = \frac{3.5167}{1.500276 + 1.63386} = 1.12205$$

It is observed that the COP decreases compared to the simple cascade refrigeration system. However, this system is more practical since it prevents the slugging of the LT compressor and prevents the entry of vapour into the LT and HT expansion valves.

Cascade systems find applications in food, pharmaceutical, and chemical processing used in petroleum and chemical industries or in laboratory environmental chambers and thermal storage equipment. A two-stage cascade is normally used in the range of –80°C. A three-stage cascade is required for evaporator temperature of –100°C. Normally during off-cycle the liquid refrigerant is stored in the reservoir at condenser pressure. In the cascade system, during the off-cycle period the temperature rises and the liquid on the LT side vaporises since its condenser temperature is around –20°C and the temperature becomes 40°C. As it vaporises, its pressure also increases. To limit the pressure rise, expansion tanks are provided. These are called *fade out tanks.* In fact, the entire charge on the LT side will be in vapour state during the off-cycle.

R13 was a popular refrigerant for the LT side. It is not ozone-friendly, hence it is not used any longer. HFC23 and R508b are commonly used these days. Azeotrope R508b consists of HFC23 and HFC16 in proportion of 46%:54% by weight. For the HT side, HFC 134a, HCFC-22, NH_3 and R507 (550/50 HFC125/HCFC143a) are commonly used. HFC refrigerants require polyolester synthetic lubricants. Hydro-treated paraffine oil is recommended for ammonia.. An oil separator must be used and it should not have more than 5 ppm carry-over.

6.8 DRY ICE MANUFACTURE

Figure 6.16 shows the *p–h* diagram for carbon dioxide. It has critical pressure and temperature of 71.8 bar and 31°C respectively. Its triple point is 5.18 bar, –56.6°C. The triple point is far above the atmospheric pressure. Hence, at atmospheric pressure CO_2 exists in solid and vapour phase. If liquid CO_2 comes out of a high-pressure cylinder into the atmosphere, it will expand along the constant enthalpy line *A–B*. At point *B* the pressure is atmospheric and the state is a mixture of solid dry ice and vapour. A pure substance cannot exist in stable liquid state at pressures below its triple point pressure. Hence, it is observed that CO_2 cannot exist in stable liquid state below 5.18 bar. In contrast, water has triple point pressure of 0.611 kPa and it can exist as subcooled liquid at all temperatures above its triple point temperature of 0.01°C and pressures above 0.611 kPa.

Solid CO_2 or dry ice at atmospheric pressure sublimes into vapour phase at –78.52°C, which is a very low temperature, hence it can readily absorb its enthalpy of sublimation and produce cooling.

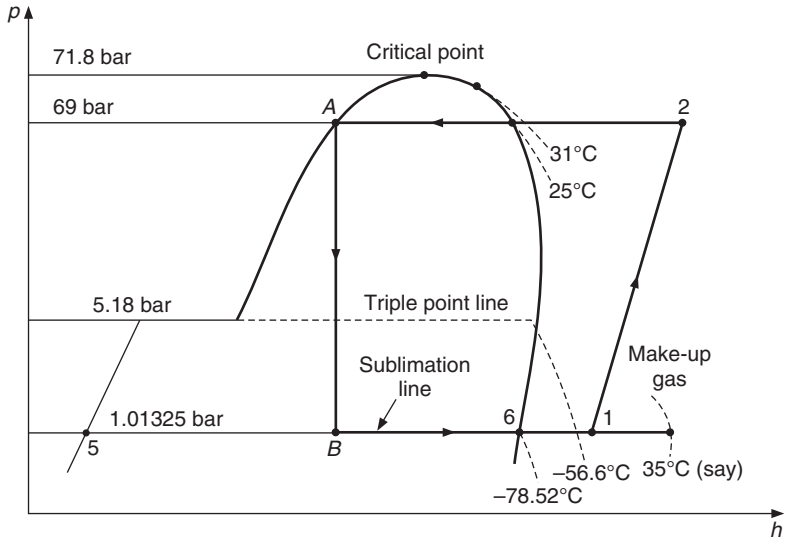

Figure 6.16 *p–h* cycle for simple vapour compression cycle for manufacture of dry ice.

Dry ice can be made by a throttling process like *A–B* starting from saturated liquid from condenser at say 25°C. For the condenser temperature to be 25°C the water from the cooling tower should also be available at temperature less than 25°C. This restriction on water temperature is because of the low critical temperature at 31°C for CO_2. At higher water temperatures, heat rejection cannot occur by condensation, it will have to carried out in the supercritical region with larger irreversibility. Hence, in such cases, a cascade refrigeration is recommended with ammonia on the HT side, and CO_2 then rejects heat to ammonia at around –20°C to –10°C in the cascade condenser. The HT side uses water for heat rejection in the condenser from ammonia.

Figure 6.17(a) shows the schematic diagram of a two-stage dry ice system if condenser heat rejection is possible at 25°C. Figure 6.17(b) shows the thermodynamic cycle diagram on *p–h* coordinates. It is observed that this is the most elementary two-stage cycle using a flash chamber with flash gas removal along 9 and desuperheating or intercooling along 2–3. The saturated liquid after condensation is at state 6 and it is throttled to state 7. The flash vapour at state 9 is adiabatically mixed with stream 3 and is passed to the HP compressor. The liquid at state 8 expands along 8–10 ending up at 10 in the solid–vapour region. The snowmaker makes dry ice at state 11. The remaining vapour at state 12 (called revert vapour) is mixed with make-up CO_2 at state 13 and enters the LP compressor. After the snowmaker has been filled with snow, a mixture of dry ice and vapour, a hydraulic ram compresses it to make dry ice. The density of dry ice is around 1500 kg/m^3.

The cycle calculations follow the procedure outlined for the two-stage systems except that additional mass and energy balance is required for the snowmaker. Mass balance and energy balance for the flash chamber yields

$$\dot{m}_6 = \dot{m}_8 + \dot{m}_9 \tag{6.29}$$

and

$$\dot{m}_6 h_6 = \dot{m}_8 h_8 + \dot{m}_9 h_9$$

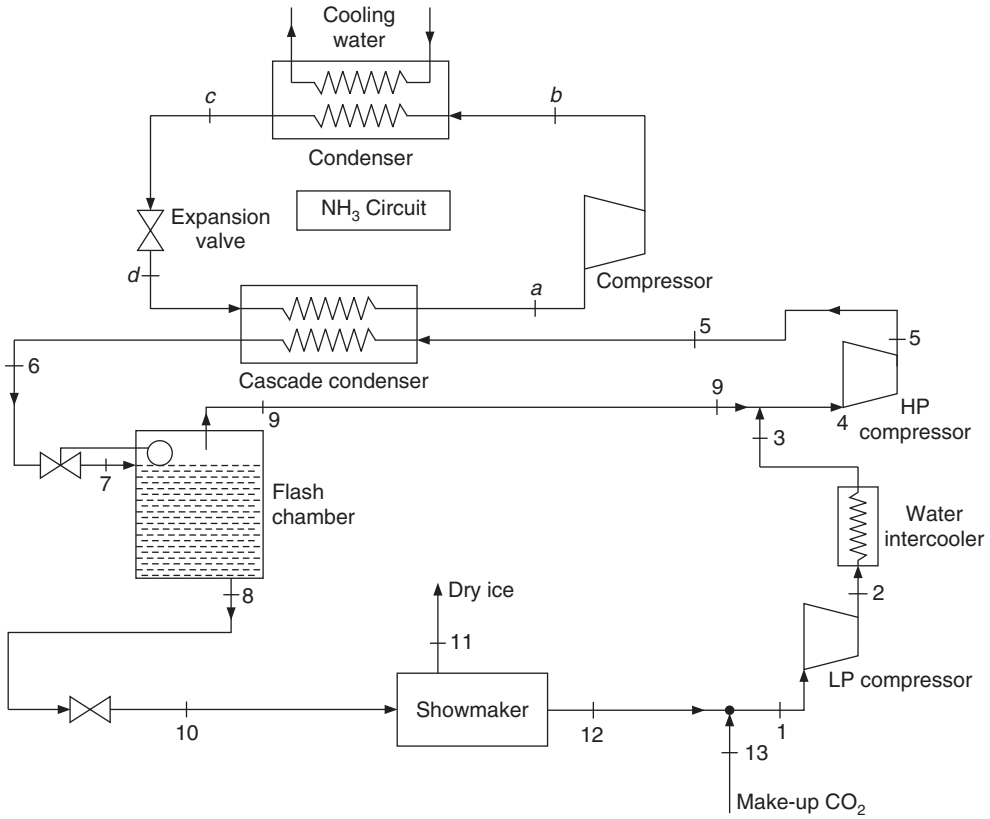

Figure 6.17(a) Schematic diagram of two-stage dry ice system with ammonia in the cascade circuit.

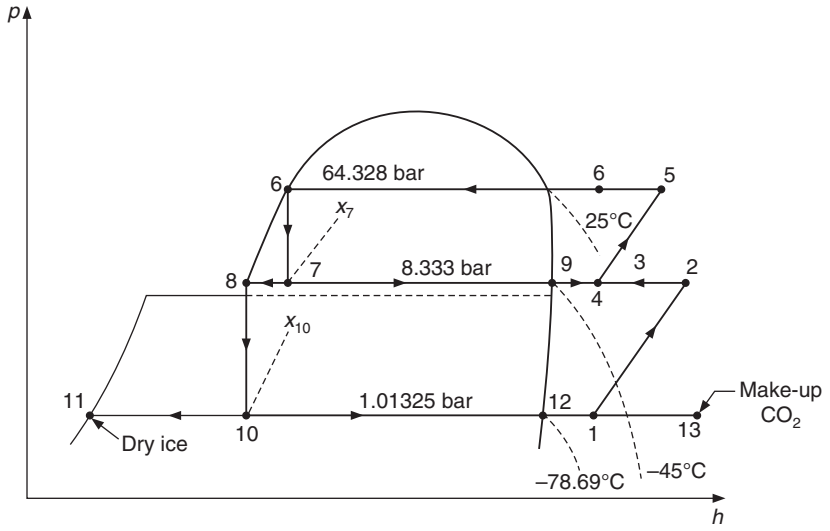

Figure 6.17(b) *p–h* diagram of CO_2 circuit for Figure 6.17(a).

Substituting from Eq. (6.29) for $\dot{m}_9$, we get

$$\dot{m}_6 h_6 = \dot{m}_8 h_8 + \dot{m}_6 h_9 - \dot{m}_8 h_9$$

or
$$\frac{\dot{m}_8}{\dot{m}_6} = \frac{h_9 - h_6}{h_9 - h_8} \tag{6.30}$$

Mass and energy balance for the snowmaker yields

$$\dot{m}_{10} = \dot{m}_{11} + \dot{m}_{12} \quad \text{and} \quad \dot{m}_{10} h_{10} = \dot{m}_{11} h_{11} + \dot{m}_{12} h_{12}$$

which are simplified to yield

$$\dot{m}_{10} h_{10} = \dot{m}_{11} h_{11} + \dot{m}_{10} h_{12} - \dot{m}_{11} h_{12}$$

or
$$\frac{\dot{m}_{11}}{\dot{m}_{10}} = \frac{h_{12} - h_{10}}{h_{12} - h_{11}} \tag{6.31}$$

The calculation starts with the specified production rate of dry ice, i.e. $\dot{m}_{11}$. The mass flow rate of make-up CO_2 will be same as the $\dot{m}_{11}$, i.e.

$$\dot{m}_{13} = \dot{m}_{11}$$

Mass flow rate at inlet to compressor $\dot{m}_1$ is same as that at inlet to snowmaker $\dot{m}_{10}$, i.e.

$$\dot{m}_1 = \dot{m}_{10}$$

Therefore, $\dot{m}_1$ is determined from Eq. (6.31), Also, for LP and HP stages we have

$$\dot{m}_1 = \dot{m}_8 \quad \text{and} \quad \dot{m}_4 = \dot{m}_6$$

Therefore the mass flow rate through the high-pressure compressor $\dot{m}_4$ is determined from Eq. (6.30). The work requirements of the compressors are as follows:

$$W_{LP} = \dot{m}_1 (h_2 - h_1)$$

and
$$W_{HP} = \dot{m}_4 (h_5 - h_4)$$

In case the water temperature is high, the cycle is not suitable for operation. The compression of gas when cold water temperature is greater than the critical temperature and other cycles have been discussed by Stickney (1932).

EXAMPLE 6.22 A dry ice plant of 1 kg/s capacity uses a two-stage refrigeration system. The heat rejection in the condenser takes place at 25°C to the water. The first stage compressor compresses CO_2 from 1.01325 bar (–78.69°C) to a pressure of 8.333 bar (–45°C). The LP vapour is desuperheated to 30°C in a water intercooler. The second stage compressor operates between 8.333 bar to 64.328 bar (25°C). Determine the state points on the cycle shown in Figure 6.17(b) and find the mass flow rates, swept flow rates and work requirement of both the compressors, condenser heat rejection and COP.

Solution:

The properties at saturation are as follows:

p (bar)	t (°C)	v_f (dm^3/kg)	v_g (dm^3/kg)	h_f (kJ/kg)	h_g (kJ/kg)	s_f (kJ/kg-K)	s_g (kJ/kg-K)
1.01325	–78.69	0.64	364.34	–259.5061	311.7526	–1.2029	1.73507
6.8364	–50	0.8669	55.407	–18.8015	318.696	–0.0813	0.2382
8.333	–45	0.8814	45.809	–9.463	319.954	–0.04063	1.40298
26.4936	–10	1.0183	14.194	60.8723	322.2971	0.2382	1.23173
64.328	25	1.4025	4.1322	159.391	280.515	0.5791	0.98346

For the *solid dry ice* at –78.69°C; entropy $s_s = -1.2029$ and enthalpy $h_s = -259.506$

The properties of superheated carbon dioxide are as follows:

t	1.0325 bar (–78.69°C)			8.333 bar (–45°C)			64.328 bar (25°C)		
(°C)	v	h	s	v	h	s	v	h	s
–30	448.75	351.14	1.9112	50.33	336.681	1.46787			
–20	467.83	359.35	1.9439	53.248	346.708	1.50848			
–10	486.84	367.64	1.9757	55.947	356.48	1.54658			
10	524.75	384.345	2.0368	61.202	375.605	1.6165			
20	543.65	392.803	2.0666	63.769	385.051	1.64916			
30	562.52	401.344	2.0955	66.296	394.454	1.68056	4.92	294.126	1.01235
90	675.3	454.516	2.255	80.945	450.629	1.85013	8.905	412.072	1.3812
100	694.05	463.685	2.2797	83.342	460.099	1.87608	9.359	424.897	1.41491
110	712.8	472.896	2.304	85.73	469.612	1.90079	9.799	437.269	1.44777
120	731.54	482.191	2.3278	88.108	479.17	1.92507	10.226	449.301	1.48018
130				90.485	488.804	1.94948	10.64	461.02	1.5102
140				92.863	498.438	1.97293	11.04	472.454	1.53804
150				95.231	508.08	1.99595	11.43	483.612	1.56421

Solution:

Referring to Figure 6.17(b), we have

$h_6 = h_f$ (25°C) = 159.391, $h_8 = h_f$ (–45°C) = –9.463, $h_9 = h_g$ (–45°C) = 319.954

h_{11} is saturated solid at –78.69 °C = h_s (–78.69°C) = –259.5061

h_{12} is saturated vapour at –78.69 °C = h_g (–78.69°C) = 311.7526

h_{13} is superheated vapour at 1.01325 bar and 30°C. From superheat table,

$h_{13} = 401.344$

For a plant of 1 kg/s capacity,

$$\dot{m}_{11} = 1 \text{ kg/s}$$

From Eq. (6.30),

$$\frac{\dot{m}_8}{\dot{m}_6} = \frac{h_9 - h_6}{h_9 - h_8} = \frac{319.954 - 159.391}{319.954 + 9.463} = 0.4874$$

From Eq. (6.31),

$$\frac{\dot{m}_{11}}{\dot{m}_{10}} = \frac{h_{12} - h_{10}}{h_{12} - h_{11}} = \frac{311.7526 + 9.463}{311.7524 + 259.506} = 0.5623$$

$$\dot{m}_1 = \dot{m}_8 = \dot{m}_{10} = 1.0 / 0.5623 = 1.7784$$

$$\dot{m}_6 = \dot{m}_8 / 0.4874 = 3.6487$$

$$\dot{m}_9 = \dot{m}_6 - \dot{m}_8 = 1.87026$$

$$\dot{m}_{12} = \dot{m}_{10} - \dot{m}_{11} = 0.7784$$

Adiabatic mixing of streams 12 and 13 yields

$$h_1 = (\dot{m}_{11}h_{11} + \dot{m}_{12}h_{12})/\dot{m}_1 = \{401.344 + 0.7784\ (311.7524)\}/1.7784 = 362.1293$$

This is a superheated state. The temperature and entropy are not known at this point. Interpolating in the superheat table for 1.01325 bar, we get

$$t_1 = -16.647^\circ\text{C},\ s_1 = 1.95456 \text{ and } v_1 = 474.203 \times 10^{-3} = 0.474203$$

State 2 is isentropic compression from 1 to 2 such that $s_1 = s_2$. Interpolating in the superheat table at 8.333 bar for $s_1 = s_2 = 1.95456$, we get

$$t_2 = 132.166^\circ\text{C},\ h_2 = 490.891 \text{ and } v_2 = 91.0 \times 10^{-3} = 0.091$$

$$W_{\text{LP}} = \dot{m}_1(h_2 - h_1) = 1.7784(490.891 - 362.1293) = 228.99 \text{ kW}$$

$$\eta_{\text{vol LP}} = 1.04 - 0.04(474.203/91.0\ ) = 0.8316$$

$$(\mathbb{V}_S)_{\text{LP}} = \dot{m}_1 v_1/\eta_{\text{vol LP}} = 1.7784(0.474.203)/0.8316 = 1.01415 \text{ m}^3\text{/s}$$

State 3 is superheated state at 30°C and 8.333 bar. From the superheat table,

$$h_3 = 394.454$$

State 4 is obtained by adiabatic mixing of state 3 and state 9 as follows:

$$h_4 = (\dot{m}_3h_3 + \dot{m}_9h_9)/\dot{m}_6 = (1.7784 \times 394.454 + 1.87026 \times 319.954)/3.6487$$
$$= 356.266$$

This is a superheated state. Temperature and entropy are not known at this point. Interpolating in the superheat table for 8.333 bar for $h_4 = 356.266$, we get

$$t_4 = -10.2185^\circ\text{C},\ s_4 = 1.54575 \text{ and } v_4 = 55.888 \times 10^{-3} = 0.055888$$

State 5 involves isentropic compression from 4 to 5. Interpolating in the superheat table for $s_4 = s_5 = 1.54575$ at 64.328 bar, we get

$$t_5 = 142.946^\circ\text{C}\ ,\ h_5 = 475.741 \text{ and } v_2 = 11.155 \times 10^{-3} = 0.011155$$

$$\eta_{\text{vol HP}} = 1.04 - 0.04\ (55.888/11.155\ ) = 0.8396$$

$$(\mathbb{V}_S)_{\text{HP}} = \dot{m}_1 v_1/\eta_{\text{vol LP}} = 3.6487\ (0.055888)/0.8396 = 0.24288\ \text{m}^3/\text{s}$$

$$W_{\text{HP}} = \dot{m}_4(h_5 - h_4) = 3.6487(475.741 - 356.266) = 435.928\ \text{kW}$$

$$Q_c = \dot{m}(h_5 - h_6) = 3.6487(475.741 - 159.391) = 1154.266\ \text{kW}$$

$$W_{\text{net}} = W_{\text{LP}} + W_{\text{HP}} = 228.99 + 435.928 = 664.918\ \text{kW}$$

Refrigeration capacity may be taken as the cooling capacity of dry ice produced, that is, Q_e = production rate of dry ice × latent heat of fusion of dry ice

$$Q_e = \dot{m}(h_{12} - h_{11}) = 1.0\ (311.7524 - (-259.506)) = 571.2584\ \text{kW}$$

$$\text{COP} = 571.2584/664.918 = 0.859$$

It is observed that the size of compressors required is very large and the COP is very low. In fact, superheating, subcooling and intercooling by refrigerant in heat exchangers has been omitted for simplicity of illustration of calculation procedure. Intercoling has been done by water alone. Intercooling to a lower temperature by CO_2 may also improve the COP. Condenser temperature of 25°C would require availability of water at 20°C, which is not possible in tropical countries. Hence, a cascade system is a more practical system. In the next example, we consider a cascade system where heat is rejected to ammonia from CO_2 which in turn rejects it to surroundings at 40°C.

EXAMPLE 6.23 A dry ice plant of 1 kg/s capacity uses a cascade refrigeration system with ammonia on the HT side. CO_2 condenses at –10°C, 26.4934 bar in a cascade condenser with ammonia evaporating at –15°C. The make-up CO_2 is available at atmospheric pressure and 30°C. The pressure after the first stage CO_2 compressor is 6.8364 bar (–50°C saturation temperature). The LP vapour is desuperheated to 30°C in a water intercooler before entry into cascade condenser. Determine the state points on the cycle shown in Figure 6.17(c) and find the mass flow rates, swept flow rates and work requirement of both the compressors, and cascade condenser heat rejection. Then find the mass flow rate, the compressor work and condenser heat rejection of ammonia circuit and the COP.

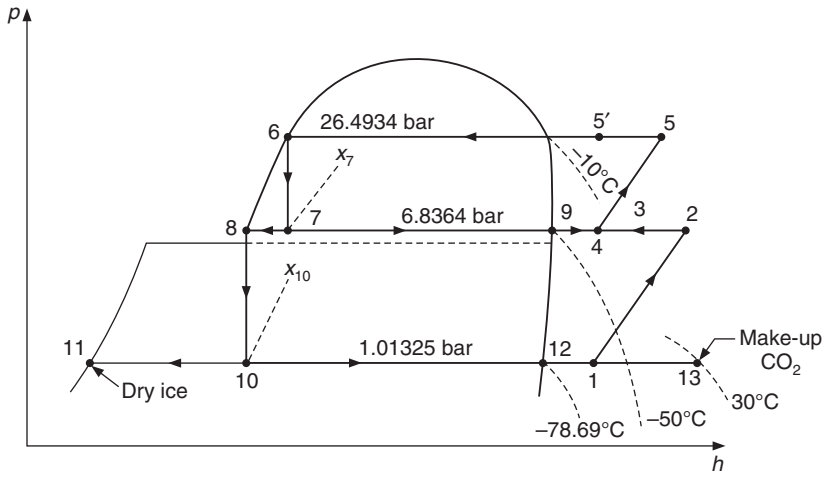

Figure 6.17(c) *p–h* diagram of CO_2 circuit of Example 6.23.

Solution:

The saturation table in Example 6.22 gives the data required for this case too. The superheat table at 6.83 bar and 26.49 bar, is as follows.

t	1.0325 bar (–78.69°C)			6.8364 bar (–50°C)			26.4934 bar (–10°C)		
(°C)	v	h	s	v	h	s	v	h	s
–30	448.75	351.14	1.9112	63.6723	339.731	1.5172			
–20	467.83	359.35	1.9439	66.9684	349.381	1.5558			
–10	486.84	367.64	1.9757	70.1883	358.858	1.5926			
10	524.75	384.345	2.0368	76.4881	377.462	1.6602	16.655	349.552	1.3284
20	543.65	392.803	2.0666	79.5842	386.699	1.6924	17.7344	362.262	1.3714
30	562.52	401.344	2.0955	82.6466	395.92	1.7233	18.7591	374.28	1.411
90	675.3	454.516	2.255	100.513	451.43	1.8906	24.2231	439.96	1.608
100	694.05	463.685	2.2797	103.446	460.808	1.9160	25.0656	450.369	1.6365
110	712.8	472.896	2.304	106.375	470.291	1.9407	25.8931	460.684	1.6638
120	731.54	482.191	2.3278	109.293	479.811	1.9652	26.7283	470.906	1.6905

Solution:

Referring to Figure 6.17(c), we have

$h_6 = h_f$ (–10°C) = 60.8723, $h_8 = h_f$ (–50°C) = –18.8015,

$h_9 = h_g$ (–50°C) = 318.696

h_{11} is saturated solid at –78.69 °C = h_s (–78.69°C) = –259.506

h_{12} is saturated vapour at –78.69 °C = h_g (–78.69°C) = 311.7524

h_{13} is superheated vapour at 1.01325 bar and 30°C. From superheat table, h_{13} = 401.344

For a plant of 1 kg/s capacity,

$$\dot{m}_{11} = 1 \text{ kg/s}$$

From Eq. (6.30),

$$\frac{\dot{m}_8}{\dot{m}_6} = \frac{h_9 - h_6}{h_9 - h_8} = \frac{318.696 - 60.8723}{318.696 + 18.8015} = 0.7639$$

From Eq. (6.31)

$$\frac{\dot{m}_{11}}{\dot{m}_{10}} = \frac{h_{12} - h_{10}}{h_{12} - h_{11}} = \frac{311.7524 + 18.8015}{311.7524 + 259.506} = 0.5786$$

$$\dot{m}_1 = \dot{m}_8 = \dot{m}_{10} = 1.0/0.5786 = 1.7282$$

$$\dot{m}_6 = \dot{m}_8/0.7639 = 2.2622$$

$$\dot{m}_9 = \dot{m}_6 - \dot{m}_8 = 0.53405$$

$$\dot{m}_{12} = \dot{m}_{10} - \dot{m}_{11} = 0.7282$$

Adiabatic mixing of streams 12 and 13 yields

$$h_1 = (\dot{m}_{11}h_{11} + \dot{m}_{12}h_{12})/\dot{m}_1 = \{401.344 + 0.7282\ (311.7524)\}/1.7282 = 363.5938$$

This is a superheated state. The temperature and entropy are not known at this point. Interpolating in the superheat table for 1.01325 bar, we get

$$t_1 = -14.8808^{\circ}\text{C},\ s_1 = 1.960179 \text{ and } v_1 = 477.56 \times 10^{-3} = 0.47786\ \text{m}^3/\text{kg}$$

State 2 is isentropic compression from 1 to 2 such that $s_1 = s_2$. Interpolating in the superheat table at 6.8364 bar for $s_1 = s_2 = 1.960179$, we get

$$t_2 = 117.95^{\circ}\text{C},\ h_2 = 477.86 \text{ and } v_2 = 108.695 \times 10^{-3} = 0.108695\ \text{m}^3/\text{kg}$$

$$W_{\text{LP}} = \dot{m}(h_2 - h_1) = 1.7282(477.86 - 363.5938) = 258.5\ \text{kW}$$

$$\eta_{\text{vol LP}} = 1.04 - 0.04(477.56/108.695\ ) = 0.8642$$

$$(\mathbb{V}_S)_{\text{LP}} = \dot{m}_1 v_1/\eta_{\text{vol LP}} = 1.7784(0.474.203)/0.8316 = 1.01415\ \text{m}^3/\text{s}$$

State 3 is superheated state at 30°C and 6.8364 bar. From superheat table

$$h_3 = 395.9197$$

State 4 is obtained by adiabatic mixing of state 3 and state 9 as follows:

$$h_4 = (\dot{m}_3h_3 + \dot{m}_9h_9)/\dot{m}_6 = (1.7287 \times 395.9197 + 0.53405 \times 318.696)/2.2622$$
$$= 377.689$$

This is a superheated state. The temperature and entropy are not known at this point. Interpolating in the superheat table for 6.8364 bar for $h_4 = 377.2689$, we get

$$t_4 = 10.246^{\circ}\text{C},\ s_4 = 1.66099 \text{ and } v_4 = 76.564 \times 10^{-3} = 0.076564\ \text{m}^3/\text{kg}$$

State 5 involves isentropic compression from 4 to 5. Interpolating in the superheat table for $s_4 = s_5 = 1.66099$ at 26.4934 bar, we get

$$t_5 = 108.9707^{\circ}\text{C},\ h_5 = 459.6224 \text{ and } v_2 = 25.8124 \times 10^{-3} = 0.0258124\ \text{m}^3/\text{kg}$$

$$\eta_{\text{vol HP}} = 1.04 - 0.04\ (76.564/25.8124\ ) = 0.9213$$

$$(\mathbb{V}_S)_{\text{HP}} = \dot{m}_1 v_1/\eta_{\text{vol LP}} = 2.2622\ (0.076564)/0.9213 = 0.188\ \text{m}^3/\text{s}$$

$$W_{\text{HP}} = \dot{m}_4(h_5 - h_4) = 2.2622(459.6264 - 377.689) = 185.35\ \text{kW}$$

The water intercooler cools the vapour from state 5 to 5′ at 30°C, 26.4934 bar. From the superheat table, we get

$$h_{5'} = 374.28$$

$$Q_c = \dot{m}_4(h_{5'} - h_6) = 2.2622(374.28 - 60.8723) = 709.0023\ \text{kW}$$

Refrigeration capacity may be taken as the cooling capacity of dry ice produced, that is, Q_e = production rate of dry ice × latent heat of fusion of dry ice

$$Q_e = \dot{m}_{11}(h_{12} - h_{11}) = 1.0\ (311.7524 - (-259.506)) = 571.2584\ \text{kW}$$

HT side

On the HT side, the SSS cycle for ammonia runs between the evaporator and the condenser temperatures of –15°C and 40°C respectively (Figure 6.17(d)). From the saturation table for ammonia at 2.363 bar (–15°C) and 15.55 bar (40°C), we get

$$h_a = h_g\ (-15^{\circ}\text{C}) = 1424.919,\ s_a = 5.5423,\ v_a = 0.509 \text{ and } h_c = 371.47$$

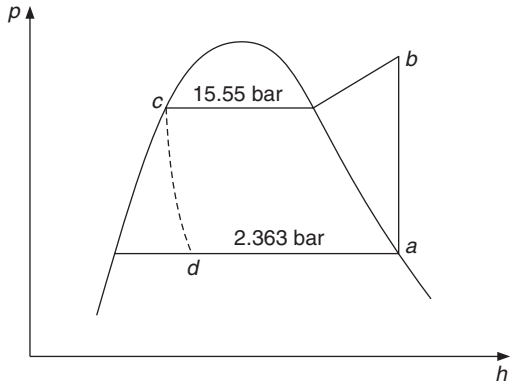

Figure 6.17(d) *p–h* diagram of HT side of Example 6.23.

At 15.55 bar the relevant portion of superheat table is as follows:

Superheat	80	100
v	0.116	0.123
h	1700.3	1751.7
s	5.5253	5.65283

Interpolating in the superheat table for $s_a = s_b = 5.5423$, we get

$$t_b = 122.67 \text{ oC},\ h_b = 1707.15,\ v_b = 0.11693$$

The mass flow rate is found by using the condenser heat rejection of CO_2 side, that is 709.0023 kW

$$\dot{m}_{\text{HT}} = \frac{709.0023}{h_a - h_c} = \frac{709.0023}{1424.919 - 371.47}\ 0.67303 \text{ kg/s}$$

$$W_{\text{HT}} = \dot{m}_{\text{HT}}\,(h_b - h_a) = 0.67303\ (1707.15 - 1424.919) = 189.95 \text{ kW}$$

$$Q_{c\ \text{HT}} = \dot{m}_{\text{HT}}\,(h_b - h_c) = 0.67303\ (1707.15 - 371.47) = 898.95 \text{ kW}$$

$$\eta_{\text{vol HT}} = 1.04 - 0.04\ (0.509/0.11693) = 0.8659$$

$$(\mathbb{V}_S)_{\text{HT}} = \dot{m}_1 v_1/\eta_{\text{vol LP}} = 0.67303\ (0.509)/0.8659 = 0.396 \text{ m}^3\text{/s}$$

$$W_{\text{net}} = W_{\text{LP}} + W_{\text{HP}} + W_{\text{HT}} = 258.5 + 185.35 + 189.95 = 633.80 \text{ kW}$$

$$\text{COP} = Q_e/W_{\text{net}} = 571.2584/633.80 = 0.901$$

The COP improves slightly from 0.859 to 0.901. It is not the improvement in COP that is important but the fact that the two-stage system cannot work unless water is available at temperature of 20°C or lower.

6.9 AUTO-CASCADE SYSTEM

A variation of cascade refrigeration system, which runs with only one compressor has become very popular. The LT and HT side refrigerants are chosen such that the evaporator pressure of LT side and the evaporator pressure of HT side are equal. The temperatures will be different. Also, their condenser pressures are equal. The condenser temperature of HT side will be around 40°C while the condenser temperature of LT side may be around – 20°C. The pressure being the same, a single compressor can compress both the refrigerants. It must be kept in mind that the selection of the refrigerant pair will satisfy a unique combination of intermediate and evaporator pressures. If a different set of temperatures is required, then a different pair of refrigerants has to be sought.

For illustration, we consider a system which uses R13 on LT side and R22 on HT side. At a pressure of 2.25 bar the saturation temperature of R13 is –65°C, while that of R22 is –22°C. Similarly at a pressure of 13.2 bar, the saturation temperature of R13 is –15°C while that of R22 is 34°C.

In the schematic diagram shown in Figure 6.18, R13 vapour at state 1 and R22 vapour at state 6 after evaporation are mixed together and compressed in a single compressor. Now the question is how to separate them, condense them and take R22 to cascade condenser and R13 to the evaporator. This is based upon the principle that if the mixture is cooled at 13.2 bar and 34°C, only R22 will condense. R13 has saturation temperature of –15 °C at 13.2 bar, hence it can condense by heat rejection only at –15°C.

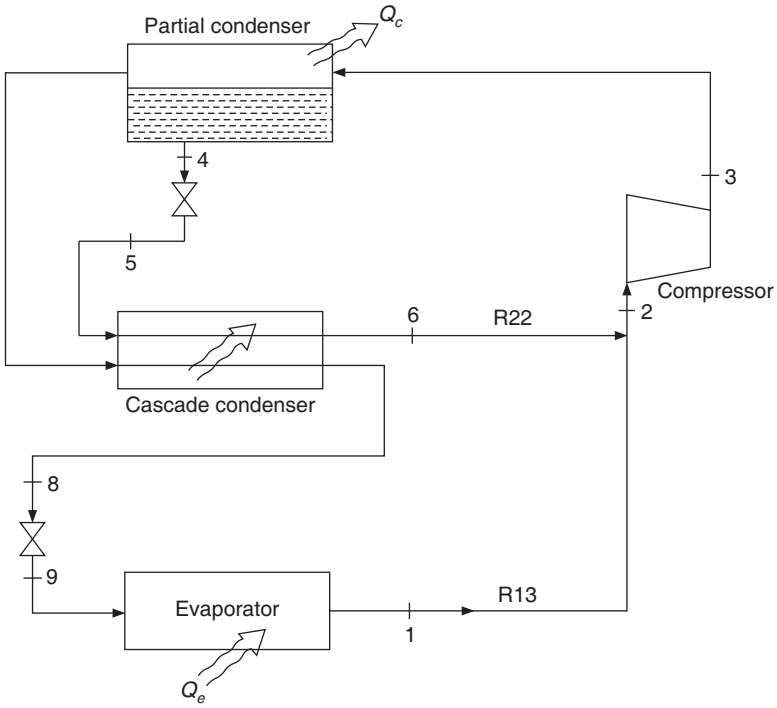

Figure 6.18 Schematic of a two-stage auto-cascade system.

In the schematic diagram, the HT side condenser is named *partial condenser* since only R22 condenses in this component by heat rejection to the surroundings. R13 which cannot condense at this temperature flows to the cascade condenser.

The R22 liquid is drained from the bottom of partial condenser at point 4. Throttling through the expansion valve 4–5 expands it, where its pressure is reduced to 2.25 bar. It goes into the cascade condenser where it evaporates at –22ºC by absorbing heat from R13, which comes from the partial condenser. R13 condenses at –15ºC. Liquid R13 passes through expansion valve 8–9 and expands to a pressure of 2.25 bar at which it absorbs heat in the evaporator at –65ºC.

In the partial condenser, the temperature is too high for R13 to condense at 13.2 bar, but R22 can condense provided its partial pressure is high

In actual practice some vapours of R13 will also condense in the partial condenser, hence the R22 liquid will contain some R13 vapours. Similarly, the vapour leaving the partial condenser will be rich in R13, but it will have some R22 liquid. In a liquid solution, the boiling of a species takes over a range of temperature depending upon its concentration in the solution. Similarly, the condensation also takes place over a range of temperatures.

There are many other pairs of refrigerants, which are used in the auto-cascade cycle since they have the same evaporator and condenser pressures. Small packaged environmental chambers use auto-cascade cycle. Hermetic compressors commercially available off-the-shelf, are used. The refrigerant mixtures are proprietary and the balancing heat exchangers are specially designed. The maximum compressor motor capacity of such units is around 7.5 kW.

REFERENCES

Schmidt H. (May 1965): Die bemessung von *kältekocompressoren* in kaskadenschaltung, *Kältechnik*, vol. 17, no. 5, pp.151–155.

Stickney, A.B. (1932): The thermodynamics of CO_2 cycles. *Refrig. Eng.*, vol. 24, pp. 334–342.

REVIEW QUESTIONS

1. The condenser and evaporator temperatures are 36°C and –24°C respectively for a two-stage NH_3 refrigeration system of 100 TR cooling capacity. A water intercooler intercools the LP vapour to 30°C and further intercooling up to saturated state is done in a flash chamber, after the refrigerant vapour is compressed to an intermediate pressure of 5.2 bar. The vapour is compressed isentropically in both compressors from the saturated vapour condition. Find the mass flow rates, swept volume flow rates and work requirements of the compressors, condenser heat rejection and the COP. The clearance volume ratio for both the compressors is 0.04.
2. The condenser and evaporator temperatures are 36°C and –24°C for a two-stage ammonia refrigeration system of 100 TR cooling capacity. The vapour get superheated to 10°C in the evaporator and at this temperature it enters the low pressure compressor. The discharge gas from the LP compressor is cooled by a water intercooler to a temperature of 30°C before it enters the flash chamber. The suction to the high pressure compressor is maintained at

15°C. The liquid refrigerant is subcooled to a temperature of 30°C. Assuming that the refrigerant vapour is compressed to an intermediate pressure of 5.2 bar and the vapour is compressed isentropically in both the compressors, determine the mass flow rates, swept volume flow rates, work requirements of both the compressors, condenser heat rejection and the COP. The clearance volume ratio for both the compressors is 0.04.

3. Work out the parameters of Question 2 for a two-stage R12 refrigeration systems except that the water intercooler is not used.
4. An R12 refrigeration system has two evaporators of 4 TR and 2 TR, respectively, kept at –4°C (Evaporator-2) and –20°C (Evaporator-1). The system uses one compressor, an individual expansion valve for each evaporator. The vapour from Evaporator-2 is throttled to the pressure of Evaporator-1. The two vapours are adiabatically mixed and compressed in the compressor. The condenser temperature is 40°C. Determine the enthalpies, temperature and entropies after throttling and adiabatic mixing. Find the mass flow rate, volumetric efficiency, swept volume rate and work requirement of compressor, condenser heat rejection and the COP.
5. An R134a refrigeration system has three evaporators of 30 TR, 20 TR and 10 TR, kept at 6°C (Evaporator-3), –4°C (Evaporator-2) and –20°C (Evaporator-3), respectively. The system uses one compressor, an individual expansion valve for each evaporator. The vapours from Evaporator-3 and Evaporator-2 are throttled to the pressure of Evaporator-1. The three vapours are adiabatically mixed before entering the compressor. The condenser temperature is 40°C. Determine the enthalpies, temperatures and entropies after throttling and adiabatic mixing. Find the mass flow rate, volumetric efficiency, swept volume rate and work requirement of compressor, condenser heat rejection and the COP.
6. A two-stage NH3 refrigeration system serves Evaporator-1 at –20°C and Evaporator-2 at –4°C. The evaporators are of 20 TR and 40 TR respectively. The vapour leaves both the evaporators in saturated state. The condenser temperature is 40°C. A water intercooler cools the LP vapours to 40°C. The subcooling HEX subcools the liquid refrigerant from 40°C to 5°C before it is fed to the main expansion valve. Find the mass flow rates, swept volume rates and work requirement of both the compressors, the condenser heat rejection and the COP.
7. A cascade refrigeration system uses R13 on the LT side and R134a on the HT side. The evaporator and condenser temperatures are –70°C and 38°C respectively. The refrigeration effect produced is 10 TR. In the cascade condenser, R13 condenses at –20°C and R134a evaporators at –26°C. Consider SSS cycles on both the LT and HT sides and determine the mass flow rates, the work requirement and swept volume rates of the two sides, condenser heat rejection and the COP. The clearance volume ratio is 0.04.

7

Absorption Refrigeration Systems

LEARNING OBJECTIVES

After studying this chapter the student should be able to:

1. Explain the basic principle of a vapour absorption refrigeration system.
2. Derive the expression for maximum COP of ideal absorption refrigeration system.
3. Understand the properties of solutions and mixtures of two substances.
4. Explain the differences between the ideal and real (nonideal) mixtures with the help of pressure–composition and temeprature–composition diagrams.
5. Explain the concepts of bubble point and dew point temperatures.
6. Find out the thermodynamic properties of ammonia–water mixtures using p–T–x and h–T–x charts.
7. Analyze the simple acqua–ammonia absorption system with the help of h–x diagram.
8. Explain the effects of presence of water vapour in the evaporator and condenser.
9. Explain the functions of dephlegmator, rectification column and exhausting column in ammonia enrichment process.
10. Draw the schematic diagram of the water-lithium bromide absorption system and explain its working principle.
11. Explain the operation of a single-vessel type and twin-vessel type water-lithium bromide systems.
12. Explain the working principle of the double-effect vapour absorption system.
13. Perform thermal analysis of water-lithium bromide absorption refrigeration system using the given data and fluid properties.
14. Explain the working principle of Platen–Munters system.
15. Discuss the properties required for ideal refrigerant–absorbent pairs for absorption refrigeration systems.
16. Compare the absorption system with the mechanical vapour compression refrigeration system.

7.1 INTRODUCTION

In the mechanical vapour compression refrigeration system the compressor not only compresses the vapour, it also drives away the vapour from the evaporator. An alternative method of driving away the vapour is to absorb it in some substance that has affinity for it and hence absorbs it readily. The absorption rate of vapour provides the potential for the removal of vapour from the evaporator. John Leslie demonstrated this phenomenon in 1910 by using two interconnected vessels, one containing water and the other containing H_2SO_4. Sulphuric acid has very strong affinity for water. The water vapour evaporating from a water containing vessel is absorbed by H_2SO_4, providing a driving force for evaporation. A vacuum pump may also be used to accelerate the evaporation process and let the water boil at a lower pressure and temperature to produce ice. The sulphuric acid thus becomes dilute after some time and its capacity to absorb water reduces. Therefore, it has to be concentrated (so that it contains very little water) by heating. Windhausen in 1878 made a machine to do this.

Ferdinand Carre in 1859 introduced the aqua–ammonia absorption refrigeration system in which ammonia was the refrigerant and water was the absorbent. Water has very strong affinity for ammonia. Hence, if the evaporator containing ammonia is connected to a vessel containing water, ammonia vapour will be absorbed and a low pressure will be created in the evaporator. The vessel where the absorption occurs is called *absorber*. It is not necessary to have pure water; a weak solution of ammonia in water will also serve the purpose to absorb ammonia. The solution that absorbs ammonia becomes a strong solution and is recycled by heating to drive off ammonia, so that a continuous supply of weak ammonia solution is available. The vessel where the refrigerant vapour is generated (or the weak solution is generated) is called *generator*.

7.2 ABSORPTION CYCLE OF OPERATION

A schematic diagram of this system is shown in Figure 7.1. The refrigerant vapour leaving the evaporator at state 6 (low temperature and low pressure vapour) is absorbed by a weak solution stream 2″ (weak in ammonia solution coming from the pressure reduction valve) and after absorbing ammonia vapour it becomes a strong solution, and leaves the absorber at state 1. When the ammonia vapour is absorbed, it becomes liquid and hence its enthalpy of condensation has to be rejected, therefore there is heat rejection Q_a in the absorber. The heat is rejected to cold water, which is recirculated to a cooling tower. A liquid pump increases the pressure of the strong solution from evaporator pressure p_1 to the condenser pressure p_2. It leaves the pump at state 1′. Thereafter, it is preheated to state 1″ in a preheating heat exchanger by the warm weak solution. Then it enters the generator where the refrigerant is librated by heating the strong solution. A steam coil or waste heat may be used for heat transfer Q_g in the generator. The weak solution is drained from generator at state 2. It is passed through the preheating heat exchanger 2–2′ and then a pressure reduction valve reduces its pressure to the absorber pressure value and it enters the absorber at state 2″.

A comparison of this absorption refrigeration system with the mechanical vapour compression refrigeration system reveals that the condenser, expansion valve and evaporator are common to the two systems. The compressor in the mechanical vapour compression system is replaced by the combination of absorber, liquid solution pump, preheating heat exchanger, generator and liquid pressure reduction valve. This ensemble removes vapour from the evaporator at state 6 and delivers high-pressure vapour to condenser at state 3 just like the compressor of the former system. The

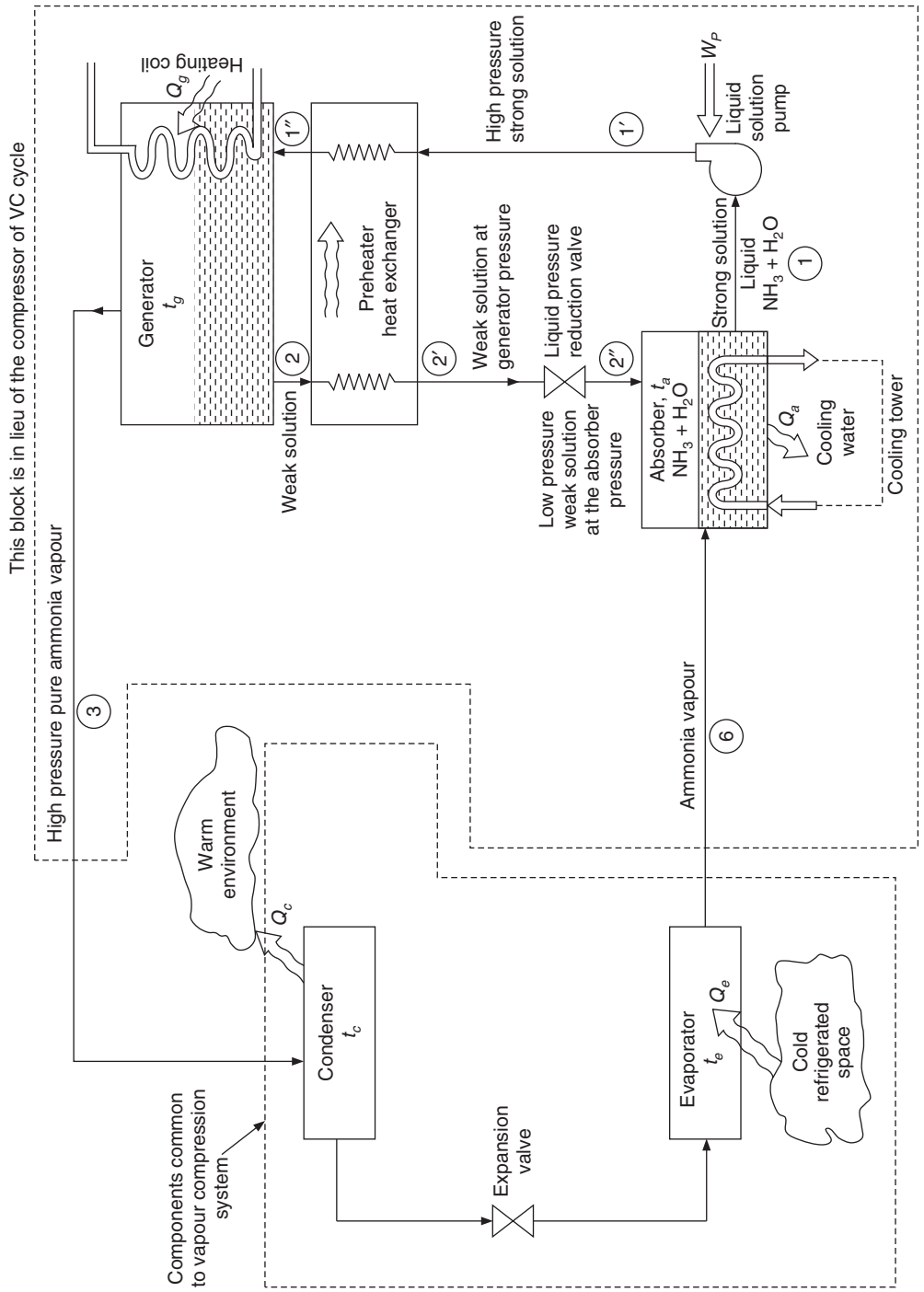

Figure 7.1 Schematic representation of ammonia absorption refrigeration cycle.

condenser requires a higher pressure since it has to reject heat Q_c to the surroundings by condensation at a higher temperature. Hence compression is required. A liquid pump does the compression in this system. A liquid pump requires much less work than a vapour compressor for the same pressure difference since the work requirement of pump is given by

$$w_P = -\int_{p_1}^{p_2} v\,dp$$

The specific volume of liquid is very small ($\approx 10^{-3}$ m^3/kg); hence the work required is also small. This is a very important feature of this system. *The high-grade energy required by this system is negligibly small. The system runs on low-grade heating energy supplied to the generator.* It should be noted that this is also a vapour compression refrigeration system; only the vapour is not directly compressed mechanically. It is absorbed in a liquid, which is then compressed. For this reason, the conventional vapour compression cycle discussed in earlier chapters is sometimes called the *mechanical vapour compression cycle*.

Ammonia vapour at state 3 is obtained by virtually driving it off from the strong solution which is heated in the generator, leaving behind a weak solution of ammonia at state 2. This weak solution is fed back to the absorber to absorb ammonia vapour. However, it is at high temperature and hence not capable of absorbing NH_3. It is passed through a preheating heat exchanger, where it preheats the strong solution towards the generator temperature t_g so that it requires less energy Q_g for heating. In this process the weak solution cools down towards the absorber temperature t_a so that it can absorb ammonia at lower temperature. Its pressure is that of generator while the absorber is at lower pressure. A constriction or a pressure reduction valve 2′–2″ reduces its pressure to absorber pressure. The generator and condenser have high pressure while the evaporator and absorber have low pressure. This is a heat-driven refrigeration system where the input is the heat transfer rate Q_g to the generator and the desired effect is the evaporator heat transfer rate Q_e. Hence the COP of the absorption refrigeration system is defined as

$$\text{COP} = \frac{Q_e}{Q_g}$$

7.3 MAXIMUM COP

The maximum COP of this heat-driven absorption refrigeration cycle is obtained by assuming the heat transfers to be isothermal and reversible, pump work to be negligible and in addition the condenser and absorber temperatures to be same. The first law applied to Figure 7.1 gives

$$Q_e + Q_g + W_p - Q_c - Q_a = 0$$

Assuming the pump work to be negligible, we get

$$Q_e + Q_g - Q_c - Q_a = 0 \tag{7.1}$$

The second law of thermodynamics is applied in the form of Clausius inequality, that is, $\oint \frac{dQ}{T} \le 0$. With the convention that heat transfer to the system is positive, we get

$$\frac{Q_e}{T_e} + \frac{Q_g}{T_g} - \frac{Q_c + Q_a}{T_c} \leq 0 \tag{7.2}$$

Substituting for $Q_c + Q_a$ from Eq. (7.1) and simplifying, we get

$$Q_e \left[\frac{T_c - T_e}{T_c T_e} \right] \leq Q_g \left[\frac{T_g - T_c}{T_c T_g} \right]$$

or

$$\text{COP} = \frac{Q_e}{Q_g} \leq \left[\frac{T_g - T_c}{T_g} \right] \left[\frac{T_e}{T_c - T_e} \right] \tag{7.3}$$

The first term on the right hand side is the efficiency of Carnot (reversible) heat engine operating between the source temperature T_g and the sink temperature T_c. This represents the part of heat transfer Q_g that can be converted into work reversibly. The second term is the COP of the reversible Carnot cycle. This COP will always be less than the COP of the mechanical vapour compression refrigeration system that uses high-grade electrical energy to drive the compressor motor.

7.4 PROPERTIES OF SOLUTIONS

An understanding of the operation of the cycle, thermodynamic characteristics and performance, all require an understanding of the properties of solutions and mixtures of two substances. A brief description of these aspects is presented in the following sections.

7.4.1 Ideal Solutions

A solution is, in general, any phase containing more than one component. The phase may be solid, liquid or gaseous. In the case of gases the concept of ideal gases makes the analysis very simple, that is, the p–v–T relation is very simple; and internal energy and enthalpy are functions of temperature alone. Similarly, the concept of ideal solutions is very useful in the study of solutions.

A gas is considered to be ideal if the cohesive forces between its molecules are negligible. A mixture of ideal gas A and ideal gas B is also an ideal gas if the intermolecular forces between the molecules of A and B are negligible in addition to the forces between like molecules. In liquids the intermolecular forces cannot be negligible, otherwise they will not be liquids. Ideal solutions are characterized by the uniformity of intermolecular forces, that is, if A and B are the constituents then the cohesive forces between A–A pairs, A–B pairs and B–B pairs are assumed to be the same. The composition of a mixture can be specified either on mass fraction basis or on mole fraction basis.

7.4.2 Mass Fraction

If a mixture of mass m consists of masses m_A and m_B of A and B respectively, then the mass fractions x_A and x_B of A and B are defined as

$$x_A = m_A/(m_A + m_B)$$

$$x_B = m_B/(m_A + m_B)$$

where

$$x_A + x_B = 1.$$

7.4.3 Mole Fraction

If M_A and M_B are the molecular weights of A and B respectively, then the number of moles n_A and n_B of A and B in the mixture is

$$n_A = m_A/M_A \quad \text{and} \quad n_B = m_B/M_B$$

The mole fractions χ_A and χ_B of A and B are defined as

$$\chi_A = n_A/(n_A + n_B)$$

$$\chi_B = n_B/(n_A + n_B)$$

where $$\chi_A + \chi_B = 1.$$

7.4.4 Raoult's Law

The partial vapour pressure of a constituent is in a sense, a measure of its tendency to escape from the liquid surface. If the liquid solution of A and B is ideal, then this tendency to escape for A molecules is the same, whether it is surrounded by A molecules or B molecules, since the intermolecular forces are the same between A and B. In such a case, the partial pressure of A is same as that of pure A liquid except that there are proportionally less molecules of A in solution than in pure A liquid. The partial vapour pressure of A is equal to the mole fraction χ_A of A in the solution multiplied by p_A°, where p_A° is the vapour pressure of pure A liquid at the temperature of solution. This is known as Raoult's law, that is,

$$p_A = \chi_A \, p_A^{\circ} \tag{7.4}$$

$$p_B = (1 - \chi_A) \, p_B^{\circ} \tag{7.5}$$

From Dalton's law of partial pressures, we have

$$p = p_A + p_B \quad \text{and} \quad \chi_A + \chi_B = 1$$

where p_B° is the partial pressure of pure B and p is the total pressure. A plot of these partial pressures is shown in Figure 7.2. It is observed that the partial pressure of A in the solution increases linearly from 0 to p_A° as its mole fraction increases from 0 to 1. For a binary ideal solution at a given temperature, the partial vapour pressures of both the constituents are straight lines when plotted against the mole fraction.

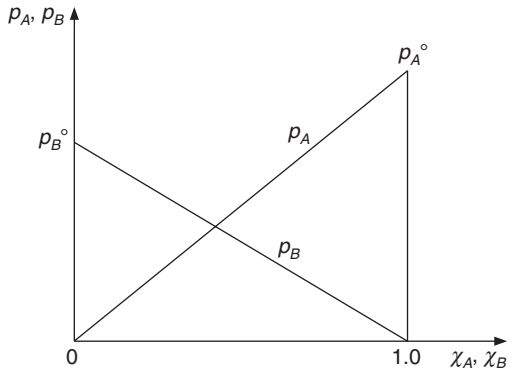

Figure 7.2 Partial vapour pressures of constituents A and B against mole fraction.

In addition, for the solutions obeying Raoult's law the change in volume and enthalpy during mixing are zero, since the intermolecular forces between its constituents are the same. The entropy change, however, is not zero. If n_A moles of A at temperature T and pressure p mix adiabatically with n_B moles of B at same temperature and pressure, the pressure of A reduces from p to p_A and the pressure of B reduces to p_B, the temperature remaining the same. The second fundamental relation of thermodynamics may be used to find the change in entropy during mixing of the gases.

$$Tds = dh - v\,dp \;;\; dh = 0 \text{ since temperature does not change.} \quad \therefore \quad Tds = -v\,\mathrm{d}p$$

$$\Delta s_A = -\frac{1}{T}\int_p^{p_A} v\,dp = -\bar{R}n_A \int_p^{p_A} \frac{dp}{p} = -\bar{R}n_A \ln \frac{p_A}{p} \quad \text{and} \quad \Delta s_B = -\bar{R}n_B \ln \frac{p_B}{p}$$

$$\Delta s_{\text{mixture}} = -\bar{R}n_A \ln \frac{p_A}{p} - \bar{R}n_B \ln \frac{p_B}{p} = -\bar{R}n_A \ln \chi_A - \bar{R}n_B \ln \chi_B$$

since $\chi_A = \dfrac{p_A}{p}, \quad \chi_B = \dfrac{p_B}{p}$.

7.4.5 Nonideal Solutions

In a solution, the constituent with the larger concentration is called *solvent* and the one with the smaller concentration is called *solute*. The solvent in a dilute solution follows the Raoult's law, that is, its partial pressure $p_A = \chi_A\, p_A^{\circ}$. This is justified since a dilute solution has a small number of solute molecules which have a negligible effect on the escaping tendency of solvent molecules whose number is large.

Raoult's law is not valid for solutions over the whole range of concentration. The constituents may not mix well beyond a certain concentration because of the repulsive forces between the unlike molecules. The *repulsive forces will increase the escaping tendency of the molecules* and thereby their partial pressure will be more than that predicted by Raoult's law, that is, $p_A > \chi_A\, p_A^{\circ}$. This is shown in Figure 7.3 where the partial pressure of both the constituents as well as that of solution is more than that predicted by Raoult's law. Near $\chi_A = 0$, constituent B is solvent hence it follows Raoult's law whereas near $\chi_A = 1$, constituent A is solvent which follows Raoult's law. At all other pressures the repulsive forces manifest themselves, hence the partial pressures of both the constituents are more than those predicted by Raoult's law. The total solution pressure is also more than that predicted by Raoult's law. Such a solution is said to have a positive deviation from Raoult's law.

On the other hand, if the constituents mix well then there will be *attractive forces between them that will reduce the escaping tendency* and thereby the partial pressure will be less than that predicted by Raoult's law, that is, $p_A < \chi_A\, p_A^{\circ}$. Figure 7.4 shows such a situation where the partial pressures of both the constituents and that of the solution are less than those predicted by Raoult's law. Such a solution is said to have a negative deviation from Raoult's law.

Another common feature observed in both Figures 7.3 and 7.4 is that in the dilute solutions, the vapour pressure of the dilute component (solute) is proportional to its mole fraction. That means that the escaping tendency of the solute is proportional to its mole fraction. This is referred to as Henery's law, that is,

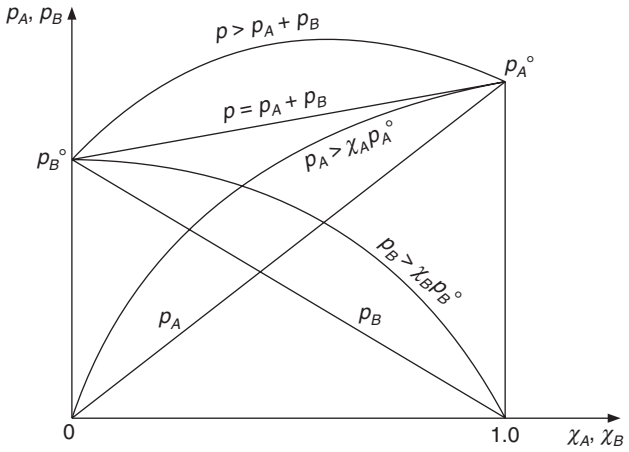

Figure 7.3 Diagram showing positive deviations from Raoult's law in case of nonideal solutions.

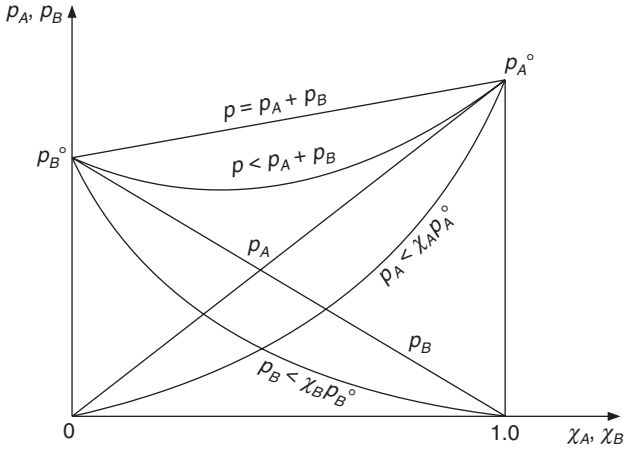

Figure 7.4 Diagram showing negative deviations from Raoult's law in case of nonideal solutions.

$$p_A = k\,\chi_A \tag{7.6}$$

where k is the proportionality constant. In Raoult's law, the proportionality constant is p_A°.

The nonideal solutions generally have the following characteristics:

(i) Those showing deviations from Raoult's law.

(ii) Those showing marked change in volume upon mixing.

(iii) The mixing either evolves or absorbs heat.

7.4.6 Temperature–Composition Diagram

For a simple compressible substance, only two independent properties are sufficient to fix the thermodynamic state. This is the case in superheated and subcooled states, where for example, both pressure and temperature are required to fix the thermodynamic state. At saturation, however,

only one property is required to fix the state since the saturation pressure and temperature are related to each other. Hence, at a fixed pressure, if a liquid (pure substance) is heated, it boils at its saturation temperature and the temperature remains constant until the whole of liquid has evaporated. Similarly, at a fixed pressure, the vapour condenses at its saturation temperature until all of it has condensed. For water at standard atmospheric pressure, boiling occurs at 100°C. For R12, boiling occurs at –29.8°C and for R22 boiling occurs at –40.8°C at standard atmospheric pressure.

Pure substances have a unique boiling point at a given pressure; further the boiling point and the condensation point temperatures are the same.

For a solution of two simple compressible substances, a minimum of three independent properties are required, that is, the composition has also to be specified in addition to the two properties required for pure individual substances. In saturated state for a binary solution, two independent properties are required to fix the thermodynamic state, for example the concentration has to be specified to fix the boiling point in addition to pressure. Two-dimensional property charts can be drawn if one of the properties is held constant. It is convenient to plot either t vs. x or h vs. x.

When a subcooled binary solution of concentration x_{A1} at state1, is heated at constant pressure p, the bubbles will make their first appearance at point C shown in Figure 7.5. The temperature t_C is called the bubble point temperature for this concentration and pressure. Similarly, when a subcooled binary solution of concentration x_{A2} is heated at constant pressure p, the bubbles will make their first appearance at point H. Pure A liquid at pressure p will have boiling point or bubble point at temperature t_A shown at $x_A = 0$ and pure B will have it at temperature t_B shown at $x_B = 0$ ($x_A = 1$). For a given pressure, if a line is drawn joining the bubble point temperatures for all concentrations, such a line is called the *bubble point curve*. This is shown by the curve *I–C–H–II* in Figure 7.5. This curve represents the saturated liquid state.

If superheated vapour with concentration x_{A1} at state 3 is cooled, then condensation will start to occur at E. This point is called the dew point temperature at concentration x_{A1} and pressure p. Similarly, vapour at state 4 when cooled, starts to condense at point K. A line joining dew points for all the concentrations for a pressure is called the *dew point curve*. This is shown by *I–E–K–II*. This curve represents the saturated vapour state. *It may be noted that these two curves are coincident for a pure substance, whereas for a solution, the bubble point and the dew point curves are not the same.*

At concentration x_{A1} the boiling starts at point C. The first vapour that comes out will have concentration $x_{A1'}$ corresponding to point C' which is the dew point at the same temperature. If heating is continued further, the temperature does not remain constant during boiling unlike for a pure substance where, the temperature remains constant during boiling. For a solution the temperature increases while the liquid evaporates, until at E all the liquid evaporates and only the saturated vapour is left behind. The region *C–E* is the two-phase region. At any point D in this region, vapour of concentration x_G is in equilibrium with liquid of concentration x_F. The saturated liquid F and the saturated vapour G are at same temperature and hence are in equilibrium. If ξ is the quality (proportion of vapour, or dryness fraction) in the two-phase mixture at D, then the mass conservation of species A yields

$$\xi_{A1} = \xi\, x_G + (1 - \xi)\, \xi_F$$

$$\therefore \qquad \xi = \frac{x_{A1} - x_F}{x_G - x_F} \tag{7.7}$$

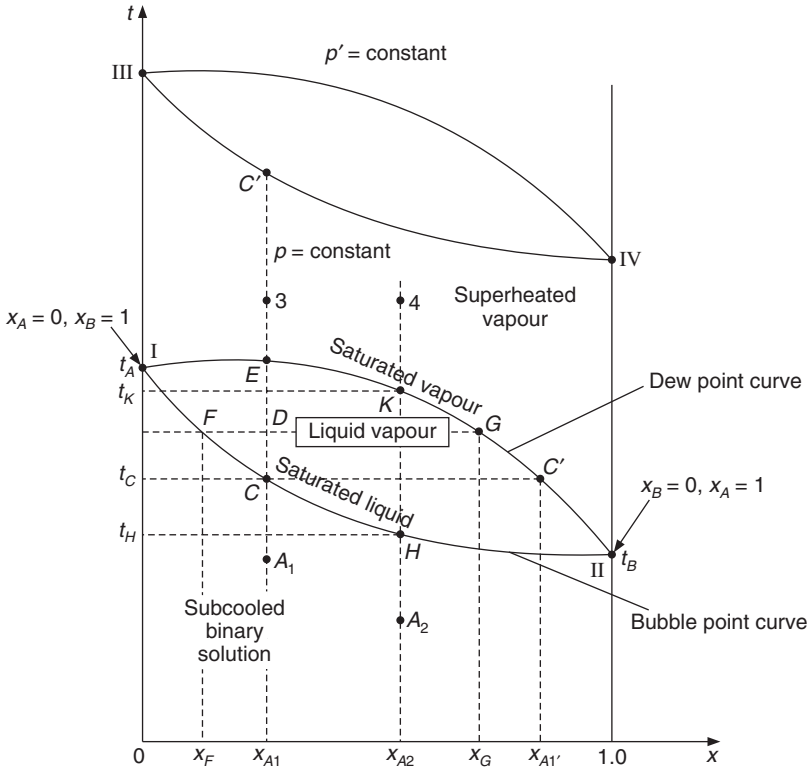

Figure 7.5 Temperature–composition diagram for a solution of two simple compressible substances.

Figure 7.5 shows another set of bubble and dew point curves for a higher pressure p'. The liquid at any point below the curve *III–C′–IV* will be subcooled liquid at pressure p'. Referring to the saturation curve for pressure p, it is observed that at points 3 and 4 it will be superheated vapour if the pressure is p while it will be subcooled liquid at pressure p'.

Figure 7.6 shows the bubble point temperature curves for nonideal solutions with positive and negative deviations along with Raoult's law solution. The bubble temperature curve of the positive deviation solution is lower than that of the ideal solution. The molecules of such solutions repel each other and the solution pressure is more than pressure p of the ideal solution, that is, $p_A + p_B > p$. Hence, at pressure p (lower pressure) the boiling point will be lower. R502, which is a mixture of R22 and R115 is an example of this. R22 has a NBP of – 40.8°C while R115 has a normal boiling point of –39.1°C. R502 has NBP of – 45.4°C, which is lower than that of both of its constituents.

The mixing of such solutions involves endothermic reaction, that is, heat has to be supplied to the solution for mixing since the constituents repel each other. In other words, during adiabatic mixing, the solution temperature decreases since the heat of solution comes from the constituents. To bring the solution back to the initial temperature, heat has to be transferred to the solution, hence the heat of solution is positive. The enthalpy of the liquid solution is given by

$$h = x_A\, h_A + (1 - x_A)h_B + (\Delta h)_s \tag{7.8}$$

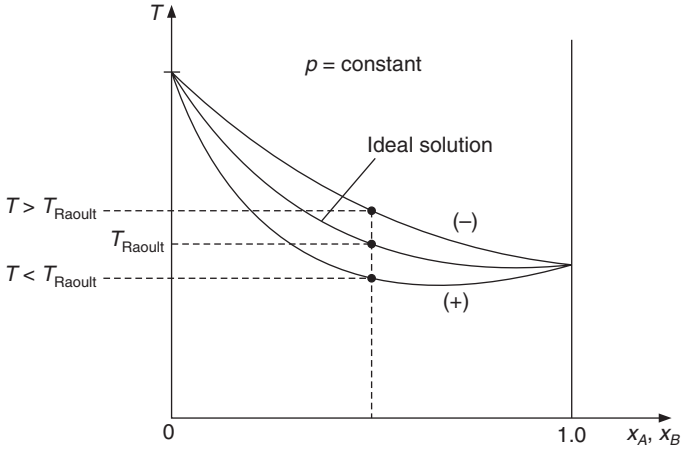

Figure 7.6 Bubble point temperature curves on temperature–composition diagram showing positive and negative deviations from Raoult's law.

where, $(\Delta h)_s$ is the heat of solution. Heat transfer to the system is considered to be positive. Hence in this case the heat of solution is positive. For ideal solutions, the heat of solution is zero. The heat of solution being positive, $h = h_f$ for the saturated liquid solution will be more than that for the ideal solution.

The forces of attraction or repulsion between the molecules of A and B in vapour state are negligible, hence the enthalpy of the mixture in vapour state in most of the cases is given by

$$h_g = x_A\, h_{gA} + (1 - x_A)\, h_{gB} \tag{7.9}$$

since the enthalpy of liquid h_f increases while h_g remains the same as that for ideal solution, the enthalpy of evaporation h_{fg} for such a solution decreases. The solution of R22 and R114 is an example of this.

By the same argument the molecules of the negative (–) deviation solution attract each other, as a result the solution pressure is less than pressure p of the ideal solution that is, $p_A + p_B < p$ and the corresponding boiling point is more than that of ideal solution. The mixing of such constituents requires exothermic reaction; as a result the solution enthalpy and temperature are more than those for ideal solution. Heat has to be rejected to bring the solution back to the initial temperature of the constituents. The heat of solution is negative. The enthalpy of saturated liquid h_f, decreases and therefore h_{fg} increases.

7.5 AQUA–AMMONIA SOLUTION

When x kg ammonia is mixed with $(1 - x)$ kg of water, the reaction is exothermic; some heat is rejected and the temperature increases. Heat has to be rejected to bring back the solution back to the initial temperature. The heat of solution $(\Delta h)_s$ is negative. If h_N and h_W are the specific enthalpies of pure liquid ammonia and water respectively, then the enthalpy of liquid solution at the temperature of the reactants, is given by

$$h = xh_N + (1 - x)h_W + (\Delta h)_s$$

7.5.1 Eutectic Points

Ammonia and water can mix well in all proportions in most of the temperature range. At 0°C the water freezes. Its freezing temperature decreases with the addition of ammonia. Similarly, pure ammonia freezes at –78°C and the addition of water decreases its freezing point. Mixtures usually exhibit eutectic points where the whole of mixture freezes uniformly without separation of any constituent. In case of ammonia–water mixture, two additional compounds, namely, $NH_3 \cdot H_2O$ and $(2NH_3) \cdot H_2O$ are formed during freezing. The first eutectic point occurs at (–92°C, $x = 0.81$), the second eutectic point occurs at (–87°C, $x = 0.57$) and the third eutectic point occurs at (–100°C, $x = 0.33$).

Thermodynamic cycle calculations of absorption cycle require values of vapour pressure, concentration, and enthalpy of solution and vapour mixture. These properties are now described below.

7.5.2 Vapour Pressure

Addition of water to liquid ammonia reduces ammonia's vapour pressure. Similarly, addition of liquid ammonia to water reduces the partial pressure of water. The total pressure of the aqua–ammonia solution is the sum of the partial pressures of both the components, which will be less than that for ideal solution.

A convenient way of expressing the vapour pressure data of aqua–ammonia solutions is available in the form of Dühring plot. This plot makes use of the following fact. *If the boiling points of two substances are close to each other, then the plot of their saturation temperatures (boiling points) at the same pressure gives a straight line*. In this plot, the boiling point of the aqua–ammonia solution is plotted against the boiling point of pure ammonia. The temperature of solution is shown on abscissa (x-axis) and the saturation temperature of pure NH_3 at the same pressure is shown on ordinate on the right hand side. The ordinate on left hand side shows the vapour pressure of pure NH_3 at the temperature indicated on the right hand ordinate. For example, solution at $x = 0.15$ and 130°C has the same vapour pressure as that of pure NH_3 at 20°C. The pressure read from the left side ordinate scale is 8.5 bar. The pressure may be accurately determined from the saturation table for NH_3 at 20°C, which is 8.574 bar. Similarly, the solution at 50°C and $x = 0.4$ has the same vapour pressure as that of pure NH_3 at 0°C. The pressure read from the plot is 4.2 bar, while the value read from the ammonia saturation table is 4.294 bar. The advantage of Dühring plot is that the temperature scales on both x and y-axes are linear and interpolation for fractional values can be done conveniently. The solution pressure can be read from the scale on the left hand side. The solution pressure is the saturation pressure of NH_3 corresponding to the temperature on the right hand side ordinate. This pressure scale is not linear, but it is logarithmic. However, a more accurate value of pressure can be read from the saturation table of NH_3 for the temperature read from the right hand ordinate of the Dühring plot. Other plots like ln (p) against $1/T$ or $1/(T + C)$ have the disadvantage that the temperature scale is not linear. However, the saturated vapour lines are straight on such a plot. It will be shown that the absorption cycle is easy to show on such a plot.

The aqua–ammonia solution shows considerable deviation from ideal solution as shown in the following example.

EXAMPLE 7.1 Compare the vapour pressure found from Dühring plot with that determined from Raoult's law for acqua–ammonia solution at 70°C and $x = 0.3$.

Solution:

From the Dühring plot the solution pressure is equal to that of pure NH_3 at 0°C, which is obtained from saturation table of NH_3 as 4.294 bar. We require mole fraction of ammonia and water to use Raoult's law. For this purpose, we take the molecular weights as $M_{\text{ammonia}} = 17$ and $M_{\text{water}} = 18$, hence for mass concentration $x = 0.3$, the mole fraction of NH_3 is

$$\chi = \frac{0.3/17}{(0.3/17) + (1 - 0.3)/18} = 0.312$$

At 70°C the saturation pressure of NH_3 is 33.12 bar, and the saturation pressure of water is 0.319 bar.

Partial pressure of NH_3 in solution, $p_N = 0.312\ (33.12) = 10.338$ bar

Partial pressure of water in solution, $p_W = (1 - 0.312)\ 0.3119 = 0.2145$ bar

Total pressure = 10.338 + 0.2145 = 10.5525 bar. This is the pressure of the solution predicted by Raoult's law and it is very much different from the actual pressure 4.294 bar of the solution.

The actual pressure for aqua–ammonia solution is much less than that for ideal solution since ammonia has strong affinity for water.

7.5.3 Vapour Concentration

Another useful plot is that of the mass fraction of NH_3 in vapour mixture that is in equilibrium with the liquid at the given temperature and concentration. It was shown in Figure 7.5 that saturated liquid with concentration x_F is in equilibrium with saturated vapour of larger concentration x_G at the same temperature. Figure 7.7 shows a representative chart that gives the mass fraction of

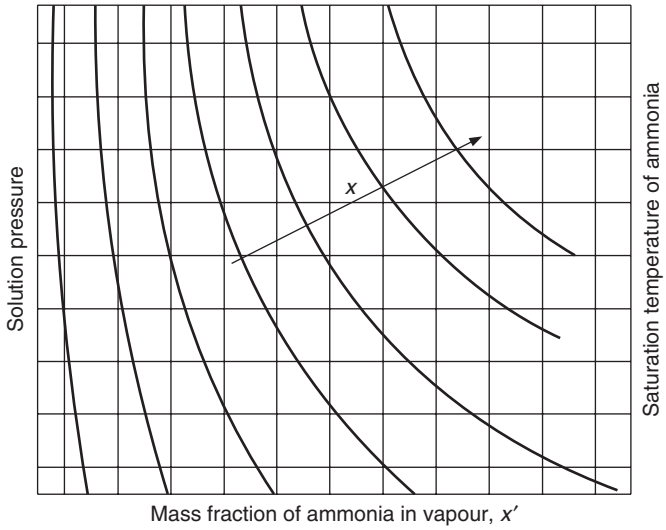

Figure 7.7 Vapour–liquid equilibrium chart for ammonia–water solution.

ammonia vapour x' (vapour phase mass fraction) on the abscissa against the saturation temperature of ammonia as ordinate on the right hand side. The ordinate on the left hand side is similar to that in Dühring plot. It is the solution pressure, which is the saturation pressure of NH_3 corresponding to temperature on right hand side scale. The figure has several curves for different mass fractions x of NH_3 (liquid phase mass fraction). It can be shown with the help of an actual chart (like that of Figure 7.7) that the vapour composition considering ideal solution, does not agree with the experimental data presented in such a chart. The following example illustrates this.

EXAMPLE 7.2 Determine the mass fraction of saturated ammonia vapour given off by an aqua-ammonia solution of mass fraction 0.3 at 70°C.

Solution:

Considering ideal solution, the partial pressures of ammonia and water as determined in Example 7.1 are:

$$p_N = 10.338 \text{ bar} \quad \text{and} \quad p_W = 0.2145 \text{ bar}$$

By interpolating in the superheat tables for ammonia and water, the specific volumes of the two are:

$$v_N = 0.1574 \text{ m}^3/\text{kg at } 10.338 \text{ bar} \quad \text{and} \quad 70^\circ\text{C}$$

and

$$v_W = 7.35 \text{ m}^3/\text{kg at } 0.2145 \text{ bar} \quad \text{and} \quad 70^\circ\text{C}$$

Let m_N and m_W be the masses of ammonia and water vapour in a sample of volume $\mathbb{V}$ m^3.
Mass fraction of ammonia in vapour mixture is given by

$$x' = \frac{m_N}{m_N + m_W} = \frac{m_N / \mathbb{V}}{m_N / \mathbb{V} + m_W / \mathbb{V}} = \frac{1/v_N}{1/v_N + 1/v_W} \tag{7.10}$$

$$\therefore \quad x' = \frac{1/0.1574}{1/0.1574 + 1/7.35} = 0.979 \quad \text{and} \quad (1 - x') = 0.021$$

The mass fraction of ammonia and water in vapour mixture are 0.979 and 0.021 respectively. In Example 7.1 it was observed that the pressure of solution is 4.294 bar. The experimental values read from an actual chart (like that of Figure 7.7) for solution concentration of 0.3 and pressure of 4.294 bar are

$$x' = 0.95 \quad \text{and} \quad 1 - x' = 0.05$$

These are different from those calculated from the ideal solution relations.

7.5.4 Enthalpy

Solution enthalpy

The solution enthalpy is given by a relation similar to Eq. (7.8) in terms of enthalpy of ammonia, water and the heat of solution, that is,

$$h = x\, h_N + (1 - x)h_W + (\Delta h)_s \tag{7.11}$$

The enthalpy of the liquid solution can be determined by using the experimental values of heat of solution. The values of solution enthalpy against ammonia mass fraction are given in the bottom part of Figure 7.8 for some temperatures and pressures. The enthalpy of liquids does not strongly

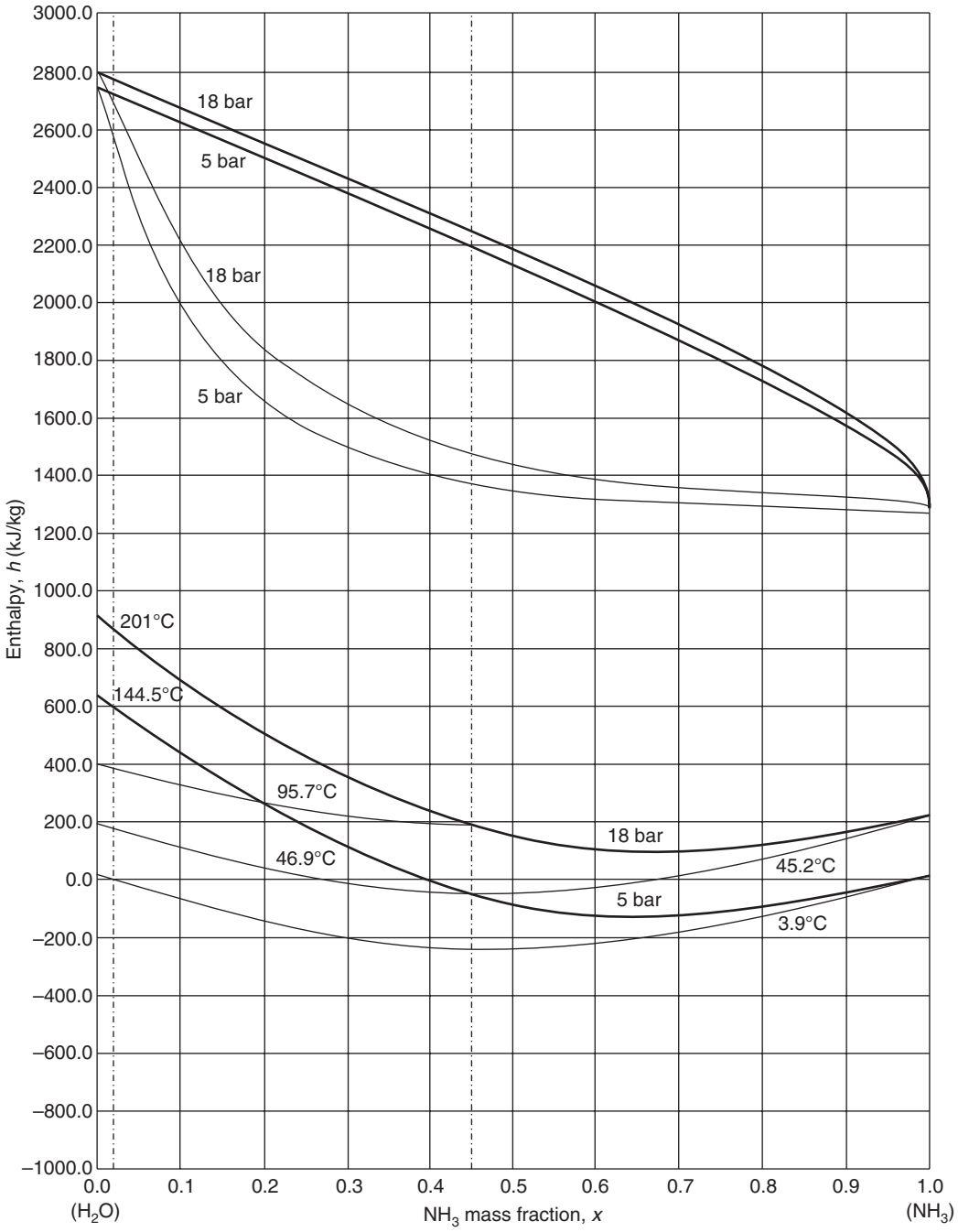

Figure 7.8 *h–x* diagram for acqua–ammonia solution.

depend upon pressure. In fact, accurate data about compressed liquids is not available. Hence, enthalpy of a subcooled liquid is considered to be the same as that of the saturated liquid at the same temperature. This implies that the enthalpy of the liquid solution is a function of temperature and mass fraction of ammonia. Therefore, isotherms have been shown in the figure against x. At $x = 0$, the solution enthalpy is that of pure water (this is zero in IIR reference) while at $x = 1$, it is that of pure ammonia.

It was observed that at each mass fraction, the solution has a unique bubble point for a given pressure. In other words at each temperature and mass fraction there is a unique pressure at which the solution is saturated liquid. This data is available in Dühring chart. Thus, isobars are also plotted in Figure 7.8.

A solution of mass fraction 0.3 at a pressure of 2 bar has a bubble point of 47°C and enthalpy of 0.0 kJ/kg. The solution of mass fraction 0.3 and pressure 2 bar will be a sub-cooled liquid below temperature of 47°C. Similarly at mass fraction 0.45 and 18 bar pressure the bubble point is 96°C and enthalpy is 200 kJ/kg.

Vapour enthalpy

It is usually assumed that the enthalpy of mixing of ammonia and water vapour is negligible. That is, the chemical reaction does not occur and no new compounds are formed during mixing as it happens for the liquid solution. Hence, the mixture enthalpy can be determined from equation similar to Eq. (7.8) if the mass fraction of ammonia vapour, x', is known. It has been seen in Example 7.2 that if the experimental data on specific volume were available, then the mass fraction and hence the enthalpy can be determined with confidence. The equation for mixture enthalpy is

$$h = x' h_{gN} + (1 - x') h_{gW} \tag{7.12}$$

where, h_{gN} and h_{gW} are the enthalpies of superheated ammonia and water vapours respectively at their partial pressures. In Example 7.2 for $x = 0.3$ and 70°C the total pressure was 4.294 bar. Water vapour has saturation pressure of 0.3119 bar at 70°C. Water vapour cannot exist at 70°C and pressure of 4.294 bar except perhaps in a metastable state. Hence the following procedure is adopted.

- Mole fraction of ammonia is determined from the given value of mass fraction.
- Partial pressures of ammonia and water vapour are determined.
- Enthalpy and specific volume of superheated water vapour and ammonia are found by interpolation in the superheat tables of water and ammonia respectively.
- Then enthalpy is determined from Eq. (7.12).

As a cross check, mass fraction of ammonia is determined from the specific volume data. This is illustrated by the following example.

EXAMPLE 7.3 Determine the specific enthalpy of saturated vapour produced by aqua–ammonia solution of mass fraction 0.3 and temperature of 70°C.

Solution:

The mass fraction $x = 0.3$ is the mass fraction of ammonia in liquid solution. In Example 7.2 it was observed that the mass fraction of ammonia in the vapour mixture (that is in equilibrium with liquid of $x = 0.3$) as determined from Figure 7.7, is $x' = 0.95$. The mass fraction of water vapour = $1 - 0.95 = 0.05$. Therefore, the mole fraction is

$$\chi' = \frac{0.95/17}{(0.95/17) + (0.05/18)} = 0.95265, \quad 1 - \chi' = 0.04735$$

$$p_N = 0.95265(4.294) = 4.091 \text{ bar and } p_W = 0.04735(4.294) = 0.2033 \text{ bar}$$

By interpolating in the superheat tables for water vapour and ammonia,

$$h_N = 1615.048 \text{ kJ/kg} \quad \text{and} \quad v_N = 0.404553 \text{ m}^3/\text{kg}$$

and $$h_W = 2629.35 \text{ kJ/kg} \quad \text{and} \quad v_W = 7.75504 \text{ m}^3/\text{kg}$$

Therefore,

$$h = 0.95(1615.048) + 0.05(2629.35) = 1665.76 \text{ kJ/kg}$$

As a cross check the mass fraction of ammonia is

$$x' = \frac{1/0.404553}{1/0.404553 + 1/7.75504} = 0.95042$$

This is very close to experimental values of 0.95 for the mass fraction of ammonia. This can still be refined by trial and error so that we get a value of mass fraction x' closer to the experimental value.

The values of specific vapour enthalpies are found by this method for various values of ammonia mass fraction x (in liquid solution) and fixed saturation pressure. The process is repeated for various pressures. These isobars are plotted on enthalpy vs. x diagram as shown in the upper part of Figure 7.8. These are referred to as *Equilibrium Construction lines.*

A liquid of concentration x at given pressure and temperature is in equilibrium with vapour of concentration x' as shown in Figure 7.7. A similar plot of enthalpy can be made against the saturated vapour concentration x'. In this diagram enthalpy is plotted against the vapour concentration x' corresponding to liquid concentration x and enthalpy is same along a horizontal line joining these two points x and x'. Several authors including *Bošnjakovic'* (1937) have presented such plots. Such a plot is also available in *Thermodynamic and Physical Properties of* NH_3–H_2O, Int. Inst. Refrigeration, Paris France, 1994 (p. 88). Park, Y.M. and Sonntag, R.E. have given a similar diagram in *ASHRAE Trans*., 96, 1, pp. 150–159,1990. Ibrahim, O.M. and Klein, S.A. in *ASHRAE Trans*., 99, 1, pp. 1495–1502 have also given this data.

The enthalpy–composition diagram for two pressures is shown in Figure 7.9 for illustration. At pressure p_1 the enthalpy of saturated liquid and saturated vapour ammonia is h_{fN} and h_{gN}, respectively, as shown in the figure at x =1 for pure ammonia. Similarly, at pressure p_1 the enthalpy of saturated liquid and vapour water is h_{fW} and h_{gW}, respectively, as shown in the figure at x = 0 for pure water. The enthalpy of saturated liquid solution at pressure p_1 and various concentrations x is determined from Eq. (7.8) by knowing the heat of solution for these conditions. The line joining h_{fW}, liquid enthalpies at various concentrations and h_{fN} is the saturated liquid line. The enthalpy of vapour mixture at pressure p_1 and various concentrations x' can be determined from Eq. (7.12). A line joining these states with h_{gW} and h_{gN} is the saturated vapour line at pressure p_1. The region between these two lines is the mixture region where the liquid exists in equilibrium with the vapour state.

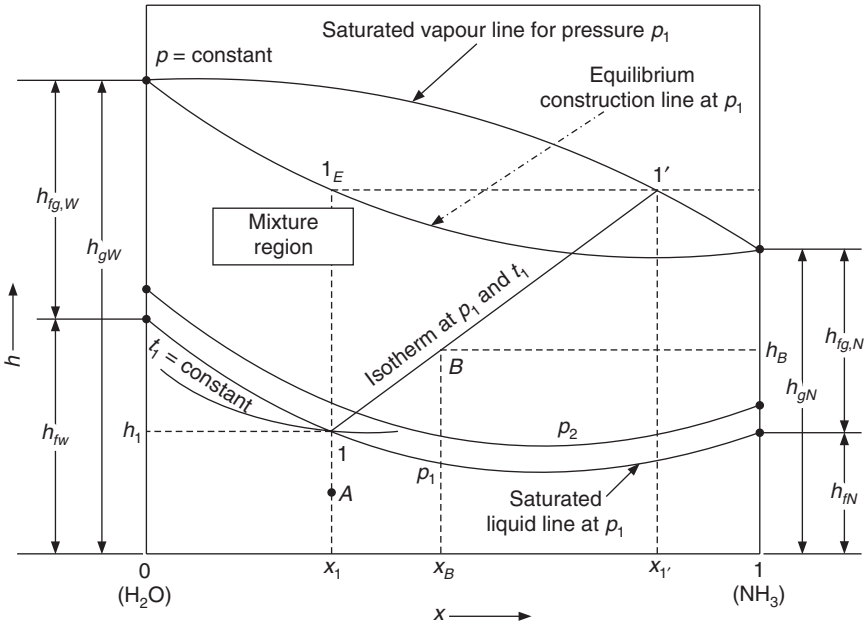

Figure 7.9 Enthalpy–composition diagram of NH_3–H_2O at a constant pressure p.

The isotherms are generally shown only in the liquid region. For constant mass fraction, the temperature is maximum at the saturated liquid state for a given pressure. For example, at concentration x_1 it occurs at point 1. This is the bubble point for pressure p_1 and concentration x_1. At a temperature lower than this or at pressure lower than this, the solution with concentration x_1 is the subcooled liquid. For example at point A, the solution is subcooled at concentration x_1 and, say, 20°C. Similarly, state 1 would be a subcooled state for pressure $p_2 > p_1$.

If one looks along an isotherm there is a unique value of x at which the solution is saturated liquid (isotherm intersects the constant pressure line p_1 at this point).

Temperatures are not shown in the vapour region or the mixture region to avoid overcrowding of the figure. The isotherm in the mixture region can be drawn with the help of the equilibrium construction line. To draw an isotherm for temperature t_1 (say 40°C) at pressure p_1, the saturated liquid state is located at point 1 as shown in Figure 7.9. A vertical line is drawn from point 1 to intersect the equilibrium construction line at point 1_E. The equilibrium construction line represents the vapour enthalpy at liquid mass fraction x. Hence, enthalpy of vapour is same as that at 1_E. Therefore, to locate the saturated vapour state a horizontal line (constant enthalpy) is drawn from point 1_E to intersect the saturated vapour line for pressure p_1 at point $1'$. Line 1–$1'$ is the isotherm at temperature t_1 and pressure p_1. The mass fraction of ammonia in saturated vapour is $x_{1'}$. At any point B with pressure p_1 in the mixture region we will have a mixture of saturated liquid (x_1, h_1) and saturated vapour ($x_{1'}$, $h_{1'}$). The dryness fraction x at this point is given by Eq. (7.7), that is, $\xi_B = (x_B - x_1)/(x_{1'} - x_1)$ and enthalpy $h_B = \xi h_{1'} + (1 - \xi)h_1$.

EXAMPLE 7.4 The enthalpy of aqua–ammonia solution is 0.0 kJ/kg and the concentration is 0.35. (a) Find the condition for this to be saturated state. (b) What is the state if the pressure is 2.0 bar? (c) What is the condition if the pressure is 4 bar?

Solution:

It is to be noted that three independent thermodynamic properties are required to fix the thermodynamic state of the liquid solution. In this example only two properties are given, hence the state will be different in the three cases asked for.

(a) It can be made out from the h–x diagram in Figure 7.8 that the line for 3 bar pressure would intersect the 50°C isotherm at $x = 0.35$ and $h = 0.0$. Hence, for saturated state the pressure should be 3.0 bar and temperature should be 50°C. This is illustrated by point A in Figure 7.10.

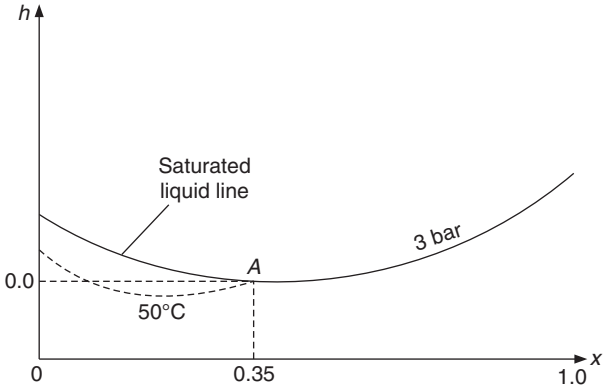

Figure 7.10 Example 7.4.

(b) At pressure of 2 bar and $x = 0.35$ it is found from the h–x diagram that enthalpy $h = -60.0$ kJ/kg. This is less than the given enthalpy of $h = 0.0$, hence the state at $x = 0.35$ and $h = 0.0$ is in two-phase region at 2 bar (the pressure is less than the saturation pressure). An isotherm passing through this point can be drawn for pressure of 2.0 bar. To draw this, one chooses a liquid state on 2.0 bar line at slightly lower value of temperature (say x_l, h_l), draws a vertical line to intersect the 2 bar equilibrium construction line and draws a horizontal line from this point on the equilibrium construction line to intersect the 2 bar saturated vapour line (say x_V', h_V'). The line joining these two points (i.e. x_1, h_1 and x_V', h_V') should pass through point B, that is, $x = 0.35$ and $h = 0.0$. If this line does not pass through B, then by trial and error, another point 2 is chosen on the 2 bar liquid state and point 2_E is located on equilibrium line followed by the horizontal line $2_E - 2'$. Line 2–2′ is drawn which passes through point B. In this case, the end points of the isotherm line are: $x_l = 0.321$, $h_l = -20$ and $x_V = 0.982$, $h_V = 1400$.

(c) At pressure of 4.0 bar and $x = 0.35$ it is found from the h–x diagram that $h = 45$ which is more than the given enthalpy, hence the liquid is in subcooled state (the pressure is more than the saturation pressure). The temperature will be observed to be 60°C at this point.

EXAMPLE 7.5 Given that for an aqua–ammonia solution $p = 2$ bar, $x = 0.41$ and $h = 210$ kJ/kg, find the state at this point.

Solution:

An inspection of the h–x diagram (Figure 7.8) reveals that at $x = 0.41$ and $h = 210$, the liquid will be a saturated liquid if the pressure is 18 bar and temperature 100°C. However it is given that the pressure is 2 bar, hence the mixture is in the two-phase region. By trial and error, an isotherm may

be drawn through this point. Following the procedure outlined in Example 7.4(b), the isotherm joins the saturated liquid state at 2 bar, $x = 0.3$ and $h = 0.0$ with the saturated vapour state at 2 bar, $x = 0.975$ and $h = 1430$ kJ/kg.

7.6 SIMPLE ABSORPTION SYSTEM

We will now look at some of the simple processes that occur in an absorption system and represent these on the h–x diagram.

7.6.1 Adiabatic Mixing

Two streams 1 and 2 of ammonia–water solutions and of different concentrations mix adiabatically in a chamber resulting in stream 3 as shown schematically in Figure 7.11(a). We will consider mass and energy conservation to find the outlet conditions of the stream 3 leaving the mixing chamber.

Overall Mass Conservation: $\dot{m}_1 + \dot{m}_2 = \dot{m}_3$

Mass Conservation for Ammonia: $\dot{m}_1 x_1 + \dot{m}_2 x_2 = \dot{m}_3 x_3$

Energy Conservation: $\dot{m}_1 h_1 + \dot{m}_2 h_2 = \dot{m}_3 h_3$

Rearranging these equations, we get

$$\frac{\dot{m}_1}{\dot{m}_2} = \frac{x_2 - x_3}{x_3 - x_1} = \frac{h_2 - h_3}{h_3 - h_1} \tag{7.13}$$

$$x_3 = x_1 + (\dot{m}_2 / \dot{m}_3)(x_2 - x_1) \tag{7.14a}$$

and

$$h_3 = h_1 + (\dot{m}_2 / \dot{m}_3)(h_2 - h_1) \tag{7.14b}$$

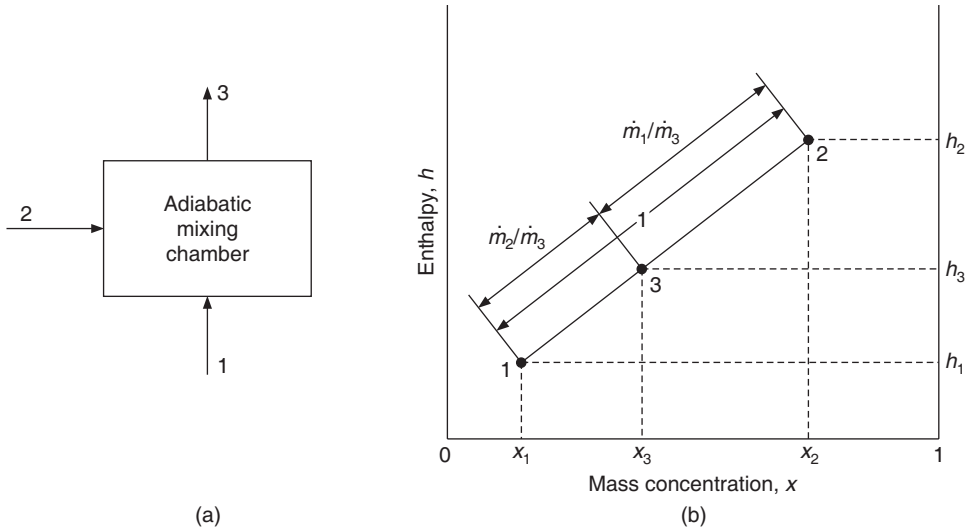

Figure 7.11 Adiabatic mixing of two solution streams.

Equations (7.14a) and (7.14b) define a straight line on the h–x diagram as shown in Figure 7.11(b). Equation (7.14a) indicates that state 3 lies on a vertical line intersecting x_1 and x_2 in proportion of $\dot{m}_2$ and $\dot{m}_1$. Similarly, Eq. (7.14b) indicates that state 3 lies on horizontal line intersecting h_1 and h_2 in proportion of $\dot{m}_2$ and $\dot{m}_1$. Therefore state 3 line lies on the line joining 1 and 2 and intersecting it in proportion of $\dot{m}_2$ and $\dot{m}_1$ as shown in Figure 7.12(b).

7.6.2 Mixing of Two Streams with Heat Rejection

Two streams 1 and 2 mix resulting in stream 3 and heat rejection Q as shown schematically in Figure 7.12(a). This type of process occurs in the absorber of absorption refrigeration systems. We consider mass and energy conservation to find the outlet conditions.

Overall Mass Conservation: $\dot{m}_1 + \dot{m}_2 = \dot{m}_3$

Mass Conservation for Ammonia: $\dot{m}_1 x_1 + \dot{m}_2 x_2 = \dot{m}_3 x_3$

Energy Conservation: $\dot{m}_1 h_1 + \dot{m}_2 h_2 = \dot{m}_3 h_3 + Q$

Rearranging these equations, we get $\dfrac{\dot{m}_1}{\dot{m}_2} = \dfrac{x_2 - x_3}{x_3 - x_1}$

$$x_3 = x_1 + (\dot{m}_2 / \dot{m}_3)(x_2 - x_1) \tag{7.15a}$$

and
$$h_3 = h_1 + (\dot{m}_2 / \dot{m}_3)(h_2 - h_1) - Q / \dot{m}_3 = h_{3'} - Q / \dot{m}_3 \tag{7.15b}$$

where $h_{3'} = h_1 + (\dot{m}_2 / \dot{m}_3)(h_2 - h_1)$ which is same as Eq. (7.14b)

These equations indicate that state 3′ will lie on a line joining states 1 and 2 and intersecting the line in proportion of $\dot{m}_2$ and $\dot{m}_1$ as in the last example and shown in Figure 7.12(b). State 3 is located vertically below state 3′ by $Q / \dot{m}_3$ as shown in Eq. (7.15b), since enthalpy at state 3 is less than that at state 3′ by $Q / \dot{m}_3$.

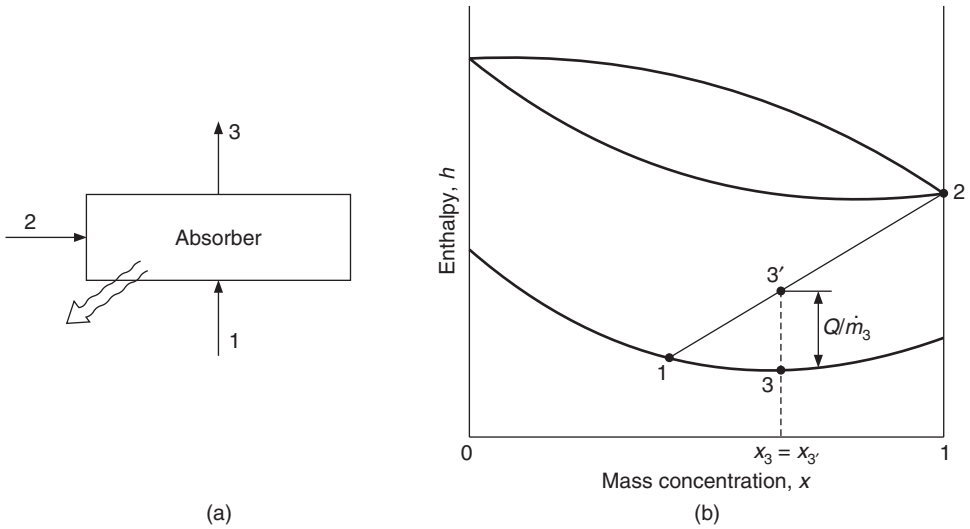

Figure 7.12 Mixing of two streams with heat transfer.

7.6.3 Heat Transfer Followed by Separation into Liquid and Vapour

This process is schematically shown in Figure 7.13(a). Heat is transferred to subcooled liquid stream 1 at the rate of Q_{12} kW, the resulting stream is put into a vessel where the liquid is separated from the bottom as state 3 and vapour comes out from top of the vessel at state 4. The mass and energy conservation yields

$$\dot{m}_1 + \dot{m}_2,\ x_1 = x_2$$

and

$$\dot{m}Q_{12} = \dot{m}_1(h_2 - h_1) \quad \text{or} \quad h_2 = h_1 + (Q_{12} / \dot{m}_1)$$

If state 1 is a sub-cooled state as shown in Figure 7.13(b), then state 2 is in the mixture region and is located vertically above it by $Q_{12} / \dot{m}_1$ as shown in the Figure 7.13(b). For the sates 3 and 4, we have

$$\dot{m}_3 + \dot{m}_4 = \dot{m}_2$$

$$\dot{m}_3 x_3 + \dot{m}_4 x_4 = \dot{m}_2 x_2$$

and

$$\dot{m}_3 h_3 + \dot{m}_4 h_4 = \dot{m}_2 h_2$$

$$\frac{\dot{m}_3}{\dot{m}_4} = \frac{x_4 - x_2}{x_2 - x_3} = \frac{h_4 - h_2}{h_2 - h_3}$$

States 3 and 4 are saturated liquid and vapour states at the same temperature. The temperature however is not known. An isotherm passing through point 2 is drawn by trial and error to locate states 3 and 4 in Figure 7.13(b).

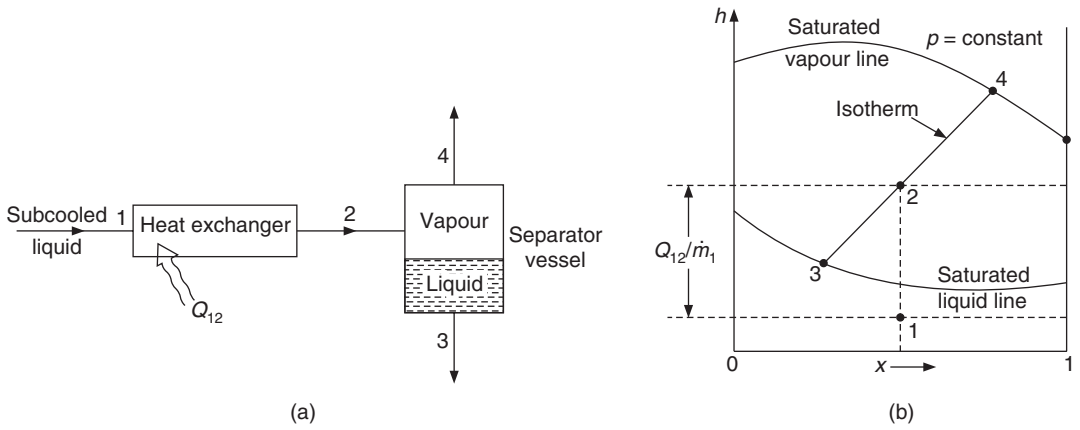

Figure 7.13 Heating of ammonia–water solution.

7.6.4 Heat Rejection Followed by Separation into Liquid and Vapour

This process is schematically shown in Figure 7.14(a). The saturated vapour at state 1 is cooled by heat rejection rate Q_{12}. State 2 is located vertically below state 1 by $Q_{12} / \dot{m}_1$ since

$$h_2 = h_1 - Q_{12} / \dot{m}_1$$

The mixture at state 2 is passed into a separation vessel where the liquid settles down and is drained from the bottom at state 3 and vapour leaves at state 4. The saturated liquid and vapour states 3 and 4 respectively are located by drawing the isotherm passing through point 2 as shown in Figure 7.14(b).

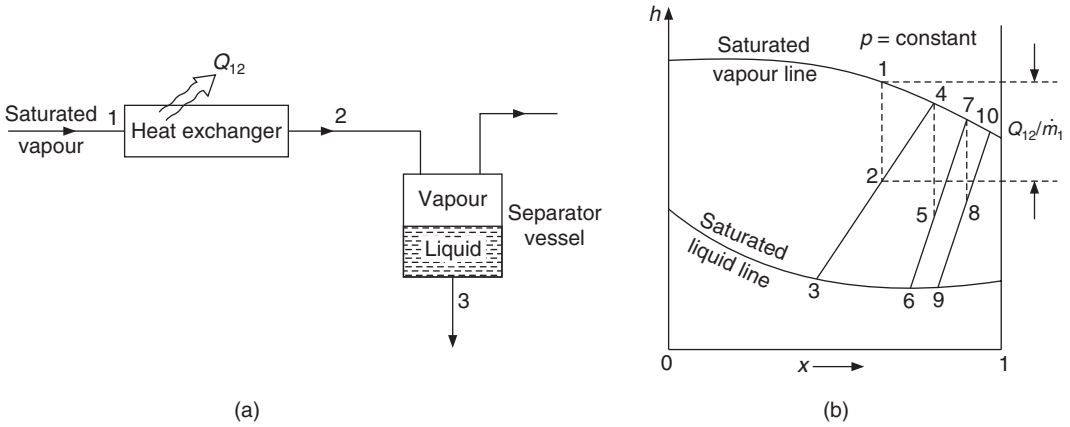

Figure 7.14 Cooling of ammonia–water mixture.

The saturated vapour at state 4 has a higher mass fraction of ammonia than at state 1. If saturated vapour at state 4 is cooled further and the mixture is separated into liquid and vapour, the vapour at state 7 turns out to be richer in ammonia. Hence, a given vapour mixture can be enriched by a number of steps each involving cooling followed by separation into liquid and vapour. This is the principle of enrichment of ammonia in the vapour mixture. It is shown in Figure 7.14(b) that if another set of cooling and separation is added, one would get even more richer vapour at state 10.

7.6.5 Throttling Process

The mass flow rate, the concentration and the enthalpy do not change during the throttling process. A throttling valve is shown schematically in Figure 7.15(a). Hence, in a throttling valve,

$$\dot{m}_4 = \dot{m}_5, \quad x_4 = x_5$$

and

$$h_4 = h_5$$

As a result, on the *h*–*x* diagram as shown in Figure 7.15(b) the points 4 and 5 are coincident. However, the pressure at point 5 is less than that at point 4. State 4 is saturated liquid state at pressure p_2 while state 5 is in the mixture region at lower pressure p_1 since there is a possibility of vapour generation due to flashing at the exit condition 5. The temperature at point 5 is determined by drawing an isotherm passing through point 5 for pressure p_1 by trial and error. The saturated liquid 5_l and saturated vapour state 5_v correspond to isotherm through point 5.

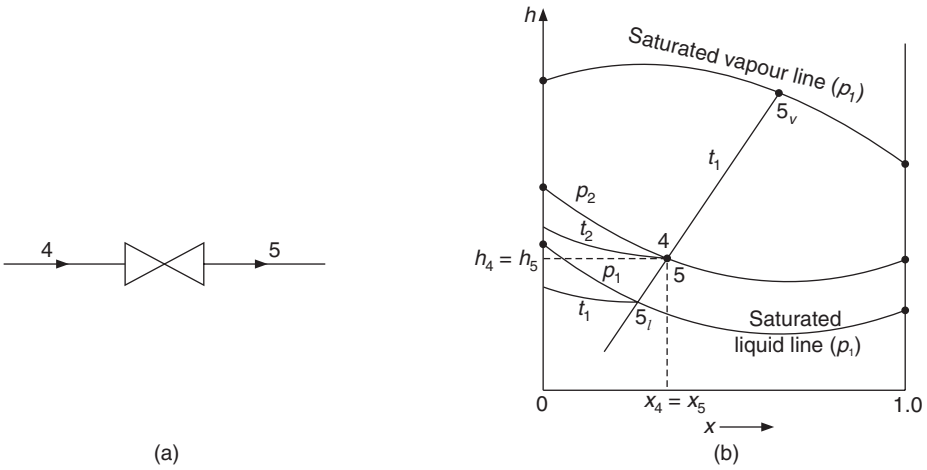

Figure 7.15 Throttling of ammonia–water solution.

EXAMPLE 7.6 The liquid solution at 15.0 bar pressure and $t = 40^{o}$ C is throttled to a pressure of 2 bar. Find the state after expansion.

Solution:

It may be determined from the *h–x* diagram that the saturated liquid state at 15 bar and 40°C has $x = 0.935$ and $h = 160$. As outlined in Examples 7.4 and 7.5 the state at 2 bar will be in the two-phase region. By trial and error the two ends of the isotherm passing through this point for 2.0 bar are found as follows. $x_l = 0.92$, $h_l = -140.0$ and $x_v = 0.995$ and $h_v = 1225$.

7.7 *h–x* DIAGRAM FOR SIMPLE ABSORPTION SYSTEM

To illustrate the representation of the absorption refrigeration system on the *h–x* diagram and to do sample cycle calculations, we consider a simple absorption refrigeration system without preheating and precooling heat exchangers as shown in Figure 7.16.

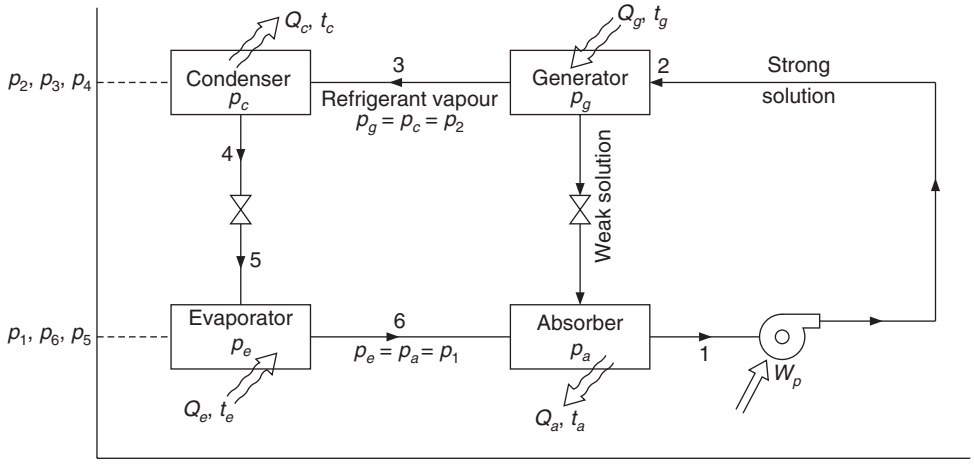

Figure 7.16 Simple ammonia–water absorption refrigeration system (without preheating and precooling heat exchangers).

EXAMPLE 7.7 In a simple absorption refrigeration system of Figure 7.16 the conditions at various points are as given in the table below. Show all the state points on the h–x diagram. Determine the mass flow rate through the evaporator and those of weak and strong solutions for 1 TR cooling capacity. Then determine the heat transfer rates through absorber, generator and the condenser. Check the energy balance and find the COP.

State	*Pressure*	*Temperature* (°C)
1	1.75	25
2	13.5	100
3	13.5	100
4	13.5	40
5	1.75	0

Solution:

It is observed that the evaporator pressure p_e is same as the absorber pressure p_a and the generator pressure p_g is same as the condenser pressure p_c, that is,

$$p_e = p_a = p_1 \quad \text{and} \quad p_g = p_c = p_2$$

In practice, flow occurs from evaporator to absorber, hence $p_e > p_a$ and similarly $p_g > p_c$. These differences are, however, small and may be neglected.

In general p_1 and p_2 are the saturation pressures at the evaporator and condenser temperatures respectively. In case the mixture entering the evaporator is not pure refrigerant ($x < 1$), all the liquid in the evaporator may not evaporate and for this mixture of liquid and vapour the pressure in the evaporator will not be saturation pressure of pure ammonia. It has been observed that during boiling and condensation the temperature does not remain constant for a binary mixture, therefore the temperatures in the condenser and evaporator will not be constant.

Both the absorber and condenser if cooled by water that passes in parallel through them, their temperatures will be same. If the cooling water passes first through the absorber and then enters the condenser, we would have $t_c > t_a$.

State 1

In the absorber, mixing occurs hence state 1 is usually a saturated state. In this case, it is located at the intersection of isobar for 1.75 bar and temperature 25°C in the liquid region. We have from the h–x diagram

$$x_1 = 0.393 \quad \text{and} \quad h_1 = -115 \text{ kJ/kg}$$

The skeleton h–x diagram in Figure 7.17 shows the states for this cycle.

States 2 and 3

In the generator boiling occurs, as a result the liquid and the vapour are in equilibrium, therefore state 2 is saturated liquid state and state 3 is saturated vapour state. Point 2 is located at the intersection of isobar for 13.5 bar and 100°C in the liquid region. To locate the saturated vapour state 3, we

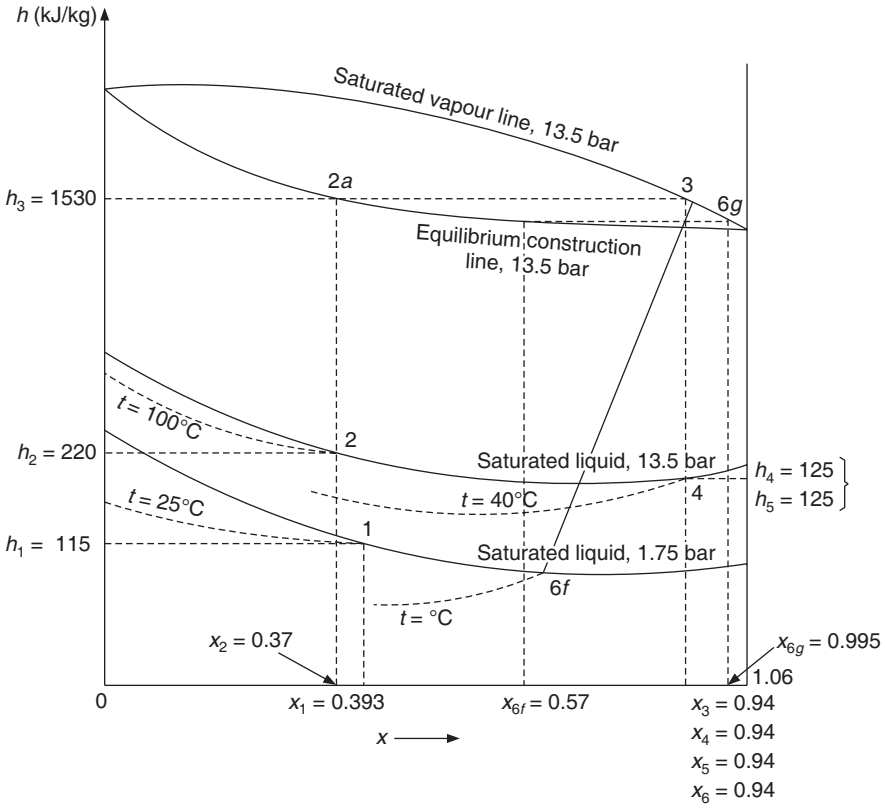

Figure 7.17 Schematic *h–x* diagram for Example 7.7.

draw a vertical line through point 2 to intersect the equilibrium construction curve for 13.5 bar at point 2*a* and then draw a horizontal line through point 2*a* to intersect the saturated vapour line for 13.5 bar at point 3. We have from the skelton *h–x* diagram,

$$x_2 = 0.37 \text{ and } h_2 = 220.0 \text{ kJ/kg} ; \; x_3 = 0.94 \text{ and } h_3 = 1530 \text{ kJ/kg}$$

State 4

The concentration of ammonia does not change in the condenser, expansion valve and evaporator, since no mass of water or ammonia is added or removed in these components.

$$\therefore \qquad x_3 = x_4 = x_5 = x_6 = \text{constant}$$

This indicates that states 3, 4, 5 and 6 all will lie on the vertical line x_3 = constant.

If it is assumed that all the vapour condenses at the exit of the condenser then we will have saturated liquid at condenser exit. This point may be located at the intersection of isobar for13.5 bar and $x_4 = 0.94$. From *h–x* diagram, it is observed that

$$h_4 = 125 \text{ kJ/kg and temperature } t_4 = 40^{\circ}\text{C}$$

It is not necessary to specify the temperature at the exit of condenser in this case, it is automatically fixed by $x_3 = x_4$ and p_2. In fact, pressure p_2 is chosen such that we obtain saturated liquid at state 4 since entry of liquid–vapour mixture into the expansion valve is not recommended.

If the solution leaving the condenser is subcooled, then the temperature will be less than 40°C, on the other hand for incomplete condensation (mixture of liquid and vapour) it will be greater than 40°C.

State 5

The enthalpy remains constant during the throttling process 4 to 5, hence,

$$x_5 = x_4 = 0.94 \text{ and } h_5 = h_4$$

If the enthalpy and concentration are the same then the points are coincident on the h–x diagram. However, pressure $p_4 = p_2 > p_1 = p_5$. Hence state 5 is in the mixture region (liquid + vapour) at 1.75 bar since the saturated liquid line for 1.75 bar is well below this point.

State 6

We have specified p_6 = 1.75 bar, t_5 = 0°C and x_6 = 0.94. Obviously, it is not a saturated vapour state, since for a saturated liquid or vapour state of two components, only two properties need be specified. In this case three properties are specified. It is, in fact, in the mixture region. The saturated pressure of NH_3 at 0°C is 4.29 bar. The evaporator pressure is given to be 1.75 bar, which is lower than 4.29 bar. The state 1.75 bar, 0°C and x = 0.94 is located by drawing the isotherm of 0°C, that is, 6f–6g and finding its intersection with $x_3 = x_6$ = 0.94 as shown in Figure 7.17. Along the isotherm the properties of saturated liquid and vapour at 0°C and 1.75 bar are:

$$h_{6f} = -245 \text{ kJ/kg} \text{ and } x_{6f} = 0.57$$
$$h_{6g} = 1300 \text{ kJ/kg} \text{ and } x_{6g} = 0.995$$

The concentration of NH_3 at inlet to evaporator is 0.94 and at the exit of evaporator it should become 0.995 if all the liquid evaporates. However, mass conservation states that it is 0.94 at the exit of evaporator. Hence, all the liquid entering the evaporator does not evaporate and some purge liquid is present at state 6.

Let the mass flow rate of mixture at point 6 be 1 kg/s and let the purge liquid contained in this be w_6 kg/s; then vapour flow rate is $(1 - w_6)$ kg/s. The liquid has concentration of 0.57 and vapour has 0.995. Mass conservation of NH_3 at exit yields

$$0.94(1) = w_6(0.57) + (1 - w_6)(0.995)$$

which yields

$$w_6 = (0.995 - 0.94)/(0.995 - 0.57) = 0.13$$

That is, there is 13% liquid left at exit of the evaporator. Therefore, enthalpy at point 6 is

$$h_6 = w_6 h_{6f} + (1 - w_6)h_{6g}$$
$$h_6 = 0.13(-245) + 0.87(1300) = 1099.15 \text{ kJ/kg}$$

For 1 TR cooling capacity,

$$\dot{m}_6 = 3.5167/(h_6 - h_4) = 3.5167/(1099.15 - 125) = 3.61 \times 10^{-3} \text{ kg/s}$$

The overall mass conservation and ammonia mass conservation for the absorber yields.

$$\dot{m}_2 + \dot{m}_6 = \dot{m}_1 \quad \text{: Overall mass conservation}$$
$$\dot{m}_2 x_2 + \dot{m}_6 x_6 = \dot{m}_1 x_1 \quad \text{:Ammonia mass conservation}$$

Solving these two equations, we get

$$\dot{m}_2 = \dot{m}_6(x_6 - x_1)/(x_1 - x_2)$$
$$= 3.61 \times 10^{-3}\ (0.94 - 0.393)/(0.393 - 0.37) = 8.5855 \times 10^{-2}\ \text{kg/s}$$
$$\dot{m}_1 = \dot{m}_6(x_6 - x_2)/(x_1 - x_2)$$
$$= 3.61 \times 10^{-3}\ (0.94 - 0.37)/(0.393 - 0.37) = 8.9465 \times 10^{-2}\ \text{kg/s}$$

Energy balance for the absorber yields

$$Q_a = \dot{m}_2 h_2 + \dot{m}_6 h_6 - \dot{m}_1 h_1$$
$$= 8.5855 \times 10^{-2}(220) + 3.61 \times 10^{-3}\ (1099.15) - 8.9465 \times 10^{-2}(-115) = 33.1445\ \text{kW}$$

Similarly for the generator,

$$Q_g = \dot{m}_2 h_2 + \dot{m}_3 h_3 - \dot{m}_1 h_1$$
$$= 8.5855 \times 10^{-2}(220) + 3.61 \times 10^{-3}\ (1530) - 8.9465 \times 10^{-2}(-115) = 34.6999\ \text{kW}$$
$$Q_c = \dot{m}_3(h_3 - h_4) = 3.61 \times 10^{-3}\ (1530 - 125) = 5.072\ \text{kW}$$

To check the overall energy balance, neglecting the pump work input, we get

Net heat rejection from system = $Q_a + Q_c = 33.1445 + 5.072 = 38.217$ kW

Net heat input into the system = $Q_g + Q_e = 34.6999 + 3.5167 = 38.216$ kW

The two are the same.

$$\text{COP} = \frac{Q_e}{Q_g} = \frac{3.5167}{34.6999} = 0.1013$$

$$\text{Circulation factor, } f = \frac{\dot{m}_1}{\dot{m}_6} = 24.782$$

EXAMPLE 7.8 Suppose a preheating heat exchanger is added to the system of Example 7.7, such that the strong solution leaves it at 40°C. Determine the heat transfer rates through various components and the COP.

Solution:

This is exactly like the system shown in Figure 7.1. The state of the strong solution at the exit of heat exchanger is determined by intersection of the isotherm for 40°C with $x_2 = x_{2'} = 0.37$.

This gives $h_{2'} = 0$ kJ/kg-K

Energy balance for the heat exchanger gives

$$\dot{m}_2(h_2 - h_{2'}) = \dot{m}_1(h_{1''} - h_{1'})$$

Substituting for various terms, we get

$$h_{1''} = h_{1'} - (\dot{m}_2/\dot{m}_1)/(h_2 - h_{2'}) = (-115.0) + (8.5855/8.9465)\ (220 - 0) = 96.123$$

From the h–x diagram at $x_1 = 0.393$ and $h_{1''} = 96.123$, the temperature $t = 70$°C. This happens to be in two-phase region at pressure of 13.5 bar. The energy balance for the absorber and the generator yields

$$Q_a = \dot{m}_2 h_{2''} + \dot{m}_6 h_6 - \dot{m}_1 h_1$$

$$= 8.5855 \times 10^{-2}(0) + 3.61 \times 10^{-3}\ (1099.15) - 8.9465 \times 10^{-2}(-115) = 14.2681 \text{ kW}$$

Similarly, for the generator,

$$Q_g = \dot{m}_2 h_2 + \dot{m}_3 h_3 - \dot{m}_1 h_{1''}$$

$$= 8.5855 \times 10^{-2}(220) + 3.61 \times 10^{-3}\ (1530) - 8.9465 \times 10^{-2}(96.123) = 15.8117 \text{ kW}$$

$Q_c = 5.072$ kW as before

Overall energy balance is checked and observed to be satisfied.

$$Q_a + Q_c = 19.340 \text{ kW} \quad \text{and} \quad Q_e + Q_e = 19.328 \text{ kW}$$

$$\text{COP} = \frac{Q_e}{Q_g} = \frac{3.5167}{15.8117} = 0.2224$$

It is observed that the COP improves from 0.1013 to 0.2224 by adding the preheating heat exchanger.

EXAMPLE 7.9 If a subcooling heat exchanger is included in Example 7.8, and it is assumed that the vapour at the exit of HEX is saturated vapour at 1.75 bar find the mass flow rates, heat transfer rates and the COP.

Solution:

The vapour leaving the evaporator is a mixture of purge liquid and vapour. The purge liquid could have evaporated in evaporator to give more refrigeration effect. The performance can be improved by installing a subcooling heat exchanger where this liquid will subcool the liquid entering the expansion valve. The schematic diagram with subcooling heat exchanger is shown in Figure 7.18. It may be assumed that the vapour at the exit of evaporator is saturated vapour at 1.75 bar.

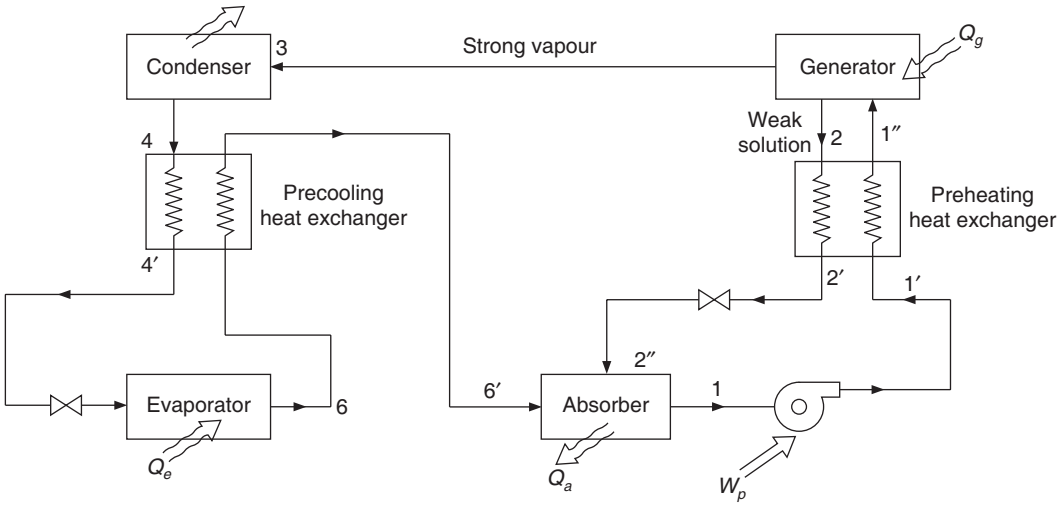

Figure 7.18 Ammonia–water vapour absorption system with preheating and precooling heat exchangers.

The enthalpy of saturated vapour is found at the intersection of $x_6 = 0.94$ and the saturated vapour line for 1.75 bar. It is observed that

$$h_{6'} = 1460 \text{ kJ/kg}$$

To find the temperature at this point a horizontal line is drawn through this point followed by a vertical line from its intersection with equilibrium construction line and the temperature is noted at the intersection of vertical line with 1.75 bar line in the liquid region,

$$t_{6'} = 40^{\circ}\text{C}$$

The condenser outlet temperature is also 40°C. Only an ideal heat exchanger with 100% effectiveness can achieve this condition. Otherwise the state at exit of evaporator will still contain some purge liquid.

For a control volume including the subcooling HEX and the evaporator, energy balance gives

$$\dot{m}_6 h_4 + Q_e = \dot{m}_6 h_{6'}$$

$$\therefore \quad \dot{m}_6 = 3.5167/(1460 - 125) = 2.6342 \times 10^{-3} \text{ kg/s}$$

By analogy with Example 7.8 the mass flow rates of weak and strong solutions are:

$$\dot{m}_2 = 6.26483 \times 10^{-2} \text{ kg/s} \quad \text{and} \quad \dot{m}_1 = 6.52825 \times 10^{-2} \text{ kg/s}$$

$$h_{1''} = h_{1'} + (\dot{m}_2/\dot{m}_1)(h_2 - h_{2'}) = -115 + (6.26483/6.52825)(220 - 0) = 96.123 \text{ kJ/kg}$$

$$Q_a = m_6 h_{6'} + m_2 h_{2''} - m_1 h_1 = 2.6342 \times 10^{-3} (1460) + 6.26483 \times 10^{-2} (0)$$
$$- 6.52825 \times 10^{-2}(-115) = 11.3534 \text{ kW}$$

$$Q_g = m_3 h_3 + m_2 h_2 - m_1 h_{1''} = 2.6342 \times 10^{-3}(1530) + 6.26483 \times 10^{-2}(220)$$
$$- 6.52825 \times 10^{-2}(96.123) = 11.5378 \text{ kW}$$

$$Q_c = m_3 h_3 - m_3 h_4 = 2.6342 \times 10^{-3}(1530 - 125) = 3.70106 \text{ kW}$$

$$Q_a + Q_c = 15.0545 \text{ kW} \quad \text{and} \quad Q_g + Q_e = 15.0545 \text{ kW}$$

$$\text{COP} = \frac{Q_e}{Q_g} = \frac{3.5167}{11.5378} = 0.3048$$

$$\text{Circulation factor,} \quad f = \frac{\dot{m}_1}{\dot{m}_6} = 24.78$$

It is observed that the COP drastically improves with the addition of preheating and subcooling heat exchangers.

7.8 DRAWBACKS OF PRESENCE OF WATER VAPOUR IN EVAPORATOR AND CONDENSER

The simple absorption system is not very efficient. If pure ammonia ($x_3 = 1$ in Figure 7.17) does not enter the evaporator, the evaporation will not be an isothermal process but the temperature will increase during evaporation. As a result, the low temperature cann7ot be achieved. Pure ammonia

will evaporate at $x = 1$ and at saturation temperature of t_e. If the concentration of ammonia entering the evaporator is $x_6 < 1$, then at evaporator pressure p_e, the liquid enters at temperature t_{el} and its temperature does not remain constant but increases to temperature t_{ev} if complete evaporation occurs. Both these temperatures are greater than t_e.

It is observed that to achieve an evaporator temperature of t_e at concentration $x_e < 1$, the evaporator pressure has to be decreased to $p_{e'}$ so that the evaporator exit temperature $t_{ev'} = t_e$. It was observed in Example 7.7 that to achieve an evaporator temperature of 0° C, the pressure required was 1.75 bar at $x_e = 0.94$ whereas the saturation pressure of ammonia at 0°C is 4.29 bar. This reduces the COP.

The additional problem is that it leads to incomplete evaporation. It was shown in Example 7.7 that the evaporator exit enthalpy of 1099.15 kJ/kg was obtained instead of 1300 kJ/kg for complete evaporation. The refrigeration effect on this account was reduced by 1300 – 1099.15 = 200.85 kJ/kg. This also reduces the COP.

It has been observed that as the boiling occurs in the evaporator for $x_e < 1$, vapour stronger in ammonia is given off leaving water in the evaporator. This water has either to be removed at frequent intervals or the vapour exit velocity has to be kept large enough to carry it to absorber.

In brief, the effects of aqua–ammonia mixture instead of pure ammonia entering the evaporator are:

(i) Evaporator temperature does not remain constant.
(ii) Lower evaporator pressure is required to obtain the given evaporator temperature
(iii) Refrigeration effect is reduced.
(iv) Some water is left behind in the evaporator, which requires a larger velocity for removal to the absorber.
(v) COP decreases.

7.9 AMMONIA ENRICHMENT PROCESS

It is obvious that the largest COP will be obtained if pure ammonia vapour leaves the generator. This however is not possible in a simple generator where only boiling occurs. The vapour leaving the generator has to be enriched in ammonia. It was shown in Section 7.6.4 that a combined process of cooling the vapour into the mixture region and separating the liquid, increases the concentration of ammonia. A number of such combination steps or stages are arranged in a vertical column called *rectification column*. At the top of this column there is a heat exchanger in which the vapour is cooled by heat rejection to cold water flowing in a coil. This is called *dephlegmator or reflux condenser* as shown in Figure 7.19. Some vapour condenses into cold liquid in this component. The cold liquid drips down into the column and cools the ascending vapour. The condensate formed during cooling is separated and collected at the plates and drips down the lower plates.

The cooling of vapour into two-phase region and separation of liquid leaves the vapour richer in ammonia. At the same time some liquid also evaporates to provide cooling of vapour, this also produces a relatively richer vapour. Several such plates are provided to achieve a higher concentration. Vapour with 100% ammonia cannot be obtained, that is, complete rectification is

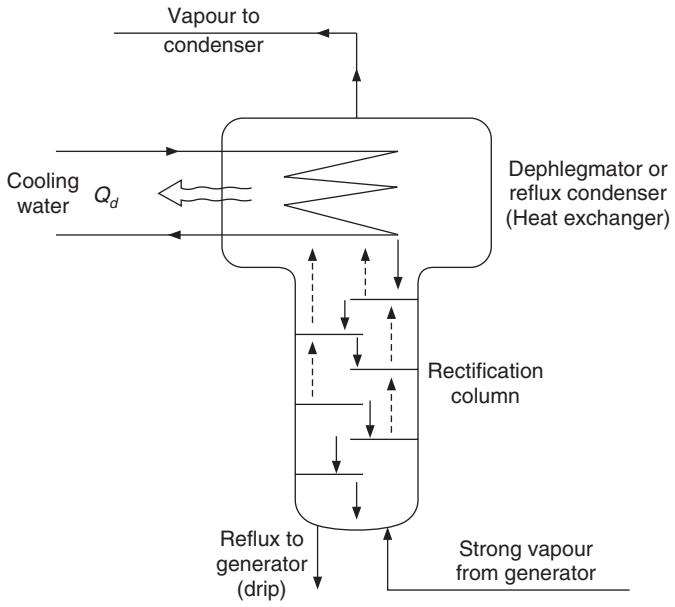

Figure 7.19 Dephlegmator and rectification column.

not possible. It is not economical and practical to enrich the vapour after a certain point since the potential for heat and mass transfer decreases towards the top of the column. The vapour temperature at each cross section must be greater than the liquid temperature (for condensation of vapour and separation of vapour) for the enrichment to occur while for 100% enrichment the two temperatures must be same at the exit. This will require a very large area. In actual system, the exit concentration is around 0.995 to 0.998. The effect of this is that the vapour exit temperature from the column may be 10–15°C higher than that for pure ammonia. For example, the vapour temperature at 15.5 bar and $x = 0.98$ is 53°C while the saturation temperature of pure ammonia at 15.5 bar is 40°C as seen from the ammonia saturation table.

The strong solution even after passing through the preheating heat exchanger is at a temperature lower than the temperature of vapour leaving the generator; hence it can also be used to cool the vapour ascending from the generator. A part of the strong solution will evaporate giving rich vapour. In this process, the strong solution will be further preheated before it enters the boiler. The vapour leaving the generator has to be cooled in the dephlegmator and the condenser anyway, so a part of it preheats the strong solution saving generator heat transfer and increasing the COP.

For this purpose the strong solution is fed into the rectification column at a point where the temperature of the descending liquid is same as that of the strong solution. The part of the rectification column below this point is called *Exhausting column or Analyzer* and the part above this is called *Rectification column.* This is shown in Figure 7.20. For analysis purpose the generator-cum-exhausting column and dephlegmator-cum-rectification column are considered separately.

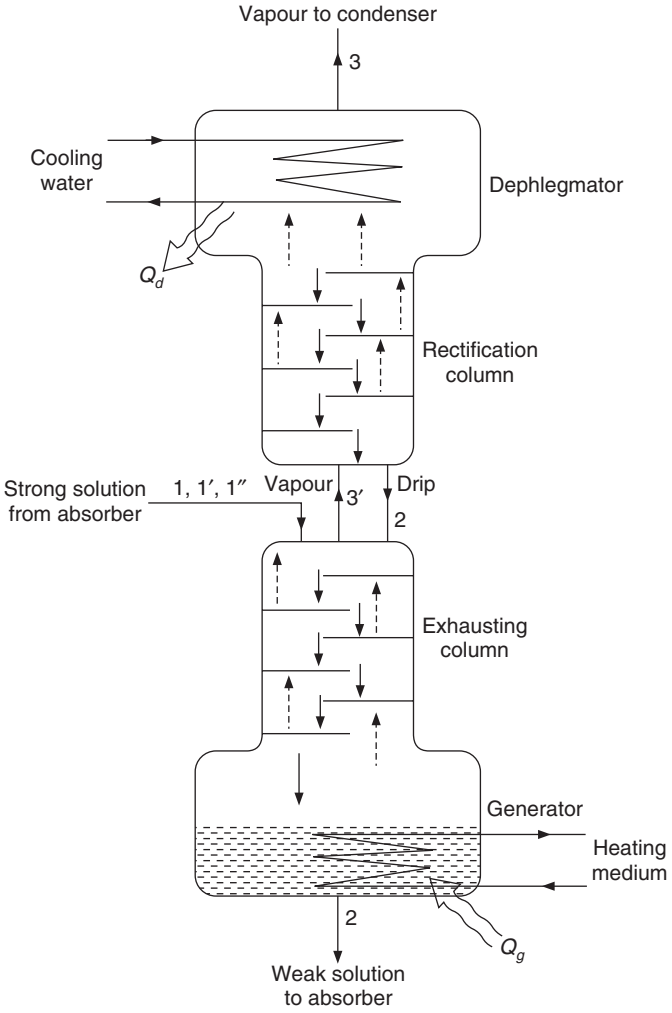

Figure 7.20 Schematic of generator-cum-exhausting column and dephelegmator-cum-rectification column used in ammonia–water systems.

7.9.1 Dephlegmator-cum-Rectification Column

The vapour is cooled in the dephlegmator and some of it condenses to form a cool liquid which drips down in the rectification column. The descending cold liquid comes into contact with the ascending vapour. The capped plates of the rectification column provide area for heat and mass transfer. The enrichment of vapour occurs due to cooling of vapour followed by its separation into liquid and vapour. Let the states of liquid and vapour at any cross section of the rectification column be L and V respectively. The temperature of vapour at any section is greater than that of liquid. Hence L and V do not lie along an isotherm. For analysis purpose we consider a control volume including the dephlegmator and a cross section through the rectification column as shown

in Figure 7.21. The mass flow rate and enthalpy of the liquid and vapour are $\dot{m}_L, h_L$ and $\dot{m}_V, h_V$ respectively. Considering overall mass conservation and mass conservation of ammonia respectively, we get

$$\dot{m}_V - \dot{m}_L = \dot{m}_3 \tag{7.16}$$

$$\dot{m}_V x_V - \dot{m}_L x_L = \dot{m}_3 x_3 \tag{7.17}$$

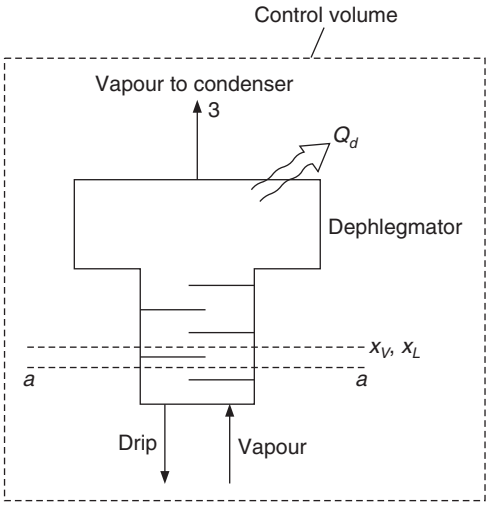

Figure 7.21 Control volume including the dephlegmator and a cross section through the rectification column.

The energy conservation yields

$$\dot{m}_V h_V - \dot{m}_L h_L = \dot{m}_3 h_3 + Q_d \tag{7.18}$$

Eliminating $\dot{m}_L$ between Eqs. (7.16) and (7.17), we get

$$\frac{\dot{m}_V}{\dot{m}_3} = \frac{x_3 - x_L}{x_V - x_L} \tag{7.19}$$

Dividing Eq. (7.18) by $\dot{m}_3$ and substituting for $\dot{m}_L / \dot{m}_3$ from Eq. (7.16), we get

$$(\dot{m}_V / \dot{m}_3)(h_V - h_L) = (h_3 - h_L) + Q_d / \dot{m}_3$$

Substituting for $\dot{m}_V / \dot{m}_3$ from Eq. (7.19), we get

$$\frac{(h_V - h_L)}{(x_V - x_L)}(x_3 - x_L) = (h_3 - h_L) + \frac{Q_d}{\dot{m}_3} \tag{7.20}$$

A straight line on the *h*–*x* diagram can represent this equation. This is shown as follows. Referring to Figure 7.22, *L* and *V* denote the liquid and vapour states on saturated liquid and vapour lines for pressure p_2. State 3 is the saturated vapour state at concentration x_3 and pressure p_2. Let

$$\frac{h_V - h_L}{x_V - x_L} = \tan \theta_1$$

where, θ_1 is the slope of the line joining L and V for a cross section. This line is extended to meet x_3 = constant line at a point P_1 shown in Figure 7.22. Then from Figure 7.22,

$$(x_3 - x_L) \tan \theta_1 = \text{Distance } P_1 - b = h_{P1} - h_L$$

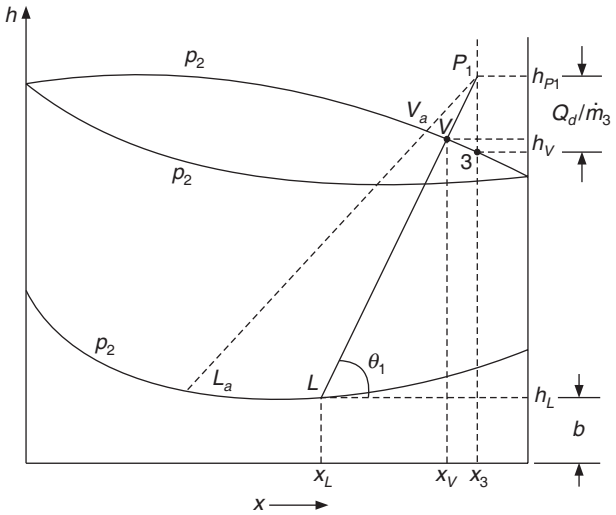

Figure 7.22 Thermodynamic process of dephlegmator-cum-rectification column.

Equation (7.20) reduces to

$$(x_3 - x_L) \tan \theta_1 = (h_3 - h_L) + \frac{Q_d}{\dot{m}_3} = h_{P1} - h_L = \text{distance } L\text{–}3 + \text{distance } 3\text{–}P_1$$

Therefore, the distance between point 3 and P_1 is equal to $\frac{Q_d}{\dot{m}_3}$, that is,

$$h_{P1} - h_3 = \frac{Q_d}{\dot{m}_3} \quad \text{or} \quad h_{P1} = h_3 + \frac{Q_d}{\dot{m}_3} \tag{7.21}$$

Equation (7.21) has been derived for an arbitrary section of the rectification column, hence Eqs. (7.20) and (7.21) must be valid for all the sections. Since h_3, $\dot{m}_3$ and Q_d are constant, the enthalpy h_{P1} of point P_1 is also constant and this is located above point 3 by an enthalpy difference of $Q_d / \dot{m}_3$ as shown in Figure 7.22. This specifies the dephlegmator heat transfer rate Q_d. Equation (7.20) is a straight line on the h–x diagram. This leads to the graphical construction that if the liquid and vapour states of a cross section of rectification column are joined by a straight line then all these straight lines for various sections meet at a common point P_1. These lines are called *operating lines* of the dephlegmator–rectification column and the point of intersection P_1 is called

the first principal pole. The operating line for any section above this section will be to the right of this line and the operating line for a section below this section will be to the left of this line.

Since, there are a number of capped plates, one must know what happens at a plate so that the total number of plates required can be fixed. A detailed analysis will require the direct contact heat and mass transfers between the liquid and the vapour. However considering the concept of equilibrium stage or theoretical plate may lead to some important conclusions. Rectification will take place only if the vapour temperature at each section is more than the liquid temperature. This is essential for the cooling of vapour and its separation into liquid and vapour of higher concentration at each plate. That is, if an isotherm is drawn for the liquid temperature it will lie to the right of the operating line since temperature along the saturated vapour line decreases towards the right. In other words the operating line for each section must be steeper than the isotherm for the liquid temperature. There is a mushroom or bubble cap on top of each plate, which prevents the escape of vapour without bubbling through the liquid. This may lead to equilibrium between the two. The vapour bubbles through the liquid and the liquid overflows. Some vapour condenses, the condensate being of lower concentration the vapour is enriched since the condensate has more water in it. Also some liquid evaporates. The vapour is also rich compared to the concentration of liquid. The combination of these leads to rectification.

The direct contact heat and mass transfer between liquid and vapour under adiabatic conditions (no heat transfer to surroundings) leads to equilibrium between the leaving streams from a plate. This implies that the liquid leaving the plate may be at the same temperature as the vapour leaving it. If the mixing is sufficient then both the leaving states will be saturated states. Suppose $P_1V_aL_a$ is the operating line for section *a–a* (see Figure 7.22). The vapour enters the section *a–a* at temperature t_{Va} and leaves it at t_{Vb}, while the liquid enters the section *a–a* at t_{Lb} and leaves it at $t_{La.}$ Under ideal conditions the temperature of the liquid t_{La} at state L_a is equal to the temperature of the vapour t_{Vb} at state V_b, that is

$$t_{La} = t_{Vb}$$

Then the operating line for the upper stage $P_1V_bL_b$ will pass through the point intersection of isotherm t_{La} with saturated vapour line at V_b. The number of equilibrium stages required to achieve the final concentration may be obtained by this construction on the *h–x* diagram. This method is called *Panchon-Savarit* method. One starts from the operating line passing through the feed state 1″, draws the isotherm for liquid temperature and draws the second operating line passing through the point of intersection of isotherm with the saturated vapour line. For enrichment of ammonia to occur in the rectification column, the operating line for each section must be steeper than the corresponding liquid isotherm. At the exit, the vapour leaving the column is in equilibrium with the liquid dripping from dephlegmator. In actual practice for a finite stage the equilibrium does not exist at the plates. In fact, the temperature of vapour V_b will be higher than the temperature of the leaving liquid requiring that the vapour state V_b lie to the left of isotherm for L_a. Hence in an actual case, the total number of plates will be more than that for the ideal case.To account for this, the plate efficiency is defined as

$$\eta_{\text{plate}} = N_{\text{theoretical}}/N_{\text{actual}}$$

There is another form of construction where the column is a packed column, packing being ceramic spheres or rings. The liquid trickles over the surface of the packing and the vapour rises through the interstitial spaces.

7.9.2 Generator-cum-Exhausting Column

The strong solution from the absorber after preheating is fed to the top of exhausting column. This provides sufficient area for intimate contact between the strong solution and the vapour leaving it. For analysis purpose, we consider a control volume including the generator and a cross section through the exhausting column as shown in Figure 7.23. *L* and *V* denote the states of the liquid and vapour at this cross section respectively. These states lie on saturated liquid and saturated vapour line respectively for pressure p_2 as shown in Figure 7.24. The temperature of vapour at any section is more than that of liquid. The state at the exit of generator is saturated liquid state 2. The mass

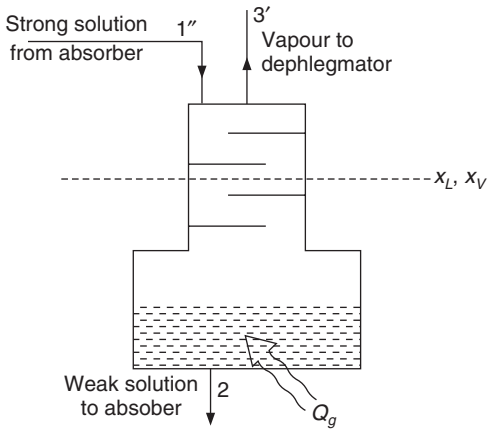

Figure 7.23 Control volume including the generator and a cross section through the exhausting column.

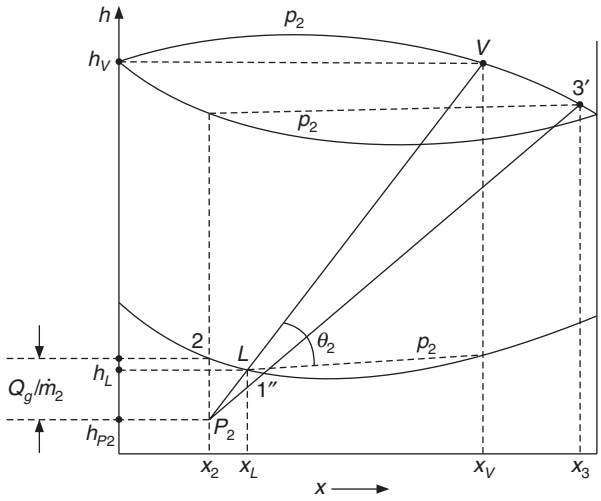

Figure 7.24 Thermodynamic process of generator-cum-exhausting column.

flow rate and enthalpy of the liquid and vapour are $\dot{m}_L, h_L$ and $\dot{m}_V, h_V$ respectively. Considering overall mass conservation and mass conservation of ammonia respectively, we get

$$\dot{m}_L - \dot{m}_V = \dot{m}_2 \tag{7.22}$$

$$\dot{m}_L x_L - \dot{m}_V x_V = \dot{m}_2 x_2 \tag{7.23}$$

The energy conservation yields

$$\dot{m}_L h_L - \dot{m}_V h_V = \dot{m}_2 h_2 - Q_g \tag{7.24}$$

Eliminating $\dot{m}_V$ between Eqs. (7.22) and (7.23), we get

$$\frac{\dot{m}_L}{\dot{m}_2} = \frac{x_V - x_2}{x_V - x_L} \tag{7.25}$$

Dividing Eq. (7.24) by $\dot{m}_2$ and substituting for $\dot{m}_V / \dot{m}_2$ from Eq. (7.22), we get

$$(\dot{m}_L / \dot{m}_2)(h_L - h_V) = (h_2 - h_V) - Q_g / \dot{m}_2$$

Substituting for $\dot{m}_L / \dot{m}_2$ from Eq. (7.25), we get

$$\frac{(h_V - h_L)}{(x_V - x_L)}(x_V - x_2) = (h_V - h_2) + \frac{Q_g}{\dot{m}_2} \tag{7.26}$$

This equation can be represented as a straight line on the *h–x* diagram as follows. Let the line joining states *V* and *L* be extended downwards to intersect the vertical line through state 2 at point P_2. Let

$$\frac{h_V - h_L}{x_V - x_L} = \tan \theta_2$$

where, θ_2 is the slope of the line joining *L* and *V* for a cross section, then

$$(x_V - x_2) \tan \theta_2 = \text{distance } VP_2 = h_V - h_{P2}$$

and Eq. (7.26) reduces to

$$(x_V - x_2) \tan \theta_2 = (h_V - h_2) + Q_g / \dot{m}_2 = h_V - h_{P2}$$

$$\therefore \qquad h_2 - h_{P2} = Q_g / \dot{m}_2 \quad \text{or} \quad h_{P2} = h_2 - Q_g / \dot{m}_2 \tag{7.27}$$

The point P_2 is called the *second principal pole* and the line *V–L–*P_2 is called the *operating line* for the exhausting column-cum-generator. Since h_2, $\dot{m}_2$ and Q_g are constant, the enthalpy h_{P2} of point P_2 is also constant and this is located below point 2 by an enthalpy difference of $Q_g / \dot{m}_2$ as shown in Figure 7.24. Equations (7.26) and (7.27) are valid for any arbitrary cross section of the column, hence operating lines for all sections must pass through P_2, that is, operating lines for all the sections with different values of *L* and *V* will pass through this point. The operating line for a section higher up than the section shown, will lie to the right of that of the section shown and for a section below it the operating line will lie to the left of the operating line shown. The exit state

of the vapour from the exhausting column is 3′ and the inlet state of the strong liquid solution is 1″. Hence the line 3′–1″–P_2 is the last operating line for the exhausting column-cum-generator. In case of pre-heating heat exchanger the enthalpy of the liquid 1″ increases while $x_{1''} = x_1$ remains constant. The point 1″ shifts upwards and raises the pole P_2 upwards, thereby decreasing the heat transfer to the generator, Q_g.

In this case too, under ideal conditions, vapour leaving a plate will be in equilibrium with the liquid dripping from it. Hence, the vapour state for a section immediately above the given section will lie at the intersection of the isotherm drawn from the liquid state. This is similar to the discussion for the rectification column-cum-dephlegmator. The procedure for drawing the operating lines is as follows. To start with, isotherm t_2 = constant is drawn. Its point of intersection with the saturated vapour line is located at point, say *a*. The first operating line would thus be P_2–*a*. This intersects the saturated liquid line, say at point *b*. An isotherm is drawn from point *b* which intersects the saturated vapour line at point *c*. Line P_2–*c* would thus become the second operating line. This procedure is continued until the operating line passes through the feed state 1″. This will be the last operating line of the generator-cum-exhausting column. In actual case the first operating line will be to the left of line P_2–*a* and the second operating line will be towards left of line P_2–*c*. The total number of stages required will be more than the theoretical number of stages. This will meet the saturated vapour line at point 3′, the inlet vapour state to the rectification column.

7.9.3 Analysis of Double Rectification Column

The vapour enriched to state 3′ (Figure 7.23) leaves the exhausting column and it is further enriched to state 3 (Figure 7.20) in the rectification column. The liquid leaving the rectification column mixes with the strong solution and is fed to the exhausting column at state 2. Here we consider the two columns combined with dephlegmator and generator as shown in Figure 7.20. The overall mass conservation and mass conservation of ammonia yields

$$\dot{m}_1 = \dot{m}_2 + \dot{m}_3 \tag{7.28}$$

$$\dot{m}_1 x_1 = \dot{m}_2 x_2 + \dot{m}_3 x_3 \tag{7.29}$$

The energy conservation yields

$$\dot{m}_1 h_{1''} + Q_g = \dot{m}_2 h_2 + Q_d + \dot{m}_3 h_3 \tag{7.30}$$

or $$(\dot{m}_2 + \dot{m}_3) h_{1''} + Q_g = \dot{m}_2 h_2 + Q_d + \dot{m}_3 h_3$$

or $$(\dot{m}_2 / \dot{m}_3)\{h_{1''} - h_2 + Q_g / \dot{m}_2\} = h_3 - h_{1''} + Q_d / \dot{m}_3 \tag{7.31}$$

Eliminating $\dot{m}_1$ in Eqs. (7.28) and (7.29), we get

$$\frac{\dot{m}_2}{\dot{m}_3} = \frac{x_3 - x_1}{x_1 - x_2} \tag{7.32}$$

Substituting Eq. (7.32) in Eq. (7.31), we get

$$\frac{h_{1''} - (h_2 - Q_g / \dot{m}_2)}{x_1 - x_2} = \frac{(h_3 + Q_d / \dot{m}_3) - h_{1''}}{x_3 - x_1} \tag{7.33}$$

Referring to Figure 7.24,

$$h_2 - Q_g / \dot{m}_2 = h_{P2}$$

$\therefore$ $$h_{1''} - (h_2 - Q_g / \dot{m}_2) = \varsigma$$

Also $$(h_3 + Q_d / \dot{m}_3) = h_{P1}$$

$\therefore$ $$(h_3 + Q_d / \dot{m}_3) - h_{1''} = \beta$$

Therefore Eq. (7.35) reduces to

$$\frac{\varsigma}{x_1 - x_2} = \frac{\beta}{x_3 - x_1} = \tan \theta_2$$

This equation is satisfied. This requires that poles P_1, P_2, the feed state 1″ and the state 3″ all lie on a straight line on the h–x diagram. This straight line is called the *principal operating line*. It is observed that as the principal operating line tends to become flat, the heat transfers to generator and the dephlegmator decrease. However this line cannot be drawn arbitrarily. The poles P_1 and P_2 are located such that all operating lines are steeper than the liquid isotherms for the corresponding section. The following example illustrates the calculation procedure for the whole system.

EXAMPLE 7.10 In an aqua-ammonia absorption refrigeration system the vapour leaving the dephlegmator may be assumed to be 100% rich saturated ammonia at 40°C. The condenser and evaporator temperature are 40°C and –20°C respectively. The absorber and generator temperature are 30°C and 170°C respectively. The weak solution leaving the generator cools down to 50°C in the preheating heat exchanger. Determine the mass flow rates and heat transfer rates on one TR basis and the COP. Figure 7.25 shows the schematic diagram of the system.

Solution:

Saturation pressures of ammonia at –20°C and 40°C are 1.9 bar and 15.54 bar respectively.

$\therefore$ Condenser and generator pressure = 15.54 bar

Evaporator and absorber pressure = 1.9 bar

Assume that equilibrium conditions exist in the generator and absorber so the exit states from these are saturated states. Further complete rectification is assumed to occur so that state 3 at dephlegmator exit is saturated vapour at 40°C.

It is observed from the h–x diagram of Figure 7.8 that the enthalpy of liquid at x =1, is zero for temperature of 0°C and 4.29 bar. This indicates that the reference state in the diagram has been chosen as 0°C, that enthalpy of liquid ammonia is zero at 0°C which is the IIR reference state. The properties of saturated ammonia given in the table in Appendix have ASHRAE reference state, that is, –40°C, hence the enthalpy values read from this table are corrected by adding 180.88 kJ/kg (the liquid enthalpy at 0°C in ASHRAE reference table).The corrected enthalpies are:

Saturated ammonia vapour at 40°C, h_3 = 1472.02 + 180.88 = 1652.9 kJ/kg
Saturated ammonia liquid at 40°C, h_4 = 371.47 + 180.88 = 552.35 kJ/kg
Saturated ammonia vapour at –20°C, h_6 = 1417.97 + 180.88 = 1598.85 kJ/kg

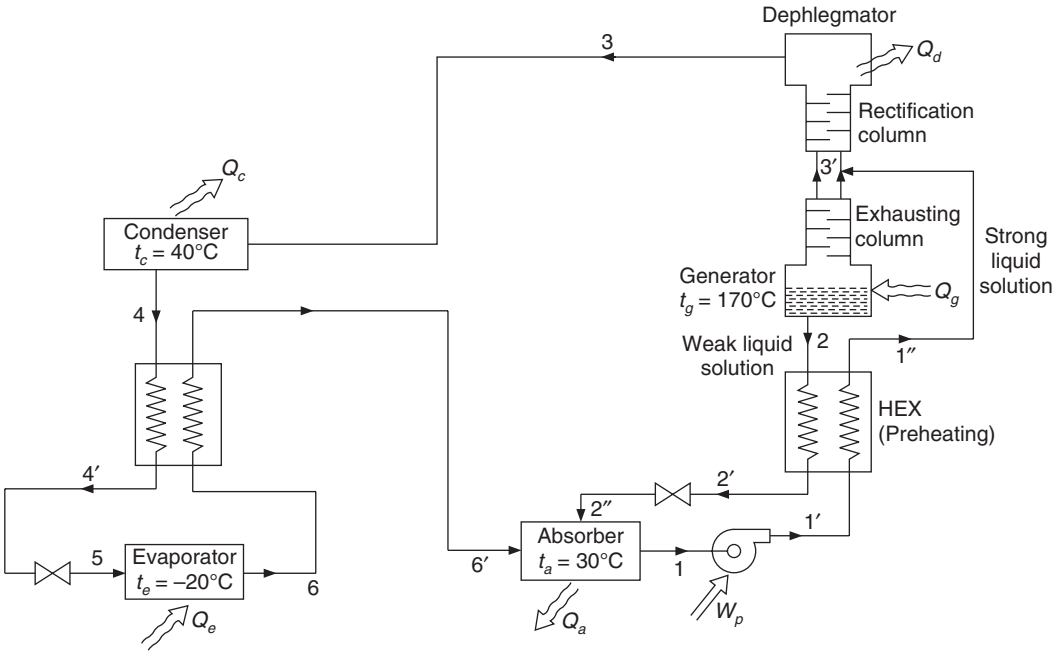

Figure 7.25 Aqua-ammonia absorption refrigeration system – Example 7.10.

From *h*–*x* diagram at absorber exit for saturated liquid at 30°C, 1.9 bar,

$$h_1 = -100.0 \quad \text{and} \quad x_1 = 0.38$$

From *h*–*x* diagram at generator exit for saturated liquid at 170°C, 15.54 bar,

$$h_2 = 665.0 \quad \text{and} \quad x_2 = 0.1$$

At HEX exit along $x_2 = 0.1$ and 50°C,

$$h_{2'} = 135.0 \quad \text{and} \quad x_{2'} = 0.1$$

For 1 TR, and $\dot{m}_6 = 3.5167/(h_6 - h_4) = 3.5167/(1598.85 - 552.35)$

$$\therefore \qquad \dot{m}_6 = 3.3604 \times 10^{-3} \text{ kg/s}$$

$$x_3 = x_4 = x_5 = x_6 = 1.0 \qquad \text{since pure ammonia leaves the dephlegmator.}$$

Following the procedure of Example 7.9,

$$\dot{m}_2 = \dot{m}_6 (x_6 - x_1)/(x_1 - x_2) = 3.3604 \times 10^{-3}(1 - 0.38)/(0.38 - 0.1) = 7.441 \times 10^{-3} \text{ kg/s}$$

$$\dot{m}_1 = \dot{m}_6 (x_6 - x_2)/(x_1 - x_2) = 3.3604 \times 10^{-3}(1 - 0.1)/(0.38 - 0.1) = 1.08 \times 10^{-2} \text{ kg/s}$$

Energy balance for the absorber yields

$$Q_a = \dot{m}_2 h_{2'} + \dot{m}_6 h_6 - \dot{m}_1 h_1$$

$$= 7.441 \times 10^{-3}(135.0) + 3.3604 \times 10^{-3}(1598.85) - 1.08 \times 10^{-2}(-100.0) = 7.457 \text{ kW}$$

Energy balance for the pre-heating heat exchanger gives

$$\dot{m}_2(h_2 - h_{2'}) = \dot{m}_1(h_{1''} - h_{1'})$$

$$h_{1''} = h_{1'} - (\dot{m}_2 / \dot{m}_1)/(h_2 - h_{2'}) = (-100.0) + (7.441/1.08)\ (665.0 - 135.0) = 265.11$$

By locating this point at $x_1 = 0.38$ on h–x diagram, it is observed that its temperature is

$$t_{1''} = 110^{\circ}\text{C}$$

Further, it is observed to be in two-phase region at 15.54 bar which is the pressure after the pump. Sometimes, it is stated that the strong solution leaving the HEX is a saturated liquid, then it can be located straight away on h–x diagram at calculated value of x_1 and along the condenser pressure liquid line of 15.54 bar (in this case).

Energy balance for the generator,

$$Q_g - Q_d = \dot{m}_2 h_2 + \dot{m}_3 h_3 - \dot{m}_1 h_{1''}$$

$$= 7.441 \times 10^{-3}(665.0) + 3.3604 \times 10^{-3}\ (1652.9) - 1.08 \times 10^{-2}(265.11) = 7.639 \text{ kW}$$

$$Q_c = \dot{m}_3(h_3 - h_4) = 3.3604 \times 10^{-3}\ (1652.9 - 552.35) = 3.698 \text{ kW}$$

To check the overall energy balance neglecting the pump work input,

Net heat rejection from the system = $Q_a + Q_c = 7.457 + 3.698 = 11.156$ kW

Net heat input into the system = $Q_g - Q_d + Q_e = 7.639 + 3.5167 = 11.155$ kW

The two are the same, which provides a check on the calculations.

For the determination of Q_d and Q_g independently, an assumption is required to draw the principal operating line. It may be observed from Figure 7.25 that the strong solution inlet state 1″ and the vapour exit state 3′ from the exhausting column would both lie on the principal operating line. This is depicted in Figure 7.26. The vapour temperature is greater than the liquid temperature at all points in rectification column and exhausting column. Hence, it is assumed that the temperature at 3′ is say, 5°C greater than that of 1″. Therefore

$$t_{3'} = 110 + 5 = 115^{\circ}\text{C}$$

The state 3′ is located by drawing the isotherm for 115°C and 15.54 bar at which for saturated liquid, we have

$$h_{3l'} = 300.0 \quad \text{and} \quad x_{3l'} = 0.33$$

And for saturated vapour, we have

$$h_{3v'} = 1625.0 \quad \text{and} \quad x_{3v'} = 0.88$$

The state $h_{3v'} = 1625.0$ and $x_{3v'} = 0.88$ is the required state for the operating line.

The states 1″ and 3′ are joined and extended to x_2 on the left hand side and extended to x_3 on the right hand side. This is the principal operating line. The enthalpies at the poles are

$$h_{P1} = 1975.0 \quad \text{and} \quad h_{P2} = -460 \text{ kJ/kg}$$

The dephlegmator and generator heat transfer rates Q_d, Q_g are calculated as follows:

$$Q_g / \dot{m}_2 = h_2 - h_{P2} = 665.0 - (-460) = 1125.0$$

$$\therefore \quad Q_g = 7.441 \times 10^{-3}\ (125.0) = 8.371 \text{ kW}$$

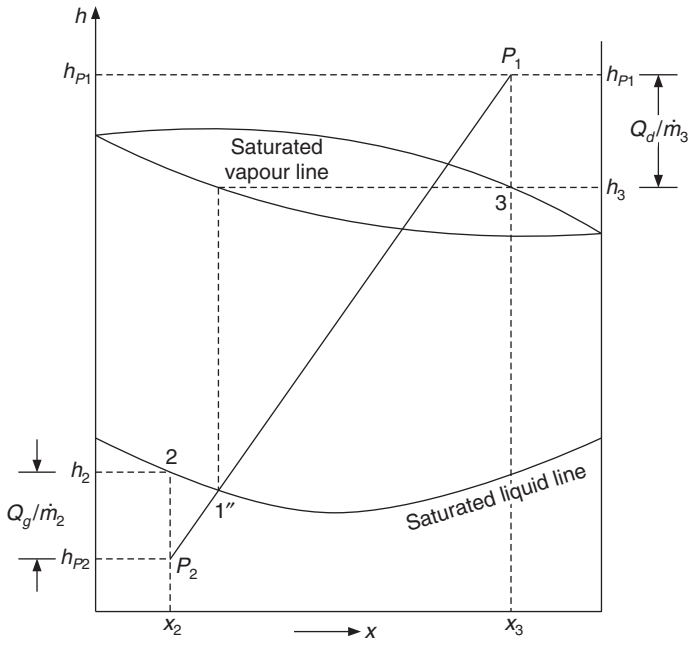

Figure 7.26 Principle operating line—Example 7.10.

$$Q_d / \dot{m}_3 = h_{P1} - h_3 = 1975.0 - 1652.9 = 322.1$$

$$\therefore \quad Q_d = 3.604 \times 10^{-3}(322.1) = 1.082 \text{ kW}$$

$$\therefore \quad Q_g - Q_d = 8.371 - 1.082 = 7.295$$

This is smaller than the value calculated by energy balance, which was 7.639 kW.

The assumed value of temperature for state 3′ has to be iterated to get a match between the two values. Also the exit state of the HEX could have been taken as saturated state to simplify the calculations.

$$\text{COP} = Q_e/Q_g = 3.5167/8.371 = 0.42$$

If it is assumed that the absorber temperature is 40°C instead of 30°C, that is, same as condenser temperature, then the expression for maximum COP is given by

$$\text{COP}_{\max} = \frac{T_g - T_c}{T_g} \cdot \frac{T_e}{T_c - T_e}$$

For $T_c = T_a = 273 + 40 = 313$ K, $T_g = 170 + 273 = 443$ K and $T_e = -20 + 273 = 253$K

$$\text{COP}_{\max} = (130/443)(253/60) = 1.2374$$

Therefore, the refrigerating efficiency is given by

$$\eta_R = \frac{\text{COP}}{\text{COP}_{\max}} = \frac{0.42}{1.2374} = 0.3394$$

The enthalpy of evaporation of water at 170°C is 2045.12 kJ/kg and $Q_g = 8.371$ kW

Mass flow rate of steam required in the generator per TR = 8.371 × 3600/2045.12 = 14.73 kg/TR-h.

Pump work

Empirical expression for specific volume of saturated aqua-ammonia liquid is

$$v_{soln} = 0.001/(1 - 0.35\, x_1) = 0.001/(1 - 0.35 \times 0.38) = 1.1534 \times 10^{-4}$$

Considering this as the average specific volume during compression, the pump work may be approximated as

$$W_p = \dot{m}_1 (p_2 - p_1)\, v_{soln} = 1.08 \times 10^{-2} (15.54 - 1.9) \times 10^2 \times 1.1534 \times 10^{-4} = 17 \text{ W}$$

This is negligibly small.

Circulation factor

An alternative calculation procedure defines a circulation factor λ, which is the ratio of mass flow rate of weak solution to the mass flow rate of vapour produced in the generator–dephlegmator. This is expressed as follows:

$$\lambda = \dot{m}_2 / \dot{m}_3 = \dot{m}_2 / \dot{m}_6 \tag{7.34}$$

$$\therefore \quad \dot{m}_2 = \lambda \dot{m}_6$$

Overall mass conservation for the absorber gives

$$\dot{m}_1 = \dot{m}_2 + \dot{m}_6 = (1 + \lambda)\, \dot{m}_6 \tag{7.35}$$

Mass conservation of ammonia for the ideal case of x_6 =1 yields

$$\dot{m}_1 x_1 = \dot{m}_6 + \dot{m}_2 x_2 = (1 + \lambda x_2)\, \dot{m}_6 \tag{7.36}$$

Subtracting Eq. (7.36) from Eq. (7.35), we get

$$\lambda = (1 - x_1)/(x_1 - x_2) \tag{7.37}$$

In this example, we have

$$\lambda = (1 - 0.38)/(0.38 - 0.1) = 2.214$$

$$\therefore \quad \dot{m}_1 = (1 + \lambda)\, \dot{m}_6 = (1 + 2.214) \times 3.3604 \times 10^{-3} = 1.08 \times 10^{-3} \text{ kg/s}$$

$$\dot{m}_2 = \lambda \dot{m}_6 = 2.214 \times 3.3604 \times 10^{-3} = 7.44 \times 10^{-3} \text{ kg/s}$$

7.10 WATER–LITHUM BROMIDE ABSORPTION REFRIGERATION SYSTEM

The absorption refrigeration system using water–lithium bromide has recently become very popular for air-conditioning systems running on low-grade energy. In this system, water is used as refrigerant while a solution of lithium bromide in water is used as absorbent. Lithium bromide is a salt, which makes a homogeneous solution when mixed with sufficient quantity of water. Lithium bromide does not evaporate when heated in the generator. This is of great advantage, since water the refrigerant can be separated from lithium bromide solution without the use of rectification column.

This simplicity has made this system more popular. The simple absorption cycle shown in Figure 7.1 can be used for the water–lithium bromide pair. Also, this system gives higher COP than that given by the aqua–ammonia refrigeration system. The drawback of the system is that water freezes at 0°C; hence the system cannot be used below about 5°C. The strong solution of lithium bromide is prone to crystallization of LiBr at higher concentration; hence a proper system design is required to prevent this.

The working principle is similar to that of the aqua–ammonia system, that is, LiBr solution, which is weak in water has affinity for water vapour and will absorb water vapour. Therefore, the water that evaporates in evaporator to give refrigeration, can be driven to absorber and absorbed by the weak LiBr solution. Evaporator has pure water while absorber has a weak solution of water in LiBr. As an example say, the absorber is fed with a weak solution of concentration, $x_{\text{LiBr}} = 0.5$ at 25°C whose saturation pressure is 8.5 mbar. The evaporator has a temperature of 5°C at which the saturation pressure of pure water is 8.7 mbar. This system is shown schematically in Figure 7.27. In such a system, water will evaporate in evaporator to give refrigeration effect, Q_e, and the resulting water vapour will be driven to absorber where it will be absorbed. A difference of pressure of (8.7 – 8.5) = 0.2 mbar is required to overcome the frictional resistance offered by the tube connecting the evaporator to the absorber.

Thus, the weak solution of water in lithium bromide acts like a compressor in drawing the vapour from the evaporator. The solution leaving the absorber must be stronger in water concentration than the one entering it. The concentration of solution is usually specified in terms of kg of LiBr per kg of solution, that is, x_{LiBr}. Hence, a solution strong in LiBr concentration (or weak solution of water in LiBr) enters the absorber and a weak solution in LiBr (or strong solution of water in LiBr) leaves it. In the aqua–ammonia system, weak solution of ammonia in water enters the absorber and strong solution of ammonia in water leaves it, since the concentration refers to that of refrigerant ammonia. An important parameter in the calculation of the system is the mass flow rate of weak solution (strong in LiBr returning from generator) required to absorb the unit mass flow rate of refrigerant vapour (water) from evaporator. This ratio is called *circulation factor*. The pressure in the evaporator and absorber is the saturation pressure of water vapour at evaporator temperature. The pressure in the generator and condenser is the saturation pressure of water vapour at condenser temperature. For example, at $t_e = 5$°C, $p_e = 8.7$ mbar. If the water is available from the cooling tower at 25°C, then the condenser temperature may be taken as 30°C at which the condenser pressure is 42.4 mbar.

The liquid pump raises the pressure from 8.7 mbar to 42.4 mbar. In the absorption refrigeration system, the vapour is absorbed in liquid and the pressure of the liquid is raised whereas in the vapour compression system, it is the pressure of the vapour that is raised. Both are essentially vapour compression refrigeration systems. The pressure difference in this case, however, is only (42.4 – 8.7 = 33.7 mbar) 3400 Pa, which is rather small. One metre height of water in a U-tube gives a pressure difference of $g \times \rho = 9.82 \times 1000 = 9820$ Pa. Therefore, for a pressure difference of 3400 Pa, only a U-tube of 3400/9820 = 0.3427 m is sufficient, which may be used as an expansion valve. Flow through a designed nozzle can also give this pressure drop as liquid water is sprayed into evaporator.

The system invariably uses a preheating heat exchanger that cools the weak solution (strong in LiBr), which becomes capable of absorbing more water vapour and at the same time the weak solution preheats the strong solution, thereby reducing the requirement of heat transfer to the

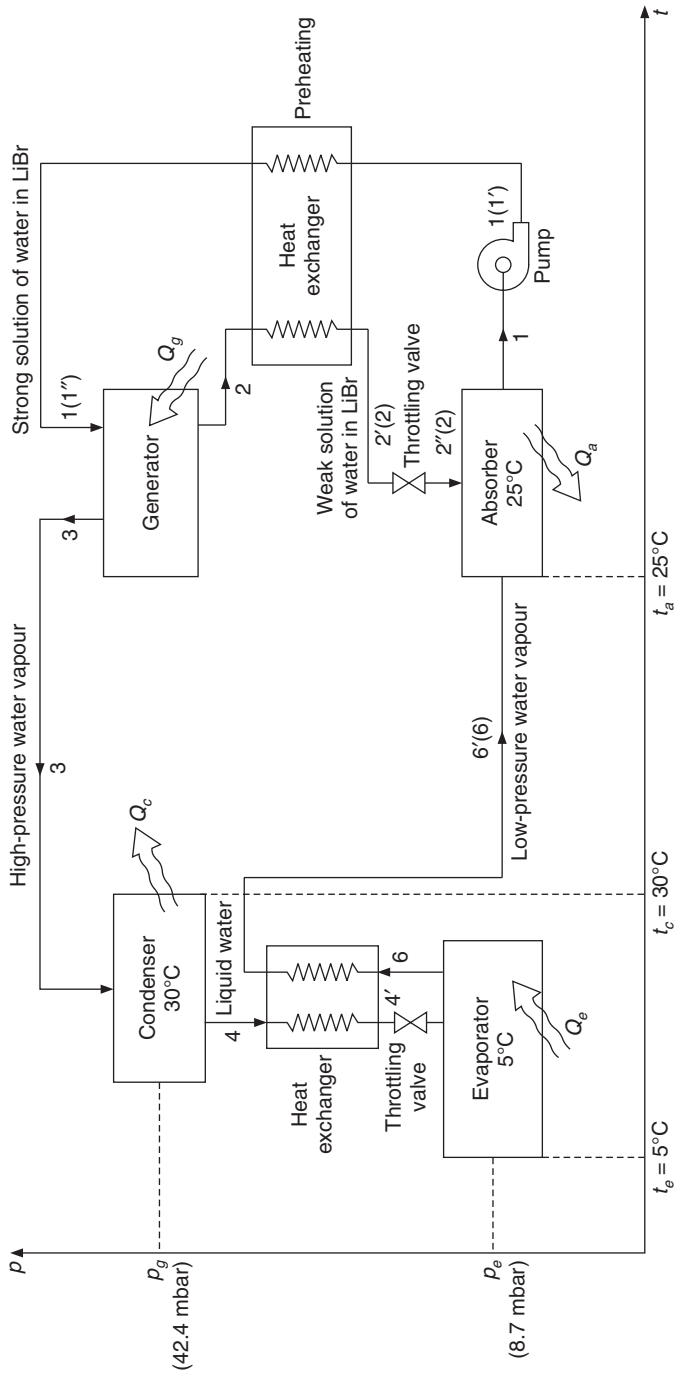

Figure 7.27 Water–lithium bromide absorption system with preheating heat exchanger and subcooling heat exchanger.

generator from an external source. Proper care has to be taken so that the weak solution (strong in LiBr) does not crystallize upon cooling in the preheating HEX. The temperature in the boundary layers near the walls of HEX tubes is small; hence some crystallization invariably occurs there. Hence, sometimes the weak solution is first mixed with the strong (which is weak in LiBr) solution already present in the absorber and re-circulated by a pump for proper absorption. This provides better heat and mass transfer since the velocity is higher apart from reducing the possibility of crystallization.

The specific volume of water vapour is very large (147 m^3/kg at 5°C). This makes the volume flow rate per TR very large. This is one of the main disadvantages of refrigeration system using water as refrigerant. Hence, very large diameter pipelines are required between the generator and the condenser and between the evaporator and the absorber, to reduce the flow velocities and the pressure drops. These pressure drops can be totally eliminated by combining the condenser and generator in one vessel and the evaporator and absorber into another vessel since pressures in these pairs are the same. One model available in the market has all the four components in a single vessel divided into two regions, a high-pressure region and a low-pressure region, by a diaphragm. This is shown in Figure 7.28. Both the evaporator and condenser pressures are below atmospheric pressure, hence a purging device is provided to remove any air leaking into the system.

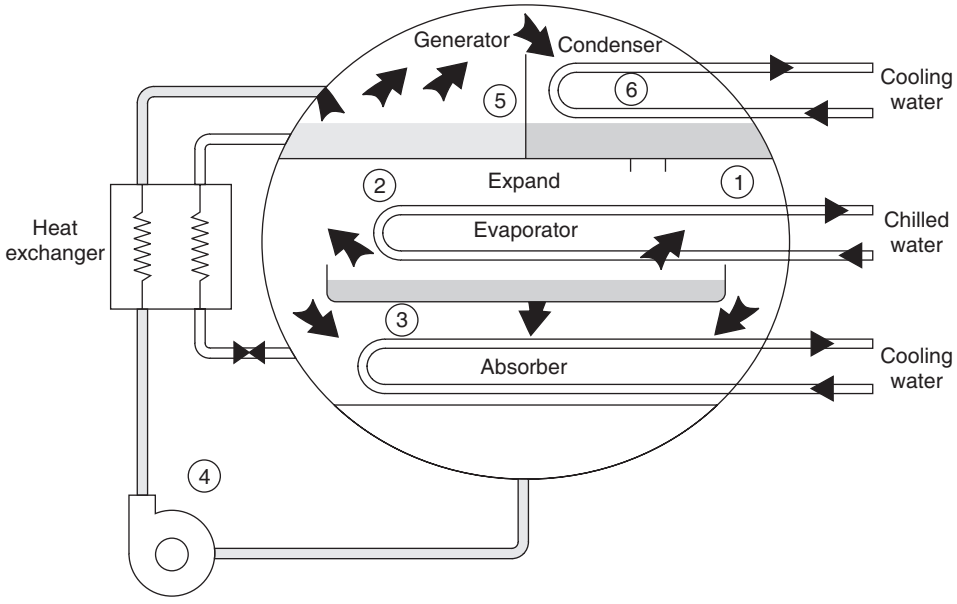

Figure 7.28 A practical single-vessel type, water–lithium bromide system.

The generator may be heated by steam or hot water. In the water chilling system employed in the absorber and condenser, the water to be chilled flows through tubes while the refrigerant water falls on to these tubes through a nozzle (expansion valve). This makes a thin film outside the tube wall from which it evaporates to produce refrigeration. The water level in the evaporator trough is not very large, that is, the tubes are not immersed in it since any depth would mean pressure will be lower at lower depth causing lower temperature and possible freezing. The pressure difference between the condenser and the evaporator is only 0.3427 m of water. A pump circulates the water

draining from the tubes. The pipe wall has conduction thermal resistance and there are convective heat transfer coefficients on both sides of the wall, therefore there is a temperature difference between the two waters. This arrangement produces a minimum chilled water temperature of 5°C. The chilled water itself can be circulated to the cooling load. However it has to be kept in mind that its pressure is 8.7 mbar or lower.

It is thus observed that a practical system uses three pumps whereas in cycle analysis it has been mentioned that only one pump is used. The power requirement of these pumps is small and a very small amount of high-grade energy is consumed by these systems.

A two-vessel system is shown in Figure 7.29. The principle of operation of this is also similar to that described above for the one-vessel system.

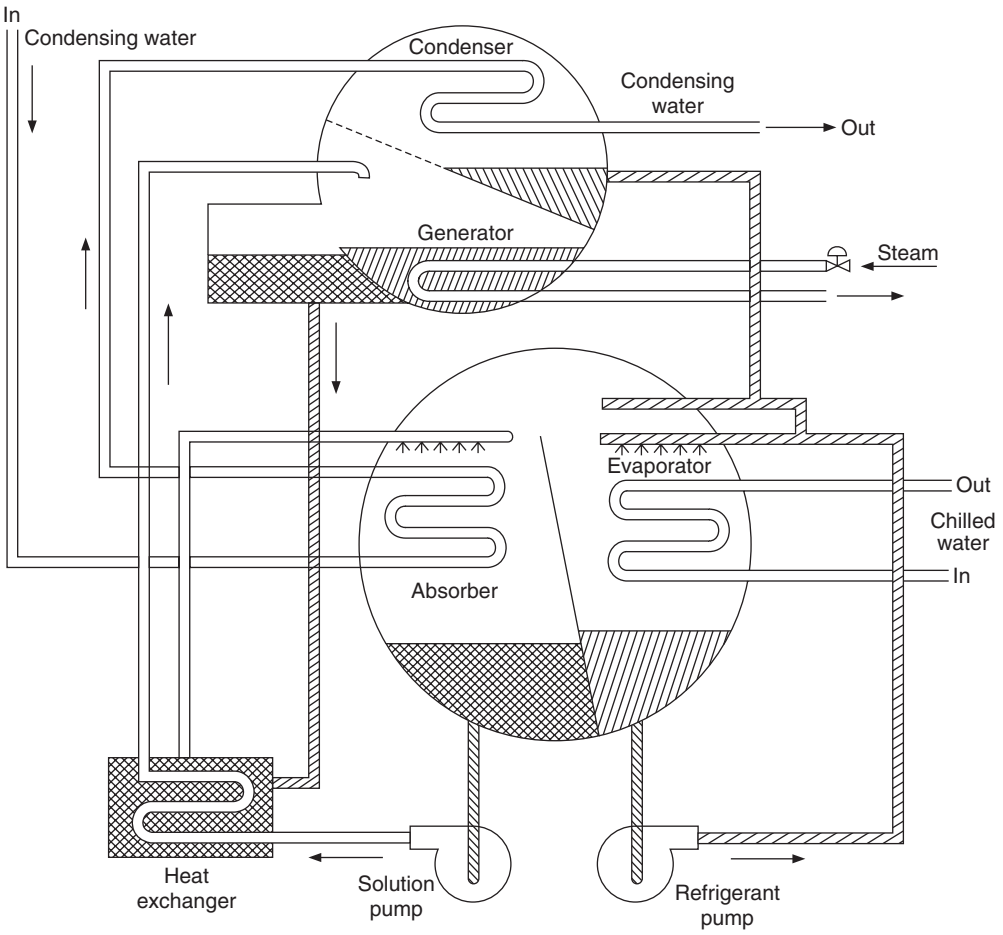

Figure 7.29 A practical, twin-vessel type, water–lithium bromide system.

7.10.1 Dual–Effect System

This system uses steam at very high pressure of 1000 kPa and high temperature in the generator compared to 120 kPa used in a single-stage system. It has typically three vessels, which are at

three different pressures as shown in Figure 7.30. Vessel-1 contains two generators, vessel-II contains the condenser and vessel-III contains the evaporator and absorber.

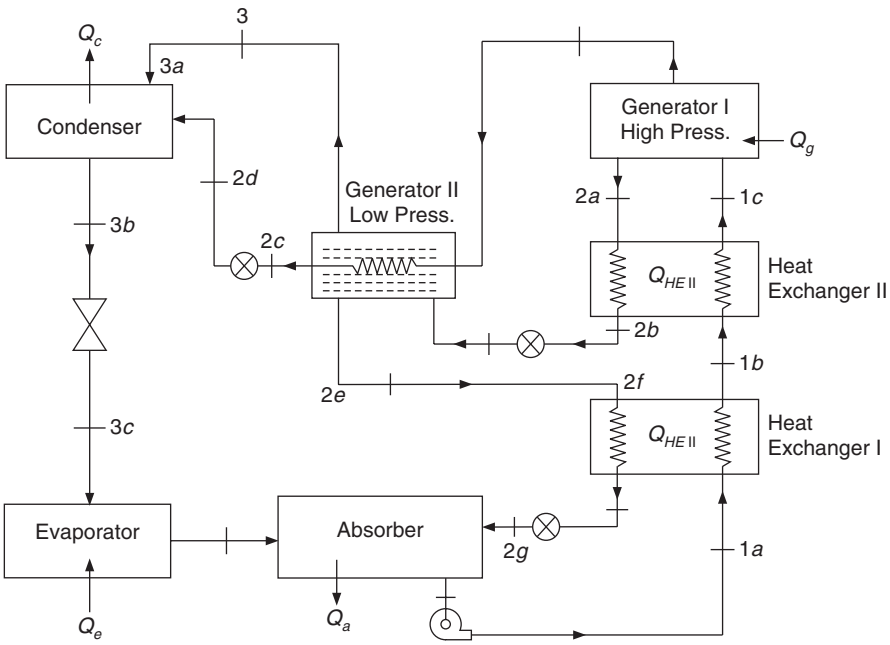

Figure 7.30 Double-effect vapour absorption system.

The first vessel (vessel–I) houses the generator and it is not combined with the condenser vessel-II since the temperature and pressure in vessel-I are higher than those in condenser. The generator (vessel-I) is divided into two generators. The high temperature steam flows through a coil kept in strong solution in generator-I. The strong solution is fed to it at 1*c* from HEX-II. During heating in generator-I, some water vapour evaporates, which cannot be taken to condenser since its pressure is more than the condenser pressure. This water vapour is used to heat the re-circulating weak solution in the coils of generator-II. It condenses on these coils.

The weak solution 2*a* from generator-I is taken to preheating HEX-II where it heats the strong solution going to generator-I from 1*b* to 1*c*. This weak solution at 2*b* is fed back to vessel–I and heated to 2*c* in generator-II by the refrigerant water vapour condensing on the coil. The weak solution passes through the expansion valve 2*c*–2*d* and is fed to the condenser vessel.

The condensate water in the generator is the refrigerant. It is taken out at state 3, passed through expansion valve 3–3*a* and sprayed in the condenser. The flash vapour formed during the expansion is condensed in the condenser. The weak solution fed at 2*d* to the condenser vessel also has some flash vapour, which is also condensed in condenser. The heat is rejected to cold water from cooling tower flowing through a coil. The condensate is the refrigerant. This is drained at 3*b*, passed through an expansion valve 3*b*–3*c* and sprayed into the evaporator in the third vessel.

The weak solution in the condenser vessel is at higher temperature and intermediate pressure. It is expanded to absorber pressure in expansion valve 2*e*–2*f* and used to preheat the strong solution

in HEX I. Then at state 2*g*, it is fed to the absorber and sprayed to absorb the water evaporating from the evaporator. The strong solution at state 1*a* is fed to preheating heat exchanger-I. It is taken to HEX-II and then to generator-I.

The double-effect absorption system has a much higher COP than that of the single-stage system.

7.10.2 Thermal Analysis

The thermal analysis of the system requires the evaluation of enthalpy and concentration at various state points of the cycle. The vapour pressure of the saturated solution at various concentrations and temperatures is conveniently represented in a plot as shown in Figure 7.31 with pure water as the base liquid. This plot gives the equivalent temperature of water whose saturation pressure is the same as the pressure of the solution with given concentration and temperature. The scale of water temperature is on the left ordinate and the solution temperature is on the abscissa. Both the scales are linear scales. The pressure scale on the right ordinate is nonlinear. Linear scales make interpolation easy. The pressure on the right ordinate gives the saturation pressure of water at the temperature indicated in the left hand scale. This pressure may also be obtained from steam tables for the temperature read from the left ordinate. This plot is based upon the data of Pennington (1955) for water–lithium bromide solution.

Typically the pressure in the absorber will be the evaporator pressure and the temperature will be 5 to 10°C more than the cooling tower water temperature. Suppose the evaporator temperature is 5°C and the absorber temperature is 45°C. Then we locate the saturated liquid state leaving the evaporator at 5°C water temperature on right ordinate or its saturation pressure 8.72 mbar on left ordinate (which are same) and 45°C abscissa. Essentially, we have located the state of saturated solution at pressure of 8.7 mbar and 40°C. This lies at $x = 0.605$. The generator pressure will be the saturation pressure at condenser temperature. The generator temperature say is 100°C while the condenser temperature is 45°C and the corresponding saturation pressure is 95.8 mbar. The saturated liquid state leaving the generator is located at left ordinate of 45°C water temperature (or 95.8 mbar on the right ordinate) and abscissa of 100°C. This lies at $x = 0.665$.

The specific enthalpy of water–lithium bromide solution for various temperatures is given in Figure 7.32 based upon the data of Lower (1960). This data is obtained from the measured values of heat of solution of water–lithium bromide solution. It is observed that for all temperatures there is a maximum value of concentration of LiBr for which it can exist in solution. For values of concentration larger than this, crystallization of LiBr will occur. This boundary line is shown by dashed line. Saturated solution and crystals of LiBr exist beyond the dashed line in the two-phase region. The crystals can be $LiBr.5H_2O$, $LiBr.3H_2O$, $LiBr.2H_2O$ or $LiBr.H_2O$. The slope of the isotherms changes as one crosses the dashed line. Ultimately, at $x_{LIBR} = 1.0$ we have anhydrous salt and near this region we have a mixture of anhydrous salt and crystals.

In these charts, the enthalpy of water has been taken to be zero at 0°C. Strictly speaking, it should have been taken to be zero at the triple point 0.01°C.

We require the enthalpy of water and water vapour too in the calculations. These may be obtained from the steam tables or to a fairly good accuracy from the following empirical correlations.

For water: $h = 4.1867\ t$ kJ/kg , where t is in °C (7.38)

For water vapour : $h = 2501 + 1.88\ t$ kJ/kg , where t is in °C (7.39)

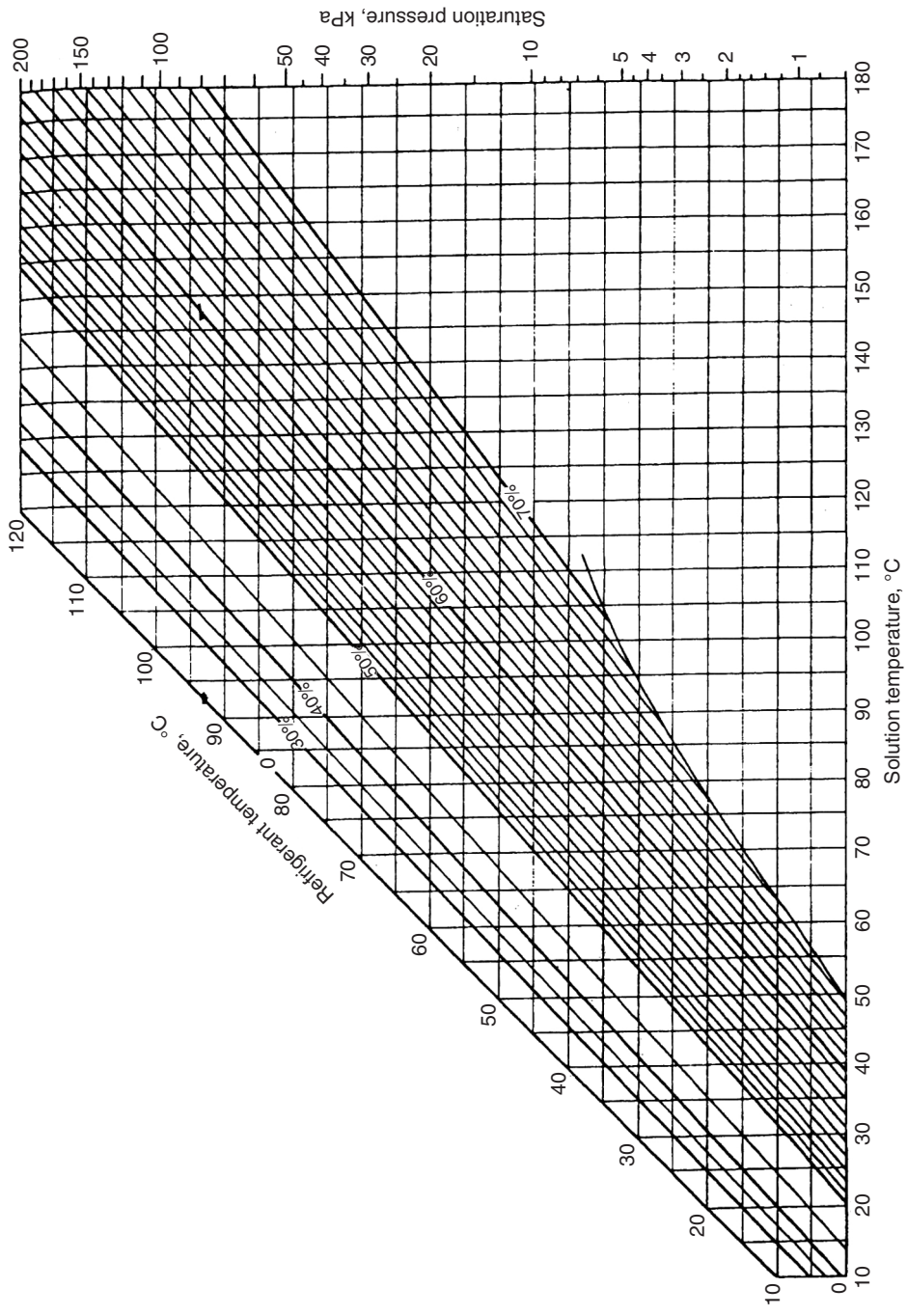

Figure 7.31 Pressure–temperature–concentration diagram for water–lithium bromide solutions.

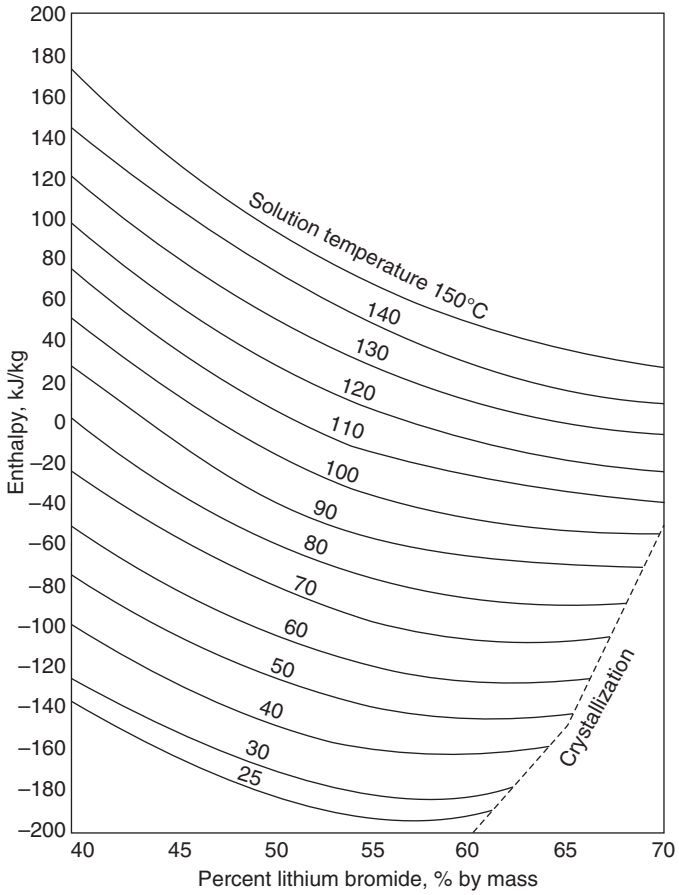

Figure 7.32 Enthalpy–temperature–concentration diagram for water–lithium bromide solutions.

EXAMPLE 7.11 Both the absorber and condenser temperatures in a LiBr absorption refrigeration system are 45°C. The generator and evaporator temperatures are 100°C and 5°C respectively. Considering the simple absorption system (Figure 7.27) but without any heat exchangers, determine the heat transfer rates in all the components on per TR basis and also find the COP.

Solution:

The evaporator and condenser pressures are 8.72 mbar and 95.8 mbar, the saturation pressures at 5°C and 45°C respectively. The absorber pressure is 8.72 mbar and generator pressure is 95.8 mbar. The procedure to determine the concentration of saturated liquid leaving the generator and the saturated liquid leaving the absorber from Figure 7.31 has been outlined above. Once this is known, the enthalpy can be read from Figure 7.32 for the given temperatures. The read values are:

$$x_1 = 0.605 \quad \text{and} \quad h_1 = -143.0 \text{ kJ/kg} \quad \text{at 8.72 bar and 45°C}$$

$$x_2 = 0.665 \quad \text{and} \quad h_2 = -23.0 \text{ kJ/kg} \quad \text{at 95.8 bar and 100°C}$$

At generator exit, enthalpy of water vapour at 100°C: $h_3 = 2501 + 1.88(100) = 2690.4$ kJ/kg

At evaporator exit, enthalpy of water vapour at 5°C: $h_6 = 2501 + 1.88(5) = 2510.4$ kJ/kg

At condenser exit, enthalpy of saturated liquid at 45°C: $h_4 = 4.1867(45) = 188.406$ kJ/kg

For 1 TR cooling capacity,

$$\dot{m}_6 = 3.5167/(h_6 - h_4) = 3.5167/(2510.4 - 188.406) = 1.5145 \times 10^{-3} \text{ kg/s}$$

The overall mass conservation and ammonia mass conservation for the absorber yields

$$\dot{m}_2 + \dot{m}_6 = \dot{m}_1 \quad \text{: Overall mass conservation}$$

At evaporator exit we have pure water vapour, hence concentration of LiBr, i.e. $x_6 = 0$

$$\dot{m}_2 x_2 + \dot{m}_6(0) = \dot{m}_1 x_1 \text{ : Mass conservation of LiBr}$$

Solving these two equations,

$$\dot{m}_2 = \dot{m}_6 x_1/(x_2 - x_1) = 1.5145 \times 10^{-3}(0.605)/(0.665 - 0.605) = 1.5271 \times 10^{-2} \text{ kg/s}$$

$$\dot{m}_1 = \dot{m}_6 x_2/(x_2 - x_1) = 1.5145 \times 10^{-3}(0.665)/(0.665 - 0.605) = 1.6786 \times 10^{-2} \text{ kg/s}$$

Energy balance for the absorber yields

$$Q_a = \dot{m}_2 h_2 + \dot{m}_6 h_6 - \dot{m}_1 h_1$$
$$= 1.5271 \times 10^{-2}(-23.0) + 1.5145 \times 10^{-3}(2510.4) - 1.6786 \times 10^{-2}(-143) = 5.851 \text{ kW}$$

Similarly for the generator,

$$Q_g = \dot{m}_2 h_2 + \dot{m}_3 h_3 - \dot{m}_1 h_1$$
$$= 1.5271 \times 10^{-2}(-23.0) + 1.5145 \times 10^{-3}(2690.4) - 1.6786 \times 10^{-2}(-143) = 6.1359 \text{ kW}$$

$$Q_c = \dot{m}_3(h_3 - h_4) = 1.5145 \times 10^{-3}(2690.4 - 188.406) = 3.8014 \text{ kW}$$

$$Q_a + Q_c = 5.851 + 3.8014 = 9.6524 \text{ kW}$$

and

$$Q_g + Q_e = 6.1359 + 3.5167 = 9.6526 \text{ kW}$$

$$\text{COP} = Q_e/Q_g = 3.5167/6.1359 = 0.573$$

The circulation factor, $\lambda = \dot{m}_2/\dot{m}_6 = 1.5271 \times 10^{-2}/1.5145 \times 10^{-3} = 10.083$

The specific volume of lithium bromide solution at 45°C and $x = 0.665$,

$$v_{sol} = 0.00055 \text{ m}^3/\text{kg}$$

The pump work = $\dot{m}_1 v_{sol}(p_2 - p_1) = 0.016786(0.00055)(95.8 - 8.72) \times 100 = 0.08$ W

The pump work is negligible since the pressure difference is very small.

EXAMPLE 7.12 Consider a preheating heat exchanger in the above example such that the strong solution leaving the absorber is heated to saturated liquid state.

Solution:

The pressure of the strong solution after it passes through the pump is 95.8 bar. This solution at 45°C and 95.8 bar is a subcooled liquid. It is observed that if this solution is heated along the $x = 0.605$ line the pressure becomes 95.8 bar at 92°C, that is, it becomes saturated at this temperature. From Figure 7.32,

$$h_{1''} = -50 \text{ kJ/kg}$$

Energy balance for the preheating heat exchanger gives

$$\dot{m}_2(h_2 - h_{2'}) = \dot{m}_1(h_{1''} - h_{1'})$$

$$h_{2'} = (-23.0) - (1.6786/1.5271)(-50.0 + 143.0) = -125.226 \text{ kJ/kg}$$

The mass flow rates and condenser heat rejection remain unchanged; the absorber and generator heat transfer rates will change. These are as follows:

$$Q_a = \dot{m}_2 h_{2''} + \dot{m}_6 h_6 - \dot{m}_1 h_1$$
$$= 1.5271 \times 10^{-2}(-125.226) + 1.5145 \times 10^{-3}(2510.4) - 1.6786 \times 10^{-2}(-143) = 4.29 \text{ kW}$$

Similarly for the generator,

$$Q_g = \dot{m}_2 h_2 + \dot{m}_3 h_3 - \dot{m}_1 h_{1''}$$
$$= 1.5271 \times 10^{-2}(-23.0) + 1.5145 \times 10^{-3}\ (2698.4) - 1.6786 \times 10^{-2}(-50.0) = 4.5748 \text{ kW}$$

$$Q_c = \dot{m}_3(h_3 - h_4) = 1.5145 \times 10^{-3}\ (2698.4 - 188.406) = 3.8014 \text{ kW}$$

$$Q_a + Q_c = 4.29 + 3.8014 = 8.0914 \text{ kW}$$

and $$Q_g + Q_e = 4.5748 + 3.5167 = 8.0914 \text{ kW}$$

$$\text{COP} = Q_e/Q_g = 3.5167/4.5748 = 0.7687$$

The circulation factor remains unchanged.

The COP increases from 0.573 to 0.7687. The COP can be further improved by including a subcooling heat exchanger as demonstrated below in Example 7.13.

EXAMPLE 7.13 Consider a subcooling heat exchanger in Example 7.12 along with the preheating heat exchanger (Figure 7.27). The vapour leaving the evaporator is superheated up to 40°C in this heat exchanger. Find the mass flow rates, the heat transfer rates and the COP.

Solution:

The enthalpy of water vapour at 40°C is given by

$$h_{6'} = 2501 + 1.88\ (40) = 2575.2 \text{ kJ/kg}$$

Energy balance across the subcooling heat exchanger gives

$\dot{m}_4(h_4 - h_{4'}) = \dot{m}_6(h_{6'} - h_6)$. The mass flow rate $\dot{m}_4$ is equal to $\dot{m}_6$, hence we get

$$h_{4'} = h_4 - (h_{6'} - h_6), \text{ or } h_{4'} = 188.406 - (2575.2 - 2510.4) = 122.606 \text{ kJ/kg}$$

This will change the mass flow through the evaporator as well as those through absorber and generator. For 1 TR cooling capacity, we have

$$\dot{m}_{6'} = 3.5167/(h_{6'} - h_4) = 3.5167/(2510.4 - 122.606) = 1.4728 \times 10^{-3} \text{ kg/s}$$

Following the procedure of Example 7.12,

$$\dot{m}_2 = \dot{m}_{6'} x_1/(x_2 - x_1) = 1.5145 \times 10^{-3}(0.605)/(0.665 - 0.605) = 1.485 \times 10^{-2} \text{ kg/s}$$

$$\dot{m}_1 = \dot{m}_{6'} x_2/(x_2 - x_1) = 1.5145 \times 10^{-3}(0.665)/(0.665 - 0.605) = 1.6323 \times 10^{-2} \text{ kg/s}$$

Energy balance for the preheating heat exchanger gives

$$h_{2'} = h_2 - (\dot{m}_1 / \dot{m}_2)/(h_{1''} - h_{1'}) = (-23.0) + (1.6323/1.485)(-50.0 + 143.0) = -125.223 \text{ kJ/kg}$$

$$\dot{Q}_a = \dot{m}_2 h_{2''} + \dot{m}_{6'} h_{6'} - \dot{m}_1 h_1$$

$$= 1.485 \times 10^{-2}(-125.223) + 1.4728 \times 10^{-3}(2576.2) - 1.6323 \times 10^{-2}(-143) = 4.2687 \text{ kW}$$

Similarly for the generator,

$$\dot{Q}_g = \dot{m}_2 h_2 + \dot{m}_{3'} h_3 - \dot{m}_1 h_{1''}$$

$$= 1.485 \times 10^{-2}(-23.0) + 1.4728 \times 10^{-3}(2698.4) - 1.6323 \times 10^{-2}(-50.0) = 4.4487 \text{ kW}$$

$$\dot{Q}_c = \dot{m}_3 (h_3 - h_4) = 1.4728 \times 10^{-3}(2698.4 - 188.406) = 3.6966 \text{ kW}$$

$$\dot{Q}_a + \dot{Q}_c = 4.2687 + 3.6966 = 7.9653 \text{ kW}$$

and

$$\dot{Q}_g + \dot{Q}_e = 4.4487 + 3.5167 = 7.9654 \text{ kW}$$

$$\text{COP} = \dot{Q}_e / \dot{Q}_g = 3.5167/4.4487 = 0.7905$$

Circulation factor, $\lambda = \dot{m}_2 / \dot{m}_{6'} = 1.485 \times 10^{-2}/1.4728 \times 10^{-3} = 10.083$

The COP increases from 0.7687 to 0.7905.

7.11 THE PLATEN–MUNTERS SYSTEM

Two students named Baltzar von Platen and Carl Munters in 1920 invented this absorption refrigeration system that does not use any moving parts like pump and is therefore free of noise and maintenance, thus ideally suited for household use. It does not use expansion device as well. The whole system is at constant total pressure and is hermetically sealed. This is very useful at places where no electric supply is available. Some hydrogen is present in the evaporator and absorber and the total pressure is equal to partial pressure of ammonia and partial pressure of hydrogen. As a result, ammonia can evaporate at a low temperature corresponding to its partial pressure. The situation is very similar to evaporation of water from a pool at room temperature into the atmosphere where total pressure is more than the saturation pressure of water. The water evaporates from the surface and is carried away by diffusion and advection. Bubbles do not form in the pool. Similarly, in the above system ammonia does not boil in the evaporator, it just evaporates from the surface and is driven to the absorber because of it affinity to the weak solution. For this reason, this system is sometimes called diffusion–absorption refrigeration system. In the absorber, only ammonia is absorbed, the hydrogen is returned to evaporator through a heat exchanger. The schematic diagram is shown in Figure 7.33.

The purpose of liquid pump in the conventional absorption system is to circulate the strong solution apart from increasing its pressure. The rise in pressure is not required in this system since it is at condenser pressure and circulation is achieved by a bubble pump, which works on the principle of coffee percolator. In a coffee percolator water is heated at the bottom of a tube, bubbles form and these rise in the tube. As they rise, they carry some water also in between the bubbles. This water falls on to the coffee beans kept in a perforated tray at the top and percolates through them to give a concoction of coffee. In the Platen–Munters system, the boiler has a hollow tube where a flame is introduced for heating. The strong solution flows into a coil around this hollow tube. Bubbles are formed in this coil. These bubbles have a lower density than the rest of the liquid

and they rise up in the riser tube. Some liquid is also trapped in between the bubbles and is transported to the level of inlet of the absorber vessel. Figure 7.34 shows the schematic representation of a small Platen–Munters system.

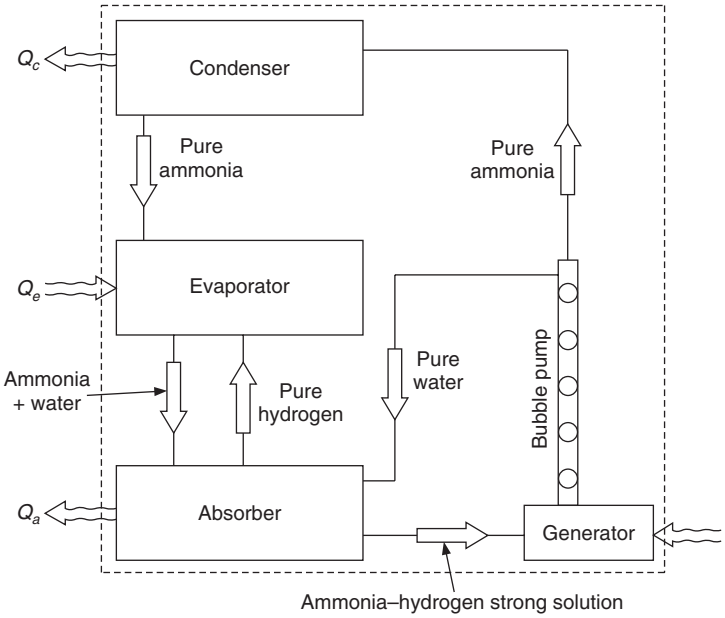

Figure 7.33 Schematic representation of Platen–Munters system.

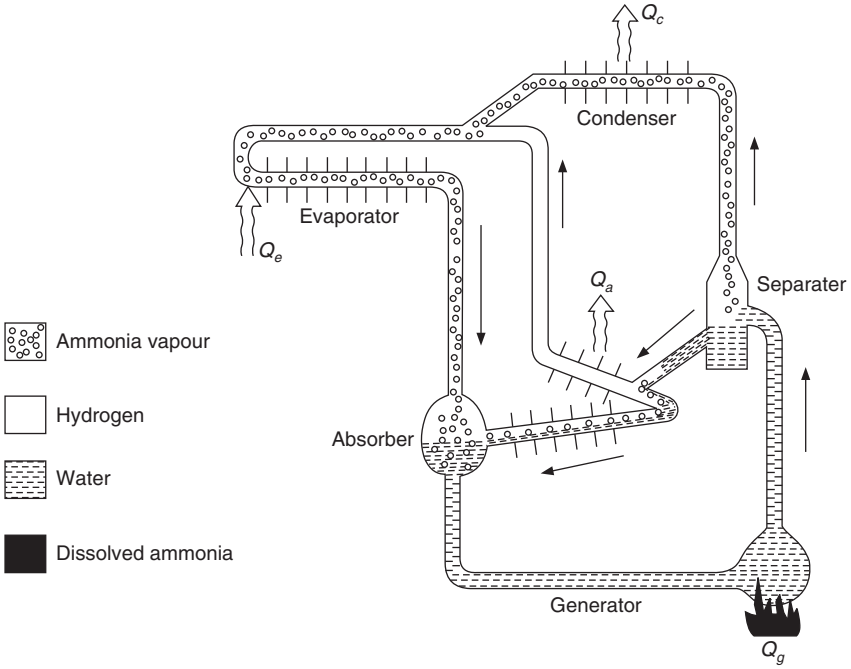

Figure 7.34 Refrigeration circuit of a small Platen–Munters system.

The vapour carried by these bubbles travels to the vertical tube and the solution that becomes weak is drained down into the annulus around the boiler. The vertical tube carrying the vapour acts as rectification column since some cold liquid drips down into this tube providing cooling and separation of vapour all along its length. There are fins on this tube to increase the heat rejection to surroundings to provide additional cooling and condensation. The dephlegmator is the inclined top tube of the condenser.

The vapour condenses in the condenser by heat rejection to the surroundings. There is a liquid seal in the form of a U tube at the exit of the condenser. This is always filled with liquid, hence it prevents the entry of vapour to the evaporator and also prevents the entry of hydrogen into the condenser. The liquid ammonia evaporates in the evaporator to produce refrigeration. The ammonia and hydrogen are drawn towards absorber because of affinity of ammonia for the weak solution. On their way these pass through a heat exchanger where the hydrogen and residual ammonia vapour returning from warm absorber are cooled. The ammonia vapour is absorbed in the absorber.

The ammonia vapour formed due to evaporation comes down in the strong solution receiver and its momentum pushes the hydrogen upwards. Even otherwise hydrogen is lighter and would rise upwards but this provides positive circulation.

The weak solution comes down in the annulus around the boiler and passes through a preheating heat exchanger to heat the strong solution. It rises up to the absorber level because of the static head provided by the bubble pump.

The heat transfer process in the evaporator is dependent upon the diffusion of ammonia from its liquid surface. If the partial pressure of ammonia in vapour phase is equal to that near the liquid surface, then the ammonia–hydrogen mixture is saturated and no further evaporation will occur (typically what occurs in an air–water vapour mixture in contact with liquid water in a container, where air gets saturated with water vapour). This occurs when there is no heat transfer to the evaporator. When heat is transferred to the evaporator, the liquid temperature goes up and the capacity of hydrogen to absorb ammonia vapour increases. The temperature of liquid ammonia increases so that the rate of heat transfer to it is equal to the evaporation rate. Typically hydrogen enters the evaporator at the top point, hence at this point partial pressure of ammonia is the smallest leading to more evaporation, therefore the temperature is the lowest here compared to the bottom part. This is unlike the vapour compression system where the temperature is uniform everywhere in the evaporator. The top part of evaporator may be used for keeping the freezing box.

A vessel is shown in the top part of the figure by dotted line. This is connected to the condenser too. This is meant for equalization of total pressure between the condenser and the absorber. If the atmospheric temperature increases, the condenser temperature and pressure would increase. This may push the liquid seal in the U tube and push ammonia vapour into the evaporator, and raise the partial pressure of ammonia and the temperature of evaporator. The pressure equalization prevents the seal from breaking by maintaining the same pressure on the two sides. Some ammonia vapour passes to the vessel, displaces some hydrogen and increases the total evaporator pressure to the same level as in the condenser.

This was very popular domestic refrigeration system at one time. However, its COP is low compared to the mechanical vapour compression system, therefore, it has been replaced except where there is no electricity or in places like hotel rooms where its silent operation gives it an edge over the other systems.

7.12 PROPERTIES OF REFRIGERANT PAIRS FOR ABSORPTION SYSTEMS

The following properties are required for ideal refrigerant–absorbent pairs for absorption refrigeration systems.

1. The molecules of refrigerant and absorbent should attract each other so that there is large negative deviation from Raoults law, and they mix well and a strong solution of refrigerant in absorbent may be obtained. Negative deviation means that the vapour pressure of the solution is much less than that of the refrigerant at the same temperature. The other way round at the same pressure, the pure refrigerant will be at a much lower temperature than that of the solution.
2. This absorption refrigeration system allows the absorber to work and reject heat at a higher temperature than the evaporator temperature although their pressure is the same. In Figure 7.27 the evaporator temperature is 5°C while the absorber temperature is 25°C and both of them have a pressure of 8.5 mbar. The large difference in pressure acts as potential for driving the vapour from evaporator and for providing a vigorous and thorough mixing in absorber. In the generator this is a great disadvantage since it becomes more difficult to drive the refrigerant from the solution requiring a larger temperature. For low-grade energy application involving solar energy this is great disadvantage.

   The large negative deviation from Raoults law means that mixing of such pairs will involve exothermic reaction and enthalpy of solution will be negative. This is not desirable, since this has to be rejected in the absorber and added over and above the enthalpy of evaporation in the generator. The strong affinity between the refrigerant and the absorbent requires more energy to evaporate them. The best pair will be one, which has a large Raoult's law deviation in the absorber and ideal solution behaviour, or even positive Raoult's law deviation in the generator.
3. There should be considerable difference in the boiling point of the two substances so that at a given pressure only the refrigerant boils off with negligible amount of absorbent. Aqua-ammonia is such a pair but the difference in boiling points is not very large. R22 as refrigerant with dibutylphthalate (DBP) as absorbent has also been used. If some absorbent passes to condenser then the heat rejection and absorption will not be isothermal leading to irreversibility. Solid absorbents do not pose this problem, since they do not evaporate upon boiling. LiBr with water as refrigerant does not pose this problem. Similarly, methanol with LiBr also goes well. LiBr can even be used with ZnBr. Several references for various combinations are available in the literature on this subject.
4. The mixture should have low viscosity so that the pump work is minimum. It should be chemically stable for the whole temperature range. Irreversible chemical reaction, polymerization and corrosion, etc. should not occur. The pair should have low freezing point.

The common pairs used in industrial refrigeration systems are aqua–ammonia and LiBr–H_2O systems. Ammonia is the refrigerant in the aqua–ammonia system and the boiling point difference between the refrigerant and the absorbent is 138 K whereas a difference of 200 K is desirable. Hence, a rectification column is required to enrich the vapours. Water is the refrigerant in the LiBr–H_2O system and salt LiBr is the absorbent. The salt does not evaporate but water freezes at 0°C, hence this system cannot be used for lower temperatures.

7.13 COMPARISON OF ABSORPTION SYSTEM WITH MECHANICAL VAPOUR COMPRESSION REFRIGERATION SYSTEM

It has been observed that the COP of the aqua–ammonia system is about one-seventh of that of single stage saturation cycle for the same evaporator and condenser temperatures. The COP of the LIBr–H_2O system is a little more than that of the aqua–ammonia system.

A direct comparison between the two is unfair, since the absorption system uses low-grade energy while the vapour compression system uses high-grade energy. The COP of the mechanical system should be multiplied by the thermal efficiency of the power plant and then the transmission losses may be included as well. Under such a scrutiny, it will appear that the vapour compression system has a slight edge over the absorption system. The need of a boiler and storage of the fuel are extra burdens for the absorption system. The irreversibility is more in the absorption system due to departure from equilibrium involving mass transfer in addition to heat transfer. The high temperature of combustion can be used in power plants to obtain better efficiency, whereas it cannot be done in an absorption system.

Equation (7.3) for the maximum COP of the absorption system indicates that COP increases with the generator temperature. However, this cannot be chosen arbitrarily since the generator pressure depends upon the condensing temperature, which ultimately limits the generator temperature. In the aqua–ammonia system an increase in the generator temperature causes a decrease in the absorber pressure, if other conditions are maintained constant. It was observed that in LiBr system, the generator temperature can be increased by having a dual–effect system and two pressure levels on the high pressure side.

Practically, the absorption system requires less maintenance than that required by the mechanical vapour compression system. The wear and tear is also less. It may operate at lower temperatures with little decrease in COP. Also, the liquid carry-over and the typical slugging of compressor is not encountered in absorption refrigeration systems. The choice is ultimately based upon economical considerations. If low cost fuel is available and electricity is expensive, then one should opt for the absorption system. If in an installation excess steam or process steam is available during the summer months and where the existing electrical load is not adequate for installing a motor-driven mechanical refrigeration system, then the absorption system is the answer.

At lower evaporator temperatures, a single-stage absorption system will serve the purose whereas the mechanical vapour compression system requires multistaging. Hence the absorption system may be more economical at lower evaporator temperatures.

REFERENCES

Bošnjakovic′, Fr., *Technische Thermodynamik*, Vol.2, 3rd edn. 1960. English Translation by P.L. Blackshear, Holt Rinehart & Winston, New York, 1965.

Lower, H. (1960): *Thermodynamische und physikalische Eigenschaften der wassrigen Lithiumbromid Losung*, Technische Hochschule Karlsruhe.

Pennington, W. (1955): How to find accurate vapor pressure of LiBr water solutions, *Refrig. Eng*. 63, 57–61.

REVIEW QUESTIONS

1. Explain the differences between an absorption refrigeration system and a mechanical vapour compression system.
2. Explain the concept of vapour absorption refrigeration system.
3. Draw a neat diagram of the simple ammonia–water absorption refrigeration system and explain its working.
4. What are the drawbacks of presence of water vapour in the evaporator and condenser of an aqua–ammonia absorption refrigeration system?
5. Explain with a neat sketch the working of a water–lithium bromide absorption refrigeration system. What are its limitations?
6. Explain the merits and demerits of the absorption system compared to the mechanical vapour compression refrigeration system.
7. Enumerate the desirable properties of refrigerant pairs for absorption systems.
8. In a single stage vapour absorption refrigeration system, the temperature of generator, condenser and evaporator are 95°C, 30°C and –5°C, respectively. Find the maximum COP obtainable from the system.
9. In an aqua–ammonia absorption refrigeration system the vapour leaving the dephlegmator is 100% rich saturated ammonia at 40°C. The condenser pressure and evaporator pressure are 20.3 bar and 2.1 bar respectively. The absorber temperature and generator temperature are 40°C and 156°C respectively. The weak solution leaving the generator is cooled down to 50°C in a preheating heat exchanger. Determine the mass flow rates and heat transfer rates on one TR basis and also find the COP. Draw the schematic diagram of the system as well.
10. In a simple water–lithium bromide absorption refrigeration system without any heat exchangers, the generator temperature is 93°C, both absorber and condenser temperatures are 40°C, and the evaporator temperature is 5°C. Determine the heat transfer rates in all the components on per TR basis and also find the COP.
11. Suppose a preheating heat exchanger is added to the system of Question 10 such that the strong solution leaving the absorber is heated to saturated liquid state. Determine the heat transfer rates in all the components and also find the improvement in the COP due to the addition of preheating heat exchanger.

8

Refrigerants

LEARNING OBJECTIVES

After studying this chapter the student should be able to:

1. Differentiate between primary and secondary refrigerants.
2. Describe the numbering system used for designating refrigerants.
3. Describe the properties of some commonly used refrigerants.
4. Explain the desirable properties of refrigerants.
5. Explain the adverse effects of oil and moisture on refrigerants.
6. Enumerate all the thermodynamic properties influencing refrigerant selection.
7. List all the possible alternative refrigerants to CFCs and HCFCs.
8. Explain what refrigerants mixtures are and how they are used in practice.
9. Explain what azeotropes are.
10. Discuss the properties of natural refrigerants and explain what the secondary refrigerants do.

8.1 INTRODUCTION

Refrigerants are used as working substances in refrigeration systems. A very large number of substances are available, which can be used as refrigerants. In fact, there is always a unique refrigerant available which is most suited for a given application and given system. In this chapter, the properties of refrigerants are discussed so that a judicious choice of refrigerant can be made based upon thermodynamic, practical, economic, ecological and other specific considerations.

Based upon the working principle, the refrigerants may be classified into primary refrigerants and secondary refrigerants.

8.1.1 Primary Refrigerants

Primary refrigerants are substances that produce refrigeration effect or absorb heat by evaporating at low temperatures and pressures. In some cases, sensible cooling also produces refrigeration effect. Examples of primary refrigerants are: air, water, ammonia, hydrocarbons, chlorofluorocarbons, etc.

8.1.2 Secondary Refrigerants

Secondary refrigerants are substances that are cooled in the refrigeration plant and transported to produce refrigeration effect at a location away from the refrigeration plant. These do not go through the cyclic processes of evaporation and condensation in a refrigeration system. Examples are: chilled water, brines and glycols, etc.

8.1.3 Types of Refrigerants

The discussion in this chapter will mainly focus upon primary refrigerants since their choice is very crucial from efficiency, economic, ecological and practical considerations point of view. It was pointed out in the history of refrigeration (Chapter 1) that the naturally occurring substances such as ethane, alcohol, NH_3, SO_2, CO_2, methyl chloride, ethyl chloride, methylamine, hydrocarbons and a number of their derivatives were used as refrigerants to start with until the need of better refrigerants was felt. As a consequence, chlorofluorocarbons (CFCs) were invented. Now that it has been found that CFCs are not eco-friendly, hence a search is again on for better refrigerants.

The refrigerants are either organic or inorganic compounds. Amongst the organic compounds these can be either hydrocarbons or halocarbons. Halocarbons contain apart from carbon and hydrogen the elements of halogen group, such as fluorine, chlorine, bromine, iodine and astatine which are part of group VII A of the periodic table. Chlorofluorocarbons contain apart from carbon and hydrogen, the elements chlorine and fluorine. All halocarbons containing chlorine and bromine cause ozone depletion. Fluorine does not cause ozone depletion. The danger of ozone depletion decreases with the presence of hydrogen atoms in the compound. The chlorine and bromine containing compounds cause maximum ozone depletion. In view of these facts, the new classification of the organic refrigerants is as follows:

HC : Hydrocarbons
FC : Fluorocarbons
HFC : Hydrofluorocarbons
HCFC : Hydrochlorofluorocarbons
CFC : Chlorofluorocarbons

8.2 DESIGNATION OF REFRIGERANTS

Thomas Migley, Jr. and Charles Kettering carried the pioneering work of synthesizing series of chlorofluorocarbons. There are a very large number of refrigerants and many of them have large chemical formulae, which become difficult to remember and express sometimes. Migley and Kettering introduced a classification to express all the refrigerants by a very convenient notation called R*abc* . This notation has been adopted by ASHRAE as well. In this notation:

a : number of carbon atoms – 1
b : number of hydrogen atoms + 1
c : number of fluorine atoms

Chlorine atoms satisfy the remaining valency of the carbon atoms. The saturated hydrocarbons are represented by C_nH_{2n+2} and unsaturated hydrocarbons by C_nH_{2n}.

The number of chlorine atoms, d, in CFCs obtained from saturated hydrocarbons will be

$$d = 2a - b - c + 5$$

Hence for the saturated case, Rabc = $C_{a+1}\ H_{b-1}\ F_c\ Cl_{(2a-b-c+5)}$.

8.2.1 Unsaturated Compounds

The CFC derived from unsaturated hydrocarbons is represented by R_1abc, that is, an additional subscript "1"is added to abc to identify it from saturated compounds.

The number of chlorine atoms in CFCs obtained from unsaturated hydrocarbons will be

$$d = 2a - b - c + 3$$

Hence, for the unsaturated case, $R_1abc = C_{a+1}\ H_{b-1}\ F_c\ Cl_{(2a-b-c+3)}$. Examples are:

R1150 = C_2H_4 : Ethylene
R1270 = CH_3CHCH_2 : Propylene
R1130 = $C_2H_2Cl_2$: Dielene or Dichloroethylene
R1120 = C_2HCl_3 : Trielene or Trichloroethylene

8.2.2 Cyclic Compounds

These also have a double bond between carbon atoms. Examples are:

C316 = $C_4Cl_2F_6$: Dichloro hexafluoro cyclic butane
C317 = C_4ClF_7 : Monochloro heptafluoro cyclic butane
C318 = C_4F_8 : Octafluoro cyclic butane

8.2.3 Brominated Refrigerants

These are denoted by putting an additional Bn at the end of abc, where n denotes the number of chlorine atoms replaced by bromine atoms. Examples are:

R13B1 = CF_3Br
R114B2 = $CBrF_2CBr_2F_2$: Dibromo tetrafluoro ethane

8.2.4 Isomers

These compounds have the same chemical formula and the same atomic weight but different chemical structures. These are distinguished from each other by adding the suffix a, b, c, etc. after the number. For example, R134a is CF_3CFH_2 . Subscripts a, b and c for isomers are not the same as the integer numbers values of a, b and c in Rabc.

8.2.5 Non-azeotropic Mixtures

By mixing two or more refrigerants the adverse properties such as flammability, low vapour density or high pressure, etc. of some refrigerants can be offset. However, the difference between the dew point temperature and the boiling point temperature (called the overlap temperature) of the mixture remains distinct. That is, at the given pressure the boiling point temperature increases as the mixture evaporates, unlike pure substances where it remains constant throughout boiling at fixed pressure. These are denoted by R400 series.

R401A : HCFC22 (53%), HFC152a (13%) and HCFC124 (34%)
R401B : HCFC22 (61%), HFC152a (11%) and HCFC124 (28%)
R401C : HCFC22 (33%), HFC152a (15%) and HCFC124 (52%)
R404A : HCFC125 (44%), HCFC143a (52%) and HFC134a (4%)
R405A : HCFC22 (45%), HCFC152a (7%), HCFC142b (5.5%) and Cycloperfluorobutane (42.5%)
R406A : HCFC22 (55%), HCFC142b (41%) and Isobutane (4%)
R409A : HCFC22 (60%), HCFC124 (25%) and HCFC142b (15%)

8.2.6 Azeotropic Mixtures

These are also mixtures of two refrigerants that improve upon the adverse properties of some refrigerants, however at the given concentration these have a unique boiling point. That is, these do not have glide temperature, the boiling point temperature remains constant until the whole of the mixture evaporates. These are denoted by R500 series. For example:

R500 consists of 73.8% by weight of R12 (CCl_2F_2) and 26.2% R152a (CH_3CHF_2)
R501 consists of 75% by weight of R22 ($CHClF_2$) and 25% R12 (CCl_2F_2)
R502 consists of 48.8% by weight of R22 ($CHClF_2$) and 51.2% R115 ($CClF_2CF_3$)
R503 consists of 40.1% by weight of R23 (CHF_3) and 59.9% R13 ($CClF_3$)
R504 consists of 48.2% by weight of R32 (CH_2F_2) and 51.8% R115 ($CClF_2CF_3$)
R507 consists of 50% by weight of R125 (CF_3CHF_2) and 50% R143a (CH_3CF_3)

8.2.7 Hydrocarbons

A few hydrocarbons are denoted as follows:

R50	Methane	CH_4
R170	Ethane	CH_3CH_3
R290	Propane	$CH_3CH_2CH_3$
R600	Butane	$CH_3CH_2CH_2CH_3$
R601	Isobutane	$CH(CH_3)_3$

8.2.8 Oxygen Compounds

Oxygen compounds have been assigned 610 series as follows:

R610	Ethyl Ether	$C_2H_5O\ C_2H_5$
R611	Methyl Formate	$HCOOCH_3$

8.2.9 Nitrogen Compounds

Nitrogen compounds have been assigned 630 series as follows:

R630	Methyl Amine	CH_3NH_2
R631	Ethyl Amine	$C_2H_5NH_2$

8.2.10 Inorganic Compounds

These are denoted by R700 series and the number *abc* is obtained by adding the molecular weight of the compound to 700. For example:

H_2	:	R702	Air	:	R729
He	:	R704	O_2	:	R732
NH_3	:	R717	A	:	R740
H_2O	:	R718	CO_2	:	R744
Ne	:	R720	SO_2	:	R764
N_2	:	R28			

8.3 SOME COMMONLY USED REFRIGERANTS

AIR: It was being used as refrigerant as late as World War I where a non-toxic medium was required. Dense air cycle was used so that the density of air was high and the size of the compressor and expander remained small and manageable. Air is very safe refrigerant and available free of cost. The coefficient of performance of air-based systems is very low. Air is still used in aircraft refrigeration systems where the operating COP is of secondary importance and low weight is of primary importance. Liquid nitrogen finds widespread applications at low temperatures. In fact, it is economical to use it for refrigeration below –100°C against the earlier recommendation to use it below –150°C (123 K).

AMMONIA: It is one of the oldest and most widely used refrigerants in large industrial applications. Its toxicity and irritability are its adverse properties; otherwise it is a naturally occurring substance, which has its natural cycle in nature, that is, it is eco-friendly. It requires a small displacement volume per TR. It is a simple molecule like water, hence its latent heat of evaporation is very high and only a small mass flow rate per TR is required. It is relatively cheap compared to other refrigerants. Its gives a high COP. It attacks cuprous alloys in presence of water. It dissolves in water in all proportions and is non-miscible with mineral oil. It is used in industrial applications where toxicity is of secondary importance. It is a strong irritant and 16–25% by volume in air is sufficient to cause burns on the skin.

CO_2: It is colourless, odourless gas which is heavier than air. It is nontoxic, non-flammable but requires a higher operating pressure. Its HP/TR is very high; hence it finds a very limited application. It was used in marine refrigeration for quite some time and was also used in theatre air-conditioning, hotel and institutional refrigeration instead of NH_3 because it is non-toxic. Its critical temperature is 31°C and critical pressure is 73.8 bar. Hence in a tropical country like India where the ambient temperatures shoot above 45°C, the regular single stage cycle cannot be used sometimes and a two-stage cycle is used or a supercritical cycle is used. Its main use is in the form of Dry Ice that sublimes at –78.3°C. Since the operating pressure is high, heavy equipment and tubes of larger

thickness have to be used. The operating cost is also high compared to other refrigerants. A two-stage system improves the COP. A cascade system is more practical. It does not cause ozone depletion, hence it is considered a safe refrigerant. However, it is one of the main substances causing global warming. It is corrosive if both water and oxygen are present simultaneously.

CH_3Cl: It is a colourless liquid with faint sweet, non-irritating odour. It is both flammable and toxic to some extent. It was used in household refrigerators with rotary and reciprocating compressors and also in commercial units up to 10 TR capacities. It reacts vigorously with aluminium. It was used as drop-in substitute for R12 during World War II when R12 was in short supply.

SO_2: It is a colourless, non-explosive and non-flammable gas. It is extremely toxic and irritating. In 1920s it was used in household refrigerators with rotary and reciprocating compressors. The refrigerant charge was small, therefore the danger of leakage was less. It has extremely noxious odour so much so that even animals cannot stand it. It causes stinging of eyes and coughing, that is what makes it unsafe. People tend to run away as soon as the leak occurs. But most of the accidents happened when people were asleep. Liquid sulphur dioxide acts as a lubricant, hence if the compressor has a water-cooled jacket so that some condensation of SO_2 occurs, then no lubricant is required in the compressor. It absorbs moisture and forms sulphurous acid that is very corrosive and seizes the compressor. It has bleaching effect on flowers, plants and furs.

H_2O: It is the cheapest and safest refrigerant. It is non-toxic, non-flammable and non-explosive. The high freezing temperature (0°C) restricts its use to high temperature refrigeration. Hence, it is principally used for comfort air-conditioning or brewage, milk or liquid chilling. The vapour density is small, hence the volume flow rates are large. Steam-jet refrigeration system, vapour compression with centrifugal compressor or absorption refrigeration with LiBr use water as refrigerant. The operating pressures are below atmospheric pressure in evaporator as well as in condenser, which requires a vacuum to be maintained in the system.

8.4 DESIRABLE PROPERTIES OF REFRIGERANTS

As a rule the selection of a refrigerant is a compromise between the conflicting desirable properties, for example, evaporator pressure should be as high as possible and at the same time the condenser pressure should be as low as possible. Both of these requirements are difficult to satisfy. Low viscosity and low surface tension are desirable but these make it difficult to provide drop-wise condensation that improves the heat transfer during condensation. Easy availability is also one of the criteria. In general, the desirable properties of refrigerants are:

1. *Above atmospheric evaporator pressure:* Refrigerant may leak from the refrigeration system if the evaporator gauge pressure is positive, that is, above atmospheric. Hence, steps are taken to make the system leaktight. However, if the evaporator pressure is below atmospheric (negative gauge pressure) the atmospheric air and water vapour may leak into the system. The water vapour will remain as free water if it is not dissolved by the refrigerant. This free water will freeze in the expansion valve where the temperature may be less than 0°C. This will choke the flow in the refrigeration system. The air that leaks into the system will not condense at room temperature and it will occupy a precious heat transfer area in the condenser. Since $Q_c = A_c U_c (T_c - T_\infty)$, if the area A_c decreases, then for the same heat transfer rate, the condensation temperature T_c must increase and the corresponding saturation

pressure p_c must also increase. Also, refrigerant will condense at its saturation temperature corresponding to its partial pressure in the mixture of air and refrigerant. The total pressure, being the sum of partial pressure of both the components, will be large, This decreases the volumetric efficiency and the mass flow rate of refrigerant and the refrigeration capacity, apart from compressing air without getting any cooling from it.

2. *Moderately low condenser pressure:* This is required so that low-weight equipment and piping may be used. Carbon dioxide has the highest condenser pressure among all the refrigerants. Table 8.2 gives the values of condenser pressure of common refrigerants at condenser temperatures of 30°C and 40°C. Power requirement is high if the condenser pressure is high. Refrigerants with low normal boiling points have a higher condenser pressure and high vapour density, for example, NH_3 and R22 have pressures of 15.54 and 15.331 bar respectively at the condenser temperature of 40°C. CO_2 has the critical temperature and pressure of 31°C and 73.8 bar respectively. Power requirement is also usually high if the condenser pressure is high. Reciprocating compressor is usually used if the condenser pressure is high, for example, for R12, R22, R40, SO_2, CO_2 and NH_3. Refrigerants with low condenser pressure have high normal boiling points and low vapour densities. The volume flow rates are high as shown in Table 8.2, hence centrifugal compressors are used for these. Examples are R11, R113 and R114. Rotary compressors are used for refrigerants with intermediate condenser pressures.
3. *Relatively high critical pressure:* As the condenser pressure approaches the critical pressure the zone of condensation decreases and the heat rejection occurs mostly in the superheated vapour region. Since the zone for isothermal heat transfer decreases, the irreversibility increases. This involves a large temperature difference between the refrigerant and the surroundings leading to large irreversibility. Power requirement also goes up since the area of superheat horn is large. The flash gas losses increase since the quality at the end of the throttling process increases. The COP is small if the refrigeration cycle is operated near the critical temperature. Hence, the refrigerant should be such that the critical temperature is large compared to normal condenser temperature. The critical temperature, pressure and specific volume are given in Table 8.1. Ethylene has critical temperature of 10.6°C while CO_2 has critical temperature of 31°C. Some low normal boiling point refrigerants like R13 and R14 and ethylene have low critical temperatures but these are mainly used on low temperature side of cascade refrigeration systems. For most common refrigerants the ratio T_{nb}/T_{cr} is 0.6 to 0.7, hence the normal boiling point is also low if the critical temperature is low.
4. *High vapour density:* The refrigerants with high vapour density require smaller compressors, velocities can be kept small, pressure drops will be small, and tubes of smaller diameter can be used.
5. *Low freezing temperature:* The refrigerant should not freeze during the normal course of operation; hence its freezing temperature should be small. Water for example cannot be used below 0°C.
6. *Low cost:* It is immaterial sometimes since the quantity of the refrigerant required is small. If the cost is low, then people may not take sufficient safeguards to prevent leakages,

for example NH_3. The prices of some of the refrigerants with high ozone depletion potential, are deliberately hiked to discourage their use.

7. *High latent heat:* High latent heat results in lower mass flow rate. If the vapour density is also high, then it will require a smaller compressor. Small mass flow rate sometimes becomes a disadvantage since it is difficult to control small flow rates. For example, NH_3 cannot be used in small refrigeration systems since it mass flow rate is very small (of the order of 0.003 kg/s per TR). The normal boiling point and latent heat/mole of similar refrigerants is usually similar from Trouten's Rule. Table 8.3 gives the values of latent heat at atmospheric pressure for most of the common refrigerants. The specific refrigeration effect is approximately equal to $h_{fg} - c_{pf}(T_c - T_e)$. The latent heat is large for H_2O and NH_3, hence the throttling loss $c_{pf}(T_c - T_e)$ is small compared to h_{fg} for ammonia.
8. *Inertness and stability:* The refrigerant should not react with materials used in the refrigeration system, that is, tubes, gaskets, compressor parts, etc. It should be non-corrosive in presence of water. It should be stable, that is, its chemical composition should not change during its use. Ammonia reacts with copper and cuprous alloys while CH_3Cl reacts with aluminium. Most of refrigerants form acids and bases in presence of water and some of them may react in presence of lubricating oil. CH_3Cl and CCl_2F_2 can form HCl that can dissolve copper from the copper tubes and deposit it on piston.
9. *High dielectric strength of vapours:* High dielectric strength is required for use of refrigerants in hermetically sealed compressors where the refrigerant vapour comes into direct contact with the motor windings and may cause short circuits.
10. *High heat transfer characteristics:* The heat transfer coefficient depends upon density, specific heat, thermal conductivity, viscosity, surface tension and latent heat or non-dimensional numbers like Reynolds Number, Prandtl Number and few other parameters for boiling and condensation. Low liquid and vapour viscosity is desirable since it leads to higher heat transfer coefficients. A higher heat transfer coefficient leads to the requirement of smaller area and results in lower pressure drop, both of which are economical and the equipment also becomes compact.
11. *Satisfactory oil solubility:* This property is discussed separately.
12. *Low water solubility:* This property is also discussed separately.
13. *Nontoxic*: Refrigerants should be nonpoisonous to human beings and foodstuff. The toxicity depends upon the percentage of vapours in air and the duration of exposure. All freons are safe. Ammonia gives an unpalatable flavour to food. SO_2 kills flowers and is a dying agent for textiles. Refrigerants have been assigned toxicity grades 1–6 by the National Board of Underwrites of USA. SO_2 is most toxic. It is placed in Group 1. A concentration of 0.5–1% and exposure of 5 min is sufficient to cause death or serious injury. NH_3 is placed in group 2. A concentration of 0.5–1% and an exposure of just ½ hour is lethal. CO_2, methane, ethane, propane and butane are in group 5. R12 is in group 6 and is considered to be the safest. This rating is, however, now questionable since a prolonged or periodic exposure is not covered by these standards. Time Weighted Average (TWA) concentration is one useful concept to which repeated eight-hour exposures five days a week are considered safe. Short Term Exposure Limit (STEL) is the maximum concentration to which workers can be exposed up to a maximum of 15 minutes.

14. *Non-irritability:* The refrigerant should not irritate the skin, eyes, nose and lungs. NH_3 irritates all mucous membranes. SO_2 also irritates the lungs.
15. *Non-flammability:* The refrigerant should not support combustion in air or lubricating oil. Freons, SO_2, CO_2, are non-flammable. All hydrocarbons, methane, ethane, propane and butane, etc. are flammable. This is rather unfortunate since propane is a refrigerant with properties similar to NH_3. In general, all chlorofluorocarbons with larger number of hydrogen atoms are flammable. NH_3 with 16–25% air makes an explosive mixture.
16. *Easy leak detection:* NH_3 and SO_2 can be detected by their characteristic smell. NH_3 has a pleasant odour in small concentrations, which becomes irritating and pungent in strong concentrations. SO_2 has an irritating smell that causes sneezing. Strong smell is an advantage in leak detection. Sometimes a strong smelling chemical like acrolein may be added to the refrigerant for detection purposes. Smell just gives an idea of leakage, it does not indicate the location of leakage. NH_3 leakage can be smelled, however, the exact location of leakage has to be determined by other means. NH_3 leaks in water-cooled condensers are very difficult to locate since NH_3 is soluble in water. Soap solution can be used to detect leaks. Soap bubbles form when the solution is placed at the site of leak. Small leaks cannot be detected by soap solution.

    Freons can be detected by Halide torch. It consists of an alcohol lamp that gives blue flame. The blue flame turns green in presence of freons impacting upon copper elements of the burner. This test is based upon Beilstein test for chlorine. SO_2 can be detected with NH_3–H_2O solution as it makes white fumes of ammonia sulphide. Similarly, ammonia can be detected by burning sulphur that will form white fumes of ammonia sulphide. A stick wetted with strong HCl yields white fumes in the presence of ammonia. It can also be detected by blue litmus paper.

    Electronic detectors are used for the detection of freons, based upon the variation of current between two platinum electrodes. All freons except R14 can be detected by this method. The presence of alcohol and CO interferes with the detection test.

    The rate of leakage is proportional to $1/\sqrt{M}$, pressure ratio, diffusion coefficient, density, kinematic viscosity and capillarity. Leakage of refrigerants may result in accidents, low evaporator pressure and should be detected early and corrected.
17. *Eco-friendly:* Refrigerants should not cause global warming or ozone depletion. This has been discussed in the chapter on history of refrigerants (Chapter 1). All chlorine containing refrigerants have a high ozone depletion potential. The CFCs are very stable and inert compounds. Once they leak into the atmosphere they will stay in the atmosphere for all times. CFCs are not soluble in water hence they are not washed down by the rain. CFCs do not have any natural cycle in nature and and are not biodegradable. Hence, once CFCs leak they stay in the atmosphere, and rise upwards very slowly due to atmospheric turbulence and reach stratosphere and ozonosphere. In this region, very energetic solar ultraviolet radiation of small wavelength and high energy content ($\varepsilon = hc/\lambda$) is present. This radiation breaks down the bromine and chlorine bonds and produces a radical and a chlorine atom as follows:

$$CCl_3F + h\nu \rightarrow CCl_2F^+ + Cl^- \tag{8.1}$$

The chlorine atom reacts with the oxygen atom, which would have otherwise formed an ozone atom. Thus, it destroys one ozone atom.

$$Cl^{-} + O \rightarrow ClO \tag{8.2}$$

ClO further reacts with an oxygen atom and destroys another ozone atom.

$$ClO + O \rightarrow Cl + O_2 \tag{8.3}$$

In this process two ozone atoms have been destroyed and the culprit chlorine atom has been regenerated and is free to destroy more ozone atoms by chain reaction. The oxygen atoms are a part of the reaction that occurs in this region to form ozone, which has provided the protective ozone layer around the earth's surface. This has sustained life on earth, otherwise the ultraviolet radiation would have destroyed life on earth. The following reaction takes place continuously in ozonosphere to capture the ultraviolet radiation.

$$O_2 + h\nu \rightarrow O + O \tag{8.4}$$

$$O + O_2 \rightarrow O_3 \tag{8.5}$$

In this process, one ozone atom and one oxygen atom have been destroyed and the culprit chlorine atom is still left behind to destroy more ozone atoms by chain reaction. Similar reactions also occur with NO and NO_2 as shown below.

$$NO + O_3 \rightarrow NO_2 + O_2 \tag{8.6}$$

$$NO_2 + O \rightarrow NO + O_2 \tag{8.7}$$

The other path for these reactions is as follows:

$$Cl^{-} + O_3 \rightarrow ClO + O_2 \tag{8.8}$$

$$ClO + ClO \rightarrow 2Cl + O_2 \tag{8.9}$$

$$OH + O_3 \rightarrow HO_2 + O_2 \tag{8.10}$$

$$ClO + HO_2 \rightarrow HOCl + O_2 \tag{8.11}$$

$$HOCl + h\nu \rightarrow Cl + OH \tag{8.12}$$

$$Cl^{-} + O_3 \rightarrow ClO + O_2 \tag{8.13}$$

The reaction of Cl with O_3 is much faster than the reaction of ClO with O because the concentration of O is much lower than O_3. As a result, ClO is much longer-lived species. The chlorine atom continues to break down ozone during its atmospheric lifetime (one to two years) during which it destroys 100,000 ozone molecules. Chlorine atoms are removed from stratosphere after forming two compounds that are relatively resistant to ultraviolet radiation. This happens at mid latitudes where there is a large concentration of NO_2. ClO is converted to $ClONO_2$. Similarly Cl may also be converted into its reservoir species HCl, that is,

$$Cl + CH_4 \rightarrow HCl + CH_3 \tag{8.14}$$

However both these reactions occur at lower altitudes after ClO and Cl have diffused downwards. These compounds can diffuse to troposphere where they react with water vapour and are removed by rain. The chain may also be regenerated if the concentration of OH ions is high. This occurs as follows:

$$OH + HCl \rightarrow H_2O + Cl \tag{8.15}$$

Other possibilities of chain termination are as follows:

$$Cl + ClO \rightarrow Cl_2O \tag{8.16}$$

$$Cl + NO \rightarrow NOCl \tag{8.17}$$

These can, however, dissociate again in the presence of long wavelength radiation.

Bromine too has similar reactions as chlorine, and bromine is much more destructive than chlorine because the compounds hydrogen bromide HBr and bromine nitrate $BrNO_2$ are more susceptible to dissociation by UV radiation; thus many more molecules of ozone are destroyed before the bromine atoms can diffuse downwards and convert to reservoir species.

The chemistry of depletion of Antarctic ozone is different from the homogeneous gas phase reactions described above. This is attributed to heterogeneous gas reactions in the presence of aerosols. These reactions occur in the 10 to 20 km altitude in the spring season during the month of October. At this time sun rises after six months of night in Antarctica and clouds make their appearance at stratospheric altitude. These clouds provide a large area for heterogeneous reaction. Reactions (8.1) to (8.3) cause maximum depletion at 40 km altitude and these reactions are not feasible below 26 km altitude because of low concentration of UV radiation. Reactions (8.8) to (8.13) are possible in the altitude range of 10 to 20 km if ClO is available. However, ClO is converted into its reservoir species $ClONO_2$ at this altitude if NO_2 is available in large quantities and Cl is converted into its reservoir species HCl. It is predicted that these convert back to Cl by following paths in the presence of clouds denoted by *particle* in the following reactions.

$$HCl + ClNO_3 + \text{particle} \rightarrow HNO_3 + Cl_2 + \text{particle} \tag{8.18}$$

$$ClNO_3 + H_2O + \text{particle} \rightarrow HOCl + HNO_3 \tag{8.19}$$

Cl_2 will photolyse rapidly in sunlit atmosphere into two chlorine atoms while HOCl will yield OH and Cl atoms. These reactions occur at a very fast rate compared to reservoir species reactions. Subsequently, ozone is depleted by reactions (8.8) to (8.13). A requirement for these reactions to occur is that HNO_3 should not rapidly photolyse to NO_2, which may convert the catalyst species back to reservoir species. Some authors rule out the possibility of reaction (8.18) stating that it requires simultaneous presence of H_2O and H_2SO_4. According to them the percentage of reservoir species reduces due to the following heterogeneous reactions:

$$NO_2 + O_3 \rightarrow NO_3 + O_2 \tag{8.20}$$

$$NO_3 + NO_2 + \text{particle} \rightarrow N_2O_5 + \text{particle} \tag{8.21}$$

$$N_2O_5 + H_2O + (\text{particle}) \rightarrow 2HN_3 \tag{8.22}$$

The Antarctic ozone levels return closer to usual pattern by November when stratospheric clouds disappear. This recovery is dominated by the wave driven transport, which brings in the ozone-rich air from higher latitudes.

The complexity of chemistry, concentration of reactants, temperature distribution and dynamics of earth's atmosphere make it very difficult to quantify the effects of CFCs on ozone depletion. The original hypothesis of Rowland and Molina (1974) has been expanded into a comprehensive and very complex theory involving about 200 reactions, feedback of temperature and concentration and dynamics of the atmosphere. The computational models calculate the latitudinal, seasonal as

well as vertical, distribution of ozone. The computer models are used to predict the present atmosphere and future atmosphere with historical emissions of CFCs.

Global warming

The other alarming issue is the global warming due to *greenhouse effect* that CFCs may cause and lead to global climate changes. CO_2 and CFCs are transparent to solar radiation, which is in the short wavelength range. However, these gases are opaque to long wavelength radiation, which is emitted by the ground surfaces at temperatures around 300 K. These gases block this long wavelength radiation trying to leave the earth's surface, thereby trapping it in the earth's atmosphere. The main concern in this regard is about increase in the atmosphere of CO_2 due to increased use of fossil fuels and deforestation. Increase in the concentration of CO_2, CFCs and a few other gases would inevitably lead to global warming. It is estimated that the atmospheric temperature of earth may rise by 3 K over the next 100 years.

Table 8.1 Chemical formula, normal boiling point, freezing temperature, critical point data, specific heat ratio and molecular weight of various refrigerants

Refrigerant	*Chemical formula*	*Normal boiling point*	*Freezing point* (°C)	*Critical temperature* (°C)	*Critical pressure* (bar)	*Critical volume* (L/kg)	$\gamma = c_p/c_v$	*Molecular weight*
R702n	H_2	–252.8	–259.2	–239.9	13.15	33.21		2.0159
R702p	H_2	–252.9	–259.3	–240.2	12.92	31.82		2.0159
R 717	NH_3	–33.35	–77.7	132.4	112.97	4.13	1.31	17.031
R718	H_2O	100	0.0	374.15	221.1	3.26	1.33	18.016
R720	Ne	–246.1	–248.6	–228.7	33.97	2.070		20.183
R728	N_2	–198.8	–210.0	–146.9	33.96	3.179		20.013
R729	Air	–194.3		–140.0	37.72	3.048	1.4	28.97
R732	O_2	–182.9	–218.8	–118.4	50.77	2.341		31.9988
R744	CO_2	–78.52	–56.6	31.0	73.8	2.14		44.01
R764	SO_2	–10.01	–73.2	157.2	78.7	1.92		64.06
R11	CCl_3F	23.7	–111	197.78	44.06	1.805	1.13	137.39
R12	CCl_2F_2	–29.8	–158	112.04	41.13	1.793	1.14	120.92
R13	$CClF_3$	–81.5	–180	28.78	38.65	1.721		104.47
R14	CF_4	–127.9	–194	–45.5	37.41	1.5	1.22	88.01
R21	$CHCl_2F$	8.8	–135	173.5	51.68	1.915	1.16	102.92
R22	$CHClF_2$	–40.8	–160	96	49.74	1.905	1.16	86.48
R23	CHF_3	–82.1	–155.0	25.83	48.33	1.948		70.02
R30	CH_2Cl_2	39.2	–96.7	235.4	59.7		1.18	84.93
R32	CH_2F_2	–51.75		78.41	58.3	2.326		52.042
R40	CH_3Cl	–12.4	–97.8	143.1	66.74	2.834	1.2	50.49
R50	CH_4	–161.5	–182.2	–82.5	46.38	6.181		16.04
R113	CCl_2FCClF_2	47.57	–35	214.1	34.37	1.736	1.09	187.39

(*Contd.*)

Table 8.1 Chemical formula, normal boiling point, freezing temperature, critical point data, specific heat ratio and molecular weight of various refrigerants (Contd.)

Refrigerant	*Chemical formula*	*Normal boiling point*	*Freezing point* (°C)	*Critical temperature* (°C)	*Critical pressure* (bar)	*Critical volume* (L/kg)	$\gamma = c_p/c_v$	*Molecular weight*
R114	$CClF_2CClF_2$	3.8	–94	145.7	32.59	1.717	1.107	170.94
R115	$CClF_2CF_3$	–39.1	–106	79.9	31.53	1.629	1.09	154.48
R123	CF_3CHCl_2	27.85		183.8	36.74	1.818		152.93
R123a	$CHClFCClF_2$	29.9		189.62	38.89			152.93
R124	CF_3CHClF	–12.05		122.5	36.34	1.786		136.475
R125	CF_3CHF_2	–48.55		66.25	36.31	1.748		120.02
R134	CHF_2CHF_2	–19.8		118.9	34.3	2.1		102.03
R134a	CF_3CH_2F	–26.15	–96.6	101.06	40.56	1.942	1.102	102.03
R141b	CH_3CCl_2F	32.1		208.0	43.39			116.9
R142b	CH_3CClF_2	–9.25	–131.0	137.1	42.46	2.3	1.135	100.495
R143a	CH_3CF_3	–47.35	–111.3	73.1	38.11	2.305		84.04
R152	CH_2FCH_2F	–24.15	–117.0	113.3	45.2	2.717	1.134	66.05
R160	C_2H_5Cl	12.0	–138.7	187.2	52.47	3.03	1.16	64.52
R170	C_2H_6	–88.8	–183.0	32.2	48.91	5.182	1.25	30.07
R216	$C_3Cl_2F_6$	35.69	–125.4	180.0	27.53	1.742		220.93
R290	C_3H_8	–42.07	–187.7	96.8	42.54	4.545	1.13	44.1
R500	Azeotrope	–33.5	–159.0	105.5	44.23	2.016		99.31
R502	Azeotrope	–45.4		82.2	40.72	1.785		111.63
R503	Azeotrope	–88.7		19.5	41.82	2.035		87.5
R504	Azeotrope	–57.2		66.4	47.58	2.023		79.2
R600	C_4H_{10}	–0.5	–138.5	153.0	35.35	4.383		58.13
R600a	$(CH_3)_3CH$	–11.73	–160.0	135.0	36.45	4.526	1.806	58.13
R611	$C_2H_2O_2$	31.8	–99.0	214.0	59.94	2.866		60.05
R630	CH_3NH_2	–6.7	–92.5	156.9	74.55		1.18	31.06
R631	$C_2H_5NH_2$	16.6	–80.6	164.6	54.7		1.15	45.08
R1130	$C_2H_2Cl_2$	47.78	–56.6	243.00	54.9		1.14	96.9
R1150	C_2H_4	–103.7	–169.0	10.6	51.14	4.37	1.21	28.05
R1270	C_3H_6	–47.7	–185.0	91.8	46.18	4.495		42.08
R1381	$CBrF_3$	–57.75	–168.0	67.0	39.62	1.342		148.93

Note:

R600	*n*-Butane	R1130	Dichloroethylene
R600a	Isobutane	R1150	Ethylene
R611	Methyltromate	R1270	Propylene
R630	Methylamine	R1381	Bromotrifluoromethane
R631	Ethylamine		

Table 8.2 Condenser pressure, compression ratio, swept flow rate, power/TR, adiabatic discharge temperature and COP at condenser temperatures of 30°C and 40°C and evaporator temperature of –15°C.

Refrig-erant	*Evapo-rator pressure* p_e (bar)	*Condenser pressure,* p_c (bar)		*Compression ratio*		*Compressor displacement,* V_P (m^3/TR)		*Power per* TR (kW/TR)		*Discharge Temperature* (°C)		*COP*	
	–15°C	40°C	30°C	40°C	30°C	40°C	30°C	40°C	30°C	40°C	30°C	40°C	30°C
R11	0.201	1.748	1.25	8.68	6.19	1.098	1.035	0.888	0.7	52	43.88	3.941	5.03
R12	1.83	9.6	7.44	4.68	4.08	0.181	0.165	1.025	0.745	48	38.33	3.416	4.7
R13	8.43	36.46	–	4.33	–	0.0517	–	1.01	–	41	–	1.832	–
R21	0.362	2.958	2.15	8.17	5.95	0.606	0.578	1.033	0.702	82	61.11	3.387	5.01
R22	2.96	15.331	11.9	4.06	4.03	0.111	0.1	0.965	0.754	71	53.33	3.627	4.66
R40	1.15	8.5	6.53	7.44	4.48	0.18	0.168	0.894	0.718	166	77.77	3.916	4.84
R113	0.069	0.7809	6.65	11.3	8.02	3.115	3.888	0.917	0.726	40	30	3.875	4.64
R114	0.47	3.454	2.53	7.26	5.42	0.627	0.57	0.992	0.783	40	30	3.528	4.49
R134a		10.167				0.181							
R152a		9.092				0.193							
R290	2.89	13.42	10.69	4.64	3.7	0.127	0.116	0.925	0.768	47	36.1	3.785	4.58
R500	2.14	11.41	8.79	5.33	4.12	0.154	0.140	0.971	0.754	53	40.6	3.605	4.65
R502	3.49	16.33	13.19	4.76	3.75	0.116	0.102	1.156	0.805	49	37.2	3.028	4.37
R600	0.565	3.87	2.87	6.85	5.07	0.354	0.439	0.903	0.711	40	31.1	3.875	4.95
R717	2.36	15.54	11.69	4.34	–	0.102	–	0.94	–	120	98.9	3.725	–
R744	14.29	64.3	–	4.5	–	0.036	–	1.411	–	68	–	2.48	–
R764	0.81	16.638	–	7.72	–	0.267	–	1.00	–	130	88.3	3.512	–
R718	0.009	0.2	–	22.92	–	13.76	–	0.877	–	320	–	3.993	–

Table 8.3 Enthalpy of evaporation at atmospheric pressure and the specific heat ratio for common refrigerants

Refrigerant	H_2O	NH_3	CO_2	C_2H_6	C_3H_8	C_4H_{10}	Isobutane	R22	R12
h_{fg} (kJ/kg)	2261	136.9	271.5	490	424.3	381.4	367.7	233.2	167.5
$\gamma = c_p/c_v$	1.33	1.31			1.126		1.086	1.116	1.126

Refrigerant	R114	R11	R13	R113	R14	R152a	R134a
h_{fg} (kJ/kg)	137.3	182.5	148.7	147.2	136.7	328.4	222.5
$\gamma = c_p/c_v$		1.11		1.09		1.134	1.102

8.5 REACTION WITH LUBRICATING OIL

The lubricating oils are either mineral oils or synthetic oils. The synthetic oils are polybutyl silicate recommended for R22, alkyl benzenes or poly alkyl glycols recommended specifically for R134a.

The lubricating oils come into direct contact with refrigerant in reciprocating compressors. There are three possible reactions that may take place:

- Some oil may get dissolved in refrigerant. This will change the pressure–temperature characteristics of the refrigerant.
- Some refrigerant may get dissolved in the oil. This will change the lubricating properties of the oil.
- Some oil is physically picked up by the high velocity refrigerant vapour. This results in a mechanical mixture that may accumulate in some component if it cannot be physically carried by the refrigerant.

Adverse effects

- Presence of lubricating oil on heat transfer surfaces appears as a film on them and hence reduces the heat transfer coefficient in the evaporator and condenser.
- The pressure and temperature, that is, the boiling point and the condensation temperature of the refrigerant change, resulting in lower COP.
- Compressor lubrication may be affected due to change in viscosity or reduction in quality of lubricating oil.

The refrigerants are immiscible, miscible or partially miscible with the mineral oils. It is the partially miscible variety that gives rise to maximum problems.

Completely miscible refrigerants

R11, R12, R21, R113 and R500 are completely miscible with mineral lubricating oils and make a homogeneous mixture. The lubricating oil should stay in compressor to provide lubrication. Once it is picked up by refrigerant vapour, it has to circulate in the refrigeration system. It has to be mechanically carried by the refrigerant. High suction velocities are required to circulate lubricating oil and bring it back to compressor. *ASHRAE Handbook* recommends the diameters of liquid and vapour lines based upon this criterion for the specified refrigerant and the cooling capacity. High velocities and the burden of carrying oil lead to larger pressure drops and more compressor power. R501 has very good solubility for the oil.

Immiscible refrigerants

NH_3, SO_2, CO_2, R13, R14 and R134a are immiscible with mineral oil. Hence, the oil can be mechanically separated. The systems using these refrigerants have to use oil separators right after the compressor. R13 and R14 are low temperature refrigerants. R15 and R152a have very low solubility for mineral oils.

Partially miscible refrigerants

R22 and R114 are partially miscible in lubricating oil. Above a certain temperature depending upon the percentage of lubricating oil, the lubricating oil is completely miscible in refrigerant and partially miscible below this temperature. This depends upon the type of lubricating oil as well. As an example, R22 with 18% oil separates at 0.5°C while R22 with 10% and 1% oil separates at –5°C and –51°C respectively.

In general, the partially miscible refrigerants pose maximum problems. To avoid these problems, either an efficient oil separator must be used or synthetic oil that is completely miscible with refrigerant must be used. Polybutyl silicate and alkyl benzenes are used with R22. Alternatively, R501, which is a mixture of R12 and R22, may be used in which the presence of R12 improves the solubility of oil. Poly alkyl glycol is used with R134a.

Oil logging

If the refrigerant velocity is not sufficient, then it cannot carry all the oil back to the compressor and there is a possibility that it may accumulate in the evaporator. This phenomenon is called oil logging of the evaporator. It must be prevented. If the evaporator area is blocked by lubricating oil, then the temperature difference ΔT_e required for the heat transfer increases since $Q_e = U_e A_e \Delta T_e$ or the evaporator cooling capacity reduces. As the refrigerant boils, a distillation process occurs and the oil is left behind. The built-up of lubricating oil may cause choking and give rise to problems in starting the compressor. The oil is lighter than R22. In the shell-and-tube heat exchanger if the refrigerant is on the shell side, then the oil will float on the surface of the refrigerant and prevent evaporation of the refrigerant as it separates. A facility for overflow of oil is provided in these evaporators. On the other hand, if the oil is heavier than NH_3, it settles down in the evaporator and blocks the tubes thereby reducing the heat transfer coefficient. The oil in these evaporators can be drained from the bottom.

In DX (Direct Expansion) coils, oil is carried by high suction velocity. R22 and R502 DX coils should have inlet at the top so that the gravity also helps in draining the oil. DX coils are used with these refrigerants at low evaporator temperatures.

Frothing of hermetic compressors

In hermetic compressors, the refrigerant comes into direct contact with the lubricant. The refrigerant being a polar substance gets adsorbed on the surface of the lubricating oil. The quantity of liquid adsorbed may continue to increase and then suddenly under adverse conditions the liquid refrigerant may start to boil. As it boils, a large quantity of vapour is formed, which traps the lubricating oil. The mixture of vapour refrigerant and lubricating oil is called *froth* and this phenomenon is called *frothing*. The froth fills the compressor cylinders with lubricating oil, depriving the crankcase of oil and thereby increasing the wear and tear. This is usually avoided by providing crankcase heaters, which may form a part of the condenser coil as well.

8.6 REACTION WITH MOISTURE

All refrigerants form acids or bases in the presence of water. These cause corrosion and are harmful to valves seats and metallic parts. These may also damage the insulation of windings of motors of hermetic compressors.

CO_2, SO_2 and NH_3 absorb water; NH_3 particularly absorbs water in all proportions whereas water is practically insoluble in R12, R113 and R114.

The water which does not go into solution with the refrigerant, remains as free water. The free water freezes at temperatures below 0°C and may choke the flow particularly if freezing occurs in the narrow orifice of the expansion valve. The water expands upon freezing. Hence if water freezes in a large quantity, the tubes may burst.

The solubility of refrigerants in water is different for different refrigerants. R22 absorbs 23 times more water than R12 can do. R11 and R113 are used only in air-conditioning systems with evaporator temperatures above 0°C, hence the solubility of water does not pose any problem.

Precautions

Dehydration of the system should be done before charging the refrigerant into the system. All traces of water should be removed. Water sticks to surfaces, hence radiant heaters should be used to evaporate it while evacuating the system. The lubricating oil should also be free of moisture. Lubricating oil stored in open is liable to absorb atmospheric moisture; hence it should be stored in closed containers. Subsequently, running the system at positive pressure would prevent entry of moisture and moist air. Permanent dryers should be installed in systems. These dryers usually contain silica gel or anhydrous calcium oxide.

8.7 THERMODYNAMIC PROPERTIES

8.7.1 Normal Boiling Point and Saturation Line

The normal boiling point is an important property of a refrigerant since many other properties are related to it. The dependence of saturation pressure on temperature for a pure substance can be obtained from Clausius–Clayperon equation, which is as follows

$$\frac{dp}{dT} = \frac{h_{fg}}{T(v_g - v_f)} \tag{8.23}$$

Assuming v_f to be negligible compared to v_g and replacing v_g by RT/p, we obtain

$$\frac{dp}{p} = h_{fg}(dT / RT^2) \tag{8.24}$$

This equation can be integrated over a small temperature range assuming h_{fg} to be constant, i.e.

$$\ln\ p = a - \frac{h_{fg}}{RT} \tag{8.25}$$

The constant "a" can be evaluated by applying the boundary condition that T_{nb} is the normal boiling point at atmospheric pressure p =1 (pressure is measured in atmospheres), that is,

$$\text{At } p = 1: \qquad T = T_{nb}, \qquad \text{hence } a = \frac{(h_{fg})_{nb}}{RT_{nb}}$$

$$\therefore \qquad \ln\ p = a\left(1.0 - \frac{T_{nb}}{T}\right) \tag{8.26}$$

This equation indicates that a plot of natural logarithm of saturation pressure against $1/T$ is a straight line.

Further according to Trouton's rule, molar entropy of evaporation at the normal boiling point has the same value for all pure substances, that is,

$$M\,\frac{(h_{fg})_{nb}}{T_{nb}} \approx 85 \text{ kJ/mol-K} \tag{8.27}$$

This is called the Trouton's number. Therefore constant "a" may be expressed as

$$a = \frac{M(h_{fg})_{nb}}{RT_{nb}} \approx \frac{85}{8.314} = 10.22 \tag{8.28}$$

The Trouton number being constant, amongst the refrigerants with similar normal boiling points, the refrigerants with light molecules (H_2O and NH_3) have the largest latent heat while the refrigerants with large molecules have a small latent heat. Mh_{fg} is the molal enthalpy of evaporation. Hence, refrigerants with similar normal boiling points have the same molal latent heat. ($\approx 10.22RT_{nb}$). According to Avogadro law, at the same pressure and temperature, the number of molecules in a given volume is the same for all gases. Hence, a compressor with fixed displacement volume will pump the same number of moles and will produce the same refrigeration capacity with similar boiling point refrigerants. The mass flow rate of the refrigerant circulated will be different depending upon the molecular weight. Another important term is h_{fg}/v_g, which is related to volumic refrigeration effect.

$$\frac{h_{fg}}{v_g} = 10.22\,p_{\text{atm}} \approx 10.2 \times 101.325 \text{ kPa}$$

$$\approx 1000 \text{ kJ/m}^3 \text{ or kPa} \tag{8.29}$$

Hence, all refrigerants with similar normal boiling points have similar volumic refrigeration effect at evaporator pressure of one atmosphere. Also the volumic refrigeration effect will be higher at higher evaporator pressures.

The normal boiling point of the refrigerant should be low so that the refrigerant can be used at low evaporator temperatures with compressor running at above atmospheric pressure.

8.7.2 Condenser and Evaporator Pressures

Both these pressures should be above the atmospheric pressure so that there is no possibility of leakage of air and moisture into the system. The vapour density is low at low evaporator pressures, thus requiring a large compressor. If the evaporator pressure is large then the condenser pressure becomes even larger, requiring high-pressure tubing and a robust compressor. Hence, for a specified evaporator temperature the refrigerant is chosen such that the evaporator pressure is close to atmospheric pressure. Table 8.2 gives evaporator pressures for various refrigerants at evaporator temperature of –15°C, and condenser pressures for condenser temperatures of 30°C and 40°C.

Refrigerants are sometimes classified as Low Normal Boiling Point and High Normal Boiling Point refrigerants.

High normal boiling point refrigerants

It is clear from the above discussion that the normal boiling point determines the evaporator pressure of the refrigerant. H_2O, R114 and R11 have high normal boiling points, hence their evaporator pressures at temperatures of 0–10°C are below atmospheric. These are also called *low pressure refrigerants.* These are normally used in water chilling plants and air-conditioning plants. The condenser pressures of these refrigerants are also below atmospheric and are provided with purge valves or units to maintain the required vacuum. The vapour density is very low because of low pressures. It is observed that the swept flow rate /TR increases as the NBP increases. Water vapour requires the largest swept flow rate/TR. This is followed by R13, R11 and R114. Centrifugal compressors are used for R11 and methyl chloride. This further puts a restriction on capacity. These refrigerants are efficient only for large capacities. R11 has now been withdrawn because of its large ozone depletion potential. R125 is replacing R11 in these systems. For R114 the volume flow rates are not large enough to use centrifugal compressor (tip speeds will be very high). Hence rotary compressors are used.

Low normal boiling point refrigerants

These refrigerants have evaporator pressures above atmospheric at evaporator temperatures of 0–10°C. It is observed from Table 8.2 that for these refrigerants the swept volume flow rate/TR is also small since the vapour density is large. However, these have high condenser pressures as well. The higher the condenser pressure, the higher is the power requirement. These refrigerants are also called *high pressure refrigerants.* CO_2, NH_3, SO_2, CH_3Cl, R12 and R22, R134a fall under this category and use reciprocating compressors. NH_3 has a large latent heat, still its swept flow rate is same as that for R22 because of its lower vapour density. Chlorofluorocarbons have low latent heats but higher vapour density. Low latent heat does not affect the COP since their specific heat ratio is also smaller due to which these require smaller compressor work. All the possible CFCs derived from methane along with their normal boiling points are shown in Figure 8.1(a). Methane has NBP of –16°C and carbon tetra fluoride has NBP of –128°C. Addition of chlorine increases the NBP while addition of fluorine atoms decreases the NBP. The same trends are observed in Figure 8.1(b) for ethane derivatives.

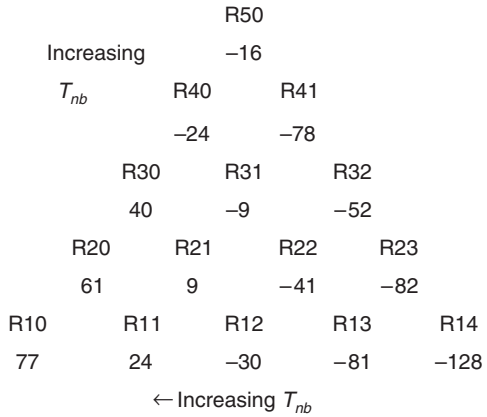

Figure 8.1(a) Normal boiling points of methane derivatives.

						R170								
						–89								
			Increasing		R160		R161							
			T_{nb}		13		–37							
				R150,a		R151,a		R152,a						
				84/57		53/16		31/–25						
			R140,a		R141,a,b		R142,a,b		R143,a					
			114/74		76/32		35/–9		5/–48					
		R130,a		R131,a,b		R132,a,b,c		R133,a,b		R134,a				
		146/131		103/88		59/47		17/12		20/–2				
	R120		R121,a		R122,a,b		R123,a,b		R124,a		R125			
	162		117/116		72/73		27/28		–12/–10		–48			
R110		R111		R112,a		R113,a		R114,a		R115		R116		
185		137		93/92		48/47		4/3		–39		–78		

← Increasing T_{nb}

Figure 8.1(b) Normal boiling points of ethane derivatives.

8.7.3 Specific Heat

The specific heat of the liquid $c_{pf} = T\,(ds/dT)_p$ should be as small as possible. On the T–s diagram, the slope of the saturated liquid line is dT/ds. Hence as seen in Figure 8.2, a small value of ds/dT will make the saturated line almost vertical. This will reduce irreversibility during throttling. The liquid can be subcooled to a larger extent if the specific heat is small. Similarly, a small value of the specific heat of vapour will make the saturated vapour line almost vertical. If both the saturated lines are vertical then as shown in Figure 8.3 the refrigeration cycle approaches the Reversed Carnot cycle.

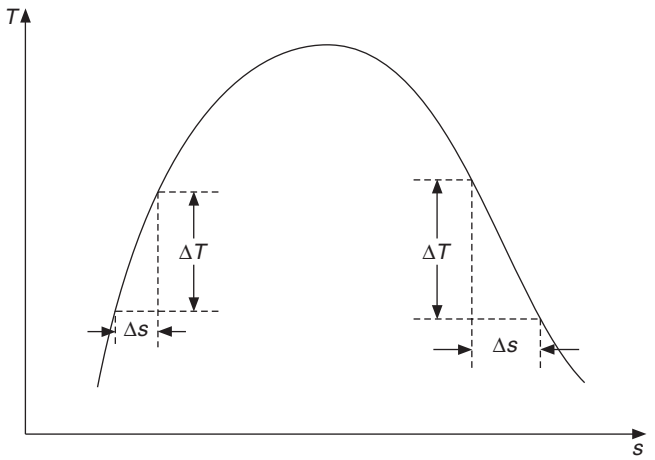

Figure 8.2 Effect of specific heats on the slopes of saturated liquid and vapour lines.

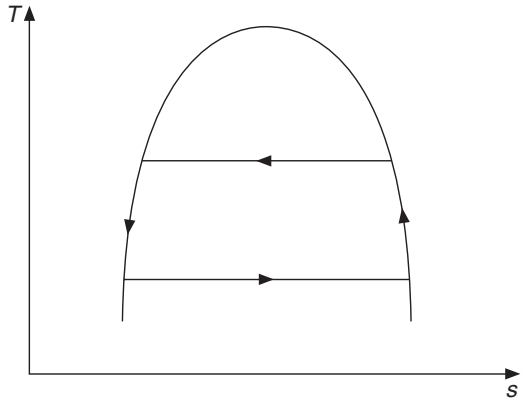

Figure 8.3 *T–s* diagram of desirable refrigerants.

The specific heat of the vapour should be in the range of 40 to 100 kJ/mol-K. If this value is low, then the slope of the saturated vapour line becomes a large negative value which results in a larger area of superheat horn. Figure 8.4 shows two kinds of constant pressure lines in the superheated region *ab* and *ac*. $[ds/dT]_p$ is larger for *ab* than for *ac,* hence the specific heat is smaller for *ac* than for *ab*. It is obvious that for a small value of c_p, the area of superheat horn is large and the COP is small. If the specific heat is large, the constant pressure line becomes flat in the superheated region, the area of superheat becomes small and the degree of superheat also becomes small, say in a subcooling heat exchanger.

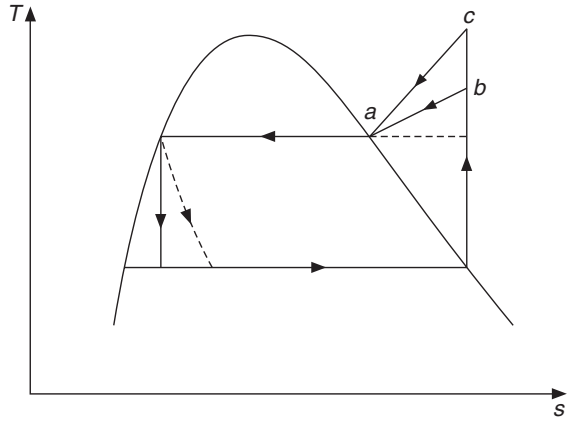

Figure 8.4 Effect of specific heat on area of superheat.

A very large value of specific heat results in positive slope of the saturated vapour line as discussed in Chapter 3 (Figure 3.12). In this case, isentropic compression starting from saturated vapour state ends up in wet region with disastrous results. It is seen that due to peculiar shape of the saturated liquid line the throttling loss is also large in this case. It is thus observed that either too large or too small values of c_p are bad. Hence, depending upon the critical temperature an optimum value of c_p is required in the range from 40 to 100 J/mol-K such that the area of superheat

horn is small. The specific heat of C–H bond is 11 J/mol-K, C–F bond has 21J/mol-K while the C–Cl bond has 25J/mol-K. The optimum value of c_p is obtained with small molecules, that is, for molecules with one or two carbon atoms. CFCs with three or more carbon atoms have larger value of c_p. This leads to wet compression. Also, these CFCs are more difficult to manufacture than those with smaller molecules. Further, these have very high critical temperatures. Those that do not have high critical temperature are flammable. The choice of refrigerants in CFCs is usually limited to those with one or two carbon atoms.

The relative performance of refrigerants is directly related to their molecular weights as well. Two laws of physical chemistry, namely the Avogadro's law and Trouton's rule explain this relation for refrigerants with similar vapour pressures. Avogadro' law states that the number of molecules in a given volume of gas depends only on the gas pressure and temperature. Hence, a given compressor running at fixed revolutions per minute will pump the same number of molecules regardless of molecular weight as long as the pressure and temperature are similar. Trouton's rule states that for a group of similar substances, Mh_{fg}/T_{nb} is constant, that is, the latent heat on molar basis is same for a group of similar group of substances. Atwood (1988) suggests that taken together, these rules mean that refrigerants with similar vapour pressures should require similar compressor displacements for equivalent molar flow rate and would result in equivalent refrigeration effect on molar basis.

The higher molecular weight members from a group of similar CFCs would exhibit minimum superheating or even wet isentropic compression. The lower molecular weight members would have lower c_p value and may result in very high superheating during isentropic compression.

The higher molecular weight refrigerants would have higher mass flow rates, lower latent heats and lower areas of superheat horn and larger values of throttling loss. The lower molecular weight refrigerants would have lower mass flow rates, higher latent heats, higher specific heats and higher areas of superheat horn. In hermetic compressors, which are cooled by suction gas, the lower mass flow rate of low molecular weight refrigerants is balanced by their higher specific heat to give equivalent cooling. Experience has shown that CFCs with molecular weights around 120 ± 40 are well suited for hermetic compressors.

8.7.4 Flammability and Toxicity

All methane derivatives with up to two hydrogen atoms and ethane derivatives with up to three hydrogen atoms are flammable.

Toxicity is not amenable to a systematization scheme since it is not a physical property but pertains to interaction with living organisms. Further confusion arises because of variable toxic effects such as "acute effect from a single but massive exposure or chronic effects from multiple low level exposures". Instead of considering TLV, toxicity is classified herein as low, moderate and high.

Hydrocarbons have low toxicity. Fluorinated compounds with no chlorine atoms have low toxicity with the exception of R161. Toxicity increases from moderate to high as the number of chlorine atoms in the CFC increase. HCFCs have lower toxicity. Figures 8.5(a) and (b) show the flammability of methane and ethane derivatives.

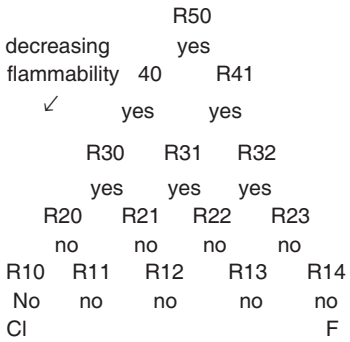

Figure 8.5(a) Flammability and toxicity for methane series. Yes and no have been used to indicate flammability.

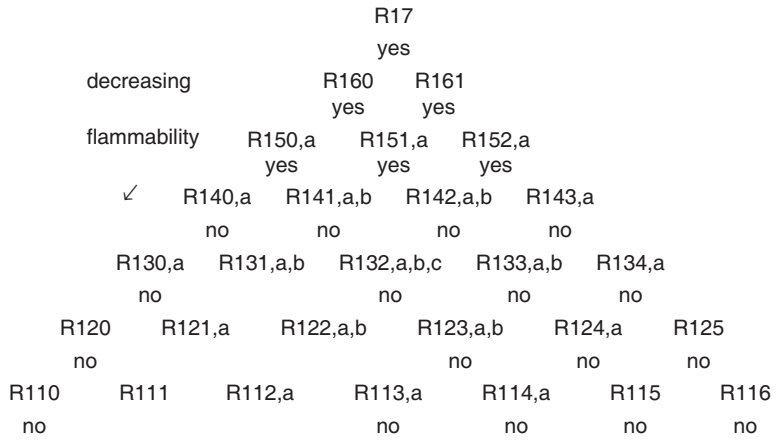

Figure 8.5(b) Flammability and toxicity for ethane series. Yes and no have been used to indicate flammability.

8.8 ALTERNATIVE REFRIGERANTS

Chlorofluorocarbons (CFCs) and hydrochlorofluorocarbons (HCFCs) are very popular as refrigerants since they cover a very wide range of normal boiling points and vapour pressures. For every specific application, a suitable CFC is available. This gives a flexibility to the industry in adapting hardware and systems to specific applications common to all the CFCs. In fact, the same compressor can give different capacities with different refrigerants avoiding the manufacture of different compressors for each cooling capacity. The thermodynamic and thermophysical properties of several CFCs proved to be especially well matched to the type of applications most sought after. Further, the inertness of CFCs to various materials gave a design flexibility, which is now taken for granted.

However, CFCs are not eco-friendly. Chlorine containing CFCs cause Ozone depletion and all of them cause global warming by greenhouse effect. These are evaluated for their eco-friendliness on the basis of Ozone Depletion Potential (ODP) and Global Warming Potential (GWP). ODP is a

measure of ozone depletion capability of a refrigerant compared to that of CFC 11, which has ODP of 1.0. GWP compares the warming effect of a gas compared to that of CO_2 by weight. ODP and GWP of some of the refrigerants are given in Table 8.4.

Now that it has been established that chlorine containing CFCs cause ozone depletion and all CFCs and HCFCs cause global warming, world community has decided to replace these. There are two international agreements in this regard, namely Montreal Protocol and Kyoto Protocol.

Table 8.4 ODP and GWP of some refrigerants

Refrigerant	*ODP*	*GWP*	*Refrigerant*	*ODP*	*GWP*	*Refrigerant*	*ODP*	*GWP*
CFC 11	1.0	1320	HCFC 123	0.02	93	HC 290	0.0	3.0
CFC 12	0.86	8500	HCFC 124		480	HC 600a	0.0	3.0
CFC 113	0.8	9300	HCFC 141b	0.11	270	HFC245fa	0.0	820
CFC 114	0.6	9300	HCFC 142b		1650	404A	0.0	3260
CFC 115	0.32	9300	HCFC 23		11700	407A		1770
R 502	0.34	5490	HFC 125	0.0	2800	407C		1530
HCFC 22	0.05	1350	HFC 134a	0.0	1300	410A		1730
Halon 1211	3.0		HFC 152a	0.0	140	Cyclic Pentane	0.0	3.0
Halon 1301	10.0		HFC 227ca	0.0	2900			

8.8.1 Montreal Protocol

In the United Nations Environment Programme Conference held in Montreal in September 1987, the decision taken to phase out ozone depleting substances (ODS) within a fixed time period is known as Montreal Protocol (MP). Some of the features of MP are as follows:

(i) Developed countries will phase out CFCs by 1996.

(ii) Developing countries will phase out CFCs by 2010 with freeze in 1999 and gradual reduction thereafter.

(iii) Developed countries will phase out HCFCs by 2030 while developing countries have been provided a grace period of ten years, that is phase out by 2040.

Global warming is another serious issue. Some naturally occurring substances mainly cause this but CFCs have very large global warming potential. Hence CFCs also have to be phased out. Kyoto Protocol refers to this.

8.8.2 Kyoto Protocol

The global warming issue was addressed by the third conference of parties to the United Nations Framework Convention on Climate Change (UNFCCC) in December 1997 held at Kyoto. This is known as Kyoto Protocol (KP). According to this, the developed countries of KP should reduce their average greenhouse gas emissions in aggregate by 5.2% below the 1990 levels within a period of 2008–2012. Developing countries do not have any obligation under KP. In KP the CFCs have been included in a basket of industrial GHGs. The basket consists of natural gases like CO_2, N_2O and CH_4 and industrial gases like PFCs and SF_6.

Kyoto Protocol has three flexible mechanisms, namely, Joint Implementation (JI), Emission Trading (ET) and Clean Development Mechanism so that the developed countries can meet their obligations of emission reduction by cooperative mechanisms with other countries. The readers may refer to Thorne (1999).

8.8.3 Total Equivalent Warming Index

This factor gives the environmental impact of GHGs from the inception of an appliance, that is, its manufacturing operations, service life and end-of-life disposal of the appliance. It includes the emission of CO_2 in generation of electricity used by the appliance apart from the emission of refrigerants including those from insulation blowing agents.

In order to comprehensively analyze global warming, the concepts of *life-cycle climate performance* and *life-cycle assessment* have also been introduced.

The ODP data is scarce, hence the prediction methods are required. Nimitz (1992) has given the following correlation for HCFCs with one or two carbon atoms.

$$\text{ODP} = 0.05013\,\text{N}_{\text{Cl}}^{1.501}\,\exp\,(-3.858/\tau)$$

where the tropospheric lifetime τ is given by

$$\tau = 0.787\left(\frac{M}{N_H}\right)\exp\,(-2.06N_{\alpha\text{Cl}} - 4.282N_{2\text{C}} + 1.359N_{\beta\text{F}} + 0.926N_{\beta\text{Cl}})$$

$N_{\alpha\text{Cl}}$ represents the number of α chlorine atoms present. The designation α means that it is attached to the same carbon atom as the hydrogen atom and β means that it is attached to the carbon atom adjacent to the hydrogen containing carbon atom. N_{H} is number of hydrogen atoms. The subscript 2C is used only if two carbon atoms are present. Duvedi and Achenie (1996) have given the following correlations:

$$\text{ODP} = 0.585602\,N_{\text{Cl}}^{-0.0035}\,\exp\left(\frac{M}{238.563}\right) \qquad \text{for one carbon atom}$$

$$\text{ODP} = 0.0949956\,N_{\text{Cl}}^{-0.0404477}\,\exp\left(\frac{M}{83.7953}\right) \qquad \text{for two carbon atoms}$$

For refrigerant mixtures,

$$\text{ODP} = \sum_i x_i\,\text{ODP}_i$$

where M is the molecular weight and x_i is the mass fraction of the ith constituent.

8.8.4 Alternatives Amongst Methane and Ethane Derivatives

The alternative refrigerants can be classified under three categories, namely:

(i) HFCs
(ii) HCFCs
(iii) Natural refrigerants like air, water, CO_2, H_2O, NH_3 and hydrocarbons.

HCFCs are transitional compounds with low ODP. Eventually, these will also have to be replaced. The presence of hydrogen atom in these compounds allows hydrolysis of these to take place in lower atmosphere where these compounds can be rained down and absorbed in the earth's surface like the other chlorine containing inorganic compounds. HFCs have high GWP, hence these are also uncertain candidates since these will also be eventually replaced.

The full array of CFCs, which contain a single carbon atom, is shown in Figure 8.6. Methane is shown at the top corner, carbon tetra fluoride in the right bottom corner and carbon tetra chloride at the left corner. R11, R12 and R22 are recognized as the best refrigerants. R11 requires a centrifugal compressor and has dominated the large water chiller plants for decades. R12 has dominated the small refrigeration systems such as the household refrigerator, automotive and mobile air conditioning since these gadgets require a small compressor. R22 requires an even smaller compressor, hence it has dominated large refrigeration and air conditioning systems. Other compounds in the table like R10, R20, R30, R40 and R21 on the left edge of the triangle are toxic. R50, R40 and R41, etc. are highly flammable. The right row of the triangle is free of chlorine atoms and therefore it has acceptable candidates under Montreal Protocol. Amongst these, only R32 is acceptable although it is flammable and has high pressure. R23 and R14 involve very high pressure and would require drastic changes in refrigeration equipment such as smaller displacement volume, large pressure and large bearing loads, etc.

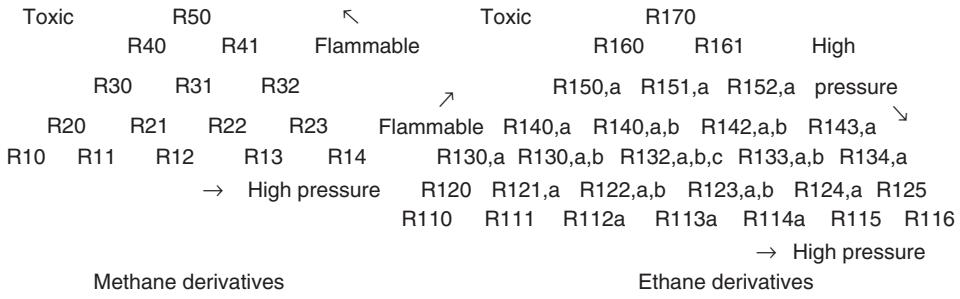

Figure 8.6 Full Array of methane and ethane derivatives used as refrigerants.

All the possible compounds with two carbon atoms are also shown in Figure 8.6. Again ethane is at the top corner, fluoroethane in the right bottom corner and chloroethane is at the left bottom corner. Here also the left row of the triangle contains toxic substances and the triangle top contains flammable substances while its right bottom contains high-pressure refrigerants. The left row of the triangle is free of chlorine atoms. R123, R124, R125, and R134 are free from toxicity and flammability problems. R124 and R125 involve high pressures.

In this group, R123 and R134a are widely used as pure refrigerants. R123 is HCFC with properties similar to R11 and is the replacement for it in water chillers. R152a is similar to R134a except flammability. R134a is very close to R12. It is being used as drop-in replacement in automotive, mobile and domestic refrigeration. R143a and R125 have a significantly higher pressure than R22 but these are promising candidates. R125 has the critical temperature of 66.04°C, hence it is not very efficient. It is non-flammable hence it becomes a candidate for mixtures.

8.9 MIXTURES

Pure refrigerants, which have low ODP and GWP are very limited and the number of diverse applications of refrigeration is ever increasing. Hence new working substances are required for specific applications. If a pure refrigerant cannot meet the requirements, then the obvious choice is to try a mixture of two refrigerants which may meet the requirements. For example, a refrigerant may be good from the thermodynamics point of view but it may be flammable or toxic. Mixing another refrigerant with it may reduce its toxicity and flammability. Some refrigerants may involve very high pressures. Mixing another refrigerant with it may reduce the working pressure. Similarly, the NBP of a refrigerant may be high and mixing another refrigerant with it may decrease its NBP. Given a compressor, different mixture refrigerants will give different cooling capacities. Hence a mixture allows variation of cooling capacity of a system. Mixtures have a long history. Earlier, attention was focused on azeotropes.

Azeotrope R500, a mixture of R115 and R12, was developed to improve the performance of R12 systems when a 50 Hz motor was used instead of the 60 Hz motor.. Similarly, R502 an azeotropic mixture of R152a and R22 was developed to improve the performance of R22 at low temperatures so that a two-stage system did not have to be used. Azeotropes behave like pure substances with unique boiling point without any glide temperature. Sometimes nonazeotropic mixtures or zeotropes also improve the performance. There is scope of improvement in many properties by using mixtures. R507A, a mixture of R125 and R134a in 50:50 proportion has properties very similar to R502 with zero ODP. R404A, a near azeotropic blend of R125, R143a and R134a is another successful R502 replacement. The normal boiling point of a refrigerant can be matched by a nonazeotropic binary mixture of two refrigerants, one of which has a larger normal boiling point and the other has a lower normal boiling point. R290 has a NBP of – 42.1°C and R600a has a NBP of –11.73°C. A 50:50 mixture of these has been proposed to replace R12 with NBP of –29.8°C.

Tertiary mixtures have also been proposed. A tertiary mixture of R22, R152a and R124 has been suggested as replacement of R12. Similarly, a tertiary mixture of R125, R143a and R134, called SUVA HP 62 by Dupont Numeris, has also been suggested as replacement of R12.

Zeotropes can cause two problems, namely:

(i) Should the refrigerant blend leak from the system, the composition of the remaining refrigerant will change since the vapour and liquid have different compositions.

(ii) Boiling and condensation occur over a range of temperatures known as glide temperature. This affects the mean temperature difference in evaporator and condenser.

Isothermal heat transfer is not possible with a blend. This may reduce the COP but in some situations it can be used to advantage to improve the performance. If the condenser is water-cooled and the evaporator is also a liquid chiller then the temperature of the cooling water will increase from t_{wi} to t_{wo} in the condenser and that of liquid to be chilled will decrease from t_{fi} to t_{fo} in the evaporator. This is shown in Figure 8.7(a) with a pure refrigerant. The temperature difference between the refrigerant and the fluids is very large at the inlets of condenser and evaporator and decreases towards their outlets. This non-isothermal heat transfer leads to irreversibility and reduction in COP.

In case of a refrigeration cycle with a blend, the blend could be chosen in such a way that the glide matches with the rise in water temperature in the condenser and decrease in liquid temperature in the evaporator as shown in Figure 8.7(b). The temperature difference between the external regime and the internal regime is uniform in both the condenser and evaporator. This actually leads to an increase in COP.

Companies and individuals have patented many refrigerants and some of them have been standardized by ASHRAE, for example, 401A, 401B, 407A, 410B, etc. Many of these are tertiary mixtures.

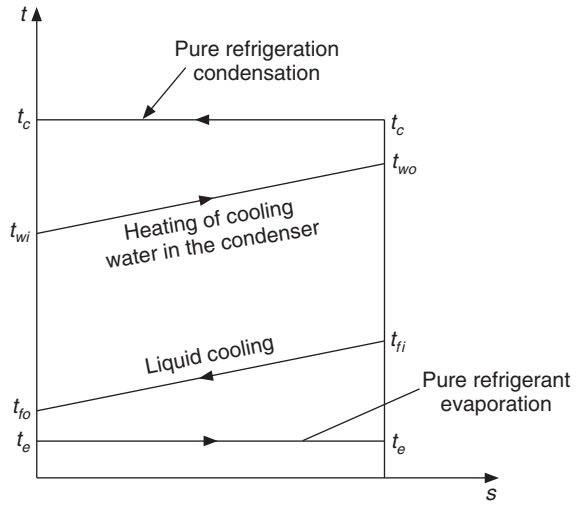

Figure 8.7(a) Refrigeration cycle with a pure refrigerant.

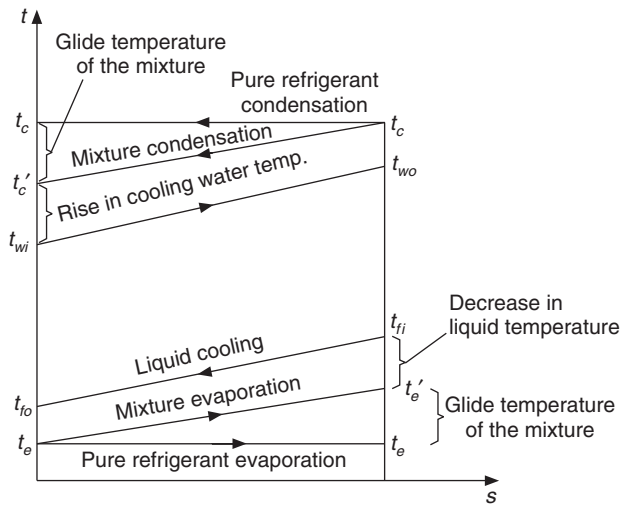

Figure 8.7(b) Refrigeration cycle with a blend of refrigerants.

8.9.1 Mixture Composition

The composition of a mixture is specified either as mole fraction or as mass fraction. Let m_1 and M_1 be the mass and molecular weight of the first component and m_2 and M_2 be those of the second component. Then the number of moles n_1 and n_2 is given by

$$n_1 = \frac{m_1}{M_1} \quad \text{and} \quad n_2 = \frac{m_2}{M_2} \tag{8.30}$$

Total number of moles $n = n_1 + n_2$

Total mass $m = m_1 + m_2$

Mole fractions χ_1 and χ_2 of the two components are

$$\chi_1 = \frac{n_1}{n} \quad \text{and} \quad \chi_2 = \frac{n_2}{n} \tag{8.31}$$

Also, $\chi_2 = 1 - \chi_1$

Mass fractions x_1 and x_2 of the two components are given by

$$x_1 = \frac{m_1}{m} \quad \text{and} \quad x_2 = \frac{m_2}{m} \tag{8.32}$$

Also, $x_2 = 1 - x_1$

It may be noted that x_1 and x_2 are the mass fractions of the liquid phase. The mass fractions of the vapour phase at the same temperature in equilibrium with the liquid phase will be denoted by $x_{1'}$ and $x_{2'}$ which are different from x_1 and x_2. It can be shown that the mass fraction and the mole fraction are related as follows:

$$x_1 = \frac{M_1\chi_1}{M_1\chi_1 + M_2\chi_2} \quad \text{and} \quad x_{1'} = \frac{M_1\chi_1}{M_1\chi_{1'} + M_2\chi_{2'}} \tag{8.33}$$

8.9.2 Temperature–Composition Diagram

Figure 8.8 (like Figure 7.5) shows the T–x diagram for a binary mixture at a pressure p. The saturation temperature of the pure first liquid is t_1° and that of the pure second liquid is t_2°. We have pure first liquid at $x_1 = 0$, that is on the left hand side.

We have subcooled liquid with composition x at point A. As this liquid is heated, the bubbles will appear at point B, that is, the liquid begins to boil. This point is called the *bubble point*; this state is called saturated liquid state and the temperature t_B is called bubble point temperature. The curve t_1°–B–t_2° is called bubble point curve or saturated liquid line since it joins the boiling points at all concentrations.

Similarly, we have superheated vapour at point E. As this is cooled, the dew makes its first appearance at point D, that is, condensation starts at this point. This is called *dew point*; this state is called saturated vapour state and the temperature t_D is called dew point temperature. The curve t_1°–D–t_2° is called dew point curve or saturated vapour line since it joins the dew points at all concentrations.

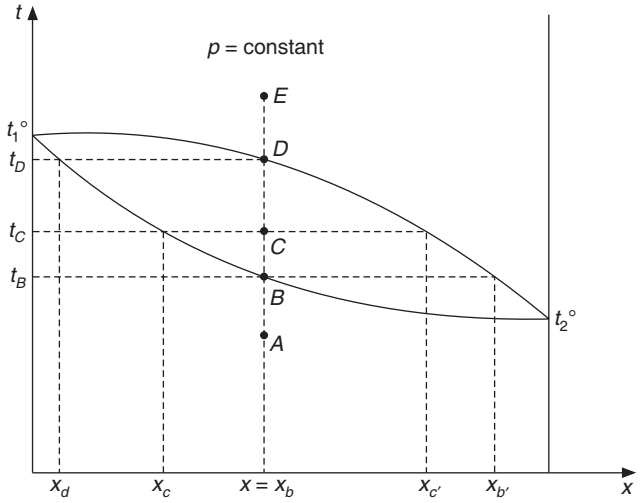

Figure 8.8 The *T–x* diagram for a binary mixture at pressure *p*.

The region below the curve $t_1{}^o$–B–$t_2{}^o$ is called the subcooled region. The region above the line $t_1{}^o$–D–$t_2{}^o$ is called superheated region. The region in between these two curves is the two-phase region. It is observed that in mixtures, the boiling point t_B and the dew point t_D are different. This implies that temperature does not remain constant during boiling.. Boiling starts at t_B and the temperature continues to rise as the liquid evaporates until the dew point temperature t_D and saturated vapour state is reached. The difference between t_D and t_B is called *glide temperature*.

In the mixture region at point C say, saturated liquid L of composition x_c is in equilibrium with vapour of composition $x_{c'}$ at the same temperature t_C. Also it is worth observing that when the boiling starts at B, the first vapour to come out has concentration $x_{b'}$. At point C the vapour has concentration $x_{c'}$ and at point D it is x_b. Hence during boiling, the vapour mass fraction varies from $x_{b'}$ to x_b. Similarly during condensation, the first liquid condensate has concentration x_d and as the condensation continues the liquid mass fraction varies from x_d to x_b. The dryness fraction ξ at point C is defined by the equation,

$$x_b = \xi x_{c'} + (1 - \xi)\, x_c \tag{8.34}$$

It was observed in Chapter 7 that ideal solutions do not involve any change in volume or temperature during mixing of the component liquids. In ideal mixtures the vapours follow the Dalton's law while the liquids follow the Raoult's law. If $p_1$and p_2 are the partial pressures of the two components in the mixture at temperature T and the total pressure is p, then from Raoult's law, we get

$$p_1 = \chi_1 p_1{}^o \tag{8.35}$$

$$p_2 = \chi_2 p_2{}^o \tag{8.36}$$

Dalton's law yields

$$p_1 = \chi_{1'} p \tag{8.37}$$

$$p_2 = \chi_{2'} p \tag{8.38}$$

and the total pressure is given by Dalton's law as follows:

$$p = p_1 + p_2 = \chi_1 p_1^{\circ} + \chi_2 p_2^{\circ} = \chi_{1'} p + \chi_{2'} p$$

Simplification yields,

$$p = \frac{p_1^{\circ} p_2^{\circ}}{p_1^{\circ} - \chi_{1'} (p_1^{\circ} - p_2^{\circ})} \tag{8.39}$$

For ideal solutions, Eq. (8.39) may be used to find by iteration the dew point temperature for given values of total pressure and vapour composition $\chi_{1'}$.

All the mixtures are invariably non-ideal. The deviation from Raoult's law is termed positive, if the mixture pressure is more than that predicted by Raoult's law. Mixing of such mixtures is endothermic, that is, it is accompanied by absorption of heat Δh_m. The enthalpy of the liquid mixture is given by

$$h_f = x_1 h_{1f} + x_2 h_{2f} + \Delta h_m \tag{8.40}$$

The bubble point temperature of such a solution is lower than that predicted by Raoult's law. In the vapour phase the deviation from ideal gas behaviour is considered by considering enthalpy dependence upon pressure and then mixing rules to account for the intermolecular forces between the molecules of various components. If h_g is the vapour enthalpy, the latent heat is the difference $h_{fg} = (h_g - h_f)$. This will be smaller for this mixture compared to that for ideal solution.

On the other hand, a mixture, which has negative deviation from Raoult's law, will exert lower pressure than the ideal mixture and it will have higher bubble point temperature than that for ideal mixture. The mixing of liquids will be exothermic and the latent heat will be larger than that for the ideal solution. The vapour phase enthalpy can be determined if the mass fraction of vapour $x_{1'}$ is known.

The heat of solution is obtained from experimental data. The mass fraction of vapour phase x_1 corresponding to liquid phase mass fraction for given temperature and pressure is also determined from experimental data. Dühirng plot for pressure, like Figure 7.7 and *h–x* plot like Figure 7.8 for aqua-ammonia, can be drawn for the mixture. Similarly, a figure like Figure 7.9 to determine vapour phase mass fraction can also be drawn. These are useful when one wants to investigate the performance for variable mass fraction, like in absorption refrigeration systems. Such details are not required when the data is needed for a fixed composition.

Some mixtures do not deviate drastically from Raoult's law behaviour. In such a case, predictions can be made based upon Raoult's law.

8.9.3 Enthalpy of Mixing

In chemical engineering textbooks the properties of non-ideal solutions are expressed in terms of deviation from that of ideal solution. The difference between the two is termed *excess property* denoted by the superscript *E*. Hence for a solution of *n* components,

$$v^E = v - v^I = \sum_{i=1}^{n} \chi_i (\overline{v}_i - v_i^*) = \Delta v_m \tag{8.41}$$

$$h^E = h - h^I = \sum_{i=1}^{n} \chi_i (\overline{h}_i - h_i^*) = \Delta h_m \tag{8.42}$$

$$g^E = g - g^I = \sum_{i=1}^{n} \chi_i (\overline{g}_i - g_i^*) = \Delta g_m \tag{8.43}$$

The superscript* denotes the reference state, which happens to be ideal solution and g denotes *Gibbs free energy*, which may be expressed in terms of fugacity f as follows:

$$g_i^E = \overline{g}_i - g_i^* = RT \ln \left(\frac{\overline{f}_i}{f_i^*} \right) \tag{8.44}$$

Substituting Eq. (8.44) into Eq. (8.43), we get

$$g^E = RT \sum_{i=1}^{n} \chi_i \ln \frac{\overline{f}_i}{\chi_i f_i^*} \tag{8.45}$$

The *activity coefficient* γ_i is defined as follows:

$$\gamma_i = \frac{\overline{f}_i}{\chi_i f_i^*} \tag{8.46}$$

Equation (8.44) may be written as follows:

$$\frac{g^E}{RT} = \sum_{i=1}^{n} \chi_i \ln \gamma_i \tag{8.47}$$

Partial molar excess Gibbs free energy $\overline{g}_i^E$ is expressed as follows:

$$\frac{\overline{g}_i^E}{RT} = \left[\frac{\partial (N g^E / (RT))}{\partial N_i} \right]_{T,p,N} = \ln \gamma_i \tag{8.48}$$

The other excess properties are expressed as follows:

$$s^E = \Delta s_m + R \sum_{i=1}^{n} \chi_i \ln \chi_i \tag{8.49}$$

$$h^E = Tds - v^E dp = g^E - Ts^E \tag{8.50}$$

Helmholtz free energy is expressed as follows:

$$A^E = u^E - Ts^E \tag{8.51}$$

Gibbs–Duhem relations for multi-component systems

$$SdT - \mathbb{V}dp + \sum_{i=1}^{n} N_i d\mu_i = 0$$

or
$$s dT - v\,dp + \sum_{i=1}^{n} \chi_i\, d\,\overline{g}_i = 0 \tag{8.52}$$

In terms of excess properties, we may write

$$s^E\, dT - v^E dp + \sum_{i=1}^{n} \chi_i\, d\,\overline{g}_i^E = 0 \tag{8.53}$$

Substituting for $d\,\overline{g}_i^E$,

$$s^E dT - v^E dp + \sum_{i=1}^{n} \chi_i d\,(RT \ln \gamma_i) = 0 \tag{8.54}$$

or
$$s^E dT - v^E dp + R\sum_{i=1}^{n} \chi_i\,(\ln \gamma_i) + RT\sum_{i=1}^{n} \chi_i\, d\,(\ln \gamma_i) = 0 \tag{8.55}$$

Substituting from Eqs. (8.47) and (8.50), we get

$$h^E \frac{dT}{T} - v^E dp + RT\sum_{i=1}^{n} \chi_i\, d\,(\ln \gamma_i) = 0 \tag{8.56}$$

From Eq. (8.48), we get

$$\frac{\overline{h}_i^E}{RT^2} = \frac{\partial (G^E / RT)}{\partial (1/T)} = -\left(\frac{\partial \ln \gamma_i}{\partial T}\right)_{p_i, v_i} \tag{8.57}$$

$$\frac{\overline{v}_i^E}{RT} = -\frac{\partial (G^E / RT)}{\partial p} = -\left(\frac{\partial \ln \gamma_i}{\partial p}\right)_{T_i, v_i} \tag{8.58}$$

Many models are available to determine activity coefficients. Some of these are in terms of product of mole fractions while others take into account molecular weight, critical properties, dipole moment, etc. UNIQUAC equation, NRTL equation, UNIFAC, modified UNIFAC, Wilson equation, NRTL equation and Van Laar equation, etc. are some of the models. Reid et al. (1987) describe these equations. Borde et al. have used UNIFAC model to find the excess enthalpy of binary solution of R134a and DMETEG by using the UNIFAC model to evaluate activity coefficient using molecular weight, critical properties, dipole moment, gyration radius, association coefficient and volume and area parameters of pure components, as well as equilibrium data, molar concentrations in liquid and vapour phases, and temperature and pressure of the mixture. Then they constructed the enthalpy–concentration diagram for this binary solution.

8.9.4 Models for Thermodynamic Properties of Pure Refrigerants and Mixtures

Evaluation of precise thermodynamic properties is of great importance in the design of refrigeration systems. *ASHRAE Handbook, Fundamentals Volume* and other reference works devote considerable

number of pages to tabulation of thermodynamic properties. It is not possible to measure these properties at all values of temperature and pressure and (in case of mixtures) composition. Hence models have to be used for their evaluation. The models contain some constants, which are evaluated from the experimental data. Apart from this, many intensive properties are defined in terms of derivatives of some other property. Hence it is convenient to resort to modelling and use computational procedure for their evaluation. Thermodynamic properties include temperature, density, pressure, internal energy, enthalpy, entropy, fugacity, Gibbs free energy , Helmholtz free energy, specific heats, speed of sound, Joule Thompson coefficient and phase equilibrium properties. Viscosity, thermal conductivity and diffusion coefficient are called transport properties. Surface tension is interfacial property.

8.9.5 Equation of State for Pure Fluids

An equation of state represents some thermodynamic property like pressure p, compressibility factor $Z = pv/RT$ or Helmholtz energy A in terms of other independent variables like temperature, density or specific volume, and for mixtures, the composition. It is capable of reproducing experimental data within the experimental accuracy over the whole range of temperatures and pressures. Models are used for evaluation of properties since it is not possible to measure them for all combinations of pressure and temperature and composition in case of mixtures. It is possible to obtain other properties by differentiation and integration of equation of state. by using thermodynamic relations. McLinden, Lemmon and Jacobsen (1998) have given a review of some of the models for pure refrigerants and mixtures. Some of the equations of state are briefly described here.

The Virial Equation of State

This equation can be derived from statistical mechanics by considering interaction between molecules. This equation expresses the deviation from ideal gas behaviour as a power series in density or pressure.

$$\frac{p}{\rho RT} = 1 + A_2\rho + A_3\rho^2 + A_4\rho^3 \tag{8.59}$$

The virial coefficients A_2, A_3 and A_4, etc. are functions of temperature. The second virial coefficient A_2 accounts for interaction between two molecules; the third virial coefficient A_3 accounts for interaction between three molecules. Virial coefficients up to A_3 are available from experimental measurements and higher order coefficients are seldom available. The virial equation of state is applicable only to vapour phase properties. The region of applicability of this equation is limited up to three coefficients only.

Cubic Equation of State

This equation includes many equations that are in common use. The original equation was proposed by van der Walls in 1873. The general form of this equation is as follows:

$$p = \frac{RT}{\mathbb{V} - b} - \frac{a}{\mathbb{V}^2 + ub\mathbb{V} + wb^2} \tag{8.60}$$

Some of the well known equations of this type are given below.

van der Walls equation

$$p = \frac{RT}{\mathbb{V} - b} - \frac{a}{\mathbb{V}^2} \tag{8.61}$$

This equation improves upon the ideal gas behaviour by including the volume of molecules b and long range attractive forces between gas molecules.

Redlich–Kwong equation

This equation is obtained by substituting $u = 1$ and $w = 0$ in Eq. (8.60). Therefore,

$$p = \frac{RT}{\mathbb{V} - b} - \frac{a}{\mathbb{V}^2 + b\mathbb{V}} \tag{8.62}$$

where

$$a = \frac{0.427478\, R^2 T_c^{2.5}}{p_c T^{0.5}} \quad \text{and} \quad b = \frac{0.08664\, RT_c}{p_c} \tag{8.63}$$

Soave Redlich–Kwong (SRK) equation

This equation was proposed by Soave (1972) and is same as the Redlich–Kwong equation except that the constants a and b are different.

$$a = \frac{0.42748\, R^2 T_c^2}{p_c^2}[1 + f(\omega)(1 - T_c^{0.5})]^2 \quad \text{and} \quad b = \frac{0.08664\, RT_c}{p_c} \tag{8.64}$$

$$f(\omega) = 0.48 + 1.574\omega - 0.176\omega^2$$

Peng–Robinson equation

This equation was proposed by Peng et al. (1976) and is obtained by substituting $u = 2$ and $w = -1$ in Eq. (8.60). Therefore,

$$p = \frac{RT}{\mathbb{V} - b} - \frac{a}{\mathbb{V}^2 + 2b\mathbb{V} - b^2} \tag{8.65}$$

$$a = \frac{0.45724\, R^2 T_c^2}{p_c}[1 + f(\omega)(1 - T_c^2)]^2 \quad \text{and} \quad b = \frac{0.07780\, RT_c}{p_c} \tag{8.66}$$

$$f(\omega) = 0.374641 + 1.54226\omega - 0.26992\omega^2$$

The advantage of cubic equation is that the density may be expressed and found as the root of cubic equation, which increases the computation speed considerably. Equation (8.60) is written in terms of $Z = p\mathbb{V}/RT$ as follows:

$$Z^3 - (1 - ug + g)Z^2 + (r - ug - ug^2 + wg^2)Z - (rg + wg^2 + wg^3) = 0 \tag{8.67}$$

where

$$r = ap/(R^2T^2) \quad \text{and} \quad g = bp/RT \tag{8.68}$$

The cubic equations are, however, not capable pf expressing the properties very accurately over a wide range of temperatures. Over a limited range they can be very accurate when fitted to the experimental data. The *cubic equation is capable of doing vapour-liquid equilibrium calculations very accurately even for mixtures*. Some more forms of cubic equations have also appeared in literature. Notable amongst them is Zhang et al. equation of state where van der Walls repulsive force is modified according to the hard sphere model. This is done by introducing another constant c as follows:

$$p = \frac{RT}{\mathbb{V}}\left(\frac{8\mathbb{V}+3b}{8\mathbb{V}-5b}\right) - \frac{a}{\mathbb{V}(\mathbb{V}+c)} \tag{8.69}$$

The accuracy of the equation is improved by the introduction of c.

Canahan–Starling–DeSaints EOS

This is another accurate equation although it is not of cubic type.

$$\frac{p\mathbb{V}}{RT} = \frac{1+y+y^2-y^3}{1-y^3} - \frac{a}{RT(\mathbb{V}+b)} \tag{8.70}$$

where $y = b/4\mathbb{V}$, a and b are empirical functions of temperature.

Martin–Hou Equation of State

This equation was proposed by Martin and Hou (1955). It combines the van der Walls repulsive term with an elaborate expanded attractive term. In this equation, critical temperature or reduced temperature is used in the exponential term.

$$p = \frac{RT}{v-b} + \frac{A_2 + B_2T + C_2\exp(-KT/T_c)}{(v-b)^2} + \frac{A_3 + B_3T + C_3\exp(-KT/T_c)}{(v-b)^3} + \frac{A_4}{(v-b)^4} + \frac{A_5 + B_5T + C_5\exp(-KT/T_c)}{(v-b)^5} \tag{8.71}$$

where there are eleven unknowns, which are fitted from experimental data. This equation is also not valid in the liquid region. The specific heat is correlated as follows:

$$c_p = c_{p1} + c_{p2}\,T + c_{p3}\,T^2 + c_{p4}\,T^3 + c_{p5}/T \tag{8.72}$$

The enthalpy of vapour is found by finding the pressure correction from Eq. (8.71) and the ideal gas enthalpy from Eq. (8.72).

The density of saturated liquid is also correlated with temperature. The enthalpy of saturated liquid is obtained from vapour phase enthalpy by using the Clausis–Clapeyron equation, that is,

$$h_g - h_f = T(v_g - v_f)\frac{dp_{sat}}{dT} \tag{8.73}$$

Downing (1988) has given the constants for various fluorocarbons to be used in this equation.

Benedict Web Rubin (BWR) Equation

This equation was introduced by Benedict et al. (1940) to cover a wide range of temperatures. In appearance it is similar to virial equation of state. This may be written as follows:

$$p = \rho RT + (B_0 RT - A_0 - C_0 / T^2)\rho^2 + (bRT - a)\rho^3 + a\alpha\rho^6 + \frac{c\rho^3 (1 + \gamma\rho^2)}{T^2} \exp(-\gamma\rho^2) \tag{8.74}$$

This equation has eight constants. The first term on the right hand side represents ideal gas. The next two terms are analogous to virial equation of state. These terms provide proper behaviour in the low-density vapour region. The last two terms are empirical. The exponential term is used to fit the isotherms in high-density compressed liquid state.

Modified Benedict Web Rubin (MBWR) Equation

The BWR equation was modified by Jacobsen and Stewart (1973) to represent the properties of nitrogen in liquid region as well as vapour region. Subsequently it has proved to be one of the most accurate equations and has been applied to hydrocarbons, cryogens, and refrigerants. It can represent properties of a fluid over a wide range of temperature, pressure and density. It expresses pressure in terms of molar density and temperature. It may be written as follows:

$$p = \sum_{i=1}^{9} a_n \rho^n + \exp(\rho^2 / \rho_c^2) \sum_{n=10}^{15} a_n \rho^{2n-17} \tag{8.75}$$

where

$$\begin{aligned}
a_1 &= RT & a_8 &= b_{17}/T + b_{18}/T^2 \\
a_2 &= b_1 + b_2 T^{0.5} + b_3 + b_4/T + b_5/T^2 & a_9 &= b_{19}/T^2 \\
a_3 &= b_6 T + b_7 + b_8/T + b_9/T^2 & a_{10} &= b_{20}/T^2 + b_{21}/T^3 \\
a_4 &= b_{10} T + b_{11} + b_{12}/T & a_{11} &= b_{22}/T^2 + b_{23}/T^4 \\
a_5 &= b_{13} & a_{12} &= b_{24}/T^2 + b_{25}/T^3 \\
a_6 &= b_{14}/T + b_{15}/T^2 & a_{13} &= b_{26}/T^2 + b_{27}/T^4 \\
a_7 &= b_{16}/T & a_{14} &= b_{28}/T^2 + b_{29}/T^3 \\
 & & a_{15} &= b_{30}/T^2 + b_{31}/T^3 + a_{32}/T^4
\end{aligned} \tag{8.76}$$

The constants a_i as seen above are functions of temperature. There are a total of 32 adjustable parameters. Mclinden et al. (1989) also proposed the following auxiliary functions for fitting the experimental data, although the final computation is based on the MBWR equation. The vapour pressure was fitted in the following form:

$$\ln p = \frac{\pi_1}{T} + \pi_2 + \pi_3 T + \pi_4 \left(1 - \frac{T}{T_c}\right)^{1.5} \tag{8.77}$$

The saturated liquid density was fitted in the following form:

$$\frac{\rho}{\rho_c} = 1 + d_1 \tau^{\beta} + d_2 \tau^{2/3} + d_3 \tau + d_4 \tau^{4/3} \tag{8.78}$$

where, $\tau = 1 - T/T_c$.

The saturated vapour density was fitted in the following form:

$$\ln\left(\frac{\rho}{\rho_c}\right) = g_1\tau^{\beta} + g_2\tau^{2/3} + g_3\tau + g_r\tau^{4/3} + g_5 \ln(T/T_c) \tag{8.79}$$

For a complete description, the MBWR equation is combined with an expression for molar heat capacity of the ideal gas, that is, vapour in the limit of zero pressure. The variation of enthalpy with pressure is evaluated from the MBWR equation and added to the ideal gas enthalpy.

Helmholtz Energy Equation of State

Recently many highly accurate equations of state have been formulated in terms of reduced molar Helmholtz energy. The general form of this equation is as follows:

$$\alpha = \frac{A}{RT} = \alpha^{id}(\delta,\tau) + \alpha^{r}(\delta,\tau) = \ln\delta - N\ln\tau + \sum_i N_i\tau^{i} + \sum_k N_k\tau^{t_k}\delta^{d_k}\exp(-\gamma\delta^{c_k}) \tag{8.80}$$

where, $\delta = \rho/\rho^*$ is the reduced density and $\tau = T^*/T$ is the inverse reduced temperature. The first term on the right hand side α^{id} is the contribution of ideal gas and the second term α^{r} is the deviation from ideal gas behaviour. γ in the exponential is a symbol function. If

$$\begin{aligned} c_k = 0,\ \gamma = 0 \\ c_k \neq 0,\ \gamma = 1 \end{aligned} \tag{8.81}$$

The constants N_k, t_k, d_k and c_k are determined from matching with experimental data using nonlinear optimization or stepwise regression analysis.

The first three terms on the right hand side of Eq. (8.80) are ideal gas terms and may be represented by

$$\alpha^{id} = \frac{H_{ref}}{RT} - \frac{S_{ref}}{R} - 1 + \ln\left(\frac{T\rho}{T_{ref}\,\rho_{ref}}\right) + \frac{1}{RT}\int_{T_{ref}}^{T} c_p^{id}\,dT - \frac{1}{R}\int_{T_{ref}}^{T}\frac{c_p^{id}}{T}\,dT \tag{8.82}$$

where, H_{ref} and S_{ref} are arbitrary reference enthalpy and entropy at the reference state T_{ref} and ρ_{ref}.

The second summation in Eq. (8.80) is the real fluid contribution. The temperature and density are non-dimensionalized with respect to T^* and ρ^* which may not be critical values.

This model is sometimes termed a *fundamental equation* because it gives a complete description of the thermodynamic properties as discussed by Tillner-Roth and Baehr (1994).

Extended Corresponding State Model

A property divided by the corresponding critical property is called the reduced property. Simple corresponding state model implies that different fluids obey the same intermolecular laws for reduced properties. This model has been applied to refrigerants by various authors including Huber and Ely (1994). The extended model implies that if the temperature, density, residual Helmholz energy and compressibility of an unknown fluid *j* are properly scaled, then these are equal to those of a known reference fluid 0 for which accurate properties are available, that is,

$$\begin{aligned} \alpha_j^r(T_j,\rho_j) &= \alpha_0^r(T_0,\rho_0) \\ \text{and} \qquad Z_j(T_j,\rho_j) &= Z_0(T_0,\rho_0) \end{aligned} \tag{8.83}$$

The superscript *r* refers to residual property. This can be combined with ideal gas properties to find the thermodynamic properties. The reference fluid is measured at conformal temperature and density:

$$T_0 = \frac{T_j}{f_j} = T_j \frac{T_0^c}{T_j^c \theta(T)} \quad \text{and} \quad \rho_0 = \rho_j h_j = \rho_j \frac{\rho_0^c}{\rho_j^c} \phi(T) \tag{8.84}$$

where the multipliers $1/f_j$ and h_j are termed equivalent reducing ratios. The shape factors θ and ϕ are functions of temperature and density and are obtained from experimental data. Some predictive methods also exist for their evaluation. This model is used for mixtures too, where the shape factors map one equation of state into another. Huber and Ely (1994) may be referred to for details.

8.9.6 Equations of State for Mixtures

The following three approaches are usually followed to evaluate the properties of mixtures.

(i) Calculation at a specific composition assuming it to be a pseudo fluid.
(ii) Application of mixing rules to parameters in the constituent pure fluid EOS
(iii) Application of mixing rules to some property of the constituent pure fluid

Pseudo Fluid Approach

A mixture of specific composition may be treated as a pseudo pure fluid. This approach has successfully worked for azeotropes such as R500, R501 and R502. Use of Martin and Hou equation for R502 is a typical example. This equation has been successfully used for R407C and R410A in the superheated region by Monte (2002). This equation cannot take into account the different compositions of liquid and vapour in equilibrium, which occur even for azeotropes at some conditions. The advantage is simplicity of using some well-tested computer programs for pure fluids.

Mixing Rules Applied to EOS Parameters

The parameters used in EOS of pure fluids can be extended to mixtures if the parameters have some physical meaning. The best example is the virial equation of state whose parameters for mixtures can be derived from statistical mechanics, for example, the second and third virial coefficients for mixtures may be written as:

$$A_{2mix} = \sum_{i=1}^{n} \sum_{j=1}^{n} \chi_i \chi_j A_{2ij} \tag{8.85}$$

$$A_{3mix} = \sum_{i=1}^{n} \sum_{j=1}^{n} \sum_{k=1}^{n} \chi_i \chi_j \chi_k A_{3ijk} \tag{8.86}$$

The virial coefficients A_{2ii} and A_{3jjj}, (e.g. $A_{211,}A_{222}$, $A_{3111,}A_{3222}$ and A_{3333}) are virial coefficients of pure refrigerants. The cross terms A_{2ij} and A_{3ijk} (where i, j and k are not the same) represent interaction between the molecules of different refrigerants. These are determined from the experimental p, $\mathbb{V}$, T data of mixtures. This equation is not applicable to liquid state of mixtures.

Cubic equations

The same approach can be used for the cubic equation. The energy and volume parameters a and b of the cubic equation for mixtures may be defined as follows:

$$a_{mix} = \sum_{i=1}^{n}\sum_{j=1}^{n} \chi_i \chi_j a_{ij} \tag{8.87}$$

and

$$b_{mix} = \sum_{i=1}^{n}\sum_{j=1}^{n} \chi_i \chi_j b_{ij} \tag{8.88}$$

The cross terms for the energy parameter a_{ij} are usually given as geometric mean of the pure components as follows:

$$a_{ij} = (1 - k_{ij})(a_i a_j)^{1/2} \tag{8.89}$$

where k_{ij} are *binary interaction parameters*, which are determined from vapour–liquid equilibrium data of the mixture. These are functions of temperature and/or composition. The cross volume parameter b_{ij} is represented as arithmetic mean of the volume or diameter parameters of pure components, b_i and b_j as follows:

$$b_{ij} = (b_i + b_j)/2 \quad \text{or} \quad b_{ij} = (b_i^{1/3} + b_j^{1/3})^3/8 \tag{8.90}$$

Sometimes a binary interaction parameter may be used with a cross volume parameter as well. The properties of mixtures with three or more components are usually modelled only in terms of constituent binary pairs.

This approach when applied to cubic equation of state has the advantage of simplicity that only one empirical binary interaction parameter is required. This is especially suited when a limited mixture data is available.

Huron and Vidal (1979) proposed an alternative to mixing rules, which directly link the excess Gibbs energy from a liquid solution model to the parameter a in SRK equation of state, Eq. (8.64). The Huron–Vidal method equates G^E expressions from Redlich–Kister or NRTL model to the excess Gibbs free energy from SRK equation at infinite pressure to obtain composition-dependent density-independent mixing rules. Subsequently, several variations have appeared which use of different equations of state or different models for excess G^E—choice of reference pressure or use relationship for excess Helmholtz energy. Peng et al. (1995) have summarized these models. Feroiu and Dan (2003) have used the general cubic equation of state to model properties of mixtures.

The extended corresponding states model for mixtures

The model of Huber and Ely can be extended to mixtures. In this method the reduced residual Helmholtz energy and compressibility factor of a fluid was put equal to that of a reference fluid and two reducing parameters, namely h_j and f_j, were used. The reducing parameters for the mixture are determined from those of pure components by the standard van der Walls mixing rules, which are as follows:

$$h_{mix} = \sum_{i=1}^{n}\sum_{j=1}^{n} \chi_i \chi_j h_{ij} \tag{8.91}$$

and
$$f_{mix}\, h_{mix} = \sum_{i=1}^{n}\sum_{j=1}^{n} \chi_i\, \chi_j\, f_{ij}\, h_{ij} \tag{8.92}$$

where the cross terms h_{ij} and f_{ij} are determined as follows:

$$f_{ij} = (f_i f_j)^{0.5}\,(1 - k_{ij}) \tag{8.93}$$

and
$$h_{ij} = (h_i^{1/3} + h_j^{1/3})^3\,(1 - I_{ij})/8 \tag{8.94}$$

where k_{ij} and I_{ij} are binary interaction parameters, which are obtained by fitting with the experimental data. Scalabrin et al. (2002) have described a model using CS principle and Helmholtz energy.

Mixing rules applied to Helmholtz energy

The Helmholtz energy of a mixture may be expressed as follows:

$$\alpha_{mix} = \sum_{j=1}^{n} [\chi_j\,(\alpha_j^{id} + \alpha_j^r) + \chi_j \ln \chi_j] + \sum_{p=1}^{n-1}\sum_{q=p+1}^{n} \chi_p \chi_q F_{pq} \alpha_{pq}^{excess} \tag{8.95}$$

The first summation consists of the contribution of each component of ideal fluid and real fluid with superscript r. The logarithm term arises from entropy of mixing of ideal gas with mole fraction χ_j. The double summation accounts for the excess Helmholtz energy. F_{pq} relate the behaviour of one binary pair with another. α_{pq}^{excess} terms are obtained by fitting the experimental data. α_j^r and α_{pq}^{excess} are evaluated at reduced temperature and density τ and δ. These are conformal temperature and density used in ECS method. The mixing rules for these parameters are as follows:

$$\tau = \frac{T^*}{T_{mix}} \quad \text{and} \quad T^* = \sum_{p=1}^{n}\sum_{q=1}^{n} k_{T,pq} \chi_p \chi_q\,(T_p^c + T_q^2)/2 \tag{8.96}$$

and
$$\delta = \frac{\rho_{mix}}{\rho^*} \quad \text{and} \quad \frac{1}{\rho^*} = \sum_{p=1}^{n}\sum_{q=1}^{n} k_{\mathbb{V},pq} \chi_p \chi_q \frac{1}{2}\left(\frac{1}{\rho_p^c} + \frac{1}{\rho_q^c}\right) \tag{8.97}$$

There are other forms of it too, which combine $k_{T,pq}$ with critical temperature and $k_{\mathbb{V},pq}$ with critical densities. If only limited data is available, then α_{pq}^{excess} is taken to be zero and $k_{T,pq}$ and $k_{\mathbb{V},pq}$ parameters are obtained from experimental data. $k_{T,pq}$ is associated with bubble point pressure and $k_{\mathbb{V},pq}$ is associated with change in volume during mixing. Again, ternary and higher mixtures are modelled in terms of their constituent binary pairs. The reader may refer to Lemmon and Jacobsen (1997) for details. This approach provides a very accurate equation of state. The properties will approach the properties of pure refrigerants as the mole fraction approaches unity. This does not occur when the cubic equation of state is used.

This rule may be also applied to MBWR equation by using the following transformation:

$$A^r(T, \rho) = A - A^{id} = -\int_{\mathbb{V}}^{\infty} (p - \rho RT)\, d\mathbb{V} \tag{8.98}$$

where, A is Helmholtz energy and $\alpha = A/RT$.

HYBRID APPROACH

One may use different equations in different regions or different equations for different properties. This may be done to:

(i) simplify the calculation of properties and reduce computation time, or

(ii) compensate for the weakness of the equation of state

Some models use Peng–Robinson equation to find the pressure and the composition at the given temperature, then an accurate equation of state is used to find the density and other thermodynamic properties.

Cubic equations of state for mixtures have certain deficiencies. Yokozeki (1996) uses van der Walls equation of state with a parameter c as follows:

$$p = \frac{RT}{\mathbb{V} + c - b} - \frac{a_c \alpha}{(\mathbb{V} + c)^2} \tag{8.99}$$

The parameters a_c, b and c are constants for a pure fluid and α is an empirical function of temperature. The usual mixing rules are used to find these parameters for mixtures. This is combined with the following equation for ideal gas specific heat:

$$c_p^{id} = c_0 + c_1 T + c_2 T^2 + c_3 T^3 \tag{8.100}$$

This approach is the standard approach for cubic equations. Then the specific heat of real gas is found as follows:

$$c_v = c_p^{id} - R + T \int_{\infty}^{\mathbb{V}} \left(\frac{\partial^2 p}{\partial T^2} \right)_{\mathbb{V}} d\mathbb{V} = c_p^{id} - R + T \int_{\infty}^{\mathbb{V}} \left(a_c \frac{\partial^2 \alpha}{\partial T^2} \right)_{\mathbb{V}} d\mathbb{V}$$

For the vapour phase, α is same as in Eq. (8.99). However for the liquid phase, a different empirical value of α is used. Yokozeki fitted separate functions to discrete properties and argued that a fewer experimental data is required to obtain accurate results.

The basic principles of properties calculation of mixtures have been described in the above discussion. There are many variations of these approaches that have been published. Many softwares are also available for the calculation of thermodynamic properties of mixtures, the notable one is REFPROP 7.0 of NIST, Boulder Colorado.

8.9.7 Cycle Diagrams for Refrigerant Mixture

Figure 8.9(a) shows the T–s diagram for a refrigerant mixture along with the SSS cycle. Similarly, Figure 8.9(b) shows the p–h diagram and the SSS cycle. In the T–s diagram, the temperature during condensation decreases from T_2 to T_3 due to the glide of the mixture. Similarly, in the evaporator the temperature increases from T_4 to T_1 due to glide temperature of the mixture. In the p–h diagram, the isotherms in the two-phase region are not horizontal lines like those for a pure refrigerant. The isotherms are inclined lines in the two-phase region for a mixture. The temperature of the coolant water T_c has to be less than T_3, the lowest temperature of the refrigerant, so that at point 3 too, heat is rejected to coolant. Similarly in the evaporator, the temperature of the product T_e has to be greater than T_1 so that it can reject heat to the refrigerant. It is observed that the external

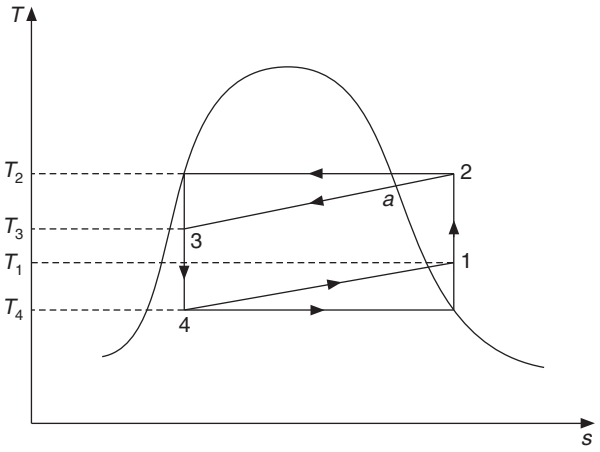

Figure 8.9(a) *T–s* diagram for a refrigerant mixture along with the SSS cycle.

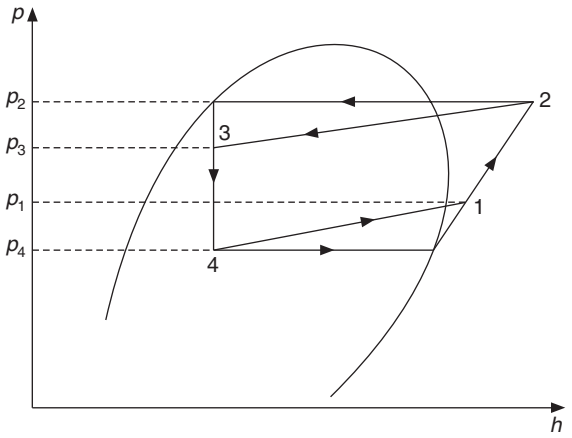

Figure 8.9(b) *p–h* diagram for a refrigerant mixture along with the SSS cycle.

region between T_e and T_c becomes very narrow. The refrigerant has to be cooled to a lower temperature and compressed to a higher pressure for a mixture compared to that for a pure refrigerant. It is desirable that the glide temperature in the condenser $(T_2 - T_3)$ and the glide temperature $(T_1 - T_4)$ in the evaporator be as small as possible so as to obtain a better COP.

In Figure 8.9(a), the condensation process is shown by *a*–3 at condenser pressure and in Figure 8.9(b) the evaporation process is shown by 4–1 at evaporator pressure. It is observed that during condensation, the first condensate liquid comes out in equilibrium with vapour at *a*. As the condensation proceeds, the composition of condensate liquid increases, that is, it follows the path *a*–3. At 3 we have saturated liquid, which passes through the expansion valve. Two-phase mixture comes out of the expansion valve. This state is shown by point 4. The evaporation in evaporator occurs along 4–1. The mass fraction varies during evaporation. The variation in composition of the refrigerant during condensation and evaporation causes variation in physical properties, which must be considered while evaluating condensation and evaporation heat transfer coefficients.

8.9.8 Azeotropes

Blends that comprise multiple components with different volatilities when used in refrigeration systems and do not change their volumetric composition or saturation temperature as they boil or condense, are called azeotropes. It has been observed that from the performance point of view, it is desirable to have refrigerant mixtures with zero glide temperature so that the dew point and the bubble point temperatures are the same. Many refrigerant blends exhibit this property at a particular composition. This composition is called *azeotropic concentration*. The components usually have a small difference in NBP but a large deviation from ideal solution. Figure 8.10(a) shows an azeotrope with positive deviation from Raoult's law while Figure 8.10(b) shows one with negative deviation.

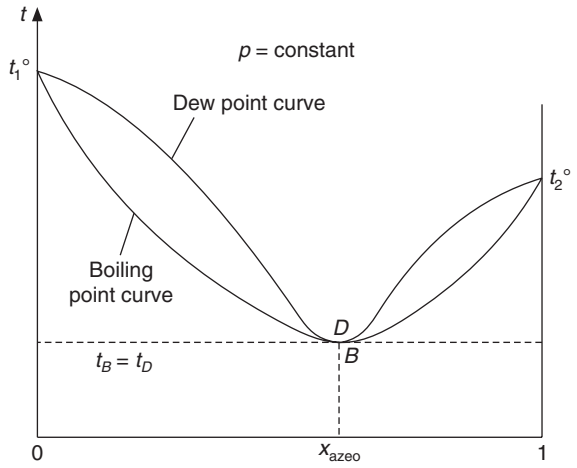

Figure 8.10(a) *T–x* diagram of a minimum boiling azeotrope.

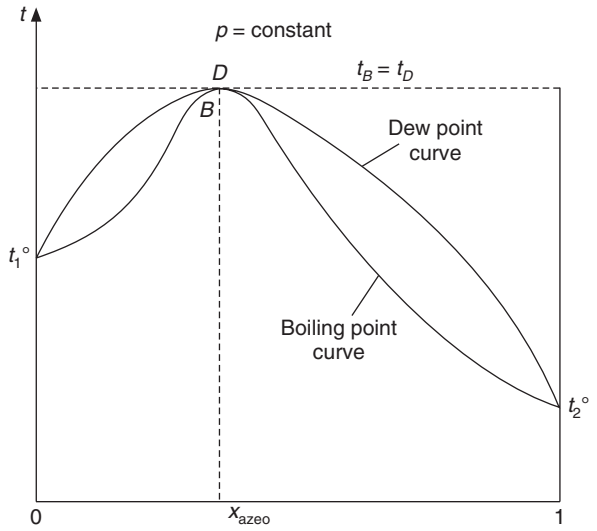

Figure 8.10(b) *T–x* diagram of a maximum boiling azeotrope.

In Figure 8.10(a) the boiling point is lower than that for Raoult's law behaviour shown by dashed line. Both dew point curve and the boiling point curve are shown. At mass fraction of x_{azeo}, both the curves meet together. This mass fraction is the azeotropic mass fraction and the mixture with this mass fraction is called azeotrope. Such a mixture will boil as a pure liquid, that is, the temperature will remain constant at $t_B = t_D$ until all the liquid evaporates at this mass fraction. The boiling point of the azeotrope is lower than the boiling point of both the components, namely t_1^o and t_2^o. For this reason, this is called the *minimum boiling azeotrope*. The enthalpy of mixing is positive in this case, hence the latent heat is lower than that of either of the components.

An azeotrope with negative deviation shown in Figure 8.10(b) has boiling point greater than that of both the components. Hence this is called the *maximum boiling azeotrope*. The mixing process is exothermic in this case. The enthalpy of mixing is negative and the latent heat is more than that of either of the components.

It should be noted that azeotropic composition is dependent upon the mixture pressure. Azeotropic composition will be different for condenser pressure and evaporator pressure, in general. However it is observed that the boiling point curve is flat near azeotropic mass fraction, hence within the range of evaporator and condenser pressures, it does not vary significantly.

According to Eiseman (1957) most of the fluorocarbon mixtures have positive deviation from Raoult's law and hence they are *minimum boiling azeotropes*. This means that at azeotropic concentration, the boiling point is less than the boiling point of the component with lower boiling point at the given pressure. Therefore the given evaporator temperature will be achieved at a higher evaporator pressure compared to the lower boiling point component. At a higher evaporator pressure, the pressure ratio will be lower and the suction vapour density will be larger, resulting in a larger mass flow rate and higher cooling capacity (although it will have lower latent heat). The saturated vapour line is represented by Eq. (8.26) as follows:

$$\ln p = a - b/T$$

Figure 8.11 shows the plot of $\ln p$ vs $1/T$ for the saturated vapour line of lower boiling component and that of the azeotrope. The saturated vapour lines for both of them are straight lines with a slope

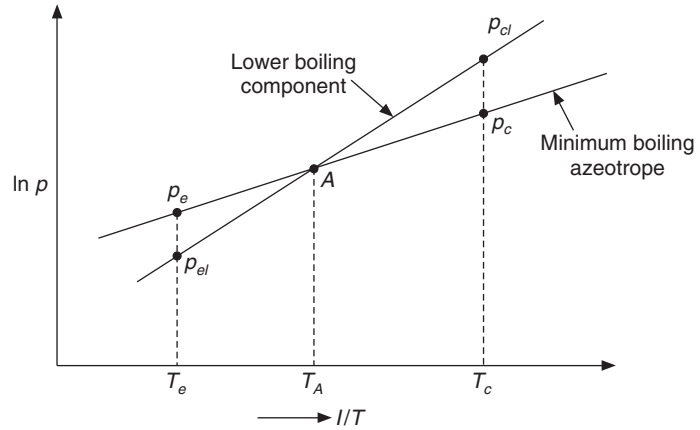

Figure 8.11 Plot of ln p against $1/T$.

of b. The azeotrope has a flat curve near the azeotropic concentration and hence its slope will be less than that of the lower boiling component as seen in the figure. It is seen that below temperature T_A, the vapour pressure of azeotrope is higher than that of the lower boiling component. At evaporator temperature T_e, the azeotrope has a pressure p_e greater than p_{el} of the lower boiling component. At condenser temperature T_c, the condenser pressure p_c of the azeotrope is lower than p_{cl} of the lower boiling component. On both these counts the pressure ratio p_c/p_e is much lower than the ratio p_{cl}/p_{el} of the lower boiling component. This results in significant saving in power requirement.

A large number of azeotropes have been found. Some of them are listed in Section 8.2.6. A few of them involve CFCs, hence these are of historical importance only since these have to be replaced. Some of them are described below to highlight the advantages they give over the pure refrigerants.

R500

R501 consists of CFC 12/HCFC 152 in proportion of 73.8/26.2 by weight. It has NBP of –33.3°C which is 3.5°C more than the lower boiling component R12 (–29.8°C). It gives more cooling capacity than R12. This refrigerant was used when 60 Hz units were used on 50 Hz AC. The speed of the motor decreases by 16.6% at 50 Hz AC, as a result the swept flow rate of the compressor decreases by the same amount. Charging a 60 Hz R12 system with R500 gave the same cooling capacity at 50 Hz AC.

R501

R501 consists of HCFC22/CFC12 in proportion of 75/25% by weight. Its NBP is lower than that of HCFC22 which is –40.8°C. This improves the performance of HCFC22 systems since it is the low boiling component. The pressure ratio of R501 is lower, the c_p/c_v ratio is lower and the suction vapour density is higher than that for HCFC22. This results in a lower adiabatic discharge temperature which in turn leads to a lower motor winding temperature for hermetic compressors. The larger mass flow rate provides further cooling of the motor winding, resulting in an even lower winding temperature. This azeotrope improves the performance of the HCFC 22 systems.

R502

R502 consists of HCFC 22 and CFC115 in proportion of 48.8/51.2% by weight. It has NBP of –45.6°C which is 4.8°C lower than that of HCFC22. This azeotrope improves the performance of the HCFC22 systems at low temperatures. It has a lower compression ratio and adiabatic discharge temperature than the corresponding values for HCFC22. In hermetic compressors, it leads to a lower motor winding temperature. In face of low temperatures applications, HCFC22 requires a two-stage system. In contrast, for the same evaporator temperature, R502 requires a single-stage system. It finds application in supermarkets where air-cooled low-temperature frozen food cabinets are used. It finds application in heat pumps as well.

R507

R507 consists of HC143a/HFC125 in proportion of 50/50% by weight. It has NBP of – 48.55°C. It has zero ozone depletion potential. It is a good replacement for R502. It gives a lower discharge temperature and a larger cooling capacity compared to R502.

R404A

R404A is a tertiary blend. It is near azeotrope (NARM). It consists of HFC125/HFC143a/HFC134a in proportion of 44/52/4% by weight. The system using it requires polyolester as lubricant because of the presence of HFC134a. Its pressure ratio is 2.4 % more than that of R502. Its discharge temperature is 5–6°C lower than that of R502. The COP is also lower. It is a good replacement for R502.

8.10 ALTERNATIVES TO VARIOUS POPULAR REFRIGERANTS

8.10.1 Alternative Refrigerants to CFC12

R12 is very extensively used in small refrigeration systems like household refrigerators, commercial refrigeration appliances, freezers and mobile air conditioning. Over the years, very efficient systems using CFC12 have been designed with reliable compressors and other compatible systems. This has led to reliability in refrigeration systems which is unheard of elsewhere by consumers. The substitute refrigerant and lubricant combination for it must also be chosen to give the same reliability as offered by CFC12. Agarwal (1999) and Agarwal (2004) has given extensive data regarding alternative refrigerants. Table 8.5 gives data for some of the alternative refrigerants, which have been investigated. Table 8.6 gives the performance data for these refrigerants for the theoretical cycle with subcooling to 32°C. Other zeotropic blends, with their composition, recommended as alternatives to R12, are given in Table 8.7.

Table 8.5 Data for CFC12 alternatives at 55°C condenser temperature and –25°C evaporator temperature.

Refrigerant	CFC12	HFC134a	HFC152a	MP66/39	HC 290/600a	HC600a Isobutane	HC290 Propane
Formula	CCl_2F_2	CH_2FCF_3	CH_3CHF_2	HCFC/HFC Blend	C_3H_8/C_4H_{10}	C_4H_{10}	C_3H_8
Molecular weight	120.93	102.03	66.05	Varies	51.12	58.13	44.1
Critical temperature	112.0	101.1	113.5	96.0	96.0	135.0	96.8
NBP (°C)	–29.79	–26.2	–25.0	–30.0	–30.0	–11.73	–42.07
p_e (bar)	1.24	1.07	0.98		1.4	0.59	2.02
p_c (bar)	13.64	14.92	13.32		14.22	7.82	19.07
$\mathbb{V}_g$ (m^3/kg)	0.1803	0.2592	0.4314		0.4142	0.8876	0.2913
h_{fg} (kJ/kg)	163.34	221.83	328.25		390.13	379.49	404.99
γ	1.126	1.102	1.134		1.104	1.086	1.126
ODP	1.0	0	0		0	0	0
GWP	3.1	0.27	0.03		< 0.01	< 0.01	< 0.01

Table 8.6 Performance of alternative refrigerants with condenser and evaporator temperatures of 55°C and –25°C respectively and subcooling to 32°C.

Refrigerant	CFC12	HFC134a	HFC152a	MP66/39	HC 290/600a	HC600a Isobutane	HC290 Propane
Vol. cap. (kJ/m^3)	1237	1185	1074		1254	626	1886
Presssure ratio	10.98	13.94	13.59	13.1	10.16	13.25	9.44
COP	Equal to HFC134a	–	> Equal to HFC134a	Equal to HFC134a	< Equal to HFC134a	> HFC 134a	> HFC 134a
Disch. temperature (°C)	120–125	115–120	135–140	125–130	105–110	100–105	105–110

Table 8.7 Other zeotropic blends with their composition, recommended as alternatives to R12

Trade Name	*ASHRAE number*	HCFCs			HFCs			HCs	
		22	124	142b	134a	152a	227ea	Butane R600	Isobutene R600a
MP39	401A	53%	34%			13%			
MP66	401B	61%	28%			11%			
MP52	401C	33%	52%			15%			
GHG	406A	55%		41%					4%
FX56	409A	60%	25%	15%					
FRIGC FR12	416A		39%		59%			2%	
Free zone 2% lube oil				19%	79%				
GHG-MP		65%		31%					4%
Hot Shot	414B	50%	39%	9.5%					1.5%
GHG X4	414A	51%	28.5%	16.5%					4%
Freeze12				20%	80%				
GHG X5		41%		15%			40%		4%

HFC 134a

This refrigerant has been extensively studied and accepted as a substitute for CFC12 in countries including North America, South America, Australia and Asia. It is expected that other countries will also adopt HFC134a. Several chemical companies are manufacturing HFC134a and almost all the major compressor manufacturers are offering models based upon this refrigerant. It is non-flammable and has zero ODP.

HFC134a is not miscible with mineral oils like naphthenic and alkyl benzene oils. This was one of the main advantages of CFC12 that made it a homogeneous mixture with mineral oils. One has to use Polyol Ester (POE) or Polyalkylene Glycol (PAG) with HFC134a. POE is used with hermetic and semi-hermetic compressors while PAG has been used mostly with mobile air conditioning systems. The oils used should be totally dry. However PAG and POE are hygroscopic substances and require enhanced controls to ensure low moisture. XH-7 and XH-9 desiccants loose fill bead driers are available globally.

Most of the metals like steel, aluminium, copper, brass, etc. are compatible with HFC134a/POE systems. Some new elastomers and plastics have been introduced though most of the common elastomers and plastics are compatible with these systems. Capillary tube plugging has been reported due to sludge generation in the initial phase of development. Metal organic salts and some unidentified oligomers are the culprits. These plugging materials come from a variety of sources such as paraffinic from motor windings, machining lubricants/greases, extracted material from elastomer/plastic, reaction products from residual chlorides and from formation of metal organic salts. It has been established that HFC134a is more sensitive to contamination of foreign material than CFC12 is. It is yet to be established whether HFC134a/POE is completely non-reactive to copper-based material of motor windings.

Process manufacturing with cleanliness is very essential for the manufacture of HFC134a system. Further it has GWP, which may be objectionable.

HFC134a has a larger latent heat but its specific volume is also larger than that of CFC12, therefore, HFC134a requires a larger compressor than that required for CFC12 for the same cooling capacity. The pressure drop in the capillary tube is 13.85 bar compared to 12.37 bar of CFC12, hence HFC134a requires a longer capillary tube.

HFC152a

HFC152a has a slightly below atmospheric pressure in the evaporator. Its normal boiling point is more than that of CFC12. Its mass flow rate is lower since its latent heat is high but the displacement volume is more since vapour is not as dense as that of CFC12. Its discharge temperature is also more since its g value is more than that of CFC12.

Hydrocarbons

Isobutane, propane and blends of isobutane/propane have been used in a number of applications. They have zero ODP and a GWP approaching zero. They are flammable, but easily available at low cost. They are compatible with existing systems and mineral lubricating oils. They have high latent heat but low vapour density (1/3 of CFC12). However, these hydrocarbons are weaker solvents which may make them susceptible to long-term sludge built-up.

Isobutane HC600a

This refrigerant has very good compatibility with the commonly used mineral oils and other materials in the CFC12 refrigeration system. Manufacturing practices similar to CFC12 can be used in this case except that some precautions must be taken since it is a flammable refrigerant. It has higher NBP and as a result the evaporator pressure is below the atmospheric pressure. The displacement volume required is 80% more than that required for CFC12. Therefore, a new compressor is required since the CFC12 compressor cannot be used. A high replacement cost is thus involved. HFC600a

has the lowest value of γ, therefore, the discharge temperature is the lowest despite the highest pressure ratio. It is not considered practical to replace CFC12 by isobutane.

Propane HC290

This refrigerant has NBP lower than that of CFC12. It has the highest pressure amongst the alternatives. It has the highest latent heat and the largest vapour density. Therefore, it requires a very small displacement compressor, 0.56 times that of CFC12. The motor size is comparable. It has the lowest pressure ratio but a similar value of γ. Hence it has a similar discharge temperature as that of CFC12.

Blends of HC600a and HC290

These two refrigerants have some contrasting properties such as NBP, pressures, latent heat and vapour density, which make their blend ideally suited as a retrofit candidate in spite of its flammability. The blend is compatible with mineral oils and usual construction materials. It has been reported that a 50:50 blend does not require any change in the system. The capillary length requires adjustment for optimum energy efficiency. The vapour pressures of HC blend (CAR 30) are almost identical to CFC12. This blend has been used in new systems of small capacity. There is increased interest in using this blend as a retrofit refrigerant in developing countries. Considerable data has been generated on refrigerant thermodynamic and thermophysical properties, flammability, toxicity, material compatibility, system reliability and safety aspects in a UNEP report. In India it is being used in domestic refrigeration systems. It has the usual problems associated with the blends. The mixture undergoes a temperature glide during boiling and condensation. If the composition is slightly affected, it may cause unstable operation.

HCFC and HCFC/HFC blends

MP39 and MP66 are known as 401A and 401B three-component HCFC/HFC blends. FX 56 is a three-component HCFC blend. Since these blends contain HCFCs, they are not the final solution to ozone depleting substances. Hence these are not being actively pursued for new equipment manufacture.

8.10.2 Alternative Refrigerants To R502

R502 is an azeotropic mixture of CFC152a and HCFC22. It was developed to improve the performance of R22 at low temperatures. Its constituent CFC115 will be phased out along with other CFCs, hence R502 will also be phased out. R507A, R404A and R407C have been proposed as promising alternatives. These are HFC-based zeotropic blends. They all have temperature glide unlike R502.

R507A

This is an azeotropic blend of HFC125 and HFC143a, 50:50 by weight. It is one of the leading alternatives to R502. HFC125 has NBP of – 48.55°C while HFC143a has NBP of – 47.35°C. The azeotrope has NBP of – 45°C. It requires a lower mass flow rate than that required by R502. The absolute pressure is higher by 9% in the condenser and 14% in the evaporator when compared to R502.

R404A

R404A is a tertiary zeotropic blend of HFC125, HFC143a and HFC134a in proportion of 44%, 52% and 4% by weight. This is a near azeotropic mixture. It has a temperature glide of 1.5°C. Its

NBP is – 46.5°C, which matches with that of R502. It has a larger latent heat compared to R502, which means that the mass flow rate is lower. However, it has lower COP than that of R502 at lower temperatures.

407C

This is also a tertiary zeotropic blend of HFC32, HFC125 and HFC134a in proportion of 20%, 20% and 40% by weight. At typical condenser temperatures, it has a temperature glide of 4°C and at typical evaporator temperatures it has a glide of 6°C. However, the actual temperature glide in the evaporator depends upon the quality of the mixture entering the evaporator. Pressure drop in the evaporator can also affect the glide by changing over to a different pressure. The actual temperature is less in the evaporator and more in the condenser.

Performance of R502 alternatives

The performance of the R502 alternatives has been investigated and is given in Table 8.8.

Table 8.8 Performance of R502 alternatives

Refrigerant	*Condenser temperature* (°C)	*Evaporator temperature* (°C)	*Cooling capacity* (kW)	*COP*
R502	40.6	–33.4	31.2	1.0
R507A	40.6	–35.8	31.2	0.92
R404A	40.6	–36.8	28.9	0.9
R407C	40.6	–43.0	18.5	0.8

Other recommended alternatives are given in Table 8.9.

Table 8.9 Zeotropic blends along with their composition, recommended as alternatives to R502

Trade name	*ASHRAE number*	*HCFC22*	*HFCs*					*HCs*	
			32	125	134a	143a	152a	Propane	Propylene
MP80	402A	38%		60%				2%	
HP81	402B	60%		38%				2%	
HP62, FX-70	404A			44%	4%	52%			
KLEA 407A	407A		20%	40%	40%				
KLEA 407B	407B		10%	70%	20%				
FX10	408A	46%		7%		47%			
R411A	411A	87.5%					11%		1.5%
R411B	411B	94%					3%		3%
G2018C		95.5%					1.5%		3%
AZ50	507			50%		50%			

8.10.3 Alternative Refrigerants To HCFC22

HCFC22 is very widely used in large refrigeration and air conditioning systems. It has very low ODP but it has to be phased out by 2030 due to its GWP. It is considered to by an alternative to other CFCs in many applications. Pure substances, which may replace HCFC22 are listed in Table 8.10. These consist of one and two carbon compounds with zero ODP. The criterion used in their selection is essentially the NBP.

Table 8.10 Characteristics of possible alternatives to HCFC22

Refrigerant	*NBP* (°C)	*Characteristics*
R23	–82	Critical temperature is very low
R32	–51.7	Flammable. Very high volumetric capacity
R125	–48.1	High GWP, low COP
R143a	–47.2	Flammable, high GWP
R134a	–26.1	Low volumetric capacity
R152a	–24.0	Flammable

Among the pure refrigerants enumerated in Table 8.10, R32, R125, R143a and R134a have been extensively studied as mixture refrigerants with other HFCs. A number of mixtures have been proposed. As a result of many years of research, two potential refrigerant mixtures, namely, R407C and R410A have emerged. Table 8.11 shows the properties of the above pure refrigerants and these two mixtures as alternatives to HCFC22.

Table 8.11 Properties of alternatives to HCFC22

Refrigerant	R22	R32	R125	R134a	R407C	R410A
Mol. wt.	86.5	52.0	120.0	102.0	86.2	72.6
NBP (°C)	–40.9	–51.7	–48.1	–26.1	–43.6	–52.7
T_c (°C)	96.2	78.2	66.2	101.2	86.7	72.5
p_c (bar)	50.5	57.9	36.6	40.7	46.2	49.5
h_{fg} (kJ/kg at 25°C)	180.3	272.5	110.4	178.0	185.8	192.6
Bubble pressure at 25°C (bar)	10.4	16.9	13.88	6.7	12.0	16.6
Sat. liquid density at 25°C (kg/m^3)	1191	961	1190	1206	1140	1065
Sat. vapour density at 25°C (kg/m^3)	44.8	47.2	90.3	32.3	43.2	64.2
Temperature glide at 1 atm (K)	0	0	0	0	7.3	0.1
Sat. liq. specific heat at 10°C	1.29	1.13	1.42	1.43	1.54	1.72
Sat. liq. specific heat at 50°C	1.46	2.42	1.93	1.57	1.79	2.20

8.10.4 Alternative Refrigarants To CFC11

CFC11 is the mainstay refrigerant of centrifugal water chillers. CFC11 has a high molecular weight and high vapour density, hence the centrifugal compressor does not require high speed. These

chillers are very efficient since they are directly coupled to the motors and hence do not require any gears. Further, CFC11 has NBP of 23.7°C, hence its storage and handling are easy operations as they are performed near atmospheric pressures.

HCFC123 has been proposed as the substitute to CFC11. It has NBP of 28°C. HCFC123 gives similar performance and has replaced CFC11 as a drop-in substitute in many installations. However, it is toxic and being HCFC, has also to be phased out. This is transitional alternative only and a long-term substitute must be identified.

Beyerlin et al. (1991) suggested that fluorinated propanes and butane may be used as CFC and HCFC substitutes. Adcock (1991) suggested that fluorinated ethers be used as substitutes. Devotta et al. (1994) studied the relative performance of HFC 245ca (Pentafluoro propane) and HFE143 ether and found it to be very close to CFC11. Their results are given in Table 8.12.

Table 8.12 Performance of alternatives to CFC11

Refrigerant	CFC11	HFC 245ca	HFE143
Formula	CCl_3F	$CF_2HCF_2CH_2F$	CH_2FOCHF_2
Molecular wt.	137.4	134.0	100.0
T_c (°C)	197.8	178.4	186.83
p_c (MPa)	4.37	3.885	4.141
NBP (°C)	23.7	25.0	30.06
p_e (MPa)	0.04	0.037	0.029
p_k (MPa)	0.175	0.172	0.145
q_e (kJ/kg)	164.9	152.2	231.91
$\mathbb{V}_s$ (m^3/MJ)	2.604	2.816	3.312
COP	6.06	5.861	6.023

The refrigerants in Table 8.12 are also not really good alternatives to CFC11 since both ether and pentafluoro propane are flammable.

8.11 NATURAL REFRIGERANTS

To cope with the environmental damage and to reduce the use of harmful refrigerants, refrigeration industry is in the process of a historical technological shift. Emphasis is shifting to the use of naturally existing substances as refrigerants, e.g. air, water, ammonia, carbon dioxide and hydrocarbons. All these are used at present, but have certain limitations. This is where the new technology is required to make robust and efficient systems.

8.11.1 Hydrocarbons

Hydrocarbons have zero ODP and very small GWP. They are already being used in many countries now. They are flammable, hence the safety issue has to be addressed. The safety measures must be used during handling, manufacturing, servicing, storage and disposal of appliance or equipment. Germany is the only country which has an approved safety standard DIN 7003 for hydrocarbons.

These refrigerants find application in household refrigerators and freezers as well as in car air conditioning. German heat pump manufacturers are in the process of switchover to R290, which requires only 40% of CFC12 charge. It gives better COP than that given by HCFC22. Some indoor swimming pool heat pumps are also using propane. European countries, namely Austria, Denmark, Germany, and Sweden apart from the UK, are using hydrocarbons in commercial systems. Some of these hydrocarbons also use secondary loop to make them perfectly safe. Apart from pure hydrocarbons, blends of hydrocarbons are also being used. These blends have already been discussed.

8.11.2 Ammonia

Ammonia has zero ODP and GWP. It has a high critical temperature, which gives good COP at normal temperatures. It has exceptionally high latent heat. It is a very good refrigerant from the thermodynamic point of view but it has some limitations. It corrodes Cu, Zn and their alloys. Hence heat exchangers cannot use copper tubes which have low thermal resistance. It is toxic and flammable. Luckily it has a distinct odour, which can warn people and animals to keep away before the concentration becomes dangerous. It is lighter than air.

Typical ammonia systems use the direct expansion coil with flooded coils as the evaporator where a certain level of liquid refrigerant is maintained in the evaporator coil. The refrigerant recirculates in the evaporator. Sometimes the recirculation pumps are also used to increase the heat transfer coefficient. Typically a very large quantity of refrigerant is required in these systems. Nowadays plate type heat exchangers or spray type shell-and-tube evaporators are used. This reduces the quantity of charge by 90% compared to the older systems. Cold storage and food processing ammonia systems in the medium capacity range are more efficient than the CFC and HCFC based systems. Typically, ammonia was used in industrial refrigeration plants. Now that low-charge systems are designed, ammonia is being used in supermarkets indirectly with brine in water chillers for centralized air conditioning plants, cold storages, ice manufacturing and skating rinks. The indirect brine systems consume 10–15% more energy than that consumed by HCFC. The use of ice-slurry for chilling reduces energy consumption by 10%. Germany and Denmark are trying to introduce 10 TR systems as well. Small systems and hermetic compressors cannot use ammonia since the mass flow rate is very small and hence cooling of the motor of hermetic compressors will not be possible.

The new low-charge systems are becoming very popular. At present, they are used for dairy products, ice-cream, meat processing, poultry processing, fish, fruit and vegetable processing, coffee, cocoa, chocolate and sugar confectionary, soft drinks and breweries. Ammonia is a good substitute for other refrigerants in direct and indirect systems.

8.11.3 Water

Water is available in abundance. It is nontoxic, nonflammable and ecofriendly. It is used in industrial cooling processes where cooling is produced by evaporating a small quantity of water which absorbs its energy from the remaining water and cools it. Steam jet refrigeration system and vacuum cooling are the systems in use. Water is also used as secondary refrigerant alone or as solvent in brines. Its disadvantages are the low volumetric refrigeration capacity, relative high pressure ratio

and vacuum pressure. Water, however, requires low maintenance. Leakage is not a problem. The heat exchanger does not require cleaning since the water is de-aerated and the dissolved oxygen is negligible, which rules out corrosion. Direct evaporation is very efficient due to the absence of any intermediate surface.

Ice slurry or binary ice

This is a novel application of water which makes it possible to use it below 0°C. Binary ice is pumpable ice slurry, which is used as ideal secondary refrigerant. It is a mixture of ice crystals 0.01 to 0.2 mm in size, water and a freezing point depressant. In brines, only the sensible heat is available for cooling. In ice slurry, apart from sensible heat, the latent heat is also available for cooling. Ice slurry thus has a very large cooling capacity. In air conditioning systems, ice slurry of 20% gives significant savings compared to 6°C chilled water. The pipe diameter can be reduced by 60%. It will result in more dehumidification due to a lower apparatus dew point.

Ice slurries are produced by (i) scrapped surface evaporators where the ice formed on a surface is scrapped by a shaft driven scrapper, (ii) vacuum freeze evaporators or vacuum ice machines or (iii) fluidized bed evaporators. In vacuum systems, the triple point pressure is maintained in a tank. Some water evaporates and absorbs heat from the remaining water in the tank, thereby freezing it. In fluidized bed evaporators, primary refrigerant evaporates outside the tubes of a vertical shell-and-tube heat exchanger. There are solid particles inside the tube, which are fluidized by upward flowing water. The ice formed on the inside surface of tubes is scrapped by solid particles and transported with water as slurry.

Ice slurries find application in meat processing, fish and food processing, quick chilling of milk, juices, etc. Ice slurries can be transported over long distances for air conditioning.

8.11.4 Carbon Dioxide

It has zero ODP and GWP of 1. It is nontoxic and inflammable. It is compatible with mineral oil and the usual construction materials can be used for it. It is heavier than air, hence if it leaks it will settle down and may cause suffocation.

The critical temperature of CO_2 is 31°C. Hence the CO_2 cycle operates as a trans-critical cycle. The heat rejection is above the critical temperature, hence there is no condensation. In this region the pressure and temperature are not saturated values and hence are not related together. High temperatures can be achieved with reasonable compressor power. This makes CO_2 very attractive for heat pump applications.

CO_2 operates at very high pressures, hence the volumetric refrigeration capacity is five times that of HCFC22. New technology is required in compressors. All components are optimally redesigned. These are small and strong to withstand high pressures. A high working pressure enables small equipment and small diameter lines to be used because of high density. A high pressure leads to a high heat transfer coefficient and a low pressure ratio. Leakage is not a problem; the gas leaked out does not have to be recovered.

CO_2 is typically used in low temperature cascade cycles. The trans-critical cycle involves high energy costs. The leakage from high pressure connections is a big problem. Leakage can be avoided by using a secondary refrigerant, which will have shorter CO_2 lines.

8.11.5 Air

Air is non-toxic, non-flammable and one of the most readily available substances, which has zero ODP and GWP. Air has been used for refrigeration for quite some time. It is used with the Bell–Coleman cycle for refrigeration. This cycle involves isentropic compression and expansion, and constant pressure heat absorption and rejection. It has low COP, large volume and weight and high operating cost. It was earlier used in marine refrigeration. It is still used in aircraft air conditioning with Bootstrap and Reduced ambient cycles. It requires less weight in aircraft application since the compressor, the motor and the evaporator are not required. Cold air is directly fed to the cabin.

Air cycle is being used in the German high speed train *ICE*. One manufacturer has used the open cycle and the other has used the closed cycle. The closed cycle unit is very compact and is mounted on roof top. Both the systems have been working since 1995. Though the CFC systems have high efficiency, these are not ecofriendly. On the other hand, though the air cycle has more energy consumption, it requires less maintenance and it is also more ecofriendly.

8.11.6 Stirling Cycle

The Stirling cycle consists of two isotherms and two constant volume processes. It operates on a closed regenerative cycle in which the working fluid is cyclically compressed and expanded at different temperature levels. The Stirling cycle gives a COP very close to that of the Reversed Carnot cycle. The working substance is either helium or air. Apart from temperatures in the range of household refrigerators, this cycle can also be used for ultra low temperature.

The Stirling cycle is more efficient than the vapour compression systems in the case of temperatures below – 23°C. Stirling cycle freezers are smaller, cheaper and efficient. They consume 12% less energy than that consumed by the CFC systems. Domestic refrigerators based on Stirling cycle are costly and have lower COP.

The Stirling cycle is typically used for cryo coolers (less than –153°C), specially for air and nitrogen liquefiers. Recent applications are miniature cryo coolers for cooling electronic devices. The Stirling cycle shows some promise for cooling at moderate temperatures as well. It is described in a later chapter.

8.12 SECONDARY REFRIGERANTS

In many applications of refrigeration and air conditioning the refrigerant cannot be used for cooling or chilling or freezing the commodity either due to safety considerations or due to toxicity or economic considerations. In air conditioning of multistorey buildings or in buildings of vast expanse where the central refrigeration plant is located at one place, it is not economical to circulate the refrigerant to all the floors or spaces for cooling purposes. It will require long refrigerant lines leading to large pressure drops and large compressor power. It will also require an enormous quantity of refrigerant. Similarly in a cold storage plant, it is not economical to circulate the refrigerant to cooling coils located at various places. In an ice manufacturing plant the cans of water cannot be cooled by the refrigerant, since here too, a very large quantity of refrigerant will be required. Ammonia because of its toxicity cannot be used for air conditioning or ice making directly. In ice skating rinks, brine is circulated in pipes below the floor.

In such cases as discussed above, it is economical to circulate water, or brine solution or glycol solution chilled in the refrigeration plant. The chilled water, brine or glycol will provide

cooling of the air or the product in the cooling coil in each floor or space. These working substances are called secondary refrigerants. Such substances cannot produce the refrigeration effect by evaporation; they only transport the refrigeration effect produced by a primary refrigerant. They also allow the use of less expensive and low pressure tubes in the heat exchangers. For example, mild steel pipes and sheets are used in these heat exchangers instead of copper, which is quite expensive.

Water is used up to 4°C since it freezes at 0° C, although ice slurries are also being effectively used at lower temperatures with the help of the boiling point depressants. Many salts are used to decrease the boiling point of water. The solution of salts in water is called brine. Some other chemicals are also used with solution in water. Sodium chloride brine is used up to –15°C and calcium chloride brine is used up to –50°C. Brine solutions are very corrosive to copper, brass and aluminium, etc. Mild steel pipes and sheets with anti-corrosive treatment are used with brines. A solution of any salt or chemical in water has a certain concentration at which the freezing point is the lowest. A solution of this concentration is called *eutectic* mixture or erohydrate, and the temperature of freezing is called the *eutectic temperature*. The eutectic concentrations and temperatures of some salts and chemicals with solution in water are given in Table 8.13. Table 8.14 gives the density, specific heat and freezing points of sodium chloride and calcium chloride brines of various concentrations. Table 8.15 gives the freezing points of aqueous solutions of glycerine, ethylene glycol and propylene glycols of various concentrations.

Table 8.13 Eutectic concentration and eutectic temperature of brines and other chemicals.

Secondary refrigerant	*Eutectic concentration* (%)	*Eutectic temperature* (°C)
Ammonium chloride	0.191	–15.7
Calcium chloride	0.324	–51.0
Ethelyne glycol	0.15	–9.3
Glycerine	0.669	–51.3
Methyl alcohol	0.695	–108.9
Potassium chloride	0.197	–10.67
Sodium chloride	0.233	–21.1
Sodium sulphate	0.049	–1.11

Table 8.14 Properties of calcium chloride and sodium chloride brines

Concentration	*Density at* 15.5°C (kg/litre)		*Sp. heat at* 15.5°C (kJ/kg-K)		*Freezing temp.* (°C)	
	$CaCl_2$	NaCl	$CaCl_2$	NaCl	$CaCl_2$	NaCl
0.05	1.044	1.035	3.86	3.92	–2.4	–2.8
0.1	1.0087	1.072	3.57	3.71	–5.4	–6.4
0.15	1.133	1.111	3.31	3.54	–10.3	–11.1
0.2	1.182	1.15	3.08	3.4	–18.0	–16.8
0.25	1.233	1.191	2.88	3.29	–29.4	–18.8
0.2987	1.29	–	2.75	–	–55	–
0.33	1.298	–	2.73	–	–46	–

Table 8.15 Freezing points of aqueous solutions

Alcohol		*Glycerine*		*Ethylene Glycol*		*Propylene Glycol*	
Conc.	°C	Conc.	°C	Conc.	°C	Conc.	°C
0.05	–2.2	0.1	–1.6	0.15	–5.3	0.5	–1.7
0.1	–4.7	0.2	–4.8	0.2	–8.8	0.1	–3.3
0.15	–6.8	0.3	–9.5	0.25	–12.2	0.15	–5.3
0.2	–10.4	0.4	–15.4	0.3	–15.8	0.2	–7.2
0.25	–14.7	0.5	–23.0	0.35	–20.0	0.25	–9.5
0.3	–19.2	0.6	–34.7	0.4	–24.7	0.3	–12.8
0.35	–25.1	0.7	–38.9	0.45	–30.0	0.35	–16.4
0.4	–29.4	0.8	–20.8	0.5	–35.8	0.4	–20.8
0.45	–33.1	0.9	–1.6			0.45	–26.1
0.5	–38.7	1.0	+17.0			0.5	–31.9
0.55	–40.3					0.55	–39.8
						0.59	–49.4

When salt is added to water, it decreases the freezing point of water. The freezing point of water decreases as the concentration of salt in it is increased. This trend continues up to the eutectic concentration, beyond which the addition of more salt increases the freezing point of water. Figure 8.13 shows the variation in freezing point with concentration for a typical brine. The eutectic concentration and temperature are indicated by x_E and t_E respectively.

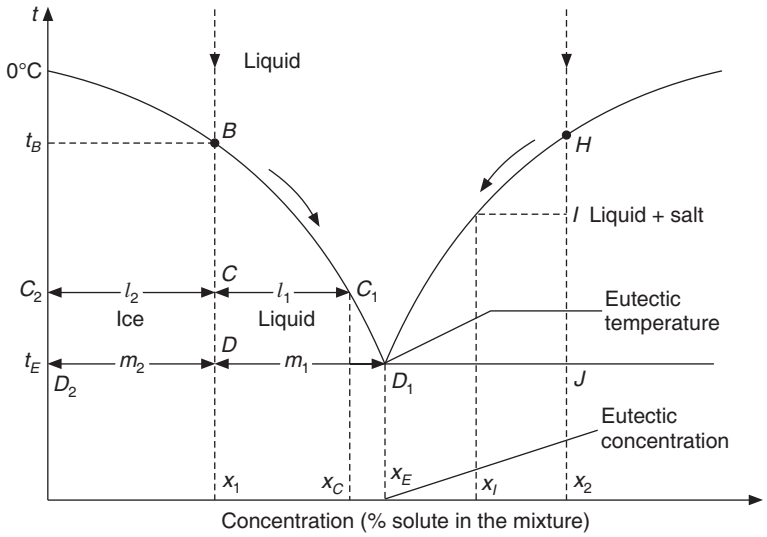

Figure 8.13 Variation of freezing point of water with salt concentration in a typical brine solution.

A solution of $x_1 < x_E$ when cooled along the arrow in the figure, will start freezing at point B where the temperature is t_B. The ice crystals will begin to form and enthalpy of freezing of ice

crystals will be required. As the temperature is lowered further, more and more crystals will continue to form. At point C it is a mixture of ice crystals and brine of concentration x_C. The mixture consists of l_1 part brine and l_2 part ice crystals. As the mixture is cooled further, the brine concentration increases, and ultimately reaches the eutectic concentration x_E. At point D, the mixture consists of m_1 part eutectic solution and m_2 part ice crystals. As more heat is removed, m_1 part eutectic solution will freeze at uniform temperature t_E. The frozen mixture is not a solution. It is a mixture of salt and frozen water, and consequently the latent heat must be corrected for the heat of solution. If the heat of solution is positive, then the effective latent heat decreases. On the other hand if the heat of solution is negative, then the effective latent heat increases. Sodium chloride when mixed in water cools the water. Heat has to be added to the solution to bring it to the original temperature, hence the heat of solution is positive.

If the initial solution has $x_2 > x_E$, then as the temperature is decreased to t_H at point H, the salt freezes out and the brine concentration decreases. At point I, it is a mixture of salt and brine of concentration x_I. As the mixture is cooled further, the concentration of brine decreases until at point J it reaches the eutectic concentration x_E.

Calcium chloride is very corrosive, hence excessive contact with the air should be avoided. Corrosion inhibitors such as sodium dichromate may be added to maintain the pH value in the range of 7 to 8.5. A sodium dichromate concentration of 2 kg/m^3 of brine is recommended. Caustic soda may also be added to correct acidity, that is if the pH value is below 7. Calcium chloride attacks fish by direct contact, hence for fish sodium chloride is used. The freezing point of calcium chloride is lower, hence it is used for low temperature applications. Ethylene glycol has a freezing point lower than that of the propylene glycol. It is also very often used. It is also very toxic and attacks food products by direct contact. These can be inhibited for corrosivity. The specific heats of these are very high.

REFERENCES

Adcock, J.L. et al. (1991): Fluorinated ethers a new series of CFC substitutes, *Proc. Int. CFC and Halon Conference*, Baltimore, MD, USA.

Agarwal, R.S. (1999): Alternative to CFCs and HCFC Impact on ODS Phase out Due to Kyoto Control Measures on HFCs, *Proc. Joint IPCC/TEAP Expert Meeting on Options for Limitation of Emissions of HFCs and PFCs*, Petten, The Netherlands, 1999, pp. 219–229.

Agarwal, R.S. (2004): Alternatives to CFCs and HCFCs for Refrigeration and Air conditioning: Emerging Trends, *Workshop on Alternate Refrigerants and Cycles*, Mechanical Engineering Department, IIT Kharagpur, Jan. 28–30.

Atwood, T. (1988): "CFCs in Transition, *International Journal of Refrigeration*," Vol. 11, No. 4, July.

Benedict, M., Webb, G.B. and Rubin, L.C. (1940): An empirical equation for thermodynamic properties of light hydrocarbons and their mixtures—methane, ethane, propane and n-butane, *J. Chem. Phy*. Vol. 8, pp. 334–345.

Beyerlien, A.L. et al. (1991): Physical property data on fluorinated propanes and butanes as CFC and HCFC substitutes, *Proc. Int. CFC and Halon Conference*, Baltimore, MD, USA.

Borde, I., Jelinek, M. and Daltrophe,N.C. (1995): Absorption system based on Refrigerant R134a, *Int. J. Refrig*., Vol. 18, No. 6, pp. 387–394.

Devotta, S. et al. (1994): Comparative assessment of some HCFCs , HFCs and HFEs as Alternative to CFC11, *Int. J. Refrigeration*, Vol. 17, No. 1, 1994.

Downing, R.C. (1988): *Fluorocarbon Refrigerants Handbook*, Prentice Hall, Englewood Cliffs, New Jersey.

Eiseman, B.J., The azeotrope of monochloro-diffluoromethane and dichloro difluoromethane, *J. American Chemical Society*, Vol. 79, No. 4, 1957, p. 6086.

Feroiu, V. and Geana, D. (2003): Volumetric and thermodynamic properties for pure and refrigerant mixtures from cubic equations of state, *Fluid Phase Equilibria*, Vol. 207, pp. 283–300.

Huber, M.L. and Ely, J.F. (1994): A predictive extended corresponding state model for pure and mixed refrigerants including an equation of state for R134a, Vol. 17, pp. 18–31.

Huron, M.J. and Vidal, J. (1979): New mixing rules in simple equations of state for representing vapour-liquid equilibria of strongly non-ideal liquid mixtures, *Fluid Phase Equilibria*, Vol. 3, pp. 255–271.

Jacobsen, R.T. and Stewart, R.B. (1973): Thermodynamic properties of nitrogen including liquid and vapour phases from 63 K to 2000 K with pressures to 10000 bar, *J. Phys. Chem. Ref. Data*, Vol. 2, pp. 757–922.

Lemmon, E.W.and Jacobsen, R.T. (1997): Thermodynamic properties of mixtures of refrigerants R32, R125, R134a and R152a, *13th Symposium on Thermophysical Properties*, Boulder, Colorado, June, 22–27.

Martin, J.J. and Hou, Y.C. (1995): Development of an equation of state for gases, *AICHE J.*, Vol. 1, pp. 142–151.

McLinden, M.O., Lemmon, E.W. and Jacobsen, R.T. (1998): Thermodynamic properties for the alternate refrigerants, *Int. J. Refrig.*, Vol 21, No. 4, pp. 322–338.

McLinden, M.O., Gallagher, J.S. et al. (1989): Measurement and Formulation of the Thermodynamic Properties of Refrigerant R134a (1,1,1,2 Tetrafluoroethane) and R123 (1,1 Dichloro-2,2,2 Tetrafluoroethane), *ASHRAE Trans*., Vol. 95, Part 2.

Molina, M.J. and Rowland, F.S. (1974): Stratospheric Sinks for Chlorofluorocarbons—Chlorine Atom Catalyzed Destruction of Ozone, *Nature*, Vol. 249, pp. 810–812.

Monte, F. de (2002): Calculation of thermodynamic properties of R407C and R410A by Martiin-Hou equation of state—part I theoretical development, *Int. J. Refrigeration*, Vol. 25, pp. 306–313.

Peng, C.L., Stein, F.P. and Gow, A.S. (1995): An enthalpy-based cubic equation of state mixing rule for cross-prediction of excess thermodynamic properties of hydrocarbon and halogenated refrigerant mixtures, *Fluid Phase Equilibria*, Vol. 1088. pp. 79–102.

Peng, D.Y. and Robinson, D.B. (1976): A new two-constant equation of state, *Ind. Eng. Chem. Fundam*, Vol. 15(1), pp. 59–64.

Reid, R.C., Prausnitz, J.M. and Poling, B.E. (1987): The Properties of Gases and Liquids, McGraw Hill Book Company.

Scalabrin, G., Piazza, G. and Cristofoli, G. (2002): A corresponding states thermodynamic model for pure and mixed refrigerants in terms of the Helmholtz energy, *Fluid Phase Equilibria*, Vol. 199, pp. 79–99.

Soave, G. (1972): Equilibrium constants from a modified Redlich-Kwong equation of state, *Chem. Eng. Sci.*, Vol. 27, pp. 1197–1203.

Thorne, S. and Lebre, E. (1999): Criteria and Indicators for Appraising Clean Development Mechanism (CDM) Projects, HELIO International, COP5.

Tillner-Roth, R. and Baehr, H.D. (1994): An international standard formulation of the thermodynamic properties of 1,1,1,2 tetrafluoroethane (HFC134a) covering temperatures from 170 K to 455 K at pressures up to 70 MPa, *J. Phys. Chem. Ref. Data*, Vol. 23, pp. 657–729.

Yokozeki, A. (1996): Thermodynamic properties of mixtures based on van der Walls equation of state : R32/R125 binary system, *Int. J. HVAC and R Res.*, Vol. 2, pp. 284–311.

Zhang, H.L., Sato H. and Watanabe, K. (1997): *Int.J. Refrig*.

REVIEW QUESTIONS

1. Which elements in refrigerants cause ozone depletion?
2. What is the new classification of organic refrigerants?
3. Explain the various methods of designation of refrigerants?
4. What are non-azeotropic and azeotropic mixtures? How do such mixtures improve upon the adverse properties of some refrigerants?
5. Name some commonly used refrigerants. Explain the utility of water as a refrigerant.
6. Enumerate all the desired properties of refrigerants.
7. What kind of refrigerants would you prefer for use with (a) rotary compressors and (b) centrifugal compressors?
8. Explain the chemical reactions that CFCs undergo in the atmosphere.
9. Explain the chemistry underlying the depletion and recovery of Antartic ozone levels.
10. Explain the issue of global warming related to increase in the concentration of CO_2 and CFCs in the atmosphere.
11. How do partially miscible refrigerants in lubricating oil pose maximum problems? How are these problems overcome? Name the refrigerants that are completely miscible with the lubricating oils.
12. Why is it necessary to keep refrigerants free from moisture?
13. Explain the characteristics and applications of Low Normal Boiling Point refrigerants and High Normal Boiling Point refrigerants.
14. How is the performance of refrigerants related to their molecular weights?

15. In spite of CFCs being suitable for every specific application from the point of view of their thermodynamic and thermophysical properties, these refrigerants are not eco-friendly. Comments on this statement and explain how these refrigerants are being contemplated to be replaced under Montreal Protocol and Kyoto Protocol.

16. Explain the potential of alternative refrigerants such as HFCs and HCFCs.

17. Give some examples to explain the importance of mixtures of refrigerants. Do such mixtures cause any problems?

18. Explain with the help of a neat diagram the term glide temperature in the context of a mixture of refrigerants.

19. What is a minimum boiling azeotrope? Explain its behaviour on a T–x diagram and compare the same with the behaviour of maximum boiling azeotrope.

20. Describe the advantages obtained with azeotropes such as R501, R502 and R507 over the pure refrigerants.

21. Name the alternative refrigerants to R12. In this context discuss the advantages obtained with HFC134a vis-a-vis R12.

22. Why is R502 needed to be phased out? Name the alternative refrigerants to R502.

23. Why is HCFC22 needed to be phased out? Name the pure substances which can replace HCFC22.

24. Can HCFC123 replace CFC11? Discuss this statement.

25. What are natural refrigerants? Discuss their potentials and limitations.

26. Explain the role of secondary refrigerants in applications of refrigeration and air conditioning systems to meet varied requirements.

9

Expansion Valves

LEARNING OBJECTIVES

After studying this chapter, the student should be able to:

1. Explain the purpose of an expansion valve in refrigeration systems.
2. Enumerate the types of expansion valves most commonly used in refrigeration systems.
3. Describe the working principle and salient features of capillary tube and the concept of balance point between the compressor and the capillary tube.
4. Discuss the effect of load variation on the balance point, and describe how the selection of capillary tubes is done and the required length is estimated using the analytical and graphical methods.
5. Explain the advantages and disadvantages of capillary tube based refrigeration systems.
6. Explain the working principle of an automatic expansion valve, and its performance under varying loads.
7. Describe the advantages, disadvantages and applications of automatic expansion valves.
8. Present a simple analysis of fluid flow through orifices.
9. Explain the working principle of a thermostatic expansion valve (TEV), and its performance under varying loads.
10. Explain the operation of the cross-charged TEV, and that of the TEV with external pressure equalizer and limit charging.
11. Describe the advantages, disadvantages and applications of TEVs.
12. Explain the working principle of high-side and low-side float valves.
13. Explain the working principle of an electronic expansion valve.
14. Discuss some of the practical problems encountered in the operation of various types of expansion devices used in refrigeration systems.

9.1 INTRODUCTION

The purpose of an expansion valve is

(i) to reduce the pressure from the condenser pressure to the evaporator pressure and

(ii) to control the mass flow rate in the refrigeration system according to some predetermined criterion.

The mass flow rate in the system should under ideal conditions be proportional to the cooling load on the plant. Sometimes, the product to be cooled is such that a constant evaporator temperature has to be maintained. In other cases, it is desirable that the liquid refrigerant should not enter the compressor. In such a case, the mass flow rate has to be controlled in such a manner that only the superheated vapour leaves the evaporator. Again, an ideal refrigeration system should have the facility to control the mass flow rate in such a way that the energy requirement is minimum and the both the required criterion of temperature and cooling load are satisfied. Some additional controls to control the capacity of the compressor and the space temperature may be required as well, so as to minimize the energy consumption. There are two basic types of controls on the compressor, namely the on-off control and the proportional control. The expansion valve used in refrigeration systems has to be compatible with the overall control system. The following five types of expansion valves are commonly used.

1. Capillary Tube
2. Automatic Expansion Valve (maintains a constant temperature in the evaporator)
3. Thermostatic Expansion Valve (maintains a constant degree of superheat in the evaporator)
4. Float type Expansion Valve
   (a) High Side Float Valve (maintains a constant level of liquid refrigerant in the evaporator)
   (b) Low Side Float Valve (maintains a constant level of refrigerant in the evaporator)
5. Electronic Expansion Valve

The capillary tube has a fixed area of flow, whereas the passage area is changed in the other types of valves in order to change the mass flow rate in response to evaporator temperature or superheat. This area is sometimes also called the area of restriction.

9.2 CAPILLARY TUBE

A refrigerant capillary tube is a narrow bore tube of constant diameter. It serves the purpose of reducing the pressure in a refrigeration system. The pressure reduction occurs owing to the following two factors:

1. The refrigerant has to overcome the frictional resistance offered by the capillary tube walls. This leads to some pressure drop.
2. The liquid refrigerant flashes (evaporates) into mixture of liquid and vapour as its pressure reduces. The density of vapour is less than that of the liquid. Hence, the average density of the refrigerant decreases as it flows in the capillary tube. The mass flow rate and the tube diameter (hence the area) being constant, the velocity of the refrigerant increases since $\dot{m} = \rho VA$. The increase in velocity or acceleration of the refrigerant also requires a pressure drop.

The word capillary is a misnomer since surface tension is not important in refrigeration application of capillary tubes. The tube diameters range from 0.4 mm to 2 mm and the length ranges from 0.6 m to 6 m.

Once a capillary tube of some dimensions has been installed in a refrigeration system, the mass flow rate through it will vary in such a manner that the total pressure drop through it matches the pressure difference between the condenser and the evaporator. For a capillary tube of given bore and length, the mass flow rate through it is totally dependent upon the pressure difference across it; the mass flow rate cannot adjust itself in response to variations in load.

9.2.1 Balance Point between the Compressor and the Capillary Tube

The compressor and the capillary tube, under steady state must arrive at some suction and discharge pressures, which allow the same mass flow rate through the compressor and the capillary tube. This state is called the *balance point*. Condenser and evaporator pressures are the saturation pressures at the corresponding condenser and evaporator temperatures. Hence, each condenser pressure corresponds to a value of saturation condenser temperature and similarly each evaporator pressure corresponds to a value of saturation evaporator temperature. Figure 9.1 shows the variation in mass flow rate through the compressor against the evaporator pressure/temperature and the capillary tube for three values of condenser temperature, namely 30°C, 40°C and 50°C.

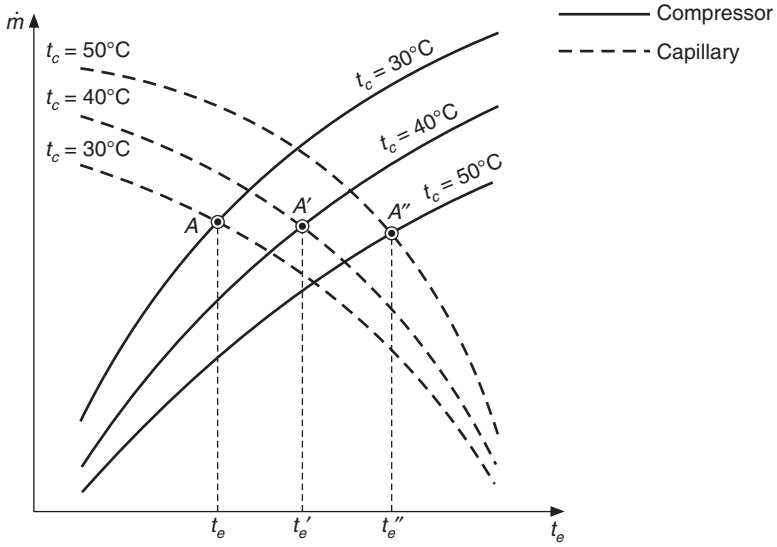

Figure 9.1 Variation in refrigerant mass flow rate through the compressor and the capillary tube with the evaporator and condenser temperatures (*A*, *A′* and *A″* are the balance points).

The mass flow rate through the compressor decreases if the pressure ratio increases since the volumetric efficiency of the compressor decreases with the increase in pressure ratio. In fact, at a particular value of the pressure ratio the volumetric efficiency and consequently the mass flow rate become zero. The pressure ratio increases when either the evaporator pressure decreases or the condenser pressure increases. Hence, the mass flow rate through the compressor decreases

with increase in condenser pressure and with decrease in evaporator pressure. The variation in mass flow rate with evaporator pressure/temperature is shown for three condenser temperatures namely 30°C, 40°C and 50°C in Figure 9.1.

The pressure difference across the capillary tube is the driving force for the refrigerant to flow through it, hence the mass flow rate through the capillary tube increases with increase in the pressure difference across it. Thus the mass flow rate through the capillary tube increases with increase in condenser pressure at a fixed evaporator pressure, or decrease in evaporator pressure at a fixed condenser pressure. The variation in mass flow rate through the capillary tube is shown for three condenser temperatures, namely, 30°C, 40°C and 50ºC in Figure 9.1. This is the opposite of the effect of pressure on the compressor mass flow rate. Hence, for a given value of the condenser pressure, there is a definite value of the evaporator pressure at which the mass flow rates through the compressor and the evaporator are the same. This pressure is the *balance point* that the system will acquire in steady state. Hence, for a given condenser temperature, there is a definite value of evaporator temperature at which the balance point will occur. Figure 9.1 shows a set of three balance points A, A' and A'' for the three condenser temperatures 30°C, 40°C and 45ºC. These balance points occur at evaporator temperatures of t_e , $t_{e'}$ and $t_{e''}$. It is observed that the evaporator temperature at balance point increases with the increase in condenser temperature.

However, the capillary tube and compressor are not at complete liberty to fix the balance point. The heat transfer rates requirement of the evaporator must also be met at that evaporator temperature that is $Q_e = U_e A_e (t_e - t_r)$, where t_r is the temperature of refrigerated space.

9.2.2 Effect of Load Variation

The situation described in Section 9.2.1 is in steady state. A sudden variation in the refrigeration load may change the balance point between the compressor and the capillary tube. The capillary tube based systems usually do not have a reservoir (accumulator) and are the flooded evaporator type systems. In a flooded evaporator the whole surface area of the evaporator is in contact with the liquid refrigerant.

Increase in refrigeration load

If the refrigeration load increases, there is a tendency for the evaporator temperature to increase. This situation is shown in Figure 9.2 for a condenser temperature of 44ºC. The balance point is shown by point A. As the load increases, the evaporator temperature rises to point C. At point C the mass flow rate through the compressor, $\dot{m}_{\text{comp}}$, is seen to more than $\dot{m}_{\text{cap}}$ through the capillary tube. In such a situation, the compressor will draw more refrigerant through the evaporator than the capillary tube can supply to it. This will lead to *starving* of the evaporator and the evaporator pressure will decrease since the compressor will try to evacuate the evaporator. But emptying of the evaporator cannot continue indefinitely. The system will take some corrective action since changes are occurring in the condenser as well.

Corrective action: Since the capillary tube feeds less refrigerant to the evaporator, the refrigerant accumulates in the condenser. The accumulation of refrigerant in the condenser reduces the effective area of the condenser that is available for heat transfer. The condenser heat transfer rate is given by, $Q_c = U_c A_c (t_c - t_\infty)$. If the heat transfer coefficient U_c and t_∞ are constant, then for the same heat transfer rate a decrease in area A_c will lead to a higher condenser temperature t_c. It is

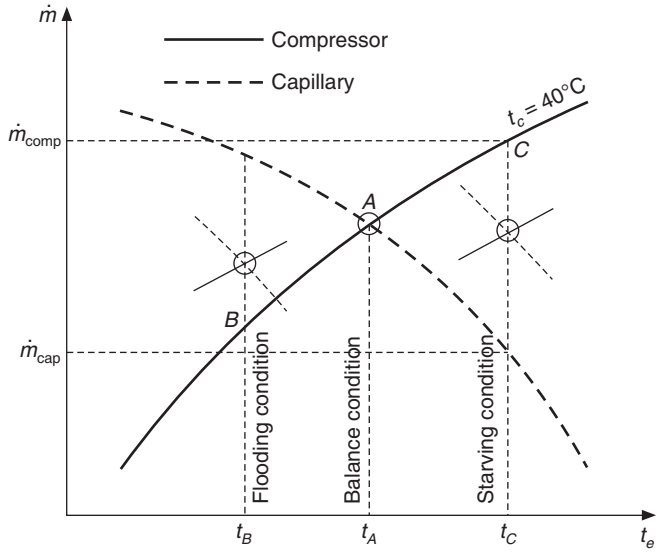

Figure 9.2 Effect of load variation on capillary tube based refrigeration systems. *A:* Design point; *B:* At low load; *C:* At high load.

observed from Figure 9.1 that an increase in condenser temperature leads to a decrease in compressor mass flow rate and an increase in capillary mass flow rate. Hence, the system will find a new balance point at a higher condenser temperature. If an accumulator were present in the system, then the extra refrigerant from the condenser will be stored in it and the condenser temperature will not increase in response to change in load.

The second possibility is that at a lower evaporator mass flow rate, the Reynolds number decreases and as a result the heat transfer coefficient U_e decreases. Or in a flooded evaporator, the reduction in mass flow rate reduces the wetted surface area and the heat transfer coefficient. Therefore, a larger temperature difference is required in the evaporator for the same amount of heat transfer. This decreases the evaporator temperature and the corresponding pressure to the previous values.

Decrease in refrigeration load

If the refrigeration load decreases, there is a tendency for the evaporator temperature to decrease, say to state *B* as shown in Figure 9.2. In this condition the capillary tube feeds more refrigerant to the evaporator than the compressor can remove. This leads to accumulation of liquid refrigerant in the evaporator causing *flooding* of the evaporator. This may lead to dangerous consequences if the liquid refrigerant overflows to the compressor causing *slugging* of the compressor. This has to be avoided at all costs; hence the capillary tube based refrigeration systems use *critical charge* as a safety measure. Critical charge is a definite amount of refrigerant that is put into the refrigeration system so that in the eventuality of all of it accumulating in the evaporator, it will just fill the evaporator up to its brim and never overflow from evaporator to compressor. (Capillary tube based systems do not use a receiver. The receiver keeps the condenser drained of liquid and the entire refrigerant is in the evaporator.) The flooding of the evaporator is also a transient phenomenon, it cannot continue indefinitely. The system has to take some corrective action.

Corrective action: Since the capillary tube is fed with more refrigerant from the condenser, the liquid seal at the condenser-exit breaks and some vapour enters the capillary tube. The vapour has a very small density compared to the liquid; as a result the mass flow rate through the capillary tube decreases drastically as suggested by Staebler [1948]. This is not desirable since the refrigeration effect, as shown in Figure 9.3, decreases and the COP also decreases. Hence, attempts are made in all the refrigeration plants to subcool the refrigerant before entry to the expansion device. A vapour-to-liquid subcooling heat exchanger is usually employed, wherein the low temperature refrigerant vapour leaving the evaporator subcools the liquid leaving the condenser as shown in Figure 9.4.

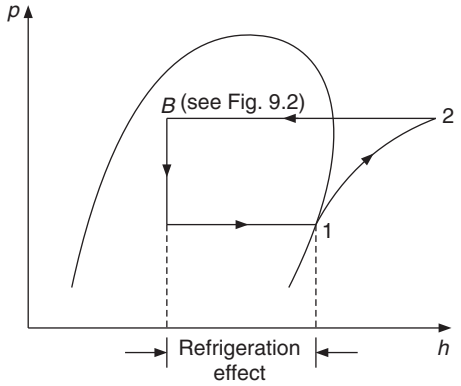

Figure 9.3 Reduction in refrigeration effect when vapour enters the capillary tube.

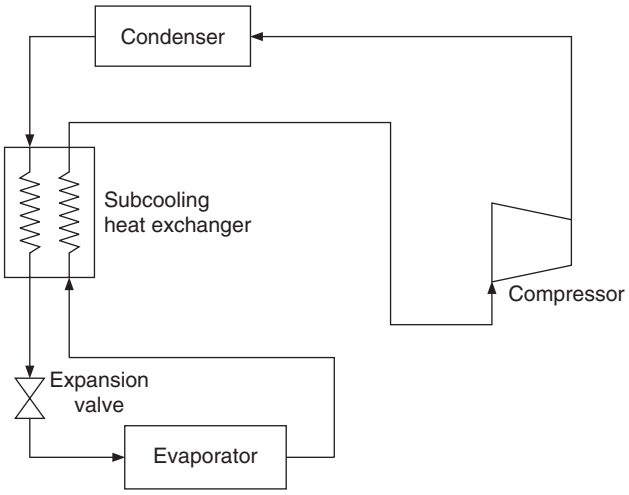

Figure 9.4 Vapour compression refrigeration system with subcooling heat exchanger.

9.2.3 Selection of Capillary Tube

For any new system, the diameter and the length of capillary tube have to be selected by the designer such that the compressor and the capillary tube achieve the balanced point at the desired evaporator temperature. There are analytical and graphical methods to select the capillary tube.

The *fine-tuning* of the length is finally done by the *cut-and-try* method. A tube longer than the design (calculated) value is installed with the expected result that the evaporating temperature will be lower than that expected. The tube is shortened until the desired balance point is achieved. This procedure is followed for mass production. If a single system is to be designed, then a tube of slightly shorter length than the design length is chosen. This tube will usually result in a higher temperature than the design value. The tube is pinched at a few spots to obtain the required pressure and temperature.

Analytical method

The analysis of flow through a capillary tube is one of the interesting problems that illustrates how a simple one-dimensional analysis yields good results. Hopkins [1950] and Cooper et al. [1957] originally suggested this method but it has been considerably modified for use with digital computers. The flow through a capillary tube is actually compressible, three-dimensional and two-phase flow with heat transfer and thermodynamic metastable state at the inlet of the tube. However, to simplify the analysis the flow is assumed to be steady, one-dimensional and in a single phase or a homogeneous mixture. One-dimensional flow means that the velocity is independent of the radius of tube. Homogeneous means annular flow or plug flow model etc., which are not considered for the two-phase flow. Figure 9.5 shows a small section of a vertical capillary tube with momentum and pressure at two ends of an elemental control volume. Considering mass conservation and momentum conservation for a control volume shown in the figure, we get:

Mass conservation:

$$\rho VA + \frac{\partial(\rho V)}{\partial y}\Delta y\, A - \rho VA = 0$$

or

$$\frac{\partial(\rho V)}{\partial y} = 0 \qquad \therefore \quad \rho V = \text{constant} \tag{9.1}$$

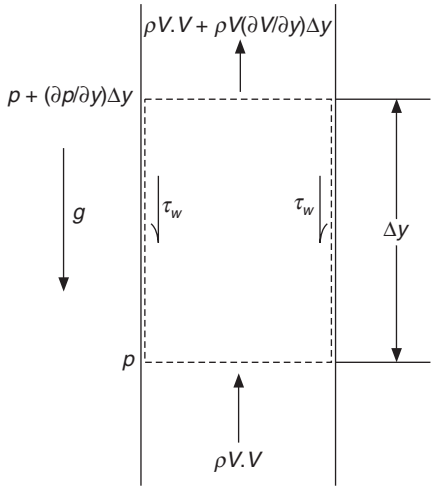

Figure 9.5 A small section of a capillary tube considered for analysis.

Momentum conservation:

The momentum theorem is applied to the control volume. According to this theorem,

$$[\text{Momentum}]_{\text{out}} - [\text{Momentum}]_{\text{in}} = \text{Total forces on control volume}$$

$$\pi R^2 \left(\rho V \cdot V + \rho V \frac{\partial V}{\partial y} \Delta y \right) - \pi R^2 (\rho V \cdot V) = -\pi R^2 \frac{\partial p}{\partial y} \Delta y - \rho_{\text{avg}} \pi R^2 \Delta y - 2\pi R \Delta y \tau_w \quad (9.2)$$

At the face $y + \Delta y$, Taylor series expansion has been used for pressure and momentum and only the first-order terms have been retained. The second-order terms with second derivatives and higher-order terms have been neglected. If the above equation is divided by $\pi R^2 \Delta y$ and limit $\Delta y \to 0$ is taken, then all the higher-order terms will tend to zero if these were included since these will have Δy or its higher power of Δy multiplying them. Also, ρ_{avg} will tend to ρ since the control volume will shrink to the bottom face of the control volume where ρ is defined. Further, neglecting the gravity, we obtain

$$\rho V \frac{\partial V}{\partial y} = -\frac{\partial p}{\partial y} - 2\frac{\tau_w}{R} \quad (9.3)$$

The wall shear stress may be written in terms of friction factor. In fluid flow through pipes the pressure decreases due to shear stress. This will be referred to as frictional pressure drop and a subscript '*f*' will be used with it and it will be written in terms of friction factor. The Darcy's friction factor is for fully developed flow in a pipe. In fully developed flow the velocity does not change in the flow direction. In our case it is increasing. Still it is a good approximation to approximate the shear stress term by friction factor. For fully developed flow the left hand side of Eq. (9.3) is zero, hence the frictional pressure drop Δp_f may be obtained from the following equation:

$$\tau_w = R\Delta p_f / (2\Delta y) \quad (9.4)$$

The friction factor is defined as

$$\Delta p_f = \rho f \frac{\Delta y}{D} \frac{V^2}{2} \quad (9.5)$$

Substituting Eq. (9.5) into Eq. (9.4), we get

$$\tau_w = \rho f \frac{V^2}{8} \quad (9.6)$$

Substituting for τ_w in Eq. (9.3), we have

$$\rho V \frac{\partial V}{\partial y} = -\frac{\partial p}{\partial y} - \frac{\rho f V^2}{2D} \quad (9.7)$$

Mass conservation Eq. (9.1) indicates that the product ρV is constant in the tube. In fact, it is called *mass velocity* and is denoted by *G*. Therefore,

$$G = \rho V$$

We have mass flow rate, $\dot{m} = (\pi D^2 / 4)\rho V$

$$\therefore \qquad \rho V = \frac{\dot{m}}{A} = G = \text{constant} \tag{9.8}$$

Hence, Eq. (9.7) is rewritten as follows:

$$G\frac{\partial V}{\partial y} = -\frac{\partial p}{\partial y} - \frac{f V G}{2D} \tag{9.9}$$

In this equation the term on the left hand side is the acceleration of fluid. The first term on the right hand side is the pressure drop required to accelerate the fluid and to overcome the frictional resistance. The second term on the right hand side is the frictional force acting on the tube wall. The friction factor depends upon the flow Reynolds number and the wall roughness for the fully developed flow. For the developing flow it is a function of the distance along the tube, in addition to Reynolds number. The flow accelerates along the tube due to vapour formation, as a result, the Reynolds number increases along the tube. The velocity and Reynolds number vary in a complex manner along the tube and these are coupled together. Hence, an exact solution of Eq. (9.9) is not possible. To a good approximation the integral of the product $f V$, that is, $\int f V\, dy$ can be calculated by assuming an average value of the product $f V$ over a small length ΔL of the capillary tube.

Accordingly, integrating Eq. (9.9) over a small length ΔL of the capillary tube, we obtain

$$G\,\Delta V = -\Delta p - (f V)_{\text{mean}}\,\frac{G}{2D}\,\Delta L \tag{9.10}$$

or
$$\Delta p = G\,\Delta V + (G/2D)\,(f V)_{\text{mean}}\,\Delta L \tag{9.11}$$

where, $\Delta V = V_{i+1} - V_i$ and $\Delta p = p_{i+1} - p_i$

and Δp is negative since $p_i > p_{i+1}$.

Equation (9.11) may be expressed as follows:

$$\Delta p = \Delta p_{\text{accln}} + \Delta p_f$$

This means that the total pressure drop over a length ΔL is the sum of that required for acceleration and that required to overcome the frictional resistance.

For laminar flow the effect of wall roughness is negligible and the friction factor is given by

$$f = 64/\text{Re} \tag{9.12}$$

For turbulent flow the friction factor increases with the increase in the roughness ratio. Moody's chart gives the variation of friction factor with Reynolds numbers for various roughness ratios. Moody's chart is available in many Fluid Mechanics textbooks. A number of empirical expressions for friction factor are also available in standard textbooks on Fluid Mechanics. One such expression for the smooth pipe, known as Blasius correlation is as follows:

$$f = 0.3164\text{Re}^{-0.25} \approx 0.32\text{Re}^{-0.25} \qquad \text{for Re} < 10^5 \tag{9.13}$$

The solution procedure for Eq. (9.11) as suggested by Hopkins [1950] and Cooper and Brisken [1957] is described below.

The condenser and evaporator temperatures t_c and t_e, the refrigerant and its mass flow rate are usually specified and the length and the bore of the capillary tube are required to be found out. Equation (9.11) is valid for a small length of the tube. Hence, the tube is divided into small lengths ΔL_i such that across each incremental length a temperature drop Δt_i of say 5 degree or 1 degree takes place depending upon the accuracy of the calculations required. The length of the tube ΔL_i for temperature to drop by, say, 1°C is found from Eq. (9.11). The temperature base is taken for calculations instead of the pressure base since the refrigerant properties are available on the basis of temperature.

1. Assume an appropriate diameter D for the tube. At condenser exit and inlet to capillary tube point "0" shown in Figure 9.6, say, the state is saturated liquid state. Hence,

$$v_0 = v_f, \quad h_0 = h_f, \quad \mu_0 = \mu_f$$

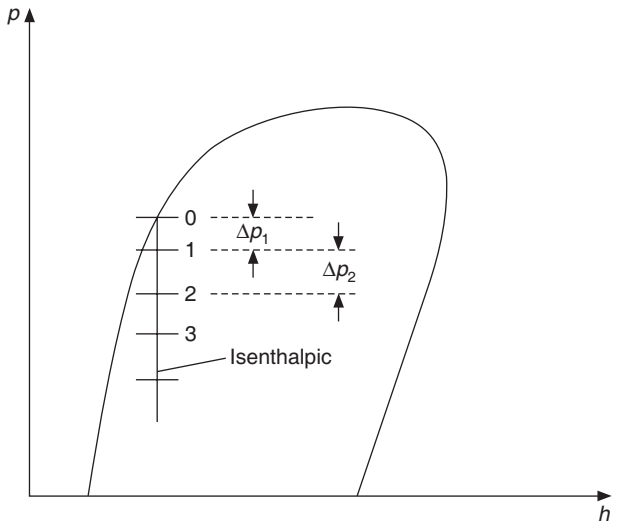

Figure 9.6 The step-wise procedure on *p–h* diagram for calculating the length of the capillary tube.

and $\dot{m}$ is known from the thermodynamic cycle calculation for the given cooling capacity.

$$\therefore \qquad \text{Re} = \frac{4\dot{m}}{\pi D \mu}$$

$$G = \frac{\dot{m}}{A} = \rho V = V/v$$

The constants in Eq. (9.11), i.e. G, $G/(2D)$ and $4\dot{m}/\pi D$ required for solution are then calculated.

2. At the inlet $i = 0$: $(\text{Re})_0 = \dfrac{4\dot{m}}{\pi D \mu_0}$, $f_0 = 0.32\ (\text{Re})^{-0.25}$ and $V_0 = v_0 G$

3. At $i = 1$ in Figure 9.6: $t_1 = t_c - \Delta t_1$, find the saturation pressure p_1 at t_1.
   The saturation properties v_{1f}, v_{1g}, h_{1f}, h_{1g} and μ_{1f} and μ_{1g} are obtained at t_1. It is assumed that the enthalpy remains constant during expansion as shown in Figure 9.6.
4. If x_1 is the dryness fraction at $i = 1$, then

$$h_0 = h_1 = x_1 h_{1g} + (1 - x_1)\, h_{1f} \tag{9.14}$$

$$\therefore \quad x_1 = \frac{h_0 - h_{1f}}{h_{1g} - h_{1f}}$$

5. Find $v_1 = x_1 v_{1g} + (1 - x_1)\, v_{1f}$
   Assuming that the viscosity of the mixture can be taken as the weighted sum of the viscosity of saturated liquid and vapour, we get

$$\mu_1 = x_1 \mu_{1g} + (1 - x_1)\, \mu_{1f}$$

$$(\mathrm{Re})_1 = \frac{4\dot{m}}{\pi D \mu_1}, \quad f_1 = 0.32(\mathrm{Re})^{-0.25} \quad \text{and} \quad V_1 = v_1 G$$

$$\Delta V = V_1 - V_0$$

$$\Delta p_1 = p_0 - p_1$$

$$(fV)_{\text{mean}} = \frac{f_0 V_0 + f_1 V_1}{2}$$

   Hence, from Eq. (9.11) the incremental length ΔL_1 of capillary tube for the first step is

$$\Delta L_1 = \frac{-\Delta p_1 - G \Delta V}{(G/2D)(f\,V)_{\text{mean}}}$$

6. For the next section $i = 2 : t_2 = t_1 - \Delta t_2$, find the saturation pressure p_2 at t_2. The saturation properties v_{2f}, v_{2g}, h_{2f}, h_{2g} and μ_{2f} and μ_{2g} are obtained at temperature t_2.
7. Assuming the enthalpy to remain constant, that is $h_2 = h_1 = h_0$, the quality x_2 is found and steps 4 and 5 are repeated to find the incremental length ΔL_2.

Steps 4 and 5 are repeated for all the intervals up to evaporator temperature and all the incremental lengths are summed up to find the total length of the capillary tube.

It is observed from Eq. (9.11) that the total pressure drop Δp is the sum of the pressure drops due to acceleration, that is, $\Delta p_{\text{accln}} = G\, \Delta V$ and the pressure drop due to friction, that is, $\Delta p_f = (G/2\Delta)(f\,V)_{\text{mean}}\, \Delta L$. It may so happen under some conditions that after a few steps of calculation, the total pressure drop required for a segment may become less than the pressure drop required for acceleration alone, i.e. $\Delta p < \Delta p_{\text{accln}}$. The increment length ΔL for this segment will turn out to be negative which has no meaning. This condition occurs when the velocity of refrigerant has reached the velocity of sound $\sqrt{\gamma RT}$. This condition is called *choked flow condition*. The velocity of fluid cannot exceed the velocity of sound in a tube of constant diameter, hence the calculation cannot proceed any further. The flow is said to be choked-flow and the mass flow rate through the tube has reached its maximum value for the selected tube diameter. For a capillary tube of constant diameter, choked-flow condition represents the minimum suction pressure that can be achieved. If further pressure drop is required, then a tube of larger diameter should be chosen in which the velocity of sound occurs at longer length.

Figure 9.7 shows the variation in mass flow rate with suction pressure for a fixed condenser pressure. The mass flow rate through the capillary tube increases as the evaporator pressure decreases. However at a pressure of p_e^* the flow is choked. If the choking occurs at some interior point of the tube, the length of the tube from this point to the exit will offer frictional resistance to the flow and the pressure must decrease to overcome this. The pressure, however, cannot decrease since the flow is choked. Hence, an adjustment in the inlet conditions occurs and the mass flow rate is reduced so that the flow will (always) be choked at the exit of the tube with reduced mass flow rate. This is typical of compressible sonic flow where the upstream influence occurs; otherwise the downstream pressure decides the mass flow rate.

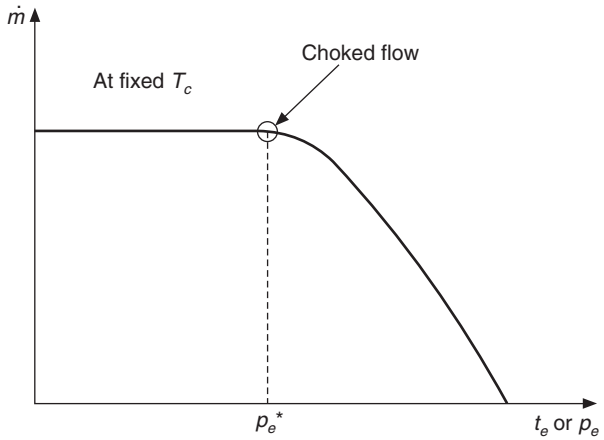

Figure 9.7 Variation in mass flow rate with suction pressure for a fixed condenser pressure.

Shortcomings of the above analysis

We have assumed that the expansion is a constant enthalpy process. This is not true since there is a large change in kinetic energy. In fact the kinetic energy increases at a very fast rate as the velocity becomes sonic and the flow becomes choked. The first law of the thermodynamics indicates that in the absence of heat transfer, the work done and the change in potential energy for a system in steady state, the sum of enthalpy and the kinetic energy must remain constant. Hence, if the kinetic energy increases then the enthalpy must decrease, as a result the quality of the refrigerant will be lower than that calculated by assuming constant enthalpy. The actual state of the refrigerant in a constant diameter adiabatic tube is represented by *Fanno line*, which is shown in Figure 9.8 on the *h*–*s* diagram along with the saturation curve. Fanno line is the solution of steady, compressible adiabatic flow with friction through a tube of constant diameter as illustrated in Shapiro [1953].

It is observed that in the early part of the capillary tube, the constant enthalpy line does not deviate very much from the Fanno line. In the latter part, the deviation from the Fanno line increases. Most of the length of the capillary tube happens to be in the latter portion where the quality and velocity changes are very significant; hence a constant enthalpy approximation may introduce a significant error.

Point *A* on the Fanno line is the point where the entropy is maximum. This point corresponds to choked flow condition. Pressure cannot drop below this value since it will require a decrease in entropy under adiabatic condition, which is not possible in a real system. This would mean violation of the second law of thermodynamics.

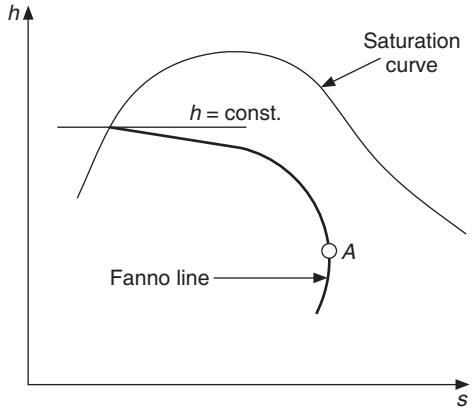

Figure 9.8 Fanno line for capillary tube on the *h–s* diagram.

Modified procedure

It is observed that the kinetic energy changes significantly in the later part of the capillary tube. In step 4 of the calculation procedure, enthalpy was assumed to be constant. To improve upon it, the quality is calculated by considering energy balance, that is, the sum of enthalpy and kinetic energy is assumed to remain constant. The quality of the mixture is not found from Eq. (9.14). Instead, the sum of enthalpy and kinetic energy is taken as constant. For the first segment, we get

$$h_0 + \frac{V_0^2}{2} = h_1 + \frac{V_1^2}{2} = h_1 + \frac{G^2 v_1^2}{2} \tag{9.15}$$

Substituting for h_1 and v_1 in terms of quality x_1 and properties at saturation, we get

$$x_1 h_{1g} + (1 - x_1) h_{1f} + \frac{G^2 [x_1 v_{1g} + (1 - x_1) v_{1f}]^2}{2} = h_0 + \frac{V_0^2}{2}$$

or

$$h_{1f} + x_1 h_{1fg} + \frac{G^2 (v_{1f} + x_1 v_{1fg})^2}{2} = h_0 + \frac{V_0^2}{2}$$

or

$$x_1^2 \left(v_{1fg}^2 \frac{G^2}{2} \right) + x_1 (G^2 v_{1f} v_{1g} + h_{1fg}) + (h_{1f} - h_0) + \left(\frac{G^2}{2} \right) v_{1f}^2 - \frac{V_0^2}{2} = 0$$

This is a quadratic equation in x_1 that can be solved to find x_1. The positive root of this equation is taken as the value of x_1. The enthalpy is usually given in kJ/kg and the velocity in m/s, hence to make the equation dimensionally consistent, the enthalpy is multiplied by 1000, that is

$$x_1^2 \left(v_{1fg}^2 \frac{G^2}{2} \right) + x_1 (G^2 v_{1f} v_{1fg} + 1000 h_{1fg}) + 1000 (h_{1f} - h_0) + \left(\frac{G^2}{2} \right) v_{1f}^2 - \frac{V_0^2}{2} = 0 \tag{9.16}$$

The remaining part of the procedure from step 5 to 6 remains the same. For all subsequent steps, the quality is calculated from Eq. (9.14).

Graphical procedure

A graphical procedure for capillary tube selection based on the data of Hopkins [2] and Whitesel has been presented in ASHRAE Handbook [8]. A representative Figure 9.9 gives the mass flow rate of R12 and R22 at various inlet pressures, subcooling and dryness fraction through a capillary tube of 1.63 mm diameter and 2.03 m length. The companion Figure 9.10 gives the flow correction factor for diameters and lengths different from those used in Figure 9.9. These plots are for choked flow conditions. Corrections for non-choked flow conditions are given in *ASHRAE Handbook*.

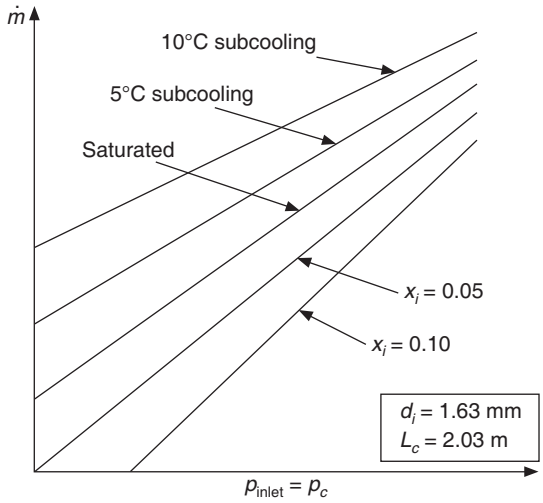

Figure 9.9 Variation of refrigerant mass flow rate with inlet state for the standard capillary tube (choked flow condition).

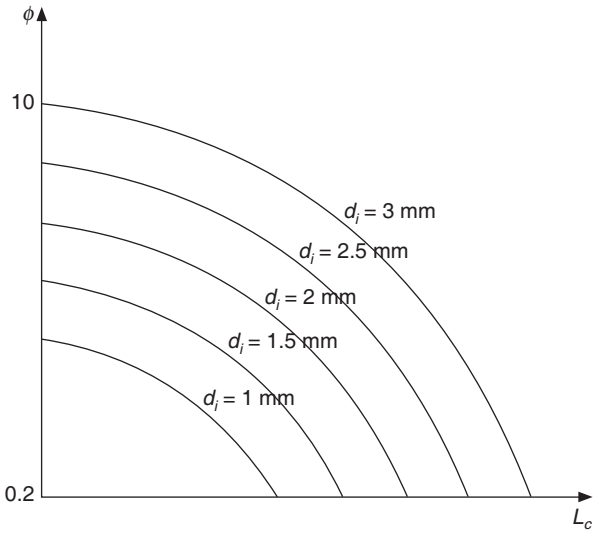

Figure 9.10 Variation of flow correction factor ϕ with capillary tube length and diameter (choked flow condition).

Advantages of capllary tube

Some of the advantages of capillary tube are:

1. It is inexpensive.
2. It does not have any moving parts hence it does not require maintenance.
3. Capillary tube provides an open connection between the condenser and the evaporator, hence during off-cycle, pressure equalization occurs between the condenser and the evaporator. This reduces the starting torque requirement of the motor since the motor starts with the same pressure on the two sides of the compressor. Hence, a motor with low starting torque (squirrel cage induction motor) can be used.

Disadvantages of the capillary tube

Some of the disadvantages of the capillary tube are:

1. It cannot adjust itself to changing flow conditions in response to daily and seasonal variation in ambient temperature and load. Hence the COP is usually low under off-design conditions.
2. It is susceptible to clogging because of the narrow bore of the tube.
3. During off-cycle the liquid refrigerant flows to evaporator because of low pressure in the evaporator. The evaporator may get flooded and the liquid refrigerant may flow to compressor and damage it when it starts. Therefore, a critical charge is used in capillary tube based systems. Further, it is used only with hermetically sealed compressors where the refrigerant does not leak so that the critical charge can be used.

9.3 AUTOMATIC EXPANSION VALVE

The automatic expansion valve acts in such a manner so as to maintain a constant pressure in the evaporator and thereby a constant temperature in the evaporator. Hence it is also known as constant pressure valve. The schematic diagram of the valve is shown in Figure 9.11.

The valve has an adjustment spring that can be adjusted to maintain the required temperature in the evaporator. This exerts force F_s on the top of the bellows. The atmospheric pressure, p_o, also acts on top of the bellows and exerts a force of $F_o = p_o A_b$, A_b being the area of the bellows. The evaporator pressure p_e acts below the bellows since this is in communication with the outlet of the orifice by the pressure equalizer holes around the pushpins. If a stuffing box is provided around the pushpins then this pressure cannot be transmitted to the bottom of bellows. An external opening is provided to feed evaporator pressure to the bottom of the bellows. The force due to evaporator pressure is $F_e = p_e A_b$. The net downward force $F_s + F_o - F_e$ is fed to the needle stand by the bellows through the pushpins. This net force along with the force due to the follow-up spring F_{fs} controls the location of the needle with respect to the orifice and thereby controls the orifice opening.

If $F_e + F_{fs} > F_s + F_o$ the needle will be pushed against the orifice and the valve will be fully closed.

On the other hand if $F_e + F_{fs} < F_s + F_o$, the needle will be away from the orifice and the valve will be open. Hence the relative magnitudes of these forces control the mass flow rate through the expansion valve.

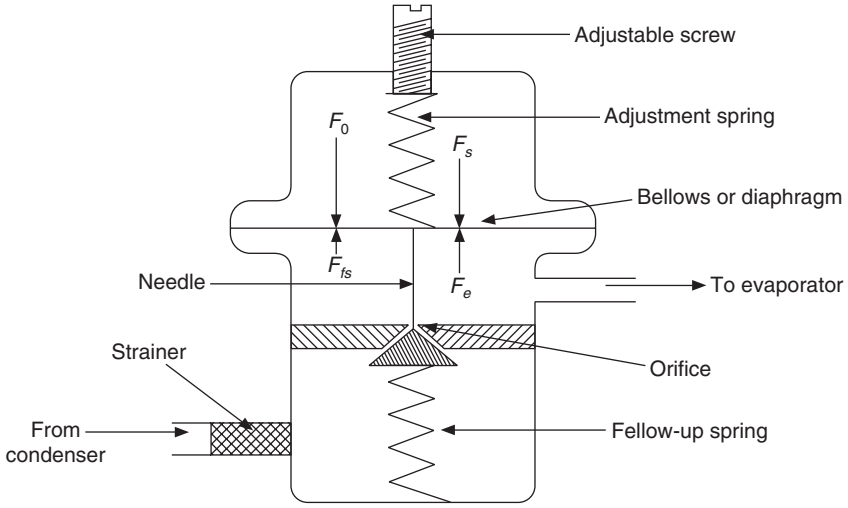

Figure 9.11 Schematic of an automatic expansion valve.

The adjustment spring is usually set such that during off-cycle the valve is closed, that is, the needle is pushed against the orifice. Hence,

$$F_{eo} + F_{fso} > F_{so} + F_o$$

where the subscript $_o$ refers to forces during off-cycle.

During the off-cycle, the refrigerant remaining in the evaporator continues to vaporize but is not taken out by the compressor. As a result the evaporator pressure rises during the off-cycle as shown in Figure 9.12.

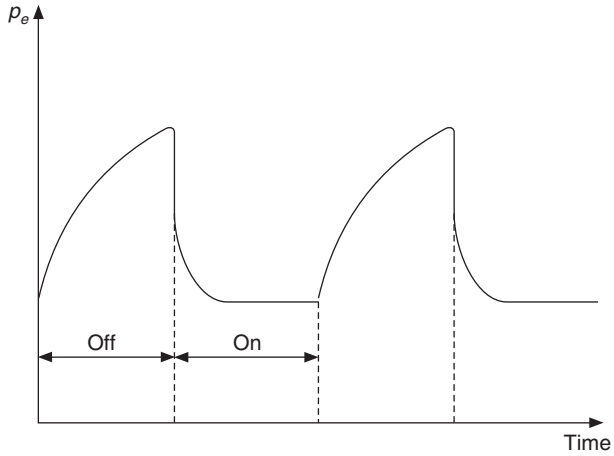

Figure 9.12 Variation of evaporator pressure during the on- and off-cycles of an automatic expansion valve based refrigeration system.

When the compressor is started after the off-cycle period, the evaporator pressure p_e starts decreasing at a very fast rate since the valve is closed; refrigerant is not fed to evaporator while the compressor removes the refrigerant from the evaporator. As p_e decreases the force F_e decreases from F_{eo} to $(F_{eo} - \Delta F_e)$. At one stage, the sum $F_e + F_{fs}$ becomes less than $F_s + F_o$, as a result the needle stand moves downwards (away from the needle stand) and the valve opens. Under this condition,

$$(F_{eo} - \Delta F_e) + F_{fso} < F_{so} + F_o$$

When the refrigerant starts to enter the evaporator, the evaporator pressure does not decrease at the same fast rate as at the starting time. Thus, the movement of the needle stand will slow down as the refrigerant starts entering the evaporator. As the needle moves downwards, the adjustment spring elongates, therefore the force F_s decreases from its off-cycle value of F_{so}, the decrease being proportional to the movement of the needle stand.

As the needle moves downwards, the follow-up spring is compressed; as a result, F_{fs} increases from its off-cycle value. Hence, the final equation may be written as

$$(F_{eo} - \Delta F_e) + (F_{fso} + \Delta F_{fs}) = (F_{so} - \Delta F_s) + F_o$$

or

$$F_e + F_{fs} = F_s + F_o = \text{constant} \tag{9.17}$$

The constant is the sum of force due to spring force and the atmospheric pressure, hence it depends upon the position of the adjustment spring. This will be the equilibrium position. Then onwards, the valve acts in such a manner that the evaporator pressure remains constant as long as the refrigeration load is constant. At this point, the mass flow rate through the valve is the same as that through the compressor.

9.3.1 Effect of Load Variation

The mass flow rate through the valve is directly proportional to the pressure drop through the orifice $(p_c - p_e)$ and the area of the orifice opening (needle position). At constant condenser pressure the mass flow rate will decrease if the evaporator pressure p_e increases or as the orifice opening becomes narrower.

Decrease in load

If the refrigeration load decreases, there is a tendency in the flooded evaporator for the evaporator temperature to decrease and thereby the evaporator pressure (saturation pressure) also decreases. This decreases the force F_e. The sum $F_e + F_{fs}$ will become less than the sum on the right hand side of Eq. (9.17) and the needle stand will be pushed downwards opening the orifice wider. This will increase the mass flow rate through the valve. This is opposite of the requirement since at lower load, a lower mass flow rate of the refrigerant is required. This is the drawback of this valve that it counteracts in an opposite manner since it tries to keep the evaporator pressure at a constant value. In Figure 9.13, point *A* is the normal position of the valve and *B* is the position at reduced load and wider opening. It is observed that both these positions are at same evaporator pressure. The compressor capacity remains the same as at *A*. The valve feeds more refrigerant to the evaporator than the compressor can remove from the evaporator. This causes accumulation of liquid refrigerant in the evaporator. This is called *flooding* of the evaporator. The liquid refrigerant may fill the

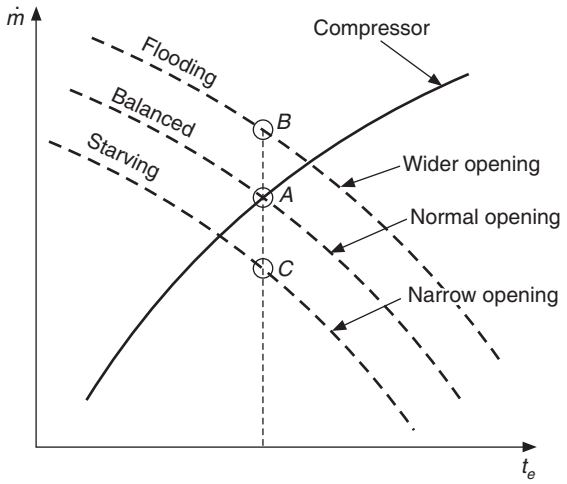

Figure 9.13 Effect of load variation on the balance point of the system using AEV.

evaporator and it may overflow to the compressor causing damage to it. Flooding of the evaporator can occur otherwise as well, if the heat transfer rate in the evaporator is made to decrease by some other means. The heat transfer rate Q_e to evaporator is expressed in terms of the overall heat transfer coefficient U_e, the heat transfer area A_e and the temperature difference Δt as follows:

$$Q_e = U_e A_e \Delta t$$

Q_e and A_e being constant, if U_e decreases then Δt increases. Δt is the temperature difference between say the cooled space and the evaporator. The evaporator temperature t_e decreases as $\Delta t = (t_e - t_r)$ increases since the temperature of the cooled space takes more time to respond. In this event too, the flooding of the evaporator may occur.

Increase in load

On the other hand if the refrigeration load increases or the evaporator heat transfer rate increases, the evaporator temperature and pressure will increase for a flooded evaporator. This will increase F_e. A look at the schematic diagram (Figure 9.11) reveals that this will tend to move the needle stand upwards, consequently making the orifice opening narrower and decreasing the mass flow rate. Again the valve counteracts in a manner opposite to what is required. This shifts the operating point from A to point C where the compressor draws out more refrigerant than that fed by the expansion valve leading to *starving* of the evaporator.

The adjustment of evaporator pressure and temperature is carried out by the adjustment spring. An increase in the tension of the adjustment spring increases F_s so that the evaporator pressure at which balance occurs, increases. That is, the regulated temperature increases.

9.3.2 Applications

The automatic expansion valves (AEVs) are simple in design and economical. In some valves a diaphragm is used in place of bellows. AEVs are used in home freezers and small commercial refrigeration systems where sealed compressors are used. Critical charge has to be used since the

system using AEV is prone to flooding. It is used in systems of less than 10 TR capacities with critical charge. Essentially, it is used wherever a constant temperature is required, for example, milk chilling units and water coolers where freezing is disastrous. In air-conditioning systems AEV is used when the humidity control is by DX coil temperature .The flooding can be prevented by putting off the refrigeration system when the desired temperature is achieved.

When the temperature of the room or the medium to be cooled reaches a desired value, some kind of control must be used to stop the compressor and start it again when the temperature increases. This is done since at temperatures lower than the desired temperature, flooding of evaporator and consequent slugging of compressor can occur. Also, some saving in energy can be realized; hence a direct control on the compressor is desirable.

In such situations, an evaporator thermostat rather than a room thermostat is recommended to prevent flooding. As the room temperature decreases, the load on the plant may decrease resulting in an increase in mass flow rate of refrigerant. Since the entire refrigerant may not evaporate in the evaporator, the liquid may enter the suction line, atmospheric moisture may freeze on its outer surface and frost it up, and eventually wet vapour may enter the compressor and causes slugging. To avoid frosting of the suction line, a thermostat can be put on the suction line slightly away from the evaporator outlet. The room temperature as well as the suction line temperature, however, affect the thermostat. The thermostat will put off the power supply to the compressor when the set value of temperature is reached. This will lead to an on-off cycle operation. The temperature variation or evaporator pressure variation will be as shown in Figure 9.12.

The initial pressure p_{e1} corresponds to the initial room temperature. The cut-off pressure for the thermostat is p_{e3}, while p_{e2} is the cut-in pressure for starting the refrigeration system.

The pressure limiting characteristics of AEV valve can be used to advantage when protection is required against overload of compressor due to high suction pressure.

9.3.3 Flow Rate Through Orifice

Let A_1 and A_2 be the areas at the inlet and the outlet of the orifice, where $A_1 > A_2$. Let V_1 and V_2 be the velocities, p_1 and p_2 the pressures and ρ_1 and ρ_2 be the densities at the inlet and outlet respectively of the orifice as shown in Figure 9.14. Then assuming steady, incompressible, inviscid flow and neglecting gravity, Bernoulli's equation may be used to write the flow rate through the orifice as follows.

Mass conservation:

$$\rho_1 V_1 A_1 = \rho_2 V_2 A_2 \tag{9.18}$$

Assuming $\rho_1 = \rho_2$, we get

$$\frac{V_1}{V_2} = \frac{A_2}{A_1}$$

Bernoulli's equation:

$$\frac{p_1}{\rho_1} + \frac{V_1^2}{2} = \frac{p_2}{\rho_2} + \frac{V_2^2}{2} \tag{9.19}$$

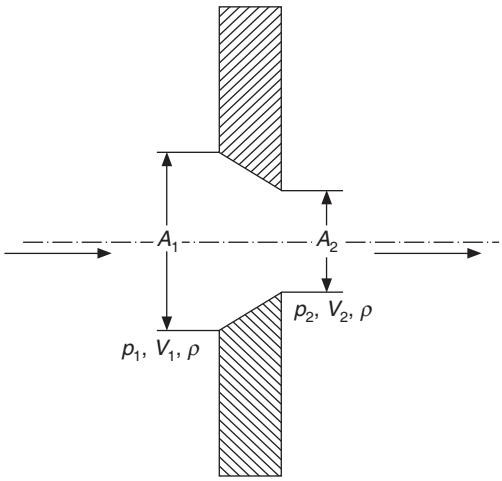

Figure 9.14 Fluid flow through the orifice of an automatic expansion valve.

Therefore,

$$\frac{p_1 - p_2}{\rho_1} = \frac{V_2^2}{2}\left(1 - \frac{V_1^2}{V_2^2}\right) = \frac{V_2^2}{2}\left(1 - \frac{A_2^2}{A_1^2}\right)$$

Ideal flow rate:

$$Q_{\text{ideal}} = A_2 V_2 = A_2 \sqrt{\frac{2(p_1 - p_2)}{\rho_1}} \frac{1}{\sqrt{1 - (A_2 / A_2)}} \tag{9.20}$$

Defining,

$$M = \frac{1}{\sqrt{1 - (A_2 / A_1)^2}}$$

we get

$$Q_{\text{ideal}} = MA_2 \sqrt{\frac{2(p_1 - p_2)}{\rho_1}} \tag{9.21}$$

The actual flow through the orifice is less than the ideal flow because viscous effects are not included in the above treatment. An empirical coefficient C_D, called *discharge coefficient*, is introduced to account for the viscous effects.

$$Q_{\text{actual}} = C_D Q_{\text{ideal}} = C_D M A_2 \sqrt{\frac{2(p_1 - p_2)}{\rho_1}} \tag{9.22}$$

Introducing the flow coefficient, $K = C_D M$

$$Q_{\text{actual}} = KA_2 \sqrt{\frac{2(p_1 - p_2)}{\rho_1}}$$

To account for compressibility, another empirical constant Y is introduced for actual mass flow rate. Hence, the mass flow rate is expressed as

$$\dot{m} = K\rho_1 Y A_2 \sqrt{\frac{2(p_1 - p_2)}{\rho_1}} \tag{9.23}$$

The area of the orifice opening is usually controlled to control the mass flow rate through the expansion valve. It is observed that the mass flow rate depends upon the difference between the condenser and evaporator pressures as well. It is curious that single-phase relations have been given above while it was shown that during expansion of high pressure liquid, the refrigerant flashes into a low pressure mixture of liquid and vapour as it flows through the expansion valve. Actually, the refrigerant remains in a thermodynamic metastable liquid state as it flows through the orifice of the expansion valve as explained by Pasqua [1953]. That is, it remains a liquid at a lower pressure and temperature during its passage through the orifice. It flashes into a mixture of liquid and vapour as soon as it emerges out of the orifice of the valve. This kind of phenomenon has been observed in the initial sections of transparent capillary tubes as well. This phenomenon is also observed in the steam nozzles.

9.4 THERMOSTATIC EXPANSION VALVE

The thermostatic expansion valve (TEV) is the most versatile expansion valve and is, therefore, most often used in refrigeration systems. It maintains a constant degree of superheat at the exit of the evaporator; hence it is most effective for dry evaporators in preventing the slugging of the compressors since it does not allow the liquid refrigerant to enter the compressor. The schematic diagram of the valve is given in Figure 9.14. The valve consists of a feeler bulb that is attached to the evaporator exit tube so that it senses the temperature at the exit of the evaporator. The feeler bulb is connected to the top of the bellows by a narrow tube. The feeler bulb and the narrow tube contain some fluid that is called power fluid. The power fluid may be the same as the refrigerant in the refrigeration system, or it may be different. In case it is different from the refrigerant, then the TEV is called *TEV with cross charge*. The pressure of the power fluid p_p is the saturation pressure corresponding to the temperature at the evaporator exit. If the evaporator temperature is t_e and the corresponding saturation evaporator pressure is p_e, then the purpose of TEV is to maintain a temperature $t_e + \Delta t_s$ at the evaporator exit, where Δt_s is the degree of superheat required from the TEV. The power fluid senses this temperature $t_e + \Delta t_s$ by the feeler bulb and its pressure p_p is the saturation pressure at this temperature. The force F_p exerted on top of bellows of area A_b due to this pressure is given by

$$F_p = A_b\, p_p \tag{9.24}$$

The evaporator pressure is exerted below the bellows through the clearance between pushpins and the body of the valves. In case the evaporator is large and has a significant pressure drop, the pressure from the evaporator exit is fed directly to the bottom of the bellows by a narrow tube. This is called pressure-equalizing connection. Such a TEV is called *TEV with pressure equalizer*. In such a TEV the clearance between the pushpins and the valve body is closed by stuffing boxes. The force F_e exerted due to this pressure p_e on the bottom of the bellows is given by

$$F_e = A_b\, p_e \tag{9.25}$$

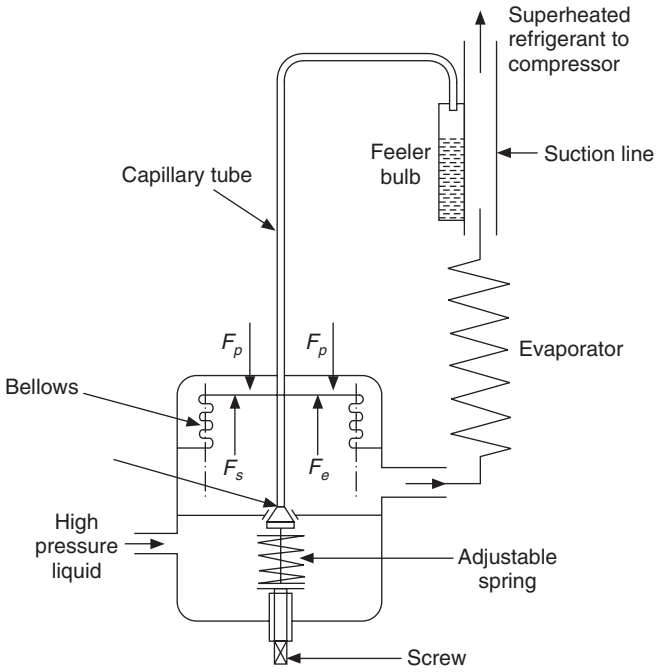

Figure 9.15 Schematic of a thermostatic expansion valve (TEV).

The difference of the two forces F_p and F_e is exerted on top of the needle stand by the pushpins. There is an adjustment spring below the needle stand that exerts an upward spring force F_s on the needle stand. There is a follow-up spring whose spring force is negligible (unlike in automatic expansion valve). In steady state, there will be a force balance on the needle stand, that is,

$$F_s = F_p - F_e \tag{9.26}$$

During off-cycle, the evaporator temperature is same as the room temperature throughout, that is, the degree of superheat Δt_s is zero. If the power fluid is the same as the refrigerant, then $p_p = p_e$ and $F_p = F_e$. Therefore any arbitrarily small spring force F_s acting upwards will push the needle stand against the orifice and keep the TEV closed. If it is *TEV with cross charge* or if there is a little degree of superheat during off cycle then for TEV to remain closed during the off-cycle, F_s should be slightly greater than $(F_p - F_e)$.

As the compressor is started, the evaporator pressure decreases at a very fast rate and hence the force F_e decreases at a very fast rate. This happens since TEV is closed and no refrigerant is fed to evaporator while the compressor draws out the refrigerant at a very fast rate and tries to evacuate the evaporator. The force F_p does not change during this period since the evaporator temperature does not change. Hence, the difference $F_p - F_e$, increases as the compressor runs for some time after starting. At one point this difference becomes greater than the spring force F_s and pushes the needle stand downwards opening the orifice. The valve is said to open up.

As the refrigerant enters the evaporator it arrests the fast rate of decrease in evaporator pressure. The movement of the needle stand also slows down. The spring, however, gets compressed as the

needle stand moves downwards to open the orifice. If F_{so} is the spring force in the rest position, that is, off-cycle, then during the open valve position

$$F_s = F_{so} + \Delta F_s$$

Eventually, the needle stand reaches a position such that

$$F_s = F_p - F_e = A_b\,(p_p - p_e) \tag{9.27}$$

That is, F_p is greater than F_e or p_p is greater than p_e. The pressures p_p and p_e are saturation pressures at temperature $(t_e + \Delta t_s)$ and t_e respectively. Hence, for a given setting force F_s of the spring, TEV maintains the difference between F_p and F_e or the degree of superheat Δt_s constant.

$$\Delta t_s \propto (F_p - F_e) \tag{9.28}$$

$$\propto F_s$$

This is irrespective of the level of p_e, that is, evaporator pressure or temperature, although the degree of superheat may be slightly different at different evaporator temperatures for the same spring force, F_s. It will be an ideal case if the degree of superheat is same at all evaporator temperatures for a given spring force.

9.4.1 Effect of Load Variation

The thermostatic expansion valve is used with the dry type evaporator. This evaporator may be a shell-and-tube type of evaporator with the refrigerant on the shell side and the liquid or brine to be cooled flowing through the tubes. The shell is not totally filled with the liquid refrigerant. The liquid refrigerant at the bottom of the shell will cool the brine flowing through the tubes, while at the top portion of the shell, the refrigerant vapour will cool the brine in the tubes. During this process, the vapour will become superheated. That is, some heat transfer area is provided in the evaporator for superheating the refrigerant vapour.

If the load on the plant increases, the evaporation rate of the liquid refrigerant increases, the level of liquid refrigerant in the shell decreases and therefore the area available for superheating the vapour increases. The degree of superheat increases, the pressure of the power fluid p_p increases, the needle stand is pushed down and the mass flow rate of the refrigerant increases. This is the ideal case. The evaporation rate of the refrigerant is proportional to the load and the mass flow rate supplied through the expansion valve is also proportional to the load.

On the other hand, if the load on the plant decreases, the evaporation rate of the refrigerant in the shell decreases, as a result the degree of superheat decreases. The thermostatic expansion reacts in such a way so as to reduce the mass flow rate through it.

The flow rate of the refrigerant in this valve is proportional to the evaporation rate of the refrigerant in the evaporator. Hence, this valve always establishes a balanced flow condition of flow between the compressor and itself.

9.4.2 Cross Charge

Figure 9.16 shows the saturated vapour line with pressure along the ordinate. The difference between p_p and p_e is proportional to the spring force F_s and their corresponding projection from the saturated

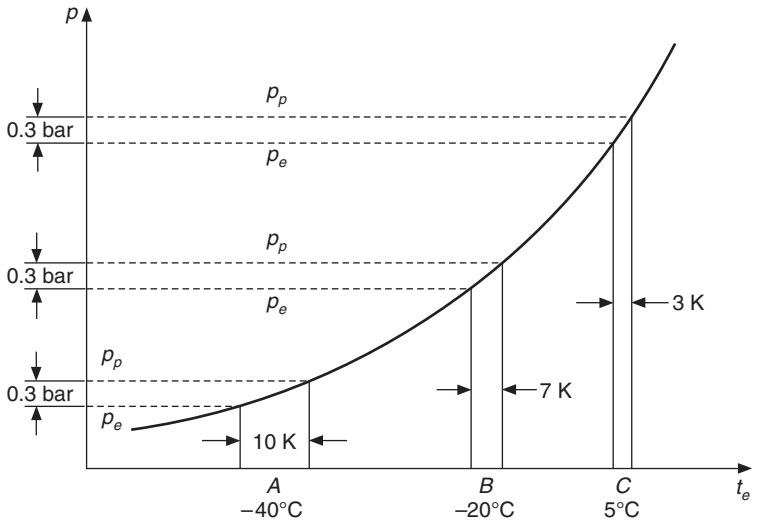

Figure 9.16 Vapour pressure curve of the refrigerant and power fluid.

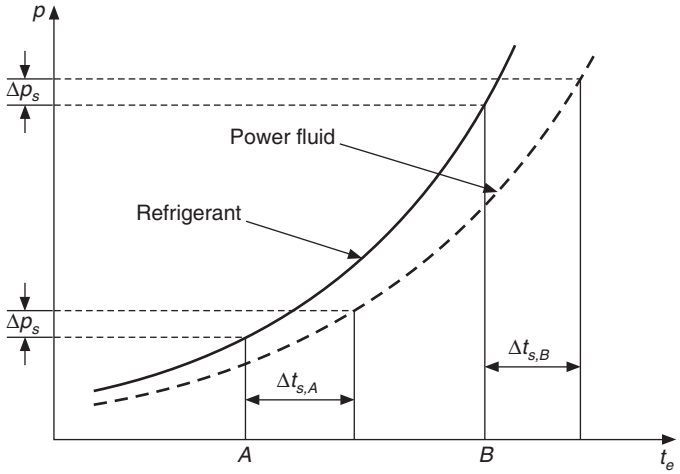

Figure 9.17 Vapour pressure curves of refrigerant and power fluid (cross-charged TEV).

vapour line is the degree of superheat given by a set of p_p and p_e. The figure shows three sets of p_p and p_e for the same spring force at three evaporator temperatures say – 40°C, –20°C and 5°C. It is observed that at location *A*, the degree of superheat is very large whereas at location *C* the degree of superheat is very small for the same spring force setting proportional to $(p_p - p_e)$. This would not have been the case if the saturated vapour line were a straight line. It is observed that if the spring is set for say a superheat of 5°C at –40°C evaporator temperature, the degree of superheat will become almost zero at higher temperatures. As a result, when the plant is started at warm temperature, there is a possibility of flooding the evaporator. If the degree of superheat is set to avoid flooding at say 5°C, then at the design point of say – 40°C, the superheat will be very large and it will starve the evaporator. This can be corrected if a fluid different from the refrigerant is used in the feeler

bulb as power fluid. Such a TEV is called *TEV with cross charge*. Figure 9.17 shows the saturated vapour line for the power fluid as well as the refrigerant in the system. The projection for p_p is taken from the saturation line for power fluid and it shows the temperature at the exit of the evaporator. The power fluid is such that at any temperature it has lower saturation pressure than that of the refrigerant in the system, so that as the evaporator temperature increases the degree of superheat increases. The projection for p_e is taken from the saturation line of the refrigerant and it indicates the evaporator temperature. Two sets of points with the same difference between p_p and p_e (equivalent to the same spring force setting) are shown in this figure. It is observed that for the three different locations shown in Figure 9.16, the degree of superheat is same in Figure 9.17 for all evaporator temperatures.

Hence cross charge helps in maintaining the same degree of superheat at all evaporator temperatures. Cross-charged valves perform satisfactorily in a narrow range of temperatures that must be specified while ordering a valve.

9.4.3 TEV with External Pressure Equalizer

The pressure drop of the refrigerant is quite significant in large evaporators, for example in direct expansion coils with a single long tube. The thermostatic expansion valve maintains $F_p - F_e = A_b(p_p - p_e)$ at a constant value equal to the spring force. The pressure p_p is the saturation pressure at $(t_e + \Delta t_s)$ while p_e is saturation pressure at t_e. In a large evaporator, due to pressure drop Δp_e, the pressure at exit is say, $p_e - \Delta p_e$ and the corresponding saturation temperature at exit of the evaporator is $t_e - \Delta t_e$. The superheat Δt_s corresponds to evaporator pressure p_e and temperature t_e. Therefore, effective superheat at evaporator exit is $t_s + \Delta t_e$. This may become very large and may result in low COP and lower volumetric efficiency of the compressor. To correct this, TEV is provided with a tapping, which feeds the pressure $p_e - \Delta p_e$ from evaporator exit to the bottom of bellows. This will result in a degree of superheat equal to the set value Δt_s. A TEV with this provision is called *TEV with External Pressure Equalizer.* In this TEV, a stuffing box is provided between the pushpins and the valve body so that the evaporator inlet pressure is not communicated to the bottom of bellows.

In any case a large evaporator pressure drop leads to a lower COP; hence a number of parallel paths or circuits are provided in the evaporator. The refrigerant is fed to these paths by a single TEV fitted with a distributor. In such a case, it is recommended that an external pressure equalizer be used and care be taken to ensure that all the paths are symmetric and have the same length. Four types of distributors are in common use at present. These are: (1) venturi type, (2) pressure drop type, (3) centrifugal type and (4) manifold type. The details of these are available in Dossat [1984].

9.4.4 Fade-out Point and Limiting Characteristics of TEV

The volume of power fluid in the feeler bulb and the connecting tube is constant, therefore the heating and cooling of the power fluid is a constant specific volume process as shown in the $p - v$ diagram of Figure 9.18. The bulb usually has some liquid in it. At point A in the figure, it is a mixture of liquid and vapour and the pressure exerted by the power fluid corresponds to its saturation temperature at A. The pressure of the power fluid increases rather rapidly as its temperature increases since the liquid evaporates and it has to be accommodated in a fixed volume. This sharp rise in pressure with temperature continues until point F on the saturation curve, where no liquid is left. A

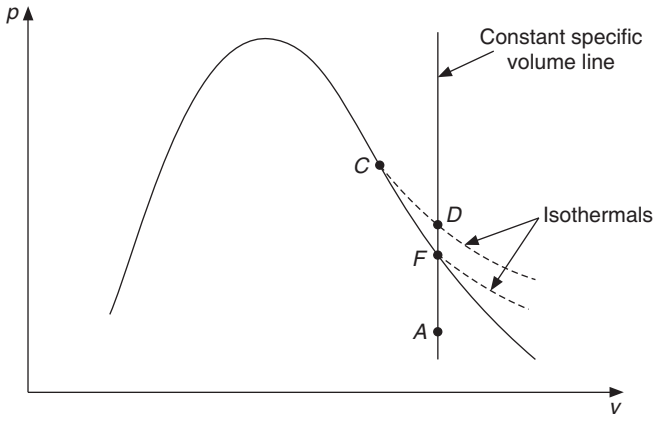

Figure 9.18 Fade-out point (*F*) depicted on the *p–v* diagram.

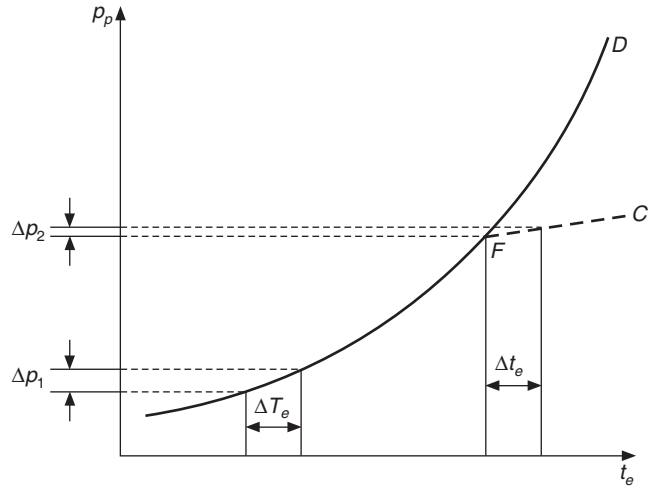

Figure 9.19 Variation of power fluid pressure with temperature in a limit charged TEV.,

rise in temperature along *F–C* does not lead to significant rise in pressure since the power fluid is in vapour state. This point *F* is called the *fade-out* point of TEV. Figure 9.19 shows the same phenomenon on the *p–T* curve where the line *F–C* is in superheated state while the line *F–D* is along the saturation curve. Since the pressure of the power fluid does not increase significantly beyond *F*, the valve does not open any wider, $p_p \approx$ constant, hence for a fixed spring setting, p_e remains almost constant and thereby limits the pressure in the evaporator to *maximum operating pressure*. It was earlier observed in Figure 4.10 that the power requirement of a reciprocating compressor is maximum at a certain evaporator pressure. This figure is reproduced in Figure 9.20. The air-conditioning systems usually operate near the peak while the refrigeration systems such as those for ice cream or frozen food operate on the left leg of the curve say at point *D* in Figure 9.20. It was shown that during pull-down, the power requirement would pass through the power peak if the evaporator were kept fully supplied with liquid. It is, however, uneconomical to provide a large electric motor to meet the power requirement of the peak for small times during pull-down.

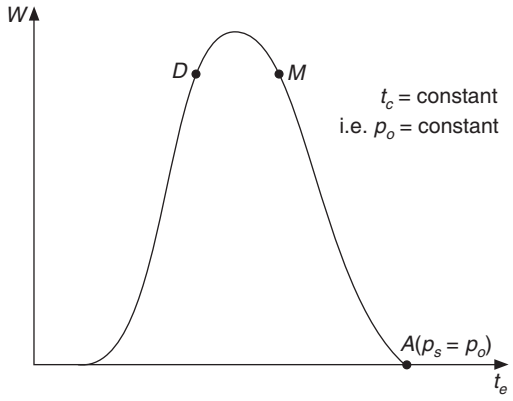

Figure 9.20 Effecty of evaporator temperature (or the suction pressure) on the power requirement of an actual reciprocating compressor.

The power requirement at the design point on the left leg is small. A motor capable of providing normal power can be used if the TEV makes the evaporator starve (reduces the mass flow rate to it) and limits the pressure during pull-down when the load is high. Charging the bulb with limited mass of power fluid so that it is entirely vapour above a maximum evaporating pressure and temperature achieves this purpose. Above this temperature the superheat increases considerably as seen in Figure 9.19 and the valve tends to shut down. Such a valve is called *limit charged or dry charged valve*. This arrangement will give slow cooling rate during pull-down. If rapid cooling is required from the refrigeration system, then this arrangement cannot be used.

The power required is proportional to mass flow rate of the refrigerant. Hence, during pull-down the design point may be reached at lower power if the mass flow rate through the compressor is manually reduced by a hand valve or done by a limit charged TEV. Once the design condition is reached the design mass flow rate is automatically restored by TEV or may be manually restored by full opening of the hand valve. But once the design condition, say the point D in Figure 9.20 is reached then for the safety of the motor, power peak should not be approached due to load variation or some other transient operating condition. This is achieved by setting the fade-out point of the TEV to a value slightly larger than the design point, say at point *F* (30 to 70 kPa above the design value at *D*) but much lower than the peak power pressure.

The limit charged valve is prone to failure known as *reversal*. The feeler bulb has vapour only. The head of the feeler bulb is usually colder than the rest of it, as a result a small amount of vapour can condense in this region. This colder region will have a lower saturation pressure that will decide the pressure of the feeler bulb and this low pressure may be insufficient to open the valve. This is avoided by keeping the head of the valve warm by internal circulation.

9.3.5 Advantages, Disadvantages and Applications of TEV

The advantages of TEV compared to other types of expansion devices are as follows:

1. The TEV provides an excellent control of refrigeration capacity as the supply of refrigerant to the evaporator matches the demand.
2. The TEV ensures that the evaporator operates efficiently by preventing starving under high load conditions.

3. The TEV protects the compressor from slugging by ensuring a minimum degree of superheat under all conditions of load, if properly selected.

However, compared to capillary tubes and AEVs, a TEV is more expensive and proper precautions should be taken during its installation. For example, the feeler bulb must always be in good thermal contact with the refrigerant tube. The feeler bulb should preferably be insulated to reduce the influence of the ambient air. The bulb should be mounted such that the liquid is always in contact with the refrigerant tubing for proper control.

The use of TEV depends upon the degree of superheat. Hence, in applications where a close approach between the fluid to be cooled and the evaporator temperature that is desired, TEV cannot be used since a very small extent of superheating is available for operation. A counterflow arrangement can be used to achieve the desired superheat in such a case. Alternatively, a subcooling HEX may be used and the feeler bulb mounted on the vapour exit line of the HEX. The valves with bellows have a longer stroke of the needle, which gives extra sensitivity compared to the diaphragm type of valve. But valves with bellows are more expensive.

A TEV is normally selected from the manufacturers' catalogues. The selection is based on the refrigeration capacity, the type of the working fluid, and the operating temperature range, etc. In practice, the design is different to suit different requirements such as single evaporators, multi-evaporators, etc.

9.5 FLOAT TYPE EXPANSION VALVE

The float valve is a type of expansion valve, which maintains the level of liquid refrigerant constant in a vessel or an evaporator. Hence, the mass flow rate of the refrigerant through the expansion valve is proportional to the evaporation rate of the refrigerant in the evaporator, which in turn is proportional to the load. There are two types of such expansion valves, namely (i) High-side level control valve and (ii) Low-side level control valve.

9.5.1 High-side Level Control Valve

This type of valve maintains the level of liquid refrigerant in the evaporator constant indirectly by maintaining a constant liquid level in the high-pressure float chamber. The float chamber is a vessel with a float. It is located at the exit of the condenser. The liquid refrigerant from the condenser enters this vessel. The float may be linked by a lever to a slide valve or to a needle valve. A typical schematic of a high-side float valve is shown in Figure 9.21. A rise in the liquid level in the vessel opens the float valve wider and allows more refrigerant to pass through it. This works on the principle of drawing liquid from the condenser as it is formed, so that no liquid is stored on the high side (except for some in the vessel for control of the float). The refrigerant fed to the evaporator is proportional to the evaporation rate. The mass flow rate of the refrigerant always matches the load. If the evaporation rate increases the valve opens wider. Instead of being of modulating type, it may be of on/off type as well. The float valve may open completely when the liquid level drops below the control point and close completely when the level reaches the control point. The liquid refrigerant is drained from the condenser as it is formed, therefore, all of it resides in the evaporator, typically a flooded type of evaporator. Hence, it is recommended that a critical charge be used in such systems to avoid flooding of the evaporator and consequent slugging of the compressor.

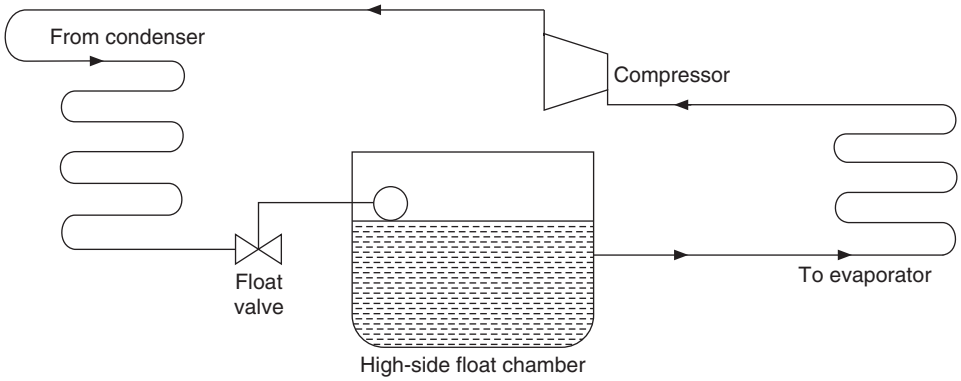

Figure 9.21 Schematic of a typical high-side float valve arrangement.

9.4.2 Low-side Level Control Valve

This type of valve maintains a constant level of liquid refrigerant in the evaporator. Obviously, this is used with a flooded type of evaporator where the entire heat transfer surface area is wetted by the liquid refrigerant. There are re-circulation type of evaporators in which the entire liquid refrigerant that is fed to the evaporator does not get evaporated in the evaporator. For this reason, the mixture of liquid and vapour emanating from the evaporator is sent to a separator vessel known as accumulator, suction separator or surge drum where the liquid is separated from the mixture and then re-circulated to the evaporator. If x is the dryness fraction of the mixture returning to the surge chamber, then the mass flow rate of the liquid through the evaporator is $\dot{m}/x$ where $\dot{m}$ is the mass flow rate through the expansion valve and also the mass flow rate of vapour to the compressor. A schematic diagram of the valve is given in Figure 9.22. The float is mounted in a vessel. The float senses the level and through a mechanical linkage operates a larger expansion valve. In larger systems like the one shown, the float is placed in a separate float chamber rather than in the surge drum or evaporator. This makes servicing of the valve easier since it can be isolated from the evaporator without shutting down the evaporator, which is kept running with a hand valve for pressure reduction. The separate float chamber senses the level of liquid refrigerant in the evaporator without being exposed to turbulence caused by boiling. The float chamber is connected to the evaporator by pipes at the bottom and at the top. These are called balance lines or equalizing lines. Insulation is provided so that the liquid in the evaporator does not evaporate since the liquid is usually at a lower temperature than that of the surrounding air.

The flow rate of the refrigerant in this valve is proportional to evaporation rate of the refrigerant in the evaporator. Hence, this valve always establishes a balanced flow condition of flow between the compressor and itself. If the load increases, the evaporating pressure and temperature have the tendency to rise in a flooded evaporator. This increases the compressor mass flow rate momentarily compared to that for the expansion valve. The valve reacts to keep the level constant by opening wider and a new balance point is reached. If the refrigeration load decreases, then there is a tendency for the evaporator temperature and the pressure to decrease. There is a momentary decrease in mass flow rate through the compressor, which will remove less refrigerant from the evaporator, the level of liquid refrigerant in the evaporator will rise prompting the valve to become narrower.

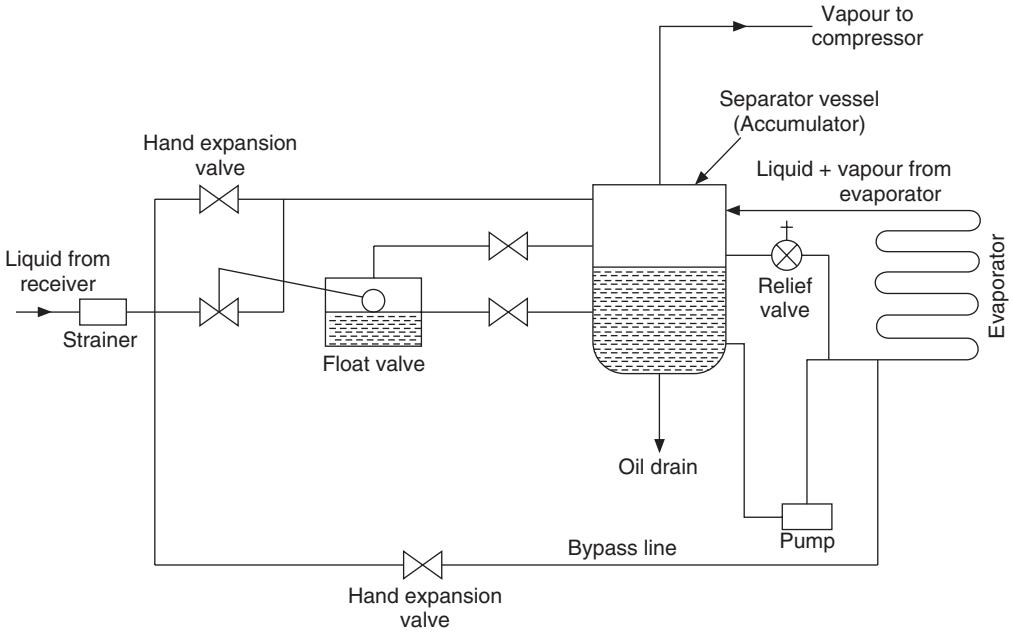

Figure 9.22 Schematic of a typical low-side float valve arrangement.

Flooded evaporators have a better heat transfer coefficient compared to the dry type evaporators, since typically only 30–40% of the area is used for the vaporization of refrigerant in the latter type. Re-circulation and sometimes liquid pumps are used to increase the heat transfer even further in flooded type evaporators of large installations. Float type valves are essentially used for large installations. These should not be used in continuous type evaporators, say DX coil, where there is no place to sense the level of the liquid refrigerant. A bypass line equipped with a hand valve is usually provided around the float valve in order to provide refrigeration in case of float valve failure.

9.6 ELECTRONIC TYPE EXPANSION VALVE

The schematic diagram of an electronic expansion valve is shown in Figure 9.23. It has an orifice and a needle in front it. The needle moves up and down in response to magnitude of current in the heating element. A small resistance allows more current to flow through the heater of the expansion valve, as a result the valve opens wider. A small negative coefficient thermistor is used if superheat control is desired. The thermistor is placed in series with the heater of the expansion valve. The heater current depends upon the thermistor resistance which in turn depends upon the refrigerant condition. Exposure of thermistor to superheated vapour permits thermistor to selfheat, thereby lowering its resistance and increasing the heater current. This opens the valve wider and increases the mass flow rate of the refrigerant. This process continues until the vapour becomes saturated and some liquid refrigerant droplets appear. The liquid refrigerant will cool the thermistor and increase its resistance. Hence in the presence of liquid droplets the thermistor offers a large resistance, which allows a small current to flow through the heater making the valve opening narrower. The

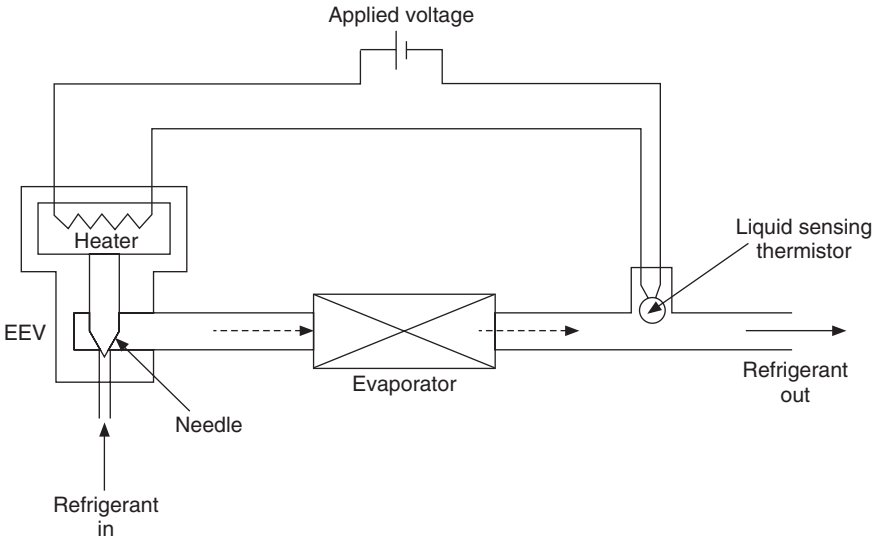

Figure 9.23 Schematic of an electronic expansion valve.

control of this valve is independent of refrigerant and refrigerant pressure; hence it works in the reverse flow direction as well. It is convenient to use it in year-round-air-conditioning systems, which serve as heat pumps in winter with reverse flow. In another version of it the heater is replaced by a stepper motor, which opens and closes the valve with greater precision giving a proportional control in response to the temperature sensed by an element.

9.7 SOME PRACTICAL PROBLEMS IN OPERATION OF EXPANSION VALVES

An oversized expansion valve will overfeed the refrigerant or hunt and not achieve the balance point. It may pass more refrigerant to the evaporator and cause flooding and consequent slugging of the compressor with disastrous results.

A small valve on the other hand would pass an insufficient quantity of the refrigerant, causing the balance point to occur at a lower temperature. The mass flow rate through the expansion valve depends upon the pressure difference between the condenser and the evaporator. The condenser temperature and consequently the pressure decrease during winter for air-cooled as well as water-cooled condensers. As a result, the pressure difference is not sufficient for balance of flow between the compressor and the expansion valve. Hence, the evaporator temperature and pressure decrease during winter months. This decreases the volumetric efficiency of the compressor and results in a lower mass flow rate and lower cooling capacity and the natural advantage of the lower condenser pressure is lost. Hence, sometimes the condenser pressure must be kept artificially high so that adequate supply of refrigerant is achieved. This may lead to disastrous results for hermetic compressors, which rely upon the refrigerant flow rate for cooling the motor. At lower mass flow rates, hermetic compressor may not get cooled sufficiently and may thus burn out.

During summer months, the mass low rate through an expansion valve is large because of large pressure difference. The corrective action taken by the system is to pass vapour through the expansion valve. This problem can also occur (i) if there is insufficient charge of refrigerant in the

system so that the liquid seal at the condenser exit is broken and vapour enters the expansion valve, or (ii) because of higher elevation of expansion valve over the condenser so that there is static pressure drop to overcome the gravitational force to reach the expansion valve, which causes flashing of the refrigerant into a mixture of liquid and vapour. This is, however, not advisable since it leads to lower COP. Hence, it is advisable to use a liquid-to-vapour subcooling heat exchanger so that the liquid is subcooled and does not flash before entry into the expansion valve.

Since the area available for refrigerant flow in the expansion device is normally very small, there is a danger of valve blockage due to some impurities present in the system. Hence, it is essential to use a filter/strainer before the expansion device, so that only the refrigerant flows through the valve and solid particles, if any, are blocked by the filter/strainer. Normally, the automatic expansion valve and thermostatic expansion valves consist of in-built filters/strainers. However, when a capillary tube is used, it is essential to use a filter/dryer ahead of the capillary to prevent entry of any solid impurities and/or unbound water vapour into the capillary tube.

REFERENCES

Staebler, L.A. (1984): Theory and Use of a Capillary Tube for Liquid Refrigerant Control, *Refrig. Eng.*, vol. 55, no.1, pp. 55.

Hopkins, N.E. (1950): Rating the Restrictor Tube, *Refrig. Eng.*, vol. 58, no. 11, pp. 1087.

Cooper, L., Chu, C.K. and Brisken, W.R. (1957): Simple Selection Method for Capillaries Derived from Physical Flow Condition, *Refrig. Eng.*, vol. 65, no.7, pp. 37.

Bolstead, M.M. and Jordan, R.C. (1948): Theory and Use of the Capillary Tube Expansion Devices, *Refrig.Eng.*,vol. 56, no. 6, pp. 519.

Shapiro, A.H. (1953): *The Dynamics and Thermodynamics of Compressible Fluid Flow*, Ronald, New York.

Whitesel, H.A. (1957): Capillary Two-Phase Flow, pt. I, *Refrig.Eng.*, vol. 65, no. 4, pp. 42.

Whitesel, H.A. (1957): Capillary Two-Phase Flow, pt. II, *Refrig.Eng.*, vol. 65, no. 9, pp. 35.

ASHRAE Handbook and Product Directory, Equipment Volume (1975): American Society of Heating Refrigerating and Air Conditioning Engineers, Atlanta, Ga.

Pasqua, P.F. (1953): Metastable Flow of Freon-12, *Refrig. Eng.*, vol. 61, no. 10, pp. 1084.

Dosat Roy J. (1984): *Principles of Refrigeration*, Wiley Eastern Limited, New Delhi.

REVIEW QUESTIONS

1. Explain the concept of balance point between the compressor and the capillary tube.
2. Discuss the effect of refrigeration load variation on the balance point.
3. Enumerate the advantages and disadvantages of the capillary tube.
4. Explain with a heat sketch the working principle of automatic expansion valve. Discuss the factors that affect the capacity of the valve.

5. Describe the working principle of thermostatic expansion valve (TEV) with the help of a neat sketch.
6. What is cross-charged TEV, and a TEV with external pressure equalizer?
7. Explain with the help of a schematic diagram the working of a typical low-side float valve arrangement.
8. Discuss the practical problems encountered in the operation of expansion valves.
9. An R12 thermostatic expansion valve uses R12 itself as the power fluid in an R12 based system operating at an evaporator temperature of 4°C. Calculate the degree of superheat if the adjustable spring is set to provide a resistance equivalent to a pressure of 60 kPa.

10

Condensers

LEARNING OBJECTIVES

After studying this chapter the student should be able to:

1. Understand the general aspects of condensers used in refrigeration systems.
2. Classify the refrigerant condensers based on the external fluid used, type of external fluid flow, and constructional features.
3. Compare air-cooled condensers with water-cooled condensers.
4. Perform design calculations of condensers, including estimation of various heat transfer coefficients involved in the design.
5. Discuss the concept of Wilson's plot to determine the individual heat transfer coefficients from the experimental data on heat transfer characteristics of heat exchangers.
6. Explain the effect of presence of air and other non-condensable gases in refrigerant condensers.
7. Explain the concept of optimum condenser pressure.

10.1 INTRODUCTION

A condenser is a heat exchanger where the refrigerant is first desuperheated and then the saturated vapour condenses into liquid state. The liquid may also be subcooled in some condensers. This is an important part of the refrigeration cycle without which the refrigerant cannot be recycled. This is the component where the heat absorbed by the evaporator at low temperature and the work of compression are rejected to the surroundings as heat transfer. The heat is rejected either to air directly or to water which in turn rejects it to the surroundings in a cooling tower. The temperature remains constant during condensation (a–3) but decreases during desuperheating (2–a) in vapour phase as shown in the T–s cycle diagram in Figure 10.1. The temperature of the coolant increases from t_{wi} to t_{wo} as shown in the figure.

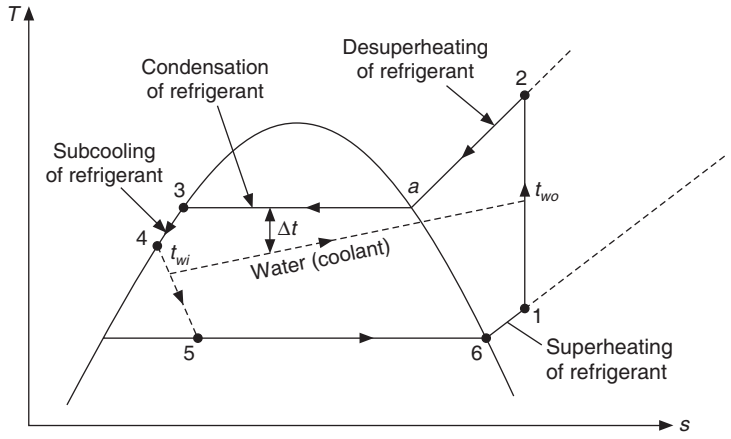

Figure 10.1 Refrigeration cycle on the *T–s* diagram.

The heat transfer coefficient, h_c, is small in vapour phase but the temperature difference between the refrigerant and the coolant Δt is large, while during condensation the heat transfer coefficient is large but the temperature difference is small. As a result, the product $h_c \Delta t$ is approximately same in both the regions; hence one may design the condenser by assuming that condensation occurs throughout the condenser.

In fact, the coolant temperature (specially in water-cooled condensers) may be less than the condenser temperature at the inlet of condenser; hence the tube wall temperature will also be less than the condenser temperature. Hence, condensation will occur at the wall even at inlet although the bulk of the vapour will be superheated.

10.2 HEAT REJECTION RATIO

The heat rejection ratio is the ratio of the heat rejected to the heat absorbed, that is,

$$R = \frac{Q_c}{Q_e} = \frac{Q_e + W_c}{Q_e} = 1 + \frac{1}{\text{COP}} \tag{10.1}$$

For a fixed condenser temperature, as the evaporator temperature decreases the COP decreases and the heat rejection ratio increases. For a fixed evaporator temperature as the condenser temperature increases the COP decreases and hence the heat rejection ratio increases. These characteristics are shown in Figure 10.2. Such curves can be drawn for all refrigerants so that the condenser heat rejection can be determined for the given T_e, T_c and TR.

10.3 TYPES OF CONDENSERS

There are essentially three types of condensers, namely:

(a) Air-cooled condensers
(b) Water-cooled condensers
(c) Evaporative condensers.

There are further classifications depending upon the geometry and the type of heat transfer.

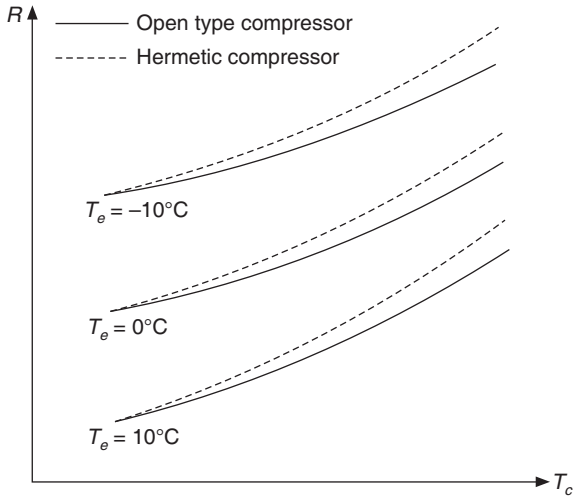

Figure 10.2 Variation of heat rejection ratio with evaporator and condenser temperatures.

Some of the salient features of the air-cooled and water-cooled condensers are as follows:

	Air cooled	*Water cooled*
Temperature difference ($T_c - T_{coolant}$)	15–20°C	6–12°C
Volume flow rate of coolant per TR	12–20 cmm	7–20 Lpm
Heat transfer area per TR	10–15 m^2	0.5–1.0 m^2
Face velocity	2–5 m/s	2–3 m/s
Power per TR	Blower: 0.1 to 0.2 hp	Pump power is very small

10.4 COMPARISON OF WATER-COOLED AND AIR-COOLED CONDENSERS

10.4.1 Advantages of Air-cooled Condensers

Air-cooled condensers are simple in construction since no pipes are required for air. Further, the disposal of warm air is not a problem and it is available in plenty. The fouling of condenser is small and the maintenance cost is low.

10.4.2 Disadvantages of Air-cooled Condensers

The specific heat of air is one-fourth of that of water and the density is one-thousandth of that of water, hence the volume flow rates required are very large. The thermal conductivity is small; hence the heat transfer coefficient is also very small. Also, the air is available at dry-bulb temperature while the water is available at a lower temperature, which is 2–3°C above the wet-bulb temperature. The temperature rise of air is much higher than that of water, therefore the condenser temperature becomes very large and the COP reduces. The use of air-cooled condensers is normally restricted to 10 TR although the blower power goes up beyond 5 TR. In systems up to 3 TR with open compressors, the condenser is mounted on the same chassis as the compressor and the compressor

motor drives the condenser fan as well. In middle-east countries where there is shortage of fresh water, air-cooled condensers are used up to 100 TR or more.

The air-cooled condensers cost two to three times more than the cost of water-cooled condensers. The water-cooled condenser requires a cooling tower since water is scarce in municipality area and has to be recycled. Water from lakes and rivers cannot be thrown back in warm state since it affects the marine life adversely. Increased first cost and maintenance cost of a cooling tower offsets the cost advantage of water-cooled condensers. Fouling of the heat exchange surface is a big problem in use of water.

10.5 COMPARISON OF WATER-COOLED AND EVAPORATIVE CONDENSERS

Evaporative condensers combine the features of cooling tower and water-cooled condenser in a single unit. In this condenser, the water is sprayed from top on a bank of tubes carrying the refrigerant and the air is induced upwards. There is a thin water film around the condenser tubes from which evaporative cooling takes place. The heat transfer coefficient for evaporative cooling is very large. The water spray countercurrent to the airflow acts as a cooling tower. The evaporative condenser is located indoors near the compressor. The refrigerant pipeline is long when the evaporative condenser is used since these pipes feed the refrigerant and run through the evaporative condenser, hence the compressor power is a little higher. The water lines are short, hence the pump power is small. In the water-cooled condenser, the condenser is located next to the compressor while the cooling tower is located outside. In this case, the compressor power is less but the water pump power is large. Both these types of condensers compete with each other up to thousands of TR.

10.6 AIR-COOLED CONDENSER

There are of two type of air-cooled condensers—natural convection type and forced convection type.

10.6.1 Natural Convection Type

These types of condensers are used for small capacity refrigeration systems such as the household refrigerators and freezers. These condensers are either of plate surface type or of finned tube type.

The plate surface type of air-cooled condenser is more common these days. In fact, the refrigerant-carrying tubes are attached to all the outer sidewalls of the refrigerator. The whole body of the refrigerator (except the door) acts like a fin. There is insulation between the outer cover that acts like fin and the inner plastic cover of the refrigerator. It is for this reason that the outer body of the refrigerator is always warm.

The finned type of tube condenser is mounted either below the refrigerator at an angle or on the rear side of the refrigerator. In case it is mounted below the refrigerator, then the warm air rises up and to assist it, an air envelope is formed by providing a jacket on the rear side of the refrigerator. The fin spacing is kept large to prevent fouling by dust.

In the older designs, the condenser tube (in serpentine form) was attached to a plate and the plate was mounted on the rear side of the refrigerator. The plate acted like a fin and warm air rose up along it. In some designs, a set of thin wires was soldered to the serpentine tube coil. The wires acted like fins for increased heat transfer area.

10.6.2 Forced Convection Type

The forced convection type condensers are used in window air conditioners, water coolers and packaged air conditioning plants. These are either chassis mounted or remote mounted. In the chassis mounted type, the compressor, the induction motor, the condenser with condenser fan, the accumulator, the HP/LP cut-out switch and the pressure gauges are mounted on a single chassis. It is called the condensing unit of rated capacity. The components are matched to condense the required mass flow rate of refrigerant to meet the rated cooling capacity. The remote mounted type is either vertical or roof mounted horizontal type. Typically, the air velocity varies between 2 m/s and 3.5 m/s for economic design with airflow rates of 12 cmm to 20 cmm per TR. The air specific heat is 1.005 kJ/kg-K and the density is 1.2 kg/m^3. Therefore, for 1 TR the temperature rise Δt_a = 3.5167/(1.2 × 1.005 × 16/60) = 10.9°C for average air flow rate of 16 cmm. Hence, the air temperature rises by 10°C to 15°C compared to 3°C to 6°C for water.

The area of the condenser seen from outside in the airflow direction is called the face area. The velocity at the face is called the face velocity. This is given by the volume flow rate divided by the face area. The face velocity is usually around 2 m/s to 3.5 m/s to limit the pressure drop due to frictional resistance. The coils of the tube in the flow direction are called rows. A condenser may have two to eight rows of the tubes carrying the refrigerant. There can be two types of finned tubing—spiral fins and continuous flat-plate fins. Figure 10.3 shows the schematic arrangement of a plate-fin type condenser. The moist air flows over the fins while the refrigerant flows inside the tubes. The fins are usually of aluminium and tubes are made of copper. Holes of diameter slightly less than the tube diameter are punched in the plates and plates are slided over the tube bank. Then the copper tubes are pressurized which expands the tubes and makes a good thermal contact between the tube and fins. This process is also known as bulleting. For ammonia condensers, mild steel tubes with mild steel fins are used. In this case the fins are either welded or galvanizing is done to make a good thermal contact between the fin and the tube. In case of ammonia, annular crimpled spiral fins are also used over the individual tubes instead of the flat-plate fins as shown in Figure 10.3.

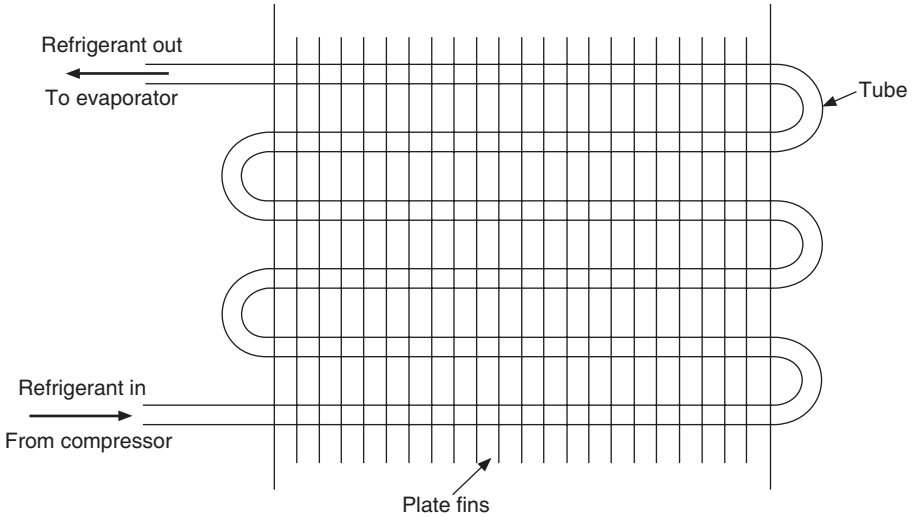

Figure 10.3 Forced convection, plate-fin-and-tube type condenser.

Finned coils are very compact. The secondary surface area is 10 to 30 times the bare pipe area; hence the finned coils are very compact and have smaller weight. Heat transfer in finned coils is very complicated. The expression for the overall heat transfer coefficient was derived in Section 2.25 for a pipe. This expression must be modified to include the presence of fins on the air side and sometimes on the refrigerant side too, so that it can be used for a condenser. In Section 2.26, expressions were derived for the mean temperature difference called the *log mean temperature difference* that can be used for parallel and counterflow heat exchangers. The air-cooled condensers are crossflow type with flow reversal on the refrigerant side. These expressions also have to be modified so that they can be used for condensers.

10.7 MEAN TEMPERATURE DIFFERENCE FOR CROSSFLOW HEAT EXCHANGER

The expression for overall heat transfer derived in Section 2.25 must be modified. The fluids are in some type of cross type of arrangement, hence the log-mean temperature difference may not be exactly valid. There is a *pure crossflow* heat exchanger, which is commonly used in steam coils for heating moist air and there is a *counter-crossflow* arrangement commonly used in condensers and evaporators. It will be shown that the *log mean temperature difference* is valid for crossflow too, if the temperature of one of the fluids remains constant like that of the refrigerant in the condenser and in the evaporator. Otherwise, it is convenient to express the mean temperature difference Δt_m for heat transfer for any heat exchanger in terms of the mean temperature difference $\Delta t_{m,cf}$ of a counterflow heat exchanger as follows:

$$\Delta t_m = F\, \Delta t_{m,cf} \tag{10.2}$$

where, F is a correction factor. In the following analysis, we derive an expression for the correction factor F for pure crossflow over a tube. It was shown that for a counterflow heat exchanger the heat transfer rate and log mean temperature difference (LMTD) are given by Eq. (2.155) as follows:

$$Q = U_o A_o\, \Delta t_m = U_o A_o\, \frac{\Delta t_2 - \Delta t_1}{\ln\,(\Delta t_2 / \Delta t_1)}$$

$$\text{LMTD} = \Delta t_m = \frac{\Delta t_2 - \Delta t_1}{\ln\,(\Delta t_2 / \Delta t_1)} \tag{10.3}$$

Figure 10.3 schematically shows the diagram of a condenser with tubes and fins. The hot fluid flows through the tubes in the x direction and hence its temperature decreases in this direction. Moist air flows through the passages between the fins. Hence, there are as many streams of it as the number of passages. This arrangement is known as unmixed flow since the air flows individually through each passage. The air contacts the fins and tubes and is heated; hence its temperature increases in the y direction. The temperature rise in each passage is different since the fin temperature decreases in the x direction. If the temperatures of air and hot fluid are denoted by t and T respectively, then

$$T = T(x) \quad \text{and} \quad t = t(x, y)$$

Suppose the dimensions of the heat exchanger in the x and y directions are L_x and L_y respectively. Let us take an elemental area (dx, dy).

If the total outside area of the heat exchanger is A_o, then the area of the element

$$(dx, dy) = dA_o = \frac{dx}{L_x}\frac{dy}{L_y}A_o$$

If the mass flow rate of air is $\dot{m}$, then the mass flow rate through the element dx is $\dot{m}\frac{dx}{L_x}$. Let the specific heat of air be c_p and the temperature rise through the control volume be dt.

If U_o is the overall heat transfer coefficient, then the heat transfer rate by convection is

$$U_o dA_o (T - t) = \dot{m}\frac{dx}{L_x}c_p\, dt \quad \text{or} \quad U_o \frac{dx}{L_x}\frac{dy}{L_y}A_o(T - t) = \dot{m}\frac{dx}{L_x}c_p\, dt \tag{10.4}$$

Thus,
$$\int_{t_1}^{t'} \frac{dt}{T - t} = \frac{U_o A_o}{\dot{m}c_p L_y}\int_0^{L_y} dy \tag{10.5}$$

where t' is the temperature of one stream. When streams from all passages mix together the outlet temperature of air will be t_2.

The temperature of the hot fluid, T, varies in the x direction only, hence Eq. (10.5) can be integrated to give

$$t' = t_1 + (T - t_1)(1 - e^{-K_1}) \tag{10.6}$$

where
$$K_1 = \frac{U_o A_o}{\dot{m}c_p} \tag{10.7}$$

Temperature distribution of warm fluid: In the elemental control volume the temperature of the warm fluid rises by dT and that of air rises by $(t' - t_1)$, the mass flow rate being $\dot{m}\frac{dx}{L_x}$, the heat transfer is given by

$$\dot{M}C_p dT = \dot{m}\frac{dx}{L_x}c_p(t' - t_1)$$

Substituting from Eq. (10.6) for $(t' - t_1)$, we get

$$\dot{M}C_p dT = \dot{m}\frac{dx}{L_x}c_p(T - t_1)(1 - e^{-K_1})$$

Integrating the above equation from T_1 to T_2, we get

$$\int_{T_1}^{T_2} \frac{dT}{T - t_1} = -\frac{\dot{m}c_p}{\dot{M}C_p}\frac{(1 - e^{-K_1})}{L_x}\int_0^{L_x} dx \tag{10.8}$$

Integrating Eq. (10.8), we find the temperature T_2 of the warm fluid at the exit of the heat exchanger as

$$T_2 = T_1 - (T_1 - t_1)(1 - e^{-K_2}) \tag{10.9}$$

where,
$$K_2 = \frac{\dot{m}c_p}{\dot{M}C_p}(1 - e^{-K_1}) \tag{10.10}$$

Energy balance for the whole heat exchanger gives

$$\dot{m}c_p(t_2 - t_1) = \dot{M}C_p(T_2 - T_1) \tag{10.11}$$

Substituting for $(T_2 - T_1)$ from Eq. (10.9), we get

$$t_2 = t_1 \frac{\dot{M}C_p}{\dot{m}c_p}(T_1 - t_1)(1 - e^{-K_2}) \tag{10.12}$$

We define the thermal capacity ratio R and effectiveness P of heat exchanger as follows:

$$R = \frac{\dot{m}c_p}{\dot{M}C_p} \quad \text{and} \quad P = \frac{t_2 - t_1}{T_1 - t_1} \tag{10.13}$$

Using Eq. (10.11), the thermal capacity ratio reduces to

$$R = \frac{\dot{m}c_p}{\dot{M}C_p} = \frac{T_2 - T_1}{t_2 - t_1} \quad \text{and} \quad RP = \frac{T_2 - T_1}{T_1 - t_1} \tag{10.14}$$

From Eq. (10.10), we get

$$K_2 = R(1 - e^{-K_1}) \tag{10.15}$$

From Eq. (10.9) and Eq. (10.14), we get

$$e^{-K_2} = (1 - RP) \qquad \text{or} \qquad -K_2 = \ln(1 - RP) \tag{10.16}$$

From Eq. (10.10), we have $K_2 = R(1 - e^{-K_1})$. Simplifying and using Eq. (10.16), we get

$$e^{K_1} = \frac{R}{R + \ln(1 - PR)} \tag{10.17}$$

The aim of this analysis is to represent the heat transfer rate in the following form:

$$Q = U_o A_o \Delta t_m \tag{10.18}$$

where Δt_m is the mean temperature difference for the crossflow heat exchanger, which is obtained by substituting $Q = \dot{m}c_p(t_2 - t_1)$ in the above equation. The required expression is

$$\Delta t_m = \frac{t_2 - t_1}{\ln\left[\dfrac{R}{R + \ln(1 - RP)}\right]} \tag{10.19}$$

For a counterflow heat exchanger, we have log mean temperature difference, which is defined as

$$\Delta t_{m,cf} = \text{LMTD} = \frac{(T_2 - t_1) - (T_1 - t_2)}{\ln\left(\dfrac{T_2 - t_1}{T_1 - t_2}\right)} = \frac{(t_2 - t_1)(R-1)}{\ln\left(\dfrac{1-P}{1-RP}\right)} \tag{10.20}$$

It is convenient to express the mean temperature difference Δt_m in terms of $\Delta t_{m,cf}$ as

$$\Delta t_m = F\, \Delta t_{m,cf} \tag{10.21}$$

where F is a correction factor. From Eqs. (10.19) and (10.20), we get

$$F = \frac{\Delta t_m}{\Delta t_{m,cf}} = \frac{\ln\left(\dfrac{1-P}{1-RP}\right)}{(R-1)\ln\left[\dfrac{R}{R + \ln(1-RP)}\right]} \tag{10.22}$$

Equation (10.22) shows that the correction F is a function of R and P only. Hence, it can be determined from Eq. (10.22). Bowman, Mueller and Nagle have given the solution for various crossflow heat exchangers, e.g. single-pass one-fluid unmixed, single-pass, both fluids unmixed, two-pass one-fluid unmixed, etc.

10.7.1 Mean Temperature Difference for Condenser

In the condenser the temperature of the refrigerant which is hot fluid may be assumed to be constant, only the temperature of the air will vary in the y direction, that is, t' will be same for all fin passages and equal to t_2. Equation (10.6) gives

$$t_2 = t_1 + (T - t_1)(1 - e^{-K_1}) \tag{10.23}$$

If there were more than one pass, we can show that Eq. (10.23) will still be applicable by replacing K_1 by NK_1 where N is the number of passes. Also, it does not matter if the crosses have flow from left to right or from right to left as long as the temperature of the refrigerant is constant. Equation (10.23) may be written as follows:

$$e^{K_1} = \frac{T - t_1}{T - t_2} \quad \text{or} \quad K_1 = \ln\left(\frac{T - t_1}{T - t_2}\right)$$

Then from Eq. (10.5), we have

$$K_1 = U_o A_o / c_p \qquad \text{and} \qquad Q = U_o A_o \Delta t_m = \dot{m} c_p (t_2 - t_1).$$

$$\therefore \qquad \Delta t_m = \frac{t_2 - t_1}{\ln\left(\dfrac{T - t_1}{T - t_2}\right)} = \frac{(T - t_1) - (T - t_2)}{\ln\left(\dfrac{T - t_1}{T - t_2}\right)} \tag{10.24}$$

EXAMPLE 10.1 Moist air is heated from 20°C to 65°C by hot water whose temperature changes from 95°C to 75°C. Determine the true mean temperature difference if the heat exchanger is of the following type: (a) pure counterflow, (b) pure parallel flow, (c) average temperature difference and (d) pure crossflow with one row of tubes.

Solution:

(a) From Eq. (10.3), mean temperature for pure counterflow is as follows:

$$\text{LMTD} = \Delta t_m = \frac{\Delta t_2 - \Delta t_1}{\ln(\Delta t_2 / \Delta t_1)}$$

We have $T_1 = 95^oC$ and $T_2 = 75^oC$ for the hot fluid and $t_1 = 20^oC$ and $t_2 = 65^oC$ for the moist air

$$\Delta t_{m,cf} = \frac{(T_2 - t_1) - (T_1 - t_2)}{\ln\left(\frac{T_2 - t_1}{T_1 - t_2}\right)} = \frac{(95 - 20) - (95 - 65)}{\ln\left(\frac{75 - 20}{95 - 65}\right)} = \frac{25}{\ln(55/30)} = 41.245°C$$

(b) For pure parallel flow the LMTD is as follows:

$$\Delta t_{m,pf} = \frac{(T_1 - t_1) - (T_2 - t_2)}{\ln\left(\frac{T_1 - t_1}{T_2 - t_2}\right)} = \frac{(95 - 20) - (75 - 65)}{\ln\left(\frac{95 - 20}{75 - 65}\right)} = \frac{65}{\ln(75/10)} = 32.26°C$$

(c) Average hot water temperature = (95 + 75)/2 = 85°C
Average moist air temperature = (20 + 65)/2 = 42.5°C
Hence average temperature difference = 85 – 42.5 = 42.5°C
This is very close to the counterflow case.

(d) For this case we have to find the correction factor F given by Eq. (10.22).

$$\text{We have } P = \frac{t_2 - t_1}{T_1 - t_1} = \frac{65 - 20}{95 - 20} = 0.6 \quad \text{and} \quad R = \frac{T_2 - T_1}{t_2 - t_1} = \frac{95 - 75}{65 - 20} = 0.57143$$

$$F = \frac{\Delta t_m}{\Delta t_{m,cf}} = \frac{\ln\left(\frac{1 - P}{1 - RP}\right)}{(R - 1)\ln\left[\frac{R}{R + \ln(1 - RP)}\right]} = \frac{\ln\left(\frac{0.4}{0.6571}\right)}{(-0.42857)\ln\frac{0.57143}{0.57143 + \ln(0.6571)}} = 0.873$$

Therefore the mean temperature difference is

$$\Delta t_m = F\,\Delta t_{m,cf} = 0.873 \times 41.245 = 36.007°C$$

10.8 FIN EFFICIENCY

The heat transfer coefficient on the air side is very low compared to the condensation or boiling heat transfer coefficient, hence fins are added on the air side to increases the heat transfer rate. It is recommended that a larger number of short, thin fins of a highly conductive material be used to increase the heat transfer rate. The fins are attached to the parent material from which heat transfer occurs. The base of the fin is at the same temperature as the parent material. The temperature along the fin length decreases due to thermal conduction resistance offered by the fin material in case of condenser; hence the fag end of the fin does not dissipate the same amount of heat as the end near

the base. Hence, although the fins increase the heat transfer area considerably, the conduction thermal resistance is also considerable. On the other hand, if the parent tube is made of copper, its thermal resistance may be negligible. The effectiveness of the fins is defined in terms of efficiency. In the following we consider a straight rectangular fin attached in the radial direction to a tube and then we consider an annular fin.

10.8.1 Rectangular Fin

Figure 10.4 schematically shows a rectangular fin of length L attached to a circular tube. The thickness of the fin is $2y$ and its thermal conductivity is k. Its temperature is denoted by t_f, while the air temperature is denoted by t. The convective heat transfer coefficient from the outer surface of the fin is h_{co}. In steady state, energy balance for the control volume gives:

$$\frac{dq_f}{dx}\Delta x + 2h_{co}(t_f - t)\Delta x = 0 \tag{10.25}$$

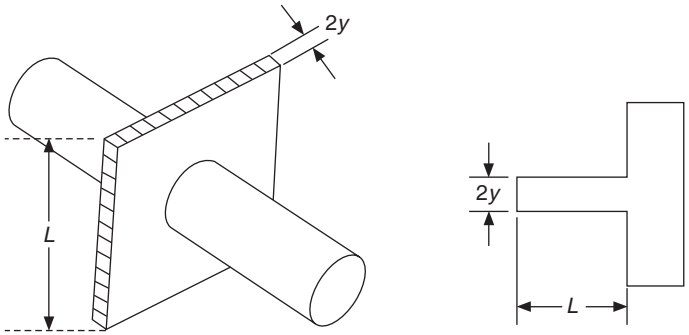

Figure 10.4 Rectangular fin attached to a circular tube.

From Fourier's law of heat conduction, considering a unit depth of fin, we have

$$q_f = -kA\frac{dt_f}{dx} = -k(2y)\times 1\frac{dt_f}{dx} \tag{10.26}$$

Defining

$$\theta = (t_f - t) \quad \text{and} \quad m^2 = h_{co}/(ky) \tag{10.27}$$

Equation (10.25) reduces to

$$\frac{d^2\theta}{dx^2} = m^2\theta \tag{10.28}$$

The fin temperature at the base $x = 0$ is t_{fb} while at $x = L$ it is assumed that fin being very thin the heat transfer is negligible, that is, at $x = L$: $dt_f/dx = 0$. In terms of θ, we have

$$\text{At } x = 0,\ \theta = \theta_b \tag{10.29a}$$

and $$\text{at } x = L, \frac{d\theta}{dx} = 0 \tag{10.29b}$$

The solution of Eq. (10.29) may be written as

$$\theta = C \cosh m(L - x)$$

which satisfies the boundary condition (10.29b).

Boundary condition (10.29a) yields $C = \theta_b/\cosh(mL)$.

$$\therefore \quad \theta = \theta_b \frac{\cosh m(L - x)}{\cosh mL} \tag{10.30}$$

The total heat transfer rate from the fin is the heat transfer rate that is conducted into the fin at $x = 0$, that is,

$$Q_f = k(2y)\left(\frac{dt}{dx}\right)_{x=0}$$

which reduces to

$$Q_f = 2\theta_b \sqrt{k\, y\, h_{co}}\ \tanh(mL) \tag{10.31}$$

By definition,

$$Q_f = A_f\, h_{co}\, (t_{fm} - t) = 2Lh_{co}(t_{fm} - t)$$

where, t_{fm} is the average temperature of the fin, A_f is the fin area, which for unit depth is equal to $2L$. Equating this equation to Eq. (11.31), we get

$$(t_{fin} - t) = \theta_b \frac{\tanh(mL)}{mL} \tag{10.32}$$

If whole of the fin is at the base temperature, then

$$Q_{f\max} = 2\, h_{co}\, L\, \theta_b \tag{10.33}$$

$$\text{Fin efficiency, } \phi = \frac{Q_f}{Q_{f\max}} = \frac{t_{fm} - t}{t_{fb} - t} = \frac{\tanh(mL)}{mL} \tag{10.34}$$

EXAMPLE 10.2 Find the effectiveness of a radial fin 1.0 mm thick and made of mild steel. The tube outer diameter is 16 mm, and the outer diameter of the fin is 37.5 mm; the air side convective heat transfer coefficient is 60.0 W/m^2-K and the thermal conductivity of mild steel is 55.0 W/m-K.

Solution:

$$m^2 = h_{co}/(ky)$$

Thickness $2y = 0.001$ m $\quad\therefore\quad y = 0.0005$ m

$$m = \sqrt{\frac{60.0}{55(0.0005)}} = 46.71 \quad \text{and} \quad L = (r_2 - r_1) = (0.0375 - 0.016)/2 = 0.01075 \text{ m}$$

$$mL = 0.4979 \quad \text{and} \quad \tanh(mL) = \tanh(0.4979) = 0.46046$$

The fin effectiveness $\phi = \tanh(mL)/mL = 0.9248$.

10.8.2 Circular Plate Fin

The straight circular plate or annular fins are more frequently used on tubes than the straight bar fins in radial direction. Crimpled fins spirally wound around the pipe are also used very frequently. However the results of circular fins are more useful in air-cooled condensers since these are more frequently used. Figure 10.5(a) shows the schematic diagrams of a circular plate fin. The circular plate in Figure 10.5(b) has a uniform thickness while the circular plate in Figure 10.5(c) has a constant area of cross section along the radius, that is, its thickness decreases along the radius.

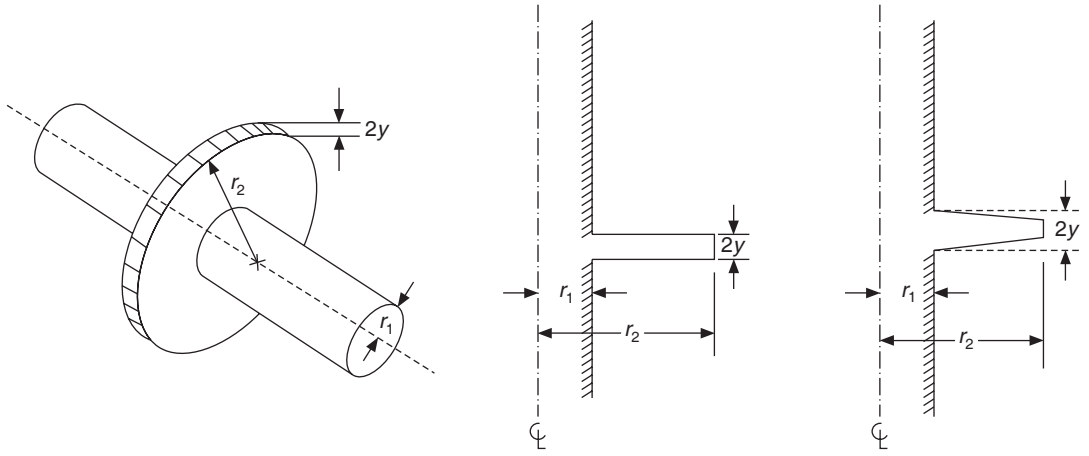

(a) Schematic diagram (b) Circular plate fin of uniform thickness (c) Circular plate fin of varying thickness

Figure 10.5 Circular plate fin.

Gardner (1945) has solved the differential equations for the two geometries in Figure 10.5 and given the temperature distribution and effectiveness. The solutions for the effectiveness are given in Eqs. (10.35) and (10.36) for the straight and tapered fins respectively.

For the fin of uniform thickness, we get

$$\phi = \frac{\sqrt{2/\xi}}{1 + r_{2c}/r_1}\left[\frac{I_1(R_a\xi)K_1(R_b\xi) - I_1(R_b\xi)K_1(R_a\xi)}{I_1(R_a\xi)K_0(R_b\xi) - I_{01}(R_b\xi)K_1(R_a\xi)}\right] \tag{10.35}$$

whereas for the fin of varying area of cross section such that $2\pi ry$ = constant

$$\phi = \frac{2r_1}{N(r_{2c}^2 - r_a^2)}\left[\frac{I_{-2/3}(2Hr_1^{3/2}/3)I_{2/3}(2Hr_{2c}^{3/2}/3) - I_{2/3}(2Hr_1^{3/2}/3)I_{-2/3}(2Hr_{2c}^{3/2}/3)}{I_{-1/3}(2Hr_1^{3/2}/3)I_{-2/3}(2Hr_{2c}^{3/2}/3) - I_{1/3}(2Hr_1^{3/2}/3)I_{2/3}(2Hr_{2c}^{3/2}/3)}\right] \tag{10.36}$$

where, $H^2 = \dfrac{h}{kr_1y} = \dfrac{N^2}{r_1}$, $r_{2c} = r_2 + y$, I and K are modified Bassel functions, and ξ is fin effectiveness.

An efficiency chart for the circular plate fin of uniform thickness is shown in Figure 10.6.

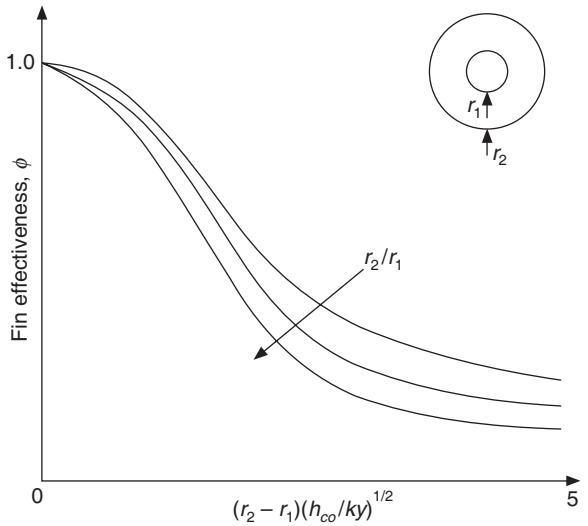

Figure 10.6 Fin efficiency curves for annular fins of constant thickness.

10.8.3 Rectangular Continuous Plate Fin

Rectangular continuous plates are commonly used as fins in the condensers and evaporators. All the tubes of all the rows pass through each plate. The exact analytical solution for the fin efficiency in such a case is not available. In fact, constant air temperature, constant convection heat transfer coefficient and constant base temperatures are all assumptions made as in the previous case. For the analysis of continuous plate fin, another assumption is made. It is assumed that there is one circular fin associated with each tube. The radius of the circular fin has to be approximated.

Figure 10.7 shows a typical plate fin-and-tube type condenser. In Figure 10.8(a) the tubes are parallel to each other while in Figure 10.8(b) the tubes in consecutive rows are staggered. The spacing between the tubes is B units within a row and C units between rows. If an equivalent circular fin of radius $r = B/2$ is chosen, it is observed that it will underestimate the total fin area. On the other hand, if a circular fin with radius $r = C/2$ is chosen then it will overestimate the area. Carrier and Anderson have shown that the area of $(B \times C - \pi r_o^2)$ associated with each fin is equivalent in performance to whole plate as a fin with all the tubes. This assigns an equal area of $B \times C$ to all the tubes. For such a fin the radius r_2 associated with Figure 10.5(a) is given by

$$B \times C - \pi r_1^2 = \pi(r_2^2 - r_1^2)$$

$$\therefore \quad r_2 = \sqrt{\frac{BC}{\pi}} \tag{10.37}$$

The efficiency for such a fin may be determined from Eq. (10.34) or Figure 10.6.

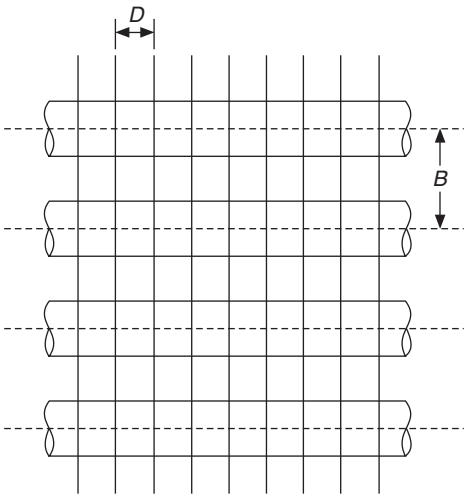

Figure 10.7 A portion of a plate fin-and-tube type condenser.

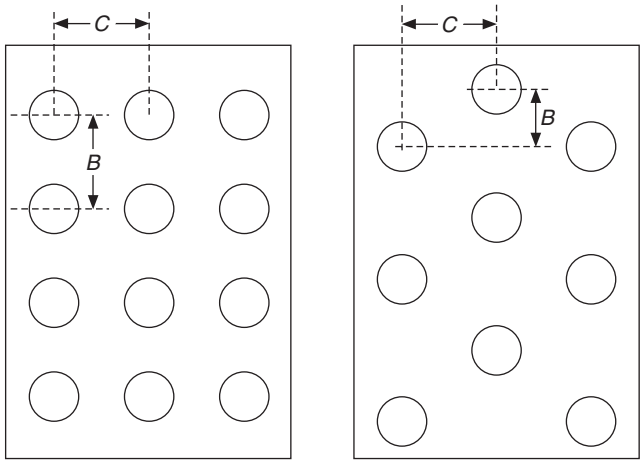

(a) Parallel tubes (b) Staggered tubes

Figure 10.8 Tube arrangements.

EXAMPLE 10.3 Find the effectiveness of a rectangular 0.3 mm thick fin made of aluminium, the spacing of the tubes in a row is 50 mm and the spacing between the rows is 40 mm. The tube outer diameter is 16 mm, air side convective heat transfer coefficient is 65 W/m^2-K and the thermal conductivity of aluminium is 202 W/m-K.

Solution:

$$r_2 = \sqrt{\frac{BC}{\pi}} = \sqrt{\frac{0.05 \times 0.04}{\pi}} = 0.02523$$

Thickness, $2y = 0.0003$ m $\quad \therefore \quad y = 0.00015$ m

$$m = \sqrt{\frac{h_{co}}{ky}} = \sqrt{\frac{65}{202(0.00015)}} = 46.316$$

and $$L = (r_2 - r_1) = 0.02523 - 0.008 = 0.01723$$

$$mL = 46.316 \times 0.01723 = 0.7981 \quad \text{and} \quad \frac{r_2}{r_1} = \frac{0.02523}{0.008} = 3.154$$

From an actual efficiency chart like Figure 10.6, the fin efficiency obtained is $\eta_f = 0.72$.

10.9 HEAT TRANSFER AREAS

Figure 10.3 shows the schematic diagram of a condenser or a cooling coil with tubes and fins. The air flows through the passages formed by the fins. The heat transfer takes place from the fins and the exposed part of the tube. The part of the tube directly under the fin transfers heat to the fin. Hence heat transfer occurs from the following areas.

1. Bare tube area between the consecutive fins. This will be denoted by A_{po}.
2. Area of the fins. This will be denoted by A_f.

These areas are expressed in terms of per m^2 of face area and per row. The face area A_{face} is the area of the condenser seen from outside, the actual flow area is less than the face area since fins have a finite thickness. Further, as the air flows through it, it has to pass between the narrow passage between the tubes. The flow area is minimum at these locations. This will be denoted by A_c. To find these areas we consider a condenser of 1.0 m height and 1.0 m width as shown in Figure 10.7. All the dimensions are in mm. The following nomenclature is used.

B: vertical spacing between the tubes in a row, mm
C: spacing between the tubes in different rows, mm
E: thickness of the fins, mm (i.e. $2y$ as shown in Figure 10.5(b))
D: centre-to-centre spacing between the fins, mm
d_o: outer diameter of the tubes, mm
d_i : inner diameter of the tubes, mm

Number of tubes per m height = $1000/B$ (tubes per m^2 face area per row)
Number of fin passages per m width = $1000/D$ (number of passages per m^2 face area)
Number of fins per m^2 face area = $1 + 1000/D \approx 1000/D$
Width of each passage = $(D - E)/1000$ (in metres)

Now the various areas are as follows:

Bare tube area, A_{po} = (tube perimeter)(number of fin passages)(number of tubes)
(width of each passage)

$$= (\pi d_o/1000)(1000/D)(1000/B)(D - E)/1000$$

$$\therefore \quad A_{po} = \frac{D - E}{DB}\pi d_o \quad (\text{m}^2 \text{ per m}^2 \text{ face area per row}) \tag{10.38}$$

Fin area, A_f = (number of fins) (two sides of fins){width of fin per row – number of tubes × area of cross section of each tube)}

$$= \left(\frac{1000}{D}\right)(2)\left\{1 \times \frac{C}{1000} - \left(\frac{1000}{B}\right)\frac{\pi(d_o/1000)^2}{4}\right\}$$

$$\therefore \quad A_f = \frac{2}{D}\left(C - \frac{\pi d_o^2}{4B}\right) \quad (\text{m}^2 \text{ per m}^2 \text{ face area per row}) \tag{10.39}$$

Minimum flow area, A_c = (number of fin passages)(width of each passage)(height – number of tubes per row × diameter of tube)

$$= \left(\frac{1000}{D}\right)\left(\frac{D-E}{1000}\right)\left\{1 - \frac{(1000/B)}{(d_o/1000)}\right\}$$

$$\therefore \quad A_c = \frac{D-E}{D}\left(1 - \frac{d_o}{B}\right) \quad (\text{m}^2 \text{ per m}^2 \text{ face area per row}) \tag{10.40}$$

Total heat transfer area,

A_o = bare tube area + fin area

or $A_o = A_{po} + A_f$ (m^2 per m^2 face area per row) (10.41)

Wetted perimeter, P = total heat transfer area/length in flow direction = $\dfrac{A_o}{C/1000}$

Hydraulic diameter, $D_h = 4A_c$/wetted perimeter

$$\therefore \quad D_h = \frac{4CA_c}{1000A_c} \tag{10.42}$$

The Reynolds number and the Nusselt numbers are based upon the hydraulic diameter.

Inside heat transfer area, $A_i = (\pi d_i/1000)$(Number of tubes) = $\pi d_i/B$

$$\therefore \quad A_i = \pi d_i/B \tag{10.43}$$

EXAMPLE 10.4 The dimensional data for three plate-fin-and-tube heat exchangers is as follows. Determine the various heat transfer areas such as the bare tube area, fin area, minimum flow area and hydraulic diameter.

	Surface I	Surface II	Surface III
Tube inside diameter d_i, mm	8.422	14.681	11.26
Tube outside diameter d_o, mm	10.2	17.17	12.68
Tube spacing B within a row, mm	25.4	38.1	43.0
Tube spacing C between rows, mm	22.0	44.45	38.0

Spacing D between fins, mm	3.175	3.277	3.175
Fin thickness E, mm	0.3302	0.4064	0.254
$A_{po} = \frac{D-E}{DB}\pi d_o$	1.1304	1.2402	0.8517
$A_f = \frac{2}{D}\left(C - \frac{\pi d_o^2}{4B}\right)$	11.832	23.419	22.42
$A_c = \frac{D-E}{D}\left(1 - \frac{d_o}{B}\right)$	0.5362	0.4813	0.6486
$A_o = A_{po} + A_f$	12.9624	24.6592	23.2717
$A_i = \pi d_i / B$	1.0417	1.2105	0.822
$D_h = \frac{4CA_c}{1000A_o}$	0.00364	0.00347	0.004236
A_o / A_i	12.444	20.371	28.31
A_{po} / A_f	0.08721	0.0503	0.038
St $Pr^{2/3}$	$0.176R^{-0.4087}$	$0.116Re^{-0.3705}$	

The experimental heat transfer characteristics for surface I and II are given by Kays and London (1955) as plots of St $Pr^{2/3}$ versus Re based upon the hydraulic diameter. These are straight lines.

10.10 OVERALL HEAT TRANSFER COEFFICIENT

The heat transfer coefficient of finned-tube condensers is expressed as follows:

$$Q = U_o A_o \Delta t_m \tag{10.44}$$

All the terms of this expression have been defined earlier except the overall heat transfer coefficient. The expression derived in Section 2.25 for the overall heat transfer coefficient has to be modified to include the effect of fins. Following the procedure of Section 2.25 the heat transfer rate through various components is written as follows:

$$Q = h_i A_i (t_R - t_{wi}) \tag{10.45}$$

$$= 2\pi k_w L \frac{t_{wi} - t_{wo}}{\ln (d_o / d_i)} \frac{1000}{B} = \frac{k_w A_i}{r_i}(t_{wi} - t_{wo}) = \frac{k_w A_{wm}}{x_w}(t_{wi} - t_{wo}) \tag{10.46}$$

$$= h_{co} A_o (t_{wo} - t) + h_{co} A_f (t_{fin} - t) \tag{10.47}$$

In Eq. (10.46) A_{wm} is the mean surface area of the pipe, $A_{wm} = \pi L(d_o + d_i)/2B$ and x_w is the thickness of the pipe, $x_w = (d_o - d_i)/2$. The term A_{wm}/x_w is an approximation to the log term, which is an exact expression for conduction heat transfer through the tube wall.

The air side heat transfer coefficient is denoted by h_{co} and the refrigerant side coefficient is denoted by h_i. The thermal conductivity of the wall material is k_w.

Also, from the definition of fin efficiency ϕ, we have

$$\phi = \frac{t_{fm} - t}{t_{wo} - t} \quad \text{where } t_{fb} = t_{wo}$$

Therefore, Eq. (10.44) may be written as follows:

$$Q = h_{co}(A_{po} + \phi A_f)(t_{po} - t) \tag{10.48}$$

Combining Eqs. (10.45), (10.46) and (10.48), we get

$$t_R - t = Q\left[\frac{1}{h_i A_i} + \frac{r_i \ln (d_o / d_i)}{A_i k_w} + \frac{1}{h_{co}(A_{po} + A_f)}\right] = \frac{Q}{U_o A_o}$$

The overall heat transfer coefficient U_o is defined as follows:

$$U_o = \frac{1}{\dfrac{A_o}{h_i A_i} + \dfrac{A_o}{A_i}\dfrac{r_i \ln (d_o / d_i)}{k_w} + \dfrac{A_o}{h_{co}(A_{po} + A_f)}}$$

This may also be written as

$$U_o = \frac{1}{\dfrac{A_o}{h_i A_i} + \dfrac{A_o}{A_i}\dfrac{r_i \ln (d_o / d_i)}{k_w} + \dfrac{1 - \phi}{(A_{po} / A_f + 1)}\dfrac{1}{h_{co}} + \dfrac{1}{h_{co}}} \tag{10.49}$$

This equation may be modified to include the deposit coefficient on either side. The deposit on the fin side usually has little effect since $1/h_{co}$ is rather large. In some cases an allowance may be made for imperfect contact between the fins and the tubes, however it is difficult to evaluate. It is negligible for good construction. The deposit coefficient for the inside coefficient is not negligible and must be included. If the deposit coefficient is h_{di}, the thermal resistance offered by it is $1/h_{di}$. The equation for overall heat transfer coefficient may be written as follows:

$$U_o = \frac{1}{\dfrac{A_o}{h_i A_i} + \dfrac{A_o}{h_{di} A_i} + \dfrac{A_o}{A_i}\dfrac{r_i \ln (d_o / d_i)}{k_w} + \dfrac{1 - \phi}{(A_{po} / A_f + 1)}\dfrac{1}{h_{co}} + \dfrac{1}{h_{co}}} \tag{10.50}$$

10.11 HEAT TRANSFER COEFFICIENTS

10.11.1 Air Side Heat Transfer Coefficient over Finned Tubes

The forced convection heat transfer coefficient for the air side depends upon the type of fins, fin spacing, fin thickness, tube diameters, etc. It can be evaluated experimentally for a particular fin-and-tube arrangement. Kays and London (1955) have carried out extensive measurements on the

fin-and-tube arrangement shown in Figure 10.7. They have presented the data in the forms of plot of St $Pr^{2/3}$ vs. Re for various geometries. On the average, the following correlation is a good fit to their data for various geometries.

$$\text{Nu} = 0.117\text{Re}^{0.65}\,\text{Pr}^{1/3} \tag{10.51}$$

The Nusselt number and Reynolds number are based upon the hydraulic diameter defined in Eq. (10.42).

Another simple expression has been proposed by the Air Conditioning and Refrigeration Institute, Arlington Va.(1972) , which is as follows:

$$h_{co} = 38V_f^{\,0.5} \tag{10.52}$$

where, V_f is the face velocity in m/s.

Pressure drop

Rich (1974) has carried out extensive measurements over the fin-tube heat exchangers and has given pressure drop plots. A correlation fitted to his data is as follows for various fin spacings for pressure drop in pascals per row. The velocity is the face velocity in m/s.

Number of fins/m	315	394	472	531	
Δp (Pa)	$7.15V^{1.56}$	$8.5V^{1.56}$	$9.63V^{1.56}$	$11V^{1.56}$	(10.53)

10.11.2 Air Side Heat Transfer Coefficient for Flow over Tube Banks

Heat transfer coefficient for flow over a horizontal tube has been presented in Section 2.20. Grimson has given correlations for average heat transfer coefficient for forced convection over tube banks in cross flow for staggered as well as in-line arrangement of tubes as shown in Figure 10.9. Face area A_f of the heat exchanger is the area seen from the flow direction and if Q_f is the volume flow rate of flow, then the face velocity V_f is given by

$$V_f = \frac{Q_f}{A_f}$$

The maximum velocity occurs between the tubes since the tubes block a part of the flow passage. If B is the spacing between tubes in the face and C is the tube spacing between rows, and d_o is the tube diameter, then maximum velocity is given by

$$V_{\max} = \frac{V_f B}{B - d_o} \tag{10.54}$$

The Reynolds and Nusselt number are defined as follows for this case:

$$\text{Re} = \frac{\rho V_{\max} d_o}{\mu} \quad \text{and} \quad \text{Nu} = \frac{h d_o}{k} \tag{10.55}$$

The Grimson's (1937) correlation is as follows

$$\text{Nu} = C\,\text{Re}^n\,\text{Pr}^{1/3} \tag{10.56}$$

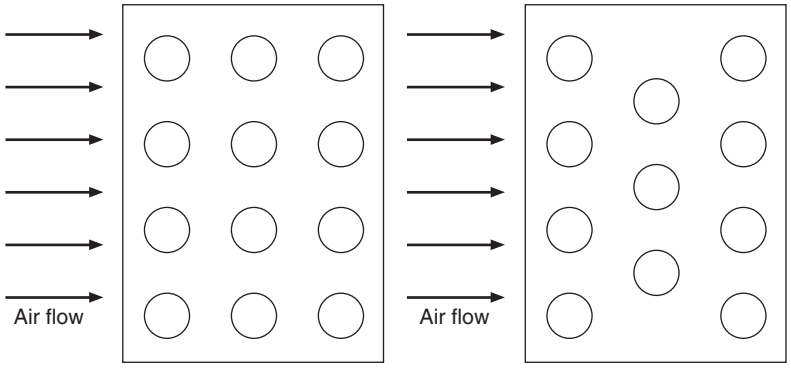

Figure 10.9 Schematic representation of plate fin-and-tube condenser with tubes-in-line and tubes staggered.

where the constants C and n are dependent upon Reynolds number and are as follows:

Re	C	n
0.4–4	0.989	0.33
4–40	0.911	0.385
40–4000	0.683	0.466
4000–40,000	0.193	0.618
40,000–400,000	0.0266	0.805

Presure drop:

Pierson and Huge have given the correlation for pressure drop for flow over tube banks as follows:

$$\Delta p = \frac{f N V^2}{2} \tag{10.57}$$

where, f is the friction factor and N is the number of rows. The friction factor is given by

$$f = \mathrm{Re}^{-0.15}\left[0.176 + \frac{0.32b}{(a-1)^{0.43} + 1.13/b}\right] \quad \text{for tubes in-line}$$
$$f = \mathrm{Re}^{-0.16}\left[1.0 + \frac{0.47}{(a-1)^{1.08}}\right] \quad \text{for staggered tubes} \tag{10.58}$$

EXAMPLE 10.5 A heat exchanger is to be designed to process 450 m^3/min of air from 10°C to 25°C. The inlet face velocity is 150 m/min. Heating medium is steam at 100°C. Type II surface is to be used. Determine the required face area, the total outside surface area, the number of rows required and kg/h of steam required. The condensation heat transfer coefficient for steam is given to be 6800 W/m^2-K.

Solution: Face area = volume flow rate /face velocity = 450/150 = 3 m^2

$$\text{LMTD} = \frac{25-10}{\ln\dfrac{100-10}{100-25}} = \frac{15}{\ln(90/75)} = 82.27$$

The properties of air at 25°C are: $\rho = 1.1774$ kg/m^3, $\mu = 1.983 \times 10^{-5}$ kg/m-s, $c_p = 1005.7$ J/kg-K and $k = 0.02624$ W/m-K

The minimum flow passage area for surface II is $A_c = 0.4813$. Therefore,

$$V_{\max} = V_f/A_c = 150/0.4813 \text{ m/min} \quad \text{and} \quad D_h = 0.00347 \text{ m}$$

$$\text{Re} = \frac{1.177(150)}{60(0.4813)} \frac{0.00347}{1.983\times10^{-5}} = 1609.8$$

$$\text{St Pr}^{2/3} = 0.116\text{Re}^{-0.3705} = 8.7543 \times 10^{-3} \quad \therefore \quad \text{Nu} = 8.3155$$

$$h_o = \frac{8.3155(0.02624)}{0.00347} = 62.88 \text{ W/m}^2\text{-K}$$

$$r_2 = \sqrt{\frac{BC}{\pi}} = \sqrt{\frac{0.0381\times0.04445}{\pi}} = 0.023218$$

Thickness $2y = 0.0004064$ m $\quad \therefore \quad y = 0.0002032$ m and $L = (r_2 - r_1) = 0.023218 - 0.008585 = 0.014633$ m. Thermal conductivity of aluminium = 202 W/m-K

$$L\sqrt{\frac{h_o}{k_{al}y}} = 0.014633\sqrt{\frac{62.88}{202(0.0002032)}} = 0.565 \text{ m}$$

From Figure 10.6, the fin effectiveness $\phi = 0.86$

Substituting these values in Eq. (10.50), we get

$$\frac{1}{U_o} = \frac{20.371}{6800} + 20.371(0.00009) + \frac{0.14}{62.88(0.91)} + \frac{1}{62.88} \quad \therefore \quad U_0 = 43.142 \text{ W/m}^2\text{-K}$$

$$Q_t = \dot{m}c_p(t_2 - t_1) = \left(\frac{450}{60}\right)1.1774\times1.0057(25-10) = 133.2125 \text{ kW}$$

$A_t\, U_o$ LMTD = 133.2125 kW $\quad \therefore \quad A_t = 133212.5/(43.142 \times 82.27) = 37.532$ m^2

$A_o = 24.6592$ m^2 per m^2 face area per row

Face area = 3 m^2

$\therefore$ Number of rows = 37.532/24.6592 (3) = 0.5

In fact, half a row is sufficient which is rounded to one row.

If the face area is reduced, the face velocity will increase. Actually a face area of 37.532/24.6592 = 1.522 m^2 is sufficient. This will increase the face velocity to 4.93 m/s and other parameters will change to: Re = 2109.64, Nu = 12.747, $h_o = 96.39$, $U_o = 59.52$, $A_t = 27.2$ and the number of rows = 0.724 ≈ 1.

10.11.3 Condensation Heat Transfer Coefficient

Outside horizontal tubes

The condensation heat transfer coefficient was discussed in Section 2.21. A typical correlation known as Nusselt's correlation for film-wise condensation outside a bank of horizontal tubes as given by Eq. (2.124) is as follow:

$$h_o = 0.725\left[\frac{k_f^3 \rho_f (\rho_f - \rho_g) g h_{fg}}{N D_0 \mu_f \Delta t}\right]^{0.25}$$

The density of liquid is much more than that of vapour, hence this expression may be approximated by

$$h_o = 0.725\left[\frac{k_f^3 \rho_f^2 g h_{fg}}{N D_o \mu_f \Delta t}\right]^{1/4} \tag{10.59}$$

This expression is exactly valid for still vapour. In this expression the subscript f refers to the properties of saturated liquid, which are evaluated at mean film temperature of $(t_{wo} + t_r)/2$. Here D_o is the outer diameter of the tube and N is the average number of tubes per column.

Several investigators have confirmed the constant to be 0.725, however, White (1948) has proposed a constant of 0.68 and Gotto et al. (1979) have proposed the value of 0.65.

For a vertical surface the constant is 1.13 instead of 0.725. Some of the features of this correlation are as follows.

(a) As thermal conductivity k_f increases, the heat transfer coefficient increases since conduction thermal resistance of the condensate film decreases.

(b) Similarly a decrease in viscosity or increase in density will offer less frictional resistance and cause rapid draining of the condensate, thereby causing an increase in heat transfer coefficient.

(c) A high value of latent heat h_{fg} means that for each kW of heat transfer there will be smaller condensate thickness and higher heat transfer coefficient.

(d) An increase in diameter means larger condensate thickness at the bottom and hence a smaller heat transfer coefficient.

(e) A large value of temperature difference will lead to more condensation and larger condensate thickness and eventually to a smaller heat transfer coefficient.

(f) An increase in the number of tubes will lead to a larger condensate thickness in the lower tubes, leading to a smaller heat transfer coefficient

In actual practice the vapour will not be still but it will move with some velocity and the condensate will splash and ripples will be caused which may lead to a larger value of heat transfer coefficient. Hence the above equation gives a very conservative estimate of the condensation heat transfer coefficient.

Outside vertical tube

For laminar flow the average heat transfer coefficient by Nusselt's correlation for condensation over a vertical tube is as follows:

$$h_o = 1.13\left[\frac{k_f^3 \rho_f (\rho_f - \rho_g) g h_{fg}}{L \mu_f \Delta t}\right]^{0.25} \tag{10.60}$$

where L is the tube length. This expression may be used in laminar flow up to $\mathrm{Re}_f = 1800$, where $\mathrm{Re}_f = 4\dot{m}/(\pi \mu_f D)$. Kirkbride rearranged this correlation in terms of *condensation number* C_o, which is defined as follows:

$$C_o = h_o\left[\frac{\mu_f^2}{k_f^3 \rho_f^2 g}\right]^{1/3} = 1.514\,\mathrm{Re}_f^{-1/3} = 1.514\,\mathrm{Re}_f^{-1/3} \tag{10.61}$$

For turbulent flow : $\mathrm{Re}_f > 1800$, the Kirkbride correlation is as follows:

$$C_o = h_o\left[\frac{\mu_f^2}{k_f^3 \rho_f^2 g}\right] = 0.0077\,\mathrm{Re}_f^{0.4} \tag{10.62}$$

Condensation inside tubes

Condensation heat transfer inside tubes causes a reduction in the area of condensation due to liquid collecting in the bottom of the tubes. The draining of the condensate may retard or accelerate the vapour flow depending upon whether it flows in the same direction as the vapour or in the opposite direction. The flow rate of vapour considerably influences the heat transfer coefficient.

(a) *Chaddock and Chato's correlation:* Chaddock and Chato suggested that condensation heat transfer coefficient inside tubes is 0.77 times that of Nusselt's heat transfer coefficient outside the tubes particularly if the vapour Reynolds number $\mathrm{Re}_g = \mathrm{Re}_f = 4\dot{m}/(\pi \mu_g D_i) < 35{,}000$. This gives the average value of the heat transfer coefficient over the length of the tube.

$$h_{TP} = 0.77 h_o$$

$$h_{TP} = 0.555\left[\frac{k_f^3 \rho_f (\rho_f - \rho_g) g h'_{fg}}{D_i \mu_f \Delta t}\right]^{0.25} \tag{10.63}$$

where the modified enthalpy of evaporation is defined as $h'_{fg} = h_{fg} + 3c_{pf}\Delta t/8$, Δt being the difference beween the temperature of the condensing refrigerant and the temperature of the surface.

(b) *Cavallini Zecchin correlation:* This correlation represents the condensation heat transfer coefficient in a manner similar to Dittus Boelter equation for turbulent flow

heat transfer inside tubes. The constant is different from that equation and an equivalent Reynolds number is used to take care of two-phase flow and incomplete condensation. The local values of heat transfer coefficient can also be found if the quality distribution is known.

$$h_{TP} = 0.05\,\mathrm{Re}_{\mathrm{eq}}^{0.8}\,\mathrm{Pr}_f^{0.33}\,k_f / D_i$$

$$\mathrm{Re}_{\mathrm{eq}} = \mathrm{Re}_f\,(1-x) + x\left(\frac{\mu_g}{\mu_f}\right)\left(\frac{\rho_f}{\rho_g}\right)^{0.5}\mathrm{Re}_g$$

where,
$$\mathrm{Re}_g = \frac{4\dot{m}}{\pi D_i \mu_g} \quad \text{and} \quad \mathrm{Re}_f = \frac{4\dot{m}}{\pi D_i \mu_f} \tag{10.64}$$

(c) *Traviss et al. correlation:* This correlation uses the Lockhart Martinilli parameter which takes into account incomplete condensation. This can also be used for evaluation of local heat transfer coefficient if the quality of mixture is known. The correlation covers a wide range of Reynolds numbers defined as $\mathrm{Re}_l = (1-x)\,\mathrm{Re}_f$, where Re_f is the Reynolds number if all the refrigerant flows in liquid phase.

$$\mathrm{Nu} = \left[\frac{\mathrm{Pr}_f\,\mathrm{Re}_f^{0.9}}{F_2}\right] F_{tt} : \text{for } 0.15 < F_{tt} < 15$$

$$F_{tt} = 0.15\,(X_{tt}^{-1} + 2.85\,X_{tt}^{-0.467}) \quad \text{and}$$

$$F_2 = 0.707\mathrm{Pr}_f\,\mathrm{Re}_l \quad \text{for} \quad \mathrm{Re}_l < 50 \quad \text{where, } \mathrm{Re}_l = (1-x)\,\mathrm{Re}_f$$

$$F_2 = 5\,\mathrm{Pr}_f + 5\ln\left[1 + \mathrm{Pr}_f\,(0.09636\,\mathrm{Re}_l^{0.585} - 1)\right] \quad \text{for} \quad 50 < \mathrm{Re}_l < 1125$$

$$F_2 = 5\,\mathrm{Pr}_f + 5\ln[1 + 5\,\mathrm{Pr}_f] + 2.5\ln\left[0.00313\,\mathrm{Re}_l^{0.812}\right] \quad \text{for} \quad \mathrm{Re}_l > 1125$$

$$X_{tt} = [(1-x)/x]^{0.9}\,(\rho_g/\rho_f)^{0.5}\,(\mu_f/\mu_g)^{0.1} : \text{Lockhart Martinilli parameter} \tag{10.65}$$

(d) *Shah's correlation:* This correlation takes into account also the pressure of the refrigerant in addition to the quality of the mixture. It can also be used to find the local condensation heat transfer coefficient. The heat transfer coefficient is a product of the heat transfer coefficient given by Dittus–Boelter equation and an additional term.

$$h_{TP} = h_L\left[(1-x)^{0.8} + \frac{3.8x^{0.76}\,(1-x)^{0.04}}{p_r^{0.38}}\right]$$

where, $p_r = p/p_{\mathrm{cri}}$ = reduced pressure

$$h_L = 0.023\,\mathrm{Re}_f^{0.8}\,\mathrm{Pr}_f^{0.4}\,k_f / D_i$$

$$\bar{h}_{TP} = h_{TP}\,(0.55 + 2.09/p_r^{0.38}) : \text{average value of heat transfer coefficient at } x = 0.5$$

(10.66)

(e) *Akers, Dean and Crosser correlation:* Akers, Dean and Crosser have proposed the following correlation when the rate of condensation or the length is very large. This is very similar to Dittus–Boelter correlation for turbulent heat transfer in tubes, except that the constant is different.

$$\frac{hD_i}{k_f} = 5.03\,\mathrm{Re}_m^{1/3}\,\mathrm{Pr}_f^{1/3} \quad \text{for} \quad \mathrm{Re}_g < 5\times10^4$$

$$= 0.0265\,\mathrm{Re}_m^{0.8}\,\mathrm{Pr}_f^{1/3} \quad \text{for} \quad \mathrm{Re}_g > 5\times10^4$$

where $$\mathrm{Re}_m = \mathrm{Re}_f\,[1 + (\rho_f/\rho_g)^{0.5}] \tag{10.67}$$

In this correlation the heat transfer coefficient is independent of the temperature difference and it increases with the increase in the liquid Reynolds number, Re_f. Sometimes, it overestimates the heat transfer coefficient.

10.11.4 Fouling Factor—Deposit Coefficient

The condenser tubes are clean when it is assembled with new tubes. However with usage some scale formation takes place in all the tubes and the value of the overall heat transfer coefficient decreases. It is a standard practice to control the hardness of water used in the condenser. Even then it is a good maintenance practice to descale the condenser once a year with 2% HCl or muric acid solution. Stoecker suggests the following values of deposit coefficients.

$1/h_{di.} = 0.00009$ J^{-1}-s-m^2 for R12 and R-22 with copper tubes

$1/h_{di.} = 0.000178$ J^{-1}-s-m^2 for steel tubes with ammonia. (10.68)

10.12 WATER COOLED CONDENSERS

10.12.1 Classification

There are, in general, four types of water cooled condensers:

1. Double-tube type
2. Shell-and-coil type
3. Shell-and-tube type, both horizontal and vertical
4. Evaporative condenser

Double-pipe type condenser

This type of condenser is used up to 10 TR capacity. The cold water flows through the inner tube and the refrigerant flows through the annulus in counterflow as shown in Figure 10.10. Headers are used at both the ends to make the length of the condenser small and reduce the pressure drop. The refrigerant in the annulus rejects a part of its heat to the surroundings by free convection and radiation. The heat transfer coefficient is usually low because of the poor liquid refrigerant drainage if the tubes are long.

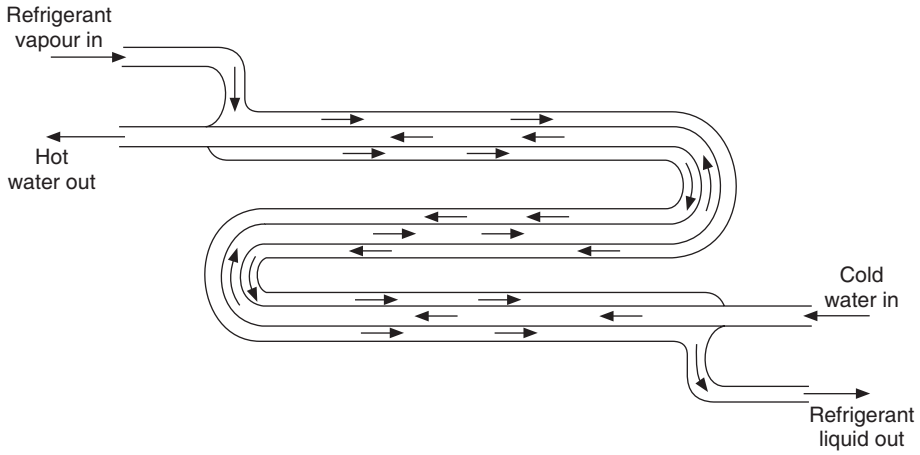

Figure 10.10 The double-tube type water-cooled condenser.

Shell-and-coil type condenser

This type of condenser may be used up to 50 TR capacity. The water flows through multiple coils which may have fins to increase the heat transfer coefficient. The refrigerant flows through the shell. In smaller capacity condensers, the refrigerant flows through coils while the water flows through the shell. Figure 10.11 shows a shell-and-coil type condenser.

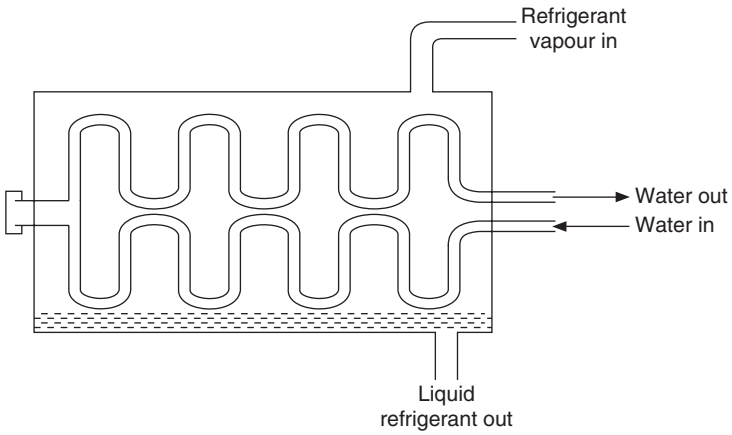

Figure 10.11 The shell-and-coil type condenser.

Shell-and-tube type condenser—both horizontal and vertical

The shell-and-tube type is the most common type of condenser, which is used from 2 TR to thousands of TR capacity. The refrigerant flows through the shell while the water flows through the tubes in single to four passes. The condensed refrigerant collects at the bottom of the shell. The coldest water contacts the liquid refrigerant so that some subcooling can also be obtained.

The liquid refrigerant is drained from the bottom to the receiver. There might be a vent connecting the receiver to the condenser for smooth drainage of the liquid refrigerant. The shell also acts as a receiver. Further the vapour refrigerant also rejects heat to the surroundings from the shell. The most common type is horizontal shell type. A schematic diagram of the horizontal shell-and-tube type condenser is shown in Figure 10.12.

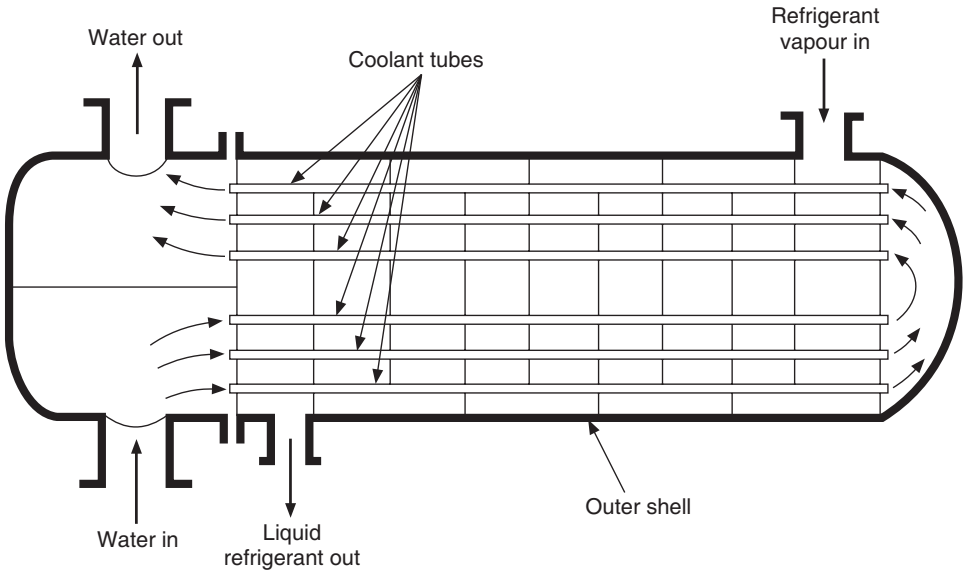

Figure 10.12 The shell-and-tube condenser with one-shell pass and two-tube pass.

The vertical shell-and-tube type condenser is usually used with ammonia in large capacity systems so that cleaning of the tubes is possible from top while the plant is running.

10.12.2 Heat Transfer Relations for Water-cooled Condenser

The heat transfer rate from the water-cooled condenser is also found in a manner similar to that for air-cooled condenser. The concept of *log mean temperature difference* for the mean temperature is still valid since it is assumed that condensation occurs throughout the length of the condenser and hot fluid (refrigerant temperature) remains constant. Considering the water and the refrigerant to be in counterflow, the heat transfer rate given by Eq. (2.155) is as follows:

$$Q = U_o A_o \, \Delta t_m = U_o A_o \, \frac{\Delta t_2 - \Delta t_1}{\ln (\Delta t_2 / \Delta t_1)} \tag{10.69}$$

$$\text{LMTD} = \Delta t_m = \frac{\Delta t_2 - \Delta t_1}{\ln (\Delta t_2 / \Delta t_1)} \tag{10.70}$$

where $\Delta t_2 = t_c - t_{wo}$ and $\Delta t_1 = t_c - t_{wi}$: t_c is the condenser temperature, t_{wi} is the water inlet temperature and t_{wo} is the water outlet temperature.

The expression for the overall heat transfer coefficient is similar to Eq. (10.39) except for the fin efficiency term

$$U_o = \frac{1}{\frac{A_o}{h_i A_i} + \frac{A_o}{h_{di} A_i} + \frac{A_o}{A_i}\frac{r_i \ln(d_o/d_i)}{k_w} + \frac{1}{h_o}} \tag{10.71}$$

In this expression, h_o is the heat transfer coefficient for condensation outside horizontal tubes as given by Eq. (10.41). The inside heat transfer coefficient h_i is the water-side heat transfer coefficient. The flow of water is invariably turbulent flow, hence it is obtained from Dittus–Boelter Eq. (2.111)

$$\text{Nu} = 0.023\ \text{Re}^{0.8}\ \text{Pr}^{0.4} \tag{10.72}$$

In case the viscosity variation is important, Side and Tate Eq. (2.112) may be used, which is as follows.

$$\text{Nu} = 0.036\ \text{Re}^{0.8}\ \text{Pr}^{1/3}\ (\mu/\mu_w)^{0.14} \tag{10.73}$$

If the Reynolds number is less than 2300, the flow will be laminar; then any of the equations mentioned in Chapter 2 may be used, for example, Hausen's correlation for the flow in the developing length given by Eq. (2.104) is as follows:

$$\overline{\text{Nu}}_d = 3.66 + \frac{0.0668(D_i/L)\,\text{Pe}}{1 + 0.04[(D_i/L)\,\text{Pe}]^{2/3}} \tag{10.74}$$

10.12.3 Finned Tubes

The condensation heat transfer coefficient is of the order of 7000 W/m^2-K for ammonia. However it is of the order of 1700 W/m^2-K for R12 and R22, whereas the water side heat transfer coefficient is high in both the cases for turbulent flow. It is advisable to add fins on the side where the heat transfer coefficient is low. In case of R12 and R2 condensers the tubes have integral external fins to augment the heat transfer rate. This is easily seen if the overall heat transfer coefficient is written in terms of the inside area as follows:

$$\frac{1}{U_i} = \frac{1}{h_i} + \frac{r_i \ln(d_o/d_i)}{k_w} + \frac{1}{h_o}\frac{A_i}{A_o} + \frac{1}{h_{di}}$$

It is observed that by increasing the area ratio A_o/A_i, that is, the outside surface area, the overall heat transfer coefficient can be increased.

10.12.4 Wilson Plot

This concept of Wilson's was introduced way back in 1915 by Wilson to determine the individual heat transfer coefficients from the experimental data on heat transfer characteristics of heat exchangers. This approach is sometimes applied to determine the condensing or boiling heat transfer coefficients of condensers and evaporators respectively.

In a water-cooled condenser, for example, a number of tests are conducted by varying the flow rates of water through it and measuring the inlet and outlet water temperatures. The total heat transfer rate is determined from

$$Q = \dot{m}_w c_{pw} (t_{wo} - t_{wi}) \tag{10.75}$$

Then the overall heat transfer coefficient U_o is determined from Eq. (10.71) for various velocities of water. If the tubes are clean, that is, deposit or scale coefficient is negligible, then Eq. (10.71) reduces to

$$\frac{1}{U_o} = \frac{A_o}{h_i A_i} + \frac{A_o}{A_i} \frac{r_i \ln (d_o / d_i)}{k_w} + \frac{1}{h_o} \tag{10.76}$$

If the water temperature does not vary very significantly during these tests, then the properties of water almost remain constant. Since during these tests no changes are made on the refrigerant side, it can be assumed that the heat transfer resistance offered by the wall separating the two fluids and the heat transfer coefficient on the refrigerant side (h_o) remains constant for all values of water flow rates. Hence, Eq. (10.76) can be written as

$$\frac{1}{U_o} = C_1 + \frac{C_2}{h_i} \tag{10.77}$$

where C_1 and C_2 are empirical constants that depend on the specifications of the heat exchangers and operating conditions, and the expressions for these can be obtained by equating Eqs. (10.76) and (10.77).

If the flow on the water side is turbulent and the variations in thermal properties are negligible, then the waterside heat transfer coefficient can be written as

$$h_i = C_3 \, . \, V^{0.8} \tag{10.78}$$

Substituting this expression in Eq. (10.77), we obtain

$$\frac{1}{U_o} = C_1 + \frac{C_4}{V^{0.8}} \tag{10.79}$$

The Wilson plot for the condenser is a plot of $1/U_o$ versus $1/V^{0.8}$ as shown in Figure 10.13. This plot is extrapolated to infinitely high velocity where $1/V^{0.8}$ tends to zero, i.e. $1/h_i$ tends to zero. Hence the intercept on the ordinate is $1/h_o + A_o r_i \ln (d_o/d_i)/(A_i k_w)$ which is equal to C_1. The thermal conduction resistance of the tube can be calculated and then the condensation heat transfer coefficient h_o can be calculated. As shown in the figure, the term $A_o/(A_i h_i)$ can also be obtained from the figure at any value of velocity.

It should be kept in mind that Wilson's plot is an approximation since drawing a straight line and extending it to meet the y-axis means that the condensation heat transfer remains constant as the velocity tends to infinity. Wilson's plot can be applied to air-cooled condensers as well. In this case as the heat transfer coefficient for air over the finned surface varies as $V^{0.65}$, $1/U_o$ will have to be plotted versus $V^{-0.65}$.

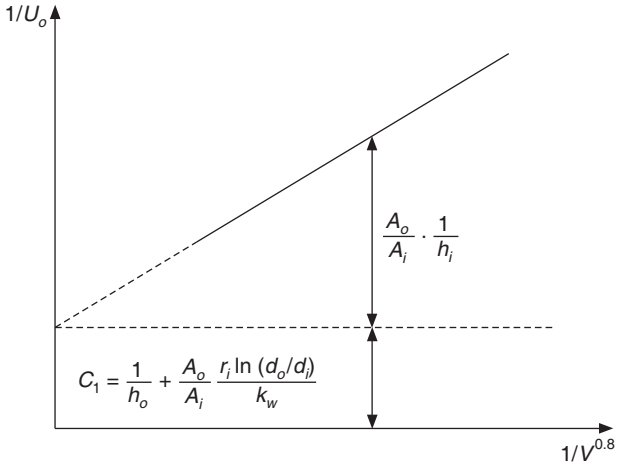

Figure 10.13 Wilson's plot.

10.12.5 Effect of Air and Noncondensables

This is usually a problem with refrigerants R11 and R113 which have been banned now due to their high ozone depletion potential. However, some air may be left behind before the system is evacuated and charged with refrigerant. If some noncondensable gase or air enters the system, it will collect in the condenser and lead to two adverse effects.

1. Condensation will take place at the saturation pressure corresponding to the condenser pressure, which will be the partial pressure of the refrigerant in the mixture of refrigerant and air in this case. The air will have its partial pressure proportional to its amount in the condenser. The total pressure will be the sum of these two partial pressures, which will be high and the compressor would have to work against this pressure ratio and hence the work requirement will increase.
2. Noncondensable gases do not diffuse throughout the condenser as the refrigerant condenses. They cling to the tubes and reduce the precious heat transfer area. The reduction in heat transfer area causes the temperature difference between the cold water and the refrigerant to increase. This raises the condenser temperature and the corresponding pressure, thereby reducing the COP.

10.12.6 Cost of Water

The total running cost of a refrigeration system is the sum of the cost of compressor power and the cost of water. The cost of water can be the cost of municipal water or the cost of running a cooling tower. The compressor power increases as the condenser temperature or the pressure increases for a fixed evaporator temperature. The water from a cooling tower is usually available at a fixed temperature equal to the wet-bulb temperature of air plus the approach temperature of the cooling tower. As the condenser temperature increases the overall *log mean temperature* increases, as a result a lower mass flow rate of cooling water is required. This reduces the cost of water at higher

condenser temperatures. Figure 10.14 shows the general trend of the total running cost of a refrigeration system. It is observed that there is a condenser pressure at which the running cost is minimum and it is recommended that the system should be run at this pressure. This poses some problems during winter operation.

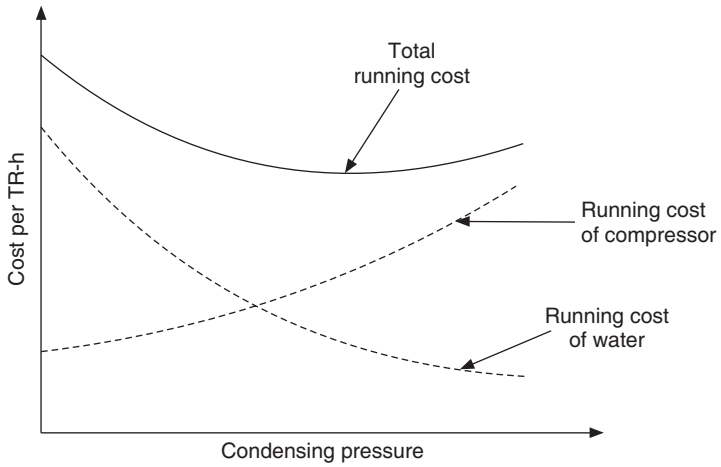

Figure 10.14 Variation of total running cost of a refrigeration system with condensing pressure.

A complete analysis of the cost should actually be carried out which should include the initial cost of the whole system, the interest on capital, the depreciation, the maintenance cost, the operator cost, and so on. The final selection of the system and the operating conditions should be such that the cost is the least over the running life of the system.

EXAMPLE 10.6 Determine the length of tubes in a two-pass 10 TR shell-and-tube R22 water-cooled condenser with 52 tubes arranged in thirteen columns as shown in Figure 10.15. The heat rejection ratio is 1.2747. The condensing temperature is 45°C. The water inlet and outlet temperatures are 30°C and 35°C respectively. The tube inner and outer diameters are 14.0 and 16.0 mm respectively. The average properties of the refrigerant and water are as follows:

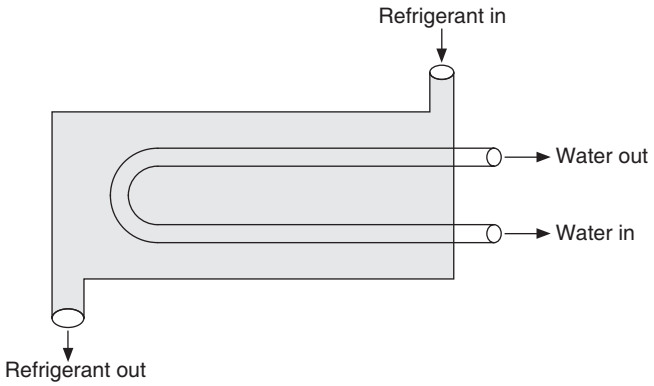

Figure 10.15 Schematic of one-shell pass and two-tube passes condenser for Example 10.6.

Water	**R22**
$\mu_w = 7.73 \times 10^{-4}$ kg/m-s	$\mu_f = 1.8 \times 10^{-4}$ kg/m-s
$k_w = 0.617$ W/m-K	$k_f = 0.0779$ W/m-K
$\rho_w = 995.0$ kg/m^3	$\rho_f = 1118.9$ kg/m^3
$c_{pw} = 4.19$ kJ/kg-K	$h_{fg} = 160.9$ kJ/kg
$1/h_s = 0.000176$ m^2-K/W	$k_{\text{copper}} = 390$ W/m-K
Nu = 0.023 Re$^{0.8}$Pr$^{0.4}$	$h_o = 0.725[k_f^3 \rho_f^2 g\, h_{fg}/(N d_o \mu_f\, \Delta t]^{0.25}$

Solution:

Heat rejection in the condenser for a 10 TR plant,

$$Q_c = 1.2747 \times 10 \times (211/60)$$
$$= 44.82695 \text{ kW}$$

This heat is rejected to water. The temperature of water goes up by 5°C. The specific heat of water is given the hence the mass flow rate of water can be found as follows. The water passes through 26 tubes at a time. Let its mass flow rate be $\dot{m}_w$. Then,

$$Q_c = \dot{m}_w c_{pw} \Delta t_w = \dot{m}_w \times 4.19 \times (35 - 30) = 44.82695 \text{ kW}$$

or $$\dot{m}_w = 44.82695/(4.19 \times 5) = 2.1397 \text{ kg/s}$$

Water flow per tube, $\dot{m}_{wt} = 2.1397/26 = 0.0823$ kg/s

Reynolds number, $$\text{Re} = \frac{4\dot{m}_{wt}}{\pi d_o \mu_w} = 4 \times \frac{0.0823}{3.1419 \times 0.014 \times 7.73 \times 10^{-4}}$$
$$= 4682.57$$

The Reynolds number is greater than 2300, hence the flow is turbulent and the inside heat transfer coefficient h_i may be found by the Dittus–Boelter equation as follows.

$$\text{Pr} = \frac{c_{pw}\mu_w}{k_w} = 4.19 \times 1000 \times 7.73 \times \frac{10^{-4}}{0.617} = 5.2494$$

$$\text{Nu} = \frac{h_i\, d_i}{k_w} = 0.023\,(4682.57)^{0.8}\,(5.2494)^{0.4} = 68.955$$

$$h_i = 68.955 \times \frac{0.617}{0.014} = 3038.922 \text{ W/m}^2\text{-K}$$

The refrigerant condenses outside the tubes. Fifty-two tubes are arranged in 13 columns. Hence on the average there are 4 tubes (56/13) in each column. Therefore we take $N = 4$ in the Nusselt correlation,

$$h_o = 0.725\left[\frac{k_f^3 \rho_f\, g h_{fg}}{N D_o \mu_f \Delta t}\right]^{1/4} = 0.725\left[\frac{(0.0779)^3 (1118.9)^2 \times 9.81 \times 160.9 \times 10^3}{4 \times 0.016 \times 1.8 \times 10^{-4}\, \Delta t}\right]^{0.25}$$

$$= 0.725\left[\frac{8.09596 \times 10^{13}}{\Delta t}\right]^{0.25}$$

or
$$h_o = \frac{0.725 \times 2.999626}{\Delta t^{0.25}} = \frac{2.17473}{\Delta t^{0.25}}$$

where, $\Delta t = t_R - t_{po}$. This is not known apriori. A suitable value has to be assumed for it and then this has to be cross checked. Therefore, the calculation procedure requires iteration. From the basic heat transfer relations, we have

$$Q_c = A_i\, h_i\, (t_{pi} - t_s) = A_i\, h_s\, (t_s - t_w)$$

or
$$Q_c = 2\pi L k_{\text{copper}} \frac{(t_{po} - t_{pi})}{\ln (d_o / d_i)}$$

or
$$Q_c = A_o\, h_o\, (t_R - t_{po})$$

The overall heat transfer coefficient U_o based upon the outside area is defined by the following equation

$$Q_c = U_o\, A_o (t_R - t_w)$$

Therefore, the overall heat transfer coefficient is given by the following equation:

$$\frac{1}{U_o} = \frac{1}{h_o} + \frac{d_o}{d_i}\frac{1}{h_s} + \frac{d_o \ln (d_o / d_i)}{2\pi k_{\text{copper}}} + \frac{d_o}{d_i}\frac{1}{h_i}$$

or
$$\frac{1}{U_o} = \frac{1}{h_o} + \frac{0.16}{0.14} 0.000176 + \frac{0.16 \ln (0.16/0.14)}{2\pi (390)} + \frac{0.16}{0.14}\frac{1}{3038.922}$$

or
$$\frac{1}{U_o} = 0.0005781 + \frac{1}{h_o}$$

If the conduction resistance due to copper wall is neglected, then

$$\frac{1}{U_o} = 0.0005772 + \frac{1}{h_o}$$

First Trial

To start the calculation, we assume $\Delta t = 5^{\circ}$C. Therefore, condensation heat transfer coefficient,

$$h_o = \frac{2.17473}{(5)^{0.25}} = 1454.316 \text{ W/m}^2\text{-K}$$

The overall heat transfer coefficient is given by

$$\frac{1}{U_o} = 0.0005781 + \frac{1}{1456.316}$$

$$\therefore \quad U_o = 790.8 \text{ W/m}^2\text{-K}$$

The wall temperature and the water temperature vary throughout the length of the tubes while the refrigerant temperature remains constant, hence we use the *log mean temperature difference* for the calculation. That is,

$$\text{LMTD} = \frac{(45-30)-(45-35)}{\ln\left(\frac{45-30}{45-35}\right)} = 12.331517$$

$$\therefore \quad Q_c = (U_o)\,(A_o)\,(\text{LMTD})$$

$$\therefore \quad A_o = \frac{Q_c}{(U_o)(\text{LMTD})} = 44.82695 \times \frac{10^3}{790.8 \times 12.331517} = 4.601 \text{ m}^2$$

Now the assumed temperature difference for the condensation heat transfer coefficient $\Delta t = (t_R - t_{po})$ is cross checked by using the condensation heat transfer coefficient and the outside heat transfer area A_o.

$$\Delta t = \frac{Q_c}{h_o A_o} = \frac{44826.95}{4.601 \times 1454.316} = 6.699 \text{ K}$$

Second Trial

Assume $\Delta t = 7^\circ$C

$$h_o = \frac{2.17473}{(7)^{0.25}} = 1336.998 \text{ W/m}^2\text{-K}$$

$$\frac{1}{U_o} = 0.0005781 + \frac{1}{1336.998}$$

$$\therefore \quad U_o = 754.123 \text{ W/m}^2\text{-K}$$

$$A_o = 44.82695 \times \frac{10^3}{754.123 \times 12.331517} = 4.82036 \text{ m}^2$$

$$\Delta t = \frac{Q_c}{h_o A_o} = \frac{44826.95}{4.82036 \times 1454.316} = 6.955 \text{ K}$$

Hence a temperature difference of 7°C is the correct answer.

We have 56 tubes of 0.016 m outside diameter. Hence, $A_o = 56\pi d_o L$

$$\therefore \quad L = \frac{A_o}{56\pi d_o} = \frac{4.82036}{56\pi \times 0.016} = 1.844 \text{ m}$$

EXAMPLE 10.7 If the configuration of Example 10.6 is used for a condenser of 25 TR capacity, determine the length of the shell-and-tube condenser.

Solution:

For a 25 TR plant, $Q_c = 1.2747 \times 25 \times (211/60) = 112.0684$ kW

$$Q_c = \dot{m}_w c_{pw} \Delta t_w = \dot{m}_w \times 4.19 \times (35 - 30) = 112.0684 \text{ kW}$$

$$\therefore \quad \dot{m}_w = \frac{112.0684}{4.19 \times 5} = 5.34933 \text{ kg/s}$$

Water flow per tube,

$$\dot{m}_{wt} = \frac{5.34933}{26} = 0.20574 \text{ kg/s}$$

Reynolds number, $$\text{Re} = \frac{4\dot{m}_{wt}}{\pi d_o \mu_w} = \frac{4 \times 0.20574}{3.1419 \times 0.014 \times 7.73 \times 10^{-4}}$$

$$\therefore \quad \text{Re} = 24206.3$$

Now, $$\text{Nu} = \frac{h_i d_i}{k_w} = 0.023 (24206.3)^{0.8} (5.2494)^{0.4} = 143.5205$$

$$\therefore \quad h_i = 143.5205 \times \frac{0.617}{0.014} = 6325.154 \text{ W/m}^2\text{-K}$$

The expression for the condensation heat transfer coefficient is the same, hence we get

$$\frac{1}{U_o} = \frac{1}{h_o} + \frac{0.16}{0.14} 0.000176 + \frac{0.16 \ln (0.16/0.14)}{2\pi (390)} + \frac{0.16}{0.14} \frac{1}{6325.154}$$

$$\therefore \quad \frac{1}{U_o} = 0.0003827 + \frac{1}{h_o}$$

First trial:

Assume $\Delta t = 5^{\circ}$C.

$\therefore$ Condensation heat transfer coefficient, $h_o = \dfrac{2.17473}{(5)^{0.25}} = 1454.316 \text{ W/m}^2\text{-K}$

The overall heat transfer coefficient is given by

$$\frac{1}{U_o} = 0.0003827 + \frac{1}{1456.316}$$

$$\therefore \quad U_o = 934.31 \text{ W/m}^2\text{-K}$$

$$A_o = \frac{Q_c}{(U_o)(\text{LMTD})} = \frac{112.0684 \times 10^3}{(934.31 \times 12.331517)} = 9.727 \text{ m}^2$$

$$\Delta t = \frac{Q_c}{h_o A_o} = \frac{112068.4}{9.727 \times 1454.316} = 7.922 \text{ K}$$

Second trial:

Assume $\Delta t = 7^{\circ}\text{C}$

$$h_o = \frac{2.17473}{(7)^{0.25}} = 1336.998 \text{ W/m}^2\text{-K}$$

$$\frac{1}{U_o} = 0.0003827 + \frac{1}{1336.998}$$

$\therefore$ $U_o = 884.451 \text{ W/m}^2\text{-K}$

$$A_o = \frac{112068.4}{884.451 \times 12.331517} = 10.275 \text{ m}^2$$

$$\Delta t = \frac{Q_c}{h_o A_o} = \frac{112068.4}{10.275 \times 1336.998} = 8.157 \text{ K}$$

Third trial:

Assume $\Delta t = 8.5^{\circ}\text{C}$

$$h_o = \frac{2.17473}{(8.5)^{0.25}} = 1273.651 \text{ W/m}^2\text{-K}$$

$$\frac{1}{U_o} = 0.0003827 + \frac{1}{1273.651}$$

$\therefore$ $U_o = 856.28 \text{ W/m}^2\text{-K}$

$$A_o = \frac{112068.4}{856.28 \times 12.331517} = 10.6133 \text{ m}^2$$

$$\Delta t = \frac{Q_c}{h_o A_o} = \frac{112068.4}{10.6133 \times 1336.998} = 8.29 \text{ K}$$

The actual value may lie somewhere between 8.3 and 8.5°C. We may assume that $\Delta t = 8.5^{\circ}\text{C}$ is good enough.

We have 56 tubes of 0.016 m outside diameter. Hence $A_o = 56\pi d_o L$

$\therefore$ $$L = \frac{A_o}{56\pi d_o} = \frac{10.6133}{56\pi \times 0.016} = 3.77 \text{ m}$$

This length is rather too long and will occupy a large floor space. Also, the pressure drop on water side will be rather high. Hence it is not recommend for use with the 25 TR plant. The shell-and-tube condenser for this 25 TR plant should have at least 100 tubes.

EXAMPLE 10.8 Determine the face area for an R12 air condenser for a 5 TR plant with condenser and evaporator temperatures of 40°C and –5°C respectively. The face velocity is 150 m/min. The inside and outside tube diameters are 11.26 mm and 12.68 mm respectively. The inlet air temperature is 27°C. The fin efficiency is 0.73 and the other dimensions of the air-cooled condenser with reference to Figures 10.7 and 10.8 are as follows:

$B = 43.0$ mm, $C = 38.0$ mm, $D = 3.175$ mm and $E = 0.254$ mm

Solution: The heat transfer areas of the condenser are calculated as follows:

Bare tube area, $A_{po} = \dfrac{D-E}{BD}\pi d_o$

$$= \frac{3.175 - 0.254}{43(3.175)} 3.14159(12.68) = 0.8523 \text{ m}^2 \text{ per m}^2 \text{ face area per row}$$

Fin area, $A_f = \dfrac{2}{D}\left(C - \dfrac{\pi d_o^2}{4B}\right)$

$$= \frac{2}{3.175}\left(38 - \frac{\pi(12.68)^2}{4(43)}\right) = 22.087 \text{ m}^2 \text{ per m}^2 \text{ face area per row}$$

Minimum flow area, $A_c = \dfrac{D-E}{D}\left(1 - \dfrac{d_o}{B}\right)$

$$= \frac{3.175 - 0.254}{3.175}\left(1 - \frac{12.68}{43}\right) = 0.6487 \text{ m}^2 \text{ per m}^2 \text{ face area per row}$$

Total heat transfer area,

$$A_o = A_{po} + A_f = 0.8523 + 22.087 = 22.9393 \text{ m}^2 \text{ per m}^2 \text{ face area per row}$$

Inside heat transfer area,

$$A_{pi} = \frac{\pi d_i}{B} = \frac{3.14159(11.26)}{43} = 0.82266 \text{ m}^2 \text{ per m}^2 \text{ face area per row}$$

Hydraulic diameter,

$$D_h = \frac{2CA_c}{1000A_o} = \frac{2(38)0.6487}{1000(22.9393)} = 4.2984 \times 10^{-3} \text{ m}$$

Area ratios:

$$\frac{A_o}{A_{pi}} = 27.8843$$

$$\frac{A_{po}}{A_f} = 0.3715$$

Condenser heat rejection

A single-stage saturation cycle is considered with R12 as the refrigerant. The enthalpies at inlet of compressor h_1 and outlet of condenser h_3 are the saturated vapour and saturated liquid enthalpies at –5°C and 40°C respectively. The enthalpy at the compressor outlet h_2 is determined for isentropic compression by interpolation in the superheat table. The values of enthalpies are as follows:

$$h_1 = 185.4 \text{ kJ/kg}$$

$$h_2 = 208 \text{ kJ/kg}$$

$$h_3 = h_4 = 74.6 \text{ kJ/kg}$$

Refrigeration effect = $h_1 - h_4 = 110.8$ kJ/kg. The mass flow rate of the refrigerant for the 5 TR cooling capacity is determined as follows:

$$\dot{m} = \frac{5 \times 211}{110.8} = 9.52166 \text{ kg/min} = 0.15869 \text{ kg/s}$$

The condenser heat rejection, $Q_c = \dot{m}(h_2 - h_3) = 0.15869\,(133.4)$

$$Q_c = 21.17 \text{ kW}$$

Condensation heat transfer coefficient:

The properties of R12 at 40°C are as follows:

$\mu_f = 0.24$ cP, $\mu_g = 0.01295$ cP, $v_f = 0.8 \times 10^{-3}$ m^3/kg , $v_g = 0.0182$, $k_f = 0.073$ W/m-K, $k_g = 0.01012$ W/m-K, $c_{pf} = 0.993$ k/kg-K and $c_{pg} = 0.624$ kJ/kg-K, 1 cP = 10^{-3} kg/m-s

$$\text{Pr}_f = \frac{c_{pf}\,\mu_f}{k_f} = \frac{0.993 \times 10^3\ (0.24 \times 10^{-3})}{0.073} = 3.264$$

$$\text{Re}_g = \frac{4\dot{m}}{\pi d_i\,\mu_g} = \frac{4 \times 0.15869}{3.14159\,(0.01126)(0.01295 \times 10^{-3})} = 1385.6435 \times 10^3$$

$$\text{Re}_f = \frac{4\dot{m}}{\pi d_i \mu_f} = \frac{4 \times 0.15869}{3.14159\,(0.01126)(0.24 \times 10^{-3})} = 74.767 \times 10^3$$

The condensation heat transfer coefficient inside the tube is found from various correlations to get an idea about the range by which it can vary.

Zecchin's correlation:

$$\text{Nu} = \frac{h_i d_i}{k_f} = 0.05\,\text{Re}_{\text{eq}}^{0.8}\ \text{Pr}_f^{1/3}$$

where,

$$\text{Re}_{\text{eq}} = (1 - x)\,\text{Re}_f + x\,\text{Re}_f \sqrt{\frac{\rho_f}{\rho_g}}$$

The refrigerant enters as vapour and leaves as saturated liquid. Hence the quality is $x = 1$ at inlet and $x = 0$ at the outlet. If we assume that the quality varies linearly with the length of the

condenser, then the average of $(1 - x)\text{Re}_f$ and $x\text{Re}_f$ is 0.5Re_f. Therefore, the equivalent Reynolds number Re_{eq} becomes

$$\text{Re}_{eq} = 0.5\,\text{Re}_f \left(1.0 + \sqrt{\frac{\rho_f}{\rho_s}}\right) = 0.5\,\text{Re}_f \left(1.0 + \sqrt{\frac{v_g}{v_f}}\right)$$

or
$$\text{Re}_{eq} = 0.5 \times 74.767 \times 10^3 \left(1 + \sqrt{\frac{0.0182}{0.8 \times 10^{-3}}}\right) = 215691.75$$

Now, $\text{Nu} = 0.05(215691.476)^{0.8}\,(3.264)^{1/3} = 1371.786$

and
$$h_i = \text{Nu}\,\frac{k_f}{d_i} = 1371.786\,\frac{0.073}{0.01126} = 8893.463\ \text{W/m}^2\text{-K}$$

Dean Ackers and Crosser's correlation:

In this correlation it is assumed that complete condensation occurs. This correlation defines a modified Reynolds number Re_m and Nusselt number is expressed in a manner similar to the Dittus–Boelter equation.

$$\text{Re}_m = \text{Re}_f \left(1.0 + \sqrt{\frac{\rho_f}{\rho_g}}\right) = \text{Re}_f \left(1.0 + \sqrt{\frac{v_g}{v_f}}\right)$$

$$\text{Nu} = \frac{h_i\,d_i}{k_f} = 0.0265\,\text{Re}_m^{0.8}\,\text{Pr}_f^{1/3}$$

$\therefore$
$$\text{Re}_m = \text{Re}_f \left(1.0 + \sqrt{\frac{v_g}{v_f}}\right) = 74767.016\,(1 + 4.869696) = 431382.95$$

$$\text{Nu} = 0.0265\ (431382.95)^{0.8}\ (3.264)^{1/3} = 1265.86$$

$$h_i = \text{Nu}\,\frac{k_f}{d_i} = \frac{1265.86 \times 0.073}{0.01126} = 8206.74\ \text{W/m}^2\text{-K}$$

Shah's correlation:

$$h_i = h_f \left(0.55 + \frac{2.09}{p_r^{0.38}}\right)$$

In this correlation h_f is single-phase heat transfer coefficient determined from Dittus–Boelter equation assuming that whole mass of refrigerant flows in liquid phase, that is,

$$\frac{h_f\,d_i}{k_f} = 0.023\,\text{Re}_f^{0.8}\,\text{Pr}_f^{1/3} = 0.023\,(74767.016)^{0.8}\,(3.264)^{1/3} = 270.362$$

$$h_f = \frac{0.073(270.362)}{0.01126} = 1752.792$$

For R12, critical pressure, $p_{cr} = 41.15$ bar and at 40°C $p_c = 9.6$ bar.

$\therefore$ $$p_r = \frac{p_c}{p_{cr}} = \frac{9.6}{41.15} = 0.2333 \text{ bar}$$

$$h_i = 1752.792\left(0.55 + \frac{2.09}{(0.2333)^{0.38}}\right) = 7333.078 \text{ W/m}^2\text{-K}$$

Air side heat transfer coefficient:

The Nusselt number for the air side is given by

$$\text{Nu} = 0.1 \text{ Re}^{0.65} \text{ Pr}^{1/3}$$

The Nusselt number is based upon the hydraulic diameter D_h and the Reynolds number is based upon the maximum velocity and the hydraulic diameter. These are given by

$$\text{Re} = \frac{U_{\max} D_h}{v} \quad \text{and} \quad \text{Nu} = \frac{h_o D_h}{k}$$

The properties of air at the mean temperature are as follows:

$$\rho = 1.1774 \text{ kg/m}^3, \mu = 1.983 \times 10^{-5} \text{ kg/m-s}, c_p = 1.005 \text{ kJ/kg-K}, k = 0.0284 \text{ W/m-K}$$

$$U_{\max} = \frac{150}{60A_c} = \frac{2.5}{0.6487} = 3.8539 \text{ m/s} \quad \text{and} \quad D_h = 4.2984 \times 10^{-3}$$

$\therefore$ $$\text{Re} = \frac{3.8539 \times 4.2984 \times 10^{-3}}{(1.983/1.1774) \times 10^{-5}} = 983.577 \quad \text{and} \quad \text{Pr} = \frac{1005 \times 1.983 \times 10^{-5}}{0.0284} = 0.7017$$

$\therefore$ $\text{Nu} = 0.1(983.577)^{0.65} (0.7017)^{1/3} = 7.835$

and $$h_o = 7.835 \times \frac{0.0284}{4.2984 \times 10^{-3}} = 51.77 \text{ W/m}^2\text{-K}$$

Overall heat transfer coefficient:

This is given by

$$\frac{1}{U_o} = \frac{A_o}{A_{pi}} \frac{1}{h_i} + \frac{A_o}{A_{pi}} \frac{1}{h_s} + \frac{1-\phi}{h_o (A_{po}/A_f + \phi)} + \frac{1}{h_o}$$

We will use the Dean Ackers and Crosser's correlation value of $h_o = 8206.74$, scale or deposit coefficient $1/h_s = 0.00009$ m^2-K/W and fin effectiveness of $\phi = 0.73$

$$\frac{1}{U_o} = \frac{27.8843}{8206.74} + 27.8843(0.00009) + \frac{1 - 0.73}{51.77(0.03715 + 0.73)} + \frac{1}{51.77}$$

$\therefore$ $U_o = 31.229$ W/m^2-K

First trial:

The air inlet temperature is given to be 27°C. The outlet temperature is not given. Assume the air outlet temperature to be 35°C.

$$\text{LMTD} = \frac{35 - 27}{\ln\left(\frac{40 - 27}{40 - 35}\right)} = 8.3725°\text{C}$$

$$Q_c = (U_o)\ (A_{ot})\ (\text{LMTD}) = 21.17 \text{ kW}$$

$$\therefore \quad A_{ot} = \frac{21.17 \times 1000}{31.229 \times 8.3725} = 80.967 \text{ m}^2$$

Normally 4 rows are used for a 5 TR condenser. Total area A_{ot} is given by

$$A_{ot} = A_{\text{face}} \times \text{number of rows} \times A_o$$

$$\therefore \quad A_{\text{face}} = \frac{80.967}{22.9393 \times 4} = 0.8824 \text{ m}^2$$

Mass flow rate of air is given by $\dot{m}_{air} = \rho A_{\text{face}} V = 1.1774 \times 0.8824 \times 2.5 = 2.5973$ kg/s

$$Q_c = \dot{m}_{\text{air}}\, c_p\, \Delta t$$

$$\therefore \quad \Delta t = \frac{Q_c}{\dot{m}_{\text{air}}\, c_p} = \frac{21.17}{2.5973 \times 1.005} = 8.11°\text{C}$$

Second trial:

We had assumed an outlet air temperature of 35°C. The calculation gives the outlet air temperature of 27 + 8.11 = 35.11°C. This is a good approximation. If a better accuracy is desired, then another trial may be done by assuming an outlet temperature of 35.1°C.

$$\text{LMTD} = \frac{35.1 - 27}{\ln\left(\frac{40 - 27}{40 - 35.1}\right)} = 8.3016°\text{C}$$

$$A_{ot} = \frac{21.17 \times 1000}{31.229 \times 8.3016} = 81.6583 \text{ m}^2$$

$$A_{\text{face}} = \frac{81.6583}{22.9393 \times 4} = 0.8899 \text{ m}^2$$

$$\dot{m}_{\text{air}} = \rho A_{\text{face}}\, V = 1.1774 \times 8899 \times 2.5 = 2.6195 \text{ kg/s}$$

$$\therefore \quad \Delta t = \frac{Q_c}{\dot{m}_{\text{air}}\, c_p} = \frac{21.17}{2.6195 \times 1.005} = 8.04°\text{C}$$

Hence, a face area of 0.89 m^2 is the answer.

Alternative method:

If one uses the ε-NTU method, the iteration can be avoided. In fact the determination of effectiveness ε is also not required. We have the following relation from the overall energy balance for the condenser.

$$Q_c = (U_o)(A_o)(\text{LMTD}) = \dot{m}_{\text{air}}\, c_p\, \Delta t$$

where, $A_{ot} = A_{\text{face}} \times \text{number of rows} \times A_o$

and $$\dot{m}_{\text{air}} = \rho A_{\text{face}} V, \quad \text{LMTD} = \frac{t_o - t_i}{\ln \dfrac{t_o - t_i}{t_c - t_o}}$$

The air inlet and outlet temperature are t_i and t_o respectively.

and $\Delta t = (t_o - t_i)$.

$$\therefore \quad \ln \frac{t_c - t_i}{t_c - t_o} = \frac{U_o A_{ot}}{\dot{m} c_p} = \text{NTU} = \frac{U_o A_{\text{face}} n A_o}{\rho A_{\text{face}} V} = \frac{U_o A_o n}{\rho V c_p} = \frac{31.229(22.9393)4}{1.1771(2.5)1005} = 0.96865$$

In general, we get

$$\frac{t_c - t_i}{t_c - t_o} = \exp(\text{NTU})$$

In this case, it is observed that the expression for NTU is independent of the face area. Hence the only unknown is the outlet air temperature t_o, which can be determined without iteration. Thus,

$$\frac{40 - 27}{40 - t_o} = \exp(\text{NTU}) = \exp(0.96865) = 2.6344$$

$$\therefore \quad t_o = 40 - \frac{13}{2.6344} = 35.06°\text{C}$$

The iteration also gave a similar result.

REFERENCES

Carrier,W.H. and Anderson, S.W. (1944): The Resistance to Heat Flow Through Finned Tubing, *ASHVE Trans*., Vol. 50, pp. 117–152.

Gardner, K.A. (1945): Efficiency of Extended Surfaces, *Trans. ASME*, Vol. 67, pp. 621–631.

Gotto, M., Hotta, H. and Tezuka, S. (1979): Film Condensation of Refrigerant Vapours on Horizontal Tube, *15th Intl. Congr. Refrig*., Venice, Paper B1–20.

Grimson, E.D. (1937): Correlations and Utilization of New Data on Flow Resistance and Heat Transfer for Cross-Flow of Gases Over Tube Banks, *Trans. ASME*, Vol. 59, pp. 583–594.

Kays, W.M. and London A.L. (1955): *Compact Heat Exchangers*, The National Press, Palo Alto, California.

Rich, D.G. (1974): The Effect of Fin-Spacing on the Heat Transfer and Friction Performance of Multi-Row Smooth Plate Fin and Tube heat Exchanger's, *ASHRAE Trans*., Vol. 79, Pt. 2, pp. 137–145.

Standard for Forced-circulation Air-cooling and Air-heating coils, Standard 410, Air Conditioning and Refrigeration Institute, Arlington, Va. 1972.

White, R.E. (1948): Condensation of Refrigerant Vapours: Apparatus and Film Coefficients for R12, *Refrigeration Eng*., Vol. 55, no. 5 , pp. 375.

REVIEW QUESTIONS

1. Describe the relative advantages and disadvantages of air-cooled, water-cooled and evaporative condensers.
2. What are the different types of air-cooled condensers?
3. Discuss the importance of heat rejection ratio.
4. Explain the significance of fin efficiency in finned-tube condensers.
5. What are the various heat transfer areas of a finned-tube condenser?
6. Derive the expression for the overall heat transfer coefficient of the finned-tube condenser.
7. Discuss the significance of various heat transfer coefficients of the finned-tube condenser.
8. What are the different types of water-cooled condensers?
9. How does the entry of air and non-condensable gases in the system affect the performance of the condenser?
10. Determine the condensing temperature of a water-cooled condenser of a refrigeration system of 55 kW cooling capacity with a COP of 5.0. The overall heat transfer coefficient of the condenser is 450 W/m^2-K and it has a heat transfer area of 18 m^2. The cooling water enters the condenser at a flow rate of 3.2 kg/s at a temperature of 30°C. Assume the specific heat of water to be 4.18 kJ/kg-K.

11

Evaporators

LEARNING OBJECTIVES

After studying this chapter the student should be able to:

1. Understand the classification of evaporators into natural convection type or forced convection type, refrigerant flow inside the tubes or outside the tubes, flooded type or dry type.
2. Discuss the salient features of natural convection coils.
3. Discuss the salient features of flooded evaporators.
4. Discuss the salient features of shell-and-tube type evaporators, shell-and-tube liquid chillers, shell-and-coil chillers, double pipe chillers (flooded and dry type), Boudelot coolers, direct expansion coils, plate surface evaporators, and finned evaporators.
5. Perform thermal design calculations on refrigerant evaporators.

11.1 INTRODUCTION

In the previous chapters, the three main components of refrigeration systems, namely, compressor, expansion valve and condenser, have been described. To complete the description of the refrigeration system, the fourth component, the evaporator is described in this chapter. This component like the condenser is also a heat exchanger. The refrigerant boils or evaporates in this component and absorbs heat from the substance being cooled which is the main purpose of a refrigeration system. The name evaporator refers to the evaporation process occurring in the heat exchanger.

11.2 CLASSIFICATION OF EVAPORATORS

There are several ways of classifying the evaporators depending upon the heat transfer process or refrigerant flow or condition of the heat transfer surface.

11.2.1 Natural and Forced Convection Type Evaporators

The evaporator may be classified as *natural convection* type or *forced convection* type. In the forced convection type, a fan or a pump is used to circulate the fluid being cooled and make it flow over the cooled heat transfer surface, which is cooled by evaporation of refrigerant. In the natural convection type, the fluid being cooled flows due to natural convection currents arising out of density difference caused by temperature difference. The refrigerant boils inside tubes and is located at top. The temperature of the fluid, which is cooled by the refrigerant, decreases and its density increases. The cooled fluid moves downwards due to its higher density and the warm fluid rises up to replace it.

11.2.2 Refrigerant Flow Inside or Outside Tubes

The heat transfer phenomenon during boiling inside and outside tubes is very different; hence, evaporators are classified as those with refrigerant flow inside the tubes and those with refrigerant flow outside the tubes.

In natural convection type evaporators and some other evaporators, the refrigerant is confined and boils inside the tubes while the fluid being chilled flows over the tubes. The direct expansion coil where the air is directly cooled in contact with the tubes cooled by refrigerant boiling inside is an example of forced convection type of evaporator where the refrigerant is confined inside the tubes.

In many forced convection type evaporators, the refrigerant is kept in a shell and the fluid being chilled is carried in tubes, which are immersed in the refrigerant. Shell-and-tube brine chillers and water chillers are mainly of this type.

11.2.3 Flooded and Dry Types

The third classification is flooded type and dry type. An evaporator is said to be *flooded type* if the liquid refrigerant covers the entire heat transfer surface. This type of evaporator uses a float type of expansion valve. An evaporator is called *dry type* when a portion of the evaporator is used for superheating the refrigerant vapour after its evaporation. This type of evaporator uses a thermostatic expansion valve.

11.3 NATURAL CONVECTION COILS

Natural convection coils are mainly used in cold storages. Long lengths of bare or finned pipes are mounted near the ceiling or along the high sidewalls of the cold storages. The refrigerant from expansion valve is fed to these tubes. The liquid refrigerant evaporates inside the tubes and cools the air whose density increases. The high-density cooled air flows downwards through the product, which is kept in the cold storage for cooling. The air becomes warm by the time it reaches the floor. Some free area like a passage is provided for warm air to rise up. The same passage is used for loading and unloading the product into cold storage.

Natural convection coils do not occupy any floor space, require low maintenance cost, can operate for long periods without defrosting the ice formed on them and do not require any special skill to fabricate them. These coils are usually welded at site.

The disadvantage is that the natural convection heat transfer coefficient of natural convection coils is very small; hence very long lengths of coils are required which may cause excessive refrigerant side pressure drops unless parallel paths are used. The large length of coils requires a

large quantity of refrigerant compared to the forced convection coils. The large quantity of refrigerant increases the time required for defrosting, since before the defrosting can start all the liquid refrigerant has to be pumped out of the evaporator tubes. The pressure balancing also takes a long time if the system trips or is to be restarted after load shedding.

Natural convection coils are very useful when low air velocities and minimum dehumidification of the product is required. Household refrigerators, display cases, walk-in-coolers, reach-in refrigerators and obviously large cold storages are few of its applications. Sufficient space should be provided between the evaporator and the ceiling to permit air circulation over top of the coil. Baffles are provided to separate the warm air and cold air plumes. Single, ceiling mounted evaporators are used for rooms of width less than 2.5 m. For rooms with larger widths, two or more evaporator coils are used.

11.4 FLOODED EVAPORATOR

Flooded evaporators are typically used in large ammonia systems. The refrigerant enters a surge drum through a float type expansion valve. The compressor directly draws the flash vapour formed during expansion. This vapour does not take part in refrigeration, hence its removal makes the evaporator more compact and pressure drop due to this is also avoided. The liquid refrigerant enters the evaporator from the bottom of the surge drum. The refrigerant boils inside the tubes as heat is absorbed by it. The mixture of liquid and vapour bubbles rises up along the evaporator tubes. The vapour is separated as it enters the surge drum. The remaining unevaporated liquid circulates again in the tubes along with the constant supply of liquid refrigerant from the expansion valve. The mass flow rate in the evaporator tubes is $f\,\dot{m}$ where $\dot{m}$ is the mass flow rate through the expansion valve and to the compressor. The term f is called *recirculation factor*. Let x_4 be the quality of mixture after the expansion valve and x be the quality of mixture after boiling in the tubes as shown in Figure 11.1. In steady state, the mass flow rate from expansion valve is same as the mass flow rate to the compressor. Hence mass conservation gives:

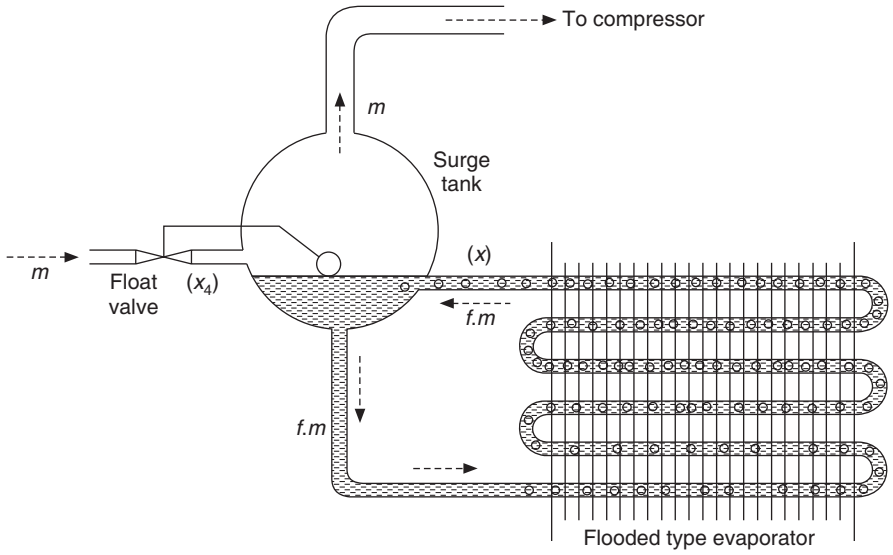

Figure 11.1 Schematic of a flooded evaporator.

$$x_4\dot{m} + x\, f\dot{m} = \dot{m}$$

$$\therefore \quad f = \frac{1 - x_4}{x}$$

For $x_4 = x = 0.25$, for example, the circulation factor is 3, that is, the mass flow rate through the evaporator is three times that through the compressor. Further, liquid refrigerant is in contact with whole of the evaporator surface, which makes it more effective. Sometimes, a liquid pump may also be used to further increase the heat transfer coefficient. The lubricating oil tends to accumulate in the flooded evaporator, hence an effective oil separator must be used immediately after the compressor.

The flooded type of evaporator is used in most of cold storages with a ceiling fan over the tubes to circulate the air. The tubes may also have fins to increase the heat transfer area.

11.5 SHELL-AND-TUBE LIQUID CHILLERS

The shell-and-tube evaporators, as the name suggests, have a shell and a large number of straight tubes arranged parallel to each other. These evaporators have a very high efficiency and require minimum floor space and headspace. They are easy to maintain and hence are very widely used. They can be either of dry type or of flooded type. In the dry-expansion type, the refrigerant flows through the tubes while in the flooded type the refrigerant is in the shell. A pump circulates the chilled water or brine. The shell diameters range from 150 mm to 1.5 m. The number of tubes may be less than 50 to several thousands and the length may be 1.5 m to 6 m. Steel tubes are used with ammonia while copper tubes are used with freons. Ammonia has a very high heat transfer coefficient, while freons have rather poor heat transfer coefficient and hence fins are used on the refrigerant side. The dry-expansion type uses fins inside the tube while the flooded type uses fins outside the tube. Outside dry-expansion type requires less charge of refrigerant and has positive lubricating oil return. The dry-expansion type refrigerator is used for small and medium capacity TR plants ranging from 2 TR to 350 TR. The flooded type is available in larger capacities ranging from 10 TR to thousands of TR.

11.5.1 Flooded Type Shell-and-Tube Evaporator

Figure 11.2 shows a flooded type of shell-and-tube type liquid chiller where the liquid (usually brine or water) to be chilled flows through the tubes in double pass just like that in a shell-and-tube condenser. The refrigerant is fed through a float valve, which maintains a constant level of liquid refrigerant in the shell. The shell is not filled entirely with tubes as shown in the end view of Figure 11.2(a). This is done to maintain the level of liquid refrigerant below the top of the shell so that liquid droplets settle down due to gravity and are not carried by the vapour leaving the shell. If the shell is completely filled with tubes, then a surge drum is provided after the evaporator to collect the liquid refrigerant.

The tube arrangement in shell-and-tube evaporators can either be of single pass type or be of multipass type. In the multipass type, the chilled liquid changes direction in the heads. The heads are bolted to the ends of the shell by flanges. These can be changed to get different passes. The tube bundles may also be of removable type. In the fixed tube bundle design the end plates containing the tubes are welded to the shell.

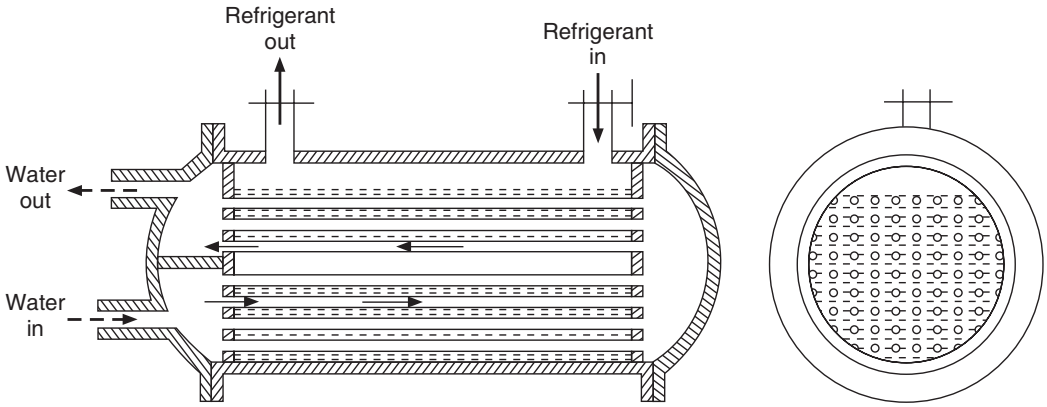

Figure 11.2 Schematic of a flooded type shell-and-tube evaporator.

Shell-and-tube evaporators are available in vertical design as well. The vertical type requires minimum floor area. The chilled water enters from the top and flows downwards due to gravity and is then taken to a pump, which circulates it to the refrigeration load. At the inlet to tubes at the top a special arrangement introduces swirling action to increase the heat transfer coefficient.

11.5.2 Dry Type Shell-and-Tube Evaporator

Figure 11.3 shows a liquid chiller with refrigerant flowing through the tubes and water flowing through the shell. A thermostatic expansion valve feeds the refrigerant into the tubes through the cover on the left. It may flow in several passes through the dividers in the covers of the shell on either side. The liquid to be chilled flows through the shell around the baffles. The presence of baffles turns the flow around creating some turbulence, thereby increasing the heat transfer

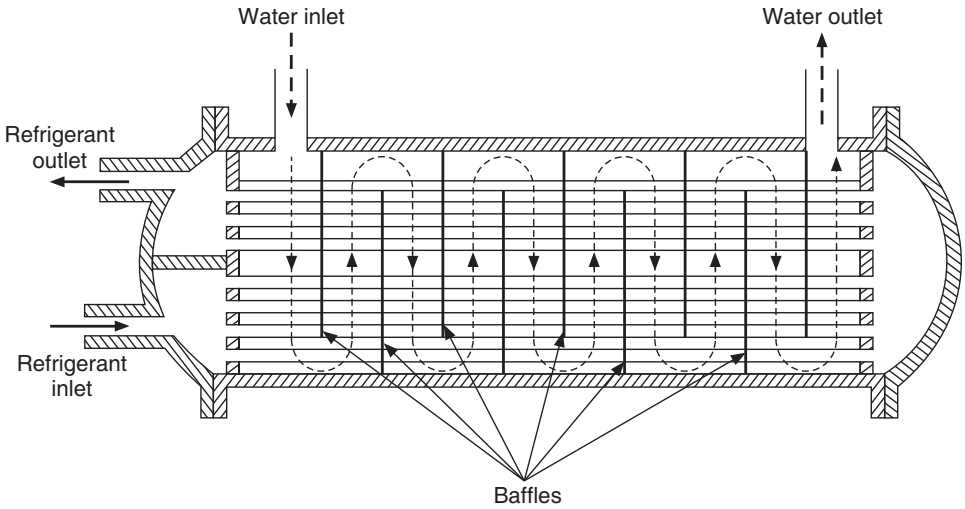

Figure 11.3 Schematic of a dry type shell-and-tube evaporator.

coefficient. This evaporator is called dry type since some of the tubes superheat the vapour. To maintain the chilled liquid velocity so as to obtain good heat transfer coefficient, the length and the spacing of segmental baffles is varied. Widely spaced baffles are used when the flow rate is high or the liquid viscosity is high. The number of passes on the refrigerant side are decided by the partitions on the heads on the two sides of the heat exchanger. Sometimes, more than one circuit is also provided. Changing the heads can change the number of passes. It depends upon the chiller load and the refrigerant velocity to be maintained in the heat exchanger.

11.5.3 Shell-and-Coil Chiller

These evaporators are of smaller capacity than the shell-and-tube chillers. They are made of one or more spiral-shaped bare tube coils enclosed in a welded steel shell. Such evaporators are usually of dry-expansion type with the refrigerant flowing in the tube and the chilled liquid in the shell as shown in Figure 11.4. In some cases the chiller operates in flooded mode with refrigerant in the shell and chilled water flowing thorough the spiral tube. The water in the shell gives a large amount of thermal storage capacity called *hold-up capacity*. This type is good for small but highly infrequent peak loads. It is used for cooling the drinking water in stainless steel tanks to maintain sanitary conditions. It is also used in bakeries and photographic laboratories.

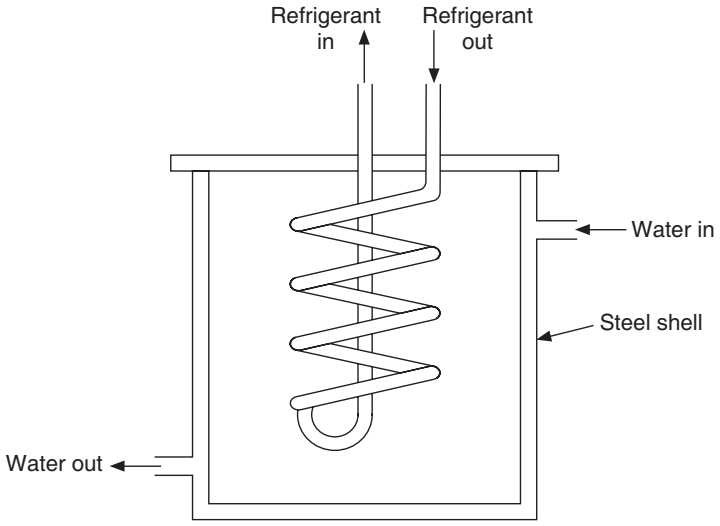

Figure 11.4 Schematic of shell-and-coil chiller.

When the refrigerant is in the shell that is in flooded mode it is called instantaneous liquid chiller. This type does not have thermal storage capacity, the liquid must be instantaneously chilled whenever required. In the event of freeze up the water freezes in the tube, which causes bursting of the tubes since water expands upon freezing. When water is in the shell, there is enough space for expansion of water if the freezing occurs. The flooded types are not recommended for any application where the temperature of chilled liquid may be below 3°C.

11.5.4 Double Pipe Chiller

This evaporator consists of two concentric tubes, the refrigerant flows through the annular passage while the liquid being chilled flows through the inner tube in counterflow. One design is shown in Figure 11.5 in which the outer horizontal tubes are welded to vertical header tubes on either side. The inner tubes pass through the headers and are connected together by 180° bends. The refrigerant side is welded, hence there is minimum possibility of leakage of refrigerant. These evaporators may be used in flooded as well as dry mode. This design requires more space compared to other designs. Shorter tubes and counterflow provide good heat transfer coefficient. This evaporator has to be insulated from outside since the refrigerant flows in the outer annulus which may be exposed to surroundings if insulation is not provided.

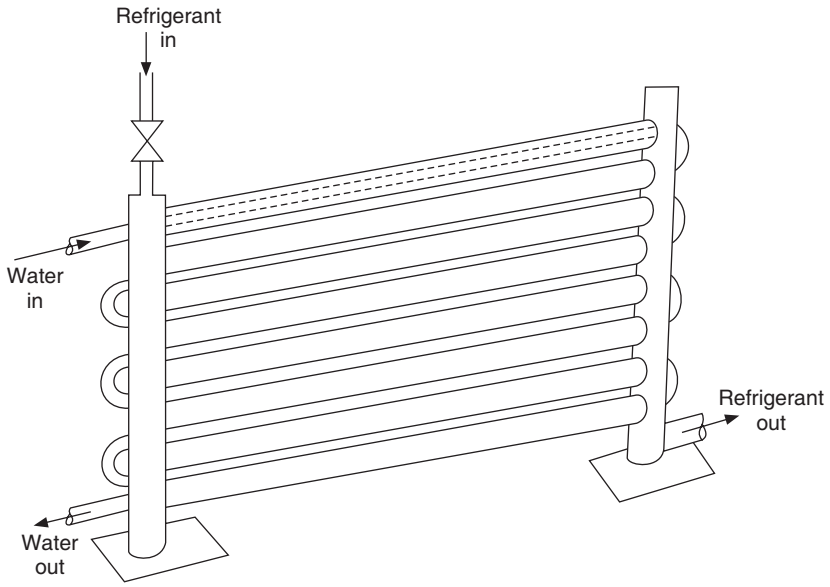

Figure 11.5 Schematic of a double pipe type evaporator.

11.5.5 Baudelot Coolers

This type of evaporator consists of a large number of horizontal pipes stacked one on top of the other and connected together by headers to make a single circuit or multiple circuits. The refrigerant is circulated inside the tubes either in flooded or dry mode. The liquid to be chilled flows in a thin layer over the outer surface of the tubes. The liquid flows down by gravity from a distributor pipe located on top of the horizontal tubes as shown in Figure 11.6. The liquid to be chilled is open to atmosphere, that is, it is at atmospheric pressure and its aeration may take place during cooling. This type of evaporator is widely used for cooling milk, wine and for chilling water for carbonation in bottling plants. The liquid can be chilled very close to its freezing temperature since freezing outside the tubes will not damage the tubes.

Another advantage is that the refrigerant circuit can be split into several parts, which permit a part of the cooling done by cold water and then chilling by the refrigerant.

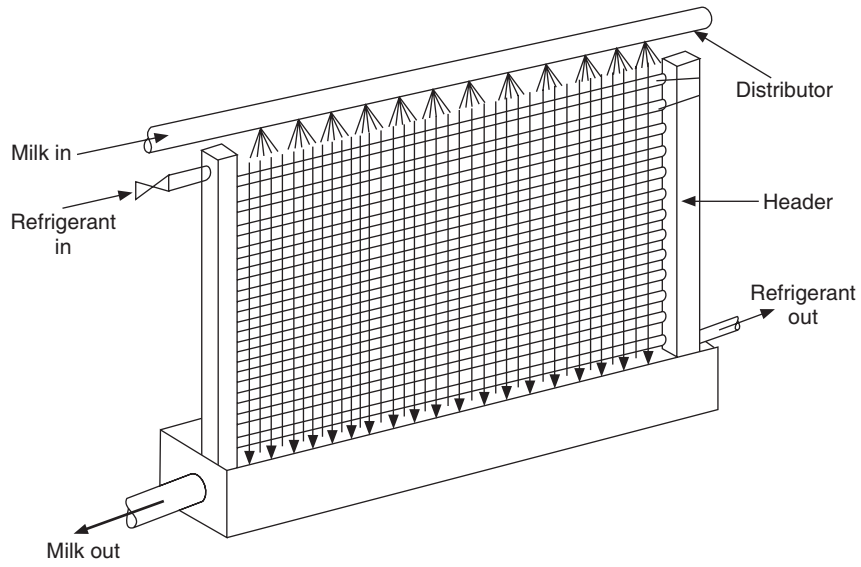

Figure 11.6 Schematic of a Baudelot type evaporator for chilling milk.

11.6 DIRECT EXPANSION COIL

This type of evaporator is used for cooling and dehumidifying the air directly by the refrigerant flowing in the tubes. An indirect method of cooling is to first chill water or brine in any of the evaporators described above and then cool the air by chilled water flowing through the tubes in another heat exchanger. The direct expansion coil type of evaporator consists of coils placed in a number of rows with fins mounted on the coil so as to increase the heat transfer area. Various fin arrangements are used. Tubes with individual spiral straight fins or crimpled fins welded to it are used in some applications like ammonia. Plate fins accommodating several rows are used in air conditioning applications with ammonia as well as freons.

The liquid refrigerant enters from top through a thermostatic expansion valve as shown in Figure 11.7. This arrangement makes the refrigerant return to compressor better rather than feeding the refrigerant from the bottom of the coil. When the evaporator is close to the compressor, a direct expansion coil is used since the refrigerant lines are short, refrigerant leakage will be less and the pressure drop will be small. If the air-cooling is required away from the compressor, it is preferable to chill water and pump it to the air-cooling coil to reduce the possibility of refrigerant leakage and excessive refrigerant pressure drop, which reduces the COP.

11.7 PLATE SURFACE EVAPORATORS

These evaporators are also called *bonded plate evaporators*. Two flat sheets of metal (usually aluminium) are embossed in such a manner that when these are welded together, the embossed portion of the two plates makes a passage for refrigerant to flow. This is shown in Figure 11.8. This type of evaporator is used in household refrigerators. In the bonded evaporator the contact resistance between the tube and the surface is eliminated.

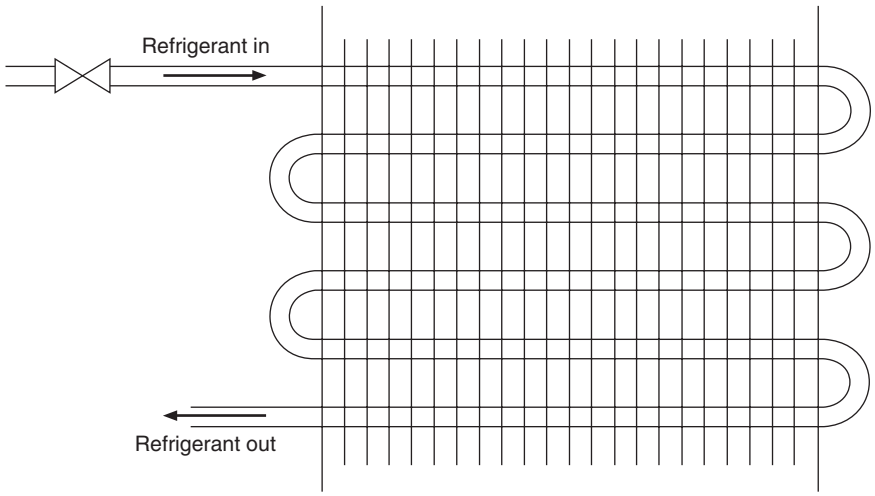

Figure 11.7 Schematic of a direct expansion fin-and-tube type evaporator.

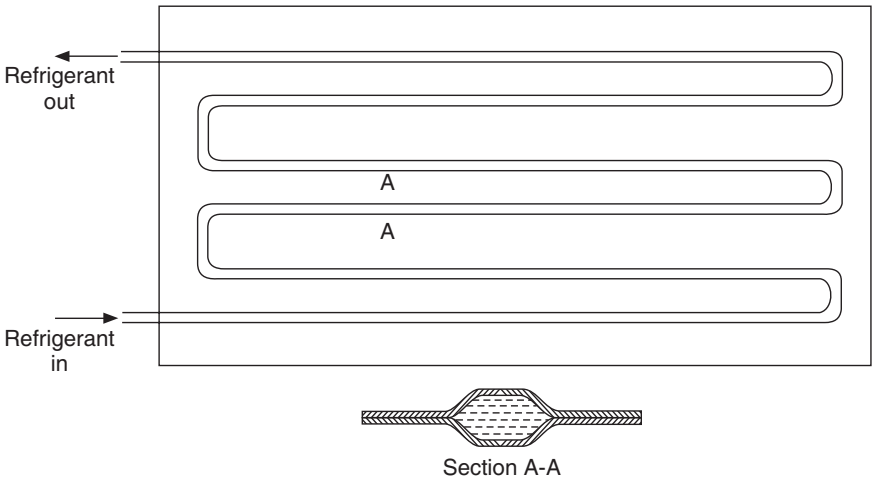

Figure 11.8 Schematic of a bonded plate evaporator.

In another type of plate surface evaporator, a serpentine tube is placed between two metal plates such that the plates press on to the tube. The edges of the plates are welded together. The space between the plates is either filled with a eutectic solution or evacuated. The vacuum between the plates and atmospheric pressure outside, presses the plates on to the refrigerant carrying tubes making a very good contact between them. If eutectic solution is filled into the void space, this also makes a good thermal contact between the refrigerant carrying tubes and the plates. Further, it provides an additional thermal storage capacity during off-cycle and load shedding to maintain a uniform temperature. These evaporators are commonly used in refrigerated trucks. Figure 11.9 shows an embedded tube, plate surface evaporator.

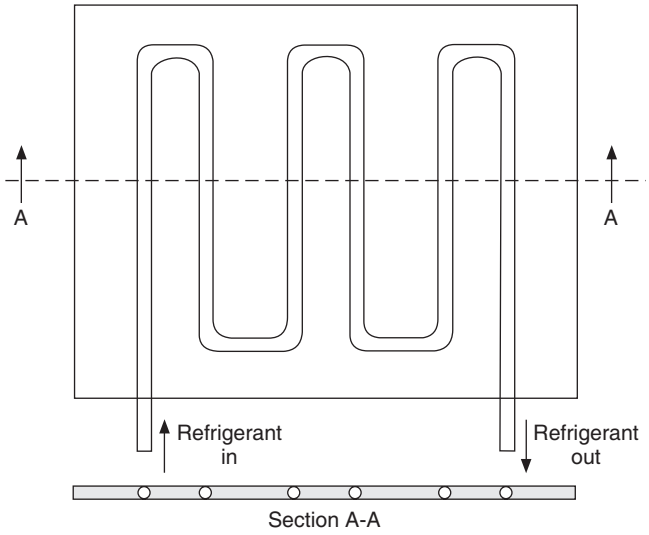

Figure 11.9 Schematic of an embedded tube, plate surface evaporator.

11.8 FINNED EVAPORATORS

Fin-and-tube evaporators are very widely used for heating and cooling of air. These have been described for heating purpose and heat rejection from condensers in Chapter 10 on condensers. As evaporators these are either direct expansion coils with the refrigerant evaporating directly inside the tubes, or heat exchangers with chilled water flowing through the tubes.

The fins increase the outside surface area of an evaporator, thereby improving its efficiency. When the air flows between the tubes, a part of the air never comes into contact with the tubes. Heat transfer takes place in the boundary layers in the vicinity of the tubes. These boundary layers are typically a few mm thick, hence most of the air forms free stream, which remains unaffected by the low temperature of the refrigerant inside the tubes. When the fins are provided, the fins cover the free passage between the tubes and hence the air that comes into contact with the bare tubes as well as the fins is cooled by the refrigerant flowing inside the tubes. For the fin temperature to be low, there should be a good contact between the fins and the tube. Slipping the fins over the tubes and then pressurizing the tubes to a very high pressure ensure a good contact of tubes with fins. Another method is to make the holes in the fins slightly smaller than the tube outer diameter, flare the holes, slip the tubes and then straighten the flares. The fin spacing is kept large for larger tubes and small for smaller tubes. Nearly 50 to 500 fins per metre length of the tube are used in heat exchangers. In evaporators, the atmospheric water vapour condenses on the fins and tubes when the metal temperature is lower than the dew point temperature. On the other hand, frost may form on the tubes if the surface temperature is less than 0°C. Hence for low temperature coils, a wide spacing with about 80 to 200 fins per metre is used to prevent the restriction of the flow passage due to the frost formation. In air-conditioning applications, a typical fin spacing of 1.8 mm is used. Addition of fins beyond a certain value will not increase the capacity of the evaporator by restricting the airflow. The frost layer has a poor thermal conductivity, hence it decreases the overall heat transfer coefficient apart from restricting

the flow. Therefore, for applications in freezers below 0°C, frequent defrosting of the evaporator is required.

The expressions of various heat transfer areas and overall heat transfer coefficients are similar to those given in Sections 10.7 and 10.8 respectively for the air-cooled condensers. There is one big difference however that changes the whole analysis. In direct expansion coil or in air-cooling coil (by chilled water), the temperature deceases, however at the same time some water vapour condenses since the temperature of the surface is less than the dew point temperature of the air. The condensation causes the outer surface of the tubes and fins to be wetted and in freezing applications, frost may also form on the surface.

11.8.1 Total Heat Transfer to Air from a Wetted Surface

When a moving stream of moist air flows over a cold surface, a film of water is formed over the surface due to condensation of water from the moist air. The thickness of the condensate layer increases along the surface. There is a thermal boundary layer next to the condensate layer. The heat transfer occurs by convection across the boundary layer with heat transfer coefficient h_{co}. Then, this heat is transferred by conduction across the water film followed by conduction across the metal wall and finally by heat transfer coefficient h_i to the refrigerant across the boundary layer inside the tube.

The moist air consists of dry air and the water vapour. The proportion of water vapour keeps on changing since it may get added or removed, hence all the calculations in air conditioning are based upon the mass flow rate of dry air. The mass flow rate of dry air is denoted by $\dot{m}_a$ kg of dry air per second (kga/s). The ratio of mass of water vapour to the mass of dry air in a given sample of moist air is called *humidity ratio* and is denoted by W kgw/kga. Hence, the mass flow rate of water vapour would be $\dot{m}_a W$ at inlet to, say, a control volume. The specific enthalpy of moist air is also specified on per kg of dry air basis and denoted by h kJ/kga. The temperature, humidity ratio and enthalpy of moist air decrease by dt, dW and dh across the control volume. The total heat transfer from the air is assumed to be dQ. The condensate rate at inlet to the control volume is $\dot{m}_w$ and it increases by dm_w across the control volume.

It is assumed that the air immediately next to the water film is saturated at the water temperature t_w. Its enthalpy is the saturation enthalpy of moist air h_{sw} and the humidity ratio is W_{sw}. Mass conservation of water vapour across the control volume gives

$$\dot{m}_a W + \dot{m}_w = \dot{m}_a (W - dW) + \dot{m}_w + dm_w$$

$$\therefore \quad \dot{m}_a dW = d\dot{m}_w \tag{11.1}$$

If the mass transfer coefficient is assumed to be h_{Do} and dA_o is the area of heat and mass transfer, then

$$\dot{m}_a dW = h_{Do} dA_o (W - W_{sw}) \tag{11.2}$$

The enthalpy of water vapour in the moist air at temperature t is $h_g(t) = h_{gt}$, the enthalpy of saturated water vapour. After condensation, its enthalpy is $h_f(t_w) = h_{fw}$, i.e. the enthalpy of saturated liquid water at temperature t_w. The condensation requires latent heat transfer, which in this case is $(h_{gt} - h_{fw})$. The condensate rate in the control volume is dm_w, hence the latent heat transfer, that is, the heat transfer rate associated with condensation is given by

$$dQ_L = h_{Do}\, dA_o (W - W_{sw})\, (h_{gt} - h_{fw}) \tag{11.3}$$

The sensible heat transfer across the thermal boundary layer is given by

$$dQ_S = h_{co}\, dA_o (t - t_w) \tag{11.4}$$

The total heat transfer is the sum of sensible and latent heat transfers, that is

$$dQ = dQ_S + dQ_L = dA_o[h_{co}(t - t_w) + h_{Do}(W - W_{sw})(h_{gt} - h_{fw})] \tag{11.5}$$

The heat transfer and mass transfer coefficients will be shown to be related as follows:

$$h_{Do} = \frac{h_{co}}{(\text{Le})(c_{pma})}$$

Therefore, Eq. (11.5) reduces to

$$dQ = \frac{h_{co}\, dA_o}{c_{pma}} \left[c_{pma}(t - t_w) + \frac{(W - W_{sw})(h_{gt} - h_{fw})}{\text{Le}} \right] \tag{11.6}$$

The enthalpy of moist air and saturated air may be expressed as

$$h = c_{pma}\, t + 2500W \quad \text{and} \quad h_{sw} = c_{pma}\, t_w + 2500W_{sw}$$

Therefore,

$$c_{pma}\,(t - t_w) = h - h_{sw} - 2500(W - W_{sw})$$

Substituting this in Eq. (11.6), we get

$$dQ = \frac{h_{co}\, dA_o}{c_{pma}} \left[h - h_{sw} + \frac{(W - W_{sw})(h_{gt} - h_{fw} - 2500\,(\text{Le}))}{(\text{Le})} \right] \tag{11.7}$$

The second term in Eq. (11.7) is negligible. Hence the total heat transfer, the sum of those associated with condensation and forced convection, is expressed as follows:

$$dQ = \frac{h_{co}\, dA_o}{c_{pma}} (h - h_{sw}) \tag{11.8}$$

In this equation the term $(h - h_{sw})$ is known as the enthalpy potential, which is the difference in enthalpy of moist air and that of saturated air at the water temperature. The total heat transfer is proportional to the enthalpy potential just like sensible heat transfer is proportional to the temperature difference and mass transfer is proportional to the difference in humidity ratio. This is a very good approximation, which simplifies the equations when heat and mass transfer occur simultaneously.

Another linear approximation over small temperature range is sometimes used to simplify the saturated enthalpy h_{sw} occurring in Eq. (11.8). This is as follows:

$$h_{sw} = a_w + b_w\, t_w \tag{11.9}$$

where the constants a_w and b_w are dependent upon the temperature.

11.8.2 Efficiency of a Wetted Fin

The efficiency of a dry bar or rectangular fin has been derived in Section 10.6.1. For a dehumidifying coil, the fin is covered with a layer of water, which introduces conduction thermal resistance to the heat transfer from the fin. Let us consider a wet fin covered with a thin layer of water of thickness y_w. Let us assume the width of the fin to be unity in a direction perpendicular to the plane of paper. An elemental length Δx of the fin is considered for analysis.

Total heat transfer from moist air to a length Δx and to both the sides of the fin is given by Eq. (11.8) with area $dA_o = 2\Delta x$ as follows:

$$dQ = \frac{2h_{co}\,\Delta x}{c_{pma}}(h - h_{sw}) \tag{11.10}$$

Suppose that the water and fin temperatures are t_w and t_f respectively. Heat transfer across the water film of thickness y_w and thermal conductivity k_w is given by

$$dQ = \frac{2k_w\,\Delta x}{y_w}(t_w - t_f) \tag{11.11}$$

Equation (11.9) gives a relation between h_{sw} and t_w. In a similar way, we may define a fictitious enthalpy h_f at fin temperature t_f, i.e.

$$h_f = a_w + b_w\, t_f \tag{11.12}$$

The temperature range between t_w and t_f is small hence the same constants a_w and b_w have been used. By using Eqs. (11.9) and (11.12), we may write Eq. (11.11) as follows:

$$dQ = \frac{2k_w\,\Delta x}{b_w y_w}(h_{sw} - h_f) \tag{11.13}$$

Combining Eqs. (11.10) and (11.13), we get

$$dQ = \frac{2h_{ow}\Delta x}{b_w}(h - h_f) = \frac{2h_{ow}\Delta x}{b_w}\Delta h_f \tag{11.14}$$

where,
$$h_{ow} = \frac{1}{c_{pma}/(b_w\, h_{co}) + y_w / k_w} \tag{11.15}$$

Now we consider an elemental length Δx of the fin and write the energy balance for it.

$$\frac{dQ_f}{dx}\Delta x = dQ \tag{11.16}$$

From Fourier's law of heat conduction, we have

$$Q_f = -2k_f y_f \frac{dt_f}{dx} \tag{11.17}$$

From Eq. (11.12), we get

$$\frac{dt_f}{dx} = \frac{1}{b_w}\frac{dh_f}{dx} = -\frac{1}{b_w}\frac{d\Delta h_f}{dx}, \quad \text{where } \Delta h_f = h - h_f \tag{11.18}$$

Substituting Eq. (11.12) in Eq. (11.18) and then substituting the resulting equation in Eq. (11.16), we obtain

$$\frac{d^2\Delta h_f}{dx^2} = \frac{h_{ow}}{k_f y_f}\Delta h_f = m^2 \Delta h_f \tag{11.19}$$

where,

$$m^2 = \sqrt{\frac{h_{ow}}{k_f\, y_f}} \tag{11.20}$$

The boundary conditions for Eq. (11.19) are as follows:

$$\text{At } x = 0,\ \Delta h_f = \Delta h_{fB} \ \text{ and } \ \text{at } x = L,\ \frac{d\Delta h_f}{dx} = 0 \tag{11.21}$$

This is similar to Eqs. (10.28) and (10.29) for the straight dry fin, hence the solution is also the same as given by Eq. (10.39), that is

$$\Delta h_f = \Delta h_{fB}\,\frac{\cosh m(L-x)}{\cosh mL} \tag{11.22}$$

By analogy with the dry fin, the effectiveness of wetted fin is given by

$$\phi_w = \frac{h - h_{fm}}{h - h_{fB}} = \frac{\tanh mL}{mL} \tag{11.23}$$

11.8.3 Overall Heat Transfer Coefficient for Wetted Fin

The overall heat transfer coefficient for a dry fin-tube heat exchanger was derived in Section 10.8. It is observed that for the wetted fin-tube heat exchanger, it is convenient to replace the temperature by enthalpy so as to obtain a simple expression for the combined sensible and latent heat transfer.

In most of the cases, copper tube is used and the conduction thermal resistance of the metal wall is negligible, that is, it is assumed that the inner and outer pipe wall temperatures are the same, i.e.

$$t_{po} = t_{pi} = t_p \tag{11.24}$$

It is further assumed that the metal and refrigerant temperatures are close together so that we may have the same coefficient b for fictitious enthalpies at pipe wall temperature and refrigerant temperature, that is

$$h_{sR} = a + b_R\, t_R \tag{11.25a}$$

$$h_{sp} = a + b_R\, t_p \tag{11.25b}$$

where, $b_R = (h_{sp} - h_{sR})/(t_p - t_R)$, h_{sp} and h_{sR} being the fictitious enthalpies at pipe temperature and refrigerant temperature t_p and t_R respectively.

Heat transfer rate to inner pipe wall is written as

$$Q = h_i A_i (t_p - t_R) = h_i A_i (h_{sp} - h_{sR}) / b_R \tag{11.26}$$

Heat transfer from bare pipe wall and the finned part is written as follows:

$$Q = \frac{h_{ow}}{b_{wp}} A_{po} (h - h_{sp}) + \frac{h_{ow}}{b_{wm}} A_f (h - h_{fm}) \tag{11.27}$$

The fin base temperature is same as the pipe temperature, hence $h_{sp} = h_{fB}$.

The coefficient b_{wm} is at mean water film temperature. It may be assumed that $b_{wp} = b_{wm}$. Hence Eq. (11.27) may be rewritten as follows:

$$Q = \frac{h_{ow}}{b_{wm}} (A_{po} + \phi_w A_f)(h - h_{sp}) \tag{11.28}$$

The overall heat transfer coefficient is defined as

$$Q = U_{ow} A_o (h - h_{sR}) \tag{11.29}$$

The overall heat transfer coefficient U_{ow} is defined from Eqs. (11.28) and (11.29).

$$\frac{1}{U_{ow}} = \frac{b_R A_o}{h_i A_i} + \frac{b_{wm}(1 - \phi_w)}{h_{ow}(A_{po}/A_f + \phi_w)} + \frac{b_{wm}}{h_{ow}} \tag{11.30}$$

This equation is similar to Eq. (10.50) for a dry tube-fin heat exchanger except for the coefficients b_R and b_{wm}. The calculation requires mean water film temperature t_{wm} and pipe wall temperature t_p to be assumed. This assumption allows the calculation of b_R and b_{wm} and then the value of U_{ow}. Then iteration may be carried to check the assumed value of temperatures. The procedure to check these values is to obtain expressions for t_p and t_{wm}. From Eqs. (11.26) and (11.29), we have for the pipe wall temperature and fictitious enthalpy

$$t_p = t_R + \frac{U_{ow} A_o (h - h_{sR})}{h_i A_i} \tag{11.31}$$

The pipe wall temperature may be checked by this expression. To obtain the expression for checking t_{wm}, we begin from the expression from Eqs. (11.10) and (11.14) as follows:

$$dQ = \frac{2h_{co}\,\Delta x}{c_{pma}} (h - h_{sw}) \quad \text{and} \quad dQ = \frac{2h_{ow}\,\Delta x}{b_w} (h - h_f)$$

When these are integrated over a length L of the fin, the enthalpy h_{sw} will be replaced by the saturated air enthalpy h_{swm} at mean water film temperature and h_f will be replaced by h_{fm} the fictitious enthalpy at mean fin temperature as follows:

$$Q = \frac{2h_{co}L}{c_{pma}} (h - h_{swm}) = \frac{2h_{ow}L}{b_{wm}} (h - h_{fm})$$

$$\therefore \quad h - h_{fm} = \frac{b_{wm}\, h_{co}}{h_{ow}\, c_{pma}} (h - h_{swm}) \tag{11.32}$$

From the definition of wet fin effectiveness, we have

$$h - h_{fm} = \phi\, (h - h_{sp}) \tag{11.33}$$

From Eqs. (11.26) and (11.29), we get

$$h - h_{sp} = \left(1 - \frac{b_R U_{ow} A_o}{h_i\, A_i}\right)(h - h_{sR}) \tag{11.34}$$

Therefore from Eqs. (11.32), (11.33) and (11.34), we obtain the expression for fictitious enthalpy at mean water film temperature

$$h_{swm} = h - \frac{c_{pma}\, h_{wo}\, \phi_w}{b_{wm}\, h_{co}} \left(1 - \frac{b_R\, U_{ow}\, A_o}{h_i\, A_i}\right)(h - h_{sR}) \tag{11.35}$$

The mean water film temperature t_{wm} is determined by trial and error from the empirical relation for saturated air enthalpy or by interpolation in moist air table such that the saturated air enthalpy at t_{wm} is equal to $h_{swm.}$

11.8.4 Mean Air Enthalpy Difference for the Wet Finned-Tube Heat Exchanger

For a heat exchanger, the enthalpy h in Eq. (11.29) is the true enthalpy of the air, which varies over the cooling coil. Similarly, it may be a chilled water-cooled heat exchanger, in which case the chilled water temperature will also rise through the heat exchanger. Therefore, a mean enthalpy difference is required in Eq. (11.29). It was shown in Chapter 10 that if the refrigerant temperature is constant then the log mean temperature difference for pure counterflow may be used as the mean temperature for crossflow heat exchanger. Similarly, for the counter-crossflow heat exchanger with more than two-tube passes and where the tube side temperature changes, it was shown that LMTD of pure counterflow is a good approximation.

Hence, in the case of crossflow wet finned-tube heat exchanger where the temperatures are replaced by fictitious enthalpy of saturated air, *log mean enthalpy difference* may be used for enthalpy difference in Eq. (11.29) which becomes

$$Q = U_{ow}\, A_o\, \Delta h_m \tag{11.36}$$

$$\Delta h_m = \frac{(h_1 - h_{sR2}) - (h_2 - h_{sR1})}{\ln \dfrac{h_1 - h_{sR2}}{h_2 - h_{sR1}}} \tag{11.37}$$

where h_1 and h_2 are the inlet and outlet air enthalpies respectively, while h_{sR1} and h_{sR2} are the fictitious enthalpies at inlet and outlet refrigerant temperature respectively. In the general case, one may also include a deposit coefficient and conduction thermal resistance of the metal wall as follows:

$$\frac{1}{U_{ow}} = \frac{b_R A_o}{h_i A_i} + \frac{b_R A_o}{h_{di} A_i} + \frac{A_o r_i \ln(r_o / r_i)}{A_i k_p} + \frac{b_{wm}(1-\phi_w)}{h_{ow}(A_{po}/A_f + \phi_w)} + \frac{b_{wm}}{h_{ow}} \tag{11.38}$$

In the estimation of overall heat transfer coefficient the evaporation heat transfer coefficient has some uncertainty as was discussed in Chapter 2. Some of the correlations for boiling heat transfer coefficient are presented in Section 11.9. The wet-finned surface side heat transfer coefficient, h_{ow} is evaluated by Eq. (11.15). It has a term y_w/k_w, which is usually small, hence the estimate of water film thickness y_w is not so critical. In case there is frost formation, the frost film thickness y_w is not small and then the estimate of it becomes critical.

It is well known that the smallest heat transfer coefficient is the controlling factor for the overall heat transfer coefficient. Therefore, h_{co} the air-side heat transfer coefficient for the fin-tube configuration is the controlling factor. For dry fins, a correlation was given in Chapter 10. For the wet fin-tube configuration the following correlation may be used to a good accuracy.

EXAMPLE 11.1 The condition of moist air at standard atmospheric pressure at the inlet of a direct expansion coil is 21°C wet-bulb temperature and 28°C dry-bulb temperature. At the exit of the coil the wet and dry-bulb temperature are 11°C and 12°C respectively. The refrigerant temperature is 5°C. Assume that a film of water of 0.125 mm average thickness covers the entire coil surface. The thermal conductivity of water is 0.571 W/m-K. The refrigerant-side heat transfer coefficient $h_i = 3400$ W/m^2-K and the air-side heat transfer coefficient $h_{co} = 56.8$ W/m^2-K. The fin effectiveness ϕ is 0.72 and surface II of Section 10.7 is used. Determine the overall heat transfer coefficient.

Solution:

Assume pipe wall temperature of 10°C and mean water film temperature of 12°C

$$t_R = 5°C,\ t_p = 10°C \text{ and } t_{wm} = 12°C$$

The enthalpies of saturated air at these temperatures are evaluated later in Example 16.7 and these are as follows:

$$h_{sR} = 18.636 \text{ kJ/kg}$$
$$h_{sp} = 29.3465 \text{ kJ/kg}$$
$$h_{sw} = 34.1728 \text{ kJ/kg}$$
$$b_R = (h_{sp} - h_{sR})/(t_p - t_R) = 10.7105/5 = 2.1421 \text{ kJ/kg-K}$$
$$b_{wm} = (h_{sw} - h_{sp})/(t_{wm} - t_p) = 2.4131 \text{ kJ/kg-K}$$

The enthalpy, the humidity ratio, and the specific volume of the inlet air are also evaluated in Example 16.7 and these are as follows:

$$h_1 = 60.763 \text{ kJ/kg},\ W_1 = 0.012784 \text{ kgw/kga and } v_1 = 0.8704 \text{ m}^3\text{/kg}$$

The specific heat of moist air is as follows:

$$c_{pma} = 1.005 + 1.88W_1 = 1.005 + 1.88(0.012784) = 1.02903 \text{ kJ/kga-K}$$

$$h_{ow} = \frac{1}{\frac{c_{pma}}{b_{wm} h_{co}} + \frac{y_w}{k_w}} = \frac{1}{\frac{1.02903}{2.4131(56.8)} + \frac{0.125 \times 10^{-3}}{0.571}} = 129.365 \text{ W/m}^2\text{-K}$$

For surface II of Section 10.7, we have

$$A_o/A_{pi} = 20.371,\ A_{po}/A_f = 0.05029,\ A_{pi} = 1.2105,\ A_o = 24.6592,$$
$$D_h = 3.47 \times 10^{-3} \quad \text{and} \quad A_c = 0.4813.$$

Neglecting the metal wall resistance and the deposit coefficient, Eq. (11.38) for the overall heat transfer coefficient reduces to

$$\frac{1}{U_{ow}} = \frac{b_R A_o}{h_i A_i} + \frac{b_{wm}(1-\phi_w)}{h_{ow}(A_{po}/A_f + \phi_w)} + \frac{b_{wm}}{h_{ow}}$$

or
$$\frac{1}{U_{ow}} = \frac{2.1421(20.371)}{3.4} + \frac{2.4131(1-0.72)}{0.129365(0.05029+0.72)} + \frac{2.4131}{0.129365}$$

or
$$\frac{1}{U_{ow}} = 12.834 + 6.78 + 18.653 = 38.268$$

$\therefore$
$$U_{ow} = 0.02613 \text{ kW/m}^2\text{-K}$$

The pipe wall temperature is checked by Eq. (11.31) as follows:

$$t_p = 5 + \frac{0.02613(20.371)(60.763 - 18.636)}{3.4} = 5 + 6.595 = 11.595°\text{C}$$

This is 1.595°C more than the assumed value. The mean water enthalpy is determined from Eq. (11.35) as

$$h_{swm} = 60.763 + \frac{1.02903(0.129365)0.72}{2.4131(0.0568)}\left[1 - \frac{2.1421(0.02613)20.371}{3.4}\right](60.763 - 18.636)$$
$$= 41.183 \text{ kJ/kg}$$

By interpolation in moist air table, it is found that at a temperature of 14.183°C, enthalpy of saturated air is 41.183 kJ/kg. This is very close to the temperature of 14°C assumed for the mean water film temperature. If better accuracy is desired, calculations may be repeated with pipe wall temperature of 11.6°C.

EXAMPLE 11.2 The direct expansion coil of Example 11.1 processes 350 cmm of moist air from 28°C dbt and 21°C wbt to 12°C dbt and 11°C wbt. The face velocity is 150 m/min. Determine the number of rows of cooling coil required.

Solution:

The enthalpy of the outlet air at wet and dry bulb temperature of 11°C and 12°C respectively has been calculated in Example 16.7. It is given by

$$h_2 = 31.7002 \text{ kJ/kga}$$

Equations (11.36) and (11.37) will be used for the calculation of total heat transfer and the area required.

$$Q = U_{ow} A_{ot} \Delta h_m$$

$$\Delta h_m = \frac{(h_1 - h_{sR2}) - (h_2 - h_{sR1})}{\ln \dfrac{h_1 - h_{sR2}}{h_2 - h_{sR1}}} = \frac{60.763 - 31.7002}{\ln \dfrac{60.763 - 18.636}{31.7002 - 18.636}} = 24.8227$$

The overall heat transfer coefficient has been calculated in Example 11.1.

Mass flow rate of dry air, $\dot{m}_a = \dfrac{350}{60(0.8704)} = 6.7019$ kga/s

Total heat transfer rate = $\dot{m}_a(h_1 - h_2) = 6.7019(60.763 - 31.7002) = 194.775$ kW

$$A_{ot} = \frac{Q}{U_{ow}\Delta h_m} = \frac{194.775}{0.02613 \times 24.8227} = 300.294 \text{ m}^2$$

The face area of the coil is given by

$$A_{\text{face}} = \text{volume flow rate /face velocity} = 350/150 = 2.333 \text{ m}^2$$

If n number of rows are used, then $A_{ot} = A_{\text{face}}\, n\, A_o$

or
$$n = \frac{300.294}{2.333(24.6592)} = 5.219$$

Hence six rows of the coil will be required to process the air.

11.9 BOILING HEAT TRANSFER COEFFICIENTS

This phenomenon was discussed in brief in Section 2.22. For the evaporators, this involves either boiling outside tubes or boiling inside tubes. Boiling outside tubes has been extensively studied under the heading of *nucleate pool boiling*. The general characteristics of nucleate pool boiling were described in Figure 2.19. In pool boiling, it is assumed that the tube or the heat transfer surface is immersed in a pool of liquid, which is at its saturation temperature. The characteristics of heat flux as function of the temperature difference between the surface and the pool were discussed in Section 2.22. For a small temperature difference, the heat transfer from the surface is by *free convection*. As the temperature difference increases, bubbles start to form at selected nucleation sites. The bubbles grow in size as heat is transferred and the evaporation of liquid occurs. After achieving a critical diameter depending upon the surface tension and other factors, the bubbles get detached from the surface and rise to the free surface where the vapour inside the bubbles is released. During the detachment process, the surrounding liquid rushes towards the void created and also during the bubble motion upwards convection heat transfer increases from its free convection value at smaller temperature differences. This region is known as *individual bubble regime*. As the temperature difference increases further, more and more bubbles are formed and it is the columns of bubbles which rise up increasing the heat transfer drastically. This regime is known as *column bubble regime*.

As the temperature difference increases further, more and more bubbles are formed, and columns of bubbles rise to the free surface. The heat transfer rate increases drastically. As the bubble columns move upwards, they also entrain some liquid that rises upwards to the free surface.

The vapour in the bubbles escapes at the free surface but the liquid returns to the bottom because of its lower temperature (and higher density) and to satisfy the mass conservation. A given surface can accommodate only a few such rising columns of bubbles and descending columns of relatively colder liquid. Hence, the heat transfer rate cannot increase beyond a certain value. It becomes maximum at some temperature difference. The maximum heat transfer rate is called the *critical heat transfer rate*.

If the temperature difference is increased beyond the critical value, then a blanket of film forms around the heat transfer surface. This vapour film offers conduction thermal resistance; as a result the heat transfer rate decreases. The film, however, is unstable and may break at times. This regime is called *unstable film regime*.

If the temperature difference is increased further, it becomes so high that radiation heat transfer becomes very important and the heat transfer rate increases because of radiation component. This regime is called *stable film boiling regime*.

As the temperature difference is increased, the temperature of the surface t_w continues to increase since conduction thermal resistance of the film becomes larger as the film thickness increases. All the heat from the surface cannot be transferred across the film and the surface temperature increases. Ultimately the temperature may approach the melting point of the metal and a severe accident may occur (if these are the tubes of a nuclear power plant). This point is referred to as the *burnout point*.

Boiling inside tubes consists of nucleate boiling as well as convective heat transfer. As the liquid evaporates, more vapour is formed which increases the average velocity and the convective heat transfer rate. Various regimes like bubbly regime, slug regime, annular regime and mist regime are observed in (a), (b), (c) and (d) as shown in Figure 2.20. The trend of heat transfer is also shown in the various regimes. The heat transfer coefficient depends upon the fraction of vapour present and the parameters of forced convection heat transfer. Various empirical correlations for the heat transfer coefficients are given in Chapter 10 on condensers.

1. Nucleate pool boiling, Rohsenow's correlation:

$$\frac{C_f \, \Delta T_x}{h_{fg} \, \mathrm{Pr}_f^s} = C_{sf} \left[\frac{Q/A}{\mu_f \, h_{fg}} \sqrt{\frac{\sigma}{g(\rho_f - \rho_g)}} \right]^{0.33}$$

where

C_f = specific heat of liquid
σ = surface tension
s = 1 for water and s = 1.7 for halocarbons
C_{sf} = 0.013 for halocarbons boiling on copper surface.

2. Forced convection boiling inside tubes:

(a) Bo Pierre's Correlation:

$x_{\text{inlet}} \approx 0.1$ to 0.16

$\bar{\mathrm{Nu}}_f = 0.0009 (\mathrm{Re}_f^2 \, K_f)^{1/2}$: *for incomplete evaporation and* $x_{\text{exit}} < 0.9$

$$\bar{\mathrm{Nu}}_f = 0.0082(\mathrm{Re}_f^2 K_f)^{1/2} \quad : \textit{for complete evaporation}$$

$$K_f = \textit{Load factor} = \frac{\Delta x h_g}{gL}$$

(b) Chaddock–Brunemann's correlation:

$$h_{TP} = 1.91 h_L\,[\mathrm{Bo}.10^4 + 1.5(1/X_{tt})^{0.67}]^{0.6}$$

$$\mathrm{Bo} = \text{Boiling Number} = \frac{Q/A}{h_{fg}(\dot{m}/A)}$$

$$X_{tt} = \left(\frac{1-x}{x}\right)^{0.9} (\rho_g/\rho_f)^{0.5} (\mu_f/\mu_g)^{0.1} \qquad \textit{Lockhart–Martinelli parameter}$$

(c) Shah's correlation:

$\psi = h_{TP}/h_L$, where h_L is given by Dittus–Boelter correlation

ψ is determined from the largest value amongst, ψ_{nb}, ψ_{cb} and ψ_{bs}

$$\mathrm{Fr}_f = \frac{G^2}{\rho_f^2 g D_i}, \quad h_L = 0.023(G(1-x)D_i/\mu_f)\mathrm{Pr}_f\, k_f/D_i$$

For vertical tubes:	$N = \mathrm{Co}$	for all values of Fr_f
For horizontal tubes:	$N = \mathrm{Co}$	for $\mathrm{Fr}_f > 0.4$
	$N = 0.38\ \mathrm{Fr}_f^{-0.8}.\mathrm{Co}$	for $\mathrm{Fr}_f < 0.4$

$$\mathrm{Co} = \left(\frac{1}{x} - 1\right)^{0.8} (\rho_g/\rho_f)^{0.5} \qquad : \textit{Convection Number}$$

$$\mathrm{Bo} = \frac{q}{Gh_{fg}} \qquad : \textit{Boiling Number}$$

For Co > 1 : convection is negligible and it will be nucleate boiling.

The values of ψ for nucleate boiling and convection boiling are given as follows

$N > 1.0$:	$\psi_{nb} = 230\ \mathrm{Bo}^{0.5}$	$\mathrm{Bo} > 0.3 \times 10^{-4}$
	$= 1 + 46\ \mathrm{Bo}^{0.5}$	$\mathrm{Bo} < 0.3 \times 10^{-4}$
	$\psi_{cb} = 1.8/\mathrm{N}^{0.8}$	ψ is larger of ψ_{nb} and ψ_{cb}
$0.1 < N \leq 1.0$:	$\psi_{bs} = \mathrm{F}.\ \mathrm{Bo}^{0.5} \exp(2.74\, N^{-0.1})$	
		ψ is larger of ψ_{bs} and ψ_{cb}
$N < 0.1$:	$\psi_{bs} = \mathrm{F}.\ \mathrm{Bo}^{0.5} \exp(2.74 N^{-0.15})$	
	$F = 14.7$	if $\mathrm{Bo} \geq 11 \times 10^{-4}$
	$F = 15.43$	if $\mathrm{Bo} < 11 \times 10^{-4}$

(d) Kandlikar correlation:

$$h_{TP} = h_L \cdot C_1 C_0^{C_2} (25\,\mathrm{Fr}_f)^{C_5} + C_3\,\mathrm{Bo}^{C_4}\,\mathrm{Fr}_f$$

For $C_0 < 0.5$: $C_1 = 1.1360$, $C_2 = -0.9$, $C_3 = 667.2$, $C_4 = 0.7$ and $C_5 = 0.3$

For $C_0 > 0.5$: $C_1 = 0.6683$, $C_2 = -0.2$, $C_3 = 1058$, $C_4 = 0.7$ and $C_5 = 0.3$

If the tube is horizontal then $C_5 = 0$ for all cases.

(e) Jung and Radermacher Correlation:

$h_{TP} = N_1 h_{sa} + F_1 h_L$: where h_L is same as above

$$h_{sa} = 207 \frac{k_f}{bd} \left(\frac{q}{k_f} \cdot \frac{bd}{T_{\text{sat}}} \right)^{0.745} \left(\frac{\rho_g}{\rho_f} \right)^{0.581} \mathrm{Pr}_f^{0.533}$$

$$bd = 0.0146\beta \left[\frac{2\sigma}{g(\rho_f - \rho_g)} \right]^{0.5} \quad : \beta = 35^\circ$$

$N_1 = 4048\, X_{tt}^{1.22}\, \mathrm{Bo}^{1.13}$: for $X_{tt} \le 1$

$N_1 = 2.0 - 0.1\, X_{tt}^{-0.28}\, \mathrm{Bo}^{-0.33}$: for $1 < X_{tt} \le 5$

$F_1 = 2.37(0.29 + 1/X_{tt})^{0.85}$

REFERENCE

Dossat, R.J. (1961): *Principles of Refrigeration*, Wiley Eastern Limited.

REVIEW QUESTIONS

1. Explain the constructional features of flooded type evaporator. What is the nature that makes this type of evaporator very efficient?
2. Explain the differences between flooded type shell-and-tube evaporator and dry type shell-and-tube evaporator.
3. Air at a temperature of 17°C enters a direct expansion type, fin-and-tube evaporator and leaves at 11°C. The refrigerant temperature is 7°C. The total refrigerant side area is 12 m^2. The bare tube and finned areas on the air-side are 10 m^2 and 212 m^2 respectively. Find the refrigerantion capacity of the evaporator. Assume only sensible heat transfer on the air-side, and counterflow type of arrangement. Take the fin effectiveness for air-side to be 0.75. The average heat transfer coefficient on the refrigerant-side and air-side are 1700 W/m^2-K and 34 W/m^2-K, respectively

12

Complete Vapour Compression System

LEARNING OBJECTIVES

After studying this chapter the student should be able to:

1. Explain the concept of complete system analysis of vapour compression refrigeration system and the characteristics of graphical and analytical methods used.
2. Explain the performance characteristics of reciprocating compressors, condensers, evaporators, expansion valves, and condensing unit and discuss the influence of operating parameters such as cooling water and brine flow rates, and inlet temperature etc. on the performance characteristics.
3. Understand how to obtain the balance point for a condensing unit by matching the characteristics of compressors and condensers.
4. Understand how to obtain the balance point and characteristic curves for a complete system assuming an ideal expansion valve.
5. Explain the effect of expansion device on system performance.
6. Understand the meaning of sensitivity analysis and its importance in optimization of the initial cost of the system.

12.1 INTRODUCTION

A vapour compression system consists of four essential components, namely compressor, condenser, expansion valve and evaporator. Their performance characteristics have been discussed in Chapters 4, 9, 10 and 11 respectively. These components never work in isolation. Their performance is interdependent. A change in cooling water temperature will change the condenser temperature, which in turn will change the performance of compressor, expansion device as well as evaporator.

It was observed in Chapter 9, that the expansion valve and compressor work in such a manner that the mass flow rate through the two components is the same, otherwise accumulation of refrigerant occurs either in the evaporator or condenser and then corrective action is taken by the system to balance the mass flow rate. The approach of finding the balance point for the two components was explained. This is a standard method of system analysis. This can be done either graphically or mathematically.

In the graphical method, the performance of the two interdependent components is plotted for the same two variables of common interest. For example, mass flow rate vs. evaporator temperature (or pressure) are plotted along *y*- and *x*-axis respectively for a combination of compressor–expansion device at constant condenser temperature. The point of intersection of two plots will indicate the conditions at which the mass flow rate and evaporator temperature will be same for the two components. This point is called the balance point and in steady state the combination will achieve these conditions.

The mass flow rate through the expansion valve can be represented by an algebraic equation in terms of evaporator and condenser temperatures. Similarly the mass flow rate through a given compressor can also be represented by an algebraic equation in terms of evaporator end condenser temperatures by regression analysis. The balance point of the two components can be obtained by simultaneous solution of the two algebraic equations. The graphical method considers only two components at a time while the system analysis by mathematical means can consider more components simultaneously. Further, time variation of parameters in the form of differential equations can simulate the dynamic performance too. Steady-state system analysis will involve simultaneous solution of algebraic equations.

In this chapter, balance points of condensing unit, compressor–evaporator combination and two-stage systems have been considered for illustration. As a first step the performance data of industrial components is presented in the form of plots or equations. The raw data for this purpose can be obtained from the catalogues of manufacturers. These are plotted either directly or after processing in terms of the required variables.

12.2 RECIPROCATING COMPRESSOR PERFORMANCE CHARACTERISTICS

The power requirement and mass flow rate of reciprocating compressor as function of evaporator temperature with condenser temperature as a parameter were presented in Chapter 4. For the purpose of balancing, the refrigeration capacity is required as a function of evaporator and condenser temperatures. This can be easily determined by considering the SSS cycle or can be obtained from the catalogue data of the manufacturers. For a swept flow rate of $\mathbb{V}_S$ running at constant rpm, the refrigeration capacity for the SSS cycle is given by

$$Q_e = \mathbb{V}_S \, \eta_{\text{vol}} \frac{h_1 - h_4}{v_1} \text{ kW} \tag{12.1a}$$

Or in terms of displacement volume $\mathbb{V}_D$ and rpm N the refrigeration capacity is given by

$$Q_e = \mathbb{V}_D \left(\frac{N}{60} \right) \eta_{\text{vol}} \frac{h_1 - h_4}{v_1 \times 3.5167} \text{ TR} \tag{12.1b}$$

At a given condenser temperature the cooling capacity associated with mass flow rate given by a compressor increases as the evaporator temperature increases. On the other hand, for a given evaporator temperature, the cooling capacity decreases with increase in condenser temperature. These characteristics are shown in Figure 12.1. In general, the following equation may represent these trends:

$$Q_e = a_1 + a_2 t_e + a_3 t_e^2 + a_4 t_c + a_5 t_c^2 + a_6 t_e t_c + a_7 t_e^2 t_c + a_8 t_e t_c^2 + a_9 t_e^2 t_c^2 \qquad (12.2)$$

where t_e and t_c are evaporator and condenser temperatures respectively and the constants a_i may be determined by curve fitting to the data using the least square method or by solving nine simultaneous equations of the type (12.2) for the nine constants a_i using nine values of Q_e from a given catalogue data for various values of t_e and t_c.

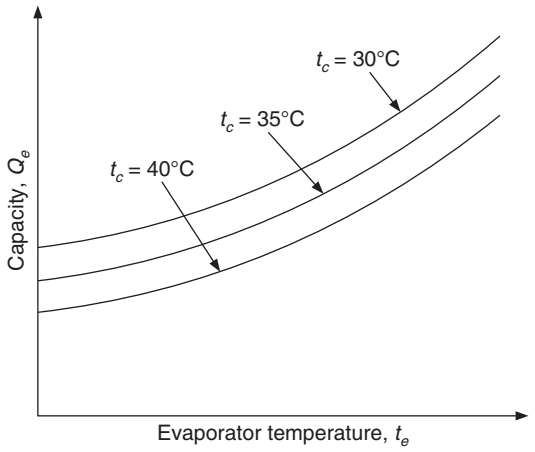

Figure 12.1 Variation of refrigeration capacity of a reciprocating compressor with evaporator and condenser temperatures at a fixed value of rpm.

12.3 CONDENSER PERFORMANCE CHARACTERISTICS

The representation of condenser performance is quite complex. A detailed analysis considers heat transfer in superheated vapour region, mixture region and subcooled region. In the superheated region, the temperature difference between the coolant and the refrigerant is large while the heat transfer coefficient from refrigerant vapour is small. In the mixture region the temperature difference is small while the condensation heat transfer coefficient is very large. Therefore, it is assumed that the total heat transfer from condenser can be found by considering it to be a single region with condensation heat transfer coefficient.

For air-cooled condensers, it is possible to represent the total heat rejection as a function of temperature difference and the overall heat transfer coefficient as follows:

$$Q_c = U_c A_c (t_c - t_\infty) \qquad (12.3)$$

where, t_∞ is the ambient temperature and t_c is the condensing temperature of the refrigerant in the condensation region.

For water-cooled condensers, one considers the water flow rate and the inlet water temperature as additional parameters. In this case too, a single region with constant condenser temperature t_c is considered. The heat transfer rate for a water-cooled condenser is expressed as follows:

$$Q_c = U_c A_c \text{ LMTD} = \dot{m}_w c_{pw} (t_{wo} - t_{wi}) \tag{12.4}$$

where $\dot{m}_w$ is the water flow rate, U_c is the overall heat transfer coefficient, t_{wi} and t_{wo} are the inlet and outlet water temperatures respectively. The log mean temperature difference LMTD is expressed as follows:

$$\text{LMTD} = \frac{t_{wo} - t_{wi}}{\ln\left\{\dfrac{t_c - t_{wi}}{t_c - t_{wo}}\right\}} \tag{12.5}$$

$$\therefore \quad \ln\left\{\frac{t_c - t_{wi}}{t_c - t_{wo}}\right\} = \frac{U_c A_c}{\dot{m}_w c_{pw}} = \text{NTU} \quad \therefore \quad \frac{t_c - t_{wi}}{t_c - t_{wo}} = e^{\text{NTU}} \tag{12.6}$$

or

$$t_{wo} = t_c - (t_c - t_{wi})\, e^{-\text{NTU}} \tag{12.7}$$

where NTU is the number of transfer units .

The matching or the determination of balance point requires that condenser characteristics be represented in the same form as done for compressor, that is, cooling capacity vs. evaporator temperature. The condenser by itself does not give cooling capacity. One finds out the condensation rate of the liquid refrigerant from the heat rejection capacity of condenser. The condensate rate multiplied by refrigeration capacity gives the cooling capacity. Hence from the given heat rejection capacity Q_c, one finds the condensate rate $\dot{m}_{\text{refrigerant}}$ for the SSS cycle as follows:

$$\dot{m}_{\text{refrigerant}} = \frac{Q_c}{h_2 - h_3} \tag{12.8}$$

The corresponding refrigeration of the condenser is given by

$$Q_e = \frac{\dot{m}_{\text{refrigerant}} (h_1 - h_4)}{3.5167} \text{ TR} \tag{12.9}$$

The condenser characteristics are shown in Figure 12.2 for a fixed value of $\dot{m}_w$ and t_{wi}. It is observed that for a fixed evaporator temperature the capacity is higher at the higher condenser temperature. A higher condenser temperature leads to a larger value of LMTD, which in turn gives a larger heat transfer rate and a larger condensate rate.

Further it is observed that at fixed condenser temperature, the cooling capacity increases with an increase in evaporator temperature. The heat rejection ratio decreases with increase in evaporator temperature, hence less heat rejection Q_c is required per TR of cooling, therefore the condensate rate of condenser can give a larger cooling capacity. Figure 12.3 shows the effect of inlet water temperature t_{wi} on TR for various condenser temperatures. The cooling capacity is zero when the inlet water temperature is equal to the condenser temperature. As the inlet water temperature

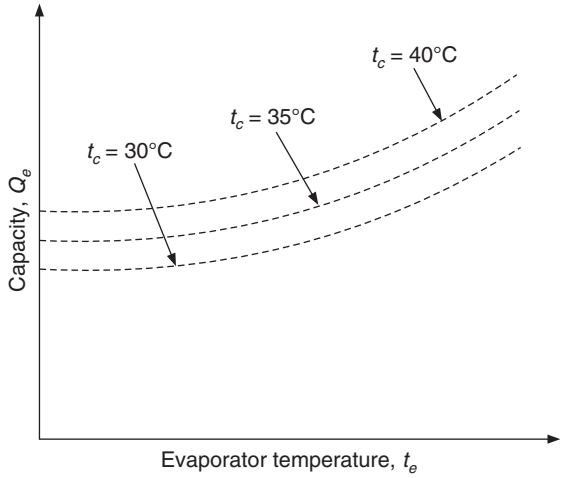

Figure 12.2 Condenser performance at a fixed value of water inlet temperature t_{wi} and a fixed value of water flow rate $\dot{m}_w$.

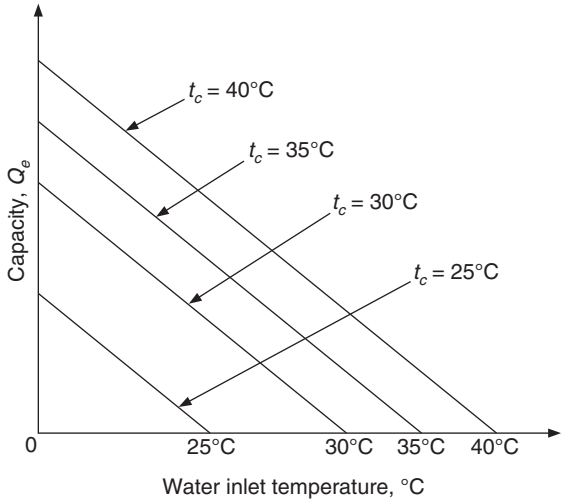

Figure 12.3 Condenser performance with water inlet temperature t_{wi} at fixed flow rate m_w.

increases for a fixed condenser temperature, the LMTD decreases, which decreases the cooling capacity. Following algebraic equation representing the curves of Figure 12.2 at constant inlet temperature and flow rate of water can represent these characteristics.

$$Q_e = b_1 + b_2 t_e + b_3 t_e^2 + b_4 t_c + b_5 t_c^2 + b_6 t_e t_c + b_7 t_e^2 t_c + b_8 t_e t_c^2 + b_9 t_e^2 t_c^2 \qquad (12.10)$$

The characteristics in Figure 12.3 are straight lines with almost same slope for all the condenser temperatures. These characteristics may be represented by the following equation:

$$Q_e = G\,(t_c - t_{wi}) \qquad (12.11)$$

12.4 EVAPORATOR PERFORMANCE CHARACTERISTICS

Evaporator is also a heat exchanger just like the condenser. Let us say that the evaporator is a brine chiller. The cooling capacity of brine chiller in TR is shown in Figure 12.4 as a function of brine flow rate on x-axis for different values of LMTD as the parameter. The brine side heat transfer coefficient h_i increases as the brine flow rate increases. As a result, the overall heat transfer coefficient increases. Figure 12.4 shows that the cooling capacity for this reason increases with flow rate for constant LMTD.

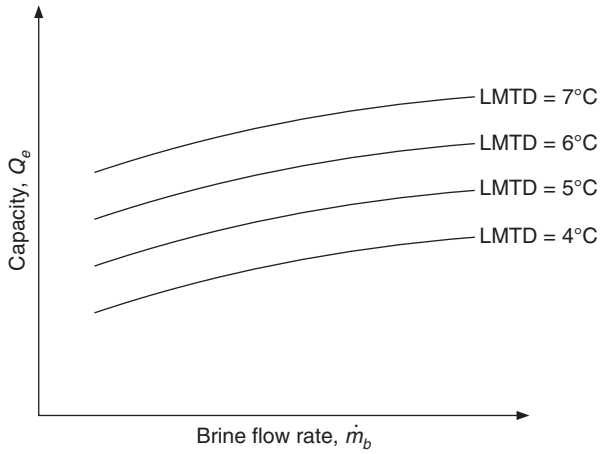

Figure 12.4 Evaporator performance against brine flow rate and LMTD as the parameter.

One can obtain the data for cooling capacity at various brine inlet temperatures from these characteristics. Say we want a plot for the brine inlet temperature t_{bi} of 10°C. We choose LMTD of 5°C and read the capacity Q_e for the chosen brine flow rate $\dot{m}_b$. Then we find the outlet brine temperature t_{bo} from the equation,

$$Q_e = \dot{m}_b c_{pb} (t_{bi} - t_{bo}) \tag{12.12}$$

Then we find the evaporator temperature t_e from the expression for LMTD which is as follows:

$$\text{LMTD} = \frac{t_{bi} - t_{bo}}{\ln\left\{\dfrac{t_{bi} - t_e}{t_{bo} - t_e}\right\}}$$

The capacity Q_e and evaporator temperature t_e are determined for different values of LMTD for a fixed brine flow rate and brine inlet temperature of 10°C. Figure 12.5 shows a plot obtained by this method. In this plot the brine flow rate is constant, hence the brine side heat transfer coefficient is constant. If the evaporation heat transfer coefficient was also constant, then the overall heat transfer coefficient will also be constant and these lines will be straight lines. The evaporation heat transfer coefficient increases with increases in evaporator temperature, hence these lines deviate from straight lines. The capacity for these lines may be expressed as follows:

$$Q_e = c_0(t_{bi} - t_e) + c_1(t_{bi} - t_e)^2 \tag{12.13}$$

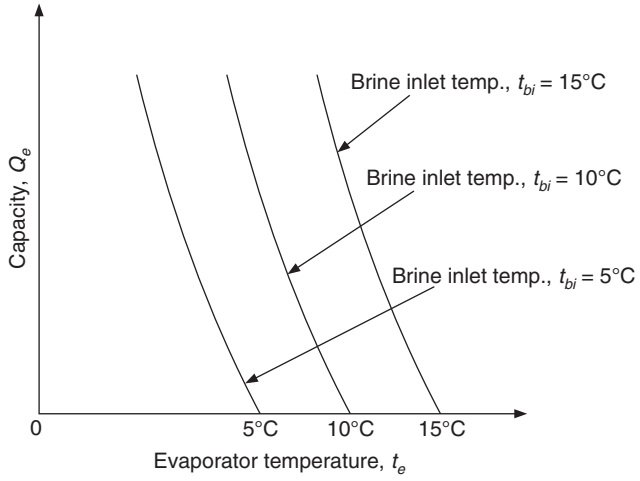

Figure 12.5 Performance characteristics of evaporator at constant brine flow rate.

12.5 EXPANSION VALVE CHARACTERISTICS

The flow characteristics of expansion valve play an important role in deciding the conditions achieved by the refrigeration system. It was shown in Chapter 9 that compressor and expansion valve seek an evaporator temperature such that the mass flow rate is same through the compressor and expansion valve. This was the result under the constraint that the condenser and evaporator have sufficiently large heat transfer areas and do not affect their performance. In this chapter it is assumed that the expansion valve is capable of providing sufficient mass flow rate at all condenser and evaporator temperatures. This is assumed to simplify the matching problem. A float type of expansion valve or TEV will meet this requirement. If the analysis is being done by a computational method, then the valve performance may also be included with some additional computational effort.

12.6 CONDENSING UNIT CHARACTERISTICS

If a graphical procedure is used to carry out performance evaluation of various components, then only two components can be considered at a time. In view of this the first sub-system considered is the condensing unit. A condensing unit is a combination of compressor and condenser. This unit draws the refrigerant from the evaporator, compresses it , condenses it into liquid refrigerant which is fed to the expansion valve. It is available as a packaged unit from manufacturers with matched set of compressor, compressor motor and condenser along with reservoir and controls. It may be an air-cooled or a water-cooled unit which may be installed as an outdoor unit.

The performance of the condensing unit as function of the evaporator temperature is obtained by combining the TR vs. evaporator temperature characteristics of compressor and condenser. First, we consider cooling capacity TR vs. evaporator temperature assuming that the compressor speed, the temperature and mass flow rate of inlet water to condenser to be constant. This matching is obtained by superimposing the compressor performance curve given in Figure 12.1 on the

condenser performance given in Figure 12.2 as shown in Figure 12.6. The intersection of the compressor and condenser characteristics is at point *A* for 30°C condenser temperature. The combination of compressor and condenser will achieve TR and t_e corresponding to this point at $t_c = 30$°C. Similarly, points *B* and *C* are the intersections at condenser temperatures of 35°C and 40°C respectively. These points are called match points and the line *A*–*B*–*C* is called the performance characteristic of the condensing unit.

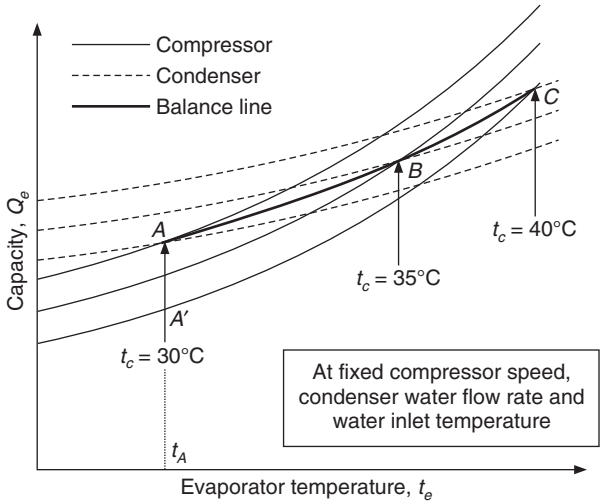

Figure 12.6 Performance characteristics of a condensing unit as a function of evaporator and condensing temperatures.

It is observed that as the evaporator temperature decreases, the condensing temperature for the combination also decreases. This is explained as follows: At lower evaporator temperatures, the volumetric efficiency and the mass flow rate through the compressor decrease. This decreases the load on the condenser. A large condenser heat transfer area is available for small mass flow rates, hence condensation can occur at lower condenser temperatures. At condenser temperature of 40°C and evaporator temperature of t_A, the compressor cooling capacity corresponds to point *A*′, while the condensing unit has the capacity corresponding to point *A*. That is, one gets a larger cooling capacity because of the reduced condenser temperature.

Figure 12.7 shows the variation of refrigeration capacity of the condensing unit with a variation in inlet water temperature to the condenser. This is obtained by superimposition of compressor characteristics of Figure 12.1 on the variation of condenser performance with inlet water temperature given in Figure 12.3. The two figures are shown side-by-side. At constant evaporator temperature of –5°C and condenser temperature of 30°C, the inlet water temperature corresponding to point *D* is required to match the two components. Points *E* and *F* are the match points at condenser temperatures of 35°C and 40°C respectively. Line DEF is the characteristics of the condensing unit at $t_e = -5$°C. It is observed that the cooling capacity decreases as the inlet water temperature increases.

These characteristics can also be obtained by simultaneous solution of Eqs. (12.2) and (12.10) for constant inlet water temperature and mass flow rate. Suppose we wish to find the condenser temperature and capacity for a given evaporator temperature t_e = 10°C. An iterative procedure may be devised as follows:

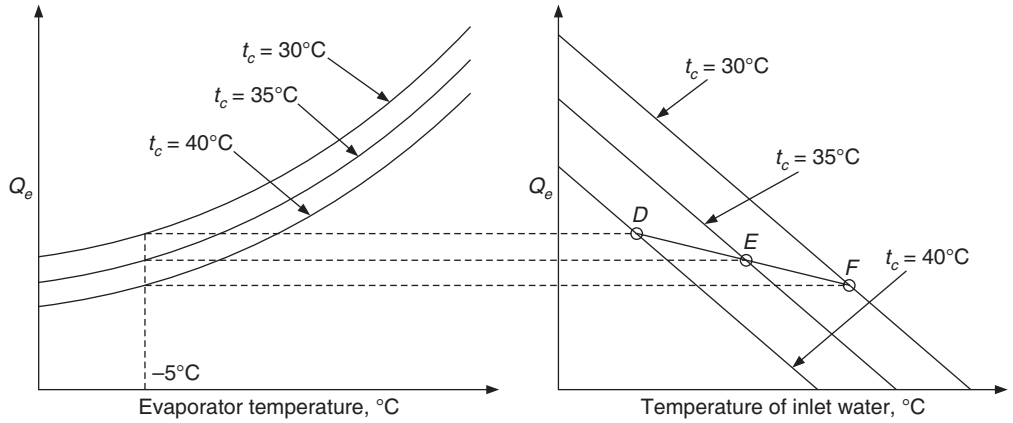

Figure 12.7 Performance of the condensing unit as a function of water temperature at condenser inlet.

(i) For $t_e = 10^oC$ assume $t_c = 35^oC$.

(ii) Find Q_e from Eq. (12.2).

(iii) Substitution of $t_e = 10^oC$ and Q_e in Eq. (12.10) will yield a quadratic equation for t_c. The value of t_c is found and checked against the assumed value of t_c (35^oC being the first iterate) and iteration is continued until the calculated value matches with the assumed value of condenser temperature.

12.7 PERFORMANCE OF COMPLETE SYSTEM—CONDENSING UNIT AND EVAPORATOR

In steady state, a balance condition must prevail between all the components, that is, between the condensing unit and the evaporator assuming that the expansion valve will provide the appropriate mass flow rate. This confluence will represent the performance of a complete single-stage vapour compression refrigeration system. The combined curves will also give insight into the off-design performance of the system and operational problems. Superimposing Figure 12.5 for the evaporator characteristics and Figure 12.6 for the condenser characteristics yields the balance point of the system. This is shown in Figure 12.8. This is for constant inlet water temperature and flow rate to the condenser, constant compressor speed and constant inlet brine temperature to the evaporator. The point of intersection of the two curves gives the refrigeration capacity and the evaporator temperature that the system will achieve. The balance point at inlet brine temperature of 10^oC would be given by $t_e = -3^oC$ and $Q_e = 35$ TR.

We can also study the response of the system in transient state utilizing Figure 12.8. In a transient state, say the evaporator temperature is 5^oC. The figure shows that at this point the condensing unit has a capacity corresponding to point *B* while the evaporator has capacity corresponding to a lower value at C. Hence the condensing unit has excess capacity. The excess capacity will reduce the temperature of the refrigerant and that of the metallic wall of the evaporator. This will continue until the balance point of 3^oC is reached at point *A*.

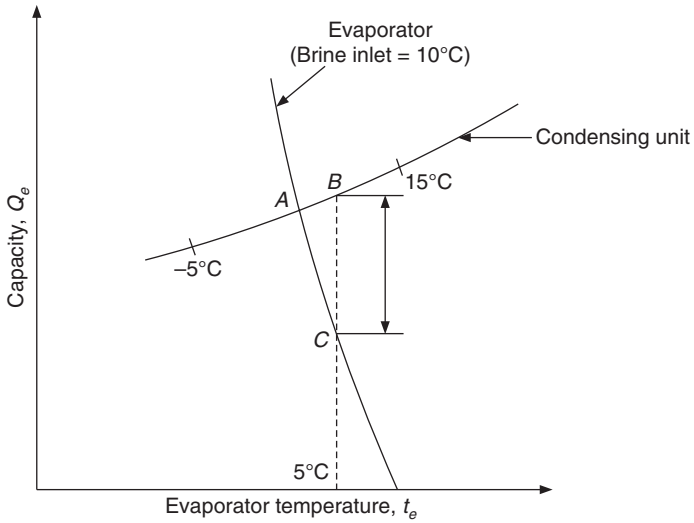

Figure 12.8 Performance of the complete system as an intersection of evaporator and condensing unit characteristics at a brine inlet temperature of 10°C.

Figure 12.9 shows the effect of brine mass flow rate compared to that at the balance point. If the brine flow rate is increased, it is observed that the cooling capacity increases to that at point *D*. At higher flow rates the overall heat transfer coefficient increases, while $(t_{bi} - t_{bo})$ decreases permitting a larger mean temperature difference between the refrigerant and the brine. Therefore with an increase in the mass flow rate of brine, the cooling capacity increases. The pump power also increases for the increased brine mass flow rate. Hence, one has to make a compromise between the increased capacity and the increased cost of pump power. Figure 12.9 also shows

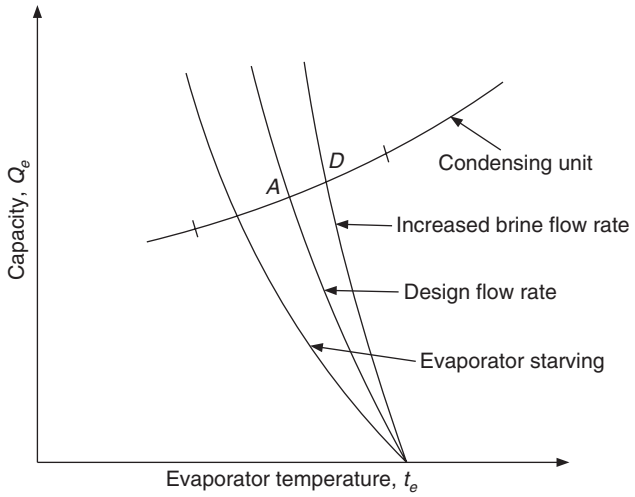

Figure 12.9 Influence of brine flow rate on system cooling capacity.

the condition for a lower brine flow rate when the heat transfer coefficient on the brine side decreases and the temperature difference ($t_{bi} - t_{bo}$) increases. This is referred to as *starving* of the evaporator. This is explained below.

12.8 EFFECT OF EXPANSION VALVE

So far we have considered the balance between the compressor, the condenser and the evaporator assuming that the expansion valve can feed sufficient refrigerant to the evaporator so that the heat transfer surface of the evaporator is wetted with the refrigerant. A thermostatic expansion valve meets this requirement. The automatic expansion valve and the capillary tube were observed in Chapter 9 to result in a condition where sufficient quantity of refrigerant could not be supplied to the evaporator. This condition was referred to as *starving* of the evaporator. Starving reduces the heat transfer coefficient in the evaporator since there is not sufficient refrigerant to wet the heat transfer surface. Consequently the cooling capacity reduces. There are other conditions too, which may lead to this situation. These are as follows:

(i) Expansion valve is too small.
(ii) Some vapour is present in the liquid entering the expansion valve
(iii) Pressure difference across the expansion valve is small.

If the charge in the system is small, then condition (ii) is likely to occur. Also if the frictional pressure drop in the liquid line is large or the valve is located at a higher elevation than the condenser, then this condition may occur. During winter months the ambient temperature is low, hence in air-cooled condensers the condenser pressure is low and the difference between the evaporator and the condenser pressure is small, as a result the starving condition (iii) is likely to occur. In the starving condition, the expansion valve does not feed sufficient refrigerant since the driving force, i.e. the pressure difference is small. The evaporator pressure also decreases in response to drop in condenser pressure. The evaporator pressure may become so low that the mass flow rate through the compressor may decrease due to lower volumetric efficiency. Hermetic compressors depend upon the mass flow rate of refrigerant for cooling the motor and the compressor. This requirement may be adversely affected under the starved condition.

12.9 CONCLUSION

The methods presented in this chapter are useful when compressor, condenser, evaporator and expansion valve have been selected and the performance of the combined system is desired. Analysis may not be useful in selecting the initial equipment. The techniques presented in this chapter are useful in predicting the system performance for off-design conditions like a change in ambient temperature, condenser inlet water temperature and brine inlet temperature, etc. The power requirement of the compressor has not been given due emphasis in the analysis. In fact, an equation similar to Eq. (12.2) may be written for this as well. This requirement can also be found from the known values of condenser and evaporator loads.

An important aspect of refrigeration system performance is the sensitivity analysis which deals with the percentage change in, say, cooling capacity with the percentage change in the capacity of the individual components such as the compressor size, heat transfer area of evaporator and condenser, etc. This can easily be done by mathematical simulation using the performance

characteristics of the components given by empirical equations. It has been shown in Stoecker and Jones (1982) that the compressor capacity has the dominant effect on system capacity and the evaporator is next in importance. An increase in compressor capacity by 10% has the effect of 6.3% increase in system capacity. A 10% increase in evaporator gives 2.1% increase while 10% increase in condenser gives 1.3% increase in system capacity. Such a data along with the relative costs of the components can be used for optimization of the initial cost of the system.

REFERENCE

Stoecker, W.F. and J.W. Jones (1982): *Refrigeration and Air Conditioning*, McGraw-Hill, New York.

REVIEW QUESTIONS

1. What is the difference between the graphical method and the analytical method for system analysis?
2. How does the cooling capacity of a reciprocating compressor vary with the evaporator temperature and the condensing temperature at a fixed value of span?
3. How does the cooling capacity of a brine chilling evaporator vary with brine flow rate, at a fixed evaporator LMTD ?
4. Describe the graphical method used to obtain the performance characteristics of a condensing unit by matching the characteristics of compressor and condenser.
5. What is meant by starving of the evaporator? Why does it cause reduction in cooling capacity?

13

Gas Cycle Refrigeration

LEARNING OBJECTIVES

After studying this chapter the student should be able to:

1. State the disadvantages and limitations of the Reversed Carnot cycle for gas refrigeration.
2. Explain the working principle of the Bell-Coleman cycle for gas refrigeration and the effect of pressure ratio on the performance of this cycle.
3. Discuss the performance of the actual Bell-Coleman cycle and the effect of isentropic efficiencies on it.
4. Discuss the effect of pressure drops on the performance of the Joule cycle.
5. State the performance advantages obtained with the regenerative Joule cycle.
6. Understand the working principles and operation of aircraft refrigeration cycles, namely simple system, bootstrap system, regenerative system, etc.
7. Perform various cycle calculations of air refrigeration systems and show these cycles on *T–s* diagrams.
8. State the significance of Dry Air Rated Temperature (DART).
9. Explain the principle of operation of vortex tube refrigeration.
10. Explain the principle of operation of pulse tube.
11. Analyze the operation of a practical Stirling cycle.
12. Gain a working knowledge of air liquefaction cycles.

13.1 INTRODUCTION

The gas cycle refrigeration was discussed in Section 3.7. It was observed that gas cycle refrigeration does not involve condensation and evaporation, therefore, large temperature differences are required for heat rejection and absorption, which leads to irreversibility and lower COP. The gases have

poor thermal conductivity, specific heat, viscosity, etc.; hence the heat transfer areas required in the heat exchangers are also very large. The gases remain far above their critical temperature during the whole of the cycle, hence they may be treated as ideal gases and some authors call gas cycle the ideal gas cycle as well.

13.2 IDEAL GAS BEHAVIOUR

Most of the gases such as O_2, N_2, air, H_2, CO_2, He and other rare gases behave like ideal gas at near ambient temperatures and pressures of a few atmospheres. The intermolecular forces are negligible in an ideal gas; hence the equation of state reduces to the simple form given by

$$pv = RT \tag{13.1}$$

It was pointed out in Chapter 2 that most of the vapours and gases behave like perfect gases, as the pressure tends to zero. In fact, as the pressure tends to zero, pv/T tends to the gas constant R which is the ratio of universal gas constant to the molecular weight of the gas, that is $R = \bar{R} / M$.

For ideal gas, it may be shown from second law that both the internal energy and enthalpy are functions of temperature only, that is,

$$h_2 - h_1 = c_p(t_2 - t_1) \quad \text{or} \quad dh = c_p\, dT \tag{13.2}$$

$$u_2 - u_1 = c_v(t_2 - t_1) \quad \text{or} \quad du = c_v\, dT \tag{13.3}$$

$$c_p - c_v = R \tag{13.4}$$

The specific heats are functions of temperature. However, for small temperature changes specific heats may be assumed to be constant. For air, the following values are a good approximation in the normal range of operation.

$$c_p = 1.005,\ c_v = 0.718 \text{ and } R = 0.287 \text{ kJ/kg-K} \tag{13.5}$$

13.3 TEMPERATURE DROP DUE TO WORK OUTPUT

The most common process used for temperature reduction is the throttling process. During throttling process where the enthalpy remains constant, the temperature of an ideal gas will remain constant. The pressure will decrease because of the obstruction offered in the path of flow. The real gases can be cooled by throttling and that too if the Joule–Thomson coefficient $[m = (\partial T/\partial h)_h]$ is positive. This requires a very high pressure and the typical cycles involving such principle are used for liquefaction of gases.

The temperature of gas can be reduced for all gases if the gas does some work in an expansion engine in pushing a piston in a cylinder. If dW is the work done in a closed system, then from the first law of thermodynamics we get

$$dU = dQ - dW \tag{13.6}$$

The change in internal energy and the corresponding drop in temperature for a given work output will be maximum if the cylinder is insulated so that the heat transfer from the surroundings, dQ, does not heat the gas, that is,

$$dU = -dW = -\dot{m}c_v\, dT \tag{13.7}$$

Similarly in a steady flow process the temperature of a gas may be reduced by letting it do some work by rotating a turbine. Again, the decrease in enthalpy will be maximum for an adiabatic process and if the changes in kinetic and potential energy are negligible. Under these conditions, in steady state from first law of thermodynamics for an open system, we get

$$dH = -dW = -\dot{m}c_p\, dT \tag{13.8}$$

A part of the work may be dissipated due to frictional heating between piston–cylinder or skin friction over the moving turbine blades if the process is not reversible. Hence a reversible adiabatic process, that is, isentropic process gives the maximum temperature drop. For a perfect gas undergoing isentropic process 1–2, the temperature ratio is given by

$$\frac{T_2}{T_1} = \left(\frac{p_2}{p_1}\right)^{(\gamma-1)/\gamma} \tag{13.9}$$

Hence if the pressure decreases in an expansion engine, the temperature also decreases.

13.4 TEMPERATURE DROP IN STEADY FLOW DUE TO CHANGE IN KINETIC ENERGY

If a gas flows through a nozzle in which the area decreases in the flow direction the velocity will increase in the flow direction, hence a part of its enthalpy is converted into kinetic energy. The enthalpy of a gas can be decreased during the passage of the gas through a nozzle. If V_1 and h_1 are the velocity and enthalpy at nozzle inlet, and V_2 and h_2 are velocity and enthalpy at its outlet respectively, then in absence of heat transfer, shaft work and change in potential energy, from the first law of thermodynamics we get

$$h_1 + \frac{V_1^2}{2} = h_2 + \frac{V_2^2}{2}$$

If the velocity at inlet is negligible, then

$$h_1 = h_2 + \frac{V_2^2}{2} \tag{13.10}$$

Assuming constant specific heat, this relation may be written as follows:

$$T_2 = T_1 - \frac{V_2^2}{2c_p} \tag{13.11}$$

For an isentropic process, T_1 and T_2 are related by Eq. (13.9).

If a gas at temperature T_1 and velocity V_1 is brought to rest adiabatically, then from the first law of thermodynamics,

$$h_{01} = h_1 + \frac{V_1^2}{2} \tag{13.12a}$$

and $$T_{01} = T_1 + \frac{V_1^2}{2} \tag{13.12b}$$

where, h_{01} is the stagnation enthalpy (state of rest, zero velocity) of gas and T_{01} is called the stagnation temperature while T_1 is called the static temperature.

It appears from Eq. (13.11) that converting a part of enthalpy of a gas into kinetic energy can reduce the temperature of the gas. However, if a thermometer is placed facing a stream with velocity V_2, it does not indicate temperature T_2 but a temperature very close to inlet temperature T_1. This is due to stagnation effect since the velocity of air reduces to zero at the bulb surface, that is kinetic energy is converted back to stagnation temperature. There will, however, be velocity gradient and temperature gradient in the flow, giving rise to viscous and thermal boundary layers on the thermometer bulb surface. A part of the kinetic energy will be lost due to viscous effects and there will be some conduction heat transfer as well. As a result, the temperature indicated by the bulb T_r would be less than T_1. The temperature T_r is called the recovery temperature and a recovery factor $a(r)$ is defined as follows:

$$a(r) = \frac{T_r - T_2}{T_{01} - T_2} \tag{13.13}$$

Therefore in a throttling process for an ideal gas, the pressure decreases in the orifice and the gas is accelerated resulting in a decrease in static temperature. However the high velocity jet is decelerated, resulting in frictional dissipation of kinetic energy, which in turn yields a temperature close to the initial temperature.

13.5 TEMPERATURE DROP IN CLOSED SYSTEM DUE TO CHANGE IN KINETIC ENERGY

In a steady flow system, change in kinetic energy is ultimately dissipated and temperature drop cannot be obtained. In a closed system the temperature drop can be observed. Consider a pressure vessel with a small hole through which issues a jet. A thermometer in the path of jet indicates a low temperature. Initially the vessel is at pressure p_1 and temperature T_1. After a while, the pressure and temperature reduce to p_2 and T_2 respectively related by Eq. (13.9) to p_1 and T_1 considering reversible adiabatic expansion of the gas inside the tank. This work of expansion is required to push the gas out of the tank in the form of a jet. Louis Caillittet used this method of expansion and reduction in temperature in 1877 to liquefy O_2. Oxygen compressed to 300 bar and cooled to –29°C (so that μ is positive) was kept in the tank from which it was suddenly released. The sudden release of pressure resulted in a mist of liquid O_2.

13.6 REVERSED CARNOT AND JOULE CYCLES FOR GAS REFRIGERATION

13.6.1 Reversed Carnot Cycle for Gas Refrigeration

These cycles were discussed in Section 3.7. The *T*–*s* and *p*–*v* cycle diagrams of Reversed Carnot refrigeration cycle using gas as refrigerant are shown in Figures 13.1(a) and (b). This cycle has been discussed in Section 3.7.1. The disadvantages of this cycle are:

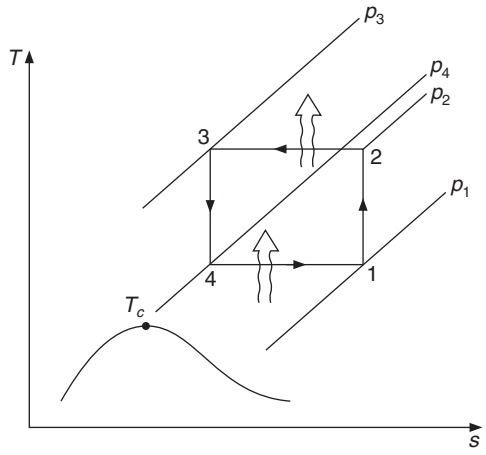

Figure 13.1(a) Reversed Carnot refrigeration cycle with gas as refrigerant on *T–s* diagram.

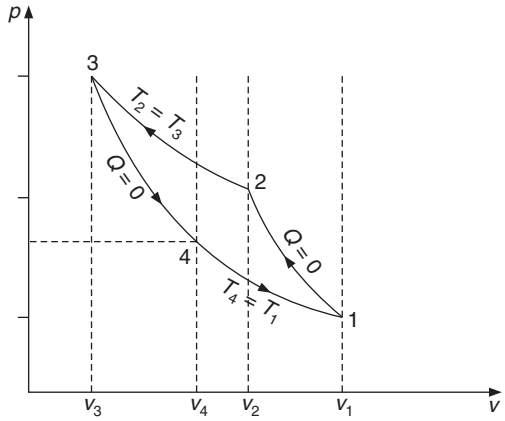

Figure 13.1(b) Reversed Carnot refrigeration cycle with gas as refrigerant on *p–v* diagram.

- Isentropic compression 1–2 is not practically feasible since compressor cannot be insulated and friction cannot be avoided. All compressors are kept at room temperature and reject heat to surroundings.
- The gas has a finite specific heat, hence isothermal heat rejection and absorption are not feasible. The isothermal heat rejection 2-3 requires an isothermal compressor since the pressure increases from p_2 to p_3. The total rise in pressure from p_1 to p_3 is very large.
- Isothermal heat absorption 4-1 requires an isothermal turbine or expander since pressure decreases from p_4 to p_1.
- The *p–v* diagram is very narrow. Any irreversibility will increase the area of work requirement drastically.
- The density of air is small, hence very large volume flow rates are required.
- Additional compressor and expander add to the initial cost and maintenance cost of the system.

13.6.2 Joule or Reversed Brayton or Bell–Coleman Cycle for Gas Refrigeration

In view of the disadvantages of the Reversed Carnot cycle mentioned in the preceding subsection, the isothermal compressor is dispensed with and whole of the compression is carried out in a single isentropic compressor with heat rejection being carried out at constant pressure. Similarly, the isothermal expander is dispensed with and the whole of expansion is carried out in an isentropic expander with heat absorption being done at constant pressure. This cycle is known as Joule cycle or Bell–Coleman cycle or Reversed Brayton cycle. The schematic diagram is shown in Figure 13.2(a). The *T–s* and *p–v* cycle diagrams are shown in Figures 13.2(b) and (c) respectively.

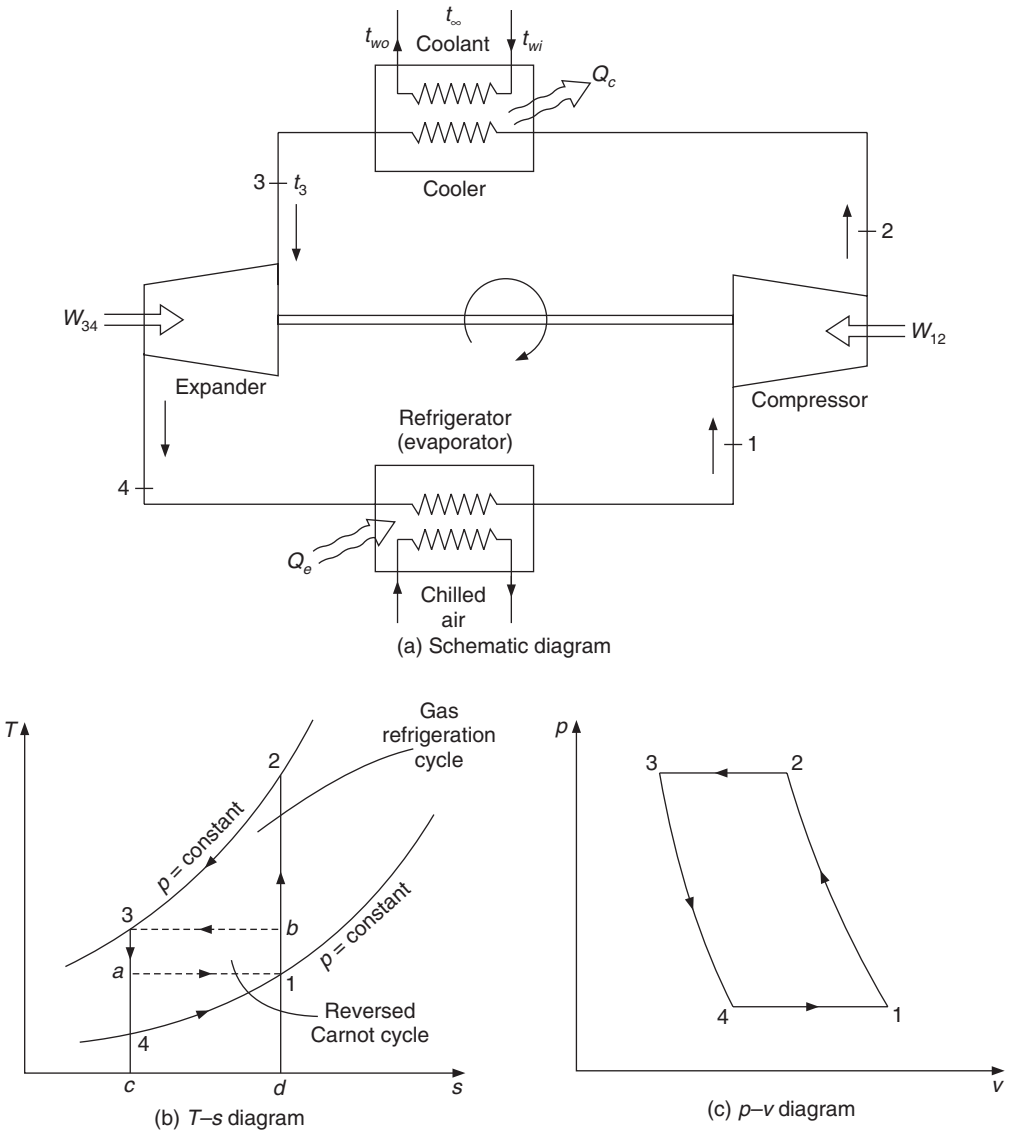

Figure 13.2 Bell–Coleman cycle for gas refrigeration.

Tbe Bell–Coleman cycle is comprised of the following processes:

Process 1–2 is isentropic compression
Process 2–3 is isobaric heat rejection
Process 3–4 is isentropic expansion
Process 4–1 is isobaric heat absorption

The corresponding Reversed Carnot cycle is also shown by 1–*b*–3–*a*–1 on the same *T*–*s* diagram for comparison purpose. The refrigeration effect of Reversed Carnot cycle is the area *a*–*c*–*d*–1–*a* whereas the refrigeration effect of Joule cycle is the area 4–*c*–*d*–1–4 which is less than that of the RC cycle by area 1–*a*–4–1. The work requirement of Joule cycle is the area 1–2–3–4–1, which is more than that of Reversed Carnot cycle by areas 1–*a*–4–1 and *b*–2–3–*b*.

In this cycle, the work output of the expander is fed back to the compressor; hence the net work is the difference of compressor work w_{12} and expander work w_{34}.

Heat is rejected to either water or surrounding air during process 2–3. The temperature at point 3 must be greater than the inlet cold-water temperature t_{wi} or the ambient temperature t_∞ as the case may be for heat transfer to take place, that is, $t_3 > t_\infty$ or $t_3 > t_{wi}$. Hence, the minimum temperature at point 3 is either t_{wi} or t_∞. The minimum pressure required for this cycle to be practical will be $p_{2\min}$ as shown in Figure 13.3. In fact, at this pressure no heat rejection can occur since $t_{2\min} = t_3 = t_{wi}$. The refrigeration effect and work requirement are both zero since the cycle has to go from 1 to $2_{\min}$ and come back from $2_{\min}$ to 1. Any practical cycle has to have temperature t_2 greater than t_3 for heat rejection to take place. One such cycle is shown by 1–2′–3′–4′–1 in which heat is rejected along 2′–3′ and refrigeration effect $c_p(t_1 - t_{4'})$ is produced along 4′–1. Another cycle with larger pressure is shown by 1–2″–3″–4″–1 in which heat is rejected along 2″–3″ and refrigeration effect $c_p(t_1 - t_{4''})$ is produced along 4″–1. It is observed that as the pressure ratio increases the refrigeration effect increases. The larger the pressure and the temperature at point 2 the smaller will be the mass flow rate for a given cooling capacity. Hence, a compromise has to be made between the mass flow rate and the pressure ratio.

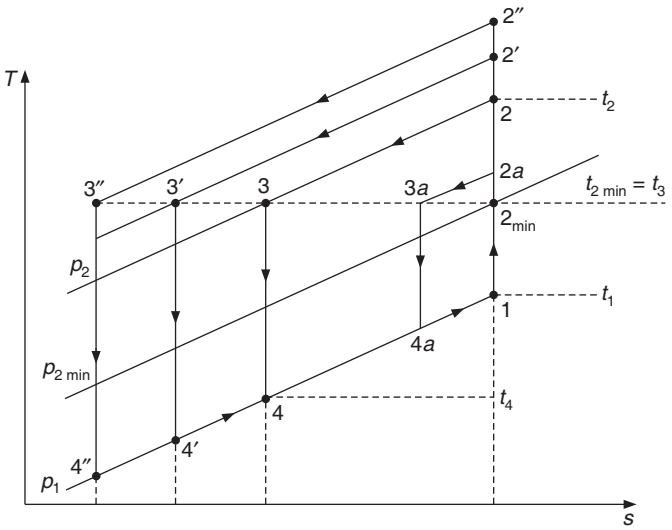

Figure 13.3 Effect of pressure ratio on the performance of the gas cycle.

The refrigerator is supposed to be maintained at temperature t_1. It is observed that the chilled air must enter at very low temperature t_4 to absorb heat in the refrigerator. This is required since the specific heat of air is small and $Q_E = \dot{m}c_p(t_1 - t_4)$. If t_4 is not small then the mass flow rate will have to be very large requiring a large compressor involving higher initial cost and running cost. This again requires a compromise between the mass flow rate and the pressure ratio.

As observed from Figure 13.2(c), the pressure ratio is the same for the isentropic processes 1–2 and 3– 4. Hence,

$$\frac{T_2}{T_1} = \left(\frac{p_2}{p_1}\right)^{(\gamma-1)/\gamma} = \frac{T_3}{T_4} \qquad \text{also,} \quad \frac{T_3}{T_2} = \frac{T_4}{T_1} \tag{13.14}$$

Compressor work is given by

$$W_{12} = W_C = \dot{m}\int_1^2 v\,dp = \dot{m}\left(\frac{\gamma}{\gamma-1}\right)(p_2v_2 - p_1v_1) = \dot{m}c_p(T_2 - T_1) \tag{13.15}$$

Similarly, the expander work is given by

$$W_{34} = W_E = \dot{m}\left(\frac{\gamma}{\gamma-1}\right)(p_3v_3 - p_4v_4) = mc_p(T_3 - T_4) \tag{13.16}$$

The heat rejection Q_c in the cooler is given by

$$Q_c = \dot{m}c_p(T_2 - T_3) \tag{13.17}$$

The heat absorption Q_e in the refrigerator is given by

$$Q_e = \dot{m}c_p(T_1 - T_4) \tag{13.18}$$

Net work = $W_{\text{net}} = W_C - W_E = Q_c - Q_e$ from first law of thermodynamics for the whole system. Substituting from Eqs. (13.15) and (13.16), we get

$$W_{\text{net}} = Q_c - Q_e = \dot{m}c_p[(T_2 - T_3) - (T_1 - T_4)] \tag{13.19}$$

$$\text{COP} = \frac{Q_e}{W_{\text{net}}}$$

$$\therefore \qquad \text{COP} = \frac{T_1 - T_4}{(T_2 - T_3) - (T_1 - T_4)} = \frac{1}{\dfrac{T_2 - T_3}{T_1 - T_4} - 1}$$

Now, $$\frac{T_2 - T_3}{T_1 - T_4} = \frac{T_2}{T_1}\left[\frac{1 - T_3/T_2}{1 - T_4/T_1}\right] = \frac{T_2}{T_1} \qquad \text{since} \quad \frac{T_3}{T_2} = \frac{T_4}{T_1} \text{ from Eq. (13.14)}$$

$$\therefore \qquad \text{COP} = \frac{1}{\dfrac{T_2}{T_1} - 1} = \frac{1}{\left(\dfrac{p_2}{p_1}\right)^{(\gamma-1)/\gamma} - 1} = \frac{1}{r^{(\gamma-1)/\gamma} - 1} \tag{13.20}$$

where, $r = \dfrac{p_2}{p_1}$ is the pressure ratio.

The COP may also be expressed as

$$\text{COP} = \frac{T_1}{T_2 - T_1} = \frac{T_4}{T_3 - T_4} = \frac{1}{z - 1} \tag{13.21}$$

where,

$$z = \frac{T_2}{T_1} = \left(\frac{p_2}{p_1}\right)^{(\gamma-1)/\gamma} \tag{13.22}$$

The expression for COP given by Eq. (13.21) is very similar to the COP of Reversed Carnot cycle. The gas has finite specific heat, hence during isobaric heat rejection, the temperature decreases from T_2 to T_3 while during isobaric heat absorption the temperature increases from T_4 to T_1. The temperature of the cold room or refrigerator is maintained at T_1 but the gas has to be cooled to a considerably lower temperature T_4 to absorb heat. The highest temperature of the cold end is T_1 and the lowest temperature of the warm end is T_3. These temperatures are those of the external regime. A Reversed Carnot cycle will work between these two temperatures and its COP will be $T_3/(T_3 - T_1)$, which is greater than the COP of Joule cycle.

$$\text{COP}_{\text{RC}} = \frac{T_3}{T_3 - T_1}$$

It is observed that the COP of the Joule cycle decreases with the pressure ratio. It was observed in Figure 13.3 that for this cycle to be practical the temperature at point 2 must be greater than T_3 so that heat can be rejected to the surroundings. For this reason the minimum pressure ratio is given by

$$\left(\frac{p_2}{p_1}\right)_{\text{min}} = \left(\frac{T_3}{T_1}\right)^{\gamma/(\gamma-1)} \tag{13.23}$$

The temperatures $T_1 = T_e + \Delta t_e$ and $T_3 = T_\infty + \Delta t_c$ where T_e and T_∞ are the temperatures in the refrigerator and ambient conditions respectively. The COP, however, is zero for this pressure ratio since the refrigeration effect is zero. The cycle 1–2*a*–3*a*–4*a*–1 shown in Figure 13.3 is a thin Joule cycle. The COP of this cycle will be very close to Reversed Carnot COP since $t_{2a} \approx t_3$ and $t_{4a} \approx t_1$.

The following table shows the variation of COP with pressure ratios for air with $\gamma = 1.4$.

Table 13.1 Variation of COP with pressure ratio for Joule cycle

$r = p_2/p_1$	1	2	3	4	5	6
COP	∞	4.56	2.71	2.05	1.72	1.5

It is observed that the COP decreases as the pressure ratio increases.

In an actual cycle there will be deviations along all the four processes. The compression and the expansion may not be isentropic and there may be some pressure drops in the heat exchangers. Also the ambient temperature may be specified along with the effectiveness of the heat exchanger to determine the temperature T_3 at the exit of the cooler. In some cases the pressure ratio may be large and may require two-stage compression with intercooling.

In the following section we consider a dense air cycle with some of these deviations.

13.6.3 Actual Bell–Coleman Cycle and Optimum COP

Effect of isentropic efficiencies

The actual cycle is shown in Figure 13.4 where the compression and expansion deviate from isentropic processes. These deviations may be accounted for by considering the empirical values of isentropic compression efficiency η_C and isentropic expansion efficiency η_E. Isentropic compression efficiency is defined as the ratio of isentropic work to the actual work while isentropic expansion efficiency is defined as opposite of this, that is, the ratio of actual work to the isentropic work. A compressor requires more work than the isentropic work while a turbine delivers less work than the isentropic work. These efficiencies are defined as

$$\eta_C = \frac{\dot{m}c_p(T_2 - T_1)}{\dot{m}c_p(T_{2'} - T_1)} = \frac{T_2 - T_1}{T_{2'} - T_1} \quad \text{and} \quad \eta_E = \frac{\dot{m}c_p(T_3 - T_{4'})}{\dot{m}c_p(T_3 - T_4)} = \frac{T_3 - T_{4'}}{T_3 - T_4} \tag{13.24}$$

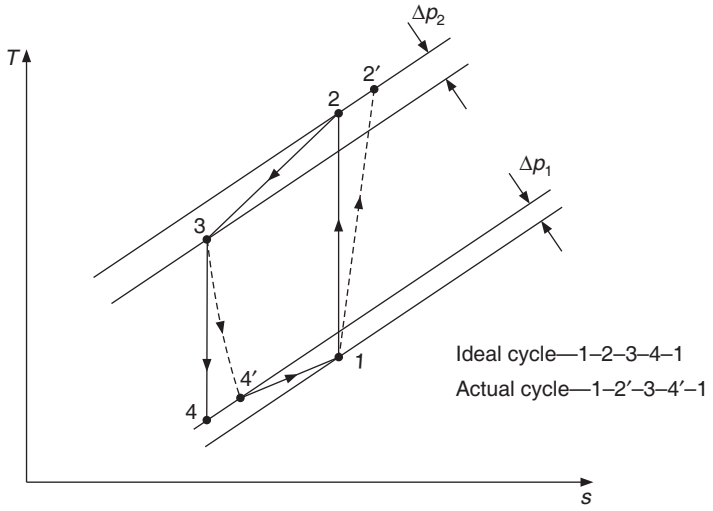

Figure 13.4 Actual Bell-Coleman cycle.

Using these definitions and Eq. (13.9), we get

$$T_{2'} = T_1 + \frac{T_1}{\eta_C}\left[\left(\frac{p_2}{p_1}\right)^{(\gamma-1)/\gamma} - 1\right] \tag{13.25}$$

or $$T_{2'} = T_1[1 + (z-1)/\eta_C] \qquad \text{where } z = (p_2/p_1)^{(\gamma-1)/\gamma}$$

Also, $$T_{4'} = T_3 - \eta_E(T_3 - T_4) = T_3 - \eta_E T_3\left[1 - \frac{T_4}{T_3}\right] = T_3 - \eta_E T_3\left[\left(\frac{p_1}{p_2}\right)^{(\gamma-1)/\gamma} - 1\right]$$

or $$T_{4'} = T_3\left[1 - \eta_E\left(1 - \frac{1}{z}\right)\right] = \left(\frac{T_3}{z}\right)\left[z - \eta_E(z-1)\right] \tag{13.26}$$

The expressions for refrigeration capacity Q_e, compressor work W_C and the expansion work W_E are as follows:

$$Q_e = \dot{m}c_p(T_1 - T_{4'}) = \dot{m}c_p T_1\left[1 - \frac{a\{z - \eta_E(z-1)\}}{z}\right] \tag{13.27}$$

where, $a = T_3/T_1$.

$$W_E = \dot{m}c_p(T_3 - T_{4'}) = \dot{m}c_p T_3\eta_E\left(1 - \frac{1}{z}\right) = \dot{m}c_p T_3\eta_E\frac{z-1}{z} \tag{13.28}$$

$$W_C = \dot{m}c_p(T_{2'} - T_1) = \frac{\dot{m}c_p T_1(z-1)}{\eta_C} \tag{13.29}$$

Substituting in the expression for COP, we get

$$\text{COP} = \xi = \frac{Q_e}{W_C - W_E} = \frac{T_1\{z(1-a) + a\eta_E(z-1)\}/z}{T_1(z-1)/\eta_C - T_3\eta_E(z-1)/z}$$

$$\therefore \quad \xi = \frac{\eta_C\{z(1-a) + a\eta_E(z-1)\}}{z(z-1) - a\eta_E\eta_C(z-1)}$$

The value of z at which COP is maximum is found by differentiating Eq. (13.30) with respect to z and putting it equal to zero. This yields an algebraic equation for z. The COP will be maximum when the value of z is one of the roots of this equation, namely

$$z^2(1 - a + a\eta_E) - 2a\,z\,\eta_E + a\eta_E(1 + a\eta_C - \eta_C) = 0 \tag{13.31}$$

For the special case when $\eta_E = \eta_C = \eta$, this equation reduces to:

$$\frac{1 - a(1-\eta)}{a\eta}z^2 - 2z + 1 + \eta(a-1) = 0 \tag{13.32}$$

It is further observed that the refrigeration effect or the COP is zero when the numerator of Eq. (13.30) is equal to zero, that is,

$$z(1-a) + a\eta(z-1) = 0 \quad \text{or} \quad z_{\xi=0} = \frac{a\eta}{1 - a(1-\eta)} \tag{13.33}$$

In the absence of expander efficiency, the COP is zero at $p_{2\min}$ and in the presence of expander efficiency the COP is zero at the value of z given by the above expression. The system just begins to work above this pressure ratio, reaches a maximum value at z given by Eq. (13.32) and decreases as the pressure ratio increases further. We look at some special cases in the following discussions.

EXAMPLE 13.1 Given that $T_1 = 270$ K and $T_3 = 313$ K and the working substance is air, find the pressure ratios corresponding to zero and maximum COP if the compressor and turbine efficiencies are same and equal to (i) 1.0, (ii) 0.99, (iii) 0.9 and (iii) 0.8.

Solution:

Case 1: $\eta_E = \eta_C = 1$

It is given that, $a = T_3/T_1 = 313/270 = 1.15926$

For this case Eq. (13.32) for the maximum COP reduces to

$$z^2 - 2az + a^2 = 0 = (z - a)^2 = 0$$

This indicates that COP is maximum at $z = a$; and substitution in Eq. (13.30) gives the maximum value of COP.

$$\xi_{\max} = \frac{z - a}{(z - 1)(z - a)} = \frac{1}{z - 1} = \frac{T_1}{T_2 - T_1} \quad \text{which is same as Eq. (13.21)}$$

$$\text{In the limit } z \to a: \ \xi_{\max} = \frac{T_1}{T_3 - T_1} = \xi_{RC} = \frac{270}{313 - 270} = 6.279$$

Case 2: $\eta_E = \eta_C = 0.99$

From Eq. (13.33) the COP is zero at

$$z_{\xi=0} = \frac{0.99a}{1 - 0.01a} = \frac{0.99(1.15926)}{1 - 0.0115926} = 1.16111$$

This corresponds to pressure ratio of $p_2/p_1 = z^{\gamma/(\gamma-1)} = z^{3.5} = 1.16111^{3.5} = 1.687$

For this case the equation for maximum COP reduces to

$$0.86123z^2 - 2z + 1.157667 = 0$$

The roots of this equation are

$$z_1 = 1.097739 \quad \text{and} \quad z_2 = 1.224515$$

The first root is less than $a = 1.15926$, hence it is not consistent. The COP will be maximum at the second root. Substituting it in Eq. (13.30), we get

$$\text{COP}_{\max} = 3.128$$

Case 3: $\eta_E = \eta_C = 0.9$

From Eq. (13.33) the COP is zero at

$$z_{\xi=0} = \frac{0.9a}{1 - 0.1a} = \frac{0.9(1.15926)}{1 - 0.115926} = 1.18014$$

This corresponds to pressure ratio of $p_2/p_1 = z^{\gamma/(\gamma-1)} = z^{3.5} = 1.18014^{3.5} = 1.7855$

Equation (13.31) for the maximum COP in this case reduces to

$$0.847855z^2 - 2z + 1.14333 = 0$$

The solution of this equation is $z = 1.38856$. The maximum COP occurs at this value of z.

The corresponding value of pressure ratio is $p_2/p_1 = z^{\gamma/(\gamma-1)} = z^{3.5} = 1.38856^{3.5} = 3.155$

$$\text{COP}_{\max} = \frac{\eta_C \{z(1 - a) + a\eta_E (z - 1)\}}{z(z - 1) - a\,\eta_E\,\eta_C (z - 1)}$$

$$= \frac{0.9\{1.38856(1-1.15926)+1.15926(0.9)0.38856}{1.38856(0.38856)-1.1592(0.9)(0.9)0.38856} = 0.9493$$

Case 4: $\eta_E = \eta_C = 0.8$
For this case from Eq. (13.33) the COP is zero at

$$z_{\xi=0} = \frac{0.8a}{1-0.2a} = \frac{0.8(1.15926)}{1-0.231952} = 1.2073$$

This corresponds to pressure ratio of $\frac{p_2}{p_1} = z^{\gamma/(\gamma-1)} = z^{3.5} = 1.2073^{3.5} = 1.9337$

Equation (13.31) in this case reduces to

$$0.82827z^2 - 2z + 1.127407 = 0$$

The solution of this equation is $z = 1.51796$. The maximum COP occurs at this value of z.

The corresponding value of pressure ratio is $\frac{p_2}{p_1} = z^{\gamma/(\gamma-1)} = z^{3.5} = 1.51796^{3.5} = 4.3093$

$$\text{COP}_{\max} = \frac{\eta_C\{z(1-a)+a\eta_E(z-1)\}}{z(z-1)-a\eta_E\eta_C(z-1)}$$

$$= \frac{0.8\{1.51796(1-1.15926)+1.15926(0.8)0.51796}{1.51796(0.51796)-1.15926(0.8)(0.8)0.51796} = 0.475$$

The values of COP at a few values of z for the four cases are given in Table 13.2.

Table 13.2 Variation of COP of Joule cycle for various isentropic efficiencies for $T_1 = 270$ and $T_3 = 313$ K

z	Case 1 $\eta = 1.0$	Case 2 $\eta = 0.99$	Case 3 $\eta = 0.9$	Case 4 $\eta = 0.8$
1.2	5.0	2.98	0.3037	–
1.3	3.333	2.7652	0.8806	0.34
1.4	2.5	2.215	0.9048	0.45
1.5	2.0	1.823	0.9073	0.474

If the values for the four cases are plotted, it will be observed that for $\eta = 0.99$, the COP is zero near $z = 1.1611$ which corresponds to a pressure ratio of 1.687. That is, at pressure ratio of 1.687 the system just starts to give some cooling. The COP reaches a maximum value of 3.128 at $z = 1.224515$ and then starts to decrease. For efficiencies values of 0.9 and 0.8 the peaks are not very sharp. For 100 % efficiency the maximum value of COP is 6.129 for $T_1 = 270$ K and $T_3 = 313$ K. This maximum occurs at $z = T_3/T_1 = a = 1.15926$. Similar results can be obtained for any other combination of T_1 and T_3. The system will not give any refrigeration for z less than a.

EXAMPLE 13.2 In a gas cycle refrigeration system working on Joule cycle, the outlet temperature from the cold space is 270 K and the temperature at inlet to turbine is 318 K. The pressure ratio is

4.0. Determine the mass flow rate, heat rejection, compressor work, turbine work, COP and the volume flow rates at inlet to compressor and at outlet of turbine for a system of 1 TR cooling capacity. The working substance is air.

Solution:

The cycle is shown in Figures 13.2(b) and (c).

$$T_2 = T_1(p_2/p_1)^{(\gamma-1)/\gamma} = T_1 z$$

$$z = (p_2/p_1)^{(\gamma-1)/\gamma} = (4)^{0.4/1.4} = (4)^{0.2857} = 1.486$$

$$T_2 = 270(1.486) = 401.22 \text{ K}$$

$$T_4 = T_3/z = 318/1.486 = 214 \text{ K}$$

For the 1 TR cooling capacity, $Q_e = \dot{m}c_p(T_1 - T_4) = 3.5167$ kW

$$\dot{m} = \frac{3.5167}{1.005(270 - 214)} = 0.062486 \text{ kg/s}$$

$$Q_c = \dot{m}c_p(T_2 - T_3) = 0.062486 \times 1.005(401.22 - 318) = 5.226 \text{ kW}$$

$$W_C = \dot{m}c_p(T_2 - T_1) = 0.062486 \times 1.005(401.22 - 270) = 8.24038 \text{ kW}$$

$$W_T = \dot{m}c_p(T_3 - T_4) = 0.062486 \times 1.005(318 - 214) = 6.531 \text{ kW}$$

$$\text{COP} = \frac{Q_e}{W_C - W_T} = \frac{3.5167}{1.70938} = 2.0573$$

$$\dot{v}_1 = \frac{\dot{m}RT_1}{p_1} = \frac{0.062486\,(0.287)\,270}{101.325} = 0.0478 \text{ m}^3/\text{s}$$

$$\dot{v}_4 = \frac{\dot{m}RT_4}{p_4} = \frac{0.062486(0.287)214}{101.325} = 0.03787 \text{ m}^3/\text{s}$$

EXAMPLE 13.3 If in Example 13.2 the isentropic compressor and turbine efficiencies are 0.8 and 0.85 respectively, then determine all the parameters of Example 13.2.

Solution:

For a pressure ratio of 4 and $\gamma = 1.4$ for air, we have

$$z = (p_2/p_1)^{(\gamma-1)/\gamma} = (4)^{0.2857} = 1.486$$

We have from Eq. (13.25),

$$T_{2'} = T_1(\,1 + (z - 1)/\eta_C) = 270(1 + (1.486 - 1)/0.8) = 434.023 \text{ K}$$

Similarly from Eq. (13.26), we have

$$T_{4'} = T_3(1 - \eta_E\,(z - 1)/z) = 318(1 - 0.85(0.486/1.486) = 229.5984 \text{ K}$$

For 1 TR cooling capacity, $Q_e = \dot{m}c_p(T_1 - T_4) = 3.5167$ kW

$$\dot{m} = \frac{3.5167}{1.005(270 - 229.5984)} = 0.08661 \text{ kg/s}$$

$$Q_c = \dot{m}c_p(T_2 - T_3) = 0.08661 \times 1.005(434.023 - 318) = 10.99 \text{ kW}$$

$$W_C = \dot{m}c_p(T_2 - T_1) = 0.08661 \times 1.005(434.023 - 270) = 14.277 \text{ kW}$$

$$W_T = \dot{m}c_p(T_3 - T_4) = 0.08661 \times 1.005(318 - 229.5984) = 7.6948 \text{ kW}$$

$$W_{\text{net}} = W_C - W_T = 6.5822 \text{ kW}$$

$$\text{COP} = \frac{Q_e}{W_C - W_T} = \frac{3.5167}{6.5822} = 0.5343$$

$$\dot{v}_1 = \frac{\dot{m}RT_1}{p_1} = \frac{0.08661(0.287)270}{101.325} = 0.06623 \text{ m}^3/\text{s}$$

$$\dot{v}_4 = \frac{\dot{m}RT_4}{p_4} = \frac{0.08661(0.287)229.5984}{101.325} = 0.056325 \text{ m}^3/\text{s}$$

EXAMPLE 13.4 In a gas cycle refrigeration system working on Joule cycle, the outlet temperature from the cold space is 270 K and the temperature at inlet to turbine is 313 K. Determine the conditions for maximum COP and its value if the working substance is air. The compressor and turbine isentropic efficiencies are 0.8 and 0.85 respectively. Also determine the temperatures at compressor and turbine outlets, mass flow rate, compressor work, turbine work and volume flow rates.

Solution:

We have

$$T_{2'} = T_1 (1 + (z - 1)/\eta_C) = 270(1 + (z - 1)/0.8) = 270(1.25z - 0.25)$$

Similarly,

$$T_{4'} = T_3(1 - \eta_E (z - 1)/z) = 313(0.85 + 0.15z)/z$$

$$\text{COP} = \frac{T_1 - T_4'}{(T_2' - T_1) - (T_3 - T_4')} = \frac{270 - 313(0.85 + 0.15z)/z}{270(1.25z - 0.25) - 270 - 313 + 313(0.85 + 0.15z)/z}$$

Defining $a = 313/270$, this expression reduces to

$$\xi = \text{COP} = \frac{z(1 - 0.15a) - 0.85a}{1.25z^2 - 1.25z - 0.85az + 0.85a}$$

Substitution of $\eta_E = 0.85$ and $\eta_C = 0.8$ in Eq. (13.30) also yields the same equation. The condition for optimum COP is obtained by putting $\frac{d\xi}{dz} = 0$. This results in the following quadratic equation:

$$(1.25 \times 0.15a - 1.25)z^2 + 2.5 \times 0.85az - 0.25 \times 0.85a - 0.85a^2 = 0$$

Substitution of $\eta_E = 0.85$ and $\eta_C = 0.8$ in Eq. (13.31) also yields the same equation.

Substitution of $a = 313/270 = 1.159259$, this equation reduces to

$$1.032639z^2 - 2.4634259z + 1.3886423 = 0$$

or

$$z^2 - 2.3855635z + 1.344751 = 0$$

The roots of this equation are:

$$z_1 = 0.9135375 \quad \text{and} \quad p_2/p_1 = z^{\gamma/(\gamma-1)} = z^{3.5} = 0.723$$

This is not correct, the pressure ratio cannot be less than one. The correct root is as follows:

$$z_2 = 1.472026 \quad \text{and} \quad p_2/p_1 = z^{\gamma/(\gamma-1)} = z^{3.5} = 3.87$$

Substituting it in Eq. (13.30), we get

$$\text{COP} = \frac{\eta_C \{z(1-a) + a\eta_E (z-1)\}}{z(z-1) - a\eta_E \eta_C (z-1)}$$

$$= \frac{0.8(1.159259 \times 0.85 \times 0.472026) - 1.472026 \times 0.159259}{1.472026 \times 0.472026 - 0.85 \times 0.81 \times 1.159259 \times 0.472026} = 0.5718$$

$$T_{2'} = 270(1.25z - 0.25) = 270(1.25 \times 1.472026 - 0.25) = 429.309 \text{ K}$$

Similarly,

$$T_{4'} = 313(0.85 + 0.15z)/z = 313(0.85 + 0.15 \times 1.472026)/1.472026 = 227.687 \text{ K}$$

For 1 TR cooling capacity $Q_e = \dot{m}c_p(T_1 - T_{4'}) = 3.5167$ kW

$$\dot{m} = \frac{3.5167}{1.005(270 - 227.687)} = 0.0826981 \text{ kg/s}$$

$$Q_c = \dot{m}c_p(T_2 - T_3) = 0.0826981 \times 1.005(429.309 - 313) = 9.6666 \text{ kW}$$

$$W_C = \dot{m}c_p(T_2 - T_1) = 0.0826981 \times 1.005(429.309 - 270) = 13.2404 \text{ kW}$$

$$W_{\text{net}} = W_C - W_T = 6.15 \text{ kW}$$

$$\text{COP} = \frac{Q_e}{W_C - W_T} = \frac{3.5167}{6.15} = 0.5718$$

$$\dot{v}_1 = \frac{\dot{m}RT_1}{p_1} = \frac{0.0826981(0.287)270}{101.325} = 0.06324 \text{ m}^3/\text{s}$$

$$\dot{v}_4 = \frac{\dot{m}RT_4}{p_4} = \frac{0.0826981(0.287)270}{101.325} = 0.06324 \text{ m}^3/\text{s}$$

13.6.4 Effect of Pressure Drops on Joule Cycle

In the above analysis it has been assumed that the pressure drops in the cooler and refrigerator are negligible. In actual practice, these components will be heat exchangers and during the passage of air through them there will be some pressure drop. Figure 13.4 show the cycle on *T*–*s* diagram, which includes the effect of isentropic efficiencies and pressure drop Δp_1 in the refrigerator and Δp_2 in the air-cooler. Therefore,

$$p_3 = p_2 - \Delta p_2 \tag{13.34}$$

$$p_4 = p_1 + \Delta p_1 \tag{13.35}$$

From Eq. (13.25), we have

$$T_{2'} = T_1[1 + (z-1)/\eta_C] \quad \text{where } z = (p_2/p_1)^{(\gamma-1)/\gamma}$$

From Eq. (13.26), we have

$$T_{4'} = T_3[1 - \eta_E\{1 - T_4/T_3\}]$$

$$\frac{T_4}{T_3} = \left(\frac{p_4}{p_3}\right)^{(\gamma-1)/\gamma} = \left(\frac{p_1 + \Delta p_1}{p_2 - \Delta p_2}\right)^{(\gamma-1)/\gamma}$$

$$= \left(\frac{p_1}{p_2}\right)^{(\gamma-1)/\gamma} \frac{(1 + \Delta p_1/p_1)^{(\gamma-1)/\gamma}}{(1 - \Delta p_2/p_2)^{(\gamma-1)/\gamma}} = \left(\frac{p_1}{p_2}\right)^{(\gamma-1)/\gamma} (1 + \Delta p_1/p_1)^{(\gamma-1)/\gamma} (1 - \Delta p_2/p_2)^{-(\gamma-1)/\gamma}$$

$$= \left(\frac{p_1}{p_2}\right)^{(\gamma-1)/\gamma} \left(1 + \alpha\frac{\Delta p_1}{p_1} + \alpha\frac{\Delta p_2}{p_2} + \ldots\right) = \frac{1}{z}\left(1 + \alpha\frac{\Delta p_1}{p_1} + \alpha\frac{\Delta p_2}{p_2} + \ldots\right) \tag{13.36}$$

where,

$$\alpha = (\gamma - 1)/\gamma \tag{13.37}$$

Define

$$A = \frac{\Delta p_1}{p_1} + \frac{\Delta p_2}{p_2} \tag{13.38}$$

Substituting Eqs. (13.34) and (13.35), the expression for $T_{4'}$ reduces to

$$T_{4'} = T_3[1 - \eta_E\{1 - T_4/T_3\}] = (T_3/z)\{z - \eta_E(z - 1 - \alpha A)\} \tag{13.39}$$

Therefore the expressions for heat transfers and work requirement reduce to following:

$$Q_e = \dot{m}c_p(T_1 - T_{4'}) = \dot{m}c_pT_1\left[1 - \frac{T_3}{T_1}\frac{1}{z}(z - \eta_E(z - 1 - \alpha A))\right] \tag{13.40}$$

$$= \dot{m}c_pT_1\{1 - a(z - \eta_E(z - 1 - \alpha A))/z\}$$

$$W_T = \dot{m}c_p(T_3 - T_{4'}) = \dot{m}c_pT_3\eta_E\{1 - (1 + \alpha A)/z\}$$

$$= \dot{m}c_pT_3\eta_E(z - 1 - \alpha A)/z \tag{13.41}$$

$$W_C = \dot{m}c_p(T_{2'} - T_1) = \dot{m}c_pT_1(z-1)/\eta_C \tag{13.42}$$

$$\text{COP} = \frac{T_1\{1 - a(z - \eta_E(z - 1 - \alpha A))/z\}}{T_1(z-1)/\eta_C - T_3\eta_E(z - 1 - \alpha A)/z}$$

or

$$\xi = \frac{\eta_C\{z - a(z - a(z - \eta_E(z - 1 - \alpha A))\}}{z(z-1) - a\eta_E\eta_C(z - 1 - \alpha A)} \tag{13.43}$$

The value of z at which COP is optimum is found by differentiating Eq. (13.43) with respect to z and putting it equal to zero. This yields an algebraic equation for z. The COP will be optimum when the value of z is one of the roots of this equation, namely

$$z^2(1 - a + a\eta_E) - 2a\eta_E z + a\eta_E\,(1 + a\eta_C - \eta_C)\,(1 + \alpha A) = 0 \tag{13.44}$$

For the special case when $\eta_E = \eta_C = \eta$, this equation reduces to:

$$\frac{1 - a(1 - \eta)}{a\,\eta}\,z^2 - 2z + (1 + \eta(a - 1))(1 + \alpha A) = 0 \tag{13.45}$$

It is further observed that the refrigeration effect or the COP is zero when the numerator of Eq. (13.43) is equal to zero, that is,

$$z(1 - a) + a\,\eta_E\,(z - 1 - \alpha A) = 0 \quad \text{or} \quad z_{\xi=0} = \frac{a\,\eta_E\,(1 + \alpha A)}{1 - a(1 - \eta_E)} \tag{13.46}$$

EXAMPLE 13.5 In a gas cycle refrigeration system working on Joule cycle, the temperature from the cold space is 270 K and the temperature at inlet to turbine is 313 K. The compressor and turbine isentropic efficiencies are 0.8 and 0.85 respectively. The pressure drop in the air-cooler is 3% of pressure and in the refrigerator it is 5% of the pressure. Determine the conditions for maximum COP and its value if the working substance is air. Also determine the temperatures at compressor and turbine exit, mass flow rate, compressor work, turbine work and volume flow rates for 1 TR cooling capacity.

Solution:

Given: $T_1 = 270$ K, $T_3 = 313$ K, $\eta_E = 0.85$, $\eta_C = 0.8$, $\Delta p_1/p_1 = 0.03$, $\Delta p_2/p_2 = 0.05$, $a = 1.15926$

Referring to Eq. (13.38), $A = \Delta p_1/p_1 + \Delta p_2/p_2 = 0.08$ and $\alpha = (\gamma - 1)/\gamma = 0.2857$ and $1 + \alpha A = 1.022857$. Substituting these values in Eq. (13.44), we get

$$0.8261z^2 - 1.97074z + 1.13631 = 0$$

The roots of this equation are: $z_1 = 0.975433$ and $z_2 = 1.41013$.

The first root is less than one, which is not realistic since the pressure ratio will also be less than one. For the second root, $p_2/p_1 = z_2^{3.5} = 3.3297$.

Substitution in Eq. (13.43) gives COP = 0.4600784

$$T_{2'} = T_1\,[1 + (z - 1)/\eta_C] = 270\,(1 + 0.41013/0.8) = 408.419 \text{ K}$$

$$T_{4'} = (T_3/z)\{z - \eta_E\,(z - 1 - \alpha A)\}$$

$$= (313/1.41013)(1.41013 - 0.85(1.41013 - 1.022857) = 239.933 \text{ K}$$

$$\dot{m} = \frac{3.5167}{1.005(270 - 239.933)} = 0.11638 \text{ kg/s}$$

$$W_T = \dot{m}c_p T_3 \eta_E\,(z - 1 - \alpha A)/z$$

$$= 0.11638(1.005)313(0.85)(1.41013 - 1.022857)/1.41013 = 8.546 \text{ kW}$$

$$W_C = \dot{m}c_p T_1 (z - 1)/\eta_C = 0.11638(1.005)\,260\,(1.41013 - 1)/0.8 = 16.1897 \text{ kW}$$

$$\text{COP} = \frac{Q_e}{W_C - W_E} = \frac{3.5167}{16.1897 - 8.546} = 0.46$$

The turbine and compressor work can be found by using $T_{2'}$ and $T_{4'}$ too.

$$\dot{v}_1 = \frac{\dot{m}RT_1}{p_1} = \frac{0.11638(0.287)270}{101.325} = 0.089 \text{ m}^3/\text{s}$$

$$\dot{v}_4 = \frac{\dot{m}RT_4}{p_4} = \frac{0.11638(0.287)239.933}{101.325} = 0.0791 \text{ m}^3/\text{s}$$

EXAMPLE 13.6 For the data of Example 13.5, find the pressure ratio at which the COP is zero and find the parameters of the example for 1 TR cooling capacity if the pressure ratio is 4.0.

Solution:

From Eq. (13.46) the COP is zero at the following value of z:

$$z_{\xi=0} = \frac{a\eta_E(1+\alpha A)}{1-a(1-\eta_E)} = \frac{1.15926(0.85)1.022857}{1-1.15926(0.15)} = 1.22$$

For $p_2/p_1 = 4 : z = (4)^{0.2857} = 1.486$

$$T_{2'} = T_1[1 + (z-1)/\eta_C] = 270(1 + 0.486/0.8) = 434.023 \text{ K}$$

$$T_{4'} = (T_3/z)\{z - \eta_E(z - 1 - \alpha A)\}$$

$$= (313/1.486)(1.486 - 0.85(1.486 - 1.022857) = 230.0806 \text{ K}$$

$$\dot{m} = \frac{3.5167}{1.005(270 - 230.0806)} = 0.087657 \text{ kg/s}$$

$$W_T = \dot{m}c_p T_3 \eta_E (z - 1 - \alpha A)/z$$

$$= 0.087657(1.005)313(0.85)(1.486 - 1.022857)/1.486 = 7.3048 \text{ kW}$$

$$W_C = \dot{m}c_p T_1 (z-1)/\eta_C = 0.087657(1.005)270(1.486 - 1)/0.8 = 14.45 \text{ kW}$$

$$\text{COP} = \frac{Q_e}{W_C - W_E} = \frac{3.5167}{14.45 - 7.3048} = 0.4922$$

$$\dot{v}_1 = \frac{\dot{m}RT_1}{p_1} = \frac{0.087567(0.287)270}{101.325} = 0.067 \text{ m}^3/\text{s}$$

$$\dot{v}_4 = \frac{\dot{m}RT_4}{p_4} = \frac{0.087657(0.287)230.0806}{101.325} = 0.05712 \text{ m}^3/\text{s}$$

13.6.5 Regenerative Joule Cycle

It was observed that the COP of the cycle decreases and becomes zero at a certain pressure ratio due to inefficiency of the expander. This can be prevented to some extent if colder air enters the turbine. This colder air is obtained by regenerative cooling of warm air at air-cooler outlet 3 by the cold air from the refrigerator outlet at 1. The schematic diagram of the system is shown in Figure 13.5(a) and the *T*–*s* diagram of the cycle is shown in Figure 13.5(b).

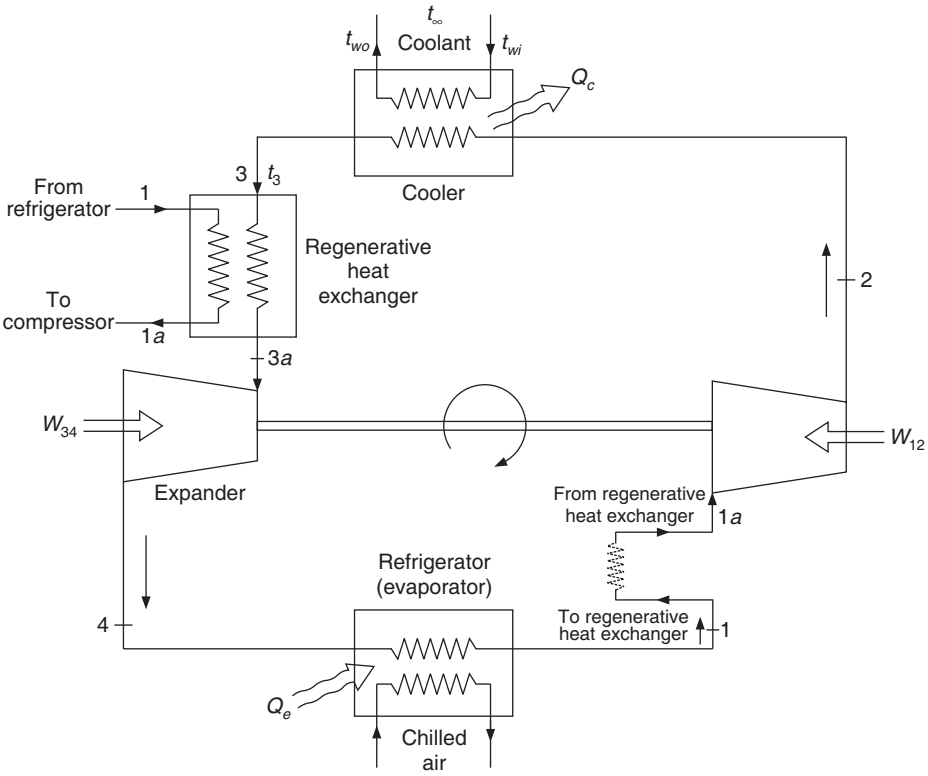

Figure 13.5(a) Schematic diagram of the regenerative Joule cycle.

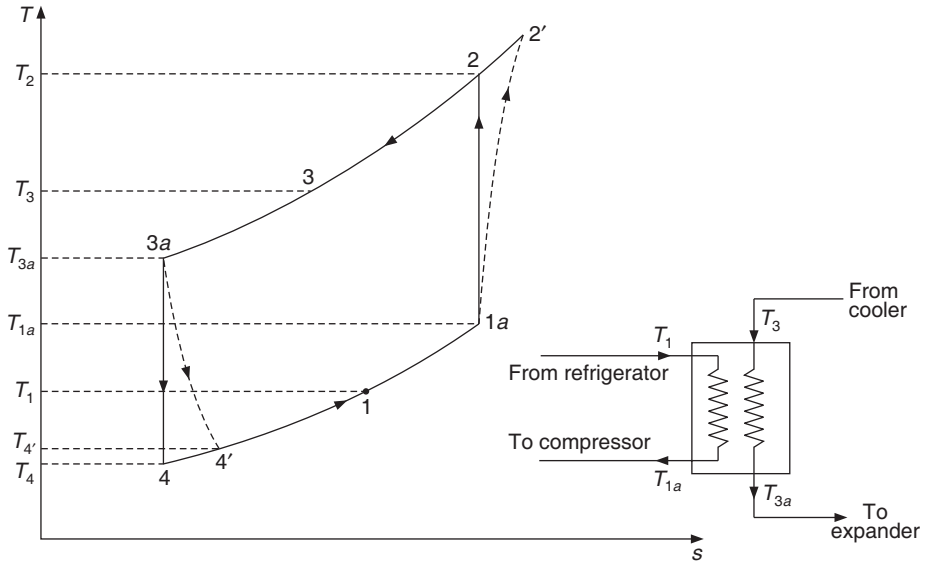

Figure 13.5(b) *T–s* diagram for the regenerative Joule cycle.

Energy balance across the heat exchanger gives

$$T_{1a} - T_1 = T_3 - T_{3a} \tag{13.47}$$

The temperature $T_1$is fixed by the temperature required in the refrigerator and the temperature of the available cold water for cooling fixes the temperature T_3. The temperatures T_{1a} and T_{3a} depend upon the effectiveness of the heat exchanger. In the ideal case when the heat exchanger has very large area, the heat exchanger effectiveness will be 100% giving

$$T_{3a} = T_1 \quad \text{and} \quad T_{1a} = T_3$$

The maximum cooling capacity available is $\dot{m}c_p(T_3 - T_1)$. In actual practice, the cooling obtained is $\dot{m}c_p(T_{1a} - T_1) = \dot{m}c_p(T_3 - T_{3a})$; hence an heat exchanger effectiveness is defined as follow:

$$\varepsilon = \frac{T_{1a} - T_1}{T_3 - T_1} = \frac{T_3 - T_{3a}}{T_3 - T_1} \tag{13.48}$$

The following ratios are introduced to study the COP of the regenerative cycle.

$$\delta = T_{1a}/T_1 = 1 + \varepsilon\,(a - 1) \tag{13.49}$$

$$\beta = T_{3a}/T_3 = 1 - \varepsilon\,(a - 1) \tag{13.50}$$

For an ideal heat exchanger,

$$\varepsilon = 1.0,\ \delta = a \ \text{ and } \ \beta = 1.0 \tag{13.51}$$

where a and z are same as defined earlier, that is,

$$a = \frac{T_3}{T_1} \quad \text{and} \quad z = \frac{T_2}{T_{1a}} = \frac{T_{3a}}{T_4} = \left(\frac{p_2}{p_1}\right)^{(\gamma-1)/\gamma} \tag{13.52}$$

The expressions for evaporator heat transfer, compressor work, turbine work and COP are as follows:

$$T_1 - T_{4'} = (T_{3a} - T_{4'}) - (T_{3a} - T_1) = \eta_E T_{3a}\,(1 - 1/z) - T_1(\beta - 1) \tag{13.53}$$

$$= \eta_E \beta T_1 (1 - 1/z) - T_1(\beta - 1)$$

$$Q_e = \dot{m}c_p(T_1 - T_{4'}) = \dot{m}c_p\eta_E\beta T_1\,(1 - 1/z) - T_1(\beta - 1) \tag{13.54}$$

$$W_C = \dot{m}c_p(T_{2'} - T_{1a}) = \dot{m}c_p(T_2 - T_{1a})/\eta_C$$

$$= \dot{m}c_p T_{1a}\,(z - 1)/\eta_C = \dot{m}c_p\delta T_1(z - 1)/\eta_C \tag{13.55}$$

$$W_T = \dot{m}c_p(T_{3a} - T_{4'}) = \dot{m}c_p\eta_B\beta T_1\,(1 - 1/z) \tag{13.56}$$

$$\text{COP} = \xi = \frac{\eta_E\beta(1 - 1/z) - (\beta - 1)}{\delta(z - 1)/\eta_C - \eta_E\beta(1 - 1/z)} = \frac{\eta_E\beta(z - 1) - (\beta - 1)z}{\delta z(z - 1)/\eta_C - \eta_E\beta(z - 1)} \tag{13.57}$$

The value of z at which COP is maximum is found by differentiating Eq. (13.57) with respect to z and putting it equal to zero. This yields an algebraic equation for z. The COP will be maximum when the value of z is one of the roots of this equation, namely

$$z^2\,\delta\,(1-\beta+\beta\,\eta_E)-2\,z\,\delta\,\beta\,\eta_E+\eta_C\,\eta_E\,\beta\,(\beta-1)+\eta_E\,\beta\,\delta=0 \tag{13.58}$$

For the special case when $\eta_E=\eta_C=\eta$, this equation reduces to:

$$\frac{\delta(1+\eta\beta-\beta)}{\eta}\,z^2-2\,z\,\delta\beta+\eta\beta\left(\beta+\frac{\delta}{\eta}-1\right)=0 \tag{13.59}$$

It is further observed that the refrigeration effect or the COP is zero when the numerator of Eq. (13.57) is equal to zero, that is,

$$(\eta_E\beta-\beta)\,z+z=\eta_E\beta \quad \text{or} \quad z_{\xi=0}=\frac{\eta_E\,\beta}{1-\beta+\eta_E\beta} \tag{13.60}$$

In case the regeneration is zero the coefficient δ reduces to 1 and β reduces to a. It can be shown that in this limit, Eq. (13.60) reduces to Eq. (13.33) and Eq. (13.58) reduces to Eq. (13.31).

EXAMPLE 13.7 Given that $T_1 = 270$ K and $T_3 = 313$ K and the working substance is air, find the pressure ratios corresponding to zero and maximum COP if the compressor and turbine efficiencies are same and equal to 0.9. For the first case consider heat exchanger with 100% effectiveness and for the second case the approach temperature between the fluids is 3 K. Compare the results with the ideal Joule cycle. Tabulate the variation of COP against z.

Solution:

Case 1: The results of ideal Joule cycle have been given in Example 13.1.

Case 2: Heat exchanger effectiveness is 100%. This gives the following values:

$$\delta = a,\ \beta = 1$$

Given: $\eta_C = \eta_E = 0.9$

Equation (13.58) for maximum COP reduces to

$$0.9az^2 - 1.8az + 0.9a = 0$$

Maximum COP occurs at z =1 and its value is

$$\xi_{\max}=\frac{0.9(z-1)}{az(z-1)/0.9-0.9(z-1)}=\frac{0.81}{az-0.81}=\frac{0.81}{1.15926-0.81}=2.3192$$

For this case, the temperature difference across the refrigerator $T_1 - T_{4'}$ is given by

$$T_1 - T_{4'} = 0.9T_1[1 - (1/z)]$$

The values of COP and the temperature difference for various values of z are given in Table 13.3.

Case 3: We assume that the heat exchanger is such that a temperature difference of 3 K occurs at both the ends, that is,

$$T_3 - T_{1a} = T_{3a} - T_1 = 3 \text{ K}$$

For the given values of $T_1 = 270$ K and $T_3 = 313$ K, we get

$$1 - \varepsilon = 3/(T_3 - T_1) = 3/(313 - 270) \quad \therefore \quad \varepsilon = 0.93023$$

$$\delta = 1 + \varepsilon\,(a - 1) = 1.148148$$

$$\beta = 1 - \varepsilon\,(a - 1) = 1.01111$$

COP is zero at $(\eta_E\beta - \beta)z + z = \eta\beta$ that is at $z = 1.012$.

Equation (13.58) for maximum COP reduces to

$$1.03206z^2 - 2.08963z + 1.0539 = 0$$

The roots of this equation are : $z_1 = 1.07316$ and $z_2 = 0.95156$

Obviously the root z_2 which is less than one, does not involve any compression and hence will not yield refrigeration.

Maximum COP is 6.273 at $z_1 = 1.07316$

The values of COP and temperature of cooling are given in Table 13.3.

Table 13.3 Variation of COP of regenerative cycle at isentropic efficiency of 0.9 and effectiveness of 1.0 and 0.093 for $T_1 = 270$ and $T_3 = 313$ K

z	Case 1: $\eta = 1.0$, $\varepsilon = 1.0$		Case 2, $\eta = 0.9$, $\varepsilon = 1.0$		Case 3: $\eta = 0.9$, $\varepsilon = 0.93023$	
	ξ	$T_1 - T_{4'}$	ξ	$T_1 - T_{4'}$	ξ	$T_1 - T_{4'}$
1.1			1.741	22.1	1.597	19.336
1.2	5.0	9.17	1.394	40.5	1.358	37.95
1.3	3.333	29.23	1.162	56.076	1.1515	53.7
1.4	2.5	46.22	0.9963	69.43	0.9944	67.2
1.5	2.0	61.33	0.872	81.0	0.8735	78.9

It was observed from the results of Table 13.3 that the minimum pressure ratio was such that z is greater than a for the Joule cycle to produce cooling. But regenerative cycle can produce cooling at pressure ratios less than $z = a$ as well. In fact the pressure ratio can be as small as possible if the heat exchanger is effective. A lower pressure ratio is desirable since it tends to give a larger COP.

It is observed from Eq. (13.53) that as the pressure ratio is reduced the temperature difference $T_1 - T_{4'}$ and therefore the specific refrigeration effect decreases. This means that for a given cooling capacity a larger mass flow rate of air will be required. It is obvious that the cycle with regeneration gives a better COP for the same temperature difference $T_1 - T_{4'}$.

The cycles discussed so far may be either open or closed at the low temperature end. The cycles open at the low temperature end have atmospheric pressure at that end since the cold air is thrown into the space for cooling. Likewise, the air drawn into compressor of such a cycle is the ambient air at room temperature. If the cycle is closed at this end then a high pressure may be maintained at this end. It can be seen from the examples where the volume flow rate was calculated that for a pressure of four atmospheres, the volume flow rate would be one-fourth of the open cycle. Such a cycle is known as *dense air cycle*.

Also, with the heat exchanger, the temperature of gas at inlet to the compressor is usually raised to near ambient temperature, which makes the compression process also similar to ordinary air compression process in which heat is rejected to the surroundings during compression. For this purpose, the compression can be thought of as reversible isothermal compression with appropriate value of isothermal compression efficiency. The expression for reversible isothermal specific work requirement in such a case is

$$w_{iso} = RT \ln (p_2/p_1) \tag{13.61}$$

If w is the actual work requirement, then the isothermal compression efficiency is defined as follows:

$$\eta_{iso} = w/w_{iso} \tag{13.62}$$

13.6.6 Cycle with Sub-atmospheric Pressure

If the refrigeration cycle is to be made open at the warm end, then the pressure at the cold end will be below atmospheric (i.e. the pressure at point 4 in Figure 13.5(b) will be below the atmospheric pressure). This requires more maintenance since the system has to be made leak-tight. Such a cycle is shown in Figure 13.6. The ambient air enters the heat exchanger (i.e. cooler of Figure 13.2(a)) and is cooled by cold air from the refrigerator. Then it passes through the turbine (expander) where its temperature and pressure are reduced. Subsequently, it enters the heat exchanger (refrigerator) and then compressed to atmospheric pressure and discharged to the atmosphere. The cycle diagram of this cycle is same as that for regenerative cycle as shown in Figure 13.5(b).

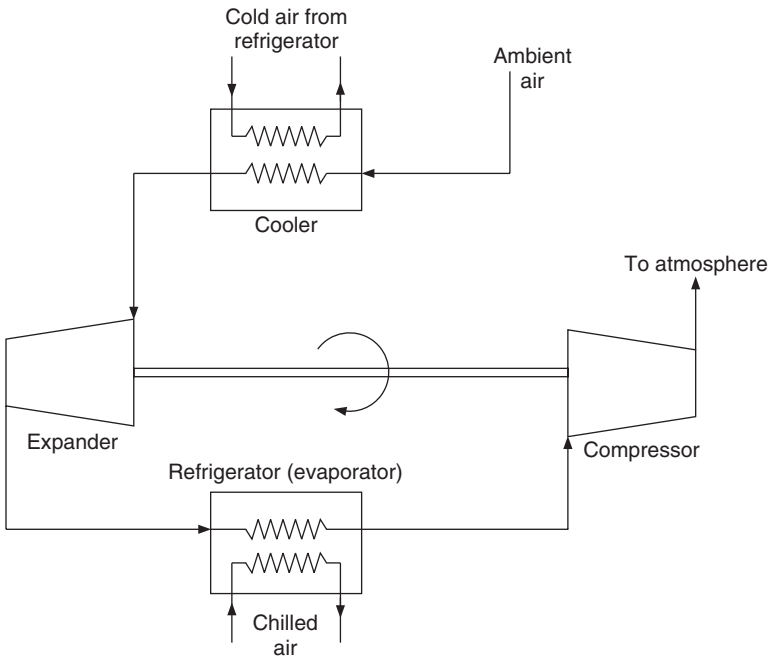

Figure 13.6 Bell–Coleman refrigeration cycle open at the warm end.

Martinovsky and Dubinsky in Odessa developed a cycle, which is open at both the ends. It is essentially a sub-atmospheric cycle. It is shown in Figure 13.7. The expanded low-pressure air from the turbine at state 6 cools another stream of atmospheric air from state 3 to state 4. It enters the cold chamber where it absorbs heat and then it enters the turbine at state 5, which is at atmospheric pressure but at a temperature lower than the ambient. The expanded low-pressure air passes from the heat exchanger to the compressor and is then exhausted to the surroundings at state 2. The compressed air does not have to be cooled in these systems. These systems may be operated at low pressure ratios; hence it is possible to use axial flow compressors and turbines which have isentropic efficiencies around 0.9.

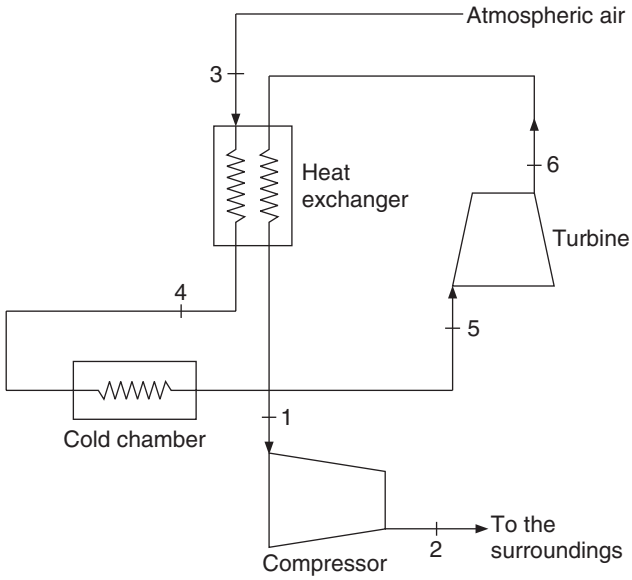

Figure 13.7 Air refrigeration cycle open at both ends.

The COP of all these cycles is strongly dependent upon the effectiveness of the heat exchanger. If a regenerator is used as in Figure 13.5(a), then a high effectiveness can be obtained.

EXAMPLE 13.8 In the sub-atmospheric refrigeration cycle of Figure 13.7, the pressure ratio is 2.0. The ambient temperature T_3 and the temperature at the exit of refrigerator T_5 are 313 K and 270 K respectively. The temperature difference at both the ends of heat exchanger between the warm and cold fluids is 3 K. For 1 TR refrigeration capacity, determine the mass flow rate, compressor work, turbine work and COP if (i) the turbine and compressor efficiencies are 0.85 and 0.8 respectively and (ii) if both the efficiencies are 0.9.

Solution:

Given: $T_3 = 313$ K and $T_5 = 270$ K, $p_2/p_1 = 2.0$, $T_1 = T_3 - 3 = 310$ and $T_4 = T_{6'} + 3$

$z = (p_2/p_1)^{(\gamma-1)/\gamma} = (2)^{0.2857} = 1.219$

Case (i): $\eta_E = 0.85$ and $\eta_C = 0.8$

$T_6 = T_5/z = 221.49$ K and $T_{6'} = T_5 - 0.85(T_5 - T_6) = 228.767$ K

$T_2 = T_1 z = (310)1.219 = 377.894$ K and $T_{2'} = T_1 + (T_2 - T_1)/0.8 = 394.8678$ K

$T_4 = T_{6'} + 3 = 231.767$ K

For 1 TR cooling capacity:

$$\dot{m} = \frac{3.5167}{1.005(T_5 - T_4)} = \frac{3.5167}{1.005(270 - 231.767)} = 0.0915 \text{ kg/s}$$

$$W_E = \dot{m} c_p (T_5 - T_{6'}) = 0.0915(270 - 228.767) = 3.7926 \text{ kW}$$

$$W_C = \dot{m} c_p (T_{2'} - T_1) = 0.0915(394.8674 - 310) = 7.804 \text{ kW}$$

$$\text{COP} = 3.5167/(7.804 - 3.7926) = 0.8766$$

Case (ii): $\eta_E = \eta_C = 0.9$

$T_{6'} = T_5 - 0.9(T_5 - T_6) = 226.3415$ K

$T_{2'} = T_1 + (T_2 - T_1)/0.9 = 385.438$ K

$T_4 = T_{6'} + 3 = 229.3415$ K

$$\dot{m} = \frac{3.5167}{1.005(T_5 - T_4)} = \frac{3.5167}{1.005(270 - 229.3415)} = 0.08606 \text{ kg/s}$$

$$W_E = \dot{m} c_p (T_5 - T_{6'}) = 0.08606(270 - 226.3415) = 3.7762 \text{ kW}$$

$$W_C = \dot{m} c_p (T_{2'} - T_1) = 0.08606(385.438 - 310) = 6.52466 \text{ kW}$$

$$\text{COP} = 3.5167/(6.52466 - 3.7762) = 1.2795$$

The COP improves considerably as the isentropic efficiencies increase to 90%.

13.7 AIRCRAFT REFRIGERATION CYCLES

Gas cycle refrigeration is used for air conditioning of commercial and military aircraft. The low speed aircraft, which usually flies at moderate altitudes, does not require artificial cooling since the outside air temperature is low at these altitudes. As a result, heat can be rejected from the cabin to the surroundings. As per accepted international norm, the air temperature and pressure vary with altitude as follows:

$$T = (T_0 - Bz) \text{ K} \tag{13.63}$$

and

$$p = p_0 (1 - Bz/T_0)^{Bz/R} \tag{13.64}$$

where $B = 0.0065$ K/m and $Bz/R = 5.26$; z is altitude in metres, $T_0 = 15^{\circ}$C and p_0 is the standard atmospheric pressure at sea level.

At an altitude of 10 km the temperature is approximately –50°C and the pressure is 0.265 bar. One may question the requirement of air conditioning at such a low ambient temperature. The pressure inside the blood vessels and other organs is one atmospheric pressure, hence human beings cannot survive at such low pressures. Human beings start to bleed through nose, ears and eyes in response to low outside pressure. The oxygen level also becomes low at low pressure, hence one has to breathe a large quantity of air to absorb the requisite amount of oxygen required

for metabolism. Also breathing in low-pressure air and absorption in the lungs by blood vessels at higher pressure causes breathing problems. As a result, the air has to be pressurized inside the cabin for comfortable conditions. The compression of air increases its temperature and one loses the advantage of low temperature.

The aircraft has a streamlined body, which should experience minimum drag. On the surface of the aircraft, the high-speed air comes to rest; as a result the surface temperature of high-speed aircraft is close to the stagnation temperature, which is quite high. The temperature rise may be of the order of 40°C. Hence heat cannot be rejected to the surroundings. For speeds near Mach one, the temperature may become intolerable. To summarize, the aircraft requires air conditioning because of the reasons enumerated at (i) to (v) of the following section.

13.7.1 Cooling Loads for Aircraft Air Conditioning

(i) The outer surface of the aircraft gets heated up due to frictional heating and this heat is transferred to the cabin.

(ii) The number of persons in the aircraft per m^2 is very large. The persons who are not used to air travel dissipate more metabolic heat due to nervousness giving rise to large occupancy load.

(iii) Lights, appliances and aircraft systems, etc. dissipate energy inside the cabin.

(iv) Incident solar radiation also heats up the cabin.

(v) Refrigeration is required for the preservation of food, beverages and medicines.

Cooling demands per unit volume of space are very high since in commercial aircraft the density of occupants is high. Transport aircraft require cooling capacity of 8 TR or more. Jet fighters flying at very high speeds need 10 to 20 TR. Missiles and other high flight systems typically require 3 TR.

Low weight and compactness are the criterion for choosing systems in aircraft. The jet aircraft has a compressor for pressurizing the air before combustion. Some of this compressed air may be used for air conditioning. Hence if the gas cycle is used for aircraft refrigeration, it will save the weight of compressor. Further, if the open cycle is used, that is, the cooled air is directly thrown into the cabin it will save the weight of heat exchanger called evaporator. The absence of these two components gives a major saving in weight making the air conditioning system compact and lightweight. The simplicity and reliability of the system makes the gas cycle very attractive for cooling the cabins of high-speed aircraft. To summarize, the advantages of the gas cycle for aircraft air conditioning are enumerated at (i) to (v) of the following section.

13.7.2 Advantages of Gas Cycle Refrigeration for Aircraft Cooling

(i) Air as a non-flammable, non-toxic refrigerant is available free of cost throughout the flight. One does not have to worry about minor leakages, thus giving the system more reliability.

(ii) Most of the jet aircraft have a compressor, hence it saves the cost and weight of one component if air is used as refrigerant. Power is provided by the turbine of jet aircraft, hence no separate prime mover is required. Any other refrigerant would require an additional compressor.

(iii) Chilled air is directly used for cooling, saving the cost and weight of the heat exchanger. Further the thermal resistance across the heat exchanger walls is also eliminated, giving it a better efficiency by direct contact heat transfer.

(iv) The pressure difference across the duct and the cabin is very small, and the pressure also is low making the ducts and pipelines of very simple design.

(v) The centrifugal compressors and turbines operate at very high rpm (around 60,000 rpm), making the equipment very compact. The motors have a very high frequency about 300 Hz compared to 50 Hz conventionally used on ground systems. This high frequency makes the motors very compact as well.

13.7.3 Classification of Aircraft Air Conditioning Systems

There are basically four types of systems that are used in aircraft air conditioning. These are as follows:

(i) Simple or the basic aircraft air conditioning system with or without evaporative cooling.

(ii) Bootstrap aircraft air conditioning system with or without evaporative cooling.

(iii) Regenerative aircraft air conditioning system.

(iv) Reduced ambient aircraft air conditioning system.

13.7.4 Simple or the Basic Aircraft Air Conditioning System with or without Evaporative Cooling

Figure 13.8(a) shows the schematic diagram and Figure 13.8(b) shows the *T*–*s* cycle diagram of this system. The aircraft moves with velocity V_1, air enters the compressor inlet with relative velocity, which is same as V_1 if the wind velocity is zero.

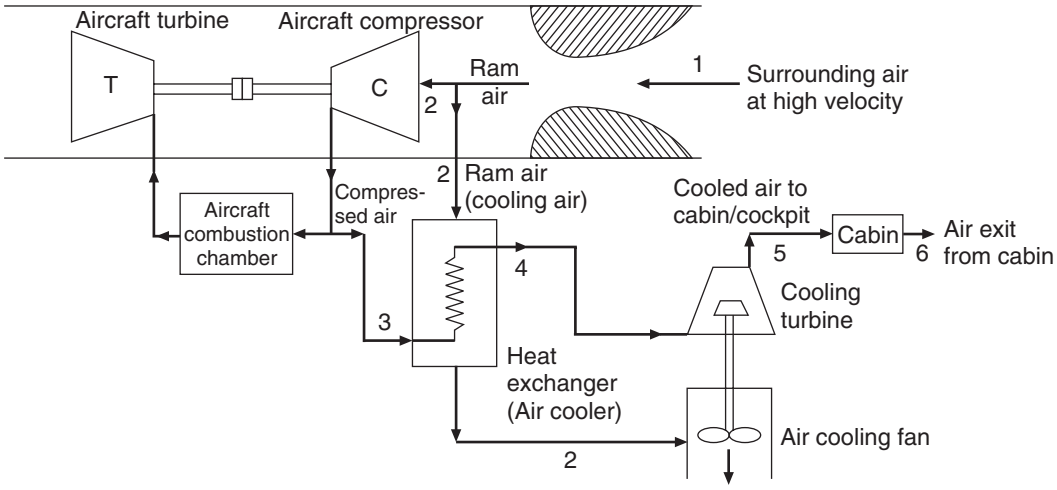

Figure 13.8(a) Schematic of simple aircraft refrigeration system without evaporative cooling.

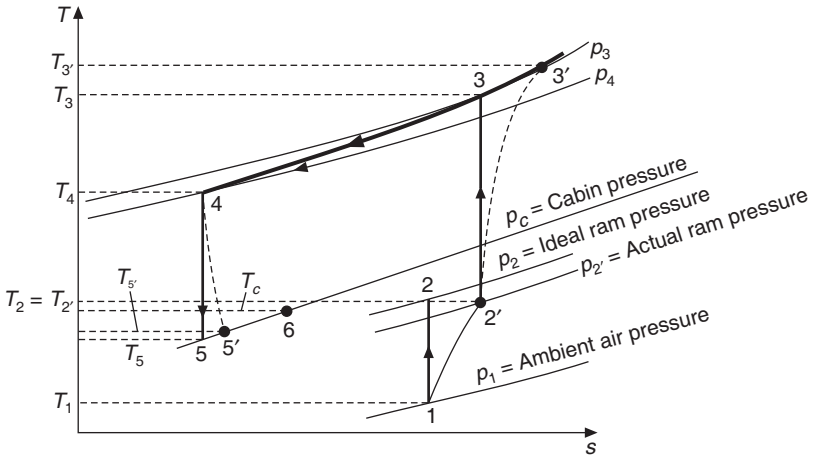

Figure 13.8(b) *T–s* diagram for the simple aircraft refrigeration system.

Ramming process

This air stream on the surface of the aircraft comes to rest and its kinetic energy is converted into internal energy or enthalpy. The final state 2 is obtained by energy conservation assuming adiabatic flow, that is,

$$h_2 = h_{01} = h_1 + \frac{V_1^2}{2} \tag{13.65}$$

where, h_{01} is called the stagnation enthalpy. Assuming perfect gas with constant specific heat, we can write Eq. (13.65) as follows:

$$T_2 = T_{01} = T_1 + \frac{V_1^2}{2c_p} = T_1 + \frac{(\gamma - 1)}{\gamma R}\frac{V_1^2}{2}$$

$$= T_1\left[1 + \frac{(\gamma - 1)}{\gamma RT_1}\frac{V_1^2}{2}\right] = T_1 + (\gamma - 1)M^2/2 \tag{13.66}$$

where, T_{01} is called stagnation temperature corresponding to inlet state 1 and M is called flight Mach number. The flight Mach number is defined as follows:

Mach number, M = speed of aircraft / ambient speed of sound = V/C

The speed of sound C at temperature T_1 is given by $(\gamma RT_1)^{0.5}$.

The pressure of the air also increases in this process due to the kinetic energy being converted into pressure rise. This process of pressure increase is called *Ram Effect*.

For reversible adiabatic (isentropic) process, we can write

$$p_2 = p_{01} = p_1\left(\frac{T_2}{T_1}\right)^{\gamma/(\gamma-1)} = p_1[1 + (\gamma - 1)M_1^2/2]^{\gamma/(\gamma-1)} \tag{13.67}$$

The process may be assumed to be adiabatic, that is, Eq. (13.66) may be assumed to be valid. However the process will not be reversible, hence all the kinetic energy is not converted into

pressure during the ramming process. This deviation from the ideal ramming process is defined as *Ram Efficiency,* η_R, and is defined as follows:

$$\eta_R = \frac{p_{2'} - p_1}{p_{01} - p_1} = \frac{p_{2'} - p_1}{p_2 - p_1} \tag{13.68}$$

The ram efficiency may be of the order of 75 to 80%.

Hence the calculation procedure is to find temperature T_2 from Eq. (13.66) and find the isentropic ram pressure p_2 from Eq. (13.67) and finally the actual pressure $p_{2'}$ from Eq. (13.68), that is,

$$p_{2'} = p_1 + \eta_R (p_2 - p_1) \tag{13.69}$$

A part of the rammed air may be used in the heat exchanger for cooling the air after compression. The major portion of the rammed air goes to the compressor.

Compression

The ram air at state 2′ is compressed to state 3′ with an isentropic efficiency of η_C. State 3 in Figure 13.8(b) will occur if the compression is isentropic. The temperature at state 3 is given in terms of pressure ratio as follows:

$$T_3 = T_{2'} \left(\frac{p_3}{p_{2'}} \right)^{(\gamma-1)/\gamma}$$

The isentropic compressor efficiency is as follows in analogy with Eq. (13.24):

$$\eta_C = \frac{T_3 - T_{2'}}{T_{3'} - T_{2'}} \tag{13.70}$$

Therefore, temperature $T_{3'}$ is given by

$$T_{3'} = T_{2'} + (T_3 - T_{2'}) / \eta_C = T_{2'} [1 + \{ (p_3 / p_{2'})^{(\gamma-1)/\gamma} - 1 \} / \eta_C] \tag{13.71}$$

The compressor work is given by

$$W_C = \dot{m} c_p (T_{3'} - T_{2'}) = \dot{m} c_p T_{2'} [(p_3 / p_{2'})^{(\gamma-1)/\gamma} - 1] / \eta_C = \dot{m} c_p T_{2'} (z - 1) / \eta_C \tag{13.72}$$

where, $$z = (p_3 / p_{2'})^{(\gamma-1)/\gamma} \quad \text{and} \quad T_{2'} = T_2 \tag{13.73}$$

Turbojet

The compressed air is taken to the combustion chamber where fuel is burned and the temperature and enthalpy of air is increased considerably. The air is passed through a turbine, which provides power for the aircraft systems. Thereafter it is expanded through a nozzle and exhausted with a high velocity providing the thrust required for the propulsion of the aircraft.

A part of the compressed air at state $T_{3'}$ is bled for the aircraft air conditioning system as shown in Figure 13.8(a).

Air cooler

The outside air is used for cooling purpose. The effective temperature of the outside air is stagnation temperature since it comes to rest in the boundary layer over the heat transfer surface. In the system of Figure 13.8(a) the ram air is used for cooling purpose. The temperature of the ram air is T_2 and it may not be possible in a finite heat exchanger to cool the compressed air from $T_{3'}$ down to temperature T_2. Instead, it is cooled to a temperature of T_4. Hence, the effectiveness of the heat exchanger ε is defined as

$$\varepsilon = \frac{T_{3'} - T_4}{T_{3'} - T_2} \tag{13.74}$$

The heat exchanger effectiveness depends upon the heat transfer area provided. A very large area will give good efficiency but the pressure drop will also increase requiring a big blower. The pressure drop in the heat exchanger is neglected in the cycle diagram shown in Figure 13.8(b) and cooling 3′–4 is assumed to occur at constant pressure.

Turbine

The cooled air at state 4 expands to state 5′ at cabin pressure p_c through the cooling turbine with efficiency η_E. State 5 in Figure 13.8(b) will occur if the expansion is isentropic. The temperature after isentropic expansion at state 5 is given as follows:

$$T_5 = T_4 \left(\frac{p_c}{p_4} \right)^{(\gamma-1)/\gamma} \tag{13.75}$$

The isentropic turbine efficiency η_E is defined in analogy with Eq. (13.24).

$$\eta_E = \frac{T_4 - T_{5'}}{T_4 - T_5} \tag{13.76}$$

The temperature $T_{5'}$ is given by

$$T_{5'} = T_4 [1 - \eta_E \{1 - (p_c / p_4)^{(\gamma-1)/\gamma}\}] \tag{13.77}$$

The cooling turbine work output and the refrigeration capacity are given by

$$W_T = \dot{m} c_p (T_4 - T_{5'}) = \dot{m} c_p \eta_E (T_4 - T_5) = \dot{m} c_p \eta_E T_4 \{1 - (p_c / p_4)^{(\gamma-1)/\gamma}\} \tag{13.78}$$

$$Q_E = \dot{m} c_p (T_c - T_{5'}) \text{ kW} = \dot{m} c_p [T_c - T_4 \{1 - \eta_E \{1 - (p_c / p_4)^{(\gamma-1)/\gamma}\}\}] / 3.5167 \text{ TR} \tag{13.79}$$

The low temperature air at $T_{5'}$ enters the cabin where it provides air conditioning and gets heated up to cabin temperature T_c of 25°C to 27°C. The cabin pressure is slightly more than the atmospheric pressure.

The refrigeration capacity, the compressor work and the turbine work are given by Eqs. (13.79), (13.72) and (13.78), respectively.

The work required for pressurization of air from pressure $p_{2'}$ to cabin pressure p_c is as follows:

$$W_P = \dot{m} c_p T_2 [(p_c / p_{2'})^{(\gamma-1)/\gamma} - 1] / \eta_C \tag{13.80}$$

The additional work required for refrigeration, W_R, is the difference between the compressor work from pressure $p_{2'}$ to p_3 and the work required for pressurization of air from ram pressure $p_{2'}$ to cabin pressure p_c.

$$\therefore \quad W_R = W_C - W_P \tag{13.81}$$

and $$\text{COP} = Q_E / W_R \tag{13.82}$$

$$\therefore \quad \text{COP} = \frac{T_c - T_4 [1 - \eta_E \{1 - (p_c / p_4)^{(\gamma-1)/\gamma}\}]}{\{T_2 [(p_3 / p_{2'})^{(\gamma-1)/\gamma} - 1] / \eta_C\} - \{T_2 [(p_c / p_{2'})^{(\gamma-1)/\gamma} - 1] / \eta_C\}} \tag{13.83}$$

The work output of the cooling turbine is used up in driving a fan for sucking air into the heat exchanger and is not available for refrigeration purpose in the *simple air conditioning system*. Similarly the ram work is dissipated in the exhaust in the *simple air conditioning system*. However, some textbooks define net work as

$$W_{\text{net}} = W_C + W_{\text{ram}} - W_T \tag{13.84}$$

This is not true for the *simple air conditioning system*.

On the other hand, some textbooks define COP as the ratio of refrigeration capacity and the compressor work, that is,

$$\text{COP}_m = \frac{Q_E}{W_C} = \frac{T_c - T_4 [1 - \eta_E \{1 - (p_c / p_4)^{(\gamma-1)/\gamma}\}]}{T_2 [(p_3 / p_{2'})^{(\gamma-1)/\gamma} - 1] / \eta_C} \tag{13.85}$$

Evaporative cooling

If the temperature at the cooling turbine exit is not sufficiently low, then some additional means are required to cool the air at inlet to turbine since a lower temperature at turbine inlet will lead to a lower temperature at its outlet. Regenerative cooling is one method and cooling the air with the help of external means in an evaporative cooler is another method. In case of evaporative cooling, the air from the exit of air cooler at point 4 is passed to another heat exchanger where it is cooled from temperature T_4 to temperature T_{4a} by evaporation of some low-boiling point liquid. The liquid used for this purpose may be refrigerant, liquid nitrogen or ether. The air enters the cooling turbine at a lower temperature T_{4a} and leaves the turbine at a still lower temperature $T_{5a'}$. The schematic diagram is shown in Figure 13.9(a) and the cycle is shown in Figure 13.9(b). If $\dot{m}_e$ is the mass flow rate of liquid and Δh_e is the change in enthalpy of the evaporating liquid, then energy balance for the evaporative heat exchanger gives:

$$\dot{m}_e \, \Delta h_e = \dot{m} c_p (T_4 - T_{4a}) \tag{13.86}$$

The temperature after expansion in the cooling turbine is given by the following equation:

$$T_{5a'} = T_{4a} [1 - \eta_E \{1 - (p_c / p_4)^{(\gamma-1)/\gamma}\}] \tag{13.87}$$

The refrigeration effect will increase in this case since $T_{5a'} < T_{5'}$. The COP should include the effort required to achieve additional cooling from T_4 to T_{4a}.

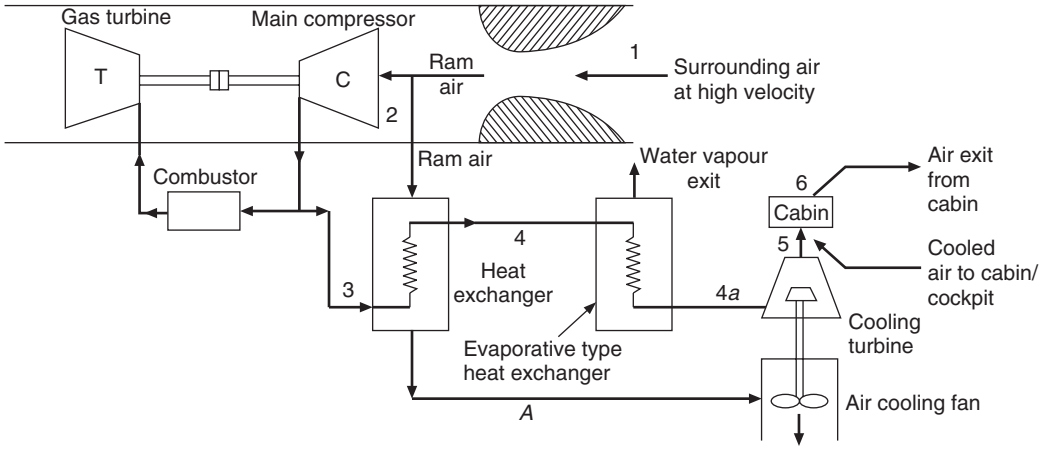

Figure 13.9(a) Schematic of simple aircraft refrigeration system with evaporative cooling.

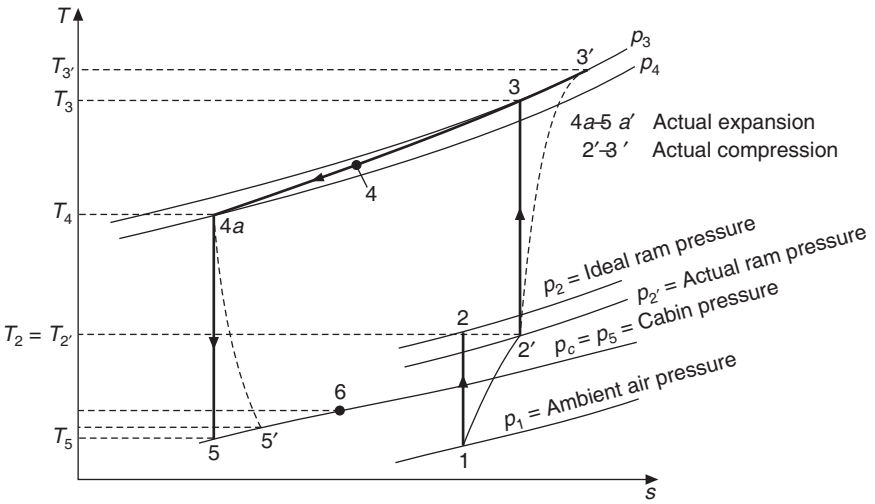

Figure 13.9(b) *T–s* diagram for the simple air evaporative cooling system of aircraft.

Blower or fan

The power output of the cooling turbine is used to run a blower, which aspirates ram air through the heat exchanger. The frictional resistance offered by the ram air is actually a drag force on the aircraft, which has to be overcome by the thrust. The blower helps in reducing this drag. The blades of the blower offer frictional resistance, which heats up the air. The blower is placed on the discharge side of the heat exchanger so that its blades do not increase the air temperature before its entry into the heat exchanger. The blower gives sufficient air-velocity in the heat exchanger to give a reasonable value of heat transfer coefficient so as to reduce the size of heat exchanger.

Ground cooling

If the system has a blower, it does not have to wait for the aircraft to move so that ram air can flow over the heat exchange surface and cool the air after compression so that air conditioning can be produced. The blower-based system can provide air conditioning when the aircraft is on the ground. Some aircraft do not have this facility. These aircraft have to be then cooled by a plug-on-type air conditioner when on ground.

Ice and moisture separator

The temperature at the turbine exit is below zero Celsius. The moisture will condense if the temperature is less than the dew point temperature and it will freeze at temperature less than 0^{o}C. The ice formation will increase the back pressure of the turbine and the volume flow rate. This will further decrease the temperature drop in the turbine since some energy is taken by the condensation and freezing process. An ice separator is used after the turbine. The ice and water are separated by inertial impact on the baffles of the separator. Sometimes warm ram from location *A* is also passed into the separator so as to melt the ice formed. The pressure drop between the inlet and the outlet of the separator is sensed and if this is more than a certain fixed value, then warm air is introduced. A PID valve controls the flow rate of the warm ram air proportional to the pressure difference.

Other controls

The cabin is a leak-tight closed shell. If the volume flow rate of air to the cabin is more than the exhaust air, the cabin pressure will tend to rise. The purpose of the air supply into the cabin is to:

(i) Remove contaminants.
(ii) Provide sufficient quantity of oxygen.
(iii) Maintain cabin pressure at a slightly higher pressure than the standard atmospheric pressure.
(iv) Maintain cabin temperature at the comfort level.

There are temperature and pressure sensors in the cabin to maintain cabin pressure and temperature. Apart from these, there is a venturimeter to sense the pressure difference between the inlet and the throat. This pressure difference is used for high-pressure control. Similarly, the pressure difference between the inlet and the outlet is also sensed. This pressure difference is used for low-pressure control. The high-pressure control maintains the upper limit while the low-pressure device maintains the lower limit of the flow rate. The controller is connected to a flow-modulating valve, which controls the supply of compressed air fed to the cabin without passing through the turbine. This also helps in controlling the cabin temperature in response to the signals from the thermostats located in the cabin.

13.7.5 Bootstrap System

If the speed of the aircraft is more than Mach 1.7, then the discharge temperature at the exit of the cooling turbine in the simple aircraft cycle would be too high for effective cooling. Essentially at higher velocities, the ram temperature T_2 is very high which has two adverse effects. Firstly, it results in higher discharge temperature $T_{3'}$ at the compressor outlet requiring more cooling. Secondly, since the ram air is used for cooling, its temperature T_2 being high the compressed air cannot be

cooled to a lower temperature, that is, T_4 is high. The remedy is to increase the pressure ratio and then expand the air through a larger pressure ratio to obtain a lower temperature. The compressed air in simple aircraft cycle was obtained from the turbo-compressor of the aircraft. This has a fixed compression ratio. Hence, an additional compressor is used to compress the air to a higher pressure.

The schematic and T–s cycle diagrams of bootstrap cycle are shown in Figures 13.10(a) and 13.10(b) respectively. In this cycle, the air is cooled to state T_4 by ram air after being compressed by the primary compressor or the supercharger of the aircraft with isentropic efficiency of η_{C1} to temperature $T_{3'}$. This is followed by compression in a secondary compressor where the isentropic compression ends up in state 5 and actual compression with isentropic efficiency η_{C2} ends up in state 5′. This is cooled again by ram air to a temperature of T_6 in a heat exchanger. Then it expands to state 7′ with isentropic efficiency η_E, state 7 being the state with isentropic expansion.

It should be noted that in this case both the heat exchangers are cooled by ram air unassisted by blower. Hence, the velocity of air in the heat exchangers will be very low compared to simple aircraft cycle. Otherwise because of high velocity, the ram air is sufficient for circulation. The heat exchangers may not be as compact as the heat exchanger of simple aircraft cycle. There will be additional drag due to frictional resistance in these heat exchangers.

The power output of the turbine is used for driving the additional compressor; hence the pressure ratio of this compressor is limited by this criterion. The power output of the turbine in simple aircraft cycle was used to run a blower.

Both the heat exchangers can cool the air up to a temperature of $T_{2'}$ if the effectiveness of the heat exchangers is 100%.

This cycle will work only when the heat exchangers have the ram air available for cooling, that is, only when the aircraft is in motion. This system does not work when the aircraft is on the ground.

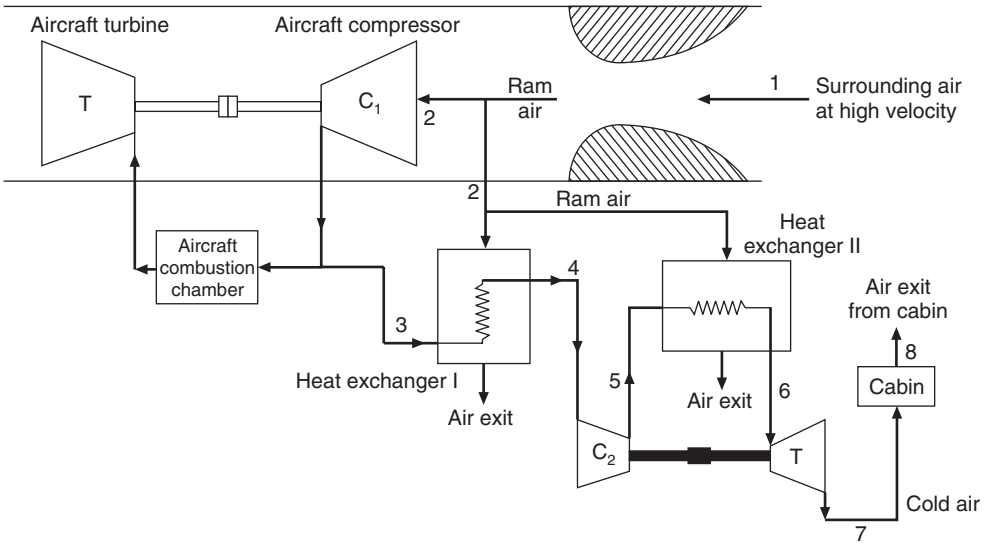

Figure 13.10(a) Schematic of bootstrap aircraft refrigeration system.

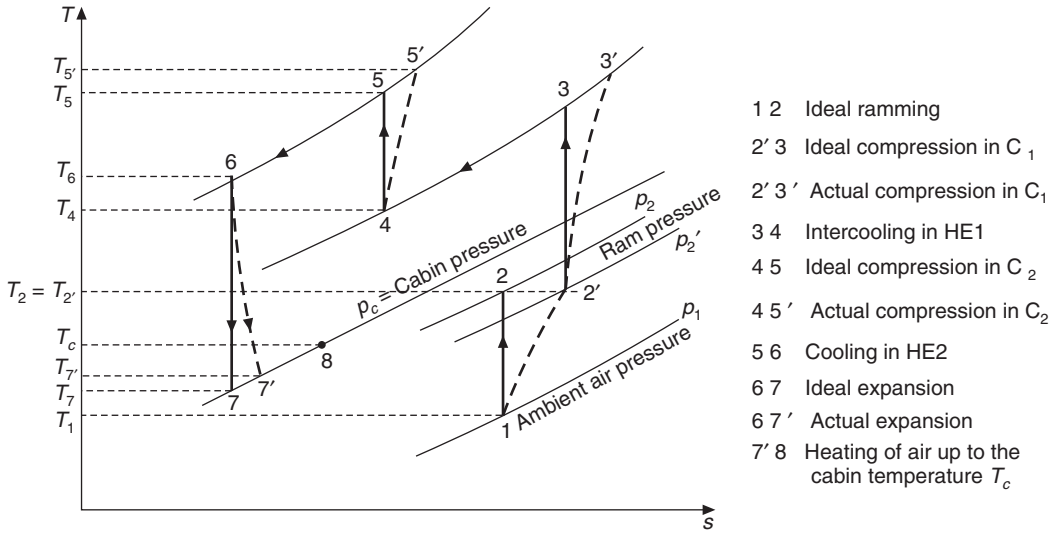

Figure 13.10(b) *T–s* diagram for the bootstrap aircraft refrigeration system.

Cycle analysis

The state after the primary compressor with isentropic efficiency η_{C1} is given by Eq. (13.71), that is,

$$T_{3'} = T_{2'} + (T_3 - T_{2'})/\eta_{C1} = T_{2'}[1 + \{(p_3/p_{2'})^{(\gamma-1)/\gamma} - 1\}/\eta_{C1}] \tag{13.88}$$

The work requirement of the primary compressor is given by

$$W_{C1} = \dot{m}c_p(T_{3'} - T_{2'}) = \dot{m}c_p(T_3 - T_{2'})/\eta_{C1} = \dot{m}c_pT_{2'}\{(p_3/p_{2'})^{(\gamma-1)/\gamma} - 1\}/\eta_{C1}$$

$$= \dot{m}c_pT_{2'}(z-1)/\eta_{C1} \tag{13.89}$$

where, $$z = (p_3/p_{2'})^{(\gamma-1)/\gamma} \tag{13.90}$$

Let the effectiveness of the first heat exchanger be ε_1 as given by Eq. (13.70), that is,

$$\varepsilon_1 = \frac{T_{3'} - T_4}{T_{3'} - T_2} \tag{13.91}$$

Therefore, $$T_4 = (1 - \varepsilon_1)T_{3'} + \varepsilon_1 T_2 \tag{13.92}$$

Substituting for $T_{3'}$ from Eq. (13.88), we get

$$T_4 = T_{2'}[1 + (1 - \varepsilon_1)\{(p_3/p_{2'})^{(\gamma-1)/\gamma} - 1\}/\eta_{C1}] = T_{2'}[1 + (1 - \varepsilon_1)(z-1)/\eta_{C1}] \tag{13.93}$$

Similarly, by analogy with Eq. (13.88), for the secondary compressor, we get

$$T_{5'} = T_4 + (T_5 - T_4)/\eta_{C2} = T_4[1 + \{(p_5/p_4)^{(\gamma-1)/\gamma} - 1\}/\eta_{C2}] = T_4[1 + (y-1)/\eta_{C2}]$$

$$= T_{2'}[1 + (y-1)/\eta_{C2}][1 + (1 - \varepsilon_1)(z-1)/\eta_{C1}] \tag{13.94}$$

where $$y = (p_5/p_4)^{(\gamma-1)/\gamma} \tag{13.95}$$

The work requirement of the secondary compressor is given by

$$W_{C2} = \dot{m}c_p(T_{5'} - T_4) = \dot{m}c_p(T_5 - T_4)/\eta_{C2} = \dot{m}c_pT_4\{(p_5/p_4)^{(\gamma-1)/\gamma} - 1\}/\eta_{C2}$$
$$= \dot{m}c_pT_4(y-1)/\eta_{C2} \tag{13.96}$$

Let ε_2 be the effectiveness of the second heat exchanger, that is,

$$\varepsilon_2 = \frac{T_{5'} - T_6}{T_{5'} - T_2} \tag{13.97}$$

Therefore, $T_6 = (1-\varepsilon_2)T_{5'} + \varepsilon_2 T_2 = T_{2'}[(1-\varepsilon_2)\{1 + (1-\varepsilon_1)(z-1)/\eta_{C1}\}\{1 + (y-1)/\eta_{C2}\} + \varepsilon_2]$ (14.98)

From the definition of isentropic turbine efficiency, we get

$$T_{7'} = T_6 - \eta_T(T_6 - T_7) = T_6[1 - \eta_T\{1 - (p_c/p_5)^{(\gamma-1)/\gamma}\}] \tag{13.99}$$

Turbine work is given by

$$W_T = \dot{m}c_p(T_6 - T_{7'}) = \dot{m}c_p\eta_T(T_6 - T_7) = \dot{m}c_p\eta_T T_6\{1 - (p_c/p_5)^{(\gamma-1)/\gamma}\}$$
$$= \dot{m}c_p\eta_T T_6(1-s) \tag{13.100}$$

where $$s = (p_c/p_5)^{(\gamma-1)/\gamma}. \tag{13.101}$$

The turbine drives the secondary compressor; hence the work requirement given by Eq. (13.96) is equal to the turbine work given by Eq. (13.100), that is,

$$\eta_T T_6(1-s) = T_4(y-1)/\eta_{C2} \tag{13.102}$$

or $$y - 1 = \eta_{C2}\eta_T(1-s)T_6/T_4 \tag{13.103}$$

$$y = \left(\frac{p_5}{p_4}\right)^{(\gamma-1)/\gamma} = \left(\frac{p_5}{p_2}\frac{p_2}{p_4}\right)^{(\gamma-1)/\gamma} = \frac{x}{z}$$

We have

$$s = \left(\frac{p_c}{p_5}\right)^{(\gamma-1)/\gamma} = \left(\frac{p_c}{p_2}\frac{p_2}{p_5}\right)^{(\gamma-1)/\gamma} = \frac{b}{x} \text{ where, } b = \left(\frac{p_c}{p_2}\right)^{(\gamma-1)/\gamma} \text{ and } x = \left(\frac{p_5}{p_2}\right)^{(\gamma-1)/\gamma} \tag{13.104}$$

Substituting the relations given by Eq. (13.104) into Eq. (13.103), we get

$$\frac{x}{z} = 1 - \eta_{C2}\eta_T\frac{T_6}{T_4}\left(1 - \frac{b}{x}\right)$$

or $$x^2 - xz\left(1 + \eta_{C2}\eta_T\frac{T_6}{T_4}\right) + \eta_{C2}\eta_T\frac{T_6}{T_4}bz = 0 \tag{13.105}$$

The total pressure ratio is given by the quadratic Eq. (13.108). It depends upon isentropic efficiencies of compressors, the effectiveness of both the heat exchangers and the pressure ratios for the primary compressor and the cabin pressure.

The COP may be defined as the ratio of refrigeration capacity to the work requirement of the primary compressor. The refrigeration capacity may be written as follows:

$$Q_E = \dot{m} c_p (T_c - T_{7'}) \tag{13.106}$$

The COP is obtained by dividing Eq. (13.106) by Eq. (13.89), that is,

$$\text{COP}_m = \frac{T_c - T_{7'}}{T_2 (z-1)/\eta_{C1}} = \frac{T_c - T_6 \{1 - \eta_T (1-s)\}}{T_2 (z-1)/\eta_{C1}} \tag{13.107}$$

This will reduce to Eq. (13.85) for the simple aircraft refrigeration system, if the secondary compressor is not used.

Ideal case

In the ideal case the effectiveness of both the heat exchangers is 100% and all the isentropic efficiencies are 100%. This implies that the temperature at the outlet of both the heat exchangers is T_2.

$$\eta_T = \eta_{C2} = \eta_{C1} = 1.0 \quad \text{and} \quad T_4 = T_6 = T_2$$

Equation (13.105) reduces to

$$x^2 - 2xz + bz = 0$$

Therefore,

$$x = z \pm \sqrt{z^2 - bz} \tag{13.108}$$

The COP in this case is given by

$$\text{COP}_m = \frac{T_c - T_7}{T_3 - T_2} = \frac{T_c - T_6 s}{T_2 (z-1)} \tag{13.109}$$

13.7.6 Aircraft Refrigeration Cycle with Regeneration

The simple aircraft cycle may not be very effective if the speed of the aircraft is high since this will result in a larger ram temperature. The ram air is used for cooling which will lead to a large temperature at the air-cooler exit, which in turn will give a higher temperature at the turbine exit. Similarly, due to inefficiency of the expander the temperature at the turbine exit will also be high. In gas cycle, it was observed that the COP becomes zero at a certain pressure ratio due inefficiency of the expander. In Section 13.6.5 it was shown that regeneration improves the COP. It was further observed that even at smaller pressure ratios it is possible to obtain a reasonable value of COP. In aircraft refrigeration too, the cooling capacity can be increased by regeneration.

Figures 13.11(a) and 13.11(b) show the schematic and *T*–*s* cycle diagrams respectively of the regenerative cycle. The air leaving the air-cooler at temperature T_4 is further cooled by a part $\dot{m}_6$ of the expanded cooled air from turbine at low temperature $T_{6'}$. This cools the warm air from temperature T_4 to a temperature T_5 in a regenerative heat exchanger. The air at temperature T_5 expands to a temperature of $T_{6'}$. Energy balance across the regenerative heat exchanger gives

$$\dot{m} (T_4 - T_5) = \dot{m}_6 (T_{6'} - T_7) \tag{13.110}$$

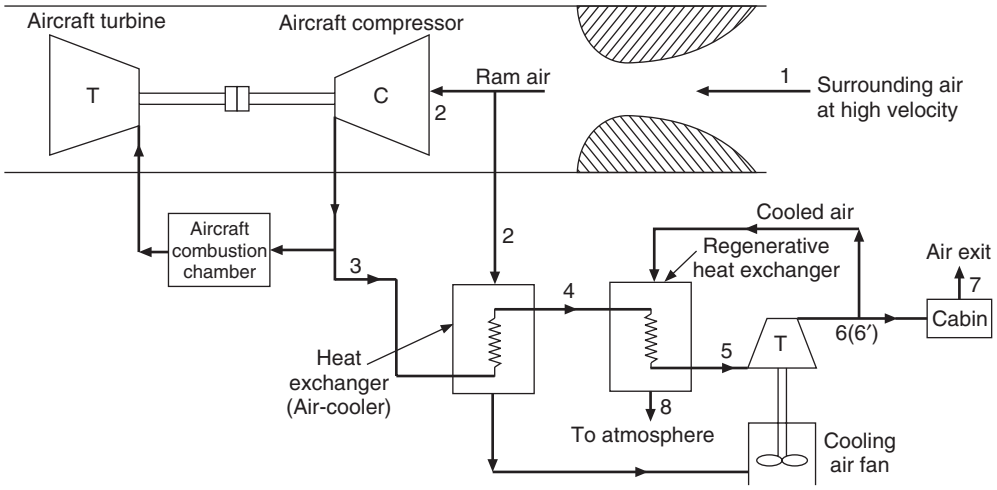

Figure 13.11(a) Regenerative aircraft refrigeration.

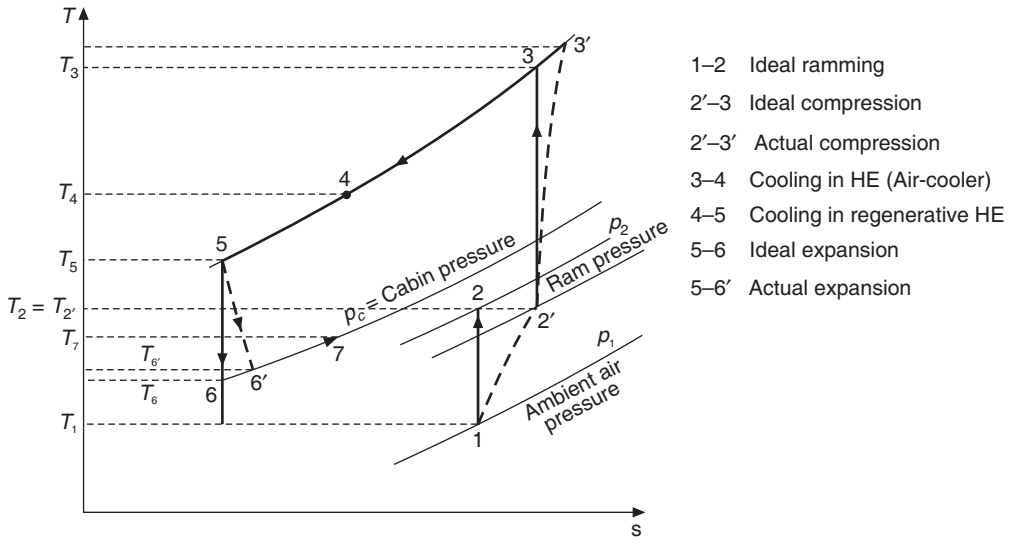

Figure 13.11(b) *T–s* diagram for regenerative aircraft refrigeration.

The temperature $T_{6'}$ is fixed by the temperature required for cabin cooling. The ram air temperature T_2 and the effectiveness of air-cooler fix the temperature T_4. The temperature T_5 depends upon the mass flow rate $\dot{m}_6$ and the effectiveness of the regenerative heat exchanger. We define the ratio of mass flow rates β as the following fraction:

$$\beta = \dot{m}_6 / \dot{m} \tag{13.111}$$

Then from Eq. (13.110) the temperature T_5 is given by

$$T_5 = T_4 - \beta(T_7 - T_{6'})$$

The isentropic turbine efficiency η_T is defined as follows:

$$\eta_T = \frac{T_5 - T_{6'}}{T_5 - T_6} \tag{13.112}$$

The temperature $T_{6'}$ is given by

$$T_{6'} = T_5 [1 - \eta_T \{1 - (p_3 / p_c)^{(\gamma-1)/\gamma}\}] = T_5 [1 - \eta_T (1 - s)] \tag{13.113}$$

where, $s = (p_3/p_c)^{(\gamma-1)/\gamma}$ and p_c is the cabin pressure.

Ideal heat exchanger

If the regenerative heat exchanger is of the counter-flow type and assumed to be ideal, then

$$T_7 = T_4$$

and $$T_5 = T_4 - \beta(T_4 - T_{6'}) = T_4(1 - \beta) + \beta T_{6'}$$

Substituting for $T_{6'}$ from Eq. (13.113), we get

$$T_5 = T_4(1 - \beta) + \beta T_5[1 - \eta_T (1 - s)]$$

or $$T_5 [1 - \beta \{1 - \eta_T (1 - s)\}] = T_4(1 - \beta)$$

Therefore,

$$T_5 = \frac{T_4 (1 - \beta)}{1 - \beta\{1 - \eta_T (1 - s)\}} \quad \text{and} \quad T_{6'} = \frac{T_4 (1 - \beta)\{1 - \eta_T (1 - s)\}}{1 - \beta\{1 - \eta_T (1 - s)\}} \tag{13.114}$$

The refrigeration capacity is given by

$$Q_E = \dot{m}(1 - \beta) c_p (T_c - T_6), \text{ which may be written as}$$

$$Q_E = \dot{m} \frac{T_4 (1 - \beta)\{1 - \eta_T (1 - s)\}}{1 - \beta\{1 - \eta_T (1 - s)\}} \tag{13.115}$$

The compressor work requirement with compressor efficiency η_C is given by

$$W_C = \dot{m} c_p (T_{3'} - T_{2'}) = \dot{m} c_p (z - 1) / \eta_C \tag{13.116}$$

where $$z = (p_3 / p_{2'})^{(\gamma-1)/\gamma}.$$

The pressure $p_{2'}$ and temperature $T_{2'}$ are given by Eqs. (13.69) and (13.66) respectively. Finally, the COP may be found as the ratio of Q_E and W_C, i.e.

$$\text{COP} = \frac{Q_E}{W_C}$$

13.7.7 Reduced Ambient Aircraft Refrigeration Cycle

The ram air temperature and pressure are very high for high speed aircraft. The ram air, therefore, cannot be used for cooling purpose since this will result in a higher temperature at turbine inlet, which in turn will give a higher temperature at turbine outlet and lower refrigeration effect. The

pressure of ram air in this case being high, it is expanded in an auxiliary turbine T_1. The resulting air is at a temperature lower than the ambient temperature (sometimes) and is effectively used for cooling the compressed air. The auxiliary turbine T_1 and the main turbine T_2 are connected by gears and the net power output is used to drive a fan. The schematic and cycle diagrams of this cycle are shown in Figures 13.12(a) and 13.12(b) respectively.

If we define $z = (p_3/p_{2'})^{(\gamma-1)/\gamma}$, then

$$T_3 = T_2[1 + (z - 1)/\eta_C] \tag{13.117}$$

If the efficiency of the auxiliary turbine is to be η_T, then

$$\eta_T = (T_2 - T_{6'})/(T_2 - T_6)$$

and
$$T_{6'} = T_2[1 - \eta_T (1 - s_1)] \quad \text{where } s_1 = (p_1/p_{2'})^{(\gamma-1)/\gamma} \tag{13.118}$$

Defining the effectiveness of heat exchanger to be $\varepsilon = (T_3 - T_4)/(T_3 - T_{6'})$, we get

$$T_4 = T_3(1 - \varepsilon) + \varepsilon T_{6'}$$

Substituting from Eqs. (13.117) and (13.118), we get

$$T_4 = (1 - \varepsilon)\, T_2[1 + (z - 1)/\eta_C] + \varepsilon T_2[1 - \eta_T (1 - s_1)] \tag{13.119}$$

The compressor work requirement is given by Eq. (13.116) as follows:

$$W_C = \dot{m} c_p (T_{3'} - T_{2'}) = \dot{m} c_p (z - 1) / \eta_C \tag{13.120}$$

If the efficiency of main turbine is η_{T1}, then

$$\eta_{T1} = (T_4 - T_{5'})/(T_4 - T_5) \tag{13.121}$$

and
$$T_{5'} = T_4[1 - \eta_T (1 - s)] \qquad \text{where } s = (p_c/p_3)^{(\gamma-1)/\gamma} \tag{13.122}$$

The refrigeration capacity is given by

$$Q_E = \dot{m} c_p (T_c - T_{5'})$$

where the temperatures $T_{5'}$ and T_4 are obtained from Eqs. (13.122) and (13.119). The COP may be obtained as the ratio of Q_E and W_C.

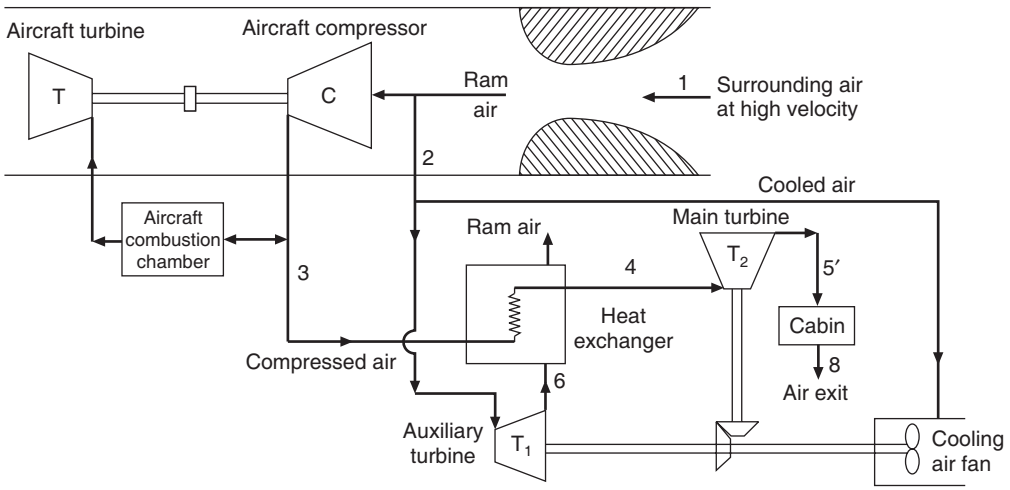

Figure 13.12(a) Reduced ambient aircraft refrigeration system.

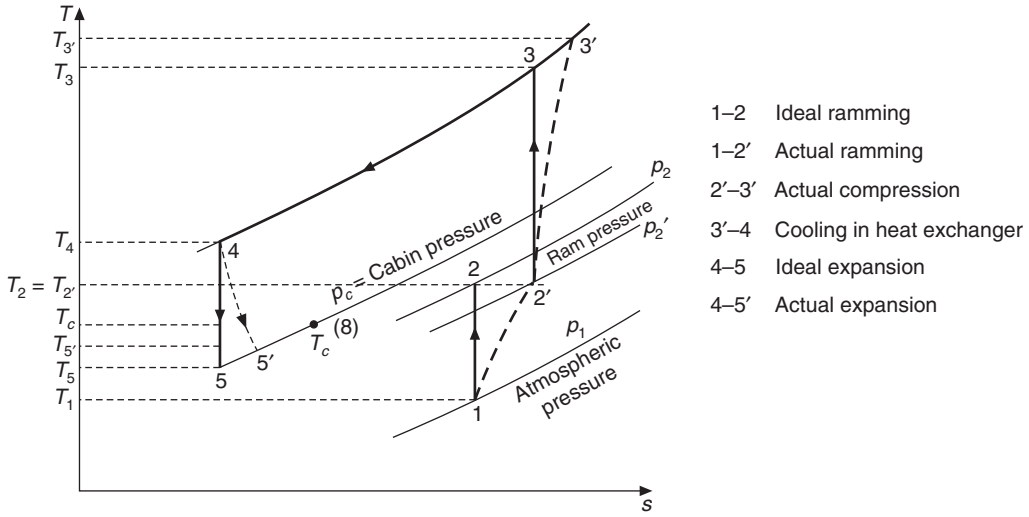

Figure 13.12(b) *T–s* diagram for reduced ambient aircraft refrigeration cycle.

13.7.8 Comparison of Various Aircraft Cycles

All the aircraft refrigeration cycles described above find application in aircraft of various sizes depending upon their speed.

The Simple system is used at moderate speeds during the flight and has the capability to provide cooling when the aircraft is on the ground since it uses a blower to cool the compressed air.

The Bootstrap system is used for high speed aircraft. It is dependent upon the availability of ram air for cooling the compressed air, hence it cannot provide cooling when the aircraft is on ground. This may be overcome by using a part of the turbine output to drive a fan that blows air through the heat exchanger. The turbine power output is usually more than that required by the blower.

As the speed of the aircraft increases, the ram temperature increases. This limits the temperature up to which the compressed air can be cooled before entry into the turbine. If the air enters the turbine at higher temperatures, then it also leaves the turbine at higher temperatures and thus the refrigeration effect is reduced. The bootstrap system has a larger pressure ratio across the turbine so that the air after the heat exchanger is cooled to a lower temperature. In the regenerative system the air is regeneratively cooled before entry into the turbine. In the reduced ambient system the ram air is expanded in a turbine to reduce its temperature for effective cooling in the heat exchanger.

13.7.9 Performance Using Moist Air

In the above calculations the air has been assumed to be dry. In actual practice the air will be moist air with certain humidity ratio W. The temperature at the exit of the cooling turbine is below the dew point temperature, hence the water vapour will condense. In fact, in many cases it is below the triple point of water, hence the water vapour in the moist air will freeze on the blades of the turbine. In the calculations for compression and the heat exchanger the specific heat of moist air should be used. The specific heat of moist air is $1.005 + 1.88W$ where the specific heat of dry air is

taken as 1.005 and W denotes the humidity of the moist air. If condensation occurs, then the dry air calculations will not give accurate results.

For the calculation purpose one may assume that the moist air at the exit of the turbine to be saturated air with the associated condensed water vapour at the same temperature (below the dew point temperature or 0°C as the case may be). For the isentropic expansion in simple cycle, we have

$$T_5 = T_4 \, (p_c/p_3)^{(\gamma-1)/\gamma} \tag{13.123}$$

$$\Delta h_{\text{isentropic}} = c_p \, (T_4 - T_5) \tag{13.124}$$

and
$$\Delta h_{\text{actual}} = \eta_T \, \Delta h_{\text{isentropic}} \tag{13.125}$$

$\therefore$
$$h_{5'} = h_4 - \eta_T \, \Delta h_{\text{isentropic}} \tag{13.126}$$

The pressure at state 5, which is the exit of turbine, is atmospheric. State 4 is above atmospheric pressure. The humidity ratio at state 4 is W_4, which indicates the water vapour content per kg of dry air at that state. This is useful since water vapour will be conserved and the humidity ratio at the exit $W_{5'}$ is equal to W_4.

13.7.10 Dry Air Rated Temperature (DART)

DART is the temperature of dry air at inlet to the cabin. If this temperature is denoted by T_i and the cabin temperature is T_c, then the cooling capacity is given by

$$Q_E = \dot{m} c_p \, (T_c - T_i) \tag{13.127}$$

Different cycles are compared based upon DART. Typical plots are shown in Figure 13.13. The speed of the aircraft in Mach number or in km/h is shown on the x-axis while DART is shown on the y-axis. As the aircraft speed increases, the ram air temperature increases which increases the temperature at the inlet to the cooling turbine. Ultimately it results in a larger value of DART.

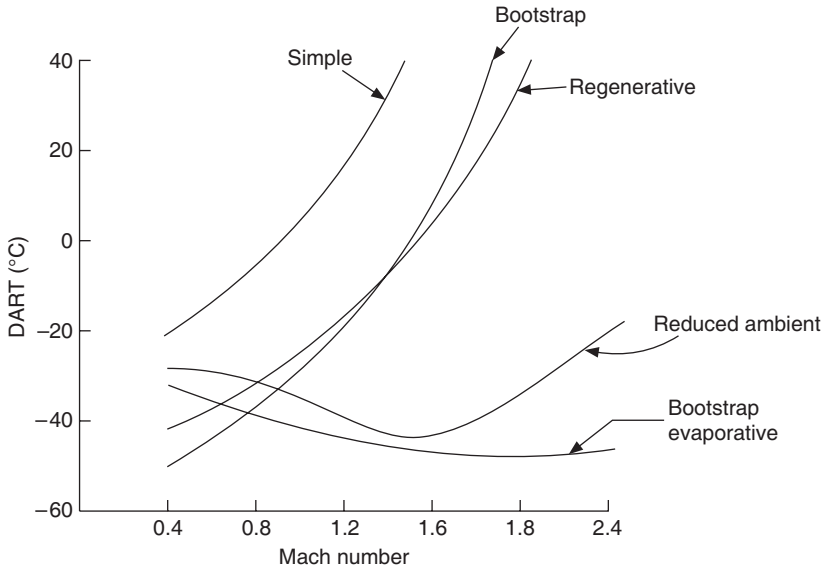

Figure 13.13 Comparison of different aircraft refrigeration cycles based upon DART.

It is observed that Simple cycle is suitable for low Mach numbers, i.e. subsonic aircraft. Regenerative cycle or bootstrap cycle should be used at high Mach numbers. For very high Mach numbers, i.e. supersonic aircraft, the reduced ambient cycle is recommended.

EXAMPLE 13.9 An aircraft is flying at a speed of 1000 km/h. The ambient temperature and pressure are –15°C and 0.35 bar respectively. The compressor and turbine and ram efficiencies are 0.8, 0.85 and 0.85 respectively. The pressure ratio of the compressor is 5.0. The heat exchanger effectiveness is 0.8 and the pressure drop in the heat exchanger is 0.1 bar. The cabin pressure is 1.06 bar and the air leaves the cabin at 25°C. Assuming simple aircraft air conditioning cycle, find the temperature and pressure at various state points, COP, mass flow rate, ram work, compressor work, expander work and volume flow rates at turbine and compressor outlets for a 1 TR capacity plant.

Solution:

Referring to Figure 13.8(b), $p_1 = 0.35$ bar, $T_1 = 273 - 15 = 258$ K, $T_6 = 298$ K, $\eta_C = 0.8$, $\eta_E = 0.85$ and $\eta_R = 0.85$

Velocity, $V = 1000 \times 1000/3600 = 277.778$ m/s

$$T_2 = T_1 + V^2/(2c_p) = 258 + (277.778)^2/(2 \times 1.005 \times 10^3) = 296.388 \text{ K}$$

$$p_2 = p_1\left(\frac{T_2}{T_1}\right)^{1.4/0.4} = 0.56874 \text{ bar} \approx 0.57 \text{ bar}$$

$$\eta_R = \frac{p_{2'} - p_1}{p_2 - p_1} \quad \therefore \quad p_{2'} = p_1 + 0.85(p_2 - p_1) = 0.35 + 0.85(0.57 - 0.35) = 0.536 \text{ bar}$$

$$p_3 = 5 \times p_{2'} = 5 \times 0.536 = 2.68 \text{ bar}$$

$$T_3 = T_2\,(p_3/p_2)^{0.4/1.4} = 296.388(5)^{0.4/1.4} = 469.4256 \text{ K}$$

$$\eta_C = \frac{T_3 - T_{2'}}{T_{3'} - T_{2'}} \quad \therefore \quad T_{3'} = T_{2'} + (T_3 - T_{2'})/\eta_C = 296.388 + (469.4256 - 296.388)/0.85$$

$$\therefore \quad T_{3'} = 512.6849 \text{ K}$$

The cooling is done by ram air, hence under ideal conditions the T_4 should be equal to T_2. Heat exchanger effectiveness ε is given to be 0.8.

$$\therefore \quad \frac{T_{3'} - T_4}{T_{3'} - T_2} = 0.8 \quad \text{or} \quad T_4 = T_{3'} - 0.8(T_{3'} - T_2) = 512.6849 - 0.8(512.6849 - 296.388)$$

$$\therefore \quad T_4 = 339.6476 \text{ K}$$

$$p_4 = p_3 - 0.1 = 2.68 - 0.1 = 2.58 \text{ bar}$$

$$T_5 = T_4\left(\frac{p_5}{p_4}\right)^{(\gamma-1)/\gamma} = 339.6476\left(\frac{1.06}{2.58}\right)^{0.2857} = 263.433 \text{ K}$$

$$\eta_C = \frac{T_4 - T_{5'}}{T_4 - T_5} \quad \therefore \quad T_{5'} - \eta_C (T_4 - T_5) = 339.6476 - 0.85(339.6476 - 263.433)$$

$\therefore \qquad T_{5'} = 274.8652$ K

For 1 TR = 3.5167 kW of cooling capacity the mass flow rate is given by

$$\dot{m} = \frac{3.5167}{c_p (T_6 - T_{5'})} = \frac{3.5167}{1.005(298 - 274.856)} = 0.15125 \text{ kg/s}$$

Ram work = $\dot{m}c_p(T_2 - T_1) = 0.15125 \times 1.005(296.388 - 258) = 5.8353$ kW

Compressor work = $\dot{m}c_p(T_{3'} - T_2) = 0.15125 \times 1.005(512.6849 - 296.388) = 32.87$ kW

Turbine work = $\dot{m}c_p(T_4 - T_{5'}) = 0.15125 \times 1.005(339.6476 - 274.8652) = 9.8474$ kW

Net work = Compressor work – Turbine work = 23.03 kW

COP = 3.5167/Net work = 3.5167/23.03 = 0.1527

The volume flow rates are found as follows:

$$\dot{V}_{CO} = \frac{\dot{m}RT_2}{p_{2'}} = \frac{0.1525(286)296.2882}{0.536 \times 10^5} = 0.2392 \text{ m}^3/\text{s}$$

$$\dot{V}_{FO} = \frac{\dot{m}RT_{5'}}{p_5} = \frac{0.1525(286)274.8652}{1.06 \times 10^5} = 0.11217 \text{ m}^3/\text{s} = 403.811 \text{ m}^3/\text{h}$$

For comparison purpose the work requirement of pressurization of air from ambient value of 0.35 bar to 1.06 bar is calculated as follows. The temperature after pressurization T_{pres} is

$$T_{\text{pres}} = 258(1.06/0.35)^{0.2857} = 354.092 \text{ K}$$

Assuming compressor efficiency of 0.8, we get

$$T_{\text{pres}'} = 258 + (354.092 - 258)/0.8 = 378.115 \text{ K}$$

$$W_{\text{pres}} = \dot{m}c_p(T_{\text{pres}'} - T_1) = 0.15125 \times 1.005(378.115 - 258) = 18.258 \text{ kW}$$

In this example the effectiveness of heat exchanger is very poor. The ram air at 296.388°C cools the compressed air to a temperature of 339.647°C. A temperature difference of 43.249°C occurs, which is rather large.

EXAMPLE 13.10 A better heat exchanger replaces the heat exchanger in Example 13.9, such that the compressed air leaves it at a temperature 10°C more than that of ram air, which provides the cooling. The pressure drop in heat exchanger is negligible. All other parameters being the same as in Example 13.9, find the parameters of Example 13.9.

Solution:

We have $T_4 = T_2 + 10 = 296.388 + 10 = 306.39$ °C

$T_{3'} = 512.685$ K , same as in Example 13.9

$$T_5 = T_4\left(\frac{p_5}{p_4}\right)^{(\gamma-1)/\gamma} = 306.39\left(\frac{1.06}{2.68}\right)^{0.2857} = 235.064 \text{ K}$$

$$\eta_C = \frac{T_4 - T_{5'}}{T_4 - T_5} \quad \therefore \quad T_{5'} = T_4 - \eta_C (T_4 - T_5) = 306.39 - 0.85(306.39 - 235.064) = 245.763 \text{ K}$$

$$\dot{m} = \frac{3.5167}{c_p (T_6 - T_{5'})} = \frac{3.5167}{1.005(298 - 245.763)} = 0.067 \text{ kg/s}$$

Ram work = $\dot{m}c_p (T_2 - T_1)$ = 0.067 × 1.005(296.388 – 258) = 2.585 kW

Compressor work = $\dot{m}c_p (T_{3'} - T_2)$ = 0.067 × 1.005(512.6849 – 296.388) = 14.564 kW

Turbine work = $\dot{m}c_p (T_4 - T_{5'})$ = 0.067 × 1.005(306.39 – 245.763) = 4.082 kW

Net work = Compressor work – Turbine work = 10.482 kW

COP = 3.5167/Net work = 3.5167/10.482 = 0.3355

$$\dot{V}_{CO} = \frac{\dot{m}RT_2}{p_{2'}} = \frac{0.067(286)296.2882}{0.536 \times 10^5} = 0.106 \text{ m}^3/\text{s}$$

$$\dot{V}_{EO} = \frac{\dot{m}RT_{5'}}{p_5} = \frac{0.067(286)245.763}{1.06 \times 10^5} = 0.0444 \text{ m}^3/\text{s} = 159.94 \text{ m}^3/\text{h}$$

The work of pressurization alone is given by

$$W_{\text{pres}} = \dot{m}c_p (T_{\text{pres}'} - T_1) = 0.067 \times 1.005\ (378.115 - 258) = 8.088 \text{ kW}$$

EXAMPLE 13.11 An aircraft flying at a speed of 1000 km/h uses the bootstrap air conditioning system. The ambient temperature and pressure are –15°C and 0.35 bar respectively. The compressor and turbine and ram efficiencies are 1.0, 1.0 and 0.85 respectively. The pressure at aircraft compressor discharge is 2.0 bar and the air is cooled to a temperature of 10°C more than the ram air temperature in both the coolers. The pressure drop in both the coolers is negligible. The cabin pressure is 1.06 bar and air the leaves cabin at 25°C. Find the temperature and pressure at various state points, COP, mass flow rate, main compressor work, auxiliary compressor work and expander work for 1 TR capacity.

Solution:

The ram air temperature and pressure are same as in Example 13.9, that is,

T_2 = 298.388 °C and $p_{2'}$ = 0.536 bar

$p_3 = p_4$ = 2.0 bar and p_c = 1.06 bar

$T_3 = T_2\ (p_3/p_2)^{0.4/1.4} = 296.388(2/0.536)^{0.4/1.4} = 431.77$ K

$T_4 = T_6 = T_2 + 10 = 306.39$ K

Referring to Figures 13.10(a) and (b), it is observed that the auxiliary compressor is driven by the expander, hence the auxiliary compressor work is equal to expander work, that is,

$$c_p\,(T_5 - T_4) = c_p\,(T_6 - T_7)$$

or $$T_4\,[(p_5/p_4)^{(\gamma-1)/\gamma} - 1] = T_6[1 - (p_c/p_5)^{(\gamma-1)/\gamma}]$$

Substituting for p_4 and p_c, we get

$$(p_5)^{0.2857}/2^{0.2857} = 2 - (1.06)^{0.2857}/(p_5)^{0.2857} \qquad (\because\ T_4 = T_6 \text{ in this case})$$

Substituting $x = (p_5)^{0.2857}$, we get

$$x^2 - 2 \times 2^{0.2857}x + (1.06)^{0.2857}2^{0.2857} = 0$$

or $$x^2 - 2.438x + 1.2395 = 0$$

The solutions of this equations are: $x = 1.7119$ and $x = 0.7261$, which correspond to

$p_5 = 6.5644$ and $p_5 = 0.3262$. The second solution is less than p_2.

Hence $p_5 = 6.5644$ bar.

$$T_5 = T_4\,(p_5/p_3)^{0.4/1.4} = 306.39(6.5644/2.0)^{0.2857} = 430.279 \text{ K}$$

$$T_7 = T_6\,(p_c/p_5)^{0.4/1.4} = 306.39(1.06/6.5644)^{0.2857} = 181.98 \text{ K}$$

$$\dot{m} = \frac{3.5167}{c_p\,(T_8 - T_7)} = \frac{3.5167}{1.005(298 - 181.98)} = 0.03016 \text{ kg/s}$$

Compressor work $W_C = \dot{m}c_p(T_3 - T_2) = 0.03016 \times 1.005(431.77 - 296.39) = 4.1035$ kW

$$\text{COP} = 3.5167/W_C = 3.5167/4.1035 = 0.857$$

The work requirement of auxiliary compressor and expander are

$$W_{C1} = 0.03016 \times 1.005(430.279 - 306.39) = 3.755 \text{ kW}$$

$$W_E = 0.03016 \times 1.005(306.39 - 181.98) = 3.771 \text{ kW}$$

These two should have been exactly the same. The error is within acceptable limits.

EXAMPLE 13.12 In the bootstrap system of Example 13.11, calculate all the parameters if the compressor and expander efficiencies are 0.8 and 0.85 respectively. All other input parameters are the same.

Solution:

Auxiliary compressor work is equal to expander work, that is,

$$c_p(T_5 - T_4)/\eta_C = \eta_E\,c_p\,(T_6 - T_7)$$

or $$T_4[(p_5/p_4)^{(\gamma-1)/\gamma} - 1]/\eta_C = \eta_E\,T_6[1 - (p_c/p_5)^{(\gamma-1)/\gamma}]$$

Substituting for p_4 and p_c, we get

$$(p_5)^{0.2857}/2^{0.2857} - 1 = 0.8 \times 0.85[1 - (1.06)^{0.2857}/(p_5)^{0.2857}]$$

Substituting $x = (p_5)^{0.2857}$, we get

$$x^2 - 1.68(2^{0.2857})\,x + 0.68(1.06)^{0.2857}2^{0.2857} = 0$$

or $$x^2 - 2.04794x + 0.842845 = 0$$

The solutions of this equation are: $x = 1.47748$ and $x = 0.57046$ which correspond to $p_5 = 3.92034$ and $p_5 = 0.1402$. The second solution is less than p_2.

Hence $p_5 = 3.92034$ bar.

$$T_5 = T_4\,(p_5/p_3)^{0.4/1.4} = 306.39(3.92034/2.0)^{0.2857} = 371.353 \text{ K}$$

$$T_{5'} = T_4 + (T_5 - T_4)/\eta_C = 306.39 + (371.353 - 306.39)/0.8 = 387.594 \text{ K}$$

$$T_7 = T_6\,(p_5/p_c)^{0.4/1.4} = 306.39(1.06/3.92034)^{0.2857} = 210.855 \text{ K}$$

$$T_{7'} = T_6 - \eta_E\,(T_6 - T_7) = 306.39 - 0.85(306.39 - 210.855) = 225.185 \text{ K}$$

$$T_3 = T_2\,(p_3/p_2)^{0.4/1.4} = 296.388(2/0.536)^{0.4/1.4} = 431.77 \text{ K}$$

$$T_{3'} = T_2 + (T_3 - T_2)/\eta_C = 296.388 + (431.77 - 296.388)/0.8 = 465.615 \text{ K}$$

$$\dot{m} = \frac{3.5167}{c_p\,(T_8 - T_{7'})} = \frac{3.5167}{1.005(298 - 225.185)} = 0.048056 \text{ kg/s}$$

Compressor work $W_C = \dot{m} c_p (T_{3'} - T_2) = 0.048056(1.005)(465.615 - 296.39) = 8.173$ kW

$$\text{COP} = 3.5167/W_C = 3.5167/8.173 = 0.43$$

The work requirement of auxiliary compressor and expander are

$$W_{C1} = 0.048056 \times 1.005(387.594 - 306.39) = 3.9218 \text{ kW}$$

$$W_E = 0.048056 \times 1.005(306.39 - 225.185) = 3.928 \text{ kW}$$

These two should have been exactly the same. These are almost the same.

EXAMPLE 13.13 In the bootstrap system of Example 13.12, calculate all the parameters if the effectiveness of the main and auxiliary heat exchangers are 0.85 and 0.9 respectively. The compressor and expander efficiencies are 0.8 and 0.85 respectively as in Example 13.12. All other input parameters are the same.

Solution:

$$T_3 = T_2\,(p_3/p_2)^{0.4/1.4} = 296.388(2/0.536)^{0.4/1.4} = 431.77 \text{ K}$$

$$T_{3'} = T_2 + (T_3 - T_2)/\eta_C = 296.388 + (431.77 - 296.388)/0.8 = 465.615 \text{ K}$$

For the main heat exchanger, we have

$$(T_{3'} - T_4)/(T_{3'} - T_2) = 0.85$$

$$\therefore \quad T_4 = 465.615 - 0.85(465.615 - 296.39) = 321.774 \text{ K}$$

$$T_5 = T_4\,(p_5/p_3)^{0.4/1.4} \quad \text{and} \quad T_{5'} = T_4 + (T_5 - T_4)/\eta_C$$

$$\therefore \quad T_{5'} = T_4 + T_4\,[(p_5/p_3)^{0.4/1.4} - 1]/0.8 = T_4(1 + 1.25R) \text{ where, } R = [(p_5/p_3)^{0.4/1.4} - 1]$$

For the auxiliary heat exchanger, we have

$$(T_{5'} - T_6)/(T_{5'} - T_2) = 0.9$$

$$\therefore \quad T_6 = T_{5'} - 0.9(T_{5'} - T_2)$$

$$= T_4(1 + 1.25R) - 0.9T_4(1 + 1.25R) + 0.9T_2$$

$$= (0.1)\,(321.774)(1 + 1.25R) + 0.9(296.39)$$

$$= 298.9284 + 40.22175R = 258.70665 + 40.22175(p_5/2\ )^{0.2857}$$

where, $R = [(p_5/2)^{0.2857} - 1]$.

The auxiliary compressor and turbine work per unit mass flow rate are given by

$$w_T = T_6 - T_{7'} = 0.85(T_6 - T_7) = 0.85T_6[1 - (1.06/p_5)^{0.2857}]$$

$$w_C = T_{5'} - T_4 = (T_5 - T_4)/0.8 = T_4[(p_5/p_3)^{0.2857} - 1]/0.8$$

Equating these two, we get

$$0.85[258.70665 + 40.22175(p_5/2\ )^{0.2857}]\ [1 - (1.06/p_5)^{0.2857}] = 321.774[(p_5/p_3)^{0.2857} - 1]/0.8$$

or $$[219.90065 + 34.1885\ (p_5/2)^{0.2857}]\ [1 - (1.06/p_5)^{0.2857}] = 402.2175(p_5/2)^{0.2857} - 402.2175$$

or $$723.6006 - 368.029(p_5)^{0.2857} - 272.5591/p_5{}^{0.2857} = 0$$

or $$x^2 - 1.96615x + 0.74059 = 0, \text{ where, } x = p_5{}^{0.2857}$$

The solutions of this equations are: $x = 1.458308$ and $x = 0.507842$ which correspond to $p_5 = 3.74518$ and $p_5 = 0.0933$. The second solution is not feasible since it is less than p_2.

Hence $p_5 = 3.74518$ bar

$$R = (p_5/2)^{0.2857} - 1 = 0.19629$$

$$T_6 = 298.9284 + 40.22175R = 306.82357$$

$$T_5 = T_4\ (p_5/p_3)^{0.4/1.4} = 321.774(3.74518\ /2.0)^{0.2857} = 384.935 \text{ K}$$

$$T_{5'} = T_4 + (T_5 - T_4)/\eta_C = 321.774 + (384.935 - 321.774)/0.8 = 400.7257 \text{ K}$$

$$T_7 = T_6\ (p_5/p_c)^{0.4/1.4} = 306.82357(1.06/3.74518\ )^{0.2857} = 213.9328 \text{ K}$$

$$T_{7'} = T_6 - \eta_E(T_6 - T_7) = 306.82357 - 0.85(306.82357 - 213.9328) = 227.8664 \text{ K}$$

$$\dot{m} = \frac{3.5167}{c_p\,(T_8 - T_{7'})} = \frac{3.5167}{1.005(298 - 227.8664)} = 0.05014 \text{ kg/s}$$

Compressor work $W_C = \dot{m}c_p(T_{3'} - T_2) = 0.05014(1.005)(465.615 - 296.39) = 8.5279$ kW

$$\text{COP} = 3.5167/W_C = 3.5167/8.5279 = 0.4124$$

The work requirement of auxiliary compressor and expander are

$$W_{C1} = 0.05014 \times 1.005(400.7257 - 321.774) = 3.97866 \text{ kW}$$

$$W_E = 0.05014 \times 1.005(306.82357 - 227.8664) = 3.9789 \text{ kW}$$

The work of auxiliary compressor and the turbine are the same.

EXAMPLE 13.14 An aircraft is flying at a speed of 1000 km/h. The ambient temperature and pressure are –15°C and 0.35 bar respectively. The compressor and turbine and ram efficiencies are 0.8, 0.85 and 0.85 respectively. The pressure ratio of the compressor is 5.0. The compressed air is cooled to a temperature of 306.388 K. The pressure drop in the heat exchanger is negligible. A regenerative heat exchanger cools the air further by 20°C. In the regenerative HEX too, cold air

leaves at 10°C less than that of the warm air. The mass flow rate of air is 0.5 kg/s. Find the cooling capacity and the COP.

Solution:

The ram air temperature and pressure, and the compressor outlet temperature are the same as in Example 13.9.

$$T_2 = 296.388 \text{ K}, p_{2'} = 0.536 \text{ bar}, T_{3'} = 512.6849 \text{ K and } p_3 = 2.68 \text{ bar}$$

Referring to Figure 13.11(b),

$$T_4 = T_2 + 10 \text{ K} = 306.388 \text{ K}$$

$$T_5 = T_4 - 20 \text{ K} = 286.388 \text{ K and } p_6 = 1.06 \text{ bar}$$

$$T_6 = T_5 (1.06/2.68)^{0.2857} = 219.72$$

$$T_{6'} = 286.388 - 0.85(286.388 - 219.72) = 229.72 \text{ K}$$

$$T_8 = T_4 - 10 = 296.388 \text{ K}$$

Let $\dot{m}_6$ be the mass flow rate of cold air used for regeneration and be the mass flow rate through the turbine, then energy balance across the regenerative HEX gives

$$\dot{m}_6 (T_{6'} - T_8) = \dot{m}(T_4 - T_5) = 20\dot{m} = 20 \times 0.5 = 10$$

$$\dot{m}_6 = 20\,\dot{m}/(296.388 - 229.72) = 0.15 \text{ kg/s}$$

The mass flow rate used for refrigeration = 0.5 – 0.15 = 0.35 kg/s

$$Q_E = (\dot{m} - \dot{m}_6)\, c_p (T_7 - T_{6'}) = 0.35 \times 1.005 (298 - 229.72) = 24.0175 \text{ kW}$$

$$W_C = (\dot{m} - \dot{m}_6)\, c_p (T_{3'} - T_{2'}) = 0.35 \times 1.005 (512.6849 - 296.388) = 76.0824$$

$$\text{COP} = Q_E/W_C = 24.0175/76.0824 = 0.3157$$

EXAMPLE 13.15 An aircraft flies at a speed of 950 km/h. The ambient temperature and pressure are –10°C and 0.55 bar respectively. It uses a reduced ambient cycle. The ram, compressor and turbine efficiencies are 0.9, 0.8 and 0.85 respectively. The exhaust air of the auxiliary turbine that runs on ram air, cools the compressed air. The effectiveness of the heat exchanger is 0.9. The compression ratio is 3.0. The cabin pressure is 1.06 bar. Find the temperature and pressure at all state points, then find the compressor work, turbine work for 1 TR cooling capacity and COP.

Solution:

Referring to Figures 13.12(a) and 13.12(b),

$$V = 950 \times 1000/3600 = 263.89 \text{ m/s}$$

$$T_2 = T_1 + V^2/2c_p = 263 + (263.89)^2/(2 \times 1.005 \times 1000) = 297.645 \text{ K}$$

$$p_2 = p_1(T_2/T_1)^{3.5} = 0.55(297.645/263)^{3.5} = 0.8481 \text{ bar}$$

$$\eta_R = 0.9 \quad \therefore \quad p_{2'} = p_1 + 0.9(p_2 - p_1) = 0.8183 \text{ bar}$$

$$p_3 = 3p_2 = 3 \times 0.8183 = 2.4549 \text{ bar}$$

$$T_3 = 297.645(3)^{0.2857} = 407.392 \text{ K}$$

$$T_{3'} = T_2 + (T_3 - T_2)/0.8 = 434.828 \text{ K}$$

Auxiliary turbine expands the ram air from 0.8183 bar to 0.55 bar

$$T_6 = T_2\,(0.55/0.8183)^{0.2857} = 265.7058 \text{ K}$$

$$T_{6'} = T_2 - 0.85(T_2 - T_6) = 270.497 \text{ K}$$

The effectiveness of the heat exchanger is 0.9.

$$T_4 = T_3 - 0.9(T_3 - T_{6'}) = 286.93 \text{ K}$$

$$T_5 = T_4\,(1.06/2.4549)^{0.2857} = 225.72 \text{ K}$$

$$T_{5'} = T_4 + 0.85(T_5 - T_4) = 234.903 \text{ K}$$

$$\dot{m} = \frac{3.5167}{c_p\,(T_8 - T_{5'})} = \frac{3.5167}{1.005(298 - 234.903)} = 0.05546 \text{ kg/s}$$

$$W_C = \dot{m}c_p\,(T_{3'} - T_2) = 0.05546 \times 1.005(434.828 - 297.645) = 7.6458 \text{ kW}$$

$$W_T = \dot{m}c_p\,(T_4 - T_{5'}) = 0.05546 \times 1.005(286.93 - 234.903) = 2.9 \text{ kW}$$

The turbine work and the ram work both are used for running the blower.

$$\text{COP} = 3.5167/\,W_C = 3.5167/7.6458 = 0.45$$

13.8 VORTEX TUBE REFRIGERATION

The molecules of a gas move in a random manner with velocities of different magnitudes in different directions. Some molecules move with larger velocities while others move with smaller velocities. Temperature is a measure of the root mean square velocity of the molecules. Hence the faster moving molecules will have higher temperature than the slower moving molecules. Maxwell with a touch of humour suggested that both cold and hot water could be drawn from a single pipe if we could capture a small demon and train him to open and close a small valve. The demon would open the valve when the slow moving molecules approach it, letting out a stream of cold water. Similarly, letting out of fast molecules will result in a warm stream.

George Ranque, a French physics student, quite by accident in 1928, invented the Vortex tube. He was conducting experiments on a vortex type pump that he had developed when to his surprise he observed cold air coming from one end and warm air from the other end. He had observed low temperature in the rotating flow of air cyclone separators. Ranque made experimental models of this device. However it could not be commercialized and was soon forgotten. The German Army during its occupation of France found these experimental models and turned them over to German physicist Rudolf Hilsch. Hilsch made some improvements on the device. However, he found that even at its best performance, it was not more efficient than the conventional methods of refrigeration in achieving low temperature.

Hence, the vortex tube has been variously known as the *Ranque Vortex Tube*, *Hilsch Vortex Tube*, *Ranque–Hilsch Vortex Tube* and *Maxwell's demon*. It has been accepted as a reliable simple and low cost device for a variety of industrial spot cooling problems.

The principle of operation is very well understood by now, however, a convincing theory of its performance has not been available. It uses compressed air and it does not have any moving parts. It is available in two designs, namely, counterflow and uniflow. These are shown in Figures 13.14 and 13.15 respectively.

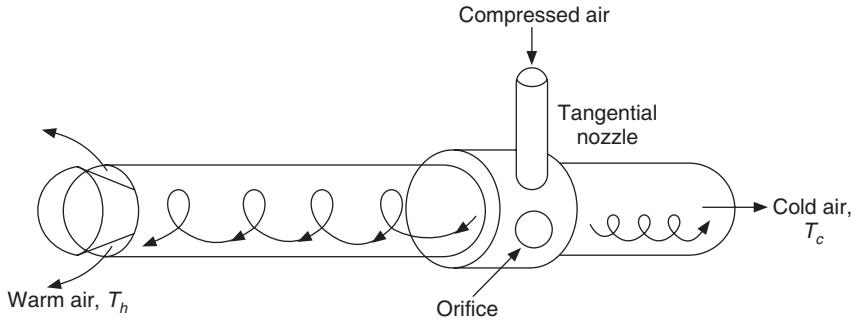

Figure 13.14 Counterflow type vortex tube.

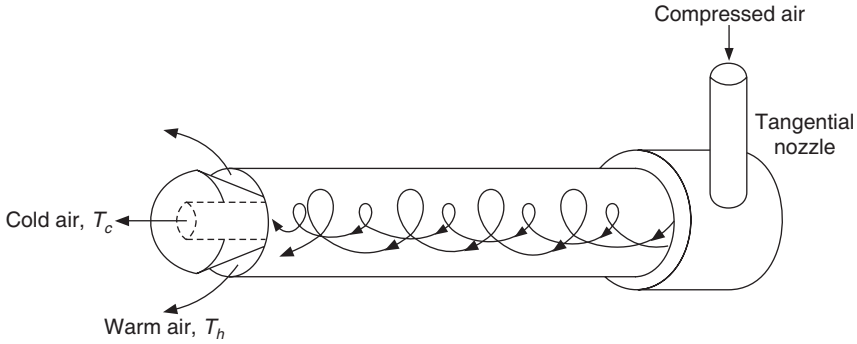

Figure 13.15 Uniflow type vortex tube.

13.8.1 Counterflow Type Vortex Tube

The geometry of the vortex tube is illustrated in Figure 13.16. Compressed air is supplied through nozzles, which are located tangentially to the internal tube diameter. The air enters tangentially at the tube inlet and rotates as a forced vortex with high velocity at the periphery and low velocity in its core. There is an orifice plate at end 2, which is close to the nozzle. The orifice diameter is half of the tube diameter. The cold air comes out of this orifice. The orifice ensures that the high velocity vortex moves towards the opposite end 3 while only the air from the core comes out of the orifice.

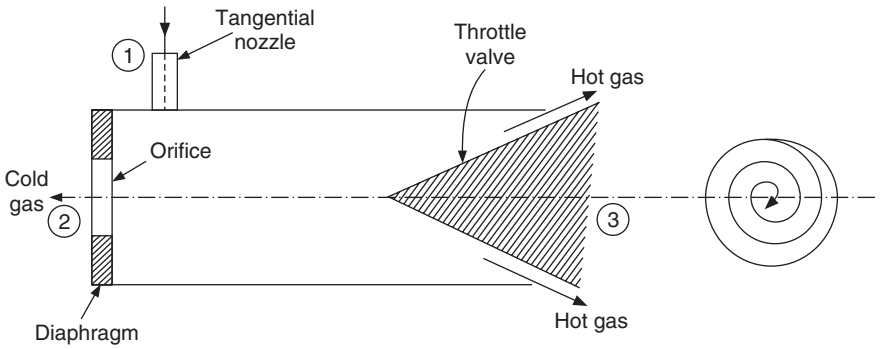

Figure 13.16 Vortex tube.

A throttle valve is provided at point 3, the opposite end of the tube to create some back pressure. The warm air will come out of this end. If the valve is closed, all the air will go out through end 2 and no cooling is produced.

As the valve is partially opened, warm air flows through end 3 and some cold air comes out through the orifice. As the valve is opened further, the flow rate of cold air through the orifice and its temperature both decrease. The temperature is minimum when the flow rate is between 1/3 to 1/4 of total flow rate. Further decrease in flow rate increases the temperature.

As the air flows through the nozzle, its kinetic energy increases and static temperature decreases. Considering the flow to be adiabatic, the stagnation temperature will remain the same as that at nozzle inlet. It rotates like a tornado and moves towards the valve 3 where some of it escapes as warm air. The air in the core which does not escape, turns back towards the nozzle. The pressure of the air at the valve, called back pressure, becomes stagnation pressure since velocity becomes zero at the valve. The pressure in the plane of nozzle is static pressure which is lower than the back pressure. As a result, the flow in the core of the tube reverses and moves backwards towards the nozzle. It rotates in the same sense as the air in the outer part of the tube, only its axial velocity component is towards the nozzle. The pressure of this stream is above atmospheric, hence its expansion to atmospheric pressure gives lower temperature.

The air near the periphery is retarded by friction at the tube wall, as a result some kinetic energy is dissipated by viscous dissipation and it becomes a warm stream. The division of two counter moving flows into a core and annuls is a concept only. Actually there is a continuous gradient of velocity and temperature along the radius. The central core of air loses momentum and kinetic energy. Work is done on the outer annulus by the core, that is it acts as a sink for the core. The difference between the two regions is in their axial velocity. Experimental evidence by smoke injection indicates a solid rotation of the core. Tests carried out with an oil-coated tube wall gave the trace a helical path on the tube wall with increasing pitch towards exit 3.

The inner core behaves like a forced vortex, that is, solid body rotation with increasing rotational velocity away from the radius, that is, $V_\theta = r\Omega$. Actually the momentum conservation requires that the velocity should be greater than this value, which implies that momentum is transferred from this layer to the outer annulus. The pressure increases in the radial direction due to centrifugal force, that is, $\partial p/\partial r = V_\theta^2/r = r\,\Omega^2$. The pressure increases in the radial direction, hence locally there is compression in the radial direction, due to which the temperature of the outer vortex increases.

The role of the orifice or the diaphragm is to block the high kinetic energy air from moving out of the orifice and thus move the air towards the valve.

13.8.2 Uniflow Type Vortex Tube

In uniflow vortex tube shown in Figure 13.15, the flow reversal does not occur since there is no opening at the nozzle end. The flow in this case too, is divided into an inner core which loses momentum to the outer vortex. The outer vortex becomes warm because of this and also due to viscous dissipation at the tube wall as well as due to compression arising out of centrifugal force. Both the vorticies move in the same direction and rotate in the same sense. The inner core comes out at lower temperature and the outer core is at higher temperature.

A turbine reduces the air temperature by removing kinetic energy of the air in the form of work output. A vortex tube divides the flow into two streams, a low temperature and low kinetic energy stream and a high kinetic energy warm stream.

A typical vortex tube has 12.5 mm inner diameter, 6.25 mm diameter of the orifice, a 350 mm long warm end and 100 mm long cold end. Three parameters determine the performance of the tube, namely:

1. The setting of the valve
2. The inlet pressure
3. The size of the hole in the orifice.

For each value of the valve setting and orifice hole, the temperature difference is maximum at a particular inlet pressure. When the vortex tube of the dimensions described above is properly adjusted, it will deliver warm air at 40°C and cold air at –55°C.

13.8.3 Analysis of the Vortex Tube

Let the inlet mass flow rate be $\dot{m}_1$ and the mass flow rate of cold and hot air be $\dot{m}_c$ and $\dot{m}_h$ respectively. The enthalpies of cold and warm air are h_c and h_h respectively. Assuming the vortex tube to be insulated, the mass and energy conservation yields:

$$\dot{m}_1 = \dot{m}_c + \dot{m}_h \tag{13.128}$$

$$\dot{m}_1 h_1 = \dot{m}_c h_c + \dot{m}_h h_h \tag{13.129}$$

Assuming the specific heat of air to be constant, we get

$$\dot{m}_1 T_1 = \dot{m}_c T_c + \dot{m}_h T_h \tag{13.130}$$

or $$\dot{m}_c (T_1 - T_c) = \dot{m}_h (T_h - T_1)$$

The cold air fraction μ is defined as follows:

$$\mu = \frac{\dot{m}_c}{\dot{m}_h} = \frac{T_h - T_1}{T_h - T_c} \tag{13.131}$$

The pressure at inlet to vortex tube is p_1 and the pressure at the exit is atmospheric pressure p_a. If the gas expands isentropically from pressure p_1 to p_a, the temperature $T_{c'}$ of the cold air is given by

$$T_{c'} = T_1 (p_a / p_1)^{(\gamma-1)/\gamma} = T_1 / z \tag{13.132}$$

where $z = (p_1 / p_a)^{(\gamma-1)/\gamma}$.

The cooling device under ideal condition should have resulted in temperature $T_{c'}$ for the whole air mass flow rate. The vortex tube gives a temperature of T_c for mass flow rate $\dot{m}_c$ of the cold stream. Hence the isentropic efficiency of the vortex tube may be defined as follows:

$$\eta_e = \frac{\dot{m}_c (T_1 - T_c)}{\dot{m}_1 (T_1 - T_{c'})} = \mu\phi \tag{13.133}$$

where, $$\phi = \frac{T_1 - T_c}{T_1 - T_{c'}} \quad \text{and} \quad T_1 - T_{c'} = T_1 (1 - 1/z) \tag{13.134}$$

To determine the COP, the energy requirement of the supply air to compress it from pressure p_a to p_1 must be determined. If the compression efficiency is assumed to be η_c, then

$$W_c = \dot{m} c_p T_a (z-1)/\eta_c \tag{13.135}$$

Therefore,
$$\text{COP} = \frac{\dot{m}_c c_p (T_1 - T_c)}{\dot{m} c_p T_a (z-1)/\eta_c} = \frac{\dot{m}_c}{\dot{m}} \frac{T_1}{T_a} \frac{1}{z} \phi \eta_c \tag{13.136}$$

If the compressed air is cooled to atmospheric pressure before entry to the vortex tube, then the COP is given by

$$\text{COP} = \frac{\mu \phi \eta_c}{z} = \frac{\eta_e \eta_c}{z} \tag{13.137}$$

The COP decreases as the pressure ratio increases.

In case of isothermal compression the work requirement is given by

$$W_c = \frac{\dot{m} c_p T_a \ln (p_1/p_a)}{\eta_c} \tag{13.138}$$

In this case the COP is given by

$$\text{COP} = \frac{\mu \phi \eta_c (1 - 1/z)}{\ln (p_1/p_a)} = \frac{\eta_e \eta_c (1 - 1/z)}{\ln (p_1/p_a)} \tag{13.139}$$

The COP is usually between 0.1 to 0.2. It is observed from Eqs. (13.137) and (13.139) that to obtain large COP the vortex tube efficiency η_e should be large and the pressure ratio z should be small. A small pressure ratio would, however, give a small cooling capacity. Equation (13.39) shows that COP decreases with increase in pressure ratio. As the cold air fraction μ increases, the cold air temperature difference ΔT_c increases until it reaches a maximum value and decreases thereafter up to full valve opening. The maximum temperature difference will not give maximum cooling since the cooling rate is a function of temperature difference and mass flow rate of cold air, that is $\mu \dot{m}_1 c_p \Delta T_c$.

Advantages and disadvantages of vortex tube

1. The design of vortex tube is very simple and only one back-pressure valve is used for control.
2. Air is the working medium whose leakage poses no problem.
3. There are no moving parts requiring maintenance.
4. It is lightweight and compact. It can be used for cooling in tight and congested spaces.
5. Initial investment is small and the system is easy to operate.

The disadvantage of the vortex tube is that its COP is very poor and the cooling capacity is very small. It finds application in spot cooling. It is used for cooling of cutting tools and machining materials for which the use of coolant is not permitted. It is used for cooling the suits worn by miners and spray painting operators.

13.9 PULSE TUBE

The pulse tube is a device to obtain low temperature by using an oscillating pressure (typically produced by a compressor) to generate oscillating gas flow in the system. Prof. Gifford noticed

that the closed end of a tube gets heated if the other end is connected to a compressor. Gifford and Longsworth reported that connecting such a tube to a compressor through a regenerator produced cooling at one end of the tube and heating at the other end. This was named *Pulse tube*. The schematic diagram of this is shown in Figure 13.17.

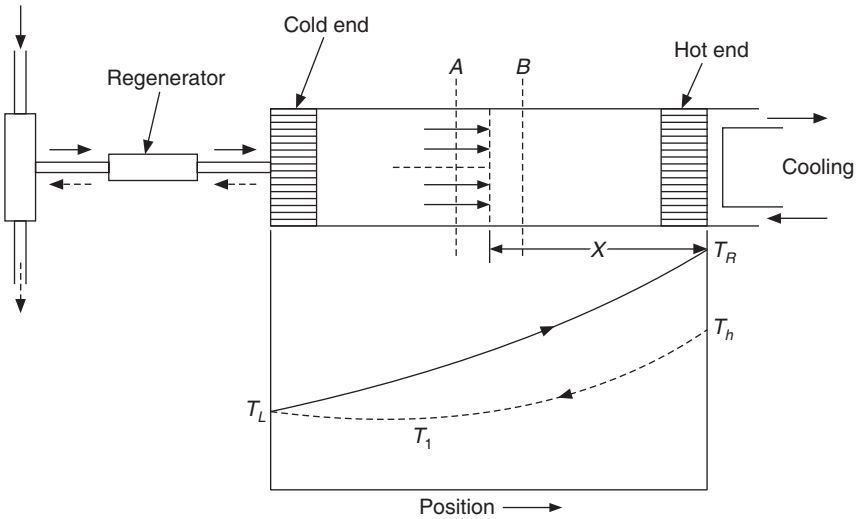

Figure 13.17 Pulse tube.

The principle of operation of this device is similar to gas cycle refrigeration. The compressed gas from the compressor is cooled to approximately the ambient temperature in the after-cooler. This cooling can occur in the reservoir of the compressor as well. The output of the compressor is periodic. As the output of compressor reciprocates, so does the flow. The flow first occurs towards the extreme right hot end of the pulse tube. The pressure in the pulse tube builds up. Then the gas flows towards the left end and the pressure in the pulse tube decreases. It can either be directly connected to the compressor or the output of compressor can be fed to it by a rotary valve. This valve introduces compressed air into pulse tube for some time and withdraws the expanded air during the rest of the cycle.

The high-pressure gas entering the pulse tube acts on a *fictitious* piston. As this pulse moves to the right, it compresses the gas present inside the tube. The temperature in the tube increases from T_L at the left to T_R at the right end as the compression occurs. This is shown by the solid curve in Figure 13.18. At the right end the heat is rejected to some cold medium and its temperature decreases to T_h. Cooling in the pulse tube cannot be obtained without this heat rejection.

Then the flow reversal occurs. The fictitious piston moves towards the left, the pressure in the tube decreases and expansion occurs towards the left. The gas temperature decreases towards the left as shown by the dashed curve in Figure 13.17. This yields gas at low temperature T_1 at the left end.

The cooling principle of pulse tube is just like the gas cycle refrigeration consisting of three steps, namely:

(i) Compression by fictitious piston
(ii) Heat rejection at the hot right end
(iii) Expansion by fictitious piston resulting in a low temperature.

Figure 13.17 shows a fictitious piston located at distance X from the hot end. Consider a small element AB of the pulse tube as shown in Figure 13.17. As the fictitious piston moves to the right the pressure in the section AB increases by Δp. The work done due to compression is given by

$$\Delta W = V_{AB}\, \Delta p \tag{13.140}$$

The temperature at the end B will increase due to this work done, as a result, the enthalpy of the gas leaving section B will be greater than that entering the section A. This is given by

$$h_B = h_A + V_{AB}\, \Delta p \tag{13.141}$$

The enthalpy progressively increases to the right, that is, the effect of heating due to compression is transferred to the right.

If the process is reversed, that is, Δp decreases from B to A, then the work is done by the gas, as a result, the enthalpy of the gas decreases. For small Δp the change in enthalpy of gas may be same in both directions. During expansion, the enthalpy decreases towards the left, that is the cooling effect is transferred to the left.

The mass of the gas, which physically moves from the cold left end to the hot right end is much less than the total gas, which fills the tube. Otherwise it is the wave that travels to the right. Only a small portion comes into contact with the hot and cold ends. Let $\mathbb{V}_h$ be the volume of the gas whose temperature is decreased to T_h at the hot end by heat rejection to the heat exchanger. During expansion this gas expands from location X_h to location X. Its pressure and temperature decrease. If T_X is the temperature at location X and p_h and p_X are pressure at hot end and location X respectively, then the sudden expansion process may be considered isentropic and we get

$$\left(\frac{T_X}{T_h}\right)^{\gamma/(\gamma-1)} = \frac{p_X}{p_h} \tag{13.142}$$

The mass of the gas at location X_h and at location X is related to pressures at the two locations as follows:

$$\frac{m_X}{m_h} = \frac{p_X}{p_h} \tag{13.143}$$

The mass of gas in volume $\mathbb{V}_h$ is given by $m_h = p_h \mathbb{V}_h / RT_h$

The mass at location X is given by the following expression:

$$m_h = m_X + \int_{x_h}^{X} \frac{p_x\, A dx}{RT_x} \tag{13.144}$$

Substituting from Eq. (13.142), we get

$$\frac{p_X}{p_h} = \frac{m_X}{m_h} = 1 - \int_{x_h}^{X} \frac{p_x\, A dx}{RT_s m_h} \tag{13.145}$$

Substituting from Eq. (13.142), we get

$$\frac{p_X}{p_h} = 1 - \frac{p_h A}{R m_h (T_h)^{\gamma/(\gamma-1)}} \int_{x_h}^{X} T_x^{1/(\gamma-1)}\, dX$$

The temperature T_x is assumed to be equal to T_X, hence

$$\frac{p_X}{p_h} = 1 - \frac{p_h A (T_h)^{1/(\gamma-1)}}{R m_h (T_h)^{\gamma/(\gamma-1)}} \int_{x_h}^{X} \frac{\mathbb{V}_h}{\mathbb{V}_x} dx$$

$$\frac{p_X}{p_h} = 1 - \frac{p_h}{m_h R T_h} \frac{\mathbb{V}_h}{\mathbb{V}_X} A(X - X_h) = 1 - \frac{\mathbb{V}_X - \mathbb{V}_h}{\mathbb{V}_X} = \frac{\mathbb{V}_h}{\mathbb{V}_X}$$

or
$$\left(\frac{T_X}{T_h}\right)^{\gamma/(\gamma-1)} = \frac{\mathbb{V}_h}{\mathbb{V}_X} \quad \text{or} \quad \frac{T_X}{T_h} = \left(\frac{\mathbb{V}_h}{\mathbb{V}_X}\right)^{(\gamma-1)/\gamma} \tag{13.146}$$

As the fictitious piston moves to the left, the volume ratio $\mathbb{V}_X/\mathbb{V}_h$ increases and it is observed from Eq. (13.146) that the temperature T_X decreases. Figure 13.18 shows the variation of temperature ratio with the volume ratio for air and helium. The polytropic index of helium is 1.66 compared to 1.44 for air; hence the temperature decreases at a faster rate for helium compared to that for air.

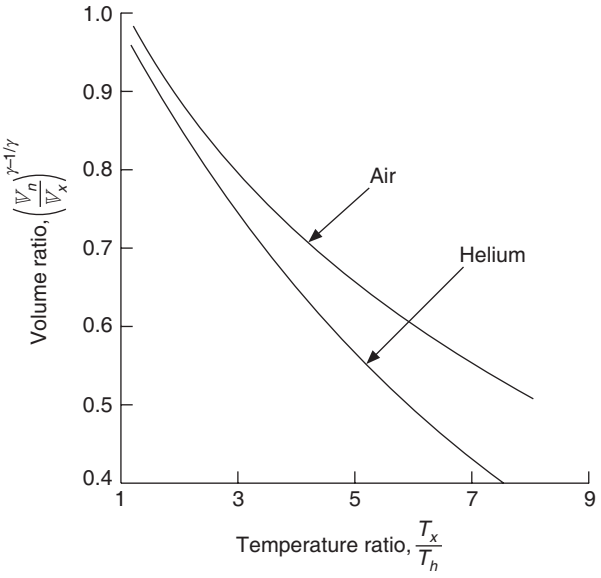

Figure 13.18 Variation of temperature ratio with volume ratio for air and helium.

It is obvious that the lowest temperature will depend upon the temperatures T_h and T_L. The temperature of cold water or the air to which heat is ejected fixes the temperature T_h. T_L the temperature of the air at inlet to pulse tube can be decreased by using a regenerator. A regenerator is a heat exchanger, which absorbs heat during one part of the cycle and rejects it during the other part. The air that leaves the pulse tube at the cold end is at a temperature lower than the ambient value, hence this can cool the matrix of the regenerator provided ahead of the pulse tube.

The low temperature gas leaving after expansion cools the regenerator matrix. In the next cycle the compressed gas that enters the regenerator at T_L is cooled by it to a temperature $T_{L'}$ before entry into the pulse tube. After compression a temperature $T_{R'}$ is achieved at the hot end and a

much lower temperature $T_{l'}$ is obtained at the end of the pulse tube. The exhaust gas leaves the regenerator at temperature $T_1 < T_L$.

A temperature of the order of 190 K may be obtained is a single-stage pressure tube with a sink temperature of 280 K. It is not possible to achieve these temperatures by multistage or cascade systems. Air cycle will face lubrication problems at such a low temperature. The pulse tube does not have any moving parts except the rotary valve, hence it is free of maintenance. The COP however is rather low. Experimental results indicate that there are optimum dimensions for its operation. The length of the cold end and its proportion to the free length of the pulse tube can be optimized.

There are three conditions for the optimum operation of the pulse tube. These are as follows:

1. The gas must reach the cold end of the pulse tube without carrying a lot of heat as measured by flow of enthalpy in the regenerator.
2. The amplitude of gas flow and oscillations in the pulse tube must be large enough to carry away the heat transfer from the cold end to the hot end for its rejection.
3. The phase relationship between the pressure and the gas flow in the pulse tube section must be appropriate to carry away the heat transfer from the cold end to hot end by flow of enthalpy.

Mikulin showed that the efficiency of the pulse tube can be increased by inserting an orifice and a reservoir at the hot end. This increases the phase shift between the pressure and the mass oscillations. The orifice pulse tube has now become the standard implementation. A single-stage pulse tube can achieve temperatures below 30 K, while a three-stage pulse tube can achieve 3.6 K as claimed by Matsubara (1994).

One-dimensional thermodynamic model based upon enthalpy flow has been given by NIST. TRW has built a pulse tube that gives output of 1 W at 35 K with 200 W power input. TRW is in the process of designing a 1.5 W unit for 55 K application with power input less than 100W, which has efficiency comparable to Stirling cycle cooler. A pulse tubes does not have moving parts like Stirling cycle, as a result, there is no friction, no wear and essentially no vibrations; hence the low-temperature pulse tube has a long life. The heat is transferred from the cold end to the hot end by physical flow of gas while the expansion and the compression are by waves. The phase difference between the pressure and the gas flow is essential to transfer the heat from cold end to the hot end. The orifice and the reservoir provide this phase shift.

Another related technology under development is thermo-acoustic engines and coolers. Loudspeakers can drive the coolers. Engine can operate at acoustic resonance. Pulse tube works at frequencies well below resonance. Effort is on to replace the Gifford–McMohan cooler by the pulse tube. What is required is the low cost, low vibration and more reliability.

13.10 STIRLING CYCLE

The temperature of a gas increases or decreases during heat absorption or heat rejection at constant pressure due to its finite specific heat. Maximum COP requires isothermal heat transfer processes. In Reversed Carnot cycle for a gas, it was observed that during isothermal heat rejection, work has to be done on it by a compressor. Similarly, isothermal heat absorption by a gas requires work output or expansion work in a turbine. The Reversed Carnot cycle has a very narrow indicator

diagram. It has a very small volumic refrigeration capacity and a small mean effective pressure, which is defined as the ratio of work done to the swept flow rate. The friction between the piston and the cylinder and in a turbine plays a dominant role. It increases the narrow area of the indicator diagram leading to large work input and low COP. Similarly in a Carnot heat engine, the frictional mean effective pressure may be more than the indicated mean effective pressure and hence no work may be delivered.

The Stirling cycle is practical in this respect. In this cycle the isentropic processes are replaced by constant volume processes as shown in Figures 13.19(a) and 13.19(b) on T–s and p–$\mathbb{V}$ coordinates. The corresponding Reversed Carnot cycle on p–v coordinates with the same maximum pressure is shown in Figure 13.1(b). It is observed that the weak points of the Reversed Carnot cycle are cut off and the area of the indicator diagram increases in Stirling cycle.

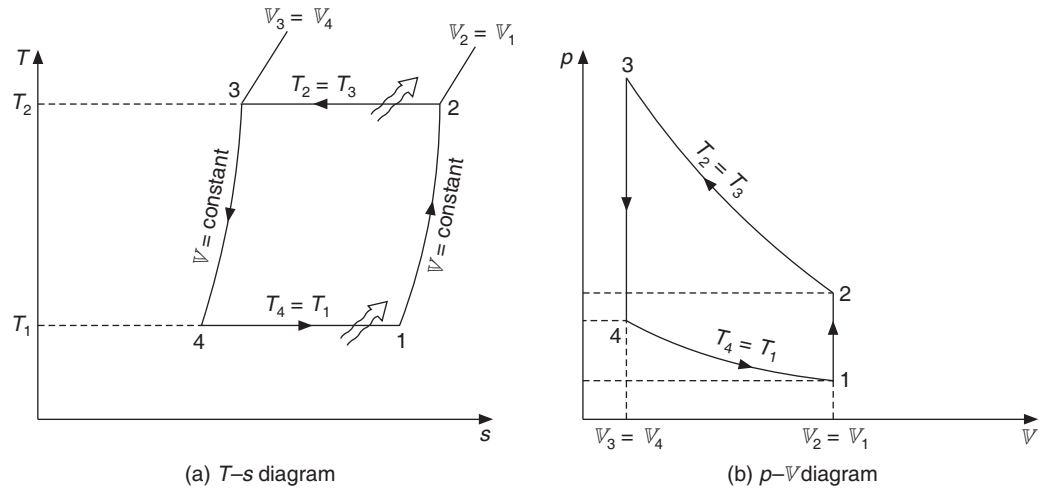

Figure 13.19 Ideal Reversed Sterling cycle.

A constant volume compression process 1–2 requires heat addition from temperature T_1 to T_2. Similarly, the constant volume heat rejection process 3–4 requires heat rejection from temperature T_2 to T_1. The heat rejection from the gas during 3–4 is used to heat the gas during 1–2.

This cycle can be easily achieved by arranging two opposed cylinders in thermal contact with each other as shown in Figure 13.20. The thermal contact between the cylinders is through a regenerator. Essentially the above two cycles are performed out of phase in the two cylinders. The

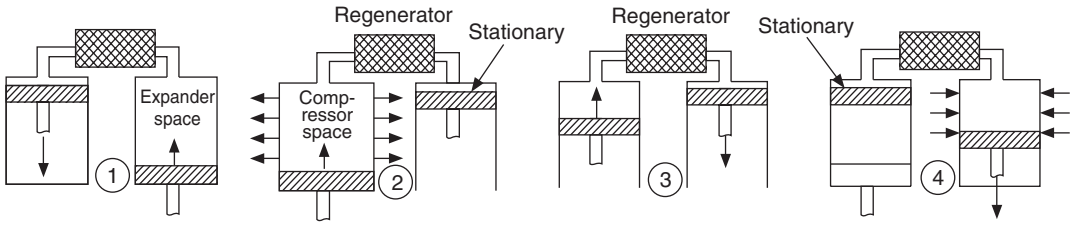

Figure 13.20 Practical Stirling cycle.

temperature of one cylinder follows the process 1–2 while that of the other cylinder follows 3–4 simultaneously by using opposed pistons. The left hand cylinder rejects heat to the surroundings (2–3) while the right hand cylinder accepts heat from the refrigerator (4–1).

Figure 13.20 shows the disposition of pistons at all the four terminal points. The processes executed are as follows:

Process 1–2: Both the pistons move from position 1 at the same speed displacing gas through the regenerator at constant volume. The regenerator is warm to start with. The cold gas from RH cylinder cools the regenerator. The gas temperature increases as it moves to LH cylinder. All the gas is heated and transferred to LH cylinder. It achieves temperature T_2.

Process 2–3: At position 2 all the gas is in left cylinder. Heat is rejected from LH cylinder to cooling medium while the piston moves. The RH piston remains stationary during this process. The motion of the piston in the LH cylinder compresses the gas isothermally by rejecting heat to the cooling medium.

Process 3–4: At position 3 while the LH piston is moving, the RH piston also starts to move at the same speed resulting in a constant volume process. The gas is transferred to the right cylinder through the cold regenerator. The regenerator becomes warm due to passage of warm gas.

Process 4–1: At position 4 all the gas has been transferred to the RH cylinder. The left cylinder becomes stationary while the right piston continues to move at the same speed. The gas in RH cylinder expands isothermally by accepting heat from the refrigerator until point 1 is reached.

The precise motion of the pistons described above cannot be achieved in practice. An approximation to this can be achieved by coupling the pistons through connecting rods and cranks that are out of phase usually by 90°. The resulting motion is sinusoidal. The indicator diagrams thus will not have sharp corners. The isothermal processes will also not be strictly isothermal.

J. Stirling invented this cycle in 1827. A.C. Kirk is credited with its application to refrigeration. He made a few machines. The constant pressure Joule cycle was more practical, hence the stirling cycle was forgotten for some time. J.W.L. Köhler reviewed this cycle and found that it offers advantages for refrigeration at low temperatures of the order of 150 K. This is the principle of the Philips air liquefaction machine as developed by Köhler and Jonkers (1954). The cycle in Philips machines is slightly different from the cycle described above. Temperatures as low as 12 K can be achieved by a two-stage cycle. There are many variations of the Stirling cycle as described by Walker (1973).

13.10.1 Analysis of Stirling Cycle

Figure 13.21 shows that the actual variation of piston motion is sinusoidal. The analysis of Stirling cycle is presented here. It involves the following assumptions.

(i) The instantaneous pressure is assumed to be the same throughout the system.

(ii) All heat exchangers including the regenerator are perfect.

(iii) The gas is assumed to be ideal.

If $\mathbb{V}_E$ and $\mathbb{V}_C$ are the maximum expander and compressor volumes respectively, then according to sinusoidal motion the instantaneous expansion and compression volumes $\mathbb{V}_e$ and $\mathbb{V}_c$ respectively are given by

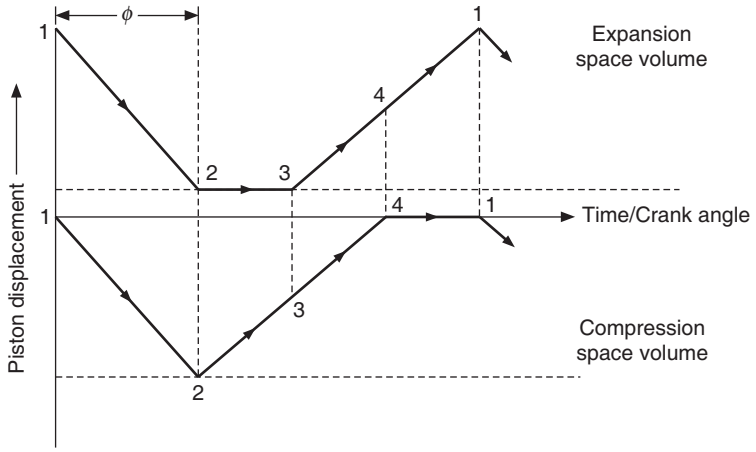

Figure 13.21 Cyclic piston displacement diagram.

$$\mathbb{V}_e = 0.5\ \mathbb{V}_E\,(1 + \cos\,\theta) \tag{13.147a}$$

$$\mathbb{V}_c = 0.5\ \mathbb{V}_C\,\{1 + \cos\,(\theta - \phi)\} \tag{13.147b}$$

where, θ is the crank angle and ϕ is the phase difference between the two pistons.

The total mass of gas in the expander, compressor and the dead space is given by

$$m_T = \frac{p_e \mathbb{V}_e}{RT_e} + \frac{p_c \mathbb{V}_c}{RT_c} + \frac{p_d \mathbb{V}_d}{RT_d} \tag{13.148a}$$

It is further assumed that instantaneous temperatures $T_e = T_E$ and $T_c = T_C$ since the compression and expansion are isothermal and heat exchangers are ideal. Hence, we get

$$m_T = \frac{p}{R}\left[0.5\,\frac{\mathbb{V}_E}{T_E}\,(1 + \cos\,\theta) + 0.5\,\frac{\mathbb{V}_C}{T_C}\,\{1 + \cos\,(\theta - \phi)\} + \frac{\mathbb{V}_d}{T_d}\right] \tag{13.148b}$$

Defining,

$$a = T_C/T_E,\ b = \mathbb{V}_C/\mathbb{V}_E \ \text{ and } \ c = \mathbb{V}_D T_C/(\mathbb{V}_E T_D) \tag{13.148c}$$

we get

$$\begin{aligned}\frac{2m_T RT_C}{p\mathbb{V}_E} &= a\,(1 + \cos\,\theta) + b\,\{1 + \cos\,(\theta - \phi)\} + 2c \\ &= a\,\cos\,\theta + b\,\cos\,(\theta - \phi) + a + b + 2c \\ &= a\,\cos\,\theta + b\,\cos\,\theta\,\cos\,\phi + b\,\sin\,\theta\,\sin\,\phi + a + b + 2c \\ &= \cos\,\theta\,(a + b\,\cos\,\phi) + b\,\sin\,\theta\,\sin\,\phi + a + b + 2c\end{aligned}$$

Assuming $a + b\,\cos\,\phi = e\,\cos\,\alpha$ and $b\,\sin\,\phi = e\,\sin\,\alpha$, the above expression can be further simplified as follows:

$$\frac{2m_T RT_C}{p\mathbb{V}_E} = \sqrt{a^2 + b^2 + 2ab\,\cos\,\phi}\,\cos\,(\theta - \alpha) + a + b + 2c \tag{13.149}$$

This is rewritten as follows:

$$\frac{K}{p} = \beta\{1 + \delta\cos(\theta - \alpha)\} \tag{13.150}$$

where, $K = 2m_T RT_C/\mathbb{V}_E$, $\beta = a + b + 2c$ and $\delta = \sqrt{(a^2 + b^2 + 2ab\cos\phi)}/\beta$

or
$$p = \frac{K}{\beta\{1 + \delta\cos(\theta - \alpha)\}} \tag{13.151}$$

Therefore the pressure is minimum at $\theta = \alpha$ and $p_{\min} = \dfrac{K}{\beta(1+\delta)}$ (13.152a)

And pressure is maximum at $\theta = \alpha + \pi$ and $p_{\max} = \dfrac{K}{\beta(1-\delta)}$ (13.152b)

Accordingly Eq. (13.151) for pressure may be written either in terms of $p_{\min}$ or $p_{\max}$ as follows:

$$p = p_{\max}\frac{1-\delta}{1+\delta\cos(\theta-\alpha)} \quad \text{and} \quad p = p_{\min}\frac{1+\delta}{1+\delta\cos(\theta-\alpha)} \tag{13.153}$$

Mean pressure may be found by integrating pressure over one cycle from $(\theta - \alpha) = 0$ to 2π.

$$p_{\text{mean}} = \frac{1}{2\pi}\int_0^{2\pi} p\,d\psi = \frac{1}{2\pi}\int_0^{2\pi} p_{\max}\frac{1-\delta}{1+\delta\cos\psi}\,d\psi = p_{\max}\sqrt{\frac{1-\delta}{1+\delta}} \tag{13.154}$$

The pressures depend upon the mass of the gas charged into the system. The maximum pressure, the minimum pressure and the mean pressure are related as above.

13.10.2 Heat Transfer and Work Done in Stirling Cycle

Heat transfer is equal to work done during isothermal expansion and compression since during these processes internal energy does not change.

Refrigeration effect

This is equal to work done or heat transfer during the expansion process, that is,

$$Q_E = W_E = \int_0^{2\pi} p\,d\mathbb{V}_e \tag{13.155}$$

Substituting $\mathbb{V}_e = \mathbb{V}_E(1 + \cos\theta)/2$ or $d\mathbb{V}_e = -0.5\,\mathbb{V}_E \sin\theta\,d\theta$, we get

$$W_E = -\mathbb{V}_E\frac{p_{\max}}{2}(1-\delta)\int_0^{2\pi}\frac{\sin\theta}{1+\delta\cos(\theta-\alpha)}\,d\theta$$

Substituting $\theta - \alpha = \psi$, we get

$$W_E = -\mathbb{V}_E\frac{p_{\max}}{2}(1-\delta)\int_{-\alpha}^{2\pi-\alpha}\frac{\sin(\psi+\alpha)}{1+\delta\cos\psi}\,d\psi$$

or $$W_E = -\mathbb{V}_E \frac{p_{\max}}{2}(1-\delta)\left[\sin\alpha \int_{-\alpha}^{2\pi-\alpha} \frac{\sin(\psi+\alpha)}{1+\delta\cos\psi}\,d\psi + \cos\alpha \int_{-\alpha}^{2\pi-\alpha} \frac{\sin(\psi+\alpha)}{1+\delta\cos\psi}\,d\psi\right]$$

Substituting for the integrals, we get

$$W_E = -\mathbb{V}_E p_{\max} \sin\alpha \frac{\pi(1-\delta)}{\delta}\left(\frac{\sqrt{1-\delta^2}-1}{\sqrt{1-\delta^2}}\right)$$
$$Q_E = W_E = -\mathbb{V}_E p_{\text{mean}} \sin\alpha \frac{\pi}{\delta}(\sqrt{1-\delta^2}-1) \tag{13.156}$$

Heat rejection during compression

This is given by

$$Q_C = W_C = \int_0^{\pi} p\,d\mathbb{V}_c$$

Substituting $\mathbb{V}_c = b\mathbb{V}_E(1+\cos(\theta-\alpha))/2$ or $d\mathbb{V}_c = -0.5\,b\mathbb{V}_E \sin(\theta-\alpha)\,d\theta$, we get

$$Q_C = -b\mathbb{V}_E \frac{p_{\max}}{2}(1-\delta)\int_0^{\pi} \frac{\sin(\theta-\pi)}{1+\delta\cos(\theta-\alpha)}\,d\theta$$
$$Q_C = -b\mathbb{V}_E \frac{p_{\max}}{2}\frac{(1-\delta)}{\delta}\ln\frac{(1-\delta\cos\alpha)}{(1+\delta\cos\alpha)} \tag{13.157}$$
$$Q_C = -b\mathbb{V}_E \frac{p_{\text{mean}}}{2}\frac{\sqrt{1-\delta^2}}{\delta}\ln\frac{(1-\delta\cos\alpha)}{(1+\delta\cos\alpha)}$$

COP = $T_E/(T_C - T_E)$ which is same as the Reversed Carnot expression. Similarly, the work done is also the same as that for the Reversed Carnot cycle.

13.10.3 Optimum Design Parameters for Stirling Cycle

There are two pistons and two volumes in Stirling cycle. Hence the product of the total swept volume, $\mathbb{V}_T$ and maximum pressure $p_{\max}$ is used as a parameter for power input. The performance index or the specific refrigeration effect is defined as follows.

$$\frac{Q_E}{p_{\max}\,\mathbb{V}_T} = \frac{\pi(\sqrt{1-\delta^2}-1)\sqrt{1-\delta}}{(1+b)\delta(1+\delta)}\sin\alpha \tag{13.158}$$

This is nondimensional refrigeration effect. If p_{mean} is used for nondimensionalization, then we get

$$\frac{Q_E}{p_{\text{mean}}\,\mathbb{V}_T} = \frac{\pi(\sqrt{1-\delta^2}-1)\sqrt{1-\delta}}{(1+b)\delta(1-\delta)}\sin\alpha \tag{13.159}$$

It is observed that the performance index is a function of δ, b and sin α. It is directly proportional to:

(i) Speed of the pistons
(ii) Total mass of the charge or the maximum pressure
(iii) Total volume of the charge, $\mathbb{V}_T$

The friction between the cylinder and the wall increases as the speed increases, hence at larger speeds Q_E may tend to decrease. Increase in the mass of the charge also has a limit decided by the storing capacity of regenerator, which reaches a saturation value for a certain charge. The areas of the heat exchangers for heat rejection and absorption also put a limit on the charge. Hence there are optimum values of speed and charge beyond which Q_E may decrease.

Equation (13.158) for the specific refrigeration effect involves the temperature ratio a, volume ratio b, phase lag between the cylinders ϕ and the dead volume ratio $X = \mathbb{V}_D/\mathbb{V}_E$. These parameters also have to be optimized. Just like other refrigeration systems, Q_E increases as the parameter $a = T_C/T_E$ decreases, that is, as T_E increases or as T_C decreases. As the volume ratio $b = \mathbb{V}_C/\mathbb{V}_E$ increases, Q_E increases. It decreases as the dead volume ratio increases, hence the dead volume should be kept as small as possible. It is optimum at approximately phase angle difference of 90° but it is fairly constant between phase angle differences of 60° and 120°.

EXAMPLE 13.16 An ideal Stirling cycle operates at 720 rpm between $T_C = 300$ K, $T_E = 250$ K and same cylinder volumes $\mathbb{V}_C = \mathbb{V}_E = 5 \times 10^{-5}$ m^3. The dead volume ratio is 1.5 and the phase angle difference between the two cylinders ϕ is 90°. The maximum pressure is 20 bar. Find the refrigeration capacity, the power requirement, and the mean and minimum pressures.

Solution:

$$a = T_C/T_E = 300/250 = 1.2;\ b = \mathbb{V}_C/\mathbb{V}_E = 1.0 \text{ and } \phi = 90^\circ$$

From Eq. (13.148c), $c = (\mathbb{V}_E/\mathbb{V}_C)(T_C/T_E) = 1.2$

From Eq. (13.150), $\beta = a + b + 2c$ and $\delta = \sqrt{(a^2 + b^2 + 2ab\cos\phi)}/\beta$

$$\beta = 1.2 + 1.0 + 2.4 = 4.6 \text{ and } \delta = \sqrt{(1.44 + 1.0)}/4.6 = \sqrt{2.44}/4.6 = 0.3395$$

$$\tan\alpha = \frac{b\sin\phi}{a + b\cos\phi} = \frac{b}{a} = \frac{1}{1.2}.\ \text{Hence } \alpha = 39.806^\circ$$

$\therefore$ $\sin\alpha = 0.6402$

Substituting in Eq. (13.158), we get

$$\frac{Q_E}{p_{\max}\,\mathbb{V}_T} = 0.1235$$

$$Q_E = 0.1235\ (20 \times 10^5)\ 2 \times 5 \times 10^{-5} = 24.7 \text{ J/cycle}$$

$$\dot{Q}_E = Q_E N/60 = 24.7(720)/60 = 296.4 \text{ W}$$

$$\text{COP} = T_E/(T_C - T_E) = 1/(\alpha - 1) = 1/(1.2 - 1) = 5.0$$

$$\dot{W} = \frac{Q_E}{\text{COP}} = 59.28 \text{ W}$$

$$p_{\text{mean}} = p_{\max}\sqrt{\frac{1-\delta}{1+\delta}} = 14.043 \text{ bar}$$

$$p_{\min} = p_{\max}\frac{1-\delta}{1+\delta} = 9.862 \text{ bar}$$

13.10.4 Actual Stirling Cycle

The above mentioned analysis is for an ideal cycle. In a practical Stirling cycle, there are a number of deviations from the ideal case. Some of these are as follows:

1. It is difficult to achieve isothermal compression and expansion. These processes will involve some temperature variation. Finkelstan has considered this aspect.
2. Regenerator may not be ideal, that is, during expansion the gas temperature may be greater than T_E and during compression less than T_C.
3. Frictional losses in compressor, expander, regenerator and heat exchanger may not be negligible. This will lead to pressure drops in these components.
4. The system is not perfectly insulated. Hence, there may be heat loss from hot gas and heat gain by cold gas which may decrease the refrigeration effect.
5. The dead volume may be large, which will decrease the COP.

13.11 AIR LIQUEFACTION CYCLES

The lowest temperature that can be achieved by vapour compression refrigeration system by using R14 in a cascade system, is –150°C. This leaves a gap of 123 K between this temperature and the absolute zero. In this range, liquefied gases are used to achieve refrigeration and the term *cryogenics* is used to describe these applications. Cryogenics involves research into the behaviour of materials near absolute zero. Adiabatic demagnetization is used to realize temperatures near absolute zero. Cryogenics is a broad field of study, the liquefaction of gases being an important aspect.

Oxygen, nitrogen, argon, neon, xenon and krypton are constituents of air. These are obtained by liquefaction and separation from atmospheric air. Pure hydrogen may be obtained by separation from coke-oven gas. Helium may be obtained by separation from helium bearing natural gas. Liquid oxygen finds many applications including steelmaking. It is used as oxidant in rocket propulsion.

13.11.1 Minimum Work Required to Liquefy a Gas

To liquefy a gas, heat must be withdrawn from gas and rejected to atmosphere at high temperature. It is impossible to achieve this process without work input due to second law limitation. The work input will be minimum if the processes involved are reversible. Figure 13.22(a) shows the schematic diagram of a reversible arrangement for liquefaction and Figure 13.22(b) shows the *T*–*s* diagram for this cycle. It involves isothermal compression of dry gas from state 1 at atmospheric pressure and temperature to state 2 at very high pressure. This is followed by isentropic expansion of the gas to saturated liquid state 3.

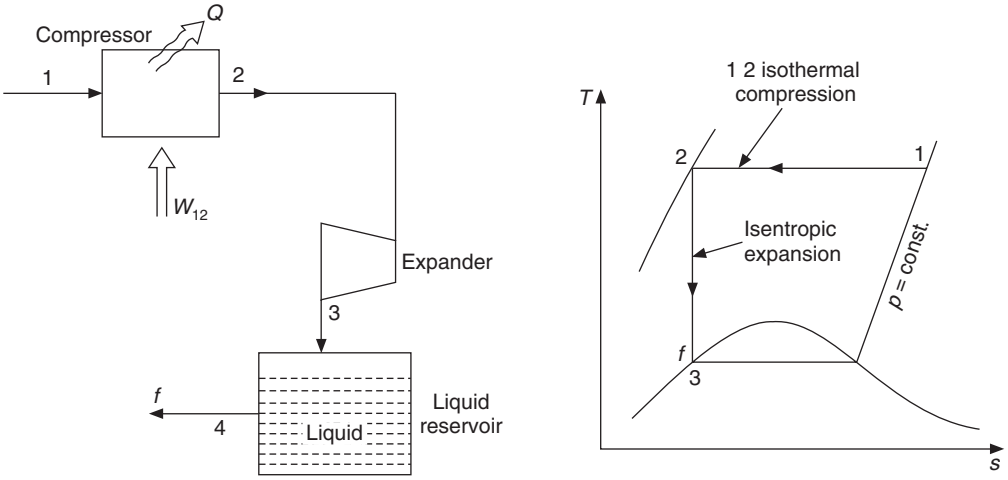

(a) Schematic diagram (b) *T s* diagram

Figure 13.22 The thermodynamically ideal liquefaction system.

Dry gas is isothermally and reversibly compressed from state 1 at atmospheric temperature and pressure to state 2 at very high pressure. The compressed gas is isentropically expanded from state 2 in a frictionless expander to state 3, which is saturated liquid state. For steady state process, we may write on per unit mass flow rate basis,

$$W_{12} = h_2 - h_1 + T_1(s_1 - s_2) \tag{13.160a}$$

$$W_{23} = h_2 - h_3 \tag{13.160b}$$

$$\therefore \quad W_{net} = W_{12} - W_{23} = T_1(s_1 - s_3) - (h_1 - h_3) \tag{13.161}$$

Equation (13.161) may be generalized in the form

$$W_{min} = T_0(s_0 - s_f) - (h_0 - h_f) \tag{13.162}$$

This is the minimum work requirement per kg of liquid gas produced. The actual work requirement is many times more than this. This system however is not practical since the pressure at point 2 is prohibitively large and irreversibility in the expander will be very large.

There are two main problems associated with liquefaction. Firstly, the irreversibility becomes very large at low temperatures. The entropy change associated with isothermal heat transfer is expressed as

$$\Delta s = (\Delta q)_{rev}/T \tag{13.163}$$

If we consider 1 J of isothermal heat transfer from 1 kg of gas at 300 K and also at 5 K temperature, the entropy change associated with it is 0.033 J/kg-K and 0.2 J/kg-K respectively. Obviously, the entropy change at 5 K is very large. This is what is meant by irreversibility being large at low temperatures. If this heat transfer at 5 K has to be ultimately rejected to atmosphere then enormous amount of work is required.

The second problem is that irreversibility during expansion to low temperature may be so large that restrained expansion alone may not liquefy the gas. Unrestrained expansion or throttling

is also required along with restrained expansion. Throttling does not always lead to cooling. This throttling process is of great importance hence we consider it here.

Throttling is a constant enthalpy process. For cooling to be produced by throttling process, the temperature must decrease as the pressure decreases, that is the derivative $(\partial T/\partial p)_h$ must be positive. This gradient is called the Joule–Thomson coefficient.

$$\mu = (\partial T/\partial p)_h \tag{13.164}$$

If $\mu < 0$, the temperature of the gas increases during expansion. An expression for μ may be obtained from the second fundamental relation of thermodynamics, that is,

$$ds = \frac{1}{T}\,dh - \frac{v}{T}\,dp \tag{13.165}$$

Since ds is an exact differential, we must have

$$\frac{\partial}{\partial p}\left(\frac{1}{T}\right)_h = -\frac{\partial}{\partial h}\left(\frac{v}{T}\right)_p = -\frac{\partial}{\partial T}\left(\frac{v}{T}\right)_p \left(\frac{\partial T}{\partial h}\right)_p \tag{13.166}$$

Simplifying it, we get

$$-\frac{1}{T^2}\left(\frac{\partial T}{\partial p}\right)_h = -\left[\frac{1}{T}\left(\frac{\partial v}{\partial T}\right)_p - \frac{v}{T^2}\right]\left(\frac{\partial T}{\partial h}\right)_p$$

By definition, $c_p = \left(\frac{\partial h}{\partial T}\right)_p$. Hence, we get

$$\mu = \frac{1}{c_p}\left[T\left(\frac{\partial v}{\partial T}\right)_p - v\right] \tag{13.167}$$

This equation is valid for liquids as well as gases. Joule Thomson coefficient may be found if the equation of state is known. For ideal gases,

$$pv = RT \quad \text{and} \quad \left(\frac{\partial v}{\partial T}\right)_p = \frac{R}{p} = \frac{v}{T} \tag{13.168}$$

For ideal gas, the Joule–Thomson coefficient is always zero. The value of Joule–Thomson coefficient is a measure of deviation from ideal gas behaviour. The value of μ may be either negative or positive depending upon pressure and temperature. The temperature at which μ is equal to zero, is called *inversion temperature* for a given pressure. Figure 13.23 schematically shows the *T–p* diagram for a gas. The constant enthalpy lines are shown by solid lines. Along each line μ is negative and becomes positive as one proceeds towards lower pressures. The temperature at which μ is equal to zero is called *inversion temperature*. It is observed that along constant enthalpy lines *a–b* and *c–d* the slope of constant enthalpy lines does not change, hence inversion does not occur along these lines. The constant enthalpy line *e–f* and all other lines show a peak where μ becomes zero. The *inversion temperature curve* may be drawn by joining peaks of constant enthalpy lines. It is observed that the inversion temperature of gas decreases with increase in pressure. The temperature increases with decrease in pressure on the left hand side of the inversion line, that is, μ is negative in this region. Other gases also behave in a similar manner.

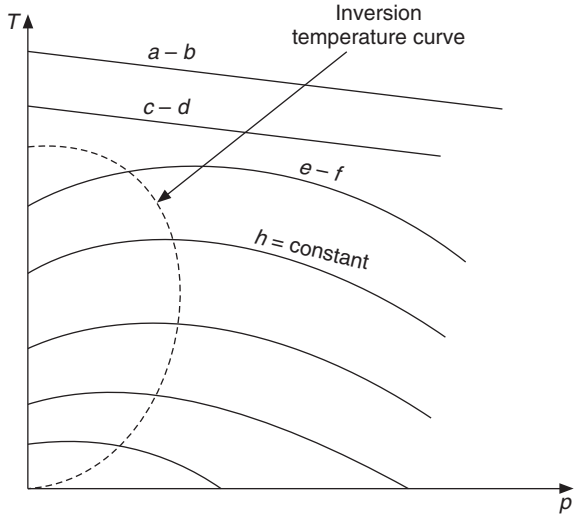

Figure 13.23 Constant enthalpy curves and the inversion curve of a real gas.

13.11.2 Linde Air-Liquefaction Cycle

Linde in Germany and Hampson in England developed this cycle simultaneously in 1895. This is the most elementary air-liquefaction cycle. It consists of an isothermal compressor, a cooler, a heat exchanger, an expansion valve and a separator as shown in Figure 13.25(a). The *T*–*s* diagram of the cycle is shown in Figure 13.24(b). The heat exchanger and separator are assumed to be perfectly insulated.

The compressor is a multi-stage compressor, which compresses dry air at ambient conditions to a very high pressure in the range of 50–200 atmospheres from state 1 to state 2. The compressed air has to be cooled to maximum possible extent so that a higher value of Joule–Thomson coefficient and a higher degree of cooling may be obtained during Joule–Thomson expansion. Hence the compressed air is first cooled from state 2 to state 3 by water from a cooling tower. The cold air from the separator that could not be liquefied returns at state 7 to the heat exchanger. This cold air cools the compressed air further to a lower temperatures in the heat exchanger. The air is cooled sufficiently to state 4 so that liquid air can be obtained after J–T expansion to one atmospheric pressure.

The expansion actually ends in a mixture region at state 5. The liquid air at state 6 is removed in the separator and the cold air at low temperature state 7 flows back to heat exchanger where it regeneratively cools the high-pressure air before being fed to J–T valve. This stream after providing cooling is fed back to the compressor along with some make-up air. The amount of make-up air is same as that of the liquefied air.

If the temperature of the air stream leaving the heat exchanger is less than the inversion temperature at that pressure, the system can pull down to conditions of liquefaction. The lower the temperature after heat exchanger the smaller will be the pull-down period. The pull-down period is the time required for the first drop of liquid to appear after the plant is started. The mechanical vapour compression system is sometimes used to cool the air before entry to heat exchanger so as to reduce the pull-down period. The state when the liquefaction of air starts will be the steady state.

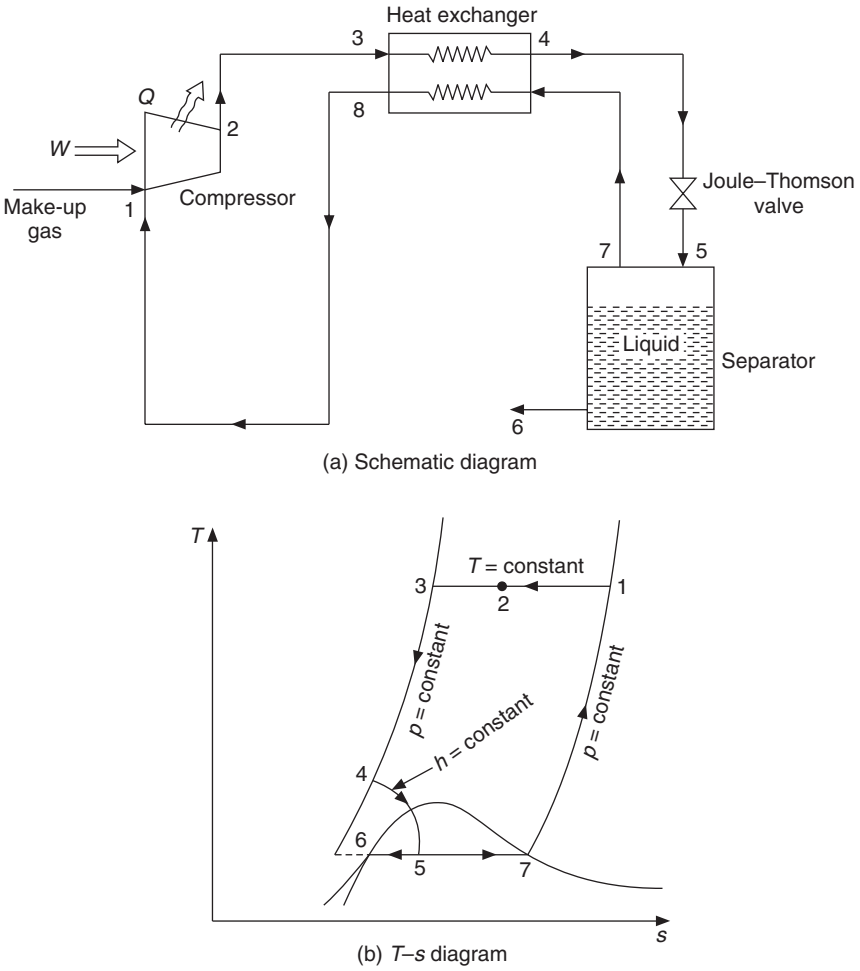

Figure 13.24 The Linde–Hampson air liquefaction system.

To get an idea about pull-down, we look at the sequence of events by tracing the air temperature as the first kg enters it at ambient conditions and trace out the successive kg of air as it is sequentially cooled.

Let us say that the first kg of air enters the heat exchanger at point 3 at 35°C. It leaves the HEX at point 4 at 35°C since cold air is not available at state 7. The temperature of this air decreases to say 5°C as it expands to state 5. It passes through the separator and whole of one kg returns at 5°C state 7 to the HEX since no liquefaction occurs.

The second kg of ambient air entering the HEX is cooled by this stream from 35°C to say 5°C if the HEX is perfect. The second kg of air enters the expansion valve at 5°C. Its temperature will reduce to say –35°C after expansion. The whole of second kg also returns to the HEX at state 7 since no liquefaction occurs. The first kg of air was cooled by 30°C while the second kg is cooled by 40°C after expansion. The cooling is more since the Joule–Thomson coefficient is larger at lower temperature.

The third kg will be cooled by even larger extent after expansion and the subsequent kg by still larger extent. Ultimately, air is sufficiently cooled by the return air so that after expansion it ends up in two-phase region at state 4 where liquid is separated and cold gaseous air is returned to heat exchanger.

It is worth noting that some gaseous air has to be returned which will precool the air entering the expansion valve. All the air entering the expansion valve cannot be liquefied. If that were to happen, then precooling will not occur and liquefaction will also not occur.

Analysis

At steady state mass and energy conservation is carried out for the combination of separator and heat exchanger. This yields

$$\dot{m}_3 = \dot{m}_6 + \dot{m}_8 \tag{13.169}$$

$$\dot{m}_3 h_3 = \dot{m}_6 h_6 + \dot{m}_8 h_8 \tag{13.170}$$

Substituting for $\dot{m}_8$ from Eq. (13.169) into Eq. (13.170),

$$\dot{m}_3 (h_3 - h_8) = \dot{m}_6 (h_6 - h_8)$$

The yield Z_L is defined as the ratio of liquefied air quantity to the compressed air quantity. The subscript L refers to Linde cycle. The above equation gives

$$Z_L = \frac{m_6}{m_3} = \frac{h_8 - h_3}{h_8 - h_6} \tag{13.171}$$

If an isothermal compression is assumed, then

$$Tds = dh - vdp$$

$$\therefore \quad -\int_1^2 v\,dp = \int_1^2 T\,ds - \int_1^2 dh = T_1 (s_2 - s_1) - (h_2 - h_1)$$

$$\therefore \quad \left| W_{12} \right| = T_1 (s_1 - s_2) - (h_1 - h_2) \tag{13.172}$$

In Figure 13.24 if the compression is isothermal then point 2 will lie on a horizontal line through 1, that is, at state a. The specific work requirement is defined in terms of kW of power per kg of liquid air produced.

$$\therefore \quad W_{Z,L} = \frac{m_3 (W_{12})}{m_6} = \frac{W_{12}}{Z_L} = [T_1 (s_1 - s_2) - (h_1 - h_2)] \frac{(h_8 - h_6)}{(h_8 - h_3)} \tag{13.173}$$

According to Eq. (13.171), the yield of Simple Linde cycle depends on states 3, 6 and 8. The denominator $(h_8 - h_6)$ is very large compared to the numerator $(h_8 - h_3)$. In the numerator h_8 must be greater than h_3 otherwise a negative number appears which has no meaning. The temperature t_8 does not have to be greater than t_3 since states 8 and 3 are at different pressures, actually t_3 is greater than t_8. The difference in enthalpy $(h_8 - h_3)$ is the most crucial factor since a small change in it may change the yield drastically. The best results are obtained for large values of enthalpy h_8 and small values of h_3. Hence sometimes, refrigeration system may be used to reduce the temperature t_3 and h_3.

Further inspection of the *T*–*s* diagram for air reveals that for isentropic compression, h_2 decreases with increase in pressure until the inversion pressure. Beyond the inversion pressure, h_2 increases with increase in pressure. Linde cycle is not very efficient, just like the SSS cycle which is also not very efficient at low temperatures.

13.11.3 Claude Air-Liquefaction Cycle

If the gas that is at high pressure, is made to do some work, its enthalpy will decrease resulting in a decrease in temperature. This is referred to as restrained expansion where the high-pressure air moves the piston of a reciprocating engine or rotates a turbine to yield some power output. This process yields a significant drop in temperature for ideal gas as well. The throttling process does not yield any work output. The pressure drop is by an irreversible expansion, which leads to a temperature drop if the Joule–Thomson coefficient is positive. This is referred to as unrestrained expansion. The Joule–Thomson coefficient is zero for ideal gas, hence unrestrained expansion of an ideal gas does not result in temperature drop. The expanders, however, cannot be used for large pressure drops. Further, the expander can be used only in the vapour region due to operational problems caused by liquid droplets striking the blades and increasing its wear and tear.

At low temperatures the conduction losses are very large and as it is, the irreversibilities are also very large. Isentropic restrained expansion therefore is not practically feasible. There are large deviations due to conduction heat transfer from say –185°C to room temperature and due to frictional irreversibility.

Fortunately despite this, restrained expansion gives a larger temperature drop than that given by unrestrained expansion. However it cannot be used alone for liquefaction since it cannot be used in two-phase region. Therefore it is used along with the Joule–Thomson valve. This combination gives the advantage that the system can work at lower pressures and give higher yield. Claude cycle does this by including an expansion engine and additional heat exchangers in addition to the components used in Linde cycle.

It was pointed out that at lower temperatures the Joule–Thomson coefficient is large and therefore the air must be cooled to maximum possible extent. The expander is essentially used for additional cooling of the air before it enters the J–T expansion valve. Its work output is usually wasted since its use will require a sophisticated and expensive control system. The schematic diagram is shown in Figure13.25(a) and the *T*–*s* diagram of the cycle is shown in Figure 13.25(b).

For convenience of analysis consider a control volume that includes both the heat exchangers and the separator. The mass and energy conservation yields the following two equations:

$$\dot{m}_3 = \dot{m}_7 + \dot{m}_{12} \tag{13.174}$$

$$\dot{m}_3 h_3 + \dot{m}_9 h_9 = \dot{m}_7 h_7 + \dot{m}_{12} h_{12} + \dot{m}_9 h_4 \tag{13.175}$$

Substituting for $\dot{m}_{12}$ from Eq. (13.174) into Eq. (13.175), we get

$$\dot{m}_3 h_3 + \dot{m}_9 h_9 = \dot{m}_7 h_7 + (\dot{m}_3 - \dot{m}_7) h_{12} + \dot{m}_9 h_4$$

or
$$(h_{12} - h_3) = (h_{12} - h_7)\dot{m}_7 / \dot{m}_3 + (h_9 - h_4)\dot{m}_9 / \dot{m}_3 \tag{13.176}$$

$\therefore$
$$Z_C = \frac{m_7}{m_3} = \frac{(h_{12} - h_3)}{(h_{12} - h_7)} + \frac{m_9}{m_3}\frac{(h_4 - h_9)}{(h_{12} - h_7)} \tag{13.177}$$

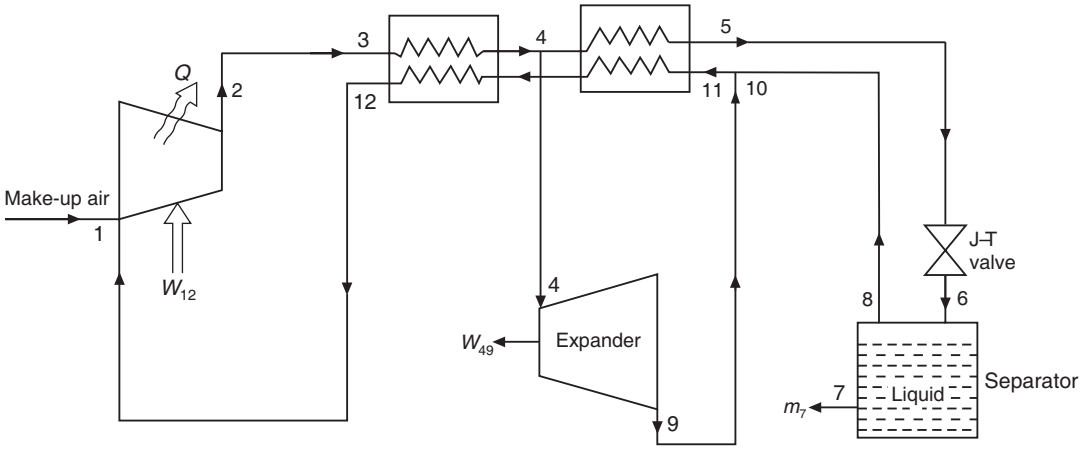

(a) Schematic diagram

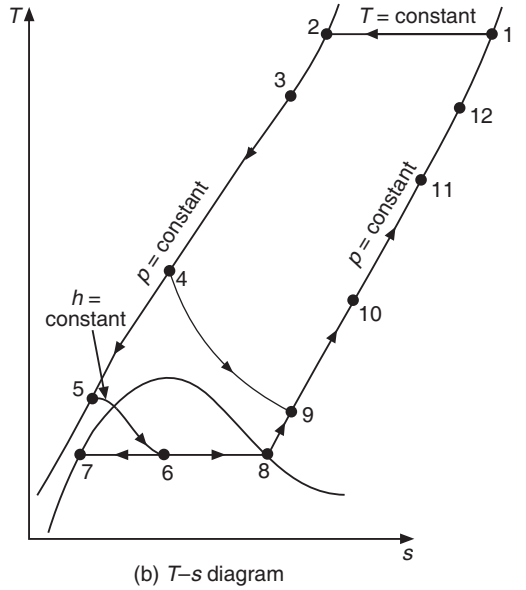

(b) *T–s* diagram

Figure 13.25 The Claude air-liquefaction system.

$$\therefore \quad Z_C = Z_L + \frac{m_9}{m_3}\frac{(h_4 - h_9)}{(h_{12} - h_7)} \tag{13.178}$$

It is obvious from Eq. (13.171) that the yield of Claude cycle is more than the yield of Linde cycle.

Assuming isothermal compression the work required is obtained by integrating the second fundamental equation of thermodynamics, namely $Tds = dh - vdp$

$$\therefore \quad W_{12} = T_1 (s_1 - s_2) - (h_1 - h_2)$$

The specific work requirement may be defined as the work per kg of liquid air produced. To find the net work the work recovered in turbine W_{49} on mass flow rate of $\dot{m}_9$ is subtracted from the isothermal work input to the compressor W_{12} on mass flow rate of $\dot{m}_3$. The mass flow rate of liquid air rate produced is $\dot{m}_7$. Therefore

$$W_{Z,C} = \frac{m_3 W_{12} - m_9 W_{49}}{m_7} = \frac{W_{12}}{Z_C} - \frac{m_9}{m_7} W_{49} = \frac{T_1(s_1 - s_2) - (h_1 - h_2)}{Z_C} - \frac{m_9}{m_7} W_{49}$$

The pressure ratio of Claude cycle is always less than that in Linde cycle. However for comparison purpose we assume that the pressure ratio is same for both Linde and Claude cycles. In such a case the work requirement of isothermal compressor W_{12} will be same for both the cycles and may be denoted as W_L. Then, substituting Z_C from Eq. (13.179), we get

$$W_{Z,C} = \frac{W_L}{Z_L + \dfrac{m_9 (h_4 - h_9)}{m_3 (h_{12} - h_7)}} - \frac{m_9}{m_7} W_{49}$$

It is also observed that the specific work requirement of Claude cycle is less than that of Linde cycle.

REVIEW QUESTIONS

1. Discuss the limitations of the Reversed Carnot cycle with gas as refrigerant.
2. Discuss the Bell–Coleman cycle (Reversed Brayton cycle) for gas refrigeration with the help of schematic, *T–s* and *p–v* diagrams. Explain the effect of pressure ratio on the performance of this cycle.
3. How does the actual Bell-Coleman cycle differ from the ideal cycle?
4. In a gas cycle refrigeration system working on Bell–Coleman cycle, the pressure ratio is 10.0. Air is drawn from the cold chamber at 263 K and the temperature at inlet to the turbine is 323 K. The working substance is air. The isentropic compressor and turbine efficiencies are 0.8 and 0.85 respectively. Determine the mass flow rate, heat rejection, compressor work, turbine work, COP and the volume flow rates at inlet to compressor and at outlet of turbine for a system of 1 TR cooling capacity.
5. For the cycle described in Question 4, determine the conditions for maximum COP and its value. Also determine the temperatures at compressor and turbine outlets, mass flow rate, compressor work, turbine work, and volume flow rates.
6. For the data of Question 5, determine all the parameters of the cycle taking into account that the pressure drop in the air-cooler is 3% of pressure and in the refrigerator it is 5% of the pressure. Also, find the pressure ratio at which the COP would become zero.
7. If in Question 4 the compressor and turbine efficiencies are both equal to 0.9, find the pressure ratios corresponding to zero and maximum COP for the case when the temperature difference between the fluids in the regenerative heat exchanger (when employed) is 3 K.

8. Why do aircraft require air conditioning? What are the advantages of using gas cycle refrigeration for aircraft air conditioning?
9. State the various air refrigeration cycles used for aircraft air conditioning and discuss their utility vis-a-vis the aircraft size and speed.
10. An aircraft is flying at a speed of 1.2 Mach. The ambient temperature and pressure at the altitude of the aircraft are –40°C and 0.2 bar respectively. The aircraft employs the simple air refrigeration system, maintaining the temperature of the cabin at 25°C and pressure at 1.0 bar. The pressure ratio of the compressor is 5. Assume the compressor, turbine and ram efficiencies to be 0.85, 0.75 and 0.9 respectively. Take $\gamma = 1.4$ and $c_p = 1$ kJ/kg-K, and the heat exchanger effectiveness to be 0.8. The pressure drop in the heat exchanger is 0.1 bar.

    Find the temperature and pressure at various state points, COP, mass flow rate, ram work, compressor work, turbine work and volume flow rates at turbine and compressure outlets for a 10 TR capacity plant.
11. The ambient temperature and pressure at the altitude of an aircraft are 0.9 bar and 10°C respectively. The pressure of ramming air is 1.013 bar. The temperature of the air is reduced by 50°C in the heat exchanger. The pressure in the cabin is 1.01 bar. The temperature of the air leaving the cabin is 25°C. The pressure of the compressed air is 3.5 bar. Assume the compression and expansion efficiencies to be both equal to 0.9. Determine the temperature and pressure at various state points, the COP, and the power required to take the cooling load of 10 TR in the cabin. Also, sketch the cycle on the *T*–*s* diagram.
12. An aircraft that has a bootstrap refrigeration system flies at an altitude where the ambient conditions are 5°C and 0.85 bar. The air pressure rises to 1.1 bar after the ramming action. The pressure at the aircraft main compressor discharge is 3.5 bar and this air is further compressed in the secondary compressor to 4.8 bar. The isentropic efficiencies of the main compressor, secondary compressor and turbine are 0.9, 0.9 and 0.8 respectively. The effectiveness of the main and auxiliary heat exchangers are 0.6 and 0.7 respectively. The pressure drop in both the heat exchangers is negligible. The cabin is maintained at 1 bar and 25°C. Calculate the COP and the power required per ton of refrigeration.
13. An aircraft flies at a speed of 1500 km/h. It employs a reduced ambient air refrigeration system. The ambient temperature and pressure are 10°C and 0.8 bar. The exhaust air of the auxiliary turbine that runs on ram air, cools the compressed air in the heat exchanger. The exhaust air leaves the auxiliary turbine at a pressure of 0.8 bar. The air from the main compressor at 6 bar is cooled in the heat exchanger and leaves it at 100°C. The cabin pressure and temperature are 1 bar and 20°C respectively. The isentropic efficiency for the main compressor is 0.85. The isentropic efficiency for both of the cooling turbines is 0.8. Draw the *T*–*s* diagram. Find the mass flow rate of air supplied to cabin for 1 TR cooling capacity, quantity of air passing through the heat exchanger if the temperature rise of ram air is limited to 80 K, the power used to drive the cooling fan, and the COP of the system.
14. An aircraft that employs a bootstrap refrigeration system flies at an altitude where the ambient conditions are 20°C and 0.9 bar. The pressure of air is increased from 0.9 bar to 1.1 bar by the ramming action. The pressures of air leaving the main and auxiliary compressors are 3 bar and 4 bar respectively. The isentropic efficiencies of compressors and turbine are 0.85

and 0.8 respectively. 50% of the total heat of air leaving the main compressor is removed in the first heat exchanger and 30% of their total heat of air leaving the auxiliary compressor is removed in the second heat exchanger using ram air. The cabin pressure and temperature are maintained at 1.02 bar and 25°C. The raming action is assumed to be isentropic. Find the power required for 1 TR cabin load. Also, find the COP of the system.

15. An aircraft that uses a simple aircraft refrigeration system with evaporative cooling flies at an altitude where the ambient pressure and temperature are 0.9 bar and 25°C respectively. The ramming action increases the pressure of air from 0.9 bar to 1 bar. The air leaves the main compressor at a pressure of 3.5 bar and its 50% heat is removed in a ram air-cooled heat exchanger and then this air passes through an evaporator for further cooling. The temperature of the air in the evaporator is reduced by 10°C. The air from the evaporator is passed through the cooling turbine and then supplied to the cabin at 1.03 bar at 25°C. The isentropic efficiency of the compressor and turbine are 0.75 and 0.7 respectively. Find the power required per ton of cooling load and the COP of the system.

16. Briefly describe the principle of operation of the vortex tube. What are its advantages and disadvantages?

17. Explain the cooling principle of pulse tube.

18. How does an actual Stirling cycle differ from the ideal cycle?

19. What is cryogenics? Explain the principle of operation of an ideal gas liquefaction system.

20. Discuss the working of Linde air-liquefaction cycle with the help of a block diagram and its *T–s* diagram.

14

Water—Steam Ejector—Refrigeration System and Thermoelectric Refrigeration System

LEARNING OBJECTIVES

After studying this chapter the student should be able to:

1. Understand the advantages and limitations of water as refrigerant.
2. Describe the principle of operation of a simple water refrigeration system.
3. Describe the principle of operation of a centrifugal compressor based water refrigeration system.
4. Explain the principle of operation of the steam-jet ejector system.
5. Explain the principle of operation of thermoelectric refrigeration.

14.1 INTRODUCTION

Water is one of the most safe, ozone friendly refrigerants. It has very high latent heat, however, it can be used above 0ºC, which is its freezing point. The specific volume of water vapour is very large which means that an enormously large volume of vapour has to be handled per TR. Table 14.1 gives the displacement volume and the compressor bore data for R12, R22, R717 and water at condenser and evaporator temperatures of 40°C and 5°C respectively using reciprocating compressor running at 1440 rpm and with volumetric efficiency of 80%, and compressor stroke equal to itsbore.

Table 14.1 Swept flow rate and reciprocating compressor bore for various refrigerants

Refrigerant	*Evaporator pressure* at 5°C (bar)	*Specific volume* (m^3/kg)	*Volume flow rate* (m^3/min-TR)	*Compressor bore = stroke* (mm)
R12	3.68	0.0478	0.0845	45.4
R22	6.02	0.404	0.0539	39.0
R717 (Ammonia)	5.08	0.244	0.0477	37.5
R718 (Water)	0.0087	147.12	13.2	244.3

It is obvious that the reciprocating compressor-based system would require an enormously large compressor, whose initial, running and maintenance cost would make the system economically unfeasible. In 1930s when centrifugal compressors were available, water refrigeration became popular for large air conditioning systems. The advantage is that water evaporating from flash chamber cools the water, hence the heat exchanger–evaporator is not required. This system is also used for pre-cooling of vegetables, concentration of fruit juices, vacuum processing of vegetables, drying up of heat sensitive fluids and chemicals and water chilling. In all these applications, water evaporating from substances cools them.

14.2 PRINCIPLE OF OPERATION

Saturation pressure of water at 5°C is 0.0087 bar, which means that if the pressure in a vessel containing water is reduced to 0.0087 bar by a vacuum pump, the water will boil at 5°C absorbing its latent heat from the water in the container. The latent heat of water at 5°C is 2489.8 kJ/kg and its specific heat is 4.18 kJ/kg-K. This means that if 1 kg of water evaporates it can cool (2489.8/4.18) 595.6 kg of water by 1°C. This is the main advantage of this system that a very small quantity of water evaporating, say, from the surface of lettuce can cool it to 5°C.

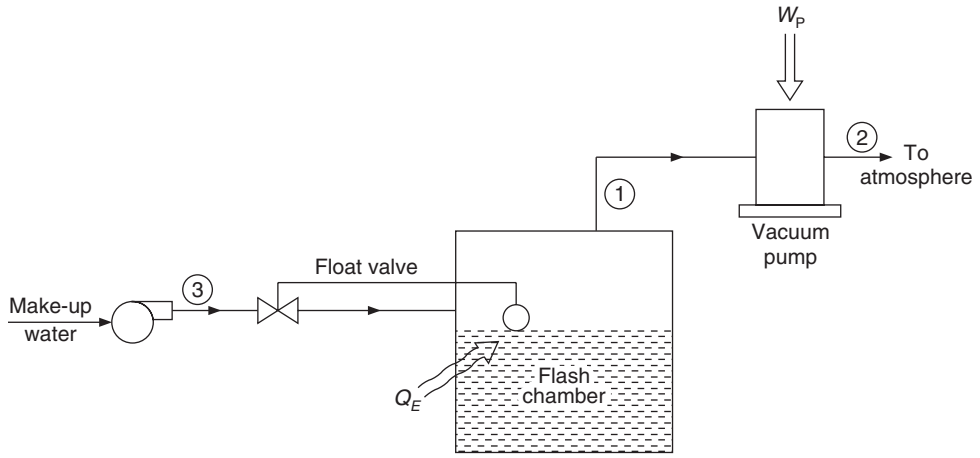

Figure 14.1 A simple water refrigeration system.

Figure 14.1 shows a simple water refrigeration system. A vacuum pump is used to maintain the pressure of 0.0087 bar by removing the water vapour formed. The water in the container flashes into water vapour, hence the container is also called *flash chamber*. Assuming that there is no leakage heat transfer, energy balance gives

$$Q_E = \dot{m}(h_1 - h_3) \tag{14.1}$$

$$W_P = \dot{m}(h_2 - h_1) \tag{14.2}$$

$$\text{COP} = (h_1 - h_3)/(h_2 - h_1) \tag{14.3}$$

EXAMPLE 14.1 A temperature of 5°C is maintained inside the flash chamber by using vacuum pump. The make-up water is supplied at 30°C. Find the volume flow rate per TR, pump work and COP. The vacuum pump efficiency is 75%.

Solution:

The following properties of water vapour are obtained from steam tables. Referring to Figure 14.1, $h_1 = h_g(5^\circ\text{C}) = 2510.8$ kJ/kg, $v_1 = 147.16$ m^3/kg, $s_1 = 9.0271$ kJ/kg-K and $h_3 = h_f(30^\circ\text{C}) = 125.6$ kJ/kg.

The enthalpy at state 2 after isentropic compression from 0.0087 bar to 1.01325 bar may be obtained either from Mollier diagram or by interpolating in superheat tables. Interpolating in the superheat tables, we get

$$h_{2'} = 3641.7 \text{ kJ/kg} \quad \text{and} \quad t_{2'} = 671.05^\circ\text{C}$$

Refrigeration effect = $q_E = h_1 - h_3 = 2385.2$ kJ/kg

Mass flow rate per TR = $\dot{m} = 211/(h_1 - h_3) = 211/2385.2 = 0.0885$ kg/min

Volume flow rate per TR = $\dot{m}v_1 = 0.0885(147.16) = 13.02$ m^3/min

Isentropic compressor work = $\dot{m}(h_{2'} - h_1) = 0.0885(3641.7 - 2510.8)/60 = 1.668$ kW

Actual compressor work = $\dot{m}(h_{2'} - h_1)/\eta_C = 1.668/0.75 = 2.224$ kW

$$\text{COP} = (211/60)/2.224 = 1.58$$

It is observed that the volume flow rate per TR is enormously large. The pump work is also large. The discharge temperature at atmospheric pressure is very high. If a condenser at say, 40°C is used at the exit of the vacuum pump, the pump work will reduce. The condensation will occur at 0.074 bar, which is also below atmospheric pressure.

14.3 CENTRIFUGAL COMPRESSOR-BASED SYSTEM

This system as shown in Figure 14.2(a) uses a centrifugal compressor 1–2 to compress the vapour from 0.0087 bar at 5°C in flash chamber to condenser pressure of 0.096 bar at 45°C condenser temperature. The condenser therefore has to be maintained at sub-atmospheric pressure, which is done by a suitable ejector system, which removes the non-condensable gases (air etc.). The air may enter the system with the make-up water or through any leak in the system apart from being initially present in the system. The chilled water from the flash chamber at 4 is passed through the load, which may be a heat exchanger of some process or cooling coil of an air conditioning system. This water becomes warm after picking up load and it is sprayed in the flash chamber for

re-evaporation. Make-up water enters at 3 through a float valve. The isentropic compression efficiency is η_C. The isentropic compression 1–2′ and the actual compression are shown on the *h*–*s* diagram of Figure 14.2(b).

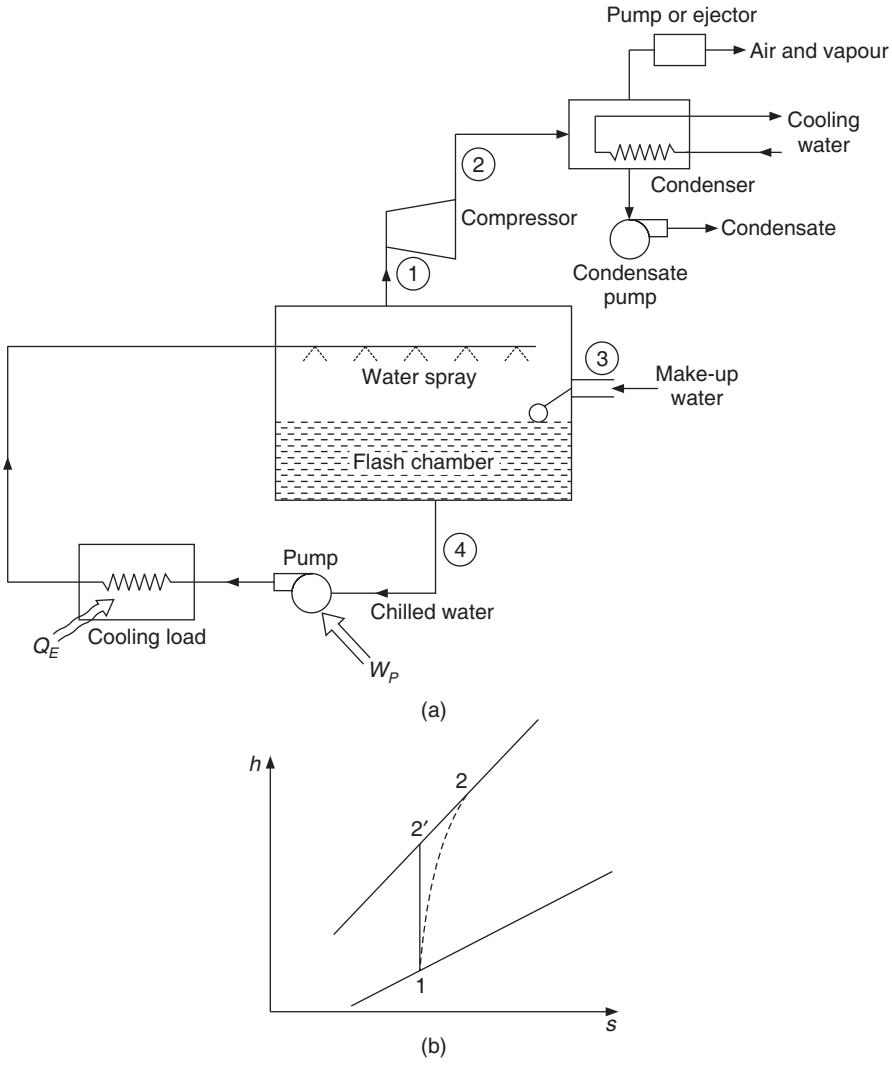

Figure 14.2 Centrifugal compressor-based water refrigeration system.

$$\text{The specific compression work, } w_C = (h_{2'} - h_1)/\eta_C = h_2 - h_1 \tag{14.4}$$

Mass and energy conservation for the flash chamber and cooling coil give

$$\dot{m}_1 = \dot{m}_3 \tag{14.5}$$

$$\dot{m}_1 h_1 = \dot{m}_3 h_3 + Q_E + \dot{m}_4 w_P \tag{14.6}$$

$$Q_E = \dot{m}_1(h_1 - h_3) - \dot{m}_4 w_P \tag{14.7}$$

The pump work is usually small, hence we get

$$Q_E = \dot{m}_1(h_1 - h_3) \quad \text{or} \quad q_E = h_1 - h_3 \tag{14.8}$$

$$\text{COP} = q_E/w_C = \eta_C(h_1 - h_3)/(h_{2'} - h_1) \tag{14.9}$$

The COP of the system depends upon the condenser pressure, flash chamber temperature, make-up water temperature, compressor efficiency, pump and ejector work. The pump and ejector work input may be negligible. The flash chamber pressure depends the cooling water temperature desired but it cannot be lower than 0.08 bar (saturation pressure at 4°C) to avoid freezing of water. The condenser pressure is around 0.096 bar corresponding to the condenser temperature of 45°C. The condenser requires a suitable ejector for purging of non-condensable gas, usually air. The ejector may use up to three stages. A mixture of air and water vapour enters the ejector. The water vapour must be removed from it and only air must be thrown outside. Hence the mixture from the first stage ejector is taken to an intermediate condenser which condenses water vapour at a pressure between the condenser pressure and atmospheric pressure. Some water vapour does not condense and passes through the second stage ejector. This goes to another condenser, which works at atmospheric pressure and removes most of the water vapour.

EXAMPLE 14.2 A chilled water air conditioning system has water cooled at 5°C in the flash chamber. A centrifugal compressor removes the flash vapours and the condenser works at 45°C. The make-up water is available at 30°C. Compressor efficiency is 80%. Neglecting pump work, find the COP and the volume flow rate of water vapour handled for a 100 TR system.

Solution:

From steam tables at 5°C: $h_1 = h_g(5°C) = 2510.8$ kJ/kg, $v_1 = 147.16$ m^3/kg, $s_1 = 9.0271$ kJ/kg-K and $h_3 = h_f(30°C) = 125.6$ kJ/kg.

Interpolating in the superheat table for 0.096 bar (45°C) for $s_{2'} = s_1 = 9.0271$, we get

$$h_{2'} = 2938.92 \text{ kJ/kg} \quad \text{and} \quad t_{2'} = 275.32°C$$

Refrigeration effect $q_E = h_1 - h_3 = 2385.2$ kJ/kg

Mass flow rate $\dot{m} = 211(100)/(h_1 - h_3) = 21100/2385.2 = 8.8462$ kg/min

Volume flow rate $\dot{m}v_1 = 8.8462(147.16) = 1301.81$ m^3/min

Isentropic compressor work $= \dot{m}(h_{2'} - h_1) = 8.8462(2938.92 - 2510.8)/60$

$= 63.12$ kW

Actual compressor work $= \dot{m}(h_{2'} - h_1)/\eta_C = 63.12/0.75 = 78.9$ kW

$$\text{COP} = (21100/60)/78.9 = 4.457$$

It is observed that the COP improves considerably compared to the previous case of Example 14.1 where the compression was carried up to atmospheric pressure. The volume flow rate is very large hence an enormously large centrifugal compressor is required which is not economically and practically feasible. The use of steam-jet ejector will allow such a large volume flow rate to be handled more efficiently.

14.4 STEAM-JET EJECTOR SYSTEM

The steam-jet ejector creates a high velocity jet which drives away the large quantity of flash vapour formed and then compresses it to condenser pressure. This is a heat-operated refrigeration system where motive steam from a boiler at high pressure p_1 and condensing at condenser pressure p_C forms the heat engine, and the processes in the flash chamber and condenser form the refrigeration system. Figure 14.3 shows the schematic diagram of the steam-jet ejector refrigeration system. The chilled water from the flash chamber is circulated through the cooling load by a pump where it is chilled by evaporation at low pressure. A float valve supplies the make-up water to flash chamber.

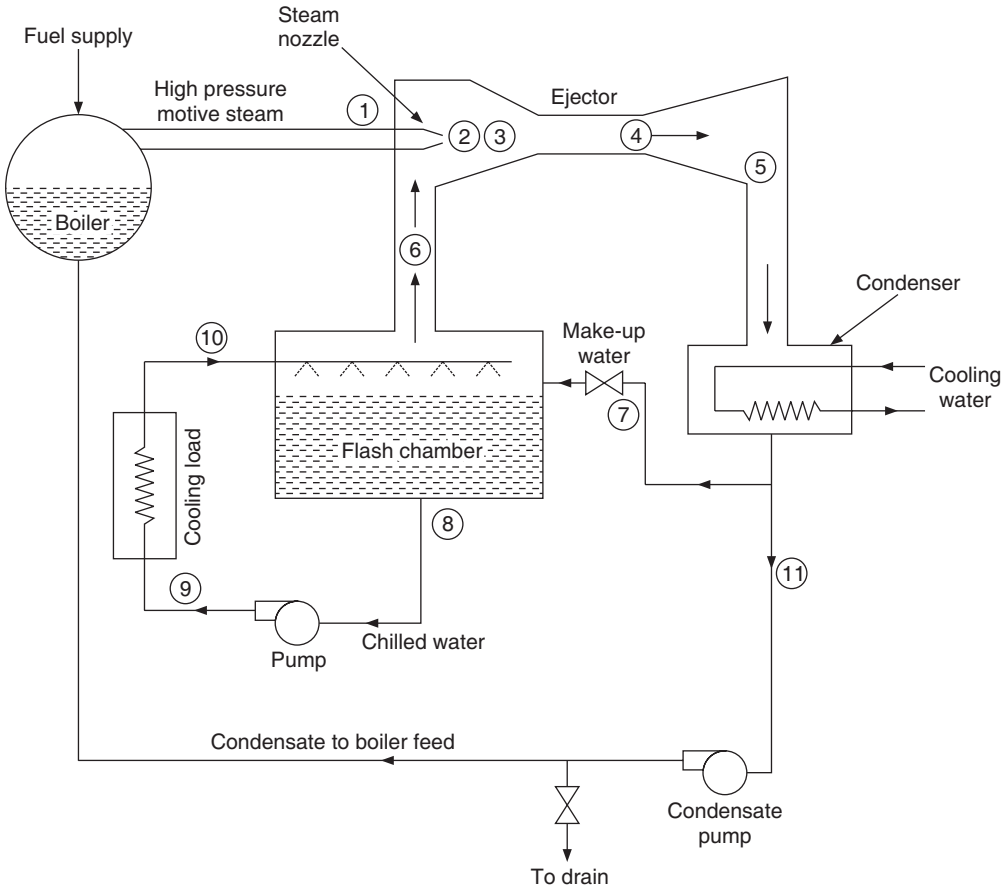

Figure 14.3 The steam-jet ejector system.

The motive steam enters the ejector through a convergent-divergent nozzle and comes out as a supersonic jet. The high velocity jet drags or carries away the flash vapour along with it by imparting a part of its momentum to water vapour. This process is called *entrainment*. Figure 14.4(a) shows the schematic diagram of the steam ejector and Figure 14.4(b) shows the pressure variation along its length. Figure 14.4(c) shows the T–s diagram for the entire steam jet cycle. The

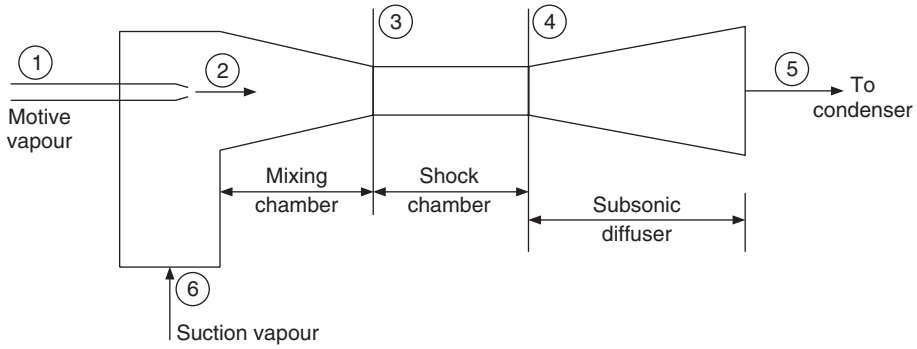

Figure 14.4(a) Schematic diagram of the steam ejector.

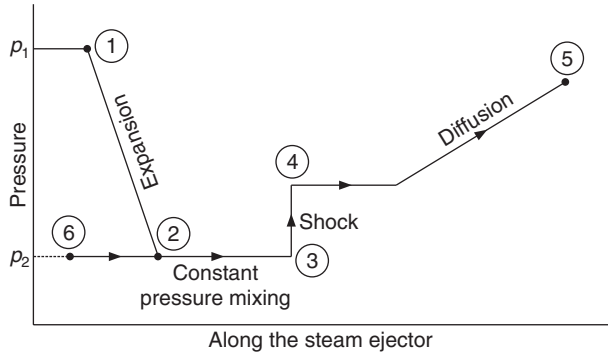

Figure 14.4(b) Pressure variation along the steam ejector.

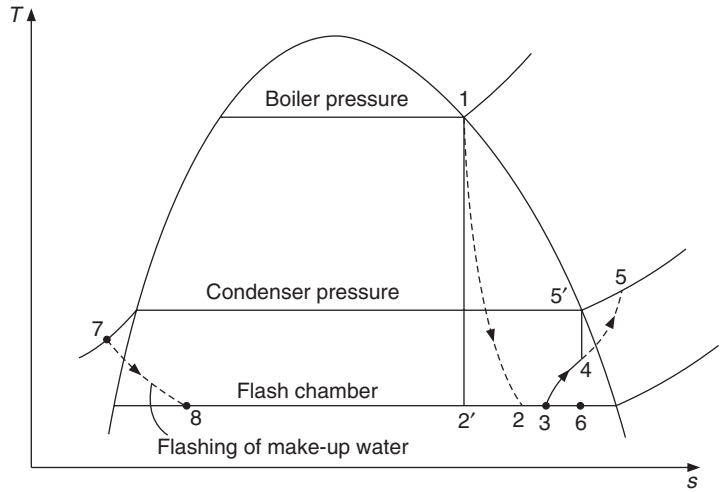

Figure 14.4(c) Thermodynamic cycle of the steam-jet ejector system.

motive steam is assumed to be dry and saturated. It expands through the nozzle and the pressure drops from p_1 to p_2. The friction and leakage heat transfer in the nozzle do not let all the enthalpy drop to be converted to kinetic energy. State 2′ is for isentropic expansion and state 2 is the actual state after expansion. The nozzle efficiency η_n is defined as follows:

$$\eta_n = \frac{h_1 - h_1}{h_{2'} - h_1} \tag{14.10}$$

The velocity at the nozzle exit is given by

$$V_2 = \sqrt{2\eta_n (h_1 - h_{2'})} \tag{14.11}$$

The nozzle efficiency is around 0.9 to 0.94 for a well-designed nozzle. The high velocity jet entrains the flash vapours from 6. The pressure p_2 is equal to p_6 but enthalpy h_2 is not same as h_6. After mixing, the state of steam is denoted by 3. This state is usually supersonic hence a shock will occur before the gas enters the diffuser. For the shock to remain stable the ejector is provided with a section whose area of cross section is constant from 3 to 4. Normal shock will occur in this region. After the shock, the mixture of motive steam and flash vapour is compressed in the diffuser from state 4 to 5. The pressure p_5 is saturation pressure corresponding to condenser temperature.

Mixing

Mass and momentum will be conserved during mixing. This yields

Mass conservation: $$\dot{m}_3 = \dot{m}_1 + \dot{m}_6 \tag{14.12}$$

Momentum conservation: $$(\dot{m}_1 + \dot{m}_6)V_3 = \dot{m}_1 V_2 + \dot{m}_6 V_6 \tag{14.13a}$$

This assumes that there is no loss in momentum and there are no forces acting between sections 2 and 3.

Assuming V_6 to be negligible, Eq. (14.13a), reduces to

$$\dot{m}_3 V_3 = \dot{m}_1 V_2 \tag{14.13b}$$

Energy equation for the mixing process is

$$\dot{m}_1 h_1 + \dot{m}_6 h_6 = \dot{m}_3 (h_3 + V_3^2 / 2) \tag{14.14}$$

There will be some loss in kinetic energy due to entrainment, which has been neglected.

Relations for normal shock

State 4 after the shock will be subsonic. Mass momentum and energy will be conserved across the shock. These are respectively as follows:

$$\dot{m}_3 / A = V_3 / v_3 = V_4 / v_4 \tag{14.15}$$

$$(p_4 - p_3)A = \dot{m}_3 (V_3 - V_4) \tag{14.16}$$

$$h_3 + \frac{V_3^2}{2} = h_4 + \frac{V_4^2}{2} \tag{14.17}$$

The state 4 consisting of p_4, v_4 and h_4, and velocity V_4 are the unknowns which are determined iteratively by the above three equations and the equation of state, that is, steam tables. The solution

of Eqs. (14.15) and (14.16) along with properties from steam tables is represented by *Rayleigh Line* while the solution of Eqs. (14.15) and (14.17) along with properties from steam tables is represented by *Fanno Line*. The intersection of these two lines gives the solution of above three equations, that is state 4.

Diffuser

Velocity at section 4 after the normal shock is subsonic and it reduces to almost zero at section 5, the end of the diffuser section. Hence

$$h_5 - h_4 = \frac{V_4^2}{2} \tag{14.18}$$

A diffuser efficiency η_d is defined to account for the frictional and other losses in the diffuser, that is,

$$\eta_d = \frac{h_5 - h_4}{h_{5'} - h_4} \tag{14.19}$$

where $h_{5'}$ represents the enthalpy of isentropic compression which may be determined from Mollier chart or from superheat steam tables.

The unknowns in the above equations are the ratio of flash vapour to the motive steam m_6/m_1 and the cross sectional areas at various sections. The solution is obtained by an iterative procedure. One iteration is required for the motive steam ratio and another iteration is required to find the relations across the normal shock. The solution has to give the desired pressure at section 5 to be the saturation pressure at condenser temperature.

Alternative method

Simplifications can be made to avoid calculations for normal shock. In this method, state 3 is considered to be that of motive steam after entrainment and state 4 is that of mixture of motive steam and the flash vapour after mixing. Assume that at state 3, both the motive steam and the flash vapours have velocity V_3. Neglecting skin friction and pressure drop between sections 3 and 4, the momentum conservation would give

$$\text{Momentum out} - \text{Momentum in} = \text{Forces on control volume} = 0$$

which yields

$$\dot{m}_1 V_3 + \dot{m}_6 V_3 = (\dot{m}_1 + \dot{m}_6) V_4 \quad \therefore \quad V_3 = V_4 \tag{14.20}$$

The energy equation for mixing is

$$\dot{m}_1 \left(h_3 + \frac{V_3^2}{2} \right) + \dot{m}_6 h_6 = (\dot{m}_1 + \dot{m}_6) \left(h_4 + \frac{V_4^2}{2} \right)$$

This is approximated as follows:

$$\dot{m}_1 h_3 + \dot{m}_6 h_6 = (\dot{m}_1 + \dot{m}_6) h_4 \tag{14.21}$$

Energy balance over control volume including states 1, 5 and 6 and neglecting kinetic energies at 1, 5 and 6 gives

$$\dot{m}_1 h_1 + \dot{m}_6 h_6 = (\dot{m}_1 + \dot{m}_6) h_5 \tag{14.22}$$

Subtracting Eq. (14.21) from Eq. (14.22), we get

$$\dot{m}_1 (h_1 - h_3) = (\dot{m}_1 + \dot{m}_6)(h_5 - h_4) \tag{14.23}$$

This is the governing equation for the steam-jet refrigeration system. The left hand side of this equation is the enthalpy drop of motive steam after entrainment and the right hand side is the energy required for compression of the mixture of motive steam and flash vapour. This equation is stated as follows:

Energy required for compression is equal to the enthalpy drop of motive steam

Further to determine state 3, an entrainment efficiency η_e is defined as follows:

$$\eta_e = \frac{h_1 - h_3}{h_1 - h_2} = \frac{h_1 - h_3}{\eta_n (h_1 - h_{2'})} \tag{14.24}$$

Let m be the mass of the motive steam required per unit mass flow rate of flash vapour, that is,

$$\dot{m} = \dot{m}_1 / \dot{m}_6 \tag{14.25}$$

From Eqs. (14.24) and (14.19), we get

$$h_1 - h_3 = \eta_e \eta_n (h_1 - h_{2'}) \text{ and } h_5 - h_4 = \eta_d (h_{5'} - h_4)$$

Substituting these on left and right hand sides of Eq. (14.23), we get

$$\dot{m} = \frac{h_{5'} - h_4}{\eta_e \eta_n \eta_d (h_1 - h_{2'}) - (h_{5'} - h_4)} = \frac{1}{\dfrac{\eta_e \eta_n \eta_d (h_1 - h_{2'})}{(h_{5'} - h_4)} - 1} \tag{14.26}$$

The state of flash vapour at 6 is obtained by considering the energy balance for the ejector, which yields

$$h_6 = (1 + \dot{m}) h_5 - \dot{m} h_1 \tag{14.27a}$$

Substituting for $\dot{m}$ from Eq. (14.26), we get

$$h_6 = h_5 - \frac{(h_{5'} - h_4)(h_1 - h_5)}{\eta_e \eta_n \eta_d (h_1 - h_{2'}) - (h_{5'} - h_4)} \tag{14.27b}$$

Considering the flash chamber and the load as control volume, we get for refrigeration load,

$$Q_E = \dot{m}_6 (h_6 - h_7) - W_{p1} \tag{14.28}$$

Energy input to the motive steam is given by

$$Q_{\text{steam}} = \dot{m}_1 h_1 - (\dot{m}_6 + \dot{m}_1) h_{12} = \dot{m}_1 h_1 - (\dot{m}_6 + \dot{m}_1)(h_{11} + w_{p2}) \tag{14.29}$$

The COP is given by

$$\text{COP} = \frac{\dot{m}_6 (h_6 - h_7) - W_{p1}}{\dot{m}_1 h_1 - (\dot{m}_6 + \dot{m}_1)(h_{11} + w_{p2})} = \frac{(h_6 - h_7) - W_{p1}/\dot{m}_6}{\dot{m} h_1 - (1 + \dot{m})(h_{11} + w_{p2})} \tag{14.30}$$

The mass flow rate of flash vapour and that of motive steam required for the given cooling capacity, in TR are obtained as follows:

$$\dot{m}_6 = \frac{211\text{TR} + W_{p1}}{h_6 - h_7}$$

$$\dot{m}_1 = \frac{(211\text{TR} + W_{p1})(h_{5'} - h_4)}{\eta_e \eta_n \eta_d (h_1 - h_{2'}) - (h_{5'} - h_4)} \tag{14.31}$$

14.4.1 Advantages and Limitations

The steam-jet ejector system has many advantages and a few limitations as described below:

Advantages

1. Commodities like vegetables that contain water can be directly cooled since each kg of water that evaporates cools 600 kg or even more of vegetables by 1°C. Lettuce in large quantity is cooled by evaporation of a small quantity of surface moisture.
2. Immersing the commodity in chilled water of flash chamber can also do the cooling. This avoids the use of heat exchanger for cooling.
3. In vacuum cooling and concentration of juices by this method, the water evaporates at low temperature, which preserves the flavour.
4. There are two pumps, otherwise there are no other moving parts and hence very little maintenance is required.
5. In plants like steel plants, petroleum plants and thermal power plants etc. where waste steam is available, it is very economical to use this system.
6. It uses low-grade energy in the boiler, hence it can be used in remote areas where electricity is not available. The pumps can also be operated by steam.
7. The flexible arrangement of units allows them to be fitted into tight quarters.

Limitations

1. It can be used only for temperatures above 4°C.
2. Condenser size is very large since not only the flash vapour but the motive steam also has to be condensed.
3. Volume flow rates of steam are very large, hence either the centrifugal compressor or the steam ejector has to be used. Centrifugal compressor is not economical to use.
4. COP is low since it uses low-grade energy.

14.4.2 Performance

To compress the vapour to high condenser pressure, the velocity at section 4 must be high. If the motive steam pressure is fixed, then velocity V_2 at nozzle exit is fixed, hence only increasing the mass flow rate of motive steam can increase V_4.

When the chilled water temperature is lower, the pressure at nozzle exit will also be lower. This will increase the compression ratio, again demanding more motive steam.

If the motive steam pressure and condenser temperature are constant, then the cooling capacity increases as the chilled water temperature increases.

The motive steam mass flow rate increases as the motive steam pressure decreases with condenser and flash chamber temperatures remaining constant. However for motive steam pressure greater than 4 bar, the variation in motive steam flow rate with pressure is insignificant. At lower flash chamber temperatures and at higher condenser temperatures, more motive steam flow rate is required. COP is obviously low for lower flash chamber temperature and higher condenser temperature.

14.4.3 Actual System

In an actual system there is an ejector attached to the condenser to maintain the condenser and to remove the non-condensable gases (usually air) which enter with the make-up water and motive steam or may leak in from cracks in the plant. Ejectors may have up to three stages. Ejectors are not very efficient devices but these are capable of handling large volume flow rates. These usually work at pressure ratio of 5 but in some cases pressure ratio up to 8 is also used. As mentioned earlier, an intermediate condenser is used between two stages of ejectors. This condenser is a direct contact type arranged vertically. Cold water drips through it while the mixture of air and water vapour flows up. Water vapour condenses and the air and the left-over water vapour go to the second stage ejector. The condenser in the steam ejector system is very large and requires a large quantity of cold water. A cooling pond or cooling tower may be used for this purpose.

To improve the COP, a two fluid system has also been tried where the motive fluid was mercury with high molecular weight. Water with low molecular weight was the refrigerant. A larger pressure ratio was required in order to separate the two components. Further, mercury is a very toxic substance, therefore, it was abandoned in favour of a slightly less efficient steam ejector system.

EXAMPLE 14.3 In a steam-jet refrigeration system, saturated steam at 5 bar, 151.8°C enters the ejector. Condenser, evaporator (flash chamber) and make-up water temperatures are 45°C, 5°C and 30°C respectively. The nozzle, entrainment and diffuser efficiencies are 92%, 65% and 80% respectively. Neglecting the normal shock, find the mass flow rate of motive steam per kg of flash vapour, refrigeration effect and COP. The properties of water are as follows:

t (°C)	p (bar)	h_f (kJ/kg)	h_g	h_{fg}	s_f (kJ/kg-K)	s_g	s_{fg}
151.8	5.0		2747.48			6.8198	
45	0.09582	188.5	2583.2	2394.9	0.6385	8.1663	7.5278
30	0.04243	125.6					
5	0.008721	21.02	2510.8	2489.78	0.0762	9.0271	8.9509

Specific volume of water at 5°C : $v_f = 0.001$ m^3/kg and $v_g = 147.16$ m^3/kg

Solution:

From steam tables, $h_1 = h_{g@5\text{ bar}} = 2747.48$ kJ and $s_1 = s_{g@5\text{ bar}} = 6.8198$ kJ/kg-K.
Considering isentropic expansion to determine state 2′, the quality x_2' is given by

$$x_2' = \frac{[s_1 - s_f\,(5°\text{C})]}{s_{fg}\,(5°\text{C})} = \frac{6.8198 - 0.0762}{8.9509} = 0.7534$$

and $$h_2' = h_f(5^o\text{C}) + x_2'\, h_{fg}\,(5^o\text{C}) = 21.02 + 0.7534(2489.78) = 1896.818 \text{ kJ/kg}$$

$$V_2 = \sqrt{2 \times 0.92 \times (2747.48 - 1896.818)1000} = 1251.09 \text{ m/s}$$

In this method state 4 cannot be determined after mixing. This state is assumed to be such that isentropic compression from this state leads to saturated vapour state at condenser pressure as shown in Figure 14.4(c).

$\therefore$ $$x_4 = \frac{[s_g\,(45°\text{C}) - s_f\,(5°\text{C})]}{s_{fg}\,(5°\text{C})} = \frac{8.1663 - 0.0762}{8.9509} = 0.9038$$

and $$h_4 = h_f(5^o\text{C}) + x_4\, h_{fg}\,(5^o\text{C}) = 21.02 + 0.9038(2489.8) = 2271.3601 \text{ kJ/kg}$$

$$h_5 = h_4 + \frac{h_5' - h_4}{\eta_d} = 2271.3601 + \frac{2583.2 - 2271.3601}{0.8} = 2661.16 \text{ kJ/kg}$$

From Eq. (14.26), we get

$$\dot{m} = \frac{1}{\dfrac{\eta_e\,\eta_n\,\eta_d\,(h_1 - h_{2'})}{(h_{5'} - h_4)} - 1}$$

$$= \frac{1}{\dfrac{(0.65)(0.92)(0.8)(2747.48 - 1896.818)}{(2583.2 - 2271.3601)} - 1} = 3.27516$$

From Eq. (14.27a),

$$h_6 = (1 + \dot{m})\,h_5 - \dot{m}h_1 = 4.27516(2661.16) - 3.27516\,(2747.48) = 2378.448 \text{ kJ/kg}$$

The vapour coming from flash chamber is wet.

$$h_7 = h_f(30^o\text{C}) = 125.6 \text{ kJ/kg}$$

Neglecting pump work the refrigeration effect is given by

$$q_E = h_6 - h_7 = 2378.448 - 125.6 = 2252.848 \text{ kJ/kg}$$

Evaporation rate per TR, $\dot{m}_6 = \dfrac{211}{2252.848} = 0.09366$ kg/min-TR = 5.619 kg/h-TR

Steam consumption rate per TR = 3.27516(5.619) = 18.405 kg/h-TR

$$h_{11} = h_f\,(45^o\text{C}) = 188.5 \text{ kJ/kg}$$

Neglecting the condensate pump work, COP is given by

$$\text{COP} = \frac{q_E}{h_1 - h_{11}} = \frac{2252.848}{2747.48 - 188.5} = 0.88$$

$$x_6 = \frac{h_6 - h_f}{h_{fg}} = \frac{2378.448 - 21.02}{2489.78} = 0.9468$$

$$v_6 = (1 - 0.9468)0.001 + 0.9468(147.16) = 139.3373$$

Volume flow rate of flash vapour is given by

$$\dot{V} = \dot{m}_6 v_6 = 5.619(139.3373) = 782.94 \text{ m}^3\text{/h-TR}$$

EXAMPLE 14.4 A steam-jet refrigeration system is supplied motive saturated steam at 5 bar. The temperature of chilled water is 5°C. The ratio of motive steam to flash vapour is 2.4. The nozzle and diffuser efficiencies are 85% and 80% respectively. Determine the states of steam before and after the shock and after the diffuser. Find the evaporation rate, steam consumption and COP.

Solution:

$h_1 = 2747.48$ and $s_1 = 6.8198$ (as in Example 14.3)

Considering isentropic expansion to determine state 2′, the quality $x_{2'}$ is given by

$$x_2' = \frac{[s_1 - s_f\,(5°\text{C})]}{s_{fg}\,(5°\text{C})} = \frac{6.8198 - 0.0762}{8.9509} = 0.7534$$

and $h_2' = h_f(5°\text{C}) + x_2'\, h_{fg}\,(5°\text{C}) = 21.02 + 0.7534(2489.78) = 1896.818$ kJ/kg

$\Delta h' = 2747.48 - 1896.818 = 850.662 \quad \therefore \quad \Delta h = 0.85(850.662) = 723.06$ kJ/kg

$$V_2 = \sqrt{2 \times 723.06 \times 1000} = 1202.54 \text{ m/s}$$

From Equation (14.13b), we get

$$\dot{m}_3 V_3 = \dot{m}_1 V_2$$

If we do the calculations on the basis of per kg of flash vapour, then

$$\dot{m}_6 = 1.0, \ \dot{m}_1 = 2.4 \quad \text{and} \quad \dot{m}_3 = 3.4$$

$$V_3 = \frac{2.4(1202.54)}{3.4} = 848.851 \text{ m/s}$$

Note: Some textbooks define an entrainment efficiency, η_e to find V_3 as follows:

$$\frac{\eta_e \dot{m}_1 V_2^2}{2} = \frac{\dot{m}_3 V_3^2}{2}$$

From Eq. (14.14), we get

$$h_3 = \frac{\dot{m}_1 h_1 + \dot{m}_6 h_6}{\dot{m}_3} - \frac{V_3^2}{2}$$

$$h_3 = \frac{2.4 \times 2747.48 + 2510.8}{3.4} - \frac{(848.581)^2}{2 \times 1000} = 2317.594 \text{ kJ/kg}$$

$$x_3 = \frac{2317.594 - 21.02}{2489.78} = 0.9224$$

$$v_3 = 0.9224(147.16) + (1.0 - 0.9224)0.001 = 135.7405 \text{ m}^3/\text{kg}$$

$$\frac{V_3}{v_3} = \frac{848.851}{135.7405} = 6.2535$$

$$h_3 + \frac{V_3^2}{2} = 2677.868$$

Equations (14.15), (14.17) and (14.16) reduce to

$$\frac{\dot{m}_3}{A} = \frac{V_3}{v_3} = \frac{V_4}{v_4} = 6.2535 \tag{i}$$

$$h_4 + \frac{V_4^2}{2} = h_3 + \frac{V_3^2}{2} = 2677.868 \tag{ii}$$

$$p_4 = p_3 + \left(\frac{\dot{m}_3}{A}\right)(V_3 - V_4) = 0.008721 + 6.2535 \times 10^{-5}\,(848.851 - V_4) \tag{iii}$$

These equations are solved iteratively to find V_4, v_4, h_4 and p_4. The following procedure is adopted.

(i) Assume V_4 and find v_4 from Eq. (i)
(ii) Find p_4 from Eq. (iii)
(iii) Find h_4 from steam tables for these values of p_4 and v_4.
(iv) Find h_4 from Eq. (ii) and see if it agrees with that of step (iii).

An approximate solution of this set is as follows:

$V_4 = 220$ m/s, $v_4 = 35.18$ m^3/kg, $p_4 = 0.04805$ bar and $h_4 = 2653.7$ kJ/kg

At $p = 0.04805$ bar, the properties at saturation are as follows:

$v_f = 0.0010048$, $v_g = 29.8019$, $h_f = 134.1054$, $h_g = 2560.0$, $s_g = 8.414$ and $t = 32.04^\circ$C

Hence, state 4 after the normal shock is superheated state and the temperature is 81°C.

Enthalpy rise after the diffuser is given by

$$h_5 - h_4 = \frac{V_4^2}{2} = \frac{(220)^2}{2 \times 1000} = 24.2 \text{ kJ/kg}$$

$$h_5' - h_4 = \eta_d\,(h_5 - h_4) = 0.8(24.2) = 19.36$$

$$h_5' = 2653.7 + 19.36 = 2673.06 \text{ kJ/kg}$$

Mollier diagram gives $p_5 = 0.55$ bar, which corresponds to 35°C.

Energy balance across the ejector gives

$$h_6 = (1 + \dot{m})h_5 - \dot{m}h_1 = 3.4(2677.9) - 2.4(2747.48) = 2510.908 \text{ kJ/kg}$$

The vapour coming from flash chamber is almost saturated vapour.

Now, $$h_7 = h_f(30^oC) = 125.6 \text{ kJ/kg}$$

Neglecting pump work the refrigeration effect is given by

$$q_E = h_6 - h_7 = 2510.908 - 125.6 = 2385.308 \text{ kJ/kg}$$

Evaporation rate per TR,

$$\dot{m}_6 = \frac{211}{2385.308} = 0.0885 \text{ kg/min-TR} = 5.3075 \text{ kg/h-TR}$$

Steam consumption per TR = 2.4(5.3075) = 12.738 kg/h-TR

Now, $$h_{11} = h_f(35^oC) = 146.5 \text{ kJ/kg}$$

Neglecting the condensate pump work, COP is given by

$$\text{COP} = \frac{q_E}{h_1 - h_{11}} = \frac{2385.308}{2747.48 - 146.5} = 0.917$$

The vapour at 6 is almost saturated, hence $v_6 = v_g(5^oC) = 147.16$
Volume flow rate of flash vapour is given by

$$\dot{V} = \dot{m}_6 v_6 = 5.3075(147.16) = 781.05 \text{ m}^3\text{/h-TR}$$

The condenser pressure is very low in this example. The ratio of motive steam has to be increased to obtain higher condenser pressures.

14.5 THERMOELECTRIC REFRIGERATION OR ELECTRONIC REFRIGERATION

Goldsmith and Douglas demonstrated a practical thermoelectric system in 1954, using semiconductors to show that cooling was possible from ordinary room temperature down to below 0°C. The basic principles date back to Seebeck effect and Peltier effect.

14.5.1 Seebeck Effect

Thomas Seebeck, a German physicist observed in 1821 thermoelectric emf when two dissimilar metals were used to make two junctions, one of which was heated and the other cooled. The emf was found to be proportional to the temperature difference between the junctions and the material combination. That is,

$$\text{e.m.f} \propto (\Delta T, \text{ material combination})$$

or $$\text{e.m.f} = \alpha_{ab}\, \Delta T = \Delta E \qquad (14.32)$$

where, α_{ab} is the differential Seebeck coefficient between the materials a and b.

$$\therefore \qquad \alpha_{ab} = \Delta E/\Delta T$$

The Seebeck coefficient is termed positive if the emf tends to drive a current in the clockwise sense, that is, the Y terminal becomes positive and the Z terminal becomes negative as shown in Figure 14.5. Seebeck coefficient is also called thermal emf coefficient or thermoelectric power. In fact, this is the principle of temperature measurement by thermocouples. Two junctions are not necessary, an emf measuring device may act as a reference junction as shown in Figure 14.6. For precise temperature measurement at one junction, the second junction is immersed in an ice bath of known temperature.

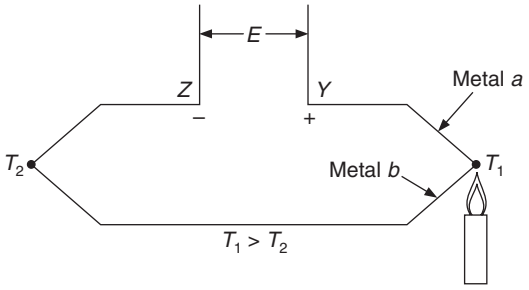

Figure 14.5 Seebeck effect.

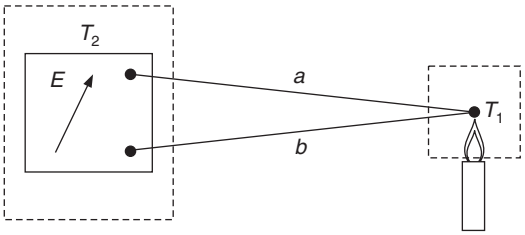

Figure 14.6 A thermocouple circuit.

14.5.2 Peltier Effect

Jean Peltier, a French scientist, observed in 1834, that if direct current was passed through a pair of junctions of dissimilar materials, there occurred heating or cooling at the junctions as shown in Figure 14.7. If the current is clockwise, there will be heating of H junction and cooling of C junction. As per Peltier observation the rate of heat transfer is proportional to the current I and depends upon the material combination. That is,

$$Q = \pi_{ab} I \tag{14.33}$$

or

$$\pi_{ab} = Q/I$$

π_{ab} is positive if the junction H is heated and C is cooled. At the hot junction the current flows from material b to material a with π_{ab} as positive while at the cold junction it flows from a to b. Heat transfer to the system is considered to be positive. For a control volume around the cold junction, Q_C is to the system which is positive if π_{ab} is positive and the current flows from a to b. If the

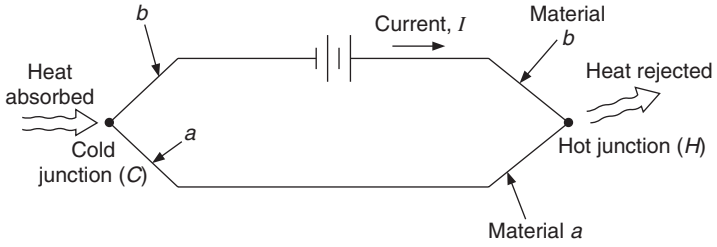

Figure 14.7 Peltier effect.

current flows from b to a then heat will be rejected at this junction. Similarly at the hot junction, with π_{ab} positive the current flows from b to a, hence heat transfer is negative and it is rejected at this junction.

14.5.3 Thomson Effect

Lord Kelvin (who was William Thomson at that time) showed theoretically that there is a close relationship between Seebeck effect and Peltier effect. He also predicted a third thermoelectric effect, which is now known as Thomson effect. This consists of reversible heating or cooling when current flows along a homogeneous conductor in which there is a uniform temperature gradient initially. It states that the rate of heating per unit length dQ/dx in the conductor is proportional to the current I flowing in it and the temperature gradient along the conductor, i.e.

$$\frac{dQ}{dx} = \tau I \frac{dT}{dx} \tag{14.34}$$

where, τ is called the Thomson coefficient.

The heat transfer due to Thomson effect is in addition to that of the Joulean effect. Thomson effect is a reversible phenomenon whereas Joulean heating is irreversible. This is of importance in refrigeration since there always exists a temperature gradient along the materials used in electronic refrigeration and the current also flows.

14.5.4 Relation between Seebeck, Peltier and Thomson Coefficients

There exists a thermodynamic relation between the three coefficients α_{ab}, π_{ab} and τ which may be derived by using the principles of irreversible thermodynamics, for example, see Zymnaski (1957). These are known as Kelvin's relations and are as follows.

$$\tau_a - \tau_b = T \frac{d\alpha_{ab}}{dT} \tag{14.35}$$

$$\pi_{ab} = \alpha_{ab} T \tag{14.36}$$

It is seen that the Thomson effect may be observed along a single conductor, whereas the Seebeck and Peltier effects can be observed only when two dissimilar conductors are joined. Seebeck and Peltier coefficients are properties of materials and not surface properties as may be imagined. It is, therefore, possible to write α_{ab} as $\alpha_a - \alpha_b$, and $\pi_{ab} = \pi_a - \pi_b$ where α_a and π_a are the absolute Seebeck and Peltier coefficients of material a. The negative sign between π_a and π_b is

required for the combined effect of the two materials. Both π_{ab} and α_{ab} are zero if the thermocouple branches are made of the same material, that is, α_{aa} and π_{aa} are zero. For a single conductor,

$$\tau_a = T\frac{d\alpha_a}{dT} \tag{14.37}$$

14.5.5 Measurement of Seebck Coefficient

If a conductor is imagined whose Thomson coefficient is zero at all temperatures, then for such a conductor from Eq. (14.37),

$$\frac{d\alpha_a}{dT} = 0 \text{ or } \alpha_a = \text{constant at all temperatures} \tag{14.38}$$

It is known that the differential Seebeck coefficient between any two conductors is zero at absolute zero temperature, hence it may be assumed that absolute Seebeck coefficient of all materials is zero at absolute zero.

Hence for our imaginary material α_a = constant = 0. That is, our imaginary conductor for which $\tau = 0$ at all temperatures has $\alpha = 0$ at all temperatures. Hence absolute Seebeck coefficient of any real conductor is equal to the differential Seebeck coefficient between the conductor and the imaginary conductor. The absolute Peltier coefficient is related to absolute Seebeck coefficient as

$$\pi_a = \alpha_a T \tag{14.39}$$

Superconductors have zero value of Seebeck coefficient. The differential Seebeck coefficient between Pb and Nb_3Sn has been measured up to critical temperature of 18 K of Nb_3Sn. Thompson coefficient of Pb has been measured above 18 K. Hence the absolute Seebeck coefficient of Pb is known at all temperatures. The absolute Seebeck coefficients of all other materials may be measured relative to lead.

The knowledge of Kelvin's relations made it possible to predict the performance of thermoelectric refrigeration system.

14.5.6 Thermoelectric Refrigeration

In 1838 Lenz, a German scientist, observed ice formation on one of the bismuth–antimony junctions. The ice melted when the direction of current flow was reversed. This experiment was repeated by many investigators but ice formation could not be observed. The bismuth and antimony used by Lenz were not pure. The impurities present in these materials acted as doping and made them semiconductors, which gave the desired effect. Altenkirsch in 1911 emphasized the importance of selecting a proper combination of materials according to a factor, which in modified form is now known as *figure of merit*.

Figure of merit of most metallic conductors is very low; hence these cannot be used for refrigeration purpose. Thermoelectric refrigeration feasibility had to wait for the development of semiconductors, which have a high figure of merit at ordinary temperatures.

Now it is possible to attain temperatures below –100°C by having systems with as many as six stages. Bismuth telluride alloys are used for this purpose. At lower temperatures their performance becomes very poor. The semi-metal bismuth and its alloys with antimony give better performance

at lower temperatures. There is a possibility of improving these properties with the application of magnetic field. Anisotropic thermoelectric elements may give better performance by reducing the thermal conductivity through boundary scattering of the phonons.

The Peltier cooling is always opposed by Joulean heating. If the current is increased, Joulean heating increases in proportion to I^2 whereas Peltier cooling increases in proportion to I only. As a result, Joulean heating tends to mask the Peltier cooling. If electrical resistance is decreased by increasing the area of cross section and decreasing the length, then the conduction heat transfer rate increases between the hot and the cold junctions. So what we actually need in a good thermoelectric material are:

1. High Peltier coefficient
2. Low electrical resistivity
3. Low thermal conductivity

$$\text{Resistivity, } \rho = \frac{\varepsilon}{IL/A} \quad \text{or} \quad \varepsilon = \rho I \frac{L}{A} \tag{14.40}$$

In an anisotropic material the directions of ε and I are different.

14.5.7 Analysis

The potential drop in a single thermocouple is usually very small, hence a number of them are connected in parallel and a high current is passed through them. For the analysis purpose, we may consider only one thermocouple and assume that:

(i) The convective heat transfer in the space between the conductors and junctions is negligible.

(ii) The thermal contact resistances between the thermocouples and the heat exchanger are negligible.

(iii) The properties α, π, ρ and k, etc. are not functions of temperature. (Thomson coefficient $\tau = T\, d\alpha/dT$ will be zero if α is not a function of temperature.)

Figure 14.8 shows a *p-n* type of semiconductor thermocouple. Let T_h and T_c be the temperatures of hot and cold junctions and let Q_c be the refrigeration effect and Q_h be the heat rejection at the other end to the surroundings.

Assume that I^2R the Joulean heat is dissipated equally at both the junctions, that is, $I^2R/2$ is dissipated at the hot junction and $I^2R/2$ at the cold junction, that is,

$$Q_j = I^2R/2 \tag{14.41}$$

The conduction heat transfer is from the hot junction to the cold junction and it may be expressed as

$$Q_{\text{cond}} = (T_h - T_c)\left[\frac{k_pA_p}{L_p} + \frac{k_nA_n}{L_n}\right] = U(T_h - T_c) \tag{14.42}$$

$$R = \frac{L_p\rho_p}{A_p} + \frac{L_p\rho_n}{A_n} \tag{14.43}$$

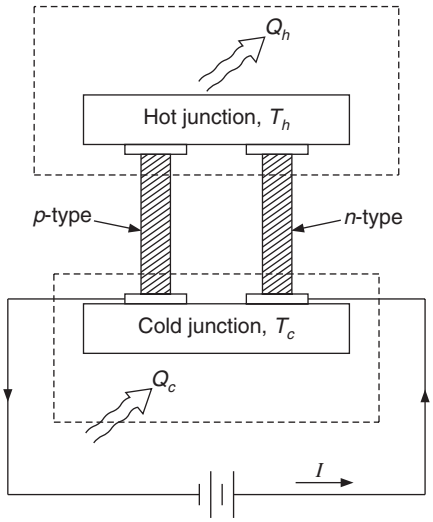

Figure 14.8 A *p–n* type of semiconductor thermocouple.

Energy balance for the control volume at the cold junction in steady state gives

$$Q_c + Q_j + Q_{\text{cond}} = \alpha_{pn}\, IT_c$$

Therefore, refrigeration effect is given by

$$Q_c = \alpha_{pn.}\, I\, T_c - \frac{I^2 R}{2} - U(T_h - T_c) \tag{14.44}$$

Energy balance for a control volume around the hot junction gives

$$-Q_h - Q_{\text{cond}} + Q_j = -\alpha_{pn.}\, I\, T_c \tag{14.45}$$

The current flows from *n*-type material to *p*-type material, hence if α_{pn} is positive the sign of thermoelectric Peltier heat transfer will be negative, that is, from the control volume to the surroundings. The heat rejection to the surroundings is

$$Q_h = \alpha_{pn}\, I\, T_h + \frac{I^2 R}{2} - U(T_h - T_c) \tag{14.46}$$

The net energy supplied to the thermoelectric refrigeration system is the difference between Q_h and Q_c, that is,

$$P = Q_h - Q_c = a_{pn} I\,(T_h - T_c) + I^2 R \tag{14.47}$$

The power input is to compensate for the power loss in Joulean effect and to counteract the Seebeck effect. This is the work done by the battery. The first term is the emf due to Seebeck effect multiplied by current I and the second term is the Joulean effect. The coefficient of performance is defined as

$$\xi = \text{COP} = \frac{Q_c}{Q_h - Q_c} = \frac{\alpha_{pn}\, I\, T_c - I^2 R/2 - U(T_h - T_c)}{\alpha_{pn}\, I\,(T_h - T_c) + I^2 R} \tag{14.48}$$

For $R = 0$ and $U = 0$: $\xi = T_c/(T_h - T_c)$, that is, in the absence of irreversibilities the COP is the Reversed Carnot value.

The properties being fixed, the COP is a function of current I. Two cases are of interest, namely (i) the current required for maximum COP and (ii) the current required for maximum refrigeration effect.

Maximum COP

The derivative of COP ξ with respect to current I is put equal to zero to obtain the condition for maximum COP.

$$\frac{d\xi}{dI} = 0 = \frac{(\alpha_{pn}T_c - IR)(\alpha_{pn} I\Delta T + I^2R) - (\alpha_{pn}\Delta T + 2IR)(\alpha_{pn}IT_c - I^2R/2 - U\Delta T)}{(\alpha_{pn}I\,\Delta T + I^2R^2)^2}$$

The denominator is positive definite hence the numerator should be equal to zero for optimum condition, that is,

$$\frac{\alpha_{pn}I^2R(T_h + T_c)}{2} + \alpha_{pn}U\Delta T^2 + 2UIR\Delta T = 0$$

Substituting $T_m = (T_h + T_c)/2$ the average temperature and $Z = a_{pn}^2/RU$ for the figure of merit, we get

$$\alpha_{pn}\, I^2R\, T_m + \alpha_{pn}U\Delta T^2 + 2\, U\, I\, R\, \Delta T = 0$$

or $$a_{pn}^2\, I^2R\, T_m/U + \alpha_{pn}^2\, \Delta T^2 + 2\alpha_{pn}\, I\, R\, \Delta T = 0$$

or $$Z\, I^2\, R\, T_m + (\alpha_{pn}\Delta T + I\, R)^2 - R^2I^2 = 0$$

or $$I^2R^2(1 + Z\, T_m) = (\alpha_{pn}\Delta T + I\, R)^2$$

or $$I_{\max} = \frac{\alpha_{pn}\Delta T}{R(\sqrt{1 + ZT_m} - 1)} \tag{14.49}$$

Substituting this in Eq. (14.18), the expression for maximum COP is obtained as follows:

$$\xi_{\max} = \frac{T_c[\sqrt{1 + ZT_m} - T_h/T_c]}{(T_h - T_c)[\sqrt{1 + ZT_m} + 1]} \tag{14.50}$$

Maximum refrigeration effect

The derivative of refrigeration effect Q_c with respect to current I is put equal to zero to obtain the condition for maximum refrigeration effect.

$$Q_c = \alpha_{pn}I\,T_c - \frac{I^2R}{2} - U(T_h - T_c)$$

$$\frac{dQ_c}{dI} = \alpha_{pn}T_c - IR = 0$$

$$\therefore \qquad I_{\max} = \frac{\alpha_{pn} T_c}{R} \tag{14.51}$$

Substituting it in the expression for COP [Eq. (14.50)] yields

$$\xi_{\max} = \frac{ZT_c^2/2 - (T_h - T_c)}{ZT_h T_c} \tag{14.52}$$

and

$$Q_{c\max} = \frac{\alpha_{pn}^2 T_c^2}{2R} - U\,\Delta T = U\left[\frac{ZT_c^2}{2} - (T_h - T_c)\right] \tag{14.53}$$

The figure of merit $Z = a_{pn}^2/UR$ appears in all these expressions. This is optimum when the product UR is minimum. The product UR may be expressed as follows:

$$UR = \left(\frac{k_p A_p}{L_p} + \frac{k_n A_n}{L_n}\right)\left(\frac{L_p \rho_p}{A_p} + \frac{L_n \rho_n}{A_n}\right) \tag{14.54}$$

or

$$UR = \rho_p k_p + \rho_n k_p \frac{A_p L_n}{A_n L_p} + \rho_n k_n + \rho_p k_n \frac{A_n L_p}{A_p L_n}/RU$$

Once the materials are chosen the physical properties ρ_p, k_p, ρ_n and k_n are fixed and optimization is done for the dimensions of the conductors as follows. A group of dimensions is defined as $x = A_p L_n / A_n L_p$, hence

$$UR = \rho_p k_p + \rho_n k_n + k_p \rho_n x + k_n \rho_p \frac{1}{x} \tag{14.55}$$

For UR to be minimum,

$$\frac{d(UR)}{dx} = 0 = k_p \rho_n - k_n \rho_p \frac{1}{x^2} \quad \text{and} \quad \frac{d^2(UR)}{dx^2} = k_n \rho_p \frac{2}{x^3} = \text{positive quantity}$$

Hence for UR to be minimum

$$x = \frac{A_p L_n}{A_n L_p} = \sqrt{\frac{k_n \rho_p}{k_p \rho_n}} \tag{14.56a}$$

and

$$UR_{\min} = (\sqrt{\rho_n k_n} + \sqrt{\rho_p k_p})^2 \quad \text{and} \quad Z_{\max} = \frac{\alpha_{pn}^2}{(\sqrt{\rho_n k_n} + \sqrt{\rho_p k_p})^2} \tag{14.56b}$$

For the special case of $k_p = k_n = k$ and $\rho_p = \rho_n = \rho$, $Z_{max} = \alpha_{pn}^2 / \rho k$

One can include a contact resistance of, say, r ohm-cm^2 at each junction and carry out the optimization. The expression for the product UR then becomes.

$$UR = \left(\frac{k_p A_p}{L_p} + \frac{k_n A_n}{L_n}\right)\left(\frac{L_p \rho_p}{A_p} + \frac{r}{A_p} + \frac{L_n \rho_n}{A_n} + \frac{2r}{A_n}\right)$$

$$= \frac{A_n}{L_n}(k_n + x k_p)\frac{L_n}{A_n}\left(\rho_n + \frac{\rho_p}{x} + \frac{2r}{L_n} + \frac{A_n}{L_n}\frac{2r}{A_p}\right)$$

$$= (k_n + x k_p)\left(\frac{\rho_p}{x}\left(1 + \frac{2r}{\rho_p L_p}\right) + \rho_n\left(1 + \frac{2r}{\rho_n L_n}\right)\right) \quad (14.57)$$

The optimization of this expression can be easily done if one assumes that the length of both the conductors is the same, that is, $L_p = L_n = L$ which reduces the expression for the product UR to

$$UR = (k_n + x k_p)\left(\frac{\rho_p}{x}\left(1 + \frac{2r}{\rho_p L}\right)\rho_n\left(1 + \frac{2r}{\rho_n L}\right)\right) \quad (14.58)$$

Differentiating this with respect to x and equating it to zero yields

$$x = \sqrt{\frac{k_n \rho_p (1 + 2r/\rho_p L)}{k_p \rho_n (1 + 2r/\rho_n L)}} \quad (14.59)$$

which yields

$$Z_{\max} = \frac{\alpha_{pn}^2}{[\sqrt{\rho_n k_n (1 + 2r/\rho_n L)} + \sqrt{\rho_p k_p (1 + 2r/\rho_p L)}]^2} \quad (14.60)$$

For the special case of $k_p = k_n = k$ and $\rho_p = \rho_n = \rho$

$$Z_{\max} = \frac{\alpha_{pn}^2 \sigma}{4k(1 + 2r\sigma/L)} \quad \text{where,} \quad \sigma = \frac{1}{\rho} \quad (14.61)$$

Insulators have small electrical conductivity, that is, large electrical resistance, which leads to large Joulean heating. The Seebeck coefficient is large for insulators, which generates large refrigeration capacity but it is masked by large Joulean heating and these materials, therefore, fail as thermoelectric refrigeration materials.

Metals have small Seebeck coefficient and large thermal conductivity. Hence these fail as thermoelectric materials since small refrigeration capacity is generated while heat conduction is very large.

The best results are obtained with semiconductors. The figure of merit $Z_{\max} = \alpha_{pn}^2/\rho k = Z_{\max} = \sigma\alpha_{pn}^2/k$. The product $\sigma\alpha_{pn}^2$ is observed to be maximum for semiconductors. Hence semiconductors are most suited for thermoelectric refrigeration. Alloys of bismuth, tellurium and antimony are used for *p*-type elements. Alloys of bismuth, tellurium and selenium are used for *n*-type elements.

According to *ASHRAE Handbook, Fundamentals Volume*, 1967, typical values of properties of these thermoelectric materials are as follows:

Seebeck coefficient = 0.00021 V/K
Thermal conductivity = 0.015 W/m-K

Electrical resistivity = 0.001 ohm-cm

Electrical contact resistance = 0.00001 to 0.0001 ohm-cm^2

The values of maximum figure of merit Z_{max} for this data for various lengths and contact resistances are as follows:

L (cm)	R (Ω-cm^2)	$1 + 2r\sigma/L$	Z_{max} (K^{-1})
–	0	1.0	0.00294
1.0	0.00001	1.02	0.00288
1.5	0.00001	1.04	0.00283
1.0	0.0001	1.2	0.00245
1.5	0.0001	1.4	0.0021

EXAMPLE 14.5 In a thermoelectric refrigeration system of 20 W cooling capacity, $T_c = -15^oC$ and $T_h = 40^oC$. Both the diameter and length of *p*-type material are 0.01 m. The length of the *n*-type material is also 0.01 m. The properties of thermoelectric materials are as follows:

$\alpha_p = 0.00015$ V/K and $\alpha_n = -0.0002$ V/K

$\sigma_p = 1000$ cm^{-1} ohm^{-1} and $\sigma_n = 1500$ cm^{-1} ohm^{-1}

$k_p = k_n = 1.2$ W/m-K

Find the area and the diameter of the *n*-type material, overall heat transfer coefficient U, the resistance R and the figure of merit Z. Then find the COP, the current, refrigeration effect, the number of thermocouple pairs and the power for the case of maximum COP and for the case of maximum cooling.

Solution:

For UR to be minimum and the *figure of merit* to be maximum, we have from Eq. (14.56a)

$$x = \frac{A_p L_n}{A_n L_p} = \sqrt{\frac{k_n \rho_p}{k_p \rho_n}}$$

We have $L_p = L_n$, $k_p = k_n$ and $\sigma = 1/\rho$, therefore,

$$\frac{A_p}{A_n} = \sqrt{\frac{\rho_n k_n}{\sigma_p k_p}} = \sqrt{\frac{1500}{1000}} = 1.225$$

$$A_p = \frac{\pi (0.01)^2}{4} = 0.00007854 \text{ m}^2 \quad \therefore \quad A_n = \frac{A_p}{1.225} = 0.00006413 \text{ m}^2$$

$$d_n = \sqrt{\frac{4A_n}{\pi}} = 0.00904 \text{ m}$$

With $L_p = L_n$, $k_p = k_n$, we get

$$U = \frac{(A_p + A_n)k}{L} = \frac{0.00014267(1.2)}{0.01} = 0.01712 \text{ W/K}$$

$$R = \frac{L\left(\frac{1}{\sigma_p A_p} + \frac{1}{\sigma_n A_n}\right)}{100} = \frac{0.01\left(\frac{1}{1000 \times 0.00007854} + \frac{1}{1500 \times 0.00006413}\right)}{100}$$

$$= 0.0023128 \text{ ohm}$$

$$UR = 0.00003959 \text{ W-ohm/K}$$

$$\alpha_{pn} = \alpha_p - \alpha_n = 0.00035 \text{ V/K}$$

$$Z = \alpha_{pn}^2 / UR = 0.003094 \text{ K}^{-1}$$

$$T_m = \frac{T_h + T_c}{2} = \frac{258 + 313}{2} = 285.5 \text{ K}$$

and $\sqrt{1 + ZT_m} = \sqrt{1 + 0.003094(285.5)} = 1.3724$

For the case of maximum COP, from Eq. (14.50),

$$\xi_{\max} = \frac{T_c[\sqrt{1 + ZT_m} - T_h / T_c]}{(T_h - T_c)[\sqrt{1 + ZT_m} + 1]} = \frac{258}{55} \frac{1.3724 - (313/258)}{1.3724 + 1} = 0.3148$$

From Eq. (14.49),

$$I_{\max} = \frac{\alpha_{pn} \Delta T}{R\{\sqrt{1 + ZT_m} - 1\}} = \frac{0.00035(55)}{0.0023128(1.3724 - 1.0)} = 22.35 \text{ amps}$$

From Eq. (14.44),

$$Q_c = \alpha_{pn} I T_c - (I^2 R/2) - U(T_h - T_c)$$

$$= (0.00035)(22.35)(258) - (22.350)^2(0.00231288)/2 - 0.01712(55)$$

$$= 0.4989 \text{ W per pair}$$

For 20 W cooling, the number of thermocouple pairs required = 20/0.4989 = 40 pairs

$$\text{Power} = \frac{Q_c}{\text{COP}} = \frac{20}{0.3148} = 62.89 \text{ W}$$

For the case of maximum cooling, we have from Eq. (14.52),

$$\xi_{\max} = \frac{ZT_c^2 / 2 - (T_h - T_c)}{ZT_h T_c} = \frac{\frac{0.003094(258)^2}{2} - 55}{0.003094 \times 313 \times 258} = 0.192$$

From Eq. (14.51),

$$I_{\max} = \frac{\alpha_{pn} T_c}{R} = \frac{0.00035(258)}{0.0023128} = 39.043 \text{ amps}$$

From Eq. (14.53),

$$Q_{e\max} = U\left[\frac{ZT_c^2}{2} - (T_h - T_c)\right] = 0.01712\left[\frac{258^2\,(0.003094)}{2} - 55\right] = 0.8213 \text{ W per pair}$$

For 20 W cooling, the number of thermocouple pairs required = 20/0.8213 = 24.35 = 25 pairs

$$\text{Power} = \frac{Q_c}{\text{COP}} = \frac{20}{0.193} = 104.17 \text{ W}$$

A thermoelectric material should be chosen such that the *figure of merit* is as large as possible so that significant refrigeration effect can be obtained. A value around 0.006 K^{-1} is reasonable. The COP increases with increase in the value of *figure of merit* and approaches $(\text{COP})_{RC}$ as $Z \to \infty$.

It has been shown that COP is maximum at a certain value of current. Similarly, the refrigeration effect is also maximum at a certain different value of current. Example 14.5 shows that if the system is designed based upon maximum COP, then the number of thermocouple pairs required is very large, that is, it will require more initial cost. If the system is designed based upon maximum refrigeration effect then it requires a less number of thermocouple pairs but the power requirement is more. That is, the initial cost is less but the running cost is more. In fact, one can consider both the running and initial costs and find the optimum number of thermocouple pairs cost-wise.

Multistage thermoelectric system

Figure 14.9 shows a two-stage thermoelectric refrigeration system. The first stage rejects heat transfer Q_1 to the second stage. This becomes the refrigeration effect of the second stage. The second stage rejects heat transfer Q_2 to the surroundings. In a multistage system, Q_2 will be rejected to the third stage. Let COP_1 and COP_2 be the coefficients of performance of the two stages. Then, we have

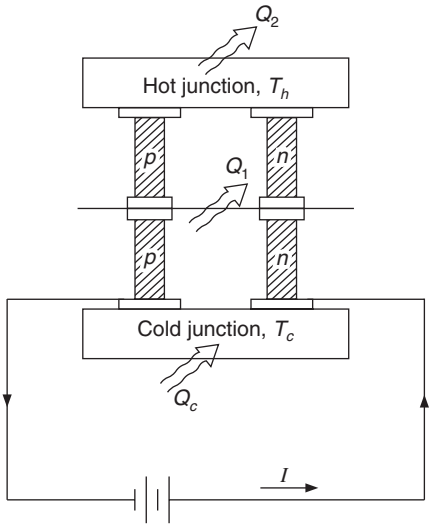

Figure 14.9 A two-stage thermoelectric refrigeration system.

$$\text{COP}_1 = \frac{Q_c}{Q_1 - Q_c} \quad \therefore \quad Q_1 = Q_c\left(1 + \frac{1}{\text{COP}_1}\right) \tag{14.62}$$

$$\text{COP}_2 = \frac{Q_1}{Q_2 - Q_1} \quad \therefore \quad Q_2 = Q_1\left(1 + \frac{1}{\text{COP}_2}\right) \tag{14.63}$$

$$\therefore \quad Q_2 = Q_c\left(1 + \frac{1}{\text{COP}_1}\right)\left(1 + \frac{1}{\text{COP}_2}\right) \tag{14.64}$$

For an n-stage system, one can write

$$Q_n = Q_c \prod_{i=1}^{n}\left(1 + \frac{1}{\text{COP}_i}\right) \tag{14.65}$$

The COP of an n-stage system may be written as follows:

$$\text{COP}_{n-\text{stage}} = \frac{Q_c}{Q_n - Q_c} = \frac{1}{\prod_{i=1}^{n}\left(1 + \frac{1}{\text{COP}_i}\right) - 1} \tag{14.66}$$

Foster has discussed the optimization of multistage systems.

Advantages of thermoelectric system

The following are the advantages offered by thermoelectric systems:

1. There are no moving parts, hence the system does not have any vibration problems and does not require significant maintenance.
2. The cooling load can be easily and precisely controlled by controlling the direct current flowing through the circuit.
3. The system is very compact and works in any orientation unlike the compressor which has to be kept in a vertical position. The elements can be directly attached to the surface to be cooled, thus saving the cost of a heat exchanger.
4. It is a very lightweight system.
5. It can be converted into a heat pump just by changing the direction of current, hence the system can be used for year-round air conditioning.
6. The system is very neat and clean compared to other systems which use refrigerant, lubricating oil and water.
7. Since it does not use refrigerant and oil, the leakage problems are not encountered. It is obviously ozone friendly.

Disadvantages of thermoelectric system

Due to limitation on the *figure of merit* for the available materials, the COP is very low and the running cost is high.

REFERENCE

Zemansky, M.W. (1957): *Heat and Thermodynamics*, McGraw-Hill Book Co., New York.

REVIEW QUESTIONS

1. Describe the advantages, limitations and applications of the water refrigeration system.
2. A temperature of 4°C is maintained inside the flash chamber by using vacuum pump. The make-up water is supplied at 25°C. Find the volume flow rate per TR, pump work and COP. The vacuum pump efficiency is 80%.
3. A chilled water air conditioning system has water cooled at 5°C in the flash chamber. A centrifugal compressor the removes the flash vapours and the condenser works at 40°C. The make-up water is available at 30°C. The efficiency of the compressor is 80%. Neglecting pump work, find the COP and the volume flow rate of water vapour handled for a 50 TR system.
4. In a stream-jet refrigeration system, dry and saturated steam at 7 bar enters the ejector. The temperature of the evaporator (flash chamber) is 4°C and that of make-up water to the flash chamber 17°C. The condenser pressure is 0.06 bar. The nozzle, entrainment and diffuser efficiencies are 0.9, 0.6 and 0.7, respectively. Assume the quality of steam at the entry to the diffuser to be 0.92. Determine the mass flow rate of motive steam per kg of flash vapour, refrigeration effect and the COP.
5. In a steam-jet refrigeration system, dry and saturated steam at 6 bar enters the ejector. The flash chamber is maintained at 5°C. The condenser temperature is 35°C and that of the make-up water is 30°C. The nozzle efficiency, entrainment efficiency and diffuser efficiency are 0.85, 0.65 and 0.80 respectively. The state of compressed vapour after isentropic compression is just saturated. Find the mass flow rate of motive steam per kg of flash vapour, refrigeration effect and the COP.
6. Explain the function of each of the basic components of a steam-jet refrigeration plant.
7. Describe with the help of a neat sketch the working of the steam-jet refrigeration cycle. Show the various state points and processes on the *T*–*s* diagram.
8. When is the steam-jet refrigeration system preferred over other systems? Explain the limitations of this system.
9. Explain the phenomena of Seebeck effect and Peltier effect.
10. Explain the importance of Thomson effect in thermoelectric refrigeration.
11. Discuss the relationship between Seebeck, Peltier and Thompson coefficients.
12. What is meant by figure of merit in thermoelectric refrigeration? State the factors governing the value of figure of merit.
13. State the three desirable properties of a good thermoelectric material.
14. Why are semiconductors most suited for thermoelectric refrigeration. Discuss.

15. In a thermoelectric refrigeration system of 120 W cooling capacity, the cold junction and the hot junction temperatures are –1°C and 35°C respectively. The diameter and length of both *p*-type and *n*-type elements are 10 mm and 12.5 mm respectively. The properties of these thermoelectric materials are :

$$\alpha_p = 170 \times 10^{-6} \text{ V/K and } \alpha_n = -190 \times 10^{-6} \text{ V/K}$$

$$\sigma_p = 1000 \text{ cm}^{-1} \text{ ohm}^{-1}, \sigma_n = 1500 \text{ cm}^{-1} \text{ ohm}^{-1}$$

$$k_p = k_n = 2 \text{ W/m-K}$$

Find the overall heat transfer coefficient U, the resistance R and the figure of merit Z. Also, find the COP, the current, refrigeration effect, the number of thermocouple pairs and the power consumption for the case of maximum COP and for the case of maximum cooling.

16. State the advantages and disadvantages of thermoelectric refrigeration.

15

Air Conditioning

LEARNING OBJECTIVES

After studying this chapter the student should be able to:

1. Acquire an understanding of the historical background of air conditioning.
2. Discuss the basis on which air conditioning systems are classified.

15.1 HISTORICAL REVIEW

The science and practice of creating a controlled climate in indoor spaces is called air conditioning. Man inhabitates all the parts of the world—from Antarctica to the African deserts. Only in a very few favoured areas of the earth's temperate zone can people live and work comfortably round the year without any air conditioning. From the earliest times, artificial cooling has been recognized as desirable. In every era people have invented primitive methods for cooling strictly as a luxury rather than as a necessity—snow, ice, and cold water when available were used for small-scale cooling. Atmospheric evaporation of water was also used crudely without much understanding of the underlying principles. The primitive method of heating for comfort, was building open fires in caves and tents. Fireplaces in medieval Europe were hardly an improvement. Ancient Romans circulated warm air in hollow floors or walls to provide radiant heating. This was an improvement over the localized radiation from a fireplace.

Around 2500 BC, the method of ice making by radiative cooling by sky at night time from water kept in shallow earthen pots was popular in dry climates in India, Egypt, and China. It was in Patliputra University in India that the first air-cooling system was introduced by inducing the cool breeze from river Ganges with the help of chimneys and natural draft methods. Evaporative cooling by inducing the air to flow through wetted straw matrix has been popular in India since a very long time. A particular variety of weed called *khus* is used for the matrix. This freshens the air by its odour apart from cooling it. Also, evaporative cooling of water kept in earthen porous pots

has been in vogue in India since a long time. Emperor Akbar was known to be very fond of cool beverages and for this purpose he used to get his ice made by radiative cooling.

Leonardo da Vinci (as described in *History of Refrigeration*, IIR Publication, 1979) in fifteenth century invented a ventilation and cooling unit for the Duke of Milan. This was essentially a great wheel, one storey high in order to draw the air.

In western societies too, the use of ice was in vogue. As the use of ice increased, the need for mechanical cooling was felt. Anderson (1953) has given the details of history of refrigeration. In 1755 mechanical cooling was achieved for the first time. Thomas Harris and John Long obtained the first patent in 1790. Jacob Perkins developed the hand-operated refrigeration system in 1834 using ether. Dr. John Gorrie of Florida, in 1851, obtained the first American patent for a cold air machine to produce ice. Dr. James Harrisson of Australia, in 1860, installed the world's first refrigeration machine for brewery, using a steam engine for power and sulphuric ether as the refrigerant. Dr. Alexander Kirk of England, in 1861, made a machine similar to Gorrie's in England. In this machine, air was compressed by a compressor, which was driven by a steam engine. It consumed 20 kg of coal to produce 4 kg of ice.

From the inception of refrigeration machine in 1755 a number of attempts were made for mechanical refrigeration by using air, water, ether, etc. as refrigerants. These attempts were based upon more of trial and error rather than on sound principles. It was around 1870 that mechanical vapour compression and absorption refrigeration systems with NH_3 as refrigerant were developed. This put the industry on a sound footing and by 1891 the refrigeration industry was firmly established and within a few years NH_3, CO_2 and SO_2 systems made the air refrigeration systems obsolete.

American Civil War stopped the supply of ice from Northern States of America to Southern States and it was Ferdinand Carre who then developed the vapour absorption system. Before that period, transportation of ice by railways in carriages insulated by cork had been a major achievement in the area of refrigerated transport.

All these machines were run at very low rpm (< 100) by steam engines. This gave a very poor compression efficiency. In 1911 the compressor rpm was raised to 300 and in 1915 a two-stage compressor was introduced.

Refrigeration systems were also used for providing cooling and dehumidification for summer comfort (air conditioning). Air conditioning systems ever since their inception were used for comfort and for industrial air conditioning. Eastman Kodak installed the first air conditioning system in 1891 in Rochester, New York for storage of photographic films. The first domestic air conditioning system was installed in a house in Frankfurt in 1894. A private library was air conditioned in St. Louis, USA in 1895. Many systems were installed in tobacco and textile factories around 1900. A casino was air conditioned in Monte Carlo in 1902. An air conditioning system was installed in a printing press in 1902 and in a telephone exchange in Hamburg in 1904. In 1904, New York Stock Exchange was air-conditioned and around the same time the theatres in Germany were air conditioned.

Willis Carrier is known as the father of air conditioning. In 1904, he designed a central air conditioning plant using air washer He is credited with the first successful attempt to reduce the humidity of air and maintain it at the required level. In 1927, Willis H. Carrier began systematic studies of the conditions of air–water vapour mixture, which was followed by the development of air conditioning equipment. Around 1930, the manufacture of air conditioning equipment started on a commercial scale. By 1950 the industry was firmly established. At present, comfort air

conditioning is widely used in residences, offices, commercial buildings, airports, and hospitals and in mobile applications such as rail coaches, automobiles, aircraft, etc. Industrial air conditioning is largely responsible for the growth of modern electronic, pharmaceutical and chemical industries, etc. Most of the present day air conditioning systems use either a vapour compression refrigeration system or a vapour absorption refrigeration system. The capacities vary from a few kilowatts to megawatts.

Air conditioning of Houston Astrodome with an area of 10 acres and height of 61 m is the major achievement. The historical twin-towers of World Trade Centre had a cooling capacity of 49,000 TR.

Energy crisis gave new challenges to the industry. This has shifted the emphasis to improved efficiencies of the components and to the application of the renewable energy sources. Also it required improved standards of insulation to control heat losses and gains. When better insulating materials and methods were available, the environmental concerns placed new restrictions on materials and methods in HVAC systems. The ban on use of CFCs has also changed the scenario. Some of the popular insulating materials containing R11 cannot be used and have to be replaced by R125. Also the R11 centrifugal compressor used for air conditioning has to be replaced. The globalization has brought in fierce competition.

Indoor air quality (IAQ) has become an essential element and poses new challenges for HVAC systems. Consumers have become conscious of thermal comfort and IAQ, and are placing increasing demands to meet the standards. The systems are becoming more and more sophisticated from the operation and control point of view. Different sophisticated control systems and strategies are being adopted for reliability in achievement of computer controlled energy optimization and in achieving the required thermal conditions.

15.2 HVAC SYSTEMS

A complete heating, ventilating and air conditioning (HVAC) system has the facility to heat, cool, humidify, dehumidify, clean and distribute the conditioned air into the room so as to meet the indoor year-round human comfort or industrial applications. In a large building or in a large installation such as shopping complex, academic complex, research laboratories and office complex, etc. different areas may require different levels of temperature, humidity and cleanliness. The regions with different requirements are divided into zones. Similarly, in a hotel too, each occupant in each room may desire a different level of temperature and humidity. In some cases, the temperature can be controlled by varying the air-volume flow rate or by supplying a little colder air and providing heaters for fine control of temperature. But in general, such vast systems are divided into zones of similar requirements and the system is integrated for energy optimization.

Sometimes the complex may be so far spread out that conditioned air from a single unit cannot be economically transported to various locations. The fan power requirement will be large and also the size of the duct to carry conditioned air and return air will occupy enormous space. In such cases, chilled water and hot water are generated at a central place and transported in underground-insulated pipes to individual buildings for efficient heating/cooling of the coils with air blown and recirculated in separate air handling units. Similarly, in high-rise buildings too, chilled water and hot water are pumped to all the floors where the individual cooling coils are used to heat/cool the air. These systems involve an heat exchanger in a central place where the water is heated/cooled.

A pump is used to transport water in a long pipe line involving heat loss/gain through insulation, followed by cooling/heating of air in another heat exchanger. It saves fan power, but involves more pump power, more heat loss/gain in pipes and an extra heat exchanger. On the other hand, if small individual units are used, the equipment will directly heat or cool the air, thus, eliminating the temperature drop in the second heat exchanger, saving pump power and also heat loss through insulation. Such systems will, however, be of maximum load that each zone needs. It may so happen that all the individual units may not utilize the maximum capacity simultaneously, but such maximum capacity has to be anyway provided for each unit. A central system of smaller total cooling/heating capacity can take care of this by meeting the requirement of maximum load in some zones while the loads in some other zones will be at their minimum. This concept is called diversity factor, which is the ratio of actual load of the whole system to the sum of the individual maximum loads in all the zones.

15.3 CLASSIFICATIONS

There are three major ways of classifying the air conditioning systems, namely (i) based upon the arrangement of equipment, (ii) based upon the major function and (iii) based upon the season.

15.3.1 Classification Based Upon Equipment Arrangement

HVAC systems can be classified into the following three categories based upon the equipment arrangement.

Central HVAC system

In this system, various matched components like compressor, condenser, pumps, cooling tower, etc. are selected and procured from those commercially available in the market and installed in a central plant room or service block. The processing of the air is done in one or more zones in air handling units (AHUs), which are supplied with the liquid refrigerant from the condenser. Direct expansion coils are used as evaporators. Sheet metal ducts to various zones distribute the air. The return air is brought back to the AHU by a duct where it is mixed with some fresh air, cooled/heated, humidified/dehumidified, sometimes reheated and passed through a filter and circulated to the room. Open type reciprocating compressors are used in systems up to 200 TR capacity, screw compressors in the intermediate range of cooling capacity and centrifugal compressor for plants of very large capacity. Sometimes, a combination of, say, centrifugal compressor and screw compressor may be used. The centrifugal compressor in used to meet the steady state demand and the screw compressor is used to augment the system during peak demand. This type of system is not really suitable for hotel or office buildings where individual room control is necessary. It is also not well suited, if the area to be served is spread out or if it is a high-rise building.

Unitary or packaged systems

Most future productions point to the increasing use of these systems. These are factory assembled or packaged units, hence good workmanship can be maintained. A single unit may serve the whole building through ductwork or without ductwork. Many units may be used in the same building connected to the same ductwork. These may be mounted on floor or on rooftop. Smaller units use hermetic compressors while larger units of 5 to 7.5 TR capacities use semi-sealed compressors so

that these require minimum of maintenance. The condenser can be air-cooled for a plant of smaller capacity. Air-cooled condensers require negligible maintenance compared to water-cooled condensers, which require a cooling tower and a water pump too. However, when many packaged units are combined together to give a larger capacity, it is advised to use a water-cooled condenser to obtain a higher COP. The air-cooled condenser may be mounted on rooftop. The unit may be hung from the ceiling. The packaged units are very convenient for single storey buildings or to serve a single floor of high-rise buildings.

Window air conditioner: These are small units of 1 TR to 3 TR cooling capacity meant for individual rooms. These may be installed on the outdoor facing wall of a room near the window or in the window frame. These units are called window air conditioners. There is a partition in the middle of a window air conditioner, which divides it into an outer part and an inner part. The compressor and the air-cooled condenser are on the outer side of the partition. An axial fan sucks the outside air from its sides and throws it straight out over the condenser rejecting heat to the surroundings. The air when sucked flows over the compressor to cool it to some extent. The evaporator (a direct expansion coil) is on the inner side of the partition inside the room. The room air is sucked by a centrifugal fan, made to flow over the evaporator, cooled, dehumidified and recirculated in the room. A single motor with shaft on either side of it, drives the condenser and the evaporator fans. There is a vent in the partition through which some fresh air is continuously introduced into the room. The water vapour that condenses on the direct expansion coil (condensate) is drained outside towards the condenser, where it is sprayed on the air-cooled condenser to obtain some evaporative cooling as well. The small motors are usually not very efficient; hence the COP of these smaller systems may be 20 to 30% less than those of the central systems. Moreover, there is no way of controlling the relative humidity precisely. Also, humidification is not possible and better filters cannot be used to clean the air properly.

Split air conditioner: The window air conditioner is usually very noisy with noise levels of 50 decibals or so. The noise emanates from the compressor and the fans. The split air conditioner is split at the level of partition. It has two distinct parts. The part containing the compressor and the air-cooled condenser along with a motor and a fan, is mounted outside the building. This eliminates the compressor and condenser fan noise from entering the room. It is called condensing unit; it rejects heat to the surroundings and produces liquid refrigerant by condensation. The other part contains the direct expansion coil and a fan. This may be called cooling unit. The liquid refrigerant from the condensing unit is brought into the room by a tube of up to 10 metre length and the vapour from the evaporator is taken out of the room by a tube of similar length and fed to the compressor. These two tubes combined together work as subcooling heat exchanger. There is drop in pressure in both these tubes, as a result the pressure ratio of the compressor is higher for the split units and the COP is smaller. The condensate from the evaporator cannot be sprayed over the condenser to obtain evaporative cooling. Hence, the condenser temperature is higher which further reduces the COP. Two separate motors are used for the two fans, which require more power. And worst of all, there is no scope of introducing fresh air into the room. The split air conditioner is recommended for private executive offices where low noise levels are required, or for interior rooms which do not have a wall facing outdoor on which window air conditioner can be mounted. The condensate from the direct expansion coil has to be drained outside by a pipe line which may get choked if not cleaned frequently.

Combination systems

These systems have already been described. There is a central plant where the water is chilled in a refrigeration system and there is a facility such as a boiler or furnace to heat the water. The hot/chilled water is supplied by insulated pipes to various buildings of a complex or different floors of a high-rise building where it cools/heats the air in a heat exchanger. This type of system is ideally suited for large buildings, large installations like shopping complex, academic complex, research laboratories and office complex, etc. In these systems various control strategies are used to carry out energy optimization by microprocessors with minimum intervention from operators.

15.3.2 Classification According to Major Function

The purpose of an air conditioning system is either to provide comfort to persons or create an environment conducive to industries. Accordingly, the system is classified as comfort air conditioning or industrial air conditioning.

Comfort air conditioning

The purpose of this is to create indoor conditions conducive to human health, comfort and efficiency. Cooling in large buildings during summer months is becoming a standard design practice these days. Even in places where summer temperatures are not high, the heat generated by people, appliances and lights has to be removed to improve the efficiency of workers in offices and for the comfort of customers in stores, restaurants, theatres, hospitals and schools.

Industrial air conditioning

This is meant for providing at least a partial measure of comfort to workers in a hostile environment and to create an environment conducive to research and industrial operations in order to maintain manufacturing tolerances in electronics, space and computer industries and all high speed automated manufacturing operations. These premises or processes require absolute control of temperature, moisture, and air purity. Paper mills, textile mills, candy manufacturing units, printing, photo-processing and host of other industries require air conditioning.

15.3.3 Classification According to Season

The air conditioning systems are classified, according to the season, either as winter air conditioning systems, summer air conditioning systems or year-round air conditioning systems. This is done since the requirements during summer and winter are different.

Summer air conditioning systems

This involves cooling of air, removal of excess moisture, removing the pollutants, dust and introducing fresh air to dilute the odours and the carbon dioxide level. Cooling is done by a refrigeration system and the removal of moisture is also done by the cooling coil. In extreme cases, dehydration by silica gel or other chemicals may be required.

Winter air conditioning systems

Winter comfort usually involves heating and humidification with air purity and movement. Circulating hot water or steam to fin tube radiators or fan coil convectors usually does the heating.

Boilers, furnaces fired by gas, oil, coal or electrical heaters are used to heat the water. Solar collectors may also be used for heating. Heat pumps are very efficient compared to electrical heating. Humidification is done by adding water vapour to the moist air. Humidifiers are simple pan type, spray type or rotary type.

Year-round air conditioning systems

These systems involve both cooling/heating and humidification/dehumidification apart from improving the purity of the air quality so that one can use them throughout the year. In true sense, these systems are called Heating Ventilating and Air Conditioning (HVAC) systems. These have automatic controls to switch them over to heating and dehumidifying systems during winter and vice-versa during summer. In fact, the modern packaged residential heat pumps with their improved designs and better refrigerants work very efficiently as heat pumps during winter and provide cooling during summer.

REFERENCES

Anderson, O.E., Jr. (1953): *Refrigeration in America*, Princeton University Press, Princeton.

IIR Publication (1979): *History of Refrigeration.*

Willis Carrier, *Father of Air Conditioning* (1991): Fetter Printing Company, Louisville, KY, USA.

REVIEW QUESTIONS

1. Explain how does a complete HVAC system work to meet the heating, ventilating and air conditioning requirements of a large complex?
2. Describe the three major ways of classifying air conditioning systems.
3. Briefly describe the working of window air conditioner and split air conditioner.

16

Thermodynamic Properties of Moist Air

LEARNING OBJECTIVES

After studying this chapter the student should be able to:

1. Define the concept of a homogeneous mixture of nonreacting gases.
2. Define the quantities used to describe the composition of a gas mixture, such as mole fraction, volume fraction and mass fraction.
3. Explain the Amagat–Leduc's law of additive volumes and Dalton's law of additive pressures, as applicable to perfect gases as well as real gases.
4. Understand the properties of saturated air, dry air and water vapour.
5. Explain the meaning of terms such as humidity ratio, degree of saturation, relative humidity and saturated air.
6. Derive the relations between relative humidity and the degree of saturation.
7. Explain the terms such as dew point, adiabatic saturation temperature, enthalpy of moist air, and humid specific heat.
8. Explain the phenomenon of adiabatic saturation of air.
9. Determine the properties of moist air given any one of the following combinations:
   (i) Dry-bulb temperature and dew-point temperature
   (ii) Dry-bulb temperature and relative humidity
   (iii) Dry-bulb and wet-bulb temperatures
   (iv) Relative humidity and wet-bulb temperature
10. Explain the concept and the underlying theory of psychrometric chart as a tool to determine the properties of moist air.

16.1 MIXTURES OF GASES

A homogeneous mixture is one whose composition is same everywhere in the domain. This is possible only when its constituents do not react chemically with each other so that the chemical composition remains unchanged. The advantage of the concept of homogeneous mixture is that it can be regarded as a single substance for all practical purposes. The problem is to determine the thermodynamic properties of a mixture from the properties of its individual constituents.

Mixtures of some of the perfect gases can be considered homogeneous, for example, air or air and water vapour. The properties of a homogeneous mixture can be represented in terms of the properties of its constituents.

A homogeneous mixture will have one temperature and one pressure, uniform all over and will be invariant in chemical composition. This implies that such a mixture may be treated as a pure substance. The next question that one may ask is, how many independent intensive properties are required to fix the thermodynamic state of a mixture? A substance which has only *pdv* work mode, is called simple compressible substance. For such a substance only two independent properties are sufficient to fix its thermodynamic state. If p and T or p and v or v and T are specified then all the other thermodynamic properties, for example, u, h, s, etc. can be determined for such a substance. For a mixture of simple compressible substances, on the other hand, one extra property, that is, the relative proportion of various components must also be specified in addition to p and T or p and v or v and T. Only then the extensive properties like enthalpy, internal energy and entropy, etc. can be determined.

The description of the mixture can be given based upon either a gravimetric analysis or a volumetric analysis. The mass fraction of a constituent is defined as the ratio of the mass of the ith constituent to the total mass in any arbitrary sample of gas.

16.2 AMAGAT–LEDUC'S LAW

This law states that the volume of a mixture of perfect gases is equal to the sum of partial volumes of the constituent gases. The partial volume is the volume that a constituent gas will occupy if it existed alone at the mixture pressure p and the mixture temperature T as shown in Figure 16.1. If $\mathbb{V}$ is the total volume and $\mathbb{V}_a$, $\mathbb{V}_b$ and $\mathbb{V}_c$ are the partial volumes of constituent gases a, b and c, then $\mathbb{V}_a + \mathbb{V}_b + \mathbb{V}_c = \mathbb{V}$. That is, $\Sigma \mathbb{V}_i = \mathbb{V}$. The proof of this for perfect gases is as follows.

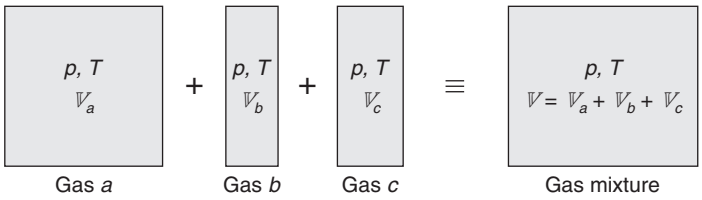

Figure 16.1 Amagat–Leduc's law of additive volumes.

If m_i (kg) and M_i (kg/kg-mole) are the mass and the molecular weight respectively of the ith constituent, then n_i the number of moles for the ith constituent is given by

$$n_i = m_i/M_i$$

Total number of moles is equal to

$$\sum_i n_i = n$$

Mole fraction is defined as

$$\chi_i = n_i / n \quad \text{and} \quad \sum_i \chi_i = 1 \tag{16.1}$$

For perfect gases,

$$p\mathbb{V}_a = n_a \bar{R}T; \; p\mathbb{V}_b = n_b \bar{R}T \quad \text{and} \quad p\mathbb{V}_c = n_c \bar{R}T$$

or in general,

$$p\mathbb{V}_i = n_i \bar{R}T \tag{16.2}$$

where, $\bar{R}$ = universal gas constant.

$$\therefore \qquad \mathbb{V}_a + \mathbb{V}_b + \mathbb{V}_c = (n_a + n_b + n_c)\,\bar{R}\,T/p = n\bar{R}T/p = \mathbb{V}$$

This is the mathematical statement of the Amagat–Leduc's law.

We have in general,

$$\Sigma\,\mathbb{V}_i = \mathbb{V} = \Sigma\, n_i\, \bar{R}T/p = n\bar{R}T/p \tag{16.3}$$

For the whole volume,

$$p\mathbb{V} = n\bar{R}T \tag{16.4}$$

Dividing Eq. (16.2) by Eq. (16.4),

$$\frac{\mathbb{V}_i}{\mathbb{V}} = \frac{n_i}{n} = \chi_i \qquad \text{(the mole fraction of species } i\text{)} \tag{16.5}$$

Hence for an ideal gas the volume fraction is the same as the mole fraction.

The gas constant for species i is defined as $R_i = \bar{R} / M_i$

The mass fraction

$$x_i = \frac{m_i}{\sum m_i} = \frac{m_i}{m} = \frac{n_i M_i}{\sum n_i M_i} \tag{16.6}$$

For ideal gas,

$$p\mathbb{V}_i = n_i \bar{R}T = (m_i / M_i)\,\bar{R}T = m_i R_i T$$

$$\Sigma\,\mathbb{V}_i = \mathbb{V} = \Sigma(m_i R_i)T/p = m\,RT/p$$

Hence the gas constant for mixture, R, may be defined as

$$R = \Sigma\,(m_i R_i) / \Sigma\, m_i \tag{16.7}$$

The previous derivations are based upon the concept of partial volume. The concept of partial pressure is also useful for the mixtures. The partial pressure of a constituent is the pressure, which will exist if this constituent alone occupied the mixture volume $\mathbb{V}$ at the mixture temperature T. The sum of partial pressures of the constituents is equal to the total pressure of the gaseous mixture. If p is the total pressure of the gaseous mixture and p_a, p_b and p_c are the partial pressures of species a, b and c, then

$$p_a + p_b + p_c = p$$

or in general

$$\Sigma p_i = p \tag{16.8}$$

This is known as *Dalton's law of additive pressures* and it is schematically represented in Figure 16.2.

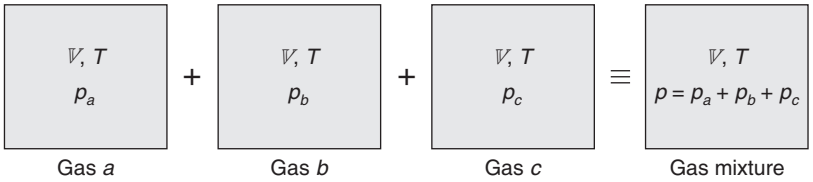

Figure 16.2 Dalton's law of additive pressures.

16.3 GIBBS–DALTON'S LAW

The pressure of a mixture of perfect gases is equal to the sum of the partial pressures of its constituent gases. (It is true for real gases as well.) Gibbs extended this Dalton's law to internal energy, enthalpy and entropy. While using it for entropy, the entropy of mixing has to be included.

The internal energy, or enthalpy, or the entropy of a mixture is equal to the sum of internal energies, or enthalpies, or entropies that each component will have, if it alone occupied the volume $\mathbb{V}$ of the mixture at the mixture temperature T, that is, at its partial pressure. We have

$$p_i \, \mathbb{V} = m_i \, R_i \, T$$

$$\therefore \quad \Sigma p_i \, \mathbb{V} = \Sigma m_i \, R_i \, T$$

From Dalton's law, $\Sigma p_i = p$

$$\therefore \quad p \, \mathbb{V} = \Sigma m_i \, R_i \, T = mRT$$

where R is the gas constant for the mixture of gases and it is equal to

$$R = \Sigma \, (m_i R_i)/m$$

which is the same result as derived using the partial volume concept.

$$p_i/p = m_i \, R_i \, / \, \Sigma (m_i R_i) = m_i R_i \, / \, (mR) = x_i \, R_i / R \tag{16.9}$$

The ratio of partial pressure of species i to the total pressure, is therefore not equal to mass fraction. It can, however, be shown to be equal to mole fraction.

$$p_i \mathbb{V} = n_i \bar{R} T$$

$$\therefore \quad \Sigma p_i \mathbb{V} = p\mathbb{V} = \Sigma n_i \bar{R} T = n \bar{R} T$$

$$\therefore \quad p_i / p = n_i / n = \chi_i \tag{16.10}$$

Now, $$n_i = (p\mathbb{V}_i)/\bar{R}T \quad \text{and} \quad \chi_i = \frac{n_i}{n} = \frac{(p\mathbb{V}_i)/\bar{R}T}{\sum (p\mathbb{V}_i)/\bar{R}T} = \frac{\mathbb{V}_i}{\mathbb{V}}$$

This shows that the mole fraction, the partial pressure ratio and the volume fraction all are equal for a mixture of perfect gases, that is,

$$\chi_i = \mathbb{V}_i / \mathbb{V} = p_i / p = n_i / n \tag{16.11}$$

Dalton's law holds true for real gases too, consequently the mixture compressibility factor can be determined.

For real gases,

$$p\mathbb{V} = n Z \bar{R} T \tag{16.12}$$

where, $Z = Z(p, T, \chi_i)$ is the compressibility factor.

For the ith component of the mixture,

$$p_i \mathbb{V} = n_i Z_i \bar{R} T \tag{16.13}$$

Further from Dalton's law of additive pressures,

$$p = p_1 + p_2 + p_3 + \ldots + p_n = \Sigma p_i$$

And also, $n = \Sigma (n_i)$

For the mixture,

$$p = \bar{R} T \, \Sigma (n_i Z_i) / \mathbb{V} = \bar{R} T n Z / \mathbb{V} \tag{16.14}$$

where Z is the compressibility factor for the mixture.

Hence,

$$Z = \Sigma (n_i Z_i) / \Sigma (n_i) = \Sigma (n_i Z_i)/n = \Sigma (\chi_i Z_i) \tag{16.15}$$

Dividing Eq. (16.13) by Eq. (16.14), we get

$$\frac{p_i}{p} = \frac{n_i Z_i}{\sum n_i Z_i}$$

whereas, for a perfect gas this partial pressure ratio is equal to mole fraction χ_i.

If the Dalton's law holds good for real gases, then it can be shown that the Amagat–Leduc's law also holds for real gases.

From the definition of partial volume and compressibility factor, we have

$$\mathbb{V}_i = n_i Z_i \bar{R} T / p$$

$$\Sigma \mathbb{V}_i = \bar{R} T \, \Sigma (n_i Z_i) / p$$

From Eq. (16.15), we have $\Sigma (n_i Z_i) = nZ$.

$\therefore$ $\Sigma \mathbb{V}_i = n \bar{R} TZ / p = \mathbb{V}$, which proves the Amagat–Leduc's law.

Also,

$\mathbb{V}_i / \mathbb{V} = n_i Z_i / \Sigma (n_i Z_i)$, whereas for an ideal gas $\mathbb{V}_i / \mathbb{V}$ is equal to the mole fraction.

Hence for a real gas, $\mathbb{V}_i / \mathbb{V} = p_i / p \neq \chi_i$.

16.4 PROPERTIES OF AIR–WATER VAPOUR MIXTURE

A pure substance is a substance which is chemically homogeneous and which remains invariant in chemical composition.

Air is a pure substance as long as it is all in vapour phase or all of it is in liquid phase. The two-phase mixture of air is not a pure substance since the liquid phase of air is richer in nitrogen.

A simple compressible substance (SCS) is one for which the only work mode is the $pd\mathbb{V}$ work mode. From the first law of thermodynamics the internal energy can be changed either by heat transfer or by work transfer. The number of independent properties required to fix the thermodynamic state is equal to the number of ways its internal energy can be changed. Hence for an SCS the internal energy can be changed by only two processes, namely, heat transfer and work ($pd\mathbb{V}$). It follows from state postulate that the intensive thermodynamic state of SCS can be described by specifying two intensive properties, namely, temperature for heat transfer and either p or $\mathbb{V}$ for the work transfer.

A mixture of nonreacting gases such as air and water vapour can be treated as an SCS. But to specify its extensive thermodynamic state, three independent properties, for example, the composition of its constituents, internal energy and volume will be required. Since it is a mixture, its composition has to be specified.

The water vapour in the air–vapour mixture will have its pressure as the partial pressure. This partial pressure is quite low and hence the water vapour may be treated as an ideal gas. If the mixture is cooled sufficiently, some water vapour may condense or solidify or if the mixture is heated some liquid may evaporate or the solid may sublime. That is, the chemical composition of the air–water vapour mixture changes, hence it cannot be treated as a pure substance. On the other hand, the only work mode is the $pd\mathbb{V}$ work mode so we will call it an SCS and hence three independent properties are required to fix its thermodynamic state.

16.4.1 Saturated Air

Saturated air is a mixture of dry air and saturated water vapour. Note that it is the water vapour in the moist air, which is saturated and not the air. The oxygen and nitrogen will be saturated at ultra low temperatures when these are in equilibrium with LN_2 and LO_2.

The total pressure of moist air is the sum of partial pressure of dry air and the partial pressure of water vapour. If the partial pressure of the water vapour corresponds to the saturation pressure of water vapour at the mixture temperature, the vapour is said to be saturated.

A closed volume of air in contact with water will become fully saturated if sufficient time is given. If it is not given sufficient time, then the water vapour will be in a superheated state. Also once the air is saturated, it cannot pick up any more water vapour.

Actually the presence of air molecules alters the saturation pressure of water by a very small amount. The saturation pressure reported in steam tables corresponds to the case when at a given temperature water vapour is in equilibrium with liquid water at the same temperature. In such a case the escaping tendency of water molecules from liquid water is exactly the same as the condensing tendency of water vapour molecules. The presence of air molecules changes the escaping tendency of the water molecules, hence the saturation pressure of the air–water vapour mixture will be slightly different from that reported in steam tables. That is, the saturation pressure of a water and water vapour system will be different from the saturation pressure of water and a mixture of water vapour and air system.

16.4.2 Dry Air

Clean air consists of dry air and water vapour. On volume basis, dry air contains 20.99% O_2, 78.03% N_2 and 0.98% traces of about fifteen gases including argon, CO_2, He, and Ne, and H_2O vapour. In some engineering applications the air is supposed to be composed of 21% O_2 and 79% N_2 by volume or 23.2% O_2 and 76.8% N_2 by mass.

The composition of dry air is nearly constant over the earth's surface and up to an altitude of 150 km. The presence of pollutants, gases and particulate matter varies from place to place depending upon the location of industries and other pollution sources.

Goff in *Trans. ASHVE*, vol. 55, p. 463 gives the following composition to determine the molecular weight of dry air.

Substance	*Molecular weight*	*% by mass*	*% by mass × molecular weight*
O_2	32	0.2095	6.704
N_2	28.016	0.7809	21.878
A	39.944	0.0093	0.371
CO_2	44.010	0.0003	0.013
		1.0000	28.966

Although somewhat arbitrary, this composition is regarded as exact in air conditioning. The molecular weight of dry air is 28.996 and the gas constant $R_a = 0.2871$ kJ/(kg mole-K), the gas constant for water being $R_w = 0.461$ kJ/(kg mole-K).

The perfect gas equation describes the properties in an excellent manner at sufficient low pressures and high temperatures. The departure from ideal gas behaviour may be considerable at other conditions. Near the saturated states (–185°C for air) there is a significant deviation from ideal gas behaviour. Luckily, this range for air is way below the air conditioning range of temperatures. In fact, near the saturated states it is called vapour and far above the critical temperature only the ideal gas behaviour is expected.

16.4.3 Virial Equation of State

For real gases a reliable equation of state may be derived from the fundamental principles of statistical thermodynamics. This equation is called the virial equation of state.

For a pure substance such as water vapour or dry air, the *virial equation of state* is given by a power series of the following form:

$$p\bar{v} = \bar{R}T + A_2 p + A_3 p^2 + ... \tag{16.16}$$

or

$$Z = p\bar{v} / \bar{R}T = 1 + A_{2'} p + A_{3'} p^2 + ... \tag{16.17}$$

where, $\bar{v}$ and $\bar{R}$ are defined on molal basis. The first term of this equation is same as that of ideal gas equation. The coefficients A_2, A_3 are second and third virial coefficients, respectively, and these represent the deviation from ideal gas behaviour. These coefficients are functions of temperatures and have to be determined experimentally. These account for forces of attraction or repulsion between molecules. The main characteristic of this equation is that it may be made to conform with experimental data as closely as desired by increasing the numbers of constants. This equation has often been used with ten or more coefficients in composing the tables of properties of refrigerants.

National Bureau of Standards Publication *Table of Thermal Properties of Gases, Circular 54* (Washington DC : Government Printing Office 1955) gives the accurately determined properties of several gases including air. This table shows that the compressibility factor of air is essentially unity in the range of –75°C to 80°C at atmospheric pressure. Hence in this range the perfect gas equation gives excellent results for dry air. The specific heat c_p of dry air varies between 1.004 and 1.007 kJ/kg-K in this range of temperatures. The average value of 1.005 is used for specific heat of dry air. Hence if the reference state of enthalpy is taken as 0°C, the enthalpy of dry air may be written as

$$h_a = 1.005t \text{ kJ/kg} \tag{16.18}$$

Properties of water vapour

The thermodynamics properties of water and steam at saturation are given in appendix for a limited range of air conditioning temperatures (0–50°C). In these tables the enthalpy of water has been taken to be zero at 0°C. In some steam tables, enthalpy and the internal energy are taken to be zero at the triple point of water, which is 0.01°C. Water boils at 100°C at atmospheric pressure of 1.01325 bar. If the pressure is reduced to 0.07384 bar, water will boil at 40°C. Similarly at a pressure of 0.0234 bar, water will boil at 20°C. During boiling the liquid water is in equilibrium with the vapour and both are called saturated states. The specific volume, the specific enthalpy and the specific entropy of saturated liquid water are denoted by v_f, h_f and s_f respectively and saturated vapour states are denoted by v_g, h_g and s_g respectively. The subscript $_{fg}$ is used to denote the difference between the saturated vapour and the saturated liquid values. Figure 16.3 shows the trend of properties of liquid water and water vapour on the *T–s* diagram. This trend is very similar to those obtained for refrigerants.

In the air-conditioning range of temperatures (0–50°C) the pressure is less than 0.08 bar. Hence the properties of low-pressure water vapour are of importance. Figure 16.3 shows several lines of constant enthalpy in the superheat region. The lines of constant enthalpy are seen to be distinctly curved above one atmospheric pressure and very near the saturated vapour line and become horizontal at lower pressures (towards the right side). This essentially shows that that the enthalpy is a function of pressure as well. For an ideal gas, enthalpy is a function of temperature alone. Hence this is a deviation from ideal gas behaviour.

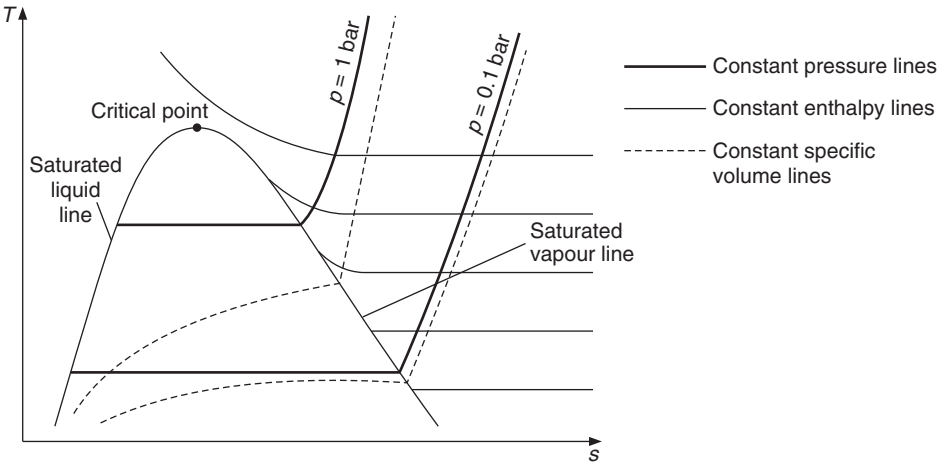

Figure 16.3 Schematic of the *T–s* diagram for water.

In fact at pressures near and below 0.08 bar the constant enthalpy lines are almost horizontal. That is, the enthalpy of superheated vapour is very nearly equal to the enthalpy of saturated vapour at the same temperature. Hence, for pressures less than 0.08 bar,

$$h_w(t) = h_g(t) \tag{16.19}$$

One need not find a virial equation of state for the steam since extensive data is available in steam tables. In fact, an empirical equation is also available to fit the enthalpy data at low pressures, that is,

$$h_w(t) = h_g(t) = 2500 + 1.88t \quad \text{kJ/kg} \tag{16.20}$$

where the temperature t is in ^oC.

The enthalpy is zero for water at 0^oC, hence the enthalpy of saturated water vapour is equal to the enthalpy of evaporation h_{fg} at 0^oC which is approximately 2500 kJ/kg. The specific heat of water vapour is 1.88 kJ/kg-K, hence the enthalpy of water vapour at a point which is at temperature t^oC is, given by

$$h_g(t) = 2500 + 1.88t \tag{16.21}$$

Equations (16.18) and (16.20) represent the enthalpy of dry air and water vapour assuming these relations to behave like ideal gases. These may be called the enthalpies at very low pressures or at zero pressure and denoted by h_a^0 and h_w^0 respectively.

$$h_a^0 = 1.005t \tag{16.22a}$$

$$h_w^0 = h_g(t) = 2500 + 1.88t \tag{16.22b}$$

The variation of enthalpy with pressure for a real gas can be considered on the lines of virial coefficients as done in Eq. (16.16).

In a manner similar to the virial equation of state, an equation may be set up for the specific enthalpy of a real gas as follows:

$$\bar{h} = \bar{h}^0 + B_2 p + B_3 p^2 + \cdots \tag{16.23}$$

where $\bar{h}$ is molal enthalpy and $\bar{h}^0$ is the molal enthalpy at zero pressure, that is if it is assumed to behave like ideal gas. The coefficients B_2 and B_3 account for the interaction between two and three molecules respectively (in ideal gas the forces are zero between molecules). These are called second and third virial coefficients of enthalpy. These can be expressed in terms of virial coefficients A_2 and A_3, etc. of the equation of state (referring to Eq. (16.17)) as follows:

Enthalpy may be considered to be a function of pressure and temperature, i.e. $h = h(p, T)$

$$\therefore \quad dh = \left(\frac{dh}{dp}\right)_T dp + \left(\frac{dh}{dT}\right)_p dT \tag{16.24}$$

The expression for enthalpy is the molal enthalpy. Similarly the volume is also molal volume and entropy is molal entropy. The over-scores have been omitted for brevity. Also,

$$dh = Tds + vdp = T\left[\left(\frac{ds}{dT}\right)_p dT + \left(\frac{ds}{dp}\right)_T dp\right] + vdp$$

or

$$dh = \left[T\left(\frac{ds}{dp}\right)_T + v\right] dp + T\left(\frac{ds}{dT}\right)_p dT$$

Therefore,

$$\left(\frac{dh}{dp}\right)_T = T\left(\frac{ds}{dp}\right)_T + v \tag{16.25}$$

From Maxwell's relations $\left(\frac{ds}{dp}\right)_T = -\left(\frac{dv}{dT}\right)_p$, we get

$$\left(\frac{dh}{dp}\right)_T = -T\left(\frac{dv}{dT}\right)_p + v \tag{16.26}$$

From virial equation of state, we get

$$\left(\frac{dv}{dT}\right)_p = \frac{\bar{R}}{p} + \left(\frac{dA_2}{dT}\right) + \left(\frac{dA_3}{dT}\right) p + \cdots \tag{16.27}$$

Substituting the above expression and the expression for v from Eq. (16.16) in Eq. (16.26), we get

$$\left(\frac{dh}{dp}\right)_T = \left(A_2 - T\frac{dA_2}{dT}\right) + \left(A_3 - T\frac{dA_3}{dT}\right) p + \cdots$$

Integrating it with respect to pressure p, we get

$$\bar{h} = \bar{h}^0 + \left(A_2 - T\frac{dA_2}{dT}\right) p + \left(A_3 - T\frac{dA_3}{dT}\right) \frac{p^2}{2} + \cdots \tag{16.28}$$

Comparing it with Eq. (16.23), we get the expressions for coefficients B_i in terms of A_i,

$$B_2 = \left(A_2 - T \frac{dA_2}{dT} \right), \quad B_3 = \frac{1}{2} \left(A_3 - T \frac{dA_3}{dT} \right), \cdots \tag{16.29}$$

For moist air, which is a mixture of dry air and water vapour, the interaction between air and water vapour molecules has to be taken into account. These interactions can be of the following type and a virial coefficient must be defined for each interaction.

One molecule of dry air interacting with one molecule of dry air	: A_{aa}
One molecule of dry air interacting with one molecule of water vapor	: A_{aw}
Three molecules of air interacting with each other	: A_{aaa}
Two molecules of air interacting with one molecule of water vapour	: A_{aaw}

Accordingly the equation of state for the mixture becomes

$$\begin{aligned} p\bar{v} &= \bar{R}T + (\chi_a^2 A_{aa} + 2\chi_a \chi_w A_{aw} + \chi_w^2 A_{ww})\, p \\ &\quad + (\chi_a^3 A_{aaa} + 3\chi_a^2 \chi_a^2 \chi_w A_{aaw} + 3\chi_a \chi_w^2 A_{aww} + \chi_w^3 A_{www})\, p^2 + \cdots \end{aligned} \tag{16.32}$$

where, χ_a is the mole fraction of dry air and χ_w is the mole fraction of water vapour.

Similarly the virial equation for enthalpy may be written as

$$\begin{aligned} \bar{h} &= \chi_a \bar{h}_a^0 + \chi_w \bar{h}_w^0 - (\chi_a^2 B_{aa} + 2\chi_a \chi_w B_{aw} + \chi_w^2 B_{ww})\, p \\ &\quad - 1/2\, (\chi_a^3 B_{aaa} + 3\chi_a^2 \chi_w B_{aaw} + 3\chi_a \chi_w^2 B_{aww} + \chi_w^3 B_{www}) p^2 \end{aligned} \tag{16.31}$$

where, $\bar{h}_a^0$ and $\bar{h}_w^0$ are the molal enthalpies at zero pressure or for ideal gas and the remaining terms in the above expression account for variation of enthalpy with pressure.

By applying these procedures of statistical thermodynamics, Goff and Gratch (JA Goff and S. Gratch, Thermodynamic Properties of Moist Air, *Trans. ASHVE*, vol. 51, pp. 125–164, 1945) have calculated accurate thermodynamics of properties of moist air at standard sea level pressure of 1.01325 bar.

For convenience in air-conditioning calculations, the enthalpy and specific volume are based upon unit mass of dry air. The specific enthalpy of moist air h has the unit kJ/kga, where kga implies per unit mass of dry air. If in a given sample of moist air, the mass of moist air is m, the mass of dry air is m_a and the mass of water vapour is m_w, then the enthalpy of moist air is written as

$$m_a h = m_a h_a + m_w h_w$$

or

$$h = h_a + (m_w/m_a)\, h_w \tag{16.32}$$

If ideal gas approximation can be made, then

$$h = h_a^0 + (m_w/m_a)\, h_w^0 \tag{16.33}$$

Substituting for enthalpies for zero pressure from Eqs. (16.22a) and (16.22b), we get

$$h = 1.005t + (m_w/m_a)\, h_g(t) \quad \text{kJ/kg} \tag{16.34a}$$

or $$h = 1.005t + (m_w/m_a)\,(2500 + 1.88t) \quad \text{kJ/kg} \tag{16.34b}$$

The term (m_w/m_a) is called the *humidity ratio*. This and other related properties of moist air are defined in the following sections. Subsequently, the expression of enthalpy will also be modified.

16.5 SPECIFIC HUMIDITY OR HUMIDITY RATIO

The composition of moist air may be expressed in terms of specific humidity or humidity ratio. This is usually denoted by the symbol W and is the ratio of the mass of water vapour to the mass of dry air in the given volume of moist air.

$$W = \frac{\text{mass of water vapour}}{\text{mass of dry air}} = \frac{m_w}{m_a} \tag{16.35}$$

let n_a and χ_a denote the number of moles and the mole fraction of dry air, and n_w and χ_w denote the number of moles and the mole fraction for water vapour, then

$$m_w = n_w M_w \text{ and } m_a = n_a M_a$$

$$\chi_a = n_a/(n_a + n_w) \text{ and } \chi_w = n_w/(n_a + n_w) \text{ and } \chi_a + \chi_w = 1$$

$$\therefore \quad W = \frac{m_w}{m_a} = \frac{n_w M_w}{n_a M_a} = \frac{\chi_w M_w}{\chi_a M_a} = \frac{18.016\chi_w}{28.966\chi_a} = 0.622\,\frac{\chi_w}{\chi_a} = 0.622\,\frac{\chi_w}{1-\chi_w} \tag{17.38}$$

These relations are true for a real gas. These can be simplified if it is assumed that water vapour behaves like a perfect gas. Perfect gas approximation is quite good for dry air.

$$p_a \mathbb{V} = \frac{m_a}{M_a}\bar{R}T, \quad p_w \mathbb{V} = \frac{m_w}{M_w}\bar{R}T \quad \text{and} \quad p_a + p_w = p$$

$$\therefore \quad W = \frac{m_w}{m_a} = \frac{p_w M_w}{p_a M_a} = \frac{18.016\,p_w}{28.966\,p_a} = 0.622\,\frac{p_w}{p_a} = 0.622\,\frac{p_w}{p - p_w}$$

$$\therefore \quad W = 0.622\,\frac{p_w}{p - p_w} \tag{16.37}$$

16.6 HUMIDITY RATIO AT SATURATION

If water vapour is added to unsaturated moist air at temperature t, its partial pressure continues to increase until it reaches the saturated state as shown in the T–s diagram of water vapour in Figure 16.4. In the figure the partial pressures of water vapour at states 1 and 2 are p_{w1} and p_{w2} respectively. The water vapour is in superheated state for both the cases and the moist air is unsaturated. At state s the partial pressure of water vapour is p_{ws}, the saturated pressure at temperature t, and it is the maximum pressure that water vapour at this temperature can achieve. The moist air at this state is called *saturated air*.

Goff has defined saturation of moist air as that condition where moist air may coexist in neutral equilibrium with the associated condensed water presenting a flat surface to it. For a curved water interface the pressure will be different on the two sides of the interface depending upon the

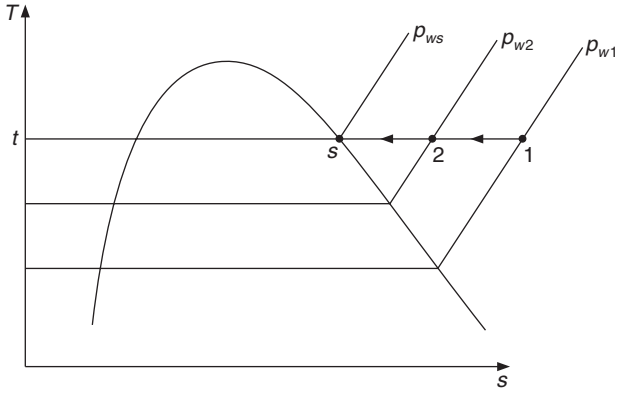

Figure 16.4 For saturated air at state *s*, the partial pressure of water vapour is equal to the saturation pressure of water.

surface tension. Vapour pressure of water represents the escaping tendency of water molecules from the liquid surface. The saturation pressure given in steam tables is the pressure of water vapour alone at temperature t in equilibrium with water at the same temperature. In case of moist air, it is not water vapour alone but a mixture of water vapour and dry that is are present over the water surface. The presence of air molecules increases the escaping tendency of water molecules. If p_{ws} is the saturation pressure of pure water with its associated vapour in equilibrium at temperature t, then the partial pressure of water vapour in saturated moist air is a little higher than $p_{ws.}$ Goff and Gratch have denoted it by $f_s\, p_{ws}$, where f_s is a function of temperature. This is greater than one, which implies that the escaping tendency of water vapour increases in the presence of air molecules. This function f_s has been tabulated by Goff and Gratch (Table 16.1).

Table 16.1 Values of factor f_s for various temperatures for Eq. (16 .38)

Temperature, °C	f_s	*Temperature*, °C	f_s
–20	1.0048	20	1.0045
–15	1.0047	25	1.0047
–10	1.0046	30	1.0048
–5	1.0045	35	1.0049
0	1.0044	40	1.0052
10	1.0044	45	1.0054
15	1.0044		

The humidity ratio at saturation is denoted by symbol W_s and may be expressed as

$$W_s = 0.622 \frac{f_s\, p_{ws}}{p - f_s\, p_{ws}} \tag{16.38}$$

The saturation pressure p_{ws} is a unique function of temperature alone, hence the humidity ratio $W_s = W_s(t)$ at saturation is also a function of temperature alone. Similarly, $f_s = f_s(p, t)$.

The absolute values of humidity may not be sufficient for some calculations. In many calculations involving evaporation of water, the relative proportion of saturation is required. Two such relative measures of saturation are used in air conditioning. These are degree of saturation and relative humidity.

16.7 DEGREE OF SATURATION

The degree of saturation represents the capacity of moist air to absorb water vapour. It is denoted by the symbol μ and defined as follows.

$$\mu = \frac{\text{humidity ratio of moist air at temperature } t}{\text{humidity ratio of saturated air at the same temperature } t} = \frac{W}{W_s} \tag{16.39}$$

16.8 RELATIVE HUMIDITY

Relative humidity is defined as the ratio of the mass of water vapour in a certain volume of moist air at a given temperature, to the mass of water vapour in saturated air of same volume and at same temperature. It is denoted by the symbol f and expressed as follows:

$$\phi = \frac{m_w}{m_{ws}} = \frac{\text{mass of water vapour in a given volume } \mathbb{V} \text{ of moist air at temperature } t}{\text{mass of water vapour in saturated air of same volume } \mathbb{V} \text{ and at the same temperature } t} \tag{16.40}$$

For a real gas, relative humidty may be expressed as

$$\phi = \frac{m_w}{m_{ws}} = \frac{m_w / M_w}{m_{ws} / M_w} = \frac{n_w}{n_{ws}} = \frac{\chi_w}{\chi_{ws}}$$

This expression can be simplified if we assume that moist air, and water vapour in particular, behaves like an ideal gas. Then, $m_w = p_w \mathbb{V}/(R_w T)$ and $m_{ws} = p_{ws} \mathbb{V}/(R_w T)$

$$\therefore \quad \phi = \frac{m_w}{m_{ws}} = \frac{p_w}{p_{ws}} \tag{16.41}$$

Therefore the relative humidity is defined as the ratio of partial pressure of water vapour in the moist air at temperature t to the saturation pressure of water vapour at temperature, t. For a mixture of non-ideal gases, relative humidity is defined as the ratio of mole fraction of water vapour, to the mole fraction of saturated air in same volume, same temperature and at same total pressure.

In some psychrometric calculations, the relations between relative humidity and degree of saturation are required. There are three such relations. These relations are derived as follows:

$$W = 0.622 \frac{\chi_w}{1 - \chi_w}; \ \therefore \ \frac{0.622}{W} = \frac{1 - \chi_w}{\chi_w}; \ \therefore \ \chi_w = \frac{W}{0.622 + W} \ \text{ and } \ \chi_{ws} = \frac{W_s}{0.622 + W_s}$$

$$\therefore \quad \phi = \frac{\chi_w}{\chi_{ws}} = \frac{W}{W_s} \cdot \frac{0.622 + W_s}{0.622 + W}$$

$$\therefore \qquad \phi = \mu \frac{0.622 + W_s}{0.622 + W} \tag{16.42}$$

The second relation is derived as follows:

$$\mu = \frac{W}{W_s} = \frac{0.622\, p_w}{0.622 (p - p_w)} \frac{p - p_{ws}}{p_{ws}} = \phi \frac{p - p_{ws}}{p - p_w}$$

Substituting $p_w = \phi\, p_{ws}$ yields

$$\mu = \phi \frac{p - p_{ws}}{p - \phi p_{ws}}$$

or $$\phi (p - p_{ws} + \mu p_{ws}) = \mu p$$

or $$\phi = \frac{\mu\, p}{p - p_{ws} + \mu p_{ws}}$$

or $$\phi = \frac{\mu}{1 - [(1 - \mu)\, p_{ws} / p]} \tag{16.43}$$

The third relation is derived as follows:

$$\mu = \frac{W}{W_s} = \frac{0.622\, \chi_w}{(1 - \chi_w)} \cdot \frac{(1 - \chi_{ws})}{0.622\, \chi_{ws}} = \phi \frac{(1 - \chi_{ws})}{(1 - \chi_w)} = \phi \frac{(1 - \chi_{ws})}{(1 - \phi \chi_{ws}) + \chi_{ws} - \chi_{ws}}$$

or $$\mu = \phi \frac{(1 - \chi_{ws})}{(1 - \chi_{ws}) + (1 - \phi)\, \chi_{ws}} = \frac{\phi}{1 + \dfrac{(1 - \phi)\, \chi_{ws}}{1 - \chi_{ws}}} = \frac{\phi}{1 + \dfrac{(1 - \phi) W_s}{0.622}} = \frac{0.622 \phi}{0.622 + (1 - \phi) W_s} \tag{16.44}$$

In most air-conditioning calculations, $p >> p_{ws}$. Therefore, $\phi \approx \mu$.

16.9 DEW POINT

Let the temperature of moist air be t and the partial pressure of water vapour be p_w. This state is shown by point A on T–s diagram for water in Figure 16.5. If moist air is cooled at constant pressure, the water vapour that is in superheated state at point A in Figure 16.5 will get de-superheated at constant pressure p_w along the path A–d and approach the saturated state d. The temperature at point d is such that p_w is equal to the saturation pressure p_{ws} at this temperature, that is,

$$p_w = p_{ws}\,(d)$$

If moist air is cooled below the point d then water vapour will condense since the saturated air will hold smaller quantity of water vapour at a lower temperature. Therefore, the temperature of incipient condensation is called *dew point*. The humidity ratio remains constant along the line A–d since no condensation occurs. At point d the humidity ratio is that of saturated air at temperature t_d, therefore

$$W(t, p_w, p) = W_s(t_d, p) \tag{16.45}$$

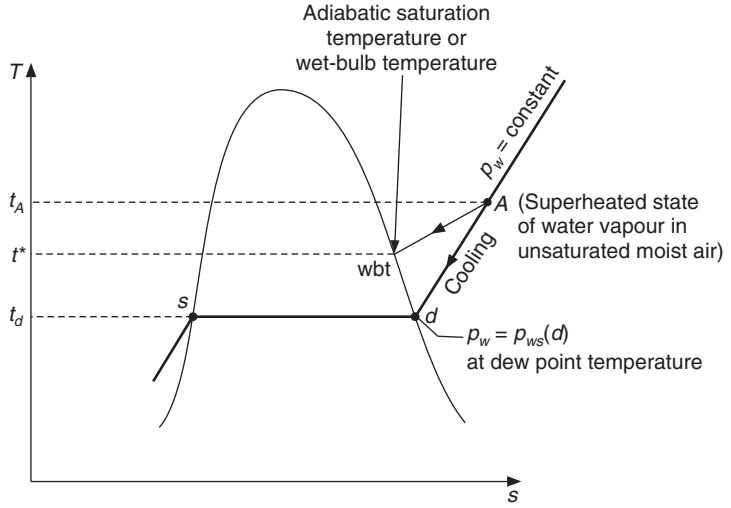

Figure 16.5 Dew point temperature and the adiabatic saturation process on *T–s* diagram.

The process of *cooling at constant pressure* is one of the practical processes to achieve saturation. The figure shows the isothermal cooling process *d–s*, wherein the air is supposed to be *saturated at constant temperature*. This is not a practical process since heat cannot be transferred without some temperature difference. The figure shows another cooling process *A–wbt*. In this process air is *cooled and saturated adiabatically* by evaporation of associated water. The temperature at saturation for this process is called adiabatic saturation temperature or wet bulb temperature, t^*, which is greater than the dew point temperature. This requires a long chamber to be achieved; however, it is practically possible to approach this process.

16.10 ENTHALPY OF MOIST AIR

Equations (16.34a) and (16.34b) can now be expressed in terms of humidity ratio, that is,

$$h = 1.005\, t + W\, h_g(t) \quad \text{kJ/kg} \tag{16.46a}$$

or

$$h = 1.005\, t + W(2500 + 1.88\, t) \quad \text{kJ/kg} \tag{16.46b}$$

The above equation may be rewritten as

$$h = (1.005 + 1.88W)t + 2500W \tag{16.46c}$$

16.11 HUMID SPECIFIC HEAT

It is observed from Eq. (16.46c) that the term $(1.005 + 1.88W)$ multiplies the temperature just as the specific heat c_p of dry air multiplies the temperature t to find the enthalpy of dry air. Hence the quantity $(1.005 + 1.88W)$ is termed the specific heat of moist air or simply the *humid specific heat* and is denoted by the symbol $c_{p\text{-}ma}$, the specific heat of moist air. The first term (1.005) is the specific heat c_p of dry air while the second term $1.88W$ is the specific heat of water vapour. Hence, the specific heat of moist air on the basis of per kg of dry air is $1.005 + 1.88(m_w/m_a)$, that is,

$$c_{p\text{-}ma} = 1.005 + 1.88W$$

In the FPS system, an average value of 0.245 Btu/lb-°F for standard air is used for the specific heat of moist air. In the SI system of units, a value of 1.0216 is used for it. This is supposed to be the humid specific heat of moist air with 50% relative humidity at 20°C and pressure of 1.01325 bar. In terms of it, the enthalpy of moist air may be written as

$$h = 1.0216t + 2500W \tag{16.46d}$$

Amongst all the expressions for enthalpy, Eq. (16.46a) is the most accurate one while Eq. (16.46d) is the least accurate.

16.12 THERMODYNAMIC WET-BULB TEMPERATURE

The thermodynamic wet-bulb temperature is also called the *adiabatic saturation temperature*. It is the temperature at which water, by evaporating into air will bring the air to saturation adiabatically at the same temperature as the water. That is, ultimately the water and saturated air temperatures are the same.

The water molecules escape from water surface and diffuse away from it. The air in the vicinity of water has a larger humidity ratio than that of the air away from it. This provides the potential or the driving force for evaporation and diffusion. As the whole mass of air approaches saturation, this potential diminishes and the rate of evaporation decreases and at saturation, this potential is zero. Therefore, a very large chamber is required to achieve saturation.

Figure 16.6 shows an arrangement by which the adiabatic saturation condition may be achieved. This is an indefinitely insulated enclosed chamber containing water. The chamber is so large that air flowing through it ultimately gets adiabatically saturated. The water evaporates under adiabatic conditions hence the enthalpy of evaporation (or latent heat of evaporation) is derived in part from air and in part from water. In this process both the water and the air are cooled to adiabatic saturation temperature t^*. Since the water in the chamber evaporates, some make-up water has to be provided. It is assumed that the make-up water is added at temperature t^*. In actual practice the temperature of the make-up water will be slightly greater than t^*. The whole process will take a long time or a longer length of the chamber would be required if the water temperature is very much different from t^*.

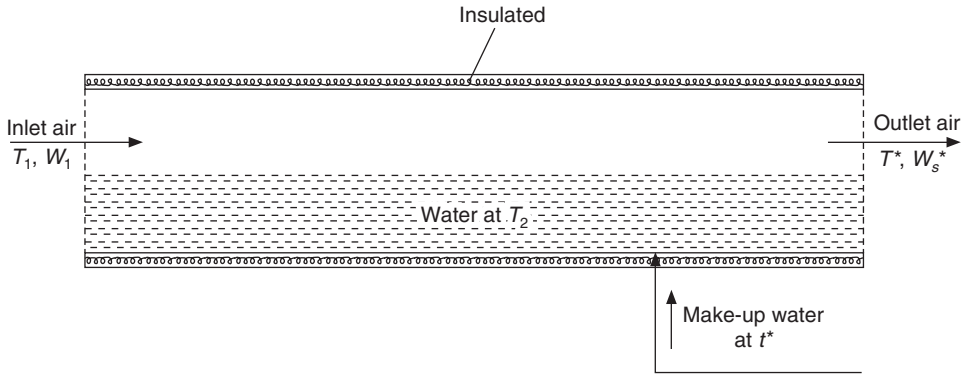

Figure 16.6 Schematic arrangement of adiabatic saturation of air.

Mass and energy conservation are carried to obtain an expression for adiabatic saturation temperature. The mass flow rate of dry air $\dot{m}_a$ remains unchanged in the chamber since dry air is not added from any other source.

Mass flow rate of water vapour at inlet $= \dot{m}_a W_1 \quad \left[\frac{\text{kga}}{\text{s}} \cdot \frac{\text{kgw}}{\text{kga}} = \frac{\text{kgw}}{\text{s}}\right]$

Mass flow rate of water vapour at outlet = $\dot{m}_a W_s^*$

Mass conservation of water gives the mass flow rate of make-up water,

$$\dot{m}_w = \dot{m}_a (W_s^* - W_1) \tag{16.47}$$

Energy balance, considering inlet and outlet air, and make-up water,

$$\dot{m}_a h_1 + \dot{m}_w h_f^* = \dot{m}_a h_s^* \tag{16.48}$$

Substituting for $\dot{m}_w$ and cancelling $\dot{m}_a$ from both sides of the equation, we get

$$h_s^* = h_1 + (W_s^* - W_1) h_f^* \tag{16.49}$$

In this expression for a fixed total pressure p, W_s^* , h_f^* and h_s^* are the functions of saturation temperature t^*, that is,

$$W_s^* = W_s^*(t^*)$$

$$h_f^* = h_f^*(t^*)$$

and $$h_s^* = h_s^*(t^*)$$

whereas, $$h_1 = h_1(W_1, t_1)$$

Therefore Eq. (16.49) states that $t^* = t^*(t_1, W_1, p)$, that is, the adiabatic saturation temperature is a function of thermodynamic properties, hence this adiabatic saturation temperature is also a thermodynamic property. Therefore, Eq. (16.49) is an *implicit equation for thermodynamic saturation temperature.*

It is to be noted that t^* is the temperature of water at adiabatic saturation. For the air-water vapour mixture, the temperature of air is also the same as that of water at saturation. For some pairs, for example, air–alcohol mixture, this temperature is not the same for air and alcohol.

The thermodynamic wet-bulb temperature is one of the properties that can be measured to a very good accuracy. Since it is called the wet-bulb temperature, *the temperature t measured with an ordinary mercury-in-glass or alcohol-in-glass thermometer is called the dry-bulb temperature.* If t and $t^*$are measured, all other properties can be determined.

The expression for humidity ratio is obtained by substituting the following expression for enthalpy into Eq. (16.49), i.e.

$$h_1 = 1.005t_1 + W_1 h_g(t_1)$$

and $$h_s^* = 1.005\, t^* + W_s^*\, h_g(t^*)$$

Thus, we have

$$1.005\, t^* + W_s^*\, h_g(t^*) = 1.005\, t_1 + W_1\, h_g(t_1) + (W_s^* - W_1)\, h_f^*$$

or $$W_1[h_g(t_1) - h_f^*] = W_s^*\, h_{fg}^* - 1.005\,(t_1 - t^*)$$

where $h_{fg}^* = h_g(t^*) - h_f^*$

$\therefore$ $$W_1 = \frac{W_s^*\, h_{fg}^* - 1.005(t_1 - t^*)}{h_g(t_1) - h_f^*}$$

For the general case the subscript 1 can be dropped, that is,

$$W = \frac{W_s^*\, h_{fg}^* - 1.005(t - t^*)}{h_g(t) - h_f^*} \tag{16.50}$$

To evaluate the humidity ratio from this expression, the properties $p_{ws}^*, h_f^*, h_{fg}^*$ and $h_g(t)$ are found from steam tables. W_s^* is determined from p_{ws}^* using $0.622 p_{ws}^*/(1.01325 - p_{ws}^*)$. Alternatively, W_s^* may be found from Goff and Gratch tables.

Expression (16.50) can be simplified by substituting for $h_{fg}^* = 2500 - 2.3067t^*$, $h_g(t) = 2500 + 1.88t$ from Eq. (16.22b) and $h_f^* = 4.1867t^*$. This substitution yields

$$W = \frac{W_s^*\,(2500 - 2.3067t^*) - 1.005(t - t^*)}{2500 + 1.88t - 4.1867t^*} = \frac{2500W_s^* - 1.3017t^* - 1.005t}{2500 + 1.88t - 4.1867t^*} \tag{16.51}$$

Another simple expression may be obtained for W if the empirical expressions are substituted for enthalpy in Eq. (16.48) as follows:

Adding and subtracting h_g^* on left hand side of Eq. (16.49), we have

$$W(h_g - h_g^*) + W h_{fg}^* = W_s^*\, h_{fg}^* - 1.005\,(t - t^*)$$

or $$W(2500 + 1.88\, t - 2500 - 1.88t^*) = (W_s^* - W)\, h_{fg}^* - 1.005\,(t - t^*)$$

or $$(1.005 + 1.88W)(t - t^*) = (W_s^* - W)\, h_{fg}^*$$

or $$c_{p\text{-}ma}\,(t - t^*) = (W_s^* - W)\, h_{fg}^*$$

or $$W = W_s^* - \frac{c_{p\text{-}ma}\,(t - t^*)}{h_{fg}^*} \tag{16.52}$$

Some empirical correlations have been proposed to determine the partial pressure of water vapour, p_w, based upon the given values of t and t^*. Once p_w is known, the humidity ratio is evaluated from $0.622\, p_w/(1.01325 - p_w)$. The correlations are:

1. *Modified Apjohn Equation*

$$p_w = p_{ws}^* - 1.8\, p\,(t - t^*)/2700 \tag{16.53}$$

2. *Modified Ferrel Equation*

$$p_w = p^*_{ws} - 0.0006p(t - t^*)(1 + 1.8\,t\,/1571) \tag{16.54}$$

3. *Carrier Equation*

$$p_w = p^*_{ws} - 1.8(p - p^*_{ws})(t - t^*)/[2800 - 1.3(1.8\,t + 32)] \tag{16.55}$$

In all these equations, temperatures are in °C, p^*_{ws} is saturation pressure at wet-bulb temperature t^*. All the pressures p, p_w and p^*_{ws} must be in same units. It may be noted that these relations can be used even if the pressure is less than the standard atmospheric pressure.

16.13 GOFF AND GRATCH TABLES

Goff and Gratch determined the virial coefficients by fitting the available experimental data on moist air and prepared a set of tables, which are considered to be very accurate to this date. These tables are also called the tables of moist air in some textbooks. These tables list the following variables of moist air at standard atmospheric pressure of 1.01325 bar.

W_s : humidity ratio of saturated air, kg of water vapour per kg of dry air, kgw/kga
v_a : specific volume of dry air at atmospheric pressure and given temperature, m^3/kga
v_s : specific volume of saturated air, m^3/kga
v_{as} : $v_a - v_s$
h_a : specific enthalpy of dry air , kJ/kga
h_s : specific enthalpy of saturated air, kJ/kga
h_{as} : $h_a - h_s$
s_a : specific entropy of dry air, kJ/kga-K
s_s : specific entropy of saturated air, kJ/kga-K
s_{as} : $s_a - s_s$

The values of specific volume, enthalpy and entropy of moist air are very closely given by the following relations:

$$v = v_a + \mu v_{as} + \overline{v} \tag{16.56}$$

$$h = h_a + \mu h_{as} + \overline{h} \tag{16.57}$$

$$s = s_a + \mu s_{as} + \overline{s} \tag{16.58}$$

where

$$\overline{v} = \frac{\mu(1-\mu)A}{1 + 1.6078\,\mu W_s} \tag{16.59}$$

$$\overline{h} = \frac{\mu(1-\mu)B}{1 + 1.6078\,\mu W_s} \tag{16.60}$$

$$\overline{s} = \frac{\mu(1-\mu)C}{1 + 1.6078\,\mu W} \tag{16.61}$$

The constants A, B and C are given in Table 16.2. For temperatures less than 35°C, these constants may be taken to be zero.

Table 16.2 The constants A, B and C for Eqs. (16.59) to (16.61)

Temperature, °C	A, m³/kga	B, kJ/kga	C, kJ/kga-K
35	1.124×10^{-4}	0.0623	1.675×10^{-4}
40	1.874×10^{-4}	0.10679	2.7221×10^{-4}
50	4.73×10^{-4}	0.26597	6.649×10^{-4}
60	1.157×10^{-3}	0.63313	1.5281×10^{-4}
70	2.828×10^{-3}	1.51	3.5538×10^{-4}
80	7.2977×10^{-3}	3.8053	8.666×10^{-4}

The entropy of mixing of air and water vapour must be added to the above result for moist air. It is obtained by integrating $Tds = dh - vdp$ at constant temperature for dry air from pressure of p_a to p and for water vapour from p_w to p. It is given by the following relation.

$$\Delta s_{\text{mixing}} = 0.1579[(1 + 1.6078\,\mu W_s)\log_{10}(1 + 1.6078\,\mu W_s - 1.6078\,\mu W_s \log_{10}\mu) - \mu(1.6078\,\mu W_s)\log_{10}(1 + 1.6078\,\mu W_s)] \quad (16.62)$$

Another convenient relation can be obtained by using the definitions of GG table variables to express the degree of saturation. We have

$$h = h_s^* - (W_s^* - W)h_f^*$$

or
$$h_a + \mu h_{as} = h_s^* - (W_s^* - W)h_f^* = h_s^* - W_s^* h_f^* + \mu W_s h_f^*$$

or
$$\mu = \frac{h_s^* - W_s^* h_f^* - h_a}{h_{as} - W_s h_f^*} \quad (16.63)$$

There are usually three sets of measurements that can be easily made, namely:

Dry-bulb temperature and dew-point temperature

Dry-bulb temperature and relative humidity

Dry-bulb and wet-bulb temperatures.

The relations discussed above can determine all other properties of moist air.

The fourth combination is relative humidity and wet-bulb temperature, in which case iteration is required to determine the properties. We will now discuss these cases with the help of solved examples given below.

EXAMPLE 16.1 The dry-bulb temperature and the dew point temperature of moist air at standard atmospheric pressure are 30°C and 20°C respectively. Determine the humidity ratio, the degree of saturation, the relative humidity, the specific enthalpy and the specific volume using the moist air table and also by using the perfect gas relations.

Solution:

From the moist air table available in the literature, we have the following values:

At 20°C : $p_{ws} = 0.023389$ bar and $W_s = 0.014758$

At 30°C : $p_{ws} = 0.042462$ bar and, $W_s = 0.027392$, $h_a = 30.185$, $h_{as} = 69.82$, $v_a = 0.8586$ and $v_{as} = 0.0376$

We know from Eq. (16.45) that the humidity ratio of moist air is equal to the humidity ratio of saturated air at the dew point temperature, that is,

Humidity ratio of moist air, $W = W_s\,(t_d) = W_s(20^\circ\text{C}) = 0.014758$

Degree of saturation, $\mu = \dfrac{W}{W_s} = \dfrac{0.014758}{0.027392} = 0.53877$

Relative humidity, $\phi = \mu \dfrac{0.622 + W_s}{0.622 + W} = 0.53877 \dfrac{0.622 + 0.027392}{0.622 + 0.014758} = 0.54946$

From Table 16.2 for A, B and C we note that for temperatures less than 35°C, these constants are zero. Hence $\bar{v}$ and $\bar{h}$ are zero. Therefore,

$$h = h_a + \mu h_{as} + \bar{h} = 30.185 + 0.53877\,(69.82) = 67.802 \text{ kJ/kga}$$

$$v = v_a + \mu v_{as} + \bar{v} = 0.8586 + 0.53877(0.0376) = 0.87886 \text{ m}^3\text{/kg}$$

Perfect gas approximation:

We have $p_w = p_{ws}(t_d)$. Therefore, $p_w = 0.023389$ bar

$$\therefore \quad W = 0.622 \frac{p_w}{p - p_w} = 0.622 \frac{0.023389}{1.01325 - 0.023389} = 0.014697$$

$$W_s = 0.622 \frac{p_{ws}}{p - p_{ws}} = 0.622 \frac{0.042462}{1.01325 - 0.042462} = 0.0272062$$

If the factor f_s is to be used for evaluation of W_s, we have from Table 16.1 , $f_s = 1.00475$

$$\therefore \quad W_s = 0.622 \frac{1.00475(0.042462)}{1.01325 - 1.00475(0.042462)} = 0.027341$$

$$\mu = \frac{W}{W_s} = \frac{0.014697}{0.0272062} = 0.54021$$

$$\phi = \mu \frac{0.622 + W_s}{0.622 + W} = 0.54021 \frac{0.622 + 0.0272062}{0.622 + 0.014697} = 0.550823$$

From steam tables, $h_g(30^\circ\text{C}) = 2555.52$ kJ/kg

$$h = 1.005\,t + W\,h_g(t) = 1.005(30) + 0.014697(2555.52) = 67.70848 \text{ kJ/kga}$$

Or by using the empirical equation,

$$h = 1.005\,t + W(2500 + 1.88t) = 1.005(30) + 0.014697(2500 + 1.88 \times 30) = 67.72141 \text{ kJ/kga}$$

Or by using the approximate equation,

$$h = 1.0216\,t + 2500\,W = 1.0216(30) + 2500(0.014697) = 67.5225 \text{ kJ/kga}$$

The partial pressure of dry air is required to determine the specific volume of dry air.

$$p_a = p - p_w = 1.01325 - 0.023389 = 0.98961 \text{ bar} = 98.961 \text{ kPa}$$

$R_a = 0.2871$ kJ/kg-K and 1 bar = 100 kPa

The value of p_a is written in kPa since the gas constant of air R_a is in kJ/kg-K. Also, the temperature should be in K for use in the perfect gas equation.

$$v_a = \frac{R_a T}{p_a} = \frac{0.2871\,(303.15)}{98.961} = 0.87926 \text{ m}^3\text{/kga}$$

It is observed that the enthalpy determined from the empirical equation is less than that determined by use of the moist air table. If the average specific heat of moist air is used, then the enthalpy is even less than that obtained from the empirical equation. The humidity ratio obtained by perfect gas approximation is less than obtained from the moist air table.

EXAMPLE 16.2 The dry-bulb temperature and the relative humidity of moist air at standard atmospheric pressure are 40°C and 30% respectively. Determine the humidity ratio, the degree of saturation, the specific enthalpy and the specific volume using the moist air table and also by using the perfect gas relations.

Solution:

From the moist air table at 40°C : $p_{ws} = 0.073838$ bar, $W_s = 0.049141$, $h_a = 40.253$, $h_{as} = 126.43$, $v_a = 0.887$ and $v_{as} = 0.0698$ and from steam tables $h_g(40^\circ\text{C}) = 2573.49$ kJ/kg

From Table 16.2 : $A = 1.874 \times 10^{-4}$ and $B = 0.10679$

We require the value of degree of saturation, μ, to determine the moist air properties. This is determined by Eq. (16.44) as follows:

$$\mu = \frac{0.622\phi}{0.622 + (1 - \phi)W_s} = \frac{0.622\,(0.3)}{0.622 + (1 - 0.3)\,0.049141} = 0.28428$$

$$\therefore \quad W = \mu\, W_s = 0.28428(0.049141) = 0.139697$$

Now,

$$\frac{\mu(1 - \mu)}{1 + 1.6078\,\mu W_s} = 0.19899$$

and

$$\bar{h} = \frac{\mu(1 - \mu)\,B}{1 + 1.6078\,\mu W_s} = 0.19899(0.10679) = 0.02125$$

$$\therefore \quad h = h_a + \mu h_{as} + \bar{h} = 40.253 + 0.28428 \times 126.43 + 0.02125 = 76.2158$$

Now, $$\bar{v} = \frac{\mu(1-\mu)A}{1+1.6078\,\mu W_s} = 0.19899(1.874\times10^{-4}) = 3.73\times10^{-5}$$

$\therefore$ $$v = v_a + \mu v_{as} + \bar{v} = 0.887 + 0.28428\times0.0698 + 3.73\times10^{-5} = 0.90688$$

Perfect gas approximation:

Given the relative humidity, the partial pressure of water vapour is given by Eq. (16.41)

$$p_w = \phi\, p_{ws} = 0.3(0.073838) = 0.0221514$$

$$W = 0.622\,\frac{0.0221514}{1.01325 - 0.0221514} = 0.0139019$$

$$W_s = 0.622\,\frac{0.073838}{1.01325 - 0.073838} = 0.0488893 \text{ and } \mu = \frac{W}{W_s} = 0.28435$$

From Table 16.1, $f_s = 1.00515$

$\therefore$ $$W_s = 0.622\,\frac{1.00515(0.073838)}{1.01325 - 1.00515(0.073838)} = 0.049161$$

which is closer to the value taken from the GG table.

$$h = 1.005\,t + Wh_g(t) = 1.005(40) + 0.0139019(2573.49) = 75.9764 \text{ kJ/kga}$$

Or by using the empirical equation,

$$h = 1.005\,t + W(2500 + 1.88t) = 1.005(40) + 0.0139019(2500 + 1.88\times40) = 76.0 \text{ kJ/kga}$$

From Dalton's law,

$$p_a = p - p_w = 1.01325 - 0.0221514 = 0.991097 \text{ bar} = 99.1097 \text{ kPa}$$

The value of p_a is written in kPa since the gas constant of air R_a is in kJ/kg-K. Also the temperature should be in K for use in the perfect gas equation.

$\therefore$ $$v_a = \frac{R_a T}{p_a} = \frac{0.2871(313.15)}{99.1097} = 0.90713 \text{ m}^3\text{/kga}$$

EXAMPLE 16.3 The dry-bulb temperature and the wet-bulb temperature of moist air at standard atmospheric pressure are 30°C and 20°C respectively. Determine the humidity ratio, the degree of saturation, the relative humidity, the specific enthalpy and the specific volume using the moist air table and also by using the perfect gas relations.

Solution:

From steam tables and moist air tables:

At 20°C : $p_{ws} = 0.023389$, $h_f^* = 83.9$, $h_{fg}^* = 2453.48$, $W_s^* = 0.014758$ and $h_s^* = 57.555$

At 30°C : $p_{ws} = 0.042462$, $h_g(t) = 2555.52$, $W_s = 0.027392$, $h_a = 30.185$, $h_{as} = 69.82$, $v_a = 0.8586$ and $v_{as} = 0.0376$

We use Eq. (16.50) to determine the humidity ratio

$$W = \frac{W_s^* h_{fg}^* - 1.005(t - t^*)}{h_g(t) - h_f^*} = \frac{0.014758(2453.48) - 1.005(10)}{2555.52 - 83.9} = 0.0105835$$

An approximate relation using the average humid specific heat is

$$W = W_s^* - c_{p\text{-}ma}(t - t^*)/h_{fg}^* = 0.014758 - 1.0216(10)/2453.48 = 0.01059412$$

This is a good approximation.

$$\therefore \quad \mu = W/W_s = 0.0105835/0.027392 = 0.386373$$

Alternatively, using Eq. (16.65),

$$\mu = \frac{h_s^* - W_s^* h_f^* - h_a}{h_{as} - W_s h_f^*} = \frac{57.555 - 0.014758(83.9) - 30.185}{69.82 - 0.027392(83.9)} = 0.387013$$

The two values are different. We use the first value.

The relative humidity is determined from Eq. (16.42) as follows:

$$\phi = \mu \frac{0.622 + W_s}{0.622 + W} = 0.386373 \frac{0.622 + 0.027392}{0.622 + 0.0105835} = 0.39664$$

The correction to enthalpy and specific volume is zero since both A and B are zero below 35.5°C.

$$h = h_a + \mu h_{as} = 30.185 + 0.386373(69.82) = 57.1615$$

$$v = v_a + \mu v_{as} = 0.8586 + 0.386373(0.0376) = 0.87313$$

$$p_w/p = W/(0.622 + W) = 0.0105835/(0.622 + 0.0105835) = 0.0167306$$

$$\therefore \quad p_w = 1.01325(0.0167306) = 0.01695232 \text{ bar}$$

This value of p_w can be checked against the values given by the three empirical equations.

Modified Apjohn Equation

$$p_w = p_{ws}^* - 1.8\, p(t - t^*)/2700 = 0.023389 - 1.8(1.01325(10))/2700 = 0.016634$$

Modified Ferrel Equation

$$p_w = p_{ws}^* - 0.00066\, p(t - t^*)(1 + 1.8\, t\,/1571)$$

$$= 0.023389 - 0.00066(1.01325)\,(10)[1 + (1.8 \times 30)/1571] = 0.01647168$$

Carrier Equation

$$p_w = p_{ws}^* - 1.8(p_w - p_{ws}^*)(t - t^*)/[2800 - 1.3(1.8\, t + 32)]$$

$$= 0.023389 - 1.8(1.01325 - 0.023389)(10)/[2800 - 1.3(1.8 \times 30 + 32)] = 0.01677$$

It is observed that the Carrier equation gives the best approximation to the partial pressure of water vapour.

EXAMPLE 16.4 The dry-bulb temperature and the relative humidity of moist air at 0.9 bar barometric pressure are 35ºC and 40% respectively. Determine the humidity ratio, the degree of saturation, the specific enthalpy and the specific volume using the moist air table and also by using the perfect gas relations.

Solution:

The moist air table cannot be used in this case since these values are valid for standard atmospheric pressure and in this case the pressure is not standard atmospheric pressure. Hence the perfect gas relations have to be used.

At 35ºC : $p_{ws} = 0.05628$ and $h_g = 2564.53$

$$p_w = \phi\, p_{ws} = 0.4(0.05628) = 0.022512$$

$$W = 0.622 \frac{p_w}{p - p_w} = 0.622 \frac{0.022512}{1.01325 - 0.022512} = 0.0159574 \text{ kgw/kga}$$

$$W_s = 0.622 \frac{p_{ws}}{p - p_{ws}} = 0.622 \frac{0.05628}{1.01325 - 0.05628} = 0.04149$$

From Table 17.1, $f_s = 1.0046$ which yields,

$$W_s = 0.622 \frac{p_{ws} f_s}{p - p_{ws} f_s} = 0.622 \frac{1.0046 \times 0.05628}{1.01325 - 1.0046 \times 0.05628} = 0.041694$$

$$\mu = \frac{W}{W_s} = \frac{0.0159574}{0.04149} = 0.38461$$

$$h = 1.005t + Wh_g(t) = 1.005(35) + 0.0159574(2564.53) = 76.09823 \text{ kJ/kg}$$

$$v_a = R_a T \frac{1 + 1.6078W}{p} = \frac{0.2871(308)(1 + 1.6078 \times 0.0159574)}{90}$$

$$= 1.00773 \text{ m}^3\text{/kga}$$

EXAMPLE 16.5 Moist air exists at dry and wet-bulb temperatures of 25°C and 40ºC respectively. The barometric pressure is 0.955 bar. Determine the humidity ratio, the relative humidity, the specific enthalpy and the specific volume.

Solution:

In this example too, the perfect gas relations have to be used since the moist air tables are for standard atmospheric pressure.

At 25ºC : $p_{ws} = 0.031693$, $h_f^* = 104.81$, $h_{fg}^* = 2441.65$

At 40ºC : $p_{ws} = 0.073838$, $h_g(t) = 2573.49$

We use Eq. (16.50) to determine the humidity ratio.

$$W = \frac{W_s^* h_{fg}^* - 1.005(t - t^*)}{h_g(t) - h_f^*} = \frac{0.02135(2441.65) - 1.005(15)}{2573.49 - 104.81} = 0.0150102$$

Now $$p_w = \frac{p.W}{0.622 + W} = \frac{0.955(0.0150102)}{0.622 + 0.015012} = 0.022503 \text{ bar}$$

$\therefore$ $$\phi = \frac{p_w}{p_{ws}} = \frac{0.022503}{0.073838} = 0.302764$$

Now $$W_s = 0.622 \frac{p_{ws}}{p - p_{ws}} = 0.622 \frac{0.073838}{1.01325 - 0.073838} = 0.0521212$$

and $$\mu = \frac{W}{W_s} = \frac{0.0150102}{0.0521212} = 0.28798$$

$\therefore$ $h = 1.005t + Wh_g(t) = 1.005(40) + 0.0150102(2573.49) = 78.8286$ kJ/kga

and $$v_a = \frac{R_a T(1 + 1.6078W)}{p} = \frac{0.2871(313.15)(1 + 1.6078 \times 0.0150102)}{95.5} = 0.963678 \text{ m}^3/\text{kga}$$

The partial pressure of water vapour can be checked against the values given by the three empirical equations.

Modified Apjohn Equation

$$p_w = p^*_{ws} - 1.8\, p\, (t - t^*)/2700 = 0.031693 - 1.8(0.955((15)/2700 = 0.022143$$

Modified Ferrel Equation

$$p_w = p^*_{ws} - 0.00066\, p\, (t - t^*)(1 + 1.8\, t\, /1571)$$

$$= 0.031693 - 0.00066(0.955)\,(15)[1 + (1.8 \times 40)/1571] = 0.0218052$$

Carrier Equation

$$p_w = p^*_{ws} - 1.8(p_w - p^*_{ws})(t - t^*)/[2800 - 1.3\,(1.8t + 32)]$$

$$= 0.031693 - 1.8(0.955 - 0.031693)(15)/[2800 - 1.3(1.8 \times 40 + 32)] = 0.022338$$

The calculated value is 0.022503. Hence the Carrier equation gives the best approximation.

EXAMPLE 16.6 Moist air exists at 25°C wet-bulb temperature and 50% relative humidity. The pressure is standard atmospheric pressure. Find the dry-bulb temperature.

Solution:

The solution has to be found by iteration. We have two relations for humidity ratio, one in terms of relative humidity and the other in terms of the wet-bulb temperature. We guess the value of temperature and find the humidity ratio by the two equations.

$$W = 0.622 \frac{\phi\, p_{ws}}{p - \phi\, p_{ws}} = 0.622 \frac{0.5 p_{ws}}{p - 0.5 p_{ws}}$$

At t =33°C : h_g = 2560.93, p_{ws} = 0.050345 : W = 0.015846

At t =34°C : h_g = 2562.73, p_{ws} = 0.053242 : W = 0.01678

At t =35°C : h_g = 2564.53, p_{ws} = 0.05628 : W = 0.01777

The second relation for humidity ratio is

$$W = \frac{W_s^* h_{fg}^* - 1.005(t - t^*)}{h_g(t) - h_f^*}$$

At 25°C : p_{ws} = 0.031693, h_f^* = 104.81, h_{fg}^* = 2441.65

At t = 33°C : W = 0.017951

At t = 34°C : W = 0.0175287

At t = 35°C : W = 0.017107

Comparing the two set of results, we observe that the answer lies between 34°C and 35°C.

At t = 34.5°C : p_{ws} = 0.054761 $\therefore$ W = 0.017248

Also, h_g = 2563.63 $\therefore$ By second relation, W = 0.01732

The two values are very close together, hence the dry-bulb temperature is 34.5°C.

EXAMPLE 16.7(a) Determine the humidity ratio, the specific enthalpy and the specific volume for moist air at standard atmospheric pressure and if the dry-bulb and the wet-bulb temperatures are 28°C and 21°C respectively.

Solution:

At 21°C : h_f^* = 88.08, h_{fg}^* = 2451.12 and W_s^* = 0.015721

At 28°C : $h_g(t)$ = 2551.9

We use Eq. (16.50) to determine the humidity ratio.

$$W = \frac{W_s^* h_{fg}^* - 1.005(t - t^*)}{h_g(t) - h_f^*} = \frac{0.015721(2451.12) - 1.005(7)}{2551.9 - 88.08} = 0.012784$$

$$h = 1.005t + Wh_g(t) = 1.005\ (28) + 0.012784(2551.9) = 60.763 \text{ kJ/kg}$$

$$p_w = pW/(0.622 + W) = 101.325\ (0.012784)/(0.622 + 0.012784) = 2.046 \text{ kPa}$$

$$p_a = p - p_w = 101.325 - 2.046 = 99.2844 \text{ kPa}$$

$$v_a = \frac{0.2871(273 + 28)}{99.2844} = 0.8704 \text{ m}^3/\text{kg}$$

EXAMPLE 16.7(b) Determine the humidity ratio and the specific enthalpy for moist air at standard atmospheric pressure, if the dry-bulb and wet-bulb temperatures are 12°C and 11°C respectively.

Solution:

At 11°C : $h_f^* = 46.21$, $h_{fg}^* = 2474.74$ and $W_s^* = 0.008197$

At 12°C : $h_g(t) = 2522.78$

We use Eq. (16.50) to determine the humidity ratio.

$$W = \frac{W_s^* h_{fg}^* - 1.005(t - t^*)}{h_g(t) - h_f^*} = \frac{0.008197(2474.74) - 1.005}{2522.78 - 46.21} = 0.007785$$

$$h = 1.005t + Wh_g(t) = 1.005(12) + 0.007785(2522.78) = 31.7002 \text{ kJ/kg}$$

EXAMPLE 16.7(c) Determine the specific enthalpy of saturated air at standard atmospheric pressure and for dry-bulb temperatures of 5°C, 10°C and 12°C.

Solution:

The humidity ratio at saturation is found from the moist air table and then the enthalpy for these temperatures are:

At 5°C : $W_s^* = 0.005424$ and $h_g = 2509.95$

At 10°C : $W_s^* = 0.007661$ and $h_g = 2519.12$

At 12°C : $W_s^* = 0.008766$ and $h_g = 2522.78$

At 5°C : $h = 1.005 + W_s^*(2500 + 1.88t) = 18.636$ and $h = 1.005 + W_s^* h_g = 18.639$

At 10°C : $h = 1.005 + W_s^*(2500 + 1.88t) = 29.3465$ and $h = 1.005 + W_s^* h_g = 29.349$

At 12°C : $h = 1.005 + W_s^*(2500 + 1.88t) = 34.1728$ and $h = 1.005 + W_s^* h_g = 34.1747$

16.14 PSYCHROMETRIC CHARTS

Using the empirical relations, the perfect gas equation, the steam tables or the Goff and Gratch table, one may conveniently solve problems involving moist air. However at times the problems become time-consuming. Also in some air conditioning calculations, iteration is required. In such cases it is convenient to use nomographs, which give a plot of various properties of moist air. This is called the *psychrometric chart*. Not only can this chart determine the properties of moist air, but the calculations for some processes can also be done on this chart itself.

A chart typically is a plot of two independent properties. Moist air requires three independent properties to fix the thermodynamic state. It was shown that if the total pressure called the barometric pressure is fixed, then only two properties are sufficient to fix the thermodynamic state since by Dalton's law the sum of partial pressure of dry air and the partial pressure of water vapour is equal to the specified pressure. This provides an additional relation and reduces the required properties from three to two. The charts are thus drawn for standard atmospheric pressure of 1.01325 bar. Most of the charts use temperature and humidity ratio as the x and y coordinates.

Richard Mollier of Dresden in 1923 introduced enthalpy and humidity ratio as the coordinates. The wet-bulb temperature lines are straight lines on this chart and most other lines are also straight lines. Goodman has suggested a procedure of constructing the h–W psychrometric chart where enthalpy is used as an oblique coordinate. The ASHRAE chart uses this procedure. A schematic of a psychrometric chart for a total pressure of say 1 bar is shown in Figure 16.7.

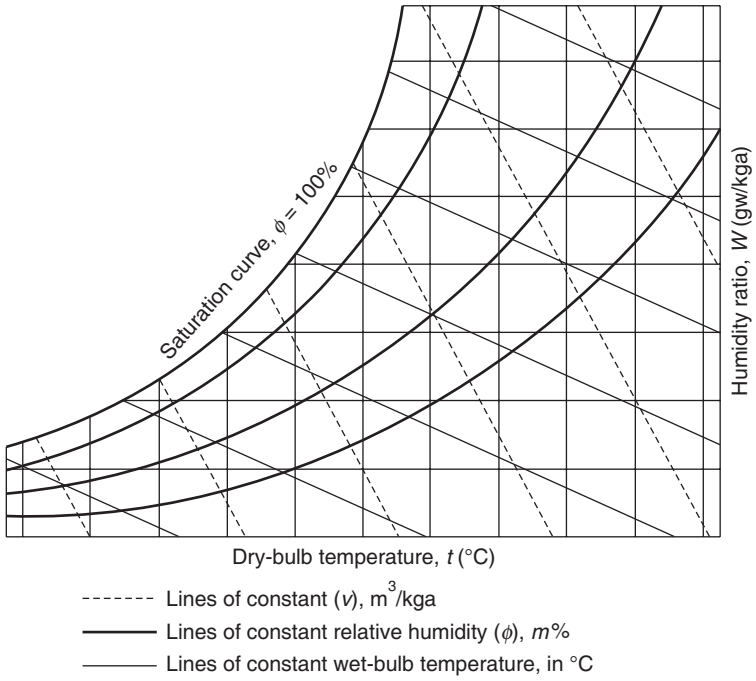

Figure 16.7 Schematic of a pyschrometric chart for a given total pressure, say 1 bar.

16.14.1 Construction of the *t*–*W* Chart

On this chart the humidity ratio W is along the ordinate and the dry-bulb temperature t is along the abscissa. One may make use of the table of properties of moist air or the perfect gas relations along with steam tables to construct this chart, the basic features of which are illustrated in Figure 16.8.

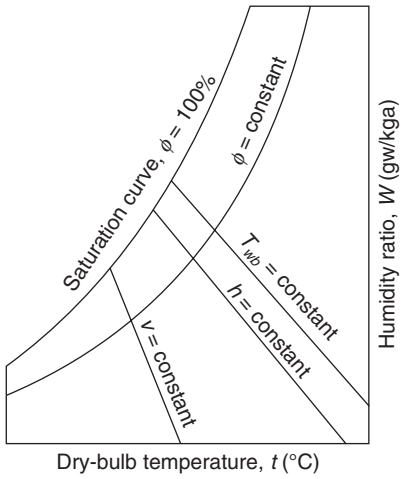

Figure 16.8 Basic features of the pyschometric chart.

Saturation curve

This is the locus of temperature and the corresponding humidity ratio at saturation, W_s. The value of W_s may be read from the moist air tables at the selected temperature and the pairs (t, W_s) plotted to give this curve at 100% relative humidity.

Constant relative humidity lines

If the perfect gas relation is used, then for a given value of relative humidity ϕ, the saturation p_{ws} is read from steam tables for the chosen temperature and the humidity ratio is calculated from the relation

$$W = 0.622 \frac{\phi\, p_{ws}}{p - \phi\, p_{ws}} \tag{16.64}$$

This gives a set of pairs (t, W) for the given ϕ which are plotted to give a ϕ = constant line.

Alternatively, if a very accurate plot is required then for a selected temperature, W_s is read from moist air table and for given ϕ, the degree of saturation and humidity ratio are obtained as under.

$$\mu = \frac{0.622\,\phi}{0.622 + (1-\phi)W_s} \quad \text{and} \quad W = \frac{0.622\,\phi W_s}{0.622 + (1-\phi)W_s} \tag{16.65}$$

Again a set of pairs (t, W) for the given ϕ is plotted to give a ϕ = constant line.

Thermodynamic wet-bulb temperature lines

From the definition of thermodynamic wet-bulb temperature, we have

$$W = \frac{W_s^* h_{fg}^* - 1.005(t - t^*)}{h_g - h_f^*} \tag{16.66a}$$

Cross multiplying and simplifying, we get

$$(W_s^* - W)\, h_{fg}^* = (1.005 + 1.88W)(t - t^*) \tag{16.66b}$$

The slope of the constant wet-bulb temperature (wbt) line is obtained by differentiating Eq. (16.66a) and is thus given by

$$\left(\frac{dt}{dW}\right)_{\text{wbt}} = \frac{-h_{fg}^* - 1.88(t - t^*)}{1.005 + 1.88W} \approx \frac{1}{1.0216}(h_{fg}^* + 1.88(t - t^*)) \tag{16.67}$$

The slope of the constant thermodynamic wet-bulb temperature line is not exactly constant. The enthalpy of evaporation is, however, very large compared to $1.88(t - t^*)$, as a result the right hand side expression is almost constant. An average value of humid specific heat 1.0216 is taken in this expression. One may take an average value of 0.01 for W and use 1.0238 for the denominator. To draw the straight line with this slope, a starting point is required. This point is obtained either from Eq. (16.66a) or Eq. (16.66b), that is,

At $t = t^*$, $W = W_s^*$, that is, on the saturation curve this line intersects it at $t = t_s$

At $W = 0$, $t = t^* + W_s^* \, h_{fg}^*/1.005$

The exact line will not be a straight line. For a given t^*, W can be calculated for the chosen t from Eq. (16.66a) and these set of pairs (t, W) can be joined to give this line.

Constant specific volume lines

The derivation of this is obtained from the perfect gas relation. Starting from the definition of humidity ratio, $W = 0.622 p_w/(p - p_w)$, it can be shown that

$$\frac{p_w}{p} = \frac{1.6078W}{1 + 1.6078W}$$

$$\therefore \quad \frac{p_a}{p} = 1 - \frac{p_w}{p} = \frac{1}{1 + 1.6078W} \tag{16.68}$$

Substituting for p_a in the perfect gas equation for v_a, we get

$$v_a = \frac{R_a T}{p_a} = \frac{(1 + 1.6078W) R_a T}{p}$$

or
$$t = \frac{v_a p}{R(1 + 1.6078W)} - 273.15 \tag{16.69}$$

Differentiating Eq. (16.69) with respect to W, we get

$$\left(\frac{dt}{dW}\right)_{v_a} = -\frac{1.6078 \, v_a p}{R_a (1 + 1.6078W)^2} \tag{16.70}$$

It is obvious from Eq. (16.70) that the slope of this line is also not exactly constant. An average value of slope may be used with a small error to draw this line, for example with $W = 0.01$, $R_a = 0.2871$ kJ/kg-K and $p = 101.325$ kPa, we get the slope as

$$\left(\frac{dt}{dW}\right)_{va} = -531.183 \, v_a \tag{16.71}$$

The point of intersection of v_a = constant line with the x-axis is found by putting $W = 0$ in Eq. (16.69), that is,

Along the x-axis : $t_0 = 352.9258 v_a - 273.15$ (16.72)

For example: at $v_a = 0.7$, $t_0 = -26.1$; at $v_a = 0.75$, $t_0 = -8.46$; at $v_a = 0.8$,

$t_0 = 9.19$; at $v_a = 0.85$, $t_0 = 26.837$; at $v_a = 0.9$, $t_0 = 44.483$

With t_0 as the starting point and the slope given by Eq. (16.71) the constant specific volume line can be drawn.

Calculation of enthalpy of moist air using chart

The psychrometric chart does not give the enthalpy straightaway. It has to be calculated using additional information. The enthalpy of moist air depends upon the dry-bulb temperature and its

water vapour content. It is convenient to express it in terms of enthalpy of saturated air from the definition of thermodynamic wet-bulb temperature, that is,

$$h = h_s^* - (W_s^* - W)\, h_f^* \tag{16.73}$$

The difference $(W_s^* - W)$ will at the most be 0.01 while h_f^* for say 25°C, is $4.1867 \times 25 = 104.67$. Hence the second term in Eq. (16.73) will be around 1.0 at the most. Therefore, for many applications enthalpy is assumed to be constant at h_s^* value along the wet-bulb temperature line. The deviation $(W_s^* - W)\, h_f^* = \Delta h$ is maximum near $W = 0$ and minimum near saturation. The plots of the constant deviation Δh are also available with t along the x-axis and t^* along the y-axis. Hence if one calculates the enthalpy of saturated air h_s^* and finds the deviation Δh from the deviation plot, the enthalpy of moist air can be found from $h = h_s^* \pm \Delta h$.

It is convenient to show the enthalpy scale near the saturation curve expressing the enthalpy of saturated moist air h_s^* at each wet-bulb temperature.

Hence for a given state, h_s^* and W_s^* can be read from the psychrometric chart along the wbt line passing through that point. The value of W is also read from the chart for the given state. Then the only unknown in Eq. (16.73) is h_f^* that can be approximated as $4.1867t^*$ or read from the steam tables.

Sensible heat ratio or sensible heat factor

The end states 1 and 2 of a process when joined by a straight line represent the condition line on the psychrometric chart as shown in Figure 16.9. The processes may involve water vapour addition or condensation and heating or cooling. The slope of this line is the ratio of change in humidity ratio ΔW to the change in dry-bulb temperature Δt. The actual angle on the psychrometric chart depends upon the scales used for humidity ratio and temperature. Say s_w kgw/kga per mm and s_t°C per mm are the scales used for humidity ratio and temperature respectively. Then the change ΔW corresponds to $\Delta W/s_w$ mm shown by distance 2–3. Similarly the change Δt in temperature corresponds to $\Delta t/s_t$ mm shown by distance 1–3. Then the tangent of angle θ is given by

$$\tan\theta = \frac{3\text{–}2}{1\text{–}3} = \frac{\Delta W}{\Delta t} \cdot \frac{s_t}{s_w} \tag{16.74}$$

The humidity ratio is generally in gw/kga, therefore s_t/s_w is usually 10^3 in most of the charts. Therefore,

$$\tan\theta = \frac{\Delta W}{\Delta t} \times 10^3$$

It will be shown later in Chapter 17 that the Sensible Heat Factor (SHF) is represented by

$$\text{SHF} = \frac{1}{1 + 2451\dfrac{\Delta W}{\Delta t}} = \frac{1}{1 + 2.451\tan\theta} \tag{16.75}$$

Therefore,

$$\tan\theta = 0.408\left(\frac{1}{\text{SHF}} - 1\right) \tag{16.76}$$

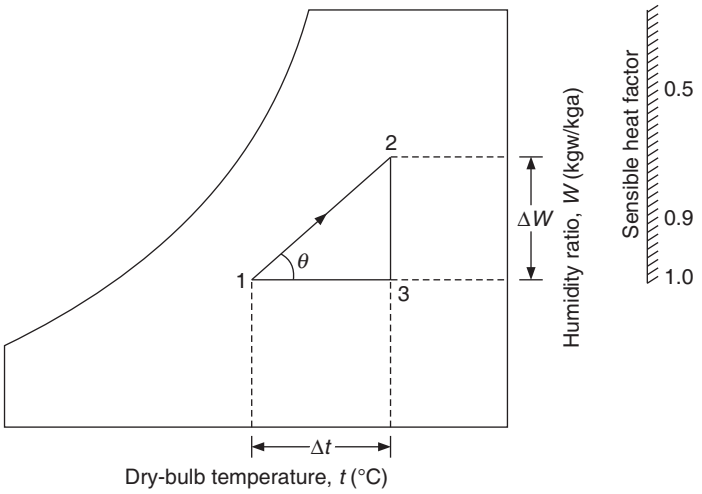

Figure 16.9 Determination of SHF for a given condition line.

A few of the values of angle θ are as follows:

(SHF = 1, $\theta = 0$); (SHF = 0.9, $\theta = 6.34^{o}$); (SHF = 0.8, $\theta = 14.04^{o}$); (SHF = 0.75, $\theta = 18.44^{o}$); (SHF = 0.7, $\theta = 23.2^{o}$); (SHF = 0.65, $\theta = 28.3^{o}$); (SHF = 0.6, $\theta = 33.7^{o}$) and (SHF = 0.5, $\theta = 45^{o}$).

The SHF scale is shown on the right hand side of the psychrometric chart. It shows lines inclined at angle θ corresponding to the SHF value given above. The charts usually have a reference point *O*. It is either 25°C, 50% RH or 26.7°C, 50% RH. The reference point is also called the *alignment circle*. The line joining the alignment circle and a point on the SHF scale will have the corresponding slope θ. The starting point of the actual process with the given SHF may be the point *A* as shown in Figure 16.10. The line *OR* is drawn with the given SHF. The actual condition line will start from point *A* and will be parallel to line *OR*. The SHF scale therefore makes it very convenient to draw the condition line on the psychrometric chart and find the end state.

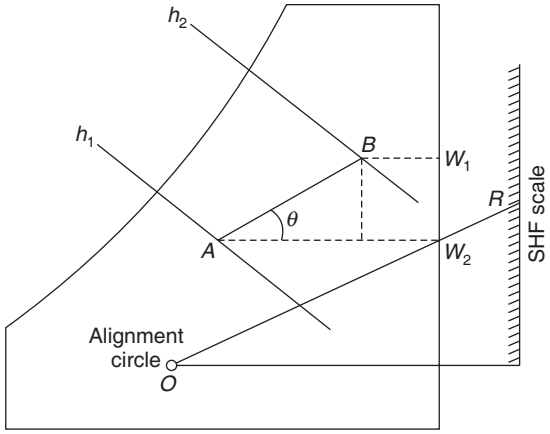

Figure 16.10 Determination of condition line and the end state with the given value of SHF.

16.14 TYPICAL AIR CONDITIONING PROCESSES

Any combination of two of the properties of moist air discussed in the preceeding section can help locate the state of air on the psychrometric chart. Such combinations are unlimited but normally the combinations of dry-bulb temperature and dew-point temperature or wet-bulb temperature are followed. The various air conditioning processes can be illustrated on the psychrometric chart by marking the end conditions of the air. For all of these processes, the air is considered at atmospheric pressure of 1.01325 bar. The various processes that are performed on air in air conditioning systems are illustrated on the psychrometric chart in Chapter 17.

REVIEW QUESTIONS

1. The dry-bulb temperature and the dew point temperature of moist air at standard atmospheric pressure are 21°C and 15°C respectively. Find the humidity ratio, the degree of saturation, the relative humidity, the specific enthalpy and the specific volume using the moist air table and also by using the perfect gas relations.
2. The dry-bulb temperature and the relative humidity of moist air at standard atmospheric pressure are 25°C and 50% respectively. Find the humidity ratio, the degree of saturation, the specific enthalpy and the specific volume using the moist air table and also by using the perfect gas relations.
3. The dry-bulb temperature and the wet-bulb temperature of moist air at standard atmospheric air are 42°C and 30°C respectively. Find the humidity ratio, the degree of saturation, the relative humidity, the specific enthalpy and the specific volume using the moist air table and also by using the perfect gas relations.
4. For Question 2, determine the quantities therein at 0.9 bar pressure of moist air.
5. The atmospheric air, on a particular day, had a dry-bulb temperature of 30°C and wet-bulb temperature of 18°C. The barometric pressure was observed to be 756 mm of Hg. Find the relative humidity, specific humidity, dew point temperature, the enthalpy of air per kg of dry air, and the volume of moisture per kg of dry air.

17

Elementary Psychrometric Processes

LEARNING OBJECTIVES

After studying this chapter the student should be able to:

1. Identify the various processes that are performed on air in air conditioning systems.
2. Perform calculations for various psychrometric processes using the psychrometric charts and equations.
3. Explain the principle of operation of an air washer and various psychrometric processes of the air washer.
4. Explain the principle of dehumidification using hygroscopic substances and hygroscopic spray.

17.1 INTRODUCTION

In air conditioning systems, the temperature, the relative humidity and the air purity have all to be maintained as per the indoor air quality (IAQ) requirements. This requires throwing away some stale air and adding an equal mass flow rate of fresh air, cooling or heating and addition or removal of water vapour, apart from removing particulate matter by appropriate filters. These processes of mixing, heat and mass transfer are carried out in various apparatus. These processes can be represented in terms of some simple fundamental processes on psychrometric chart and calculations carried out. In all these processes, a steady state is assumed and the total pressure is assumed to be constant since the conditions in air conditioning systems change at a slow rate and the total pressure drop through the equipment is at the most of the order of 25 mm of water, which is negligible. The actual process will be a combination of a few of these fundamental

processes. The fundamental psychrometric processes that the air undergoes in air conditioning systems are described in the following sections.

17.2 SENSIBLE HEATING OR COOLING OF MOIST AIR

During summer months, the buildings gain heat due to heat transfer from outdoors through the building structure, incident solar radiation, lights, appliances and persons, etc. This heat gain by the room has to be removed by processing the room air through the cooling coil of the air conditioning plant. This is a heat gain for the building but the air has to be cooled by the plant, hence it is called *cooling load.* In winter months, the heat loss from the building structure to the surroundings may be more than the sum of heat gains by solar radiation, lights, appliances and persons, etc. and the room air may require heating. This is heat loss for the building but the room air requires heating, hence it is called *heating load*. These category of loads give rise to a change in temperature, hence these are called *sensible loads*. The word *sensible* has been in use for temperature change since it can be sensed by human senses, in contrast when water evaporates at constant temperature, it cannot be sensed by thermometer or by our senses, hence it is called the *latent* heat transfer process.

Sensible heating or cooling is a process in which heat transfer can be represented in terms of change in dry-bulb temperature. Sensible cooling can, however, occur only when the temperature of the cooling surface is more than the dew point temperature of air; otherwise some condensation will also occur, which is a latent heat transfer process.

Moist air with mass flow rate $\dot{m}_{a1}$ kg of dry air/s enters an insulated duct at a temperature t_1, humidity ratio W_1 and enthalpy h_1 as shown in Figure 17.1(a). At the outlet of the duct these parameters are $\dot{m}_{a2}$, t_2, W_2 and h_2. There is a heating system in the insulated duct, which may be an electrical heater or hot water flowing through a cooling coil. Steady flow is considered; mass and energy conservation are applied to the system.

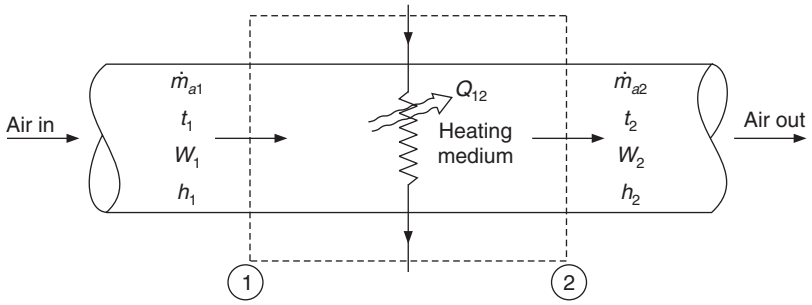

Figure 17.1(a) Schematic of a heating device for heating of moist air.

Mass conservation

A control volume is shown in the figure by a dashed line. No water vapour or dry air is added to this control volume. Hence,

Mass conservation of dry air gives

$$\dot{m}_{a1} = \dot{m}_{a2} = \dot{m}_a \tag{17.1}$$

Mass conservation of water vapour gives

$$\dot{m}_{a1} W_1 = \dot{m}_{a2} W_2 \quad \therefore \quad W_1 = W_2 = W \tag{17.2}$$

Energy conservation gives

$$\dot{m}_a h_1 + Q_{12} = \dot{m}_a h_2$$

$$\therefore \quad Q_{12} = \dot{m}_a (h_2 - h_1) \tag{17.3}$$

We have from the empirical relation for enthalpy

$$h_1 = 1.005 t_1 + W_1(2500 + 1.88 t_1) \quad \text{and} \quad h_2 = 1.005 t_2 + W_1(2500 + 1.88 t_2)$$

$$\therefore \quad Q_{12} = \dot{m}_a (1.005 + 1.88 W_1)(t_2 - t_1)$$

Hence sensible heat transfer Q_S may be expressed as follows:

$$Q_S = Q_{12} = \dot{m}_a c_{p\text{-}ma} (t_2 - t_1) = \dot{m}_a c_{p\text{-}ma} \, \Delta t \ \text{kW} \tag{17.4}$$

where, $c_{p\text{-}ma}$ is called the specific heat of moist air or humid air specific heat. If c_{pa} and c_{pw} are the specific heats of dry air and water vapour respectively, then $c_{pa} + (m_w/m_a)c_{pw}$ is the specific heat of moist air. We have c_{pa}= 1.005 and c_{pw} =1.88 and $W = m_w/m_{a.}$ Therefore the specific heat of moist air is expressed as follows:

$$c_{p\text{-}ma} = 1.005 + 1.88 W \tag{17.5}$$

A horizontal line on the psychrometric chart shows this process since the humidity ratio remains constant. This is shown on the psychrometric chart in Figure 17.1(b).

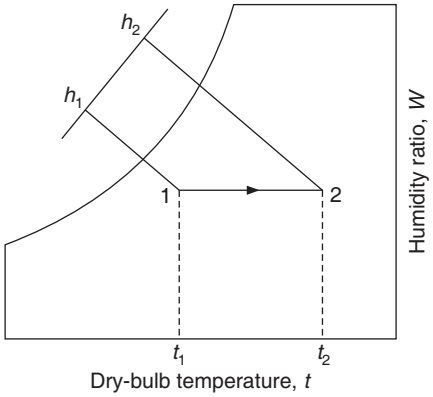

Figure 17.1(b) Sensible heating process.

Commercial air conditioning equipment are rated in terms of volume flow rate of standard air, that is, air at 1.01325 bar, 20°C and 50% relative humidity. The density of standard air is 1.2 kg of dry air per m^3 (kga / m^3). Humid specific heat of standard air is 1.0216 kJ/kg-K. Also, the volume flow rate is specified in m^3/min or cubic metre per minute, abbreviated cmm.

If the volume flow rate is Q_v cmm of standard air, then

$$m_a = 1.2\ Q_v/60 \text{ kga/s}$$

and with $c_{p\text{-}ma} = 1.0216$ kJ/kg-K

$$Q_S = 1.2 \times 1.0216\ Q_v \Delta t/60$$

or
$$Q_S = 0.0204\ Q_v \Delta t \text{ kW} \tag{17.6}$$

If the supply air volume rate is given at conditions other than the standard atmosphere, then the equivalent standard air volume flow rate can be calculated as follows:

$$Q_{v,\text{ standard}} = (1 + W)\ Q_v/(1.2v_a) \tag{17.7}$$

where, Q_v , W and v_a are the volume flow rate, humidity ratio and specific volume respectively under the given conditions.

17.3 HUMIDIFICATION

This process will occur if spraying water or adding water vapour to moist air humidifies the air. In air conditioning systems, water vapour gets added to the room air when the outdoor humid air infiltrates through gaps and crevices in the building. The fresh air introduced for ventilation purpose also adds water vapour to the room air. Human beings dissipate a part of their metabolic heat by perspiration, which adds water vapour to the room air, and the respiration process also adds water vapour to the room air. Appliances like coffee urns, cooking food and warm showers may also add water vapour to the room air. Water vapour may further come in along with the products brought into the room. It may be seen that all these processes involve addition of water vapour to room air.

To model these processes, the system considered is schematically shown in Figure 17.2(a) where moist air enters an insulated duct and water is sprayed inside the duct. *It is assumed that all the water that is sprayed evaporates*. The notations for the inlet and outlet variables are same as in the preceding section. It is assumed that the air retains all the water vapour added. The make-up water flow rate is $\dot{m}_w$ and the enthalpy of water is h_w. There is no heat transfer to the surroundings. The mass flow rate of dry air remains constant like in the last case.

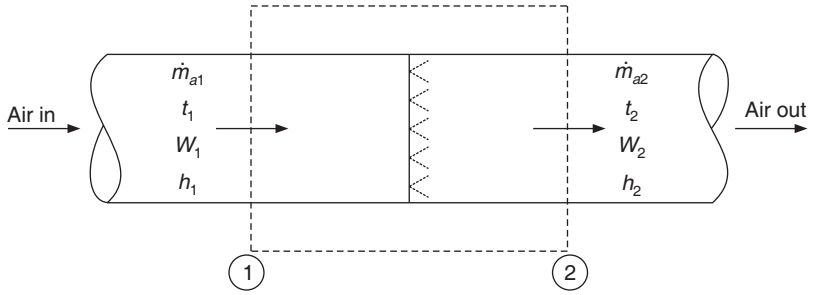

Figure 17.2(a) Schematic of a humidifying device for adding water vapour to moist air.

Mass conservation of water vapour

The mass flow rate of water vapour entering the system is $\dot{m}_a W_1$; similarly that of leaving the system is $\dot{m}_a W_2$. Hence, we get

$$\dot{m}_w = \dot{m}_a(W_2 - W_1) \tag{17.8}$$

Energy conservation

Energy added by water vapour to the moist air is $\dot{m}_w h_w$, hence we get

$$\dot{m}_a(h_2 - h_1) = \dot{m}_w h_w \tag{17.9}$$

Substituting for $\dot{m}_w$ from Eq. (17.8) into Eq. (17.9) and cancelling $\dot{m}_a$, we get

$$(h_2 - h_1) = (W_2 - W_1)\, h_w \tag{17.10}$$

Substituting empirical relations for enthalpy, namely, $h = 1.005t + Wh_g(t)$, we get

$$1.005(t_2 - t_1) + W_2 h_g(t_2) - W_1 h_g(t_1) = (W_2 - W_1)\, h_w$$

or
$$1.005(t_2 - t_1) + W_2\{h_g(t_2) - h_g(t_1)\} = (W_2 - W_1)\{h_w - h_g(t_1)\} \tag{17.11}$$

Also $h_g(t_2) - h_g(t_1) = 2500 + 1.88t_2 - 2500 - 1.88t_1 = 1.88(t_2 - t_1)$. Hence Eq. (17.11) reduces to

$$(1.005 + 1.88W_2)(t_2 - t_1) = (W_2 - W_1)\{h_w - h_g(t_1)\} \tag{17.12a}$$

Alternatively, we can also obtain

$$(1.005 + 1.88W_1)(t_2 - t_1) = (W_2 - W_1)\{h_w - h_g(t_2)\} \tag{17.12b}$$

This equation indicates that the dry-bulb temperature may increase or decrease depending upon the right hand side of the above equation, that is

If $h_w > h_g(t_1)$: Then from Eq. (17.12b), $t_2 > t_1$, that is, air will be sensibly heated and humidified. This is shown by line 1–2′ on the psychrometric chart in Figure 17.2(b). This process occurs if steam is injected into air stream since h_w can be greater than $h_g(t_1)$ only for steam.

If $h_w < h_g(t_1)$: Then from Eq. (17.12b), $t_2 < t_1$, that is, air will be sensibly cooled and humidified. This is shown by line 1–2″ in Figure 17.2(b). This process typically occurs in water spray systems. This should be expected as well, since the liquid water evaporates to become water vapour, which requires latent heat. The latent heat comes from the air, which is cooled.

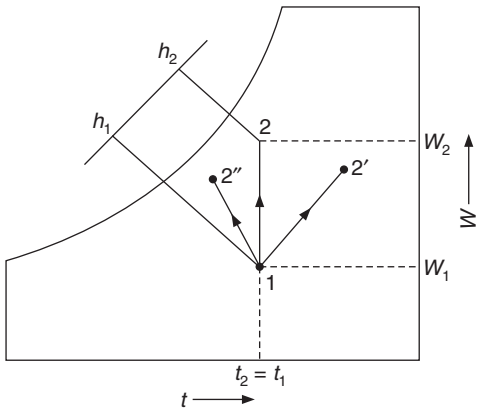

Figure 17.2(b) Humidification process.

If water at temperature t_w is sprayed into the stream of moist air, then $h_w = h_f(t_w) = 4.1867t_w$ while $h_g(t_1) = 2500 + 1.88t_1$. Hence, h_w is always less than $h_g(t_1)$ and water spray will always lead to sensible cooling and humidification of moist air if all the water evaporates.

Also, from Eq. (17.12a)

$$\frac{\Delta W}{\Delta t} = \frac{1.005 + 1.88 W_2}{h_g(t_1) - h_w} \approx \text{constant} \tag{17.13}$$

Hence, a straight line on the W–t psychrometric chart represents this process.

If $h_w = h_g(t_1)$: Then from Eq. (17.12a) $t_2 = t_1$, that is the temperature remains constant. This process is shown by vertical line 1–2 in Figure 17.2(b). This is the pure humidification process.

Equation (17.10) is very similar to the definition of wet-bulb temperature. If water is injected at wet-bulb temperature of air, that is, $h_w = h_f^*$ then the process follows the wet-bulb temperature line 1–2^* as shown in Figure 17.2(c). If the water temperature is less than the wet-bulb temperature of air, then it follows 1–2a and if it is greater than wbt then it follows 1–2c.

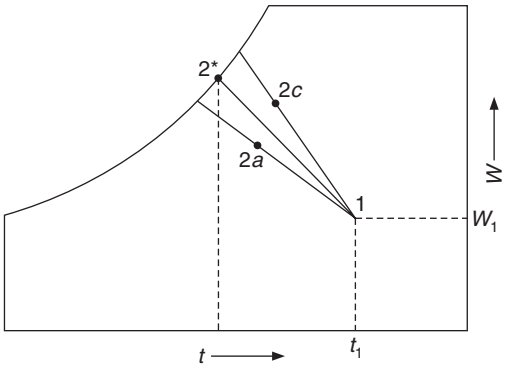

Figure 17.2(c) Process with liquid water injection.

17.4 PURE HUMIDIFICATION

It is observed that pure humidification without any change in temperature will occur if water is added at enthalpy $h_g(t_1)$ to the moist air. This requires $4.1867t_w = 2500 + 1.88t_1$. In actual practice, this is not possible. However, in the processes of addition of water vapour due to infiltration, respiration and perspiration, etc. the water is not added to the system but water vapour is added to the room air at nearly the room temperature. In such a case, it is possible to approximate the pure humidification process.

In case $t_1 = t_2$, the enthalpies at the inlet and outlet are:

$$h_1 = 1.005t_1 + W_1 h_g(t_1) \quad \text{and} \quad h_2 = 1.005t_1 + W_2\, h_g(t_1)$$

$$\therefore \qquad h_2 - h_1 = (W_2 - W_1) h_g(t_1)$$

This process may be considered to be the latent heat transfer process since the temperature remains constant. Let Q_L denote the heat transfer rate in such a process. Then,

$$Q_L = \dot{m}_a(h_2 - h_1) = \dot{m}_a(W_2 - W_1)\, h_g(t_1) = \dot{m}_a(W_2 - W_1)(2500 + 1.88t_1) \qquad (17.14)$$

In most of the pure humidification processes like infiltration and perspiration, etc. the temperature cannot be ascertained accurately, therefore the second term $1.88t_1$ is neglected compared to 2500 in Eq. (17.14). Hence, Eq. (17.14) is approximated as

$$Q_L = \dot{m}_a 2500(W_2 - W_1)$$

For standard air we have $\dot{m}_a = \rho_{\text{standard}}\, Q_v/60 = (1.2)\, Q_v/60$

$$\therefore \qquad Q_L = (1.2)2500\, Q_v\, \Delta W/60$$

or

$$Q_L = 50\, Q_v\, \Delta W \text{ kW} \qquad (17.15)$$

In an air conditioning system, the water vapour added to the room has to be removed by condensation in the cooling coil (evaporator), hence it is considered a *cooling load*. While loss of water vapour from room air has to be made up by addition of water vapour in the humidifier, which is considered a *heating load*. Equation (17.15) is a simple equation to account for such latent heat loads.

17.5 COMBINED HEATING AND HUMIDIFICATION OR COOLING AND DEHUMIDIFICATION

In winter months the air has to be heated and humidified by the air conditioning equipment before it is fed to the air conditioned space. Heat and water vapour are removed from the air in the air conditioned space. During summer months the air is cooled and dehumidified by the air conditioning equipment. Heat and water vapour are added to the air in the air conditioned space. We consider the heating and humidification process in the following discussion. We consider an insulated duct as shown in Figure 17.3(a). The notations for the inlet and outlet are the same as in the previous cases. Again, $\dot{m}_w$ is the mass flow rate of water that evaporates and it is also the mass flow rate of make-up water. Again it is assumed that mass conservation for dry air is satisfied since there is no leakage in the system. The mass flow rate for water vapour and the energy conservation lead to the following:

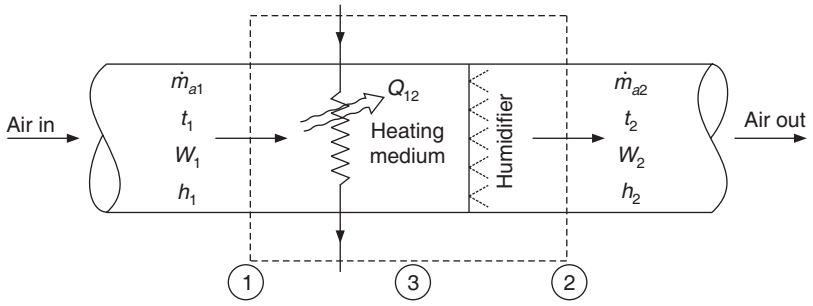

Figure 17.3(a) Schematic of a heating and humidification device by water spray following sensible heating.

Mass conservation of water vapour

$$\dot{m}_a W_1 + \dot{m}_w = \dot{m}_a W_2 \tag{17.16}$$

or $$\dot{m}_w = \dot{m}_a (W_2 - W_1)$$

Energy conservation

Energy added by water vapour is $\dot{m}_w h_w$, hence energy balance for the control volume gives

$$\dot{m}_a h_1 + \dot{m}_w h_w + Q_{12} = \dot{m}_a h_2 \tag{17.17}$$

Substituting for $\dot{m}_w$, we get

$$Q_S = \dot{m}_a (h_2 - h_1) - \dot{m}_a (W_2 - W_1) h_w$$

If water is sprayed into air stream, it will evaporate and absorb its latent heat from air and cool it. On the other hand, addition of water vapour does not require evaporation. It was shown that pure humidification requires $h_w = h_g(t_1)$ which means that water vapour is added at temperature t_1.

This process is shown by straight line 1–2 on the psychrometric chart in Figure 17.3(b). The process 1–2 can be represented by the sum of sensible heat transfer along the horizontal line1–3 (this will actually be Q_S) followed by latent heat transfer along the vertical line 3–2 (which will be Q_L).

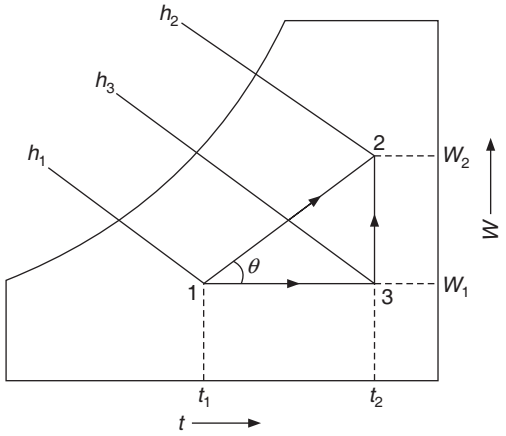

Figure 17.3(b) Heating and humidification process by water spray following sensible heating.

The sensible heat transfer rate is given by

$$Q_S = \dot{m}_a (h_3 - h_1) = \dot{m}_a C_{p\text{-}ma} (t_2 - t_1) \tag{17.18}$$

where $c_{p\text{-}ma} = 1.005 + 1.88 W_1$, is the humid specific heat.

Latent heat transfer rate is given by

$$Q_L = \dot{m}_a (h_2 - h_3)$$

Substituting $h_2 = 1.005 t_2 + W_1 h_g(t_2)$ and $h_3 = 1.005 t_2 + W_2 h_g(t_2)$, we get

$$Q_L = \dot{m}_a (W_2 - W_1) h_g(t_2) \tag{17.19}$$

Hence the total heat transfer is equal to the sum of Q_S and Q_L given by Eqs. (17.18) and (17.19),

$$\begin{aligned} Q_{\text{total}} &= \dot{m}_a[(1.005 + 1.88W_1)(t_2 - t_1) + (W_2 - W_1)(2500 + 1.88t_2)] \\ &= \dot{m}_a[\{1.005t_2 + W_2(2500 + 1.88t_2)\} - \{1.005t_1 + W_1(2500 + 1.88t_1)\} \\ &\qquad + 1.88W_1t_2 - 1.88W_1t_1] \\ &= \dot{m}_a(h_2 - h_1) \end{aligned} \tag{17.20}$$

which is expected from first law of thermodynamics in the absence of any work done. The sensible and latent heat transfers increase the enthalpy of moist air from h_1 at inlet to h_2 at the outlet.

Again, if the volume flow rate of standard air is specified as Q_v cmm, then

$$\dot{m}_a = 1.2(Q_v)/60 = 0.02Q_v \text{ kga/s}$$

Equations (17.18) and (17.20) are rewritten as

$$\begin{aligned} Q_{\text{total}} &= 0.02\ Q_{\text{v}}\ \Delta h\ \text{kW} \\ Q_S &= 0.0204Q_v\ \Delta t\ \text{kW} \\ Q_L &= 50Q_v\ \Delta W\ \text{kW} \\ Q_{\text{total}} &= Q_v(0.0204\ \Delta t + 50\ \Delta W)\ \text{kW} \end{aligned}$$

On a t–W psychrometric chart, this line can be conveniently drawn in terms of sensible heat transfer ratio (SHR) or sensible heat factor (SHF).

17.5.1 Sensible Heat Factor

Sensible heat factor or sensible heat ratio is the ratio of sensible heat transfer to the total heat transfer, that is,

$$\text{SHR} = \frac{Q_S}{Q_S + Q_L} = \frac{Q_S}{Q_{\text{total}}} = \frac{h_3 - h_1}{h_2 - h_1} = \frac{c_{p\text{-}ma}\,\Delta t}{\Delta h} = \frac{c_{p\text{-}ma}\,\Delta t}{c_{p\text{-}ma}\,\Delta t + \Delta W\, h_g(t_2)} = \frac{1}{1 + \dfrac{h_g(t_2)}{c_{p\text{-}ma}}\dfrac{\Delta W}{\Delta t}} \tag{17.21}$$

If approximations are used for Q_S and Q_L, then the equation for SHR can be simplified as follows:

$$\text{SHR} = \frac{0.0204Q_v\,\Delta t}{0.02Q_v\,\Delta h} = \frac{0.0204\,\Delta t}{0.0204\,\Delta t + 50\,\Delta W} = \frac{1}{1 + \dfrac{50}{0.0204}\dfrac{\Delta W}{\Delta t}} = \frac{1}{1 + 2451\dfrac{\Delta W}{\Delta t}} \tag{17.22}$$

The scales on the psychrometric chart are (usually) as follows:

Scale on temperature axis : 1 cm = 1°C scale factor s_t = 1°C/cm

Scale on humidity ratio axis : 1 cm = 0.001 kgw/kga, scale factor $s_W = 10^{-3}$ kgw/kga/cm

$$\tan\theta = \frac{\text{distance 2–3}}{\text{distance 1–3}} = \frac{\Delta W}{\Delta t}\frac{s_t}{s_W} = 0.001\frac{\Delta W}{\Delta t}$$

The value of tan θ is in terms of the actual distance on the chart, hence the scales have been defined. The scale factor s_t may be 2°C per cm and s_W may be 0.002 kgw/kga per cm, also leading to the same expression for tan θ.

$$\text{SHR} = \frac{1}{1 + 2.451 \tan \theta}$$

or
$$\tan \theta = 0.408 \left(\frac{1}{\text{SHR}} - 1 \right) \tag{17.23}$$

The sensible heat factor varies between 0 and1. It is equal to one for sensible heat transfer and zero for pure latent heat transfer. For an efficient air conditioning system, SHR lies between 0.75 and 0.8. One does not have to calculate the value of SHR to draw the process line on the psychrometric chart. To make its use convenient, a SHR nomograph is drawn on the right hand side of the chart and an *alignment circle* is shown either at (25°C, 50% RH) or at (26.7°C and 50% RH). A line with given SHR is drawn by joining the alignment circle to the SHR value located on the nomograph. Then the actual line passing from inlet state point 1 is drawn parallel to this line, as shown in Figure 17.3(c).

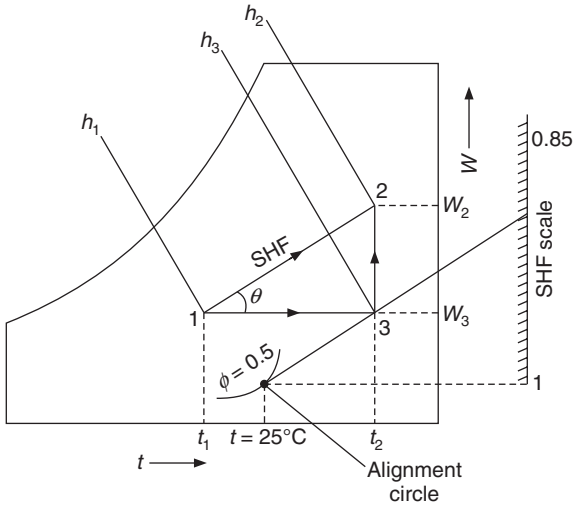

Figure 17.3(c) Determination of the process line making use of a SHR nomograph.

17.6 ADIABATIC MIXING OF TWO STREAMS OF MOIST AIR

In many air conditioning processes two streams are mixed to obtain either some desired condition of temperature and humidity or some desired purity of air. This mixing usually occurs under adiabatic conditions and the pressures of the two streams are usually the same. Figure 17.4(a) shows adiabatic mixing of two streams marked 1 and 2.

Mass conservation of dry air

$$\dot{m}_{a1} + \dot{m}_{a2} = \dot{m}_{a3} \tag{17.24}$$

Mass conservation of water vapour

$$\dot{m}_{a1} W_1 + \dot{m}_{a2} W_2 = \dot{m}_{a3} W_3 \tag{17.25}$$

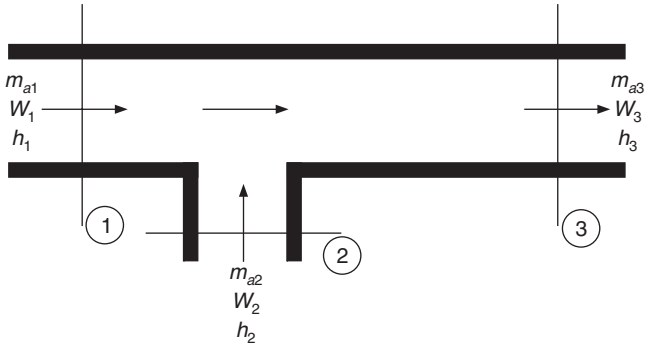

Figure 17.4(a) Adiabatic mixing of two streams of moist air.

Energy conservation

$$\dot{m}_{a1}h_1 + \dot{m}_{a2}h_2 = \dot{m}_{a3}h_3 \tag{17.26}$$

The value of $\dot{m}_{a3}$ is substituted in Eq. (17.25) from Eq. (17.24) leading to

$$\dot{m}_{a1}(W_1 - W_3) = \dot{m}_{a2}(W_3 - W_2)$$

or

$$\frac{W_1 - W_3}{W_3 - W_2} = \frac{\dot{m}_{a2}}{\dot{m}_{a1}} \tag{17.27}$$

This indicates that W_3 can be located by dividing the distance between $W_1$and W_2 in proportion of $\dot{m}_{a2} : \dot{m}_{a1}$ as shown in Figure 17.4(b) on the psychrometric chart. State 3 lies somewhere on this line. Similarly, Eq. (17.26) is modified to

$$\frac{h_1 - h_3}{h_3 - h_2} = \frac{m_{a2}}{m_{a1}} \tag{17.28}$$

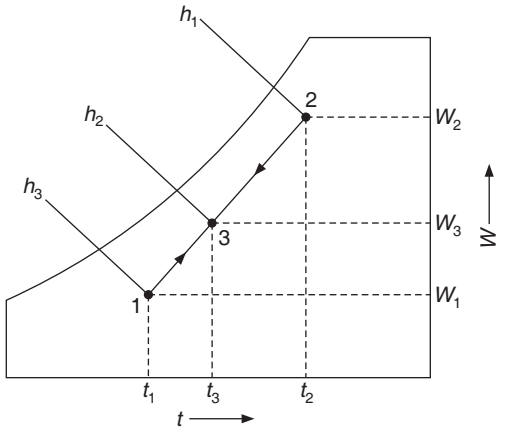

Figure 17.4(b) Adiabatic mixing of two air streams.

This indicates that h_3 can be located by dividing the distance between h_1 and h_2 in proportion of $\dot{m}_{a2} : \dot{m}_{a1}$ as shown in Figure 17.4(b) on the psychrometric chart.

On psychrometric chart, state 3 lies on the line joining states 1 and 2 and dividing it in proportion of $\dot{m}_{a2} : \dot{m}_{a1}$ as shown in Figure 17.4 (b). This makes it easy to locate the adiabatic mixed state on the chart without making any calculations. The humidity ratio and enthalpy at state 3 are found from the following relations, which are derived from Eqs. (17.24), (17.25) and (17.26).

$$W_3 = (\dot{m}_{a1} W_1 + \dot{m}_{a2} W_2)/(\dot{m}_{a1} + \dot{m}_{a2})$$

and

$$h_3 = (\dot{m}_{a1} h_1 + \dot{m}_{a2} h_2)/(\dot{m}_{a1} + \dot{m}_{a2}) \tag{17.29}$$

Substituting the empirical relation for enthalpy in Eq. (17.26), we get

$$\dot{m}_{a1}\{1.005t_1 + W_1(2500 + 1.88t_1)\} + \dot{m}_{a2}\{1.005t_2 + W_2(2500 + 1.88t_2)\}$$

$$= \dot{m}_{a3}\{1.005t_3 + W_3(2500 + 1.88t_3)\}$$

In this expression the terms multiplying 2500 cancel out in view of Eq. (17.25), that is, $2500(\dot{m}_{a1} W_1 + \dot{m}_{a2} W_2 = \dot{m}_{a3} W_3)$. Hence, the above equation reduces to

$$\dot{m}_{a1}(1.005 + 1.88W_1)t_1 + \dot{m}_{a2}(1.005 + 1.88W_2)t_2 = \dot{m}_{a3}(1.005 + 1.88W_3)t_3 \tag{17.30}$$

If it is assumed that the humid specific heat $c_{p\text{-}ma}$ is approximately constant, that is,

$$c_{p\text{-}ma} = 1.005 + 1.88W_1 \approx 1.005 + 1.88W_2 \approx 1.005 + 1.88W_3$$

Then Eq. (17.30) reduces to

$$\dot{m}_{a1} t_1 + \dot{m}_{a2} t_2 = \dot{m}_{a3} t_3 \tag{17.31}$$

This is similar to Eq. (17.27), hence by analogy with Eq. (17.28),

$$\frac{t_1 - t_3}{t_3 - t_2} = \frac{m_{a2}}{m_{a1}} \tag{18.32}$$

Hence, following the arguments given above, on *t–W* psychrometric chart too state 3 lies on the line joining states 1 and 2 and dividing it in proportion of $\dot{m}_{a2} : \dot{m}_{a1}$.

17.7 ADIABATIC MIXING OF TWO STREAMS WITH CONDENSATION

In case warm air with high humidity ratio mixes adiabatically with cold air of lower humidity, there is a possibility that the mixed air may contain more moisture than saturated air at the mixture air temperature can hold. In such a case, the excess moisture will condense out as *fog*. This state will be a mechanical mixture of saturated air and the associated condensed water vapour at the mixed air temperature. On the psychrometric chart, the state 3 which is the point of intersection of line 1–2 in proportion of $\dot{m}_{a2} : \dot{m}_{a1}$ will lie to the left of saturation curve, that is, in the fog region as shown in Figure 17.4(c).

The state 3 consists of saturated air at state 4 and condensed water vapour. If $\dot{m}_c$ is the condensation rate and h_{f4} is the enthalpy of condensate, then mass and energy conservation between states 3 and 4 gives

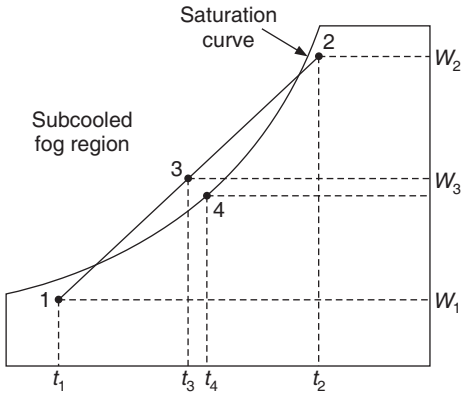

Figure 17.4(c) Adiabatic mixing of two air streams resulting into fog.

$$\dot{m}_{a3} = \dot{m}_{a4}$$

$$\dot{m}_c = \dot{m}_{a3}(W_3 - W_4)$$

$$\dot{m}_{a3} h_3 = \dot{m}_{a3} h_4 + \dot{m}_c h_{f4} = \dot{m}_{a3}(W_3 - W_4) h_{f4}$$

or
$$h_4 = h_3 - (W_3 - W_4) h_{f4} \tag{17.33}$$

A close observation reveals that this is the equation of the thermodynamic wet-bulb temperature line corresponding to the wet-bulb temperature at state 4.

While doing the construction on psychrometric chart it is immediately known that state 3 lies in the fog region. However, if the calculations are done by using moist air table or perfect gas equations, it is not immediately obvious that state 3 is in fog region unless one checks and finds out that W_3 is greater than the humidity ratio of saturated air $W_s(t_3)$. State 4 can be determined by satisfying Eq. (17.33) by trial and error. It is observed that $t_4 \approx t_3$. Hence in the trial-error solution, a value of $t_4 \approx t_3$ is assumed and h_{f4} is found from steam tables, $W_s(t_4) = W_4$ and $h_s(t_4) = h_4$ are found from moist air tables, and substituted in Eq. (17.33) to check if the choice of t_4 is correct. If Eq. (17.33) is not satisfied, then iteration is carried until the correct value of t_4 is obtained.

EXAMPLE 17.1 Moist air enters an insulated duct at the rate of 10 kga/min at 20°C, 50% relative humidity and standard atmospheric pressure. If it is heated by a heater of 1 kW capacity, find the outlet state.

Solution:

At 20°C, from steam tables : $p_{ws} = 0.023389$ bar and $h_g = 2537.38$ kJ/kg

$$W_1 = \frac{0.5(0.023389)}{1.01325 - 0.5(0.023389)} = 0.0072627 \text{ kgw/kga}$$

$$h_1 = 1.005(20) + 0.0072627(2537.38) = 38.52818 \text{ kJ/kga}$$

$\dot{m}_a = 10/60$ kga/s and $Q_{12} = 1$ kW

If the empirical equation is used to find the enthalpy at state 1, we get

$$h_1 = 1.005(20) + 0.0072627(2500 + 1.88 \times 20) = 38.5238 \text{ kJ/kga}$$

The two values are very close. From Eq. (17.3), we have

$$Q_{12} = \dot{m}_a(h_2 - h_1), \qquad \therefore \quad h_2 = h_1 + Q_{12}/\dot{m}_a$$

or

$$h_2 = 38.52818 + 1(60)/10 = 44.52818 \text{ kJ/kga}$$

This is a process of sensible heating, hence the humidity ratio remains constant during this process. The temperature t_2 can be found by using the empirical equation for enthalpy as follows:

$$h_2 = 1.005t_2 + W_1(2500 + 1.88t_2) = (1.005 + 1.88W_1)t_2 + 2500W_1$$

$$\therefore \qquad t_2 = \frac{h_2 - 2500W_1}{1.005 + 1.88W_1}$$

or

$$t_2 = \frac{44.52818 - 2500 \times 0.0072677}{1.005 + 1.88 \times 0.0077627} = 25.89°\text{C}$$

This value of t_2 gives $W_2 = 0.007262$ kgw/kga.

EXAMPLE 17.2 Moist air enters an insulated duct at the rate of 10 cmm at 10°C, 40% relative humidity and standard atmospheric pressure. If it is heated by a heater of 2.5 kW capacity, find the outlet state.

Solution:

This is sensible heat transfer process, hence we use Eq. (17.6) to obtain the result.

$$Q_S = 0.0204\, Q_v \Delta t \text{ kW}$$

$$\therefore \qquad t_2 = t_1 + \frac{Q_S}{0.0204 Q_v} = 10 + \frac{2.5}{0.0204 \times 10} = 22.255°\text{C}$$

Equation (17.6), however, is meant for standard air with a density of 1.2 kga/m^3 and humid specific heat of 1.0216 kJ/kga-K. As a check, we do the exact calculations to find the error introduced by this empirical equation.

At 10°C : $p_{ws} = 0.01228$ bar, $h_g = 2519.12$ kJ/kg

$$W_1 = \frac{0.4(0.01228)}{1.01325 - 0.4(0.01228)} = 0.00303 \text{ kgw/kga}$$

$$h_1 = 1.005(10) + 0.00303(2519.12) = 17.6829 \text{ kJ/kga}$$

$$c_{p\text{-}ma} = 1.005 + 1.88(0.00303) = 1.0106964$$

$p_w = 0.4(0.01228) = 0.004912$, hence, $p_a = 1.01325 - 0.004912 = 1.008338$ bar

$$\rho_a = 1.008338 \times 100 / (0.2871 \times 283) = 1.241 \text{ kga/m}^3$$

$$\rho = \rho_a(1 + W_1) = 1.241(1 + 0.00303) = 1.2448 \text{ kg/m}^3$$

$$\dot{m}_a = 10 \times \rho_a = 10 \times 1.241 = 12.41 \text{ kga/min}$$

$$\dot{m} = 10 \times \rho = 10 \times 1.2448 \text{ kg/min}$$

$$Q_S = Q_{12} = \dot{m}_a(h_2 - h_1) = 2.5$$

$$\therefore \quad h_2 = h_1 + 2.5/\dot{m}_a = 17.6829 + 2.5 \times 60/12.41 = 29.77 \text{ k/kg}$$

Also, $$h_2 = c_{p\text{-}ma}\, t_2 + 2500 W_1$$

$$\therefore \quad t_2 = \frac{29.11 - 0.00303 \times 2500}{1.0106964}$$

$$= \frac{22.195}{1.010696} = 21.96\ ^{o}\text{C}$$

The approximate value found by using the empirical equation was 22.255°C.

Another method is to first find the equivalent standard volume flow rate for the volume flow rate specified at the given conditions.

We have $\dot{m}_a = 1.2 Q_{vs} = \rho_a Q_v = 1.241 \times 10$

$\therefore$ Volume flow rate of equivalent standard air, $Q_{vs} = 12.41/1.2 = 10.3417$ cmm

$Q_S = 0.0204\, Q_v \Delta t$ gives, $\Delta t = 2.5/(10.3417 \times 0.0204) = 11.85°\text{C}$

$\therefore \quad t_2 = 10 + 11.85 = 21.85^{o}\text{C}$

This value of t_2 is closer to the exact result as found above.

EXAMPLE 17.3 Moist air at 40°C, 30% relative humidity and standard atmospheric pressure flows at the rate of 10 kga/s through an insulated duct. Water at 20°C is sprayed at the rate of 0.05 kg/s. Find the outlet air state if all the water evaporates.

Solution:

At 40°C : $p_{ws} = 0.073838$ bar, $h_g = 2573.49$ kJ/kg

$$W_1 = \frac{0.3(0.073838)}{1.01325 - 0.3(0.073838)} = 0.013902 \text{ kgw/kga}$$

$$h_1 = 1.005(40) + 0.013902(2573.49) = 75.9764 \text{ kJ/kga}$$

$$h_w = h_f(20^{o}\text{C}) = 83.9 \text{ kJ/kg}$$

The enthalpy of water h_w is less than $h_g(40^{o}\text{C})$, hence the air will be sensibly cooled.

From Eq. (17.8), $\dot{m}_a(W_2 - W_1) = \dot{m}_w = 0.05$

$\therefore \quad W_2 = 0.013902 + 0.005 = 0.018902$

$$(1.005 + 1.88 W_2) = 1.005 + 1.88 \times 0.018902 = 1.0405$$

From Eq. (17.22a), we have $(1.005 + 1.88 W_2)(t_2 - t_1) = (W_2 - W_1)\{h_w - h_g(t_1)\}$

$\therefore \quad (t_2 - t_1) = (W_2 - W_1)(83.9 - 2573.49)/1.0405 = -11.96^{o}\text{C}$

$\therefore \quad t_2 = 40 - 11.96 = 28.04^{o}\text{C}$

i.e. $\quad t_2 = 28.04\ ^{o}\text{C}$ and $W_2 = 0.018902$

EXAMPLE 17.4 Moist air enters an insulated duct at the rate of 10 kga/s at 20°C, 50% relative humidity and standard atmospheric pressure. It is heated by a heater of 25.0 kW capacity and steam at the rate of 0.1 kg/s is injected at 100°C. Find the outlet state, and the sensible and latent heat transfer rates.

Solution:

At 20°C, from steam tables : $p_{ws} = 0.023389$ bar and $h_g = 2537.38$ kJ/kg
At 100 °C : The enthalpy of steam $h_{st} = h_g = 2675.44$ and $\dot{m}_s = 0.1$ kg/s

$$W_1 = \frac{0.5(0.023389)}{1.01325 - 0.5(0.023389)} = 0.0072627 \text{ kgw/kga}$$

$$h_1 = 1.005(20) + 0.0072627(2537.38) = 38.52818 \text{ kJ/kga}$$

$$\dot{m}_a = 10 \text{ kga/s} \quad \text{and} \quad Q_{12} = 25.0 \text{ kW}$$

From Eq. (17.8), $\dot{m}_a(W_2 - W_1) = 0.1 \quad \therefore \quad W_2 = 0.0172627$

$\therefore \quad c_{p\text{-}ma2} = (1.005 + 1.88W_2) = 1.005 + 1.88 \times 0.0172627 = 1.03745$

Energy balance gives

$$\dot{m}_a(h_2 - h_1) = \dot{m}_s h_{st} + Q_{12} = 0.1(2675.44) + 25.0 = 292.544$$

$$h_2 = 38.52818 + 29.2544 = 67.7826$$

$$h_2 = (1.005 + 1.88W_2)t_2 + 2500W_2$$

$\therefore \quad t_2 = (67.7826 - 2500 \times 0.0172627)/1.03745 = 23.737°C$

For the inlet condition the humid specific heat is

$$c_{p\text{-}ma1} = (1.005 + 1.88W_1) = 1.01865$$

Total heat transfer $Q_T = \dot{m}_a(h_2 - h_1) = 292.544$ kW

Sensible heat transfer, $Q_S = \dot{m}_a c_{p\text{-}ma1}(t_2 - t_1) = 10 \times 1.01865 \times 3.737 = 38.0672$ kW

Latent heat transfer $Q_L = Q_T - Q_S = 254.4769$ kW

Actually it can be shown that the latent heat transfer is

$$Q_L = \dot{m}_a(h_2 - h_3) = 10(2500 + 1.88t_2)(W_2 - W_1) = 254.46 \text{ kW}$$

The approximate expression will give, $Q_L = 2500\,\dot{m}_a(W_2 - W_1) = 250.0$ kW

EXAMPLE 17.5 Moist air enters an insulated duct at the rate of 10 kga/s at 10°C, 40% relative humidity and standard atmospheric pressure. Steam is injected into the duct at the rate of 0.3 kg/s at 100°C. Determine the outlet state of moist air.

Solution:

From Example 17.2, we have

$W_1 = 0.00303$ kgw/kga, $h_g(10°C) = 2519.12$ kJ/kg and $h_1 = 17.6829$ kJ/kga

At 100°C : The enthalpy of steam $h_{st} = h_g = 2675.44$ kJ/kg and $\dot{m}_s = 0.3$ kg/s

From Eq. (17.8), $W_2 - W_1 = 0.3/10 = 0.03$

$\therefore \quad W_2 = 0.00303 + 0.03 = 0.03303$

$\therefore \quad (1.005 + 1.88W_2) = 1.005 + 1.88 \times 0.03303 = 1.0671$

Hence from Eq. (17.12a),

$\therefore \quad (t_2 - t_1) = (W_2 - W_1)(2675.44 - 2519.12)/1.0671 = 4.395°C$

$\therefore \quad t_2 = 10 + 4.319 = 14.395°C$

Alternatively, the energy equation for the insulated duct gives

$$\dot{m}_a(h_2 - h_1) = \dot{m}_s h_{st} \quad \text{or} \quad h_2 = h_1 + \dot{m}_s h_{st}/\dot{m}_a = 17.6829 + 0.3 \times 2675.44/10 = 97.9461$$

This also gives $t_2 = (h_2 - 2500W_2)/(1.005 + 1.88W_2) = 14.4046°C$

We get $t_2 = 14.395°C$ by the approximate method and $t_2 = 14.4046°C$ by the better method.

At first glance the answer seems to be correct since it satisfies the mass and energy conservation equations. A closer look indicates otherwise.

From Goff and Gratch table we find that the humidity ratio of the saturated air at 14.395°C is

$$W_s(14.395°C) = 0.01028$$

The result of the above calculation is that $W_2 = 0.03303$. One cannot add more water vapour than that at saturation. Hence the moist air cannot hold 0.03303 kgw of water vapour per kg of dry air. It will at the most become saturated and the remaining steam will condense and remain in the form of suspended water vapour just like in FOG or condense as water.

Assuming that the suspended water is at same temperature as the saturated air at final temperature (unknown) we may write the energy equation as follows:

$$\dot{m}_a(h_2 - h_1) = \dot{m}_s h_{st} - \dot{m}_c h_c \tag{17.34}$$

where the subscript c refers to condensate.

The moist air at the outlet will be saturated, hence $h_2 = h_s(t_2)$ and $W_2 = W_s(t_2)$

This can be solved by trial and error.

First trial: Assume $t_2 = 30°C$. From Goff and Gratch table

$$W_s = 0.027392,\ h_s = 100.006 \text{ and } h_f = 125.81$$

$$\dot{m}_a(W_2 - W_1) = 10(0.027392 - 0.00303) = 0.24362$$

$$\dot{m}_c = \dot{m}_s - \dot{m}_a(W_2 - W_1) = 0.3 - 0.24362 = 0.05638$$

The right hand side of Eq. (17.34) $= 0.3 \times 2675.44 - 0.05638 \times 125.81 = 795.539$

The left hand side of Eq. (17.34) $= 10(100.006 - 17.6829) = 823.3171$

The two sides are not equal, hence we do another trial.

Second trial: Assume $t_2 = 29°C$. From Goff and Gratch table,

$$W_s = 0.025735,\ h_s = 94.878 \text{ and } h_f = 121.63$$

$$\dot{m}_a(W_2 - W_1) = 10(0.025735 - 0.00303) = 0.22705$$

$$\dot{m}_c = \dot{m}_s - \dot{m}_a(W_2 - W_1) = 0.3 - 0.22705 = 0.07295$$

The right hand side of Eq. (17.34) = $0.3 \times 2675.44 - 0.07295 \times 121.63 = 793.76$

The left hand side of Eq. (17.34) = $10(94.878 - 17.6829) = 771.95$

Again the two sides of the equation are not exactly equal, hence we do another trial.

Third trial: Assume $t_2 = 29.5^oC$. From Goff and Gratch table

$$W_s = 0.0265635,\ h_s = 97.442 \text{ and } h_f = 123.72$$

$$\dot{m}_a(W_2 - W_1) = 10(0.0265635 - 0.00303) = 0.235335$$

$$\dot{m}_c = \dot{m}_s - \dot{m}_a(W_2 - W_1) = 0.3 - 0.235335 = 0.064665$$

The right hand side of Eq. (17.34) = $0.3 \times 2675.44 - 0.064665 \times 123.72 = 794.66316$

The left hand side of Eq. (17.34) = $10(97.442 - 17.6829) = 797.59.95$

The two sides are very close to each other, hence the outlet air will be saturated air at 29.5^o in the FOG region or saturated air with condensate.

EXAMPLE 17.6 Moist air enters a cooling coil at 40°C dry-bulb temperature, 50% RH and standard atmospheric pressure. It leaves the cooling coil as saturated air at 20°C. The condensate also leaves at 20°C. The mass flow rate of air is 100 kga/min. Determine the condensate rate and the cooling capacity in TR. The schematic diagram is given in Figure 17.5.

Solution:

At 40°C : $p_{ws} = 0.073838$ bar and $h_g = 2573.49$ kJ/kg

At 20°C : $p_{ws} = 0.023389$, $W_s = 0.014758$, $h_s = 57.555$, $h_g = 2537.33$, $h_f = 83.9$

$$W_1 = 0.622 \frac{0.5(0.073838)}{1.01325 - 0.5(0.073838)} = 0.02352032$$

$$W_2 = W_s(20^oC) = 0.014758$$

$$h_1 = 1.005 \times 40 + 0.02352032(2573.49) = 100.7293 \text{ kJ/kga}$$

State 2 is saturated state at 20°C. The enthalpy from Goff and Gratch table is 57.555. while the empirical equation gives

$$h_2 = 1.005 \times 20 + 0.014758(2537.38) = 57.5466 \approx \text{given } h_s = 57.555$$

Mass balance yields

$$\dot{m}_w = \dot{m}_a(W_2 - W_1) = (100/60)(\ 0.02352032 - 0.014758) = 0.0146 \text{ kgw/s}$$

Energy balance yields

$$\dot{m}_a h_1 = \dot{m}_a h_2 + Q_{12} + \dot{m}_w h_f \quad \text{or} \quad Q_{12} = \dot{m}_a[h_1 - h_2 - (W_2 - W_1)h_f]$$

$$\therefore \quad Q_{12} = (100/60)[100.7293 - 57.555 - (0.02352032\text{-}0.014758)83.9] = 70.732 \text{ kW}$$

$$= 70.732/3.5167 = 20.113 \text{ TR}$$

Condensate rate = 0.0146 kg/s

Cooling capacity = 20.113 TR

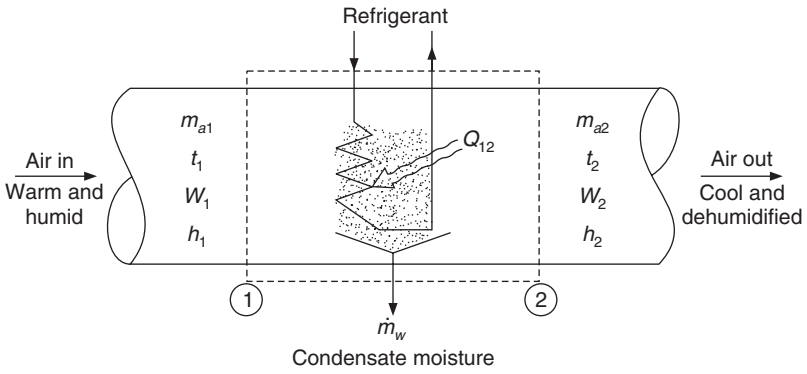

(a) Schematic device for cooling and dehumidification

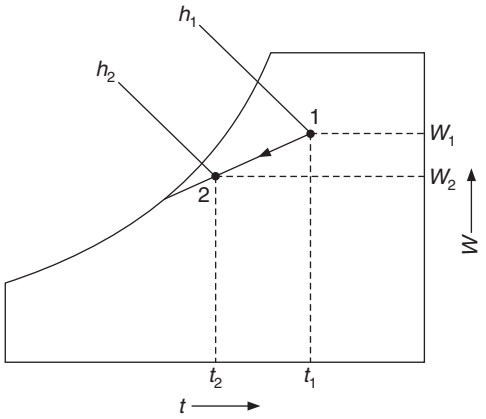

(b) Cooling and dehumidification process

Figure 17.5 Example 17.6.

EXAMPLE 17.7 One stream of moist air at 40°C dry-bulb temperature and 40% relative humidity is adiabatically mixed with another stream at 30°C dry-bulb temperature and 15°C dew point temperature. Both the streams are at standard atmospheric pressure. Determine the humidity ratio, the enthalpy and the temperature of the mixed air stream if the mass flow rates of the two streams are 500 kga/min and 200 kga/min respectively.

Solution:

From steam tables, we find

At 40°C: $p_{ws} = 0.073838$ bar and $h_g = 2573.49$ kJ/kg

At 30°C: $h_g = 2555.52$ kJ/kg

At 15°C: $W_s = 0.010692$ kgw/kga from Moist air table.

First stream:

$$W_1 = 0.622 \frac{0.4(0.07338)}{1.01325 - 0.4(0.073838)} = 0.018675 \text{ kgw/kga}$$

$$h_1 = 1.005(40) + 0.018675(2573.49) = 88.25998 \text{ kJ/kg}$$

Second stream:

$$W_2 = W_s\ (15^{\circ}\text{C}) = 0.010692 \text{ kgw/kga}$$

$$h_2 = 1.005(30) + 0.010692(2555.52) = 57.4736 \text{ kJ/kg}$$

Mass and energy conservation from Eqs. (17.25) and (17.26) yields

$$W_3 = \frac{\dot{m}_{a1}W_1 + \dot{m}_{a2}W_2}{m_{a3}} = \frac{500\,(0.018675) + 200\,(0.010692)}{700} = 0.016394 \text{ kgw/kga}$$

$$h_3 = \frac{\dot{m}_{a1}h_1 + \dot{m}_{a2}h_2}{\dot{m}_{a3}} = \frac{500\,(88.25998) + 200\,(57.4736)}{700} = 79.4639 \text{ kJ/kg}$$

The temperature t_3 may be determined from the empirical expression for enthalpy, that is,

$$h_3 = 1.005t_3 + W_3(2500 + 1.88t_3)$$

$$\therefore \quad t_3 = \frac{h_3 - 2500W_3}{1.005 + 1.88W_3} = \frac{79.4639 - 2500\,(0.016394)}{1.005 + 1.88\,(0.016394)} = 37.148^{\circ}\text{C}$$

Also,
$$t_3 \approx \frac{\dot{m}_{a1}t_1 + \dot{m}_{a2}t_2}{\dot{m}_{a3}} = \frac{500\,(40) + 200\,(30)}{700} = 37.143^{\circ}\text{C}$$

The two results are very close to each other, hence the approximation of assuming constant humid specific heat gives a reasonable accurate result.

EXAMPLE 17.8 In Example 17.7 if the volume flow rates are given to be 500 cmm and 200 cmm respectively for the two streams, other data remaining the same, find the enthalpy, the humidity ratio and the temperature of the mixed air stream.

Solution:

The dry air mass flow rates of the two streams have to be found so that mass and energy conservation can be applied. For this purpose, the specific volumes of the dry air for the two streams are determined as follows:

The humidity ratio and enthalpy of the streams are the same as those determined in Example 17.7.

$$v_{a1} = R_aT_1(1 + 1.608W_1)/p = 0.2871(313)(1 + 1.608 \times 0.018675)/101.325$$

$$= 0.9135 \text{ m}^3\text{/kga}$$

$$\therefore \quad \dot{m}_{a1} = 500/0.9135 = 547.343 \text{ kga/min}$$

$$v_{a2} = R_aT_2(1 + 1.608W_2)/p = 0.2871(303)(1 + 1.608 \times 0.010692)/101.325$$

$$= 0.8733 \text{ m}^3\text{/kga}$$

$$\therefore \quad \dot{m}_{a2} = 200/0.8733 = 229.017 \text{ kga/min}$$

$$\therefore \quad \dot{m}_{a3} = \dot{m}_{a1} + \dot{m}_{a2} = 547.343 + 229.017 = 776.36 \text{ kga/min}$$

$$W_3 = \frac{\dot{m}_{a1}W_1 + \dot{m}_{a2}W_2}{\dot{m}_{a3}} = \frac{547.343(0.018675) + 229.017(0.010692)}{776.36} = 0.01632 \text{ kgw/kga}$$

$$h_3 = \frac{\dot{m}_{a1}h_1 + \dot{m}_{a2}h_2}{\dot{m}_{a3}} = \frac{547.343(88.25998) + 229.017(574736)}{776.36} = 79.178 \text{ kJ/kg}$$

$$\therefore \quad t_3 = \frac{h_3 - 2500W_3}{1.005 + 1.88W_3} = \frac{79.178 - 2500(0.01632)}{1.005 + 1.88(0.01632)} = 37.0558°\text{C}$$

The results are very close to those in Example 17.7.

EXAMPLE 17.9 One stream of air with flow rate of 4 kga/s at 0°C and 90% relative humidity mixes adiabatically with another stream of air with a flow rate of 1 kga/s at 35°C and 70% relative humidity. Find the state of the mixed air.

Solution:

From moist air table, at 0°C, $W_{s1} = 0.0037895$. The degree of saturation at 90% relative humidity is found from the equation $\mu_1 = 0.622\phi_1/[0.622 + (1 - \phi_1)W_{s1}] = 0.89945$

$$\therefore \quad W_1 = \mu W_{s1} = 0.89945(0.0037895) = 0.00340847$$

$$h_1 = 1.005(0) + 0.00340847[2500 + 1.88\ (0)] = 8.5212 \text{ kJ/kga and } \dot{m}_{a1} = 4 \text{ kga/s}$$

Similarly at 30°C from moist air table, $W_{s2} = 0.036756$. At 70% relative humidity,

$$\mu_1 = 0.622\phi_1/[0.622 + (1 - \phi_1)\ W_{s1}] = 0.687806,\ W_2 = 0.025281$$

$$h_2 = 1.005(35) + 0.025281[2500 + 1.88\ (35)] = 100.04104 \text{ kJ/kga}$$

and $\dot{m}_{a2} = 1$ kga/s

Considering adiabatic mixing,

$$W_3 = \frac{\dot{m}_{a1}W_1 + \dot{m}_{a2}W_2}{\dot{m}_{a3}} = \frac{4(0.00340847) + (0.025281)}{5} = 0.007783 \text{ kgw/kga}$$

$$h_3 = \frac{\dot{m}_{a1}h_1 + \dot{m}_{a2}h_2}{\dot{m}_{a3}} = \frac{4(8.5212) + (100.04104)}{5} = 26.8252 \text{ kJ/kg}$$

$$\therefore \quad t_3 = \frac{h_3 - 2500W_3}{1.005 + 1.88W_3} = \frac{26.825168 - 2500(0.007783)}{1.005 + 1.88(0.007783)} = 7.226°\text{C}$$

At $t_3 = 7.226$°C, $W_s = 0.0063378$

The humidity ratio W_3 is greater than the saturated value at 7.226°C, hence the mixed air state is in fog region. If 4 is the state of saturated air at wet-bulb temperature corresponding to state 3 then from Eq. (17.33),

$$h_4 = h_3 - (W_3 - W_4)\ h_{f4} = 26.8252 - (0.007783 - W_4)4.1868 \times t_4 \qquad (17.35)$$

This has to be satisfied by trial and error.

From moist air table,

At 8° C : $W_s = 0.006683$

At 9° C : $W_s = 0.007157$

Assume $t_4 = 8.8^oC$:

$$W_4 = 0.0070622,\ h_4 = 1.005(8.8) + 0.0070622(2500 + 1.88 \times 8.8) = 26.61634$$

and $$(W_3 - W_4)4.1868 \times t_4 = 0.0265$$

From Eq. (17.33), $h_4 = 26.7987$: It is not satisfied.

Assume $t_4 = 8.88^oC$:

$$W_4 = 0.00710012,\ h_4 = 1.005(8.88) + 0.0071002(2500 + 1.88 \times 8.88) = 26.7932$$

and $$(W_3 - W_4)4.1868 \times t_4 = 0.02539$$

From Eq. (17.33), $h_4 = 26.7998$: It is almost satisfied.

$\therefore$ Condensate rate = $\dot{m}_{a3}(W_3 - W_4) = 5(0.007783 - 0.00710012) = 0.003414$ kg/s

EXAMPLE 17.10 The sensible and latent heat loads for an air-conditioned room are 25 kW and 10 kW respectively. The supply airflow rate to the room is 100 cmm. Find the sensible heat factor, and the increase in temperature and humidity ratio of the supply air.

Solution:

$$Q_S = 25 \text{ kW and } Q_L = 10 \text{ kW and } Q_v = 100 \text{ cmm}$$

From Eqs. (17.6) and (17.15), we have

$$Q_S = 0.0204\ Q_v \Delta t \text{ kW}$$

$$Q_L = 50\ Q_v \Delta W \text{ kW}$$

$\therefore$ $$\Delta t = 25/(0.0204 \times 100) = 12.255^oC$$

$$\Delta W = 10/(50 \times 100) = 0.002$$

$$\text{SHF} = Q_S/(Q_S + Q_L) = 25/35 = 0.7143$$

$$\tan\theta = \Delta W/\Delta t = 0.0001632$$

If the scale on the W-axis is 10^{-3} kgw/kga per cm and that on t-axis is 1^oC per cm, then

$$\tan\theta = 1000 \times \Delta W/\Delta t = 0.1632 \quad \therefore \quad \theta = 9.269^o$$

Equation (17.23) gives the same result, i.e.

$$\tan\theta = 0.408\left(\frac{1}{\text{SHR}} - 1\right) = 0.408[(35/25) - 1] = 4.08/25 = 0.1632$$

17.8 AIR WASHER

Figure 17.6 shows the schematic arrangement of an air washer. It has a chamber with a sump at the bottom of it. Nozzles are mounted at the top of it. The water from the sump is heated or cooled and pumped to the nozzles from where it is sprayed into the chamber such that the whole chamber is full of fine water droplets. The air is drawn in the horizontal direction through a filter. There are drift eliminators at inlet and outlet to reduce the carryover of fine water droplets. The whole chamber may be assumed to be insulated.

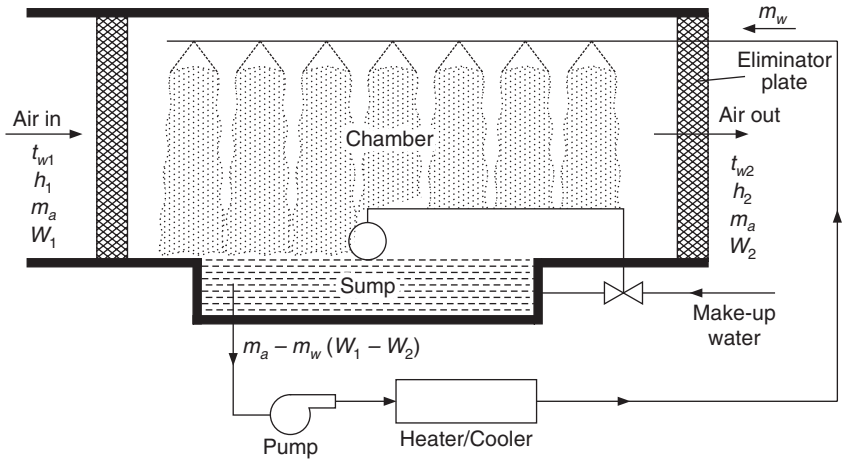

Figure 17.6 Air washer.

17.8.1 Adiabatic Saturation

If the water is neither heated nor cooled and is just recirculated, then after some time it achieves the wet-bulb temperature of the inlet air t_1^* (if Lewis number of air is assumed to be equal to 1), that is, $t_{w1} = t_{w2} = t_1^*$. Some water evaporates taking its enthalpy of evaporation in part from air and in part from water. In steady state the water temperature becomes constant and the air is adiabatically cooled along the wet-bulb temperature line as shown later by line $1 - 2_s^*$ in Figure 17.7. The temperature at point 2_s^* is the wet-bulb temperature of inlet air t_1^*. In practice, the air cannot be saturated in a finite air washer. The outlet state will be $2D$ on the wet-bulb temperature line as shown in the figure. The efficiency of the air washer is defined as follows:

$$\eta = \frac{t_1 - t_2}{t_1 - t_{2s}^*} = \frac{t_1 - t_2}{t_1 - t_1^*} = \frac{W_1 - W_2}{W_1 - W_s^*} \tag{17.36}$$

17.8.2 Spray Washer with Cold/Hot Water Circulation

This is a very versatile system with whose help heating, cooling, humidification and dehumidification can be carried out. A year-round air conditioning system can be obtained with the help of this device. Energy balance for Figure17.6 gives

$$\dot{m}_a h_1 + \dot{m}_w c_{pw} t_{w1} = \dot{m}_a h_2 + \{\dot{m}_w - \dot{m}_a (W_2 - W_1)\} c_{pw} t_{w2}$$

or

$$\dot{m}_a (h_2 - h_1) = \dot{m}_w c_{pw} (t_{w1} - t_{w2}) + \dot{m}_a (W_2 - W_1) c_{pw} t_{w2} \tag{17.37}$$

In case of adiabatic saturation, $t_{w1} = t_{w2} = t_1^*$. In this case the above equation reduces to

$$h_2 - h_1 = (W_2 - W_1) h_f^*$$

This is the equation for the wet-bulb temperature line.

The enthalpy of saturated air at inlet and outlet wet-bulb temperatures may be written as

$$h_{2s}^* = h_2 + (W_{2s}^* - W_2)\, h_{f2}^* \tag{17.38a}$$

$$h_{1s}^* = h_1 + (W_{1s}^* - W_1)\, h_{f1}^* \tag{17.38b}$$

If we assume that $h_{f2}^* \approx h_{f1}^*$ and $W_{2s}^* \approx W_{1s}^*$, then from Eqs. (17.38a) and (17.38b), we get

$$h_{2s}^* - h_{1s}^* = h_2 - h_1 - (W_2 - W_1)\, h_f^*$$

Hence Eq. (17.37) reduces to

$$\dot{m}_a\,(h_{2s}^* - h_{1s}^*) \approx \dot{m}_w c_{pw}\,(t_{w1} - t_{w2}) \tag{17.39}$$

This equation implies that the following processes may occur in the air washer:

(i) If $t_{w1} > t_{w2}$, that is, hot water is sprayed, then $h_{2s}^* > h_{1s}^*$, as a result the wet-bulb temperature of the outlet air increases.

(ii) If $t_{w1} < t_{w2}$, that is, cold water is sprayed, then $h_{2s}^* < h_{1s}^*$, as a result the wet-bulb temperature of the outlet air decreases.

(iii) If $t_{w1} = t_{w2}$, then $h_{2s}^* = h_{1s}^*$ as a result the wet-bulb temperature of the outlet air remains constant.

The processes that can occur in the air washer are shown on the psychrometric chart in Figure17.7.

Heating and humidification 1–2*A*($t_w > t_1$): If externally heated water is circulated in the washer such that its mean surface temperature is greater than the dry-bulb temperature of air, then heating as well as humidification will occur as shown by process 1–2*A*.

Pure humidification 1–2*B*($t_w = t_1$): If the mean surface temperature of water is equal to the dry-bulb temperature of air, then sensible heating cannot take place and pure humidification will occur as shown by line 1–2*B*. In this case also the water has to be heated since the enthalpy of air increases. The temperature of water tends to decrease along the washer since evaporation occurs.

Cooling and humidification 1–2*C*($t_w < t_1$): If the mean surface temperature of water is less than the dry-bulb temperature of air but greater than the wet-bulb temperature of air, then the process 1–2*C* occurs. This lies above the wet-bulb temperature line passing through point 1, In this case too, the enthalpy of air increases hence the water has to be heated.

Adiabatic saturation 1–2*D*($t_w = t_1^*$): If the water is circulated by pump without heating or cooling then the water attains the wet-bulb temperature of air (if Lewis number is equal to one). The air is cooled and humidified along the wet-bulb temperature line 1–2*D*.

Cooling and humidification 1–2*E*($t_d < t_w < t_1^*$): In this process the water is cooled such that its temperature is less than the wet-bulb temperature of air, but greater than the dew point temperature of air. The enthalpy of air decreases.

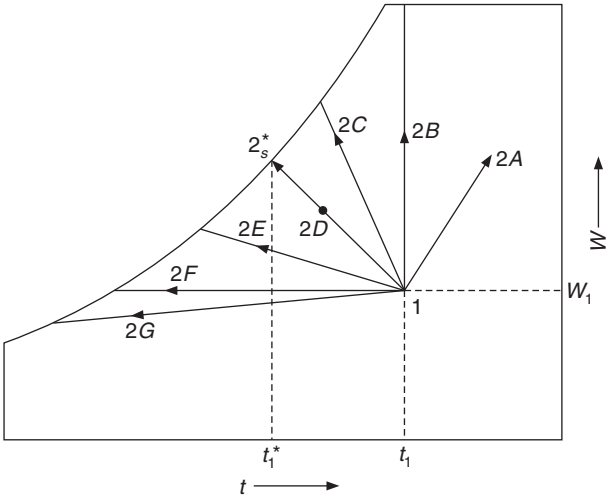

Figure 17.7 Various psychrometric processes of an air washer.

Sensible cooling 1–2F($t_d = t_w$): In this process the average surface temperature of water is equal to the dew point temperature of air. The humidity ratio of air remains constant. The enthalpy of air decreases hence the water has to be externally cooled.

Cooling and dehumidification 1–2G($t_w < t_d$): In this process the mean surface temperature of water is less than the dew point temperature of air. The air is cooled and dehumidified. This process is similar to what happens in a cooling coil.

EXAMPLE 17.11 Air enters an air washer at 30°C and 60% relative humidity at flow rate of 10 kga/s. The cooled water is sprayed at 8°C and at the rate of 10 kg/s. Find the enthalpy of the leaving air if the washer efficiency is 85%. The enthalpy of saturated air may be represented by the following equation.

$$h_s = 9.3625 + 1.7861t + 0.0035t^2 + 0.00098855t^3 \text{ kJ/kga} \tag{17.40}$$

From moist air table at 30°C, $W_s = 0.02732$ kgw/kga. For 60% relative humidity, we find the degree of saturation from the equation, $\mu = 0.622\phi/[0.622 + (1 - \phi)] = 0.487255$

$$W_1 = \mu W_s = 0.487255(0.02732) = 0.01336645$$

$$h_1 = 1.005(30) + 0.01336645(2500 + 1.88 \times 30) = 64.32 \text{ kJ/kga}$$

First we calculate the state of outlet air assuming it to be 100% effective and saturated. In Eq. (17.37) we neglect the evaporation rate to obtain

$$\dot{m}_a(h_1 - h_s) = \dot{m}_w c_{pw}(t_s - t_{w1})$$

or $$10(64.32 - 9.3625 + 1.7861t_s + 0.0035t_s^2 + 0.00098855t_s^3) = 10 \times 4.1867 \times (t_s - 8)$$

or $$38.4519 - 5.9729t_s - 0.01135t_s^2 - 0.00098855t_s^3 = 0$$

Assume $t_s = 13.9$: The left hand side of the above equation is : 0.581

Similarly for, $t_s = 13.95$: LHS = 0.237

$$t_s = 13.97 \quad : \text{LHS} = 0.1$$

$$t_s = 13.985 : \text{LHS} = 0.0028$$

From Eq. (17.40) at $t_s = 13.985$: $h_s = 39.2648$ kJ/kga
From the definition of adiabatic saturation efficiency,

$$\eta = 0.85 = \frac{64.32 - h_2}{64.32 - 39.2648}$$

$$\therefore \qquad h_2 = 43.0231 \text{ kJ/kga}$$

17.9 ADIABATIC DEHUMIDIFICATION

Hygroscopic substances like silica gel or activated alumina are commonly used in this process. It consists of a large horizontal drum, which rotates at very low rpm about its vertical axis. The drum has a large length of ribbon coated with silica gel. In one-half of the drum the room air is made to flow which gets dehumidified. The silica gel, which has adsorbed the water vapour, has to be reactivated. This is done in the other half of the drum through which heated outside air is made to flow, which absorbs water vapour from the silica gel. As the drum rotates the air passes from room air-side to the outdoor air-side.

Dehumidification in this case is based upon the principle of adsorption where the vapour is drawn into the void spaces of adsorbent by capillary action and condenses as a subcooled liquid. This reduces the vapour pressure at the surface of the adsorbent which results in mass transfer from the air stream. As the void spaces and pores get filled with water, the capillary attraction decreases and the dehumidification rate falls. Figure 17.8 shows the adsorption process by line 1–2. During adsorption, the heat of adsorption is released which heats up the adsorbent and the air stream, hence the process lies above the constant wet-bulb temperature line. The heat of adsorption is very large for both silica gel and alumina.

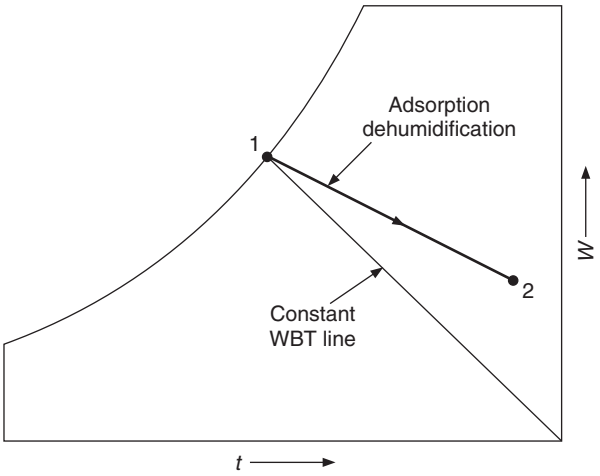

Figure 17.8 Adsorption dehumidification process.

17.10 DEHUMIDIFICATION BY HYGROSCOPIC SPRAY

Substances like calcium chloride, sodium chloride, lithium chloride and glycols, etc. are hygroscopic substances. Their solution in water has lower vapour pressure than that of water at the same temperature. Figure 17.9 curve *A* gives the vapour pressure of water, curve *B* gives the vapour pressure of 80% ethylene glycol and curve *C* gives that of 90% ethylene glycol. The vapour pressure of water is p_{vA}, which is greater than p_{vB} of 80% triethylene glycol at the same temperature. The condition line for water at this temperature is 1–*a* while that for the 80% triethylene is 1–*s*. Obviously, the triethylene solution will absorb more water vapour from air if this is sprayed in an air washer compared to water spray. The vapour pressure of the triethylene solution is lower, hence more water vapour from the air will diffuse and be absorbed by the hygroscopic solution spray. If the spray liquid is cooled, then its vapour pressure will be still lower resulting in more mass transfer and cooling as well. Air will be cooled and dehumidified as shown in the figure.

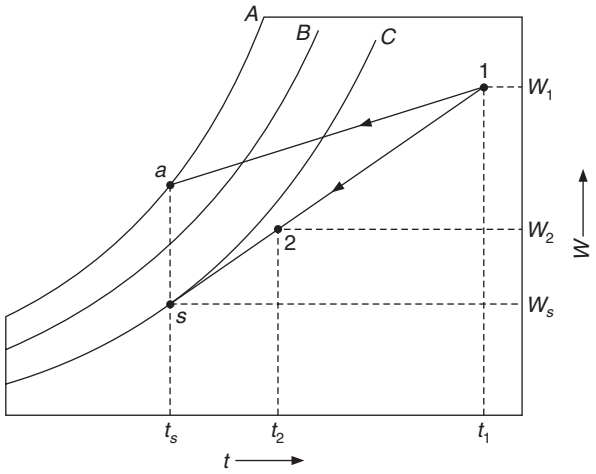

Figure 17.9 Dehumidification of air by hygroscopic solutions.

It is observed from the figure that an increase in the concentration at the given temperature results in a higher vapour pressure and a decrease in temperature at the given concentration reduces the vapour pressure.

The outlet state cannot be the saturated state in a finite equipment. It is predicted by an *approach factor* similar to the definition of efficiency.

$$\text{Approach factor} = \frac{t_1 - t_2}{t_1 - t_s} = \frac{W_1 - W_2}{W_1 - W_s}$$

where state 2 is the outlet state and the subscript *s* refers to condition of hygroscopic liquid or the saturated state. Line 1–2–*s* shows a condition line on the psychrometric chart for 80% ethylene glycol.

Hygroscopic sprays are also used in low temperature applications to prevent the formation of frost on the cooling coils. The solution has a lower freezing temperature than that of water and acts as antifreeze. Sodium chloride and calcium chloride sprays on cooling coil are frequently used for

this purpose. Diethylene glycol is used for dehydrating the natural gas. LiCl is used for dehumidification. The recovery of hygroscopic sprays requires the heating of the solution to vaporize water. Solar energy may also be used for this purpose.

17.11 SPRAYED COILS

One modification of air washer is to combine the recirculated spray with the cooling coil. The water is sprayed on the cooling coil. The removed foreign matter from air, washes the surface of the cooling coil and keeps it clean. The rate of sensible heat transfer also increases from the coil since the coil will have a lower temperature. Figure 17.10 shows the process on psychrometric chart. Line 1–2 is the condition line of the cooling coil with 2 as the leaving air state. For the sprayed coil, further cooling occurs along the constant wet-bulb temperature line 2–3–*s*. The leaving air state is 3, which is at a lower temperature.

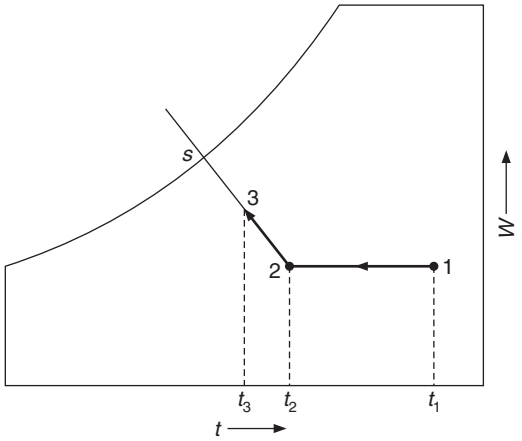

Figure 17.10 Psychrometric process for the sprayed coil.

REVIEW QUESTIONS

1. Moist air enters an insulated duct at the rate of 0.5 m^3/s at 10°C and 50% relative humidity and standard atmospheric pressure. It is heated by a heater of 12 kW capacity. Find the outlet state.
2. Moist air enters an insulated duct at the rate of 100 cmm at 20°C, 50% relative humidity and standard atmospheric pressure. It is heated by a heater of 40 kW capacity and picks up 45 kg/h of steam at 100°C. Find the outlet state, the sensible and latent heat transfer rates.
3. One stream of moist air of 7000 m^3/h at a dry-bulb temperature of 27°C and humidity ratio of 0.010 kg/kga is adiabatically mixed with another stream with 120,000 m^3/h of air at a dry-bulb temperature of 35°C and 55% RH. Both the streams are at standard atmospheric pressure. Determine the dry-bulb temperature and the wet-bulb temperature of the mixed air stream.

4. Moist air at 1 bar enters the heating section of an insulated duct at a rate of 140 cmm, 25°C, 75% relative humidity. The air then leaves the humidifying section at 25°C and 60% relative humidity. The humidifier supplies saturated steam at 2.25 bar. Determine the following:

(a) The temperature and relative humidity of air at the exit of the heating section.
(b) The rate of heat transfer in the heating section.
(c) The rate at which steam is supplied in the humidifying section.

5. Air at 40°C dry-bulb temperature and 20% relative humidity is passed through an adiabatic humidifier at the rate of 150 cmm. The outlet condition is 30°C dry-bulb temperature and 20°C wet-bulb temperature. Determine the dew point temperature, the quantity of water vapour added to the air per minute and the humidifier efficiency.

6. Moist air at 12°C dry-bulb temperature and 90% relative humidity is preheated sensibly before passing to the air washer in which water is recirculated. The relative humidity of the air coming out of the air washer is 80%. The air is again reheated sensibly to obtain the final desired condition of 40°C dry-bulb temperature and 25°C wet-bulb temperature. Find the following:

(a) Temperature of the air at the exit of preheating.
(b) Additional water required in the air washer.
(c) Humidifying efficiency of the air washer.

7. One stream of moist air flowing at 0.2 kg/s, 45°C dry-bulb temperature and 10% relative humidity is mixed with another stream flowing at 0.3 kg/s at 25°C dry-bulb temperature and humidity ratio of 0.018 kgw/kga. After mixing, the resulting mixed stream is heated to a temperature of 40°C using a heater. Find the temperature and relative humidity of air after mixing. Also, find the heat transfer rate in the heater and the relative humidity of air at the exit of the heater.

18

Wetted Surface Heat Transfer—Psychrometer, Straight Line Law and Psychrometry of Air Conditioning Processes

LEARNING OBJECTIVES

After studying this chapter the student should be able to:

1. Understand the phenomenon of combined heat and mass transfer from a wetted surface.
2. Understand the theory underlying the psychrometer and the practical use of thermometer.
3. Explain the difference between the thermodynamic wet-bulb temperature and the psychrometer wet-bulb temperature.
4. Discuss the straight line law for air–water mixtures and its usefulness in psychrometry.
5. Explain the concept of apparatus dew point temperature and bypass factor of cooling coils.
6. Explain the functioning of the simple summer air conditioning system under different conditions.
7. Discuss the concept of Effective Room Sensible Heat (ERSH) load, Effective Room Latent Heat (ERLH) load, and Effective Sensible Heat Factor (ESHF).
8. Discuss the situation of high latent cooling load and reheating.
9. Understand how the desired humidity control may be maintained in a room.
10. Explain the concept of degree days used for winter heating.
11. Explain the types of processes used in winter air conditioning.
12. Solve problems involving psychrometry of air conditioning processes.

18.1 INTRODUCTION

In Chapter 16 the properties of moist air have been discussed. The relations amongst the properties were also determined. The psychrometric chart was found to be very convenient to use for standard atmospheric pressure. The trend these days, however, is to use computer software to find the properties and for doing psychrometric calculations rather than use the psychrometric chart.

In any case we must know the thermodynamic state of moist air by knowing its pressure and at least two other properties. Pressure and temperature can be measured easily and precisely. A third property related to moisture content of air has also to be measured. The thermodynamic wet-bulb temperature cannot be measured. Similarly, the humidity ratio is also difficult to measure since most techniques available for it, involve errors. It was pointed out in Chapter 17 that relative humidity, dew point temperature and wet-bulb temperature are possible to measure. Amongst these three, the wet-bulb thermometer is a very convenient and economic device for humidity measurement. It is a reliable instrument if judiciously used. One of the most intriguing problems is the relation between the thermodynamic wet-bulb temperature and the wet-bulb temperature. This relation can be derived if the combined heat and mass transfer from a wetted surface is understood. Similarly, a cooling coil also involves combined heat and mass transfer from a wetted surface. Hence the combined heat and mass transfer is first discussed in the following Section 18.2 and then the related processes are taken up.

18.2 HEAT AND MASS TRANSFER RELATIONS

The wet-bulb thermometer induces evaporation of water from the wick. This involves fundamentals of heat and mass transfer. There are many other equipment like cooling and dehumidifying coils, spray washer and cooling tower, etc. which also involve combined heat and mass transfer with evaporation. Hence we consider evaporation of water from a free surface. This was briefly discussed in Section 2.20 where convection and mass transfer from a boundary layer were discussed. Suppose a free water surface at temperature t_w is exposed to a stream of moist air at temperature t_∞, humidity ratio W_∞ and velocity U_∞. There will be momentum, thermal and mass transfer boundary layers in the vicinity of the free water surface. The velocity will vary from zero to U_∞, the temperature will vary from t_w to t_∞ and the humidity ratio will vary from W_{sw} to W_∞. The moist air in the immediate vicinity of water surface is assumed to be saturated at temperature t_w. W_{sw} denotes its humidity ratio.

Considering u to be the velocity component in the x-direction, that is, along the free surface and v to be the velocity component in the y-direction, which is perpendicular to free surface and considering two-dimensional, steady, incompressible, laminar and constant properties flow, the basic equations for the flow and heat transfer in the boundary layer are as given below. The reader may refer to Eckert and Drake (1959).

Mass conservation or continuity equation:

$$\frac{\partial u}{\partial x} + \frac{\partial v}{\partial y} = 0 \tag{18.1}$$

Momentum equations:

$$u\frac{\partial u}{\partial x} + v\frac{\partial u}{\partial y} = \nu\frac{\partial^2 u}{\partial y^2} \tag{18.2}$$

$$\frac{\partial p}{\partial y} = 0$$

$$u\frac{\partial t}{\partial x} + v\frac{\partial t}{\partial y} = \alpha\frac{\partial^2 t}{\partial y^2} \tag{18.3}$$

where, v and α are kinematic viscosity and thermal diffusivity respectively.

The equation for mass transfer in terms of humidity ratio is not available in many textbooks, hence it is briefly derived here. We consider a control volume as shown in Figure 18.1. The water vapour flow rate through the left face a–b is $\rho_a uW$ per unit area and that from the bottom face a–d is $\rho_a vW$ per unit area. On the right face d–c at $x + \Delta x$, the water vapour flux is expanded in Taylor series and only the first two terms are retained, that is, $\rho_a uW + \Delta x\, \partial(\rho_a uW)/\partial x$. Similarly on the top face $\rho_a vW + \Delta y\, \partial(\rho_a vW)/\partial y$ is retained. The mass transfer by diffusion into the control volume is represented by m_{wx} and m_{wy} in the x and y directions. These mass transfers are actually dependent upon the gradient of the humidity ratio as follows:

$$m_{wx} = -\rho_a D\frac{\partial W}{\partial x} \quad \text{and} \quad m_{wy} = -\rho_a D\frac{\partial W}{\partial y} \tag{18.4}$$

where, D is the diffusion coefficient for diffusion of water vapour into moist air.

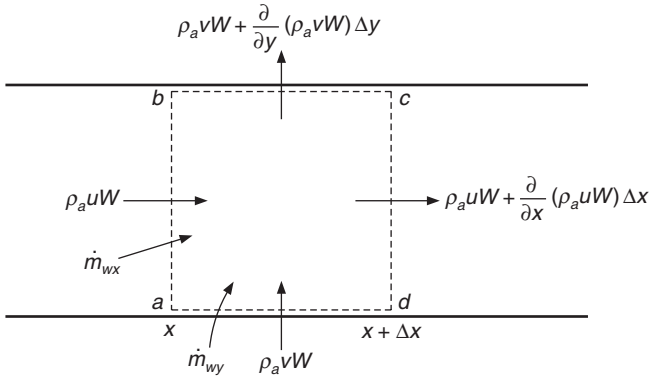

Figure 18.1 A control volume.

Assuming ρ_a to be constant and further assuming that there is no source of water vapour generation in the control volume, the mass conservation of water vapour for the control volume yields:

$$\rho_a\frac{\partial(uW)}{\partial x} + \rho_a\frac{\partial(vW)}{\partial y} + \frac{\partial}{\partial x}(m_{wx}) + \frac{\partial}{\partial y}(m_{wy}) = 0 \tag{18.5}$$

Differentiating Eq. (18.5) and substituting from Eqs. (18.1) and (18.4) it reduces to:

$$\rho_a\left[u\frac{\partial W}{\partial x} + v\frac{\partial W}{\partial y}\right] = \rho_a D\left[\frac{\partial^2 W}{\partial x^2} + \frac{\partial^2 W}{\partial y^2}\right] \tag{18.6}$$

In the boundary layer approximation, the second derivative in the x-direction is negligible compared to the second derivative in the y-direction, and we get

$$u\frac{\partial W}{\partial x}+v\frac{\partial W}{\partial y}=D\frac{\partial^2 W}{\partial y^2} \tag{18.7}$$

It is observed that Eqs. (18.2), (18.3) and (18.7) are same except for the coefficients on the right hand side. The boundary conditions for these three equations can also be made same if the following nondimensionalization scheme is followed.

$$\bar{u}=\frac{u}{U_\infty},\qquad \bar{t}=\frac{t-t_w}{t_\infty-t_w}\qquad \text{and}\qquad \bar{W}=\frac{W-W_{sw}}{W_\infty-W_{sw}} \tag{18.8}$$

The solution of the momentum boundary layer Eqs. (18.1) and (18.2) is known as Blasius solution. This solution is valid for temperature and humidity ratio too, since the equations and boundary conditions are similar. This requires the following substitution:

$$\eta=\frac{yU_\infty}{\sqrt{2\nu x}},\qquad \bar{u}=\frac{df}{d\eta}\qquad \text{and}\qquad v=\sqrt{\frac{\nu U_\infty}{2x}}\,(f'\eta-f) \tag{18.10}$$

Substitution yields

$$-f\frac{d}{d\eta}(f')=\frac{d^2}{d\eta^2}(f') \tag{18.11}$$

$$-f\frac{d\bar{t}}{d\eta}=\frac{\alpha}{\nu}\frac{d^2\bar{t}}{d\eta^2} \tag{18.12}$$

$$-f\frac{d\bar{W}}{d\eta}=\frac{D}{\nu}\frac{d^2\bar{W}}{d\eta^2} \tag{18.13}$$

The boundary conditions are as follows:

$$\begin{aligned}&\text{At } \eta=0: \quad \bar{u}=\bar{t}=\bar{W}=0\\ &\text{At } \eta\to\infty: \ \bar{u}=\bar{t}=\bar{W}=1\end{aligned} \tag{18.14}$$

It is observed that if $\alpha/\nu = 1$ and $D/\nu = 1$, the solution for temperature and humidity ratio is the same as the Blasius solution $f(\eta)$ for the velocity profile. This is known as Reynold's analogy. In this case,

$$\bar{u}=\bar{t}=\bar{W}=f'(\eta) \tag{18.15}$$

The skin friction coefficient C_f is given by $\tau_w/(0.5\,\rho\,U_\infty^2)$ where $\tau_w = (\partial u/\partial y)_{y=0}$.

$$C_f=2\sqrt{\frac{U_\infty}{2\nu x}}\,f''(0)=2\frac{\nu}{U_\infty}\sqrt{\frac{U_\infty}{\nu x}}\,\frac{1}{\sqrt{2}}\,f''(0)=2c\,\mathrm{Re}_x^{1/2} \tag{18.16}$$

The heat transfer from the free water surface occurs by molecular conduction, that is, $-k\partial T/\partial y$. Then it is convected to the remainder of fluid. It is convenient to relate it to the convective heat transfer coefficient as follows:

$$h_c(t_\infty - t_w) = k\left(\frac{\partial t}{\partial y}\right)_{y=0} = k(t_\infty - t_w)\sqrt{\frac{U_\infty}{2\nu x}}\left(\frac{d\bar{t}}{d\eta}\right)_{\eta=0} = k(t_\infty - t_w)\sqrt{\frac{U_\infty}{2\nu x}}\, f''(0)$$

This may be conveniently written as follows:

$$\frac{h_c x}{\nu} = \frac{x}{\nu}\sqrt{\frac{U_\infty}{\nu x}}\,\frac{1}{\sqrt{2}}\, f''(0) \quad \text{or} \quad \mathrm{Nu}_x = c\,\mathrm{Re}_x^{1/2} \tag{18.17}$$

where, Nu_x is Nusselt number based upon distance x and Re_x is the Reynolds number. The constant c has a value of 0.332.

Similarly, the evaporation rate is related to mass transfer coefficient h_D as follows:

$$\begin{aligned} h_D(W_{sw} - W_\infty) &= \rho_a D\left(\frac{\partial W}{\partial y}\right)_{y=0} = \rho_a D(W_{sw} - W_\infty)\sqrt{\frac{U_\infty}{2\nu x}}\left(\frac{d\bar{W}}{d\eta}\right)_{\eta=0} \\ &= \rho_a D(W_{sw} - W_\infty)\sqrt{\frac{U_\infty}{2\nu x}}\, f''(0) \end{aligned} \tag{18.18a}$$

This relation may be conveniently written as follows:

$$\frac{h_D x}{\rho_a D} = \sqrt{\frac{U_\infty}{\nu x}}\,\frac{1}{\sqrt{2}}\, f''(0) \quad \text{or} \quad \mathrm{Sh}_x = c\,\mathrm{Re}_x^{1/2} \tag{18.18b}$$

where, Sh_x is Sherwood number based upon distance x.

Hence, for the special case of $\nu/\alpha = \nu/D = 1$

$$\mathrm{Nu}_x = \mathrm{Sh}_x = C_f/2 \tag{18.19}$$

This is known as Reynold's analogy.

In the general case $\nu/\alpha \neq 1$ and $\nu/D \neq 1$. The ratio ν/α is known as Prandtl number and ν/D is known as Schmidt number. That is

$$\mathrm{Pr} = \nu/\alpha \text{ and } \mathrm{Sc} = \nu/D$$

The Nusselt number and Sherwood number for the general case of laminar flow reduce to

$$\mathrm{Nu}_x = h_c\, x/k = c\ \mathrm{Re}_x^{1/2}\ \mathrm{Pr}^{1/3} \tag{18.20a}$$

and

$$\mathrm{Sh}_x = h_D\, x/\rho_a D = c\ \mathrm{Re}_x^{1/2}\ \mathrm{Sc}^{1/3} \tag{18.20b}$$

For turbulent flow over a wetted flat plate, it is expected that the functional dependence of Nu and Sh will be similar. In fact, for turbulent flow over a flat plate, cylinder, sphere and packed beds, the dependence of Nu and Sh is similar. For a body with characteristic length L in turbulent flow,

$$\frac{h_c L}{k} = a\,\mathrm{Re}^b\ \mathrm{Pr}^c \quad \text{and} \quad \frac{h_D L}{\rho_a D} = a\,\mathrm{Re}^b\ \mathrm{Sc}^c$$

$$\therefore \quad \frac{h_e}{h_D} = \frac{k}{\rho_a D}\left(\frac{D}{\alpha}\right)^c \tag{18.21}$$

or
$$\frac{h_c}{h_D c_{p,a}} = \left(\frac{\alpha}{D}\right)^{1-c}$$

The dimensionless group $h_c/(h_D c_{p,a})$ is called the Lewis number, Le, in air conditioning practice while in chemical engineering textbooks (α/D) is called the Lewis number.

$\therefore$
$$\text{Le} = \frac{h_c}{h_D c_{p,a}} \tag{18.22}$$

Kusuda (1965) has given an empirical correlation for Lewis number in turbulent flows. That is,

$$\text{Le} = \left(\frac{\alpha}{D}\right)^{2/3} \quad \text{For forced convection} \tag{18.23a}$$

$$\text{Le} = \left(\frac{\alpha}{D}\right)^{0.48} \quad \text{For free convection} \tag{18.23b}$$

The values of α, D and the ratio α/D are given in Table 18.1 for dry air and saturated air.

Table 18.1 Values of α, D and α/D for dry air and saturated air at various temperatures

Temperature	$\alpha \times 10^5$ (m^2/s)		$D \times 10^5$	α/D	
(°C)	$\mu = 0$	$\mu = 1$	(m^2/s)	$\mu = 0$	$\mu = 1$
10	1.987	1.984	2.325	0.855	0.854
15	2.047	2.042	2.397	0.854	0.852
20	2.121	2.116	2.488	0.853	0.851
25	2.191	2.183	2.570	0.852	0.849
30	2.261	2.248	2.655	0.851	0.846
35	2.330	2.315	2.742	0.85	0.844
40	2.403	2.379	2.828	0.849	0.841
45	2.475	2.441	2.917	0.848	0.837
50	2.547	2.495	3.004	0.848	0.83
55	2.619	2.547	3.097	0.846	0.822

18.3 THEORY OF PSYCHROMETER

The wet-bulb thermometer with some variations has been in use for more than a century. It consists of an ordinary (usually mercury-in-glass) thermometer whose sensing element is covered with a moistened cloth wick. A thermocouple covered with a wick can also be used. Air or moist air is made to flow over the wick either by whirling it or by forced circulation. When a dry-bulb thermometer and a wet-bulb thermometer are included in the same unit, it is called a psychrometer.

Let V be the average velocity of moist air at temperature t and let t_∞ be the temperature of surroundings, $t_\infty \neq t$. Let t_{db} be the temperature indicated by the dry-bulb thermometer and t_{wb} be the temperature indicated by the wet-bulb thermometer. Figure 18.2 shows a hand-held psychrometer. It consists of two thermometers, wet-bulb thermometer and dry-bulb thermometer.

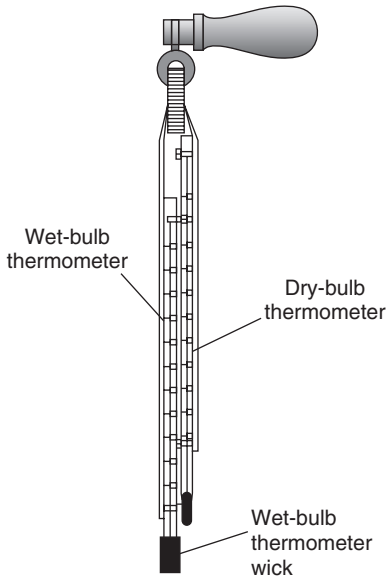

Figure 18.2 Sling psychrometer.

18.3.1 Dry-bulb Thermometer

Let us first analyze the heat transfer for dry-bulb thermometer. If we neglect the stagnation effect and conduction heat transfer along the stem of the thermometer, then in steady state, t_{db} will be such that the total heat transfer rate by convection and radiation from the dry-bulb thermometer is zero.

If $t_\infty > t$: $h_R(t_\infty - t_{db}) + h_c(t - t_{db}) = 0$ (18.24)

Then $t_\infty > t_{db} > t$: $t = t_{ab} - \dfrac{h_R}{h_c}(t_\infty - t_{db})$ (18.25)

Equation (18.25) allows the true dry-bulb temperature t of air to be found from the reading t_{db} of dry-bulb thermometer.

18.3.2 Wet-bulb Thermometer

The wet-bulb in Figure 18.2 will receive heat by radiation from the surroundings and by convection from the air stream. As a result, some water vapour will evaporate giving a depression in temperature. In steady state, latent heat transfer rate from the wick will be equal to the sum of heat transfer rates by radiation and by convection.

Evaporation rate/area = $h_D(W_{s,wb} - W)$

Latent heat transfer rate/area = $h_{fg,wb}h_D(W_{s,wb} - W)$ (18.26)

Latent heat transfer rate from wick = Heat transfer to bulb by convection and radiation

$\therefore$ $h_{fg,wb}\,h_D(W_{s,wb} - W) = h_c(t - t_{wb}) + h_R(t_\infty - t_{wb})$ (18.27)

From Eq. (18.22), we have, $h_D = h_c/\text{Le}c_{p,a}$. Substitution of this results in,

$$\frac{h_{fg,wb}}{\text{Le}c_{p,a}}(W_{s,wb} - W) = t - t_{wb} + \frac{h_R}{h_c}(t_\infty - t_{wb}) \tag{18.28}$$

$$\therefore \quad W = W_{s,wb} - \frac{\text{Le}c_{p,a}}{h_{fg,wb}}\left[1 + \frac{h_R(t_\infty - t_{wb})}{h_c(t - t_{wb})}\right](t - t_{wb}) \tag{18.29}$$

$$\therefore \quad W = W_{s,wb} - K(t - t_{wb}) \tag{18.30}$$

where,
$$K = \frac{\text{Le}c_{p,a}}{h_{fg,wb}}\left[1 + \frac{h_R(t_\infty - t_{wb})}{h_c(t - t_{wb})}\right] \tag{18.31}$$

$$c_{p,a} = 1.005 + 1.80W$$

If we calculate $c_{p,a}$ at the mean humidity ratio, that is,

$$c_{p,a} = 1.005 + \frac{1.88}{2}(W + W_{s,wb}) \tag{18.32}$$

then Eq. (18.27) becomes

$$h_{fg,wb}(W_{s,wb} - W) = \{1.005 + 0.94(W_{s,wb} + W)\}\text{Le}\left[t - t_{wb} + \frac{h_R}{h_c}(t_\infty - t_{wb})\right]$$

$$= \{1.005 + 1.88W_{s,wb} + 0.94(W_{s,wb} - W)\}\text{Le}\left[t - t_{wb} + \frac{h_R}{h_c}(t_\infty - t_{wb})\right]$$

Collecting the terms with $(W_{s,wb} - W)$, we have

$$(W_{s,wb} - W)\left[h_{fg,wb} + 0.94(t - t_{wb})\,\text{Le}\left\{1 + \frac{h_R}{h_c}\frac{(t_\infty - t_{wb})}{(t - t_{wb})}\right\}\right]$$

$$= \{1.005 + 1.88W_{s,wb}\}\,\text{Le}(t - t_{wb})\left\{1 + \frac{h_R}{h_c}\frac{(t_\infty - t_{wb})}{(t - t_{wb})}\right\}$$

$$\therefore \quad (W_{s,wb} - W) = \frac{\{1.005 + 1.88W_{s,wb}\}(t - t_{wb})}{\dfrac{h_{fg,wb}}{\text{Le}\left\{1 + \dfrac{h_R}{h_c}\dfrac{(t_\infty - t_{wb})}{(t - t_{wb})}\right\}} + 0.94(t - t_{wb})}$$

or
$$W = W_{s,wb} - K_1(t - t_{wb}) \tag{18.33}$$

where
$$K_1 = \frac{1.005 + 1.88W_{s,wb}}{\dfrac{h_{fg,wb}}{\text{Le}\left\{1 + \dfrac{h_R}{h_c}\dfrac{(t_\infty - t_{wb})}{(t - t_{wb})}\right\}} + 0.94(t - t_{wb})} \tag{18.34}$$

Equation (18.33) may be used to find the value of W from the measured value of t_{wb}. The dry-bulb temperature t is found from Eq. (18.25). Evaluation of K_1 is the main problem in psychrometry. The various terms of K_1 are evaluated as follows:

Le is found from Eq. (18.23a) with (α/D) found from Table 18.1.

$W_{s,wb}$ may be calculated from, $W_{s,wb} = 0.622 \dfrac{p_{w,s}}{p - p_{w,s}}$ where $p_{w,s} = p_{w,s}(t_{db})$

$W_{s,wb}$ may be read from moist air tables, $h_{fg,wb}$ is also read from steam tables. The formula for h_R/h_c will be given later.

There are two special cases that commonly exist.

Special case I

The first case is that the temperature of the surroundings t_∞ may be equal to dry-bulb temperature t. For this special case, Eq. (18.34) reduces to

$$t_\infty = t \qquad K_1 = \frac{1.005 + 1.88 W_{s,wb}}{\dfrac{h_{fg,wb}}{\text{Le}\left\{1 + \dfrac{h_{R,t}}{h_c}\right\}} + 0.94(t - t_{wb})} \tag{18.35}$$

where $h_{R,t}$ means h_R evaluated for $t_\infty = t$.

Special case II

If the wet-bulb is perfectly shielded, then $h_R = 0$ and

$$K_1 = \frac{1.005 + 1.88 W_{s,wb}}{\dfrac{h_{fg,wb}}{\text{Le}} + 0.94(t - t_{wb})} \tag{18.36}$$

18.3.3 Radiation and Convection Heat Transfer Coefficients

$$q_{\text{radiation}} = \sigma \varepsilon_{wb} [T_\infty^4 - T_{wb}^4] = h_R (t_\infty - t_{wb})$$

$$\sigma = 5.669 \times 10^{-8} \text{ W/m}^2\text{-K}^4$$

$$h_R = 5.669 \varepsilon_{wb} \frac{\left[\left(\dfrac{T_\infty}{100}\right)^4 - \left(\dfrac{T_{wb}}{100}\right)^4\right]}{(t_\infty - t_{wb})} \text{ W/(m}^2\text{-K)} \tag{18.37}$$

where ε_{wb} is the surface emissivity of wet bulb.

For flow around a cylinder the heat transfer coefficient in non-dimensional form as given by McAdams (1954) is as follows:

$$\frac{h_c d}{k_f} = 0.615 \left(\frac{d \rho_f V}{\mu_f}\right)^{0.466} \qquad \text{for } 40 < \text{Re} < 400 \tag{18.38a}$$

$$= 0.174 \left(\frac{d \rho_f V}{\mu_f} \right)^{0.618} \qquad \text{for } 4000 < \text{Re} < 40{,}000 \tag{18.38b}$$

where, d is the wet-bulb diameter. k_f, ρ_f, μ_f are the properties of moist air at the mean film temperature t_f.

Psychrometers usually operate in laminar flow regions. It will be clear from the following discussion that it is not necessary to operate in turbulent flow regions.

$$\frac{h_{R,t}}{h_c} = \frac{5.669 \, \varepsilon_{wb(d)} \left[(T_\infty / 100)^4 - (T_{wb} / 100)^4 \right]}{0.615 \dfrac{k_f}{d} \left(\dfrac{d \rho_f V}{\mu_f} \right)^{0.466} (t_\infty - t_{wb})} \tag{18.39}$$

It is observed that for larger velocities, the flow is turbulent and Eq. (18.38b) was used. It is observed that $h_{R,t}/h_c$ decreases with decrease in dry-bulb and wet-bulb temperatures. Further, it increases very rapidly with decrease in V for $V < 2.5$ m/s. At velocities above 5.0 m/s, it is less dependent on V particularly for small bulb diameters, say for example $d = 3.75$ mm. It is possible to use Eq. (18.35) with a little modification as shown below for the general case too, when the temperature of the surroundings is not the same as the dry-bulb temperature.

$$K_1 = \frac{1.005 + 1.88 W_{s,wb}}{\dfrac{h_{fg,wb}}{\text{Le} \left\{ 1 + \dfrac{h_{R,t}}{h_c} \dfrac{(T_\infty / 100)^4 - (T_{wb} / 100)^4}{(T / 100)^4 - (T_{wb} / 100)^4} \right\}} + 0.94 (t - t_{wb})}$$

EXAMPLE 18.1 A psychrometer indicates a wet-bulb temperature of 10°C and dry-bulb temperature of 25°C. The diameter of the dry-bulb is 6.0 mm. The wet-bulb with wick has bulb diameter of 7.25 mm. The air velocity is 5 m/s. Find the humidity ratio for the following cases. (i) Both the thermometers are unshielded and surroundings are at same temperature as the dry-bulb temperature (ii) Both the thermometers are unshielded and surroundings are at mean temperature of 30°C. (iii) Both the thermometers are shielded. (iv) Only the wet-bulb is shielded.

Solution:

The properties of air are as follows:

At 10°C : $k = 0.02489$ W/m-K and $\nu = 13.575 \times 10^{-6}$ m^2/s

At 25°C : $k = 0.02608$ W/m-K and $\nu = 15.432 \times 10^{-6}$ m^2/s

At 10°C : From steam tables, $h_{fg,wb} = 2477.11$ kJ/kg. From moist air table, $W_{s,wb} = 0.007661$ kgw/kga and from Table 18.1, $\alpha/D = 0.855$

Lewis number Le = $(\alpha/D)^{2/3} = 0.9008$

Reynolds numbers:

For the dry-bulb, Re = $5 \times 6 \times 10^{-3}/(15.432 \times 10^{-6}) = 1944$

For the wet-bulb, Re = $5 \times 7.25 \times 10^{-3}/(13.575 \times 10^{-6}) = 2670.35$

Convective heat transfer coefficients:

For the dry-bulb: $h_c = \frac{k_f}{d} 0.615 \text{Re}^{0.466} = \frac{0.02608}{0.006} 0.615 \times (1944)^{0.466} = 91.11 \text{ W/m}^2\text{-K}$

For the wet-bulb: $h_c = \frac{0.02489}{0.00725} 0.615 \times (2670.35)^{0.466} = 83.43 \text{ W/m}^2\text{-K}$

Radiation heat transfer coefficients:

The emissivity of both the bulbs is assumed to be 0.9.

For the dry-bulb:

$$h_R = 5.669 \varepsilon_{wb} \frac{\left[\left(\frac{T_\infty}{100}\right)^4 - \left(\frac{T_{wb}}{100}\right)^4\right]}{(t_s - t_{wb})} = 5.669 \times 0.9 \frac{3.03^4 - 2.98^4}{30 - 25} = 5.538 \text{ W/m}^2\text{-K}$$

For the wet-bulb with $t_\infty = t$: $h_R = 5.669 \times 0.9 \frac{2.98^4 - 2.83^4}{25 - 10} = 5.006 \text{ W/m}^2\text{-K}$

For the wet-bulb with $t_\infty \neq t$: $h_R = 5.669 \times 0.9 \frac{3.03^4 - 2.83^4}{30 - 10} = 5.139 \text{ W/m}^2\text{-K}$

Case (*i*): $t_\infty = t_{db} = 25^\circ\text{C}$. From Eq. (18.35), we have

$$K_1 = \frac{1.005 + 1.88 W_{s,wb}}{\frac{h_{fg,wb}}{\text{Le}\left\{1 + \frac{h_{R,t}}{h_e}\right\}} + 0.94(t - t_{wb})} = \frac{1.005 + 1.88(0.007661)}{\frac{2477.11}{0.9008\left\{1 + \frac{5.006}{83.43}\right\}} 0.94(25 - 10)} = 0.0003908$$

From Eq. (18.33),

$$W = W_{s,wb} - K_1(t - t_{wb}) = 0.007661 - 0.0003908(25 - 10) = 0.0017986 \text{ kgw/kga}$$

Case (*ii*): $t_\infty = 30^\circ\text{C}$ and $t_{db} = 25^\circ\text{C}$

From Eq. (18.25), $t = t_{db} - \left(\frac{h_R}{h_c}\right)_{db} (t_\infty - t_{db}) = 25 - \frac{5.538}{91.11}(30 - 25) = 24.696^\circ\text{C}$

From Eq. (18.34):

$$K_1 = \frac{1.005 + 1.88 W_{s,wb}}{\frac{h_{fg,wb}}{\text{Le}\left\{1 + \frac{h_R}{h_c} \frac{(t_\infty - t_{wb})}{(t - t_{wb})}\right\}} + 0.94(t - t_{wb})}$$

$$= \frac{1.005 + 1.88(0.007661)}{\frac{2477.11}{0.9008\left\{1 + \frac{5.139}{83.43} \frac{(30 - 10)}{(24.696 - 10)}\right\}} + 0.94(24.696 - 10)}$$

or $K_1 = 0.0003996$

From Eq. (18.33), $W = 0.007662 - 0.0003996(24.696 - 10) = 0.0017884$ kgw/kga

Case (*iii*): Both the thermometers are shielded, hence h_R is zero for both the bulbs. From Eq. (18.36), we get

$$K_1 = \frac{1.005 + 1.88W_{s,wb}}{\frac{h_{fg,wb}}{\text{Le}} + 0.94(t - t_{wb})} = \frac{1.005 + 1.88(0.007661)}{\frac{2477.11}{0.9008} + 0.94(25 - 10)} = 0.000368814$$

From Eq. (18.33), $W = 0.007661 - 0.000368814(25 - 10) = 0.0021288$ kgw/kga.

Case (*iv*): Wet-bulb is shielded but dry-bulb is not shielded. Hence h_R is not zero for the dry-bulb. Therefore, $t_{db} = 25^oC$ and $t = 24.696^oC$. From Eq. (18.36), we get

$$K_1 = \frac{1.005 + 1.88(0.007661)}{\frac{2477.11}{0.9008} + 0.94(24.696 - 10)} = 0.000368852$$

From Eq. (18.33), $W = 0.007661 - 0.000368852(24.696 - 10) = 0.00224035$ kgw/kga.

EXAMPLE 18.2 In Example 18.1 if the air velocity is 1 m/s, find the humidity ratio for the four cases.

Solution:

Reynolds numbers:

For the dry-bulb, $\text{Re} = 1 \times 6 \times 10^{-3}/(15.432 \times 10^{-6}) = 388.8$

For the wet-bulb, $\text{Re} = 1 \times 7.25 \times 10^{-3}/(13.575 \times 10^{-6}) = 534.07$

Convective heat transfer coefficients:

For the dry-bulb: $h_c = \frac{k_f}{d} 0.615\,\text{Re}^{0.466} = \frac{0.02608}{0.006} 0.615 \times (388.8)^{0.466} = 43.037$ W/m^2-K

For the wet-bulb: $h_c = \frac{0.02489}{0.00725} 0.615 \times (534.07)^{0.466} = 39.411$ W/m^2-K

Radiation heat transfer coefficients:

These will remain the same as in Example 18.1.

Case (*i*): $t_\infty = t_{db} = 25^oC$. From Eq. (18.35), we have

$$K_1 = \frac{1.005 + 1.88W_{s,wb}}{\frac{h_{fg,wb}}{\text{Le}\left\{1 + \frac{h_{R,t}}{h_c}\right\}} + 0.94(t - t_{wb})} = \frac{1.005 + 1.88(0.007661)}{\frac{2477.11}{0.9008\left\{1 + \frac{5.006}{39.411}\right\}} 0.94(25 - 10)} = 0.0004154$$

From Eq. (18.33):

$$W = W_{s,wb} - K_1(t - t_{wb}) = 0.007661 - 0.0004154(25 - 10) = 0.00143 \text{ kgw/kga}$$

Case (*ii*)*:* $t_\infty = 30^oC$ and $t_{db} = 25^oC$

From Eq. (18.25), $t = t_{db} - \left(\frac{h_R}{h_c}\right)_{db}(t_\infty - t_{db}) = 25 - \frac{5.538}{43.037}(30 - 25) = 24.357°C$

From Eq. (18.34):

$$K_1 = \frac{1.005 + 1.88W_{s,wb}}{\frac{h_{fg,wb}}{\text{Le}\left\{1 + \frac{h_R}{h_c}\frac{(t_\infty - t_{wb})}{(t - t_{wb})}\right\}} + 0.94(t - t_{wb})}$$

$$= \frac{1.005 + 1.88(0.007661)}{\frac{2477.11}{0.9008\left\{1 + \frac{5.139}{39.411}\frac{(30 - 10)}{(24.357 - 10)}\right\}} + 0.94(24.357 - 10)}$$

or $K_1 = 0.000435517$

From Eq. (18.33), $W = 0.007662 - 0.000435517(24.357 - 10) = 0.0014083$ kgw/kga.

Case (*iii*)*:* Both the thermometers are shielded, hence h_R is zero for both the bulbs. From Eq. (18.36), we get

$$K_1 = \frac{1.005 + 1.88W_{s,wb}}{\frac{h_{fg,wb}}{\text{Le}} + 0.94(t - t_{wb})} = \frac{1.005 + 1.88(0.007661)}{\frac{2477.11}{0.9008} + 0.94(25 - 10)} = 0.000368814$$

This result is same as in Example 18.1.

From Eq. (18.33), $W = 0.007661 - 0.000368814(25 - 10) = 0.0021288$ kgw/kga.

Case (*iv*)*:* Wet-bulb is shielded but the dry-bulb is not shielded. Hence h_R is not zero for the dry-bulb. Therefore, $t_{db} = 25^oC$ and $t = 24.357^oC$. From Eq. (18.36), we get

$$K_1 = \frac{1.005 + 1.88(0.007661)}{\frac{2477.11}{0.9008} + 0.94(24.357 - 10)} = 0.000368895$$

From Eq. (18.33),

$$W = 0.007661 - 0.000368895(24.357 - 10) = 0.002365 \text{ kgw/kga}$$

18.3.4 Practical Use of Psychrometer

The use of psychrometer requires a number of precautions to be taken so as to obtain a reasonably accurate reading. There are several factors that affect the reading.

There are two types of psychrometers, namely the sling type and aspiration type, in common use. Both use two thermometers with the bulb of one covered with a moistened wick The two sensing bulbs are separated from each other so as to avoid radiation exchange between them. Sometimes a radiation shield is also used.

In the sling type, the air circulation is obtained by whirling the psychrometer. This is widely used in places where air velocities are small. The aspiration type uses a motor driven blower for air circulation. The two bulbs are mounted on the suction side of the blower so that the energy added by the blower does not affect the reading. In most of the psychrometers, mercury-in-glass thermometers are used. However, platinum resistance thermometers, thermocouples and bimetallic elements may also be used.

The purpose of the wick is to provide a thin film of water around the wet-bulb. Cotton or linen cloth of soft mesh gives satisfactory results. The wick should be such that water rises along it by capillary action as the water evaporates from it. The other end of the wick should be immersed in a reservoir of water. The wick should be perfectly clean and preferably distilled water may be used to prevent salt deposits in the pores. The wick should snugly fit the bulb, otherwise some portions of the bulb may remain dry, which may cause erroneous readings. The wick should not have any sizing or encrustations so that the water film is continuous around the bulb. It is desirable that wick should extend 25 to 50 mm beyond the sensing bulb to help reduce conduction heat transfer along the stem of the thermometer. The temperature of the water used for saturating the wick should be close to wet-bulb temperature, otherwise the thermometer will take more time to reach the wet-bulb temperature.

The application of the wet-bulb thermometer for the measurement of temperatures below freezing requires discarding the wick and instead freezing a thin layer of ice on the wet-bulb. Some uncertainty may exist as to whether ice or subcooled water is in equilibrium with the wet-bulb. The wet-bulb is, therefore, not very reliable and convenient to use for temperatures below freezing.

18.3.5 Correlation between the Thermodynamic Wet-bulb Temperature and Psychrometer Wet-bulb Temperature

The thermodynamic wet-bulb temperature cannot be measured in the laboratory, it can at the most be approached in a limiting case. It is a thermodynamic property, and hence its measurement requires the establishment of an equilibrium. A wet-bulb temperature indicated by wet-bulb thermometer depends upon the heat and mass transfer rates and is therefore a function of Re, Pr and Sc, etc. apart from the thermodynamic state of moist air. Hence, there is a distinct difference between the thermodynamic wet-bulb temperature and the wet-bulb temperature read on a wet thermometer. An interesting problem is the relation between the psychrometer wet-bulb temperature and the thermodynamic wet-bulb temperature. This is considered in the following: The thermodynamic wet-bulb temperature by definition is given by

$$h + (W_s^* - W) h_f^* = h_s^* \tag{18.40}$$

The enthalpies h and h_s^* may be expressed as

$$h = 1.005t + Wh_g(t), \quad h_s^* = 1.005t^* + Wh_g(t^*) \quad \text{and} \quad h_g(t) = 2500 + 1.88t$$

Substituting in Eq. (18.40), we get

$$1.005t + Wh_g(t) + (W_s^* - W) h_f^* = 1.005t^* + W_s^* h_g(t^*)$$

or $$W_s^* [(h_g(t^*) - h_f^*] - W[h_g(t^*) - h_f^*] + Wh_g(t^*) = 1.005(t - t^*) + Wh_g(t)$$

or $$(W_s^* - W) h_{fg}^* = 1.005(t - t^*) + W[h_g(t) - h_g(t^*)] = (1.005 + 1.88W)(t - t^*)$$

The humid specific heat is written as $c_{p,a} = 1.005 + 1.88W$, hence we get

$$(W_s^* - W)h_{fg}^* = c_{p,a}(t - t^*) \tag{18.41}$$

$\therefore$
$$W = W_s^* - \frac{c_{p,a}}{h_{fg}^*}(t - t^*) \tag{18.42}$$

or
$$W = W_s^* - K^*(t - t^*) \tag{18.43a}$$

where
$$K^* = \frac{c_{p,a}}{h_{fg}^*} \tag{18.43b}$$

For t_{wb} measured by a wet-bulb thermometer, we have from Eqs. (18.30) and (18.31),

$$W = W_{s,wb} - K(t - t_{wb}) \tag{18.30}$$

$$K = \frac{\text{Le}\, c_{p,a}}{h_{fg,wb}}\left[1 + \frac{h_R}{h_c}\frac{(t_\infty - t_{wb})}{(t - t_{wb})}\right] \tag{18.31}$$

From Eqs. (18.43) and (18.30), we get

$$\frac{t - t_{wb}}{t - t^*} = \frac{W_{s,wb} - W}{W_s^* - W}\frac{h_{fg,wb}}{h_{fg}^*}\frac{1}{\text{Le}\left(1 + \dfrac{h_R}{h_c}\dfrac{(t_\infty - t_{wb})}{(t - t_{wb})}\right)} \tag{18.44}$$

$$\frac{h_R}{h_c}\frac{(t_\infty - t_{wb})}{(t - t_{wb})} > 0 \quad \text{and} \quad \text{Le} < 1 \quad W_{s,wb} \approx W_s^* \quad \text{and} \quad h_{fg,wb} \approx h_{fg}^*$$

For a shielded wet-bulb thermometer, h_R is zero and Le is less than one. Hence the right-hand side of Eq. (18.44) will always greater than one. Therefore the wet-bulb temperature t_{wb} will always be less than the thermodynamic wet-bulb temperature t^*. However, for an unshielded wet-bulb thermometer t_{wb} may be equal to t^* if

$$\text{Le}\left[1 + \frac{h_R}{h_c}\frac{(t_\infty - t_{wb})}{(t - t_{wb})}\right] = 1 \tag{18.45}$$

that is, if the radiation heat transfer to the wet-bulb compensates for Le number being less than unity. For an unshielded wet-bulb thermometer, there is a particular velocity at which the two are equal. In the following the general relation between the wet-bulb temperature and the thermodynamic wet-bulb temperature is derived. From Eqs. (18.30) and (18.43a), we get

$$t - t_{wb} = \frac{W_{s,wb} - W}{K} \quad \text{and} \quad t - t^* = \frac{W_s^* - W}{K^*}$$

$\therefore$
$$t_{wb} - t^* = \frac{W_s^* - W}{K^*} - \frac{W_{s,wb} - W}{K} = \frac{W_s^*}{K^*} - \frac{W_{s,wb}}{K^*} + \frac{W_{s,wb}}{K^*} - \frac{W_{s,wb}}{K} + \frac{W}{K} - \frac{W}{K^*}$$

or
$$t_{wb} - t^* = \frac{W_s^* - W_{s,wb}}{K^*} + \frac{W_{s,wb} - W}{K}\left[\frac{K}{K^*} - 1\right]$$

$\therefore$
$$t_{wb} - t^* + \frac{W_{s,wb} - W_s^*}{K^*} = \left(\frac{K}{K^*} - 1\right)(t - t_{wb}) \tag{18.46}$$

In the temperature ranges of t_{wb} to t^*, we can write a linear correlation between W and t since the temperature range $(t_{wb} - t^*)$ is very small.

$$W_{s,wb} = A + Bt_{wb} \tag{18.47}$$
$$W_s^* = A + Bt^*$$
$$W_{s,wb} - W_s^* = B(t_{wb} - t^*)$$

with this combination, Eq. (18.46) reduces to

$$(t_{wb} - t^*) + \frac{B(t_{wb} - t^*)}{K^*} = \left(\frac{K}{K^*} - 1\right)(t - t_{wb})$$

or
$$\frac{(t_{wb} - t^*)}{(t - t_{wb})} = \frac{K/K^* - 1}{1 + B/K^*} \tag{18.48}$$

Equation (18.48) represents the deviation $(t_{wb} - t^*)$ in terms of wet-bulb depression, $(t - t_w)$. The psychrometric wet-bulb coefficient K is given by Eq. (18.31).

The constant B can be evaluated for saturated moist air at various temperatures as given in Table 18.2.

Table 18.2 The values of constant B in Eq. (18.47) at various temperatures and standard atmospheric pressure

Temperature	*B*	*Temperature*	*B*
5°C	0.000382	35°C	0.002158
10°C	0.00052	40°C	0.0002
15°C	0.0007	60°C	0.0004
20°C	0.000936	80°C	0.00075
25°C	0.001242	100°C	0.0014
30°C	0.00164	120°C	0.00255

Special case I ($t_\infty = t$):

When the mean temperature of surroundings is same as the air temperature, we substitute the value of K from Eq. (18.31) in Eq. (18.48) . Thus, we have

$$K = \frac{\text{Le}\, c_{p,a}}{h_{fg,wb}}\left[1 + \frac{h_{R,t}}{h_c}\right] \qquad K^* = \frac{c_{p,a}}{h_{fg}} \quad \text{and since} \quad h_{fg,wb} \approx h_{fg}^*$$

$\therefore$
$$\frac{(t_{wb} - t^*)}{(t - t_{wb})} = \frac{\text{Le}\left\lfloor 1 + h_{R,t}/h_c \right\rfloor - 1}{1 + B/K^*} \tag{18.49}$$

The thermodynamic wet-bulb temperature is equal to psychrometric wet-bulb temperature if the right hand side of this equation is zero, which occurs at

$$\text{Le}\left\lfloor 1 + h_{R,t}/h_c \right\rfloor = 1 \qquad \text{that is, when} \qquad 1 + h_{R,t}/h_c = 1/\text{Le}$$

Special case II:

For a shielded wet-bulb thermometer, $h_R = 0$ and Eq. (18.31) reduces to

$$K = \frac{\text{Le}\, c_{p,a}}{h_{fg,wb}}$$

This when substituted in Eq. (18.48) yields

$$\frac{(t_{wb} - t^*)}{(t - t_{wb})} = \frac{\text{Le} - 1}{1 + B/K^*} \tag{18.50}$$

The right hand side of this equation is always less than zero, therefore for a shielded wet-bulb, the psychrometric wet-bulb temperature is always less than the thermodynamic wet-bulb temperature independent of velocity.

EXAMPLE 18.3 If the dry-bulb and the wet-bulb temperatures are 25°C and 10°C respectively, find $h_{R,t}/h_c$ and $(t_{wb} - t^*)/(t - t_{wb})$ for velocities of 0.5, 1.0, 2.0, 3.0, 4.0, 5.0, 6.0, 8.0, 10.0 and 12.0 m/s for wet-bulb diameters of 7.25 mm and 3.75 mm.

Solution:

We will assume $t_\infty = t$ and use Eq. (18.49) for the unshielded and Eq. (18.50) for the shielded psychrometer.

From Example 18.1, we have: Le = 0.9008, $h_{R,t} = 5.006$ and $h_{fg}^* = 2477.11$, $\nu = 13.575 \times 10^{-6}$ m^2/s and $k = 0.02489$ W/m-K

From Table 18.2, $B = 0.00052$

In this range of temperature, the humidity ratio from Example 18.1 is, $W = 0.002$ kgw/kga

$\therefore$ $c_{pa} = 1.005 + 1.88(0.002) = 1.00876$

and $K^* = c_{pa}/h_{fg}^* = 1.00876/2477.11 = 0.000407$

Hence, $1 + B/K^* = 2.27691$

We have

$$\text{Re} = V \times 7.25 \times 10^{-3}/13.575 \times 10^{-6}$$

$$h_c = (0.02489/0.00725)0.615\ \text{Re}^{0.466} : \text{Re} < 4000$$

$$h_c = (0.02489/0.00725)0.174\ \text{Re}^{0.618} : \text{Re} > 4000$$

The results of the calculations for the wet-bulb diameter of 7.25 mm are shown in the following table.

V	0.5	1.0	2.0	3.0	4.0	5.0	6.0	8.0	10.0	12.0
Re	267.03	534.07	1008.14	1602.2	2136.28	2670.35	3204.42	4272.56	5340.7	6408.84
h_c	28.53	39.41	54.44	65.76	75.194	83.43	90.83	104.71	120.2	134.53
$h_{R,t}/h_c$	0.175	0.127	0.092	0.076	0.66	0.6	0.55	0.048	0.042	0.037
$(t_{wb} - t^*) \times 100/(t - t_{wb})$	2.58	0.665	–0.72	–1.345	–1.723	–1.983	–2.177	–2.465	–2.710	– 2.88

For a bulb diameter of 3.75 mm,

$$\text{Re} = V \times 3.75 \times 10^{-3}/13.575 \times 10^{-6}$$

$$h_c = (0.02489/0.00375)0.615\ \text{Re}^{0.466} : \text{Re} < 4000$$

$$h_c = (0.02489/0.00375)0.174\ \text{Re}^{0.618} : \text{Re} > 4000$$

The results of the calculations for the wet-bulb diameter of 3.75 mm are shown in the following table.

V	0.5	1.0	2.0	3.0	4.0	5.0	6.0	8.0	10.0	12.0
Re	138.12	276.24	552.49	828.73	1104.97	1381.21	1657.46	2209.94	2762.43	3314.92
h_c	40.57	56.04	74.41	93.51	106.92	118.69	129.16	147.69	163.87	178.41
$h_{R,t}/h_c$	0.123	0.09	0.0672	0.0535	0.05	0.042	0.039	0.034	0.0305	0.028
$(t_{wb} - t^*) \times 100/(t - t_{wb})$	0.526	−0.822	−1.693	−2.237	−2.5	−2.685	−2.82	−3.02	−3.14	−3.25

Shielded wet-bulb thermometer:

From Eq. (18.50), we get

$$\frac{(t_{wb} - t^*)}{(t - t_{wb})} \times 100 = \frac{\text{Le} - 1}{1 + B/K^*} \times 100 = \frac{0.9008 - 1.0}{2.27691} \times 100 = -4.357$$

EXAMPLE 18.4 If the dry-bulb and the wet-bulb temperatures are 45°C and 30°C respectively, find $h_{R,t}/h_c$ and $(t_{wb} - t^*)/(t - t_{wb})$ for velocities of 0.5, 1.0, 2.0, 4.0, 6.0, 8.0, 10.0 and 12.0 m/s for wet-bulb diameters of 7.25 mm and 3.75 mm.

Solution:

We will assume $t_\infty = t$ and use Eq. (18.49) for the unshielded and Eq. (18.50) for the shielded psychrometer.

From Table 18.1, $\alpha/D = 0.851$, $\text{Le} = (\alpha/D)^{2/3} = 0.898$, and $h_{fg}^* = 2429.8$, $\nu = 15.985 \times 10^{-6}$ m^2/s and $k = 0.02647$ W/m-K

$$h_{R,t} = 5.669 \times 0.9\ [(3.18)^4 - (3.03)^4]/15 = 6.113$$

From Table 18.2, $B = 0.00164$

For the given temperatures the humidity ratio from the psychrometric chart, $W = 0.0206$ kgw/kga

$\therefore$ $c_{pa} = 1.005 + 1.88(0.0206) = 1.043728$

and $K^* = c_{pa}/h_{fg}^* = 1.043728/2429.8 = 0.0004295$

$\therefore$ $1 + B/K^* = 4.81676$

We have

$$\text{Re} = V \times 7.25 \times 10^{-3}/15.985 \times 10^{-6}$$

$$h_c = (0.02647/0.00725)0.615\ \text{Re}^{0.466} : \text{Re} < 4000$$

$$h_c = (0.02647/0.00725)0.174\ \text{Re}^{0.618} : \text{Re} > 4000$$

The results of the calculations for the wet-bulb diameter of 7.25 mm are shown in the following table.

V	0.5	1.0	2.0	4.0	6.0	8.0	10.0	12.0
Re	226.78	453.55	907.1	1814.2	2721.3	3628.4	4535.5	5442.6
h_c	28.12	38.84	53.65	74.103	89.515	102.36	115.55	129.33
$h_{R,t}/h_c$	0.217	0.157	0.114	0.082	0.068	0.056	0.053	0.047
$(t_{wb} - t^*) \times 100/(t - t_{wb})$	1.953	0.817	0.0067	−0.58	−0.84	−1.004	−1.13	− 1.236

For a bulb diameter of 3.75 mm,

$$\text{Re} = V \times 3.75 \times 10^{-3}/15.985 \times 10^{-6}$$

$$h_c = (0.02647/0.00375)0.615\ \text{Re}^{0.466} : \text{Re} < 4000$$

$$h_c = (0.02647/0.00375)0.174\ \text{Re}^{0.618} : \text{Re} > 4000$$

The results of the calculations for the wet-bulb diameter of 3.75 mm are shown in the following table.

V	0.5	1.0	2.0	4.0	6.0	8.0	10.0	12.0
Re	117.29	234.59	469.19	938.38	1407.57	1876.76	2345.95	2815.14
h_c	39.98	55.23	76.29	105.37	127.29	145.55	161.5	175.82
$h_{R,t}/h_c$	0.153	0.111	0.08	0.058	0.048	0.042	0.038	0.035
$(t_{wb} - t^*) \times 100/(t - t_{wb})$	0.733	−0.054	−0.623	−1.036	−1.222	−1.335	−1.412	−1.47

Shielded wet-bulb thermometer:

From Eq. (18.50), we get

$$\frac{(t_{wb} - t^*)}{(t - t_{wb})} \times 100 = \frac{\text{Le} - 1}{1 + B/K^*} \times 100 = \frac{0.898 - 1.0}{4.81676} \times 100 = -2.1176$$

EXAMPLE 18.5 If the dry-bulb and the wet-bulb temperatures are −1°C and −6°C respectively, find $h_{R,t}/h_c$ and $(t_{wb} - t^*)/(t - t_{wb})$ for velocities of 0.5, 1.0, 2.0, 4.0, 6.0, 8.0, 10.0 and 12.0 m/s for wet-bulb diameters of 7.25 mm and 3.75 mm.

Solution:

We will assume $t_\infty = t$ and use Eq. (18.49) for the unshielded and Eq. (18.50) for the shielded psychrometer.

Extrapolating in Table 18.1, $\alpha/D = 0.858$, $\text{Le} = (\alpha/D)^{2/3} = 0.903$, and $h_{sg}^* = 2835.68$, $\nu = 11.5946 \times 10^{-6}$ m^2/s and $k = 0.0236198$ W/m-K

$$h_{R,t} = 5.669 - 0.9[(2.72)^4 - (2.67)^4]/5 = 3.995$$

From moist air table, $B = 0.0001973$

For the given temperatures the humidity ratio from psychrometric chart, $W = 0.0004$ kgw/kga

$\therefore \quad c_{pa} = 1.005 + 1.88(0.0004) = 1.005752$

and $\quad K^* = c_{pa}/h_{fg}^* = 1.005752/2835.68 = 0.0003547$

$\therefore \quad 1 + B/K^* = 1.55628$

We have

$$\text{Re} = V \times 7.25 \times 10^{-3}/11.5946 \times 10^{-6}$$

$$h_c = (0.0236198/0.00725)0.615\ \text{Re}^{0.466} : \text{Re} < 4000$$

$$h_c = (0.0236198/0.00725)0.174\ \text{Re}^{0.618} : \text{Re} > 4000$$

The results of the calculations for the wet-bulb diameter of 7.25 mm are shown in the following table.

V	0.5	1.0	2.0	4.0	6.0	8.0	10.0	12.0
Re	312.64	625.29	1250.58	2501.16	3751.75	5002.33	6252.91	7503.49
h_c	29.14	40.252	55.6	76.8	92.77	107.58	123.49	138.22
$h_{R,t}/h_c$	0.964	0.07	0.05	0.0366	0.03	0.0265	0.024	0.022
$(t_{wb} - t^*) \times 100/(t - t_{wb})$	−0.638	–2.18	–3.3	−4.11	−4.476	−4.7	−4.85	−4.96

For a bulb diameter of 3.75 mm,

$$\text{Re} = V \times 3.75 \times 10^{-3}/11.5946 \times 10^{-6}$$

$$h_c = (0.0236198/0.00375)0.615\ \text{Re}^{0.466} : \text{Re} < 4000$$

$$h_c = (0.0236198/0.00375)0.174\ \text{Re}^{0.618} : \text{Re} > 4000$$

The results of the calculations for the wet-bulb diameter of 3.75 mm are shown in the following table.

V	0.5	1.0	2.0	4.0	6.0	8.0	10.0	12.0
Re	161.71	323.43	646.85	1293.7	1940.56	2587.4	3234.3	3881.12
h_c	41.43	57.24	79.06	109.2	131.915	150.84	167.37	182.21
$h_{R,t}/h_c$	0.0964	0.07	0.05	0.0366	0.03	0.0265	0.024	0.022
$(t_{wb} - t^*) \times 100/(t - t_{wb})$	−0.638	–2.18	–3.3	−4.11	−4.476	−4.7	−4.83	−4.96

Shielded wet-bulb thermometer:

From Eq. (18.50), we get

$$\frac{(t_{wb} - t^*)}{(t - t_{wb})} \times 100 = \frac{\text{Le} - 1}{1 + B/K^*} \times 100 = \frac{0.903 - 1.0}{1.55628} \times 100 = -6.233$$

The results of Examples 18.3, 18.4 and 18.5 for the deviation of the psychrometer wet-bulb temperature from the thermodynamic wet-bulb temperature are plotted in Figures 18.3 and 18.4 for wet-bulb diameters of 7.25 mm and 3.75 mm respectively. These lines are calculated from Eq. (18.49) for the unshielded wet-bulb for the case when $t_\infty = t$.

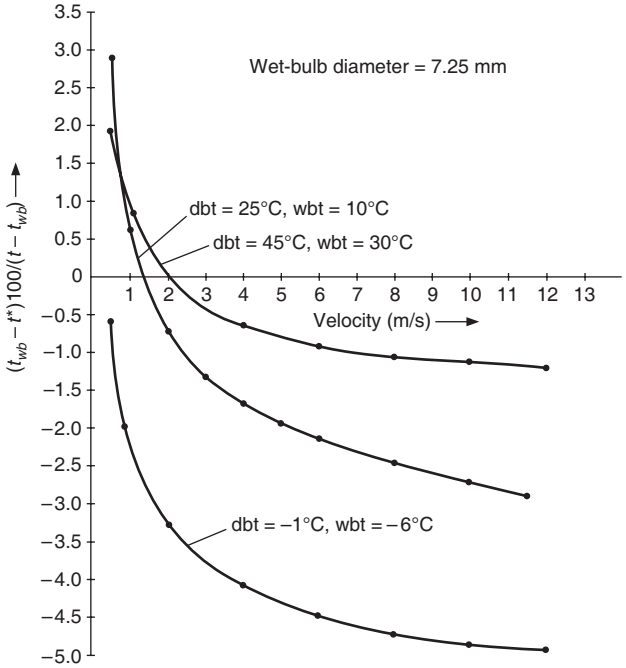

Figure 18.3 Deviation of the psychrometer wet-bulb temperature from the thermodynamic wet-bulb temperature for wet-bulb diameter of 7.25 mm.

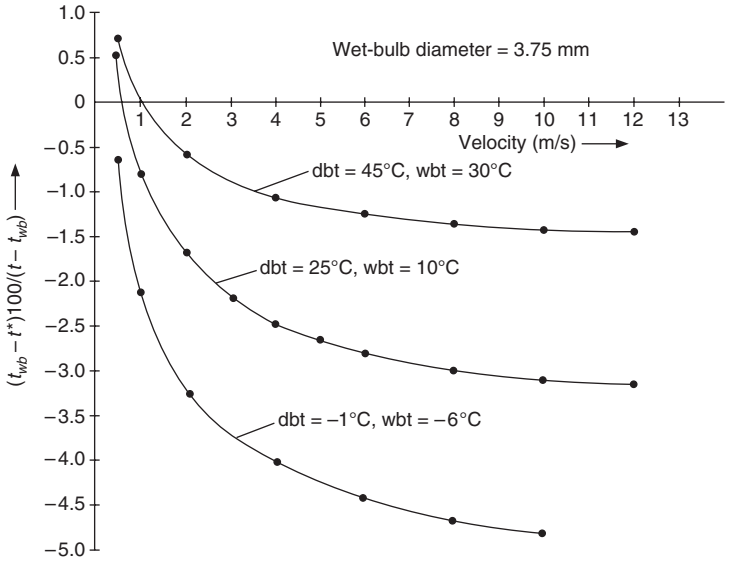

Figure 18.4 Deviation of the psychrometer wet-bulb temperature from the thermodynamic wet-bulb temperature for wet-bulb diameter of 3.75 mm.

Unshielded $t_\infty = t$

The unshielded wet-bulb temperature gives very high values of positive deviation at velocities less than 0.5 m/s. At one particular velocity, $t_{wb} = t^*$ and beyond it t_{wb} is less than t^*. This changeover velocity increases with increasing dry-bulb temperature. At velocities greater than 5 m/s the deviation is almost constant. That is one need not use velocity more than 5 m/s for the measurement. Figure 18.4 shows that for the smaller bulb diameters the changeover velocities are lower and the asymptotic negative values of deviation ($t_{wb} < t^*$) are also larger.

Shielded

The shielded wet-bulb thermometer usually gives a larger negative deviation than an unshielded one. In this case $h_{R,t}$ and therefore the deviation is independent of velocity as seen from Eq. (18.50).

Although we have shown the results for only three temperatures in Figures 18.3 and 18.4, several general observations may be made from these figures.

In general, at lower dry bulb temperatures particularly near freezing, the deviation is large. Also the deviation is large for larger depression ($t - t^*$).

- Under atmospheric conditions when the wet-bulb depression is less than 11°C for unshielded mercury-in-glass thermometer at velocities greater than 0.5 m/s and no unusual radiation exists, t_{wb} differs from t^* by less than 0.3°C.
- If thermocouple is used (smaller diameter) then at relatively lower velocities same accuracy can be obtained.
- When the wet-bulb depression is large but unshielded psychrometer may be used at $t_\infty = t$, then equations should be used to determine the exact t^*.
- When t_∞ is different from t or if the temperatures are to be measured in sunshine, both the thermometers should be shielded.
- For majority of the engineering problems, the wet-bulb temperature obtained from a properly operated unshielded psychrometer may be used directly as the thermodynamic wet-bulb temperature.

18.4 HUMIDITY STANDARDS

For any measurement, a primary standard is required. The standard for humidity measurement must measure a property related to moisture content, and measurement must be consistent with the definition of thermodynamic property.

Humidity ratio

Humidity ratio can be measured by gravimetric method and is considered to be the primary standard. The water vapour from a known volume of moist air of known density is removed by a desiccant such as P_2O_5. The precision measurement of the mass of water vapour is carried out using the National Bureau of Standards gravimetric standard hygrometer that includes a humidity generator capable of supplying a constant source of moist air over a long period of time. Atmospheric producer may also be used as humidity standard. Atmospheric producer is a precise air conditioning system. Most atmospheric producers operate on the principle of altering the condition of saturated atmosphere in a precisely calculable way. The precision of the device is primarily dependent upon how precisely the saturation is achieved. The humidity ratio of saturated air is given by

$$W_s = 0.622 \frac{p_{ws}}{p - p_{ws}}$$

At a given temperature, W_s is inversely proportional to p. Hence it is easier to saturate the air at higher total pressures.

Amdur and White have described a two-pressure type atmosphere producer. The air is compressed and then saturated at high pressure and known temperature. Then it is throttled to atmospheric pressure in a test chamber where relative humidity is determined by precisely measuring the two pressures.

It is known that by mixing salt in water, the vapour pressure of the salt solution can be reduced. The precise vapour pressures of a saturated salt solution of known concentration are known at various temperatures. If the salt is kept in a bottle the air in the bottle will have a particular relative humidity, which can be used for calibration. This method is used for the calibration of small digital hygrometers.

18.5 OTHER METHODS OF MEASURING HUMIDITY

Dew point indicator

The temperature of a mirror surface is reduced until incipient condensation occurs on it. The mirror allows both the dew droplet and its image to be seen easily. One type of mirror uses a thin polished silver thimble containing ether. Aspiration of air across the thimble causes ether to evaporate and cool the thimble.

Dry ice, liquid air, mechanical refrigeration or thermoelectric refrigeration may also be used for cooling the mirror surface. Some models have a pump, which compresses air and then the compressed air is expanded to atmospheric pressure to produce cooling. It is difficult to measure the temperature of a surface and thus the point of incipient condensation may be uncertain. The heat transfer and the mass transfer rates (aspiration) affect the temperatures. Some models use the thermoelectric device for cooling the mirror and the detection of dew point is also automatically done by an electronic circuit.

Hygrometer

The hygrometer gives a direct reading of relative humidity.

Mechanical hygrometer

Human hair is hygroscopic and its length varies with relative humidity. In a mechanical hygrometer, the human hair element is connected by a simple mechanical linkage to a pointer. Unfortunately the length of human hair length is affected by dry-bulb temperature as well. Its reliability is ± 3%. It has a large time lag.

Dunmore electric hygrometer

It depends upon the hygroscopic and electrical characteristics of LiCl salt solution in H_2O. The electrical resistance of a thin layer of unsaturated LiCl will vary with relative humidity. The change in electrical resistance can be measured and correlated with relative humidity. This hygrometer is well suited to remote sensing.

18.6 COOLING AND DEHUMIDIFICATION THROUGH COOLING COIL

18.6.1 Straight Line Law

The state of moist air as it passes through the cooling coil can be represented on psychrometric chart if the values of t and W for moist air are known at few points along the path. A line joining these points is known as *condition line* for the cooling coil.

The moist air in immediate contact with the surface of cooling coil including fins attains the temperature of the coil while the moist air away from the surface of cooling coil may remain unaffected. That is, there are viscous, thermal and mass transfer boundary layers near the surface through which velocity, temperature and humidity ratio vary from surface value to free stream value. This results in significant temperature and humidity variations in the moist air. If the air could be uniformly contacted, that is, if the boundary layers are not present, then all the air will be cooled to the temperature of the cooling coil and it will leave as saturated air at the temperature of coil. One can imagine that uniformly contacted air will be cooled sensibly at constant humidity ratio along 1–2 as shown in Figure 18.5. Then for a uniformly contacted air, combined sensible and latent cooling will occur along the saturation curve 2–3 where condensation occurs along with cooling.

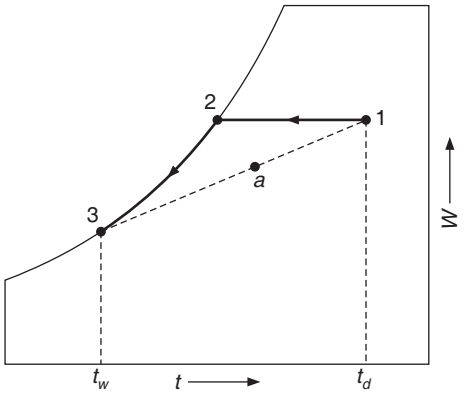

Figure 18.5 Cooling and dehumidification of air.

In practice the moist air cannot be uniformly contacted because of the boundary layers. Approach to point 3 is also impossible since the temperature difference and the humidity ratio difference between the air and the cooling surface, required for heat and mass transfer, approach zero. As a result, very large cooling coil area will be required to approach point 3.

In the actual process, moist air in the immediate vicinity of the cooling coil acquires its temperature and the condensation may occur at the inlet itself if the cooling coil temperature is less than the dew point temperature of inlet air t_d, that is, condensation occurs even though the main body of air is unsaturated. As a result, the process is that of cooling and dehumidification right from the inlet and may follow the path 1–a–3. The moisture condenses from the initial dew point temperature t_d of moist air to the final saturation temperature t_w. The temperature of the cooling coil including fins is not uniform, hence the temperature at point 3 is some sort of average temperature of the cooling coil. In the following analysis it is assumed for simplicity that the whole of coil is at uniform temperature. The condition line 1–a–3 has been shown to be

a straight line. This is known as *straight line law* and was developed by Keevil and Lewis (1928) as follows.

A vertical surface at a uniform temperature, t_w, less than the dew point temperature t_d of the inlet air is considered. The inlet temperature and humidity ratio of the moist air are t_1 and W_1 respectively.

The moist air in the immediate vicinity of the surface is cooled below its dew point at the inlet as well. Hence condensation starts at the inlet itself and the condensate rate $\dot{m}_w$ increases along the surface. The heat transfer process is the combined sensible and latent heat transfer process. The temperature of the surface is uniform t_w all along it and the air in its immediate vicinity will be saturated. The humidity ratio of the saturated air is W_{sw}. Consider an elemental area dA of the surface as shown in Figure 18.6. At inlet to this area, the average temperature and humidity ratio of air are t and W respectively while the condensate rate is $\dot{m}_w$. The average temperature of the moist air reduces to $t - dt$ at the exit of dA as it is sensibly cooled and its humidity ratio reduces to $W - dW$ as moisture condenses out of it. The condensate rate increases to $\dot{m}_w + d\dot{m}_w$ at the exit of area dA where $d\dot{m}_w$ is the condensation rate over the area dA.

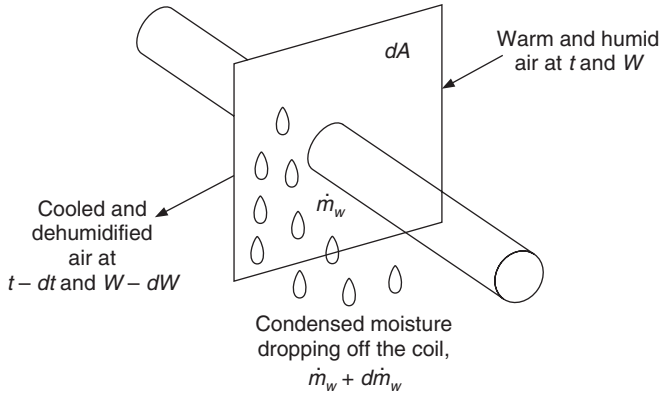

Figure 18.6 Elemental area dA of the cooling surface.

Let h_c and h_D be the convective heat and mass transfer coefficients respectively and $c_{p\text{-}ma}$ be the average humid specific heat. The temperature difference $t - t_w$ is the driving force for sensible heat transfer. The sensible heat transfer dq_S is the decrease in the enthalpy of moist air due to convective heat transfer to the surface. This is expressed as

$$dq_S = -c_{p\text{-}ma}\, dt \tag{18.51}$$

$$= h_c\, dA\,(t - t_w) \tag{18.52}$$

$W - W_{sw}$ is the driving force for mass transfer. Mass conservation of water vapour implies that increase in the condensate rate is due to mass transfer by advection and is equal to $\dot{m}_a dW$. This is expressed as follows:

$$d\dot{m}_w = -\dot{m}_a dW \tag{18.53}$$

$$= h_D\, dA(W - W_{sw}) \tag{18.54}$$

Combining Eqs. (18.51 and 18.52) and Eqs. (18.53) and (18.54), we get

$$\int_{t_1}^{t} \frac{dt}{t - t_w} = -\frac{h_c}{\dot{m}_a c_{p\text{-}ma}} \int_0^A dA \tag{18.55}$$

$$\int_{W_1}^{W} \frac{dW}{W - W_{sw}} = -\frac{h_D}{\dot{m}_a} \int_0^A dA \tag{18.56}$$

Assuming h_c, h_D, t_w and W_{sw} to be constants, Eqs. (18.55) and (18.56) are integrated to yield

$$\ln\left(\frac{t - t_w}{t_1 - t_w}\right) = -\frac{h_c}{\dot{m}_a c_{p\text{-}ma}} \tag{18.57}$$

$$\ln\left(\frac{W - W_{sw}}{W_1 - W_{sw}}\right) = -\frac{h_D}{\dot{m}_a} \tag{18.58}$$

The heat and mass transfer coefficients are related through Lewis number as follows:

$$h_D = \frac{h_c}{\text{Le}\, c_{p\text{-}ma}} \tag{18.59}$$

Therefore, Eq. (18.58) reduces to

$$\ln\left(\frac{W - W_{sw}}{W_1 - W_{sw}}\right) = -\frac{h_c}{\dot{m}_a \,\text{Le}\, c_{p\text{-}ma}} \tag{18.60}$$

A comparison of Eqs. (18.57) and (18.60) yields

$$\frac{t - t_w}{t_1 - t_w} = \left(\frac{W - W_{sw}}{W_1 - W_{sw}}\right)^{\text{Le}} \tag{18.61}$$

It has been observed in Table 18.1 that Lewis number for moist air is of the order unity. Assuming Lewis number to be equal to one, Eq. (18.61) is a straight line on t–W psychrometric chart starting from (t_1, W_1) and joining it to saturated state (t_w, W_{sw}) on saturation curve as shown in Figure 18.7(a).

The state of moist air at locations 2 and 3, etc. along the surface lies on line 1–s as shown in Figure 18.7(a). As the cooling surface area increases, the exit air state approaches the saturated state s.

In actual practice, however, saturated state cannot be achieved. The potential for sensible heat transfer ($t - t_w$) and potential for mass transfer ($W - W_{sw}$) decrease as one approaches the saturated state, e.g. $(t_2 - t_w) > (t_3 - t_w)$. The heat and mass transfer rates decrease as $t \to t_w$ and for a given heat transfer very large area will be required for moist air temperature to become equal to t_w. In fact, the condition line will look like 1–2–3–4 in actual practice, that is, it will become parallel to the saturation curve.

However, for the ideal case of constant surface temperature of wetted surface the condition line is 1–s. It is convenient to locate the point s if the SHF of line 1–s is known, by its intersection with the saturation curve whose empirical equations are as follows:

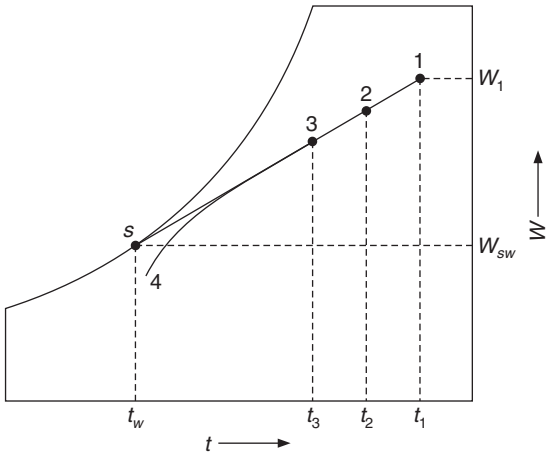

Figure 18.7(a) Principle of straight line law for air–water mixtures.

$$1000W_s = 3.9665859 + 1.868155\frac{t}{10} + 1.7747316\left(\frac{t}{10}\right)^2 \text{ where } t \text{ is in °C} \qquad (18.62)$$

$$1000W_s = 3.7839708 + 2.8665433\frac{t}{10} + 0.6423378\left(\frac{t}{10}\right)^2 + 0.30925\left(\frac{t}{10}\right)^3 \qquad (18.63)$$

The surface temperature should be at least equal to the dew point temperature of inlet air otherwise condensation cannot occur, surface will not be wetted and mass transfer cannot occur. Hence for $t_w > t_d$, the straight line law is not valid. For $t_w = t_d$, the condition line is a horizontal line as shown in Figure 18.5.

18.6.2 Actual Coil Condition Line

In Figure 18.5 two alternatives are shown. Condition line 1–2–3 would occur if the whole mass of moist air is uniformly contacted. Condition line 1–3 would occur if a wetted surface at uniform temperature $t_w < t_d$ cools the moist air. In a cooling coil consisting of a number of rows the coil surface temperature decreases with each row, that is, the first row will be at higher temperature, compared to that of the second row which in turn will be higher than the surface temperature of the third row and so on, as a result the condition line would be a curved line that can be assumed to be a composite of a series of straight lines, one for each row. The straight lines keep becoming steeper as the surface temperature decreases and keep becoming shorter since the cooling potential decreases. Usually maximum cooling is performed in the first row and the extent of cooling decreases in successive rows. The potential for heat and mass transfer decreases as the saturation curve is approached.

It is not possible to obtain the saturated state in a cooling coil of finite area. The condition line becomes parallel to the saturation curve near the saturated state. Further the surface temperature is not uniform in actual practice. There are boundary layers around the fins and on the metal tube in which the temperature varies. The temperature in the fins also varies. The metal surface temperature is always higher than the chilled water temperature or refrigerant temperature and less than the air

temperature. The chilled water temperature is also not constant in the coil. Therefore the metal surface temperature varies throughout. Effective surface temperature is that uniform surface temperature which will produce the same heat transfer and condensate rate as the actual coil.

18.6.3 Apparatus Dew Point and Bypass Factor

It is observed that the condition line may be approximated by a straight line as shown in Figure 18.7(b) if the inlet air state 1 and the outlet air state 2 are joined together. In actual practice the condition line when extended to meet the saturation curve intersects it at a temperature, which is the effective temperature of the cooling coil and is called the *apparatus dew point* (ADP), since it is like the dew point of the apparatus. This is a useful concept since the surface temperature varies with each row and along the fins. Also the air cannot be cooled to saturated state because of boundary layers. The definition of *apparatus dew point* along with bypass factor makes it very convenient to carry out psychrometric calculations. A coil will be 100% efficient if it can cool all the air up to coil temperature t_w and make it 100% saturated. The actual outlet state is state 2 which is away from the saturated state. Hence the efficiency of the cooling coil is given by

$$\eta = \frac{t_1 - t_2}{t_1 - t_{ADP}} \tag{18.64}$$

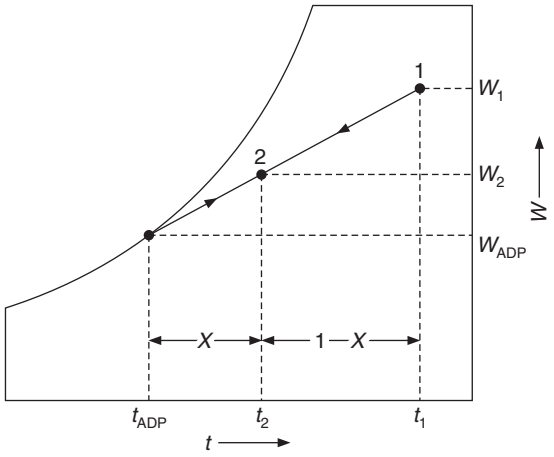

Figure 18.7(b) Mixing of perfectly contacted air and bypassed air.

However in air-conditioning calculations, by convention, inefficiency of the cooling coil is defined and it is called the *bypass factor*. It is denoted by X, where

$$X = \frac{t_2 - t_{ADP}}{t_1 - t_{ADP}} \tag{18.65}$$

As the name suggests this is the quantity of air which bypasses the cooling coil, assuming that the remaining air is uniformly contacted.

If X is the bypass factor and $\dot{m}_a$ is the mass flow rate of dry air, then $(1 - X)\,\dot{m}_a$ part of the air is perfectly contacted, that is, it is cooled from (t_1, W_1) to (t_{ADP}, W_{ADP}), while $X\,\dot{m}_a$ part of the air is bypassed, that is, it leaves the coil unaffected at t_1, W_1. The mixing of perfectly contacted air and bypassed air results in state 2 as shown schematically in Figure 18.7(b).

Energy conservation yields

$$X\dot{m}_a c_{p\text{-}ma} t_1 + (1 - X)\dot{m}_a c_{p\text{-}ma} t_{ADP} = \dot{m}_a c_{p\text{-}ma} t_2$$

$$\therefore \quad X(t_1 - t_{ADP}) = (t_2 - t_{ADP}) \quad \text{or} \quad t_2 = t_1 X - (1 - X)t_{ADP} \tag{18.66}$$

Now,
$$X = \frac{t_2 - t_{ADP}}{t_1 - t_{ADP}} = \frac{W_2 - W_{ADP}}{W_1 - W_{ADP}} \tag{18.67}$$

If X_1 is the bypass factor of one row of tubes, then the bypass factor of two rows of identical tubes may be obtained as follows. If t_3 is the temperature after the second row of tubes, then

$$t_3 = X_1 t_2 + t_{ADP}(1 - X_1) \tag{18.68}$$

Substituting for t_2 from Eq. (18.66), we get

$$t_3 = X_1[t_1 X_1 + t_{ADP}(1 - X_1)] + t_{ADP}(1 - X_1)$$
$$= t_1 X_1^2 + t_{ADP}(1 - X_1^2) = t_1 X_2 + t_{ADP}(1 - X_2)$$

or the bypass factor of two rows,

$$X_2 = X_1^2 \tag{18.69}$$

or for n rows of tubes

$$X_n = X_1^n \tag{18.70}$$

The validity of this derivation depends upon the rows being identical and the same surface temperature of all the rows and that of moist air. In actual case, greater turbulence of the air entering the second row gives a lower bypass factor than the first. The method is, however, very convenient and hence it is used.

The bypass factor of a cooling coil (inefficiency) decreases with decrease in spacing and increase in the number of rows. It increases with increase in face velocity since at higher velocities the moist air gets less time to contact the coil surface. Table 19.3 shows the bypass factors of some of the coils. The values given here should be taken as guidelines only for the selection of the cooling coil. Over the years the fin design (corrugated, stamping, turbulence promotion) have considerably improved the efficiency of the cooling coils.

Table 18.3 Typical bypass factors for various cooling coils

Depth of coils / *Face velocity* / *No of rows*	*Without spray*		*With spray*	
	3.2 fins/cm (8 fins/inch)	5.6 fins/cm (14 fins/inch)	3.2 fins/cm	5.6 fins/cm
	1.5–3 m/s	1.5–3 m/s	1.5–3 m/s	1.5–3 m/s
2	0.42–0.55	0.22–0.38		
3	0.27–0.4	0.1–0.23		
4	0.19–0.3	0.05–0.14	0.12–0.22	
5	0.12–0.23	0.02–0.09	0.08–0.14	0.08–0.1
6	0.08–0.18	0.01–0.06	0.06–0.11	0.01–0.08
8	0.03–0.08		0.02–0.05	0.01–0.05

The outlet temperature of air from a cooling coil depends upon the bypass factor of the cooling coil and the apparatus dew point or the effective surface temperature of the cooling coil. For example in Figure 18.7(c), if the apparatus dew point temperature is t_w then the outlet state will be 2 with a bypass factor of X. On the other hand if the apparatus dew point is t_{w1}, then the outlet state is 2′ with a bypass factor of X. In case of another apparatus dew point t_{w2}, the line 1–t_{w2} may become tangent to the saturation curve and then an ADP lower than this cannot be achieved.

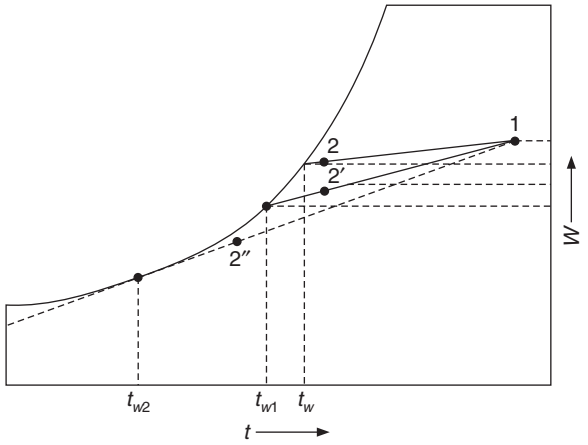

Figure 18.7(c) Cooling and dehumidification.

It is further observed that the sensible heat factor is higher for line 1–2 than that for 1–2′ or that for 1–2″. Hence a sensible heat factor lower than that for 1–2″ cannot be achieved. A lower apparatus dew point requires a lower evaporator temperature, which would imply a lower coefficient of performance for the refrigeration plant.

A sensible heat factor of 0.75 is considered to be the best from refrigeration plant economy point of view. A lower sensible heat factor occurs when the latent heat load is high since SHF = RSH/(RSH + RLH). This occurs when large outdoor air is required, or when occupancy load is high or during monsoon months. For such cases one chooses a cooling coil with a low bypass factor if choosing low ADP is not economical. The typical bypass factors for various applications are summarized in Table 18.4 and 18.5.

Table 18.4 Typical bypass factors

X	*Type of application*	*Examples*
0.3–0.5	A small total load or a load which is somewhat larger with low SHF (high latent load)	Residences
0.2–0.3	Comfort application with relatively small total load or a low SHF with somewhat larger load	Residences, small retail shops, factories
0.05–0.1	High internal sensible load or requiring large amount of outdoor air for ventilation	Departmental stores, dark rooms, restaurants, VIP lounges, factories, banks, cold storages
0.0–0.1	All outdoor air application	Hospitals, operation theatres, factories, insect rearing, microorganism labs, incubators, ICUs, dark rooms, battery rooms of telephone exchanges.

Table 18.5 Bypass factors for 2, 4, 6 and 8 row coils at various velocities and fin spacing

Air vel. (m/s)	*No. of fins per cm*														
	1.2 (3 per inch)		1.7 (4 per inch)		2.4 (6 per inch)		3.2 (8 per inch)				5.12 (13 per inch)		6 (15 per inch)		
	4	6	4	6	4	6	2	4	6	8	4	6	2	4	6
1.5	0.42	0.27	0.32	0.2	0.21	0.1	0.42	0.19	0.08	0.03	0.052	0.012	0.22	0.05	0.01
2	0.45	0.3	0.39	0.24	0.25	0.12	0.46	0.26	0.1	0.05	0.076	0.022	0.26	0.07	0.02
2.5	0.48	0.33	0.42	0.27	0.28	0.15	0.50	0.26	0.13	0.06	0.099	0.032	0.3	0.1	0.03
3	0.5	0.36	0.46	0.3	0.31	0.18	0.53	0.28	0.16	0.07	0.12	0.042	0.34	0.13	0.04
3.5	0.52	0.38	0.47	0.32	0.34	0.2	0.55	0.3	0.18	0.08	0.14	0.052	0.38	0.14	0.05

Coils with more than or equal to 3–2 fins/cm are considered to be efficient and coils with 4, 6, 8 rows are commonly used for air conditioning. The choice depends upon the application as indicated in Table 18.4. For cooling applications, 2 m/s face velocity is economical and the value 2.5 m/s to 4 m/s is generally used. Higher velocities result in more fan power and pressure drop. For cooling coils, face velocities more than 3 m/s are never used. It is always better to choose a larger coil rather than using a higher velocity. In the case of cooling coils for food freezing where the air temperatures are very low and water vapour freezes, fin spacing of 1.2 to 2.4 fins/cm is used to provide sufficient space for frosting and airflow in the event of frosting.

18.7 AIR CONDITIONING SYSTEM

It will be shown in the chapter on load calculations that the air-conditioned space in summer months gains heat through building structure, ingress of warm outdoor air and internal heat gains from occupants, appliances, lights and computers, etc. These are called sensible heat loads and for the room this is called Room Sensible Heat load, abbreviated RSH. Similarly the space or room gains moisture due to sweating, respiration, ingress of outdoor humid air and internal heat gains like cooking, hot showers, etc. These heat gains unlike sensible heat gains do not result in a rise in temperature. This is called Room Latent Heat load and abbreviated RLH. In summer months these are cooling loads since the air conditioning system has to cool and dehumidify the air, which is circulated in the room to remove these heat loads. In winter the directions of RSH and RLH will be opposite of those in summer requiring heating and humidification of air to maintain the required indoor design conditions. These loads are picked up by the conditioned air, which is supplied to the room. Hence the air conditioning problem essentially involves the determination of temperature, humidity ratio and mass flow rate at which the conditioned air should be supplied to the room so as to maintain a steady-state condition in the room and pick up the sensible and latent heat loads.

The indoor design condition prevails in a room from working plane level to the return air duct. Hence the return air conditions are the same as the indoor design conditions, say the dry-bulb temperature t_i and the humidity ratio W_i. The return air from the room is diluted with fresh air, cooled and dehumidified by cooling coil and circulated to the room.

18.7.1 Simple Air Conditioning System

An air conditioning system in which all the return air is recirculated is called the simple air conditioning system. Figure 18.8 shows the schematic diagram of the simple summer air conditioning system with sensible and latent heat gains as RSH and RLH. If instead of RLH the moisture gain G kgw/s is specified, then RLH is given by

$$\text{RLH} = 2500G \text{ kW} \tag{18.71}$$

The total room heat load is denoted by RTH and is the sum of RSH and RLH, that is

$$\text{RTH} = \text{RSH} + \text{RLH} \tag{18.72}$$

Let $\dot{m}_a$ be the mass flow rate of dry air equivalent to supply air quantity Q_{vs} cmm of dry air. Also, let t_s and W_s be the dry-bulb temperature and humidity ratio of supply air. Then the energy balance for Figure 18.8 yields

$$\text{RSH} = \dot{m}_a c_{p\text{-}ma}(t_i - t_s) = 0.0204\, Q_{vs}(t_i - t_s) \text{ kW} \tag{18.73}$$

$$\text{RLH} = \dot{m}_a (h_{fg})_0 (W_i - W_s) = 2500G = 50\, Q_{vs}(W_i - W_s) \text{ kW} \tag{18.74}$$

Also,
$$\text{RTH} = \dot{m}_a (h_i - h_s) = 0.02\, Q_{vs}\, (h_i - h_s) \tag{18.75}$$

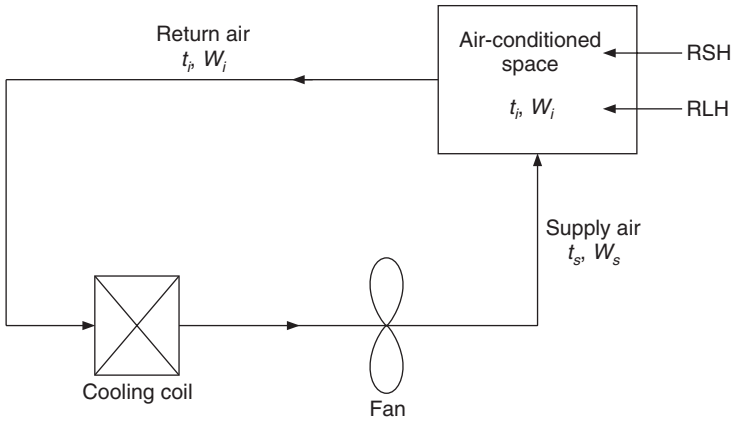

Figure 18.8 Simple summer air conditioning system.

Given RSH and RLH we have two equations in three unknowns, namely t_s, W_s and Q_{vs}. Hence one of the variables is either known in advance or fixed from experience. If the supply air state is saturated state then W_s and t_s are related together. There can be many solutions of Eqs. (18.73) and (18.74). For each Q_{vs} there will be fixed t_s and W_s, which will meet the requirement. All the solutions will have the same sensible heat factor, which is called Room Sensible Heat Factor and abbreviated RSHF.

$$\text{RSHF} = \frac{\text{RSH}}{\text{RSH} + \text{RLH}} = \frac{0.0204(t_i - t_s)}{0.0204(t_i - t_s) + 50(W_i - W_s)} = \frac{1}{1 + 2451\dfrac{\Delta W}{\Delta t}} \tag{18.76}$$

All the possible values of t_s, W_s and Q_{vs} will lie on a straight line with this slope called RSHF line drawn from the room air state t_i, W_i as shown in psychrometric chart in Figure 18.9. States (t_{s1}, W_{s1}), (t_{s2}, W_{s2}) and (t_{s3}, W_{s3}) on the RSHF line, all satisfy RSH and RLH simultaneously. The point of intersection of RSHF line with the saturation curve is called *apparatus dew point*, abbreviated ADP. This is the effective temperature of the cooling coil. The state of air at this point is saturated air. In actual practice it is not possible to achieve this state. The volume flow rate of air is minimum if the air is supplied to the room at ADP. This from Eqs. (18.73), (18.24) and (18.75) is given by

$$Q_{v,\min} = \frac{\text{RSH}}{0.0204\,(t_i - t_{\text{ADP}})} = \frac{\text{RLH}}{50\,(W_i - W_{\text{ADP}})} = \frac{\text{RTH}}{0.02\,(h_i - h_{\text{ADP}})} \tag{18.77}$$

The volume flow rate will progressively increase as one moves away from ADP along the RSHF line. The volume flow rate at (t_{s3}, W_{s3}) will be greater than that at ADP. Similarly, the volume flow rate at (t_{s2}, W_{s2}) will be greater than that at (t_{s3}, W_{s3}).

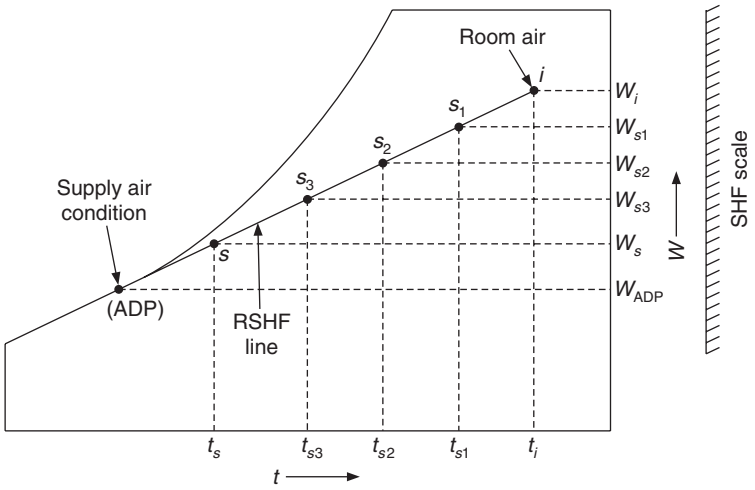

Figure 18.9 Simple summer air conditioning process.

In the actual case, the coil will have a certain bypass factor X and the supply air state will correspond to s rather than ADP as shown in Figure 18.9. A finite value of bypass factor increases the supply air temperature, humidity ratio and the supply air volume flow rate. The RSH and RLH are met by the supply air quantity Q_{vs}, which is available at temperature ($t_i - t_s$) lower than the return air. The temperature difference ($t_i - t_s$) is called the *dehumidified temperature rise* and the corresponding volume flow rate Q_{vs} is called the *dehumidified air quantity* $(\text{cmm})_d$.

$$\text{Dehumidified temperature rise} = t_i - t_s \tag{18.78}$$

$$\text{Dehumidified air quantity } (\text{cmm})_d = \text{RSH}/[0.0204(t_i - t_s)] \tag{18.79}$$

EXAMPLE 18.6 The indoor design conditions are 25°C and 50% relative humidity. The RSH and RLH are 100 kW and 20 kW respectively. (i) Find the minimum volume flow rate and the volume flow rate at supply air temperatures of 14°C, 15°C and 16°C. (ii) If the bypass factor of the cooling coil is 0.15, find the supply air state and the volume flow rate.

Solution:

(i) The humidity ratio at 25°C, 50% RH can be found either by using the vapour pressure of water vapour from steam tables or by using Goff and Gratch tables.

$$\text{At } 25^{\circ}\text{C: } p_{ws} = 0.031693 \text{ bar}, \quad W_i = 0.622 \frac{0.5(0.031639)}{1.01325 - 0.5(0.031639)} = 0.0098822$$

$$\text{From GG table, } W_s = 0.02017, \quad \mu = \frac{0.622\phi}{0.622 + (1-\phi)W_s} = \frac{0.622(0.5)}{0.622 + 0.5(0.02017)}$$

$$\therefore \qquad \mu = 0.492022 \quad \text{and} \quad W = \mu W_s = 0.0099241 \text{ kgw/kga}$$

The apparatus dew point is not given. This may be obtained either by using the psychrometric chart or by iteration.

$$\text{RSHF} = 100/(100 + 20) = 0.833$$

Drawing a line with this RSHF from 25°C and 50% RH intersects the saturation curve at 12.2°C.

$$\text{RSH} = 0.0204 Q_{vmin} (25 - t_{\text{ADP}}) = 100 \text{ kW}$$

$$\text{RLH} = 50 Q_{vmin} (0.0099241 - W_{\text{ADP}}) = 20 \text{ kW}$$

$$\frac{\text{RSH}}{\text{RLH}} = \frac{100}{20} = \frac{0.0204(25 - t_{\text{ADP}})}{50(0.0099241 - W_{\text{ADP}})}$$

or $$(25 - t_{\text{ADP}}) = 250(0.0099241 - W_{\text{ADP}})/0.0204$$

This equation is solved by iteration by using the values of W_s from GG table at various temperatures.

At 12°C :	$W_s = 0.008766$;	Right-hand side = 14.1924	and	Left-hand side = 13.0
At 13°C :	$W_s = 0.00937$;	Right-hand side = 6.79	and	Left-hand side = 12.0
At 12.2°C :	$W_s = 0.0088868$;	Right-hand side = 12.712	and	Left-hand side = 12.8
At 12.19°C :	$W_s = 0.0088808$;	Right-hand side = 12.786	and	Left-hand side = 12.81

The iteration gives an apparatus dew point of 12.19°C which is as good as 12.2°C obtained from the psychrometric chart.

$$Q_{vmin} = 100/[0.0204(25 - 12.19)] = 382..67 \text{ cmm}$$

$$\text{At } t_s = 14^{\circ}\text{C}, \; Q_{vs} = 100/[0.0204(25 - 14)] = 445.63 \text{ cmm}$$

$$\text{At } t_s = 15^{\circ}\text{C}, \; Q_{vs} = 100/[0.0204(25 - 15)] = 490.196 \text{ cmm}$$

$$\text{At } t_s = 16^{\circ}\text{C}, \; Q_{vs} = 100/[0.0204(25 - 16)] = 544.66 \text{ cmm}$$

(ii) The bypass factor is given to be 0.15. From the definition of bypass factor, we have

$$t_{s1} = t_{\text{ADP}} + X(t_i - t_{\text{ADP}}) = 12.19 + 0.15(25 - 12.19) = 14.1115^{\circ}\text{C}$$

$$\text{Dehumidified temperature rise} = 25 - 14.1115 = 10.8885^{\circ}\text{C}$$

Dehumidified air quantity = 100/(0.0204(10.8885) = 450.196 cmm

18.7.2 Summer Air Conditioning System with Ventilation and Zero Bypass Factor

In all air conditioning systems a certain amount of fresh outdoor air has to be introduced to dilute the odours, pollutants and carbon dioxide exhaled by occupants. The amount of fresh air introduced depends upon the level of activity of occupants in the space. The simple air conditioning system is modified accordingly. If $\dot{m}_{a0}$ kg/s or Q_{v0} cmm is the fresh air that is added, then the same amount of return air has to be rejected. The drawback of this system is that the return air rejected is at lower temperature and lower humidity ratio than the fresh air that is introduced. Hence effectively the fresh air has to be cooled to the return air temperature, which is an extra cooling load on the cooling coil.

Figure 18.10 shows the schematic diagram of the system. Out of the total return air $\dot{m}_{as}$, a quantity $\dot{m}_{ar}$ is recirculated, that is, it is returned to the cooling coil and $\dot{m}_{a0}$ is rejected to the surroundings. The recirculated air is at the state t_i, W_i. Fresh air of mass flow rate $\dot{m}_{a0}$ at t_0, W_0 is adiabatically mixed with the return air resulting in mixed air at state t_1, W_1, which enters the cooling coil. Temperature t_1 and humidity ratio W_1 are greater than t_i and W_i, hence this causes additional load on cooling coil. Adiabatic mixing is described by

$$\dot{m}_{as} h_1 = \dot{m}_{ar} h_i + \dot{m}_{a0} h_0 \tag{18.80}$$

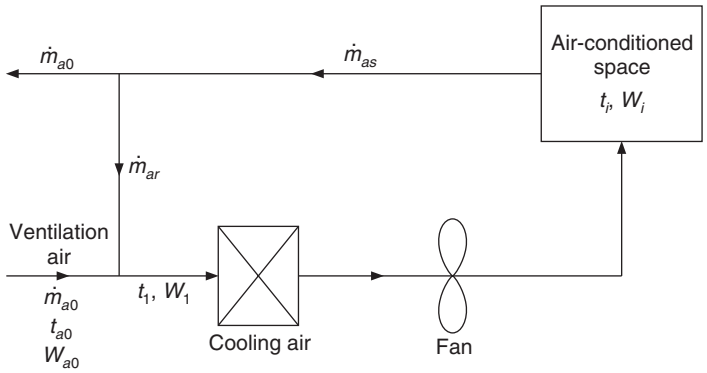

Figure 18.10 Simple summer air conditioning system with ventilation air.

The mixed air is cooled to state 2 in the cooling coil. State 2 is saturated state since the bypass factor of the cooling coil is assumed to be zero. The cooling load Q is expressed as

$$Q = \dot{m}_{as} (h_1 - h_2) \tag{18.81}$$

Substituting Eq. (18.80) in (18.81), we get

$$Q = \dot{m}_{ar} h_i + \dot{m}_{a0} h_0 - \dot{m}_{as} h_2 = (\dot{m}_{as} - \dot{m}_{a0}) h_i + \dot{m}_{a0} h_0 - \dot{m}_{as} h_2$$

or

$$Q = \dot{m}_{as} (h_i - h_2) + \dot{m}_{a0} (h_0 - h_i) \tag{18.82}$$

The air enters the room at enthalpy h_2 and leaves at enthalpy h_i, hence the first term in this expression is the total cooling load of the room. The second term is the amount by which the fresh

air has to be cooled to the return air condition. This is called the *total outside air load* or *ventilation load*. This has sensible as well as latent parts called *outside air sensible heat* (OASH) and *outside air latent heat* (OALH). For Q_{v0} cmm flow rate of standard fresh air, these quantities may be expressed as follows:

$$\text{OASH} = 0.0204Q_{v0}(t_0 - t_i) \tag{18.83}$$

$$\text{OALH} = 50Q_{v0}(W_0 - W_i) \tag{18.84}$$

The total of these two quantities is the *outside air total heat* (OATH) given by

$$\text{OATH} = \text{OASH} + \text{OALH} = 0.02Q_{v0}(h_0 - h_i) = m_{ao}(h_0 - h_i) \tag{18.85}$$

The total load on the cooling coil is the sum of room load and outside air load. The sensible and latent parts of it are denoted by *total sensible heat* (TSH) load and *total latent heat* (TLH) load. The sum of latent and sensible loads is denoted by *grand total heat* (GTH) load.

$$\text{TSH} = \text{RSH} + \text{OASH} \tag{18.86}$$

$$\text{TLH} = \text{RLH} + \text{OALH} \tag{18.87}$$

$$\text{GTH} = \text{TSH} + \text{TLH} \tag{18.88}$$

In line with RSHF for the room a grand sensible heat factor (GSHF) is defined for the cooling coil as follows:

$$\text{GSHF} = \frac{\text{TSH}}{\text{TSH} + \text{TLH}} \tag{18.89}$$

The state of moist air through the cooling coil has the slope of GSHF. This is shown by a line on psychrometric chart just like the RSHF line. RSHF satisfies the room loads while GSHF satisfies the cooling coil loads. The supply air state satisfies both the room load and the cooling coil load, hence it must lie at the intersection of RSHF and GSHF lines.

Figure 18.11 shows these lines on the psychrometric chart. It has been assumed for simplicity that the bypass factor of the cooling coil is zero, therefore the supply air leaves the cooling coil at

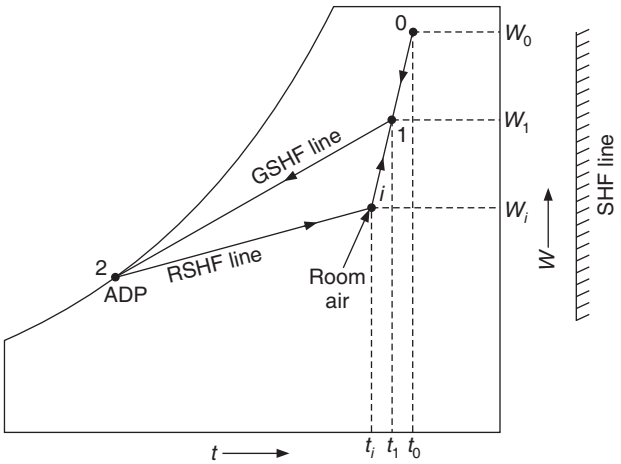

Figure 18.11 Simple summer air conditioning processes with ventilation air.

saturated state 2, which is also the apparatus dew point of the cooling coil. This is also the point of intersection of RSHF and GSHF lines. The state (t_i, W_i) is the return air state and state (t_0, W_0) is outdoor air state. The state (t_1, W_1) at the inlet to cooling coil is obtained by adiabatic mixing of return air and outdoor air. That is, it lies on the line *i*–0 dividing it in proportion of $\dot{m}_{a0} : \dot{m}_{ar}$.

Supply air state 2 is such that RSH and RLH are met along the line 2–*i*, hence this line has the slope of RSHF. Similarly, line 1–2 is such that the cooling coil load is met along it hence it, has the slope of GSHF. The direction of arrow on the RSHF line indicates that supply air picks up the room loads along it. Similarly, the direction of arrow on GSHF line indicates cooling of mixed air.

EXAMPLE 18.7 The room air leaves an air-conditioned space at 25°C, 50% relative humidity. The bypass factor of the cooling coil is zero. The outdoor air is at 45°C, 30% relative humidity. The dehumidified air quantity is 600 cmm and 80% of this by mass is recirculated. The apparatus dew point is 12°C. Determine RSH, RLH, OASH, OALH, RTH and OATH.

Solution:

From Example 18.6 : $W_i = 0.0099241$
From GG table, at 45°C, $W_s = 0.065411$ and at 12°C $W_s = 0.008766$

$$\text{For outdoor condition, } \mu = \frac{0.622\phi}{0.622 + (1-\phi)W_s} = \frac{0.622(0.3)}{0.622 + 0.7(0.065411)} = 0.27943$$

$$\therefore \qquad W_0 = \mu\, W_s = 0.27943(0.065411) = 0.018278$$

Considering adiabatic mixing of return air and outdoor air, we get

$$t_1 = 0.8(25) + 0.2(45) = 29^{\circ}\text{C}$$

$$W_1 = 0.8(0.0099241) + 0.2(0.018278) = 0.011595 \text{ kgw/kga}$$

The supply air state 2 is the apparatus dew point of the cooling coil since the bypass factor is zero. Considering the given volume flow rate to be that of standard air, we get

$$\text{RSH} = 0.0204(600)(25 - 12) = 159.12 \text{ kW}$$

$$\text{RLH} = 50(600)(0.0099241 - 0.008766) = 34.743 \text{ kW}$$

$$\text{RTH} = 159.12 + 34.743 = 193.863 \text{ kW}$$

Fresh air flow rate, $Q_{v0} = 0.2(600) = 120$ cmm

$$\text{OASH} = 0.0204(120)(45 - 25) = 48.96 \text{ kW}$$

$$\text{OALH} = 50(120)(0.18278 - 0.0099241) = 50.123 \text{ kW}$$

$$\text{OATH} = 48.96 + 50.123 = 99.083 \text{ kW}$$

$$\text{GTH} = \text{RTH} + \text{OATH} = 193.863 + 99.083 = 292.946 \text{ kW}$$

If the volume flow rate is not that of standard air but the actual volume flow rate of air at inlet to cooling coil, then we have to find the specific volume of dry air at state1 and then the mass flow rate of dry air. This will be followed by the determination of loads from enthalpies at various points. The specific volume of dry air at state 1 is given by

$$v_a = \frac{R_a T_1 (1 + 1.6078 W_1)}{p} = \frac{0.2871(302)(1 + 1.6078 \times 0.011595)}{101.325} = 0.87166 \text{ m}^3/\text{kga}$$

$$\dot{m}_a = \frac{600}{60\,(0.87166)} = 11.47236 \text{ kga/s}$$

$$h_i = 1.005(25) + 0.0099241(2500 + 1.88 \times 25) = 50.40168 \text{ kJ/kga}$$

$$h_0 = 1.005(45) + 0.018278(2500 + 1.88 \times 45) = 92.46632 \text{ kJ/kga}$$

$$h_1 = 1.005(29) + 0.011595(2500 + 1.88 \times 29) = 58.76435 \text{ kJ/kga}$$

$$h_{\text{ADP}} = 1.005(12) + 0.008766(2500 + 1.88 \times 12) = 34.17276$$

$$\text{RTH} = \dot{m}_a(h_i - h_{\text{ADP}}) = 11.47236(50.40168 - 34.17276) = 186.184 \text{ kW}$$

$$\text{OATH} = 0.2\,\dot{m}_a(h_0 - h_i) = 0.2 \times 11.47236(92.46632 - 50.40168) = 96.516 \text{ kW}$$

$$\text{GTH} = \dot{m}_a(h_1 - h_{\text{ADP}}) = 11.47236(58.76435 - 34.17276) = 282.1236 \text{ kW}$$

It is observed that the calculations based upon the mass flow rate give slightly different results than those for standard air.

EXAMPLE 18.8 The room air leaves an air-conditioned space at 25°C, 50% relative humidity. The bypass factor of the cooling coil is zero. The outdoor air is at 45°C, 30% relative humidity. The outdoor air quantity is 100 cmm. RSH and RLH are 200 kW and 50 kW respectively. Determine the supply air state, mass flow rate of supply air, state at inlet to cooling coil, OASH, OALH, RTH and OATH and total cooling load.

Solution:

From Example 19.7, $W_i = 0.0099241$ and $W_0 = 0.018278$

$h_i = 50.40168$ kJ/kga and $h_0 = 92.46632$ kJ/kga

RSHF = RSH/(RSH + RLH) = 200/250 = 0.8

The supply air state is saturated air state at apparatus dew point. The RSHF line and GSHF line will both meet the saturation curve at ADP. The ADP can be found by iteration. The slope of the line joining ADP to (t_i, W_i) is same as that of RSHF line. We guess ADP and check the slope of this line. The slope of RSHF line is given by

$$\frac{\Delta W}{\Delta t} = \frac{1}{2451}\left(\frac{1}{\text{RSHF}} - 1\right) = \frac{0.25}{2451} = 0.000102$$

At $t_{\text{ADP}} = 11.5$: $W_s = 0.0084815$ and $\Delta W/\Delta t = 0.0001069$

At $t_{\text{ADP}} = 11.6$: $W_s = 0.0085384$ and $\Delta W/\Delta t = 0.0001034$

At $t_{\text{ADP}} = 11.7$: $W_s = 0.0085953$ and $\Delta W/\Delta t = 0.0000991$

At $t_{\text{ADP}} = 11.65$: $W_s = 0.0085668$ and $\Delta W/\Delta t = 0.0001017$

At $t_{\text{ADP}} = 11.64$: $W_s = 0.0085611$ and $\Delta W/\Delta t = 0.00010$

Therefore the apparatus dew point is 11.64°C.

$$h_{ADP} = 33.2884 \text{ kJ/kga}$$

$$\text{OASH} = 0.0204(100)(45 - 25) = 40.8 \text{ kW}$$

$$\text{OALH} = 50(100)(0.018278 - 0.0099241) = 41.77 \text{ kW}$$

$$\text{OATH} = 40.8 + 41.77 = 82.57 \text{ kW}$$

$$\text{TSH} = 200 + 40.8 = 240.8 \text{ kW}$$

$$\text{TLH} = 50 + 41.77 = 91.77 \text{ kW}$$

$$\text{GTH} = 332.57 \text{ kW}$$

$$\text{GSHF} = 240.8/332.57 = 0.724$$

Supply air volume flow rate is given by

$$Q_{vs} = \text{RSH}/[0.0204(t_i - t_{ADP})] = 200/(0.0204 \times 13.36) = 733.826 \text{ cmm}$$

The specific volume of outdoor air is given by

$$v_{a0} = \frac{R_a T_0 (1 + 1.6078 W_0)}{p} = \frac{0.2871(318)(1 + 1.6078 \times 0.018278)}{101.325} = 0.9275 \text{ m}^3/\text{kga}$$

$$\dot{m}_{a0} = \frac{100}{60(0.9275)} = 1.79691 \text{ kga/s}$$

The specific volume of supply air is given by

$$v_{as} = \frac{0.2871(286.64)(1 + 1.6078 \times 0.00856116)}{101.325} = 0.8176 \text{ m}^3/\text{kga}$$

$$\dot{m}_{as} = \frac{733.826}{60(0.8716)} = 14.9586 \text{ kga/s}$$

$$\dot{m}_{ar} = \dot{m}_{as} - \dot{m}_{a0} = 13.1617 \text{ kga/s}$$

Adiabatic mixing of recirculated and outdoor air yields

$$h_1 = (\dot{m}_{ar} h_i + \dot{m}_{a0} h_0) / \dot{m}_{as} = 55.4547 \text{ kJ/kga}$$

$$W_1 = (\dot{m}_{ar} W_i + \dot{m}_{a0} W_0) / \dot{m}_{as} = 0.0109276$$

$$t_1 = (h_1 - 2500 W_1)/(1.005 + 1.88 W_1) = 27.435$$

$$\text{OATH} = \dot{m}_{a0} (h_0 - h_i) = 75.5864 \text{ kW}$$

$$\text{GTH} = \dot{m}_{as} (h_1 - h_{ADP}) = 331.578 \text{ kW}$$

Also $\text{GTH} = \text{RSH} + \text{RLH} + \text{OATH} = 325.5864 \text{ kW} = 92.58 \text{ TR}$

The two results are slightly different essentially because OATH is different if standard air volume flow rate is used and when the mass flow rate of outdoor air is used.

18.7.3 Summer Air Conditioning System with Ventilation and Non-zero Bypass Factor

The conditions of moist air in this case are shown in Figure 18.12. In this figure, *i*–2 is the RSHF line. It was seen that if the bypass factor is zero, the supply air state is ADP itself satisfying the room loads. If the bypass factor is not zero, then the supply air state 2 in this case has to lie away from the saturated state at the intersection of GSHF and RSHF lines. This is shown by the new position of state 2. The apparatus dew point lies at the intersection of GSHF line with the saturation curve. It is observed that to satisfy the bypass factor of the cooling coil, the apparatus dew point gets lowered to state s' compared to the same state without the bypass factor. States s', 1 and 2 are related as follows.

$$X = \frac{t_2 - t_{s'}}{t_1 - t_{s'}} = \frac{W_2 - W_{s'}}{W_1 - W_{s'}} = \frac{h_2 - h_{s'}}{h_1 - h_{s'}} \tag{18.90}$$

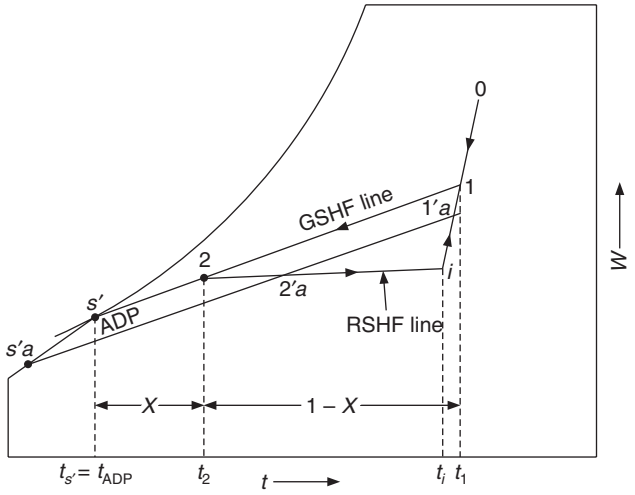

Figure 18.12 Summer air conditioning processes with ventilation air and finite bypass factor.

The effect of bypass factor is to lower the apparatus dew point, hence it reduces the performance of the refrigeration system. Also the GSHF line changes to 1–2–s'. The supply air temperature at the new point 2 is high, the dehumidified temperature rise $(t_i - t_2)$ is lower and the dehumidified air quantity will be larger.

The calculation procedure is, however, not straightforward. The bypass factor depends upon state 1 of mixed air. State 1 is obtained by adiabatic mixing of outdoor air and supply air. The outdoor air quantity is usually known by the ventilation or fresh air requirement. The supply air quantity has to be calculated to satisfy the room loads, RSHF and GSHF. Hence state 1 cannot be found unless supply air quantity is known. Therefore with the given bypass factor and GSHF, the supply air state cannot be found in a straightforward manner.

The solution procedure involves trial and error. It is known that the condition line 1–2–s' has the slope of GSHF. The supply air state 2 must lie at the intersection of GSHF line with RSHF line such that point 2 satisfies the bypass factor X of the cooling coil. Hence, one draws another GSHF

line $1a'$–$2'a$–$s'a$ which intersects the RSHF line at state $2'a$. It is checked if state $2'a$ satisfies the bypass factor of the cooling coil Eq. (18.90). If it does not, another line $1'b$–$2'b$–$s'b$ (not shown in the figure) is drawn parallel to GSHF and the bypass relation is checked. That is, the GSHF line is floated parallel to its slope until the bypass relation is satisfied between 1, 2 and the apparatus dew point. Another GSHF line $1'c$–$2'c$–$s'c$ similarly drawn (not shown in the figure) may not also satisfy the bypass relation. Line 1–2–s', however, satisfies the bypass relation and point 2 lies on both RSHF and GSHF lines, hence 2 is the supply air state.

The state of the mixed air 1 also floats along the line i–0, dividing it in proportion of $\dot{m}_{a0} : \dot{m}_{ar}$. Once the supply air state is known, the dehumidified temperature rise and the dehumidified air quantity are found by the relations,

$$\text{Dehumidified temperature rise} = t_i - t_2$$

$$\text{Dehumidified air quantity (cmm)}_d = \text{RSH}/[0.0204(t_i - t_2)]$$

$$= \text{TSH}/[0.0204(t_1 - t_2)]$$

Effect of bypass factor

If the bypass factor increases:

(i) The supply air state moves towards the return air state i.

(ii) The dehumidified temperature rise decreases

(iii) The dehumidified air quantity increases

(iv) The fresh air volume flow rate remaining fixed, the recirculated air volume flow rate increases.

(v) The apparatus dew point decreases which decreases the COP of the refrigeration plant and that in turn increases the running cost. The cooling coil of the higher bypass factor will be less costly.

An approximate method has been suggested to find the supply air state without resorting to iteration. This method is known as Effective Room Sensible Heat Factor Method. It is described in the following section.

18.7.4 Effective Room Sensible Heat Factor

It is observed that the calculation of supply air state and volume flow rate for the given RSH, RLH, Q_{v0}, t_0, W_0, t_i, W_i and X require iteration. The GSHF line is floated on the psychrometric chart and state 1 is found such that Q_{v0}, Q_{vs} and the bypass factor of the cooling coil satisfy it. To avoid iteration an approximate procedure called *Effective Sensible Heat Factor* method is introduced. The use of bypass factor requires that state 1 be known apriori so that the line 1–ADP can be intersected in proportion of X. This is not known. The approximate method uses the room design condition and the line i–ADP, divides it in proportion of X to find the supply air state.

The airflow rate at the inlet to the cooling coil is the sum of Q_{v0} and Q_{vr}. The bypass factor X implies that X part of the air never comes into contact with the cooling coil while the $(1 - X)$ portion is perfectly contacted by the cooling coil, that is leaves the cooling coil at t_{ADP} and W_{ADP}. Therefore as shown schematically in Figure 18.13, the XQ_{v0} part of the outdoor fresh air bypasses the cooling coil and enters the room directly. Since it enters the room directly, it adds to the room sensible and latent heat loads.

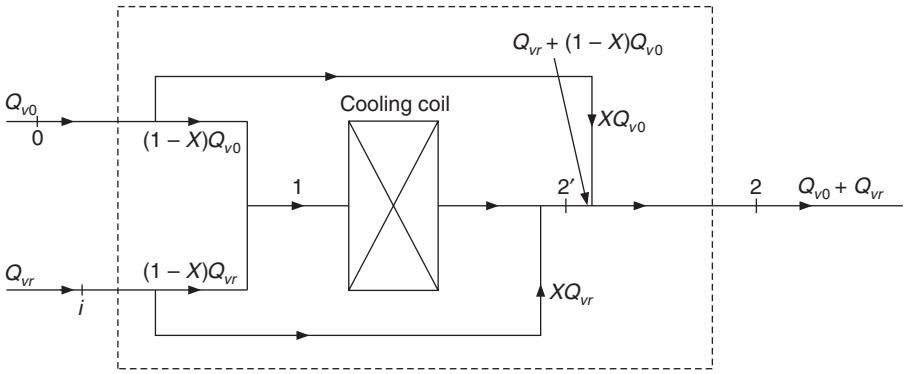

Figure 18.13 Schematic diagram equivalent to the system of Figure 18.10.

The XQ_{vr} part of the recirculated air also enters the room directly, but it does not change the room loads since it is at (t_i, W_i), the room design condition whereas the outdoor air is at (t_0, W_0). Hence the effective loads of the room change and these are called *Effective Room Sensible Heat* (ERSH) load and *Effective Room Latent Heat* (ERLH) load. These are given as follows.

$$\text{ERSH} = \text{RSH} + X(\text{OASH}) \tag{18.91}$$

$$\text{ERLH} = \text{RLH} + X(\text{OALH}) \tag{18.92}$$

$$\text{ERTH} = \text{ERSH} + \text{ERLH}$$

$$\text{ESHF} = \frac{\text{ERSH}}{\text{ERSH} + \text{ERLH}} \tag{18.93}$$

In Figure 18.13, $(1 - X)Q_{vr}$ and $(1 - X)Q_{v0}$ pass through the cooling coil and the outlet state of the cooling coil is 2′. The air at state 2′ is adiabatically mixed with bypassed air XQ_{v0} at (t_0, W_0) to yield the supply air state 2. The adiabatic mixing of these two streams yields

$$XQ_{v0}\,\rho_0\,t_0 + [(1 - X)\,Q_{v0}\,\rho_0 + Q_{vr}\,\rho_i]\,t_{2'} = (Q_{v0}\,\rho_0 + Q_{vr}\,\rho_i)t_2$$

or

$$X\dot{m}_{a0}\,t_0 + [(1 - X)\,\dot{m}_{a0} + \dot{m}_{ar}]t_{2'} = (\dot{m}_{a0} + \dot{m}_{ar})t_2 \tag{18.94}$$

In the psychrometric chart (Figure 18.14) for this process, state 2′ lies on line 0–2 extended such that the ratio of lengths 2–2′ and 0–2 is given by

$$2\text{–}2' : 0\text{–}2 = X\dot{m}_{a0} : [(1 - X)\,\dot{m}_{a0} + \dot{m}_{ar}]$$

In this figure, the triangle *s* 2 2′ and the triangle *s i* 1 may be assumed to be similar. In that case, the ratio of the sides of triangles has the same proportion, that is,

$$\frac{s\text{–}2}{s\text{–}2'} = \frac{s\text{–}1}{s\text{–}i} \quad \text{or} \quad \frac{s\text{–}2'}{s\text{–}i} = \frac{s\text{–}2}{s\text{–}1} = X \tag{18.95}$$

This is an assumption only since 2–2′ and *i*–1 are not parallel to each other. However, the points 2 and 2′ are very close in practice and point 0 is far away, hence it is a good approximation. This result, although approximate, has far-reaching implications. *This implies that the state 2′ is obtained by dividing the line i–s in the proportion of X and* $(1 - X)$.

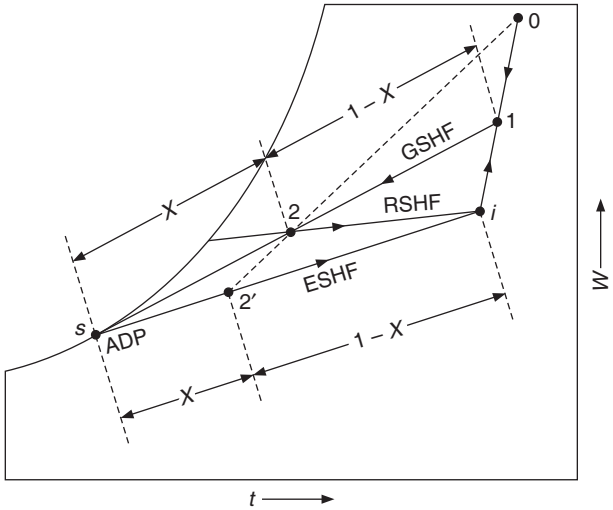

Figure 18.14 Psychromatic process of Effective Room Sensible Heat (ERSH) Load.

The conditioned air at 2′ first meets the bypassed outdoor air load and becomes state 2 which meets the room loads. Therefore state 2′ is able to take care of the loads RSH, RLH and the bypassed outside air loads X OASH and X OALH. *This implies that state 2′ lies on ESHF line, which is line i–s*. Point 2′ is at the exit of cooling coil hence 2′ divides the line *i–s* in proportion of X and $1 - X$. Therefore,

$$\text{ERSH} = 0.0204\, Q_{vs}\, (t_i - t_{2'}) = 0.0204(1 - X)(t_i - t_{\text{ADP}})$$

or
$$Q_{vs} = \frac{\text{ERSH}}{0.0204\,(t_i - t_{2'})} = \frac{\text{ERSH}}{0.0204\,(t_i - t_{\text{ADP}})(1 - X)} \tag{18.96}$$

The iteration is avoided by this procedure. ERSH, ERLH and ESHF are calculated, then the ESHF line is divided in proportion of X and $(1 - X)$ to locate the state 2′. State 2′ is so close to state 2 that lies on RSHF line, that one need not calculate the state 2. Although it is said that iteration is avoided, actually it is still required since ADP at which the ESHF line meets the saturation curve is not known. If the calculation is done on psychrometric chart, then the ESHF line is drawn and ADP is located. If calculations are done manually, then iteration is required to find ADP.

Carrier Corporation Handbook has given ESHF tables, in which the dew points are given for various values of ESHF for a number of room air states (t_i, ϕ_i), where ϕ is the relative humidity. The use of these tables avoids the iteration required for finding the ADP.

EXAMPLE 18.9 The room air leaves an air-conditioned space at 25°C, 50% relative humidity. The bypass factor of the cooling coil is 0.15. The outdoor air is at 45°C, 30% relative humidity. The outdoor air quantity is 120 cmm. RSH and RLH are 160 kW and 35 kW respectively. Determine the ESHF, apparatus dew point, the supply air state on ESHF and the actual supply air state, the state at inlet to cooling coil, OASH, OALH, OATH and the total cooling load.

Solution:

From Example 18.8, $W_i = 0.0099241$ and $W_0 = 0.018278$

$$h_i = 50.40168 \text{ kJ/kga} \quad \text{and} \quad h_0 = 92.46632 \text{ kJ/kga}$$

$$\text{OASH} = 0.0204(120)(45 - 25) = 48.96 \text{ kW}$$

$$\text{OALH} = 50(120)(0.018278 - 0.0099241) = 50.123 \text{ kW}$$

$$\text{ERSH} = \text{RSH} + (0.15)\text{OASH} = 160 + 0.15(48.96) = 167.344 \text{ kW}$$

$$\text{ERLH} = \text{RLH} + (0.15)\text{OALH} = 35 + 0.15(50.123) = 42.518$$

$$\text{ESHF} = \text{ERSH}/(\text{ERSH} + \text{ERLH}) = 167.344/209.862 = 0.7974$$

The ESHF line drawn from the supply air state will meet the saturation curve at ADP. The ADP can be found by iteration. The slope of the line joining ADP to (t_i, W_i) is same as that of ESHF line. We guess ADP and check the slope of this line. The slope of ESHF line is given by

$$\frac{\Delta W}{\Delta t} = \frac{1}{2451}\left(\frac{1}{\text{ESHF}} - 1\right) = 0.00010366$$

At $t_{\text{ADP}} = 11.4$: $W_s = 0.0084246$ and $\Delta W/\Delta t = 0.00011025$

At $t_{\text{ADP}} = 11.5$: $W_s = 0.0084815$ and $\Delta W/\Delta t = 0.0001086$

At $t_{\text{ADP}} = 11.6$: $W_s = 0.0085384$ and $\Delta W/\Delta t = 0.00010341$

At $t_{\text{ADP}} = 11.59$: $W_s = 0.0085327$ and $\Delta W/\Delta t = 0.00010375$

Hence the apparatus dew point is taken as 11.59°C.

The approximate supply air state 2′ is given by

$$t_{2'} = t_{\text{ADP}} + 0.15(t_i - t_{\text{ADP}}) = 11.59 + 0.15(25 - 11.59) = 13.6015^{\circ}\text{C}$$

$$W_{2'} = 0.0085327 + 0.15(0.0099241 - 0.0085327) = 0.0087414$$

$$Q_{vs} = \text{ERSH}/[0.0204925 - 13.6015)] = 719.668 \text{ cmm}$$

$$Q_{vr} = Q_{vs} - Q_{v0} = 719.668 - 120 = 599.668 \text{ cmm}$$

To find the actual supply air state 2, we consider adiabatic mixing using volume flow rates instead of mass flow rates, that is, we consider adiabatic mixing of bypassed air XQ_{v0} at t_0 and $[(1 - X)Q_{v0} + Q_{vr}]$ at $t_{2'}$. This gives

$$719.668t_2 = 0.15(120)45 + [0.85(120) + 599.668)]t_{2'}$$

$$\therefore \quad t_2 = 14.387^{\circ}\text{C}$$

The actual volume flow rate is found by satisfying RSH with supply air temperature.

$$\text{RSH} = 160 = 0.0204\, Q_{vs}(25 - 14.387)$$

$$\therefore \quad Q_{vs} = 739.012$$

$$\therefore \quad Q_{vr} = 739.012 - 120 = 610.012 \text{ cmm}$$

Again using the volume flow rates for adiabatic mixing at inlet to cooling coil, we get

$$t_1 = (619.012 \times 25 + 120 \times 45)/739.012 = 28.2476^{\circ}\text{C}$$

$$W_1 = (619.012 \times 0.0099241 + 120 \times 0.018278)/739.012 = 0.0112806$$

$$t_{ADP} = 11.59^oC \quad \text{and} \quad W_{ADP} = 0.085327$$

$$\Delta W/\Delta t = 0.00016496 \quad \text{and} \quad GSHF = 0.7121$$

$$OATH = 48.96 + 50.123 = 99.083 \text{ kW}$$

$$TSH = 160 + 48.96 = 208.96 \text{ kW}$$

$$TLH = 35 + 50.123 = 85.123 \text{ kW}$$

$$GTH = 294.083 \text{ kW}$$

From these values GSHF = 208.96/294.083 = 0.7105
This agrees with the GSHF found from $\Delta W/\Delta t$.

EXAMPLE 18.10 The room air leaves an air-conditioned space at 25°C, 50% relative humidity. The bypass factor of the cooling coil is 0.15. The outdoor air is at 45°C, 30% relative humidity. RSH and RLH are 160 kW and 35 kW respectively. The outdoor mass flow rate is 20% of the supply air. Find the supply air state, total outside air load and total cooling load.

Solution:

From Example 18.10, $W_i = 0.0099241$ and $W_0 = 0.018278$

$$h_i = 50.40168 \text{ kJ/kga} \quad \text{and} \quad h_0 = 92.46632 \text{ kJ/kga}$$

The state 1 at inlet to cooling is obtained by adiabatic mixing of outside and return air.

$$t_1 = 0.8(25) + 0.2(45) = 29^oC$$

$$W_1 = 0.8(0.0099241) + 0.2(0.18278) = 0.0115948$$

This allows the supply air state to be expressed in terms of bypass factor and apparatus dew point.

$$t_2 = t_{ADP} + 0.15(29.0 - t_{ADP}) = 4.35 + 0.85t_{ADP} \quad \text{(i)}$$

$$W_2 = W_{ADP} + 0.15(0.0115948 - W_{ADP}) = 0.0017392 + 0.85W_{ADP} \quad \text{(ii)}$$

$$RSH = 0.0204\, Q_{vs}(25 - t_2) = 160$$

$$RLH = 50Q_{vs}(0.0.0099241 - W_2) = 35$$

Dividing RSH by RLH, we get

$$\frac{RSH}{RLH} = \frac{160}{35} = \frac{0.0204(25 - t_2)}{50(0.0099241 - W_2)}$$

Simplifying, we get

$$W_2 = \frac{86.194 + t_2}{11204.48} \quad \text{(iii)}$$

The unknowns in Eqs. (i), (ii) and (iii) are t_2, W_2, t_{ADP} and W_{ADP}, out of which t_{ADP} and W_{ADP} are related. Hence, we have to solve three equations for three unknowns by iteration.

Assume $t_{ADP} = 11.5$, $W_{ADP} = 0.0084815$

From Eqs. (i) and (ii) : $t_2 = 14.125$ and $W_2 = 0.008953$

From Eq. (iii), $W_2 = 0.0089485$

These two values of W_2 do not agree, hence we try another value of t_{ADP}.

Assume $t_{ADP} = 11.51$, $W_{ADP} = 0.00848719$

From Eqs. (i) and (ii) : $t_2 = 14.1335$ and $W_2 = 0.008954231$

From Eq. (iii), $W_2 = 0.0089533$

The two values agree now reasonably well, hence $t_{ADP} = 11.51^oC$

Dehumidified cmm = RSH/[0.0204(25 – 14.335) = 721.77 cmm

$v_2 = 287.1335(0.2871)(1 + 1.6078 \times 0.00895423)/101.325 = 0.82593$ m^3/kga

$\dot{m}_{as} = 721.77/60(0.82593) = 14.576$ kga/s

$\dot{m}_{a0} = 0.2(14.576) = 2.9152$ kga/s

$h_i = 50.40168$ kJ/kga and $h_0 = 92.46632$ kJ/kga

OATH = $\dot{m}_{a0}(h_0 - h_i) = 122.627$ kW

RTH = 160 + 35 = 195 kW

GTH = 195 + 122.627 = 317.627 kW = 90.32 TR

18.7.5 High Latent Cooling Load and Reheating

In the following situations the latent heat load may be very high and comparable to sensible heat load.

(i) Large internal latent heat gain due to occupants like in assembly halls, auditoriums and cinema halls.

(ii) Outdoor conditions may be very humid like in coastal areas, where infiltration and fresh air requirement may give rise to large latent heat loads.

(iii) High humidity requirement of processes.

In these cases the slope of the GSHF line will be large and it might lead to a situation where

(i) GSHF line may not intersect the saturation curve at all, or

(ii) GSHF line intersects the saturation curve at a very low value of ADP.

In the first case no cooling coil can meet the cooling load independently and in the second case the evaporator temperature of the refrigeration system becomes very low requiring large power consumption. In such cases a larger apparatus dew point is used and reheat is used to meet the room loads.

Figure 18.15 shows the reheat process and the condition lines for such a case. In this figure line i–s_1 is the original ESHF line for a very low ADP, say 3°C. We choose s_2 say at 11°C as the new ADP and i–s_2 as the modified ESHF line. State 2′ is the supply air state, which divides the modified ESHF line in proportion of bypass factor X and $1 - X$. The process 2–3 is the reheat process. Point 3 lies on the RSHF line. Point 2 represents the actual state at the exit of the cooling coil on the GSHF line. The points 2 and 2′ are very close together and the reheat line can be shown from point 2′ itself to a good approximation. It is observed that RSHF is so small that the RSHF

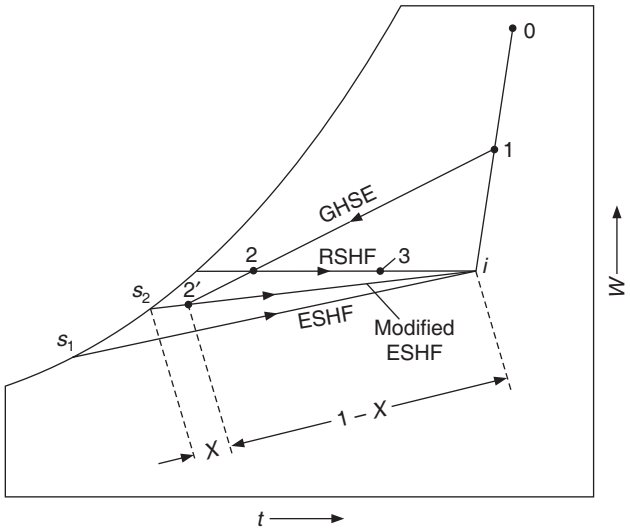

Figure 18.15 Psychrometric processes for high latent cooling load and reheating.

line does not intersect the GSHF line or the saturation curve in this case. Hence reheat has to be used to meet the room loads. The following example illustrates this situation.

EXAMPLE 18.11 The outdoor dry-bulb and wet-bulb temperatures are 40°C and 28°C respectively. The indoor design conditions in a laboratory are 25.5°C and 50% relative humidity. The RSH and RLH are 70 kW and 40 kW respectively. There are 200 persons in the laboratory and ventilation requirement is 0.56 cmm per person. Find the supply air state.

Solution:

At 25.5 °C : $W_s^* = 0.02809$, therefore $\mu = 0.622\phi / [0.622 + (1 - \phi)W_s^*] = 0.48177$

$$W_i = \mu W_s^* = 0.48177(0.02809) = 0.010233$$

At 28°C : $W_s^* = 0.024226$, $h_{fg}^* = 2434.55$, $h_f^* = 117.36$

At 30°C : $h_g = 2573.49$

$$W_0 = \frac{W_s^* h_{fg}^* - 1.005(t - t^*)}{h_g(t) - h_f^*}$$

The fresh air requirement for 200 persons $Q_{v0} = 200(0.56) = 112$ cmm

$$\text{OASH} = 0.0204(112)(40 - 25) = 33.1296 \text{ kW}$$

$$\text{OALH} = 50(112)(0.0191103 - 0.010233) = 49.672 \text{ kW}$$

$$\text{RSHF} = 70/(70 + 40) = 0.636$$

The RSHF is very small, hence an efficient cooling coil with bypass factor of 0.05 will be required. This is a high latent heat situation, hence reheat may also be required.

Taking $X = 0.05$

ERSH = 70 + 0.05(33.1296) = 71.6565 kW

ERLH = 40 + 0.05(49.672) = 42.4836 kW

ESHF = 71.6565/(71.6565 + 42.4836) = 0.6278

We will find $\Delta W/\Delta t$ corresponding to ESHF, guess ADP and check if the assumed ADP gives the required $\Delta W/\Delta t$.

$$\frac{\Delta W}{\Delta t} = \frac{1}{2451}\left(\frac{1}{\text{ESHF}} - 1\right) = 0.00024189$$

At $t_{ADP} = 5^oC$: $W_s = 0.005424$ and $\Delta W/\Delta t = 0.000234585$

At $t_{ADP} = 4^oC$: $W_s = 0.005054$ and $\Delta W/\Delta t = 0.000240884$

At $t_{ADP} = 3^oC$: $W_s = 0.004707$ and $\Delta W/\Delta t = 0.0002456$

At $t_{ADP} = 3.8^oC$: $W_s = 0.0049846$ and $\Delta W/\Delta t = 0.000241862$

The apparatus dew point is very small and will make the refrigeration system very inefficient. In fact if a higher bypass factor were chosen, the ESHF line will not intersect the saturation curve at all. The only way to meet the RSHF and have respectable ADP is to introduce reheat. We assume that we will have an apparatus dew point of 11°C and find the reheat required to achieve it.

Assume $t_{ADP} = 11^oC$, $W_{ADP} = 0.008197$

$$\text{Modified ESHF} = \frac{1}{1 + 245\Delta W/\Delta t} = \frac{1}{1 + 2451(0.010233 - 0.008197)/(25.5 - 11)} = 0.74396$$

$$\text{Also, Modified ESHF} = \frac{\text{ERSH} + \text{Reheat}}{\text{ERSH} + \text{ERLH} + \text{Reheat}}$$

$$0.74396 = \frac{71.6565 + \text{Reheat}}{71.6565 + 42.4836 + \text{Reheat}}$$

Reheat = 51.787 kW

$$(\text{cmm})_d = \frac{\text{ERSH} + \text{Reheat}}{0.0204(t_i - t_{ADP})(1 - X)} = \frac{71.6565 + 51.787}{0.0204(25.5 - 11)(1 - 0.05)} = 439.285 \text{ cmm}$$

$Q_{vr} = 439.285 - 112 = 327.285$ cmm

For an approximate calculation, we use volume flow rates for adiabatic mixing of outdoor air and fresh air to find the state 1 at inlet to cooling coil.

$$t_1 = [327.285(25.5) + 112(40)]/439.285 = 29.197^oC$$

Temperature of the air leaving the cooling coil is

$$t_2 = t_{ADP} + 0.05(t_1 - t_{ADP}) = 11 + 0.05(29.197 - 11) = 11.91^oC$$

The supply air state at inlet to room is found by using RSH and the calculated volume flow rate as follows:

$$\text{RSH} = 0.0204(439.285)(25.5 - t_3) = 70 \text{ kW}$$

$$t_3 = 25.5 - 70/(0.0204 \times 439.285) = 17.69^{\circ}\text{C}$$

Similarly, $W_3 = 0.010233 - 40/(50 \times 439.285) = 0.008412$ kgw/kga

The method of reheat is also used for the control of humidity in air conditioning systems.

18.7.6 Humidity Control

The desired humidity may be maintained in the room if the supply air enters the room at a predetermined volume flow rate and proper humidity ratio falling on the RSHF line. The problem usually arises when the latent heat load is high. In such a case the humidity tends to increase. There are three methods to handle high latent heat loads so as to maintain the proper humidity ratio.

(i) Reducing the Apparatus dew point
(ii) Using Reheat
(iii) Using face and bypass dampers

In Figure 18.16 the GSHF line 1–s_1 does not intersect the RSHF line, hence the room loads cannot be satisfied by this choice of ADP. By reducing the ADP to s_2, the GSHF line 1–s_2 intersects the RSHF line at point 2 and the room loads can be satisfied.

If the latent heat load is very severe the RSHF line may never intersect the saturation curve or the GSHF line. The RSHF line may be so steep that it does not intersect the GSHF line regardless of the extent to which ADP is decreased. The problem is avoided as discussed earlier by using reheat along process 2–3. State 2 is the outlet state of cooling coil for some commonly used ADP and state 3 is at inlet to the room. The solution procedure for this case has already been discussed.

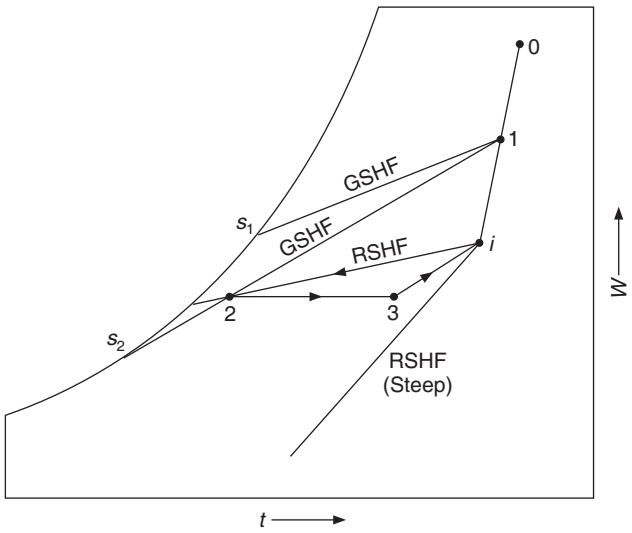

Figure 18.16 Psychrometric processes for humidity control.

The third method uses face-and-bypass dampers to control humidity. Air with volume flow rate Q_{v1} can be supplied at temperature t_2 at point 2 on GSHF line, say 1–2–s_1. To remove more moisture, only a small portion of volume flow rate is passed through the coil and the remaining portion is bypassed at the inlet state 1. At smaller flow rates through the cooling coil, its ADP reduces to say s_2, and the air is cooled to a lower temperature t_3. This is then adiabatically mixed with bypassed air at state 1. The mixed air at state 4 has the same temperature t_2 but lower humidity ratio W_4 compared W_2.

18.7.7 All Outdoor Air Application

In a hospital operation theatre, intensive care units, artificial incubators for infants and some chemical processes, there is no recirculation of room air since it may be contaminated. In these places, 100% outdoor air is cooled and supplied to the room. This is done to avoid the spread of microorganisms. This however increases the load on the plant. The GSHF line starts from the outdoor air state 0 and room loads have to be satisfied at supply air flow rate along the RSHF line 2–*i*. The following three situations occur in practice.

1. The bypass factor is so selected that the dehumidified air quantity is equal to fresh air.
2. If the dehumidified air quantity is less than the fresh air requirement, then two possibilities exist to increase the dehumidified air quantity
   (i) If the difference is small, then select a coil with larger bypass factor so that the air enters the room at a higher temperature requiring more dehumidified air quantity.
   (ii) If the difference is large, then the same coil is used but the air is reheated so that it enters the room at a higher temperature requiring more dehumidified air quantity.
3. The dehumidified air quantity is more than the fresh air flow rate. In this case the fresh air flow rate is increased.

EXAMPLE 18.12 The outdoor dry-bulb and wet-bulb temperatures are 38°C and 28°C respectively. The indoor design conditions of an operation theatre and anaesthesia room in Kolkata are 24°C and 50% relative humidity. The RSH and RLH are 15 kW and 3 kW respectively. The fresh air requirement is 50 cmm. Find the supply air state and the dehumidified air quantity. Take a bypass factor of 0.05.

Solution:

At 24°C : $W_s^* = 0.018963$, therefore $\mu = 0.622\phi/[0.622 + (1 - \phi)W_s^*] = 0.4924926$

$W_i = \mu\, W_s^* = 0.4924926\ (0.018963) = 0.009339$

At 28°C : $W_s^* = 0.024226$, $h_{fg}^* = 2434.55$, $h_f^* = 117.36$

At 38°C : $h_g = 2569.91$

$$W_0 = \frac{W_s^* h_{fg}^* - 1.005(t - t^*)}{h_g(t) - h_f^*} = 0.0199504$$

The fresh air requirement for 200 persons, $Q_{v0} = 200(0.56) = 112$ cmm

$$\text{OASH} = 0.0204(50)(38 - 24) = 14.28 \text{ kW}$$

$$\text{OALH} = 50(50)(0.01995 - 0.009339) = 26.528 \text{ kW}$$

$$\text{ERSH} = 15 + 0.05(14.28) = 15.714 \text{ kW}$$

$$\text{ERLH} = 3 + 0.05(26.528) = 4.3264 \text{ kW}$$

$$\text{ESHF} = 15.714 /(15.714 + 4.3264) = 0.7841$$

We will find $\Delta W/\Delta t$ corresponding to ESHF, guess the ADP and check if the assumed ADP gives the required $\Delta W/\Delta t$.

$$\frac{\Delta W}{\Delta t} = \frac{1}{2451}\left(\frac{1}{\text{ESHF}} - 1\right) = 0.00011233$$

We guess the value of ADP and find the slope of line *i*–ADP and see if it agrees with the above value.

At $t_{ADP} = 9^oC$: $W_s = 0.007157$ and $\Delta W/\Delta t = 0.000145476$

At $t_{ADP} = 10^oC$: $W_s = 0.007661$ and $\Delta W/\Delta t = 0.000119867$

At $t_{ADP} = 10.1^oC$: $W_s = 0.0077146$ and $\Delta W/\Delta t = 0.000116873$

At $t_{ADP} = 10.2^oC$: $W_s = 0.00776682$ and $\Delta W/\Delta t = 0.000113836$

At $t_{ADP} = 10.3^oC$: $W_s = 0.0078218$ and $\Delta W/\Delta t = 0.000110755$

Hence we assume that ADP is 10.2^oC. The dehumidified air quantity is given by

$$(\text{cmm})_d = \frac{15.714}{0.0204(24 - 10.2)(1 - 0.05)} = 58.756 \text{ cmm}$$

This is more than the fresh air requirement. Therefore, we recalculate using this as the volume flow rate.

$$\text{OASH} = 0.0204(58.756)(38 - 24) = 16.7807 \text{ kW}$$

$$\text{OALH} = 50(58.756)(0.01995 - 0.009339) = 31.173 \text{ kW}$$

$$\text{ERSH} = 15 + 0.05(16.7807) = 15.839 \text{ kW}$$

$$\text{ERLH} = 3 + 0.05(31.173) = 4.5586 \text{ kW}$$

$$\text{ESHF} = 15.839/(15.839 + 4.5586) = 0.7765$$

Corresponding to this ESHF, $\Delta W/\Delta t = 0.00011745$ and from the above iteration, the ADP may be taken as, 10.1^oC. The dehumidified air quantity is given by

$$(\text{cmm})_d = \frac{15.839}{0.0204(24 - 10.1)(1 - 0.05)} = 58.7975 \text{ cmm}$$

This is almost same as the new fresh air requirement. The supply air temperature is given by

$$t_{2'} = t_{ADP} + 0.05(24 - 10.1) = 10.795^oC$$

EXAMPLE 18.13 The outdoor dry-bulb temperature is 32^oC and the relative humidity is 50%. The indoor design conditions are 24^oC and 50% relative humidity. The RSH and RLH are 15 kW

and 3 kW respectively. The cooling coil cools only the outdoor air, which is then mixed with the recirculated air as shown in Figure 18.17(a). The bypass factor is 0.1. The supply air volume flow rate is 180 cmm. Find the supply air state, its mass flow rate, state at the exit of the cooling coil and the total cooling load.

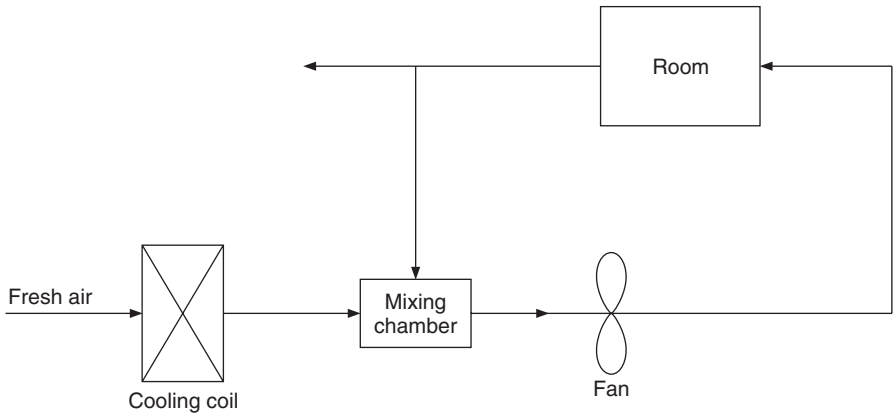

Figure 18.17(a) Conditioning plant for Example 18.13.

Solution:

At 32°C and 50% relative humidity: $W_s = 0.030793$

$$\therefore \quad \mu = 0.622\phi / [0.622 + (1 - \phi)W_s^*] = 0.48792$$

$$W_0 = \mu\, W_s^* = 0.48177(0.030793) = 0.0150246$$

$$h_0 = 1.005(32) + 0.0150246(2500 + 1.88 \times 32) = 70.6254 \text{ kJ/kga}$$

From Example 18.12: $W_i = 0.009339$ and $h_i = 47.8892$ kJ/kga

$$\text{RSH} = 15 = 0.0204\,(180)(24 - t_s) \quad \therefore \quad t_s = 19.915\ ^{o}\text{C}$$

$$\text{RLH} = 3 = 50(180)(0.009339 - W_s) \quad \therefore \quad W_s = 0.009 \text{ kgw/kga}$$

$$v_{as} = \frac{0.2871(292.915)(1 + 6078 \times 0.009)}{101.325} = 0.84197 \text{ m}^3\text{/kga}$$

$$\dot{m}_{as} = 180 / (60 \times 0.84197) = 3.563 \text{ kga/s}$$

$$h_s = 42.8515 \text{ kJ/kga}$$

The process is shown on the psychrometric chart in Figure 18.17(b). The outdoor air is cooled along the line 0–2–ADP. State 2 is at the outlet of the cooling coil. This also lies on the RSHF line *i*–*s* extended, the state *s* being the supply air state. This state has been evaluated above. The ADP is not known. Point 2 divides the line 0-ADP in proportion of X and $1 - X$. A simple construction is done to find the ADP. Line 0–*i* is extended to point *A* such that the line ADP–*A* is parallel to RSHF line *i*–*s*–2. By similarity of triangles, the point *i* also divides 0–*A* in proportion of X and $1 - X$. Hence,

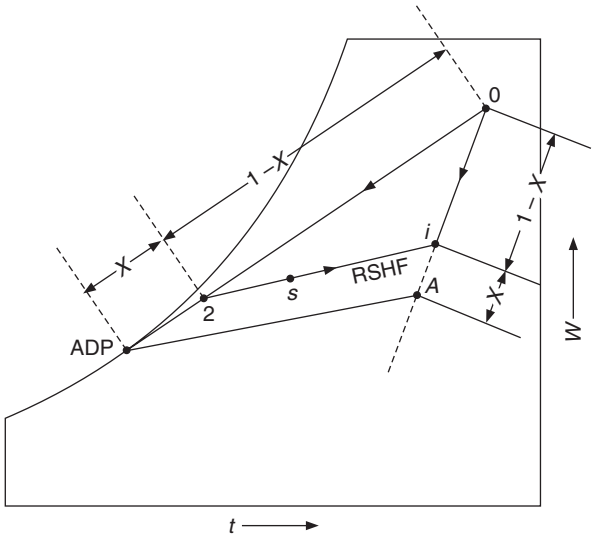

Figure 18.17(b) Process on psychrometric chart for the system of Figure 18.17(a).

$$\frac{W_i - W_A}{W_0 - W_A} = \frac{t_i - t_A}{t_0 - t_A} = X = 0.1 \quad \therefore \quad (t_i - t_A) = 0.1(t_0 - t_A) \quad \therefore \quad t_A = 23.111°\text{C}$$

$$(W_i - W_A) = 0.1(W_0 - W_A) \qquad \therefore \qquad W_A = 0.00870742$$

Line *A*–ADP has the slope of RSHF.

$$\text{RSHF} = \text{RSH}/(\text{RSH} + \text{RLH}) = 15/18 = 0.83333$$

$$\frac{\Delta W}{\Delta t} = \frac{1}{2451}\left(\frac{1}{\text{RSHF}} - 1\right) = 0.0000816$$

We guess the value of ADP and find the slope of line *A*–ADP and see if it agrees with the above value.

At $t_{\text{ADP}} = 11°\text{C}$: $W_s = 0.008197$ and $\Delta W/\Delta t = 0.000042145$

At $t_{\text{ADP}} = 10°\text{C}$: $W_s = 0.007661$ and $\Delta W/\Delta t = 0.000079812$

At $t_{\text{ADP}} = 9.9°\text{C}$: $W_s = 0.0076106$ and $\Delta W/\Delta t = 0.000083203$

At $t_{\text{ADP}} = 9.95°\text{C}$: $W_s = 0.0076358$ and $\Delta W/\Delta t = 0.000081423$

Hence we assume that ADP is 9.95 °C. The state 2 is given by

$$t_2 = t_{\text{ADP}} + 0.1(t_0 - t_{\text{ADP}}) = 12.155°\text{C}$$

$$W_2 = W_{\text{ADP}} + 0.1(W_0 - W_{\text{ADP}}) = 0.00837468$$

$$h_2 = 33.3319 \text{ kJ/kg}$$

The mass flow rate $\dot{m}_{a2}$ is found by considering adiabatic mixing of cooled air at state 2 and the recirculated air at state *i*.

$$\dot{m}_{a2} h_2 + (\dot{m}_{as} - \dot{m}_{a2}) h_i = \dot{m}_{as} h_s$$

$$\dot{m}_{a2} = \dot{m}_{as} (h_i - h_s)/(h_i - h_2) = 1.233 \text{ kga/s}$$

$$\text{Cooling load} = \dot{m}_{a2} (h_2 - h_0) = 1.233(70.6254 - 33.3319) = 45.98 \text{ kW}$$

18.7.8 Winter Air Conditioning

In winter the outdoor relative humidity is very high while the humidity ratio is low since at lower temperatures air can hold less moisture. Infiltration of outdoor air into the space causes a decrease in indoor humidity ratio, hence water vapour has to be added to the conditioned supply air. The occupancy load adds moisture to the room air, the net result being that room latent heat load may be negligibly small. The heating load is therefore predominantly the sensible load. The outdoor humidity ratio being small, the fresh air requirement reduces the humidity ratio. Hence humidification of supply air is, in general, a requirement apart from heating.

There is heat transfer from the building to the surroundings because of lower outdoor air temperature. Solar energy will add heat through walls and the glass. Internal loads like occupancy, lights and appliances, etc. are always there and may compensate for the heat loss. The summer peak loads occur between 4 to 6 PM since the outdoor air temperature is maximum around 3 PM and there is time lag in heat transfer through the thickness of walls and roof. On the other hand, winter peak loads occur early in the morning when solar heat gains through walls and glass may not occur. Aa a result, winter heating loads are always less than the summer cooling loads.

Winter air conditioning for comfort involves heating and humidification. There are two recommended procedures for winter air conditioning. These are explained with the help of psychrometric chart in Figure 18.18. In this figure, point 0 represents the outdoor air state while point *i* denotes the room design condition, which is in general at lower temperature than summer design condition. The supply air state *s* is at a higher temperature and humidity ratio than the room design condition since the conditioned air is cooled and dehumidified as it enters the room from state *s* to *i* along the RSHF line. Mixing of recirculated air at state *i* and outdoor air at state 0 results in state 1 at which it enters the air conditioning apparatus. The supply air state *s* is obtained by sensible heating from near dew point 3 corresponding to point *s*. Two types of processes and equipment can be used to achieve the state near 3.

(i) Preheating the mixed air from state1 to a point 2 which lies on the wet-bulb temperature line corresponding to dew point 3 of supply air state. Process 2–3 is adiabatic saturation by spray of water, which is recirculated by heating/cooling. Sensible heating along 3–*s* usually by an electric heater follows this process.

(ii) State 3 is obtained from state 1 in an air washer with spray and recirculation of heated water. The air is heated and humidified in this process. This is followed by sensible heating along 3–*s*.

In both these processes, saturation state cannot be achieved at point 3 due to air washer efficiency and efficiency of the adiabatic saturation process. The actual end point will be below point 3 depending upon the efficiency of air washer. Supply air and ventilation air rates are usually the same as those for summer air conditioning.

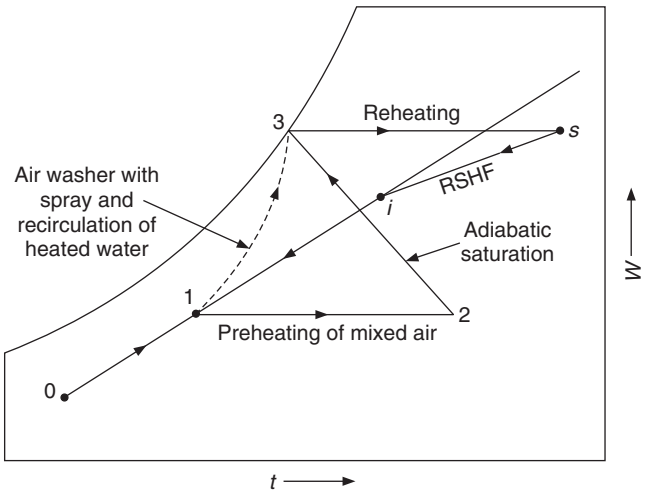

Figure 18.18 Winter air conditioning processes.

The concept of *degree days* is used for winter heating. It has been observed that fuel consumption is directly proportional to temperature difference between a reasonable comfortable indoor temperature of 18.5°C and outdoor air temperature. If the outdoor air temperature is 18.5°C, then the fuel consumption is zero.

If the mean outdoor air temperature is one degree less than 18.5°C for a 24 hours period, then it is called one *degree day*. If in a place the average outdoor temperature for 30 days is 12°C, then the *degree days* are

$$(18.5 - 12)\ 30 = 195\ \textit{degree days}$$

Another concept, which is required is the heat loss Q_L in kW per degree temperature difference inside and outside. This is essentially the product of heat transfer coefficient and total wall and roof area. This is useful along with the concept of *degree day* since $Q_L \times$ (degree days) will have the unit of kW, the total heat loss. The steam consumption S for heating of a building is found by the equation,

$$S = \frac{Q_L\ (\text{degree days})\ (24)\ (3600)}{1055}$$

where, it is assumed that 1 kg of steam gives approximately 1055 kJ of energy.

EXAMPLE 18.14 In a winter air conditioning system, an air washer of 90% efficiency is used with heated water followed by sensible heating by an electric heater. The indoor design conditions are 22°C and 50% relative humidity. The outdoor design conditions are 0°C and 70% relative humidity. Room heat loss is 200 kW and vapour loss may be neglected. The supply air and ventilation air rates are 800 cmm and 500 cmm respectively. The spray water flow rate is 150 kg/min and make-up water is available at 20°C. Find the heat transfer in various processes.

Solution:

$$\text{RSH} = 0.0204\ Q_v(t_s - t_i) \quad \therefore \quad t_s = 22 + 200/(0.0204 \times 800) = 34.255^{\circ}\text{C}$$

At 22°C and 50% relative humidity: $W_s = 0.016741$

$$\therefore \quad m = 0.622\phi/[0.622 + (1 - \phi)W_s^*] = 0.49336$$

$$W_i = \mu W_s^* = 0.49336\ (0.016741) = 0.00825935$$

At 0°C and 70% relative humidity: $W_s = 0.0037895$

$$\therefore \quad \mu = 0.622\phi/[0.622 + (1 - \phi)W_s^*] = 0.6987$$

$$W_0 = \mu W_s^* = 0.6987\ (0.0037895) = 0.0026478$$

State 1 is obtained by adiabatic mixing of fresh air at state 0 and return air at state *i*. We use the volume flow rate as approximation instead of mass flow rates.

$$t_1 = [(800 - 500) \times 22 + 500 \times 0]/800 = 8.25°C$$

$$W_1 = [(800 - 500) \times 0.00825935 + 500 \times 0.0026478]/800 = 0.004752$$

$$h_1 = 1.005 \times 8.25 + 0.004752(2500 + 1.88 \times 8.5) = 20.245\ \text{kJ/kga}$$

The process is shown in Figure 18.19. The process in air washer follows the path 1–3. If it had 100% efficiency, the outlet state will be the saturated state 3*s*. Process 3–*i* is sensible heating process, hence

$$W_3 = W_i = 0.008259$$

The efficiency of washer is 90%, hence

$$\eta = 0.9 = \frac{W_3 - W_1}{W_{3s} - W_1} = \frac{0.008259 - 0.004752}{W_{3s} - 0.004752} \quad \therefore \quad W_{3s} = 0.008649$$

The temperature t_{3s} is found either from psychrometric chart or by interpolation in moist air table.

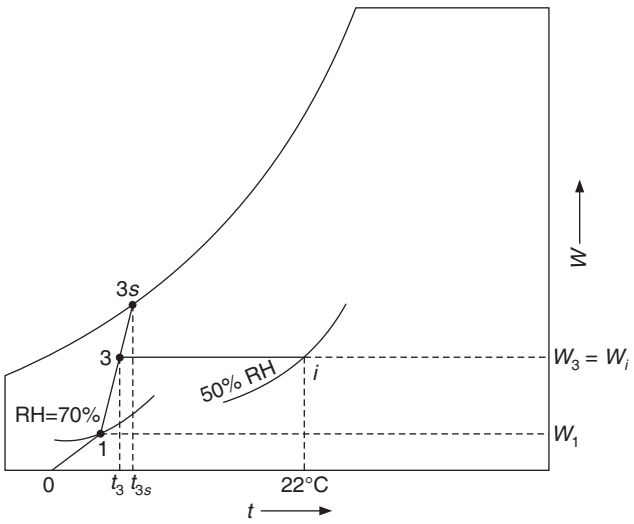

Figure 18.19 Psychrometric processes of Example 18.14.

At 11°C : $W_s = 0.008197$ and at 12°C: $W_s = 0.008766$, interpolating for $W_{3s} = 0.008649$,
$t_{3s} = 11.7944$ °C

Again using the air washer efficiency, we find the temperature at point 3 as follows:

$$\eta = 0.9 = \frac{t_3 - 8.25}{11.7944 - 8.25} \quad \therefore \quad t_3 = 11.44°\text{C}$$

From psychrometric chart, we find that the wet-bulb temperature at point 3 is

$$t_3^* = 11.4°\text{C}$$

$$h_3 = 1.005 \times 11.44 + 0.008259(2500 + 1.88 \times 11.44) = 32.322 \text{ kJ/kga}$$

The temperature of the water leaving the air washer may be assumed to be the same as the wet-bulb temperature of the leaving air, that is

$$t_{w2} = 11.4°\text{C}$$

The specific volume of the air leaving the washer is given by,

$$v_{a3} = \frac{0.2871(284.44)(1 + 1.6078 \times 0.008259)}{101.325} = 0.8166$$

The mass flow rate of dry air through the washer is $\dot{m}_a = 800/0.8166 = 979.67$ kga/min

Energy balance across the air washer gives

$$\dot{m}_a(h_3 - h_1) = \dot{m}_w c_{pw}(t_{w1} - t_{w2})$$

$$t_{w1} = t_{w2} + (979.67/150)(32.322 - 20.245)/4.1868 = 30.239 \text{ °C}$$

Evaporation rate = make up water flow rate = $\dot{m}_a(W_3 - W_1)$

$$\Delta \dot{m}_w = 979.67(0.008259 - 0.004752) = 3.4357 \text{ kg/min}$$

Heat added to make-up water = $3.4357 \times 4.1868(30.239 - 20)/60 = 2.455$ kW

Heat added to increase the temperature of spray water from 11.4°C to 30.239°C

$$Q_{13} = 150 \times 4.1868(30.239 - 11.4)/60 = 197.188 \text{ kW}$$

Total heat added to water = 197.188 + 2.455 = 199.643 kW

Sensible heat added to air during process 3–*i*.

$$Q_{3i} = 0.0204(800)(34.255 - 11.44) = 372.34 \text{ kW}$$

Net heat added to water and air = 372.34 + 199.643 = 571.984 kW

EXAMPLE 18.15 In Example 18.14 of winter air conditioning if preheating followed by adiabatic saturation and reheating is used, find the heat transfer in various processes assuming a saturation efficiency of 90%.

Solution:

The states 1 and 3*s* will remain the same as in Example 18.15 since the humidity ratio at point 2 is same as that at point 1. Also, the humidity ratio at point 3 is same as that point *i*. Therefore when we use adiabatic saturation efficiency of 0.9, we will get the same state 3*s* as in Example 18.14

$$t_{3s} = 11.7944^{o}\text{C}$$

The adiabatic saturation occurs at wet-bulb temperature of 11.7944°C. From the psychrometric chart it is seen that this wbt line intersects $W = 0.004752$ at $t = 21.5^{o}$C. This is state 2 in Figure 18.18.

Adiabatic saturation does not require heating or cooling of water. The temperature at the end of adiabatic saturation t_3 is found from adiabatic saturation efficiency as follows:

$$\eta = 0.9 = \frac{21.5 - t_3}{21.5 - 11.7944} \quad \therefore \quad t_3 = 12.765°\text{C}$$

Preheating of air from 8.25°C to 21.5°C requires

$$Q_{12} = 0.0204(800)(21.5 - 8.25) = 216.24 \text{ kW}$$

Sensible heating from state 3 to state *i* requires

$$Q_{3i} = 0.0204(800)(34.255 - 12.765) = 350.717 \text{ kW}$$

$$\text{Total heating} = 216.24 + 350.717 = 566.957 \text{ kW}$$

This amount is comparable to total heating in the Example 18.41 of 571.984 kW

REFERENCES

Amadur, E.J. and White, R.W. (1965): Two pressure Relative Humidity Standards in *Humidity and Moisture,* Volume 3: *Fundamentals and Standards*, edited by Arnold Wexler and William A. Wildback, New York Reinhold Publishing Corporation.

Eckert, E.R.G. and Drake, Jr., R.M. (1959): *Heat and Mass Transfer*, McGraw-Hill Book Company, New York.

Kusuda, T. (1965): Calculation of the Temperature of a Flat Plate Wet Surface under Adiabatic Conditions with Respect to Lewis Relation in *Humidity and Moisture*, Vol. 1: *Principles and Methods of Measuring Humidity in Gases*, edited by Robert E. Ruskin, Reinhold Publishing Corporation.

McAdams, W.H. (1954): *Heat Transmission*, McGraw-Hill Book Company, New York.

REVIEW QUESTIONS

1. In Example 18.1, find the humidity ratio for the four cases if the air velocity is 1 m/s and the values obtained from a sling psychrometer are $t_{db} = 30°\text{C}$ and $t_{wb} = 20°\text{C}$.
2. For the velocities and wet-bulb diameters of Example 18.3, find $h_{R,t}/h_c$ and $(t_{wb} - t^*)/(t - t_{wb})$ if the dry-bulb and the wet-bulb temperatures are 30°C and 20°C respectively.

3. The RSH and RLH of a room are 300 kW and 100 kW respectively. The room is maintained at 25°C dry-bulb temperature and 50% relative humidity. If the air supplied to the room is at 18°C, find the minimum amount of air supplied to the room in m^3/s and the volume flow rate at the supply temperature. If the bypass factor of the cooling coil is 0.20, find the supply air state and the volume flow rate.
4. The room air condition of an air-conditioned space is 25°C, 50% relative humidity. The outdoor air is at 40°C and 50% relative humidity. The RSH and RLH of air-conditioned space are 30 kW and 6 kW, respectively. The ventilation requirement is such that the outdoor air quantity is 100 cmm. The bypass factor of the cooling coil is zero. Determine the supply air state, mass flow rate of supply air, state at inlet to cooling coil, OASH, OALH, RTH, OATH, and the total cooling load.
5. If the bypass factor of the cooling coil in Question 4 is 0.15, RSH = 20 kW, RLH = 5 kW, the return air is mixed with outside air before entering the cooling coil in the ratio 4:1 by mass, the room air condition and the outdoor air condition being the same, then determine the ESHF, apparatus dew point, the supply air state on ESHF, and the actual supply air state, the state at inlet to cooling coil, OASH, OALH, OATH, and the total cooling load.
6. The RSH and RLH of an air-conditioned space are 60 kW and 40 kW respectively. The indoor design conditions are at 24°C and 50% relative humidity. The outdoor design conditions are 34°C and 40% relative humidity. The outdoor air is mixed with re-circulated air in the ratio of 1:3 (by mass). A reheat coil is used along with a cooling and dehumidifying coil. Air is supplied to the conditioned space at 14°C. The bypass factor of the cooling coil is 0.15 and the barometric pressure is 101.325 kPa. Find the mass flow rate of supply air, the required cooling capacity of the cooling coil and heating capacity of the reheat coil.
7. The outside air at 5°C and 60% relative humidity is first passed over heating coils and heated until its wet-bulb temperature becomes equal to the room wet-bulb temperature. The air is then passed through an adiabatic saturator and is finally heated to 45°C before being supplied to the room. Find the heat added to both the heating coils, if 500 kg of air is supplied per minute to a hall maintained at 21°C and 40% relative humidity.

19

Comfort—Physiological Principles, IAQ and Design Conditions

LEARNING OBJECTIVES

After studying this chapter the student should be able to:

1. Explain the need for creating a thermally comfortable environment.
2. Define thermal comfort, metabolic rate, basal metabolic rate, and understand the values of metabolic heat generated by various activates performed continuously by an average person.
3. Understand the energy balance equations and models of human body.
4. Estimate the various heat transfer rates from a human body.
5. Calculate the respiratory losses from a human body.
6. Describe the effect of thermal resistance of clothing and moisture resistance on the design of air conditioning systems.
7. Define the effective clothing efficiency and intrinsic clothing efficiency.
8. Define the moisture permeability index.
9. Estimate the heat transfer from a nude person and from a clothed person.
10. Discuss the thermoregulatory mechanisms used by human body to fight against heat and cold.
11. Explain the various physiological hazards resulting from heat exposure.
12. Calculate the various heat transfer coefficients—radiative, convective, and evaporative—so as to estimate the heat transfer from the body.
13. Discuss the importance of psychometric parameters and environmental indices that describe the thermal environment.
14. Define effective temperature and standard effective temperature.

15. Draw the ASHRAE comfort chart and mark the comfort zones for summer and winter conditions.
16. Define Predicted Mean Vote (PMV) and Predicted Percentage of Dissatisfied (PPO).
17. Discuss the factors affecting thermal comfort and explain how to maintain good indoor air quality.
18. Identify suitable indoor design conditions for thermal comfort.
19. Explain the criteria followed for selecting suitable outside design conditions.

19.1 INTRODUCTION

Man has always attempted to create a thermally comfortable environment. This is reflected in traditions of building design all around the world by natural means in ancient history, and by air conditioning in the present day. ISO standard 7730 defines *thermal comfort as that condition of mind, which expresses satisfaction with thermal environment.* This is a universally accepted definition, but also a definition which is most difficult to relate to physical parameters. Thermal environments are considered together with other factors such as air quality, light and sound level when we have to evaluate the working environment in air conditioning.

Man can be considered to be a homo-exothermic machine that continuously generates heat and maintains constant internal organ temperature over a wide range of external conditions. The heat generation varies from 100 W for a sedentary person to 1000 W for a person doing strenuous work.

Human body can also be thought of as a heat engine with main body function being to convert the chemical energy of food into work for the proper functioning of organs like heart, lungs, kidneys and for the day-to-day activities. Due to second law limitation, all the chemical energy of food cannot be converted into work, a major chunk of it has to be rejected to the surroundings.

19.2 MECHANICAL EFFICIENCY OF HUMANS

The efficiency of human body is defined as the ratio of mechanical work W done by the muscles to the metabolic heat M generated for it, that is, $\eta = W/M$. It is unusual for η to be more than 5 to 10%; for most activities, it is close to zero. The maximum value in activities like sports is 20 to 24%. It is quite significant in activities like walking on a grade, climbing a ladder, bicycling, lifting, etc. It can be estimated in some cases. For example, a person of 80 kg weight walking up a 10% grade at 1m/s velocity would be lifting a weight of 784 N (80 kg × 9.8 N/kg) over a height of 0.1 m every second, for a work rate of 78.4 N-m/s = 78.4 W. Or if the same person rises in half a second from sitting position, his centre of gravity is raised by say 0.3 m. The work rate is 784 × 0.3 / 0.5 = 470.4 W. In most of the cases, inside the air-conditioned spaces for persons doing sedentary work, the work rate is negligible.

19.3 METABOLIC HEAT

The rate of production of chemical energy from food is called *metabolic rate M*. The metabolic rate depends upon the activity, the person and the environmental conditions. It is measured in

met unit. One met is the energy produced by an average sedentary person (seated, quiet) per unit of body surface area called Dubois area, i.e.

$$1 \text{ met} = 58.2 \text{ W/m}^2 \tag{19.1}$$

The Dubois area is the surface area in m^2 of a person of m kg weight and h m height, and is given as proposed by Dubois in 1916 as follows.

$$A_D = 0.202(m)^{0.425} (h)^{0.725} \text{ m}^2 \tag{19.2}$$

For an average person 1.73 m tall and 70 kg weight (average by US standard) the Dubois area is around 1.8 m^2. Such a person seated at rest would dissipate a total of $1.8 \times 58.2 = 104.76 \approx 100$ W. The minimum energy is required in the state of sleep, essentially for the functioning of internal organs, like heart, lungs, kidneys and intestines, etc. This is called the basal metabolic rate, and it is around 0.7 met.

An average young person 20 years of age has energy capacity of 12 met units. This capacity decreases with age, reducing to 7 met units at the age of 70 years. Women, in general, have a maximum capacity 30% lower than men. Marathon runners and trained athletes exert about 20 met units. Activities requiring more than 5 met units are tiring and exhausting for untrained persons below or above 35 years of age. The metabolic heat values generated by various activities performed continuously by an average person (Dubois area 1.8 m^2) are given in Table 19.1. Such a metabolic activity referred to as $M_{act.}$

Table 19.1 Typical metabolic heat generation values for various activities

Activity	W/m^2	met
Resting		
Sleeping	40	0.7
Seated , quiet	60	1.0
Standing, relaxed	70	1.2
Walking (on the level)		
0.89 m/s	115	2.0
1.34 m/s	150	2.6
1.79 m/s	220	3.8
Office Activities		
Reading, seated	55	1.0
Writing	60	1.0
Typing	65	1.1
Filing, seated	70	1.2
Filing, standing	80	1.4
Walking	100	1.7
Lifting/Packing	120	2.1
Driving/Flying		
Car	60–115	1.0–2.0
Aircraft, routine	70	1.2
Aircraft, instrument landing	105	1.8
Aircraft, fighter	140	2.4
Heavy vehicle	185	3.2

(*Contd.*)

Table 19.1 Typical metabolic heat generation values for various activities (contd.)

Activity	W/m^2	met
Miscellaneous Occupational Activities		
Cooking	95–115	1.6–2.0
House cleaning	115–200	2.0–3.4
Seated, heavy limb movement	130	2.2
Machine Work		
Sawing (table saw)	105	1.8
Light (electrical industry)	115–140	2.0–2.4
Heavy	235	4.0
Handling 50 kg bags	235	4.0
Pick and shovel work	235–280	4.0–4.8
Miscellaneous		
Leisure activities		
Dancing, social	140–235	2.4–4.4
Calisthenics/exercise	175–235	3.0–4.0
Tennis, singles	210–270	3.6–4.0
Basketball	290–440	5.0–7.6
Wrestling, competitive	410–505	7.0–8.7

The measurement of metabolic rates is difficult. The level of accuracy depends upon how well is the activity defined. For well-defined activities with $M < 1.5$ met, Table 19.1 is quite accurate. For tasks with $M > 5$, if the task is not well defined or the task can be done in several ways, there can be large errors. The rate of metabolic heat produced is most accurately measured by the rate of respiratory oxygen consumption and carbon dioxide production. An empirical expression for metabolic rate is as follows:

$$M = 352.2[((0.23\ RQ)\ 0.77)\ V_{O_2}/A_D]\ \text{W/m}^2 \tag{19.3}$$

where

RQ = respiratory quotient, molar ratio of V_{CO2} exhaled to V_{O_2} inhaled.

V_{O_2} = volumetric rate of oxygen consumption in litre/min at standard temperature and pressure (STPD) of 0°C and 101.325 kPa

The respiratory quotient, RQ, depends upon activity, diet and physical condition of the person. For an average adult, it is 0.83 for light sedentary work ($M < 1.5$) and 1.0 for heavy exertion. If RQ can be estimated, M can be determined. A 10% error results in only 3% error in the metabolic rate.

Another slightly less accurate method of estimating the metabolic rate is by measuring the heart rate. The oxygen consumption can be correlated with heart rate. From the measured value of heart rate, oxygen consumption can be estimated, then M is determined from Eq. (19.3). The physical condition of a person, heat, emotional factors, muscles used, etc. also affect the heart rate, hence this is at the most an approximate method. Table 19.2 gives the heart rate and oxygen consumption for some activities.

Table 19.2 Heart rate and oxygen consumption at different activity levels

Level of exertion	*Oxygen consumption,* Lpm	*Heart rate,* beat/min
Light work	< 0.5	< 90
Moderate work	0.5–1.0	90–110
Heavy work	1.0–1.5	110–130
Very Heavy Work	1.5–2.0	130–150
Extremely Heavy Work	> 2.0	150–170

In extremely cold weather, to ward of the cold the body generates additional metabolic heat through shivering and muscle tension. This can raise M as much as three times its normal sedentary value. Hence total metabolic heat generated is equal to the sum of M_{act} and $M_{shiv.}$

A part of the metabolic energy is spent as work W (W/m^2) by the muscles. The difference between M and W, that is, $M - W = M(1 - \eta)$ has to be rejected by the body to the surroundings. This is a function of activity and basal metabolic rate and varies with sex, age and race. The blood circulation transports this energy to the lungs and to the capillary bed near the skin from where it is transferred to the surroundings. The feeling of comfort occurs, if the body does not have to take any extra action to reject it. Thermal comfort is therefore also defined as *that condition of mind in which satisfaction is expressed with the thermal environment*. It requires subjective evaluation from thermal point of view since this is "condition of mind".

19.4 ENERGY BALANCE AND MODELS

Human body rejects this heat ($M - W$) continuously in winter as well as in summer. Hence the thermal environment tends to influence the skin and the interior body temperature profoundly. The body certainly takes actions to regulate the body temperature within close limits. The heat exchange takes place from human body from

(i) Skin, Q_{sk}
(ii) Respiration, Q_{res}.

Q_{sk} consists of heat transfer by

- convection C
- Radiation R
- Evaporation E_{sk}

while Q_{res} consists of

- Convective heat loss C_{res} by respiration
- Evaporative heat loss E_{res} by respiration

all expressed in W/m^2 of body area.

Hence, in general,

$$M - W = \pm Q_{sk} \pm Q_{res} \pm Q_s \tag{19.4}$$

$$= (\pm C \pm R + E_{sk}) + (\pm C_{res} + E_{res}) \pm Q_s \tag{19.5}$$

where Q_s is the rate of energy stored in the body.

The body, under ordinary conditions is in unsteady state. During summer, if the temperature of the surroundings and the ambient air is more than the body temperature, then C, R and C_{res} all have negative sign, that is, heat is transferred to the body by convection and radiation. In such a case the sum of C, R, C_{res} and $M - W$ has to be rejected to the surroundings by evaporative cooling $E_{sk} + E_{res}$. The sum being large, there is a tendency for body temperature to rise, that is, some energy is stored in the body and Q_s is positive. On the other hand, during winter season, heat rejection from the body may be more than the heat production rate, as a result there is a tendency for the body temperature to fall, that is, Q_s is negative. The storage term is zero in steady state. It is negligibly small when body activity and surroundings are relatively stable (no rapid changes). It may be large when conditions are unstable and abnormal exposure occurs.

Two models have been proposed for energy balance of human body. These are: Steady-State Energy Balance and Two-node Transient Energy Balance.

The steady-state model due to Fanger (1970,1982) assumes Q_s to be zero. The body is assumed to be in thermal neutrality, there is no shivering, and vaso-regulation is not considered.

The two compartment (or two-node) model by Gagge et al. (1971,1986) represents the body as two concentric cylinders. The inner cylinder represents the body core (skeleton, muscle and internal organs). The outer cylinder represents the skin surface. The temperature of each compartment is considered to be uniform, t_{cr} and t_{sk}. The metabolic heat production, external work and respiratory loses are associated with core. The core and the skin compartments exchange heat through direct contact and also, through the thermoregulatory–controlled peripheral blood flow. If a is the fraction of body mass in skin compartment, m is the total body mass, c_{pb} is the body specific heat (3.49 kJ/kg-K) and q is time, then the rate of change of temperature of the skin and core is expressed as

$$\alpha m\, c_{pb}\left(\frac{dt_{sk}}{d\theta}\right) = A_D(Q_{cr,sk} - C - R - E_{sk}) \tag{19.6}$$

and

$$(1 - \alpha)\, m\, c_{pb}\left(\frac{dt_{cr}}{d\theta}\right) = A_D\,(M - W - C_{res} - E_{res} - Q_{cr,sk}) \tag{19.7}$$

where, $Q_{cr,sk}$ is the rate of energy transport from core to skin, W/m^2, by conduction through body tissue and convection through blood flow. The average body temperature may be defined as

$$t_b = \alpha t_{sk} + (1 - \alpha) t_{cr}$$

Both the models involve energy exchange with environment, which is discussed below.

19.5 ENERGY EXCHANGE WITH ENVIRONMENT

19.5.1 Sensible Heat Transfer

The sensible heat exchange from the skin to the surroundings has to pass through the clothing. The heat transfer through clothing involves all the three modes—conduction, convection and radiation—hence, it is usually represented by a single thermal resistance R_{cl}. The paths of heat transfer from skin to clothing and from clothing to surroundings are treated to be in series. The

analysis is done on per unit body area called Dubois area. Actually, the areas for convection heat transfer and radiation heat transfer are different since, arm pits and the space between legs do not take part in radiation heat transfer. However, for simplicity these are considered to be the same. The clothing area A_{cl} is different from body area, A_D. The ratio of these two is denoted by $f_{cl} = A_{cl}/A_D$.

The heat transfer rates by convection and radiation respectively from the clothing are

$$C = f_{cl}\, h_c(t_{cl} - t) \tag{19.8}$$

$$R = f_{cl}\, h_R\, (t_{cl} - t_R) \tag{19.9}$$

where

A_{cl} = area of clothing

A_D = body surface area.

$$f_{cl} = A_{cl}/A_D$$

where

h_c = convective heat transfer coefficient,W/m^2-K

h_R = linear radiative heat transfer coefficient, W/m^2-K

t_{cl}, t_R and t are clothing, mean radiant and air temperatures respectively, ^{o}C.

Equations (19.8) and (19.9) are usually combined together to represent sensible and radiative heat transfer in terms of an operative temperature t_o and a combined heat transfer coefficient, i.e.

$$C + R = f_{cl}\, h(t_{cl} - t_o) \tag{19.10}$$

where

$$h = h_R + h_c \tag{19.11}$$

$$t_o = (h_R\, t_R + h_c t) / h \tag{19.12}$$

The *operative temperature* t_o is the average of the mean radiant temperature and air temperature weighted by their respective heat transfer coefficients.

Introducing the clothing resistance R_{cl}, heat transfer from skin to clothing is written as

$$C + R = \frac{t_{sk} - t_{cl}}{R_{cl}} \tag{19.13}$$

Combining Eqs. (19.10) and (19.13) to eliminate the clothing temperature we get

$$C + R = \frac{t_{sk} - t_o}{\left(R_{cl} + \dfrac{1}{f_{cl}\, h}\right)} \tag{19.14}$$

19.5.2 Evaporative Heat Transfer

The driving force for evaporation of water from body is the difference between the water vapour pressure at the skin and that in the ambient environment. The evaporative heat loss from skin depends upon this pressure difference and the wetted area of the body. By analogy with sensible heat transfer, the total resistance to evaporation is modelled as $R_{e,cl} + 1/f_{cl}\, h_e$ and the evaporation rate is expressed as

$$E_{sk} = \frac{w(p_{sk,s} - p_w)}{(R_{e,cl} + 1/f_{cl}\, h_e)} \tag{19.15a}$$

where

$p_{sk,s}$ = saturation pressure at skin temperature
p_w = partial pressure of water vapour in ambient air
$R_{e,cl}$ = evaporative heat transfer resistance of clothing, W/m^2 - kPa
h_e = convective evaporation heat transfer resistance of clothing
w = fraction of the skin surface that is wetted.

$$E_{max} = \frac{(p_{sk,s} - p_w)}{(R_{e,cl} + 1/f_{cl}\, h_e)} \tag{19.15b}$$

The maximum skin evaporative heat transfer rate E_{max} occurs when the whole body is wetted that is, when $w = 1$.

The evaporative heat loss from the skin is due to two factors:

1. Evaporation of sweat secreted due to thermoregulatory control mechanisms (E_{rsw})
2. Heat transfer due to the natural diffusion of water vapour through the skin (E_{dif})

$$E_{sw} = E_{rsw} + E_{dif} \tag{19.16}$$

The regulatory sweating heat transfer is given by

$$E_{rsw} = \dot{m}_{rsw}\, h_{fg} \tag{19.17}$$

where, $\dot{m}_{rsw}$ is the rate at which sweat is secreted, kg/s-m^2 and, h_{fg} = 2430 kJ/kg at 30^{o}C.

The portion of the body that must be wetted to evaporate the regulatory sweat, E_{rsw}, is

$$w_{res} = E_{rsw}/E_{max} \tag{19.18}$$

The skin wettedness due to diffusion alone is 0.06 for normal conditions. If regularity sweating is taking place from w_{res} fraction of body area, then diffusion can occur from 6% of the dry part of the body, that is, $0.06(1 - w_{res})$ part of the body. An estimate of diffusion evaporative heat transfer is

$$E_{dif} = 0.06(1 - w_{res})E_{max} \tag{19.19}$$

The wetted area may be expressed as

$$w = 0.06 + 0.94\, E_{rsw}/E_{max} \tag{19.20}$$

Skin wettedness is strongly correlated with warm discomfort, and it is also a measure of thermal stress. It is difficult for the wettedness to exceed 0.8 and the practical upper limit for sustained activity for a healthy acclimatized person is 0.5.

19.5.3 Respiratory Losses

The air is inhaled at ambient temperature, and exhaled nearly saturated at a temperature t_{ex}, that is, slightly cooler than the core temperature t_{cr}. The sensible (C_{res}) and latent heat transfer (E_{res}) due to respiration are:

$$C_{res} = \dot{m}_{res}\, c_{pa}\, (t_{ex} - t)/A_D \tag{19.21}$$

$$E_{res} = \dot{m}_{res}\, h_{fg}\, (W_{ex} - W)/A_D \tag{19.22}$$

where

$\dot{m}_{res}$ = pulmonary ventilation rate, kg/s
W_{ex} and t_{ex} = humidity ratio and temperature of exhaled air.
W_a and t = humidity ratio and temperature of ambient air.
c_{pa} = specific heat of moist air
h_{fg} = latent heat of water at $t_{ex.}$

Fanger (1970) has proposed the following correlation for m_{res} in terms of met unit

$$m_{res} = K_{res}\, M \tag{19.23}$$

where $K_{res} = 0.00516$ kg-m^2/kJ or 0.3 kg/h-met.

Since t_{ex} and W_{ex} are near body temperature, Fanger has proposed the following correlations

$$t_{ex} = 32.6 + 0.066t + 32W_a \tag{19.24}$$

$$W_{ex} = 0.0277 + 0.000065t - 0.8W_a \tag{19.25}$$

As an approximation W_a is determined for standard air (20°C, 50% RH, sea level), the second term is neglected in Eq. (19.25) and standard values are used for h_{fg} and c_{pa} to obtain

$$C_{res} + R_{res} = [0.0014\, M(34 - t) + 0.0173\, M(5.87 - p_w)]/A_D \tag{19.26}$$

19.5.4 Effect of Clothing

The thermal and moisture resistance of clothing has been included in Eqs. (19.14) and (19.15). Many formulations have been used depending upon applications to describe the effect of clothing.

Thermal insulation of clothing

R_{cl} has been used to describe thermal resistance. Clothing insulation is another term used for it. Clothing ensemble consists of a number of pieces of clothing. For practical purpose, it is assumed to be a single equivalent uniform layer of insulation over the whole body. Its insulating value is denoted by a unit called "clo" as proposed by Gagg et al. (1941).

$$1 \text{ clo} = 0.155 \text{ m}^2\text{-K/W}$$

The term *intrinsic clothing insulation* (I_{cl}) is equivalent to R_{cl} that was defined in Eq. (19.13), i.e.

$$R_{cl} = \kappa I_{cl}$$

where, κ is the unit conversion factor of 0.155 m^2-K/W. Intrinsic insulation is a measure of the resistance to sensible heat transfer from skin through the clothing layer. The term κI_{cl} can be used in Eqs. (19.13) and (19.14) to replace R_{cl}. In fact, a *total clothing insulation* I_t can be defined as follows in Eq. (19.14).

$$C + R = \frac{(t_{sk} - t_o)}{(R_{cl} + 1/f_{cl}\, h_e)} = \frac{t_{sk} - t_o}{\kappa I_t} \tag{19.27}$$

where,
$$I_t = \frac{I_{cl} + 1}{\kappa f_{cl} h} \tag{19.28}$$

The total clothing insulation I_t depends upon the convective heat transfer coefficient h which varies from situation to situation. Hence the expression of I_t is not a general expression like I_{cl}. Since some of the comfort indicies are defined in terms of nude person, one can define a total insulation I_a for a nude person. This is equal to $1/(\kappa\, h)$ in Eq. (19.28) assuming that the emissivity of clothing is same as that of naked body, and shape of clothing is also same as that of naked body. Sensible heat transfer from a naked person per unit area is given by $(C + R) = t_p h(t_{sk} - t_o)$.

Effective clothing efficiency and intrinsic clothing efficiency

Sometimes it is convenient to express Eq. (19.14) as follows:

$$(C + R) = \frac{(t_{sk} - t_o)}{(R_{cl} + 1/f_{cl} h)} = F_{cle}\, h\, (t_{sk} - t_o) = F_{cl} f_{cl}\, h\, (t_{sk} - t_o) \tag{19.29}$$

where
$$F_{cle} = I_a / I_t = (1/h)/(R_{cl} + 1/(f_{cl} h)) \tag{19.30}$$

and
$$F_{cl} = \frac{F_{cle}}{f_{cl}} \tag{19.31}$$

where *F_{cle} is called the effective clothing efficiency and F_{cl} is called the intrinsic clothing efficiency*. This defines the effectiveness of clothing on sensible heat transfer and it is the ratio of thermal resistance offered by a nude person to that offered by a clothed person. Comparing Eqs. (19.10) and (19.29), we get

$$F_{cl} = (t_{cl} - t_o)/(t_{sk} - t_o) \tag{19.31a}$$

and
$$I_{cl} = (1/\kappa f_{cl} h)(1/F_{cl} - 1) \tag{19.31b}$$

Hence F_{cl} and I_{cl} can be determined from measured values of temperatures t_{sk}, t_{cl} and t_o, and estimated values of f_{cl} and h. Table 19.3 due to McCullogh and Jones (1984), gives the clothing insulation for various ensembles. Table 19.4 from the same source gives the values of insulation for individual garments. For the ensembles, which are not listed in Table 19.3, ensemble insulation can be determined from the following formula with the values for individual garments $I_{clo,i}$ taken from Table 19.4.

$$I_{cl} = 0.835 \sum_i I_{clo,i} + 0.161 \tag{19.32}$$

If $I_{clo,i}$ is not available for a particular garment, it can be estimated from the following equation

$$I_{clo,i} = (0.534 + 0.135 t_f)\left(\frac{A_G}{A_D}\right) - 0.0545 \tag{19.33}$$

where, t_f is the thickness of the fabric in mm and A_G is the body surface area covered by the garment in m^2.

Table 19.3 Typical insulation values for clothing ensembles

Ensemble description	I_{cl}, clo	I_r, clo	f_{cl}
Walking shorts, short-sleeve shirt	0.41	1.05	1.11
Fitted trousers, short-sleeve shirt	0.50	1.12	1.14
Fitted trousers, long-sleeve shirt	0.62	1.22	1.19
Same as above, plus suit jacket	0.96	1.54	1.23
Loose trousers. Long sleeve-shirt, long-sleeve sweater, T-shirt	1.01	1.56	1.28
Loose trousers. Long sleeve-shirt, long-sleeve sweater, suit jacket, long underwear bottoms. T-shirt	1.3	1.83	1.33
Sweat pants, sweat shirt	0.77	1.37	1.19
Knee-length skirt, short-sleeve shirt, panty hose(no socks), sandals	0.54	1.1	1.26
Knee-length skirt, long-sleeve shirt, full slip, panty hose (no socks)	0.67	1.22	1.29
Knee-length skirt, long-sleeve shirt, half slip, panty hose (no socks), long sleeve-sweater	1.10	1.59	1.46
Ankle-length skirt, long sleeve-shirt, suit jacket, panty hose (no socks)	1.1	1.59	1.46
Long sleeve coveralls, T-shirt	0.72	1.3	1.23
Overalls, long sleeve shirt, long underwear tops and bottoms, flannel long-sleeve shirt	1.0	1.55	1.28

Table 19.4 Garment insulation values

Garment description	clo	*Garment description*	clo	*Garment description*	clo
Underwear		**Shirts and Blouses**		**Dresses and Skirts**	
Men's Briefpanties	0.04	Sleeveless, scoop-neck	0.12	Shirt (thin)	0.14
Bra	0.03	blouse		Shirt (thick)	0.23
T-shirt	0.01	Short-sleeve, dress shirt	0.19	Long-sleeve shirt dress (thin)	0.33
Full slip	0.08	Long-sleeve, dress shirt	0.25	Long-sleeve shirt dress	0.47
Half slip	0.16	Long-sleeve, flannel shirt	0.34	(thick)	
Long underwear top	0.14	Short sleeve, knit sport shirt	0.17	Short-sleeve shirt dress	0.29
Long underwear	0.20	Long sleeve, sweat shirt	0.34	(thin)	
bottoms	0.15			Sleeveless scoop neck (thin)	0.23
Footwear		**Trousers and Coveralls**		Sleeveless scoop neck	0.27
Ankle-length athletic	0.02	Short shorts	0.06	(thick) i.e. jumper	
socks		Walking shorts	0.08	**Sweaters**	
Calf-length socks	0.03	Straight trousers (thin)	0.15	Sleeveless vest (thin)	0.13
Knee socks (thick)	0.06	Straight trousers (thick)	0.24	Sleeveless vest (thick)	0.22
Panty hose stockings	0.02	Sweat pants	0.28	Long-sleeve (thin)	0.25
Sandals/thongs	0.02	Overalls	0.30	Long-sleeve (thick)	0.36
Slippers(quilted, pile	0.03	Coveralls	0.49	Long sleeve pajamas (thick)	0.57
lined)		**Sleepwear and Robes**		Short-sleeve pajamas	0.42
Boots	0.01	Sleeveless, short gown	0.18	Long-sleeve, long wrap robe	0.69
Suit Jackets and		(thin)		(thick)	
Vests (lined)		Sleeveless, long gown	0.20	Long-sleeve, short wrap robe	0.48
Sleeveless vest (thin)	0.36	(thin)		(thick)	
Sleeveless vest (thick)	0.44	Short-sleeve hospital gown	0.31	Short-sleeve, short robe(thin)	0.34
Double-breasted (thin)	0.42	Long sleeve, long gown	0.46		
Double-breasted (thick)	0.48	(thick)			
Sleeveless vest (thin)	0.10				
Sleeveless vest (thick)	0.17				

Clothing surface area f_{cl}

This can be measured by photographic methods or it can be estimated from the available data for similar clothing. A rough estimate is given by

$$f_{cl} = 1.0 + 0.31 I_{cl} \tag{19.34}$$

The values for a few ensembles are given in Table 19.3.

Evaporative resistance of clothing

Intrinsic evaporative resistance of clothing $R_{e,cl}$ can be defined in analogy with $R_{cl.}$ It is a measure of the resistance to latent heat transfer from skin through the clothing as used in Eq. (19.15). A total evaporative resistance to latent heat transfer is defined as

$$E_{sk} = \frac{w(p_{sk,s} - p_w)}{(R_{e,cl} + 1/f_{cl} h_e)} = \frac{w(p_{sk,s} - p_w)}{R_{e,t}} \tag{19.35}$$

where

$$R_{e,t} = R_{e,cl} + 1/f_{cl} h_e. \tag{19.36}$$

In analogy with thermal efficiency of clothing, Nishi and Ibamoto (1969) define *permeation efficiency* F_{pcl} so that Eq. (19.35) may be written as

$$E_{sk} = w F_{pcl} h_e (p_{sk,s} - p_o) \tag{19.37}$$

where the permeation efficiency F_{pcl} is defined as

$$F_{pcl} = \frac{1}{R_{cl} f_{cl} h_e} = \frac{1/f_{cl} h_e}{R_{e,cl} + 1/f_{cl} h_e} \tag{19.38}$$

Combined sensible and latent heat transfer

It is a common practice in air conditioning to combine sensible and latent heat transfers by using analogy between heat and mass transfer to correlate convective heat and mass transfer coefficients. If the mass transfer rate is expressed as $\dot{m} = \rho_a h_D (W_{sk,s} - W)$, then the convective heat transfer coefficient h_c and mass transfer coefficient h_D are related as follows:

$$h_c = \text{Le } c_{p\text{-}ma} h_D \tag{19.39}$$

where Le is Lewis number and $c_{p\text{-}ma}$ is moist air specific heat.

On the other hand, if the mass transfer rate is expressed as $\dot{m} = h_e(p_{sk,s} - p_w)$ and the heat transfer rates as $\dot{m} h_{fg,sk}$ then the evaporative heat transfer coefficient h_e and h_c are related as

$$h_e = (\text{LR}) h_c \tag{19.40}$$

where, LR is Lewis ratio which is approximately equal to 16.5 K/kPa. This is called Lewis ratio in contrast to Lewis number and $c_{p\text{-}ma}$ used in Eq. (19.39). In fact, enthalpy of evaporation and relation $W = 0.622\, p_w/(p - p_w)$ between humidity ratio and partial pressure of water vapour, p_w is also used in converting Eq. (19.39) into Eq. (19.40). The values of $c_{p\text{-}ma}$ and p_w are taken for standard air at 20°C, 50% RH.

Moisture permeability index

For a naked person, these correlations can be used straightaway. However, for a clothed person a moisture permeability index i_m has to be defined to correlate the evaporative heat transfer coefficient $h_{e'}$ and convective heat transfer coefficient $h_{c'}$ from clothing, that is,

$$i_m\,(\text{LR}) = \frac{h_{e'}}{h_{c'}} \tag{19.41}$$

where

$h_{e'}$ = overall convective evaporative heat transfer coefficient $1/R_{et}$, W/m^2-kPa

$h_{c'}$ = overall sensible heat transfer coefficient (inclusive of radiation) $1/R_t$, W/m^2-K

The normal range of moisture permeability is $0.3 < i_m < 0.5$. An average value of $i_m = 0.4$ is reasonably accurate.

Total heat transfer rate is as follows:

$$\begin{aligned} q_{\text{total}} &= C + R + E_{sk} \\ &= h'(t_{sk} - t_o) + w\,h_{e'}\,(p_{sk,s} - p_w) = h'(t_{sk} - t_o) + w\,h'\,i_m\,(\text{LR})\,(p_{sk,s} - p_w) \\ &= h'[(t_{sk} + w\,i_m\,(\text{LR})\,p_{sk,s}) - (t_o + w\,i_m\,(\text{LR})\,p_w)] \end{aligned} \tag{19.42}$$

The term $t_{sk} + wi_m(\text{LR})p_{sk,s}$ describes the skin surface while $t_o + wi_m(\text{LR})p_w$ describes the environmental air condition. Combinations of t_o and p_w that yield the same value of the sum ($t_o + wi_m(\text{LR})p_w$) will result in the same total heat transfer from the skin. The skin parameters and air parameters are related together and it is a useful concept.

19.5.5 Heat Transfer from a Nude Person or Any Arbitrary Surface

To elabobrate this concept, first we consider the total heat transfer from a nude person which is actually equivalent to total heat transfer from an arbitrary wetted surface at temperature t_s and saturation water pressure $p_{s,s}$. The first subscript refers to surface while the second subscript refers to saturated state. The terms w and i_m will not appear in this expression.

$$q_{\text{total},n} = h_c(t_c - t) + h_e(p_{s,s} - p_w) = h_c[(t_c - t) + (\text{LR})(p_{s,s} - p_w)] \tag{19.43a}$$

$$= h_c[(t_c + (\text{LR})\,p_{s,s}) - (t + (\text{LR})\,p_w)] \tag{19.43b}$$

Any combination of environmental conditions t and p_w resulting in the same value of the sum ($t + (\text{LR})\,p_w$) will result in the same value of total heat transfer.

The wet-bulb temperature is another important concept. This is called adiabatic saturation temperature, that is, if the air becomes saturated by contact with a surface (the bulb of the wet-bulb thermometer) under adiabatic conditions ($q_{\text{total}} = 0$), the surface temperature is called t_{wb}. In this case, the sensible heat transfer is equal to latent heat transfer so that the net heat transfer is zero. Equation (19.43) yields

$$t_{wb} + (\text{LR})\,p_{wb,s} = t + (\text{LR})\,p_w$$

or

$$t_{wb} = t + (\text{LR})\,p_w - (\text{LR})\,p_{wb,s} \tag{19.44}$$

where, $p_{wb,s}$ is the saturation pressure of water at the wet-bulb temperature t_{wb}.

19.5.6 Conditions for Constant Heat Loss from a Clothed Person and Environmental Indicies

As pointed out earlier, the total heat loss from a clothed person is constant if the sum of environmental conditions ($t_o + wi_m$ (LR) p_w) is constant. From human comfort point of view, one can define a combination of temperature and relative humidity as a single parameter (temperature) that will give the same total heat transfer rate as the given environmental condition t_o and p_w. There are at least three conditions of relative humidity for which single temperature can be defined.

Adiabatic equivalent temperature

For zero relative humidity, $W = 0$, $p_w = 0$. If t_{ad} is the temperature at $p_w = 0$ which gives the same total heat transfer rate as the given environmental condition, then

$$t_{ad} + wi_m \text{ (LR) } (0) = t_o + wi_m \text{ (LR) } p_{w,}$$

i.e.
$$t_{ad} = t_o + wi_m \text{ (LR) } p_w \tag{19.45}$$

Humid operative temperature

This is the temperature of saturated air t_{oh} (100% relative humidity) that yields the same heat transfer rate as the actual environment That is,

$$t_{oh} = t_o + wi_m \text{ (LR) } p_w - wi_m \text{ (LR) } p_{oh,s} \tag{19.46}$$

This temperature was earlier defined as the *effective temperature*. The definition of effective temperature has now been changed as given below.

Effective temperature

This is the temperature of air with 50% relative humidity that yields the same total heat transfer rate as the actual environment. Hence,

$$ET^* = t_o + wi_m \text{ (LR) } p_w - 0.5\ wi_m \text{ (LR) } p_{ET^*,\,s} \approx t_o + 0.5\ wi_m \text{ (LR) } p_{ET^*,\,s} \tag{19.47}$$

where $p_{ET^*,s}$ is the saturation pressure at ET^* in kPa. Some textbooks refer to ET^* as the *modified effective temperature*.

19.6 THERMOREGULATORY MECHANISMS

Human beings take precautions, such as suitable choice of clothes to assist the body in maintaining its heat balance, and to optimize thermal comfort, for example, by removing jumper, rolling up sleeves or putting on a jacket. However, the body has involuntarily-initiated mechanisms for adjusting itself against heat or cold exposures. The basic purpose of these adjustments is to prevent drastic change in interior body temperature that may impair the vital organs.

The control system that regulates body responses against heat or cold is very complex and not fully understood. Two sets of sensors for the control system are known. They are located in the skin and hypothalamus. The skin sensors are cold sensors, which start the body's defence against cooling, when the skin temperature falls below 33.7°C. The hypothalamus sensor is a heat sensor, which starts the body's cooling function when the body's core temperature exceeds 36.8°C.

According to two-node model of Gagge (1971), the body is in a state of physiological thermal neutrality if the average skin and core temperatures are $t_{sk,n} = 33.7^{o}C$ and $t_{cr,n} = 36.8^{o}C$ respectively. Thermoregulatory control processes like vasomotor regulation, sweating and shivering are controlled by five signals, namely, warm signal and cold signal from the core ($WSIG_{cr}$ and $CSIG_{cr}$), warm and cold signals from the skin ($WSIG_{sk}$ and $CSIG_{sk}$), and the warm signal from the body $WSIG_{b}$. The reader is referred to Gagge (1971) for further reading.

The neutral zone is the temperature range of 28°C to 31°C for an unclothed person and 23°C to 27°C for normally clothed (0.6 clo) sedentary people. In neutral zone, the physiological system is able to maintain its thermal equilibrium with the environment and the normal body temperature without any regulatory effort. That is, the body needs to take no particular action, and there is absence of body cooling or heating, and further there is no increase in the evaporation heat loss.

19.6.1 Thermoregulatory Mechanism against Cold

Zone of vasomotor regulation against cold

If the environmental temperature decreases, the rate of heat loss from the skin to environment increases, the body responds by constricting the blood vessels adjacent to the skin, thereby decreasing the blood flow and heat transfer to the skin. The skin acts as an insulating layer. The heat generation term, Q_s, in Eq. (19.4) becomes negative, skin and adjacent tissues are cooled by heat loss to the environment but the temperature of deep skin tissues is maintained constant. This is called *zone of vasomotor regulation against cold.* This is a very narrow temperature range.

Zone of metabolic activity against cold

If the environment temperature falls below this range, restriction of blood vessels does not provide adequate protection against cold and the temperature of superficial and deep tissues may fall. This is prevented by another central reaction, and this zone is called *zone of metabolic activity against cold*. The body generates heat through muscular tension, shivering or spontaneous increase in activity. This increase in body heat generation prevents Q_s from remaining negative and also prevents the body surface temperature from further decreasing.

An alternative control reaction in the *zone of behavioural regulation against cold* involves putting more clothing or increased activity (e.g. walking faster). If all the control reactions prove inadequate, the body is unable to combat cooling of its tissues and disastrous results may occur. This final range of conditions is known as *zone of inevitable body cooling*. If the temperature falls 2°C below 37°C, people suffer major losses in efficiency (e.g. in manual dexterity under arctic conditions), and core temperatures below 31°C can be lethal.

Over a wide range of environmental conditions of cold, the body maintains the temperature of the internal crucial organs at the expense of energy loss from and possible deprivation of peripheral tissues. The farther the superficial tissue is (e.g. hands and feet) from the central body mass, the more readily its temperature falls. Also, if the ratio of surface area to the mass is large (e.g. ear versus torso) the temperature will fall very rapidly.

19.6.2 Thermoregulatory Mechanism against Heat

On the warm side of the neutral mid-point, there exists a narrow *zone of vasomotor regulation against heat.* This responds by dilating the blood vessels near the skin and allowing the blood flow

as close as possible to the skin. This may double or even triple the conductance of the heat to the superficial (skin) tissues. The skin temperature increases, providing a greater temperature difference for heat loss by convection and radiation. This further increases $p_{sk,s}$ also in Eq. (19.15), thereby increasing the evaporative loss. The skin temperature comes closer to the temperature of deep tissues.

If in spite of the increase in blood flow, the core temperature rises to about 37°C, the body enters its second line of defence called the *zone of evaporative regulation against heat*, where the body reacts in a powerful manner to prevent further rise in skin temperature. The sweat glands become highly active drenching the body surface with perspiration. If humidity ratio and velocity of air permit sufficient evaporation, further rise in body temperature may be prevented. This is the last line of defence. If atmospheric humidity is high or velocity is small or person has donned extra clothing, then the upper limit of evaporation E_{sk} decreases the term Q_s which becomes positive in Eq. (19.5) and the body enters the *zone of inevitable body heating*. If the core temperature rises more than 2°C over 37°C, people suffer major losses in efficiency. The rise of deep body temperature above 43°C may be fatal.

At the same time, excessive perspiration from the skin is equally dangerous. The body salts also come out with perspiration, the lack of which may lead to cramps and loss of water from body may lead to dehydration. Human beings are the only species, that are bestowed with this powerful mechanism of cooling by sweating. The dogs have to stick out their tongue for evaporation heat transfer.

19.6.3 Physiological Hazards Resulting from Heat Exposure

Several physiological hazards occur when Q_s is positive and the body enters the zone of inevitable heating, the extent and severity of which depends upon the extent and time duration of body temperature rise.

Heat exhaustion

Heat exhaustion is due to failure of normal blood circulation. Symptoms of heat exhaustion include fatigue, headache, dizziness, vomiting, and abnormal mental reactions such as irritability. Severe heat exhaustion may cause fainting. This does not cause any permanent damage and the patient recovers when removed to a cooler place.

Heat cramps

Heat cramps result from the loss of salt due to excessive perspiration from the body. These are painful muscle spasms, which may be avoided by proper replacement of salt.

Heat stroke

Heat stroke is the most serious hazard. When body is exposed to excessive heat, the body temperature may rise rapidly to 41°C or more. The sweating ceases at this temperature and the subject may enter a coma, with death imminent. Persons experiencing heat stroke may suffer permanent brain damage.

19.7 HEAT TRANSFER COEFFICIENTS

The values of various heat transfer coefficients—radiative, convective and evaporative—are required so as to estimate the heat transfer from the body.

19.7.1 Radiative Heat Transfer Coefficient

The linearized radiative heat transfer coefficient can be expressed as

$$h_r = 4\varepsilon\sigma(A_r/A_D)[273.16 + (t_{cl} + t_r)/2]^3 \quad (19.48)$$

where

ε = average emissivity of clothing or body surface

σ = Stefan–Boltzman constant, 5.67×10^{-8} W/m^2-K^4

A_r = effective radiation area of body, m^2

t_{cl} and t_r = average clothing temperature and mean radiant temperature respectively.

The ratio A_r/A_D is 0.7 for a sitting person and 0.73 for a standing person. The emissivity is close to unity unless special highly reflective clothes are used. The temperature of clothing t_{cl} may not be known hence its value has to be guessed and iteration carried out. Fortunately, h_r is nearly constant for indoor environment and a value of 4.7 W/m^2-K may be used to a good approximation. If emissivity is different from unity, then

$$h_r = \varepsilon\, 4.7 \text{ W/m}^2\text{-K} \quad (19.49)$$

19.7.2 Convective Heat Transfer Coefficient

Convective heat transfer occurs due either to the air movement or due to the body movement. Table 19.5 gives these coefficients for walking persons or moving air; it is recommended that the larger of the two values must be taken. Care must be taken for seated and reclining persons since, the effective heat transfer area may reduce considerably due to additional contact with chair in the reclining position.

These coefficients have been evaluated at standard atmospheric pressure of 101.325 Pa. These may be corrected for atmospheric pressure p_1 (if significantly different from 101.325 kPa) as follows:

$$h_{cc} = h_c(p_1/101.33)^{0.55} \quad (19.50)$$

The combined coefficient h is the sum of h_r given by Eq. (19.49) and h_c reported in Table 19.5.

Table 19.5 Equations for convection heat transfer coefficient h_c [W/m^2-K] where V is in m/s

Equation	*Limits*	*Condition*	*Remarks/Sources*
$h_c = 8.3\ V^{0.5}$	$0.2 < V < 4.0$	Seated with moving air	Mitchell (1974)
$h_c = 3.1$	$0.0 < V < 0.2$		
$h_c = 2.7 - 8.7\ V^{0.67}$	$0.15 < V < 1.5$	Reclining with	Colin and Houdas (1967)
$h_c = 5.1$	$0.0 < V < 0.15$	moving air	
$h_c = 8.6\ V^{0.53}$	$0.5 < V < 2.0$	Walking in still air	V is the walking speed Nishi and Gagge (1970)
$h_c = 5.7(M - 0.85)^{0.39}$	$1.1 < M < 3.0$	Active in still air	Gagge et al. (1971)
$h_c = 6.5\ V^{0.39}$	$0.5 < V < 2.0$	Walking on treadmill in still air	V is the treadmill speed Nishi and Gagge (1970)
$h_c = 14.8\ V^{0.69}$	$0.15 < V < 1.5$	Standing person in	Developed from the data
$h_c = 4.0$	$0.0 < V < 0.15$	moving air	of Seppeman et al. (1972)

19.7.3 Evaporative Heat Transfer Coefficient

The evaporative heat transfer coefficient h_e for the outer layer of a nude or clothed person can be estimated from convective heat transfer coefficient using the Lewis relationship given in Eq. (19.40), that is,

$$h_e = (\text{LR})\, h_c \quad [\text{W/m}^2\text{-kPa}] \tag{19.51}$$

where, Lewis ratio LR ≈ 16.5 K/kPa for typical indoor conditions. The corrected value h_{cc} may be used if the atmospheric pressure is significantly different from standard atmospheric pressure.

19.8 ENVIRONMENTAL PARAMETERS

The seven psychrometric parameters used to describe the thermal environment are dry-bulb temperature t, wet-bulb temperature t_{wb}, dew point temperature t_{dp}, partial pressure of water vapour p_w, relative humidity ϕ, humidity ratio W. Apart from this the air velocity V and the mean radiant temperature $\bar{t}_r$ also have to be specified. The mean radiant temperature is the uniform temperature of an imaginary enclosure in which the radiant heat transfer from the human body equals the radiant heat transfer in the actual non-uniform enclosure. This can be calculated from the given temperature distribution of various regions of the room and the view factors between each region and the human body.

$$\bar{t}_r = \sqrt[4]{\sum_i F_{pi}(t_i + 273)^4} - 273 \tag{19.52}$$

where, t_i is the temperature of the ith surface and F_{pi} is the view factor between the person and the ith surface.

The view factor for a high ceiling is less than that for a low ceiling, hence less radiant heat is transferred from a room with high ceiling than that from a low ceiling room.

19.8.1 Environmental Indices

Three such indices have been defined by Eqs. (19.45), (19.46) and (19.47). These are used to describe a thermal environment and the stress it causes on human beings. It combines two or more parameters such as t, $\bar{t}_r$, W and V into a single variable. There are two types of indices—rational and empirical. The rational index is based upon theoretical concepts. The empirical index is based upon measurements carried out on subjects.

19.8.2 Effective Temperature

This is the most common environmental index that combines temperature and humidity ratio into a single index. Two environments with the same *ET* should evoke the same thermal response although they have different temperature and humidity ratio. The original concept of effective temperature was developed by Houghton et al. (1923). It is the temperature of slowly moving (15–25 m/min) saturated air at *ET*, which indicates the same feeling of warmth or cold as some other atmospheric condition of given t and W with $t = \bar{t}_r$.

Nowadays, effective temperature is also called *humid operative temperature*, as defined in Eq. (19.46). Gagge et al. (1971) have defined a new effective temperature based upon Eq. (19.47).

Some authors prefer to call it modified effective temperature ET^*. This is the temperature of environment at 50% relative humidity that results in same total heat loss from the skin as the actual environment. It combines the effects of t, $\bar{t}_r$ and p_w into a single index. Skin wettedness w and permeability index i_m are constant for a given ET^*. At the upper limit of sweat regulation, skin wettedness w approaches one and at the lower limit w approaches 0.06. A constant value of ET^* from Eq. (19.47) means that

$$t_o + 0.5\, wi_m\, (\text{LR})\, p_{ET^*,s} = \text{constant} \tag{19.53}$$

The slope of this line on, say, t–p_w psychrometric chart depends upon w and i_m. At low values of w the line is almost vertical, while for w =1 the constant ET^* line is almost horizontal. ET^* depends upon clothing and activity. Hence it is not possible to generate a universal ET^* chart. A standard set of conditions representative of typical indoor applications is used to define *standard effective temperature* (SET^*). These conditions are as follows:

$$I_{cl} = 0.6 \text{ clo},\ i_m = 0.4,\ M = 1.0 \text{ met},\ V < 0.1 \text{ m/s and } \bar{t}_r = t$$

19.9 APPLICATION OF PHYSIOLOGICAL PRINCIPLES TO COMFORT AIR CONDITIONING PROBLEMS

The concept of comfort has psychological as well as physiological connotations. It is difficult to precisely estimate it. It is not only affected by temperature and relative humidity but also by velocity, body activity and clothing, etc.

Acclimatization is another important factor that must be considered while trying to quantify the parameters for human comfort. In winter, we become adjusted to somewhat cooler temperatures than in summer. People living in warm climate, feel comfortable in warmer surroundings than their northern neighbours.

It is difficult to quantify all these effects in a single parameter. It is not possible to include psychological parameters in a rational index based on thermal analysis. An empirical index may describe these. The research conducted by ASHRAE has resulted in the concept of a single empirical parameter called *Effective Temperature, which is defined as that index that correlates the combined effects of air temperature, air humidity and air movement upon human comfort.* It was established by conducting experiments involving trained subjects who compared comfort conditions in adjoining air conditioned test rooms. *Effective Temperature is the temperature of slowly moving* (0.1 to 0.15 m/s) *saturated air at ET that gives the same feeling of warmth or cold as the given atmospheric condition.* Based upon these results, ASHRAE comfort chart has been evolved. This chart is reproduced in Figure 19.1. This chart is applicable for persons seated at rest or doing light work in reasonable still air with mean radiant temperature equal to surrounding air dry-bulb temperature. The chart has dry-bulb temperature along the x-axis and wet-bulb temperature along the y-axis. Lines of constant effective temperature are shown with a negative slope, and lines of constant relative humidity from 20% to 100% relative humidity are shown with positive slope. In the top part, the percentage of persons feeling comfort during summer at various effective temperatures is shown. It is observed that 100% persons feel comfortable during summer at 21.7°C (71°F) effective temperature. Such a condition may be achieved by various combinations of temperature and relative humidity.

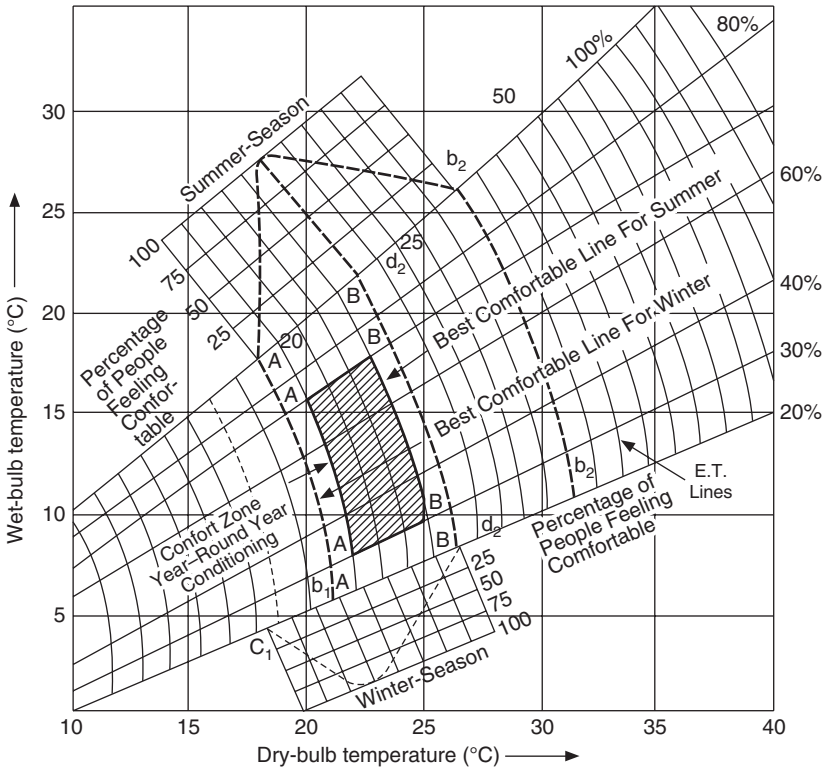

Figure 19.1 Comfort chart.

It is a common practice in India to design comfort air conditioning for summer to give a dry-bulb temperature of 25°C (76–77°F) and relative humidity of 50%. In the lower part of the figure, the percentage of persons feeling comfort during winter at various effective temperatures is shown. It is observed that during winter, 100% normally clothed persons feel comfortable at effective temperature of 20°C (67–68°F). During winter, the condensation on the inner surface of (say) a double glazed window is a problem. If the indoor relative humidity is more than 25–30%, the condensation will occur during the winter climate of northern USA. Also, if the air is not humidified, then relative humidity may fall to as low as 10%. This kind of dry condition may cause over-dehydration of skin and excessive drying-out of floors, veneered furniture, books and other hygroscopic surfaces.

The air velocity also changes the normal effective temperature. At higher velocities, one gets the same level of comfort as at higher dry-bulb temperatures.

It was realized that no person can feel comfortable with air at 100% relative humidity, since this will not allow evaporation of sweat from the skin. Also, this is conducive to fungal growth and bacterial growth on surfaces, and it causes allergic reactions in human beings. Similarly, very low values of relative humidity cause dehydration as discussed above. Hence, comfort zone should be confined to relative humidity between approximately 20% and 80%. As a result, it was observed that defining an Effective Temperature at 50% relative humidity would be more meaningful. This

temperature is called *Modified Effective Temperature*. This has been derived and discussed. The empirical one is discussed later.

19.10 PREDICTION OF THERMAL COMFORT AND THERMAL SENSATION

In this section, some of the empirical indices developed by ASHRAE and some authors are discussed. Thermal comfort is a condition of mind that expresses satisfaction with the thermal environment. Since it is condition of mind, it requires subjective evaluation. Empirical equations are used to correlate comfort perceptions to specific physiological responses. Some of the terms used in this context are as follows:

Occupied zone

It is the zone in a room where comfort conditions are to be maintained. It is specified as the height up to 1.8 m from the floor, leaving 0.6 m near floor and all the walls.

Acceptable thermal environment

An environment according to ASHRAE standard 55–92 that is acceptable to at least 80% of the occupants from thermal point of view.

Thermal sensation

This is a conscious thermal feeling commonly graded into seven categories of cold, cool, slightly cool, neutral, slightly warm, warm and hot. It requires subjective evaluation.

19.10.1 PMV–PPD

Predicted Mean Vote (PMV Index) predicts the mean value of the subjective ratings of a group of large number of people in a given thermal environment. The response of the group is given in a seven point sensation scale ranging from –3 to +3.

PMV = –3 : corresponds to thermal sensation of cold
= –2 : cool
= –1 : slightly cool
= 0 : neutral
= 1 : slightly warm
= 2 : warm
= 3 : hot

Even when PMV is zero for a given environment, there will be some persons who will be dissatisfied although dressed similarly and doing the same level of activity.

To predict how many people are dissatisfied in a given thermal environment, the PPD Index (Predicted Percentage of Dissatisfied) has been introduced. In the PPD Index, people who vote –3, –2, +2 and +3 on the PMV scale are regarded as thermally dissatisfied. The curve of PPD versus PMV is as shown in the Figure 19.2. It is observed that there are always some people who are never satisfied since PPD never goes below 5%.

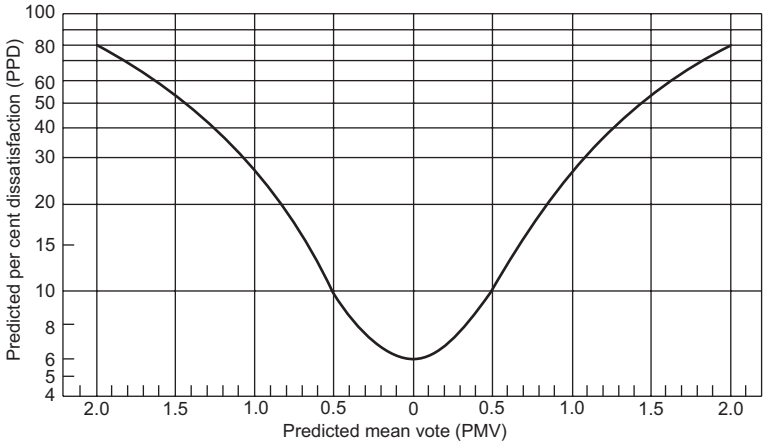

Figure 19.2 Predicted percentage of dissatisfied (PPD) as a function of predicted mean vote (PMV).

19.10.2 Conditions For Thermal Comfort

Rohles and Nevins (1971) and Rohle (1971), correlated comfort level with temperature, humidity ratio, sex and length of exposure based upon studies on 1600 college-age students. The data of these experiments was used to develop empirical equations for predicting thermal sensation. These are given in Table 19.6. A seven-point thermal sensation scale similar to PMV is used. The data given in this table defines conditions that maximize thermal acceptability of environment for a set of similar people.

Table 19.6 Equations for predicting thermal sensation for men, women and men women combined

Exposure period, h	*Sex*	*Regression equation*
		t = dry-bulb temperature, °C p_w = vapour pressure, kPa
1.0	Male	$Y = 0.220t + 0.233p_w - 5.673$
	Female	$Y = 0.272t + 0.248p_w - 7.245$
	Combined	$Y = 0.245t + 0.248p_w - 6.475$
2.0	Male	$Y = 0.221t + 0.270p_w - 6.024$
	Female	$Y = 0.283t + 0.210p_w - 7.694$
	Combined	$Y = 0.252t + 0.240p_w - 6.859$
3.0	Male	$Y = 0.212t + 0.293p_w - 5.949$
	Female	$Y = 0.275t + 0.255p_w - 8.622$
	Combined	$Y = 0.243t + 0.278p_w - 6.802$

Note: Y value ranges from –3 to +3 where –3 is cold, –2 is cool , –1 is slightly cool, 0 is comfortable, +1 is slightly warm, +2 is warm and +3 is hot

The table is for young adult subjects with sedentary activity and wearing clothing with a thermal resistance of approximately 0.5 clo, velocity < 0.2 m/s and $\bar{t}_r = t$

19.10.3 Steady-State Energy Balance and PPD–PMV Model

Empirical equations are developed by considering steady-state energy balance. If body is near thermal neutrality then according to Fanger (1982), for a given metabolic activity M, the skin temperature t_{sk} and regulation rate E_{rsw} are the only two physiological parameters influencing heat balance. Heat balance, however, does lead to thermal comfort all the time. It is in a very narrow range that thermal comfort occurs.

Based upon the data of Rohles and Nevins, the following empirical relations are obtained for t_{sk} and E_{rsw} that provide thermal comfort.

$$t_{sk} = 35.7 - 0.0275(M - W) \text{ °C} \tag{19.54a}$$

$$E_{rsw} = 0.42(M - W - 58.15) \text{ W/m}^2 \tag{19.54b}$$

$(C + R)$ can be evaluated from Eq. (19.14) and E_{sk} from Eq. (19.15) by substituting these relations. Then, energy balance Eq. (19.5) can be used to determine the six environmental and personal parameters that optimize comfort in steady state. Fanger (1982) used this data, Eq. (19.26) for C_{res} and E_{res} and several assumptions to yield the following equation for neutral sensation.

$$\begin{aligned} M - W &= (C + R) + E_{rsw} + C_{res} + E_{res} \\ &= 3.96 \times 10^{-8} f_{cl}[(t_{cl} + 273)^4 - (\overline{t_r} + 273)^4] - f_{cl}\, h_c(t_{cl} - t) \\ &\quad + 3.05[5.73 - 0.007(M - W) - p_w] + 0.42\,[(M - W) - 58.15] \\ &\quad + 0.0173M(5.87 - p_w) + 0.0014M(34 - t) \end{aligned} \tag{19.55}$$

where

$$\begin{aligned} t_{cl} &= 35.7 - 0.0275(M - W) - \kappa I_{cl}\,(M - W) - 3.05 \\ &\quad [5.73 - 0.0077(M - W) - p_w] - 0.42[(M - W) - 58.15] \\ &\quad - 0.0173M(5.87 - p_w) - 0.0014M(34 - t) \end{aligned} \tag{19.56}$$

Fanger used the following relations for h_c and f_{cl}:

$$h_c = \text{larger of } 2.38\,(t_{cl} - t)^{0.25} \text{ and } 12.1\sqrt{V} \tag{19.57}$$

$$f_{cl} = 1.0 + 0.2\, I_{cl} \qquad \text{if } I_{cl} < 0.5 \text{ clo} \tag{19.58}$$

$$f_{cl} = 1.0 + 0.1\, I_{cl} \qquad \text{if } I_{cl} > 0.5 \text{ clo} \tag{19.59}$$

If Eq. (19.55) is satisfied for the thermal environment, then it is in the neutral zone. Usually the left hand side of Eq. (19.55) will be different from the right hand side. Let L be this difference, that is, calculated by using Eqs. (19.55), (19.56) and (19.57). This imbalance in energy balance can be used to define the PMV index and PPD as follows:

$$\text{PMV} = [0.303 \exp(-0.036M) + 0.028]L \tag{19.60}$$

$$\text{PPD} = 100 - 95 \exp[-(0.03353(\text{PMV})^4 + 0.2179(\text{PMV})^2)] \tag{19.61}$$

19.10.4 Two-node Transient Energy Balance TSENS—DISC Model

Empirical equations can be developed by using the two-node model described in Eqs. (19.6) and (19.7). If the empirical expressions presented above are substituted in the transient energy balance Eqs. (19.6) and (19.7), then t_{sk} and t_{cr} can be found at any time θ by numerical integration. These are then used to find thermal sensation, TSENS, and thermal discomfort, DISC, from empirical expressions.

TSENS and DISC are based upon the 11 point scale that is similar to PMV scale except for the extra terms ±4 (very hot/cold) and ±5 (intolerably hot and cold). Recognizing the same positive/negative convention for warm/cold discomfort, DISC is defined as:

5 intolerable
4 limited tolerance
3 very uncomfortable
2 uncomfortable and unpleasant
1 slightly uncomfortable but acceptable
0 comfortable

TSENS is defined in terms of deviation of the mean body temperature t_b from cold and hot set points representing the lower and upper bounds for the zone of evaporative regulation, t_{bc} and t_{bh}, respectively, where

$$t_{bc} = (0.194/58.15)(M - W) + 36.301 \tag{19.62}$$

$$t_{bh} = (0.347/58.15)(M - W) + 36.669 \tag{19.63}$$

TSENS is then given by

$$\text{TSENS} = 0.4685(t_b - t_{bc}) \qquad t_b < t_{bc} \tag{19.64a}$$

$$= 4.7\varepsilon_{ev}\,(t_b - t_{bc})/(t_{bh} - t_{bc}) \qquad t_{bc} < t_b < t_{bh} \tag{19.64b}$$

$$= 4.7\varepsilon_{ev} + 0.4685(t_b - t_{bh}) \qquad t_{bh} < t_b \tag{19.64c}$$

where, ε_{ev} is the evaporative efficiency (assumed to be 0.85).

Thermal discomfort, DISC is numerically equal to TSENS when t_b is below the set point t_{bc} and is related to skin wettedness when the body temperature is regulated by sweating:

$$\text{DISC} = 0.4685(t_b - t_{bc}) \qquad t_b < t_{bc} \tag{19.65a}$$

$$= 4.7\,\frac{E_{rsw} - E_{rsw,reg}}{E_{max} - E_{rsw,reg} - E_{dif}} \qquad t_b \le t_{bc} \tag{19.66b}$$

where, $E_{rsw,reg}$ is given by Eq. (19.54b).

Following observation can be made regarding the two-node TSENS–DISC model.

TSENS is the predicted thermal sensation, and DISC is the predicted thermal discomfort. DISC is similar to TSENS except that it accounts for discomfort due to skin wettedness (sweating). In non-sweating conditions, TSENS is not different from DISC. For example, cold-sensation is not different from cold discomfort.

In the zone of evaporative thermal regulation, comfort and thermal sensation are not the same variables. At $ET^* = 41.4^oC$, regulation by evaporation fails.

Practically, all physiological variables predicted by the two-node model are dependent upon the ambient temperature and independent of vapour pressure p_w except at relative humidity greater than 80%, where these become functions of vapour pressure as well.

The advantage of this method is that the above-mentioned empirical relations can thermally evaluate any given thermal environment for comfort.

19.11 STANDARD EFFECTIVE TEMPERATURE AND MODIFIED COMFORT CHART

The comfort, it is observed depends upon dry-bulb temperature (DBT), relative humidity (RH), air velocity and mean radiant temperature (MRT). Dry-bulb temperature affects the convection and evaporation from body, while relative humidity affects the evaporation from the body. Air velocity affects both evaporation and convection. Dry-bulb temperature (DBT) and relative humidity (RH) are under the direct control of air conditioning systems, while velocity is a matter of air distribution. MRT can be only partially controlled. This involves warm ceilings, cold floors and sunlit windows during summer and cold windows during winter. The most commonly used instrument to determine MRT is *vernon's globe thermometer*, which consists of a hollow copper sphere 152.4 mm in diameter with flat black paint coating, and a thermometer bulb at its centre. This bulb exchanges heat by radiation and convection with surroundings and when it comes to an equilibrium, the thermometer indicates this temperature. An estimate of MRT is given by the following equation based upon the globe temperature T_g, air temperature T both in kelvin and air velocity V in m/s.

$$T^4_{mrt} = T_g^4 + 0.247 \times 10^9 \, V^{0.5} \, (T_g - T) \tag{19.66}$$

It is obvious that a single variable cannot define comfort since it involves at least four parameters, DBT, RH, V, and MRT. The most common index with the widest range of applications is the *Effective Temperature ET** which is the temperature of environment with 50% relative humidity that results in same heat loss from the skin as the actual environment. It combines DBT and RH. But it depends upon clothing and activity, hence it is not possible to generate universal charts, which can be used for given DBT and RH. Equation (19.47) and the heat transfer relations can be used to find effective temperature for various clothing and metabolic activities using computer programs. Hence, a *Standard Effective Temperature SET* has been defined for typical indoor conditions. These conditions are:

Clothing insulation	= 0.6 clo
Moisture permeability index (i_m)	= 0.4
Metabolic activity level	= 1 met
Air velocity	= 0.1 m/s
Ambient temperature	= mean radiant temperature (MRT)

It was observed that the definitions of humid operative temperature and effective temperature, both involved the operative temperature, which is the mean of MRT and DBT weighted by respective heat transfer coefficients. For usual practical applications it is convenient to take the operative temperature as the mean of MRT and DBT, that is,

$$t_o = (t_{mrt} + t)/2 \tag{19.67}$$

This is also called the *adjusted dry bulb temperature.* Under the conditions of *SET*, $t_{mrt} = t = t_o$. Operative temperature and effective temperature are used in ASHRAE Standard 55 to define comfort conditions.

EXAMPLE 19.1 Calculate the operative temperature if the dry-bulb and globe temperatures are 25°C and 28°C respectively, and air velocity is 0.15 m/s.

Solution:

We have from Eq. (19.66),

$$T_{mrt} = [T_g^4 + 0.247 \times 10^9 V^{0.5}(T_g - T)]^{0.25}$$

or $$T_{mrt} = [(273 + 28)^4 + 0.247 \times 10^9 (0.15)^{0.5} (28 - 25)]^{0.25} = 303.6 \text{ K} = 30.6^\circ\text{C}$$

$\therefore$ $$t_o = (25 + 30.6)/2 = 27.8^\circ\text{C}$$

The operative temperature shows the combined effect of velocity and radiation. In Example 19.1, the operative temperature is 2.8°C more than the dry-bulb temperature because of radiation and convection. This environment will probably be uncomfortable at any value of relative humidity.

In Europe, *dry resultant temperature* is used for most practical purposes. This is defined as

$$t_{res} = \frac{t_{mrt} + (10V)^{0.5} t}{1 + (10V)^{0.5}} \tag{19.68}$$

In Example 19.1,

$$t_{\text{res}} = \frac{30.6 + (10 \times 0.15)^{0.5}\, 25}{1 + (10 \times 0.15)^{0.5}} = 27.52^\circ\text{C}$$

which is close to the operative temperature. At velocity of 0.1 m/s, $10V = 1.0$, hence the *dry resultant temperature* reduces to $t_{res} = (t_{mrt} + t)/2$.

ASHRAE Standard 55-1992 gives the acceptable ranges of operative temperature (dry-bulb temperatures since, $t_{mrt} = t$) and relative humidity for people in typical summer and winter clothing during light and sedentary activities (≤ 1.2 met) as in Figure 19.3. This is called the modified comfort chart or *SET* chart. Two sets of comfort zones are shown, the one on left side is for winter and the one on right side is for summer. The ranges are based on 10% dissatisfaction criterion. The coordinates of the two comfort zones are as follows.

Winter: The lower boundary is at 2°C dew point temperature and the upper boundary is at 18°C wet-bulb temperature. The slanting side boundaries correspond to 20°C and 23.5°C effective temperature (measured along 50% relative humidity line). The operative temperature is in the range of 20°C to 23.5°C along the 18°C wbt line and from 20.5°C to 24.5°C along the 2°C dew point line. The effective temperature lines are loci of constant comfort and thermal sensation.

Summer: The lower boundary is at 2°C dew point temperature and the upper boundary is at 20°C wet-bulb temperature. The slanting side boundaries correspond to 23°C and 26°C effective temperature. The operative temperature is in the range of 22.5°C to 26°C along the 20°C wbt line and from 23.5°C to 27°C along the 2°C dew point line.

19.11.1 Practical Limits on Humidity for Comfort

Human body is capable of tolerating considerable variation in relative humidity. However, there are lower and upper limits. Humidity affects the evaporation of water from mucosal and sweating bodily surfaces and its diffusion from deep tissues. High humidity supports growth of pathogenic and allergenic organisms, certain fungi, mycotoxins and house mites. Respiratory health is a problem at high humidity. This growth is enhanced in the presence of fibre board, dust, lint, skin particles and dandruff. Fungal infections are likely at relative humidity greater than 70%. The upper boundary of comfort zone is limited by this criterion. Taking into account the seasonal change in clothing in

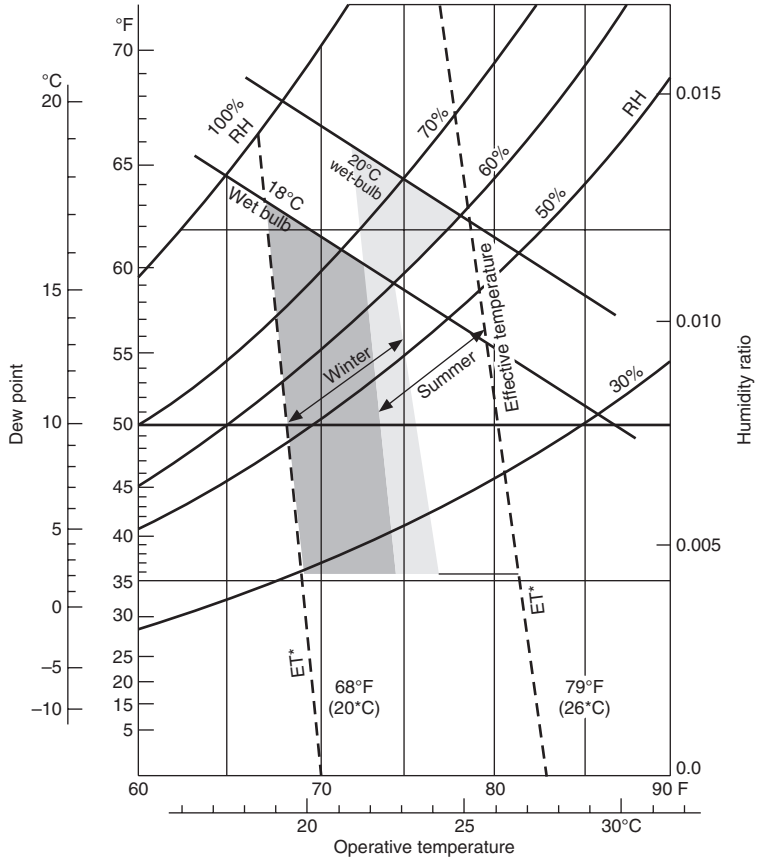

Figure 19.3 Modified comfort chart showing the acceptable ranges of operative temperature and humidity for people in typical summer and winter clothing during light and sedentary activity (≤ 1.2 met).

summer and winter, a wbt of 18ºC during winter and 20ºC during summer is suggested as the upper boundary.

At low humidity, the nose and throat become dry and eye irritation starts. A dusty atmosphere can exacerbate a low humidity skin condition. Eye irritation increases with time in the low humidity environment. The lower limit of comfort zone is kept as 2ºC dew point. This corresponds to 20% PPD.

The effect of age, adaptation, sex and individual variation is discussed in *ASHRAE Handbook*. A brief discussion is provided below.

19.11.2 Individual Variation

Every individual has a slightly different liking, hence there is a variation in comfort level felt by individuals, all other conditions like clo value, activity level being the same. The comfort zone is based upon 90% acceptance and 10% discomfort. This accounts for individual variation. Internal body temperature has a rhythm, it is lowest in the morning and highest in the afternoon. This also does not affect the comfort zone drastically.

19.11.3 Age

Metabolism decreases slightly with age. Recent studies have shown that thermal environments preferred by older people are same as those preferred by younger people. It appears that decrease in metabolism is compensated by the lower evaporative loss in older people. Further, older people are normally sedentary and have lower activity level compared to younger people and may, therefore, prefer higher temperatures on account of this.

19.11.4 Adaptation

Recent studies have shown that it has very little influence on comfort level.

19.11.5 Sex

In women the skin temperature and hence evaporative loss is lower compared to men. This balances the slightly lower metabolism in women. Women normally wear light clothing compared to men and may, therefore, prefer a slightly higher temperature on account of this reason.

19.12 EFFECT OF OTHER VARIABLES ON COMFORT

The other variables that affect comfort are, draught conditions, asymmetry in thermal radiation, vertical temperature gradient and floor temperature.

19.12.1 Draught

This is an undesirable local cooling of human body caused by air movement. This is the most annoying factor in offices and also in automobiles, aircraft and railways. The heat loss from the skin caused by draught depends upon the average air velocity and the turbulence intensity. Due to the way cold sensation in the skin works, the degree of discomfort felt depends upon not only the level of heat loss but also the fluctuation of skin temperature. Highly turbulent flow is more annoying. The more the steep drops in temperature due to fluctuating turbulent flow, the more will be discomfort signals sent by cold sensors. It has been found that fluctuations with a frequency of 0.5 Hz are the most uncomfortable, while fluctuations with frequencies more than 2 Hz are not felt. The percentage of people predicted to be dissatisfied because of draught, may be found from the equation

$$\mathrm{DR} = (34 - t)(V - 0.05)^{0.622}\,(36.96\ \mathrm{SD} + 3.14) \tag{19.69}$$

where, SD is the standard deviation in air velocity, SD = $V \times Tu$, Tu being the turbulence intensity which may be expressed as $100V_{sd}/V$. Turbulence intensity between 30% and 60% is observed in conventionally ventilated spaces. In rooms with displacement ventilation, Tu is low. Sensations of Tu are felt at head and feet. Higher values of Tu may be acceptable at lower speeds.

In fact, each 9.1 m/min (0.152 m/s) increase in velocity is equivalent to 1°C temperature rise, in the sense that at higher velocities more heat can be transferred from the body and hence a higher temperature is acceptable. If 25°C is chosen as the *SET*, then the effective draught temperature t_{ed} may be defined as

$$t_{ed} = (t - 25) - 7.65(V - 0.152) \tag{19.70}$$

There seems to be no minimum value of air movement for comfort, but an upper limit is 0.8 m/s and above which the papers start to fly.

Sedentary persons are more sensitive to draught than active persons. Acceptable operative temperature for active persons can be correlated as

$$t_{o,\ active} = t_{o,\ sedentary} - 3.0(1 + \text{clo})(\text{met} - 1.2)\ ^\circ\text{C} \quad (19.71)$$

19.12.2 Asymmetry in Thermal Radiation

On a winter day, if one faces a blazing bonfire, after some time the back starts to feel uncomfortably cold. This feeling cannot be removed by moving closer to fire, This is what is meant by discomfort due to asymmetry in heat sources. Warm ceilings and cold windows give maximum discomfort while cold ceilings and warm windows give least discomfort.

19.12.3 Vertical Temperature Gradient

A 3°C temperature difference between the head and the feet gives discomfort to 5% people.

19.12.4 Floor Temperature

The floor temperature can affect the mean radiant temperature. If the floor is too cold, the occupants feel cold discomfort and the tendency is to increase the air temperature in the room during winter months. This depends on the type of shoes used since heat is transferred from feet to the floor. For normal shoes, it has been observed that floor temperature between 19°C and 29°C leads to 10% dissatisfied people with sedentary activities. The recommended floor temperature for bare foot persons depends upon the flooring material The range for rugs is 21°C to 28°C, while for hard linoleum wood it is 24°C to 28°C and for concrete it is 26°C to 28.5°C.

19.12.5 Effect of Clothing

Fanger gives dry-bulb temperatures at 50% relative humidity for various clo values at which most people felt zero sensation, that is PPD value of zero. These are as follows:

clo *value*	0	0.5			1.0		1.25		1.5
Temp, °C	29	28	27	26	25	24	24	22	22
Velocity, m/s	0.5–1.0	0.0–1.0	0.2–0.3	0–0.1	0.5–1.0	0.2–0.3	1.0–1.5	0.1–0.15	0.5–1.0

It is obvious that at higher clo values, larger velocities will give comfort and at clo values more than 1, dry-bulb temperature lower than 25°C is required for comfort at 50% relative humidity.

19.13 INDOOR AIR QUALITY

Definition

There is no exact definition of *Indoor Air Quality* (IAQ) and no single instrument can measure it. ANSI/ASHRAE Standard 62–1989 states that acceptable indoor quality is the air in which there is no known contaminant at harmful level concentration as determined by cognizant authorities. It further states that for comfort, indoor air quality may be said to be acceptable, if not more than 50% of the occupants can detect any odour and not more than 20% experience discomfort, and not

more than 10% suffer from mucosal irritation and not more 5% experience annoyance, far less than 2% of the time.

If proper air quality is maintained, then:

(i) The environment is free of odours and contaminants
(ii) The occupants feel comfortable
(iii) The productivity of the occupants increases
(iv) And it has direct impact on the health of the occupants.

There are two main reasons for the awareness of poor IAQ in recent years. Firstly, people spend more of their time indoors since both the office and the housing complexes normally have HVAC systems. Secondly, the use of more effective insulations and more tight and sealed shell of the building, have both reduced the outdoor air and supply air requirements leading to poor dilution and removal rates of pollutants from the room. This has certainly reduced the energy consumption, but the pollutants get trapped and recirculate in the building since the windows cannot be opened. Poor indoor air quality at work, is the most common complaint of persons. Besides being uncomfortable, workers can become ill from the air they breathe inside the body leading to *sick building syndrome*. *Sick building syndrome* includes headache, coughing, dizziness, fatigue, nausea, rashes, breathing problems, and irritation of the eyes, nose and throat. In most cases, these complaints last while the worker is in the building. However, in some cases workers can get serious illness because of poor indoor air. Building related illnesses include Legionnaires' disease, humidifier fever, chronic fatigue syndrome, and multiple chemical sensitivity.

19.13.1 Pollutants

Maintaining good indoor air quality involves: keeping gaseous and particulate contaminants below some acceptable level, these include CO_2, CO and other gases, radioactive materials, microorganisms, viruses, allergens and suspended particulate matter.

The pollutants in occupied rooms come from the following six sources

1. The occupants, who emit CO_2, water vapour, solid particles (flakes of skin, hair, dandruff, nail flakes, lint from clothing) odours and biological aerosols.
2. Smoking (now prohibited) that produces CO, CO_2, other gases and vapours, solid particles, liquid droplets, volatile organic compounds (VOC) and odours. Many of these contaminants have short-term and long-term risks to human health.
3. Building materials, furnishings and their emissions. The structural components, surface finishes, furniture, adhesives used in furniture, upholstery, carpets give out odours, VOC, solid particles, dust and house mites.
4. The activities of the persons and the equipment they use, gives off gaseous and solid emissions and produce odours. These include printers, copiers, fax machines, and computers. The surface coatings of these items of equipment emit pollutants. All electrical equipment become hot, burn their coating of paint and emit dust and odours. VOCs may also be produced.
5. The outdoor air supplied as fresh air, may be polluted. The quality of outdoor may have to be assessed. Monitoring the level of CO in the outdoor air is a good practice since, it

is well correlated with oxides of nitrogen, aromatic hydrocarbons and other urban pollutants.

6. The air supply and recirculating system of the air-conditioning plant may be contaminated due to dirty air filters particularly when wet. These and silencers are potential sources of fungi. Condensate trays can breed bacteria, viruses and fungi. These should be of self-draining type and regularly cleaned. Humidifiers using spray water or wetted surface pose a bigger problem because of continuous presence of water. Dry steam is safe. The ducts may harbour dust and give contamination if not properly cleaned. Other possible pollutants are: toxic materials, radioactive materials, materials with infectious or allergenic potentials, the presence of irritants, extreme thermal conditions and objectionable odours.

Carbon dioxide and other common gases

All mammals exhale carbon dioxide as a by-product of metabolism, hence its level is high indoors than outdoors. In crowded places like auditoriums, its level can be pretty high. It is not a health risk, but it is easily measurable, therefore, it is an effective indicator of the ventilation effectiveness of the space. It gives an indirect indication of the potentially unacceptable level of harmful gases. Environmental protection agencies recommend a maximum level of 1000 ppm (1.8 g/m^3) of harmful gases in indoor spaces.

Carbon monoxide is a by-product of incomplete combustion in automobile engines and tobacco smoking. Buildings near the parking lots and shipping docks have potential of higher concentration of CO. Its level near 15 ppm can be a potential health problem. This reduces the oxygen carrying capacity of the haemoglobin in the blood and the reaction varies with humans, but the effect is cumulative. Headaches and nausea are common symptoms of levels above the tolerance level. Improperly vented and leaking furnaces, chimneys, water heaters, and incinerators are the potential sources of CO.

Sulphur oxides are the by-products of combustion of sulphur containing fuels. These may leak indoors or may come from combustion systems within the building. In the moist mucous membranes, these form sulphuric acid that causes irritation of the upper respiratory tract and induces episodic attacks in individuals with asthmatic tendencies.

Oxides of nitrogen are also produced during combustion of fuel with air at high temperatures. Their presence usually means lower levels of CO. These are also brought in from the outdoor air, however sometimes indoor combustion contributes to their high concentration. Opinion seems to differ on the health effects of different levels of oxides of nitrogen.

Radon is a naturally occurring radioactive gas that results from decay of radium. This has received a great deal of attention in areas where its level is high. This has the potential of causing lung cancer. Radon gas may enter the building from the soil through cracks in the slab floors and basement walls, or through water supply, or from building material containing uranium or thorium. The rate of radiation entering from soil, depends upon the pressure difference; hence pressurization of the rooms will reduce the rate of radiation entering a building. Its levels should be kept below 4 pico curies per litre of air for safety of the occupants.

Volatile organic compounds

Combustion sources, building materials, cleaning agents and solvents, plants and animals emit all sorts of organic compounds. Their levels are usually low, but some occupants are hypersensitive

and a few others may have recently become conscious of their presence. Formaldehyde gas is one of the most common VOCs. It is irritating to eyes and mucous membranes. It seems to cause a diversity of problems in asthmatic patients and immunoneurological reactions in others, and is considered to be a potential cancer hazard. It is used in the manufacture of carpets, pressed wood, fibre boards, insulations, textiles, paper products, cosmetics, shampoos, phenolic plastics and several building products. These products continue to outgas formaldehyde for a long period of time but mostly during the first year. Acceptable limit is 1 ppm as a time weighted 8 hour average but in homes 0.1 ppm is the accepted upper limit.

Particulate matter

A typical sample of outdoor air may contain soot, smoke, silica, clay, decayed animal and vegetable matter, lint and plant fibre, metallic fragments, mould spores, bacteria, plant pollens and other living material. These pollutants come in all variety of sizes from 0.01 μm to sizes of leaves. When suspended in air, these are called *aerosols*. The outdoor air containing aerosols, is brought indoors and these may be additionally contaminated by human activities, furniture and equipment. The indoor environment may be conducive to growth of microbial and infectious organisms. Environmental tobacco smoke is one of the major concerns, since there is evidence of its role in lung diseases and cancer. Allergies are the most common problems of modern society. Indoor environment may contain many of the allergens found outdoors, and occupants may be sensitive to fibres, dust and moulds from carpets and beddings.

Chemicals

Chemicals that cause health problems come from various sources. There are cleaning chemicals and pesticides in all the buildings. Copying machines give off ozone. Glues and correction fluids give offensive vapours. Printing machines also give off volatile compounds. Then laboratories store all kind of chemicals. Smoking makes so many passive smokers. Cosmetics, soaps and lotions all give off volatile compounds. Preparation of food gives out odours, which may be appetizing and harmful at the same time. If asbestos is used as insulation, then broken insulation will be a pollutant. Lead from paint is most harmful. Exhaust from vehicles and industrial pollution may also leak into the building.

Humidity

Humidity affects the evaporation of water from mucous containing surfaces and the sweating body surfaces. It also affects the diffusion of water from deep tissues. Low relative humidity with less than 2°C dew point temperature, tends to give a dry nose and throat and causes eye irritation. A dusty atmosphere with low humidity can have synergetic effect on skin condition. High humidity promotes the growth of pathogenic and allergenic organisms, certain fungi, mycotoxins and house mites. Their growth is further enhanced by the presence of high cellulose material such as fibreboard, dust, lint, skin particles and dandruff. Fungal infections are more likely when relative humidity exceeds 70%. The increase in humidity decreases the odour intensity due to tobacco, smoke. Initial adaptation to an odour is very rapid and perception decreases with time. The irritation of eyes and nose at low humidity, generally increases as the time passes. To minimize eye irritation, humidity should be in the range of 45–60%. The minimum perception of odours, generally occurs in the humidity range of 45–60%.

19.13.2 The Methods to Control Contaminants

The four basic methods to maintain proper indoor air quality are:

1. Source elimination or modification
2. Dilution or use of outdoor air
3. Source air distribution
4. Air cleaning.

Source elimination

In new buildings or retrofitting, the materials and furnishings free of pollutants may be specified. In existing buildings, all the undesirable contaminants not essential for the functioning of the building, may be removed from the building. It is law in India that smoking is prohibited in all buildings. If implemented properly, it will reduce the impact on air conditioning systems. Paints, solvents, volatile organic compounds, and insecticides should not be stored in the building.

Dilution or use of outdoor air

In all air conditioning systems, fresh air or ventilation air, which is outdoor air, is introduced to meet the ventilation requirement of the occupants. This air is at a higher temperature and has higher relative humidity during summer. This has to be cooled and dehumidified before being introduced into the space, hence economics usually requires that a minimum quantity of fresh outdoor air be used. It is assumed that the outdoor air is free of contaminants and will not cause discomfort. This may not be true in some localities where there are strong contaminant sources near the building. ASHRAE Standard 62 gives the ambient air quality standard based upon the published reports of the United States Environmental Protection Agency. In India, no such data is available. This data is used for the specification of contaminants in ambient air. According to this data, short-term values of SO_2, CO_2, CO, and oxidants (O_3) are 0.14, 35, 9 and 0.12 ppm respectively. Yearly averages of $SO_{2,}$- particles (PM 10) and NO_x are 80, 50 and 100 μg/m^3 respectively.

In all air conditioning systems, an amount equal to the fresh air is exhausted from the system, the remaining air is recirculated as shown in the schematic diagram (Figure 19.4) of an air

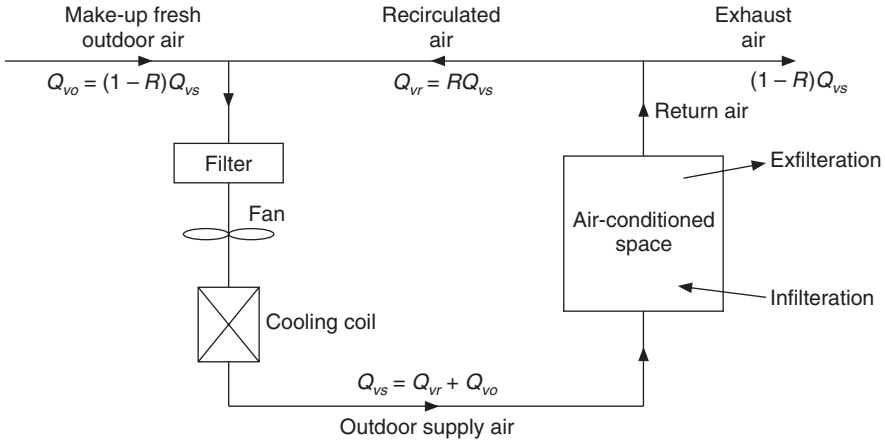

Figure 19.4 Schematic diagram of an all air conditioning system.

conditioning system. There is always some infiltration of outdoor air through cracks, interstices, gaps in floors and walls and ceilings. This is uncontrolled and is dependent upon the prevailing wind and stack effect. There is always an equal amount of exfiltration. It cannot be relied upon to reduce the level of contaminants and for ventilation. There is always mass conservation of all the species of contaminants. For an air conditioning system the following are the mass conservation of air and species.

$$Q_{vs}(C_i - C_s) = N \tag{19.72}$$

$$Q_{vo} + Q_{vr} = Q_{vs} \text{ and } Q_{vr} = RQ_{vs} \text{ and } Q_{vo} = (1 - R)Q_{vs}$$

Mixing of recirculated air and outdoor air:

$$(1 - R)Q_{vs}C_o + RQ_{vs}C_i = Q_{vs}C_s$$

or

$$(1 - R)C_o + RC_i = C_s \tag{19.73}$$

where

Q_{vs} = supply air to the room, cmm
R = recirculation ratio, that is, RQ_{vs}, cmm is recirculated to the room
Q_{vo} = $(1 - R)Q_{vs}$ fresh air volume flow rate, cmm
C_i, C_s and C_o = concentrations of contaminants in the air leaving the room, entering the room and the outdoor air respectively
N = production rate of species in the room.

EXAMPLE 19.2 There are ten persons in a room generating 3 litres/min of CO_2. The air leaving the room has the maximum possible concentration of 1000 ppm (0.1%) of CO_2. The recirculaion ratio is 0.75 and the outdoor air has 35 ppm of CO_2. Determine the volume flow rates of supply air and outdoor air.

Solution:

$$C_i = 0.001,\ C_o = 0.000035$$

From Eq. (19.73),

$$C_s = 0.25(0.000035) + 0.75(0.001) = 0.00075875$$

From Eq. (19.72),

$$Q_{vs} = \frac{3}{C_i - C_s} = \frac{3}{60(0.001 - 0.00075875)} = 207.25 \text{ litres/s}$$

The recirculation ratio being 0.75, the fresh air is $Q_{vo} = 0.25Q_{vs} = 0.25 \times 207.25 = 51.8$ l3 litres/s

If all fresh air is to be used for reducing the concentration of contaminants, then

$$Q_{vo}(C_i - C_o) = N$$

$$\therefore \quad Q_{vo} = \frac{3}{60(0.001 - 0.00035)} = 51.813 \text{ litres/s}$$

That is, 5.1813 litres/s per person is required for ventilation.

In any room, the air distribution is never perfect. All the supplied air should enter the occupied zone of the room with a sufficient low velocity, so that draft is not felt, and it should remove all the contaminants, bring about temperature and humidity equalization. The occupied zone of the room is the space between the floor and 1.8 m above the floor leaving 0.6 m from the walls or fixed air conditioning equipment. All of supply air does, not enter the occupied zone, say S portion of it bypasses and goes directly to the exhaust of the room. Of this, R part is recirculated. S is called the *occupied zone bypass factor*.

If Q_{vos} is the volume flow rate of outdoor air that is supplied to the room, then SQ_{vos} bypasses the room. Of this R portion, that is, SRQ_{vs} unused outdoor air is returned to the room and $S(1-R)Q_{vos}$ is exhausted. Hence the total outdoor air actually supplied to the room is $Q_{vo} + SRQ_{vos}$ and, this is equal to Q_{vos}, that is,

$$Q_{vos} = Q_{vo} + SRQ_{vos}$$

$$\therefore \quad Q_{vos} = \frac{Q_{vo}}{1 - RS}$$

Effectiveness of outdoor air use, E_o, with which outdoor air is used in the room is defined as follows:

$$E_o = \frac{\text{outdoor air flow rate} - \text{unused outdoor air rate exhausted}}{\text{outdoor air flow rate}} = \frac{Q_{vo} - S(1-R)Q_{vos}}{Q_{vo}}$$

It can thus be shown that

$$E_o = \frac{1 - S}{1 - RS} \tag{19.74}$$

The ventilation effectiveness E_o denotes the fraction of outdoor air used in occupied zone.

The room bypass factor, S, is related to the *ventilation efficiency* E_v of the room, which is the fraction of the supply air delivered to the room and is equal to $(1 - S)$. This is also called *stratification factor*. The ventilation efficiency depends upon the room shape as well as the location and design of supply air diffusers and return air inlets. It is obvious that it is not the same as the effectiveness of outdoor air use, E_o.

EXAMPLE 19.3 In a room, because of partitions and poor locations of supply air outlets and return air inlets, 50% of the supply air bypasses the occupied zone. Determine the fraction of outdoor air effectively utilized, if the circulation factor is increased from 0.5 to 0.8.

Solution:

Equation (19.74) gives the effective utilization of outdoor air. We have $S = 0.5$ and $R = 0.5$ and 0.8.

$$\text{At } R = 0.5: \qquad E_o = \frac{1 - 0.5}{1 - 0.5 \times 0.5} = 0.667$$

$$\text{At } R = 0.8: \qquad E_o = \frac{1 - 0.5}{1 - 0.5 \times 0.8} = 0.833$$

The outdoor air utilization improves at larger recirculation ratio since, a larger proportion of bypassed fresh air is fed back to the room.

Standard 62 describes two methods by which acceptable indoor air quality can be achieved by use of outdoor air.

The first of these specifies the ventilation rate at which the outdoor must be delivered to the space. Table 19.7 gives the outdoor air requirement for ventilation for various commercial facilities. These values are based upon physiological considerations, subjective evaluation and experience. Outdoor air treatment is also suggested when the contaminant levels become high. Rooms installed with exhaust air system, such as toilet rooms and bathrooms, kitchen, and smoking lounges, may be provided with make-up air from adjacent spaces provided the quality of air is below the threshold limit of contaminants. If these recommendations are followed, proper IAQ can be maintained.

The second procedure provides a direct solution to acceptable IAQ by restricting the concentration of all known contaminants to some specified acceptable levels. The quantitative values of contaminants are specified from various sources in Standard 62. But for odours, a subjective evaluation by an impartial observer is required.

Air cleaning may be used to reduce the outdoor air requirements below those given in Table 19.7. Some contaminants may not be reduced by the air cleaning process. Then, these contaminants become the factors that control the fresh air requirement.

ANSI/ASHRAE standard created a lot of controversy, primarily because of the requirement for large quantities of outdoor air compared to what had been the previous practice to use.

Table 19.7 Outdoor air requirement for ventilation

Application	*Outdoor air requirement,* (litres/s per person)	*Expected occupancy per* (100 m^2)	*Remarks*
Food and Beverage Service			
Dining Rooms	13		
Cafeteria, fast food	10	70	
Bars, cocktail lounges	15	70	Supplementary smoke removal equipment required
Kitchen (cooking)	8	100	Make-up required for kitchenhood
Hotels, Motels, Resorts, Dormitories			
Lobbies	8	30	
Conference rooms	10	50	
Assembly rooms	8	120	
Dormitory sleeping areas	8	20	
Gambling casinos	15	120	
Offices			
Office space	10	7	
Reception area	8	60	
Data entry area, communications	10	60	Some office equipment may require local exhaust
Conference rooms	10	50	

(*Contd.*)

Table 19.7 Outdoor air requirement for ventilation (contd.)

Application	*Outdoor air requirement,* (litres/s per person)	*Expected occupancy per* (100 m^2)	*Remarks*
Public Spaces			
Public rest rooms	25		Normally supplied by transfer air
Locker and dressing rooms	25		Local mechanical exhaust, no recirculation
Smoking lounge	30	70	Normally supplied by transfer air
Specialty Shops			
Barber	8	25	
Beauty	13	25	
Reducing salons	8	20	
Florist	8	8	Ventilation for plant growth.
Clothing, furniture, hardware, drugs, fabric	8	8	
Supermarkets	8	8	
Sports and Amusement			
Spectator	8	150	
Game rooms	13	70	
Playing floors (gymnasium)	10	30	
Ballrooms and discos	13	100	
Bowling alleys (seating area)	13	70	
Theaters			
Ticket booth	10	60	
Lobbies	10	150	Special ventilation will be needed
Auditorium	8	150	To eliminate special stage effects
Stage, studio	8	70	(e.g. dry ice vapours. mists etc.)
Transportation			
Waiting rooms	8	100	Ventilation within vehicles may require special considerations
Platform	8	100	
Vehicles	8	50	
Workrooms			
Meat processing	8	10	Freezing storage not covered by this. Ventilation from adjoining spaces if continuous occupancy
Photo studios	8	10	
Pharmacy	8	20	
Bank vaults	8	5	

(*Contd*.)

Table 19.7 Outdoor air requirement for ventilation (contd.)

Application	*Outdoor air requirement,* (litres/s per person)	*Expected occupancy per* (100 m^2)	*Remarks*
Education			
Classrooms	8	50	
Laboratories	10	30	
Training shop	10	30	
Music rooms	8	50	
Libraries	8	20	
Auditoriums	8	150	
Smoking lounges	20	70	
Hospitals, Nursing and Convalescent Homes			
Patient rooms	13	10	
Medical procedures	8	20	
Operating rooms	15	20	
Recovery and ICU	8	20	
Physical therapy	8	20	
Correctional Facilities			
Cells	10	20	
Dining halls	8	100	
Guard stations	8	40	

Application	*Outdoor air requirement,* (litres/s-m^2)	*Expected occupancy per* (100 m^2)	*Remarks*
Garages, Repair, Service Stations			
Enclosed parking garage	7.5		Distribution at location of workers and running engines. System for positive engine exhaust withdrawl
Auto repair rooms	7.5		
Hotel			
Bedrooms	15		
Living rooms	15		
Baths	18		Installed capacity for intermittent use

(*Contd.*)

Table 20.7 Outdoor air requirement for ventilation (contd.)

Application	*Outdoor air requirement,* (litres/s-m^2)	*Expected occupancy per* (100 m^2)	*Remarks*
Retail Stores, Sales and Showrooms			
Basement and street	1.5	30	
Upper floors	1.0	20	
Storage rooms	0.75	15	
Dressing rooms	1.0		
Malls and arcades	1.0	20	
Shipping and receiving	0.75	10	
Warehouses	0.25	5	
Clothiers, furniture	1.5		
Pet shops	5.0		
Ice arenas	2.5		
Swimming pools	2.5		Humidity control requires larger values
Public places, corridors and utilities	0.25		
Public rest rooms	2.5		
Dark rooms	2.5	10	
Duplicating, printing rooms	2.5		
Education: locker rooms	2.5		
Education: corridors	0.5		
Autopsy rooms	2.5		

Space air distribution

If the contaminants exist in the building, then the air is supplied at a slightly lower temperature from outlets near the floor level. The supply air rises vertically up, carrying the pollutants with it towards the return air inlet located in or near the ceiling. There exists a vertical temperature gradient in the room (< 3°C). The air and the pollutants are not allowed to mix in the occupied zone. This type of ventilation s called *displacement ventilation*.

In clean rooms, the supply air moves with a uniform velocity (like a plug) in one direction taking the contaminants with it. The air may be supplied from the floor and exhausted from the ceiling or vice-versa.

Localized cooling is resorted to in large shopfloors near the location of workers. Similarly, localized ventilation may remove contaminants from a work-station.

If contamination sources are localized, then these can be removed before they spread into the room by properly locating exhaust fans or by judiciously locating supply air diffusers and return air inlets. Care is required, since air cannot be directed by suction alone, it can spread before it moves towards the suction (exhaust) fan.

Air cleaning

If the outdoor air is polluted, it may have to be cleaned. Also, to reduce the outdoor air requirement, the return air may be cleaned before being cooled/heated. Contaminants may be removed from the air stream by absorption, by physical adsorption, by chemisorption, by catalyst and by combustion. Some of these processes may remove the particulate matter as well. Absorbers are the life-support systems in space vehicles and submarines. Air washers used for humidification may remove some gases and particulate matter as well. Water with some reagents added to it, or some liquids, may be used for absorption. The quality of contaminants in the liquid must be monitored.

Adsorption involves adhesion of molecules to the surface where they accumulate in metastable liquid state unlike absorption, in which they are dissolved or made to react with a substance. Adsorbents have typically large surface and pore areas. Activated charcoal is widely used as an adsorbent. It is not effective with light gases like ammonia and ethylene.

Chemisorption unlike adsorption involves surface binding by chemical reaction. It is a monomolecular layer phenomenon. Only certain contaminants will be acted upon by a given chemisorber. It improves with increase in temperature. It is not exothermic but may require heating. It is not reversible; the presence of water improves its efficiency.

The action of a catalyst is similar to chemisorption in as much as the reaction occurs at the surface. However, a catalyst just promotes the reaction and the chemical composition of the catalyst does not change, as a result it can be used for a long time. A catalyst can break down the contaminant molecules into smaller molecules or it can combine with oxygen. Catalytic combustion is also possible at lower temperatures as is done in automobile exhaust.

Odours are a cause of nuisance; they persist even when all contaminants are reduced to acceptable limits. In such a case, masking is resorted . This involves introduction of pleasant odours to cover or mask the offending odours.

Removal of particulate matter

Particles are present in various shapes, sizes, and concentrations. Different methods are required for removing different sizes of particles. Filters of various types are used. Smaller particles are difficult to remove and require special and expensive filters.

The mechanisms like straining, direct interception, inertial deposition, diffusion and electrostatic precipitation are used for separation of particles. The filters may be of the following types:

(i) Fibrous-media unit filters
(ii) Renewable media filters
(iii) Electric air cleaners
(iv) Combination air cleaners.

The selection criterion for a filter is the degree of cleanliness required and the size of particles to be removed. The operating cost and initial cost increases as the size of particles decreases. The three important parameters that can be used to compare the performance of filters are:

(i) Efficiency
(ii) Air flow resistance
(iii) Dust-holding capacity.

Efficiency is the fraction of particulate matter removed by a filter. If an air stream with C_i of 200 μg/m^3 is passed through a filter of efficiency E_f = 60%. Then 0.6 × 200 = 120 μg/m^3 will be removed by the filter and $(1 - E_f)C_i$ = 80 μg/m^3 will be left. Smaller particles are most difficult to clean. The efficiency of a dry filter increases with dust load since the capture area increases. Air flow resistance is the total drop in pressure of the dust-laden gas as it flows through the filter. The pressure drop increases as the square of the volume flow rate. If the rated flow rate is Q_r and the rated pressure drop is Δp_r, then at volume flow rate Q, the pressure drop is given by

$$\Delta p = \Delta p_r \, (Q_r/Q)^2$$

The dust holding capacity is defined at the rated volume flow rate. If the volume flow rate is increased beyond the rated value, the dust holding capacity will reduce. The efficiency of the cleaner will decrease and the pressure drop will increase if the dust holding capacity of the filter is exceeded (filter is not cleaned).

Air cleaning has been used for many years to improve the indoor air quality to protect heat exchangers from dust accumulation, and to remove the dust from recirculating in the room. The emphasis nowadays is to economically satisfy the IAQ norms.

The performance of an air cleaning system can be studied by taking the example of a room in which, infiltration, exfiltration and exhaust are ignored. The ventilation efficiency is $E_{v,}$ which is equal to $1 - S$, S being the room bypass factor. This represents the fraction of the supply air delivered to the occupied zone. This is not the same as the outdoor air use E_o. The fraction of the return air Q_r (m^3/s) recirculated is R, that is, RQ_r (m^3/s) is recirculated and $Q_r(1 - R)$ (m^3/s) is exhausted and an equal amount of fresh air is actually taken in. However, in this case the outdoor air quantity taken in is Q_{vo} m^3/s. There can be two locations of the filter of efficiency E_f, location A is before the mixing of fresh air with the recirculated air, while location B is after the mixing. In polluted areas the outdoor air has to be filtered as done in location B, or there can be a separate filter for the outdoor air and location A can then be used.

Filter location A:

Concentration of the pollutants leaving the room	$= C_s$ (kg/m^3)	
Concentration of the pollutants in outdoor air	$= C_o$ (kg/m^3)	
Rate of addition of pollutants in the room	$= \dot{N}$ kg/s	
Ventilation efficiency	$= E_v$	
Volume flow rate of fresh air entering the occupied zone and leaving with concentration C_s	$= E_v \, Q_o$ (m^3/s)	
Volume flow rate of recirculated air entering the occupied zone and leaving with concentration C_s	$= E_v \, RQ_r$ (m^3/s)	
The concentration of pollutants in recirculated air after it has passed through filter of efficiency E_f	$= (1 - E_f)C_s$	
$\therefore$ Increase in pollutants in fresh air leaving the room	$= E_v Q_o(C_s - C_o)$	(19.75)

$\therefore$ Increase in pollutants in recirculated air leaving the room $= E_v R Q_r [C_s - (1 - E_f) C_s]$

$$= E_v R Q_r E f C_s \tag{19.76}$$

The increase in Eqs. (19.75) and (19.76) is due to generation rate $\dot{N}$ in the room. Hence,

$$E_v Q_o (C_s - C_o) + E_v R Q_r E f C_s = \dot{N}$$

$$\therefore \quad Q_o = \frac{\dot{N} - E_v R Q_r E_f C_s}{E_v (C_s - C_o)} \tag{19.77}$$

Filter location B:

In this case the concentration of pollutants after the filter reduces to: $C_o(1 - E_f)$

$\therefore$ Increase in pollutants in fresh air leaving the room = $E_v Q_o (C_s - C_o(1 - E_f))$

$$\therefore \quad E_v Q_o (C_s - C_o (1 - E_f)) + E_v R Q_r E_f C_s = \dot{N}$$

$$\therefore \quad Q_o = \frac{\dot{N} - E_v R Q_r E_f C_s}{E_v (C_s - C_o (1 - E_f))} \tag{19.78}$$

EXAMPLE 19.4 In a constant volume air conditioning system, the filter used has 70% efficiency for environmental tobacco smoke (ETS). It is located in the return air path before the filter. This maintains the ETS level below 200 μg/m^3 in the occupied zone. There are seven occupants producing 125 mg/min of ETS. Fresh air at the rate of 10 litres/s per person is supplied. Ventilation efficiency is 80%. The outdoor air is free of ETS. Determine the total supply air flow rate and check if it is reasonable.

Solution:

N = 1250 mg/min, E_v = 0.8, E_f = 0.7, C_s = 200 μg/m^3, C_o= 0,

Q_o = 10 × 10 × 60 litres/min = 6 m^3/min

From Eq. (19.78),

$$Q_o E_v (C_s - C_o) = \dot{N} - E_v R Q_r E_f C_s$$

$$\therefore \quad 6.0 \times 0.8(200 - 0) = 1250 - 0.8(0.7)\, RQ_r\, (200)$$

$$\therefore \quad RQ_r = 0.259 \text{ m}^3/\text{min}$$

Total supply air flow rate for 10 persons = $Q_o + RQ_r$ = 6.0 + 2.59 = 8.59 cmm

Total supply air flow rate for seven persons = $8.59 \times \frac{7}{10} = 6.0$ cmm

In a room of 100 m^2 floor area, seven persons can be accommodated in an office space. A conservative estimate of cooling capacity for 100 m^2 is 6.5 TR and the supply air flow rate required is 65 cmm. The volume flow rate can be safely increased and a filter of 10% efficiency will maintain the required concentration.

EXAMPLE 19.5 In Example 19.4 if the filter is located at location B, that is, after mixing of fresh air, then determine the total volume flow rate.

Solution:

From Eq. (19.78),

$$-RQ_r(0.8)(0.7) \times 200 + 1250 - 6.0(0.8)[200 - (1.0 - 0.7) \times 0.0]$$

$\therefore$ $RQ_r = 0.259$ m^3/min which is the same result as in previous example.

19.14 INSIDE DESIGN CONDITIONS

The choice of inside design condition depends upon physiological conditions and economic factors. The inside design condition depends upon the outdoor design condition, the clothing worn by the occupants, the level of activity and the period of occupancy. As the summer passes, the temperature may be allowed to fall to 20°C and humidity corresponding to 2°C dew point. There is some evidence that incidence of common cold is less if the working environment has relative humidity ≥ 50%.

It is recommended that a dry-bulb-temperature of 5°C to 20°C less than the outdoor temperature should be selected with preferred value of 25°C and 50% to 60% relative humidity. During winter, the inside temperature of 21°C may be acceptable. The inside design temperature has significant effect on heat gain, plant capacity, capital cost of the plant and the running cost, and ultimately the energy consumption. The chosen value of outdoor dry-bulb temperature will also affect the system performance. Relaxation of t_o may not maintain the inside design temperature for a short period of peak summer, but it will involve lower overall cost.

An ideal inside design condition should meet the following requirements:

(i) The indoor design conditions must fall within the summer and winter comfort zones shown in Figure 19.5.

(ii) The relative humidity should be greater than 40% and less than 60%,and never exceed 70%.

(iii) Average velocity should be less than 0.15 m/s. However, for dry-bulb temperatures greater than 26°C, higher velocities may be acceptable.

(iv) The dew point should be greater than 2°C.

(v) The temperature difference between feet and head should be as small as possible, normally not exceeding 1.5°C and never more than 3°C.

(vi) The floor temperature should be greater than 17°C but less than 26°C.

(vii) The radiant temperature asymmetry should not be more than 5°C vertically and 10°C horizontally.

(viii) Carbon dioxide content should not exceed 0.1%.

ASHRAE Standard 55 gives the indoor design conditions for comfort in terms of *operative temperature* and *effective temperature*.

As stated earlier, the *operative temperature* is the average of the mean radiant temperature and dry-bulb temperature. It is referred to as *adjusted dry-bulb temperature* as well. It is the uniform temperature of an imaginary enclosure in which an individual exchanges the same heat transfer by convection and radiation as in the actual environment. Vernon's globe thermometer is most commonly used to determine the mean radiant temperature. This thermometer consists

of a hollow sphere of 152.4 mm diameter and flat black paint coating, and a thermocouple or a thermometer at its centre. The thermal equilibrium between the surroundings and the sphere by convection and radiation heat transfer gives a steady-state temperature, called globe temperature t_g. The mean radiant temperature is defined as a combination of air velocity dry-bulb temperature and globe temperature as follows:

$$T_{mrt}^4 = T_g^4 + CV^{0.5}(T_g - T)$$

where V is velocity in m/s and $C = 0.247 \times 10^9$. The operative temperature $t_o = (t_{mrt} + t)/2$.

The effective temperature is the temperature of an environment at 50% relative humidity that results in the same total heat loss from the skin as in the actual environment. This is a composite of temperature and humidity. Various combinations of temperature and relative humidity can result in the same effective temperature. All such combinations will result in the same heat loss from the skin. This depends upon the clothing and activity. Hence universal charts for its use cannot be generated. A *Standard Effective Temperature* has been defined for typical indoor conditions. The conditions for this are as follows:

Clothing insulation = 0.6, Moisture permeability index = 0.4, Metabolic activity = 1.0 met, air velocity < 0.1 m/s and ambient temperature = mean radiant temperature.

Based upon 10% dissatisfied criterion (i.e. Predicted Percentage Dissatisfied, PPD), the acceptable ranges of operative temperatures and humidity for people in typical summer and winter clothing during light and sedentary activity (≤ 1.2 met) have been given in Figure 19.5. The comfort zone defined therein is as follows.

Winter: Operative temperature t_o = 20°C to 23.5°C at wet-bulb temperature of 18°C. The bottom boundary of the comfort zone is at dew point of 2°C and operative temperature of 20.5°C to 24.5°C. The slanting side boundaries are between the effective temperatures of 20°C and 23.5°C.

Summer: Operative temperature t_o = 22.5°C to 26°C at 20°C wet-bulb temperature and 23.5°C to 27°C at 2°C dew point temperature (lower boundary of comfort zone in Figure 19.3) The slanting side boundaries of summer zone correspond to 23°C and 26°C effective temperature lines.

It must be noted that the upper and lower humidity lines are based upon considerations of dry skin, eye irritation, respiratory health problems, microbial growth, maintenance of furniture, and other moisture-related effects. For higher relative humidity, one must take care to avoid condensation on the building surfaces and materials by controlling those surface temperatures.

It is obvious that the winter and summer comfort zones overlap. ASHRAE Standard 55–1992 recommends the following range of operative temperatures (Table 19.8).

Table 19.8 Operative comfort temperatures for sedentary or slightly active people ((≤ 1.2 met) at 50% relative humidity

Season	*Description of typical clothing*	I_{cl} (clo)	*Operative temperature range* (°C)	*Optimum operative temperature* (°C)
Winter	Heavy slacks, long sleeve shirt, and sweater	0.9	20–23.5	22
Summer	Light slacks and short sleeve shirt	0.5	23–26	24.5
	Minimal	0.05	26–29	27

In India it is customary to take 25°C (or 25.5°C) and 50% RH in summer for optimum comfort. This corresponds to modified effective temperature of 25.2°C. In winter in India 21°C at 50% RH is taken for optimum comfort. This corresponds to modified effective temperature of 19.9°C. The current practice and the recommendation of the Defence Institute of Physiology and Allied Sciences, Chennai are as follows (Table 19.9).

TABLE 19.9 Inside design conditions for human comfort (trade practice)

Season	*Climate*	*Optimum inside range* (°C) DBT at 50% RH		*Inside design conditions*	
		Range	*Optimum*	*DBT* (°C)	*RH* (%)
Summer	Hot and dry (arid climate)	23.9–26.7	23.9	25.0 ± 1	50 ± 5
	Hot and humid	23.9–26.7	24.2	25.5 ± 1	50 ± +5
Winter	All	21–23.6	22	21	50 ± 5
Monsoon	All	23.9–26.7	24.2	25.5 ± 1	50 ± 5

There is economic sense in not adopting too low a temperature inside during summer when occupancy is short term, e.g. in a shop, foyer of theatre. A foyer at 28°C when the outside temperature is 43°C gives an immediate impression (fading with time) of comfort upon entry. The worst the outdoor condition the more will be the feeling of comfort by a slight decrease in temperature. On the other hand, an auditorium should be at 22.5°C because audience is present for several hours during which 25°C would be high for western dress code. Table 19.10 gives the inside design conditions for summer comfort as a function of outdoor air temperature and the period of stay. This is an old recommendation and may be used as a guideline. Table 19.11 gives the inside design conditions for winter comfort in various places.

Table 19.10 Inside design conditions for summer comfort

Outdoor design temp.	*Occupancy over 40 minutes*			*Occupancy under 40 minutes*		
DBT (°C)	DBT	WBT	RH	DBT	WBT	RH
26.7	23.9	18.3	60	24.4	18.9	61
	25.0	17.2	67	25.5	17.8	47
	24.1	16.1	35	26.7	16.7	36
29.4	24.4	18.9	61	25.0	19.4	61
	25.6	17.8	67	26.1	18.3	48
	26.7	16.7	36	27.2	17.2	36
32.2	25.0	19.4	61	25.6	20.6	64
	26.1	18.3	48	26.7	19.4	52
	27.2	17.2	36	27.3	16.3	40

(*Contd.*)

Table 19.10 Inside design conditions for summer comfort (contd.)

Outdoor design temp.	*Occupancy over 40 minutes*			*Occupancy under 40 minutes*		
DBT (°C)	DBT	WBT	RH	DBT	WBT	RH
35.0	25.6	20.6	64	26.1	21.1	65
	26.7	19.4	52	27.2	20.0	52
	27.8	18.3	40	28.3	18.9	41
37.8	26.1	21.1	65	27.2	21.7	63
	27.2	20.0	52	28.3	20.6	50
	28.3	18.9	41	29.4	19.4	38
40.6 and above	26.7	21.7	65	27.2	22.2	65
	27.8	20.6	52	28.3	21.1	54
	28.9	19.4	42	29.4	20.0	21

Table 19.11 Indoor design conditions for winter comfort

Type of space	*Temparature range* (°C)
Auditoriums	22–23.5
Ball rooms	20–22
Bathrooms (General)	23.5–26.7
FACTORIES (Light work)	15.5–20
(Heavy work)	14.5–20
Homes	22–24.5
HOSPITALS (Operating room)	21–25
(Patients room)	23–24.5
Hotel bedrooms & bathrooms	22–24.5
Kitchens and laundries	19
Public buildings	21–23.5
Stores	21–23.5
Theater lounges	21
Toilets	21

19.15 OUTDOOR DESIGN CONDITIONS

The outdoor temperature varies almost sinusoidally throughout the day. It is minimum one hour before the sunrise, say at 4:30 AM solar time and is maximum at 3:00 PM solar time. During the night, earth looses energy to the sky by long wavelength radiation. According to one model the sky is considered to be a blackbody at absolute zero temperature. The radiation leaving the surface is absorbed by water vapour present in the moist air, the absorption coefficient is given by $K = 0.56 - 0.08\sqrt{p_{ws}}$ where p_{ws} is the saturation pressure of water vapour in millibar. Further, if C

is the cloud cover factor and $F_{ss} = 0.5(1 + \cos \theta)$, the shape factor between the surface and the sky, the long wavelength can be expressed as

$$I_{lw} = 5.77\ F_{ss}\ (1 - C)\ K\ (T_s/100)^4 \tag{19.79}$$

For example for a surface at 15°C, $p_{ws} = 1.71$ kPa = 17.1 milibar $\therefore$ $K = 0.229$
Assuming $F_{ss} = 1$ and $C = 0.0$,

$$I_{lw} = 5.77(0.229)(2.88)^4 = 90.9\ \text{W/m}^2$$

The earth is at its lowest temperature just before dawn by loosing energy to a clear sky at night time. As the sun rises it starts to warm up the earth surface. This heat is transferred to the layer immediate next to earth's surface and is then convected upwards. The temperature of the air continues to rise since the upper layer of earth continues to convect the heat stored in it even in the afternoon hours. The maximum temperature occurs between 2 to 3 PM solar time. The variation of temperature is almost sinusoidal and may be expressed as

$$t_o = t_{15} - D[1 - \sin\ (\theta\pi - 9\pi)/12] \tag{19.80}$$

where, D is the daily range and t_{15} is the temperature at 15 hours solar time, θ being the hour.

In India the temperature is at its peak during the last week of June just before the pre-monsoon showers.

In the absence of weather change, humidity ratio may be assumed to be constant throughout the day until the air is cooled to its dew point at night time. The relative humidity is maximum during the morning hours and minimum during the afternoon hours. This can be seen along a constant humidity ratio line on the psychometric chart. As the temperature increases the capacity of the air to hold water vapour (p_{ws} and W_s) increases, as a result the relative humidity deceases during the afternoon hours. Evaporation of water from various water sources and evaporation from vegetation has little effect. Similarly, condensation due to nocturnal cooling also has little effect. In case the dew occurs, the relative humidity approaches 100%. The wet-bulb temperature and the dew-point temperature remain almost constant throughout the day. There is a wide variation in dry-bulb temperature and relative humidity round the year and from place to place depending upon the geographical location and height above sea level. In such a case, a judicious choice has to be made regarding the outdoor design condition. If one chooses the highest possible temperature that ever occurred in a place, then the plant will have excess design capacity during most of the year and it is not a sound economical practice. Choosing a lower temperature has the effect of reducing the capital cost but it will lead to dissatisfaction during peak summer hours.

Cities are usually warmer than the surrounding country side since the mass of the congregation of buildings absorbs solar energy during day time and releases it during the evening hours. The climate of the region, local morphology, thermal properties of the congregation of buildings and surfaced roads—all influence the temperature in the urban areas. Each building in an urban complex has its own mini-climate. The mean annual temperatures are usually higher by 0.5 to 1 K than their surroundings. It has been observed that in some cities the evening dry-bulb temperature during peak summer may be up to 5 K higher than that of the surroundings.

One has to take into account the temperature rise due to global warming. Global warming forecasts vary considerably but something like 0.25 K rise in a decade is acceptable. Considering a life of 60 years on the average for the building an on the average a life of 25 years for the air conditioning plant, a rise of 0.5 K seems to be reasonable.

Hourly temperature, wind velocity, relative humidity and solar radiation data is recorded in many meteorological centres throughout the world. ASHRAE has considered this data for cities of USA and Canada for the four summer months, namely June to September, a total of 2928 hours. They have reported the frequency of occurrence of 1%, 2.5%, 5% and 10% temperature. A temperature corresponding to 1% record say 35°C means that the temperature at the location is equal to more than 35°C for 2928 × 1/100 = 29 hours of the summer months. Similarly the 5% record value will mean a temperature which is equaled or exceeded for 146 hours of summer. Obviously the 5% recorded temperature will be lower than that of the 1% value. The recommendation is that outdoor design temperature should be chosen according to the building type. For light construction 1% value should be chosen, for medium construction 2.5% value, and for heavy construction 5% value should be chosen. For very heavy construction 10% value should be resorted to.

The outside design temperature may be taken as average of daily maximum temperatures of the summer months for 30 years. These temperatures are given in Table 19.12 for various cities of India. The relative humidity given in this table corresponds to the hour when the maximum temperature occurs. This is rather old data and requires modification.

Table 19.12 Outdoor design conditions

Place	*Latitude north*		*Latitude east*		*Summer*		*Monsoon*		*Winter*	
					DBT	RH	DBT	RH	DBT	RH
	deg	min	deg	min	°C	%	°C	%	°C	%
Agra	27	10	78	02	42.5	20	35.5	58	9.0	65
Ahmedabad	23	02	72	35	43.5	25	32.5	82	15.5	45
Ahmed Nagar	19	03			42.2	20	38.3	60	10.0	55
Ajmer	26	27	74	37	42.0	20	34.0	60	7.0	45
Aligarh	27	32			42.2	20	37.5	58	8.9	67
Allahbad	25	27	81	44	43.5	20	35.0	58	9.0	85
Ambala	33	23	76	46	43.5	20	35.0	60	7.0	70
Amritsar					43.0	20	33.0	55		
Asansol	23	41	86	57	42.5	26	32.5	85	11.0	50
Auragabad	19	53			42.0	25	32.5	65	12.5	60
Bangalore	12	58	77	35	25.5	45	28.0	82	14.5	78
Baroda	22	18	73	15	43.5	25	31.1	68	15.6	58
Belgaum	15	30			37.8	35	27.8	80	14.4	71
Bellary	15	05			40.6	28	34.4	50	18.3	70
Bhopal	23	16	77	25	41.0	20	33.5	70	7.0	50
Bhubaneswar	20	15			38.0	45	32.5	85	13.5	55
Calicut	11	15			35.5	55	29.5	88	22.0	70
Chennai	13	04	80	15	40.0	40	28.5	88	18.0	60
Cochin	09	58	76	14	35.0	58	29.5	88	22.0	70
Coimbatore	11	00	76	58	39.5	40	28.5	88	18.0	60

(*Contd.*)

Table 19.12 Table 19.12 Outdoor design conditions (contd.)

Place	*Latitude north*		*Latitude east*		*Summer*		*Monsoon*		*Winter*	
					DBT	RH	DBT	RH	DBT	RH
	deg	min	deg	min	°C	%	°C	%	°C	%
Cuttack	20	29	85	52	41.0	40	32.5	85	13.0	20
Dehradun	30	19	78	02	40.5	25	32.5	65	5.5	70
Delhi	28	53	77	12	43.5	20	35.0	60	7.0	70
Durgapur					42.5	26	32.5	85	11.0	50
Guwahati	26	11	91	45	32.5	60	31.0	80	7.5	26
Gaya	24	49	85	01	43.5	18	32.5	78	10.0	60
Goa	15	25			32.0	70	29.0	86	18.5	72
Hydrabad	17	26	78	27	42.5	28	29.5	82	12.5	60
Indore	22	43	75	54	41.5	30	32.0	70	10.0	65
Jabalpur	23	16			43.0	25	34.0	70	7.0	75
Jaipur	26	55	75	50	43.5	20	35.0	50	7.5	65
Jamshedpur	22	49	86	11	43.5	87	32.5	78	10.0	75
Jodhpur	26	18	73	01	43.5	23	35.0	52	7.5	52
Kanpur	26	26	80	22	43.0	23	36.0	58	7.0	80
Kathmandu	27	42	85	12	29.5	65	24.5	80	7.0	78
Kolkata	22	32	88	20	38.0	50	33.0	85	9.0	22
Lucknow	26	52	80	56	43.0	26	34.5	64	9.0	65
Madurai	09	55	78	07	38.5	35	34.5	50	20.0	72
Mumbai	18	54	72	49	35.0	60	28.5	88	18.0	60
Mysore	12	18	76	42	38.0	38	29.5	69	19.0	70
Nagpur	21	09	79	07	44.0	18	29.5	82	15.5	58
Ooty	11	24			23.0	45	19.0	62	3.0	60
Patna	25	37	85	10	40.0	26	32.5	78	10.0	60
Pune	18	32	73	51	40.0	28	28.5	82	10.0	50
Raipur	21	14	81	39	43.5	22	33.5	68	10.0	70
Ranchi	23	23	85	21	38.0	46	29.0	76	9.0	60
Roorkee	29	51	77	53	41.0	25	34.0	77	4.5	85
Rourkela	21	28			43.5	87	30.5	80	12.0	41
Shillong	25	34	91	53	29.5	50	23.5	82	3.0	50
Shimla	31	06	77	10	25.0	35	21.5	88	-1.0	05
Tiruchirapalli	10	49	78	42	40.0	40	35.0	55	21.0	80
Trivendrum	08	29	76	57	33.5	60	29.5	80	22.0	70
Varanasi	25	18	83	01	43.0	25	34.5	65	10.0	80
Vellore	12	55	78	09	40.0	45	35.5	62	13.0	88
Vijayawada	16	33			43.5	30	34.5	60	12.5	65
Visakhapatnam	17	42	82	18	33.5	64	30.5	80	18.0	60

Reliable data is not available for Indian cities. The various air conditioning companies use slightly different design conditions. The Bureau of Indian Standards (BIS) in collaboration with Central Building Research Institute (CBRI) Roorkee and Indian Meteorological Department

considered the hourly record of temperature and relative humidity for 10 years during the summer months of April, May and June, that is, a total of 2184 hours. The values were calculated for 10%, 5%, 2.5% and 1% occurrence. These values were reported in IS-7806-1975 for only sixteen cities of India. A 5% occurrence would mean a temperature, which is equaled or exceeded for 2184 × 5/100 = 109 hours. These values are given for sixteen Indian cities in Table 19.13.

Table 19.13 Outside design conditions for summer

City	DBT (°C)				WBT (°C)			
	1%	2.5%	5%	10%	1%	2.5%	5%	10%
Ahmedabad	42.8	41.7	40.7	39.5	27.6	27.2	26.9	26.4
Amritsar	42.5	41.5	40.3	38.4	27.9	26.9	26.3	25.3
Bhopal	41.7	40.8	39.8	38.5	25.3	24.8	24.4	23.8
Chennai	39.2	37.8	36.9	35.5	28.5	28.2	27.8	27.4
Coimbatore	36.7	35.9	34.9	33.7	28.3	27.4	26.7	25.9
Delhi	43.0	42.9	41.4	40.3	28.1	27.2	26.4	25.8
Hydrabad	39.5	38.7	37.9	36.7	25.3	24.4	23.9	23.5
Jodhpur	43.5	42.5	41.3	40.0	27.9	27.2	26.5	25.8
Kolkata	39.5	38.3	37.4	35.6	29.3	29.2	28.8	28.4
Lucknow	42.8	41.9	41.0	39.5	28.3	27.7	27.2	26.5
Mumbai	34.5	33.8	33.6	32.8	28.4	28.0	27.8	27.4
Nagpur	42.9	42.0	41.1	39.9	27.5	26.2	25.6	25.1
Patna	42.4	41.1	39.9	38.3	28.0	27.8	27.4	27.1
Roorkee	42.5	41.4	40.6	39.2	27.8	26.9	26.1	25.6
Trivendrum	32.9	32.4	31.8	31.2	27.2	26.9	26.7	26.4
Visakhapatnam	38.4	37.0	36.0	35.1	30.4	29.7	29.3	28.8

Similarly for winter, 99%, 97.5% and 95% values have been reported by ASHRAE. A 97.5% value means that the outdoor temperature equals or exceeds this value for 97.5% hours during the coldest month. Table 19.14 gives the mean of annual extremes, 99% and 97.5% values for some of the Indian cities. The daily range DR is also reported in this table. The mean of annual extremes is seen to be the lowest temperature in this table. This is recommended for an uninsulated building with low heat capacity, more than normal glass area and occupied during the coldest period of the day. The 99% value is recommended for buildings with moderate heat capacity, some internal heat loads and day time occupancy. For massive buildings the 97.5% value is recommended.

For cooling load the peak load conditions correspond to maximum solar load rather than the maximum outdoor dry-bulb temperature. The cooling load will not be the same for a building of same size and orientation in Delhi and Chennai. It changes with the orientation of the building. Peak solar load for the east facing room may occur at 8:00 AM solar time while for the west facing room it may occur at 4:00 PM solar time. Thus heat gain calculations may have to be done for different times of the day and different days of the year to fix the maximum cooling capacity requirement.

Table 19.14 Winter outside design conditions

City	*Winter*			*Summer*
	Mean of annual extremes	99%	97.5%	*Outdoor daily range*
Ahemdabad	0.4	11.7	13.3	15.56
Bangalore	11.7	13.3	14.4	14.44
Chennai	16.1	17.8	18.9	10.59
Kolkata	9.4	11.1	12.1	12.22
Mumbai	16.7	18.3	19.4	7.22
Nagpur	7.2	10.6	12.2	16.67
New Delhi	1.7	3.9	5.0	14.44

Table 19.15 gives the average wind velocity and the prevailing wind direction during summer, winter and monsoon months for some of the Indian cities.

Table 19.15 Average wind velocities for Indian cities (km/h)

Place	*Summer*			*Monsoon*			*Winter*		
		Direction			*Direction*			*Direction*	
	Velocity	*Morn.*	*Eve.*	*Velocity*	*Morn.*	*Eve.*	*Velocity*	*Morn.*	*Eve.*
Agra	7.3	W/SW	NW/W	6.0	W/E	W/SW	4.4	W/C	NW/N
Ahemdabad	8.0	SW/NW	W/SW	6.8	SW/W	SW/W	6.0	NE/E	NW/NE
Ajmer	10.5	W/SW	W/SW	8.3	W/SW	W/SW	2.6	C/NW	C/W
Allahabad	13.4	W/E	NW/NW	23.7	W/E	W/E	7.4	C/W	C/W
Ambala	6.0	SE/C	NW/W	3.7	C/SE	SE/NW	4.1	C/NW	NW/C
Asansol	9.2	E/SE	E/SE	7.6	E/SE	E/NE	5.4	NM/W	NW/N
Bangalore	8.9	W/SW	NW/W	11.8	W/SW	W/NW	8.3	E/NE	E/NE
Baroda	9.4	SW/W	SW/W	7.9	SW/W	SW/W	4.4	C/NE	C/N
Bhopal	8.9	W/NW	W/NW	8.2	W/NW	W/NW	3.4	W/NW	W/NW
Chennai	19.0	S/SW	SE/S	17.3	SW/W	SE/E	17.7	NW/NE	NE/N
Cochin	8.6	NE/E	NW/W	8.1	C/NE	NW/W	6.6	NE/E	W/NW
Coimbatore	6.2	SW/C	SW/S	8.7	SW/C	SW/S	4.4	NE/E	E/NE
Cuttack	6.2	SW/C	SW/S	3.6	C/SW	C/SW	1.8	C/W	C/SE
Darjeeling	7.8	C/W		5.5	C/E		3.3	C/E	
Dehradun	3.7	C/W	SW/W	2.3	C/SE	SW/W	2.5	C/E	W/C
Delhi	6.8	W/SE	NW/W	5.0	W/SE	E/W	4.6	W/C	NW/W
Guwahati	3.1	C/NE	NE/E	2.1	C/NE	W/NE	2.0	C/NE	C/NE
Gaya	9.7	NE/C	NE/N	8.6	NE/C	E/SE	5.2	C/W	NW/N
Hydrabad	10.3	W/C	NW/W	13.9	W/C	W/NW	5.2	C/SE	E/SE
Indore	9.1	W/NW	W/NW	8.2	W/NW	W/W	3.3	C/NE	NE/N

(*Contd.*)

Table 19.15 Average wind velocities for Indian cities (km/h) (contd.)

Place	*Summer*			*Monsoon*			*Winter*		
		Direction			*Direction*			*Direction*	
	Velocity	*Morn.*	*Eve.*	*Velocity*	*Morn.*	*Eve.*	*Velocity*	*Morn.*	*Eve.*
Jabalpur	4.9	W/SW	SW/NW	5.0	W/SW	SW/W	2.3	C/SE	C/NE
Jaipur	9.7	W/NW	W/NW	7.3	W/NW	SW/W	5.7	NW/E	NW/C
Jamshedpur	6.8	W/C		6.5	W/E		2.4	C/W	
Jodhpur	17.3	SW/W	SW/W	14.7	SW/W	SW/S	11.1	NW/C	NE/N
Kanpur	12.8	E/W	NW/W	10.3	E/SW	E/W	3.7	C/W	NW/W
Kathmandu	2.2			1.5			2.0		
Kolkata	8.1	S/SW	S/SW	5.6	S/SW	S/SW	3.3	C/N	C/NW
Lucknow	4.1	C/E	C/E	3.1	C/E	C/E	2.1	C/W	C/W
Madurai	7.3	NW/W	W/E	7.0	NW/W	W/SW	6.2	NE/N	E/NE
Mumbai	10.8	NW/W	NW/W	16.9	W/SW	W/NW	10.7	NE/E	NW/W
Mysore	9.9	W/SW	WS/W	12.4	SW/W	W/SW	9.5	NE/E	E/NE
Nagpur	10.7	NW/N	W/NW	9.2	W/SW	W/SW	5.5	N/NE	E/C
Ooty	4.4	C/E	NE/C	8.5	W/NW	W/SW	5.0	C/SE	C/NE
Patna	8.3	E/W	NE/E	6.3	E/C	E/NE	3.6	C/SW	W/C
Pune	14.7	W/NW	W/NW	14.4	W/SW	W/NW	6.0	C/S	C/W
Raipur	8.3	SW/W	C/W	8.7	SW/W	W/SW	2.9	C/NE	C/NE
Ranchi	7.9	SW/S	NW/E	7.4	W/SW	NW/E	5.7	NW/C	NW/N
Roorkee	5.2	C/SE	NW/SE	3.3	C/S	SE/NW	2.9	C/NW	NW/C
Shillong	6.0	C/SW	C/SW	2.8	C/SE	C/S	2.5	C/NW	C/N
Shimla	6.2	C/NE	SW/NW	3.6	C/N	C/NE	6.0	S/SE	S/SE
Tiruchirapally	7.4	W/SW	W/NW	10.0	W/SW	W/NW	5.5	C/N	NE/E
Trivendrum	8.3	NW/N	W/NW	10.7	NW/N	NW/W	4.6	C/NE	SW/W
Varanasi	5.7	E/SE	NW/N	6.3	C/E	NE/N	3.8	C/SW	W/NE
Vellore	6.2	C/NW	SW/NW	6.5	W/NW	W/SW	3.9	C/NE	NE/E
Visakhapatnam	9.1	SW/W	SW/S	7.4	SW/S	SW/W	4.7	W/NE	E/SE

Note: C denotes Calm

REFERENCES

ANSI/ASHRAE Standard 62-1989, Ventilation for Acceptable Indoor Air Quality, American Society of Heating Refrigerating and Air Conditioning Engineers, Atlanta, Inc., GA, 1989.

ANSI/ASHRAE, Standard 55-1992, *Thermal Environmental Conditions for Human Occupancy*, American Society of Heading, Refrigerating and Air Conditioning Engineers, Inc., Atlanta, GA, 1992.

ASHRAE Handbook of Fundamentals Volume, American Society of Heating, Refrigerating and Air Conditioning Engineers, Inc., Atlanta, 1997.

Fanger, P.O. (1970): *Thermal Comfort Analysis and Applications in Environmental Engineering*, McGraw-Hill, New York.

Fanger, P.O. (1982): *Thermal Comfort*, R.E. Kreiger Publishing.

Fanger, P.O., A.K. Mclikov, H. Hanzawa and J. Ring (1988): Air Turbulence and Sensation of Draught, *Energy and Building*, 12, 21–39, Elsevier, Amsterdam.

ISO Standard 7730 (1984): *Moderate Thermal Environments—Determination of PMV and PPD indicies* and *Specifications of the Conditions for Thermal Comfort*.

REVIEW QUESTIONS

1. Briefly describe the different modes of heat rejection from human body.
2. Briefly describe the different modes of energy exchange between human body and the environment.
3. What are human body's thermoregulatory mechanisms against cold and against heat ?
4. What are the values of various heat transfer coefficients used to estimate the heat transfer from the body ?
5. Explain the significance of environmental indices used in comfort studies.
6. What is effective temperature? How does it account for human comfort ?
7. What information is provided by comfort chart?
8. How does the PMV index predict thermal comfort in a given thermal environment ?
9. How is Standard Effective Temperature (SET) defined ? Discuss.
10. Enumerate the factors that affect comfort. Briefly explain each factor.
11. Briefly describe the sources of indoor air pollution.
12. What do you mean by sick building syndrome? What are the factors that affect IAQ in a building?
13. What are the methods used to maintain a proper indoor air quality?
14. Enumerate all the conditions and factors governing the choice of inside design conditions.
15. Enumerate all the conditions and factors governing the selection of outdoor design conditions, and discuss the typical summer design conditions for major Indian cities.

20

Solar Radiation

LEARNING OBJECTIVES

After studying this chapter the student should be able to:

1. Understand the importance of solar radiation in air conditioning calculations.
2. Explain the significance of the four important locations of the earth during its orbital motion around the sun.
3. Define solar angles, namely longitude, latitude, declination, and hour angle.
4. Define derived solar angles and find their relations with solar angles.
5. Explain direct solar radiation, sky radiation and reflected radiation.
6. Calculate direct, diffuse and reflected components of solar radiation on the earth's surface using ASHRAE clear sky model.
7. Explain the effect of external shading to reduce solar radiation entering an air-conditioned space.

20.1 INTRODUCTION

The temperature, the relative humidity, the wind velocity and the intensity of solar radiation at a place constitute the *thermal environment* of the place. The thermal environment depends upon solar radiation and the meteorological effects. The location and physical influences such as topography, ocean currents also affect the climate. The meteorological effects are, in general, influenced by sun and hence, ultimately the thermal environment is determined by the solar energy alone. This chapter deals with the various aspects of solar radiation.

20.2 SUN

The mass of the sun is 332,830 times that of the earth and the diameter of its sharp circular boundary is approximately 1,389,640 km. The sun also rotates about its axis but not as a rigid body. The period of rotation at its equator is 25 earth days, and at 40° latitude, the period of rotation is 27 days.

Interior: The interior of the sun is at a pressure of about a billion atmospheres and a temperature of many billion kelvin. Fusion of hydrogen and helium occurs at this temperature and pressure and this process releases tremendous amount of energy.

Photosphere: The bright boundary of the sun seen from earth is a thin layer of low pressure and density. Most of the sun's thermal radiation is emitted from this layer. This layer is at the temperature of approximately 6000 K.

Chromosphere and corona: It is a thin layer of very low pressure. It is seen during total eclipse as a ring of red light surrounding the sun. Corona consists of rarified gases extending up to about a million km or more.

20.3 EARTH

The earth has a mean diameter of 12,640 km and it is almost spherical in shape. Its period of rotation about its axis is 24 hours, which is the definition of hour. It completes one revolution around the sun in 365 days, 5 hours 48 minutes and 46 seconds = 365.242199 mean solar days. To account for the difference of 0.242199 day, Gregorian correction is introduced, that is as follows.

Every fourth year is considered to be leap year with 366 days, hence the discrepancy is

$$365 \times 3 + 366 - 365.242199 \times 4 = 0.0312037 \text{ day extra.}$$

Every 400 years, the discrepancy is 3.12037 days extra. Hence, to account for it the century years that are divisible by four are not leap years.

In 4000 years, the discrepancy becomes 1.2037 days, which is corrected, hence the discrepancy reduces to 0.02037 day.

Over a period of 20,000 years, the discrepancy will be one day.

The earth has a core of approximately 2560 km diameter, where most of its mass is concentrated, and it is harder than steel. This is enclosed in *mantle*, which forms 70% of its mass. The outer crust of earth has only 1% of its mass. The mean specific gravity is approximately 5.52.

The earth moves in an approximately elliptic orbit around the sun. The sun is actually located slightly off the centre. The earth is closest to the sun on January 1 and farthest on July 1, as a result it receives 7% more solar radiation in January than in July. The various seasons, variations in daylight hours and solar radiation intensity variation on the earth surface are due to the tilt of the axis of rotation of earth by 23.5° with respect to its orbit around the sun.

Figure 20.1 shows the position of earth at four important locations in its path around the sun. On the left side of the figure, is the location on 22nd June that is called *summer solstice*. The North Pole is tilted exactly by 23.5 degrees towards the sun, as a result the northern hemisphere receives more solar radiation, and it has summer. The southern hemisphere has winter at this time. There is

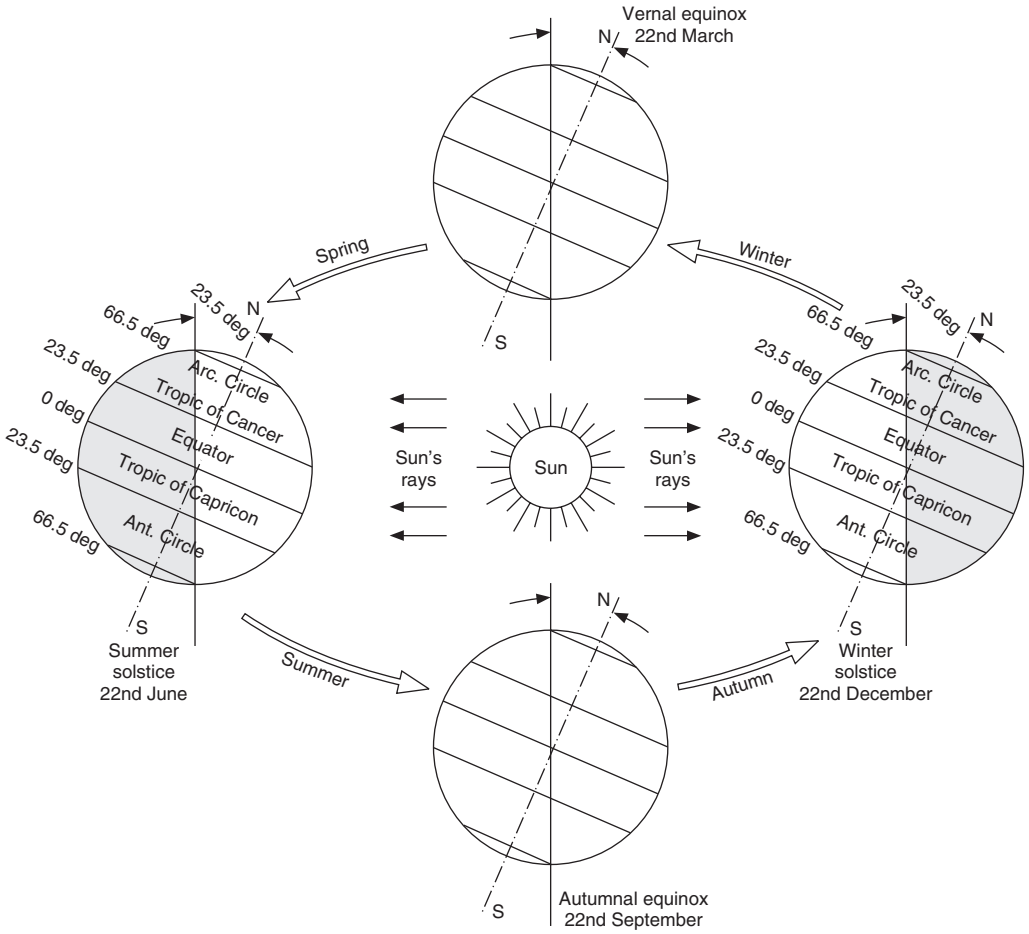

Figure 20.1 Position of earth at four important locations in its orbit around the sun.

continuous darkness or night on latitudes above 66.5°S and continuous daylight on latitudes above 66.5°N. The solar radiation is perpendicular to 23.5°N latitude. Similarly, on the right side of the figure is the location on 22nd December that is called *winter solstice*. The North Pole is tilted exactly by 23.5 degrees away from the sun, as a result the southern hemisphere receives more solar radiation, and it has summer, while the northern hemisphere has winter. There is continuous darkness or night on latitudes above 66.5°N and continuous daylight on latitudes above 66.5°S. The solar radiation is perpendicular to 23.5°S latitude.

September 22 is known as *autumnal equinox*, when both the North and South poles are equidistant from the sun, as a result there is 12 hours day and 12 hours night throughout the earth. Similarly, March 22nd is called *vernal equinox*. At both the equinoxes the solar radiation is perpendicular to Equator.

The earth is also divided into torrid, temperate and frigid zones. The torrid zone is from 23.5°S to 23.5°N. The sun is vertically overhead (at zenith) at least once a year in this zone. At the

Equator, the sun is at zenith on September 22 and March 22, while it is at zenith on June 22 at 23.5°N latitude. On December 22, it is at zenith at 23.5°S latitude.

The *temperate zone* is between 23.5°N and 66.5°N and between 23.5°S and 66.5°S. In these zones the sun appears above the horizon daily but it is never at the zenith.

Frigid zones are between 66.5°N and 90°N and between 66.5°S and 90°S. In these zones the sun is below the horizon and above the horizon for at least one full day yearly.

20.4 BASIC SOLAR ANGLES

The location of a point on the surface of earth can be precisely determined if the longitude and the latitude of the place are known.

20.4.1 Longitude

The plane perpendicular to the axis of the earth's rotation and passing through its centre is called the *equatorial plane*. It divides the earth into two equal halves. North pole is located in the upper half at the location of the axis of rotation. When viewed from top of North pole, the earth rotates in anticlockwise manner. The imaginary line joining N pole to the S pole is called *longitude*. The longitude passing through Greenwich is referred to as 0° longitude. The equatorial plane can be divided into 360 degrees and the longitudes joining N pole to the S pole may be labelled according to the angle on equatorial plane. Lines of longitude thus range from 0° to 180° East or West of the longitude passing through Greenwich (180°E and 180°W being one and the same—the international date line). Lines of longitude together with the lines of latitude form a grid on which the position of any place can be specified.

20.4.2 Latitude

In the position of the point *P* shown in Figure 20.2, the line *OP* is the radius of earth and *OQ* is the projection of *OP* on the equatorial plane. The angle between *OP* and its projection *OQ* is called the

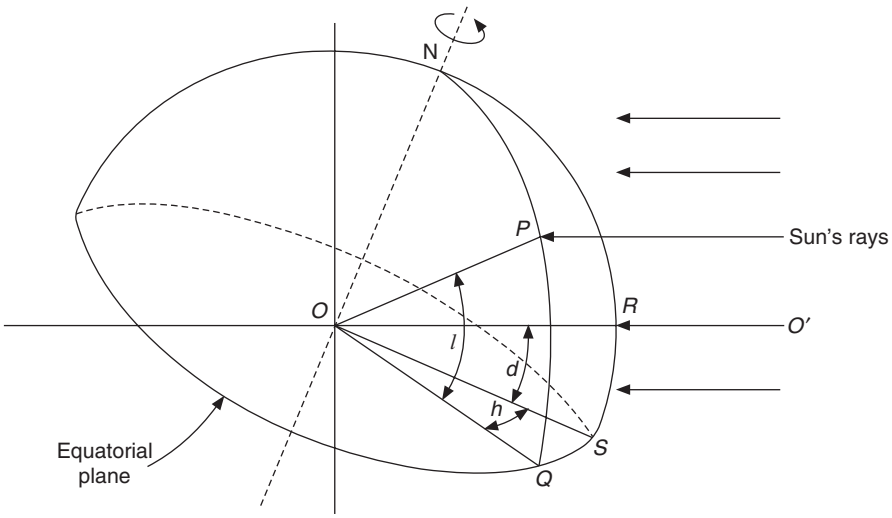

Figure 20.2 Definition of latitude (*l*), declination (*d*) and hour angle (*h*).

latitude of the place *P*. This angle is indicated by $\angle l$. The latitude of North pole, N, is 90°, while that of point *Q* at Equator is 0°. The latitude is either north or south of equator and it is indicated as, say, 30° North or 30° South.

20.4.3 Declination

Figure 20.2 shows the upper-half of the earth with its equatorial plane and the axis of rotation. It faces the sun on its right hand side and is tilted towards it, that is, this is the position during summer in northern hemisphere. Line *OR* when extended joins the centre of the earth to the centre of the sun. The sun's rays are shown by arrows parallel to this line. The projection of *OR* on the equatorial plane is *OS*. The $\angle ROS$ between the line joining the centre of earth to the centre of sun *OR*, and its projection on equatorial plane *OS* is called the *declination angle*. This is denoted by *d*. This also can be either north or south of the equator. It is negative when it is south of equator, and positive when it is north of equator. Its maximum value is 23.5° on approximately June 22, that is, Summer Solstice and the minimum value is –23.5° on approximately December 22, that is, Winter Solstice. At equinoxes (September 22 and March 22), it is zero. Two empirical expressions have been proposed for the calculation of the declination angle.

$$d = 23.45 \sin[360 \times (284 + n)/365] \tag{20.1}$$

where

n is the day number starting from 1st January.

$$d = 0.3963723 - 22.9132745 \cos N + 4.0254304 \sin N - 0.3872050 \cos 2N + 0.05196728 \sin 2N - 0.1545267 \cos 3N + 0.08479777 \sin 3N \tag{20.2}$$

with $N = (n - 1)(360/365)$.

The value of declination angle on 1st, 8th, 15th and 22nd day of each month is given in Table 20.1 (see Section 20.5).

20.4.4 Hour Angle

In the position of the earth shown in Figure 20.2, the longitude *NS* faces the sun, that is, there is solar noon on this longitude. On the longitude, *NPQ* passing through point *P*, it is still forenoon. As the time passes, the longitude *NPQ* moves towards the solar noon, that is, *NPQ*, and its projection *OQ* moves towards *OS*.

The angle measured between *OS* and *OQ* in the earth's equatorial plane is called the *hour angle*. It is denoted by $\angle h$. At solar noon, the lines *OS* and *OQ* will be coincident and the hour angle will be zero. *OQ*, the projection of *OP*, completes one revolution, that is, revolves by 360° in 24 hours. Hence, the hour angle for each hour is 360/24 = 15°.

The point *Q* shown in the Figure 20.2 is before noon. The hour angle actually expresses the time of the day with respect to solar noon.

20.5 TIME

The angle of incidence of sun's rays is required for solar radiation calculations for a given location at a given time of the day and of the year. The position of the sun relative to earth is determined if the three basic angles namely, latitude, declination and hour angle are known. The hour angle is measured

with respect to solar noon. On each day this is a unique time when the longitude of the place faces the sun. Hence, it is convenient to measure the time also with respect to solar noon on a day.

This time reckoned with respect to solar noon is called *solar time.* Obviously, every location or city will have a different solar time depending upon its longitude. Every country has a precisely defined longitude or city with respect to which its standard time is measured. For India, it is measured with respect to 82.5° longitude passing through the city of Allahabad. This is called *Indian Standard Time*.

It has been internationally recognized that the time reckoned from midnight at Greenwich meridian is called *Greenwich civil time* or *Universal time*, that is, GMT or GCT. Midnight is 0 hour and noon is 12 hour.

Local civil time

Local civil time (LCT) is reckoned from the precise longitude of the observer. On a location towards 1° east of it, the local civil time will be 4 minutes more advanced at the same instant whereas on a meridian towards 1° west of it will be 4 minutes less advanced. The earth takes 24 × 60 = 1440 minutes to cover 360 degrees that leads to a difference of four minutes for each degree difference in longitude. The sunrise and solar noon will occur earlier on any meridian to the east of a given location.

Local solar time or solar time

At every location, a day is of 24 hour duration for each day of the year. The watch measures it and it has no less or no more than two revolutions of 12 hours for each day. The earth moves in an elliptical orbit around the sun. At its nearest point to the sun, it moves faster and at its farthest point from the sun it moves slower. The tilt of the axis by 23.5° also causes a systematic difference of the length of a day. Hence the time measured by the apparent diurnal motion of the sun is called *true solar time, local solar time or apparent solar time* and is slightly different from the local civil time due to irregularities of earth's rotation, obliquity of earth's orbit and other factors. The difference between local solar time and local civil time is called *equation of time* (EOT). Therefore,

$$\text{LST} = \text{LCT} + \text{EOT} \tag{20.3}$$

The equation of time accounts for irregularities of earth's rotation, obliquity of earth's orbit and other factors. Equation of time and declination angle are tabulated in Table 20.1 for each week of every month.

Table 20.1 Declination angle and equation of time for various days and months

Day / *Month*	*1st of month*		*8th of month*		*15th of month*		*22nd of month*	
	Decli. (deg:min)	*Eq. of time* (min:sec)	*Decli.* (deg:min)	*Eq. of time* (min:sec)	*Decli.* (deg:min)	*Eq. of time* (min:sec)	*Decli.* (deg:min)	*Eq. of time* (min:sec)
January	−(23:08)	−(3:16)	−(22:20)	−(6:26)	−(21:15)	−(9:12)	−(19:50)	−(11:27)
February	−(17:18)	−(13:34)	−(15:13)	−(14:14)	−(12:55)	−(14:15)	−(10:27)	−(13:41)
March	−(7:51)	−(12:36)	−(5:10)	−(11:04)	−(2:25)	−(9:14)	0:21	−(7:12)

(*Contd.*)

Table 20.1 Declination angle and equation of time for various days and months (contd.)

Month \ Day	*1st of month*		*8th of month*		*15th of month*		*22nd of month*	
	Decli. (deg:min)	*Eq. of time* (min:sec)	*Decli.* (deg:min)	*Eq. of time* (min:sec)	*Decli.* (deg:min)	*Eq. of time* (min:sec)	*Decli.* (deg:min)	*Eq. of time* (min:sec)
April	4:16	−(4:11)	6:56	−(2:07)	9:30	−(0:15)	11:57	1:19
May	14:51	2:50	16:53	3:31	18:41	3:44	20:14	3:30
June	21:57	2:25	22:47	1:15	23:17	−(0:09)	23:27	−(1:40)
July	23:10	−(3:33)	22:34	−(4:48)	21:39	−(5:45)	20:25	−(6:19)
August	18:12	−(6:17)	16:21	−(5:40)	14:17	−(4:35)	12:02	−(3:04)
September	8:33	−(0:15)	5:58	2:03	3:19	4:29	0:36	6:58
October	−(2:54)	10:02	−(5:36)	12:11	−(8:15)	13:59	−(10:48)	15:20
November	−(14:12)	16:20	−(16:22)	16:16	−(18:18)	15:29	−(19:59)	14:02
December	−(21:41)	11:14	−(22:38)	8:26	−(23:14)	5:13	−(23:27)	1:47

EXAMPLE 20.1 Indian Standard Time (IST) corresponds to longitude of 82°30′. Find the local civil time and the local solar time at 8:00 am IST on 22nd March in Kolkata, Jodhpur, Dibrugarh and Bhuj, the longitudes of these cities being 88°27′, 73°01′, 96° and 67° respectively.

Solution:

The equation of time on 22nd March from Table 21.1 is –7′12″.

Kolkata: Longitude correction = (88°27′ – 82°30′) × 4 min = 5°57′ × 4 min
= [(5 + (57/60)] × 4 min = 23′48″

Kolkata is to the east of Allahabad, hence its LCT will be more advanced.

∴ LCT Kolkata = 8:00 + 23′48″ = 8h 23′48″

∴ LST = LCT + EQT = 8:00 + 23′48″ – 7′12″ = 8h16′36″

Jodhpur: Longitude correction = (73°01′ – 82°30′) × 4 min = –9°29′ × 4 min
= – [(9 + (29/60))] × 4 min = –37′56″

∴ LCT Jodhpur = 8:00 – 37′56″ = 7 h 22′4′

∴ LST = 7 h 22′4″ – 7′12″ = 7 h 14′52″

Dibrugarh: Longitude correction = (96 – 82°30′) × 4 min = 54 min

∴ LCT Dibrugarh = 8 h 54′ and LST = 8 h 46′48″

Bhuj: Longitude correction = (67° – 82°30′) × 4 min = – 62 min

∴ LCT Bhuj = 6 h 58′ and LST = 6 h 50′48″

20.6 Derived Solar Angles

The three basic angles, namely, latitude, hour angle and sun's declination angle have been defined. Apart from these, there are several angles that are useful in solar radiation calculations. Such

angles include *altitude angle* β, *zenith angle* ψ and *azimuth angle* γ. For a wall with normal in the direction *n*, the *angle of incidence of sun's rays* θ and *wall-solar azimuth angle* α is also defined.

Figure 20.3 shows the horizon for the location of an observer at point *P*. Point *O* is the centre of the earth and point *Z* vertically overhead at *P* is called the zenith. To an observer on earth (*P*), the sun rises at SU on the horizon, moves in a circular path and sets at SS on the horizon as shown in Figure 20.3. The path of the sun for a typical day is shown in the figure. The location of the sun is also shown in afternoon hours.

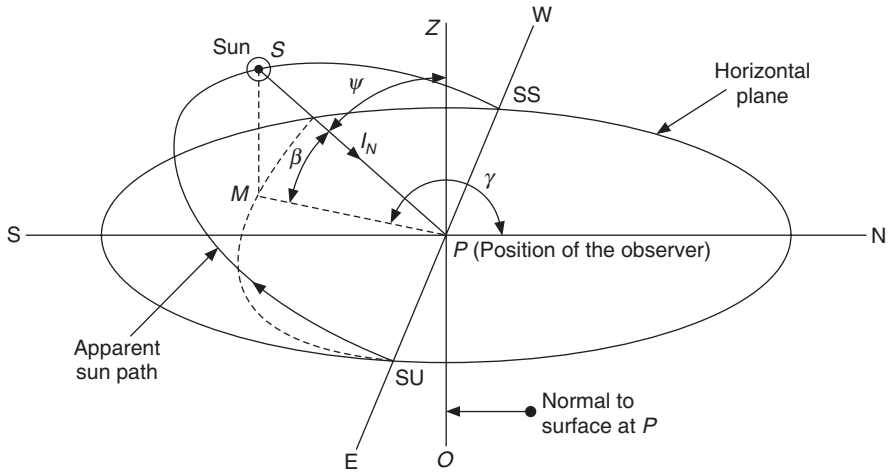

Figure 20.3 Definition of altitude angle, zenith angle and azimuth angle.

A vector I_N shows the sun's ray, which is in a direction joining *S* and *P*. The projection of the sun's ray on the horizon at this instant is *PM*. The path of the projection on the horizon is shown by a dashed line. The angles defined in this figure are as follows:

Altitude angle β: an angle measured in a vertical plane between the sun's ray *SP* and its projection *PM* on the horizon.

Zenith angle ψ: an angle measured in a vertical plane between the sun's ray *SP* and line *PZ* (extension of *OP*). It is observed from the figure that $\beta + \psi = \pi/2$.

Azimuth angle γ: an angle measured in the horizontal plane from due North, *PN*, to the projection of sun's ray *PM* on horizon.

To obtain relations between the derived angles and the basic angles we consider a coordinate system in which all these lines can be defined. Let Figure 20.4 represent a coordinate system with *z*-axis coincident with the axis of rotation of earth. The plane *x*–*y* lies in the same plane as the earth's equatorial plane. This figure can be compared to Figure 20.3. It is assumed that sun's rays are parallel and lie along the line joining the centre of earth to the centre of sun, that is, along I_N. The *x*–axis is chosen such that the projection of the sun's ray on equatorial plane is along this axis, that is, the longitude passing through it has solar noon. Hence, it is assumed that the sun's rays lie in the *x*–*z* plane. This is the same configuration as shown in Figure 20.2 where the longitude *NS* faces the sun. Point *O* is the centre of earth and *P* is the location of observer. The latitude, hour and declination angles are shown just like in Figure 20.2.

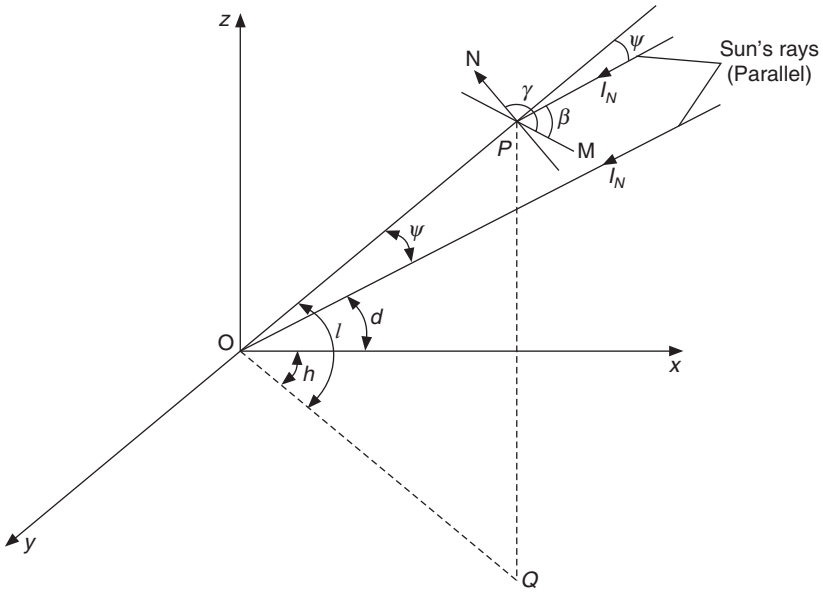

Figure 20.4 Relationships between solar angles.

The horizon is shown by a rectangle around point *P*. The angle between the sun's rays and *OP* extended is shown as zenith angle ψ. The projection of sun's ray on horizon is *PM* and the angle between I_N and *PM* is the altitude angle β in the *x*–*z* plane. The line *PN* on the horizon is due north and it is perpendicular to *OP*. *PN* lies in the plane *O*–*Q*–*P*–*N*.

The angles $\angle\psi$, $\angle\beta$ and $\angle\delta$ are in the *x*–*z* plane while $\angle h$ is in equatorial plane.

In Figure 20.4 let a_1, b_1 and c_1 be the direction cosines of *OP* with respect to *x*, *y*, *z* axes. And, let a_2, b_2 and c_2 be the direction cosines of I_N.

$$a_1 = \cos l \cos h \ , \ b_1 = \cos l \sin h \text{ and } c_1 = \sin l$$

The sun's ray I_N is in *x*–*z* plane. Hence, $a_2 = \cos d$, $b_2 = 0$ and $c_2 = \sin d$

20.6.1 Zenith Angle ψ

The zenith angle is the angle between *OP* and I_N. Hence $\cos \psi = a_1 a_2 + b_1 b_2 + c_1 c_2$

Therefore,

$$\cos \psi = \cos l \cos h \cos d + \sin l \sin d \tag{20.4}$$

20.6.2 Altitude Angle β

Since the altitude angle $\beta = \pi/2 - \psi$, we may write

$$\sin \beta = \sin\left(\frac{\pi}{2} - 4\right) = \cos \psi$$

$$\therefore \qquad \sin \beta = \cos l \cos h \cos d + \sin l \sin d \tag{20.5}$$

20.6.3 Azimuth Angle

To find a relation between the azimuth angle and the basic angles, we have to follow an inverse approach. If the direction cosines of a line are known, the direction cosines of its projection may be expressed by using the following example. In Figure 20.4, line OQ lies in the x–y plane and its direction cosines are:

$$a_3 = \cos h, \quad b_3 = \sin h \quad \text{and} \quad c_3 = 0$$

Direction cosines of OP are:

$$a_1 = \cos l \cos h, \quad b_1 = \cos l \sin h \quad \text{and} \quad c_1 = \sin l$$

The line OQ is the projection of OP in the x–y plane and the angle $\angle POQ = l$.

Hence if the direction cosines of a line (say OP) are known, then the direction cosines of a line that makes an angle l with it (line OQ) are obtained by dividing the direction cosines of the line by cos l.

The sun's azimuth angle $\gamma$is the angle between due north (PN) and the projection of sun's rays on horizon, that is, PM.

Direction cosines of PM

The line PM is the projection of sun's ray I_N on horizon making an angle β with it. The direction cosines of sun's ray being $a_2 = \cos d$, $b_2 = 0$ and $c_2 = \sin d$, the direction cosines of PM (a_4, b_4 and c_4) are obtained by dividing the direction cosines of I_N by cos β, that is,

$$\alpha_4 = \cos d/\cos \beta, \quad b_4 = 0 \quad \text{and} \quad c_4 = \sin d/\cos \beta$$

Direction cosines of PN

The lin PN points towards north from point P and is perpendicular to OP. Its projection in the x–y plane will be $PN \cos (90^o + l) = -PN \sin l$ and it makes an angle l with the z-axis. Therefore,

$$a_5 = -\sin l \cos h, \quad b_5 = -\sin l \sin h \quad \text{and} \quad c_5 = \cos l$$

Also, since OP and PN are perpendicular to each other, hence, $a_1a_5 + b_1b_5 + c_1c_5 = 0$. It is observed that it is identically satisfied.

$$\cos \gamma = a_4 a_5 + b_4 b_5 + c_4 c_5$$

$$\cos \gamma = \sec \beta (\cos l \sin d - \cos d \sin l \cos h) \tag{20.6}$$

From Eqs. (20.5) and (20.6), it may be shown that

$$\sin \gamma = \sec \beta \cos d \sin h \tag{20.7}$$

Also,
$$\tan \gamma = \frac{\cos d \sin h}{\cos l \sin d - \cos d \sin l \cos h} = \frac{\sin h}{\cos l \tan d - \sin l \cos h} \tag{20.8}$$

20.6.4 Solar Noon

At solar noon the hour angle $\angle h = 0$, that is, OQ the projection of OP coincides with the x–axis. OP and OQ both lie in the x–z plane at solar noon. Referring to Figure 20.3, the azimuth angle $\gamma$is equal to zero if the sun rises in northeast ($l < d$) and sets in northwest. It is equal to π if the sun rises

in the southeast ($l > d$). It can be shown by putting $h = 0$ in Eq. (20.5) that the altitude angle β at noon is given by

$$\sin \beta = \cos l \cos d + \sin l \sin d = \cos (l - d) \text{ or } \cos (d - l)$$

i.e. $$\beta_{\text{noon}} = \frac{\pi}{2} - \left| (l - d) \right| \tag{20.9}$$

Also at solar noon, $h = 0$, therefore from Eq. (20.7), $\sin \gamma = 0 \quad \therefore \quad \gamma = 0$ or π

From Eq. (20.6) at $h = 0$,

$$\cos \gamma = \sec \beta_{\text{noon}} \sin (d - 1) = \frac{\sin (d - l)}{\sin \left| (l - d) \right|}$$

if $l > d$: $\cos \gamma = -1 \quad \therefore \quad \gamma = \pi$ (20.10a)

if $l < d$: $\cos \gamma = 1 \quad \therefore \quad \gamma = 0$ (20.10b)

For $l = d$: γ is undefined. The sun rises exactly in the east and sets in the west and is directly overhead at solar noon, that is, at point Z in Figure 20.3.

The zenith angle, altitude angle and azimuth angle can be calculated if the latitude declination and hour angle are known However, the proper sign convention must be followed.

20.6.5 Time of Sunrise and Sunset

The altitude angle β is equal to zero at sunrise and sunset since the sun is at horizon at that time. If the solar time for sunrise is denoted by h_0, then from Eq. (20.5),

$$0 = \cos l \cos h_o \cos d + \sin l \sin d$$

$$\cos h_0 = -\tan l \tan d \tag{20.11}$$

$$\cos \gamma_0 = \sin d / \cos l \tag{20.12}$$

Sign convention

North latitudes are positive and south latitudes are negative.

Declination is positive in summer between March 22 and September 22, otherwise it is negative.

Hour angle is measured on either side of solar noon and it is limited to $0 < h < \pi$.

If $h < \pi/2$, cos h is positive and if $h > \pi/2$, cos h is negative.

Azimuth is measured clockwise from North for hour angles before noon and it is measured anticlockwise from North for hour angles in afternoon hours.

The azimuth angle is limited to $0 < \gamma < \pi$. In Eq. (20.6), cos γ is positive if $\gamma < \pi/2$ and cos γ is negative if $\gamma > \pi/2$.

20.7 ANGLE OF INCIDENCE

The above-mentioned angles are useful for solar radiation calculations on horizontal surfaces. For surfaces other than horizontal, it is convenient to express the position of sun relative to the surface in terms of the incidence angle θ. For vertical surfaces, the use of wall solar azimuth angle α is also convenient. Figure 20.5 shows a vertical surface in the x–z plane. It also shows a plane tilted

at an angle ϕ with respect to the vertical plane. The normal to the vertical surface is the y–axis while the normal to the tilted surface is PN which lies in the y–z plane since the surface is tilted about the x–axis.

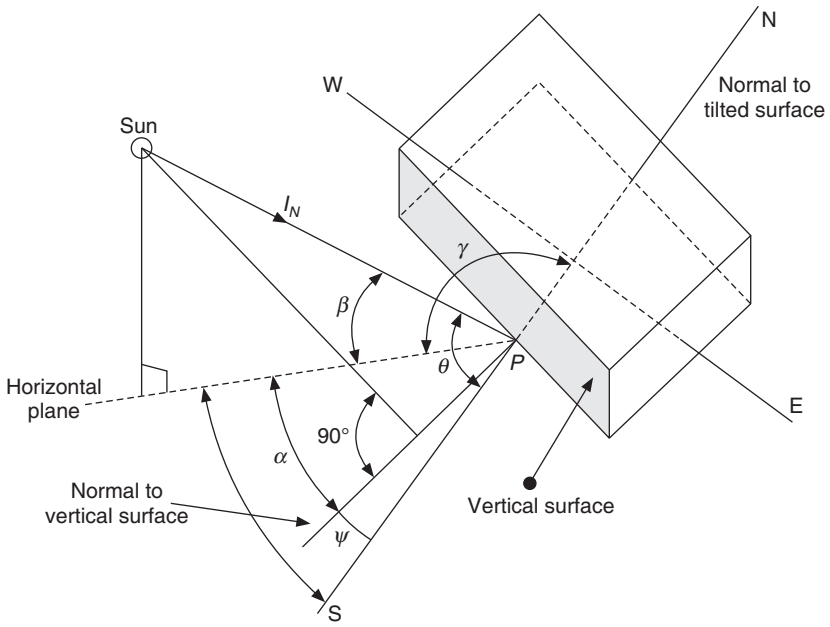

Figure 20.5 Calculation of incident solar angle for vertical surfaces.

The sun's angle of incidence θ is the angle between the sun's rays and the normal to the tilted surface.

The *wall solar azimuth angle* α is the angle measured in the horizontal plane between the normal to the vertical surface (y-axis) and the horizontal projection of the sun's rays. Thus, α is associated with a definite vertical wall position and may be used to determine the sun's azimuth angle γ. For example, for an east-facing wall in the morning hours

$$\alpha = (\pi/2) - \gamma \quad \text{if } l < d$$

and

$$\alpha = \gamma - (\pi/2) \quad \text{if } l > d$$

For a north-facing wall, $\alpha = \gamma$ if $l < d$. The wall will not be sunlit if $l > d$.

The relation for the angle of incidence is derived by using the direction cosines of sun's ray and the normal to the tilted surface. The direction cosines of sun's ray are:

$$a_1 = \cos\beta \sin a, \quad b_1 = \cos\beta \cos\alpha \quad \text{and} \quad c_1 = \sin\beta$$

The direction cosines of normal to the tilted surface are (in the y–z plane):

$$a_2 = 0, \; b_2 = \cos\phi \quad \text{and} \quad c_2 = \sin\phi$$

$$\cos\theta = a_1 a_2 + b_1 b_2 + c_1 c_2 = 0 + \cos\beta \cos\alpha \cos\phi + \sin\beta \sin\phi$$

i.e.

$$\cos\theta = \cos\beta \cos\alpha \cos\phi + \sin\beta \sin\phi \tag{20.13}$$

If the surface is vertical ($\phi = 0$), then

$$\cos\theta = \cos\beta\cos\alpha \tag{20.14}$$

If the surface is horizontal ($\phi = \pi/2$) then

$$\cos\theta = \sin\beta = \cos\psi \tag{20.15}$$

Thus, for a horizontal surface the incidence angle is equal to zenith angle.

EXAMPLE 20.2 Determine the smallest and the largest altitude angle in Delhi.

Solution:

The maximum altitude occurs on June 22 when $d = 23.5^o$ and the minimum occurs on December 22 when $d = -23.5^o$.

At solar noon from Eq. (20.9), $\beta_{noon} = 90° - (l - d)$

The latitude of Delhi is 28.583333°

June 22 : $\beta_{noon} = 90 - (28.58333 - 23.5) = 84.92^o$

December 22 : $\beta_{noon} = 90 - (28{,}58333 + 23.5) = 37.92^o$

EXAMPLE 20.3 Calculate the sun's altitude and azimuth angles at 7:30 am solar time on August 1 for Kolkata with latitude 22°39′N and longitude 88°27′E.

Solution:

From Table 20.1, declination angle on August 1, $d = 18^o12' = 18.2^o$

Hour angle at 7:30 am : $h = (12 - 7.5) \times 15 = 67.5^o$

Latitude angle, $l = 22 + (39/60) = 22.65^o$

From Eq. (20.5),

$$\sin\beta = \cos l\cos h\cos d + \sin l\sin d$$
$$= \cos 22.65°\cos 67.5°\cos 18.2° + \sin 22.65°\sin 18.2°$$
$$= (0.9229)(0.3827)(0.95) + (0.3851)(0.3123) = 0.45578$$

$\therefore \quad \beta = 27.115°$

From Eq. (20.6),

$$\cos\gamma = \sec\beta(\cos l\sin d - \cos d\sin l\cos h)$$
$$= (1/0.8901)[(0.92287)(0.31233) - (0.94997)(0.3851)(0.38268)]$$
$$= 0.14824/0.8901 = 0.16655$$

$\therefore \quad \gamma = 80.4126°$

The azimuth angle is 80.4126° east of north.

EXAMPLE 20.4 Find the time of sunrise and the azimuth angle on August 1 in Kolkata.

Solution:

On August 1 from Table 20.1, declination $d = 18.2^o$ and equation of time = −6′17″

At the time of sunrise, angle $\beta = 0$. From Eq. (20.11), we get

$$\cos h_o = -\tan l \tan d = -\tan 22.65^\circ \tan 18.2^\circ = -(0.41728)(0.32878) = -0.1372$$

$\therefore$ $h_o = 97.8856^o$

The hour angle is measured from solar noon.

$\therefore$ Time of sunrise = (12 – 97.8856/15) = 5.47429 hours

= 5 h 28′ 27″ Solar time

From Eq. (20.3),

LST = LCT + equation of time

= IST + longitude correction + equation of time

Indian Standard Time corresponds to 82.5°E longitude whereas the longitude of Kolkata is 88°27′E (88.45°). Therefore, the time in Kolkata is more advanced than IST by (88.45 – 82.5) × 4 minutes = 23.8 minutes = 23 min 48 s.

Time of sunrise = 5 h 28′27″ – 23′48″ + 6′17″= 5 h 10′56″ am Indian Standard Time.

From Eq. (20.12),

$$\cos \gamma_o = \sin d/\cos l = \sin 18.2^\circ/\cos 22.65^\circ = 0.31233/0.92287 = 0.3384$$

$\therefore$ $\gamma_o = 70.218^o$ east of north.

EXAMPLE 20.5 Find the LST, LCT and IST for sunrise, and daylight hours in Kolkata and Delhi on April 15.

Solution:

On April 15 from Table 20.1, declination $d = 9.5^o$ and equation of time = –0′15″

Latitudes of Kolkata and Delhi are 22.65° and 28.58333° respectively.

Longitudes of Kolkata and Delhi are 88.45° and 77.2° respectively.

Kolkata:

From Eq. (20.11), $\cos h_0 = -\tan l \tan d = -\tan 22.65^\circ \tan 9.5^\circ = -0.069829$

$\therefore$ $h_0 = 94.0042^o = 94.0042/15 = 6.2669$ hours measured from solar noon

Sunrise, Local Solar Time, LST = 12 – 6.2669 = 5.733 am = 5 h 43′59″

Longitude correction for Kolkata = (88.45 – 82.5) × 4 = 23.8 min = 23′48″

Local Civil Time, LCT = LST – equation of time = 5 h 43′59″ +15″= 5h 44′14″

IST = LCT – longitude correction = 5h 44′14″ – 23′48″ = 5 h 20′26″

Daylight hours = 2 × 6.2669 = 12.5338 hours = 12 h 32′2″

Delhi:

$$\cos h_o = -\tan l \tan d = -\tan 28.58333^o \tan 9.5^o = -0.09117$$

$\therefore$ $h_o = 95.2312^o = 95.2312/15 = 6.3487$ hours measured from solar noon

Sunrise, Local Solar Time , LST = 12 – 6.3487 = 5.65125 am = 5 h 39′4″

Longitude correction for Delhi = (77.2 – 82.5) × 4 = –21.2 min = 21′12″

Local Civil Time, LCT = LST – equation of time = 5 h 39′4″ + 15″ = 5 h 39′19″

IST = LCT – longitude correction = 5 h 39′19″ + 21′12″ = 6 h 0′31″

Daylight hours = 2 × 6.3487 = 12.6975 hours = 12 h 41′51″

On September 22 and March 22, declination angle $d = 0.0$

$$\cos h_o = -\tan l \tan 0.0 = 0.0 \quad \therefore \quad h_o = 90^o = 6 \text{ hours}$$

There will be exactly 12 hours of daylight.

EXAMPLE 20.6 Determine the altitude and azimuth angles on April 15 in Kolkata and Delhi at solar noon, 1:00 pm and 3:00 pm solar time. Also, find the wall solar azimuth angle for a south-facing wall.

Solution:

Calcutta:

$$l = 22.65°, \; d = 9.5°$$

At solar noon:

$$h = 0° \text{ and } \beta_{noon} = \pi/2 - (l - d) = 90° - 22.65° + 9.5° = 76.85^o$$

$$\cos \gamma = -1 \quad \therefore \quad \gamma = -180^o \text{ and wall solar azimuth angle } \alpha = 0.0$$

At 1:00 pm: $h = 15^o$

$$\sin \beta = \cos 22.65° \cos 15° \cos 9.5° + \sin 22.65° \sin 9.5° = 0.9427$$

$$\therefore \quad \beta = 70.522^o$$

$$\cos \gamma = \sec 70.522° (\cos 22.65° \sin 9.5° - \cos 9.5° \sin 22.65° \cos 15°)$$

$$= -0.6438$$

$$\therefore \quad \gamma = 130.078^o \text{ west of north}$$

$$\therefore \quad \alpha = 180 - \gamma = 49.928^o$$

At 3:00 pm: $h = 45^o$

$$\sin \beta = \cos 22.65° \cos 45° \cos 9.5° + \sin 22.65° \sin 9.5° = 0.7072$$

$$\therefore \quad \beta = 45.006^o$$

$$\cos \gamma = \sec 45.006° (\cos 22.65° \sin 9.5° - \cos 9.5° \sin 22.65° \cos 45°)$$

$$= -0.1645$$

$$\therefore \quad \gamma = 99.468^o \text{ west of north}$$

$$\therefore \quad \alpha = 180 - \gamma = 80.532^o$$

Delhi:

$$l = 28.5833^o, \; d = 9.5^o$$

At solar noon: $h = 0°$ and $\beta_{noon} = \pi/2 - (l - d) = 90° - 28.58333° + 9.5° = 70.917^o$

$$\cos \gamma = -1 \quad \therefore \quad \gamma = -180^o \text{ and wall solar azimuth angle } \alpha = 0°$$

At 1:00 pm: $h = 15^o$

$$\sin \beta = \cos 28.58333° \cos 15° \cos 9.5° + \sin 28.58333° \sin 9.5° = 0.9155$$

$\therefore \quad \beta = 66.28^{o}$

$\cos \gamma = \sec 66.28° (\cos 28.58333° \sin 9.5° - \cos 9.5° \sin 28.58333° \cos 15°)$

$= -0.7728$

$\therefore \quad \gamma = 140.608^{o}$ west of north

$\therefore \quad \alpha = 180 - \gamma = 39.392^{o}$

At 3:00 pm: $h = 45^{o}$

$\sin \beta = \cos 28.5833° \cos 45° \cos 9.5° + \sin 28.5833° \sin 9.5° = 0.6913$

$\therefore \quad \beta = 43.739^{o}$

$\cos \gamma = \sec 43.739° (\cos 28.58333° \sin 9.5° - \cos 9.5° \sin 28.58333° \cos 45°)$

$= -0.2612$

$\therefore \quad \gamma = 105.142^{o}$ west of north

$\therefore \quad \alpha = 180° - \gamma = 74.857^{o}$

EXAMPLE 20.7 Determine the altitude and azimuth angles on June 22 in Kolkata and Delhi at 7:00 am solar time. Also find the wall solar azimuth angle for a south-facing wall.

Solution:

Calcutta:

$l = 22.65°$, on June 22 $d = 23.45°$, equation of time = –1′40″

At 7:00 am: $h = 75^{o}$

$\sin \beta = \cos 22.65° \cos 75° \cos 23.45° + \sin 22.65° \sin 23.45° = 0.3724$

$\therefore \quad \beta = 21.58624^{o}$

$\cos \gamma = \sec 21.58624° (\cos 22.65° \sin 23.45° - \cos 23.45° \sin 22.65° \cos 75°)$

$= 0.2966$

$\therefore \quad \gamma = 72.74^{o}$ east of north

The sun rises in the north of east and sets in the north of west. The south-facing wall will be shaded.

Delhi:

$l = 28.58333°$, on June 22 $d = 23.45^{o}$, equation of time = –1′40″

At 7:00 am: $h = 75^{o}$

$\sin \beta = \cos 28.58333° \cos 75° \cos 23.45° + \sin 28.58333° \sin 23.45° = 0.399$

$\therefore \quad \beta = 23.51^{o}$

$\cos \gamma = \sec 23.51° (\cos 28.58333° \sin 23.45° - \cos 23.45° \sin 28.58333° \cos 75°)$

$= 0.2572$

$\therefore \quad \gamma = 75.096^{o}$ east of north

In Delhi too, the sun rises in the north of east and sets in the north of west. The south-facing wall will be shaded.

EXAMPLE 20.8 Calculate the sun's incidence angle for a south-facing surface tilted back from the vertical position by 30 degrees at 3:00 p.m. solar time on June 8 in Kolkata.

Solution:

From Table 21.1 on June 8 : $d = 22^o\ 47' = 22.7833^o$

$l = 22.65^o$ and $h = 45^o$. The first step is to find the angle β from Eq. (20.3).

$$\sin \beta = \cos l \cos h \cos d + \sin l \sin d$$
$$= \cos 22.65^o \cos 45^\circ \cos 22.7833^o + \sin 22.65^o \sin 22.7833^o$$
$$= (0.9229)(0.7071)(0.92197) + (0.3851)(0.38725) = 0.75078$$
$$\therefore \quad \beta = 48.6583^o$$
$$\cos \gamma = \sec \beta (\cos l \sin d - \cos d \sin l \cos h)$$
$$= 1.51389\ [(0.9229)(0.3872) - (0.92197)(0.3851)(0.7071)] = 0.160957$$
$$\therefore \quad \gamma = 80.7375^o$$

The azimuth angle is less than 90^o, hence for the south-facing vertical surface $\alpha = \gamma$
Given that $\phi = 30^o$, hence from Eq. (20.8)

$$\cos \theta = \cos \beta \cos \alpha \cos \phi + \sin \beta \sin \phi$$
$$= \cos 48.6583^\circ \cos 80.7375^\circ \cos 30.0^\circ + \sin 48.6583^\circ \sin 30.0^\circ$$
$$= (0.66055)(0.16096)(0.866) + (0.75078)(0.5) = 0.467468$$
$$\therefore \quad \theta = 62.13^o$$

20.8 SOLAR RADIATION INTENSITY

The solar radiation intensity varies throughout the day and from day to day. In order to develop empirical correlations for the intensity, some basic concepts are required. These are first discussed and then the correlations are developed.

The energy received from the sun closely resembles that radiated by a blackbody at 5982°C (≈ 6000°C). The spectral distribution of solar radiation intensity at the outer fringes of atmosphere has a peak of 2130 W/m^2 occurring at about 450 nm in the green part of the visible spectrum. The spectrum of wavelength of solar radiation stretches from 290 nm to about 4750 nm. This radiation intensity reduces considerably at the earth's surface. Approximately 40% of the total energy is received in the narrow visible range (380 nm to 780 nm), 51% in the near infrared range (780 nm to 3500 nm) and 9% in the ultraviolet range.

20.8.1 Solar Constant

When the earth is at its mean distance from the sun, the solar radiation intensity incident upon a surface normal to sun's rays at the outer fringes of atmosphere is called solar constant. A recent review of existing data by Iqbal (1983) indicates that

$$\text{Solar constant} = 1367 \text{ W/m}^2 \tag{20.16}$$

Its maximum value is 1413 W/m^2 in January and minimum value is 1333 W/m^2 in July. On a cloudless day a total of about 1025 W/m^2 reaches the earth surface when the sun is at zenith, about 945 W/m^2 is received directly from the sun and 80 W/m^2 from the sky as diffuse radiation.

The radiation intensity I (W/m^2) incident upon a surface is the sum of direct solar radiation, I_D, sky radiation, I_d, and the radiation reflected by the surrounding surfaces I_r. In heat transfer textbooks the sum of these three radiations is referred to as irradiation, i.e.

$$I = I_D + I_d + I_r \tag{20.17}$$

20.8.2 Direct Beam Radiation

The solar radiation, which reaches from the sun directly is called *direct beam radiation*. This radiation has the property that a mirror specularly reflects it. The direct beam radiation intensity normal to sun's rays is denoted by I_N.

The area of a surface seen from the direction of sun's rays is $A \cos \theta$ if the angle of incidence is θ and the actual area of the surface is A. Hence the total radiation incident upon the surface is $I_N A \cos \theta$. Therefore, radiation intensity incident upon a surface with an angle of incidence θ, denoted by I_D, is given by

$$I_D = I_N \cos \theta \tag{20.18}$$

20.8.3 Sky Radiation

This radiation is otherwise known as diffuse radiation or scattered radiation. This radiation comes from the entire sky vault, hence the name sky radiation is also used for it. The intensity of solar radiation attenuated during its passage in the atmosphere is due to following reasons.

1. When direct radiation strikes the dry air molecules N_2 and O_2, the radiation particularly of shorter wavelengths (of the order of size of O_2 and N_2 molecules) is scattered in all directions. The absence of shorter wavelengths in solar radiation reaching the earth's surface, is the reason for the blue colour of sky.
2. The water vapour molecules present at lower altitudes also scatter the radiation.
3. Most of the ultraviolet radiation of low wavelengths is absorbed by ozone as it passes through the ozone layer. The low wavelength radiation has the highest energy ($\varepsilon = hc/\lambda$), hence its elimination by ozone layer protects life on the earth's surface. Some gases and water vapour also absorb the radiation during its passage through atmosphere. Asymmetric molecules such as ozone, water vapour, carbon dioxide and CFCs, etc. have higher absorptivities (and hence higher emissivities) than those of symmetrical molecules such as N_2 and O_2.
4. The dust particles present in the atmosphere also scatter the radiation. The familiar red colour at sunset results from scattering of longer wavelength radiation by dust or cloud particles near the earth's surface.

20.8.4 Reflected Radiation

Some of the radiation incident upon a surface may be reflected depending upon its reflectivity. If the surface has a good surface finish like polished steel or glass, then the reflection is specular (in a particular direction). A dull surface will reflect the radiation diffusely in all the directions.

20.9 THE RADIATION INTENSITY ON EARTH'S SURFACE

The depletion of monochromatic radiation (radiation of a particular wavelength) by the atmosphere is directly proportional to its intensity and the quantity of material passed through. When the sun is at zenith (directly overhead) the sun's rays have to travel a minimum distance through the atmosphere and the solar radiation intensity will be maximum. This is shown by the distance *KP* in Figure 20.6. This minimum depth is known as *unit air mass*. During the rest of the day the sun's

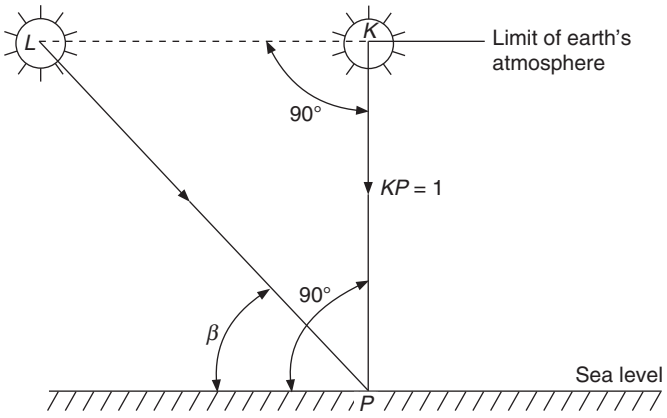

Figure 20.6 Depletion of solar radiation by the earth's atmosphere.

rays have to travel a longer distance through the atmosphere and this distance is maximum at sunrise and sunset. The distance travelled at any other time is shown by line LP in Figure 20.6. As a measure of this distance, air mass is defined as follows:

$$\text{Air mass, } m = LP/KP$$

Figure 20.6 also shows the altitude angle β of sun's ray *LP*.

$$\therefore \qquad m = \frac{LP}{KP} = \text{cosec } \beta \tag{20.19}$$

The sun's rays that reach the polar regions have to trace a longer distance than that in tropical regions and have a larger air mass. Sometimes a correction is made to air mass for atmospheric pressure, for example

$$m = \text{cosec } \beta \text{ (actual atmospheric pressure)/(standard atmospheric pressure)}$$

where β the altitude angle depends on the location, time of the day, and the day of the year. The smallar the altitude angle, the larger will be the depletion of radiation.

Figure 20.7 shows the spectral distribution of direct beam solar radiation as published by the American Society of Heating Refrigerating and Air Conditioning Engineers (ASHRAE). The outer curve shows the solar radiation at the outer fringes of atmosphere and the middle curves show the radiation incident on a surface at sea level for two air masses, namely $m = 1$ ($\beta = 90^{o}$) and $m = 5$ ($\beta = 11.5^{O}$). These two curves are for a water precipitable depth of 30 mm and dust level scale of 400 (moderately dusty atmosphere). The area under the upper curve is the solar constant. The area under the other curves is the direct beam radiation that would be incident on a surface normal to sun's rays on the earth's surface. The ratio of this area to the solar constant is called *transmission factor* which is 0.633 for m =1 and 0.276 for $m = 5$.

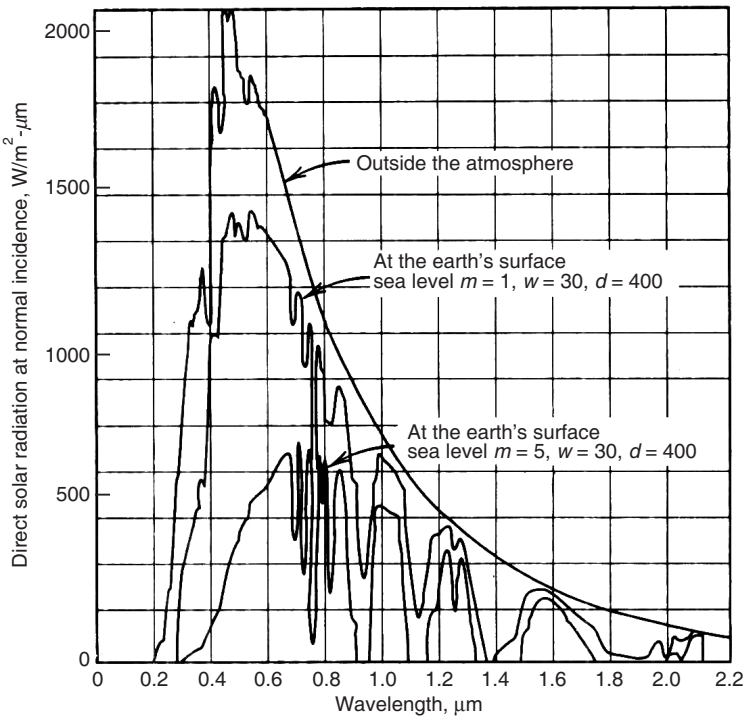

Figure 20.7 Spectral distribution of direct solar irradiation at normal incidence during clear days.

Moon (1940) has correlated the experimental data of several investigators to find the overall transmissivities of monochromatic radiation as it passes through atmosphere by including four factors mentioned above. The overall monochromatic transmissivity τ°_{λ} is defined as follows.

$$\tau^{\circ}_{\lambda} = \frac{\text{intensity for a given wavelength on earth's surface}}{\text{intensity for a given wavelength on outer fringes of atmosphere}} \tag{20.20}$$

Moon (1940) has determined these transmissivities for various wavelengths for specific dust level and precipitable water level and constructed the curves given in Figure 20.7.

20.9.1 ASHRAE Clear Sky Model

Most environmental control problems on earth's surface occur during clear days when the heating effect of sun's rays is maximum. The value of direct beam radiation component incident on earth's surface per unit area normal to sun's rays as per ASHRAE (1989) Clear Sky Model is given by

$$I_N = A \exp(-B \operatorname{cosec} \beta) \tag{20.21}$$

where

A = solar radiation W/m^2 in absence of atmosphere ($m = 0$)
B = atmospheric extinction coefficient
β = altitude angle

Table 20.2 gives the values of A and B for 21st of each month for atmospheric clearness index C_N of unity. The values of clearness index are available for most of the non-industrial locations in the USA.

Table 20.2 Constants for ASHRAE Clear Sky Model in Eq. (20.21), kW/m^2

	Jan	Feb	Mar	Apr	May	June	July	Aug	Sep	Oct	Nov	Dec
A	1.230	1.213	1.186	1.136	1.104	1.088	1.085	1.107	1.152	1.192	1.220	1.223
B	0.142	0144	0.156	0.180	0.196	0.205	0.207	0.201	0.177	0.160	0.149	0.142
C	0.058	0.060	0.071	0.097	0.121	0.134	0.136	0.122	0.092	0.073	0.063	0.057

CIBSE guide (1980) has also given the values of direct beam radiation intensity I_N on earth surface for surfaces normal to sun's rays, on horizontal surface $I_N \sin \beta$, on vertical surface $I_N \sin \beta \cos \alpha$ and for surfaces inclined to vertical surfaces at various angles. Some of these values are given in Table 20.3.

Table 20.3 Intensity of direct solar radiation with clear sky in W/m^2, 0–300 m above sea level

β, degrees	5	10	15	20	25	30	35	40	50	60	70	80
I_N	210	388	524	620	688	740	782	814	860	893	912	920
I_{DH}	18	67	136	212	290	370	450	523	660	773	857	907
I_{DV}	210	382	506	584	624	642	640	624	553	447	312	160

The solar radiation intensity increases at higher elevations since the sun's rays have to travel a smaller distance through the dense air medium near the earth's surface. Table 20.4 gives the percentage increase in solar radiation intensity with varying heights.

Table 20.4 Percentage increase in direct solar radiation with height above sea level

Height above sea level, m	*Solar altitude angle*, degrees									
	10	20	25	30	35	40	50	60	70	80
1000	32	22	18	16	14	13	12	11	10	10
1500	50	31	26	23	21	18	16	15	14	14
2000	65	40	33	29	27	24	21	19	18	18
3000	89	52	43	37	34	31	27	24	23	22

Note: The sky radiation decreases at higher elevations. It decreases by approximately 30% at 1000 m and by 60% at 1500 m above sea level.

Diffuse radiation

Diffuse radiation is difficult to determine since it does not have any preferential direction. Diffuse radiation is typically of shorter wavelength since N_2 and O_2 molecules scatter the radiation that has wavelengths similar to size of these molecules. During extremely cloudy days, only diffuse radiation may not reach the earth's surface. ASHRAE clear sky model suggests the following correlation for it.

$$I_d = CI_N \tag{20.22}$$

The value of constant C is given in Table 20.2. This is the following ratio:

$$C = \frac{\text{intensity of diffuse radiation on a horizontal surface}}{\text{intensity of direct beam normal radiation on a surface}} \tag{20.23}$$

Galanis and Chatigny (1986) have suggested the following correction for clearness index:

$$I_d = CI_N/(C_N)^2 \tag{20.24}$$

A horizontal surface (ground) can see the whole of sky, hence it radiates to the whole of sky and its configuration factor with respect to sky $F_{gs} = 1$. It has two subscripts, g for the surface (ground in this case, otherwise it will be w for wall), and s for sky. This is also called shape factor, view factor or angle factor. The two basic relations for this are mentioned in Chapter 2.

For a non-horizontal surface (wall), the shape factor has to be used since this is less than one, that is,

$$I_d = C\, I_N F_{ws} \tag{20.25}$$

If a surface (wall) is tilted by an angle ϕ with respect to vertical plane, then its shape factor with respect to ground (horizontal surface) is given by

$$F_{wg} = 0.5(1 - \sin\phi) \tag{20.26}$$

where the subscript w refers to wall and g refers to ground, the horizontal surface.

The shape factor between the ground and the wall, F_{gw}, is found from the reciprocity theorem,

$$A_w F_{wg} = A_g F_{gw} \tag{20.27}$$

The radiation that leaves the inclined surface is either incident on the ground or it goes to sky.

$$\therefore \quad F_{wg} + F_{ws} = 1$$

$$\text{or} \quad F_{ws} = 1 - F_{wg} = 1 - 0.5(1 - \sin\phi) = 0.5(1 + \sin\phi)$$

$$\therefore \quad F_{ws} = 0.5(1 + \sin\phi) \tag{20.28}$$

$$A_s F_{sw} = A_w F_{ws}$$

where F_{ws} is the shape factor between an inclined surface and the sky.

It is a common belief that sky is a uniform radiator of diffuse radiation. In that case a vertical surface will see only half of the sky whereas a horizontal surface will see full of the sky. Therefore we expect that $I_{dV} = 0.5I_{dH}$. However, it is well documented that east wall will receive more radiation than the horizontal surface during morning hours. Actually, diffuse radiation intensity from a solid angle around the sun is much more than that from the rest of the sky. During morning hours, east wall receives more diffuse radiation. The west wall receives more diffuse radiation than the horizontal surface during the evening hours. The ratio of diffuse radiation on vertical surface to the horizontal surface is given by

$$I_{dV}/I_{dH} = 0.55 + 0.437\cos\theta + 0.313\cos^2\theta \qquad \text{for } \theta > 2^\circ \tag{20.29}$$

$$= 0.45 \text{ for } \theta < 2^\circ$$

where θ is the angle of incidence.

20.9.2 Intensity of Direct Beam on a Surface

The value of I_N is the intensity of direct beam radiation on a surface normal to sun's rays. Its component may be found on any arbitrary surface by taking its projection on the given surface. Figure 20.8 shows the radiation incident on a horizontal surface. The sun's rays will make an angle equal to the altitude angle β with the horizontal surface as shown in the figure. It is seen that the rays passing through the portion NL strike the surface LM. If the intensity on the horizontal surface is I_{DH}, then

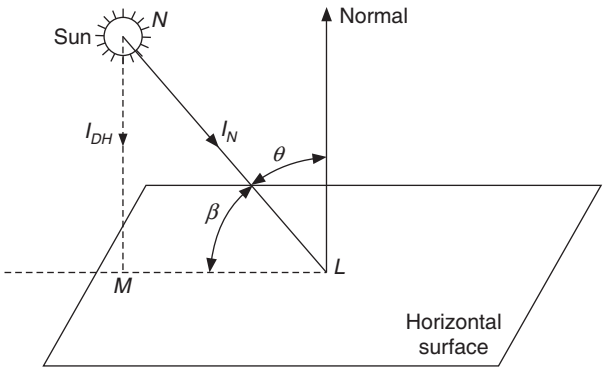

Figure 20.8 Incident angle for a horizontal surface.

$$I_{DH} = I_N \sin \beta \tag{20.30}$$

Figure 20.9 shows the direct beam radiation incident on a vertical surface. Its projection on the horizontal plane along $PA = I_N \cos \beta$. The component of this along the normal to the surface $PB = I_{DV} = I_N \cos \beta \cos \alpha$. This result could have also been obtained by using the incidence angle relation derived in Eq. (20.14) and substituting for incidence angle θ, i.e.

$$I_{DV} = I_N \cos \theta = I_N \cos \beta \cos \alpha \tag{20.31}$$

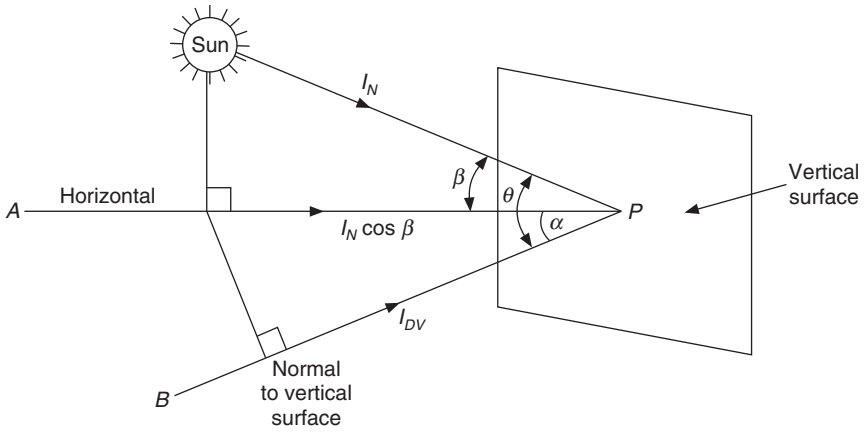

Figure 20.9 Direct solar radiation on a vertical surface.

For a tilted surface using the relation for the incidence angle given in Eq. (20.13),

$$I_{D\phi} = I_N \cos \theta = I_N (\cos \beta \cos \alpha \cos \phi + \sin \beta \sin \phi) \tag{20.32}$$

In general, the direct beam radiation intensity (W/m^2) upon a surface will be denoted by I_D. The sum of direct beam and diffuse radiation on a surface, that is, total radiation intensity I_t is given by

$$I_t = I_D + I_d F_{ws} = I_N (\cos \theta + CF_{ws}) \tag{20.33}$$

20.9.3 Reflected Radiation

This will in general be diffuse radiation unless it is reflected by a polished surface. The direct beam radiation I_D as well as the diffuse sky radiation I_d are reflected by surface. The most common case is the reflection of solar energy from ground to a tilted surface or a vertical wall. The average reflectivity of the ground may be assumed to be ρ_g. In such a case the radiation reflected by the ground and incident upon a surface is given by

$$Q_r = \rho_g A_g F_{gw} (I_{DH} + I_{dH})$$

Using the reciprocity theorem $A_w F_{wg} = A_g F_{gw}$, we get

$$Q_r = \rho_g A_w F_{wg} (I_{DH} + I_{dH})$$

$$\therefore \quad I_r = \frac{Q_r}{A_w} = \rho_g F_{wg} (I_{DH} + I_{dH}) \tag{20.34}$$

Using Eq. (20.22) for I_d ($I_{dH} = I_d$) and Eq. (20.30) for I_{DH}, we get

$$I_r = \rho_g F_{wg} I_N (C + \sin \beta) \tag{20.35}$$

Substituting Eqs. (20.33) and (20.35) in Eq. (20.17), the total radiation intensity on a surface is given by

$$I = I_N (\cos \theta + CF_{ws}) + \rho_g F_{wg} I_N (C + \sin \beta) \tag{20.36}$$

EXAMPLE 20.9 Find the direct, diffuse and total radiation on a horizontal surface in Delhi on June 22 at 3:00 pm IST. For Delhi the longitude is 77°12′ and the latitude is 28°35′.

Solution:

Equation of time and declination angles on June 21 from Table 21.1 are –1′40″ and 23°27′ respectively.

The time in Delhi is less advanced than IST.

Longitude correction = (77°12′ – 82°30′) × 4 min = –5°18′ × 4 min

= –(5 + 18/60) × 4 min = 21′12″

$\therefore$ LCT Delhi = 3:00 – 21′12″

$\therefore$ LST = LCT + equation of time = 3:00 – 21′12″ – 1′40″ = 2 h 37′08″

$\therefore$ Hour angle $\angle h = 15(2 \text{ h } 37'08'') = 15(2.6189) = 39.2833^\circ$

declination $\angle d = 23^\circ 27' = 23.45^\circ$

latitude $\angle l = 28^\circ 35' = 28.5833^\circ$

$$\sin \beta = \cos l \cos h \cos d + \sin l \sin d$$

$$= \cos 28.5833^\circ \cos 39.2833^\circ \cos 23.45^\circ + \sin 28.5833^\circ \sin 23.45^\circ$$

$$= 0.813994$$

$\therefore \quad \beta = 54.4831^\circ \qquad \sin \beta = 0.813944$

$$\cos \gamma = \sec \beta (\cos l \sin d - \cos d \sin l \cos h)$$

$$= [\cos 28.5833^\circ \sin 23.45^\circ - \cos 23.45^\circ \sin 28.5833^\circ \cos 39.2833^\circ]/\cos 54.4831^\circ$$

$$= 0.016717$$

$$\therefore \quad \gamma = 89.04213^{o}$$

From Table 21.2 for the month of June, $A = 1.088$, $B = 0.205$ and $C = 0.134$

From Eqs. (20.21) and (20.22),

$$I_N = A \exp(-B \operatorname{cosec} \beta) = A \exp(-B/\sin \beta) = 1.088 \exp(-0.205/0.813944)$$
$$= 0.84576 \text{ kW/m}^2$$

For a horizontal surface, $I_{DH} = I_N \sin \beta = 0.84576 \times 0.813944 = 0.6884 \text{ kW/m}^2$

$$I_d = C\, I_N = 0.134(0.84576) = 0.11333 \text{ kW/m}^2$$

Total radiation incident on horizontal surface = $I_{DH} + I_d = 0.6884 + 0.11333 = 0.80173 \text{ kW/m}^2$

EXAMPLE 20.10 A surface is inclined at an angle of 60° with the vertical surface facing south-west. Determine the incidence angle at 3:00 pm solar time on April 15 in New Delhi. Determine all the components of radiation.

Solution:

From Example 20.6, we have $\angle d = 9.5^{o}$, $\angle l = 28.58333^{o}$, $\angle \beta = 43.739^{o}$ and $\angle \gamma = 105.142^{o}$ west of north and $\angle h = 45^{o}$.

The normal to the south-west facing surface makes an angle of 45° with due north.

Therefore wall solar azimuth angle $\angle \alpha = 105.142° - 45° = 60.142^{o}$

Given that $\angle \phi = 60^{o}$

$$\cos \theta = \cos \beta \cos \alpha \cos \phi + \sin \beta \sin \phi = \cos 43.734° \cos 60.142° \cos 60°$$
$$+ \sin 43.739° \sin 60° = 0.7786$$

$$\therefore \quad \theta = 38.87^{o}$$

From Table 20.2 in April : $A = 1.136$, $B = 0.18$ and $C = 0.097$

From Eq. (20.21) : $I_N = A \exp(-B \operatorname{cosec} \beta) = 1.136 \exp(-0.18 \operatorname{cosec} 43.739°)$

$$\therefore \quad I_N = 0.87561 \text{ kW/m}^2$$

$$I_D = I_N \cos \theta = 0.87561(0.7786) = 0.68175 \text{ W/m}^2$$

From Eq. (20.28) $F_{ws} = 0.5(1 + \sin \phi) = 0.5(1 + \sin 60°) = 0.933$

This is the shape factor between the wall and the sky. For a vertical surface, it is 0.5 and for a horizontal surface it is 1.0. For inclined surfaces: $0.5 < F_{ws} < 1.0$. It will be less than 0.5 if the surface is inclined towards the horizontal surface from the vertical position.

$$I_d = C\, I_N\, F_{ws} = 0.097(0.87561)(0.933) = 0.0792 \text{ kW/m}^2$$

For a horizontal surface:

$$I_{DH} = I_N \sin \beta = 0.87561 \sin 43.739° = 0.60537$$

$$I_d = CI_N = 0.097(0.87561) = 0.084934$$

Assuming a reflectivity of 0.32 for fresh concrete,

$$\text{Reflected radiation from horizontal surface} = 0.32(I_{DH} + I_d)$$
$$= 0.32(0.60537 + 0.084934) = 0.2209 \text{ kW/m}^2$$

Shape factor between the tilted surface and ground, $F_{wg} = 1 - F_{ws} = 1 - 0.933 = 0.067$
Reflected radiation I_r incident upon tilted surface = $F_{wg}(0.2209) = 0.067(0.2209) = 0.0148$ kW/m^2

Hence the radiation incident on inclined surface consists of I_D, I_d and I_r.

20.10 SHADING OF SURFACES FROM DIRECT RADIATION

External shading is the best way to prevent direct solar radiation from entering an air-conditioned space. An opaque shade will prevent the entry of direct radiation but the diffuse sky and ground reflected radiation would still be incident. For a partially opaque shading, some direct radiation may also enter. Hence, an important problem is to determine if a surface is sunlit and if so what is the sunlit fraction. A window may be partially shaded due to its setback (recessed) from the plane of the wall; a flat roof may be partially shaded by parapet walls around its perimeter or a nearby building may shade another building.

Another case is the well-designed architectural projections to completely shade the window during summer and admit solar radiation during winter. These are overhangs on windows and awnings.

The orientation of the surface with respect to the direction of sun's rays decides the sunlit portion, hence each shading problem should be analyzed independently. However, there are some common features in all problems. In all the cases, an isometric sketch must be made to show the relationship between the sun's rays and the surfaces involved. Considering sun's ray passing through corner of setback or corner of overhang or corner of parapet walls does this. The point where this ray (from corner) strikes the window plane or the roof surface is located and a rectangular parallelepiped is constructed such that the sun's ray is the principal diagonal of it.

20.10.1 Shading of Roof by Parapet Walls

Suppose a flat roof is partially shaded by parapet walls of height a. The two walls are named *wall* 1 and *wall* 2 respectively. The wall solar azimuth angle is α_1 for wall 1 and α_2 for wall 2. A ray passing through the corner of the walls and striking the roof will shade a portion x parallel to wall 1 and a portion y parallel to wall 2.

The angle between the sun's ray and its projection on horizontal plane is the altitude angle β.

If the length and breadth of the roof are L_1 and L_2 respectively along walls 1 and 2, then the roof area = L_1L_2. Sunlit portion = $(L_1 - y)(L_2 - x)$ and the sunlit fraction F_s is given by

$$F_s = \frac{(L_1 - y)(L_2 - x)}{L_1 L_2}$$

which can be shown to be

$$F_s = 1 - a \cot \beta (\cos \alpha_1/L_2 + \cos \alpha_2/L_1) + (a \cot \beta)^2 \cos \alpha_1 \cos \alpha_2/L_1 L_2 \qquad (20.37)$$

where a is the height of the parapet wall and x and y can be found out to be:

$$x = a \cot \beta \cos \alpha_1 \qquad (20.38)$$

$$y = a \cos \beta \cos \alpha_2 \qquad (20.39)$$

EXAMPLE 20.11 Find the sunlit fraction of a roof in Delhi at 3:00 pm solar time on April 15. The roof is aligned with E-W-N and South directions and its dimensions are 20 m × 20 m. The parapet walls are of 1.0 m height.

Solution:

Consider wall 1 to be east facing and wall 2 to be north facing. From Example 21.6, we have at 3:00 pm solar time on April 15,

$$\angle d = 9.5^{\circ},\ \angle l = 28.58333^{\circ},\ \angle \beta = 43.739^{\circ} \text{ and } \angle \gamma = 105.142^{\circ} \text{ west of north}$$

$\therefore$ $$\alpha_2 = 180^{\circ} - \gamma = 180^{\circ} - 105.142^{\circ} = 74.858^{\circ}$$

and $$\alpha_1 = 90^{\circ} - \alpha_2 = 90^{\circ} - 74.858^{\circ} = 25.142^{\circ}$$

$\therefore$ From Eqs. (20.38) and (20.39),

$$x = 1.0 \cot 43.739^{\circ} \cos 74.858^{\circ} = 0.9461 \text{ m}$$

$$y = 1.0 \cot 43.739^{\circ} \cos 25.142^{\circ} = 0.273 \text{ m}$$

Sunlit part of roof = $(20 - 0.9461) \times (20 - 0.273) = 375.876 \text{ m}^2$

Sunlit fraction $F_s = 375.876/400 = 0.9397$

20.10.2 Shading of Window by Setback

Figure 20.10 shows a window of height a and width c, setback from the plane of wall by b units. The wall solar azimuth angle of the plane of wall is α. The sun's ray passing through the corner G at the plane of wall is considered. This ray strikes the plane of the window at point I. The portion $(c - x)\ (a - y)$ will be sunlit.

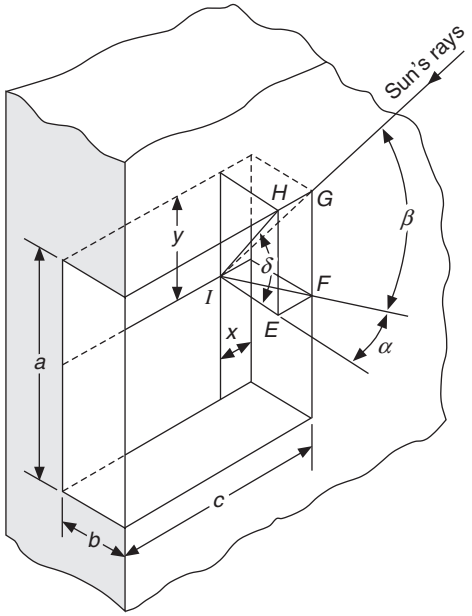

Figure 20.10 Shading of window set back from the plane of a building surface.

We can consider a horizontal plane through point I and construct a rectangular parallelepiped such that the sun's ray GI is the principal diagonal of it. Again, IF is the projection of the sun's ray on the horizontal plane.

$$\therefore \qquad \angle GIF = \beta \quad \text{and} \quad \angle EIF = \alpha$$

Let $\angle HIE$ be δ. This is called the sun's profile angle for this window.

$$x = IE \tan \alpha = b \tan \alpha \text{ since } IE \text{ is equal to the setback } b \tag{20.40a}$$

$$y = IE \tan \delta = b \tan \delta \tag{20.40b}$$

The angle δ is related to α and β. To find this relation, we consider

$$\tan \delta = \frac{HE}{EI} = \frac{GF}{EI}$$

$$GF = IF \tan \beta \quad \text{and} \quad EI = IF \cos \alpha$$

$$\tan \delta = \frac{\tan \beta}{\cos \alpha} \tag{20.41}$$

$$\therefore \qquad \text{Area of the sunlit portion} = (c - x)(a - y) = ac - cy - ax + xy$$

$$\therefore \qquad \text{Sunlit fraction, } F_s = \frac{(c - x)(c - y)}{ac} = 1 - \frac{y}{a} - \frac{x}{c} + \frac{xy}{ca}$$

or
$$F_s = 1 - r_1 \tan \delta - r_2 \tan \alpha + r_1 r_2 \tan \alpha \tan \delta \tag{20.42}$$

where $r_1 = b/a$ and $r_2 = b/c$.

EXAMPLE 20.12 Determine the sunlit fraction of a south-facing window 1.8 m high and 2.0 m wide and set back by 0.2 m. The location is Delhi at 3:00 pm solar time on April 15.

Solution:

From Example 21.6 we have on April 15 at 3:00 pm solar time

$$\angle d = 9.5^\circ,\ \angle l = 28.58333^\circ,\ \angle \beta = 43.739^\circ \text{ and } \angle \gamma = 105.142^\circ \text{ west of north}$$

For south-facing window $\alpha = 180° - \gamma = 74.858°$. From Eq. (20.41),

$$\tan \delta = \frac{\tan \beta}{\cos \alpha} = \frac{\tan 43.739°}{\cos 74.858°} = 3.6632$$

We have from Eqs. (20.40a) and (20.40b),

$$x = b \tan \alpha = 0.2 \tan 74.858° = 0.739 \text{ m}$$

$$y = b \tan \delta = 0.2\ (3.6632) = 0.7326 \text{ m}$$

We have $a = 1.8$ and $c = 2.0$. Hence from Eq. (20.42),

$$F_s = \frac{(c - x)(a - y)}{ac} = \frac{(2.0 - 0.739)(1.8 - 0.7326)}{3.6} = 0.3739$$

20.10.3 Overhang to Completely Shade the Window

Using an overhang it is possible to completely shade the whole of window. Suppose a window has a setback of b units. The overhang is located e units above the window and protrudes by f units out of the plane of wall and protrudes by g units on both the sides of the window. The height of the window is a units.

The wall solar azimuth angle of plane of wall is α. The sun's ray passing through the corner of the overhang is considered. It strikes the plane of the window at a point that lies at the bottom of the window *and hence completely shades the window*.

We can consider a horizontal plane through a point at the bottom of the window, and construct a rectangular parallelepiped such that the sun's ray is the principal diagonal of it. In this case too, Eq. (20.41) is valid, that is,

$$\tan \delta = \frac{\tan \beta}{\cos \alpha} \tag{20.43}$$

The height of the overhang from the bottom of the window = $a + e$. It can be shown that

$$f = (a + e) \cot \delta - b \tag{20.44}$$

and

$$g = f \tan \alpha \tag{20.45}$$

EXAMPLE 20.13 A south-facing window 1.5 m high and 2.0 m wide is set back from the plane of building by 0.2 m. It is desired to install a solid overhang 0.3 m above the window such that it will completely shade the window on April 15 at 9:00 am to 3:00 pm solar time in Kolkata. Calculate the dimensions of the overhang.

Solution:

9:00 am and 3:00 pm both have hour angle of 45°, hence all other angles will be same for them.

Latitude of Kolkata $\angle l$ =23.65°, declination angle on April 15 from Table 21.1

$$\angle d = 9.5^\circ \text{ and } \angle h = 45^\circ$$

$$\sin \beta = \cos l \cos d \cos h + \sin l \sin d = (0.92287)(0.9863)(0.7071) + 0.3851(0.16505)$$

$$= 0.70718$$

$$\therefore \quad \beta = 45.006^\circ$$

$$\cos \gamma = \sec \beta (\cos l \sin d - \cos d \sin l \cos h) = 1.4144[0.92287(0.165) - 0.9863(0.3851)\ 0.7071$$

$$= -0.1645$$

$\therefore$ $\gamma = 99.468°$ east of north. It is more than 90°. Hence the sun rises south of east. The wall solar azimuth angle for south-facing wall will be 180° – 99.468°.

$$\alpha = 180° - 99.468° = 80.532°$$

$$\cot \delta = \frac{\cos \alpha}{\tan \beta} = \frac{0.1645}{1.0002} = 0.16445$$

Therefore from Eqs. (20.44) and (20.45),

$$f = (a + e) \cot \delta - b = (1.5 + 0.3)(0.16445) - 0.2 = 0.096 \text{ m}$$

$$g = f \tan \alpha = 0.096\ (5.996) = 0.576 \text{ m}$$

EXAMPLE 20.14 Repeat Example 20.13 for 11:00 am solar time with $\angle h = 15^{\circ}$.

Solution:

$$\sin \beta = (0.92287)(0.9863)(0.9659) + 0.3851(0.16505) = 0.9428$$

$$\therefore \quad \beta = 70.522^{\circ} \text{ and } \sec \beta = 2.999$$

$$\cos \gamma = 2.999[0.92287(0.165) - 0.9863(0.3851)(0.9659)\ ] = -0.644$$

$$\therefore \quad \gamma = 130.08^{\circ} \text{ east of north}$$

$$\alpha = 180^{\circ} - 130.08^{\circ} = 49.922^{\circ}$$

$$\cot \delta = \frac{\cos \alpha}{\tan \beta} = 0.2273$$

$$f = (a + e) \cot \delta - b = (1.5 + 0.3)(0.2273) - 0.2 = 0.209 \text{ m}$$

$$g = f \tan \alpha = 0.209(1.1885) = 0.248 \text{ m}$$

EXAMPLE 20.15 Repeat Example 20.13 for solar noon with $\angle h = 0^{\circ}$.

Solution:

$$\sin \beta = (0.92287)(0.9863)(1.0) + 0.3851(0.16505) = 0.9738$$

$$\therefore \quad \beta = 76.852^{\circ}$$

$$\cos \gamma = 4.3964[0.92287(0.165) - 0.9863(0.3851)\ (1.0)] = -1.0$$

$$\therefore \quad \gamma = -180^{\circ}$$

$$\therefore \quad \alpha = 0$$

$$\cot \delta = \frac{\cos \alpha}{\tan \beta} = \frac{1.0}{4.281} = 0.2336$$

$$f = (a + e) \cot \delta - b = (1.5 + 0.3)\ (0.2336) - 0.2 = 0.2205 \text{ m}$$

$$\gamma = f \tan \alpha = 0.209(0.0) = 0.0 \text{ m}$$

It is observed that the altitude angle increases as solar noon is approached. The above calculation gives the impression that the front protrusion overhang should be increased and the side protrusion be decreased as solar noon approaches. However, inspection reveals that as the altitude increases, the sun's ray coming from corner of the overhang will strike the window below its bottom-most point, that is the whole window will remain shaded up to solar noon and even up to 3:00 pm ($\angle h = 45^{\circ}$).

Further it is observed that August 29 and April are symmetric with respect to June 22 and the declination angle will be larger than 9.5° during this period.

Hence the overhang calculated in Example 20.13 will shade the window from 9:00 am to 3:00 pm on each day between April 15 and August 29.

REFERENCES

ASHRAE Handbook of Fundamentals Volume (1989): American Society of Heating Refrigerating and Air Conditioning Engineers, Inc., Atlanta, Ga.

Galanis, N. Charigny, R. (1986): A Critical Review of the ASHRAE Solar Radiation Model, *ASHRAE Transactions*, Vol. 92, Pt.1.

Iqbal, M. (1983): *An Introduction to Solar Radiation*, Academic Press, Toronto.

Moon, P. (1940): Proposed Standard Radiation Curves for Engineering Use, *Journal of the Franklin Institute*, Vol. 230, Nov. 1940, pp. 583–617.

Threlkeld, J.L. (1962): *Thermal Environmental Engineering*, Prentice-Hall, Inc. N.Y.

REVIEW QUESTIONS

1. Find the local solar time at 9:00 am IST on 22nd October in Kolkata located at 88°27′E and 22°39′N.
2. Find the smallest and the largest altitude angle in Kolkata.
3. Find the sum's altitude and azimuth angles at 8.30 am solar time on 1st February for Delhi with latitude 28.58333° and longitude 77.2°.
4. Find the sunrise, sunset and total sunshine hours at Kolkata (latitude 22°39′N) on 15th January.
5. Find the altitude and azimuth angles on 15 August in Delhi at solar noon, 2:00 pm and 4:00 pm solar time. Also, find the wall solar azimuth angle for a south-facing wall.
6. Find the direct, diffuse and total radiation on a horizontal surface in Kolkata on 22nd December at 3.00 pm IST. The longitude at Kolkata is 88°27′E and the latitude is 22°39′N.
7. A surface is inclined at an angle of 30° with the vertical surface facing south-east. Determine the incidence angle at 3.00 pm solar time on 22nd December in Delhi. Also, find all the components of radiation.
8. Find the sunlit fraction of a roof in Delhi at 3.00 pm solar time on 22nd December. The roof is aligned in the E-W-N and south directions and its dimensions are 25 m × 25 m. The height of parapet walls is 1.5 m.
9. Find the sunlit fraction of a south-facing window 2 m × 2 m and set back by 0.25 m. The location is Kolkata at 3.00 pm solar time on 22nd December.
10. Repeat solved Examples 20.13, 20.14 and 20.15 for Delhi and analyse the results obtained.

21

Load Calculations

LEARNING OBJECTIVES

After studying this chapter the student should be able to:

1. Calculate the steady-state, one-dimensional heat transfer rate through homogeneous and non-homogeneous walls, through walls separated by an air cavity, and through composite walls consisting of a combination of homogeneous and non-homogeneous walls and air spaces.
2. Assimilate the solar radiation properties of various surfaces and diathermanous materials, in particular the common window glass.
3. Explain the phenomenon of heat transfer through glass, and define the term 'solar heat gain factor' (SHGF).
4. Explain and define the term 'shading coefficient' as applied to glazed portions of the glass.
5. Analyze mathematically the phenomenon of heat balance for the glass.
6. Discuss the phenomenon of periodic heat transfer through walls and roofs.
7. Explain the meaning and use of the term 'sol-air temperature' in heat transfer calculations, including those of composite walls.
8. Describe the methods used to determine heat gain from a wall.
9. Understand the concept of equivalent temperature difference for walls and roofs exposed to the sun.
10. Analyze and use the *Z*-transform methods for design load calculations.
11. Explain the methods used for estimating infiltration.
12. Explain the purpose of vapour barriers.
13. Perform load calculations of buildings for selection of air conditioning equipment, after taking into account various types of heat transfers.

21.1 INTRODUCTION

The control of thermal environment in a building requires measures to counteract the heat and moisture gain (or loss) by a building. Heat transfer occurs if there is a temperature difference between the interior space and the external environment. Both heat and mass transfer occur through the exchange of air by leakage through cracks, crevices, openings and door openings in the building. Solar radiation affects the heat transfer through opaque as well as diathermanous materials, the transmission through the latter being very significant.

The intensity of solar radiation varies from a minimum at sunrise and sunset, to maximum at solar noon. The air temperature also varies in response to solar radiation, being minimum about one hour before the sunrise and maximum about three hours after solar noon. The building material also has thermal capacity due to which it stores energy and delays the transmission of energy. Heat transfer in buildings is always periodic. Steady-state heat transfer seldom occurs in buildings, however steady-state analysis provides a convenient tool for some calculations. This is considered in the following section.

21.2 STEADY-STATE HEAT TRANSFER THROUGH A HOMOGENEOUS WALL

In this section, steady-state heat transfer through solid boundaries of a building is considered. Heat transfer through the building is assumed to be steady if the indoor and outdoor conditions do not vary with time. The indoor air conditions are: t_i, W_i and p: interior surface temperature = t_{si}, and still air, that is, $V < 0.25$ m/s. The outdoor air conditions are: t_o, W_o and p: exterior surface temperature = t_{so}, and air velocity V m/s. To begin with let us consider steady-state heat transfer through a building wall (Figure 21.1).

It is assumed that the wall is homogeneous, single-layered and has a uniform thermal conductivity k_w. The length and width of the wall perpendicular to the plane of paper are assumed to be very large compared to the thickness of the wall so that heat transfer may be considered to be one-dimensional. The inside and outside surface temperature of the wall are t_{wi} and t_{wo} respectively. Heat transfer rate per unit area of the wall may therefore be expressed as

$$q = h_o(t_o - t_{wo}) = \frac{k_w\,(t_{wo} - t_{wi})}{x_w} = h_i\,(t_{wi} - t_i) \tag{21.1}$$

where, h_i and h_o are heat transfer coefficients from the inner and outer surfaces of the wall, that is, the sum of convective and radiative heat transfer coefficients as outlined in Chapter 2. If h_{ci} and h_{co} are convective heat transfer coefficients from the inner and outer surfaces of the wall respectively, and ε is emissivity, then the combination of convection and radiation from the surface gives

$$q = h_{ci}\,(t_{wi} - t_i) + \sigma\,\varepsilon\,(T_{wi}^4 - T_{si}^4) \tag{21.2}$$

$$= h_{ci}\,(t_{wi} - t_i) + h_{ri}\,(t_{wi} - t_{si}) \qquad \text{where } h_{ri} = \frac{\sigma\,\varepsilon(T_{wl}^4 - T_{si}^4)}{t_{wi} - t_{si}}$$

$$= \left\{ h_{ci} + h_{ri}\,\frac{(t_{wi} - t_{si})}{(t_{wi} - t_i)} \right\} (t_{wi} - t_i) = h_i\,(t_{wi} - t_i)$$

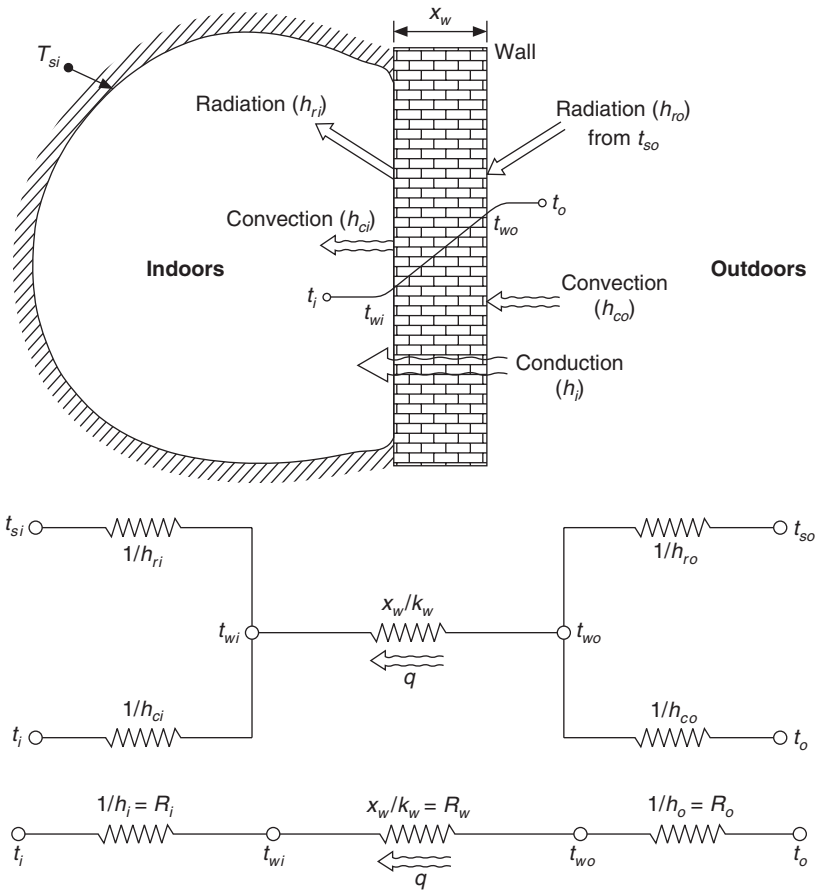

Figure 21.1 Steady-state heat transfer through a building wall and the corresponding resistance network.

$$\therefore \qquad h_i = h_{ci} + h_{ri}\frac{(t_{wi} - t_{si})}{(t_{wi} - t_i)} \quad \text{and similarly} \quad h_o = h_{co} + h_{ro}\frac{(t_{so} - t_{wo})}{(t_o - t_{wo})} \tag{21.3}$$

where, $$h_{ro} = \frac{\sigma\varepsilon(T_{wo}^4 - T_{so}^4)}{t_{wo} - t_{so}}$$

and σ is Boltzmann constant, i.e. $\sigma = 5.669 \times 10^{-8}$ W/m^2-K^4

It is a common practice to define an overall heat transfer coefficient U_o such that

$$q = U_o\,(t_o - t_i) \tag{21.4}$$

The expression for U_o may be obtained from Eq. (21.4) by the procedure outlined in Chapter 2. This expression is as follows:

$$\frac{1}{U_o} = \frac{1}{h_i} + \frac{x_w}{k_w} + \frac{1}{h_o} \quad \text{or} \quad U = U_o = \frac{1}{R_t} = \frac{1}{\sum_n R_n} \tag{21.5}$$

where R_n are the thermal resistances, for example, $R_i = 1/h_i$ and $R_o = 1/h_o$ are the combined convective and radiative resistances for the inside surface and the outside surface respectively, and $R_w = x_w/k_w$ is the thermal conduction resistance of the wall material. The total resistance is the sum of these three resistances, i.e.

$$R_t = R_i + R_w + R_o \tag{21.6}$$

21.3 NON-HOMOGENEOUS WALL

Most of the building materials are composite in nature consisting of layers of materials such as brick, cement plaster and finishing materials like linoleum, etc. The building walls may also consist of non-homogenous blocks like hollow bricks, cavities and air spaces.

Figure 21.2 shows the cross-section of a hollow block where the two outer surfaces are at different temperatures t_1 and t_2. The heat transfer will be by a combination of convection and conduction through the outer layers and by radiation and convection in the air spaces. Since it is difficult to evaluate theoretically the heat transfer rate through non-homogeneous materials, the heat transfer rate per unit area q is experimentally determined and expressed in the following convenient form

$$q = C(t_1 - t_2) \tag{21.7}$$

where C is the thermal conductance in W/m^2-K and is similar to convective heat transfer coefficient. It is determined experimentally.

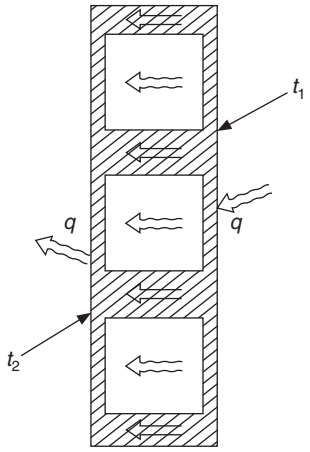

Figure 21.2 Heat transfer through a non-homogeneous wall.

Figure 21.3 shows two parallel walls separated by an air cavity. Assuming that the convective heat transfer coefficient is the same for two walls of the cavity, the overall convective heat transfer coefficient is expressed as

$$\frac{1}{U_o} = \frac{1}{h_c} + \frac{1}{h_c} = \frac{2}{h_c}$$

$$\therefore \quad U_o = h_c/2 \tag{21.8}$$

and

$$q = (h_c/2)\,(t_1 - t_2) + h_r\,(t_1 - t_2) = (h_c/2 + h_r)(t_1 - t_2) \tag{21.9}$$

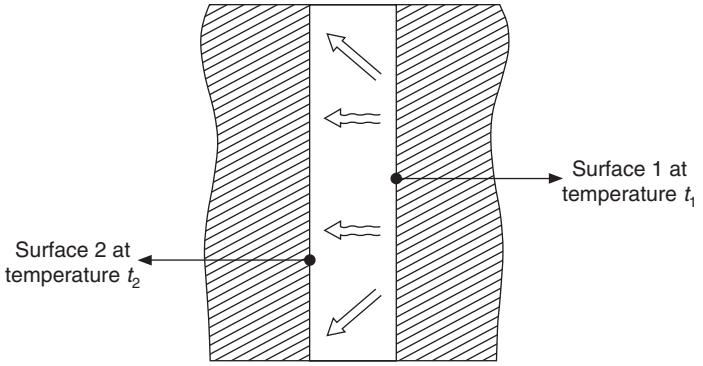

Figure 21.3 Heat transfer through an air space in the wall.

Assuming the surfaces to be flat and parallel walls, the radiation heat transfer rate is expressed as

$$Q_r = \sigma E_A (T_1^4 - T_2^4) \qquad \text{where, } E_A = \frac{1}{\frac{1-\varepsilon_1}{\varepsilon_1 A_1} + \frac{1}{A_1 F_{12}} + \frac{1-\varepsilon_2}{\varepsilon_2 A_2}}$$

In this case $A_1 = A_2$ and $F_{12} = 1$.

$$\therefore \qquad E_A = \frac{A_1}{\frac{1}{\varepsilon_1} + \frac{1}{\varepsilon_2} - 1} \qquad \text{and} \qquad h_r = \sigma E \frac{(T_1^4 - T_2^4)}{(t_1 - t_2)}, \qquad \text{where } E = \frac{1}{\frac{1}{\varepsilon_1} + \frac{1}{\varepsilon_2} - 1} \tag{21.10}$$

The heat transfer rate per unit area is measured in the same way as for the inhomogeneous materials block by introducing thermal conductance C as follows.

$$C = (h_c/2) + h_r \tag{21.11}$$

In general, for a composite wall consisting of layers of materials and non-homogeneous blocks, the overall heat transfer coefficient may be expressed as

$$\frac{1}{U_o} = \frac{1}{h_i} + \sum_n \frac{x_{nw}}{k_{nw}} + \sum_m \frac{1}{C_m} + \frac{1}{h_o} \tag{21.12}$$

Most buildings have forced convection heat transfer along the outer wall or roof and natural convection along the interior walls or narrow air spaces. The heat transfer coefficient depends upon surface characteristics like roughness and emissivity, etc. The magnitude and direction of outdoor air velocity is also unpredictable, hence there is always some uncertainty in finding the values of surface heat transfer coefficients. The surface heat transfer coefficient varies from 6 W/m^2-K to 35 W/m^2-K for free and forced convection respectively.

Table 21.1 gives the experimentally determined values of surface heat transfer coefficients h_i and h_o as given in *ASHRAE Handbook of Fundamentals Volume*, 1999. These are specially useful when the surroundings temperatures are same as the air temperature. It is observed that these values are given for three values of emissivity ε, namely $\varepsilon = 0.05$, 0.5 and 0.9. The surface with $\varepsilon = 0.05$ is a highly reflective surface since reflectivity $\rho = (1 - \alpha) = (1 - \varepsilon) = 0.95$. It is further observed that the effect of radiation is particularly significant for low velocities, that is for free convection. For forced convection, its relative magnitude decreases.

Table 21.1 Surface heat transfer coefficient (convective heat transfer coefficients)

$h = 7.9 + 0.9V$	For very smooth surfaces [W/m^2-K]
$h = 9.1 + 1.06V$	For smooth wood and plaster
$h = 11.4 + 1.41V$	For cast concrete and smooth brick
$h = 11.9 + 1.76V$	For rough surfaces

where velocity V is in km/h.

Average values of surface heat transfer coefficients (W/m^2-K)

Surface orientation	*Air velocity* (km/h)	*Direction of heat flow*	*Surface emissivity*		
			Non-reflective		*Reflective*
			0.90	0.20	0.05
Horizontal	Still air	Up	9.26	6.25	4.31
		Down	6.13	2.10	1.25
Vertical	Still air	Horizontal	8.29	4.20	3.35
Any position	25	Any	34.0	–	–
Any position	12.5	Any	22.7	–	–
Sloping (45)	Still air	Up	9.09	5.0	4.15
Sloping (45)	Still air	Down	7.50	3.41	2.56

Applicable for mean temperature of 10°C to 32°C when ambient air and surrounding surfaces are at the same temperature.

Table 21.2(a) gives the thermal properties like density, thermal conductivity, specific heat and thermal conductance for specific thickness for various materials used in building construction.

Table 21.2(a) Thermal conductivities and conductance of building and insulating materials

Material and Description	*Density* (kg/m^3)	*Thermal conductivity* (W/m-K)	*Thermal conductance* (W/m^2-K)	c_p (kJ/kg-K)
Brick				
Face	2000	1.32		0.84
Common	1600	0.77		0.84
Fire brick	2000	1.04–1.09		0.96
Concrete	2400	1.4–2.9		0.88
Sand and gravel or stone aggregate (concretes with more than 50% quartz)	2240	1.3–2.6		
Sands having higher conductivities in the higher range	2080	1.0–1.9		
Limestone concrete	1920	1.14		
Limestone concrete	1600	0.79		
RCC	2240	0.91		

(*Contd.*)

Table 21.2(a) Thermal conductivities and conductance of building and insulating materials (contd.)

Material and Description	*Density* (kg/m^3)	*Thermal conductivity* (W/m-K)	*Thermal conductance* (W/m^2-K)	c_p (kJ/kg-K)
Hollow clay tiles				
1 cell deep (10 cm)	–	–	5.11	
2 cell deep (20 cm)	–	–	3.07	
3 cell deep (30 cm)	–	–	2.27	
Lime mortar	1700	0.76		
Marble	2600	2.97		
Cement plaster sand aggregate	1860	0.72		
Cement plaster sand aggregate 10 mm			75.5	0.84
Cement plaster sand aggregate 20 mm			37.8	0.84
Cement plaster	1885	0.865		0.796
Cement mortar 1 : 3	1540	1.39		–
Cement mortar 1 : 6	1643	1.39		–
Asbestos cement board	1970	0.39		
Asbestos cement board 6.4	1900	–	93.7	–
Gypsum or plaster board 9.5	800		17.6	1.09
Gypsum or plaster board 12.7 mm	800		12.6	1.09
Plywood 6.4 mm	540	0.12	18.2	
Vegetable fiber board				
Sheathing regular density 12.7 mm	290		4.3	
Sheathing intermediate density 12.7 mm	350		5.2	
Hard board				
Medium density	800	0.105		
High density	1010	0.144		
Particle board medium density	800	0.135		
Carpet and fibrous pad			2.73	
Carpet and rubber pad			4.6	1.38
Tile-asphalt, linoleum, vinyl, rubber			113.6	1.26
Glass fiber, organic bonded	64–140	0.036		
Cellular glass	136	0.05		
Cork board	104–128	0.04		
Expanded polysterene	20.5	0.039		
Expanded polystyrene	16	0.037		
Mineral wool				
Board type	240	0.048		
Full type	150	0.039		
Metals				
Aluminium (110)	2660	221.5		0.9
Mild steel	7600	45.3		0.5
Stainless steel	7680	15.6		0.46

(*Contd.*)

Table 21.2(a) Thermal conductivities and conductance of building and insulating materials (contd.)

Material and Description	*Density* (kg/m^3)	*Thermal conductivity* (W/m-K)	*Thermal conductance* (W/m^2-K)	c_p (kJ/kg-K)
Woods				
Fiber board	270	0.049		
Red oak	659–749	0.16–0.18		
White pine	500	0.112		
Ply	544	0.1		
Hard	720	0.158		1.63
Soft, hem-fir, spruce-pine-fir	392–502	0.107–0.13		1.63
Glass window				
A	2700	0.78		
B	2640	0.756		
Borosilicate	2200	1.09		
Pyrex	2250	1.09		
Flint	3956	7.36		
Straw wheat	31	0.045		
Gypsum solid	1250	0.043		

At average temperature of 32.2°C and temperature difference of 5.6°C, E is the effective emittance. Values for other temperatures and for thickness of 40 mm and 90 mm are available in *ASHRAE Handbook of Fundamentals Volume*, 1997.

For many common building sections, the values of U_o, including walls, floors, doors, windows and skylights are given in *ASHRAE Handbook of Fundamentals Volume*, 1997. However, these are for the door and window constructions used in the USA.

Approximate values for some of the walls and roof constructions commonly used in tropical countries are given in Table 21.2(b). Otherwise, U_o values can be calculated from the thermophysical properties given in Table 21.2(a) and surface heat transfer coefficients given in Table 21.1.

Table 21.2(b) Overall heat transfer coefficients (W/m^2-K)

Details of the structure	*Thickness* (mm)	*Mass* (kg/m^2)	*Interior finish*		
			15 mm plaster on wall		
			(1)	(2)	(3)
Walls					
1. Solid brick face and common	20	425	2.72	2.56	2.33
	30	600	1.99	1.87	1.7
	40	845	1.53	1.48	1.42

(*Contd.*)

Table 21.2(b) Overall heat transfer coefficients (W/m^2-K) (contd.)

Details of the structure	*Thickness* (mm)	*Mass* (kg/m^2)	*Interior finish* 15 mm plaster on wall (1)	(2)	(3)
Common brick only	20	390	2.33	2.21	1.99
	30	585	1.76	1.70	1.53
	40	780	1.42	1.36	1.31
2. Stone	20	490	3.80	3.58	3.01
	30	735	3.12	2.96	2.61
	40	980	2.67	2.56	2.27
	60	1485	2.04	1.99	1.82
3. Poured concrete, density 2240 kg/m^3	15	340	4.26	3.92	3.29
	20	455	3.80	3.58	3.01
	25	571	3.46	3.24	2.78
	30	684	3.12	2.95	2.56
	15	195	1.76	1.70	1.53
	20	259	1.42	1.36	1.31
	25	322	1.19	1.14	1.08
	30	390	1.02	0.97	0.85
	15	73	0.74	0.74	0.74
	20	98	0.57	0.57	0.57
	25	122	0.45	0.45	0.45
	30	146	0.40	0.40	0.40
4. 33.8 cm brick + 1.25 cm plaster on both sides		720	1.54		
5. 22.5 cm brick + 1.25 cm plaster on both sides		500	2.01		
6. 30 cm cavity wall + 1.25 cm plaster on both sides		240	1.60		
7. 20 cm cavity wall + 1.25 cm plaster on both sides		190	1.95		
Roofs					
1. 11.25 RCC slab +11.25 lime concrete +1.25 cm plaster		450	2.31	2.64	
2. 11.25 RCC slab + 7.25 lime concrete + 1.25 cm plaster		390	2.63	3.07	
Solid Wooden Door [Thermal conductivity = 0.159 W/m-K]					
Actual thickness, mm	20	28	35	41	54	67
U (W/m^2-K)	3.63	3.12	2.73	2.44	2.04	1.76

Table 21.2(c) Overall heat transfer coefficients for fenestration

Type of glass		*U–Value* (W/m-K)	
		No shading	*Shading*
Vertical panels			
Glass			
Outdoor exposure	Winter	6.42	4.88
	Summer	6.02	4.59
Indoor partition			4.1
Prime window plus Storin			
Single plastic sheet			
Outdoor exposure	Winter	6.19	
	Summer	5.68	
Indoor partition		3.97	
Horizontal glass sheet			
Outdoor exposure	Winter		
	Summer		
Indoor partition			

Table 21.3 Reflectance and emittance of various surfaces

Material	*Reflectivity,* ρ	*Emissivity,* ε
Aluminium foil bright	0.92–0.97	0.05
Aluminium sheet	0.8–0.95	0.12
Aluminium coated paper polished	0.75–0.84	0.2
Steel galvanized bright	0.7–0.8	0.25
Aluminium paint	0.3–0.7	0.5
Wood, paper, glass, masonry, non-metallic	0.05–0.15	0.9

Table 21.4 Thermal resistance of plane air spaces

Orientation of space	*Direction of heat flow*	*Thermal resistance* [(K-m^2)/W]									
		Air space thickness 13 mm					*Air space thickness* 20 mm				
		E = 0.03	0.05	0.2	0.5	0.82	0.03	0.05	0.2	0.5	0.82
Horizontal	Up	0.37	0.36	0.27	0.17	0.13	0.41	0.39	0.28	0.18	0.13
45^o Slope	Up	0.43	0.41	0.29	0.19	0.13	0.52	0.49	0.33	0.20	0.14
Vertical	Horizontal	0.43	0.41	0.29	0.19	0.14	0.62	0.57	0.37	0.21	0.15
45^o Slope	Down	0.44	0.41	0.29	0.19	0.14	0.62	0.58	0.37	0.21	0.15
Horizontal	Down	0.44	0.41	0.29	0.19	0.14	0.62	0.58	0.37	0.21	0.15

To find the heat transfer through floor or from the walls and floor of basement, the temperature difference between the ground and inside air is required. The heat transfer coefficient will depend upon the floor or wall material and the thermal conductivity of the ground. Mitalas (1982) has given overall heat transfer coefficients for basement walls and floor. The ground temperature is taken as the sum of average winter temperature and the amplitude of ground temperature variation about the average temperature. The data about these temperatures is given in *ASHRAE Handbook Fundamentals Volume*, 1977 for various locations in the USA. No such data is available for Indian cities. In this absence of this data, a temperature difference of 2.5°C is assumed.

EXAMPLE 21.1 Determine the overall heat transfer coefficient for the combination of a roof and a false ceiling. The wall and the roof have overall heat transfer coefficients of 2.3 W/m^2-K and 2.0 W/m^2-K respectively. The false ceiling is made of 12.7 mm vegetable regular density fiber board. The distance between the false ceiling and the roof is 0.6 m. The ceiling has an area of 1200 m^2 (30 × 40) and perimeter of 140 m.

Solution:

Let the outdoor, indoor, and air space temperatures be t_o, t_i and t respectively.

The conductance of fiber board C_{fc} = 4.3 W/m^2-K from Table 21.2(a) and the surface heat transfer coefficient for still air from Table 21.1, h_i = 9.26 W/m^2-K. Hence the overall heat transfer coefficient for the combination of roof and false ceiling is given by

$$\frac{1}{U_{fc}} = \frac{1}{h_i} + \frac{1}{C_{fc}} + \frac{1}{h_i} = \frac{1}{9.26} + \frac{1}{4.3} + \frac{1}{9.26} \qquad \therefore \quad U_{fc} = 2.22945$$

Heat transfer from air space to the wall is given by

$$Q_w = 2.3(0.6)(140)(t_o - t) + 2.0(1200)(t_o - t) = 2593.2(t_o - t) = C_1(t_o - t)$$

Heat transfer from air space to roof is given by

$$Q_r = 2400(t_o - t_i)$$

Heat transfer from air space through the false ceiling to the room air is given by

$$Q = 1200(2.22945)\ (t - t_i) = 2675.34\ (t - t_i) = C_2(t - t_i)$$

$$\frac{1}{U_o A_o} = \frac{1}{C_1} + \frac{1}{C_2} = \frac{1}{2593.2} + \frac{1}{2675.34} = 0.0007594 \qquad \therefore \quad U_o A_o = 1316.6815$$

$$\therefore \qquad U_o = \frac{1316.6815}{1200} = 1.0973 \text{ W/m}^2\text{-K}$$

21.4 SOLAR RADIATION PROPERTIES OF SURFACES

A part of the solar radiation incident upon a building surface may be reflected, part absorbed and the remainder may be transmitted through the surface. In general, we have

$$\rho + \alpha + \tau = 1 \tag{21.13}$$

where ρ is the reflectivity of the surface, α the absorptivity and the τ transmittivity.

For opaque materials $\tau = 0$, hence

$$\rho + \alpha = 1 \tag{21.14}$$

We should keep in mind that Kirchhoff's law ($\varepsilon = \alpha$) is not valid for a surface irradiated by solar radiation, since reflectivity α corresponds to short wavelength (high temperature) solar radiation and emissivity ε corresponds to long wavelength (low temperature) radiation. Table 21.5 shows the absorptivities for various surfaces, both for low-temperature and solar radiation. The colour of the surface does not make a significant difference for long wavelength (room temperature) radiation but is very significant for solar radiation. The table shows that in the temperature range of 10°C to 40°C, a black and a white surface has the same absorptivity. For solar radiation, a dull black surface may have an absorptivity of 0.98, while a glossy white surface may have an absorptivity of 0.3. The absorptivity of metallic surfaces is much higher for solar radiation than for room temperature radiation.

Table 21.5 Absorptivities for various surfaces for solar radiation and long wavelength radiation

Surface	*Emissivity or absorptivity*		*Absorptivity for solar radiation*
	10°C to 40°C	550°C	
A small hole in a large box, sphere, furnace or enclosure	0.97–0.99	0.97–0.99	0.97–0.99
Black non-metallic surfaces such as asphalt, carbon slate, paint and paper	0.90–0.98	0.90–0.98	0.85–0.98
Red brick and tile, concrete and stone, rusty steel and iron, dark paints (red, green and brown, etc.)	0.85–0.95	0.75–0.90	0.65–0.80
Yellow and buff brick and stone, firebrick and clay	0.85–0.95	0.70–0.85	0.50–0.70
White or light-cream brick, tile, paint or paper, plaster, whitewash	0.85–0.95	0.60–0.75	0.30–0.50
Window glass	0.90–0.95		
Bright aluminium paint; gilt or bronze paint	0.4–0.6		0.3–0.5
Dull brass, copper, or aluminium; galvanized steel; polished iron	0.2–0.3	0.3–0.5	0.4–0.65
Polished brass, copper, monel metal	0.02–0.05	0.05–0.15	0.3–0.5
Highly polished aluminium, tin plate, nickel, chromium	0.02–0.04	0.05–0.1	0.1–0.4

The reflectivity of a surface may be determined by Eq. (21.14) with the value of α obtained from Table 21.5. The reflectivities and absorptivities vary with the wavelength of the incident radiation. The reflectivity values given in Table 21.6 are the average values over the entire solar spectrum. Reflectivities of polished aluminium and flat white paint are known to vary considerably in the solar spectrum, that is, from wavelength of 0.3 μm to 2.3 μm. The reflectivities of various ground surfaces increase with the angle of incidence. Table 21.6 has presented this data for the angle of incidence θ in the range from 30° to 70°.

Table 21.6 Solar reflectivities for various ground surfaces

Ground surface	*Reflectivity* $\theta = 30 - 70^{o}$	*Reflectivity* ASHRAE (1)
Bituminous parking lot surface	0.1–0.12	0.1
Bituminous and gravel roof	0.13–0.14	
Crushed rock surface	0.18–0.2	
Old concrete	0.24–0.26	0.22
Bright green grass	0.22–0.3	0.23
New concrete	0.33–0.36	0.32

21.5 RADIATION PROPERTIES OF DIATHERMANOUS MATERIALS

Materials that are capable of transmitting thermal radiation are called diathermanous materials. The incident solar radiation may be considered to be unpolarized. It gets polarized into two mutually perpendicular directions as it passes through a material. One component vibrates in the plane perpendicular to the plane of glass and the other vibrates in the plane of glass. Fresnel's laws give the reflectivity of a material as a function of the angle of incidence and refraction index. In the following, only the unpolarized radiation is considered. The discussion that follows is based on a paper by Parmelee (1945). The properties are considered be dependent upon wavelength.

Figure 21.4 shows monochromatic solar radiation of intensity I_λ incident upon a single glass sheet of thickness L. Let r be the fraction of radiation reflected from a single glass surface. This is different from reflectivity, since reflectivity involves multiple reflections from the top and bottom surfaces of the glass. Let a be the fraction available after absorption during each passage through the glass plate.

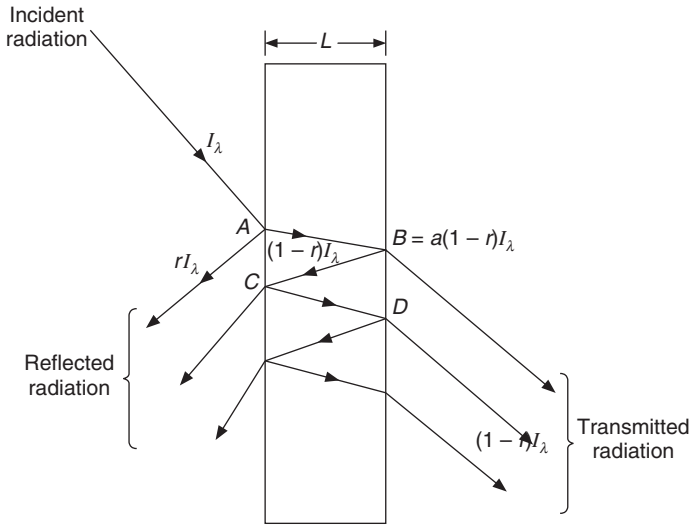

Figure 21.4 Solar radiation incident upon a single glass sheet.

- At point A, I_λ is incident, $r\,I_\lambda$ is reflected and $(1 - r)I_\lambda$ is transmitted.
- At point B, the intensity reduces to $a(1 - r)I_\lambda$, of this $ra(1 - r)\,I_\lambda$ is reflected from bottom surface of glass plate and $a(1 - r)^2 I_\lambda$ is transmitted through the glass.
- At point C, the intensity reduces to $a^2 r(1 - r)I_\lambda$. Of this $a^2 r^2\,(1 - r)I_\lambda$ is reflected from top surface of glass plate and $a^2 r\,(1 - r)^2 I_\lambda$ is transmitted through the glass towards the incident side. This forms a part of the reflected radiation from the top surface.
- At point D, the intensity reduces to $a^3 r^2(1 - r)I_\lambda$. Of this, $a^3 r^3(1 - r)I_\lambda$ is reflected from bottom surface of glass plate and $a^3 r^2(1 - r)^2 I_\lambda$ is transmitted through the glass. This forms a part of the transmitted radiation.

The net reflection through the glass plate may be written as the series:

$$\rho_\lambda = r + ra^2\,(1 - r)^2 + r^3 a^4\,(1 - r)^2 + \ldots = r + ra^2\,(1 - r)^2[1 + r^2 a^2 + r^4 a^4 + \ldots]$$

Now, $$(1 - r^2 a^2)^{-1} = 1 + r^2 a^2 + r^4 a^4 + \ldots \quad (\text{if } ra < 1)$$

$$\therefore \qquad \rho_\lambda = r + \frac{r(1 - r)^2 a^2}{1 - r^2 a^2} \tag{21.15}$$

The net transmitted radiation is written as the series

$$\tau_\lambda = a(1 - r)^2 + r^2(1 - r)^2 a^3 + r^4(1 - r)^2 a^5 + \ldots = a(1 - r)^2\,(1 + r^2 a^2 + r^4 a^4 + \ldots)$$

$$\therefore \qquad \tau_\lambda = \frac{a(1 - r)^2}{1 - r^2 a^2} \tag{21.16}$$

The monochromatic absorptivity is given by $\alpha_\lambda = 1 - \rho_\lambda - \tau_\lambda$. Simplification yields

$$\alpha_\lambda = 1 - r - \frac{a(1 - r)^2}{1 - ar} \tag{21.17}$$

21.5.1 Absorption Coefficient *a*

The absorbed radiation or the attenuation in the intensity of radiation is proportional to the intensity of radiation and the length of path travelled in the glass palate. This may be expressed as

$$-dI_\lambda = KI_\lambda\,dL$$

Integrating it along the path of transmitted ray AB, we get

$$a = \frac{I_{\lambda B}}{I_{\lambda A}} = e^{-KL'} \tag{21.18}$$

where, $L' = L/\cos\,\theta_2$.

The refractive index $n = \sin\,\theta_1/\sin\,\theta_2$

$$\therefore \qquad \cos\,\theta_2 = (1 - \sin^2\,\theta_1/n^2)^{0.5}$$

K is known as *extinction coefficient* and its values are given in Table 21.7.

Table 21.7 Values of extinction coefficient for various type of glasses

Type of glass	*K* (1/m)
Double strength, a quality	7.638
Clear plate	6.85
Heat absorbing	129.92
Heat absorbing	271.26

From Fresnel's relations the component reflectivities for the perpendicular component $r_\perp$ and parallel component $r_\parallel$ are

$$r_\perp = \frac{\sin^2(\theta_1 - \theta_2)}{\sin^2(\theta_1 + \theta_2)} \quad \text{and} \quad r_\parallel = \frac{\tan^2(\theta_1 - \theta_2)}{\tan^2(\theta_1 + \theta_2)} \tag{21.19}$$

It may be assumed that both the components are of equal intensity and r may be taken as

$$r = 0.5(r_\perp + r_\parallel), \quad r = \frac{1}{2}\left[\frac{\sin^2(\theta_1 - \theta_2)}{\sin^2(\theta_1 + \theta_2)} + \frac{\tan^2(\theta_1 - \theta_2)}{\tan^2(\theta_1 + \theta_2)}\right] \tag{21.20}$$

The expressions for reflectivity ρ, transmittivity τ and absorptivity α and for the parallel and perpendicular components are exactly same as those given by Eqs. (21.15), (21.16) and (21.17) for common value of absorption coefficient a but for respective values of single surface reflectivities $r_\parallel$ and $r_\perp$.

Parmelee has also given the transmissivities and reflectivities for a combination of two separate glass sheets.

The value of single surface glass reflectivity r for a glass with refraction index of 1.526 varies very slowly for incidence angle from 0 to 60° and thereafter it changes very fast with θ. The variation is approximately as given in Table 21.8.

Table 21.8 Values of single surface reflectance *r* for various angles of incidence

θ, deg	0	30	40	60	70	80	90
r	0.035	0.045	0.05	0.1	0.2	0.4	1.0

EXAMPLE 21.2 Determine the monochromatic transmissivity, reflectivity, and absorptivity for clear glass and heat absorbing glass 6.35 mm thick and with refractive index of 1.526 when the angle of incidence is 30°.

Solution:

For clear glass:

From Table 21.7, we find that for clear glass $K = 6.85\ \text{m}^{-1}$. $\sin\theta = \sin 30^\circ = 0.5$

$$L' = 0.00635[1.0 - (0.5/1.526)^2]^{0.5} = 0.006721\ \text{m}$$

From Eq. (21.18),

$$\therefore \qquad a = \exp(-6.85 \times 0.006721) = 0.955$$

From Table 21.8, at $\theta = 30^{o}$: $r = 0.045$
Therefore, from Eqs. (21.15) and (21.16)

$$\rho_\lambda = 0.045 + \frac{0.045(1-0.045)^2\,(0.955)^2}{1-(0.045)^2\,(0.955)^2} = 0.0825$$

$$\tau_\lambda = \frac{0.955(1-0.045)^2}{1-(0.045)^2\,(0.955)^2} = 0.872$$

$$\alpha_\lambda = 1 - \rho_\lambda - \tau_\lambda = 0.0455$$

Hence, for clear glass with small extinction coefficient, the transmissivity is very large compared to absorptivity and reflectivity.

For heat absorbing glass:

We see from Table 21.7 that $K = 271.26\ m^{-1}$

$\therefore$ $a = \exp(-271.26 \times 0.006721) = 0.16152$

$\therefore$ $$\rho_\lambda = 0.045 + \frac{0.045(1-0.045)^2\,(0.16152)^2}{1-(0.045)^2\,(0.16152)^2} = 0.0461$$

and $$\tau_\lambda = \frac{0.16152(1-0.045)^2}{1-(0.045)^2\,(0.16152)^2} = 0.1473$$

and $$\alpha_\lambda = 1 - \rho_\lambda - \tau_\lambda = 0.8066$$

Thus, for heat absorbing glass the absorptivity is very large compared to reflectivity and transmissivity.

21.5.2 Composition of Window Glass

Parmelee has stated that the composition of common window glass usually lies within the following limits (Table 21.9).

Table 21.9 Common composition of window glass

SiO_2	Na_2O	CaO	MgO	Al_2O_3	Fe_2O_3
70–73	12–15	9–14	0–3	0–1.5	0–0.15

The absorption characteristics depend upon the percentage of ferrous oxide. Heat absorbing glass may have up to 0.5% Fe_2O_3. The refractive index for most of the glasses is 1.526.

The transmissivity of window glass varies with wavelength for different percentages of Fe_2O_3. The solar radiation falls in the range of 0.3–2.3 μm. The glass containing small percentages of Fe_2O_3 has a constant transmissivity over the whole range of solar radiation. The transmissivity of heat absorbing glass varies considerably over the range of solar radiation. It is further observed that the transmissivity of window glass is zero for wavelengths greater than 4.5 μm. This is of

great significance, since it makes the window glass opaque to long wave-length radiation emitted at room temperature, while it is almost transparent to solar radiation. Therefore, glass acts as a one-way trap for solar energy. The solar radiation can be trapped by it. This is referred to as greenhouse effect by the glass. This property of glass makes it the most suitable cover plate of all the solar collectors.

Table 21.10 gives the values of transmissivity and absorptivity for two types of glass as a function of the angle of incidence.

Table 21.10 Transmissivity and absorptivity of glass

Glass		*Angle of incidence,* deg						
		0	20	40	50	60	70	80
4 mm*	Transmissivity	0.87	0.87	0.86	0.84	0.79	0.67	0.42
	Absorptivity	0.05	0.05	0.06	0.06	0.06	0.06	0.06
6 mm!	Transmissivity	0.84	0.84	0.83	0.80	0.74	0.62	0.38
	Absorptivity	0.08	0.08	0.08	0.08	0.10	0.09	0.09

* Ordinary clear glass, ! plate or float clear glass.

21.5.3 Heat Gain through Fenestration

Fenestration refers to any glazed aperture in the building and it involves a glazing material—either glass or plastic—framing and dividers, external shading devices and internal shading devices. Glass has sound-proofing effect. It creates a proper ambience in an otherwise enclosed space so that occupants feel to be in touch with the surroundings.

The fenestration affects the heat transfer into and out (summer and winter) of the building. Fenestrations also cause infiltration or ventilation if operable and provide natural lighting—which may reduce the artificial lighting.

When radiation strikes a window, about 8% is reflected, 5 to 50% is absorbed depending upon the composition and thickness of the glass, and the remaining is transmitted indoors. A part of the absorbed radiation is transferred indoors and a part is transferred outdoors. Then, there is heat transfer by combined convection–conduction through the glass. Therefore,

Total heat transfer through the glass = transmitted radiation + inward flow of absorbed energy + convection–conduction heat transfer.

The first two components are called the Solar Heat Gains. The third component is by the overall heat transfer coefficient.

The window is usually framed and sunlight strikes it at different angles of incidence throughout the day. The analysis requires details of monochromatic properties of radiation and also variation of solar radiation with angle of incidence. The properties τ_λ, α_λ, ρ_λ are sometimes difficult to evaluate. The equations required to do these calculations use computer programs. Stephen et al. (1994) and Dariush (1994) have given the details of the calculation procedure. The details of this method, called the *spectral method*, are available in *ASHRAE Handbook of Fundamentals Volume*. There are two methods in common use for the evaluation of heat gain through glass, namely (i) spectral method and (ii) solar heat gain factor method. The spectral method involves the

evaluation of *Solar Heat Gain Coefficient* (SHGC), that is, the fraction of incident radiation that enters the glazing and becomes heat gain. This includes the transmitted and inward flow of absorbed radiation, i.e.

$$q_i = I_t \text{ SHGC} \quad \text{W/m}^2$$

where I_t is the total incident radiation on the glazing. It does not include the heat transfer by temperature difference across the glazing. In multiple panes glazing, SHGC requires a term to allow for the inward flow of absorbed radiation from each layer. The second method involving SHGF is rather simple. There are two versions of it. One of them involves finding the transmittance and absorptivity of glass for direct beam and diffuse radiation at given angles and then multiplying it by the incident direct beam and diffuse radiation to find SHGF. The second version considers the overall heat balance for the glazing to find SHGF. These methods are described below.

21.5.4 Solar Heat Gain Factor (SHGF)

The solar heat gain from a unit area of double-strength sheet glass (DSA) for a given orientation and solar time is called *solar heat gain factor* (SHGF). This takes into account the transmitted and the inward flow of absorbed radiation. The transmitted part is called *transmitted solar heat gain factor* (TSHGF) and the absorbed part that flows inwards is called *absorbed solar heat gain factor* (ASHGF). Both of these are calculated by using the intensities of direct beam radiation I_D and diffuse sky radiation I_d with respective values of transmissivity for direct and diffuse radiation.

The transmittance τ_D of DSA glass to direct beam radiation incident at an angle θ and the transmittance τ_d to diffuse radiation is given as per ASHRAE recommendation by the following series.

$$\tau_D = \sum_{j=0}^{5} t_j (\cos\theta)^j \quad \text{and} \quad \tau_d = 2\sum_{j=0}^{5} \frac{t_j}{j+2} \tag{21.21}$$

where t_j is the transmission coefficient whose values are given in Table 21.11.

Table 21.11 Values for transmissivity and absorptivity coefficients in Eqs. (21.21) and (21.22)

j	0	1	2	3	4	5
a_j	0.01154	0.77674	–3.94657	8.57811	–8.38135	3.01188
t_j	–0.00885	2.71235	–0.62062	–7.07329	9.75995	–3.89922

In a similar manner, the absorptivity α_D of direct beam radiation incident at an angle θ and absorptivity α_d for diffuse radiation by DSA glass are given by

$$\alpha_D = \sum_{j=0}^{5} a_j (\cos\theta)^j \quad \text{and} \quad \alpha_d = 2\sum_{j=0}^{5} \frac{a_j}{j+2} \tag{21.22}$$

The values of the absorption coefficient a_j are also given in Table 21.11.

Hence the transmitted solar heat gain factor is given by

$$\text{TSHGF} = I_D \sum_{j=0}^{5} t_j (\cos\theta)^j + 2I_d \sum_{j=0}^{5} \frac{t_j}{j+2} \tag{21.23}$$

The absorbed solar heat gain factor is given by

$$\text{ASHGF} = I_D \sum_{j=0}^{5} a_j (\cos\theta)^j + 2I_d \sum_{j=0}^{5} \frac{a_j}{j+2} \tag{21.24}$$

21.5.5 Shading Coefficient

The transmissivity of DSA glass at normal incidence and for standard solar spectrum is 0.87. Hence at normal incidence the SHGC for DSA glass is 0.87, that is, it will transmit 87% of the incident radiation. For other fenestrations, this coefficient is different. The comparative effectiveness of various combinations of shadings and glazings is expressed in terms of a *shading coefficient* (SC), which is defined to determine solar heat gain through fenestration under similar solar conditions in terms of values of DSA.

$$\text{SC} = \frac{\text{solar heat gain of fenestration for a particular incidence angle}}{\text{solar heat gain of DSA glass at normal incidence of solar spectrum}} = \frac{\text{SHDC}}{0.87}$$

The shading coefficient applies to glazing portion and not to the frame. This is valid for single pane and double pane glazings, and for many tinted single pane glazing. Manufacturers give the values of SHGC from which SC can be determined.

$$\text{Transmitted Solar Heat Gain TSHG} = \text{SC (TSHGF)}$$
$$\text{Absorbed Solar Heat Gain ASHG} = \text{SC (ASHGF)}N_i$$

where N_i is the inward flowing fraction of absorbed solar heat gain, that is, $N_i = h_i/(h_i + h_o)$.

The tabulated values of SC use $h_i = 8.29$ W/m^2-K for still indoor air and $h_o = 22.7$ W/m^2-K for wind velocity of 3.4 m/s. This gives a value of N_i equal to 0.2675. The shading coefficient increases with increase in the value of h_i.

It may be noted that the term shading, used in the above context, does not refer to a physically shading device. It is to account for the fenestration material being different from the standard DSA clear single pane glass (with $\tau = 0.86$, $\rho = 0.08$ and $\alpha = 0.06$) exposed to standard solar spectrum. Table 21.12 gives the values of transmissivity and shading coefficients for two values of h_o.

Table 21.12 Shading coefficients for two types of glass and for two values of h_o

Type of glass	*Thickness* (mm)	*t*	*Shading coefficient*	
			h_o =17 W/m^2-K	h_o = 23 W/m^2-K
Clear glass	3.2	0.86	1.0	1.0
	6.4	0.78	0.94	0.95
	9.5	0.72	0.9	0.92
	12.7	0.67	0.87	0.88
Heat-absorbing	3.2	0.64	0.83	0.85
	6.4	0.46	0.69	0.73
	9.5	0.33	0.60	0.64
	12.7	0.24	0.53	0.58

Blinds, shadings and drapes or curtains are commonly used next to the window to decrease the solar heat gain. These are called internal shadings. These are not as effective as the external shadings. External shadings are very useful, when the altitude angle is large and the sun is high up in the sky. Fixed shadings like overhang and window setback are used extensively in tropical and subtropical zones. In temperate zones (23.5° N to 66.5° N and S latitudes), the altitude angles are small, and the sun never appears at the zenith, as a result the external shading is not very effective. Sometimes, motorized, automatic external shades are used but these involve maintenance problems. Hence, internal shadings are relied upon. Venetian blinds and roller shades are commonly used. These should have white or cream colour and reflective surface, which can be adjusted to reflect back the incident radiation. The comparative effectiveness of various combinations of shades and glazings are expressed in terms of the shading coefficient. ASHRAE (1997) has given extensive tables for various shades.

Double glazing reduces the noise considerably, if the air gap is more than 100 mm. This is an additional benefit. Further, a higher relative humidity can be maintained in winter since, the inner glazing temperature is higher and, it does not allow condensation. The glazing should be leak tight, otherwise condensation will occur in the air space of double glazing, which is difficult to remove.

Reflective plastic coatings applied on the inside surface of glass are quite useful. These are not applied on the outer surface because of possible degradation due to weathering.

Shading coefficient of drapery is a complex function of the colour, reflectiveness and weave of the fabric. The shading coefficient depends upon the reflective nature of the fabric, the ratio of the open area between the fibres and the total area, and the fullness of the drape. The washing of the curtains may remove the reflective coating applied to them.

21.6 HEAT BALANCE FOR THE GLASS

In this section we consider the energy balance for the glass plate to give a firm footing to the ideas expressed above. Let us take the case of a window. The external shading, other than that by setback, has not been considered, and the internal shading due to Venetian blinds or drapery has also not been included. The convection and radiation heat transfers q_{co} and q_{Ro} respectively without door can be combined together as outside surface heat transfer. Similarly, q_{ci} and q_{Ri} are combined as inside surface heat transfer. Direct solar radiation, diffuse sky radiation and reflected radiation are incident upon the outer surface of the window. A part of this may be reflected, a part transmitted, and a part absorbed by the glass. The outer glass surfaces will exchange long wavelength radiation with sky and outside surrounding surfaces. Similarly, the inner surface will exchange long wavelength radiation with the indoor surfaces. In general, the rate of heat gain by the indoor environment through the glass may be written as

$$q_i = F_s \tau_D I_D + \tau_d I_d + \tau_r I_r + h_i(t_{gi} - t_i) \tag{21.25}$$

The angles of incidence for direct beam, sky radiation and reflected radiation are in general, different; hence the products $\tau_D I_D$, $\tau_d I_d$ and $\tau_r I_r$ have to be evaluated separately. Table 21.10 may be used for the values of τ_D for a given value of the angle of incidence. The sky radiation comes from all directions and τ_d depends upon it. Parmeele has suggested that for usual calculations, an angle of incidence of 60° may be taken for a vertical wall. The use of a mean angle of incidence for sky radiation and reflected radiation will give satisfactory results. The temperature of the inside glass surface is $t_{gi.}$ F_s is the sunlit fraction of the window for direct beam radiation. The shading of

window is neglected for sky and reflected radiation since these are different and come from all directions.

The glass plate absorbs energy and loses some energy by convection and radiation to the indoor and outdoor surroundings. The energy balance for the glass gives

$$F_s I_D \alpha_D + I_d \alpha_d + I_r a_r = h_i (t_{gi} - t_i) + h_o (t_{go} - t_o) \pm q_{gs} \tag{21.26}$$

The left-hand side of this equation is the heat gain by absorption and the right-hand side is heat rejection by convection and radiation. The storage of energy in the glass is denoted by q_{gs} that may be negligible for glass with low value of solar absorptivity. In many situations the thickness of glass plate is small, and the glass temperature may be assumed to be a uniform value t_g, that is,

$$t_{gi} = t_{go} = t_g \tag{21.27}$$

Equation (21.26) then reduces to

$$(h_i + h_o)t_g - (h_i t_i + h_o t_o) = F_s I_D \alpha_D + I_d \alpha_d + I_r \alpha_r$$

$$\therefore \quad t_g = (F_s I_D \alpha_D + I_d \alpha_d + I_r \alpha_r + h_i t_i + h_o t_o)/(h_i + h_o) \tag{21.28}$$

$$\therefore \quad h_i (t_g - t_i) = \frac{F_s I_D \alpha_D + I_d \alpha_d + I_r \alpha_r}{\left(1 + \frac{h_o}{h_i}\right)} + \frac{h_i h_o (t_o - t_i)}{h_i + h_o}$$

Substituting this in Eq. (21.25), we get

$$q_i = (F_s \tau_D I_D + \tau_d I_d + \tau_r I_r) + \frac{F_s I_D \alpha_D + I_d \alpha_d + I_r \alpha_r}{\left(1 + \frac{h_o}{h_i}\right)} + U_o (t_o - t_i) \tag{21.29}$$

where $1/U_o = 1/h_i + 1/h_o$.

Equation (21.29) may be written as follows:

$$q_i = \text{SHGF} + U_o (t_o - t_i) \tag{21.30}$$

where,
$$\text{SHGF} = F_s \tau_D I_D + \tau_d I_d + \tau_r I_r + \frac{F_s I_D \alpha_D + I_d \alpha_d + I_r \alpha_r}{\left(1 + \frac{h_o}{h_i}\right)} \tag{21.31}$$

The indoor surface temperatures, that is, the temperature of walls, roof and floor, are different. Likewise, the outdoor surface temperatures of the surroundings such as road, parking lot and lawns etc are also different. Hence, the indoor and outdoor surface temperatures are difficult to evaluate. In most cases we may assume $t_{si} = t_i$. If the glass views the ground surface, the surrounding surfaces temperatures and the sky temperature during daylight hours may be assumed to be equal to the air temperature, that is, $t_{so} = t_o$. However, at night time if the glass faces the sky, the effective sky temperature is around –55°C, which may be used. Equation (21.29) does not take into account the external or internal shading. The sum of the first two terms in Eq. (21.29) is termed Solar Heat Gain Factor and abbreviated SHGF. The SHGF has been evaluated for wooden sash windows (with 85% glass area) for various latitudes, window orientations and solar time. The tables for this

have been prepared by Carrier Air Conditioning Corporation. These are presented in Table 21.13. These tables are applicable under the following conditions.

(i) The windows are wood-sash windows with 85% glass area. For metal sash windows, the value read from the table may be multiplied by 1/0.85 = 1.17.
For metallic frames, heat gain may further increase due to larger thermal conductivity of metal. Hence, to account for it the area of the opening in the wall (rather than the glass area) is used for metal windows.

(ii) The tables are applicable when, there is no haze in the air. For hazy conditions, a maximum of 15% reduction may be made. Haze results from contaminants in the air due to automobile or industrial pollution. This is more pronounced in the afternoon, when the ground temperature increases and upward currents are formed.

(iii) The tables are valid for sea level. For higher elevations, an increase of 2.5% per 300 m height may be made.

(iv) The tables are valid for sea level dew point of 19.3°C, which corresponds to 4 cm of precipitable water vapour content of atmosphere. For a dew point higher by 5°C, subtract 6.3% and for a dew point smaller by 5°C, add 6.3%.

(v) The tables are valid for North latitudes. For South latitudes, for December and January add 7%. In southern hemisphere, peak summer occurs in December–January and sun is closer to earth by 3% in January than in July.

Table 21.13 Solar heat gain through ordinary glass (W/m^2)

0° North Latitude		**am**							**pm**							**0° South Latitude**
Time of year	Exposure	6	7	8	9	10	11	Noon	1	2	3	4	5	6	Exposure	Time of year
	North	0	142	205	233	246	252	259	252	246	233	205	142	0	South	
	North–East	0	375	492	486	426	300	167	63	44	41	35	19	0	South–East	
	East	0	365	464	426	293	136	44	44	44	41	35	19	0	East	
June	South–East	0	117	132	85	47	44	44	44	44	41	35	19	0	North–East	Dec.
21	South	0	19	35	41	44	44	44	44	44	41	35	19	0	North	22
	South–West	0	19	35	41	44	44	44	44	47	85	132	117	0	North–West	
	West	0	19	35	41	44	44	44	136	293	426	464	366	0	West	
	North–West	0	19	35	41	44	44	63	300	420	486	492	375	0	South–East	
	Horizontal	0	88	274	464	603	685	713	685	603	464	274	89	0	Horizontal	
	North	0	117	170	192	205	208	211	208	205	192	170	117	0	South	
	North–East	0	372	483	473	391	271	136	50	44	41	35	35	0	South–East	
	East	0	382	479	438	303	136	44	44	44	41	35	35	0	East	
July																Jan.
23	South–East	0	145	164	114	57	44	44	44	44	41	35	19	0	North–East	21
and	South	0	19	35	41	44	44	44	44	44	41	35	19	0	North	and
May	South–West	0	19	35	41	44	44	44	44	57	114	164	145	0	North–West	Nov.
21																21
	West	0	19	35	41	44	44	44	136	303	438	479	382	0	West	
	North–West	0	19	35	41	44	50	136	271	391	473	482	372	0	South–East	
	Horizontal	0	91	287	476	615	703	735	703	615	476	287	91	0	Horizontal	

(*Contd.*)

Table 21.13 Solar heat gain through ordinary glass (W/m^2) (contd.)

0° North Latitude		am							pm						0° South Latitude	
Time of year	Exposure	6	7	8	9	10	11	Noon	1	2	3	4	5	6	Exposure	Time of year
	North	0	54	88	98	104	107	107	107	104	98	88	54	0	South	
	North–East	0	347	445	420	322	192	76	44	44	41	38	19	0	South–East	
	East	0	407	514	467	325	145	44	44	44	41	38	19	0	East	
Aug. 24 and April 20	South–East	0	211	249	205	110	47	44	44	44	41	38	19	0	North–East	Feb. 20 and Oct. 23
	South	0	19	35	41	44	44	44	44	44	41	38	19	0	North	
	South–West	0	19	35	41	44	44	44	47	110	205	249	211	0	North–West	
	West	0	19	35	41	44	44	44	147	325	467	514	407	0	West	
	North–West	0	19	35	41	44	44	16	192	322	420	444	347	0	South–East	
	Horizontal	0	98	965	473	650	738	773	738	650	473	306	98	0	Horizontal	
	North	0	19	38	41	44	44	44	44	44	41	38	19	0	South	
	North–East	0	300	372	319	215	97	44	44	44	41	38	19	0	South–East	
	East	0	423	527	476	338	148	44	44	44	41	38	19	0	East	
Sept. 22 and March 22	South–East	0	300	372	318	215	98	44	44	44	41	38	19	0	North–East	March 22 and Sept. 22
	South	0	19	35	41	44	44	44	44	44	41	38	19	0	North	
	South–West	0	19	35	41	44	44	44	98	215	319	372	300	0	North–West	
	West	0	19	35	41	44	44	44	148	338	476	527	426	0	West	
	North–West	0	19	35	41	44	44	44	98	215	319	372	295	0	South–East	
	Horizontal	0	101	315	514	662	757	789	757	662	514	315	101	0	Horizontal	
	North	0	19	38	41	44	44	44	44	44	41	38	19	0	South	
	North–East	0	211	249	205	110	47	44	44	44	41	38	19	0	South–East	
	East	0	407	514	467	325	145	44	44	44	41	38	19	0	East	
Oct. 23 and Feb. 20	South–East	0	347	445	420	322	192	76	44	44	41	38	19	0	North–East	April 20 and Aug. 24
	South	0	54	88	98	104	107	107	107	104	98	88	54	0	North	
	South–West	0	19	38	41	44	44	76	192	322	420	444	347	0	North–West	
	West	0	19	38	41	44	44	44	145	325	467	514	407	0	West	
	North–West	0	19	38	41	44	44	44	47	110	205	249	211	0	South–East	
	Horizontal	0	98	306	473	650	738	773	738	650	473	306	98	0	Horizontal	
	North	0	19	35	41	44	44	44	44	44	41	35	19	0	South	
	North–East	0	145	164	114	57	44	44	44	44	41	35	19	0	South–East	
	East	0	382	479	438	303	136	44	44	44	41	35	19	0	East	
Nov. 21 and Jan. 21	South–East	0	372	483	473	391	271	136	50	44	41	35	19	0	North–East	May 21 and July 23
	South	0	117	170	192	205	208	211	208	205	192	170	117	0	North	
	South–West	0	19	35	41	44	50	136	271	39	473	483	372	0	North–West	
	West	0	19	35	41	44	44	44	136	303	438	479	382	0	West	
	North–West	0	19	35	41	44	44	44	44	57	114	164	145	0	South–East	
	Horizontal	0	91	287	476	615	703	735	703	615	476	287	91	0	Horizontal	
	North	0	19	35	41	44	44	44	44	44	41	35	19	0	South	
	North–East	0	117	132	85	47	44	44	44	44	41	35	19	0	South–East	
	East	0	366	463	426	293	136	44	44	44	41	35	19	0	East	

(*Contd.*)

Table 21.13 Solar heat gain through ordinary glass (W/m^2) (contd.)

0° North Latitude					**am**				**pm**						**0° South Latitude**	
Time of year	Exposure	6	7	8	9	10	11	Noon	1	2	3	4	5	6	Exposure	Time of year
Dec. 22	South–East	0	375	492	486	420	306	167	63	44	41	35	19	0	North–East	June 21
	South	0	142	205	233	246	252	259	252	246	233	68	142	0	North	
	South–West	0	19	35	41	44	63	167	300	420	486	292	375	0	North–West	
	West	0	19	35	41	44	44	44	136	293	426	464	366	0	West	
	North–West	0	19	35	41	44	44	44	44	47	85	132	117	0	South–East	
	Horizontal	0	88	274	464	603	686	713	685	603	464	275	88	0	Horizontal	
10° North Latitude					**am**				**pm**						**10° South Latitude**	
Time of year	Exposure	6	7	8	9	10	11	Noon	1	2	3	4	5	6	Exposure	Time of year
	North	60	139	160	142	139	136	129	136	139	142	158	139	6	South	
	North–East	173	413	483	442	334	205	88	44	44	41	35	25	6	South–East	
	East	170	423	489	438	309	129	44	44	44	41	35	19	6	East	
June 21	South–East	57	155	173	136	79	44	44	44	44	41	35	25	6	North–East	Dec. 22
	South	6	25	35	41	44	44	44	44	44	41	35	25	0	North	
	South–West	6	25	35	41	44	44	44	44	70	135	173	154	57	North–West	
	West	6	25	35	41	44	44	44	129	309	438	489	423	170	West	
	North–West	6	25	35	41	44	57	80	205	334	442	483	413	173	South–East	
	Horizontal	13	139	338	524	647	735	767	735	647	524	338	139	13	Horizontal	
	North	16	107	123	110	104	90	94	98	104	110	123	107	16	South	
	North–East	132	401	467	420	34	177	69	44	44	41	35	22	3	South–East	
	East	158	426	498	448	309	136	44	44	44	41	35	22	3	East	
July 23 and May 21	South–East	82	100	208	177	101	44	44	44	44	41	35	22	3	North–East	Jan. 21 and Nov. 21
	South	3	22	35	41	44	44	44	44	44	41	35	22	3	North	
	South–West	3	22	35	41	44	44	44	44	101	177	208	180	82	North–West	
	West	3	22	35	41	44	44	44	136	309	448	498	426	158	West	
	North–West	3	22	35	41	44	44	69	177	344	420	466	401	132	South–East	
	Horizontal	9	132	338	524	662	744	779	744	662	524	338	132	9	Horizontal	
	North	3	47	50	47	47	44	44	44	47	47	50	47	3	South	
	North–East	54	356	410	350	252	107	44	44	44	41	35	22	3	South–East	
	East	79	435	514	470	328	145	44	44	44	41	35	22	3	East	
Aug. 24 and April 20	South–East	57	249	297	268	189	85	44	44	44	41	35	22	3	North–East	Feb. 20 and Oct. 23
	South	3	22	35	41	44	44	44	44	44	41	35	22	3	North	
	South–West	3	22	35	41	44	44	44	85	189	268	297	249	57	North–West	
	West	3	22	35	41	44	44	44	145	252	470	514	435	79	West	
	North–West	3	22	35	41	44	44	44	107	47	350	410	356	54	South–East	
	Horizontal	6	120	331	527	672	763	788	763	672	527	331	120	6	Horizontal	
	North	3	19	35	41	44	44	44	44	44	41	35	19	3	South	
	North–East	3	281	325	252	142	54	44	44	44	41	35	19	3	South–East	
	East	3	410	517	476	334	148	44	44	44	41	35	19	3	East	

(*Contd.*)

Table 21.13 Solar heat gain through ordinary glass (W/m^2) (contd.)

10° North Latitude					**am**				**pm**						**10° South Latitude**	
Time of year	Exposure	6	7	8	9	10	11	Noon	1	2	3	4	5	6	Exposure	Time of year
Sept. 22 and Mar. 22	South–East	3	306	401	385	297	177	66	44	44	41	35	19	3	North–East	Mar. 22 and Sept. 22
	South	3	19	35	50	76	85	88	85	76	60	41	19	3	North	
	South–West	3	19	35	41	44	44	66	177	297	385	401	306	3	North–West	
	West	3	19	35	41	44	44	44	148	334	476	517	410	3	West	
	North–West	3	19	35	41	44	44	44	54	142	252	325	281	3	South–East	
	Horizontal	3	98	306	505	653	741	779	741	653	505	54	98	3	Horizontal	
Oct. 23 and Feb. 20	North	0	16	32	41	44	44	44	44	44	41	32	15	0	South	April 20 and Aug. 24
	North–East	0	183	208	454	88	44	44	44	44	41	32	15	0	South–East	
	East	0	372	489	457	315	126	44	44	44	41	32	15	0	East	
	South–East	0	325	464	470	388	256	145	57	44	41	32	15	0	North–East	
	South	0	57	126	173	205	240	230	224	205	173	126	57	0	North	
	South–West	0	16	32	41	44	57	245	256	388	470	464	325	0	North–West	
	West	0	16	32	41	44	44	44	126	315	457	489	372	0	West	
	North–West	0	16	32	41	44	44	44	44	88	139	208	183	0	South–East	
	Horizontal	0	69	268	438	609	694	726	693	609	438	268	69	0	Horizontal	
Nov. 21 and Jan. 21	North	0	13	28	38	41	44	44	44	41	38	28	13	0	South	May 21 and July 23
	North–East	0	85	117	54	41	44	44	44	41	38	28	13	0	South–East	
	East	0	312	451	416	293	123	44	44	41	38	28	13	0	East	
	South–East	0	312	483	508	461	328	221	98	54	38	28	13	0	North–East	
	South	0	110	205	287	303	328	334	328	303	287	205	110	0	North	
	South–West	0	13	28	38	54	98	221	344	461	508	483	312	0	North–West	
	West	0	13	28	38	41	44	44	123	293	416	451	312	0	West	
	North–West	0	13	28	38	41	44	44	44	41	54	117	85	0	South–East	
	Horizontal	0	54	196	413	551	637	662	637	552	413	196	54	0	Horizontal	
Dec. 22	North	0	13	28	38	41	44	44	44	41	38	28	13	0	South	June 21
	North–East	0	47	88	54	41	44	44	44	41	38	28	13	0	South–East	
	East	0	271	432	410	287	132	44	44	41	38	28	13	0	East	
	South–East	0	312	486	514	470	382	233	114	72	38	28	13	0	North–East	
	South	0	158	233	297	344	366	379	366	344	297	233	158	0	North	
	South–West	0	13	28	38	73	114	233	382	470	514	486	312	0	North–West	
	West	0	13	28	38	41	44	44	132	287	410	432	271	0	West	
	North–West	0	13	28	38	41	44	44	44	41	54	88	47	0	South–East	
	Horizontal	0	44	208	378	527	609	637	608	527	379	208	44	0	Horizontal	
20° North Latitude					**am**				**pm**						**20° South Latitude**	
Time of year	Exposure	6	7	8	9	10	11	Noon	1	2	3	4	5	6	Exposure	Time of year
	North	88	129	104	79	60	54	47	54	60	79	104	129	88	South	
	North–East	256	486	454	385	262	120	47	44	44	44	38	28	9	South–East	
	East	256	467	505	451	303	129	44	44	44	44	38	28	9	East	

(*Contd.*)

Table 21.13 Solar heat gain through ordinary glass (W/m^2) (contd.)

20° North Latitude		am							pm							20° South Latitude
Time of year	Exposure	6	7	8	9	10	11	Noon	1	2	3	4	5	6	Exposure	Time of year
June 21	South–East	88	196	230	208	138	66	44	44	44	44	38	28	9	North–East	Dec. 22
	South	10	28	38	44	44	44	44	44	44	44	38	28	9	North	
	South–West	10	28	38	44	44	44	44	66	139	208	230	196	88	North–West	
	West	10	28	38	44	44	44	44	129	303	451	505	467	256	West	
	North–West	10	28	38	44	44	44	47	50	262	385	454	486	256	South–East	
	Horizontal	35	189	382	555	681	732	789	732	681	555	382	189	35	Horizontal	
	North	63	88	73	54	47	44	44	44	47	54	73	88	63	South	
	North–East	224	416	435	350	230	98	44	44	44	41	38	25	9	South–East	
	East	237	467	514	457	312	145	44	44	44	41	38	25	9	East	
July 23 and May 21	South–East	98	221	268	249	180	91	44	44	44	41	38	25	9	North–East	Jan. 21 and Nov. 21
	South	10	25	38	41	44	44	44	44	44	41	38	25	9	North	
	South–West	10	25	38	41	44	44	44	91	180	249	268	221	98	North–West	
	West	10	25	38	41	44	44	44	145	312	457	514	467	237	West	
	North–West	10	25	38	41	44	44	44	98	23	350	435	416	224	South–East	
	Horizontal	25	174	372	552	681	757	792	757	681	552	372	173	25	Horizontal	
	North	19	32	25	41	44	44	44	44	44	41	35	32	19	South	
	North–East	142	350	372	281	158	57	44	44	44	41	35	32	19	South–East	
	East	167	448	521	470	334	161	44	44	44	41	35	32	19	East	
Aug. 24 and April 20	South–East	92	281	357	341	309	173	63	44	44	41	35	22	6	North–East	Feb. 20 and Oct. 23
	South	6	22	35	44	63	76	82	76	63	44	35	22	6	North	
	South–West	6	22	35	41	44	44	63	173	309	341	356	281	91	North–West	
	West	6	22	35	41	44	44	44	161	334	471	520	448	167	West	
	North–West	6	22	35	41	44	44	44	41	157	281	372	350	142	South–East	
	Horizontal	16	151	338	527	662	241	779	741	662	527	338	151	16	Horizontal	
	North	0	19	35	41	44	44	44	44	44	41	35	19	0	South	
	North–East	0	262	274	186	69	44	44	44	44	41	35	19	0	South–East	
	East	0	410	514	470	328	142	44	44	44	41	35	19	0	East	
Sept. 22 and Mar. 22	South–East	0	312	429	442	379	265	129	47	44	41	35	35	0	North–East	Mar. 22 and Sept. 22
	South	0	25	69	120	164	199	205	199	164	120	69	69	0	North	
	South–West	0	19	35	41	44	47	129	265	379	442	429	429	0	North–West	
	West	0	19	35	41	44	44	44	142	328	470	514	410	0	West	
	North–West	0	19	35	41	44	44	44	44	69	186	274	262	0	South–East	
	Horizontal	0	95	293	483	626	710	735	710	625	483	293	95	0	Horizontal	
	North	0	13	28	38	41	44	44	44	41	38	28	13	0	South	
	North–East	0	139	164	91	41	44	44	44	41	38	28	13	0	South–East	
	East	0	312	464	445	315	155	44	44	41	38	28	13	0	East	
Oct. 23 and Feb. 20	South–East	0	287	461	506	470	375	233	85	41	38	28	13	0	North–East	April 20 and Aug. 24
	South	0	66	158	240	293	334	350	334	293	298	156	66	0	North	
	South–West	0	13	28	38	41	85	233	375	470	513	461	287	0	North–West	

(*Contd.*)

Table 21.13 Solar heat gain through ordinary glass (W/m^2) (contd.)

20° North Latitude		am							pm						20° South Latitude	
Time of year	Exposure	6	7	8	9	10	11	Noon	1	2	3	4	5	6	Exposure	Time of year
	West	0	13	28	38	41	44	44	155	315	366	464	312	0	West	
	North–West	0	13	28	38	41	44	44	44	41	91	164	139	0	South–East	
	Horizontal	0	57	215	401	539	618	656	618	539	401	215	57	0	Horizontal	
	North	0	10	25	35	41	41	41	41	41	35	25	9	0	South	
	North–East	0	76	82	44	41	41	41	41	41	35	25	9	0	South–East	
	East	0	224	404	401	287	136	41	41	41	35	25	9	0	East	
Nov. 21 and Jan. 21	South–East	0	230	454	517	498	426	287	145	50	35	25	9	0	North–East	May 21 and July 23
	South	0	88	218	315	388	429	445	429	388	315	217	88	0	North	
	South–West	0	10	25	35	50	145	287	426	498	517	454	230	0	North–West	
	West	0	10	25	35	39	41	41	136	287	401	404	224	0	West	
	North–West	0	10	25	35	39	41	41	41	41	35	82	76	0	South–East	
	Horizontal	0	16	151	319	461	542	568	460	460	319	151	16	0	Horizontal	
	North	0	6	22	35	38	41	41	41	38	35	22	6	0	South	
	North–East	0	44	57	38	38	41	41	41	38	35	22	6	0	South–East	
	East	0	177	372	382	268	107	41	41	38	35	22	6	0	East	
Dec. 22	South–East	0	186	438	527	502	423	306	189	63	35	22	6	0	North–East	June 21
	South	0	79	233	350	416	461	370	461	461	350	233	79	0	North	
	South–West	0	9	22	35	63	189	306	422	502	527	438	186	0	North–West	
	West	0	6	22	35	38	41	41	107	268	382	372	177	0	West	
	North–West	0	6	22	35	38	41	41	41	38	38	38	44	0	South–East	
	Horizontal	0	13	44	290	426	508	536	508	426	290	290	12	0	Horizontal	

30° North Latitude		am							pm						30° South Latitude	
Time of year	Exposure	6	7	8	9	10	11	Noon	1	2	3	4	5	6	Exposure	Time of year
	North	104	91	57	44	44	44	44	44	44	44	51	91	104	South	
	North–East	331	438	410	305	173	60	44	44	44	44	38	32	16	South–East	
	East	340	492	508	451	309	139	44	44	44	44	38	32	16	East	
June 21	South–East	132	237	284	284	230	139	54	44	44	44	38	32	16	North–East	Dec. 22
	South	16	32	38	44	44	60	66	60	47	44	38	32	16	North	
	South–West	16	32	38	44	44	44	54	138	230	284	284	237	132	North–West	
	West	16	32	38	44	44	44	44	138	309	451	508	492	341	West	
	North–West	16	32	38	44	44	44	44	60	173	310	410	438	331	South–East	
	Horizontal	60	192	413	568	685	757	789	757	685	568	413	192	60	Horizontal	
	North	69	63	76	41	44	44	44	44	44	41	44	63	69	South	
	North–East	293	413	388	281	145	50	44	44	44	41	38	28	13	South–East	
	East	315	489	517	457	132	139	44	44	44	41	38	28	13	East	
July 23 and May 21	South–East	132	259	315	315	262	167	69	44	44	41	38	28	13	North–East	Jan. 21 and Nov. 21
	South	13	28	38	44	63	85	95	85	63	44	38	28	13	North	
	South–West	13	28	38	41	44	44	44	167	262	315	315	259	132	North–West	

(*Contd.*)

Table 21.13 Solar heat gain through ordinary glass (W/m^2) (contd.)

30° North Latitude		am							pm						30° South Latitude	
Time of year	Exposure	6	7	8	9	10	11	Noon	1	2	3	4	5	6	Exposure	Time of year
	West	13	28	38	41	44	44	44	139	312	457	517	489	315	West	
	North–West	13	28	38	41	44	44	44	50	145	281	388	413	293	South–East	
	Horizontal	47	208	388	535	675	744	776	744	675	555	388	208	47	Horizontal	
	North	19	25	34	41	41	44	44	44	41	41	35	25	19	South	
	North–East	173	340	315	208	85	44	44	44	41	41	35	25	6	South–East	
	East	208	148	520	467	322	145	44	44	41	41	35	25	6	East	
Aug. 24 and April 20	South–East	177	309	401	407	353	258	123	47	41	41	35	25	6	North–East	Feb. 20 and Oct. 23
	South	6	25	41	85	148	183	199	183	148	85	41	25	6	North	
	South–West	6	25	35	41	41	47	123	259	353	407	401	309	117	North–West	
	West	6	25	35	41	41	44	44	145	322	467	520	464	208	West	
	North–West	6	25	35	41	41	44	44	44	85	208	315	340	173	South–East	
	Horizontal	19	148	338	508	631	710	741	710	631	508	338	464	19	Horizontal	
	North	0	16	32	38	41	44	44	44	41	38	32	16	0	South	
	North–East	0	233	283	126	447	44	44	44	41	38	32	16	0	South–East	
	East	0	391	498	454	325	151	44	44	41	38	32	16	0	East	
Sept. 22 and Mar. 22	South–East	0	309	413	430	445	356	211	79	41	38	32	16	0	North–East	Mar. 22 and Sept. 22
	South	0	28	57	189	256	309	311	309	259	189	57	28	0	North	
	South–West	0	16	32	38	41	789	211	356	445	479	413	309	0	North–West	
	West	0	16	32	38	41	44	44	151	325	454	498	391	0	West	
	North–West	0	16	32	38	41	44	44	44	47	126	284	233	0	South–East	
	Horizontal	0	70	571	426	565	637	668	637	564	426	256	79	0	Horizontal	
	North	0	9	25	35	38	41	44	41	38	35	25	9	0	South	
	North–East	0	104	123	57	38	41	44	41	38	35	25	9	0	South–East	
	East	0	249	426	416	297	136	44	41	38	35	25	9	0	East	
Oct. 23 and Feb. 20	South–East	0	230	448	515	502	429	290	148	47	35	28	9	0	North–East	April 20 and Aug. 24
	South	0	57	180	290	382	438	457	438	382	290	180	57	0	North	
	South–West	0	9	25	35	47	148	290	429	502	514	448	230	0	North–West	
	West	0	9	25	35	38	41	44	136	297	416	426	249	0	West	
	North–West	0	9	25	35	38	41	44	41	38	57	123	104	0	South–East	
	Horizontal	0	19	155	315	451	539	564	539	451	315	155	19	0	Horizontal	
	North	0	23	19	28	35	38	38	38	35	28	19	3	0	South	
	North–East	0	25	50	28	35	38	38	38	35	28	19	3	0	South–East	
	East	0	85	34	366	262	110	38	38	35	28	19	3	0	East	
Nov. 21 and Jan. 21	South–East	0	88	401	508	511	451	328	202	73	28	19	3	0	North–East	May 21 and July 23
	South	0	32	215	344	432	486	502	486	432	344	216	32	0	North	
	South–West	0	3	19	28	73	202	328	451	511	508	401	88	0	North–West	
	West	0	3	19	28	35	38	38	110	262	366	344	85	0	West	
	North–West	0	33	19	28	35	38	38	38	35	28	50	25	0	South–East	
	Horizontal	0	6	85	224	343	429	457	429	344	224	85	6	0	Horizontal	

(*Contd.*)

Table 21.13 Solar heat gain through ordinary glass (W/m^2) (contd.)

30° North Latitude					**am**				**pm**						**30° South Latitude**	
Time of year	Exposure	6	7	8	9	10	11	Noon	1	2	3	4	5	6	Exposure	Time of year
	North	0	0	13	28	235	38	38	38	35	28	13	0	0	South	
	North–East	0	0	32	28	35	38	38	38	35	28	13	0	0	South–East	
	East	0	0	290	331	252	101	38	38	35	28	13	0	0	East	
Dec. 22	South–East	0	0	360	495	511	451	340	227	88	28	13	0	0	North–East	June 21
	South	0	0	202	356	448	502	514	502	448	356	202	0	0	North	
	South–West	0	0	13	28	88	227	341	451	511	495	360	0	0	North–West	
	West	0	0	13	28	35	38	38	101	88	331	290	0	0	West	
	North–West	0	0	13	28	35	38	38	38	35	28	32	0	0	South–East	
	Horizontal	0	0	55	189	306	385	413	385	306	189	60	0	0	Horizontal	
40° North Latitude					**am**				**pm**						**40° South Latitude**	
Time of year	Exposure	6	7	8	9	10	11	Noon	1	2	3	4	5	6	Exposure	Time of year
	North	101	63	38	41	44	44	44	44	44	41	38	63	101	South	
	North–East	372	420	353	230	495	60	44	44	44	41	38	32	19	South–East	
	East	397	508	511	448	300	139	44	44	44	41	38	32	19	East	
June 21	South–East	161	278	344	350	312	224	107	44	44	44	38	32	19	North–East	Dec. 22
	South	19	32	38	60	110	139	170	139	110	60	38	32	19	North	
	South–West	19	32	38	41	44	44	107	224	312	350	344	278	161	North–West	
	West	19	32	38	41	44	44	44	139	300	448	511	508	397	West	
	North–West	19	32	38	41	44	44	44	44	95	230	353	420	372	South–East	
	Horizontal	98	259	423	565	662	732	748	732	662	565	423	259	98	Horizontal	
	North	76	44	38	41	44	44	44	44	44	41	38	44	76	South	
	North–East	334	401	331	208	82	44	44	44	44	41	38	32	16	South–East	
	East	372	508	517	454	309	136	44	44	44	41	38	32	16	East	
July 23 and May 21	South–East	170	303	375	394	347	259	132	47	44	41	38	32	16	North–East	Jan. 21 and Nov. 21
	South	16	32	41	82	139	199	218	199	139	82	41	32	16	North	
	South–West	16	32	38	41	44	47	132	259	347	394	375	303	170	North–West	
	West	16	32	38	41	44	44	44	136	309	454	517	508	372	West	
	North–West	16	32	38	41	44	44	44	44	82	208	331	401	334	South–East	
	Horizontal	76	230	397	539	640	710	735	710	640	539	397	230	76	Horizontal	
	North	22	25	35	41	44	44	44	44	44	41	35	25	22	South	
	North–East	214	322	259	145	50	44	44	44	44	41	35	25	9	South–East	
	East	265	464	511	457	319	142	44	44	44	41	35	25	9	East	
Aug. 24 and April 20	South–East	151	331	435	461	438	338	208	79	44	41	35	25	9	North–East	Feb. 20 and Oct. 23
	South	9	25	76	161	218	306	322	306	218	161	76	25	9	North	
	South–West	9	25	35	41	44	79	208	338	438	461	435	331	151	North–West	
	West	9	25	35	41	44	44	44	142	319	457	511	464	265	West	
	North–West	9	25	35	41	44	44	44	44	50	145	259	322	215	South–East	
	Horizontal	23	148	315	473	584	647	675	647	584	473	315	148	28	Horizontal	

(*Contd.*)

Table 21.13 Solar heat gain through ordinary glass (W/m^2) (contd.)

40° North Latitude					**am**				**pm**						**40° South Latitude**	
Time of year	Exposure	6	7	8	9	10	11	Noon	1	2	3	4	5	6	Exposure	Time of year
	North	0	16	28	38	41	41	44	41	41	38	28	16	0	South	
	North–East	0	161	183	82	41	41	44	41	41	38	28	16	0	South–East	
	East	0	366	470	438	312	142	44	41	41	38	28	16	0	East	
Sept. 22 and Mar. 22	South–East	0	300	454	511	495	420	284	129	44	38	28	16	0	North–East	Mar. 22 and Sept. 22
	South	0	38	139	256	347	385	442	385	347	256	139	38	0	North	
	South–West	0	16	28	38	44	129	284	420	495	511	454	300	0	North–West	
	West	0	16	28	38	41	41	44	142	312	438	470	366	0	West	
	North–West	0	16	28	38	41	41	44	41	41	82	183	161	0	South–East	
	Horizontal	0	66	211	391	483	555	577	555	483	391	211	66	0	Horizontal	
	North	0	16	19	32	35	38	38	38	35	32	19	6	0	South	
	North–East	0	110	104	38	35	38	38	38	35	32	19	6	0	South–East	
	East	0	269	369	385	278	132	38	38	35	32	19	6	0	East	
Oct. 23 and Feb. 20	South–East	0	266	416	508	514	454	338	199	63	32	19	6	0	North–East	April 20 and Aug. 24
	South	0	66	186	328	432	486	511	486	432	328	186	66	0	North	
	South–West	0	6	19	32	63	199	338	454	514	508	416	256	0	North–West	
	West	0	6	19	32	35	38	38	123	278	385	369	268	0	West	
	North–West	0	6	19	32	35	38	38	38	35	38	104	110	0	South–East	
	Horizontal	0	25	91	202	319	388	407	388	319	202	91	25	0	Horizontal	
	North	0	0	9	22	28	32	35	32	28	22	9	0	0	South	
	North–East	0	0	38	22	28	32	35	32	28	22	9	0	0	South–East	
	East	0	0	287	315	233	104	35	32	28	22	9	0	0	East	
Nov. 21 and Jan. 21	South–East	0	0	344	454	492	454	366	221	85	22	9	0	0	North–East	May 21 and July 23
	South	0	0	186	328	438	498	524	498	438	328	186	0	0	North	
	South–West	0	0	9	22	85	221	366	454	492	454	344	9	0	North–West	
	West	0	0	9	22	28	32	35	104	233	315	287	0	0	West	
	North–West	0	0	9	22	28	32	35	32	28	22	38	0	0	South–East	
	Horizontal	0	0	50	136	230	290	325	290	230	136	50	0	0	Horizontal	
	North	0	0	6	19	28	32	32	32	28	19	6	0	0	South	
	North–East	0	0	22	19	28	32	32	32	28	19	6	0	0	South–East	
	East	0	0	227	271	215	98	32	32	28	19	6	0	0	East	
Dec. 22	South–East	0	0	276	423	467	448	363	230	95	22	6	0	0	North–East	June 21
	South	0	0	161	312	423	498	520	498	423	312	161	0	0	North	
	South–West	0	0	6	22	95	230	363	448	467	423	278	0	0	North–West	
	West	0	0	6	19	28	32	32	98	215	271	227	0	0	West	
	North–West	0	0	6	19	28	32	32	32	28	19	22	0	0	South–East	
	Horizontal	0	0	25	101	173	240	268	240	173	101	25	0	0	Horizontal	
50° North Latitude					**am**				**pm**						**50° South Latitude**	
Time of year	Exposure	6	7	8	9	10	11	Noon	1	2	3	4	5	6	Exposure	Time of year
	North	91	38	38	41	44	44	44	44	44	41	38	38	91	South	
	North–East	397	394	296	158	50	44	44	44	44	41	38	32	25	South–East	
	East	438	517	511	429	297	129	44	44	44	41	38	32	25	East	

(*Contd.*)

Table 21.13 Solar heat gain through ordinary glass (W/m^2) (contd.)

50° North Latitude		am							pm							50° South Latitude
Time of year	Exposure	6	7	8	9	10	11	Noon	1	2	3	4	5	6	Exposure	Time of year
June 21	South–East	202	322	397	426	404	309	192	73	44	41	38	32	25	North–East	Dec. 22
	South	25	32	50	123	215	274	293	274	215	123	50	32	25	North	
	South–West	25	32	38	41	44	72	192	309	391	426	397	322	202	North–West	
	West	25	32	38	41	44	44	44	129	297	429	511	517	428	West	
	North–West	25	32	38	41	44	44	44	44	50	158	297	394	397	South–East	
	Horizontal	139	271	420	546	621	675	694	675	621	546	420	271	139	Horizontal	
	North	66	35	38	41	44	44	44	44	44	41	38	35	66	South	
	North–East	360	369	274	139	47	44	44	44	44	41	38	32	19	South–East	
	East	413	508	514	445	303	136	44	44	44	41	38	32	19	East	
July 23 and May 21	South–East	205	338	423	451	429	344	221	82	44	41	38	32	19	North–East	Jan. 21 and Nov. 21
	South	19	32	66	158	252	309	334	309	252	158	66	32	19	North	
	South–West	19	32	38	41	44	82	221	344	429	451	423	338	205	North–West	
	West	19	32	38	41	44	44	44	136	303	445	514	508	413	West	
	North–West	19	32	38	41	44	44	44	44	47	139	274	369	360	South–East	
	Horizontal	104	237	375	502	593	647	666	647	593	502	375	237	104	Horizontal	
	North	25	25	32	38	41	44	44	44	41	38	32	25	25	South	
	North–East	240	297	221	98	41	44	44	44	41	38	32	25	25	South–East	
	East	297	457	498	445	309	142	44	44	41	38	32	25	25	East	
Aug. 24 and April 20	South–East	167	350	454	495	483	416	281	126	41	38	32	25	12	North–East	Feb. 20 and Oct. 23
	South	13	28	114	230	331	410	435	410	331	230	114	28	12	North	
	South–West	13	25	32	38	41	126	281	416	483	495	454	350	167	North–West	
	West	13	25	32	38	41	44	44	142	309	445	498	457	297	West	
	North–West	13	25	32	38	41	44	44	44	41	98	221	297	140	South–East	
	Horizontal	41	145	281	413	505	565	584	565	505	413	281	145	41	Horizontal	
	North	0	12	25	32	38	38	38	38	38	32	25	12	0	South	
	North–East	0	183	145	50	38	38	38	38	38	32	25	12	0	South–East	
Sept. 22 and Mar. 22	East	0	322	435	410	293	136	38	38	38	32	25	12	0	East	Mar. 22 and Sept. 22
	South–East	0	271	438	511	514	457	331	177	54	32	25	12	0	North–East	
	South	0	35	161	293	413	473	498	473	413	293	161	35	0	North	
	South–West	0	12	25	32	54	177	331	457	514	511	438	271	0	North–West	
	West	0	12	25	32	38	38	38	136	293	410	435	322	0	West	
	North–West	0	12	25	32	38	38	38	38	38	50	145	183	0	South–East	
	Horizontal	0	47	155	278	372	442	467	442	372	278	155	47	0	Horizontal	
	North	0	0	12	22	28	32	35	32	28	22	12	0	0	South	
	North–East	0	91	63	22	28	32	35	32	28	22	12	0	0	South–East	
	East	0	230	132	331	249	110	35	32	28	22	12	0	0	East	
Oct. 23 and Feb. 20	South–East	0	218	350	457	495	454	363	218	76	22	12	0	0	North–East	April 20 and Aug. 24
	South	0	54	167	312	432	495	527	495	432	312	167	54	0	North	
	South–West	0	0	12	22	76	218	363	454	495	457	350	218	0	North–West	

(*Contd.*)

Table 21.13 Solar heat gain through ordinary glass (W/m^2) (contd.)

50° North Latitude		am							pm						50° South Latitude	
Time of year	Exposure	6	7	8	9	10	11	Noon	1	2	3	4	5	6	Exposure	Time of year
	West	0	0	12	22	28	32	35	110	249	331	312	230	0	West	
	North–West	0	0	12	22	28	32	35	32	28	22	63	91	0	South–East	
	Horizontal	0	6	60	142	227	271	297	271	227	139	60	6	0	Horizontal	
	North	0	0	3	12	19	25	28	28	19	12	3	0	0	South	
	North–East	0	0	16	12	19	25	28	28	19	12	3	0	0	South–East	
	East	0	0	161	202	180	88	28	28	19	12	3	0	0	East	
Nov. 21 and Jan. 21	South–East	0	0	196	300	401	401	338	211	66	12	3	0	0	North–East	May 21 and July 23
	South	0	0	107	221	366	451	483	451	366	221	107	0	0	North	
	South–West	0	0	3	12	66	211	338	410	401	300	196	0	0	North–West	
	West	0	0	3	12	19	25	28	88	180	202	160	0	0	West	
	North–West	0	0	3	12	19	25	28	25	19	12	16	0	0	South–East	
	Horizontal	0	0	12	41	95	148	167	148	95	41	12	0	0	Horizontal	
	North	0	0	0	9	16	19	22	19	16	12	0	0	0	South	
	North–East	0	0	0	9	16	19	22	19	16	12	0	0	0	South–East	
	East	0	0	0	85	148	73	22	19	16	12	0	0	0	East	
Dec. 22	South–East	0	0	0	129	338	366	315	196	78	12	0	0	0	North–East	June 21
	South	0	0	0	98	312	413	445	413	312	98	0	0	0	North	
	South–West	0	0	0	9	78	196	315	366	338	129	0	0	0	North–West	
	West	0	0	0	9	16	19	22	73	148	85	0	0	0	West	
	North–West	0	0	0	9	16	19	22	19	16	9	0	0	0	South–East	
	Horizontal	0	0	0	16	60	104	126	104	60	16	0	0	0	Horizontal	

EXAMPLE 21.3 Determine the total heat transfer through a south-facing window at 3:00 pm solar time on 15 April in Delhi. The window has 6 mm clear glass, with width of 2.0 m and height of 1.8 m, and it is set back by 0.2 m from the plane of the building. The outdoor and the indoor temperatures are 45°C and 25°C respectively.

Solution:

From Example 20.10 of Chapter 20 we have in Delhi at 3:00 pm on April 15,

$$b = 43.739^{o},\ \gamma = 105.142^{o} \text{ and } \alpha = 180^{\circ} - 105.142^{\circ} = 74.858^{o}$$

$$I_N = 0.87561 \text{ kW/m}^2$$

$$I_{dH} = 0.097 \times 0.87561 = 0.084934 \text{ kW/m}^2$$

$$\cos\theta = \cos\beta\ \cos\alpha = 0.1887 \quad \therefore \quad \theta = 79.123^{\circ} \approx 80^{\circ}$$

$$I_{DV} = I_N \cos\theta = 0.16526 \text{ kW/m}^2$$

$$I_{dV}/I_{dH} = 0.55 + 0.437 \cos\theta + 0.313 \cos^2\theta = 0.6436$$

$$I_{dV} = 0.084934\ (0.6436) = 0.05466 \text{ kW/m}^2$$

The sunlit fraction $F_s = 0.3739$ from Example 20.12 of Chapter 20.

For $\theta \approx 80^{o}$, from Table 21.1, transmissivity for direct beam radiation $\tau_D = 0.38$ and $\alpha_D = 0.09$, therefore, $\rho_D = 1 - \tau_D - \alpha_D = 0.53$

For diffuse radiation, $\tau_d = 0.79$, $\alpha_d = 0.06$ and $\rho_d = 0.15$ have been assumed.

The outer surface and inner surface heat transfer coefficients are taken from Table 21.1 as $h_i = 8.29$ W/m^2-K and $h_o = 34$ W/m^2-K for still air and a wind velocity of 24 km/h.

$$\therefore \qquad U_o = (1/h_o + 1/h_i) = 6.665 \text{ W/m}^2\text{-K}$$

The temperature of the glass is given by Eq. (21.28) as

$$t_g = \frac{0.3739(0.09)(165.26) + 0.06(54.66) + 34.0(45) + 8.29(25)}{34 + 8.29} = 41.2885°\text{C}$$

In absence of shading, $t_g = 41.508°$C

From Eq. (21.29),

$$q_i = (F_s\, \tau_D\, I_D + \tau_d\, I_d + \tau_r\, I_r) + \frac{F_s\, I_D\, \alpha_D + I_d\, \alpha_d + I_r\, \alpha_r}{\left(1 + \frac{h_o}{h_i}\right)} + U_o(t_o - t_i) \qquad (21.29)$$

Neglecting the reflected radiation,

$$q_i = [0.3739(0.38)(165.26) + 0.79(54.66)] + [0.3739(0.09)(165.26) + 0.06(54.66)]/(1 + 34/8.29) + 6.665\ (45 - 25)$$

$$= 66.662 + 1.733 + 133.3 = 201.695 \text{ W/m}^2$$

In absence of sunlit fraction, this sum is as follows.

$$q_i = 105.98 + 3.567 + 133.3 = 242.847$$

Substituting the value of $t_g = 41.508°$C in Eq. (21.25) results in

$q_i = 242.83$ W/m^2 which is almost same as the above result.

The first expression in Eq. (21.29) is the transmitted radiation, the second expression is the absorbed radiation that is transmitted indoors and the third expression is convective heat transfer.

It is observed that the portion of absorbed radiation that enters the space is 3.567/242.847, that is, about 1.5% of the total heat transfer.

If the window has 85% glass area then the transmitted and absorbed radiation =

$$(105.98 + 3.567)0.85 = 93.1 \text{ W/m}^2$$

The value given in Table 21.13 for 30°N latitude for April 20, 3:00 solar time south-facing glass is 85 W/m^2. This is quite close.

If the ASHRAE recommended procedure is used and Eqs. (21.21) and (21.22) are used to find the values of τ_D, τ_d, α_D and α_d and subsequently Eqs. (21.23) and (21.24) are used to find TSHGF and ASHGF, we get

$$\tau_D = 0.44479 \text{ and } \tau_d = 0.399505\ ;\ \alpha_D = 0.065314 \text{ and } \alpha_d = 0.02704$$

These values are distinctly different from the tabulated values.

$$\text{TSHGF} = 0.44479(165.26) + 0.399505(54.66) = 93.3429 \text{ W/m}^2$$

$$\text{ASHGF} = \frac{0.065314(165.26) + 0.02704(54.66)}{\left(1 + \frac{34}{8.29}\right)} = 2.40561 \text{ W/m}^2$$

$$\text{TSHGF} + \text{ASHGF} = 95.748 \text{ W/m}^2$$

For a typical wooden sash window SHGF = 0.85(95.748) = 81.386 W/m^2, which is a better approximation to the tabulated value despite the fact that transmissivities and absorptivities for direct beam and diffuse radiation are different from the tabulated values.

21.7 PERIODIC HEAT TRANSFER THROUGH WALLS AND ROOFS

We have studied steady-state heat transfer through building walls, roof and window glass. The steady-state assumption may be made if both the indoor and the outdoor thermal environments are time independent. Though it is a requirement to keep the indoor temperature and humidity constant, the outdoor conditions vary almost periodically, hence steady-state heat transfer rarely occurs in the outer walls of a building. The indoor temperature is usually less than the outdoor temperature during summer months. This temperature difference gives rise to heat gain by the interior. The incident solar radiation on the walls is absorbed by it, stored and at a later instant of time transmitted indoors. Both of these driving potentials, vary erratically with time. However, if we limit ourselves to clear days, solar radiation intensity is periodic with time and the outdoor air temperature is also essentially periodic with time.

The wall has a thermal capacity, as a result it stores a certain amount of energy passing through it, and it is released at a later time to the interior and the exterior. To illustrate it, we first consider steady-state heat transfer through the wall with an overall heat transfer coefficient U_o. The outside and inside surface heat transfer coefficients are h_o and h_i respectively. The outside wall temperature is, say, $t_{woa} < t_o$.

$$q = U_o(t_o - t_i)$$

As the sun rises, the solar radiation intensity increases and the outside wall temperature increases and becomes more than the outdoor air temperature t_o. The outside wall temperature becomes, say, $t_{wob} > t_o$. The heat transfer from the wall occurs to outdoors as well as indoors.

In the evening hours, the solar radiation intensity decreases which decreases the outside wall temperature to, say, $t_{woc} < t_o$. The interior wall temperature may be greater than t_{woc} at some points. This gives rise to a peak in the wall temperature that travels towards indoors. Eventually, this peak will reach the inner surface and hence there will be a periodic temperature variation in the indoor wall temperature t_{wi}. Thick walls with large thermal inertia will damp the temperature wave, whereas thin walls with smaller thermal inertia will have smaller damping effect. For thin walls, the temperature variation at the outer wall will be immediately felt on the interior wall.

The outside wall temperature decreases during night-time due to radiation to the sky which is at an effective temperature of about –55°C. In the early morning hours, the outside surface temperature may become less than the indoor wall temperature. Hence, both the diurnal variation of outdoor temperature and the periodic nature of solar radiation intensity play a key role in the determination of heat gain through walls.

21.7.1 Hourly Outdoor Temperature

The hourly outdoor temperature varies periodically between the outdoor design temperature and a minimum temperature. The maximum outdoor temperature occurs around 3:00 pm solar time, and the minimum occurs one hour before sunrise. The difference between the design temperature and

the minimum temperature is called *daily range, DR*. The variation of outdoor air temperature may be represented as

$$t = t_o - (X)DR$$

where t_o is the design outdoor temperature, DR is daily range and X is the percentage of daily range given in Table 21.14.

Table 21.14 Percentage of daily range for outdoor air temperature variation

Time (h)	*Percent*	*Time* (h)	*Percent*	*Time* (h)	*Percent*	*Time* (h)	*Percent*
1	87	7	93	13	11	19	34
2	92	8	84	14	3	20	47
3	96	9	71	15	0	21	58
4	99	10	56	16	3	22	68
5	100	11	39	17	10	23	76
6	98	12	23	18	21	24	82

Figure 21.6 shows diurnal variation of outdoor air temperature typical for May–June in Northern India. Typical variation of incidence of direct solar radiation and diffuse sky radiation may be determined from the equations given in Chapter 20. The reflected radiation, if significant, may also be evaluated by the procedure given in Chapter 20. Similarly, the sunlit fraction may also be evaluated. Figure 21.6 also shows the variation of direct solar radiation I_{DH} and diffuse sky radiation $I_{dH,}$ and total radiation ($I_{DH} + I_{dH}$) incident upon an unshaded horizontal surface.

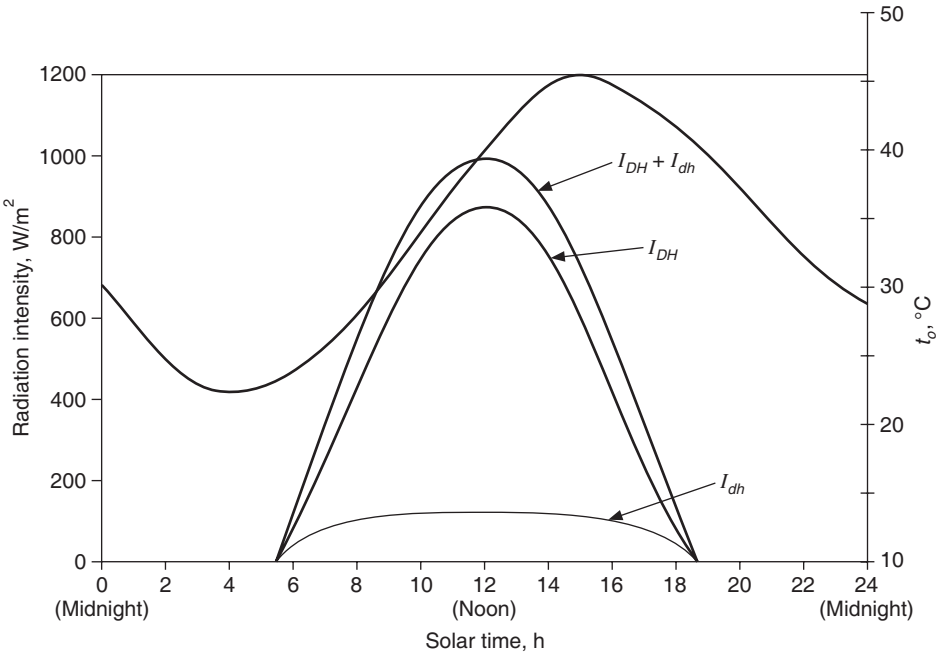

Figure 21.6 Variation of direct, diffuse and total solar radiation on a unshaded horizontal surface and variation of outside air temperature with time under clear sky conditions.

21.7.2 Sol-air Temperature

It has been found convenient to combine the effects of outdoor air temperature and absorbed solar radiation into a single quantity for heat transfer calculations. The heat transfer rate per unit area q_o from outdoor environment to the wall with outer surface temperature t_{wo} and absorptivity α, is given by

$$q_o = h_o(t_o - t_{wo}) + \alpha_D I_D + \alpha_d I_d + \alpha_r I_r$$

This may be simplified as follows by assuming $\alpha_D = \alpha_d = \alpha_r = \alpha$. The absorptivity varies only slightly with the angle of incidence, so that we can combine all radiation components into a single quantity, that is, $I = I_D + I_d + I_r$ the total radiation intensity (sum of direct, diffuse sky, and ground reflected). Thus,

$$q_o = h_o(t_o - t_{wo}) + \alpha I = h_o [t_o + \alpha (I/h_o) - t_{wo}] \tag{21.30}$$

The rate of heat transfer may be conveniently expressed as

$$q_o = h_o (t_e - t_{wo}) \tag{21.31}$$

where,
$$t_e = t_o + \alpha (I/h_o) \tag{21.32}$$

The fictitious temperature t_e in Eq. (21.32) is called the *sol-air temperature*. It is dependent upon the absorptivity of the surface. It was first introduced by Mackey and Wright (1944).

The solar radiation intensity and outdoor air temperatures are periodic in nature; hence the sol-air temperature may be expressed as a Fourier series. If θ is the time measured in hours from midnight then the *sol-air temperature* is expressed as

$$t_e = t_{em} + M_1 \cos \omega_1\theta + N_1 \sin \omega_1\theta + M_2 \cos \omega_2\theta + N_2 \sin \omega_2\theta + ... \tag{21.33}$$

where, the constants t_{em}, M_1, M_2, N_1 and N_2, etc. are given by the method of fitting the Fourier series expansion to the hourly data on solar radiation and temperature as follows.

$$t_{em} = \frac{1}{24}\int_0^{24} t_e \, d\theta, \quad M_n = \frac{1}{12}\int_0^{24} t_e \cos \omega_n\theta \, d\theta \quad \text{and} \quad N_n = \frac{1}{12}\int_0^{24} t_e \sin \omega_n\theta \, d\theta \tag{21.34}$$

$\omega_1 = \pi/12$ radians per hour or 15 degrees per hour and $\omega_n = n\omega$. Alternatively, Eq. (21.33) may be written as

$$t_e = t_{em} + \sqrt{M_1^2 + N_1^2} \cos (\omega_1\theta - \psi_1) + \sqrt{M_2^2 + N_2^2} \cos (\omega_2\theta - \psi_2) + \cdots$$

or
$$t_e = t_{em} + t_{e1} \cos (\omega_1\theta - \psi_1) + t_{e2} \cos (\omega_2\theta - \psi_2) + \cdots \tag{21.35}$$

where,
$$t_{e1} = \sqrt{M_1^2 + N_1^2} \quad \text{and} \quad t_{e2} = \sqrt{M_2^2 + N_2^2} \quad \text{and} \quad \tan \psi_n = \frac{N_n}{M_n} \tag{21.36}$$

In Eq. (21.36), the quadrant in which ψ_n lies is decided by the requirement that sin ψ_n has the sign of N_n and cos ψ_n has the sign of M_n. As an illustration, we consider the following example.

EXAMPLE 21.4 Find the Fourier series for the sol-air temperature, for a horizontal surface in Delhi on June 1. It is given that the outdoor design temperature for Delhi is 43.3°C, wet-bulb temperature is 23°C, daily range is equal to 13.889°C. The outer surface heat transfer coefficient $h_o = 22.7$ W/m^2-K and absorptivity of the surface, $\alpha = 0.09$.

Solution:

For Delhi: longitude = 77.2°, latitude = 28.5833°.

On June 1 from Tables 20.1 and 20.2, declination = 23.95°, $A = 1.088$, $B = 0.205$ and $C = 0.134$

We find the altitude angle β from Eq. (20.5):

$$\sin \beta = \cos 28.5833° \cos 23.95° \cos h + \sin 28.5833° \sin 21.95°$$

where, h is, hour angle.

$$I_N = \text{A} \exp(-B \operatorname{cosec} \beta),\ I_{DH} = I_N \sin \beta \quad \text{and} \quad I_d = CI_N \text{ and } I_H = I_{DH} + I_d$$

The results are given in Table 21.15 for various solar times.

Table 21.15 Incident solar radiation in Delhi on June 1

Solar time, h	sin β	cosec β	β, deg	I_N	I_{DH}	I_d	I_H
6.00	0.1788	5.5916	10.302	0.35478	0.06184	0.04633	0.10817
7.00	0.3896	2.5665	20.932	0.64288	0.25049	0.08615	0.33664
8.00	0.5861	1.7063	35.879	0.76686	0.44944	0.10276	0.5522
9.00	0.7547	1.325	49.0	0.82921	0.62584	0.11111	0.73695
10.00	0.8842	1.131	62.152	0.86285	0.76293	0.11562	0.87855
11.00	0.9655	1.0357	77.59	0.87987	0.84952	0.1179	0.96742
12.00	0.9933	1.0067	83.367	0.88512	0.87919	0.11861	0.9978

Sunrise occurs at: cos h_o = tan 23.95° tan 28.5833°, h_o = 102.684° = 5 h 9′16″ solar time. In the above table, the afternoon values are not given, since these are the same as those for the corresponding morning hours of solar time. The sol-air temperature is found from $t_e = t_o + \alpha I/h_o$. The hourly outdoor temperature variation is obtained by using % of *DR* given in Table 21.14. The results are as follows:

Table 21.16 Outdoors air temperature and sol-air temperature at various solar times

Solar time	*Outdoor air temp*, t_o (°C)	*Sol-air temp*, t_e (°C)	*First harmonic* $\omega_1 = 15\theta$	*Second harmonic* $\omega_2 = 30\theta$	*Solar time*	t_o (°C)	*Sol-air*, t_e (°C)	$\omega_1 = 15\theta$	$\omega_2 = 30\theta$
12 midnight	31.911	31.911	0	0	12 noon	40.106	79.666	180	360
1 am	31.217	31.217	15	30	1 pm	41.772	80.128	195	390
2 am	30.522	30.522	30	60	2 pm	42.883	77.715	210	420
3 am	29.967	29.967	45	90	3 pm	43.3	77.518	225	450
4 am	29.55	29.55	60	120	4 pm	42.883	64.776	240	480
5 am	29.411	29.411	75	150	5 pm	41.911	55.268	255	510
6 am	29.688	33.98	90	180	6 pm	40.383	44.171	270	540

(*Contd.*)

Table 21.16 Outdoors air temperature and sol-air temperature at various solar times (contd.)

Solar time	*Outdoor air temp*, t_o (°C)	*Sol-air temp*, t_e (°C)	*First harmonic* $\omega_1 = 15\theta$	*Second harmonic* $\omega_2 = 30\theta$	*Solar time*	t_o (°C)	*Sol-air*, t_e (°C)	$\omega_1 = 15\theta$	$\omega_2 = 30\theta$
7 am	30.383	43.73	105	210	7 pm	38.577	38.577	285	570
8 am	31.633	53.526	120	240	8 pm	36.772	36.772	300	600
9 am	33.439	62.657	135	270	9 pm	35.244	35.244	315	630
10 am	35.522	70.354	150	300	10 pm	33.885	33.885	330	660
11 am	37.883	76.239	165	330	11 pm	32.744	32.744	345	690
Total							1175.0		

$$t_{em} = \frac{1175.0}{24} = 48.958; \quad M_1 = \frac{1}{12}\sum_{i=1}^{24} t_{ei} \cos \omega_1\theta = \frac{-293.0}{12} = -24.42;$$

$$N_1 = \frac{1}{12}\sum_{i=1}^{24} t_{ei} \sin \omega_1\theta = \frac{-64.13}{12} = -5.344; \quad M_2 = \frac{1}{12}\sum_{i=1}^{24} t_{ei} \cos \omega_2\theta = \frac{93.041}{12} = 7.753;$$

$$N_2 = \frac{1}{12}\sum_{i=1}^{24} t_{ei} \sin \omega_2\theta = \frac{13.922}{12} = 1.16; \quad \sqrt{M_1^2 + N_1^2} = 25.0; \sqrt{M_2^2 + N_2^2} = 7.84;$$

$$\psi_1 = \tan^{-1}\frac{N_1}{M_1} = 192.35°; \quad \psi_2 = \tan^{-1}\frac{N_2}{M_2} = 8.51°$$

The expression for the first two terms of sol-air temperature reduces to:

$$t_e = 48.958 + 25.0 \cos (15\theta - 192.35^o) + 7.84 \cos (30\theta - 8.51^o) \qquad (21.37)$$

This includes only two harmonics. For a reasonable accuracy, one may use up to five to six harmonics. The following table shows a comparison of t_e given by Eq. (21.37).

θ	0	2	4	6	8	10	12	14	16	18	20	22
t_e, Table 21.16	31.91	30.52	29.55	33.98	53.53	70.35	79.67	77.72	64.77	44.67	36.77	33.85
t_e, Eq. (21.37)	32.29	30.02	29.24	35.85	51.66	70.31	81.13	77.66	62.93	46.55	36.50	33.35

Considering that only two terms are taken into account, the accuracy is limited; this has been done only to illustrate the procedure for a horizontal surface. The variation of t_e is very significant for a vertical surface, hence a large number of terms of the Fourier series have to be taken into account.

21.7.3 Conduction Equation for Periodic Heat Transfer

With this definition of sol-air temperature, the problem of periodic heat transfer through a wall formed by a single homogeneous material can be investigated. Figure 21.7 shows the schematic diagram.

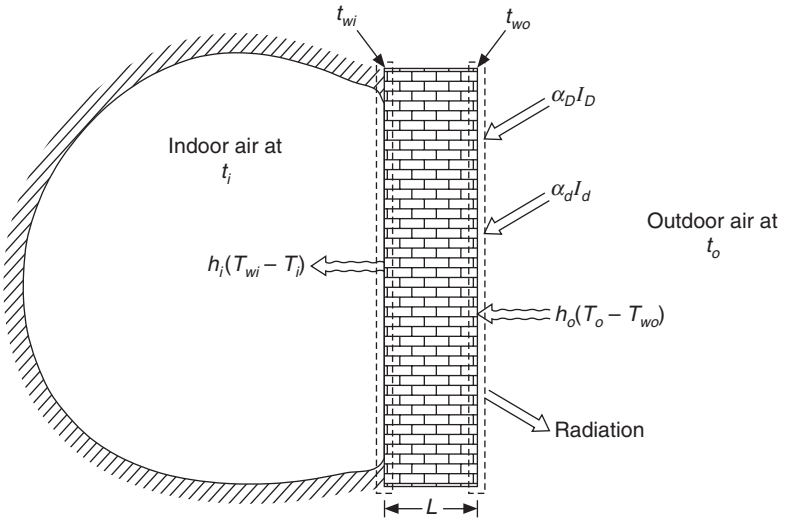

Figure 21.7 Unsteady heat transfer through a building wall.

We assume that:

(i) The wall is of very large height and length so that heat transfer occurs only in the x-direction.
(ii) The density, thermal conductivity and specific heat of the wall are constant.
(iii) The surface heat transfer coefficients h_i and h_o are constant.
(iv) Absorptivity a is independent of the angle of incidence.
(v) The variation of t_o and I is periodic in nature.
(vi) The indoor temperature t_i is maintained at constant value.

The heat transfer through the wall is described by the conduction equation,

$$\frac{\partial t_w}{\partial \theta} = \alpha_w \frac{\partial^2 t_w}{\partial x^2} \tag{21.38}$$

where $\alpha_w = k_w/(\rho_w c_w)$ is thermal diffusivity of the wall material.

The boundary conditions for Eq. (21.38) at the inner and outer surfaces involve convective heat transfer with surface heat transfer coefficients h_i and h_o and surface temperatures t_{wi} and t_{wo} respectively.

$$\text{At } x = L : q_i = -k_w \left(\frac{\partial t_w}{\partial x}\right)_{x=L} = h_i(t_{wi} - t_i) \tag{21.39a}$$

$$\text{At } x = 0 : q_o = -k_w \left(\frac{\partial t_w}{\partial x}\right)_{x=0} = h_o(t_o - t_{wo}) \tag{21.39b}$$

The solution to Eq. (21.38) subject to boundary conditions (21.39a) and (21.39b) has been given by Alford, Ryan and Urban (1939). This may be obtained by separation of variables with a

little patience. It consists of a steady-state linear variation and periodic components. The general solution is as follows.

$$t_w = A + Bx + \sum_{1}^{\infty} (C_n \cos p_n mx + D_n \sin p_n mx)\, e^{-m^2 \omega \theta} \tag{21.40}$$

where, $m = \sqrt[4]{-1}$ and A, B, C_n, D_n and p_n are constants. The coefficients A, B, C_n and D_n may be either real or complex, however the solution will be a real part of these. The solution to Eq. (21.38) subject to boundary conditions (21.39a) and (21.39b) as given by Alford, Ryan and Urban for the inside wall temperature t_{wi} is as follows.

$$t_{wi} = t_i + \frac{1}{h_i}[U(t_{em} - t_i) + V_1 t_{e1} \cos(\omega_1 \theta - \psi_1 - \varphi_1) + V_2 t_{e2} \cos(\omega_2 \theta - \psi_2 - \varphi_2) + \cdots] \tag{21.41}$$

where $$\frac{1}{U} = \frac{1}{h_i} + \frac{1}{k_w} + \frac{1}{h_o};\ V_n = \frac{h_i h_o}{\sigma_n k_w \sqrt{Y_n^2 + Z_n^2}} \quad \text{and} \quad \sigma_n = \sqrt{\frac{\omega_n}{2\alpha_w}} \tag{21.42}$$

$$Y_n = \left(\frac{h_i h_o}{2\sigma_n^2 k_w^2} + 1\right) \cos \sigma_n L \sinh \sigma_n L + \left(\frac{h_i h_o}{2\sigma_n^2 k_w^2} - 1\right) \sin \sigma_n L \cosh \sigma_n L + \frac{(h_i + h_o)}{\sigma_n k_w} \cos \sigma_n L \cosh \sigma_n L \tag{21.43}$$

$$Z_n = \left(\frac{h_i h_o}{2\sigma_n^2 k_w^2} + 1\right) \sin \sigma_n L \cosh \sigma_n L - \left(\frac{h_i h_o}{2\sigma_n^2 k_w^2} - 1\right) \cos \sigma_n L \sinh \sigma_n L + \frac{(h_i + h_o)}{\sigma_n k_w} \sin \sigma_n L \sinh \sigma_n L \tag{21.44}$$

$$\varphi_n = \tan^{-1} \frac{Z_n}{Y_n}$$

The rate of heat transfer from the inside wall is given by

$$q_i = h_i (t_{wi} - t_i) \tag{21.45}$$

Substituting for t_{wi} from Eq. (21.41), we get

$$q_i = U[\{(t_{em} + \lambda_1 t_{e1} \cos(\omega_1 \theta - \psi_1 - \varphi_1) + \lambda_2 t_{e2} \cos(\omega_2 \theta - \psi_2 - \varphi_2) + \ldots\} - t_i] \tag{21.46}$$

where, $$\lambda_n = V_n / U. \tag{21.47}$$

The form of Eq. (21.47) is very interesting. The heat transfer rate q_i continuously changes with time but it can be calculated by multiplying the overall heat transfer coefficient U (of steady-state heat transfer) by an equivalent temperature difference which accounts for periodic variation of sol-air temperature and the storage characteristics of the wall.

The quantity λ appearing in Eq. (21.46) is called the *decrement factor*; this factor decreases the amplitude of the harmonic in the inside surface temperature compared to the same harmonic in the sol-air temperature. The angle, φ, is the angular displacement or the time lag between the harmonic of sol-air temperature and the harmonic of the inside surface temperature. To illustrate the solution, we consider the following example.

EXAMPLE 21.5 The flat roof of a building in Delhi is sunlit throughout the day on June 1. The variation of sol-air temperature is given by Eq. (21.37). The roof is made of 150 mm of concrete. The indoor design air temperature is 25°C. Determine the rate of heat transfer to the room below the roof throughout the day and also the heat transfer rate if the storage effect of the wall is neglected.

Solution:

We have from Table 21.2(a) for concrete:

$$c_{p_w} = 0.88 \text{ kJ/kg-K}, \quad k_w = 1.73 \text{ W/m-K} \quad \text{and} \quad \rho_w = 1920 \text{ kg/m}^3$$

$$\alpha_w = \frac{k_w}{\rho_w c_{p_w}} = \frac{1.73}{880 \times 1920} = 1.0239 \times 10^{-6} \text{ m}^2/\text{s}$$

The overall heat transfer coefficient with $h_i = 8.29$ and $h_o = 34$ W/m^2-K is given by

$$\frac{1}{U} = \frac{1}{8.29} + \frac{0.15}{1.73} + \frac{1}{34} \qquad \therefore \quad U = 4.224 \text{ W/m}^2\text{-K}$$

$$\omega_1 = 2\pi/24 = 0.2168 \text{ radians per hour} = 7.2722 \times 10^{-5} \text{ radians per second}$$

$$\sigma_1 = \sqrt{\frac{\omega_1}{2\alpha_w}} = \sqrt{\frac{7.2722 \times 10^{-5}}{2 \times (1.0239 \times 10^{-6})}} = 5.95922 \text{ m}^{-1}$$

$$\sigma_2 = \sqrt{\frac{\omega_2}{2\alpha_w}} = \sqrt{\frac{2\omega_1}{2\alpha_w}} = \sqrt{2}\sigma_1 = 8.4286 \text{ m}^{-1}$$

$$\sigma_1 L = 5.95922 \times 0.15 = 0.89388 \quad \text{and} \quad \sigma_2 L = 1.2643$$

$$\frac{h_o h_i}{2\sigma_1^2 k_w^2} = \frac{34(8.29)}{2(5.95922)^2 (1.73)^2} = 1.326$$

$$\frac{h_o h_i}{2\sigma_2^2 k_w^2} = 0.663; \quad \frac{h_o h_i}{2\sigma_1 k_w} = 4.1021 \quad \text{and} \quad \frac{h_o h_i}{2\sigma_2 k_w} = 2.9$$

From Eqs. (21.43) and (21.44),

$$Y_1 = 2.326(0.6264)(1.01777) + 0.326(0.77951)(1.4268) + 4.1021(0.62639)(1.4268) = 5.51165$$

$$Z_1 = 2.326(0.77951)(1.4268) - 0.326(0.6264)(1.01777) + 4.1021(0.77951)(1.01777) = 5.6336$$

$$Y_2 = 1.663(0.30172)(1.6291) - 0.337(0.9534)(1.9115) + 2.9(0.30172)(1.9115) = 1.8758$$

$$Z_2 = 1.663(0.9534)(1.9115) + 0.337(0.30172)(1.6291) + 2.9(0.9534)(1.6291) = 7.7006$$

From Eqs. (21.44) and (21.47)

$$\varphi_1 = \tan^{-1}\frac{Z_1}{Y_1} = \tan^{-1}\frac{5.6336}{5.51165} = 45.627°$$

and

$$\varphi_2 = \tan^{-1}\frac{Z_2}{Y_2} = \tan^{-1}\frac{7.7006}{1.8758} = 76.31°$$

$$\lambda_1 = \frac{34(8.20)}{4.224(8.4286)(1.73)\sqrt{Y_1^2 + Z_1^2}} = 0.8212$$

and

$$\lambda_2 = \frac{34(8.20)}{4.224(8.4286)(1.73)\sqrt{Y_2^2 + Z_2^2}} = 0.5774$$

$$t_{em} = 48.958 - 25 = 23.958, \quad \lambda_1 = 25(0.8212) = 20.53$$

and

$$\lambda_2 = 7.86(0.5574) = 4.5268$$

Therefore from Eq. (21.46),

$$q_i = 4.224[23.958 + 20.53 \cos(15\theta - 192.35^o - 45.627°) + 4.5268 \cos(30\theta - 8.51° - 76.31°)]$$

or

$$q_i = 4.224[23.958 + 20.53 \cos(15\theta - 238°) + 4.5268 \cos(30\theta - 85°)] \quad (21.48)$$

If the heat storage effects are neglected, then $\lambda_1 = \lambda_2 = 1$. If the time lag is neglected, then $\varphi_1 = \varphi_2 = 0$ and then Eq. (21.48) reduces to

$$q_i = 4.224[23.958 + 25.0 \cos(15\theta - 192.35°) + 7.86 \cos(30\theta - 8.51°)] \quad (21.49)$$

Equations (21.48) and (21.49) show the heat transfer rates with and without lag and decrement factors. If the situations of Eqs. (21.48) and (21.49) are plotted, it will be observed that the curve pertaining to Eq. (21.48) would lag the curve pertaining to Eq. (22.49) by approximately 2.7 hours. The maximum value of q_i is 85% of the peak value of Eq. (21.49) that would occur if the storage effect is negligible.

Mackey and Wright (1946) have extended a similar analysis to cover composite walls. Stewart (1948) has extended the procedure to several practical wall constructions. The general form of solution for composite walls is identical to the above solution. However, the formulations of λ_n and ϕ_n became more and more complicated as the number of layers was increased. Stephensan and Mitelas (1967) and Mitelas (1972) have suggested the *transfer function method*, which has been adopted by ASHRAE (1997). A transfer function is a set of coefficients relating heat transfer into inner surface of the wall or roof with the heat transfer at previous instants of time and the temperatures at various instants of time. The method is very simple to apply, however, it requires a computer for implementation.

There are three methods, which are in use to determine the heat gain from a wall. Two of them are based upon the periodic solution obtained in Eq. (21.46) and the third is the *Z*-transform method based upon transfer functions mentioned above. These methods are described below.

21.7.4 Decrement Factor–Time Lag Method

The solution given by Eq. (21.46) for instantaneous heat transfer rate at time θ, may be written as follows:

$$q_{i\theta} = U(t_{em} - t_i) + U\,[\lambda_1 t_{e1} \cos(\omega_1\theta - \psi_1 - \phi_1) + \lambda_2 t_{e2} \cos(\omega_2\theta - \psi_2 - \phi_2) + ...] \quad (21.50)$$

The first term represents the mean heat transfer rate over the 24-hour period. In the second term, the first harmonic of sol-air temperature is damped by a factor λ_1 and delayed by time ϕ_1. Similarly, the second harmonic is also damped by a factor λ_2 and delayed by time ϕ_2. The same is the fate all higher-order harmonics.

The sol-air temperature at time θ is given by Eq. (21.35) as follows:

$$t_{e\theta} = t_{em} + t_{e1} \cos(\omega_1\theta - \psi_1) + t_{e2} \cos(\omega_2\theta - \psi_2) + ... \quad (21.51)$$

$$\therefore \quad t_{e1} \cos(\omega_1\theta - \psi_1) + t_{e2} \cos(\omega_2\theta - \psi_2) + ... = (t_{e\theta} - t_{em})$$

or $$\lambda\,[t_{e1} \cos\{\omega_1(\theta - \phi) - \psi_1\} + t_{e2} \cos\{\omega_2(\theta - \phi) - \psi_2\} + ...] = \lambda\,(t_{e,\,\theta-\phi} - t_{em})$$

The effect of delay and damping of the harmonics of sol-air temperature may be combined together as shown above where λ is kind of representative of all λ_s and ϕ represents all ϕ_s. Therefore, we may write the unsteady part of heat transfer as follows:

$$q_{i\theta} = U(t_{em} - t_i) + U\,\lambda(t_{e,\theta-\phi} - t_{em}) \quad (21.52)$$

where $t_{e,\theta-\phi}$ is the sol-air temperature ϕ hours before time θ at which the heat transfer is calculated and λ is the decrement factor.

If the values of decrement factor λ and time lag ϕ are provided, then this becomes a simple method to determine the heat gain by the interior.

It has been pointed out that the wall has thermal inertia or thermal capacity equal to mc_p. If ρ is the density, A is the area and Δx is wall thickness then $mc_p = \rho A c_p \Delta x$. The thermal capacity of almost all the building construction materials is approximately 0.84 kJ/kg-K. Hence, the thermal capacity is mainly dependent upon the wall thickness and density.

The wall because of its thermal inertia absorbs a part of the energy that is being transferred through it. Its temperature rises and it rejects heat to the surroundings as well as indoor at a later instant of time. All the energy absorbed by it is not transmitted indoors. This ratio of energy transmitted indoor and the total amount absorbed is called the decrement factor. If the wall has larger thickness then it will have larger inertia and smaller decrement factor and for same reason the time lag will also be large. Thin walls will have smaller inertia, hence the effect of variation in outdoor temperature will be immediately felt indoors.

Figures 21.8 and 21.9 from *ASHRAE Handbook* show the variation of time lag and decrement factor as a function of wall thickness. Table 21.17 gives the values of these for a few construction materials. It is observed that for a wall thickness more than 600 mm, the decrement factor is so small that the second term in Eq. (21.50) may be neglected, reducing it to

$$q_{i\theta} = U(t_{em} - t_i)$$

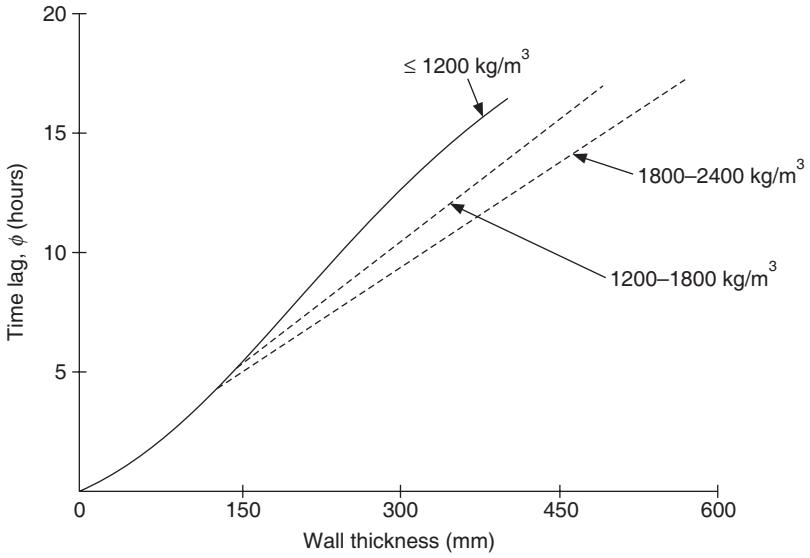

Figure 21.8 Variation of time lag with wall thickness and density.

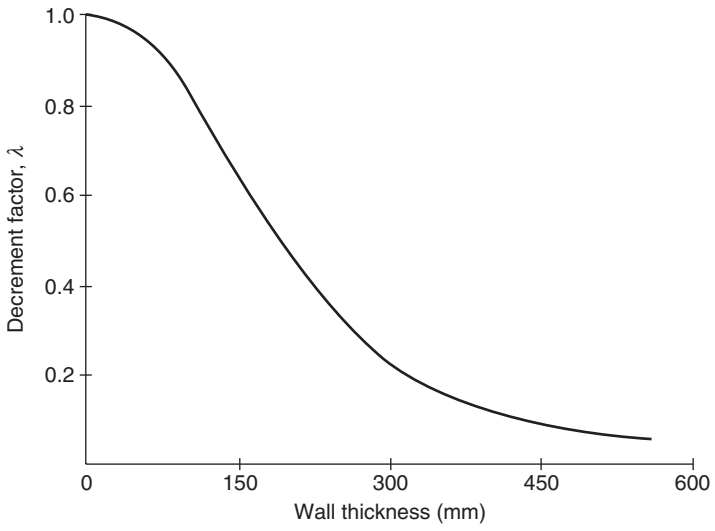

Figure 21.9 Variation of decrement factor with wall thickness.

That is, heat transfer rate is constant over the 24-hour period. Traditionally, all the historic buildings, temples and places of assembly have high ceilings and heavy construction. The temperature in these buildings remains almost constant for 24 hours in summer as well in winter.

On the other hand, for very thin walls, the time lag, ϕ, is negligible and the decrement factor, λ, is of the order of unity. Hence,

$$q_i = U(t_e - t_i)$$

That is, the variation of change in sol-air temperature is immediately felt indoors.

EXAMPLE 21.6 Consider a 150-mm concrete roof of dark colour with density of 1920 kg/m^3 on June 1 in Delhi and find out the heat transfer rate at 5:00 pm solar time by decrement factor–time lag method. The design outdoor and indoor temperatures are given as 43.3°C and 25°C respectively.

Solution:

We take $h_i = 8.29$, $h_o = 34$ and $k_w = 1.73$ W/m-K and hence $U = 4.224$ W/m^2-K as in Example 21.5.

From Figure 21.8 and 21.9, we find that

$$\lambda = 0.64 \quad \text{and} \quad \phi = 5 \text{ hours}$$

The sol-air temperature for this combination of temperatures on June 1 has been given in Table 21.16. Time lag of 5 hours means that we have to find the sol-air at solar noon to determine the heat transfer rate at 5:00 pm. From Table 21.16 at solar noon, $t_{e,\theta-\phi} = 79.66$°C and $t_{em} = 48.958$°C.

Hence from Eq. (21.52),

$$q_i = 4.224(49.958 - 25) + 0.64(4.224)(79.666 - 48.958) = 184.2 \text{ W/m}^2$$

The solution as given by Eq. (21.48) is

$$q_i = 4.224[23.958 + 20.53 \cos (15\theta - 238) + 4.5268 \cos (30\theta - 85)$$

At 5:00 pm, $\theta = 17$ hours, this yields, $q_i = 192.21$ W/m^2-K

Considering the fact that this solution also considers only two harmonics the accuracy seems to be good. In general, this method does not give accurate results. Its advantage is that it requires minimum calculations.

EXAMPLE 21.7 Find the heat transfer rate through a dark coloured flat roof of negligible mass, say asbestos roof used in a factory in Delhi, at 5:00 pm solar time.

Solution:

For negligible mass the time lag, ϕ, is negligible and the decrement factor, λ, is of the order of unity. From Table 21.16, sol-air temperature at 5:00 pm is 55.268°C. Hence,

$$q_i = 4.224(55.268 - 25) = 127.809 \text{ W/m}^2.$$

21.7.5 Equivalent Temperature Difference (ETD) or Cooling Load Temperature Difference (CLTD) Method

The steady-state heat transfer rate is expressed in terms of the product of overall heat transfer coefficient and the temperature difference. Equation (21.46) for the unsteady-state heat transfer rate, has a similar form too. The overall heat transfer coefficient U multiplies the mean temperature difference and the harmonics. The harmonics depend upon thermo-physical properties of the wall and the solar radiation intensity. Equation (21.46) may be expressed as follows:

$$q_i = U \, \Delta t_E \tag{21.53}$$

where, $$\Delta t_E = [(t_{em} - t_i) + \lambda_1 t_{e1} \cos (\omega_1 \theta - \psi_1 - \phi_1) + \lambda_2 t_{e2} \cos (\omega_2 \theta - \psi_2 - \phi_2) + ...] \tag{21.54}$$

Δt_E is called the *equivalent temperature difference*. It depends upon the outdoor and indoor temperatures t_o and t_i respectively, intensity of solar radiation which in turn depends upon the latitude of the place, the day, the time and orientation of wall apart from absorptivity of the surface and thickness, density and specific heat, etc. of the wall.

Carrier Air Conditioning Corporation *Handbook of Air Conditioning System Design* gives the values of equivalent temperature differences for walls and roofs. The density of the wall/roof is expressed in terms of wall mass, m, which is essentially the mass of unit area of the wall. If ρ is the density in kg/m^3 and Δx is the wall thickness, then $m = \rho \Delta x$ kg/m^2. The tables in this handbook give Δt_E for m = 106, 319, 532 and 744 kg/m^2 and for eight wall orientations, namely, NE, E, SE, S, SW, W, NW and N (shaded) at hourly values of solar time. This table is reproduced in Table 21.17.

Equivalent temperature differences for the roof are given for the roof exposed to sun, the roof covered with water, the roof sprayed with water, and for shaded roofs. The hourly values at various solar times are given for mass, m, of 53, 106, 212, 319 and 524 kg/m^2. This table is reproduced in Table 21.18.

The limitations and corrections to be applied, while using the tables are as follows.

(i) These tables have been prepared for July 1, at 40° N latitude, but these can be used for 0 to 50° latitude, for the hottest summer period. Corrections are also suggested for latitude and month.

(ii) A temperature difference between outdoor and indoor $(t_o - t_i)$ = 8.33°C (15°F) has been used. To correct for the actual temperature difference, add or subtract $[(t_o - t_i) - 8.33]$ from the tabulated value. This is referred to as Δt correction.

(iii) Absorptivity of 0.9 for dark colour wall has been used. This value also can be corrected for, if required.

(iv) A specific heat of 0.84 kJ/kg-K has been used.

(v) An outdoor daily range in dry-bulb temperature of 11.1°C (20°F) has been used for evaluation of sol-air temperature. This may be corrected as follows.

(a)	For each °C *DR*	:	add 0.25°C to Δt_E for medium construction
	less than 11.1°C	:	add 0.5°C to Δt_E for heavy construction
		:	no correction for light construction
(b)	For each °C *DR*	:	subtract 0.25°C from Δt_E for medium construction
	more than 11.1°C	:	subtract 0.5°C from Δt_E for heavy construction
		:	no correction for light construction
(c)	Maximum correction	:	2°C for medium and 3°C for heavy construction

For southern hemisphere, it is recommended that the tabulated values of Δt_E given for south wall be used for north wall and vice-versa.

Table 21.17 Equivalent temperature difference for walls of dark colours, sunlit and shaded walls in °C at 40°N latitude – 1 July [m is mass density in kg/m^2]

Exposure	m	*Time*											
		6	7	8	9	10	11	12	1	2	3	4	5
		←			am		→	noon	←		pm		→
North–East	106	2.8	8.3	12.2	12.8	13.3	10.6	7.8	7.2	6.7	7.2	7.8	7.8
	319	–0.55	1.1	–1.1	2.8	13.3	12.2	11.1	8.3	5.6	6.1	6.7	7.2
	532	1.1	1.7	2.2	2.2	2.2	5.5	8.8	8.3	7.8	6.7	5.5	6.1
	744	2.8	2.8	3.1	3.3	3.3	3.3	3.3	5.5	7.8	8.9	7.8	6.7

(*Contd.*)

Table 21.17 Equivalent temperature difference for walls of dark colours, sunlit and shaded walls in °C at 40°N latitude – 1 July [*m* is mass density in kg/m^2] (contd.)

Exposure	*m*	*Time*											
		6	7	8	9	10	11	12	1	2	3	4	5
		←			am		→	noon	←		pm		→
East	106	0.55	9.5	16.7	18.3	20.0	19.4	17.8	11.1	6.7	7.2	7.8	7.8
	319	−0.55	−0.55	0	11.7	16.7	17.2	17.2	10.6	7.8	7.2	6.7	7.2
	532	2.8	2.8	3.3	4.4	7.8	11.1	13.3	13.9	13.3	11.1	10.0	8.9
	744	6.1	5.5	5.6	5.0	4.4	5.0	5.6	8.3	10.0	10.6	10.0	9.4
South–East	106	5.5	3.3	7.2	10.6	14.4	15	15.6	14.4	13.3	10.6	8.9	8.3
	319	0.55	0.55	0	17.1	11.1	7.8	15.6	14.4	13.9	11.7	10.0	8.3
	532	3.0	3.9	3.3	3.3	3.3	6.1	8.8	9.4	10.0	10.6	10.0	8.9
	744	5.0	4.4	4.4	4.4	4.4	3.9	3.3	6.1	7.8	8.3	8.9	10.0
South	106	−0.55	−1.1	−2.2	0.55	2.2	7.8	12.2	15.0	16.7	15.6	14.4	11.1
	319	−0.55	−1.7	−2.2	−1.17	−1.1	3.9	6.7	11.1	13.3	13.9	14.4	12.8
	532	2.2	2.2	1.1	1.1	1.1	1.7	2.2	4.4	6.7	8.3	8.9	10.0
	744	3.9	3.3	3.3	2.8	2.2	2.2	2.2	2.2	2.2	3.8	5.6	7.2
South–West	106	−1.1	−2.2	−2.2	−1.1	0	2.2	3.3	10.6	14.4	18.9	22.2	22.8
	319	1.1	0.55	0	0	0	0.55	1.1	4.4	6.7	13.3	17.8	19.4
	532	3.9	2.8	3.3	2.8	2.2	2.8	3.3	3.9	4.4	6.7	7.8	10.6
	744	4.4	4.4	4.4	4.4	4.4	3.9	3.3	3.3	3.3	3.3	4.4	5.0
West	106	−1.1	−1.7	−2.2	−1.1	0	1.7	3.3	7.7	11.1	17.7	22.2	25.0
	319	1.1	0.55	0	0	0	1.1	2.2	3.9	5.6	10.6	14.4	18.9
	532	3.9	3.9	3.3	3.3	3.3	3.3	3.3	3.9	4.4	5.5	6.7	9.4
	744	6.7	6.1	5.5	5.0	4.4	4.4	4.4	5.0	5.5	5.5	5.5	6.1
North–West	106	−1.7	−2.2	−2.2	−1.1	0	1.7	3.3	5.5	6.7	10.6	13.3	18.3
	319	−1.1	−1.7	−2.2	−1.7	−1.1	0	1.1	3.3	4.4	5.5	6.7	11.7
	532	2.8	2.2	2.2	2.2	2.2	2.2	2.2	2.2	2.2	2.7	3.3	5.0
	744	4.4	3.9	3.3	3.3	3.3	3.3	3.3	3.3	3.3	3.3	3.3	3.9
North	106	−1.7	−1.7	−2.2	−1.7	−1.1	0.55	2.2	4.4	5.5	6.7	7.8	7.2
(Shaded)	319	−1.7	−1.7	−2.2	−1.7	−1.1	−0.55	0	1.7	3.3	4.4	5.6	6.1
	532	0.55	0.55	0	0	0	0	0	0.55	1.1	1.7	2.2	2.8
	744	0.55	0.55	0	0	0	0	0	0	0	0.55	1.1	1.7
Exposure	*m*	*Time*											
		6	7	8	9	10	11	12	1	2	3	4	5
		←			pm		→	mid night	←		am		→
North–East	106	7.8	6.7	5.6	4.4	3.3	2.2	1.1	0.0	−1.1	−1.7	−2.2	−1.1
	319	7.8	7.2	6.7	6.1	5.6	4.4	3.3	2.2	1.1	0.55	0	0.55
	532	6.7	6.7	6.7	6.1	5.6	5.0	4.4	3.9	3.3	3.3	2.8	2.8
	744	5.5	5.5	5.5	5.5	5.5	5.5	5.5	5.0	5.0	4.4	3.9	3.9

(*Contd.*)

Table 21.17 Equivalent temperature difference for walls of dark colours, sunlit and shaded walls in °C at 40°N latitude – 1 July [*m* is mass density in kg/m^2] (contd.)

Exposure	*m*	*Time*											
		6	7	8	9	10	11	12	1	2	3	4	5
		←			pm	→		mid night	←		am		→
East	106	7.8	6.7	5.6	4.4	3.3	2.2	1.1	0	−0.55	−1.1	−1.7	−1.7
	319	7.8	7.2	6.7	6.1	5.6	4.4	2.8	2.2	1.7	0.55	0.55	0
	532	7.8	7.8	7.8	7.2	6.7	6.1	5.6	5.0	4.4	5.9	3.9	3.3
	744	8.9	7.8	6.7	7.2	7.8	7.8	7.8	7.2	7.2	6.7	6.7	6.7
South–East	106	7.8	6.7	5.6	4.4	3.3	2.2	1.1	0.0	−0.55	−0.55	−1.1	−1.1
	319	7.8	7.2	6.7	6.1	5.5	4.4	3.3	2.8	2.2	1.7	1.7	1.1
	532	7.8	7.2	6.7	6.1	5.5	5.5	5.5	5.0	5.0	4.4	4.4	3.8
	744	8.9	8.3	7.8	7.2	6.7	6.7	6.7	6.1	6.1	5.5	5.5	5.0
South	106	8.9	6.7	5.6	3.9	3.3	1.7	1.1	0.55	0.55	0	0	−0.55
	319	11.1	8.3	6.7	5.5	4.4	3.3	2.2	1.1	0.55	0.55	0	−0.55
	532	10.0	8.3	7.8	6.7	5.6	5.0	4.4	4.4	3.8	3.33	3.3	2.8
	744	7.8	8.3	8.9	8.9	7.8	6.7	5.5	5.5	3.0	5.0	4.4	3.9
South–West	106	23.3	16.7	13.3	6.7	3.3	2.2	1.1	0.55	0.55	0	−0.55	−0.55
	319	20.0	19.4	18.9	11.1	5.6	3.9	3.3	2.8	2.2	2.2	1.7	1.7
	532	12.2	12.8	13.3	12.8	12.2	8.3	5.6	5.5	5.0	5.0	4.4	3.9
	744	5.6	8.3	10.0	10.6	11.1	7.2	4.4	4.4	4.4	4.4	4.4	4.4
West	106	26.7	18.9	12.2	7.8	4.4	2.8	1.1	0.55	0	0	−0.55	−0.55
	319	22.2	22.8	20.0	15.6	8.9	5.5	3.3	2.8	2.2	1.7	1.7	1.1
	532	11.1	13.9	15.6	15.0	14.4	10.6	7.8	6.7	6.1	5.5	5.0	4.4
	744	6.7	7.8	8.9	11.7	12.2	12.8	12.2	11.1	10.0	8.8	8.3	7.2
North–West	106	22.2	20.6	18.9	10.0	3.3	2.2	1.1	0	−0.55	−0.55	−1.1	−1.1
	319	16.7	17.2	17.8	11.7	6.7	4.4	3.3	2.2	1.7	0.55	0	−0.55
	532	6.7	9.4	11.1	11.7	12.2	7.8	4.4	3.9	3.9	3.3	3.3	2.8
	744	4.4	5.0	5.6	7.8	10.0	10.6	11.1	8.8	7.2	6.1	5.5	5.0
North	106	6.7	5.5	4.4	3.3	2.2	1.1	0	0	−0.55	0.55	−1.1	−1.1
(Shaded)	319	6.7	6.7	6.7	5.5	4.4	3.3	2.2	1.1	0.55	0	−0.55	−1.1
	532	2.8	2.8	4.4	3.9	3.3	2.7	2.2	1.7	1.7	1.1	1.1	0.55
	744	2.2	2.8	3.3	3.9	4.4	3.9	3.3	2.2	1.7	1.1	1.1	0.55

Table 21.18 Equivalent temperature difference for roofs of dark colour, sunlit and shaded roofs in °C at 40° N latitude – 1 July [*m* is mass density in kg/m^2]

Exposure	*m*	*Time*											
		6	7	8	9	10	11	12	1	2	3	4	5
		←			am	→		noon	←		pm		→
Exposed	53	–2.2	–3.3	–3.9	–2.8	−0.55	3.9	8.3	13.3	17.8	21.1	23.8	25.6
to sun	106	0	−0.55	–1.1	−0.55	1.1	5.0	8.9	12.8	16.7	20.0	22.8	23.9
	212	2.2	1.7	–1.1	1.7	3.3	5.5	8.9	12.8	15.6	18.3	21.1	22.2
	318	5.0	4.4	3.3	3.9	4.4	6.1	8.9	12.2	15.0	17.2	19.4	21.1
	524	7.2	6.7	6.1	6.1	6.7	7.2	8.9	12.2	14.4	15.6	17.8	19.4

(*Contd.*)

Table 21.18 Equivalent temperature difference for roofs of dark colour, sunlit and shaded roofs in °C at 40° N latitude – 1 July [*m* is mass density in kg/m^2] (contd.)

Exposure	*m*	*Time*											
		6	7	8	9	10	11	12	1	2	3	4	5
		← am →						noon	← pm →				
Covered	106	–2.8	–1.1	0	1.1	2.2	5.5	8.9	10.6	12.2	11.1	10.0	8.6
with water	212	–1.7	–1.1	–0.55	–0.55	0	2.8	5.6	7.2	8.3	8.3	8.9	8.3
	318	–0.55	–1.1	–1.1	–1.1	–1.1	–1.1	2.8	3.9	5.5	6.7	7.8	8.3
Sprayed	106	–2.2	–1.1	0.0	1.1	2.2	4.4	6.7	8.3	10.0	9.4	8.9	8.3
with water	212	–1.1	–1.1	–0.55	–0.55	0.0	1.1	2.8	5.0	7.2	7.8	7.8	7.8
	318	–0.55	–1.1	–1.1	–1.1	–1.1	0.0	1.1	2.8	4.4	5.5	6.7	7.2
Shaded	106	–2.8	–2.8	–2.2	–1.1	0.0	1.1	3.3	5.0	6.7	7.2	7.8	7.2
	212	–2.8	–2.8	–2.2	–1.7	–1.1	0.0	1.1	2.8	4.4	5.5	6.7	7.2
	318	–1.7	–1.7	–1.1	–1.1	–1.1	–0.55	0	1.1	2.2	3.3	4.4	5.0
Exposure	*m*	*Time*											
		6	7	8	9	10	11	12	1	2	3	4	5
		← pm →						mid night	← am →				
Exposed	53	25.0	22.8	19.4	15.6	12.2	8.9	5.5	3.9	1.7	0.55	–0.55	–1.7
to sun	106	23.9	22.2	19.4	16.7	13.9	11.1	8.3	6.7	4.4	3.3	2.2	1.1
	212	22.8	21.7	19.4	17.8	15.6	13.3	11.1	9.4	7.2	6.1	5.0	3.3
	318	21.7	21.1	20.0	18.9	17.2	15.6	13.9	12.2	10.0	8.9	7.2	6.1
	524	20.6	20.6	19.4	18.9	18.9	17.8	16.7	15.0	12.5	11.1	10.0	7.8
Covered	106	7.8	6.7	5.5	3.3	1.1	0.55	0.55	–0.55	–1.1	–1.7	–2.2	–2.8
with water	212	8.3	7.8	6.7	5.5	3.9	2.8	1.7	0.55	–0.55	–1.1	–1.7	–1.7
	318	8.9	8.3	7.8	6.7	5.6	4.4	3.3	2.2	1.7	1.1	0.55	0.0
Sprayed	106	7.8	6.7	5.6	3.3	1.1	0.55	0.0	–0.55	–1.1	–1.1	–1.7	–1.7
with water	212	7.8	7.2	6.7	5.0	3.9	2.2	1.7	0.55	0.0	0.0	–0.55	–0.55
	318	7.8	7.2	6.7	6.1	5.5	4.4	3.3	2.2	1.1	0.55	0.0	–0.55
Shaded	106	6.7	5.5	4.4	2.8	1.1	0.55	0.0	–0.55	–1.7	–2.2	–2.8	–2.8
	212	6.7	6.1	5.5	4.4	3.3	2.2	1.1	0.0	–0.55	–1.7	–2.2	–2.8
	318	5.5	5.5	5.5	5.0	4.4	3.3	2.2	1.1	0.55	0.0	–0.55	–1.1

1. Based on 35°C DBT outdoor design temperature and 26.7°C indoor design temperature (constant), and daily range of 11.1°C.
2. For other conditions, use the same corrections as given for walls.
3. For peaked roofs use the roof area projected on a horizontal plane.

Correction for latitude and other months with different solar radiation intensity

The values of Δt_E in Tables 21.17 and 21.18 are correct for east and west walls in any latitude during the hottest weather. The equivalent temperature difference for any wall or roof for any latitude and month is approximated as

$$\Delta t_E = (\Delta t_E)_{\text{shaded}} + \frac{R_s}{R_m}[(\Delta t_E)_{\text{sun}} - (\Delta t_E)_{\text{shaded}}] = \frac{R_s}{R_m}(\Delta t_E)_{\text{sun}} + \left(\frac{R_s}{R_m} - 1\right)(\Delta t_E)_{\text{shaded}} \tag{21.55}$$

where

R_s = maximum solar radiation intensity for the wall or horizontal roof found from the empirical equation for the month and latitude desired.

R_m = maximum solar heat gain factor (SHGF) for July and 40°N for the given orientation of wall or horizontal roof as given in Table 21.13.

$(\Delta t_E)_{\text{shaded}}$ = equivalent temperature difference for the same wall or roof in shade at the desired time of the day, corrected if necessary for design conditions

$(\Delta t_E)_{\text{sun}}$ = equivalent temperature difference for the same wall or roof exposed to sun at the desired time of the day, corrected if necessary for design conditions

Correction for light or medium colour

The absorptivity of dark colour is taken as 0.9. The absorptivities of medium and light colours are conventionaly taken as 0.7 and 0.5 respectively. Hence, for light colour the corrected equivalent temperature difference is

$$\Delta t_E = (\Delta t_E)_{\text{shaded}} + (0.5/0.9)[(\Delta t_E)_{\text{sun}} - (\Delta t_E)_{\text{shaded}}] = 0.55(\Delta t_E)_{\text{shaded}} + 0.45(\Delta t_E)_{\text{sun}} \tag{21.56}$$

For medium colour the corrected equivalent temperature difference is

$$\Delta t_E = (\Delta t_E)_{\text{shaded}} + (0.7/0.9)[(\Delta t_E)_{\text{sun}} - (\Delta t_E)_{\text{shaded}}] = 0.78(\Delta t_E)_{\text{shaded}} + 0.22(\Delta t_E)_{\text{sun}} \tag{21.57}$$

Light colours are white and cream, etc.
Medium colours are light green, light blue, gray, etc
Dark colours are dark blue, dark red, dark brown, etc.

Combined correction for latitude, month and colour

$$\Delta t_E = 0.55 \frac{R_s}{R_m} (\Delta t_E)_{\text{sun}} + \left(1.0 - 0.55 \frac{R_s}{R_m}\right) (\Delta t_E)_{\text{shaded}} \tag{21.58}$$

$$\Delta t_E = 0.78 \frac{R_s}{R_m} (\Delta t_E)_{\text{sun}} + \left(1.0 - 0.78 \frac{R_s}{R_m}\right) (\Delta t_E)_{\text{shaded}} \tag{21.59}$$

EXAMPLE 21.8 The walls are made of 22.5 cm common brick and 1.25 cm plaster on both the sides and the roof is 15 cm concrete and 1.25 cm plaster on inside with and without 50 mm expanded polystyrene insulation. The location is Delhi with outdoor design temperature of 43.3°C and Daily Range of 13.89°C. The indoor temperature is 25°C. Determine the equivalent temperature differences from 2:00 pm to 6:00 pm solar time. The outdoor wind velocity is 25 kmph.

Solution:

The properties of common brick and plaster from Table 21.2(a) are:

$\rho_{\text{brick}} = 1600$ kg/m^3, $k_{\text{brick}} = 0.77$ W/m-K, $\rho_{\text{plaster}} = 1885$ kg/m^3,
$k_{\text{plaster}} = 0.865$ W/m-K, $\rho_{\text{concrete}} = 1920$ and $k_{\text{concrete}} = 1.73$ W/m-K
and $k_{\text{ep}} = 0.037$ W/m-K, $\rho_{\text{ep}} = 30$ kg/m^3

From Table 21.1: $h_i = 8.29$ W/m^2-K and $h_o = 34$ W/m^2-K

For walls:

$$\frac{1}{U} = \left(\frac{1}{8.29}\right) + \left(\frac{0.0125}{0.865}\right) + \left(\frac{0.225}{0.77}\right) + \left(\frac{0.0125}{0.865}\right) + \left(\frac{1}{34}\right) = 0.47115$$

$\therefore$ $U = 2.122$ W/ m^2-K

$m = 1600(0.225) + 1885(0.0125 \times 2) = 407.125$ kg/m^2

For roof without insulation:

$$\frac{1}{U} = \left(\frac{1}{8.29}\right) + \left(\frac{0.15}{1.37}\right) + \left(\frac{0.0125}{0.865}\right) + \left(\frac{1}{34}\right) = 0.2512$$

$\therefore$ $U = 3.981$ W/m^2-K

$m = 1920(0.15) + 1885(0.0125) = 311.56$ kg/m^2

For roof with insulation:

$$\frac{1}{U} = \left(\frac{1}{8.29}\right) + \left(\frac{0.05}{0.037}\right) + \left(\frac{0.15}{1.37}\right) + \left(\frac{0.0125}{0.865}\right) + \left(\frac{1}{34}\right) = 1.6025$$

$\therefore$ $U = 0.624$ W/m^2-K

$m = 1920(0.15) + 1885(0.0125) + 30(0.05) = 313.06$ kg/m^2

$t_o - t_i = 43.3 - 25 = 18.3^oC$

$\therefore$ Δt_E correction $= 18.3 - 8.33 = 9.97^oC$

$DR = 13.89^oC$: Medium construction:

$\therefore$ DR correction $= 0.25(13.89 - 11.1) = 0.695^oC$

Total correction to $\Delta t_E = 9.97 - 0.695 = 9.275^oC$

The wall mass is 407.125 kg/m^2 whereas the tabulated values are for $m = 319$ and $m = 532$. Therefore, linear interpolation is done to find the values for $m = 407.125$. This gives us:

South wall:

Solar time	Δt_E at $m = 319$	Δt_E at $m = 532$	*Interpolated* Δt_E *at* $m = 407.125$	*Corrected* Δt_E	Q (W/m^2) $U \times (\Delta t_E)_{corr}$
2:00 pm	13.3	6.7	10.569	19.844	42.11
3:00 pm	13.9	8.3	11.583	20.858	44.26
4:00 pm	14.4	8.9	12.124	21.399	45.41
5:00 pm	12.8	10.0	11.641	20.916	44.38
6:00 pm	11.1	10.0	10.641	19.915	42.26
7:00 pm	8.3	8.3	8.3	17.575	37.29
8:00 pm	6.7	7.8	7.153	16.43	34.86

The maximum heat gain for the south wall occurs at 4: 00 pm.

For other walls the corrected Δt_E and the heat transfer rates are as follows:

Solar time	*East wall*		*West wall*		*North wall*	
	Corrected Δt_E	Q (W/m^2) $U \times (\Delta t_E)_{corr}$	*Corrected* Δt_E	Q (W/m^2) $U \times (\Delta t_E)_{corr}$	*Corrected* Δt_E	Q (W/m^2) $U \times (\Delta t_E)_{corr}$
2:00 pm	19.35	41.06	14.139	30.39	11.665	24.75
3:00 pm	18.088	38.38	17.765	37.7	12.558	26.65
4:00 pm	17.633	37.42	20.489	43.48	13.41	28.46
5:00 pm	17.178	36.45	24.244	51.45	14.01	29.73
6:00 pm	16.723	35.49	26.882	57.04	14.361	30.47
7:00 pm	16.723	35.49	28.393	60.25	14.361	30.47
8:00 pm	16.43	34.86	27.454	58.26	15.023	31.88

For east wall the maximum heat gain occurs at 2:00 pm solar time, while for the west wall it occurs at 7:00 pm solar time, and for north wall the maximum occurs at 8:00 pm solar time.

For roof:

Solar time	Δt_E *at* $m = 212$	Δt_E *at* $m = 318$	*Interpolated* Δt_E *at* $m = 311.56$	*Corrected* Δt_E	Q (W/m^2) $U \times (\Delta t_E)_{corr}$	
					$m = 311.56$	$m = 313.06$
2:00 pm	15.6	15.0	15.042	24.317	96.81	15.17
3:00 pm	18.3	17.2	17.276	26.55	105.7	16.57
4:00 pm	21.1	19.4	19.518	28.793	114.62	17.97
5:00 pm	22.2	21.2	21.27	30.545	121.6	19.06
6:00 pm	22.8	21.7	21.776	31.051	123.61	19.38
7:00 pm	21.7	21.1	21.141	30.416	121.07	18.98
8:00 pm	19.4	20.0	19.958	29.233	116.38	18.24

It is observed that maximum heat gain for the roof occurs at 6:00 pm.

An underdeck insulation of 50 mm reduces the heat gain from the roof by 84%. Hence, it is recommended that 50 mm of EP insulation should be used for all roofs exposed to solar radiation.

21.8 *Z*-TRANSFORM METHODS

The *Z*-transform methods are more accurate than the other two methods described above. For this reason, the *Z*-transform methods are frequently used for both the design load calculations and building energy analysis. There are two formulations of these methods, which are based upon

(a) either response factors

(b) or conduction transfer functions.

The heat transfer rate at any instant of time at a wall node is represented by the sum of three series in time. The first series uses the interior temperatures at node *j* at present and past times. The coefficients of this series are called *response factors*. The second series uses the exterior temperatures at node *j* at present and past times. The coefficients of this series are also called response factors. The third series uses the heat flux at node *j* at present and previous times. The coefficients of this series are also called response factors.

The exterior and interior temperatures may be air temperatures, sol-air temperatures, or surface temperatures depending upon the application.

The conduction transfer functions replace the temperature history with heat flux history.

The application of transfer functions is relatively easy, however, their determination is rather a difficult task. The analytical procedure for their determination by a number of methods is given in Spitler (1996).

The heat flux at the *j*th exterior surface for time θ is given by

$$q_{out,j,\theta} = -Y_o t_{is,j,\theta} - \sum_{n=1}^{N_y} Y_n t_{is,j,\theta-\delta\theta} + X_o t_{os,j,\theta} - \sum_{n=1}^{N_x} X_n t_{os,j,\theta-\delta\theta} + \sum_{n=1}^{N_q} \varphi_n q_{out,j,\theta-\delta\theta} \qquad (21.60)$$

The coefficients Y_o, Y_1. Y_2 and Y_3, etc. are multiplied by interior surface temperatures at times θ, $\theta-1$, $\theta-2$, $\theta-3$ hours, etc. Similarly X_0, X_1, X_2 and X_3 are multiplied by exterior temperatures at times θ, $\theta-1$, $\theta-2$, $\theta-3$ hours, etc. φ_1, φ_2 and φ_3 etc. are multiplied with heat flux at times θ, $\theta-1$, $\theta-2$, $\theta-3$ hours, etc.

$$q_{in,j,\theta} = -Z_o t_{is,j,\theta} - \sum_{n=1}^{N_y} Z_n t_{is,j,\theta-\delta\theta} + Y_o t_{os,j,\theta} - \sum_{n=1}^{N_x} Y_n t_{os,j,\theta-\delta\theta} + \sum_{n=1}^{N_q} \varphi_n q_{in,j,\theta-\delta\theta} \qquad (21.61)$$

where

subscript *os* : outer surface

subscript *is* : inner surface

$q_{out,j,\theta}$: heat flux at exterior surface

$q_{in,j,\theta}$: heat flux at interior surface

Y_n : cross CTF coefficient, that is this relates q_{out} with t_{is} and q_{in} with $t_{os.}$

X_n : exterior CTF coefficients, relates to exterior temperatures at past times

Z_n : interior CTF coefficients, relates to interior temperatures at past times

f_n : CTF coefficients, relates to heat flux at past times.

When the calculation of heat flux is started the temperatures and heat flux at past times are not known. Hence, some values are assumed to start the calculations and then iterations follow until the values do not change for the first day. Then one marches on to the second day. The initial values of heat flux multiplying φ_1, φ_2 and φ_3, etc. are taken to be zero. In the calculation of the value for the second hour, φ_1 is taken as the value of flux calculated at first time θ.

21.9 INFILTRATION

Infiltration should not be confused with the fresh air requirement of a space, which is required for the ventilation of the occupants and for dilution of odours. Infiltration is the uncontrolled leakage of outdoor air through the cracks and crevices in the building, around the doors and windows, light fittings, joints between walls and floor, through the building material itself and through door openings. Infiltration is always associated with an equal amount of exfiltration to maintain mass conservation of air. The buildings are designed and constructed to limit infiltration, as much as possible, to minimize the energy use. This is done by sealing the building envelope where possible, using vestibules and revolving doors, or maintaining a pressure within. Infiltration is principally due to

(i) Wind pressure
(ii) Stack effect
(iii) Door openings due to people leaving and coming into the building.

The indoor–outdoor temperature difference also affects infiltration. The estimation of infiltration for a building is often the most uncertain part of cooling/heating load calculation. There are three prevalent methods for estimating infiltration, namely (i) the air-change method, (ii) the crack length method using tables and (iii) the recent ASHRAE method of estimating the pressure drop due to wind and stack followed by evaluation of infiltration using the experimental data given in plots.

21.9.1 Air-Change Method

This method is not recommended for use by students and novices in the field of air conditioning. Experience and judgment are required to obtain satisfactory results. Experienced engineers assess the building type, construction and usage and based upon their experience assume certain air changes per hour for the building. The usual range is from 0.5 air changes per hour (rather low) to 2 ACH (really high), one ACH being the thumb rule for most buildings. But some engineers assume zero air change as well. This approach usually gives a conservative estimate of the design load.

One air change means that the total volume of the air in the room will be replaced by fresh air in one hour. If V m^3 is the volume of the room, then one ACH implies an infiltration rate of V m^3 per hour. In general infiltration in m^3/s is given by

$$Q_v = \frac{(\text{ACH})(V)}{3600} \text{ m}^3/\text{s} \tag{21.62a}$$

Table 21.19(a) gives the recommended air changes for residences and Table 21.19(b) gives that for cold storages.

Cobientz and Achenbach (1963) have given an empirical equation for determining the air changes. This is as follows:

$$\text{Number of air changes} = a + bV + c(t_o - t_i) \tag{21.62b}$$

where V is the velocity in m/s, and the constants a, b and c are given in Table 21.19(c).

Table 21.19(a) Recommended air changes for residences

Kind of room	*Number of air changes/hour*
Rooms with no windows or exterior doors	0.5
Rooms with windows or exterior doors on one side	1.0
Rooms with windows or exterior doors on two sides	1.5
Rooms with windows or exterior doors on three sides	2.0
Entrance halls	2.0

Table 21.19(b) Recommended air changes for cold storages

Storage room capacity, m^3	10	20	50	100	200	400	600	1000	1500	2000	3000
Air changes per day	32	21.5	13	8.8	6	4.1	3.4	2.5	2.0	1.7	1.4

Table 21.19(c) Infiltration constants for Eq. (21.62b)

Quality of construction	*A*	*b*	*c*
Tight	0.15	0.010	0.007
Average	0.20	0.015	0.014
Loose	0.25	0.020	0.022

21.9.2 Crack Length Method

Fluid flow through crevices, cracks and openings requires a driving force, which may be the inertia (wind velocity), pressure difference or temperature difference. All these driving forces are present in air-conditioned buildings. Wind striking a surface comes to stagnation, and the wind pressure increases. The temperature difference gives rise to density difference between the inside and the outside (chimney effect) resulting in pressure difference. In summer, we can imagine a column of cold heavy air inside the building and a column of warm light air outside the building. The inside pressure will be more at the bottom, giving rise to exfiltration. In winter, the situation is opposite to this. This is a simple situation; but the openings like windows and doors at various floors, and service shafts, staircases and elevators complicate the picture.

In general the pressure difference occurs due to three effects, i.e.

$$\Delta p = \Delta p_w + \Delta p_{st} + \Delta p_p \tag{21.63}$$

where, Δp_w is due to wind velocity, Δp_{st} is due to stack effect and Δp_p is due to pressurization of the building. The buildings are sometimes pressurized to reduce the infiltration. The inside pressure being more, some indoor air leaks out through the cracks.

The pressurization is done by introducing more make-up or fresh air than the quantity of air exhausted. This has to be properly controlled, otherwise the openings on each floor can depressurize the building, that is, the designer has to find a value of Δp_p that can actually be achieved in the system after accounting for leakage through the openings.

Pressure drop and infiltration due to wind

The rate of inflow (or outflow) into a building depends upon the pressure drop (arising due to the above mentioned forces) across the boundary surface and upon the resistance to flow through cracks, crevices and other openings. It also depends upon the crack area, type of crack and crack passage. In residences and low-height commercial buildings, the infiltration is mainly due to wind velocity. The velocity pressure or velocity head for velocity V may be expressed as $\rho(V^2/2)$ Pa. Taking the standard air density of 1.2 kg/m^3 and 1 mm of water = 9.81 Pa, the velocity pressure is expressed as

$$p_V = (1.2/2)V^2/(9.81) = 0.0612V^2 \text{ mm of water} \quad : V \text{ in m/s} \tag{21.64a}$$

$$p_V = 0.00472V^2 \text{ mm of water} \quad : V \text{ in km/h} \tag{21.64b}$$

The wind pressure causes a small amount of leakage of air even through brick and concrete. For a 25-cm plastered brick wall at 24 km/h wind velocity, the infiltration through the wall has been found to be equal to 0.000356 cmm/m^2 of wall area.

The wind velocity causes an increase in pressure inside the building as well, hence the pressure difference across the windward side wall will be at the most 64% of the above value, that is, $0.64p_V$. Another argument given is that all the kinetic energy is not converted into pressure head. If V_i is the initial velocity and V_f the final velocity after passage through, say a crack, then from Bernoulli's equation, we have

$$\Delta p = \frac{\rho(V_i^2 - V_f^2)}{2}$$

The final velocity V_f is not known and is not easily predictable. Hence, to predict the pressure drop we define a pressure coefficient C_p as follows:

$$\Delta p_V = \frac{C_p \rho V_i^2}{2} \text{ Pa} \tag{21.65}$$

The infiltration rate due to pressure difference caused by wind velocity is expressed as

$$Q_V = AC\,(\Delta p_V)^n \tag{21.66}$$

where, C is a flow coefficient, A is the area of the crack and $0.4 < n < 1$.

For non-weather stripped windows, an empirical expression for Q_V is

$$Q_V = 0.125\,(\Delta p)^{0.63} \text{ litre/s per metre of crack length} \tag{21.67}$$

where Δp is in pascal.

In general, the determination of flow coefficient and power n in Eq. (21.66) requires experimental data. The pressure rise is positive if $V_i > V_f$. The pressure coefficient may be positive or negative. *ASHRAE Cooling and Heating Load Calculation Mannual*, 2nd ed., 1992 gives data for the values of C_p for low-rise and high-rise buildings as reproduced here in Figure 21.10 and Figure 21.11 respectively. The pressure coefficient is positive for infiltration and negative for exfiltration. There is a low-pressure region called *wake* on the leeward side of a building. As seen in the figures, the pressure is positive on the windward side, and changes to negative values on the

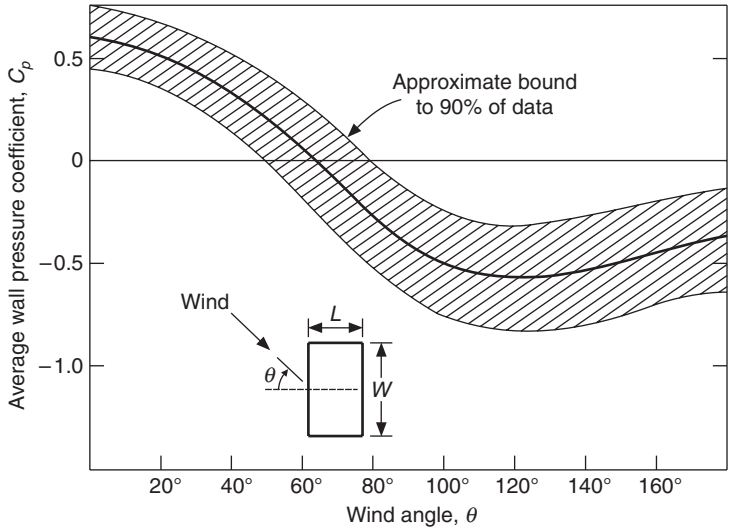

Figure 21.10 Variation of wall averaged pressure coefficients for a low-rise building.

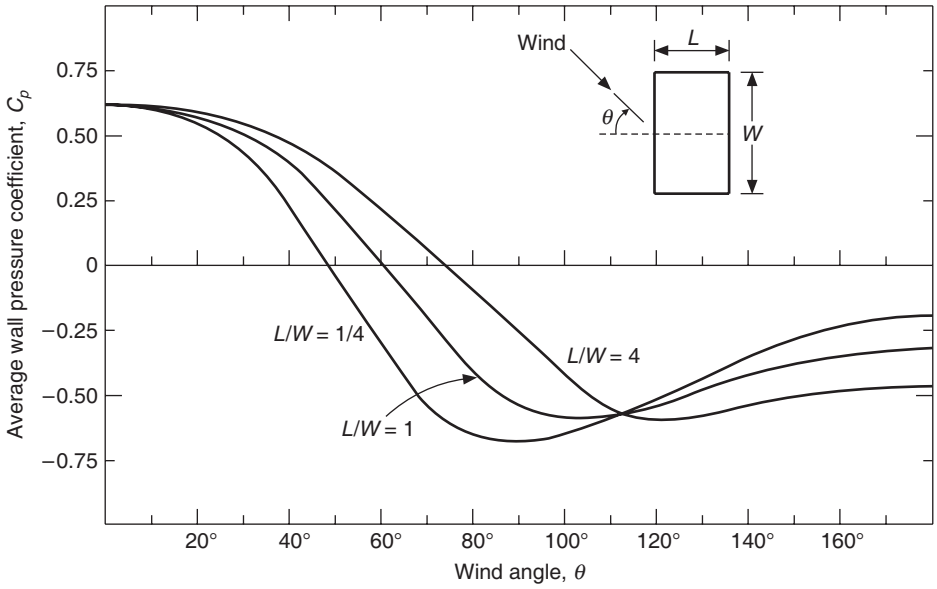

Figure 21.11 Wall averaged pressure coefficients for a high-rise building.

leeward side. If the wind strikes a wall normal to the surface, the pressure rises and the value of C_p is largest (around 0.64). If it strikes at an angle, then the value of C_p decreases. A building is called high-rise building if its height is three times the crosswind width.

EXAMPLE 21.8 A twelve-storey building is 36 m high and say 36 m wide normal to the wind and 24 m across the wind. Find the pressure rise on all its sides from Figure 21.11 if a wind of 24 km/h blows normal to the long dimension.

Solution: It can be observed from Figure 21.11 that,

$C_p = 0.6$ on windward side

$C_p = -0.3$ on leeward side

$C_p = -0.6$ on sides of the building (90° to the wind)

Using Eqs. (21.64b) and (21.65), we get

Windward side: $\Delta p_V = C_p \rho V_i^2/2 = 0.6(0.00472)(24)^2 = 1.63$ mm of water

Leeward side : $\Delta p_V = -0.3(0.00472)(24)^2 = -0.816$ mm of water

Sides of the building : $\Delta p_V = -0.6(0.00472)(24)^2 = -1.63$ mm of water

Once the pressure drop is known, the coefficient K is determined from Tables 21.20, 21.21 or 21.22 for the window, door or curtain wall respectively and the infiltration is determined from Figures 21.12, 21.13 and 21.14 respectively. Figures 21.12 and 22.13 give the infiltration depending upon the values of K, per meter length of the crack, which is usually the perimeter of the window or door. Figure 21.14 gives infiltration for one room or one floor.

The use of storm sashes and storm door is very common, and it reduces the infiltration by about 35%.

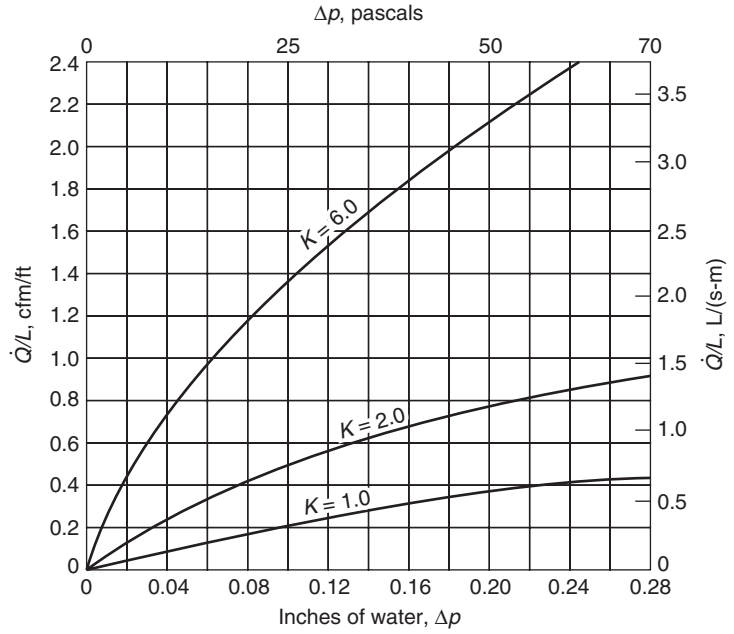

Figure 21.12 Window and door infiltration characteristics.

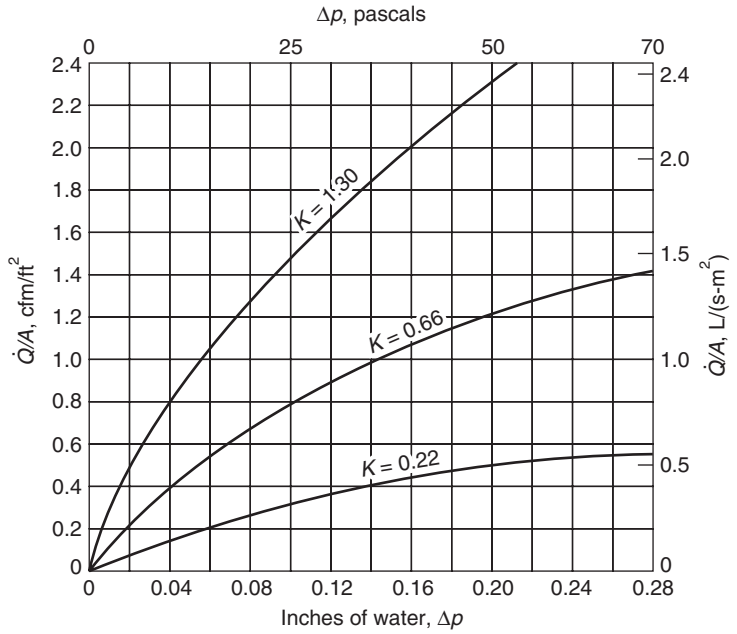

Figure 21.13 Curtain wall infiltration for one room or one floor.

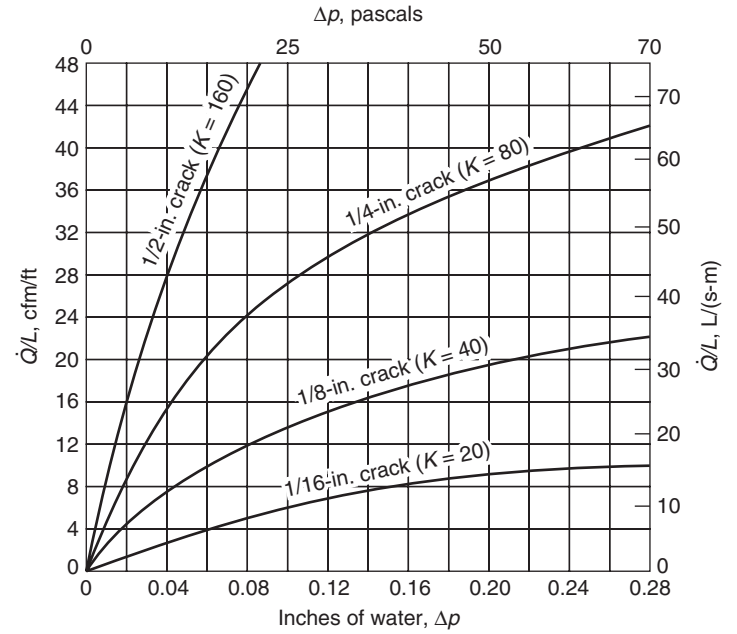

Figure 21.14 Infiltration through cracks around a closed swinging door.

Table 21.20 Window classification for Figure 21.12

	Wood double–hung (locked)	*Other types*
Tight fitting window $K = 1.0$	Weather stripped, average gap (0.4 mm, 1/64″ crack)	Wood casement and awning windows, weather stripped metal casement windows; weather stripped
Average fitting window $K = 2.0$	Non-weather stripped, average gap (0.4 mm, 1/64″ crack)	All types of vertical and horizontal sliding windows, weather-stripped. If gap is average (0.4 mm) this could be tight fitting
	Or	
	Weather stripped large gap (2.38 mm, 3/32″)	Metal casement windows, non-weather stripped. Note if the gap is large (2.38 mm) this could be a loose fitting
Loose-fitting window $K = 6.0$	Non-weather stripped. Large gap (2.38 mm, 3/32″)	Vertical and horizontal sliding windows, non-weather stripped.

Table 21.21 Door classification for Figure 21.12

Tight-fitting door, $K = 1.0$	Very small perimeter gap and perfect fit, weather stripping—often characteristic of new doors
Average–fitting door, $K = 2.0$	Small perimeter gap having stop trim fitting properly around door and weather stripped
Loose-fitting door, $K = 6.0$	Larger perimeter gap having poorly fitting stop trim and weather-stripped or small perimeter gap with no weather stripping

Table 21.22 Curtain wall classification for Figure 21.13

Leakage coefficient	*Description*	*Curtain wall construction*
$K = 0.22$	Tight-fitting wall	Constructed under close supervision of workmanship on wall joints. When joint seals appear inadequate, they must be redone.
$K = 0.66$	Average-fitting wall	Conventional construction procedure followed
$K = 1.30$	Loose-fitting wall	Poor construction quality control or an older building having separated wall joints.

Pressure drop and infiltration due to stack effect

The stack effect is important in tall buildings. During winter days, the outdoor temperature is lower and thereby the density is higher. Considering a column of air outdoors, the pressure near the ground will be higher than that inside the building. Inside the air-conditioned building, the temperature is higher, density is less and hence the pressure is less at the bottom. Hence at the ground level, infiltration occurs from a higher outdoor pressure to a lower indoor pressure. Buoyancy of the warm indoor air leads to upward flow, resulting in a higher inside pressure at the top of the building leading to exfiltration there. During summer, the outdoor air is warmer, the temperature near the ground is maximum, density is the lowest and the pressure is the lowest. The indoor temperature being uniform and less, the pressure is more than the outdoor pressure, leading to exfiltration at the bottom. The situation reverses towards the top of the building where the indoor pressure is less than the outside pressure, leading to infiltration.

It is observed that both during winter and summer, the pressure variation is such that at some floor (height) the outdoor pressure is equal to the indoor pressure. This is called the *neutral level*. Theoretically, the neutral level will be at the mid-height of the building, if the cracks and other openings are uniformly distributed in all the floors in the vertical direction. Usually, larger openings occur in the lower part of the building due to doors. Theoretical pressure difference with no internal separations is given by

$$\Delta p_{st} = gh(\rho_o - \rho_i) = \frac{p_o gh}{R_a}\left(\frac{1}{T_o} - \frac{1}{T_i}\right) \tag{21.68}$$

where, R_a is the gas constant for air (= 287.3 J/kg-K), T_o and T_i are outdoor and indoor temperatures in K, p_o = 101325 Pa and g = 9.81 m/s^2. The height h is measured from the neutral point.

There is resistance to vertical airflow in a building depending upon the passage through the staircases and elevator. Assuming the resistance to be the same on all the floors, the pressure drop given by Eq. (21.68) may be corrected by a single coefficient for all the floors. This coefficient is called the *draft coefficient*, C_d, which relates the actual pressure drop Δp_s to the theoretical pressure drop Δp_{st}, i.e.

$$C_d = \frac{\Delta p_s}{\Delta p_{st}} \tag{21.69}$$

The draft coefficient depends upon the tightness of the doors in elevators and stairwells. Its value ranges from 1.0 for buildings with no doors in the stairwells to 0.65–0.85 for most modern buildings. The pressure drop due to stack effect is added to that due to wind, and infiltration is determined from Figures 21.12 to 21.14.

An older expression recommended by ASHRAE for infiltration due to stack effect is

$$Q_V = 0.172A\sqrt{h(t_i - t_o)} \ \text{m}^3/\text{s} \tag{21.70}$$

where, A is the area available for flow from a floor. This gives velocity $V = Q_V/A$ and

$$\Delta p_{st} = \frac{pV^2/2}{C_p} = \frac{(1.2/2)(0.172)^2[h(t_i - t_o)]}{0.64} = 0.028h(t_i - t_o)\ \text{Pa} \tag{21.71}$$

The stack effect is small for low-rise buildings and wall infiltration is low, therefore only the infiltration due to wind effect need be considered. It is possible to predict that one side of the building will experience infiltration and the other side will experience exfiltration. However, the buildings do not have the same length of cracks on all the sides so that infiltration and exfiltration cancel out. There may be some obscure cracks. To account for these, it is recommended that for low-rise buildings, infiltration from all the sides be considered with normal (windward side) wind pressure and the air may be assumed to leave from the roof.

The stack effect is dominant in high-rise buildings. All pressure effects as well as leakage through windows; doors and walls must be considered. The pressure coefficient approach is used for high-rise buildings, since stack pressure causes exfiltration at lower levels and infiltration at higher than the neutral level during summer.

21.9.3 Infiltration Due to Door Openings

Figures 21.15 and 21.16 give the infiltration rate into air-conditioned space based upon the data available from *ASHRAE Cooling and Heating Load Calculation Manual*, 2nd ed., 1992 due to door openings for swinging doors. The infiltration rate is given in Figure 21.15 in terms of pressure difference and a traffic coefficient *C*. Figure 21.16 gives the traffic coefficient that depends upon the traffic rate (people per hour per door) and the door arrangement. Two types of doors have been considered. The single-bank door type opens directly into the air-conditioned space. The vestibule-type door consists of two doors in an enclosed space at the entrance to the air-conditioned space. These are two doors in series so as to form an air lock between them.

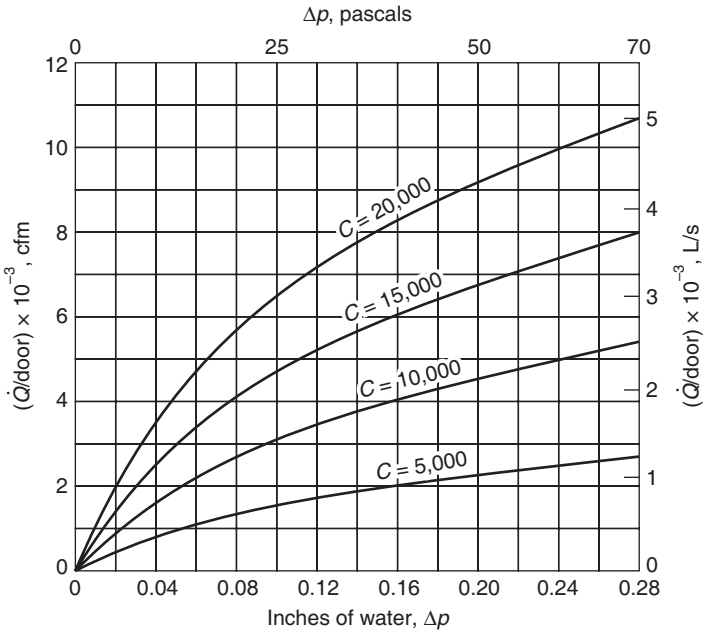

Figure 21.15 Swinging-door infiltration characteristics with traffic.

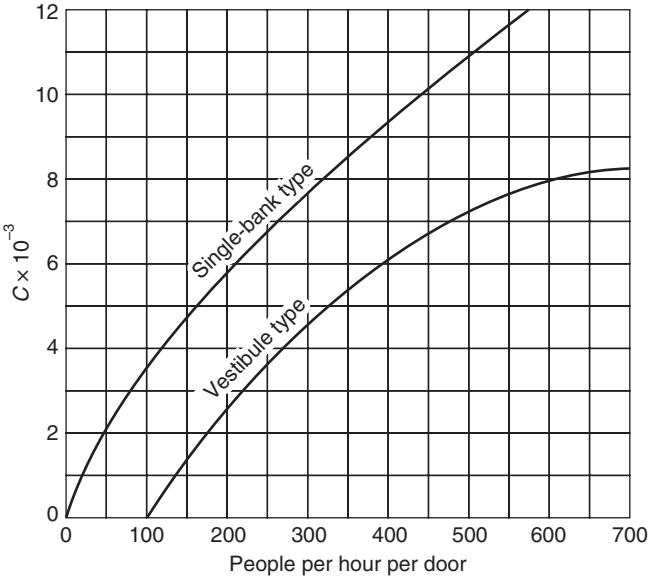

Figure 21.16 Flow coefficient dependence on traffic rate.

EXAMPLE 21.9 If the outdoor and indoor temperatures are 40°C and 25°C respectively, find the pressure drop due to wind pressure and stack effect on the first (ground) and twelfth floor in Example 21.8.

Solution:

The pressure difference due to wind has been found in Example 21.8. There are more openings (doors) in the lower part of the building; hence it is assumed that the neutral pressure level occurs at the fifth floor instead of the middle sixth floor.

For first floor the height h is 15 m. In Eq. (21.69) assuming $C_d = 0.8$,

$$\Delta p_{st} = \frac{0.8(101325)(15)9.81}{287.3}\left(\frac{1}{313} - \frac{1}{298}\right) = -6.677 \text{ Pa} = -\frac{6.677}{9.81} = -0.681 \text{ mm of water}$$

Equation (21.71) gives $\Delta p_{st} = 0.028(15)(-15) = -6.3$ Pa, which is quite close to the result of Eq. (21.67). The negative sign indicates that during summer months there is exfiltration near the ground floor. Also, if t_o is taken as 35°C then it reduces to – 0.461 mm of water.

For twelfth floor, height h is 21 m, therefore $\Delta p_{st} = -0.681(21/15) = 0.9534$ mm of water.

In this case, the sign has been taken to be positive since during summer infiltration occurs at floors above the neutral level.

Adding the pressures due to wind (Example 21.8) and stack effect, we get the total Δp as

Orientation	1st *floor*	12th *floor*
Windward	0.949	2.5834
Leeward	–1.497	0.1374
Sides of bldg.	–2.311	–0.6766

This table indicates that air will infiltrate into the building on all the floors on the windward side. There will be exfiltration on the sides of the building on all the floors. On the leeward side, there will be exfiltration up to tenth floor and infiltration on eleventh and twelfth floors.

EXAMPLE 21.10 Assuming conventional curtain wall construction and 36 m of window crack length on each side with average gap and average fitting, estimate the leakage from twelfth floor neglecting leakage from the roof. The building is 36 m in windward direction and has 24 m sides

Solution:

From Table 21.20 the K-factor for the window is $K = 2.0$. From Figure 21.11, for Δp of 2.5834 mm, 0.1374 mm and – 0.6766 mm the infiltration is 0.77, 0.075 and –0.23 L/s per m crack length. Total crack length = 36 m.

From Table 21.21 the K-factor for the wall is, $K = 0.66$. From Figure 21.13, for Δp of 2.5834 mm, 0.1374 mm and – 0.6766 mm the infiltration is 0.81, 0.05 and – 0.45 L/s per m^2. The wall area on windward side is $36 \times 3 = 108$ m^2 and 72 m^2 on the sides.

On windward side:

Infiltration from windows: $0.77 \times 36 = 27.72$ L/s

Infiltration from walls : $0.81 \times 108 = 87.48$ L/s

Total Infiltration = 115.2 L/s

On leeward side:

Infiltration from windows: $0.075 \times 36 = 2.7$ L/s

Infiltration from walls : $0.05 \times 108 = 5.4$ L/s

Total Infiltration = 8 L/s

On side walls:

Infiltration from windows: $2(-0.23 \times 36) = -16.56$ L/s

Infiltration from walls : $2(-0.45 \times 72) = -64.8$ L/s

Total Infiltrations = –81.36 L/s

Net infiltration = 115.2 + 8.1 – 81.36 = 41.94 L/s

EXAMPLE 21.11 A single story building is oriented so that one of its walls faces 24 km/h wind. There are six double-hung windows 1.5 m wide and 1.0 m high on windward and leeward side each and five similar windows on both the side walls. There is one double swinging door on all the sides of 2.0 m height and 1.8 m width. All windows and doors are of average-fitting type.

Solution:

The stack effect is negligible for single-storey building and most of the infiltration is through cracks.

It is observed from Figure 21.14 that, $C_p = 0.6$ on windward side, Δp_V is calculated from Eqs. (21.64b) and (21.65).

Windward side: $\Delta p_V = C_p\, \rho V_i^2/2 = 0.6(0.00472)(24)^2 = 1.63$ mm of water

From Tables 21.20 and 21.21 the K-factor for the doors and windows is read as $K = 2.0$.

From Figure 21.14, the leakage per m crack length is 0.54 L/s per m of crack length

Crack length for each double-hung window is 3 × (height) + 2 × (width) = 7.5 m

Total crack length for six windows = 45 m

Crack length for door = 3 × 2 + 2 × 1.8 = 9.6 m

Therefore, total crack length for windward and leeward side = 2 × (45 + 9.6) = 109.2 m

The crack length on the side walls = 2 × (37.5 + 9.6) = 94.2 m

It has been observed that pressure is negative on leeward side and on side walls, hence there is a possibility that air will enter from the windward side and leave from the other sides. However, it has been suggested that infiltration should be assumed to occur inwards from all the walls and air might leave from the roof in a single-storey building.

Therefore, total crack length = 109.2 + 94.2 = 203.4 m

Total infiltration for the space = 203.4 × 0.54 L/s = 109.8 L/s

EXAMPLE 21.12 Estimate the infiltration from a double swinging door of 2.0 m height and 1.8 m width located on the first (ground) floor on the windward side of the 12-storey building of Example 21.9. The door has 3.2 mm cracks and the traffic rate is 350 persons per hour.

Solution:

The total pressure drop due to wind and stack effects is 0.949 mm of water.

Crack length = 9.6 m

From Figure 21.12, Q_v at 0.949 mm pressure drop and $K = 40$ (3.2 mm cracks) is 10.8 L/s per m of crack length.

Infiltration = 10.6 × 9.6 = 103.88 L/s

Vestibule-type of door will reduce the infiltration by 30%.

Infiltration for vestibule type of door = 0.7 × 103.88 = 72.716 L/s

From Figure 21.16 for vestibule-type of door, traffic coefficient for 350 persons = 5000.

From Figure 21.15 at pressure drop of 0.949 mm of water and traffic coefficient 5000, the infiltration = 360 L/s = 21.24 cmm.

21.9.4 Empirical Procedure Recommended By Carrier Handbook

Carrier Handbook has given extensive set of tables for evaluation of infiltration in m^3/h per metre crack length through double-hung windows at various velocities or pressure drops. This data is presented in Table 21.23. Table 21.24 from the same source gives the infiltration through various doors in cmm per metre crack length for various wind velocities. Tables 21.25 and 21.26 give infiltration through swinging doors on adjacent walls and opposite walls respectively.

Table 21.27 gives the infiltration through 1.82 m revolving door and 0.9 m swinging doors due to traffic under various service conditions.

Table 21.23 Infiltration through windows (cubic metre per hour per metre of crack length)

Type of window or door	*Wind velocity*				
km/h	8	16	24	32	40
m/s	2.2	4.4	6.77	8.9	11.1
Wooden double-hung windows					
1. Non-weather stripped (average fit)	0.7	2.0	3.6	5.5	7.4
2. Weather stripped (average fit)	0.4	1.2	2.2	3.3	4.6
3. Non-weather stripped (poor fit)	2.5	6.4	10.3	14.3	18.4
4. Weather stripped (poor fit)	0.6	1.8	3.2	4.7	6.6
5. Masonry wall not caulked around window frame	3.3	0.7	1.3	1.9	2.5
6. Masonry wall caulked around window frame	0.1	0.2	0.3	0.4	0.5
7. Wooden frame structure around window frame	0.2	0.6	1.0	1.6	2.1
Residential casement window					
1. 0.4 mm crack	0.6	1.7	3.1	4.3	5.6
2. 0.8 mm crack	1.3	3.0	4.8	7.1	11.7

Table 21.24 Infiltration through doors (cubic metre per minute per metre of crack length)

Type of door	*cmm per m of crack length*					
	Wind velocity (kmph)					
	8	16	24	32	40	48
Glass door						
Good installation (3.2 mm crack)	0.3	0.6	0.9	1.21	1.49	1.77
Average installation (4.26 mm crack)	0.45	0.93	1.3	1.86	2.23	2.7
Poor installation (6.4 mm crack)	0.6	1.21	1.77	2.42	2.42	3.53
Ordinary wood or metal door						
Well fitted, weather-stripped	0.04	0.06	0.08	0.12	0.16	0.2
Well fitted, non-weather stripped	0.08	0.11	0.17	0.24	0.31	0.39
Poorly fitted, non-weather stripped	0.08	0.21	0.34	0.48	0.61	0.78
Factory door (3.2 mm crack)	0.3	0.6	0.9	1.21	1.49	1.77

Table 21.25 Infiltration through doors on adjacent walls

Type of door	cmm per m^2 area		cmm *Standing open*	
	No use	*Average use*	*Vestibule*	*No vestibule*
Revolving door				
Normal operation	0.24	1.58	–	–
Panels open	–	–	34	25
Glass door 4.75 mm crack	1.37	3.0	20	14
Wood door	0.3	1.98	20	14
Small factory door	0.23	1.98		
Garage and shipping room door	0.61	1.37		
Ramp garage door	0.61	2.06		

For wind velocity of 12 km/h

Table 21.26 Infiltration through doors on opposite walls

% of time the second door is open	*cmm per pair of doors % of time the first door is open*				
	10	25	50	75	100
10	2.8	7	14	21	28
25	7.1	18	35	53	71
50	14	35	71	106	142
75	21	53	106	159	210
100	28	71	142	210	180

For wind velocity of 12 km/h

Table 21.27 Infiltration through door opening (Infiltration in m^3 per hour per person per opening)

Application	1.82 m *revolving door*	0.91 m *swinging door*	
		No vestibule	*Vestibule*
Bank	11.0	13.62	10.2
Barber shop	6.78	8.52	6.48
Soda shop	9.36	11.88	9.0
Cigar store	34.0	51.0	38.2
Departmental store (small)	11.0	13.62	10.2
Dress shop	3.42	4.26	3.0
Drug store	9.36	11.88	9.0
Restaurant	3.4	4.26	3.0
Hospital room	4.2	5.9	3.822
Lunch room	6.8	8.52	4.2
Men's room	4.56	6.3	3.24
Shoe store	4.56	6.0	4.44

For doors on windward side with wind velocity of 12 kmph.
For other wind velocities multiply by velocity ratio.
For other doors multiply by 0.6 .Vestibules decrease infiltration by 30% if usage is light.
For heavy usage, vestibules serve no purpose.

EXAMPLE 21.13 Estimate the infiltration through the building of Example 21.11 with wind velocity of 24 km/h using the infiltration rate given by tables.

Solution:

In this method the pressure coefficient is not used to find the pressure drop.

The windows are weather-stripped and average fit, hence from Table 21.23, at 24 km/h, we get infiltration rate = 2.2 m^3/h per m crack length = 0.611 L/s per m crack length.

Figure 21.12 gave an infiltration rate of 0.54 L/s per m crack length, which is close to 0.611 L/s

Total crack length in Example 21.11 was = 203.4 m

Total infiltration = $0.611 \times 203.4 = 124.3$ L/s

Now we find infiltration from the empirical Eq. (21.67) for non-weather-stripped window at 24 km/h.

At 24 km/h $\Delta p_V = 0.00472\ (24)^2 = 2.72$ mm of water = $2.72 \times 9.81 = 26.67$ Pa

For non-weather-stripped windows Infiltration = $0.125(0.64\ \Delta p)^{0.63}$ m^3/s per m of crack where Δp is in Pa.

Therefore Infiltration = $0.125(0.64 \times 26.67)^{0.63} = 0.746$ L/s per m crack length.

From Table 21.23 for non-weather-stripped window, the infiltration rate = 3.6 m^3/h = 1.0 L/s

This result is 25% more than the empirical result.

21.10 WATER VAPOUR TRANSFER THROUGH BUILDING

The driving force for vapour transfer is the difference in humidity ratio or the difference in partial pressure of water vapour. This difference exists across the walls, partition walls, roof and floor since the indoor and outdoor humidity ratios are different. The vapour transfer gives rise to latent heat load. Similarly this difference exists across the insulation on ducts and chilled water pipes. As the vapour moves through a structure or insulation, its temperature decreases and it will condense if its temperature becomes less than the dew point temperature. The latent heat load due to this may not be very large but the condensed water will increase the thermal conductivity of insulation and spoil it. For this reason, the migration of water vapour poses serious problems for the insulation on chilled water lines and suction lines, cold storage, frozen cold storage and refrigerator, etc. This will spoil the wood, cause rusting of steel and is very unhygienic since it causes fungal growth. The wet walls are bad from aesthetic point of view too.

Fick's law of diffusion, which is stated as follows, governs vapour migration,

$$\dot{m}_w = -KA\frac{dp_v}{dx} = KA\frac{p_{vo} - p_{vi}}{L} = MA\Delta p \tag{21.72}$$

where p_{vo} and p_{vi} are the outdoor and indoor partial pressures of water vapour respectively and L is the thickness of the structure. The constant K is called *permeability*. It has units of g-cm/(h-m^2-cm of Hg). The constant M is called *permeance* and it has the units of g/(h-m^2-cm of Hg). The values of permeability and permeance of some common materials are given in Table 21.28.

Table 21.28 Permeability and permeance of some common construction materials

Material	*Permeability, K* g-cm/(h-m^2-cm of Hg)	*Permeance coefficient* g/(h-m^2-cm of Hg)
Construction materials		
Concrete	2.2	–
Brick (10 cm)	2.2	0.22
Asbestos cement board	–	0.15
Plaster (1.25 cm)	–	4.0
Gypsum	–	12.6
Wood	0.28–0.38	–

(*Contd.*)

Table 21.28 Permeability and permeance of some common construction materials (contd.)

Material	*Permeability, K* g-cm/(h-m^2-cm of Hg)	*Permeance coefficient* g/(h-m^2-cm of Hg)
Insulating materials		
Still air	83	–
Mineral wool	80	–
Thermocole	1.38–4.0	–
Expanded polyurethane	0.28–1.1	–
Foils		
Aluminium (1 mil)	–	0
Polyethylene (2 mil)	–	0.43
(4 mil)	–	0.022
(6 mil)	–	0.017

To avoid damage due to migration of water vapour, vapour barriers are used. These are applied on the warm side of the insulation or wall where the vapour pressure is large. In cold storages, these are applied next to the inside face of wall before the insulation. In colder climates, the inside of the room has a larger vapour pressure. In chilled-water pipe lines, a vapour barrier is applied outside the insulation. The vapour barriers are essentially of three types:

(i) Structural barriers like plastic or aluminium sheets. These have zero permeance.

(ii) Membrane barriers like aluminium foils or plastic films, etc. These are very popular and are quite often bonded with insulation. These must be perfectly sealed for the vapour barrier to be effective.

(iii) Coatings as barriers. Asphalt and resin coatings on the surfaces are also used as vapour barriers.

21.11 LOAD CALCULATIONS—GENERAL CONSIDERATIONS

During the summer months buildings gain energy by radiation through glass, heat transfer through structure, infiltration, ventilation air and due to internal heat gains. The air conditioning equipment has to cool the air, hence this load is called *cooling load*. On the other hand during winter months the building loses energy to the surroundings, hence the air has to be heated in air conditioning equipment and it is called *heating load*.

The load calculation will be as accurate as the data on which it is based. The precise calculation of load plays an important role in the selection of air conditioning equipment and on its satisfactory operation. Hence sufficient care must be taken to consider all the important factors while doing load calculations.

The outdoor design conditions have to be chosen with care depending upon building construction. For heavy construction, 5% design temperature is recommended while for medium construction 2.5% design temperature is recommended. Still some authors recommend that one should measure the temperature at the site on the hottest day of the year. The longest day during

summer is June 21, but the hottest and the most humid day may occur sometime in July. Similarly for heating, the coldest day may occur sometime in January or February instead of December 21.

The outdoor air temperature is maximum at 3:00 pm but the maximum cooling load for a building with medium construction occurs between 5–7 pm and much later for a building with heavy construction. This is due to time lag for heat to be transferred through the structure. For heavy construction the attenuation factor is also very large, hence the load is also less compared to medium construction. The direct radiation through glass, particularly the glass on the west side of buildings and to some extent the glass on the south side, may advance the time of maximum load between 5 pm and 6 pm. For this reason, it is recommended that minimum glass be used on the west side of a building.

The usage of building also decides the time of maximum load. For an office building which is not used beyond 5 pm, the maximum cooling load calculations are done between 4 pm and 5 pm. For heating load calculations if the building is not used at night time, the load calculation is done for early morning hours. The role of various loads also depends upon usage. In most cases, radiation load through glass, heat transmission through the building structure, infiltration and ventilation loads are important. But in case of auditoriums, theaters and places of assembly, the occupancy load is dominant. In restaurants, the maximum load will occur during lunch and dinner times and amongst the two, the dinner time load will be higher.

The mass of the building stores energy during the hot part of the day. During night time and early morning hours the building is cooled by radiation to sky and becomes ready to absorb radiation as the sun rises. This is referred to as *flywheel effect* where the thermal inertia of the building stores the energy and releases it later for smooth operation. Hence if the cooling load design is done on a 24-hour basis, the loads will be lower but not suited to meet the peak loads. Therefore the design is done for peak loads.

The heat transmission through building structure, radiation heat transfer through glass and infiltration have already been discussed. In the following sections the internal, ventilation and system heat gains are discussed.

21.12 INTERNAL HEAT GAINS

The heat gains that occur due to activities within the indoor space are called internal heat gains. These are essentially due to occupancy, lights and equipment. These may sometime be a very significant part of cooling load in modern office buildings, so much so that even during onset of winter, cooling may be required in the building. Any heat transfer to the indoor air is ultimately the cooling load. A part of the heat from the internal heat sources is directly convected to the air and a part is radiated to the walls, from where it is convected to the air at a later instant of time. To account for this time lag, an empirical cooling load factor is assigned to each type of internal load. The second alternative is to consider the heat balance including convection and radiation to and from the interior surfaces to account for these loads.

21.12.1 Occupancy

It was mentioned that human beings give off heat at a metabolic rate, which depends upon their level of activity. This heat transfer is partly by temperature difference between the body and the air and hence, it is called *sensible heat transfer*. The sensible heat transfer occurs by convection and

radiation. A part of the heat rejection from the body is by evaporation of sweat and evaporation from lungs and deep tissues. This does not require temperature difference, hence it is called *latent heat transfer*. The proportion of sensible and latent heat transfer rates depends upon the inside design temperature; the lower the indoor temperature the larger will be the proportion of sensible heat transfer. Table 21.29 gives heat gain from occupants in air-conditioned spaces. This data is based upon the metabolic heat generation given in the section on Comfort. It may be noted that the data in the last three columns is the adjusted data according to normal percentage of men, women and children expected in the occupancy for the listed application. It is assumed in this table that the heat gain from an adult female is 85% of that from an adult male and that the heat gain from children is 75% of that from an adult male. If the exact proportion is known, then the exact value may be calculated instead of the adjusted data. The data is quite reliable but large errors creep in because of the poor estimates of the period of occupancy and the number of occupants. Care should always be taken to be realistic about the number of people present. The whole office staff will seldom be present; similarly attendance in a lecture hall may be poor. On the other hand, a theatre will always be full; in fact on occasions it may have more people than it is designed for. Traditionally, most of the buildings (other than theatres and auditoriums) are designed with too large an allowance for occupancy. A normal density for an office block is 9 m^2 per person, as an average over the whole air-conditioned space whereas for executive offices it may be 20 m^2 per person and as high as 6 m^2 in open office areas. For restaurants 2 m^2 per person is reasonable, and densities for departmental stores may reach 4.3 m^2 to 1.7 m^2 per person during peak hours. In cinemas, theatres and concert halls the seating arrangement and walking space provides the necessary information but in dance halls, discos and nightclubs the estimates are an open conjecture varying around 0.5 m^2 per person. The heat gain from occupants in cold storages is given in Table 21.30.

Table 21.29 Heat gain from occupants

Type of activity	*Typical application*	*Total heat adults, male*	*Adjusted heat liberated*		
			Sensible heat (W)	*Latent heat* (W)	*Total heat* (W)
Seated at rest	Theater—matinee	114	66	31	97
	Theater – Evening	114	72	31	103
Seated : very light work	Offices, hostels, restaurants, residences	132	72	45	117
Moderately active work	Offices, hostels, residences	139	73	59	132
Standing light work; Walking	Departmental store, retail store	162	73	59	132
Walking slowly, standing	Bank, chemist shop	162	73	73	146
Sedentary work	Restaurants	144	81	81	162
Light bench work	Factory	235	81	139	220
Moderate dancing	Dance halls	264	89	160	249

(*Contd.*)

Table 21.29 Heat gain from occupants (contd.)

Type of activity	*Typical application*	*Total heat adults, male*	*Adjusted heat liberated*		
			Sensible heat (W)	*Latent heat* (W)	*Total heat* (W)
Walking 4.8 km/h: light machine work	Factory	293	293	110	183
Bowling	Bowling alley	440	425	170	255
Moderately heavy work	Factory	293	110	183	293
Heavy machine work; lifting	Factory	469	170	225	425
Athletics	Gymnasium	586	528	208	320

Table 21.30 Heat gain from people in cold storage rooms (light work)

Room dry bulb temperature (°C)	7	2	–18	–23
Sensible heat gain (W)	174	192	262	273
Latent heat gain (W)	33	33	33	33
Total heat gain (W)	207	225	295	306

The latent and sensible heat loads from the occupants are calculated separately. The latent heat load is assumed to become cooling load instantly, whereas the sensible heat gain is partially delayed since the radiated component is absorbed by the indoor surfaces and then transferred to the air. The energy convected from the warm body becomes an instantaneous load. This is usually 30% of the sensible load and the remaining part is the radiation heat transfer. ASHRAE has suggested that Cooling Load Factor (CLF) be used to estimate the radiation heat transfer, hours after entry into the space. The values of sensible heat transfer from Table 21.29 are multiplied by CLF determined from Table 21.31. CLF for latent heat is 1.0. Thus,

Sensible load due to occupancy = Gain per person from Table 21.29 × Number of people × CLF from Table 21.31.

Table 21.31 Sensible heat cooling load factors for persons

Hours after each entry into space	*Total hours in space*							
	2	4	6	8	10	12	14	16
1	0.49	0.49	0.50	0.51	0.53	0.55	0.58	0.62
2	0.58	0.59	0.60	0.61	0.62	0.64	0.66	0.70
3	0.17	0.66	0.67	0.67	0.69	0.70	0.72	0.75
4	0.13	0.71	0.72	0.72	0.74	0.75	0.77	0.79
5	0.10	0.27	0.78	0.76	0.77	0.79	0.80	0.82

(*Contd.*)

Table 21.31 Sensible heat cooling load factors for persons (contd.)

Hours after each entry into space	*Total hours in space*							
	2	4	6	8	10	12	14	16
6	0.08	0.21	0.79	0.80	0.80	0.81	0.83	0.85
7	0.07	0.16	0.34	0.82	0.83	0.84	0.85	0.87
8	0.06	0.14	0.26	0.84	0.85	0.86	0.87	0.88
9	0.05	0.11	0.21	0.38	0.87	0.88	0.89	0.90
10	0.04	0.10	0.18	0.30	0.89	0.89	0.90	0.91
11	0.04	0.08	0.15	0.25	0.42	0.91	0.91	0.92
12	0.03	0.07	0.13	0.21	0.34	0.92	0.92	0.93
13	0.03	0.06	0.11	0.18	0.28	0.45	0.93	0.94
14	0.02	0.06	0.10	0.15	0.23	0.36	0.94	0.95
15	0.02	0.05	0.08	0.13	0.20	0.30	0.47	0.95
16	0.02	0.04	0.07	0.12	0.17	0.25	0.38	0.96
17	0.02	0.04	0.06	0.10	0.15	0.21	0.31	0.49
18	0.01	0.03	0.06	0.09	0.13	0.19	0.26	0.39

21.12.2 Load Due To Electric Lighting

Luminous intensity is defined, by international agreement, in terms of brightness of molten platinum at a temperature of 1755ºC. It is expressed in the unit of *candela.* The luminous energy per unit solid angle is called candela. The density of luminous flux is the amount of luminous energy (uniform) received by one m^2 area. This is also called *lux.*

In production of luminous energy by electrical lighting, certain amount of electrical energy is liberated. Most of the energy appears as heat. A small part, which is initially light, is also dissipated into heat after multiple reflections.

The standard of illumination in a room depends upon the area of surface in the room, its colour, and reflective properties and also on the method of light production. The fluorescent tube light fittings are more efficient than the tungsten lamps.

The efficiency of fluorescent lamps deteriorates with age. Initially a 40 W tube might produce 2000 lux with liberation of 48 watts. It will produce only 1600 lux after 7500 hours of life with liberation of 48 W. The fluorescent fittings require 20% more power than the rated capacity. For example, a 100 W fluorescent light will consume 120 W of electricity. The additional 20 watts is liberated directly as heat from the control gear (choke).

Typical standard of light in an office space is 500 lux. This requires a power supply of 14 to 20 W/m^2 of floor area. Thus an office of dimensions 9 m × 6 m will require 1080 W. This is in absence of natural light.

Some of the energy liberated from the light source is in the form of radiation. This is absorbed by the surfaces and transferred by convection to the air at a later instant of time. A recessed light fixture will transfer heat to the surrounding surface by radiation. A hanging light will transfer heat

to the air by convection as well. Sometimes the return air grilles and luminaire are combined together so that the return air is directly heated by the lights and only a small portion is incident into the room. The air extracted through luminaire can be thrown out of the room too; in that case it will not be considered a part of cooling load. However, most of the air is recirculated. If ceiling void is used as return air path, one manufacturer (Westinghouse) has suggested that only 60–70% heat is liberated into the room for older fluorescent tubes.

Lights are very often turned off to save energy. A light left on for 24 hours approaches an equilibrium state where the cooling load is equal to power input. The heat gain from electric lights may be determined from

$$Q = W F_u F_s \text{ (CLF)} \tag{21.73}$$

where

W = lamp rating in watts
F_u = use factor, the ratio of wattage in use to the total installed wattage
F_s = special allowance factor
CLF = Cooling Load Factor from Table 21.32.

The special allowance factor is for the fluorescent and metal halide fixtures or for the fixtures that are ventilated or installed in such a way that only a part of their heat goes into the room. For fluorescent fixtures, it accounts for ballast losses and the recommended value is 1.20. For sodium lamps, it varies from 1.04 to 1.37. For ventilated or recessed fixtures, manufacturer's data may be used. Heat gain from fluorescent fixtures is assumed to be 41% convective and 59% radiative. Heat gain from incandescent fixtures is assumed to be 80% radiative and 20% convective.

The cooling load factor accounts for the radiation heat transfer from the light fixture to the surrounding surface. The radiation is absorbed by the surfaces, their temperature rises and heat is transferred by convection to the air, thereby it becomes the cooling load.

Table 21.32 Cooling load factors for two kinds of light fixtures

Number of hours after lights are turned on	*Fixture X Hours of operation*		*Fixture Y Hours of operation*	
	10	16	10	16
0	0.08	0.19	0.01	0.05
1	0.62	0.72	0.76	0.79
2	0.68	0.75	0.81	0.83
3	0.69	0.77	0.84	0.87
4	0.73	0.80	0.88	0.89
5	0.75	0.82	0.90	0.91
6	0.78	0.84	0.92	0.93
7	0.80	0.85	0.93	0.94
8	0.82	0.87	0.95	0.95
9	0.84	0.88	0.96	0.96

(*Contd.*)

Table 21.32 Cooling load factors for two kinds of light fixtures (contd.)

Number of hours after lights are turned on	*Fixture X Hours of operation*		*Fixture Y Hours of operation*	
10	0.85	0.89	0.97	0.97
11	0.32	0.90	0.22	0.98
12	0.29	0.91	0.18	0.98
13	0.26	0.92	0.14	0.98
14	0.23	0.93	0.12	0.99
15	0.21	0.94	0.09	0.99
16	0.19	0.94	0.08	0.99
17	0.17	0.40	0.06	0.24
18	0.15	0.36	0.05	0.20

Fixture *X* is a recessed light, which is not vented. The supply and return air registers are below the ceiling or through the ceiling space and grille. Fixture *Y* is a vented or free hanging light. The supply air registers are below or through the ceiling with the return air registers around the fixtures and through the ceiling space.

21.12.3 Power Dissipation from Miscellaneous Equipment

These equipment consist of electric motors, office equipment (computers, printers, copiers, faxes, etc.), kitchen appliances, hospital equipment, laboratory equipment, etc. The estimates tend to be subjective because of lack of data on frequency of use, the breakdown of radiative and convective component of heat transfer and the efficiency of the device. One can either find the heat dissipated for each equipment by finding the frequency of use and actual heat gain or by estimating on the basis of W/m^2 floor area.

When an electric motor is used and both the motor and the machine are in the conditioned space, then the power drawn from the mains appears as heat gain to the room. To be precise the total power dissipated is expressed as

$$Q_m = \frac{F_l F_u P}{\eta_m} \text{ watt} \tag{21.74a}$$

where

P = rated power of the motor, power drawn from the mains is P/η_m
F_l = motor load factor, fraction of rated load delivered by motor. All motors do not run at full load all the time
F_u = motor use factor, if the use is intermittent then, F_u = hours of use/24
η_m = motor efficiency.

If the motor is outside, then heat gain is given by

$$Q_m = F_l F_u P h_t \text{ watt} \tag{21.74b}$$

where, h_t is the transmission efficiency since P is the shaft power.

If the motor is in the conditioned space and the driven machine is outside,

$$Q_m = \frac{F_l F_u P(1-\eta_m)}{\eta_m} \text{ watt} \tag{21.74c}$$

It is a common practice to assume that the radiative and convective parts are 70% and 30% respectively for the equipment heat gain. Electronic equipment that uses fans for cooling have higher proportion of convective component. Laser printers and copiers were measured to have only 11% and 14% as the radiative fraction. The monitors of the computers had around 25% radiative fraction.

Heat gain from appliances—electric, gas or steam—makes the estimate subjective since the exact usage schedule, load factor, effect of thermostatic control and efficiencies of the variety of appliances are usually not known. If this data is not available, then the hourly heat gain is estimated as

$$Q_a = 0.5 \times Q_i \text{ watt} \tag{21.75a}$$

where, Q_i is the nameplate rating or catalogue rating.

For office equipment, the nameplate values are drastic overestimates. The actual steady-state heat gains have been observed to be 14–35% of the nameplate ratings.

In hooded appliances, the convective heat gain is assumed to be removed by the hood. Radiation fraction is up to 32% of the rated value. Hence, the heat gain from hooded appliances may be written as

$$Q_a = 0.5(0.32)Q_i = 0.16Q_i \text{ watt} \tag{21.75b}$$

Fuel-fired appliances consume about 60% more energy than that by electric appliances. When this appliance is under an effective hood, then the air receiving the convected heat transfer, latent heat and combustion products is exhausted, only the radiation fraction (32%) is dissipated to the room. Hence, Eq. (21.75b) is modified to

$$Q_a = \frac{0.16Q_i}{1.6}$$

For unhooded appliances, the sensible and latent heat gains are estimated as 30% and 70% of the total value.

ASHRAE Handbook, HVAC Applications Volume, 1999, may be consulted for a variety of appliances.

Software offices and laboratories and with computer terminals at most desks, the PCs, printers and copiers may have a heat gain as high as 50 W/m^2. General offices have been found to have an appliance load less than 10 W/m^2.

21.13 SYSTEM HEAT GAIN

The heat added or removed by components of the air conditioning system are put under this category. These components have to be estimated during design. The actual values are found after the system has been designed. The various components of this system are given below.

21.13.1 Heat Transfer to Supply Air Duct

The supply air normally flows at temperature of 11°C to 17°C through the duct. If the duct passes through an unconditioned space having a temperature of 30°C to 40°C, there will be some heat transfer or heat gain by the supply air before it reaches the conditioned space. This will reduce the cooling capacity of the system. It is recommended that long runs of ducts in unconditioned spaces, be insulated to reduce heat gain. This leakage heat transfer rate may be estimated as follows.

$$Q = UA\,(t_i - t_s) \tag{21.76}$$

where

U = overall heat transfer coefficient
A = outer surface area of the duct
t_s = average temperature of the supply air
t_i = temperature of the unconditioned space.

The overall heat transfer coefficient is given by $\dfrac{1}{U} = \dfrac{1}{h_i} + \dfrac{1}{k} + \dfrac{1}{h_o}$ (21.77)

The outside heat transfer coefficient may be taken as 10 W/m^2-K, thermal conductivity of the insulation will vary between 0.03 and 0.07, a conservative estimate is k = 0.045 W/m-K. The inside convective thermal resistance ($1/h_i$) is given by

$$1/h_i = 0.0286\, D^{0.25}\, V^{-0.8} \qquad \text{for circular ducts} \tag{21.78a}$$

$$1/h_i = 0.286\, [2AB/(A+B)]^{0.25}\, V^{-0.8} \qquad \text{for rectangular ducts} \tag{21.78b}$$

where

D = internal diameter of the duct, in m
A = internal width of the rectangular duct, in m
B = height of the rectangular duct, in m
V = average velocity of supply air, in m/s.

ASHRAE Handbook of Fundamentals Volume, 1993, gives an expression for the change in temperature as the air flows through the duct. If t_{s1} is the inlet supply air temperature, then t_{s2} the temperature after leakage heat transfer, is given by following expression.

$$t_{s2} = \frac{t_{s1}\,(y-1) + 2t_i}{y+1} \quad \text{or} \quad \Delta t = (t_{s2} - t_{s1}) = \frac{2\,(t_i - t_{s1})}{y+1} \tag{21.79}$$

where

$y = 503\,\rho DV/UL$ for circular pipes (21.80a)

$y = 2010\,\rho AV/UPL$ for rectangular ducts (21.80b)

with P as perimeter of duct and L as length.

For V = 8 m/s and 75 mm diameter duct, $1/h_i$ = 0.0284 m^2-K/W and for V = 20 m/s and 75 mm diameter $1/h_i$ = 0.0243 m^2-K/W. Therefore, it is observed that the inside heat transfer coefficient and hence the overall heat transfer coefficient are both almost independent of the duct air velocity. The U values for insulation thickness of 25, 50 and 75 mm are 1.47, 0.81 and 0.56 W/m^2-K respectively assuming $1/h_i$ = 0.026 and k = 0.045 and the values of y from Eq. (21.80a) are 400DV,

726DV and 1046DV respectively. Then assuming an air density $\rho = 1.165$ kg/m^3 and $L = 1$ metre, we get the following equations for the temperature drop per metre length from Eq. (21.79)

$$\Delta t = \frac{t_i - t_{s1}}{200\,DV} \qquad \text{for 25 mm lagging of } k = 0.045 \text{ W/m-K} \qquad (21.81a)$$

$$\Delta t = \frac{t_i - t_{s1}}{363\,DV} \qquad \text{for 50 mm lagging of } k = 0.045 \text{ W/m-K} \qquad (21.81b)$$

$$\Delta t = \frac{t_i - t_{s1}}{523\,DV} \qquad \text{for 75 mm lagging of } k = 0.045 \text{ W/m-K} \qquad (21.81c)$$

The above-mentioned procedure can be followed, if the duct dimensions and velocities, etc. are known. During the design stage, these are not known, and hence an empirical procedure has to be adopted for a good estimate.

The recommended thumb rule is that if the duct is not insulated, and all of it passes through unconditioned space, then 5% of the Room Sensible Heat Load should be taken as the leakage heat transfer to the duct. If only say X% of the total duct is in the unconditioned space, then (5X %) of RSH may be taken as leakage heat transfer loss.

21.13.2 Supply Air Leakage Loss

The leakage of supply air from the duct is a serious loss, except when it leaks into conditioned space. Then also, it may disturb the air distribution in the room, since leakage will go to arbitrary places depending upon the workmanship of the duct. Experience indicates that supply air leakage from the entire length of supply air ducts, whether large or small, averages around 10%. Workmanship is the greatest variable, duct leakages from 5% to 30% have been observed. *Handbook of Air Conditioning System Design* by Carrier Air Conditioning Company recommends that:

1. If the duct is bare and runs within the air-conditioned space then no heat gain/loss be considered.
2. If the duct is furred or insulated and the duct runs within the conditioned space, no gain/loss be considered.
3. If the whole of the duct and all the supply air ducts are outside the conditioned space, then assume 10% of the RSH loss due to leakage. When only a part of the duct is outside the conditioned space, include that fraction of 10% as the leakage loss.

21.13.3 Heat Gain from Air Conditioning Fan

Some energy is added to the air due to inefficiency of the fan and due to compression of the air. The fan can be a draw-through system, that is, fan is located after the cooling coil. In this case, the heat will be added to the cooled air, hence the heat gain should be added to the Room Sensible Heat Load. On the other hand, if the fan is blow-through system, then it adds energy to the air before it passes through the cooling coil and it is added to the Grand Sensible total heat load.

The fan efficiencies η_f are about 70% for central plants and about 50% for the packaged units. The efficiency of motor and transmission, η_m, may be about 85%. If the total pressure drop is say,

h mm of H_2O and the supply air flow rate is Q_{vs} m^3/s, then the shaft power in watts is $9.81Q_{vs}h$. Considering the efficiencies, the total energy required in watts is $9.81Q_{vs}h/(\eta_f . \eta_m)$. If the motor is not in the conditioned space, then the inefficiency of the motor does not appear as heat gain and the heat gain is $9.81Q_{vs}h/(\eta_f)$.

The fan pressure requirement is determined by the total pressure drop through filters, ducts, grilles, cooling coil, etc. The approximate values of pressure drops in the system are:

Package units	12.5–25 mm of water
Moderate duct work, low velocity system	20–37.3 mm of water
Considerable duct work, low velocity system	30–50 mm of water
Moderate duct work, high velocity system	50–100 mm of water
Considerable duct work, high velocity system	75–150 mm of water

The dehumidified temperature rise varies from 8°C to 14°C. This requires volume flow rate of 16 cmm to 9 cmm per TR with a sensible heat ratio of 0.75. Rough estimates can be obtained from this data.

Tables have been prepared for the estimate of fan heat gain for known pressure drop and dehumidified temperature rise. *In the absence of this information, the thumb rule is that fan heat gain may be assumed to be 5% of Room Sensible Heat Load.*

21.13.4 Safety Factor

For a number of items, intelligent guesses have been made or sound engineering practice has been followed. The heat gain will be as good as the reliability of accurate data used. There can be probable errors in the data and estimates. Hence, as safety factor, 5% of RSH is considered to be the additional heat gain.

Thus the total room sensible heat gain is the subtotal RSH plus the percentage additions to allow for (i) supply duct heat gain, (ii) supply duct leakage losses, (iii) fan horsepower and (iv) safety factor.

21.13.5 Return Air Duct Heat and Leakage Gain

The procedure for leakage heat transfer is the same as that followed for supply air duct. If the return air duct is within the conditioned space, then there is virtually no temperature difference since the return air temperature is same as the room design temperature (unlike supply air where the supply air temperature may be from 11°C to 17°C and room temperature 25°C). The length of the return air duct is usually very small. Leakage heat transfer has to be evaluated from the portion that is outside the conditioned space.

The return air pressure is usually negative, hence the leakage in this case is of outdoor warm humid air into the system. For the return air duct running within the conditioned space, no heat gain is considered.

For a duct running outside the conditioned space, heat gain up to 3% of RSH may be considered depending upon the proportion of duct length outside. This is added to the grand total heat load (GTH).

21.13.6 Heat Gain from Dehumidifier Pump

The dehumidifier pump required to pump chilled water to the dehumidifier adds heat to the system. The efficiencies vary from 50% for small pumps to 75% for large pumps. This depends upon the chilled water temperature rise (smaller flow rates are used for larger temperature rise requiring lower pump power) and the total pressure drop of water. It varies from 0.5% to 5% of GTH.

The percentage addition to GTH to compensate for various external losses consists of (i) heat and leakage gain to return air ducts, (ii) heat gain from dehumidifier pump, (iii) and the heat gain to the dehumidifier and piping system, and (iv) fan power gain for a blow-through system.

Chilled water flows through the dehumidifier. If the chilled water piping runs outside the conditioned space there will be heat gain by leakage heat transfer. To account for this, the following estimates for the dehumidifier piping losses, are made:

(a) Very little external piping : 1% of GTH
(b) Average external piping : 2% of GTH
(c) Extensive external piping : 4% of GTH

These losses are also added to GTH.

21.14 COOLING LOAD ESTIMATE

Cooling loads are classified as external and internal. The external ones come from outside and the internal ones are produced within the air-conditioned space. It is called room load if it falls directly on the room and supply air has to compensate for it. The ventilation load, return air loads and dehumidifier loads, etc. fall directly on the equipment, hence these are included in the total loads. Further, it is convenient to classify the loads as sensible and latent heat loads.

Room Sensible Heat Load (RSH)

These loads tend to cause temperature rise and predominantly these loads are as follows:

(i) Heat transmission through building structures like walls and roofs by conduction, convection and radiation.
(ii) Heat transmission by radiation through transparent windows and other glass.
(iii) Heat transmission through partition walls and floor, etc.
(iv) Sensible heat addition by infiltration.
(v) Internal sensible heat produced by occupants.
(vi) Internal sensible heat gains from lights, appliances and motors, etc.
(vii) Sensible heat extracted from materials or products brought into the air-conditioned space.
(viii) Additional sensible heat gain, which cannot be accounted for under the above headings and uncertainties in the above headings. These are included as a safety factor.
(ix) Supply air duct heat gain and supply air leakage and power input by fan.

The sum total of (i) to (ix) is called the Room Sensible Heat Load (RSH).

Room Latent Heat Load (RLH)

These loads tend to cause a rise in humidity ratio and are as follows:

(i) Latent heat addition by infiltration.
(ii) Latent heat addition by occupants.
(iii) Latent heat addition by cooking, hot baths or moisture producing equipment in air-conditioned space.
(iv) Latent heat addition by materials or products brought into the air-conditioned space.
(v) Additional latent heat gain, which cannot be accounted for under the above headings and uncertainties in the above headings. These are included as a safety factor.

The sum total of (i) to (v) is called the Room Latent Heat Load (RLH).

Grand Total Heat Load (GTH)

This is also classified as total sensible heat load (TSH) and total latent heat load (TLH). These loads consist of the following components:

Total Sensible Heat Load (TSH)

(i) RSH
(ii) Ventilation air sensible heat load called OASH.
(iii) Return air duct heat gain, sensible part of return air duct leakage, dehumidifier pump power and heat loss from dehumidifier and other pipes.

The sum total of (i) to (iii) is called the Total Sensible Heat Load (TSH).

Total Latent Heat Load (TLH)

(i) RLH
(ii) Ventilation air latent heat load called OALH
(iii) Latent part of return air duct leakage

The sum total of (i) to (iii) is called the Total Latent Heat Load (TLH).
The sum of TSH and TLH is called the Grand Total Heat Load (GTH).

21.15 HEATING LOAD ESTIMATE

This was briefly discussed while discussing the psychrometry of winter air conditioning in Chapter 18. Here also the estimate is based upon the maximum heat loss that will occur from a room or building during the coldest part of the day and during severe weather conditions. Brief spells of very severe weather conditions are not taken into account.

The heating load for a building is maximum during the early morning hours before sunrise. Hence solar radiation is not considered in calculations, that is, time lag and decrement factor are not considered. The load is calculated as follows:

(i) Heat transmission from the walls, roofs, windows and doors is calculated on the basis of steady-state heat transfer based upon temperature difference between the inside and the outside by the equation,

$$Q = U_o A_o (t_i - t_o)$$

(ii) Solar radiation through windows and other glass in not important since the load is calculated before sunrise.

(iii) Sensible and latent heat gains from occupants

(iv) Heat gain from lights, appliances and motors, etc.

(v) Latent heat addition by cooking, hot baths or moisture producing equipment in air-conditioned space.

(vi) Sensible and latent heat addition by materials or products brought into air conditioned space.

(vii) Sensible and latent heat gain by infiltration

(viii) Supply air duct heat loss, latent and sensible heat loss due to leakage of air from supply air duct.

(ix) Sensible and latent heat loss due to leakage of air from return air duct.

The sum is classified under the headings of sensible and latent heat loads for the room and the total heat load.

During winter months the outside humidity ratio is very low, hence infiltration decreases the room humidity ratio while occupancy and appliances increase it. The net result may be a very small room latent heat load. The ventilation load decreases the humidity ratio; as a result the humidification of air is required by the air-conditioning apparatus. The heat is lost to the surroundings while occupancy, lights and appliances add heat to the room and reduce the heating load. Supply air duct and return air duct lose warm air (compared to surroundings), hence it is a heating load.

The cooling load estimate is illustrated by the following example.

EXAMPLE 21.14 Determine the various cooling loads for the single-storey, 4 m high building with 20 m wide wall facing north and 30 m long wall facing west. The west, north and south walls have four, one and two windows respectively, each of which is 2 m wide and 1.5 m high. There is one door 1.5 m wide and 2 m high, each on the east, south and north walls. The place is near Kolkata having the same longitude and 20^o latitude. The highest load occurs say on June 21. Ten per cent of the supply air duct runs in the non-conditioned space.

The inside design conditions are: 25^{o}C dbt and 50% relative humidity.

The outdoor design conditions are: 43^{o}C dbt, 27^{o}C wbt, 12^{o}C daily range, and 25 km/h wind velocity.

Occupancy : 100 persons doing office work

Lighting : 15,000 W fluorescent and 4000 W incandescent

The walls are : 241 mm common brick with 12.5 mm plaster on both the sides

The roof : 112.5 mm RCC and 112.5 mm lime concrete

The floor : 200 mm concrete

Door : 37.5 mm hard wood

Window glass: 6.35 mm plane window glass

$h_o = 35$ W/m^2-K, $h_i = 8.5$ W/m^2-K, $k_{brick} = 0.77$ W/m-K, $k_{plaster} = 1.15$ W/m-K, $k_{rcc} = 1.73$ W/m-K, $k_{limec} = 0.71$ W/m-K, $k_{wood} = 0.158$ W/m-K and $k_{glass} = 0.78$ W/m-K, $\rho_{brick} = 1800$ kg/m^3, $\rho_{plaster} = 1860$ kg/m^3, $\rho_{rcc} = 2200$ kg/m^3, $\rho_{limec} = 1550$ kg/m^3.

Solution:

Overall heat transfer coefficients

Walls:

$$U_o = \frac{1}{\frac{1}{h_o} + \frac{x_p}{k_p} + \frac{x_b}{k_b} + \frac{x_p}{k_p} + \frac{1}{h_i}} = \frac{1}{\frac{1}{35} + \frac{0.0125}{1.15} + \frac{0.241}{0.77} + \frac{0.0125}{1.15} + \frac{1}{8.5}} = 2.008 \text{ W/m}^2\text{-K}$$

Wall mass, $m = 0.241(1800) + 2(0.0125)\ (1860) = 480.3$ kg/m^2

Roof: $$U_o = \frac{1}{\frac{1}{35} + \frac{0.1125}{0.71} + \frac{0.1125}{1.73} + \frac{0.0125}{1.15} + \frac{1}{8.5}} = 2.62 \text{ W/m}^2\text{-K}$$

Mass, $m = 0.1125(2200) + 0.1125(1550) + 0.0125(1860) = 445.1$ kg/m^2

Floor: Assuming that free convection heat transfer coefficient for floor is also 8.5 W/m^2,

$$U_o = \frac{1}{\frac{0.2}{1.73} + \frac{1}{8.5}} = 4.3 \text{ W/m}^2\text{-K}$$

Door: $$U_o = \frac{1}{\frac{1}{35} + \frac{0.0375}{0.158} + \frac{1}{8.5}} = 2.607 \text{ W/m}^2\text{-K}$$

Window: $$U_o = \frac{1}{\frac{1}{35} + \frac{0.00625}{0.78} + \frac{1}{8.5}} = 6.52 \text{ W/m}^2\text{-K}$$

Areas:

West: Glass : $4(2 \times 1.5) = 12$ m^2; Door : 0.0; Wall : $30 \times 4 - 12 = 108$ m^2

South: Glass : $2(2 \times 1.5) = 6$ m^2; Door : 3 m^2 ; Wall : $20 \times 4 - 6 - 3 = 71$ m^2

East: Glass : = 0 m^2; Door : 3 m^2 ; Wall : $30 \times 4 - 0 - 3 = 117$ m^2

North: Glass : $(2 \times 1.5) = 3$ m^2; Door : 3 m^2 ; Wall : $20 \times 4 - 3 - 3 = 74$ m^2

Roof: 600 m^2

Floor: 600 m^2

Corrections to Δt_E: $(t_o - t_i) = 43 - 25 = 18^oC$ $\therefore$ Correction for $(t_o - t_i) = 18 - 8.3 = 9.7^oC$

Correction for *DR*: Difference in *DR* = 12 – 11.1 = 0.9: Correction = $0.25 \times 0.9 \approx 0.25^oC$

Total Correction = 9.7 + 0.25 = 9.95 ^{o}C

Interpolation for wall and roof mass: The wall mass is 480 kg/m^2 while the values are tabulated for $m = 319$ and 532 kg/m^2. Let Δt_{E1} and Δt_{E2} be the values of equivalent temperatures at $m = 319$ and 532 respectively.

Then, the interpolated value for $m = 480$ is $\Delta t_E = \Delta t_{E1} + \dfrac{480 - 319}{532 - 319}(\Delta t_{E2} - \Delta t_{E1})$

$= \Delta t_{E1} + 0.7558(\Delta t_{E2} - \Delta t_{E1})$

Similarly, for the roof we have $m = 445$ while values are tabulated for $m = 318$ and 524.

Hence, the interpolated value for $m = 445$ is $\Delta t_E = \Delta t_{E1} + 0.6146(\Delta t_{E2} - \Delta t_{E1})$

The interpolated values for various *solar times* are given in the following table.

Solar time	*East*	Δt_E	*South*	Δt_E	*West*	Δt_E	*North*	Δt_E	*Roof*	Δt_E
2:00 pm	Δt_{E1}: 7.8 Δt_{E2}: 13.3	12.0	13.3 6.7	8.31	5.4 4.4	4.67	3.3 1.1	1.64	15 14.4	14.63
3:00 pm	Δt_{E1}: 7.2 Δt_{E2}: 11.1	10.15	13.9 8.3	9.67	10.6 5.5	6.74	4.4 1.7	2.36	17.2 16.6	16.22
4:00 pm	Δt_{E1}: 6.7 Δt_{E2}: 10.0	9.19	14.4 8.9	10.24	14.4 6.7	8.58	5.5 2.2	3.0	19.4 17.8	18.42
5:00 pm	Δt_{E1}: 7.2 Δt_{E2}: 8.9	6.48	12.3 10.0	10.68	18.9 9.4	11.72	6.1 2.8	3.6	21.1 19.4	20.05
6:00 pm	Δt_{E1}: 7.8 Δt_{E2}: 7.8	7.8	11.1 10.0	10.27	22.2 11.1	13.81	6.7 2.8	3.75	21.7 20.6	21.02
7:00 pm	Δt_{E1}: 7.2 Δt_{E2}: 7.8	7.65	8.3 8.3	8.3	22.8 13.9	16.07	6.7 2.8	3.75	21.1 20.6	20.79
8:00 pm	Δt_{E1}: 6.7 Δt_{E2}: 7.8	7.53	6.7 7.8	7.53	20.0 15.6	16.67	6.7 4.4	4.96	20.0 19.4	19.63
9:00 pm	Δt_{E1}: 6.1 Δt_{E2}: 7.2	6.93	5.5 6.7	6.4	15.6 15.0	15.15	5.5 3.9	4.29	18.9 18.9	18.9

Applying the correction to Equivalent temperature by adding 9.95°C, we get Δt_E corrected as follows:

Solar time	*East*	*South*	*West*	*North*	*Roof*
2:00 pm	21.95	18.26	14.62	11.59	24.58
3:00 pm	20.1	19.62	16.69	12.31	26.17
4:00 pm	19.14	20.19	18.53	12.93	28.37
5:00 pm	18.43	20.63	21.67	13.55	30.0
6:00 pm	17.75	20.22	23.76	13.7	30.97
7:00 pm	17.6	18.25	26.02	13.7	30.74
8:00 pm	17.48	17.48	26.62	14.91	29.58
9:00 pm	16.88	16.35	25.1	14.24	28.85

The outdoor air temperatures, $\Delta t = t_o - t_i$ and SHGFs are as follows:

Solar time	2:00	3:00	4:00	5:00	6:00	7:00	8:00	9:00
% DR	3	0	3	10	21	34	47	58
t_o, °C	42.64	43	42.64	41.8	40.48	38.92	37.36	36.04
$\Delta t = t_o - t_i$	17.64	18	17.64	16.8	15.48	13.92	12.36	11.04
SHGF : West	303	451	505	467	256			
SHGF : South	44	444	38	28	9			
SHGF : North	60	79	104	129	88			

Sensible Heat Gains

Heat Gains from Walls, Roof, Floor and Windows

For walls and roof, heat gain is calculated by $U_oA\ \Delta t_E$

For doors it is calculated by $U_oA\ \Delta t$: It could have been calculated by using $(\Delta t_E)_{\text{corrected}}$ for m = 106 kg/m^2. This is an assumption, which is good for east and north walls.

For windows: The solar heat gain is found by multiplying SHGF by the area of glass. The convective heat transfer rate is found by $U_oA\ \Delta t$ as recommended.

For floor, the temperature difference has been assumed to be 2.5°C.

For partition walls, it is recommended that the temperature on the partition side be taken as $(t_o - 2.5)$ *so that the temperature difference is* $(\Delta t\ - 2.5)$.

The results are given in the following table:

Solar time	2:00	3:00	4:00	5:00	6:00			
Walls : U_o = 2.008; $AU_o\Delta t_E$								
West : $108 \times 2.008 \times \Delta t_E$	3170.5	3619.5	4018.5	4699.5	5153.0	5643.0	5773.0	5443.0
South : $71 \times 2.008 \times \Delta t_E$	2603.0	2797.0	2878.5	2941.0	2833.0	2602.0	2492.0	2331.0
East : $117 \times 2.008 \times \Delta t_E$	5157.0	4722.0	4497.0	4330.0	4170.0	4135.0	4107.0	3966.0
North : $74 \times 2.008 \times \Delta t_E$	1722.0	1829.0	1921.0	2013.0	2036.0	2136.0	2215.0	2116.0
Roof : $600 \times 2.62 \times \Delta t_E$	38640.0	41139.0	44598.0	47160.0	48685.0	48323.0	46500.0	45352.0
Floor : $600 \times 4.3 \times 2.5$	6450.0	6450.0	6450.0	6450.0	6450.0	6450.0	6450.0	6450.0
Windows: U_o = 6.5; $AU_o\Delta t$								
West : $12 \times 6.5 \times \Delta t$	1376.0	1404.0	1376.0	1310.0	1207.0	1086.0	964.0	861.0
South : $6 \times 6.5 \times \Delta t$	688.0	702.0	688.0	650.0	603.0	543.0	482.0	431.0
North : $3 \times 6.5 \times \Delta t$	344.0	351.0	344.0	325.0	301.0	272.0	241.0	215.0
Doors : U_o = 2.607, total area 9.0 m^2 ; $9 \times 2.607 \times \Delta t$	414.0	422.0	414.0	394.0	363.0	327.0	290.0	259.0
Glass : Area × SHGF	3636.0	5412.0	6060.0	5604.0	3072.0	0.0	0.0	0.0
West : 12 × SHGF	264.0	264.0	228.0	168.0	54.0	0.0	0.0	0.0
South : 6 × SHGF	180.0	237.0	312.0	387.0	264.0	0.0	0.0	0.0
Subtotal	64644.0	69348.0	73785.0	**76439.0**	75192.0	71517.0	69514.0	67424.0

It is observed that the heat gain through walls, roof, windows and doors is maximum at 5:00 pm. This is usually the case for a building with medium construction. Solar radiation is maximum at solar noon and the air temperature is maximum at 3:00 pm. Sol-air temperature will be maximum around 1:00 pm. The time lag seems to be about 4 hours.

Maximum heat gain from walls, roof windows and doors at 5:00 pm = 76439.0 W.

Infiltration

Windows: The windows are double-hung windows and are assumed to be non-weather-stripped and poor fit (worst possible case) Wind velocity is 25 kmph. Interpolating in Table 21.23, we get

Infiltration rate = 10.3 + (14.3 – 10.3)/8 = 10.8 m^3/h per m crack length.

Total crack length for seven windows = 7(2 × 2 + 3 × 1.5) = 59.5 m

Infiltration through all the windows = 59.5 × 10.8 = 642.6 m^3/h

Doors: Assume that the doors are non-weather-stripped poor fit. From Table 21.24, infiltration at 24 km/h and 32 km/h are 0.17 and 0.24 cmm per m^2 respectively. Interpolating, we get

Infiltration rate = 0.17 + (0.24 – 0.17)/8 = 0.179 cmm = 10.8 m^3/h per m crack length

For three doors, total crack length = 3(2 × 1.5 + 3 × 2) = 27 m

Infiltration through all the doors = 27.0 × 10.8 = 291.6 m^3/h

Door openings: Assume that traffic is 50 persons per hour, that is, half the persons go out. Since they go out they will come back too. Hence there will be 2 × 50 = 100 door openings per hour. In the absence of data on door, we assume that the doors are of swinging type with only one half in operating condition, the other half being closed. Hence we take the data from Table 21.27 for 0.91 m swinging hospital door (office door is not listed).

Infiltration rate = 5.9 m^3/h per person

Infiltration due to door opening = 5.9 × 100 = 590.0 m^3/h

Total Infiltration = 642.6 + 291.6 + 590.0 = 1524.2 m^3/h

Let us find the air changes corresponding to the infiltration rate, volume of the room = 20 × 30 × 4 = 2400 m^3

Therefore the number of air changes = 1524.2/2400 = 0.635 air changes.

As a thumb rule, one air change is assumed in such offices. It is observed that the actual air change is less than one.

From Eq. 21.62(b) for loose fit and from Table 21.19(c), we have a = 0.25, b= 0.02 and c = 0.022.

V = 25 km/h = 6.94 m/s, $t_o - t_i$ = 43 – 25 = 18°C

Air changes = $a + bV + C\,(t_o - t_i)$ = 0.25 + 0.02 × 6.94 + 0.022(18) = 0.7848 air changes.

This is close to the result from the empirical values in Tables 21.23, 21.24 and 21.27.

Cooling load due to Infiltration

Outdoor: t_o = 43°C and t_o^* = 27°C

From psychrometric calculations:

W_o = 0.016 kgw/kga, RH = 29%, h = 85.0 kJ/kga

Indoor: t_i = 25°C and RH = 50% : From psychrometric calculations:

W_i = 0.01 kgw/kga, h = 50.85 kJ/kga

Infiltration = 1524.2 m^3/h = 25.4 cmm = Q_v

Sensible heat gain due to infiltration (OASH) = 20.4 Q_v (43 – 25) = 20.4 × 25.4 × 18
= 9327.0 W (B)

Latent heat gain due to infiltration (OALH) = 50000(25.4)(0.016 – 0.01) = 7620.0 W (C)

Occupancy

Assume that the occupants do moderate work. From Table 21.13.10, sensible and latent heat load per person is 73 watts and 59 watts respectively. Therefore, for 100 persons

Occupancy load, sensible for 100 persons = 7300 W (D)

Occupancy load, latent for 100 persons = 5900 W (E)

Lighting: 15, 000 W fluorescent = 1.25 × 15,000 = 18,750 W

4000 W tungsten = 4000 W

Lighting sensible load = 22,750 W (F)

Room Sensible Heat Gain (RSH)

A. Heat gain from walls, roof, floor ,windows and doors	= 76,439.0 W
B. Infiltration	= 9327.0 W
D. Occupancy	= 7300.0 W
F. Lighting	= 22,750.0 W
Appliances	= 0.0
Sub total A	= 11,5816.0 W
Safety factor 5%	= 5791.0 W
Sub-total B	= 12,1607.0 W

System heat gains

(a) Leakage heat transfer in the 10% SA duct in non-conditioned space	= 0.5% of RSH
(b) Leakage of supply air in the 10% SA duct in non-conditioned space	= 1.0% of RSH
(c) Fan motor	= 5.0% of RSH
(d) Return air runs in conditioned space	= 0.0%
(e) There is no dehumidifier	= 0.0%
Total system heat gain	= 6.5% of RSH
6.5% of sub-total B	= 7904 W
Room Sensible Heat Gain (RSH)	**= 129511 W**

Room Latent Heat Gain

C. Infiltration	= 7620.0 W
E. Occupancy	= 5900.0 W
Appliances	= 0.0
Sub-total A	= 13,520.0
Safety factor 5%	= 676 W
Sub-total B	= 14,196.0 W

System heat gains

Leakage in 10% of the supply air duct outside the non-conditioned space = 1% of RLH
System heat gain 1% of sub-total B = 142.0 W

Room Latent Heat Gain (RLH) = 14338.00 W

Ventilation: The ventilation requirement is the fresh air requirement for persons. The minimum value from the table in Carrier Handbook is 0.33 cmm per person.
For 100 persons, fresh outdoor air requirement = 33.0 cmm

Outside Air Sensible Heat Load (OASH) = 20.4(33.0)(43 – 25) = 12118 W

Outside Air Latent Heat Load (OALH) = 50000(33)(0.016 – 0.01) = 9900.0 W

OATH = 22,018 W

Total Sensible Heat Load, TSH, = 129,511.0 + 12,118.0 = 141,629.0 W

Total Latent Heat Load, TLH = 14,338 + 9700 = 24238.0 W

Grand Total Heat Load, GTH = 141,629.0 + 24,238.0 = 165,867.0 W

Cooling Load = 165,867/3516.7 = 47.16 TR

On per Unit Area Basis = 0.0786 TR per m^2 or 0.8 TR per 10 m^2

Supply Air Flow Rate

This is determined by Effective Sensible Heat Factor method.

ERSH = RSH + X(OASH) and

ERLH = RLH + X(OALH)

We assume a bypass factor X of 0.15, which is typical of comfort air conditioning

ERSH = 129,511 + (0.15)12118 = 131,329 W

ERLH = 14,338 + (0.15)9900 = 15,823 W

ERTH = ERSH + ERLH = 13,1329 + 15,823 = 147,152 W

ESHF = ERSH/ERTH = 131,329/147,152 = 0.89247

The apparatus dew point is not known. A suitable value above 10°C may be assumed for it and supply airflow rate can be found by trial and error satisfying ERSH, ERLH and the bypass factor. In the following calculations, we use the indoor condition, i.e. Apparatus dew point table given in Carrier Handbook. The ADP table for 25°C indoor temperature and 50% relative humidity is as follows.

ESHF	1.00	0.94	0.84	0.77	0.73	0.7	0.68	0.65	0.63
ADP (°C)	13.89	13.33	12.22	11.11	18.0	8.89	7.78	5.55	2.78
ADP (°F)	57	56	54	52	50	48	46	42	37

Interpolating in this Table for ESHF = 0.89247, we get ADP = 55.05°F = 12.8°C

We assume that the supply air state calculated by using ESHF line is very close to the one on intersection of RSHF line and GSHF lines. We denote this state by 2′ while the actual state is denoted by 2.

Dehumidified temperature rise under this assumption,

$$\Delta t = (t_i - t_{2'}) \approx (t_i - t_2) + (1 - X)(t_i - t_{ADP}) = (1 - 0.15)(25 - 12.8) = 10.37^oC$$

Hence, the air enters the room at $t_{2'} = (25 - 10.37) = 14.63^oC$

$$\therefore \quad (\text{cmm})_d = \frac{\text{ERSH}}{20.4(1 - X)(t_i - t_{ADP})} = \frac{131,329}{20.4 \times 10.37} = 620.8 \text{ cmm}$$

$\therefore$ Supply air flow rate $= Q_{vs} = 620.8$ cmm

Given outside air flow rate $= Q_{vo} = 33$ cmm

$\therefore$ Recirculatd air flow rate $= Q_{vr} = 620.8 - 33 = 587.8$ cmm

Assuming adiabatic mixing of outdoor air and recirculated air and assuming that the densities of the streams are approximately the same,

Temperature of mixed air,

$$t_1 = \frac{Q_{vr}\, t_i + Q_{vo}\, t_o}{Q_{vs}} = \frac{588(25) + 33(43)}{620.8} = 29.95°C$$

This is the inlet state to the cooling coil. Using bypass factor and apparatus dew point,

$$t_2 = t_{ADP} + X(t_1 - t_{ADP}) = 12.8 + 0.15(25.95 - 12.8) = 14.77$$

This is very close to $t_{2'} = 14.67^oC$.

REFERENCES

Alford, J.S., Ryan J.E. and Urban F.O. (1939): *ASHVE Trans*., Vol. 45, pp. 387–392.

ASHVE Trans. (1944): Vol. 50, p. 293.

ASHVE Trans. (1948): Vol. 54, pp. 281–296.

ASHRAE Handbook Fundamentals Volume (1993): American Society of Heating, Refrigerating and Air Conditioning Engineers, Inc., Atlanta, Ga, 26.33–26.34.

ASHRAE Handbook of Fundamentals Volume (1989): American Society of Heating, Refrigerating and Air Conditioning Engineers, Inc., Atlanta, Ga, 26.33–26.34.

ASHRAE Handbook of Fundamentals Volume (1997): American Society of Heating, Refrigerating and Air Conditioning Engineers, Inc., Atlanta, Ga.

ASHRAE Trans., Vol. 69, p. 31.

Carrier Air Conditioning Co., *Handbook of Air Conditioning System Design* (1965): McGraw Hill, New York.

Cobientz, C.W. and Achenbach, F.R. (1963): Field measuremets of air infiltration in ten electrically heated houses, *ASHRAE Trans*, Vol. 69, pp. 358–365.

Mackey, C.O. and Wright L.J., Jr. (1944): Periodic heat flow—Homogeneous walls and roofs, *ASHVE Trans*., p. 293.

Mackey, C.O. and Wright L.J., Jr. (1946): Periodic heat flow—Composite walls and roof.

Mitalas, G.P. (1982): Basement Heat Loss Studies at DBR/NRC, National Research Council of Canada, Division of Building Research, Ottawa.

Parmelee, G.V. (1945): Transmission of Solar Radiation through Flat Glass, *ASHVE Trans*., Vol. 51, pp. 317–350.

Spitler, J.D. (1996): Annotated Guide to Load Calculation Models and Algorithms, *ASHRAE*.

Stewart, J.P. (1948): Solar heat gain through walls and roof for cooling load calculations, *ASHVE Trans*., Vol. 54, pp. 361–388.

REVIEW QUESTIONS

1. A composite wall consists of four different materials as shown below. The thermal conductivities of the materials used are : $k_A = 20$ W/m-°C, $k_B = 10$ W/m-°C, $k_C = 7$ W/m-°C, $k_D = 25$ W/m-°C. If $T_1 = 45$°C and $T_2 = 25$°C, calculate the rate of heat flow through this wall assembly per unit breadth. Assume one-dimensional heat flow only. Also, show the electrical analogue of the problem.

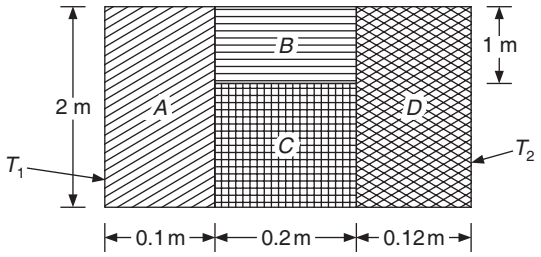

2. A window, set back by 0.25 m from the plane of the building, has 6 mm clear glass of width 2 m and height 1.8 m. The outdoor and indoor temperatures are 35°C and 25°C respectively. Find the total heat transfer through this south-facing window at 3:00 pm solar time on 15 April in Kolkata.

3. The 150-mm concrete, flat roof of a building in Kolkata is sunlit throughout the day on June 1. The indoor design air temperature is 25°C. Find the rate of heat transfer to the room below the roof throughout the day if the variation of sol-air temperature is given by Eq. (21.37).

4. The 150-mm concrete roof of dark colour with density of 1920 kg/m^3 is subjected to outdoor and indoor temperatures of 45°C and 25°C respectively. Find the heat transfer rate at 3:00 pm solar time on June 1 in Kolkata.

22

Room Airflow and Duct Design

LEARNING OBJECTIVES

After studying this chapter the student should be able to:

1. Name the elements of a typical heating ventilating and air conditioning (HVAC) system.
2. Explain the working of a typical air conditioning system with the help of a schematic diagram.
3. Understand the basics of the air distribution system in order to determine the velocity and temperature distribution in a room.
4. Explain the phenomena of losses occurring at inlet and discharge of air ducts due to sudden and smooth changes in area, etc.
5. Explain the phenomenon of airflow through ducts with fan.
6. Explain the important requirements of an air conditioning duct and the general rules to be followed in the design of ducts.
7. Design air conditioning ducts using the velocity reduction method, equal pressure drop method and static region method.
8. Understand the fundamentals behind the desirability of maintaining uniform distribution of air in the air-conditioned space.
9. Explain the parameters involved in a good air distribution system design.

22.1 INTRODUCTION

The purpose of air conditioning systems is to control temperature, relative humidity, air purity and air distribution. In this chapter, the attention is focused on the air distribution in the room. A properly designed and functioning Heating Ventilating and Air Conditioning (HVAC) system will provide a comfortable environment. The elements of the HVAC system include:

- Outdoor fresh air intake through a damper
- Mixed-air plenum with return air control
- Air filters
- Face and bypass dampers
- Heating and cooling coils
- Humidification and/or dehumidification
- Supply air fans
- Exhaust air fans
- Duct work, supply air outlets and return air inlets
- Refrigeration system or a self-contained heating and cooling unit
- Water chiller
- Boiler
- Controls

In an air-conditioned space the ducts, electrical wires, control wires, water lines and other services are located below the roof. A false ceiling is provided to improve the aesthetics of the room. The duct that supplies the conditioned air to the room, called supply air, is located between the ceiling and the false ceiling. The duct that returns the air from the room to the cooling coil is called return air duct. This is also located between the ceiling and the false ceiling. In some cases the space between the ceiling and the false ceiling itself is used as the return air path.

Figure 22.1 shows the airflow arrangement in a typical air conditioning system.

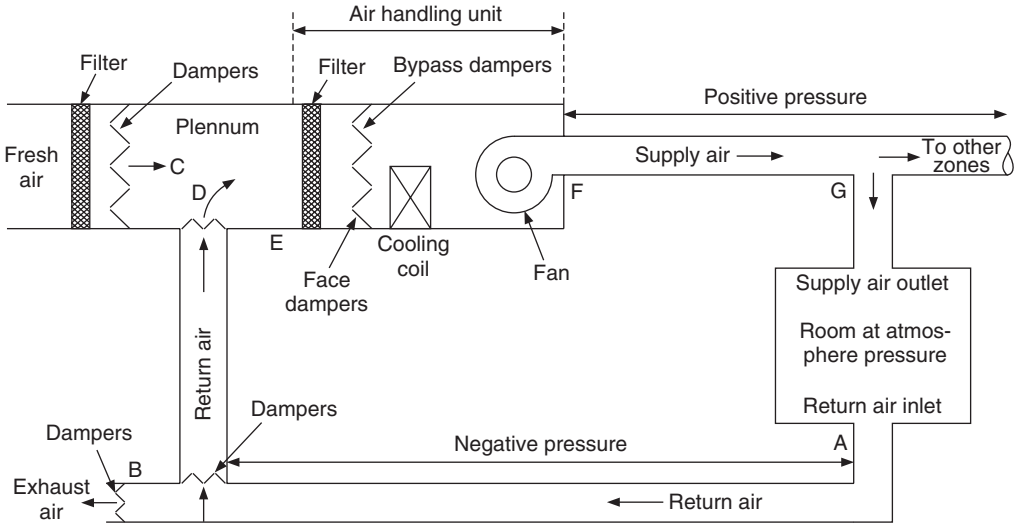

Figure 22.1 Simplified schematic of a typical air conditioning system.

The return air is drawn from the room at point A through the return air duct A–B. Some of the stale return air is thrown out at point B through dampers. Equal amount of fresh air through a filter and damper is taken at point C and mixed with the return air at point D in the plennum. The mixed air flows through a filter and then enters the cooling coil. Some of the air may be bypassed by the

control system from entering the cooling coil. The face dampers control the flow of air through cooling coil while bypass dampers control the flow of bypassed air. In the system shown, a blower or fan draws the air (or forces the air) through the cooling coil. The conditioned air is supplied to the room by supply air duct F–G.

The pressure in the room is either atmospheric or slightly greater than atmospheric. The pressure of the air decreases all along the path from A to point E at the entrance to the air handling unit. The pressure on the suction side of the fan is negative gauge pressure. The pressure in the supply air duct F–G is positive gauge pressure.

The air should be distributed in the room in such a way that the temperature, the relative humidity and the velocity conform to the comfort requirements, and in addition the air purity is maintained in the occupied zone. The occupied zone is the space in the room up to 1.8 m above the floor level and 0.6 m from all the walls. From the comfort point of view the conditions in the room may be maintained within the comfort zone given in Table 22.1. This table shows the combinations of temperature and relative humidity, which conform to comfort zone to be maintained in the room.

Table 22.1 Combinations of temperature and relative humidity for comfort

Humidity (%)	*Winter temperature* (°C)	*Summer temperature* (°C)
30	20.3–24.44	23.3– 26.7
40	20.3–24.2	23.0– 26.4
50	20.3– 23.6	22.8– 26.1
60	20.3– 23.3	22.5– 25.55

The room air distribution should be such that the variation of temperature within a room from one corner to another is not more than 1°C, and from one room to another room not more than 2°C. Further, the air distribution system should ensure that the velocities in the occupied zone are in the range of 0.1 to 0.15 m/s. The preferred direction of airflow is from the side towards the face of a person. Air velocity directed towards the back or the feet is undesirable. The maximum permissible velocity is 0.25 m/s for a sitting person and 0.35 m/s for a moving person.

22.1.1 Draft

As the air velocity increases, the convective heat transfer rate from the body increases and one gets a feeling of cold. This is referred to as *draft condition* or *chill factor* under freezing conditions. Draft is a localized feeling of coolness or warmth felt by the body due to air movement and temperature, other parameters like humidity and mean radiant temperature being constant. At higher velocities, comfort may be achieved at higher temperatures. An increase in velocity by 0.15 m/s causes the same increase in heat transfer rate as a 1° decrease in the dry-bulb temperature would cause. The draft is measured with respect to a temperature of 24.4°C (at the centre of the room) with air moving at 0.15 m/s. The difference in effective temperature for comfort at velocity V m/s is given by

$$\Delta t_e = (t - 24.4) - 7.656(V - 0.1516) \tag{22.1}$$

Besides being uncomfortable, workers can become ill from the air they breathe inside while at work. Symptoms of "*sick building syndrome*" include headaches, coughing, dizziness, fatigue, nausea, rashes, breathing problems, and irritation of the eyes, nose and throat. In most cases, these complaints only last while the workers are in the building. Workers can also get serious illnesses because of poor indoor air. "Building related illnesses" include Legionnaires' disease, humidifier fever, chronic fatigue syndrome, and multiple chemical sensitivity.

Over the years very leak-tight building shells have been designed which have reduced the infiltration and the cooling load considerably. Better insulation materials and application methods have also reduced the cooling load. On account of these, the supply air requirement has also reduced considerably. It has become a challenging task to distribute the reduced quantity of supply air uniformly in the room and it is equally challenging to collect the pollutants and separate them. This has in turn led to *sick building syndrome*. To understand the basics of the air distribution system, we summarize here the required concepts of fluid mechanics outlined in Chapter 2. Three basic concepts or laws are used to determine the velocity and temperature distribution in a room. These are *mass conservation, momentum conservation* and *energy conservation*. Mass conservation can either be applied to a control volume or it may be applied to an elemental control volume and in the limit of control volume tending to zero, it may be obtained as an equation valid at all the points of flow regime. The latter case requires that the medium be fairly dense or the concept of continuum be valid so that the limit of elemental control volume tending to a point may be taken, the equation in this case is called the *continuity equation*.

22.2 CONTINUITY EQUATION

Mass can neither be created nor be destroyed. The flow in the air conditioning ducts is usually a steady flow and in general the pressure and temperature changes being small the density is almost constant. The velocities are usually very small compared to the velocity of sound, as a result the flow may be considered incompressible. The continuity equation or the mass conservation equation for a duct shown in Figure 22.2 will remain constant, that is,

$$\dot{m} = \rho_1 V_1 A_1 = \rho_2 V_2 A_2 \tag{22.2}$$

If the area of cross section increases in the flow direction as shown in Figure 22.2, the velocity will decrease, that is if $A_2 > A_1$ then $V_2 < V_1$ since density $\rho_1 = \rho_2$.

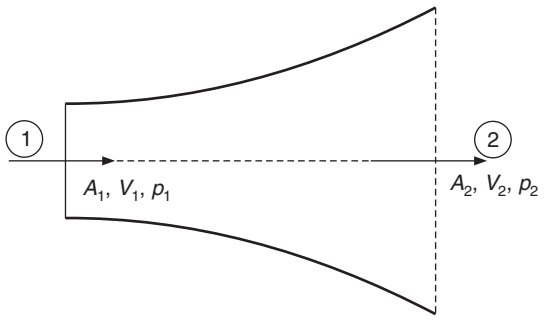

Figure 22.2 The continuity equation for steady flow of air through a duct.

For a continuum, the continuity equation, valid at any point in a flow field in incompressible flow, is as follows.

$$\nabla \cdot \bar{V} = 0 \quad \text{or} \quad \frac{\partial u}{\partial x} + \frac{\partial v}{\partial y} + \frac{\partial w}{\partial z} = 0 \tag{22.3}$$

where $\bar{V}$ is the velocity vector, u, v and w are the velocity components in x-, y- and z-directions, respectively.

EXAMPLE 22.1 The velocity at section 1 in Figure 22.2 is 3 m/s and the diameter of the duct is 0.5 m. Find the velocity at section 2 where the diameter is 1.0 m. The temperature of the air is 16°C throughout the duct and the pressure is standard atmospheric pressure. Find the mass flow rate of air as well.

Solution:

We have $V_1 = 3.0$ m/s; $d_1 = 0.5$ m and $d_2 = 1.0$ m, gas constant for air $R = 287.1$ J/kg-K
Assuming the density of air to be constant, from Eq. (23.2), we get

$$V_2 = V_1\,(A_1/A_2) = V_1(\pi d_1^2/4)/(\pi d_2^2/4) = V_1(d_1/d_2)^2 = 3(0.5)^2 = 0.75 \text{ m/s}$$

$$\rho_1 = \frac{p}{RT} = \frac{101325}{(287.1)(273+16)} = 1.2212 \text{ kg/m}^3$$

$$\therefore \qquad \dot{m} = \rho_1 V_1 A_1 = \frac{1.2212\pi(0.5)^2\,(3.0)}{4} = 0.7193 \text{ kg/s}$$

22.3 MOMENTUM CONSERVATION

Momentum conservation involves the application of Newton's second law of motion to a fluid control volume. This essentially means that the rate of change of momentum for the control volume with respect to time and the momentum flux across the control volume is equal to the sum of the forces acting on the control volume. In this case too, we may either apply the momentum theorem to a control volume or find out the equation valid for all the points of the flow field in the limit of continuum. For a control volume in steady state, we may write the momentum theorem in x-direction as follows:

$$(\text{Momentum})_{\text{out}} \text{ in } x\text{-direction} - (\text{Momentum})_{\text{in}} \text{ in } x\text{-direction} = \Sigma F_x \tag{22.4}$$

The forces consist of surface forces like shear stress and body force like gravity. For example, consider a fluid flowing through a duct shown in Figure 22.2. The shear stress acting on the walls of the duct and the force due to gravity are neglected. We consider only the pressure forces. The pressures at inlet and outlet are gauge pressures, that is, measured relative to atmospheric pressure. Atmospheric pressure acts on the outer boundary. The circumferential component of atmospheric pressure cancels out and the component in the x-direction is taken care of by the gauge pressures. The momentum theorem yields:

$$\dot{m}V_2 - \dot{m}V_1 = p_1A_1 - p_2A_2 + F_x \tag{22.5}$$

where F_x is the resisting force acting on the support of the duct.

The mass conservation for this control volume is given by

$$\dot{m} = \rho_1 V_1 A_1 = \rho_2 V_2 A_2 \quad \text{where, for incompressible flow, } \rho_1 = \rho_2$$

Substituting this in the momentum Eq. (22.5), we get

$$\rho V_2^2 A_2 - \rho V_1^2 A_1 = p_1 A_1 - p_2 A_2 + F_x \tag{22.6}$$

EXAMPLE 22.2 Referring to Figure 22.2, at the inlet the velocity V_1= 3 m/s, A_1 = 0.2 m^2, p_1 = 50 Pa gauge. The area at the outlet A_2 = 0.4 m^2 and the density may be assumed to be constant and equal to 1.2 kg/m^3. Find the pressure p_2 and the force acting on the support.

Solution:

From mass conservation equation, $V_2 = V_1 A_1 / A_2 = 3(0.2/0.4) = 1.5$ m/s

$$\therefore \quad \dot{m} = \rho V_1 A_1 = 1.2(3.0)0.2 = 0.72 \text{ kg/s}$$

It is given that the flow is frictionless; hence we use Bernoulli's equation to find the pressure at the outlet p_2.

$$p_2 = p_1 + \rho(V_1^2 - V_2^2)/2$$

or
$$p_2 - p_1 = \rho V_1^2[1 - (A_1/A_2)^2]/2 = 1.2(9)(1 - 0.25)/2 = 4.05 \text{ Pa}$$

The rise in pressure in a diverging passage is called *regain*. In this case it is equal to 4.05 Pa, under the assumption of frictionless flow. In real flow when friction is considered, region will be less than this value.

$$\therefore \quad p_2 = 50 + 4.05 = 54.05 \text{ Pa}$$

Substituting in Eq. (22.5), we get

$$F_x = \dot{m}(V_2 - V_1) + p_2 A_2 - p_1 A_1 = 0.72(1.5 - 3.0) + 54.05(0.4) - 50(0.2)$$

or
$$F_x = -1.08 + 21.62 - 10.0 = 10.54 \text{ N}$$

F_y = 0.0 since there is no change in momentum in y-direction.

It is observed that this method can give only gross results for a system. The details of velocity profiles, pressure distribution, shear stress etc. cannot be obtained by this method. For these details, we have to consider the momentum equation for continuum. Considering the stress–strain rate relations for a Stokesian fluid, the momentum equations valid at any point in the flow field for incompressible flow with constant fluid properties, called *Navier Stokes equations*, are as follows:

$$\rho(\partial \bar{V} / \partial t + \bar{V}.\nabla \bar{V}) = -\nabla p + \mu \nabla^2 \bar{V} + \rho g \tag{22.7}$$

where, g is the acceleration due to gravity and μ is the coefficient of viscosity.

In the absence of shear stress, these equations reduce to *Euler's equations*, namely

$$\rho(\partial \bar{V} / \partial t + \bar{V}.\nabla \bar{V}) = -\nabla p + \rho g \tag{22.8}$$

Integrating these equations along a streamline or integrating them between any two points in irrotational flow, we get

$$p + \rho V^2/2 + \rho gz = \text{constant} \tag{22.9}$$

This is known as *Bernoulli's equation*. This was derived from energy equation in Chapter 2.

22.4 ENERGY EQUATION

For a continuum, considering the convection of energy by fluid and Fourier's law for conduction heat transfer, neglecting viscous dissipation and work done by pressure, the energy equation valid at any point in the flow field for steady incompressible flow with constant fluid properties, is as follows:

$$\rho c_p \left(\frac{\partial T}{\partial t} + \bar{V}.\nabla T \right) = k\nabla^2 T \tag{22.10}$$

One seeks solutions of Navier Stokes equations and the energy equation to find the velocity and temperature distribution in a flow field that may be the room space. In case of study of pollutants generated or introduced into the room, one seeks the solution of the concentration of pollutant species in the room. The governing equation for species concentration $C(x, y, z, t)$ is very similar to energy equation. This equation is as follows:

$$\rho c_p \left(\frac{\partial C}{\partial t} + \bar{V}.\nabla C \right) = k\nabla^2 C \tag{22.11}$$

22.5 STATIC, DYNAMIC AND TOTAL PRESSURE

The Bernoulli's Eq. (22.9) is applicable to ideal fluid, that is, in the absence of viscosity or shear stress. It consists of three terms and these are called:

$p = p_s$	: static pressure with units of pascal.
$p_v = \rho V^2/2$	: velocity pressure. This also has units of pascal
ρgz	: pressure due to datum or the potential energy

In the absence of shear stress, the sum of these pressures is constant and it is called total pressure p_T. That is, the Bernoulli's equation is written as follows:

$$p_s + p_v + \rho gz = p_T = \text{constant}$$

It is possible to convert kinetic energy into pressure by reducing the velocity as a consequence of change in the area of cross section of the duct. Similarly, the potential energy, that is, the elevation of the duct can be changed into static pressure.

The pressures can be written in terms of millimetre or metre of water column too. In such a case, Bernoulli's equation is written as follows:

$$\frac{p_1}{\rho g} + \frac{V_1^2}{2g} + z_1 = \text{constant} \tag{22.12}$$

If there is a fan in the duct, which adds energy H_f, and if H_l is the loss in energy to overcome frictional effects, then

$$\frac{p_1}{\rho g} + \frac{V_1^2}{2g} + z_1 + H_f = \frac{p_2}{\rho g} + \frac{V_2^2}{2g} + z_2 + H_l \tag{22.13}$$

Both H_f and H_l are gain in head and loss in head and the unit of both is m or mm. In fact, dimensions of both $p/(\rho g)$ and V^2/g are in metre.

EXAMPLE 22.3 For the duct layout of Figure 22.2, $A_1 = 0.4$ m^2 and $A_2 = 1.6$ m^2. The volume flow rate is 200 cmm. The static pressure at inlet $p_1 = 30$ mm gauge of water and the pressure drop in the duct due to friction is 10 mm of water. Find the static pressure p_2.

Solution:

We rewrite Eq. (22.13) as follows.

$$\frac{p_2}{\rho g} = \frac{p_1}{\rho g} + \frac{(V_1^2 - V_2^2)}{2g} + z_1 - z_2 + H_f - H_l$$

In this equation the dimensions are in metre of air column.

$H_f = 0.0$, $p_1 = 0.03$ m of water gauge, $H_l = 0.01$ m of water, $Q_v = 200$ cmm, we find V_1 and V_2 from $Q_v = V_1A_1 = V_2A_2$.

$$V_1 = 200/0.4 = 500 \text{ m/min} = 8.33 \text{ m/s} \quad \text{and} \quad V_2 = 200/(1.6 \times 60) = 2.083 \text{ m/s}$$

$$\frac{(V_1^2 - V_2^2)}{2g} = \frac{(8.33)^2 - (2.083)^2}{2 \times 9.81} = 3.318 \text{ m of air}$$

$$= 3.318 \times 1.2/1000 = 0.00398 \text{ m of water}$$

$$= 39.0625 \text{ Pa}$$

$$\therefore \quad \frac{p_2}{\rho g} = 0.03 + 0.00398 + 0.0 - 0.0 + 0.0 - 0.01 = 0.024 \text{ m of water}$$

$$\therefore \quad p_2 = 1000 \times 9.81 \times 0.024 = 235.44 \text{ Pa}$$

In this case there is gain in velocity pressure by 39.0625 Pa due to reduction in velocity in the increasing area section. The velocity pressure is explained below.

Velocity pressure (dynamic pressure)

The expression for the velocity pressure can be simplified if one considers air of standard density of 1.2 kg/m^3. The expression for velocity pressure reduces to

$$p_v = (1.2/2)V^2 = 0.6V^2 \text{ Pa} \quad \text{and} \quad V = 1.291\sqrt{p_v} \text{ m/s} \tag{22.14}$$

Also $\quad 1 \text{ bar} = 10^5 \text{ Pa} = 10.2 \text{ m of water}$

$$\therefore \quad 1 \text{ Pa} = 1.02 \times 10^{-4} \text{ m of water} = 0.102 \text{ mm of water}$$

$$\therefore \quad 1 \text{ mm of water} = 9.81 \text{ Pa}$$

$$\therefore \quad p_v = 0.6V^2 \text{ Pa} = 0.6V^2/(9.81) \text{ mm of water} = 0.0612V^2 = \left(\frac{V}{4.04}\right)^2 \text{ mm of water}$$

$$p_v = \left(\frac{V}{4.04}\right)^2 \text{ mm of water} \quad \text{and} \quad V = 4.04\sqrt{p_v} \text{ m/s} \tag{22.15}$$

EXAMPLE 22.4 In Example 22.2 the velocity and pressure at inlet are 3 m/s and 50 Pa respectively. At the outlet these are 1.5 m/s and 54.05 Pa respectively. Find the velocity pressures at inlet and outlet, and show that the total pressure is constant.

Solution:

At inlet, $p_{v1} = 0.6V_1^2 = 0.6(3)^2 = 5.4$ Pa = 0.5504 mm of water

At outlet, $p_{v2} = 0.6V_2^2 = 0.6(1.5)^2 = 1.35$ Pa = 0.1377 mm of water

Also 50 Pa = 50/9.81 = 5.097 mm of water and 54.05 Pa = 5.5097 mm of water

At inlet, $p_{s1} + pv_1 = 50 + 5.4 = 55.4$ Pa = 5.097 + 0.5504 = 5.6474 mm of water

At outlet, $p_{s2} + p_{v2} = 54.05 + 1.35 = 55.4$ Pa = 5.5097 + 0.1377 = 5.6474 mm of water

Hence the total pressure is the same at inlet and at outlet. It was expected since Bernoulli's equation was used to determine $p_{s2.}$

22.6 PRESSURE DROP

The pressure of the fluid in the duct decreases due to three main reasons:

(i) Friction and turbulence
(ii) Change in area
(iii) Sudden change in the flow direction.

The pressure drop is grouped into two categories, *frictional pressure drop* and the *minor loss*. The minor loss is due to area change and change in the direction of the flow. In the presence of friction there will be some pressure drop to overcome the frictional resistance, this pressure drop is denoted by Δp_L. In this case the total pressure will decrease in the flow direction by Δp_L.

$$p_{T1} = p_{T2} + \Delta p_L$$

or
$$p_{s1} + p_{v1} = ps_2 + p_{v2} + \Delta p_L \tag{22.16}$$

Turbulence and friction dissipate kinetic energy and cause an increase in internal energy and temperature. The drop Δp_L in pressure causes adiabatic expansion, which leads to a drop in temperature. Hence the temperature does not change appreciably due to these two factors.

If there is a fan between the two sections, then the fan will add energy to the fluid and the total pressure will increase. Equation (22.16) may then be rewritten as follows:

$$p_{s1} + p_{v1} + FTP = p_{s2} + p_{v2} + \Delta p_L \tag{22.17}$$

where, *FTP* is the fan total pressure.

Conversion of velocity pressure into static pressure

The static pressure in a duct may increase in the flow direction if the velocity decreases. This occurs because of the conversion of kinetic energy into pressure head. This pressure rise is called *Static Regain*. It occurs if the area increases in the flow direction as in a diffuser. All of us have experienced this phenomenon while holding a hand in front of a stream of water from a hose; we feel the velocity pressure as the kinetic energy is converted to pressure.

22.6.1 Frictional Pressure Drop and Friction Factor

One of the simplest solutions of Navier Stokes equations is for steady, fully developed, laminar incompressible flow in a circular duct of radius R. This is known as Hagen–Poiseuille flow. Fully developed flow implies that the velocity profile does not change in the flow direction, hence the momentum also doe not change in the flow direction. It has been shown in Chapter 2 that the parabolic velocity profile for this case is given by,

$$U = 2\bar{U}[1 - (r/R)^2] = U_{\max}\,[1 - (r/R)^2] \tag{22.18}$$

The maximum velocity $U_{\max}$ occurs at duct centre and is twice the average velocity $\bar{U}$, where, $\bar{U} = Q/(\pi R^2)$ is the average velocity in the duct. The average velocity $\bar{U}$ is related to pressure gradient as follows:

$$\bar{U} = \left(\frac{dp}{dx}\right)\frac{R^2}{8\mu} \tag{22.19}$$

The shear stress at the duct wall is given by the following expression:

$$\tau_w = \mu\left(\frac{dU}{dr}\right)_{r=R} = \frac{4\mu\bar{U}}{R} \tag{22.20}$$

There are two ways of defining the friction factor, namely the Fanning friction factor and the Darcy Weisbach friction factor. These are defined as follows. The Fanning friction factor is essentially the skin friction coefficient and is non-dimensional wall shear stress.

$$\text{Fanning friction factor, } f = \frac{\tau_w}{0.5\rho\bar{U}^2} \tag{22.21}$$

Substituting for τ_w from Eq. (22.20), we get

$$f = \frac{4\mu\bar{U}}{R(0.5\rho\bar{U}^2)} = \frac{16\mu}{\rho\bar{U}d} = \frac{16}{\text{Re}} \tag{22.22}$$

where, Re = $\rho\bar{U}d/\mu$ is the Reynolds number.

Darcy Weisbach friction factor f' is defined to evaluate the frictional pressure drop Δp_f in a length L of a duct of diameter d , that is,

$$f' = \frac{\Delta p_f}{(\rho\bar{U}^2/2)(L/d)}$$

or

$$\Delta p_f = f'\frac{L}{d}\frac{\rho\bar{U}^2}{2} \tag{22.23}$$

Substituting for Δp_f from Eq. (22.19) by taking $dx = L$ and $dp = \Delta p_f$, we get

$$f' = \frac{8\mu\bar{U}L}{R^2}\frac{d}{L}\frac{2}{\rho\bar{U}^2} = \frac{64}{\text{Re}} \tag{22.24}$$

It is observed that Darcy Weisbach friction factor is four times the Fanning friction factor.

$$f' = 4f \tag{22.25}$$

The textbooks give different explanations for the relation (22.25). One of the common methods is to define d as the hydraulic diameter, $d_h = A/P = \pi d^2/4(\pi d) = d/4$ and express the pressure drop in terms of Fanning friction factor as follows:

$$\Delta p_f = f \frac{L}{d_h} \frac{\rho \bar{U}^2}{2}$$

In Eq. (22.23) the hydraulic diameter $d_h = 4A/P = d$, as is conventional, is used. The readers are referred to textbooks by Streeter (1981) and White (1987) for details regarding this and for correlations for friction factor.

Equation (22.24) applies to only laminar flow where the Reynolds number is less than 2300. For turbulent flow, the expression given by Colebrook and White is used for Fanning friction factor, namely,

$$\frac{1}{\sqrt{f}} = -4 \log_{10} \left[\frac{k_s}{3.7 d} + \frac{1.255}{(\mathrm{Re})\sqrt{f}} \right] \tag{22.26}$$

where k_s is the average roughness of the inner pipe wall expressed in same units as the diameter d. Evaluation of f from this equation requires iteration since f occurs on both the sides of it. ASHRAE (1997) gives the following form for the determination of friction factor, i.e.

$$f_1 = 0.11(k_s/D_h + 0.68/\mathrm{Re})^{0.25} \tag{22.27}$$

If f_1 determined from the above equation equals or exceeds 0.018, then f is taken to be same as f_1. If it is less than 0.018, then f is given as follows:

$$f = 0.85 f_1 + 0.0028 \tag{22.28}$$

Another straightforward equation suggested by Haaland (1983) is as follows:

$$\frac{1}{f^{1/2}} \approx -1.8 \log_{10} \left[\frac{6.9}{\mathrm{Re}} + \left(\frac{k_s/d}{3.7} \right)^{1.11} \right] \tag{22.29}$$

These equations can be simplified for sheet-metal ducts, which have $k_s \approx 0.00015$ m.

Further, properties of moist air at standard atmospheric pressure of 101.325 Pa, 20°C, 43% relative humidity, were taken by Fritzsche as $\rho = 1.2$ kg/m^3 and $\mu = 1.8 \times 10^{-5}$ Pa-s to yield the following relation.

$$\Delta p_f = \frac{0.01422 V^{1.852} L}{D^{1.269}} \text{ Pa} \tag{22.30}$$

This can be rearranged by using the volume flow rate $\dot{Q}_v = \pi D^2 V/4$, to give

$$\Delta p_f = \frac{0.022243 \dot{Q}_v^{1.852} L}{D^{4.973}} \text{ Pa} \tag{22.31}$$

or

$$\Delta p_f = \frac{0.002268 \dot{Q}_v^{1.852} L}{D^{4.973}} \text{ mm of water} \tag{22.32}$$

Or in terms of V and $\dot{Q}_v$, by eliminating D

$$\Delta p_f = \frac{0.012199 V^{2.4865} L}{\dot{Q}_v^{0.6343}} \text{ Pa} \tag{23.33}$$

Friction factor chart is also available which has flow rate in m^3/s on the ordinate and friction loss in Pa/m of the duct on the abscissa. The velocity and the duct diameter are the parameters. It should be kept in mind that this chart and the Fritzsche's equations given above are valid for standard air and duct roughness of 0.00015 m. If the duct has acoustic lining or is made of fibre glass, concrete or plastic, then it may have a different roughness. In such a case with little effort, Eq. (22.26) may be solved on PC numerically. The values given by Fritzsche's equations may be corrected for actual temperature and other environmental conditions by using the following correction factor.

$$\text{Correction factor, } C = \left(\frac{\rho}{1.2}\right)^{0.9} \left(\frac{\mu}{1.8 \times 10^{-5}}\right)^{0.1} \tag{22.34}$$

Fritzsche's equations have been used to develop friction charts with friction loss $\Delta p_f/L$ (Pa/m) on the abscissa and flow rate Q_v in m^3/s on the ordinate. These charts for low and high velocities, respectively, are shown in Figures 22.3 and 22.4. The duct diameter D and the velocity V are the parameters in these plots. These are valid for pipe roughness $k_s \approx 0.00015$ m, standard atmospheric pressure of 101.325 Pa, 20°C, 43% relative humidity. These charts are applicable for GI sheet metal ducts and should not be used for plastic, fiber glass, concrete or wooden ducts. For small differences in the density and temperature of air the pressure drop Δp_f may be corrected as follows.

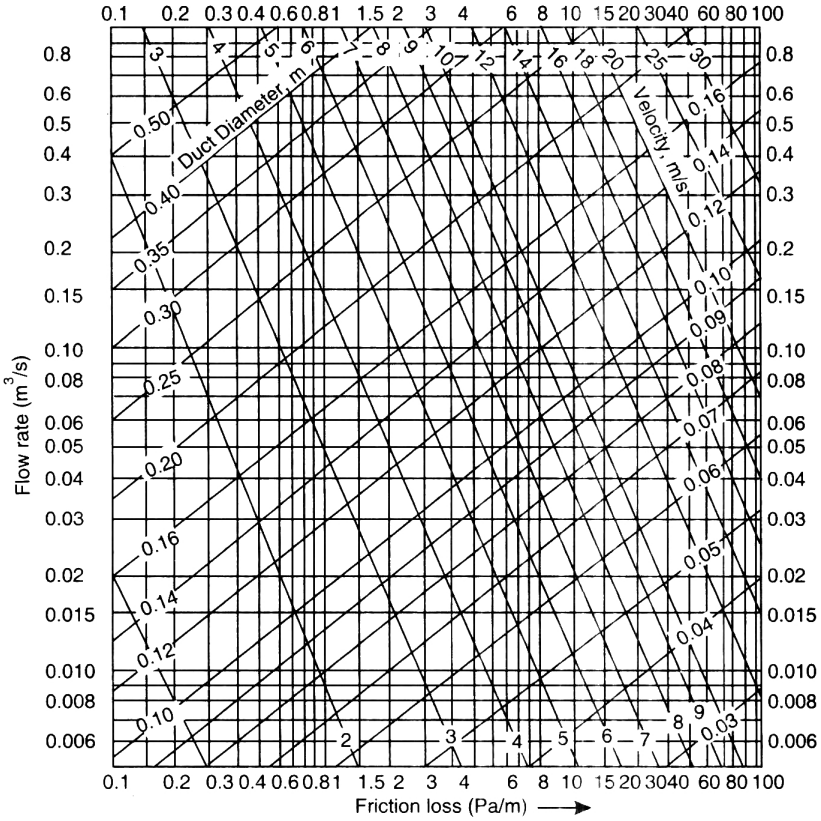

Figure 22.3 Flow rate vs. friction loss for low velocities.

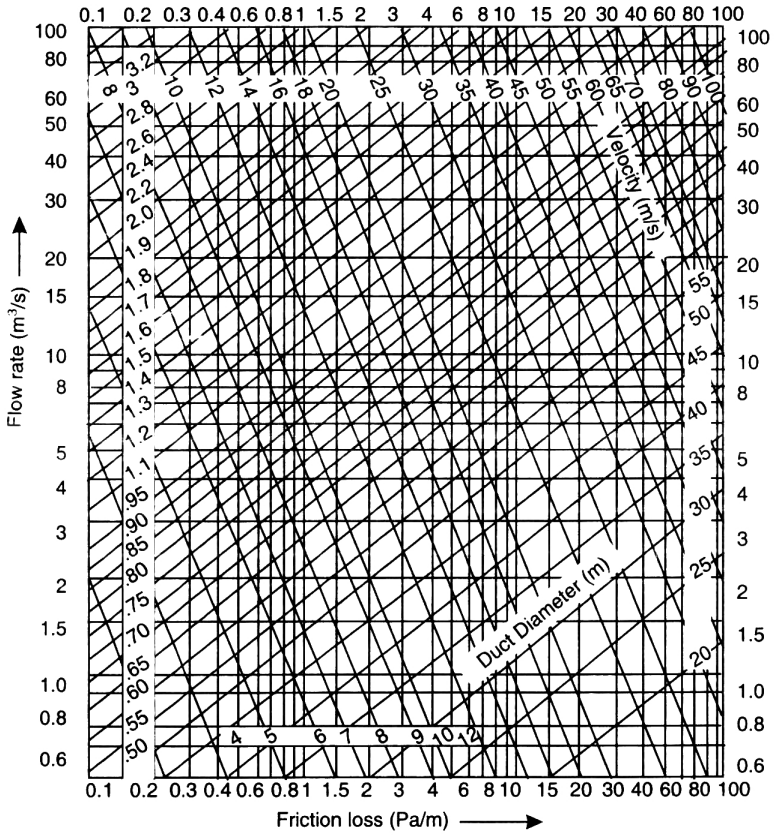

Figure 22.4 Duct friction chart for high velocities.

$$\Delta p_f \propto \rho \tag{22.35a}$$

$$\Delta p_f \propto T^{-0.857} \tag{22.35b}$$

The effects of pressure drop rate are considerable for ducts made of materials other than GI sheets. Some typical correction factors are given in Table 22.2.

Table 22.2 Correction factors for pressure drop in ducts of various materials

Material	*Absolute roughness, k_s* (mm)	*Correction factor for various Δp_f* (Pa/m)			
		0.5	1.0	2.0	5.0
G.I. sheet steel	0.015	1.0	1.0	1.0	1.0
G.I. sheet steel spirally wound	0.075	0.95	0.94	0.93	0.92
Aluminium sheet	0.05	0.93	0.91	0.9	0.88
Cement or plaster	0.25	1.07	1.08	1.08	1.09
Fair faced brick	1.3	1.42–1.41	1.50–1.45	1.54–1.48	1.63–1.54
Rough brick	5.0	2.18–1.97	2.46–2.04	2.62–2.12	2.76–2.23

The pressure drop in spiral ducts depends upon the extent of tightening of the spiral. The pressure drop rate in a flexible duct could double if the duct is only 75% extended. The guidelines laid down by manufacturers should be followed to determine the pressure drop rate. Ducts made of permeable cloth are also used in industrial applications. The air diffuses uniformly at low velocity throughout the length of the duct. These are usually made of polypropylene, polyester and nylon. Cloth is a hygroscopic substance, hence it is not recommended since it may cause the growth of microorganisms. The cloth duct also acts as a filter and may need periodic laundering. Cement ducts may be used for underground air distribution and for corrosive materials. Fibre glass ducts are used for low velocity application. The fibre glass provides insulation as well as acoustic lining.

22.7 CONVERSION FROM CIRCULAR TO RECTANGULAR DIMENSIONS

The circular cross section has the minimum value of perimeter to the area of cross section, i.e. *P/A*. Hence, the frictional resistance offered by walls is minimum for ducts with circular cross section. However, circular ducts are not convenient since they occupy large areas. Hence, ducts with rectangular cross section are used in air conditioning. The corners of rectangular ducts contain recirculating eddies which cause loss of energy. This becomes worse if the aspect ratio exceeds four. The empirical equations for pressure drop and friction coefficient are available for circular ducts; hence it is convenient to find the sizes of circular ducts for given volume flow rates and velocities. After this the size may be converted to rectangular dimensions. *The conversion from circular section to rectangular section is done in such a way that for the same surface* roughness*, the volume flow rate and the rate of pressure drop is the same in two ducts*.

The pressure drop in a circular duct of diameter d, velocity V, and length L, and Fanning friction factor f is given by

$$\Delta p = \frac{2\rho f L V^2}{d} \tag{22.36}$$

For circular ducts, $A = \pi d^2/4$ and $P = \pi d$ which gives $d = 4A/P$. Substituting this in Eq. (22.26) for pressure drop, we get

$$\Delta p = \frac{\rho f L V^2}{2}\frac{P}{A} \tag{22.37}$$

Volume flow rate is given by the relation $V = Q/A$. Therefore, we have

$$Q = \sqrt{\frac{2\Delta p}{fL}}\sqrt{\frac{A^3}{P}} \tag{22.38}$$

It has been assumed that for the rectangular duct and the circular duct the volume flow rate Q, pressure drop Δp, friction actor f, density ρ and length L are the same, hence from Eq. (22.38), $\sqrt{A^3/P}$ must be the same for the two ducts. If a and b are the dimensions of the rectangular duct, then $P = 2(a + b)$ and $A = ab$ and then equating $\sqrt{A^3/P}$, we get

$$\sqrt{\frac{\pi^3 d^6}{64\pi d}} = \sqrt{\frac{(ab)^3}{2(a+b)}} \tag{22.39}$$

Simplifying, it yields

$$d = 1.265 \sqrt[5]{\frac{(ab)^3}{(a+b)}} \tag{22.40}$$

Equation (22.40) is approximated as follows:

$$d = 1.3 \frac{(ab)^{0.625}}{(a+b)^{0.25}} \tag{22.41}$$

If the surface roughness values of the circular and rectangular ducts are not the same and are f_c and f_r respectively, then we may write

$$d = 1.265 \sqrt[5]{\frac{f_c (ab)^3}{f_r (a+b)}} \tag{22.42}$$

If all other parameters are the same, the preferred duct sections are as follows:

1. Spirally-wound circular
2. Circular duct rolled from flat sheet
3. Square
4. Rectangular with aspect ratio not exceeding 3.

Calculations for the duct design are usually done in terms of circular ducts. Then for a calculated value of diameter the equivalent duct dimensions, the width a and depth b of rectangular duct are found either from Eq. (22.41) or from Table 22.3. One of the duct dimensions, usually the depth b, is fixed from the availability of ceiling height and the width a is found from Eq. (22.41) by iteration. An approximate value may be obtained from Table 22.3 (ASHRAE 1989) and then the exact value is found by iteration from Eq. (22.41). In Table 22.3 the first row and the first column indicate the dimensions a and b of rectangular duct, while the values in the middle of the table indicate equivalent circular diameters. The dimensions are in centimetre. In fact, the table is valid for all dimensions; the dimension of diameter will be same as that of the sides. For dimensions more than100 cm the table does not give the results. These can be calculated easily from Eq. (22.41).

Round ducts require minimum duct material for a given flow rate and velocity. However, the space around the circle is wasted and the duct occupies a large part near the ceiling requiring the false ceiling to be located at lower heights. Further it does not give an aesthetic look. A square duct is closest to circular duct from the friction rate point of view. All buildings have supporting beams and the ducts have to run below them. The beams reduce the clear height available for the ducts. In air-conditioned spaces, architects do not provide liberal ceiling heights. As a result, it is not possible to use square ducts either. Rectangular ducts are used in most cases. The duct material requirement increases with increase in aspect ratio and so does the friction rate or the pressure drop rate.

Table 22.3 Equivalent diameters for rectangular ducts of given dimensions

Side a of rectangular duct	*Diameter d of circular duct*																
	b=4.0	4.5	5.0	5.5	6.0	6.5	7.0	7.5	8.0	9.0	10.0	11.0	12.0	13.0	14.0	15.0	16.0
3.0	3.8	4.0	4.2	4.4	4.6	4.8	4.9	5.1	5.2	5.5	5.7	6.0	6.2	6.4	6.6	6.8	7.0
3.5	4.1	4.3	4.6	4.8	5.0	5.2	5.3	5.5	5.7	6.0	6.3	6.5	6.8	7.0	7.2	7.4	7.6
4.0	4.4	4.6	4.9	5.1	5.3	5.5	5.7	5.9	6.1	6.4	6.8	7.1	7.3	7.6	7.8	8.1	8.3
4.5	4.6	4.9	5.2	5.4	5.6	5.9	6.1	6.3	6.5	6.9	7.2	7.5	7.8	8.1	8.4	8.6	8.9
5.0	4.9	5.2	5.5	5.7	6.0	6.2	6.4	6.7	6.9	7.3	7.6	8.0	8.3	8.6	8.9	9.1	9.4
5.5	5.1	5.4	5.7	6.0	6.3	6.5	6.8	7.0	7.2	7.6	8.0	8.4	8.7	9.0	9.4	9.6	9.8

Side a of rectangular duct	6	7	8	9	10	11	12	13	14	15	16	17	18	19	20	22	24	26	28	30	*Side a of rectangular duct*
6	6.6																				6
7	7.1	7.7																			7
8	7.4	8.2	8.8																		8
9	8.0	8.6	9.3	9.9																	9
10	8.4	9.1	9.8	10.4	10.9																10
11	8.8	9.5	10.2	10.8	11.4	12.0															11
12	9.1	9.9	10.7	11.3	11.9	12.5	13.1														12
13	9.5	10.3	11.1	11.8	12.4	13.0	13.6	14.2													13
14	9.8	10.7	11.5	12.2	12.9	13.5	14.2	14.7	15.3												14
15	10.1	11.0	11.8	12.6	13.3	14.0	14.6	15.3	15.8	16.4											15
16	10.4	114	12.2	13.0	13.7	14.4	15.1	15.7	16.3	16.9	17.5										16
17	10.7	11.7	12.5	13.4	14.1	14.9	14.5	16.1	16.8	17.4	18.0	18.6									17
18	11.0	11.9	12.9	13.7	14.5	15.3	16.0	16.6	17.3	17.9	18.5	19.5	19.7								18
19	11.2	12.2	13.2	14.1	14.9	15.6	16.4	17.1	17.8	18.4	19.0	19.6	20.2	20.8							19
20	11.5	12.5	13.5	14.4	15.2	15.9	16.8	17.5	18.2	18.8	19.5	20.1	20.7	21.3	21.9						20
22	12.0	13.1	14.1	15.0	15.9	16.7	17.6	18.3	19.1	19.7	20.4	21.0	21.7	22.3	22.9	24.1					22
24	12.4	13.6	14.6	15.6	16.6	17.5	18.3	19.1	19.8	20.6	21.3	21.9	22.6	23.2	23.9	25.1	26.2				24
26	12.8	14.1	15.2	16.2	17.2	18.1	19.0	19.8	20.6	21.4	22.1	22.8	23.5	24.1	24.8	26.1	27.2	28.4			26
28	13.2	14.5	15.6	16.7	17.7	18.7	19.6	20.5	21.3	22.1	22.9	23.6	24.4	25.0	25.7	27.1	28.2	29.5	30.6		28
30	13.6	14.9	16.1	17.2	18.3	19.3	20.2	21.1	22.0	22.9	23.7	24.4	25.2	25.9	26.7	28.0	29.3	30.5	31.6	32.8	30
32	14.0	15.3	16.5	17.7	18.8	19.8	20.8	21.8	22.7	23.6	24.4	25.2	26.0	26.7	27.5	28.9	30.1	31.4	32.6	33.8	32
34	14.4	15.7	17.0	18.2	19.3	20.4	21.4	22.4	23.3	24.2	25.1	25.9	26.7	27.5	28.3	29.7	31.0	32.3	33.6	34.8	34
36	14.7	16.1	17.4	18.6	19.8	20.9	21.9	23.0	23.9	24.8	25.8	26.6	27.4	28.3	29.0	30.5	32.0	33.0	34.6	35.8	36
38	15.0	16.4	17.8	19.0	20.3	21.4	22.5	23.5	24.5	25.4	26.4	27.3	28.1	29.0	29.8	31.4	32.8	34.2	35.5	36.7	38
40	15.3	16.8	18.2	19.4	20.7	21.9	23.0	24.0	25.1	26.0	27.0	27.9	28.8	29.7	30.5	32.1	33.6	35.1	36.4	37.6	40
42	15.6	17.1	18.5	19.8	21.1	22.3	23.4	24.5	25.6	26.6	27.6	28.5	29.4	30.4	31.2	32.8	34.4	35.9	37.3	38.6	42
44	15.9	17.5	18.9	20.2	21.5	22.7	23.9	25.0	26.1	27.2	28.2	29.1	30.0	31.0	31.9	33.5	35.2	36.7	38.1	39.5	44
46	16.4	17.8	19.2	20.6	21.9	23.2	24.3	25.5	26.7	27.7	28.7	29.7	30.6	31.6	32.5	34.2	35.9	37.4	38.9	40.3	46
48	16.5	18.1	19.6	20.9	22.3	23.6	24.8	26.0	27.2	28.2	29.2	30.2	31.2	32.2	31.1	34.9	36.6	38.2	39.7	41.2	48
50	16.8	18.4	19.9	21.3	22.7	24.0	25.2	26.4	27.6	28.7	29.8	30.8	31.8	32.8	33.7	35.5	37.3	38.9	40.4	42.0	50
52	17.0	18.7	20.2	21.6	23.1	24.4	25.6	26.8	28.1	29.2	30.3	31.4	32.4	33.4	34.3	36.2	38.0	39.6	41.2	42.8	52
54	17.3	19.0	20.5	22.0	23.4	24.8	26.1	27.3	28.5	29.7	30.8	31.9	32.9	33.9	34.9	36.8	38.7	40.3	42.0	43.6	54
56	17.6	19.3	20.9	22.4	23.8	25.2	26.5	27.7	28.9	30.1	31.2	32.4	33.4	34.5	35.5	37.4	39.3	41.0	42.7	44.3	56

(*Contd.*)

Table 22.3 Equivalent diameters for rectangular ducts of given dimensions (contd.)

Side a of rectangular duct	6	7	8	9	10	11	12	13	14	15	16	17	18	19	20	22	24	26	28	30	*Side a of rectangular duct*
58	17.8	19.5	21.1	22.7	24.2	25.5	26.9	28.2	29.3	30.5	31.7	32.9	33.9	35.0	36.0	38.0	39.8	.41.7	43.4	45.0	58
60	18.1	19.8	21.4	23.0	24.5	25.8	27.3	28.7	29.8	31.0	32.2	33.4	34.5	35.5	36.5	38.6	40.4	42.3	44.0	45.8	60
62	18.3	20.1	21.7	23.3	24.8	26.2	27.6	29.0	30.2	31.4	32.6	33.8	35.0	36.0	37.1	39.2	41.0	42.9	44.7	46.5	62
64	18.6	20.3	22.0	23.6	25.2	26.5	27.9	29.3	30.6	31.8	33.1	34.2	35.5	36.5	37.6	39.7	41.6	43.5	45.4	47.2	64
66	18.8	20.6	22.3	23.9	25.5	26.9	28.3	29.7	31.0	32.2	33.5	34.7	35.9	37.0	38.1	40.2	42.2	44.1	46.0	47.8	66
68	19.2	20.8	22.5	24.2	25.8	27.3	28.7	30.1	31.4	32.6	33.9	35.1	36.3	37.5	38.6	40.7	42.8	44.7	46.6	48.4	68
70	19.2	21.0	22.8	24.5	26.1	27.6	29.1	30.4	31.8	33.1	34.3	35.6	36.8	37.9	39.1	41.3	43.3	45.3	47.2	49.0	70
72	19.4	21.3	23.1	24.8	26.4	27.9	29.4	30.8	32.2	33.5	34.8	36.0	37.2	38.4	39.6	41.8	43.6	45.9	47.8	49.7	72
74															40.0	42.3	44.4	46.4	48.4	50.3	76
76															40.5	42.6	44.9	47.0	49.0	50.8	76
78															40.9	43.3	45.5	47.5	49.5	51.5	78
80															41.3	43.8	46.0	48.0	50.1	52.0	80
82															41.8	44.2	46.4	48.6	50.6	52.6	82
84															42.2	44.6	46.9	49.2	51.1	53.2	84
86															42.6	45.0	47.4	49.6	51.6	53.7	86
88															43.0	45.4	47.9	50.1	52.2	54.3	88
90															43.4	45.9	48.3	50.6	52.8	54.8	90
92															43.8	46.3	48.7	51.1	53.4	55.4	92
94															44.3	46.8	49.2	51.5	53.7	55.8	94
96															44.6	47.2	49.5	52.0	54.4	56.3	96

Side a of rectangular duct	32	34	36	38	40	42	44	46	48	50	52	56	60	64	68	72	76	80	84	88	*Side a of rectangular duct*
32	35.0																				32
34	36.0	37.2																			34
36	37.0	38.2	39.4																		36
38	38.1	39.2	40.4	41.6																	38
40	39.0	40.2	41.4	42.6	43.8																40
42	39.9	41.1	42.4	43.6	44.8	45.9															42
44	40.8	42.0	43.4	44.6	45.8	46.9	48.1														44
46	41.7	43.0	44.3	45.6	46.8	47.9	49.1	50.3													46
48	42.6	43.9	45.2	46.5	47.8	48.9	50.2	51.3	52.6												48
50	43.5	44.8	46.1	47.4	48.8	49.8	51.2	52.3	53.6	54.7											50
52	44.3	45.7	47.1	48.3	49.7	50.8	52.2	53.3	54.6	55.8	56.9										52
54	45.0	46.5	48.0	49.2	50.6	51.8	53.2	54.3	55.6	56.8	57.9	60.1									54
56	45.8	47.3	48.8	50.1	51.5	52.7	54.1	55.3	56.5	57.8	58.9	61.3	63.4								56
58	46.6	48.1	49.6	51.0	52.4	53.7	55.0	56.2	57.5	58.8	60.0	62.3	64.5	71.5							58
60	47.3	48.9	50.4	51.8	53.3	54.6	55.9	57.1	58.5	59.8	61.0	63.3	65.7	67.7	69.8						60
62	48.0	49.7	51.2	52.6	54.2	55.5	56.8	58.0	59.4	60.7	62.0	64.3	66.7	68.9	71.0	73.0					62
64	48.7	50.4	52.0	53.4	55.0	56.4	57.7	59.0	60.3	61.6	62.9	65.3	67.7	70.0	72.1	74.2	76.2				64
66	49.5	51.1	52.8	54.2	55.8	57.2	58.6	59.9	61.2	62.5	63.9	66.3	68.7	71.1	73.2	75.3	77.4	79.3			66

(*Contd.*)

Table 22.3 Equivalent diameters for rectangular ducts of given dimensions (contd.)

Side a of rectangular duct	32	34	36	38	40	42	44	46	48	50	52	56	60	64	68	72	76	80	84	88	*Side a of rectangular duct*
68	50.2	51.8	53.5	55.0	56.6	58.0	59.5	60.8	62.1	63.4	64.8	67.3	69.7	72.1	74.4	76.5	78.5	80.6	82.5		68
70	50.9	52.5	54.2	55.8	57.3	58.8	60.3	61.7	63.0	64.3	65.7	68.3	70.7	73.1	75.4	77.6	79.7	81.8	83.7	85.7	70
72	51.5	53.2	54.9	56.5	58.0	59.6	61.1	62.6	63.9	65.2	66.6	69.2	71.7	74.1	76.4	78.8	80.6	82.9	84.9	86.9	72
74	52.1	53.9	55.6	57.2	58.8	60.4	61.9	63.3	64.8	66.1	67.5	70.1	72.7	75.1	77.4	79.9	83.2	84.1	86.1	88.1	74
76	52.7	54.6	56.3	57.9	59.5	61.2	62.7	64.1	65.6	67.0	68.4	71.0	73.6	76.1	78.4	80.9	84.2	85.2	87.3	89.3	76
78	53.3	55.2	57.0	58.6	60.3	62.0	63.4	64.9	66.4	67.9	69.3	71.8	74.5	77.1	79.4	81.8	84.2	86.3	88.5	90.5	78
80	53.9	55.8	57.6	59.3	61.0	62.7	64.1	65.7	67.2	68.7	70.1	72.7	75.4	78.1	80.4	82.6	85.2	87.5	89.6	91.7	80
82	54.5	56.4	58.2	60.0	61.7	63.4	64.9	66.5	68.0	69.5	71.0	73.6	76.3	79.0	81.4	83.8	86.2	88.6	90.7	92.8	82
84	55.1	57.0	58.9	60.7	62.4	64.1	65.7	67.3	68.8	70.3	71.3	74.5	77.2	79.9	82.4	84.8	87.2	89.6	91.9	94.0	84
86	55.7	57.6	59.5	61.3	63.0	64.8	66.4	68.0	69.5	71.1	72.6	75.4	78.1	80.8	83.3	85.8	88.2	90.6	92.9	95.1	86
88	56.3	58.2	60.1	62.0	63.7	65.4	67.0	68.7	70.3	71.8	73.4	76.3	79.0	81.6	84.2	86.8	89.2	91.6	93.9	96.3	88
90	56.9	58.8	60.7	62.6	64.4	66.0	67.8	69.4	71.1	72.6	74.2	77.1	79.9	82.5	85.1	87.8	90.2	92.6	94.9	97.3	90
92	57.4	59.4	61.3	63.2	65.0	66.8	68.5	70.1	71.8	73.3	74.9	77.9	80.8	83.4	86.0	88.7	91.2	93.6	95.9	98.3	92
94	57.9	60.0	61.9	63.8	65.6	67.5	69.2	70.8	72.5	74.1	75.6	78.7	81.7	84.3	86.9	89.6	92.1	94.6	96.9	99.3	94
96	58.4	60.5	62.4	64.4	66.2	68.2	69.8	71.5	73.2	74.3	76.3	79.4	82.6	85.2	87.8	90.5	93.0	95.6	97.9	100.3	96

22.8 MINOR LOSSES

These pressure looses occur whenever the magnitude or the direction of velocity changes. The magnitude change may be due to change in the area of the cross section of the duct and the direction changes are due to bends in the duct. These are expressed in terms of downstream velocity pressure. The losses occurring at inlet and discharge of the ducts, sudden and smooth changes in area, etc. are described below.

22.8.1 Losses at Inlet to Ducts

Figure 22.5 shows the streamline pattern at the inlet to a duct. The fan in the duct aspirates the air into the duct, which accelerates the otherwise stationary air into the duct. The air comes from all the directions. The streamline close to the wall turns around by 180°. Similarly the other streamlines also turn through some angle. Only the streamline along the duct axis enters the duct straight. The net effect of these curved streamlines is that a vortex is formed at the inlet. The flow inside this vortex is recirculatrory and turbulent leading to loss of pressure and energy. The area available to the flow decreases, becomes minimum at a point and then increases due to this vortex. The minimum area is called *vena contracta* and denoted by A_c. If the duct area of cross section is A, then an area coefficient C_A is defined as follows:

$$C_A = A_c/A \tag{22.43}$$

The pressure distribution is also shown in the figure. The static pressure and total pressure are gauge pressures. As *vena contracta* is approached, the area decreases; velocity and the velocity pressure increases and thereby the static pressure decreases. In absence of losses, the total pressure would have remained constant. However in this case the total pressure decreases, that is, the static pressure

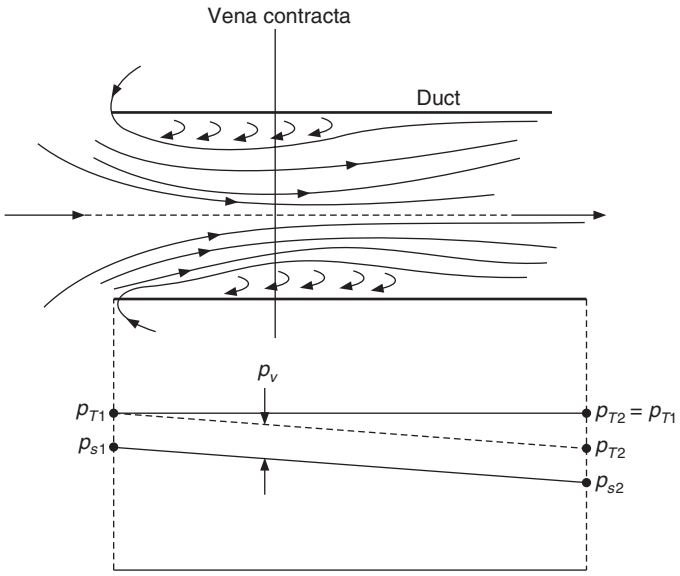

Figure 22.5 A simple duct system (straight section).

drops to overcome losses due to *vena contracta*. In the absence of these losses the velocity would have been larger for the same pressure drop. Hence a velocity coefficient is defined as follows:

$$C_v = \frac{\text{actual velocity at vena contracta}}{\text{velocity that would occur in absence of losses}} \tag{22.44}$$

The entry coefficient is the product of area coefficient and the velocity coefficient, that is,

$$C_E = C_A C_v \tag{22.45}$$

The actual volume flow rate is given by

$$Q_{\text{actual}} = C_E\, Q_{\text{ideal}} \tag{22.46}$$

The coefficient C_E is of the order of 0.85.

Entrance losses from a room to a duct are strongly dependent upon the entrance geometry. Sharp edges or protrusions in the entrance cause large losses. A little rounding can significantly reduce the losses. Reentrant entrance has smaller losses.

22.8.2 Losses at Discharge from Ducts

The pressure at the outlet of the duct has to be atmospheric pressure since there are no restraining walls. The velocity just at the exit remains unchanged and as the fluid comes out of the duct, it finds more outside area and the velocity decreases. The static pressure (which is gauge pressure in this case) reduces to zero at the outlet. The total energy leaving the duct is therefore the kinetic energy $\rho V^2/2$ of the air stream, which is dissipated.

Effect of grille

If a grille is placed at the outlet, some effort will be required for the fluid to flow through the passages of the grille; as a result, there will be some drop in static pressure. The static pressure just inside the grille in this case will be more than the atmospheric by the extent of pressure drop. The velocity usually remains unchanged during the flow through the passage unless there is a large change in area. If there is a loss of Δp_s across the grille, the total energy dissipated would be $\Delta p_s + \rho V^2/2$.

22.8.3 Loss in Sudden Expansion and Static Regain

Figure 22.6 shows a sudden enlargement of the duct where the area A_1 of the duct is suddenly increased to A_2. This causes a decrease in velocity and an increase in static pressure. The fluid cannot execute sharp 90° bends at the site of abrupt area change since the velocity gradient becomes very large giving rise to large shear stress. Therefore there will be two sitting eddies at the corners providing a cushion to the main flow. These eddies will have recirculatory turbulent flow which will cause dissipation of kinetic energy. A control volume shown by dashed line is considered for analysis. Newton's second law of motion is applied to this control volume in the following form for steady flow.

Momentum out – Momentum in = Net force in the x-direction

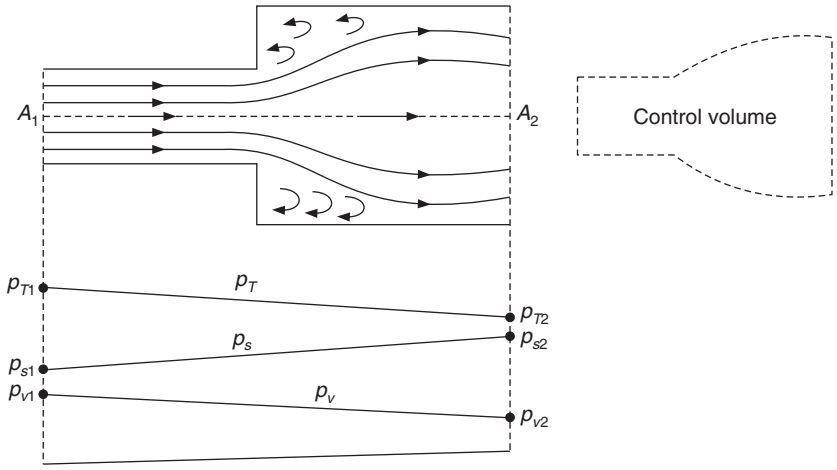

Figure 22.6 Sudden enlargement of the duct.

The forces due to shear stresses are neglected and only the force due to pressure is considered. In steady flow the mass flow rate $\dot{m} = \rho VA$ will be constant at all cross sections. Hence assuming the density ρ to be constant,

$$\rho V_1 A_1 = \rho V_2 A_2 \tag{22.47}$$

The area A_2 is greater than A_1, hence velocity V_2 will be less than V_1.

Momentum theorem may be written as

$$\dot{m}(V_2 - V_1) = A_2(p_{s1} - p_{s2})$$

or
$$\rho V_2 A_2 (V_2 - V_1) = A_2(p_{s1} - p_{s2}) \tag{22.48}$$

The static pressure increases since the kinetic energy decreases. This rise in static pressure is called static regain, denoted by SR, which is given by

$$\text{SR} = (p_{s2} - p_{s1}) = \rho V_2 (V_1 - V_2) \tag{22.49}$$

The total pressure decreases from p_{T1} to p_{T2}, hence the pressure loss may be expressed as

$$\Delta p_l = p_{T1} - p_{T2} = (p_{s1} - p_{s2}) + (p_{v1} - p_{v2}) = \rho(V_2^2 - V_1 V_2) + \rho(V_1^2 - V_2^2)/2$$

$$= \rho(V_1 - V_2)^2/2 \tag{22.50}$$

Substituting from Eq. (22.47), we get

$$\Delta p_l = \frac{1}{2}\rho V_2^2 \left(\frac{A_2}{A_1} - 1\right)^2 = \frac{1}{2}\rho V_1^2 \left(1 - \frac{A_1}{A_2}\right)^2 = K_{SE} p_{v2} \tag{22.51}$$

The coefficient K_{SE} is called the *dynamic loss coefficient* due to sudden expansion. The actual loss is more than this since viscous effects have not been included in this derivation. If the area ratio A_2/A_1 is denoted by λ, then we may write

$$\lambda = A_2/A_1$$

$$K_{SE} = (\lambda - 1)^2 \tag{22.52}$$

As the area A_2 increases the loss coefficient increases.

Area A_2 is greater than A_1, hence the loss coefficient K_{SE} is greater than 1. Some authors define the loss coefficient based upon the inlet velocity pressure p_{v1} as follows:

$$\Delta p_l = \frac{1}{2}\rho V_1^2 \left(1 - \frac{A_1}{A_2}\right)^2 = K'_{SE} p_{v1}$$

In this case the coefficient K'_{SE} is always less than one. If A_2 happens to be a room, that is, $A_1/A_2 \to 0$, then $\Delta p_l \to 0.5\rho V^2$. This implies that all the kinetic energy is dissipated.

The maximum value of regain will be as follows:

$$\text{SR} = p_{v1} - p_{v2} - \Delta p_l$$

Substituting for Δp_l, we get

$$\text{SR} = 0.5\rho(V_1^2 - V_2^2) - 0.5\,\rho V_2^2 \left(\frac{A_2}{A_1} - 1\right)^2 = \rho(V_1 V_2 - V_2^2)$$

$$\therefore \qquad \text{SR} = 2(\lambda - 1)p_{v2} \tag{22.53}$$

This is same as the expression given by Eq. (22.49).

22.8.4 Loss in Gradual Expansion

Figure 22.7 shows a gradual expansion of the included angle 2θ. The angle θ is 90° for sudden enlargement and 0° for a straight section. For small angles, there is no turbulence and the friction is neglected for the ideal case, hence there will be no loss in total pressure. Hence, we may write

$$p_{T1} = p_{T2} \quad \text{or} \quad p_{s1} + p_{v1} = p_{s2} + p_{v2}$$

or

$$p_{v1} - p_{v2} = p_{s2} - p_{s1}$$

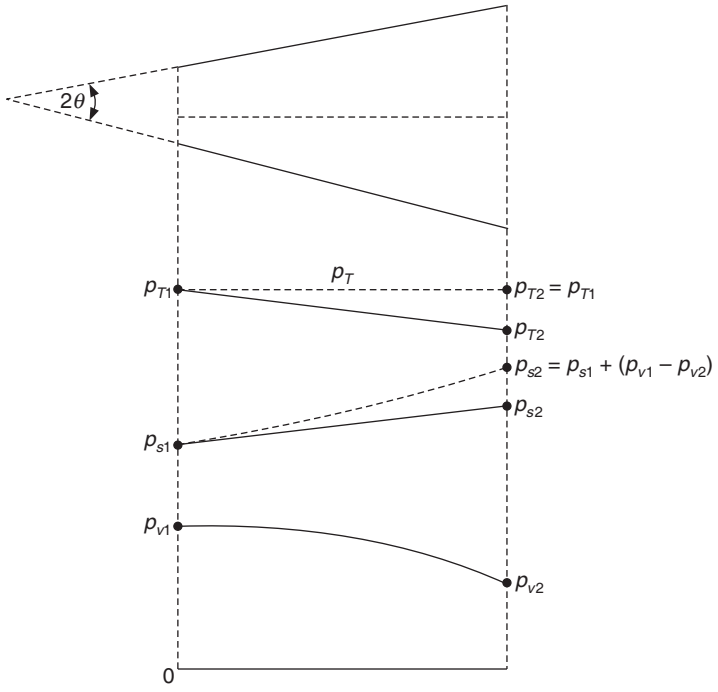

Figure 22.7 Gradual enlargement of the duct.

Therefore for the ideal case of no friction, the rise in static pressure is equal to drop in dynamic pressure and the static regain is given by

$$\text{SR} = p_{s2} - p_{s1} \tag{22.54}$$

The figure shows the ideal case by dashed lines and the actual case by solid lines. In the actual case, the total pressure will decrease by Δp_l and regain will be less than the ideal value. Therefore, static regain is given by

$$\begin{aligned} \text{SR} &= p_{s2} - p_{s1} = p_{v1} - p_{v2} - \Delta p_l \\ &= R(p_{v1} - p_{v2}) \\ \Delta p_l &= (1 - R)(p_{v1} - p_{v2}) = K_E\,(p_{v1} - p_{v2}) \end{aligned} \tag{22.55}$$

K_E is called the loss coefficient for the gradual expansion. The loss coefficient K_{SE} is maximum for the abrupt expansion. K_r denotes the ratio of K_E and K_{SE}.

$$\therefore \qquad K_r = K_E/K_{SE} \tag{22.56}$$

where K_{SE} is given by Eq. (22.52). The value of loss coefficient K_r for various half angles θ is as follows.

Angle θ	5	7	10	20	30	40
K_r	0.17	0.22	0.28	0.45	0.59	0.73

The loss coefficient for angles greater than 40° to 60° is so excessive that it is better to use the coefficient for sudden expansion with K =1. This is due to flow separation in the diffuser. In the diffuser the pressure increases in the flow direction. Viscous effects retard the flow in the boundary layer at the walls. In addition the pressure rise also retards the flow. As a result, the flow leaves the boundary layer and tends to flow backwards near the wall, giving rise to a recirculatory separation bubble. This causes loss in total pressure. For small angles the length of expansion becomes very large, hence most of the loss is due to friction. Included angle of 5° has the minimum loss and angles more than 18° cause flow separation. The loss coefficient for angles greater than 40° to 60° is so large that it is better to use sudden expansion rather than gradual expansion. This is due to flow separation in the boundary layer due to adverse pressure gradient in the diffuser section. The flow near the wall in the boundary layer is retarded by friction. It will continue to flow due to its inertia if the pressure decreases in the flow direction. In the diffuser the pressure increases in the flow direction. This further retards the flow, which cannot continue to flow in the streaming direction. It leaves the boundary region and tends to flow backwards in the direction of decreasing pressure. This leads to recirculating flow and turbulent flow, which causes excessive pressure drop.

22.8.5 Sudden Contraction

The airflow through a sudden reducer is shown in Figure 22.8. Two vorticies are formed due to sharp corners of the sudden reducer. One vortex is located in the large duct and the other is located in the narrower duct. The velocity is larger in the narrower duct; hence major loss occurs in this part of the duct from vena contracta to downstream velocity V_2. By analogy with the treatment of sudden expansion, we can show by using the momentum theorem between the vena contracta and the outlet that,

$$\Delta p_l = p_{Tc} - p_{T2} = \rho(V_c - V_2)^2/2 = \rho V_2^2\,(V_c/V_2 - 1)^2/2 \tag{22.57}$$

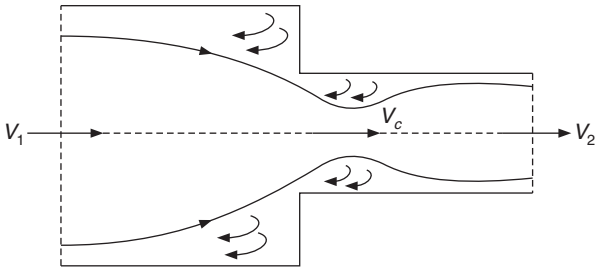

Figure 22.8 Sudden contraction.

The coefficient of area is defined for the vena contracta as follows:

$$C_c = A_c/A_2 = V_2/V_c \tag{22.58}$$

The pressure loss may be written as follows:

$$\Delta p_l = \rho V_2^2(1/C_c - 1)^2/2 \tag{22.59}$$

The loss in the duct of larger area, which is the upstream part, has been neglected in this expression. Textbooks on Fluid Mechanics indicate that C_c for water flow is about 0.62 for the circular orifice, which gives a value of 0.376 for $(1/C_c - 1)^2$. Hence in terms of velocity pressure $p_{v2} = \rho V_2^2/2$, we get

$$\Delta p_l = 0.376\, p_{v2} \tag{22.60}$$

The theory of vena contracta is not well developed, hence some textbooks write this as a correlation in terms of area ratio or diameter ratio for circular ducts. For circular tubes the following correlation is a good approximation.

$$\Delta p_l = K_{sc}\, p_{v2}$$
$$K_{SC} = 0.42[1 - (d_2/d_1)^2] \tag{22.61}$$

In general, the pressure loss may be expressed in terms of a loss coefficient K_c such that,

$$\Delta p_l = K_c\, p_{v2}$$

For flow of air in rectangular ducts the coefficient K_c has been observed to be 0.5 for sudden contraction. For gradual expansion the value of K_c is not very large. For a few angles of gradual expansion, these values are as follows:

Angle, θ	30	45	60
K_r	0.02	0.04	0.07

The values of vena contracta determined by Weisbach with experiments on water for various area ratios are as follows:

A_2/A_1	0.1	0.2	0.3	0.4	0.5	0.6	0.7	0.8	0.9	1.0
C_c	0.624	0.632	0.643	0.659	0.681	0.712	0.755	0.813	0.892	1.0

22.8.6 Minor Losses in Bends, Elbows and Tees

In this case too, the loss is expressed as a fraction of dynamic pressure in the bend. The area of the bend is usually constant and hence the calculation of the velocity pressure is straightforward. Otherwise the area has to be estimated from the geometry and the velocity pressure calculated. The loss depends upon the curvature of the section, the slope of the section and the angle through which the air stream is turned.

Figures 22.9(a) and (b) show the plan of the ducts of rectangular and circular cross-section respectively with a 90° bend. R_t and R_c denote the throat radius and the centreline radius of the duct respectively. Figure 22.9(c) shows a duct, which turns around by an angle θ only. The curvature is usually expressed as the ratio R_t or R_c to the width a parallel to the radius, that is R_c/a.

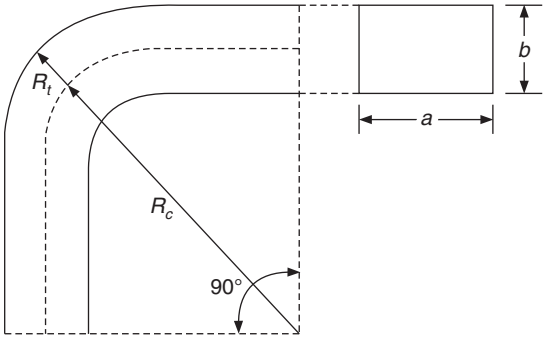

Figure 22.9(a) Duct of rectangular cross section with 90° bend.

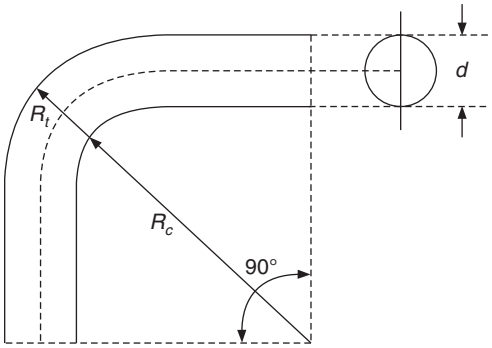

Figure 22.9(b) Duct of circular cross section with 90° bend.

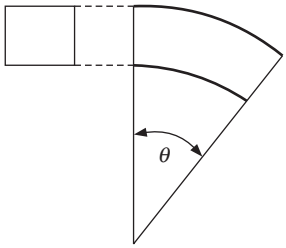

Figure 22.9(c) A duct turning around by an angle θ only.

For ducts with large radius of curvature to width ratio, there is less likelihood of flow separation and secondary flows leading to losses of kinetic energy. If the bend is gradual, then the skin friction plays a major role. However, smooth bends are more expensive to make and more unsightly in appearance. A good value of R_c/a is 1.0. A bend of 45° has a K value of 0.6 times that of 90° bend. Two 90° bends smoothly joined together will have a K value of 1.8 times that of 90° bends.

The aspect ratio (a/b) of the duct also affects the loss coefficient. A large aspect ratio offers a large value of K and hence is not desirable. A square cross section has minimum loss coefficient. The loss coefficient can be reduced by two methods, namely

1. Splitter blades
2. Turning vanes

Splitters are used when the a/b ratio is large and R_t/a is small. They divide the duct into several subsections of smaller aspect ratio which reduces the secondary flows and turbulence, thereby the pressure loss is also reduced. The noise also reduces. Experiments suggest that the pressure loss depends more strongly upon the curve ratio, that is, the heel/throat ratio, where heel is the outer radius for each passage. It is recommended that the duct be divided into sub-passages such that each passage has the same curve ratio, that is, referring to Figure 22.10, we get

$$C = \frac{R_0}{R_1} = \frac{R_1}{R_2} = \cdots = \frac{R_n}{R_{n+1}} \tag{22.62}$$

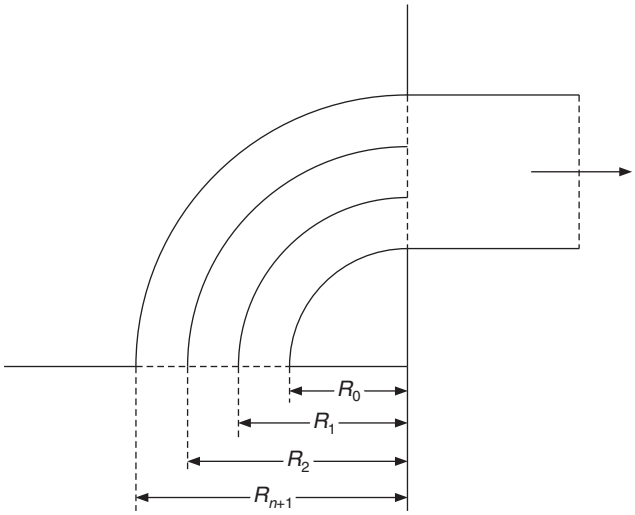

Figure 22.10 90 degree rectangular section with splitter vanes.

Therefore, $$R_1 = R_0/C,\ R_2 = R_1/C = R_0/C^2,\ ...,\ R_{n+1} = \frac{R_0}{C^{n+1}}$$

Therefore, $$C = \left(\frac{R_0}{R_{n+1}}\right)^{1/(n+1)} = k^{1/(n+1)} \quad \text{where,} \quad k = \frac{R_0}{R_{n+1}} \tag{22.63}$$

It is observed that the first splitter is closer to the throat than it is to the heel. In fact, more splitters are put closer to the throat where the scope of turning for the fluid is very sharp. It is seldom necessary to use more than two splitters since it is expensive to make splitters.

One of the best ways to reduce the energy loss in the bends is to use the mitred bend, which contains a number of aerofoil shaped turning vanes. Simple types of vanes are also used. This may have double the loss compared to an ordinary bend with R_c/a equal to unity. Table 23.4 gives the values of loss coefficient K for various bends.

Table 22.4 Pressure loss in elbows, bends and tees

90° circular elbow	R_c/d	K
	Miter	1.3
	0.5	0.9
	1.0	0.33
	1.5	0.24
	2.0	0.19

90°	b/a	R_c/a	K	b/a	R_c/a	K	b/a	R_c/a	K	b/a	R_c/a	K
rectangular	4.0	Miter	1.35	2.0	Miter	1.47	1.0	miter	1.5	0.25	Miter	1.38
elbow	4.0	0.5	1.25	2.0	0.5	1.1	1.0	0.5	1.0	0.25	0.5	0.96
	4.0	0.75	0.6	2.0	0.75	0.5	1.0	0.75	0.41	0.25	0.75	0.37
	4.0	1.0	0.37	2.0	1.0	0.28	1.0	1.0	0.22	0.25	1.0	0.19
	4.0	1.5	0.19	2.0	1.5	0.13	1.0	1.5	0.09	0.25	1.5	0.07

(*Contd.*)

Table 22.4 Pressure loss in elbows, bends and tees (contd.)

θ^o circular or rect. bend	(θ^o/90) times the value of K for a similar 90° bend								
Miter with turning vanes	: K = 0.1 to 0.35 depending on manufacturer's recommendation								
Miter Tee with vanes	: K same as that for equivalent elbow								
90°-section with splitter vanes	R_c/a	R_1/a	K	L_e/a	R_c/a	R_1/a	R_2/a	K	L_e/a
	Miter	0.5		28	Miter	0.3	0.5		22
	0.5	0.4	0.7	19	0.5	0.2	0.4	0.45	16
	1.0	1.0	0.13	7.2	0.75	0.4	0.7	0.12	
	1.5		0.12		1.0	0.7	1.0	0.1	
					1.5	1.3	1.6	0.15	

22.8.7 Loss in Branches

Figure 22.11 shows a branch marked 3 taken from the main duct 1–2. There will be pressure loss since the flow direction as well as the area changes. The exact value of loss depends upon the way the branch is constructed. *ASHRAE Handbook of Fundamentals Volume* (1997) Section 32.7 gives extensive information on loss coefficients. Losses occur along 1–2 as well as along 1–3. There will also be static regain depending upon the area A_2 or velocity V_2. The static regain reduces due to losses in the section. The static regain factor is around 0.9 for well-designed and constructed circular ducts with no reducing section, which increases the velocity. The regain factor may be small in rectangular ducts of large aspect ratio or in branches immediately after a branch or some other disturbance.

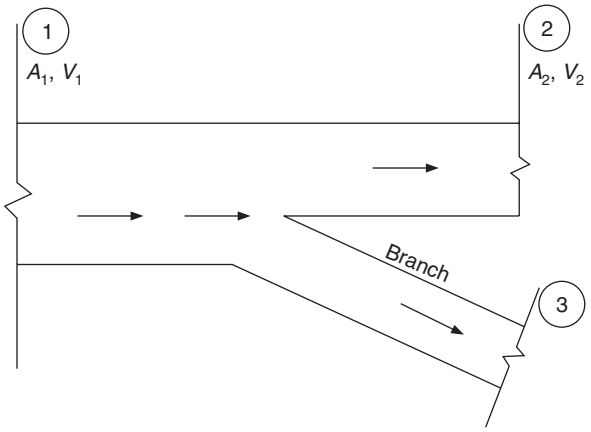

Figure 22.11 A branch take-off and a straight through duct in a duct run.

An approximate value of regain factor R = 0.75 may be taken for a straight-through duct section. For the branch 1–3 in Figure 22.11, for example, the loss coefficient depends upon the ratio of the velocity in the branch to the velocity in the main duct. These loss coefficient are given in Table 22. 5.

Table 22.5 Loss coefficient, *K* for branch take-offs

Take-off Angle	*Ratio of velocity in branch to velocity in main duct*						
(deg)	0.4	0.6	0.8	1.0	1.5	2.0	3.0
90	6.5	3.1	2.0	1.5	0.95	0.74	0.62
60	5.0	2.2	1.3	0.77	0.47	0.47	0.58
45	3.5	1.3	0.64	0.43	0.4	0.45	0.54

22.9 AIRFLOW THROUGH DUCT SYSTEMS WITH FAN

Figure 22.12 shows a simple duct on the suction as well as on the discharge side of a fan.

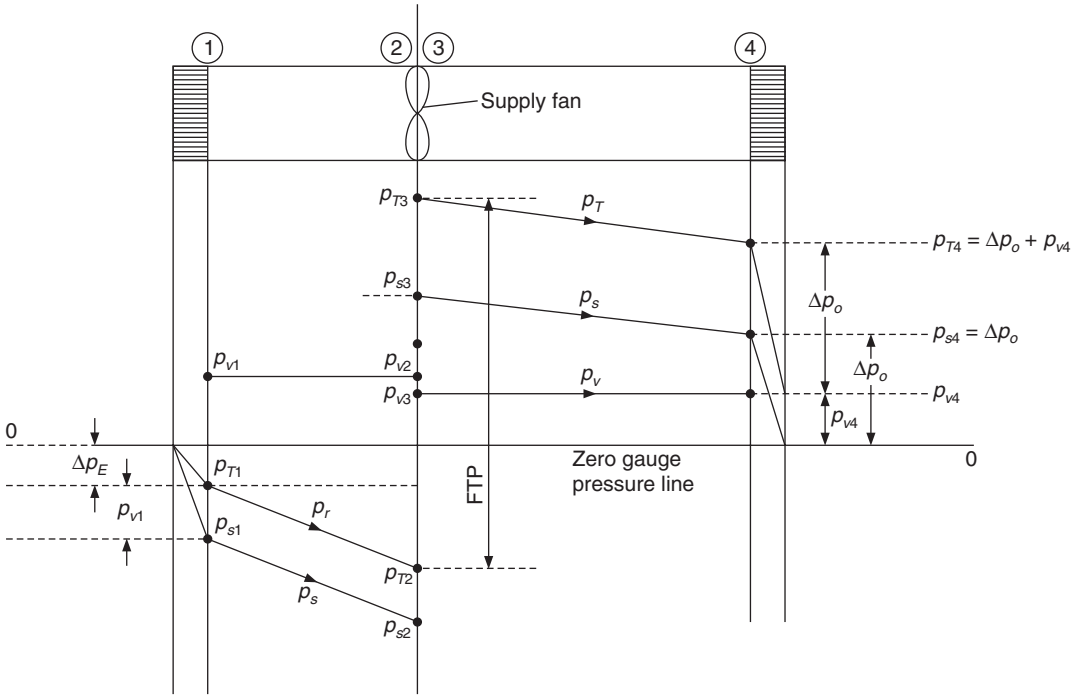

Figure 22.12 Straight inlet and outlet ducts with a simple fan system.

Loss on the inlet side

There are grilles on the inlet opening as well as on the outlet opening. The air outside the duct is stationary and is accelerated from rest to duct velocity V_1 past the vena contracta. There will be loss due to vena contracta and due to inlet grille. Let this loss be called *entry loss* equal to Δp_E. The outside static pressure is atmospheric, hence the corresponding gauge pressure is zero. Therefore,

$$p_{so} = p_{vo} = p_{To} = 0 \tag{22.64}$$

If p_{s1}, p_{v1} and p_{T1} are the pressures just inside the duct, then

$$p_{To} = p_{T1} + \Delta p_E \quad \therefore \quad p_{T1} = -\Delta p_E \tag{22.65}$$

$$p_{s1} = p_{T1} - p_{v1} = -(\Delta p_E + p_{v1}) \tag{22.66}$$

The static pressure at section 1 is negative. If the pressure drop at inlet Δp_E is zero, then the static pressure at inlet is negative of the velocity pressure. Actually it has a larger negative value since it has to overcome the inlet pressure drop too. In the duct 1–2 the velocity remains the same since the area of cross section is constant, that is,

$$p_{v2} = p_{v1} \tag{22.67}$$

There is a drop in static pressure to overcome the frictional resistance Δp_{12} offered by the duct 1–2.

$$\therefore \qquad p_{s2} = p_{s1} - \Delta p_{12} \tag{22.68}$$

and
$$p_{T2} = p_{T1} - \Delta p_{12} \tag{22.69}$$

From Eq. (22.65), we get

$$p_{T2} = -(\Delta p_E + \Delta p_{12}) \tag{22.70}$$

Also,
$$p_{s2} = -(\Delta p_E + p_{v1} + \Delta p_{12}) \tag{22.71}$$

The total pressure at the fan inlet p_{T2} consists of loss of energy through the duct up to this point. It consists of frictional loss over the inlet grille, the loss past vena contracta and frictional loss in the duct.

Loss on discharge side

It is easier to start determination of this from the discharge side. Say the frictional pressure drop across the outer grille is Δp_o and the velocity pressure at the outlet is p_{v4}. Hence the total pressure at the outlet is given by

$$p_{T4} = \Delta p_o + p_{v4} \tag{22.72}$$

The static gauge pressure outside is zero, The static pressure at point 4 must be greater than that outside by Δp_o.

$$\therefore \qquad p_{s4} = \Delta p_o = p_{T4} - p_{v4} \tag{22.73}$$

The frictional pressure drop in the discharge duct 3–4 is Δp_{34}. Therefore,

$$p_{s3} = p_{s4} + \Delta p_{34}$$

and
$$p_{v3} = p_{v4}$$

Therefore,

$$p_{T3} = p_{v4} + \Delta p_{34} + \Delta p_o \tag{22.74}$$

Flow occurs from 1 to 2, hence p_{T1} must be greater than p_{T2}. Similarly, flow occurs from 3 to 4 hence p_{T3} must be greater than p_{T4}. Also p_{T3} must be greater than p_{T2} and the difference between these two is supplied by the fan. Therefore,

$$\text{FTP} = p_{tf} = p_{T3} - p_{T2} = p_{v4} + \Delta p_{34} + \Delta p_o + \Delta p_{12} + \Delta p_E \tag{22.75}$$

Hence the fan total pressure consists of the following five components:

(i) pressure loss at inlet and past vena contract near inlet
(ii) frictional pressure in suction duct or the return air duct
(iii) frictional pressure drop across the supply air duct
(iv) frictional pressure drop across outlet grille
(v) kinetic energy loss at outlet

In actual practice Δp_{12} will include the frictional pressure drop in return air duct, filters, dampers, cooling coil, air washer, heating coil and humidifier, etc. The fan static pressure FSP and fan velocity pressure FVP may be defined as follows:

$$\text{FSP} = \text{FTP} - \text{FVP} \tag{22.76}$$

where FVP = p_{v3}

$$\text{Fan power, } W = \dot{Q}_v(\text{FTP}) \quad \text{watt} \tag{22.77}$$

where, $\dot{Q}_v$ is the volume flow rate in m^3/s and FTP is in Pa.

22.10 AIR DUCT DESIGN

The heating/cooling loads, occupancy usage and the choice of heating/cooling coil decide the volume flow rate of supply air in any HVAC system. Once this is known, a suitable velocity has to be chosen based upon either frictional pressure drop or the noise level limitation criterion.

Table 22.6 gives the recommended velocities in the main and branch supply and return air ducts from noise level and friction point of view for various applications. It is observed that 600 m/min or 10 m/s is the maximum permissible velocity in stores, banks and cafeteria. In some industrial applications velocities more than 10 m/s are also used. Table 22.7 gives the recommended velocities at intakes to various sections of the supply and return air ducts. Table 22.8 gives the recommended velocities from sound level point of view from the outlets. Table 22.9 gives the recommended return duct inlet face velocities. A good design practice is to follow these guidelines.

Table 22.6 Recommended maximum duct velocities (mpm) for low velocity systems

Application	*Noise level point of view*		*Friction factor point of view*			
	Velocity	*Sound level*	*Main ducts*		*Branch ducts*	
	(mpm)	(dB)	*Supply*	*Return*	*Supply*	*Return*
Residences	180	40	300	240	180	180
Apartments, hotel bed rooms, hospital rooms	300	40	450	390	360	300
Offices, libraries	360	60	600	450	480	360
Theatres and auditorium	240	30	390	330	300	240
Cinema	240	35	390	330	300	240
Stores, banks & restaurants	450	40	600	450	480	360
Cafetaria	540	60	600	450	480	360
Studios	120	30	240	180	120	120

Table 22.7 Recommended air velocities for intakes to various sections of duct

	Public building velocity (mpm)	*Office building velocity* (mpm)
Outside air intakes, mixing air intakes, recirculation intakes, return intakes and bypass intakes	244–305	244–305
Air washer	137–168	
Discharge opening, fan	366–548	
Main duct	305–457	366–457
Branch duct	244–305	244–305
Riser duct	152–232	152–228
Inlet opening to rooms	92–107	92–107
Exit opening to rooms	92–114	
Main return ducts	152–244	244–305
Branch return duct		152–244
Riser return duct		152
Return inlet		92–114
Intake fans		244–305

Table 22.8 Recommended velocities from noise level point of view from the outlets

Applicaton	*Velocity* (mpm)
Broadcasting studio	90–150
Residences, private office theatres	150–225
Cinema halls	300
General offices	300–375
Stores, upper floor	450
Stores, main floor	600

Table 22.9 Return duct inlet face velocities

Applicaton	*Velocity* (mpm)
Above occupied zone	240
Within occupied zone (not near seat)	180–240
Within occupied zone (near seat)	120–180
Door or wall louvers	60–90
Undercut area	60–90

If the volume flow rate is known and the air velocity has been chosen, the duct size can be determined from the following equation:

$$\dot{Q}_v = VA \tag{22.78}$$

For a circular duct the diameter is given by

$$d = \sqrt{4\dot{Q}_v / \pi} \tag{22.79}$$

If we choose a larger velocity, the duct size and therefore the initial cost will reduce while the pressure drop and the fan power will increase, thereby increasing the operating cost. On the other hand, a duct of larger area of cross section will have higher initial cost and lower operating cost. This will, however, occupy larger space that could be used for other useful purposes. In most cases, there is a conflict between the air conditioning engineers and the architects. Architects normally do not fully appreciate the need of providing liberal areas for ducts. This puts constraints on the design. Apart from this, the support beams also come in the way of the path of ducts, hence the height of the duct has to be reduced to keep a respectable ceiling height. This may increase the aspect ratio of the duct causing more frictional pressure drop.

Hence an air conditioning engineer has to design the duct keeping in mind the best possible aspect ratio, bends, expanding and contracting sections, branches etc. within the noise level constraint and providing proper ambience and respectable ceiling height. In doing so a number of compromises have to be made. In any case, the following aspects should be kept in mind while designing the duct system.

1. The duct should be taken by the shortest path to the space to be air conditioned.
2. The aspect ratio of the duct should be as near unity as possible, the maximum aspect ratio should be less than 4:1. Sharp bends in the duct should be avoided. If it is necessary to have them, then turning vanes should be used to reduce the pressure loss. A larger aspect ratio requires more material, and the pressure drop is also large.
3. The velocities should be within the permissible limit if the noise level is a limitation, otherwise they should not be very large leading to large frictional pressure drop.
4. Ducts should be made of galvanized iron (GI) sheets or aluminium sheet. In case other materials are used, then the corresponding friction factor should be used.
5. Dampers should be provided in all branches to balance the flow in the whole zone.

22.10.1 Duct Material and Construction

Ducts are usually made of GI sheets or aluminium sheets. Aluminium sheet is used when heavy ducts cannot be used or moisture resistance is required. Heavy gauge black steel may be used for kitchen exhaust. Equations (22.26) to (22.29) consider an average roughness of 0.15 mm. For other materials the pressure drop is different. A correction factor given in Table 22.2 may be used.

Duct classification according to pressure and velocity

There is no agreement amongst practitioners regarding classification of duct systems. However, classification like low velocity, mean velocity and high velocity systems is in common use.

Low velocity systems: The maximum mean velocity is less than 10 m/s.

Medium velocity systems: The maximum mean velocity is between 10 m/s and 15 m/s.

High velocity systems: In these systems the maximum mean velocity is between 15 m/s and 20 m/s. The velocity should be kept as low as possible. In the extreme case it should not exceed 20 m/s.

There is a classification based upon the total pressure drop as well. This is as follows:

Low pressure system: The static gauge pressure is within –500 Pa to 500 Pa. The acceptable maximum velocity is less than 10 m/s.

Medium pressure system: The static gauge pressure is within –750Pa to 1000 Pa.

High pressure system: The static gauge pressure is within –750 Pa to 2599 Pa.

Large negative pressures are not recommended in comfort air conditioning systems. The ducts are made of sheet metal and despite the reinforcement provided, these may tend to collapse at sub-atmospheric pressures.

Ducts for large positive pressures are essentially used in industrial exhaust systems and in the systems used for pneumatic conveying. High pressure and high velocity ducts have to withstand larger forces due to steady value of large pressure, and unsteady large forces due to turbulence. This requires the use of sheets of larger thickness and cross bracing, and the use of tie rods as well as transverse angle iron reinforcements. The recommended gauge (thickness) of GI sheet used also depends upon the longest side and it is as given in Table 22.10.

Table 22.10 Recommended gauge of GI sheets for various systems

Length of side (cm)			*Gauge of GI sheet*
Low pressure	*Medium pressure*	*High pressure*	
Up to 30	–	–	26
30–75	Up to 45	–	24
75–135	45–120	Up to 120	22
135–210	120–180	120–180	20
Above 210	Above 180	180–240	18
–	–	Above 240	16

22.10.2 Duct Design Methods

Three methods are in common use for duct design. These are as follows:

1. Velocity Reduction Method
2. Constant Equal Friction Method or Equal Pressure Drop Method
3. Static Regain Method

To obtain a general feel of what happens in the design, we discuss the volume flow rate vs. pressure drop characteristics with respect to the skeleton friction diagram reproduced in Figure 22.13. We consider the design of the duct system shown in Figure 22.14 as an example.

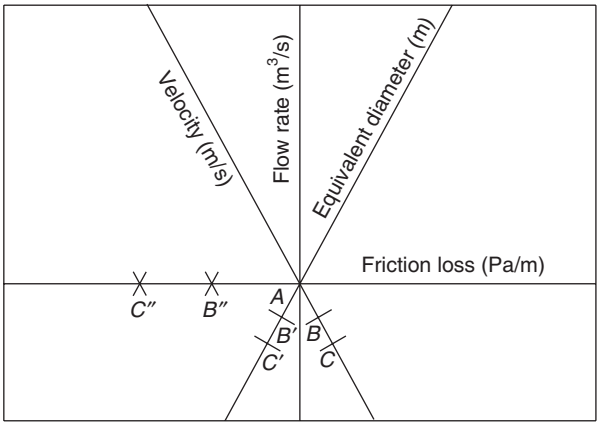

Figure 22.13 A skeleton friction loss chart.

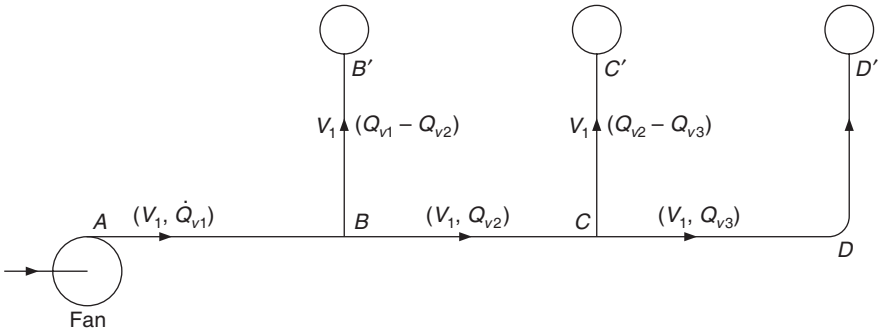

Figure 22.14 A typical air conditioning duct layout.

The volume flow rate $\dot{Q}_1$ at the fan outlet is specified and a velocity V_1 for the main supply air duct has been selected. From Eq. (22.79) the diameter d_1 is given by

$$d_1 = \sqrt{4\dot{Q}_{v1} / \pi}$$

The location of $V_1$and $\dot{Q}_{v1}$ is shown at point *A* in Figure 22.14. The rate of pressure drop as found from Eq. (22.30) is Δp_1 (Pa/m). A branch with volume flow rate $\dot{Q}_{v1} - \dot{Q}_{v2}$ is taken at point *B*. In the subsequent section, *B*–*C*, the volume flow rate is $\dot{Q}_{v2}$ m^3/s. If the velocity is kept the same as that at inlet, that is V_1, then at reduced volume flow rate the duct diameter reduces to d_2 and the pressure drop rate increases to Δp_2 corresponding to point *B* as in Figure 22.13. Similarly, for the volume flow rate of $\dot{Q}_{v3}$ in section *C*–*D* the diameter reduces to d_3 and the pressure drop increases to Δp_3 (Point *C*). The increase in pressure drop rate will increase the fan power and the risk of regenerated noise also increases.

The other extreme is to keep the duct size the same throughout the duct. This leads to lower pressure drops, for example, in Figure 22.13 corresponding to point *B′* in section *B*–*C* and corresponding to *C′* in section *C*–*D*. This will involve more cost since a duct of lower area of cross section should have been used at lower volume flow rates. The velocities in sections *B*–*C* and *C*–*D* will be very low giving rise to static regain. The total pressure drop will also be small.

These are two extreme cases. One can compromise to keep the same rate of pressure drop throughout the duct. This will lead to diameters corresponding to points B'' and C'' in Figure 22.13 for the sections B–C and C–D respectively. At these design values, the diameters as well as velocities decrease in downstream direction. It is observed that there will be some static regain in this case also due to lower velocities.

If the duct diameter is increased further then it will lie somewhere along B''–B' in Figure 22.13 and it will give more static regain. It is possible to decide the diameter in section B–C such that static regain is equal to total pressure drop due to friction in section B–C.

Control of flow rate to branches

It is expected that the static pressure at C is sufficient to deliver the required flow rate $\dot{Q}_{v2} - \dot{Q}_{v3}$ to the branch towards C' and also enough to deliver the flow rate $\dot{Q}_{v3}$ to branch towards D'. Similar considerations are required for the branch at B as well. If the pressure at B is more than that required, then it is decreased by a damper in the branch towards B'. The damper absorbs the excess pressure and delivers the correct flow rate; otherwise there will be a larger flow rate towards B'.

Sometimes it is possible to design the duct such that the pressure in all the branches is the same. Then the sizes of the ducts B–B', C–C' and D–D' decide the flow rate making it possible to obtain the desired flow rate without dampers.

Balancing procedure

The duct run having the largest pressure drop is called the *Index Run*. This is usually the longest duct run, but may not be so all the time. The total pressure drop in this run is used for finding the power requirement of the fan and for specification of the fan. The index run is useful in balancing of the flow as well.

There are standard procedures for balancing the flow by adjusting the dampers. In Figure 22.14, there may be a main damper I in the main branch, damper II in branch towards B', damper III towards branch C' and damper IV towards C–D–D'. The correct procedure for balancing the flow is called *proportional balancing* developed by Harrison et al. (1965). In brief this is as follows:

(i) The settings of safety overload cutouts on the supply air fan motor starter are checked.

(ii) The main system damper I is partly closed and the supply air fan is switched on.

(iii) The index run is identified and its terminal damper (damper IV in Figure 22.14) is fully opened and the flow rates are measured. These will be less than the design value since the system damper is partially closed.

(iv) Working backwards, the next damper (say III in Figure 22.14) is adjusted such that the flow rate through this is in the same proportion of index flow as the design value.

(v) Working backwards successively all the branch dampers are adjusted in this manner.

(vi) System checks are made and the system damper is fully opened. The total flow rate is measured and the fan speed is adjusted to give the design conditions.

In the following sections the three duct design procedures are discussed.

22.10.3 Velocity Reduction Method

A suitable mean velocity is chosen for the main duct at a location just after the fan discharge. This may be limited either by noise level or from frictional resistance point of view. The duct size for the given volume flow rate is determined from Eq. (22.79). The volume flow rate reduces after the first branch. If the same velocity is maintained then the pressure drop is excessive and if the duct size is kept same then the duct cost will be excessive. Hence the choice of correct velocity is not straightforward. One has to rely upon experience to choose the velocity. As discussed above, the velocity and the pressure should be sufficient to meet the requirement of the subsequent sections.

One approach is to work backwards. Choose the last air distribution terminal, which may be supply grille, supply diffuser or variable air volume supply device. Manufacturers give recommendations for the velocity at the grille inlet to ensure proper air distribution. This fixes the velocities at the two extremes, the inlet and outlet of the index run. Good engineering judgement and common sense may then be used to obtain proportional velocities after each branch between the two ends. Due care has to be taken so as not to exceed the velocities recommended by the manufacturer. Similarly, the volume flow rates should not be near the upper and the lower limits recommended by the manufacturer.

EXAMPLE 22.5 Choose the appropriate velocities in various sections of the duct and find the duct sizes for the layout shown in Figure 22.14. The volume flow rates in branches B', C' and D' are 1 m^3/s each. The velocity downstream of the fan is 8.5 m/s and the velocity at the outlet should be 3.5 m/s.

Solution:

The velocity at point D' is 3.5 m/s, hence at point C also it is 3.5 m/s. At point B, the velocity is 8.5 m/s just before the branch. Common sense suggests that the velocity in section B–C should be the the mean of 8.5 and 3.5, that is, 6 m/s. Therefore, we find the areas, diameters and the pressure drops for various sections with the chosen velocities from Eqs. (22.78) and (22.79), that is

$$A = \dot{Q}_v / V \quad \text{and} \quad d = \sqrt{4\dot{Q}_v / \pi}$$

$$\Delta p_f = \frac{0.012199 V^{2.4865} L}{Q_v^{0.6343}} \qquad \text{for section } A\text{–}B$$

or

$$\Delta p_f / L = \frac{0.012199 (8.5)^{2.4865}}{(3)^{0.6343}} = 1.24334 \text{ Pa/m}$$

The results are given in the following table:

Section	$\dot{Q}$ (m^3/s)	V (m/s)	A (m^2)	d (m)	$\Delta p/L$ (Pa/m)
A–B	3	8.5	0.3529	0.67035	1.24334
B–C	2	6.0	0.333	0.6515	0.6734
C–D′	1	3.5	0.2857	0.603	0.2749

22.10.4 Equal Pressure Drop Method

The velocity after the fan is chosen by noise level or frictional resistance criterion. The pressure drop per metre length is determined from Eq. (22.32). The pressure drop rate or friction factor is assumed to be the same throughout the length of the duct. Substitution of $V = \dot{Q}_v/A$ in Eq. (22.31) yields:

$$d = \frac{0.4652\,\dot{Q}_v^{0.3724}}{(\Delta p_f / L)^{0.20108}} \tag{22.80}$$

If the friction rate or the frictional pressure drop per unit length $\Delta p_f/L$ is constant then this equation gives a very simple relation for the determination of duct diameter in terms of volume flow rate as it decreases along the duct run. This method is commonly used for finding the duct dimensions for low velocity systems. In this method the duct velocity reduces downstream as shown by A–B''–C''. The static pressure will continue to decrease in the downstream direction. Hence at each successive branch, the static pressure will be smaller. Because of this the branches near the fan will tend to have larger volume flow rate. This is corrected by providing and adjusting the dampers in all branches. For example, the dampers to branches B' and C' in Figure 22.14 will adjust the flow rates to the design value. A duct calculator is available to find the solution of Eq. (22.80) for various friction rates. The total pressure drop is easily found by multiplying the friction rate by the length of index run. Following alternatives may also be used for design.

1. It is not necessary to choose a velocity in the section immediately following the fan. It can be velocity in any section thought to be critical for the design. Then the duct can be designed based upon $\Delta p_f/L$ in the critical section.
2. Instead of choosing an appropriate velocity, we can choose an appropriate friction rate and the limiting maximum mean velocity based upon experience indicating the friction rate to be suitable. The duct is sized based upon the friction rate. This method is commonly used with pressure drop rate of 0.8 Pa/m and maximum velocity in the range of 8.5 to 9 m/s. ASHRAE (1997) quotes a range of 9 to 20 m/s leaving the exact choice to the designer.

EXAMPLE 22.6 Find the duct dimensions by the equal friction method for the system shown in Figure 22.14. Assume a pressure drop rate of 0.8 Pa/m and maximum velocity of 8.0 m/s.

Solution:

Substituting $\Delta p_f/L = 0.8$ in Eq. (22.80), we get

$$d = 0.48655\ Q_v^{0.3724}$$

The velocity is determined from $V = 4Q_v/(\pi d^2)$

The solution for various sections of Figure 22.14 is as follows:

Section	$\dot{Q}$ (m^3/s)	d (m)	V (m/s)
A–B	3	0.7325	7.119
B–C	2	0.62298	6.42
C–D′	1	0.4865	5.378
B–B′	1	0.4865	5.378
C–C″	1	0.4865	5.378

In section *A–B* we could have chosen a velocity of 8 m/s. This gives $\Delta p_f/L$ = 1.0694 Pa/m. This is more than 0.8 Pa/m. Hence we accept a velocity lower than 8 m/s.

22.10.5 Static Regain Method

It was observed in Figure 22.13 that if the diameter of the duct is kept constant, the velocity reduces. A part of kinetic energy is converted to static pressure. This was called *regain*. However, all the decrease in kinetic energy is not converted into pressure. In general, the regain is about 75% of the decrease in velocity pressure. This increased static pressure is then available to be offset by friction and other losses in the downstream duct. In the static regain method of duct design, it is assumed that static regain after each branch is equal to the pressure loss in the subsequent section of the duct. For example, R denotes the static regain and p_{vA} and p_{vB} are the velocity pressures in sections A and B respectively, then after branch B, we get

$$R(p_{vA} - p_{vB}) = \Delta p_{fBC} + \Delta p_{mBC} \tag{22.81}$$

where, Δp_{fBC} denotes the frictional pressure loss and Δp_{mBC} denotes the minor losses in *B–C*.

The solution of this equation requires the magnitude of velocity in section *B–C*. This is not known apriori. Hence a guess is made for it and both the left hand and right sides of the above equation are evaluated and checked. Then iteration is required to find the velocity, which makes the left hand side expression equal to the right hand side expression.

This method is commonly used for medium and high velocity systems, where a large kinetic energy is initially available and it decreases downstream as it is converted into static pressure. The ducts may tend to become very large. Hence, sometimes only a part of the duct is sized according to this method and other methods are adopted for the remaining part.

EXAMPLE 22.7 Find the duct dimensions by the static regain method for the system of Figure 22.14, assuming a static regain of 0.75. The velocity at inlet to the duct is 8.5 m/s and the length *B–C* is 10 m and *C–D′* = 20 m. The loss coefficient for the elbow, K = 0.22.

Solution:

Section *B–C:*
The minor loss is neglected in this section and only the frictional pressure drop is considered in Eq. (22.81).

$$p_{vA} = 0.5\rho V_A^2 = 0.6(8.5)^2 = 43.35 \text{ Pa}$$

$$p_{vB} = 0.6V_B^2$$

Equation (22.33) is used to find the frictional pressure drop, which is as follows:

$$\Delta p_f = \frac{0.012199 V^{2.4865} L}{\dot{Q}_v^{0.6343}} \text{ which gives } \Delta p_f = \frac{0.012199 V_B^{2.4865} 10}{\dot{Q}_B^{0.6343}}$$

Therefore for section *B–C*, Eq. (22.81) reduces to:

$$0.75(43.35 - 0.6V_B^2) = 0.0785816V_B^{2.4865}$$

Choosing various velocities, the left and the right hand sides are as follows:

V_B (m/s)	LHS (Pa)	RHS (Pa)
7.0	10.4525	9.9243
7.05	10.146	10.10
7.06	10.08	10.136
7.055	10.1146	10.118

Hence a velocity of 7.055 m/s satisfies Eq. (22.81) in section *B–C*.

Section *C–D′:*

$$p_{vB} = 0.6V_B^2 = 0.6(7.055)^2 = 29.8638 \text{ Pa}$$

Similar approach is followed for this section except that the elbow loss has to be included in this case. The elbow loss is equal to $0.22(0.5\rho V_C^2)$. Equation (23.81) reduces to:

$$R(p_{vB} - p_{vC}) = \frac{0.012199 V_C^{2.4865}}{(1)^{0.6343}} + 0.22 \times 0.6V_C^2$$

Simplifying it, we get

$$0.75(29.8638 - 0.6V_C^2) - 0.132V_C^2 = 0.012195 \times 20 \times V_C^{2.4805}$$

or

$$22.3978 - 0.582V_C^2 = 0.24398V_C^{2.4805}$$

Choosing various velocities the left hand and the right hand sides are as follows:

V_B (m/s)	LHS (Pa)	RHS (Pa)
5.0	7.848	13.3
4.5	10.612	10.27
4.55	10.349	10.556
4.54	10.402	10.384
4.535	10.428	10.498
4.531	10.444	10.446

Hence a velocity of 4.531 m/s satisfies Eq. (22.81) in section *C–D′*.

Hence, the duct size, the pressure drops and regain for various sections are as follows:

Section	$\dot{Q}$ (m^3/s)	V (m/s)	p_v	A (m^2)	d (m)	$\Delta p_f + \Delta p_m$	Δp_{regain}
A–B	3	8.5	43.35	0.3529	0.6704	12.433	0
B–C	2	7.055	29.8638	0.2835	0.6	10.118	10.115
C–D′	1	4.531	12.318	0.2207	0.53	13.159	13.159

EXAMPLE 22.8 Find the duct dimensions by the equal friction method assuming a velocity at inlet to be 8.5 m/s.

Solution:

Example 22.7 considers duct design for an initial velocity of 8.5 m/s in section *A–B* by the static regain method. To compare the results with the equal friction method, we repeat the equal friction method with this initial velocity.

For $V = 8.5$ m/s from Eq. (22.33) the pressure drop rate is found to be 1.24334 Pa/m. Substituting this value in Eq. (22.80), we get

$$d = \frac{0.4652\,\dot{Q}_v^{0.3724}}{(1.24334)^{0.20108}} = 0.44526\,Q_v^{0.3724}$$

The solution for various sections of Figure 22.14 is as follows:

Section	$\dot{Q}$ (m^3/s)	d (m)	V (m/s)	Δp_f
A–B	3	0.6704	8.5	12.443
B–C	2	0.5764	7.665	12.433
C–D′	1	0.44526	6.422	30.311

The elbow loss = $0.22(0.6)(6.422)^2 = 5.444$ Pa

It is observed that the velocities are larger and the diameters are smaller in the equal friction method compared to the static regain method. The pressure drop is significantly large in the equal friction method. The design by equal friction method would require more fan power while a lower duct cost.

22.11 ROOM AIR DISTRIBUTION

The air has to be uniformly distributed in the occupied zone to ensure that temperature, humidity and velocity are within acceptable limits. In some cases, the zone of the room above 1.8 m is used for mixing the air and reducing its velocity. A few of the important terms used are explained here.

Blow or throw

Throw or blow is the distance travelled by air in the horizontal direction after leaving the outlet and reaching a velocity of 15 m/min (0.25 m/s), the velocity being measured 1.8 m above the floor level. The desirable throw is a maximum of ¾th of the distance to the opposite wall. A large throw would imply that the cold supply air jet will hit the opposite wall and lose some of its cooling effect.

Drop

Drop is the vertical distance that the primary air moves after leaving the supply air outlet to reach a velocity of 15 m/min (0.25 m/s) at the end of its throw.

The above meaning of the terms, i.e. *throw* and *drop* of free-stream jets is illustrated in Figure 22.15.

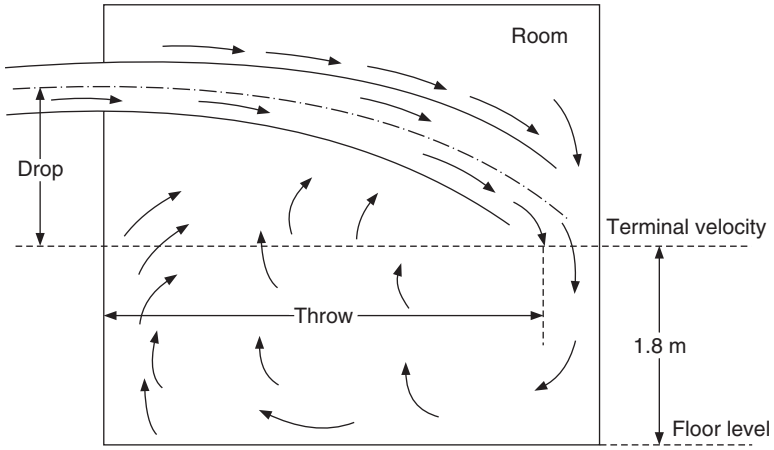

Figure 22.15 Meaning of throw and drop.

The conditioned air is introduced into the room at an optimum location with sufficient velocity so that entrainment of room air and mixing with the room air occurs. For cooling applications, this mixing will carry away the stored energy from the warm room air. Additionally, it carries away the contaminants generated in the room. The aim is to provide good mixing without creating uncomfortable draft, and to maintain a uniform temperature in the occupied zone within the limits of noise level and pressure drops. The mixing is also supposed to counteract the natural convection and radiation effects within the room.

22.11.1 Behaviour of Jets

The conditioned air is introduced into the room through supply air outlets openings such as grilles, perforated panels, ceiling diffusers, etc. at a velocity higher than that required in the occupied zone. The supply air temperature may be higher or lower than the room air temperature depending upon the heating/cooling application. The high velocity jet drags some of the room air along with it, that is, it imparts some of its kinetic energy to the room air. This phenomenon is called *entrainment* and the air set into motion by this effect is called *entrained air*. The supply air coming out of the slot is called the *primary air*.

The velocity profile at a distance from the outlet grille depends upon the average velocity at the face of the opening. If there are no adjustment bars in the grille, then it comes out as a free jet. *A free jet has four important zones*. The centreline velocity $(\bar{V}_x)$ in any zone is related to initial velocity (V_0) as shown in Figure 22.16. It is a fact that irrespective of the type of opening, the jet acquires a circular shape. In zone I, velocity $\bar{V}_x$ remains almost constant and in zone II it starts to decrease. In these two zones the air is essentially primary air. In zone III which is the most significant zone, the centreline velocity $(\bar{V}_x)$ is related to initial velocity V_0, diameter d_0 and area A_0 as follows:

$$\frac{\bar{V}_x}{\bar{V}_0} = K\frac{d_0}{x} = K'\frac{\sqrt{A_0}}{x} \tag{22.82}$$

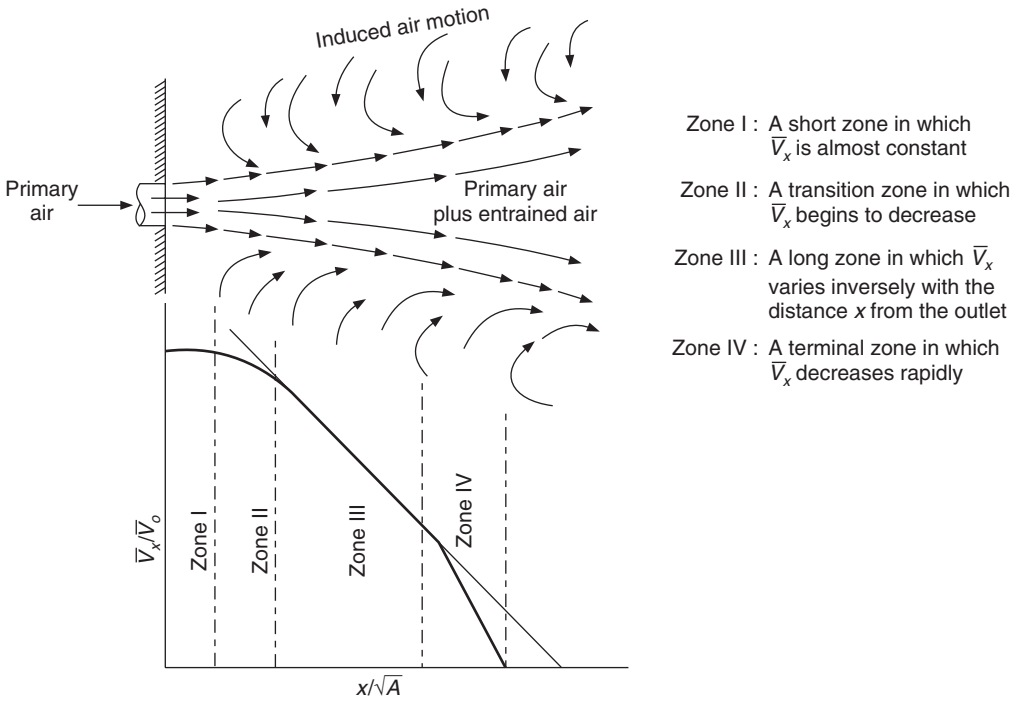

Figure 22.16 Behaviour of a free air jet.

or
$$\bar{V}_x = \frac{K' Q_0}{\sqrt{A_0}\, x} \tag{22.83}$$

where

$K' = (4/p)^{0.5} K = 1.13K$

x = distance from outlet to the point of measurement of $\bar{V}_x$.

The constant K is about 6 for free jets and approximately one for ceiling diffusers. Q_0 is the volume flow rate of primary air and $A_0 = Q_0/V_0$. This equation is for a free jet with supply air at the same temperature as the room air. The exact equation for a circular jet or plane jet is as follows:

$$\frac{\bar{V}_x}{\bar{V}_0} = \frac{7.41\sqrt{A_0}}{x[1 + 57.5(r/x)^2]^2} \tag{22.84}$$

For a rectangular jet with slot width b, the equation is as follows:

$$\frac{\bar{V}_x}{\bar{V}_0} = \frac{2.4\sqrt{b}}{\sqrt{x}} [1 - \tanh\,(7.64 y/x)] \tag{22.85}$$

where y is the normal distance from the central plane.

In case the outlet has a grille with free area A_{fa} and vena contracta with area A_v occurs, then the velocity distribution of Eq. (22.82) may be expressed as follows:

$$\frac{\bar{V}_x}{\bar{V}_0} = K' \frac{Q_0}{x\sqrt{A_0 C_d R_{fa}}} \tag{22.86}$$

where, $$R_{fa} = A_{fa}/A_0 \text{ and } C_d = A_v/A_{fa} \tag{22.87}$$

Induction ratio or entrainment ratio

The air supplied by the supply air outlet is called *primary air*. At the edges of the primary air jet, some kinetic energy is imparted to the room air, which starts to move in the direction of primary air. This is called *secondary air* or *entrained air*. The sum of these two is called *total air*. The total volume flow rate along the path of jet increases due to entrainment and the width of the jet also increases. The volume flow rate Q_x and the centreline velocity $\bar{V}_x$ at any location x are given by

$$R = \frac{Q_x}{Q_0} = C\frac{\bar{V}_0}{V_x} = \text{Induction Ratio} \tag{22.88}$$

The constant C has a value of 2 for a free round jet and $\sqrt{2}$ for a long slot jet. In zone IV of the free jet shown in Figure 22.16 the velocity $\bar{V}_x$ is very low and Eq. (22.88) with these constants gives a 20% larger value.

When a jet is projected within a few cm from a surface, it attaches itself to the surface due to Coanda effect, just like tea or coffee coming out of a kettle attaches itself to the kettle outlet. Actually a low pressure region is created as the jet entrains the air (imparts kinetic energy) from a narrow region between the jet and the surface. This creates a recirculatory region and the jet attaches itself to the surface as shown in Figure 22.17(a). This surface effect usually increases the throw and reduces the drop. This is shown in Figure 22.17(b). If the supply jet air temperature is less than the room air temperature, then the jet drops towards the floor as shown in Figure 22.17(c). In addition to primary and secondary streams, air motion develops due to natural convection effects as well, for example, air tends to rise along heated walls and move downwards along cool walls. The dependence of blow and throw on various parameters may be expressed as follows:

$$\text{Blow} = f(\text{supply air velocity, temperature difference } t_i - t_s \text{ and } R)$$

$$R = f(\text{primary air velocity and perimeter of primary air stream})$$

The expression for throw L may be obtained from Eq. (22.86) for $\bar{V}_x$ = 15 m/min = 0.25 m/s

$$L = \frac{K'}{0.25}\frac{Q_0}{\sqrt{A_0 C_d R_{fa}}} \tag{22.89}$$

The following characteristics of air jets are useful to be known in connection with room air distribution.

1. The surface effect increases the throw and reduces the drop compared to free jet.
2. The surface effect is more if the outlet is slightly away from the surface. This allows the jet to spread over the surface after impact.
3. If the jet is spread after discharge the surface effect will be larger.
4. A spreaded discharge from the outlet has a smaller throw and a smaller drop.
5. The drop depends more strongly upon the volume flow rate. The use of more number of outlets with smaller volume flow rate each, decreases the drop.

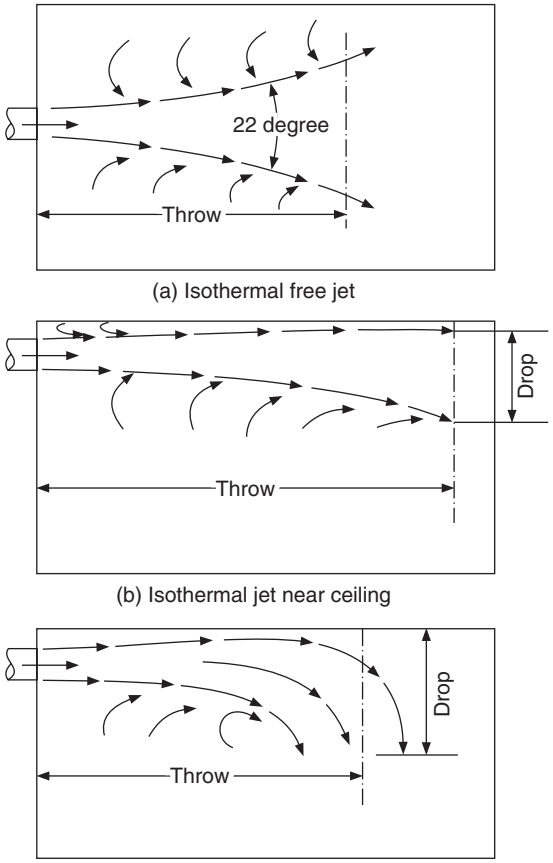

Figure 22.17 Illustration of surface effect.

22.11.2 Room Air Motion

The air entrained by the jet comes from all parts of the room towards the jet periphery. This sets the whole of the room air in motion. The difference in temperature between the wall and the air causes natural convection currents in the room. The buoyancy effects are significant whenever the average velocity is less than 0.25 m/s. The regions of the room where the velocity is less than 0.45 m/min are called *stagnant* regions. It requires about 8 to 10 air changes to avoid these regions. The method adopted in room air distribution design is that high velocity air should not enter the occupied zone. All the mixing should take place above this region. The relation between the centreline velocities and the temperature difference for a jet is given by

$$\Delta t_x = 0.8\,\Delta t_o\,\frac{\bar{V}_x}{\bar{V}_o} \tag{22.90}$$

where, $\Delta t_x = (t_r - t_x)$ and $\Delta t_o = (t_r - t_o)$. The room air temperature and supply air temperatures are indicated by t_r and t_o respectively, and t_x is the temperature at any location x.

Figure 22.18 shows the air flow velocity and temperature distributions for high sidewall grille. Equation (22.89) may be used to find the throw. Equation (22.90) may be used to find the temperature distribution. The jet enters the room with a velocity of 5.0 m/s and $\Delta t_o = -11.1^oC$. The velocity reduces to 1.0 m/s in the middle of the room and to 0.5 m/s on the right wall and the temperature on right wall is $\Delta t_x = -0.9^oC$. The isovelocity envelopes are shown for three velocities, namely 1.0 m/s, 0.5 m/s and 0.25 m/s. The temperatures differences Δt_x with respect to centre room temperature are, $-1.8°$, $-0.9°$ and -0.45^oC at the extremes of these envelopes. The temperature in the entire occupied space is about -0.45^oC below the room temperature and the room air velocity is less than 0.25 m/s.

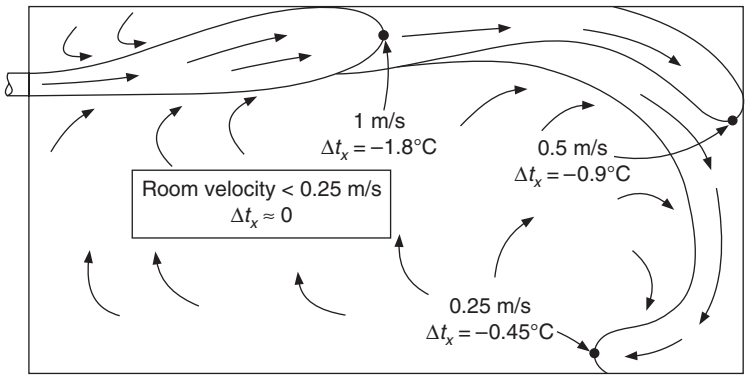

Figure 22.18 Airflow velocity and temperature distribution patterns using high side outlets installed on a high sidewall.

22.11.3 Distribution Patterns of Outlets

The best airflow pattern is one in which the whole room air is set into motion and no stagnation zone or zone of draft occurs in the occupied zone. In the following, the room airflow and temperature and velocity distribution patterns are discussed for various locations of supply air outlets. An envelope without any hatching shows the primary air. The areas with hatching indicate the secondary air. Arrows show the natural convection currents, and the wavy lines show the stagnation zones.

High side wall grille discharging air horizontally

Figure 22.19(a) and (b) show the supply air outlet located high up on the sidewall near the ceiling for the case of cooling and heating respectively. The air jet is thrown horizontally. The cold air jet being heavier stays near the ceiling and drops down after some distance depending upon the inlet velocity, volume flow rate and temperature difference. The jet tends to get attached with the ceiling depending upon the distance from ceiling. The details of the flow pattern have been discussed in Figure 22.18. The deflector in the outlet may be set to control the drop and throw. A throw of 3/4 of the room width is recommended. A larger throw may lead to draft conditions.

In case of heating, it s observed that the sidewall jet leads to stagnation zone near the floor since the warm air being lighter will tend to stay near the ceiling. The stagnation zone has a higher temperature gradient. The air has to be injected into the stagnation zone to avoid it. Overthrow may minimize the stagnation zone. *This arrangement is good for cooling. It provides rapid*

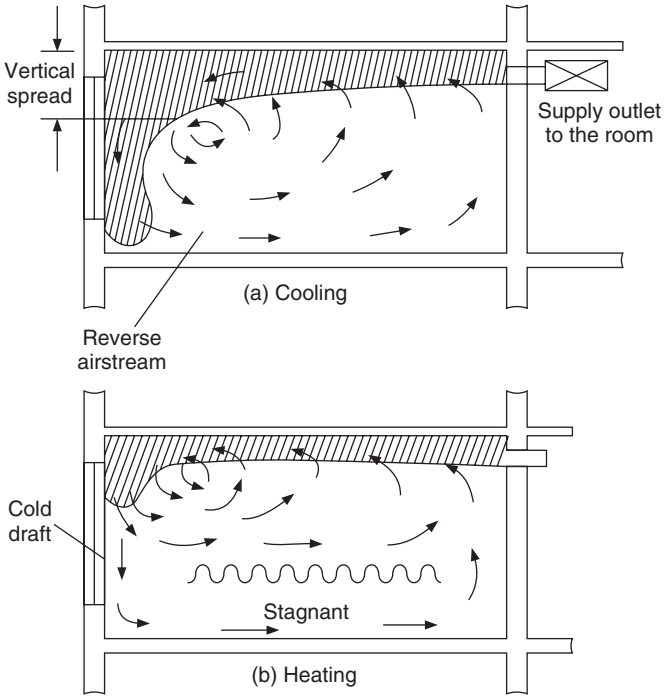

Figure 22.19 Airflow distribution patterns using high side wall outlets.

temperature equalization and no stagnation zones. It is used mainly in mild climates on second and higher floors of the building. It is not recommended for cold climates with unheated floors since it results in a large vertical temperature gradient.

Ceiling diffuser

The ceiling diffuser is very popular in all kind of applications since it can be mounted at any location in a large room where a sidewall diffuser cannot throw supply air. The ceiling diffuser throws air radially in all directions at a small angle but for all practical purpose it is near horizontal. The entrainment is very large, which reduces the high momentum of the jet very rapidly. This feature allows it to handle large volume flow rates at high velocities. The details of room airflow pattern are shown in Figures 22.20(a) and (b) for cooling and heating respectively.

The cold air tends to stay near the ceiling since it is heavier. It moves towards the sidewalls and drops down along all the sidewalls after some distance. The walls being at higher temperature, the natural convection currents rise up along the walls and are entrained by the cold air jet. The ceiling diffusers require a high-dehumidified temperature rise of 13°C to 17°C. These are good for cooling just like the high sidewall grille.

Floor registers

These outlets are mounted on the floor, or near the floor along a wall with a certain distance away from it. These are also called perimeter type outlets. These are good for heating applications particularly when the floor is over an unheated space and the wall has a large glass area. The jet can be of spreading type or of a non-spreading type.

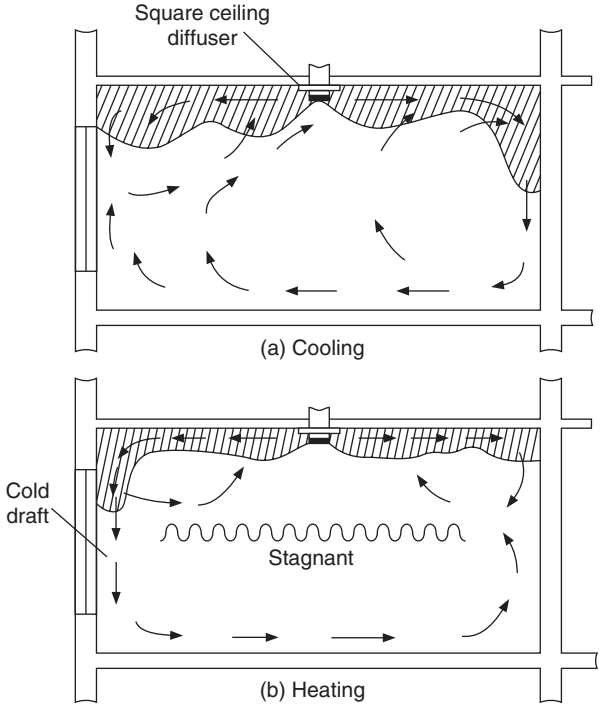

Figure 22.20 Airflow distribution patterns using ceiling diffusers.

The non-spreading type floor registers are shown in Figures 22.21(a) and (b) for cooling and heating applications. In the cooling application the total air rises up, hits the ceiling and fans out. Thereafter it falls downwards because of its larger density. On the opposite wall, air rises up along the warm wall due to buoyancy and then comes down. There may be two stagnation zones, even then this may be satisfactory for cooling.

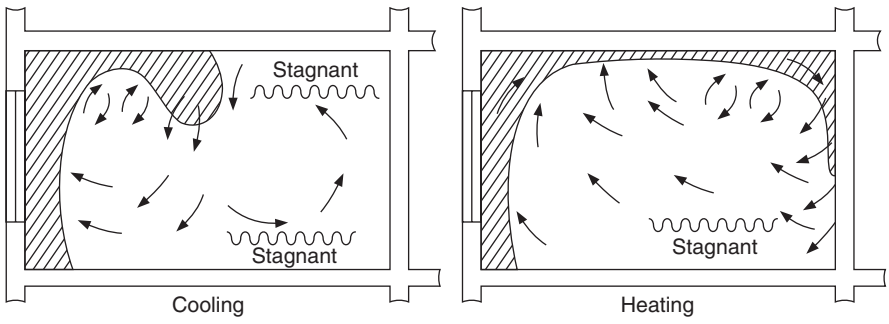

Figure 22.21 Airflow distribution patterns of floor registers, non-speading vertical jet type.

In the heating application, the warm air rises up because of its lower density, follows the ceiling, hits the opposite wall and then comes down. There is a stagnation zone near the floor. The

air comes down along the cold walls. If there is a glass area, then more air will come down. The warm air at top gives rise to stratification, which is a problem.

The elevation and side view of spreading type floor register are shown in Figure 22.22(a). The flow patterns for cooling and heating applications are shown in Figures 22.22(b) and (c) respectively. It is observed that this type of floor register is not good for cooling because the vertical throw is reduced due to its spreading nature. The throw is not sufficient to reach the ceiling. It turns back which leaves the room to be cooled by weak convection currents. A higher velocity may improve the air distribution. It is, however, good for the heating application since with the wide spread available the buoyancy increases the throw.

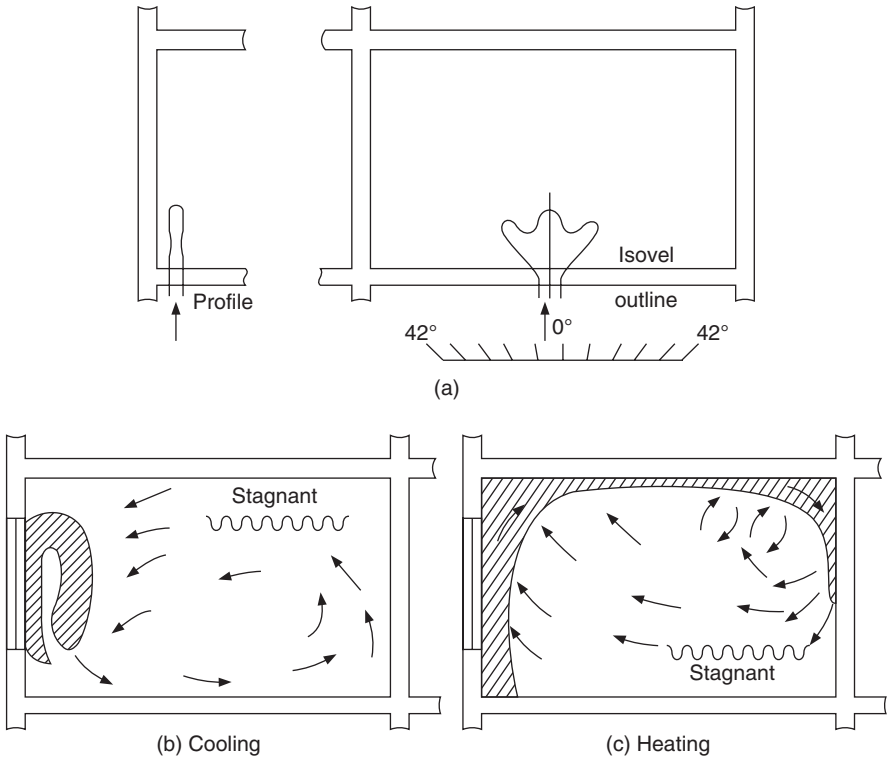

Figure 22.22 Airflow distribution patterns of floor registers, spreading vertical jet type.

When people are seated for example in theatres, floor registers cannot be used. Floor registers can be used in stores where persons are moving around. These require lower dehumidified temperatures rise and large volume flow rates. The dust collection is a problem.

Low side wall outlet discharging horizontally

These outlets are shown in Figures 22.23(a) and (b) respectively for cooling and heating applications. In cooling the supply air being at low temperature and heavier remains near the floor only. The entrained air also remains near the floor giving a low temperature in the occupied zone. In case of

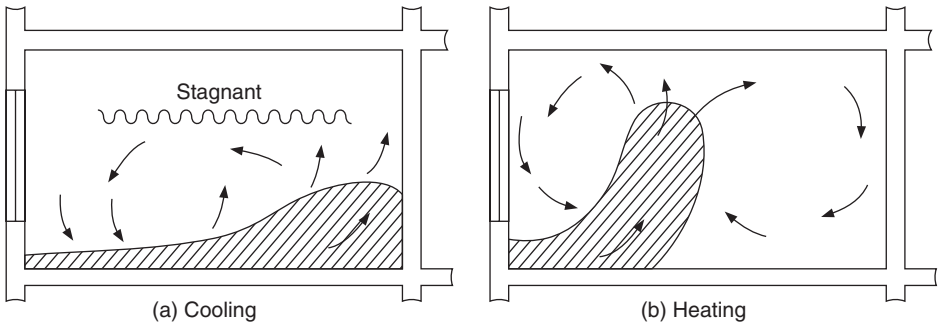

Figure 22.23 Airflow distribution patterns of low sidewall outlets discharging air horizontally.

heating the total air rises up slightly due to its lower density but still remains in the occupied zone. The floor registers throwing air horizontally also have similar air distribution pattern. These are not recommended for comfort applications.

Ceiling diffuser discharging air vertically

These outlets are shown in Figures 22.24(a) and (b) respectively. In case of cooling the cold supply air drops down to the floor. The secondary air also drops down to the floor and then the total air fans out and rises along the walls. It gives stagnation zones near the ceiling. In case of heating the density of supply air being small, it does not fall to the same extent as the cold air. The total air drops down and hits the floor but does not rise along the walls. This type of ceiling diffuser is either used for cooling or for heating. It cannot be used for both the applications. For cooling, low supply air volume flow rate velocity and dehumidified temperature rise are required whereas for heating high supply air volume is required.

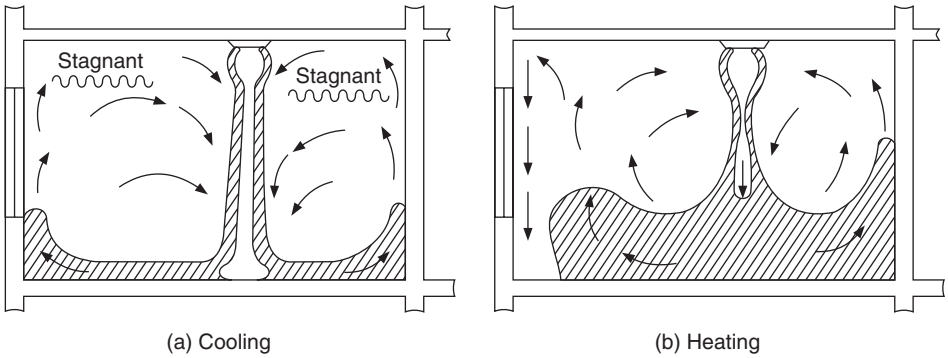

Figure 22.24 Airflow distribution patterns of ceiling diffusers discharging air vertically.

22.11.4 Return Air Inlets

The air velocity decreases as one moves away from the supply air outlet. The return air intakes are located away from the supply air outlets. The air approaches the return air intakes from all the directions and according to ASHRAE the location of these intakes has negligible effect on the

room air motion. From the energy conservation point of view, maximum heat transfer should be acquired from the supply air, that is, in cooling applications the warmest air should return and in heating applications the coolest air should return. The stagnation region is usually the best location for return air openings. In some applications with high ceilings like atriums, skylights or large vertical surfaces and where the highest areas are not occupied, air stratification is a desirable energy saving technique. In such cases the return air inlets are not located in these areas.

1. Hence the return air intakes may be located in stagnation regions except in high ceiling rooms.
2. Further the inlets are located to minimize the short circuits.
3. If there are some pollutants being generated in the room, then the return air intake should be located high up in these areas so that the pollutant does not diffuse into the rest of the room and is removed immediately after generation without causing drafts or stratification in the occupied zone. In case of dust or cotton lint in textile mills, the return air inlets are located near the floor for maximum efficiency.
4. Return air inlets should be located in areas of maximum load so as to remove the warm/cold air immediately after picking up the cooling/heating load.
5. The maximum velocity is 240 m/min for inlets located above the occupied zone and 180 m/min for those located in the occupied zone. This is done to avoid drafts near the inlets. The velocity should be particularly low if the return air intakes are located near the ear level so that excessive noise is not created.
6. A floor return is good but it tends to collect dust.

22.11.5 Noise

The diffuser always produces some noise. The noise due to air motion does not have clear-cut frequency characteristics, but it interferes with speech. The speech interfering characteristic is different at different frequencies. Higher decibles may be tolerable at lower frequencies than at lower frequencies. Noise criterion (NC) curves have been proposed to specify the decible levels, which cause some speech interference at various frequencies. Two such curves are shown in Figure 22.25 to illustrate that NC = 30 curve passes through 57, 48, 42, 35 and 32 dB at 63, 125, 250, 500 and 1000 Hz frequencies respectively. Similarly NC = 40 curve passes through 64, 57, 50, 45 and 22 dB at these very frequencies respectively. NC curves are simple means of specifying sound level limits for an environment by a single number.

NC = 30 is considered to be quiet. Sound levels of NC above 50–55 are considered noisy. Recording studios and concert halls require NC = 15–20. In restaurants, service areas, NC = 40–45 may be acceptable. The full set of these curves are available in *ASHRAE Handbook of Fundamentals Volume*, 1997.

ASHRAE Handbook gives another set of curves called *room criterion* (RC) curves. These are similar to NC curves except at low and high frequencies. These are specifically meant for HVAC system design. These are better approximation to a well-balanced neutral sounding spectrum. These also show low frequencies where noise may induce lightweight construction material such as ceiling tiles to vibrate and rattle.

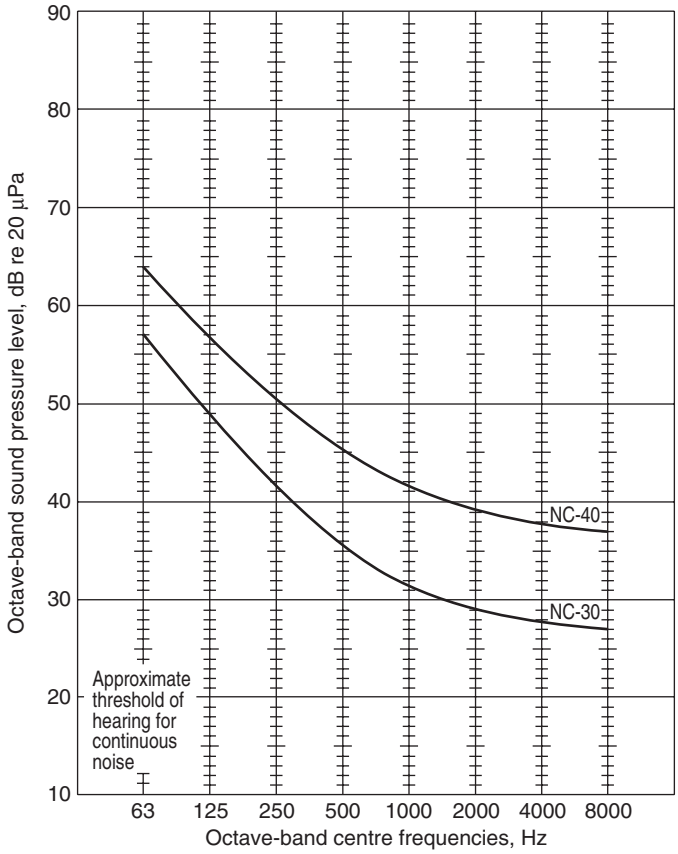

Figure 22.25 NC curves for specifying design level in terms of maximum permissible sound pressure level for each frequency band.

22.12 AIR DISTRIBUTION SYSTEM DESIGN

This part of the design involves choice and location of the supply air outlets and return air inlets; deciding the volume flow rate from load and then the throw and outlet velocity keeping noise level and uniform air distribution on mind. The outlets may be located on the basis of comfort but sometimes the architectural design and the functional requirements of the building override comfort.

It has been observed that the perimeter type floor outlets with vertical discharge are best for heating if the heating requirement is critical, particularly in the presence of large glass area. The air tends to flow downwards by natural convection on glass surface, which is counteracted by the vertically upward jet. This type of outlet is quite good for cooling as well.

The high sidewall outlet with horizontal discharge towards the exterior wall is quite good for cooling. It is good for heating too, if the heating requirement is not critical.

If the heating requirement is low, then the ceiling diffuser or high sidewall diffuser is good for cooling.

In commercial buildings, the floor space is very useful and valuable. Also the perimeter of the room may have cabinets, shelves and other decorative furniture making it unavailable for supply

air outlets. The overhead system is most practical in many situations. In all cases the ideal system cannot be used, hence the air conditioning equipment should be properly selected and located. Manufacturers give extensive catalogue data about grilles and diffusers but there is no substitute for experience, common sense and good judgment.

Equation (22.1) has been proposed as a measure of draft. This is good measure of the velocity and temperature distribution in a room. It is modified as follows to give a measure of effective draft temperature (EDT)

$$\text{EDT} = (t_x - t_r) - 7.656(\bar{V}_x - \bar{V}_r) \tag{22.91}$$

where, the subscript r refers to average room condition and x refers to any location in the room. The value of $\bar{V}_r$ is 0.15 m/s. This equation accounts for the sense of cooling produced by air motion involving convection of heat from the body. A change in velocity of value 0.1306 m/s = 7.84 m/min is equivalent to 1° C in temperature.

In Eq. (22.91) during summer application, both the terms are negative; hence any velocity greater than 0.15 m/s adds to feeling of coolness. On the other hand in winter applications if at some location $\bar{V}_x > \bar{V}_r$, this will reduce the effect of temperature and the warmth. Hence it is possible that EDT may become zero easily at any location in the room.

Experience indicates that –1.7°C < EDT < 1.1°C and velocity < 0.36 m/s are good for providing comfort to most of the sedentary people.

Air distribution performance index (*ADPI*)

The ADPI is percentage of the places of measurement in the room where –1.7°C < EDT < 1.1°C. If it is met in all the places, then ADPI is 100%. The type of diffuser and its location is selected such that this criterion is met. If the type of diffuser to be used has been selected, then ADPI is the criterion for selecting the throw. The cooling/heating capacity per unit area, called loading, is important in this context. Heavy loading lowers the ADPI.

Each type of diffuser has a characteristic length which is given in Table 22.11.

Table 22.11 Characteristic length of several diffuser types as in *ASHRAE Handbook of Fundamentals Volume*, 1997

Type of diffuser	*Characteristics length, L*
High sidewall grille	Distance to wall, perpendicular to jet
Circular ceiling diffuser	Distance to closest wall or intersecting jet
Ceiling slot diffuser	Distance to wall or mid-plane between jets

ASHRAE Handbook of Fundamentals volume 1997, has given tables for the ratio of throw X to characteristic length L, which will give maximum ADPI. The throw is based upon the distance reached by the jet where the velocity becomes 15 m/min (50 fpm). For the ceiling slot diffuser, it is based upon 30 m/min (100 fpm). Some data from this table is as follows (Table 22.12). Column 3 gives the X/L ratio for maximum ADPI given in column 4. Column 5 gives the minimum ADPI that would be obtained in the range of X/L given in column 6.

Table 22.12 The ratio of throw (*X*) to characteristic length (*L*) length for maximum ADPI

Type of diffuser	*Room loading* (kJ/min-m^2)	*X/L for maximum ADPI*	*Maximum ADPI*	*For ADPI greater than*	*Range of X/L*
High sidewall	14.4	1.8	68	–	–
grille	10.8	1.8	72	70	1.5–2.2
	7.2	1.6	78	70	1.2–2.3
	3.6	1.5	85	80	1.0–1.9
Circular ceiling	14.4	0.8	76	70	0.7–1.3
diffuser	10.8	0.8	83	80	0.7–1.3
	7.2	0.8	88	80	0.5–1.5
	3.6	0.8	93	90	0.7–1.3
Sill grille,	14.4	1.7	61	60	1.5–1.7
Straight vanes	10.8	1.7	72	70	1.4–1.7
(linear diffuser)	7.2	1.3	86	80	1.2–1.8
Straight vanes	3.6	0.9	95	0	0.8–1.3

The recommended procedure for choosing the type and size of diffuser is as follows:

1. For a given room size and the load, find the volume flow rate.
2. Select the type of diffuser from comfort point of view or other considerations.
3. Determine the room characteristic length from Table 22.11.
4. Select the recommended throw-to-length ratio from Table 22.12.
5. Calculate the throw.
6. Choose the appropriate diffuser from the manufacturer's catalogue data.
7. Check that noise criterion and total pressure, etc. are within limits.

The performance of the diffusers is usually available in a manufacturer's catalogue. The performance data consists of size of the outlet, free area for various sizes, outlet velocity, velocity pressure, total pressure capacity, throw and noise criterion. The data for a typical round diffuser, a typical linear diffuser (vertical slot jet, sidewall or ceiling) and a high sidewall diffuser are given in Tables 22.13, 22.14 and 22.15 respectively. In the case of the linear diffuser the length of the diffuser can be the entire length of the room. However, throw is given for a length of 1.22 m and NC is based upon 3.05 m length. The throw values are given for three terminal velocities. The minimum throw refers to a terminal velocity of 0.254 m/s. The medium throw refers to a terminal velocity of 0.51 m/s and the maximum throw refers to a terminal velocity of 0.76 m/s.

Table 22.13 Performance data for typical round diffuser

Size (m)	*Neck velocity* (m/min)	*Velocity pressure,* (mm of water)	*Total pressure* (mm of water)	*Flow rate* (m^3/min)	*Radius of diffuser* (m)			*NC*
					Min.	Mid.	Max.	
0.25	122	0.25	0.68	6.23	0.91	1.22	2.13	–
	183	0.58	1.57	9.34	1.22	1.83	3.05	17
	244	1.0	2.74	12.32	1.52	2.44	3.96	26

(*Contd.*)

Table 22.13 Performance data for typical round diffuser (contd.)

Size (m)	*Neck velocity* (m/min)	*Velocity pressure,* (mm of water)	*Total pressure* (mm of water)	*Flow rate* (m^3/min)	*Radius of diffuser* (m)			*NC*
					Min.	Mid.	Max.	
	305	1.6	4.32	15.43	2.13	3.05	4.88	33
	366	2.3	6.17	18.55	1.44	3.66	6.1	39
0.3	122	0.25	0.66	8.9	0.91	1.52	2.44	–
	183	0.58	1.5	13.3	1.52	2.13	3.66	17
	244	1.0	2.7	17.8	1.82	3.05	4.57	26
	305	1.6	4.2	22.2	2.44	3.66	5.79	33
	366	2.3	6.0	26.6	3.05	4.27	7.01	39
0.46	122	0.25	0.75	20.1	1.52	2.13	3.66	–
	183	0.58	1.75	30.0	2.13	3.35	5.49	21
	244	1.0	3.05	40.2	3.05	4.57	7.32	30
	305	1.6	4.8	50.1	3.66	5.79	9.14	37
	366	2.3	6.86	60.0	4.57	6.71	10.97	43
0.61	122	0.25		35.7	1.83	2.74	4.57	–
	183	0.58		53.2	2.74	4.27	6.71	19
	244	1.0		71.0	3.66	5.79	9.14	28
	305	1.6		89.0	4.88	7.01	11.28	35
	366	2.3		106.7	5.79	8.53	13.71	41

Table 22.14 Performance data for typical linear diffuser (vertical slot, side wall or ceiling)

Size (mm)	*Area* m^2/m	*Total pressure* (mm of water)	*Flow rate* (m^3/min)	*Radius of diffuser* (m)			*NC*
				Min.	*Mid.*	*Max.*	
76	0.0293	0.51	5.39	2.13	2.13	2.13	–
		1.45	8.92	3.66	3.96	4.27	17
		2.77	12.45	5.49	5.79	6.1	26
		4.62	16.07	7.01	7.31	7.62	33
		5.71	17.84	7.62	7.62	7.92	36
101	0.0424	0.51	7.71	2.74	2.74	2.74	–
		1.45	12.91	4.88	4.88	5.18	18
		2.77	18.12	6.7	7.01	7.31	27
		4.62	23.22	8.23	8.23	8.23	34
		5.71	25.83	9.14	9.14	9.14	37
152	0.0674	0.51	12.36	3.05	3.05	3.605	–
		1.45	20.53	5.49	5.49	5.49	19
		2.77	28.8	7.62	7.62	7.62	28
		4.62	36.97	9.45	9.45	9.45	35
		5.71	41.06	9.75	9.75	9.75	38

Table 22.15 Performance data for adjustable-type, high sidewall diffuser

Size (m)	*Area* (m^2)	*Flow rate* (m^3/min)	*Velocity* (m/min) p_v in mm of water	*Deflection degrees*	*Total pressure* (mm of water)	*Radius of diffuser* (m)		
						Min.	Mid.	Max.
0.2 × 0.1	0.017	2.0	122	0	0.432	1.83	2.44	4.57
0.18 × 0.13			p_v = 0.254	22.5	0.483	1.52	1.83	3.66
0.15 × 0.15				45	0.739	0.91	1.22	2.44
0.25 × 0.1	0.02	2.55		0	0.432	2.13	3.05	5.18
0.2 × 0.13				22.5	0.483	1.83	2.44	4.27
0.18 × 0.15				45	0.739	0.91	1.52	2.74
0.3 × 0.1	0.024	2.97		0	0.432	2.13	3.35	5.79
0.25 × 0.13				22.5	0.483	1.83	2.74	4.57
0.2 × 0.15				45	0.739	1.22	1.52	2.74
0.41 × 0.1	0.031	3.82		0	0.432	2.44	3.66	6.4
0.3 × 0.13				22.5	0.483	1.83	3.05	5.18
0.25 × 0.15				45	0.739	1.22	1.83	3.35
0.46 × 0.1	0.036	4.39		0	0.432	2.74	3.96	7.01
0.36 × 0.13				22.5	0.483	2.13	3.05	5.49
0.3 × 0.15				45	0.739	1.22	1.83	3.35
0.2 × 0.1	0.017	3.11	183	0	0.965	2.74	3.96	5.79
0.18 × 0.13			p_v = 0.559	22.5	1.092	2.13	3.05	4.57
0.15 × 0.15				45	1.626	1.22	2.13	3.05
0.25 × 0.1	0.02	3.68		0	0.965	2.74	4.57	6.4
0.2 × 0.13				22.5	1.092	2.13	3.66	5.18
0.18 × 0.15				45	1.626	1.52	2.13	3.05
0.3 × 0.1	0.024	4.39		0	0.965	3.05	4.88	7.10
0.25 × 0.13				22.5	1.092	2.44	3.96	5.49
0.2 × 0.15				45	1.626	1.52	2.44	3.35
0.41 × 0.1	0.031	5.8		0	0.965	3.66	5.79	7.92
0.3 × 0.13				22.5	1.092	3.05	4.57	6.4
0.25 × 0.15				45	1.626	1.83	2.74	3.96
0.46 × 0.1	0.036	6.65		0	0.965	3.96	5.79	8.53
0.36 × 0.13				22.5	1.092	3.06	4.57	6.71
0.3 × 0.15				45	1.626	2.13	3.05	4.27
0.2 × 0.1	0.017	4.1	244	0	1.752	3.35	4.88	6.71
0.18 × 0.13			p_v = 1.016	22.5	1.981	2.74	3.96	5.49
0.15 × 0.15				45	2.972	1.83	2.44	3.35
0.25 × 0.1	0.02	4.95		0	1.752	3.96	5.18	7.31
0.2 × 0.13				22.5	1.981	3.05	4.27	5.79
0.18 × 0.15				45	2.972	1.83	2.74	3.66

(*Contd.*)

Table 22.15 Performance data for adjustable-type, high sidewall diffuser (contd.)

Size (m)	*Area* (m^2)	*Flow rate* (m^3/min)	*Velocity* (m/min) p_v in mm of water	*Deflection degrees*	*Total pressure* (mm of water)	*Radius of diffuser* (m)		
						Min.	Mid.	Max.
0.3 × 0.1	0.024	5.95	244	0	1.752	4.27	5.79	7.92
0.25 × 0.13			p_v = 1.016	22.5	1.981	3.35	4.57	6.4
0.2 × 0.15				45	2.972	2.13	2.74	3.96
0.41 × 0.1	0.031	7.64		0	1.752	4.88	6.1	9.14
0.3 × 0.13				22.5	1.981	3.96	5.49	7.31
0.25 × 0.15				45	2.972	2.44	3.35	4.57

EXAMPLE 22.9 A laboratory is to be air-conditioned for summer cooling. It has ceiling height of 3.5 m. The total volume flow rate is 162 m^3/min with a load of 14.42 kJ/min-m^2 (0.0684 TR/m^2). The total cooling load is 14 TR. Find the specification of (a) circular ceiling diffuser if 12 equally spaced diffusers are used, (b) circular ceiling diffusers if six of them are used, (c) high sidewall diffuser if it is used on both the sides, and (d) vertical slot diffuser for winter application.

Solution:

(a) There are 12 ceiling diffusers equally spaced in the laboratory. The characteristic length in this case is the distance from a ceiling diffuser to the line of intersection between two ceiling diffusers. This is given by

$$L = 21.75/8 = 2.73 \text{ m}$$

From Table 22.12, *X*/*L* for maximum ADPI = 0.8. Therefore.

$$\text{Throw } X = 0.8 \times 2.73 = 2.2 \text{ m}$$

The volume flow rate of each diffuser = 162/12 = 13.5 m^3/min.

An inspection of Table 22.13 for 0.25 m circular ceiling diffuser shows by interpolation that the volume flow rate of 13.5 m^3/min can be obtained at neck velocity of 267 m/min.

By interpolation the maximum throw = 4.4 m and minimum throw = 1.75 m

Total pressure drop by interpolation = 3.34 mm of water.

The maximum throw is much larger than the required throw of 2.2 m; hence this arrangement will not be economical.

(b) This arrangement has 6 ceiling diffusers equally spaced in the laboratory. The characteristic length in this case also is the distance from a ceiling diffuser to the line of intersection between two ceiling diffusers. This is given by

$$L = 21.75/6 = 3.65 \text{ m}$$

From Table 22.12, *X*/*L* for maximum ADPI = 0.8. Therefore.

$$\text{Throw } X = 0.8 \times 3.65 = 2.92 \text{ m}$$

The volume flow rate of each diffuser = 162/6 = 27.0 m^3/min.

An inspection of Table 22.13 for 0.54 m circular ceiling diffuser shows by interpolation that the volume flow rate of 27.0 cmm can be obtained at neck velocity of 163.8 m/min.

By interpolation the maximum throw = 4.88 m and the minimum throw = 1.95 m.

Total pressure drop by interpolation = 1.43 mm of water.

The throw is again very large compared to that desired, but it is satisfactory compared to case (a).

(c) High sidewall grille:

If we decide to have grille along only one wall, the characteristic length in this case is the width of the laboratory, that is,

$$L = 9.375 \text{ m}$$

From Table 22.12, *X/L* for maximum ADPI = 1.8. Therefore,

$$\text{Throw } X = 1.8 \times 9.375 = 16.875 \text{ m}$$

This is a very large throw, which cannot be attained by any of the slot diffusers; hence we decide to have slot diffuser on both the sides. This makes the throw to be half of the previous value, that is, throw $X = 8.437$ m.

The volume flow rate for each side is half of total m^3/min, that is, 81 m^3/min.

We choose the diffuser set (0.41 × 0.1, 0.3 × 0.13 and 0.25 × 0.15) at 244 m/min velocity and angle of 0^o. The maximum throw is 9.14 m, which is good enough and the volume flow rate is 7.64 m^3/min.

Therefore the number of grilles required = 81/7.64 = 10.6 = 11

Eleven grilles (0.41m × 0.1m, 0.3 × 0.13 and 0.25 × 0.15) should therefore be used on the two side walls.

Total pressure drop is 1.752 mm of water.

(d) The characteristic length in this case is the ceiling height, that is,

$$L = 3.5 \text{ m}$$

For a load of 14.4 kJ/min- m^2 from Table 22.12, the throw is given by

$$X = 1.7L = 1.7 \times 3.5 = 5.95 \text{ m}$$

It is observed from Table 22.14 that for a 76 mm diffuser, at flow rate of 12.45 m^3/min the throw is 5.95 m. This is acceptable. This volume flow rate is for one-metre length of the diffuser. The length of diffuser required for total volume flow rate of 162 m^3/min is given by

Total diffuser length = 162/12.45 = 13 m. This has to be equally spread on two sides of the room. It gives four diffusers each of length 3.25 m.

Total pressure drop is 2.77 mm of water.

REFERENCES

ASHRAE Handbook of Fundamentals Volume (1989): American Society of Heating, Refrigerating and Air Conditioning Engineers, Inc. Atlanta, GA.

ASHRAE Handbook of Fundamentals Volume (1997): American Society of Heating, Refrigerating and Air Conditioning Engineers, Inc. Atlanta, GA.

REVIEW QUESTIONS

1. Explain with the help of a schematic diagram the functioning of a typical air-duct system.
2. What are the sources of pressure losses in air ducts? How can they be kept low?
3. Discuss the important air-duct design considerations.
4. Discuss the various methods used to classify air ducts.
5. Briefly describe the different methods of duct design.
6. A typical air-duct system is shown below:

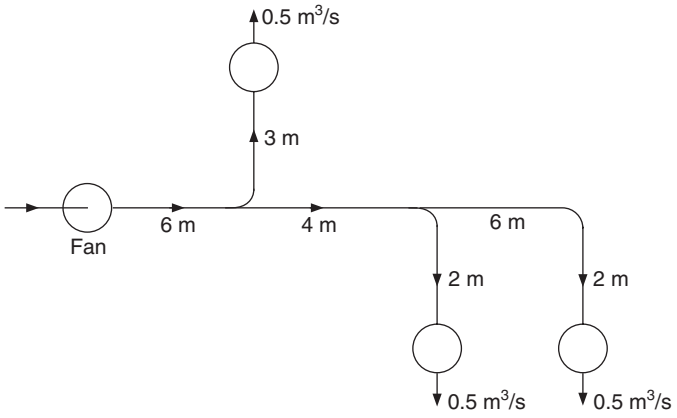

Find the duct sizes using the static-regain method. The air velocity in the first section is not to exceed 8 m/s. Also, estimate the static pressure in the index run of the duct network. Assume a pressure drop of 20 Pa at each of the outlet grilles.

7. A typical air-duct system is shown below:

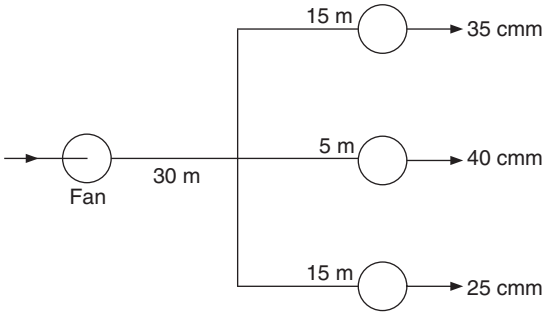

The velocity downstream of the fan is 400 m/min. The ducts can of rectangular section and one side of each duct is 60 cm. Find the duct sizes by the equal friction method and the maximum pressure loss.

8. For Question 6, design the duct system using (a) the velocity method and (b) equal friction method. Assume a dynamic loss coefficient of 0.3 for upstream to downstream and 0.8 for upstream to branch and for the elbow. Assume dynamic loss coefficients for the outlets as 1.0. Find the FTP required for each case and the amount of dampering required.

23

Fans

LEARNING OBJECTIVES

After studying this chapter the student should be able to:

1. Explain the types of fans used in air conditioning systems.
2. Sketch and explain the characteristics of forward-curved blades, radial blades and back-curved blades type of centrifugal fans.
3. Sketch and explain the characteristics of vaneaxial fans.
4. Define the fan laws.
5. Describe the application of centrifugal and vanexial fans.

23.1 INTRODUCTION

In all *air conditioning systems*, the warm and humid air has to be aspirated from the conditioned space, mixed with fresh air and passed over the cooling coil and finally the conditioned air is distributed to the space. The movement of the air through ductwork is done by fan. The fan induces air motion in the room. Free convection also causes air motion in the room. The selection of a fan is very crucial for the efficiency of the air distribution system, control of noise level, indoor air quality and comfort to the occupants.

Air conditioning systems normally use three type of fans, namely, centrifugal, axial and vaneaxial.

The *centrifugal fan* is very widely used in air conditioning systems whenever there is considerable ductwork or pressure drop, the volume flow rate may be small or large. It is relatively quiet in operation and has good efficiency. Small units like window air conditioners

and package units use simple drum type centrifugal fans whereas larger units use fans with aerofoil shaped blades.

The *axial fan* does not produce a large pressure rise but it can give a very large volume flow rates. The noise level in an axial fan is high compared to a centrifugal fan. Most of the exhaust fans are of this type.

The *vaneaxial fan* is mounted at the centreline of the duct. It gives axial flow of air. Normally the rotating blades impart rotational velocity and energy to the air stream. The vaneaxial fan has guide vanes both at inlet and outlet of the wheel to reduce the rotation of axial stream in order to prevent the wastage of energy.

23.2 PERFORMANCE OF FANS

The fan performance or fan characteristics include the pressure rise, the efficiency, and the power requirement as a function of volume flow rate. The rotation of impeller imparts kinetic energy (velocity pressure) to the fluid and also increases the static pressure due to diverging passage area between the blades. If 1 and 2 denote the states at the inlet and outlet of the fan, then the total pressure rise across the fan denoted by FTP is given in pascals as follows:

$$\text{FTP} = \Delta p_t = p_{02} - p_{01} = (p_2 - p_1) + \rho_a (V_2^2 - V_1^2)/2 \tag{23.1}$$

This can be converted into mm of water column by the following conversion factor:

$$1 \text{ mm of water column} = 9.81 \text{ pascals} \tag{23.2}$$

The total pressure in the above expression is denoted by p_0.

If the volume flow rate of air is Q_v m^3/s, then the power imparted to air is given by

$$W = Q_v \, \Delta p_t/60 \text{ watts} \tag{23.3}$$

When, Q_v is in m^3/min and Δp_t is in pascals

$$W = 9.81 \, Q_v \, \Delta p_t/60 = 0.1635 \, Q_v \, \Delta p_t \text{ watts} \tag{23.4}$$

where pressure is in mm of water column. If the mass flow rate of air is specified as $\dot{m}$ kg/s, then the total work and specific work are given by

$$W = \dot{m} \Delta p_t / \rho_a \; ; \qquad w = \Delta p_t / \rho_a \tag{23.5}$$

The total pressure of fan is proportional to the square of tip velocity of the blade. If rpm and impeller diameter are denoted by N and D (in m) respectively, then

$$\text{FTP} \propto \rho_a D^2 N^2 \tag{23.6}$$

The volume flow rate is proportional to the fan area and velocity, that is,

$$Q_v \propto D^2 (DN) \propto D^3 N \tag{23.7}$$

$$W \propto \rho_a \, D^5 N^3 \tag{23.8}$$

The fan efficiency is defined either in terms of static pressure rise or in terms of total air power. The expressions given above are those for air power. The shaft power is denoted by W_{shaft}, the total efficiency and static efficiency are defined as follows:

$$\eta_t = Q_v \, \Delta p_t / W_{\text{shaft}} \tag{23.9}$$

$$\eta_s = Q_v \, \Delta p / W_{\text{shaft}} \tag{23.10}$$

Centrifugal fan

The general configuration of a centrifugal fan is shown in Figure 23.1. It consists of an impeller, which is driven by a motor either directly or through a belt and pulley arrangement. The blades are mounted on the impeller. The air enters along the axis and is discharged at periphery through scroll casing.

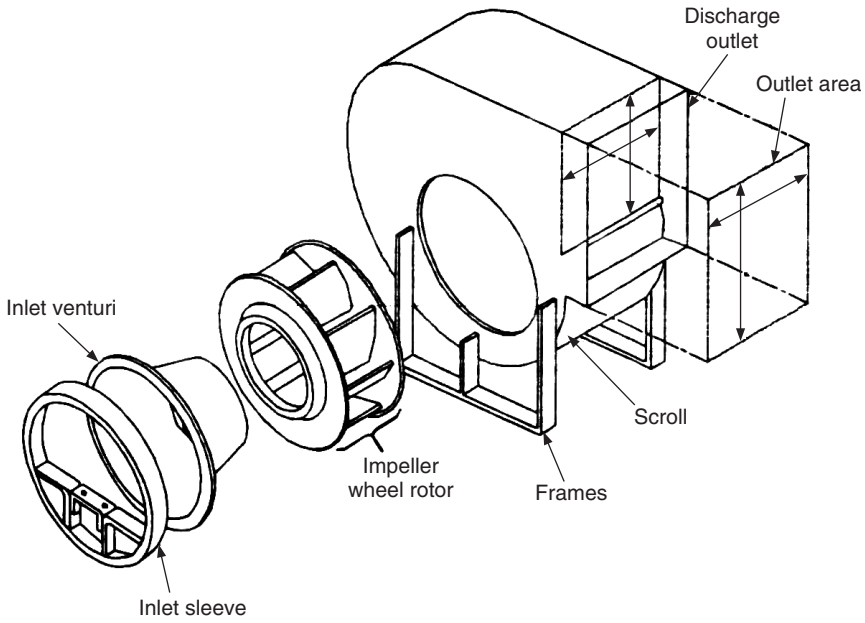

Figure 23.1 Centrifugal fan components.

Let $U_1$and U_2 denote the tangential or peripheral velocities at inlet and outlet of the blade respectively. Let $C_{r1}$and C_{r2} denote the relative velocities at inlet and outlet of the blade respectively. These velocities are tangent to the blade surface. Let C_1 and C_2 denote the total fluid velocities at inlet and outlet of the blade respectively. The air enters the blade passage with relative velocity C_{r1} radially and leaves with relative velocity C_{r2} at angle β_2 with the peripheral velocity U_2. The angle β_2 for three forms of blade design (backward curved, radial, forward curved) together with their respective velocity triangles are shown in Figure 23.2.

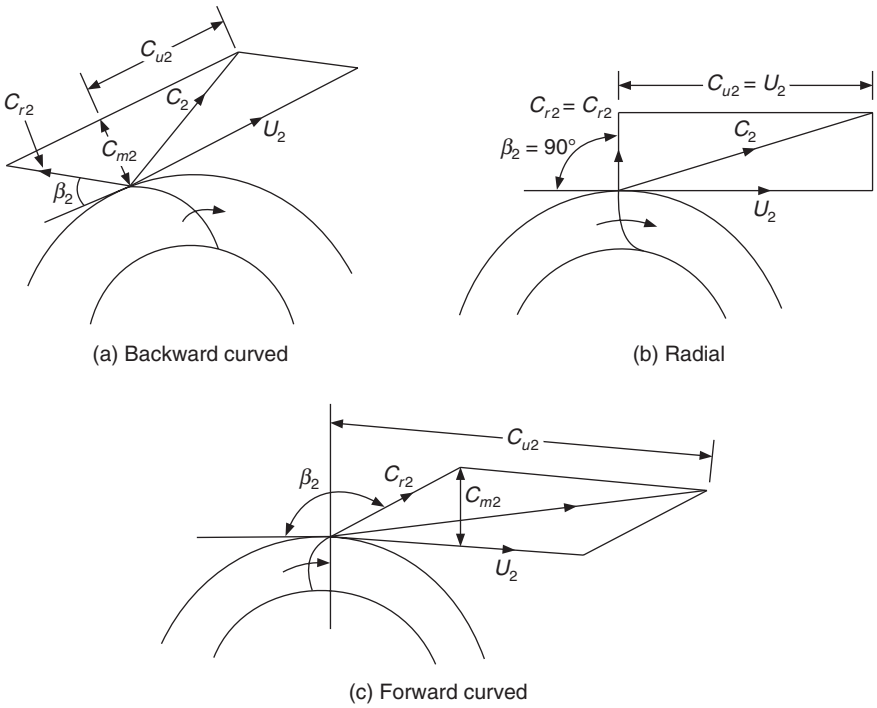

Figure 23.2 Blade design and their corresponding outlet velocity triangles for centrifugal fans.

The velocity diagram and the energy equation are same as those for the centrifugal compressor (see Chapter 4). It was shown that for centrifugal compressors the specific work requirement is given by Eqs. (4.75) and (4.76) as follows:

$$w = C_{u2}U_2 - C_{u1}U_1 = \frac{U_2^2 - U_1^2}{2} + \frac{C_2^2 - C_1^2}{2} + \frac{C_{r2}^2 - C_{r1}^2}{2} \tag{23.11}$$

where C_{u1} and C_{u2} are the components of velocities $C_1$and C_2 in the peripheral direction. C_{m2} denotes the radial component or meridonal component of velocity C_2 as shown in Figure 23.2.

Normally radial entry or entry along the axis is assumed in all fans which yields

$$C_{u1} = 0 \tag{23.12}$$

The expression for C_{u2} for the three blade types is as follows:

Backward curved blades : $C_{u2} = U_2 - C_{m2} \cot \beta_2$ (23.13a)

Forward curved blades : $C_{u2} = U_2 + C_{m2} \cot \beta_2$ (23.13b)

Radial blades : $C_{u2} = U_2$ (23.13c)

The expression for work requirement of a fan with backward curved blades as given by Eq. (23.11) reduces to

$$w = C_{u2}U_2 = U_2(U_2 - C_{m2} \cot \beta_2) \tag{23.14}$$

For an impeller with inner and outer diameters of D_1 and D_2 respectively, and the inlet and outer shroud widths of b_1 and b_2 respectively the volume flow rate is given by

$$Q_v = \pi D_1 C_{m1} b_1 = \pi D_2 C_{m2} b_2 \tag{23.15}$$

The characteristics of centrifugal compressors were discussed in terms of head and flow coefficients. The head coefficient μ was defined as the ratio of specific work to the square of tip speed, that is,

$$\mu = w/U_2^2 \tag{23.16}$$

Similarly, the flow coefficient was defined as the ratio of flow velocity to the tip velocity, that is,

$$\varphi = C_{m2}/U_2 \tag{23.17}$$

In terms of these coefficients the specific work of fans may be expressed as follows:

$\mu = 1 - \cos \varphi$ for a fan with backward curved blades
$\mu = 1 + \cos \varphi$ for a fan with forward curved blades
$\mu = 1$ for a fan with radial blades

23.3 FAN CHARACTERISTICS

The fan characteristics are presented in the form of a plot of pressure rise, power requirement and efficiency against the volume flow rate of the fan. Figure 23.3 shows the typical characteristics for fans with forward blades.

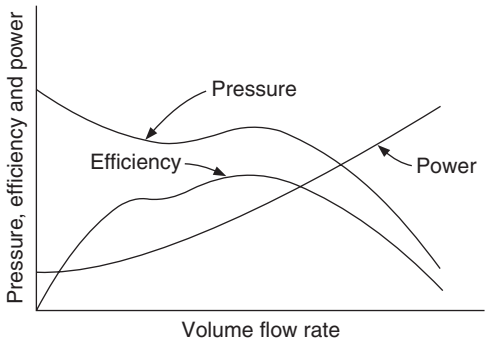

Figure 23.3 Typical characteristics of fans with forward-curved blades.

The pressure developed by a fan with forward-curved blades is highest for a given diameter and speed. This curve has a characteristic dip in pressure, that is, as the volume flow rate increases from zero value the pressure rise starts to decrease and then reaches a peak value and decreases thereafter. This is also referred to as point of inflection. The efficiency increases with volume flow rate and decreases after reaching a maximum value. The maximum efficiency and pressure occur approximately at the same volume flow rate. The power requirement increases monotonically with the volume flow rate. The pressure rise is rather flat in the region of maximum efficiency. The design point of the fan is usually chosen in the region of maximum efficiency. A small change in pressure drop, due to say filter or damper operation, will change the volume flow rate significantly

in this region. The power requirement of the motor will increases drastically in this region for a small change in pressure. This may overload the motor. These fans never have efficiency greater than 75%.

Figure 23.4 shows the fan characteristics for a fan with radial blades. In this type of fan the pressure developed decreases in the region of maximum efficiency. The power requirement also increases in a steep manner in this region. However a small change in pressure does not change the volume flow rate drastically as occuring in the case of the fan with forward-curved blades.

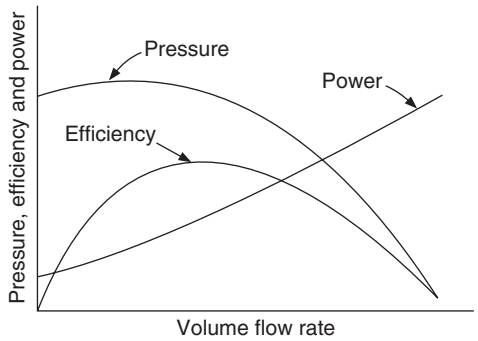

Figure 23.4 Typical characteristics of fans with radial blades.

Figure 23.5 shows the characteristics of fans with backward-curved blades. This has a steep drop in total pressure and a flat power curve in the region of maximum efficiency. Hence the volume flow rate remains almost unchanged with a small drop in pressure. The power requirement increases with volume flow rate, reaches a peak and then decreases with increase in volume flow rate. The power curve is almost flat in the region of maximum efficiency, which is referred to as non-overloading characteristics. The efficiency of this fan may be as high as 80% with sheet metal construction and 90% for aerofoil-shaped blades. These have to be run at higher speeds compared to fans with forward-curved blades to develop the same pressure.

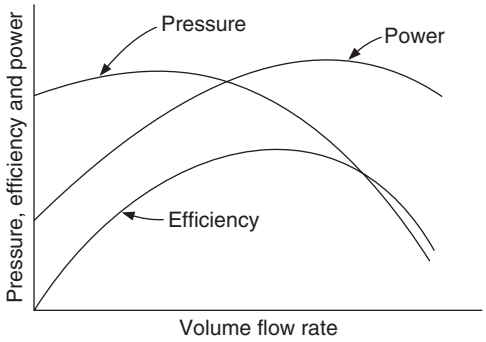

Figure 23.5 Typical characteristics of fans with backward-curved blades.

Fans with forward-curved blades are smaller and have lower speed. For small pressure drops, say up to 7.5 mm of water, these are quieter and cheaper compared to fans with backward-curved blades. The radial blade fans develop the highest pressure for same radius and speed but they are noisy.

The noise emitted by a fan is proportional to the tip speed of the impeller and the air velocity leaving the wheel. Also the noise level is proportional to the pressure developed regardless of the blade type. Backward-curved blades generally create less noise.

23.4 VANEAXIAL FAN

Figure 23.6 shows a view of the vaneaxial fan mounted at the centreline of the duct. It has guide vanes at inlet and outlet. The outlet vanes reduce the rotational component of velocity. The characteristics of this fan are shown in Figure 23.7. The power requirement is almost flat, it reaches a peak and then decreases at lower volume flow rates. The pressure drops steeply in the region of maximum efficiency. These characteristics are similar to fan with backward-curved blades.

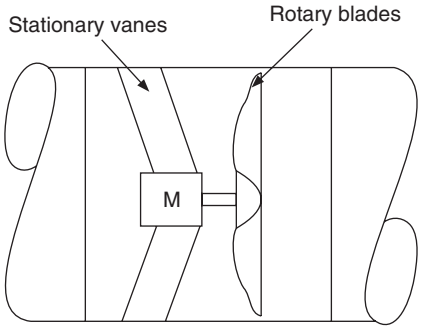

Figure 23.6 Vaneaxial fan.

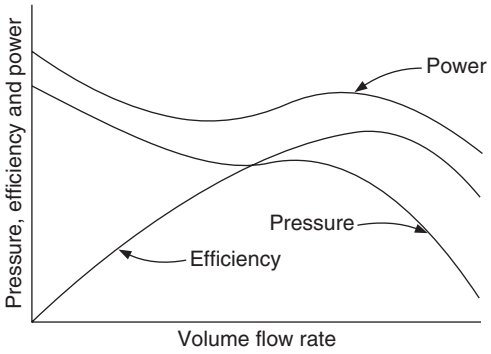

Figure 23.7 Typical characteristics of vaneaxial fans.

23.5 FAN LAWS

There are a number of simple relations between fan capacity, pressure, speed and power. These are referred to as fan laws. The three main fan laws are as follows.

1. Capacity Q_v is directly proportional to fan speed N, i.e. $Q_v \propto D^3 N$.
2. The fan pressure (static pressure, velocity pressure and total pressure) is proportional to the square of fan speed, i.e. FTP $\propto \rho_a D^2 N^2$.
3. The fan power is proportional to the cube of fan speed, i.e. $W \propto \rho_a D^5 N^3$.

Another three laws are as follows:

1. The pressure and power are proportional to density if the fan speed and capacity are constant.
2. The speed, capacity and power are inversely proportional to square root of density at constant pressure.
3. The capacity, speed and pressure are inversely proportional to density, and the power is inversely proportional to the square of density at a constant mass flow rate.

EXAMPLE 23.1 A centrifugal fan with wheel diameter of 925 mm and outlet area of 0.71 m^2 runs at 700 rpm consuming 5.2 hp and gives a volume flow rate of 4.25 m^3/s with a total pressure rise of 71.1 mm of water. The temperature of air is 0°C and the pressure is 1.01325 bar. (a) Determine the fan power and efficiency. (b) If the air temperature is 35°C and barometric pressure is 85 kPa, determine the volume flow rate, FTP and the fan power requirement. (c) Estimate the capacity, total pressure and power requirement when the speed is increased to 1000 rpm.

Solution:

(a) 71.1 mm of $H_2O = 71.1 \times 9.81 = 697.5$ Pa
Fan power = $Q_v \Delta p = 4.25 \times 697.5 = 2.964$ kW
Shaft power = 5.2 hp = $5.2 \times 0.746 = 3.879$ kW
Fan efficiency = 2.964/3.879 = 76.4 %

(b) The density will change with air temperature and pressure.
The volume flow rate will remain unchanged. $Q_v = 4.25$ m^3/s
FTP and power are proportional to density. Hence,

$$\text{FTP} = 697.5\left(\frac{273+0}{273+35}\right)\frac{85}{101.325} = 518.63 \text{ Pa}$$

$$W = 2.964\left(\frac{273+0}{273+35}\right)\frac{85}{101.325} = 2.204 \text{ kW}$$

(c) From the first fan law, as the fan speed is increased $Q_{v2} = Q_{v1}(N_2/N_1)$
$= (4.25)(1000/700) = 6.07$ m^3/s
From the second fan law, $p_{02} = p_{01}(N_2/N_1)^2 = 71.1(1000/700)^2 = 145.1$ mm of water
From the third fan law, $W_2 = W_1(N_2/N_1)^3 = 5.2(1000/700)^3 = 15.16$ hp

23.6 FAN SELECTION

Fans with radial blades are not usually used in air conditioning systems. Some of the characteristic features of the fans useful in fan selection are discussed below:

Backward-curved blade fans

These fans have the highest efficiency amongst all centrifugal fans. Their use results in lower power consumption. These fans have the highest speed of operation for a given duty. For these reasons these fans are used in low, medium and high-pressure HVAC systems. However, these fans have power limiting characteristics. The power requirement is maximum near the maximum efficiency. If a motor of this capacity is chosen then at larger volume flow rates the power requirement decreases avoiding the overloading of motor.

Backward-curved blade fans are used in industrial applications, also resulting in significant saving in power consumption. Aerofoil-shaped blades give the best efficiency, however, erosion of blades can occur due to pollutants in the industrial atmosphere.

Forward-curved blade fans

Forward-curved blade fans are used in low pressure HVAC systems such as domestic furnaces, package units, etc. These fans have the lowest efficiency and operate at the lowest speed. There is a dip in the pressure vs. volume flow rate curve to the left of the pressure peak. The highest efficiency occurs to the right of the pressure peak. The design point of this fan is selected towards far right of the pressure peak. The power requirement increases continuously with the increase in volume flow rate.

Vaneaxial fans

This fan is used in low, medium and high pressure HVAC systems. Its blades usually have aerofoil shape, which leads to relatively high efficiency at medium and high pressures. The highest pressure as shown in Figure 23.7 occurs at medium flow rates unlike centrifugal compressors where it occurs at lower flow rates. There is a break to the left of peak pressure, which is due to aerodynamic stall. Application in this region is avoided. It is possible to change the pitch of blades to meet different applications.

Maximum fan speed

In a rotating fan, stresses are developed in shaft, blades and in the back plate. For a rotating shaft, a critical speed is defined which depends upon the shaft material, mass, diameter and the distance between bearings. The maximum allowable speed must be much less than the critical speed, otherwise bending and torsional stresses may approach the yield stress. ASHRAE (1993) recommends that maximum speed should be less than 66% of critical speed but 55% is a safe limit. The maximum velocity occurs at the fan tip, giving rise to centrifugal forces but unlike centrifugal compressor, the blades of centrifugal fan are mounted in a wheel, hence the tip speed is not important. The fans should be statically and dynamically balanced.

Margins in fan selection

Some margins or safety factors are used in the selection of fans. It is expensive to use excessive margins. The margins are required to take care of design errors, late changes reported in required performance, unforeseen installation difficulties, mistakes in duct erection by misinterpretation of the design and leakage of air. As a thumb rule the volume rate is selected to be 5% more than the actual value and FTP is taken 10% more than the actual value. The motor of a forward-curved blade fan is given a margin of 35% while that of backward-curved fan is given 25% margin. The motor should be capable of achieving full speed in 18 seconds. The starter has to be selected according to this criterion.

Manufacturer's fan data

Manufacturers give plots with the region of preferred operation shown in them. Static pressure is given in all the plots. Some manufacturers do not provide total pressure. It may be computed by finding the outflow velocity from the capacity and the outlet dimensions. In some cases manufacturers give the fan performance data in a tabular form. One table is provided for each

wheel diameter. For a given volume flow rate the outlet velocity is given. Then for several rpm, the pressure rise and power input are given. As an example, Table 23.1 gives this data for a backward-curved blade fan of 600 mm wheel diameter and an outlet area of 0.479 m^2.

Table 23.1 Performance data for backward-curved blade fan

Q_v	*Outlet velocity*	0.7 kPa		0.8 kPa		0.9 kPa		1.0 kPa		1.1 kPa		1.2 kPa	
(m^3/s)	(m/s)	rpm	kW	rpm	kW	rpm	kW	rpm	kW	rpm	kW	rpm	kW
4.32	9	679	5.2	732	6.06	778	6.9	825	7.68				
4.78	10	664	5.48	721	6.48	770	7.46	819	8.43	864	9.47		
5.27	11	654	5.82	704	6.82	755	7.98	808	9.02	855	10.1	900	11.2
5.75	12	656	6.38	699	7.31	743	8.43	790	9.47	840	10.5	887	11.7
6.23	13	663	7.12	702	7.98	741	8.87	781	9.84	825	11.0	871	12.3
6.72	14	674	7.9	710	8.72	747	9.62	781	10.6	817	11.6	855	12.7

EXAMPLE 23.2 A HVAC system requires 5.5 m^3/s at 1.1 kPa total pressure rise. Determine the speed, the power, the total efficiency if a fan of 600 mm wheel diameter of Table 23.1 is used.

Solution:

Table 23.1 gives the static pressure rise. To find the total pressure rise the velocity pressure is determined at the outlet and added to static pressure. Interpolation is also required.

Set A: At 1.0 kPa

At $Q_v = 5.27$ m^3/s: $p_v = \rho_a V^2/2 = 1.2\ (11)^2/2 = 72.6$ Pa

$\therefore$ $\Delta p_t = \Delta p_s + p_v = 1000 + 72.6 = 1072.6$ Pa

At $Q_v = 5.75$ m^3/s: $p_v = \rho_a V^2/2 = 1.2\ (12)^2/2 = 86.4$ Pa

$\therefore$ $\Delta p_t = \Delta p_s + p_v = 1000 + 86.4 = 1086.4$ Pa

Interpolating, we get at $Q_v = 5.5$ m^3/s,

$$\Delta p_t = 1072.6 + (5.5 - 5.27)/(5.75 - 5.27)(1086.4 - 1072.6) = 1079.21 \text{ Pa}$$

Similarly, interpolating for power and rpm, we get at volume flow rate of 5.5 m^3/s:

$$\text{Power} = 9.02 + (5.5 - 5.27)/(5.75 - 5.27)\ (9.47 - 9.02) = 9.235 \text{ kW}$$

$$\text{rpm} = 808 - (5.5 - 5.27)/(5.75 - 5.27)(808 - 790) = 799.375 \text{ rpm}$$

Set B: At 1.1 kPa

At $Q_v = 5.27$ m^3/s: $p_v = \rho_a V^2/2 = 1.2\ (11)^2/2 = 72.6$ Pa

$\therefore$ $\Delta p_t = \Delta p_s + p_v = 1100 + 72.6 = 1172.6$ Pa

At $Q_v = 5.75$ m^3/s: $p_v = \rho_a V^2/2 = 1.2\ (12)^2/2 = 86.4$ Pa

$\therefore$ $\Delta p_t = \Delta p_s + p_v = 1100 + 86.4 = 1186.4$ Pa

Interpolating, we get at $Q_v = 5.5$ m^3/s , $\Delta p_t = 1179.21$ Pa

$$\text{Power} = 10.1 + (5.5 - 5.27)/(5.75 - 5.27)(10.5 - 10.1) = 10.292 \text{ kW}$$

$$\text{rpm} = 855 - (5.5 - 5.27)/(5.75 - 5.27)(855 - 840) = 847.81$$

We have set A at total pressure of 1079.21 Pa and set B at total pressure of 1179.21 Pa

Interpolating between these two sets for a total pressure of 1.1 kPa, we get

Shaft power = 9.457 kW

rpm = 809.55

Power transferred to the air at total pressure rise of 1.1 kPa and volume flow rate of 5.5 m^3/s:

$$W = Q_v \, \Delta p_t = 5.5 \, (1.1) = 6.05 \text{ kW}$$

Total efficiency $\eta_t = W/W_{\text{shaft}} = 6.05/9.457 = 63.97\%$

23.7 SYSTEM CHARACTERISTICS

The pressure drop in a duct system consists of frictional losses and minor losses both of which are dependent upon the square of velocity and the volume flow rate. The volume flow rate of supply air depends upon the cooling load and the duct system is accordingly designed for it. For a given volume flow rate, the average velocities in various sections and the pressure drop is found by either the constant friction method or by the static regain method. The pressure drop will change if the volume flow rate changes. The volume flow rate is changed depending upon the variation in load by changing the rpm either by changing the pulley ratio or by the frequency-controlled motor. The sum of pressure drops including frictional and in various fittings like elbow, tee, etc. can be added up to give

$$\Delta p = K_1 \, p_{v1} + K_2 \, p_{v2} + K_3 \, p_{v3} + \ldots \tag{23.18}$$

If A_i is the area of a section of a duct, then $V_i = Q_v/A_i$ gives the velocity in this section, and the velocity pressure $p_{vi} = \rho \, (Q_v/A_i)^2/2$. Therefore the expression of pressure drop is

$$\Delta p = \sum \frac{K_i \rho}{2A_i^2} \, Q_v^2 \approx K Q_v^2 \tag{23.19}$$

The pressure drop in the duct system varies with the square of volume flow rate. This curve will be a parabola on Q_v vs. Δp plot. The pressure drop is zero at $Q_v = 0$. Figure 23.8 shows the fan and system performance characteristics. The design point is the intersection A where the system characteristics OA and the fan characteristics have the same volume flow rate and pressure drop. If the system pressure drop reduces due to say cleaning of filter or opening of a damper, then the characteristics will shift to OB with larger volume flow rate.

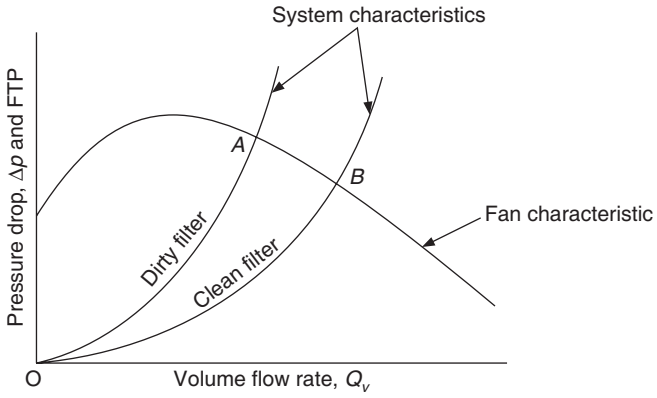

Figure 23.8 Fan and system performance curves.

23.8 DUCTWORK IN SERIES AND PARALLEL

In a HAC system the ductwork may consist of a single run in various segments where the volume flow rate is the same but the duct sizes are different and as a result the pressure drop is different. Such a duct may be considered as the series network. On the other hand if the main duct branches into various ducts then these may be considered in parallel. Analysis of such a system can be conveniently done by considering the electrical analogy with Eq. (23.19) by writing it as follows:

$$\Delta p = RQ_v^2 \tag{23.20}$$

where Δp is equivalent to potential difference, $R = K$ is equivalent to resistance and Q_v is equivalent to current, the only difference from current flow being that the square of flow rate appears in Eq. (23.19).

23.8.1 Series Connection

Figure 23.9 shows the equivalent electrical analogue of a single duct with different resistances R_1, R_2 and R_3 along its length. The velocities will be different in these sections due to different duct dimensions. We have

$$\Delta p_1 = R_1 Q_v^2,\ \Delta p_2 = R_2 Q_v^2 \text{ and } \Delta p_2 = R_3 Q_v^2$$

$$\Delta p = \Delta p_1 + \Delta p_2 + \Delta p_2 = (R_1 + R_2 + R_3) Q_v^2 = RQ_v^2$$

or
$$\Delta p = RQ_v^2 \tag{23.21}$$

where,
$$R = R_1 + R_2 + R_3 \tag{23.22}$$

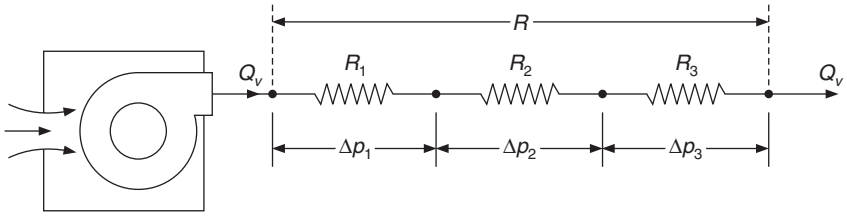

Figure 23.9 Flow resistances in series.

23.8.2 Parallel Connection

Figure 23.10 shows the equivalent electrical analogue of a ductwork consisting of parallel paths with the flow getting dividing into three branches. The volume flow rate in the branches is different but the pressure drop in the branches is the same. We have

$$\Delta p = R_1 Q_{v1}^2,\ \Delta p = R_2 Q_{v2}^2 \quad \text{and} \quad \Delta p = R_3 Q_{v3}^2 \tag{23.23}$$

$$R_1 = \Delta p / Q_{v1}^2,\ R_2 = \Delta p / Q_{v2}^2 \quad \text{and} \quad R_3 = \Delta p / Q_{v3}^2$$

We have
$$Q_v = Q_{v1} + Q_{v2} + Q_{v3}$$

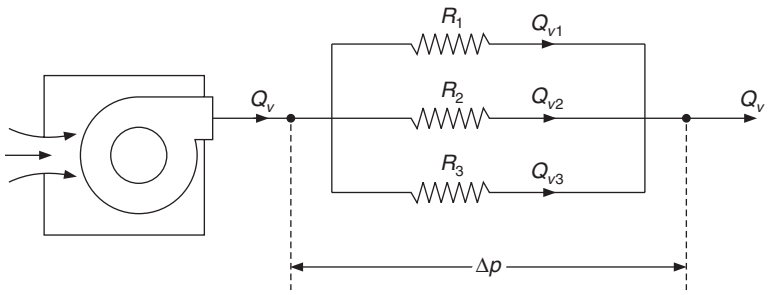

Figure 23.10 Flow resistances in parallel.

Substituting from Eq. (23.23), we get

$$\sqrt{\frac{\Delta p}{R}} = \sqrt{\frac{\Delta p}{R_1}} + \sqrt{\frac{\Delta p}{R_2}} + \sqrt{\frac{\Delta p}{R_3}}$$

or

$$\frac{1}{\sqrt{R}} = \frac{1}{\sqrt{R_1}} + \frac{1}{\sqrt{R_2}} + \frac{1}{\sqrt{R_3}} \tag{23.24}$$

23.9 EFFECT OF CHANGE IN FAN SPEED

It was shown in Eq. (23.6) that the fan total pressure (FTP) is proportional to the square of speed. The volume flow rate Q_v is proportional to speed (Eq. (23.7)). The FTP increases at a rate faster than the volume flow rate Q_v when the speed is increased. The fan characteristics are shown for two speeds $N_1$and N_2 in Figure 23.11. It is observed that as the fan speed is increased from $N_1$to N_2, the point of operation shifts from a lower pressure at A to a higher pressure at B. The power requirement also shifts from point A' to a higher value at point B'. Increase in fan speed increases the total fan pressure though the noise level may also increase.

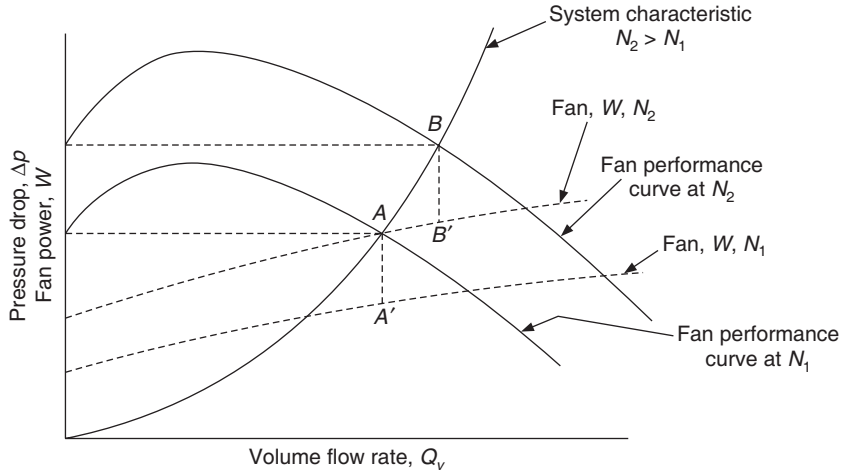

Figure 23.11 Effect of change in fan speed.

23.10 EFFECT OF CHANGE IN AIR DENSITY

The fans are rated for standard air density. The velocity pressure is directly proportional to actual density. The pressure loss or the system pressure is also proportional to density. Figure 23.12 shows the fan characteristics for two values of air densities ρ_1 and ρ_2 with $\rho_2 > \rho_1$. The system characteristics are also shown. As the density increases, the point of operation shifts from *A* to *B*. It is observed that FTP and the fan power requirement increase with increase in density. The volume flow rate decreases slightly at the point of operation.

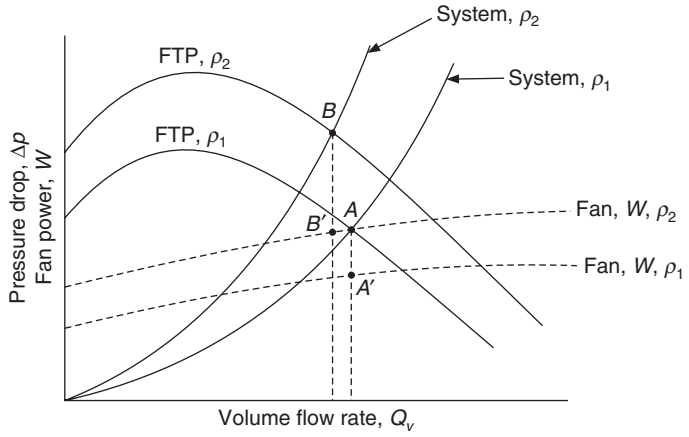

Figure 23.12 Effect of change in air density.

EXAMPLE 23.3 A duct system has a total pressure drop of 548.18 Pa at a volume flow rate of 5.2 m^3/s. A backward curved blade fan of 920 mm wheel diameter and outlet area of 0.71 m^2 running at 600 rpm is used, whose characteristics are as follows:

Q_v, m^3/s	2.5	3.5	3.75	4.25	4.75	5.2	5.65	6.0	Fan characteristics
FTP, Pa	523	540	523	490	448	410	373	336	
η	70	78	81	83	83	82	80	76	
W, hp	2.8	3.15	3.2	3.4	3.45	3.5	3.6	3.7	

(a) Draw the fan and the system characteristics and determine the power drawn, volume flow rate and efficiency at the operating point. (b) If the fan output is reduced to 3 m^3/s by a damper, determine the loss in power due to damper closing. (c) What should be done to obtain FTP of 548.19 Pa at volume flow rate of 5.2 m^3/s? (d) Determine the speed at which the fan should be run to achieve a volume flow rate of 5.0 m^3/s. (e) A filter is included in the system. The pressure drop across the clean filter is 40 Pa. The filter becomes dirty after use and the pressure drop in the filter becomes 110 Pa, find the FTP and the volume flow rate with the dirty filter.

Solution:

(a) The resistance of the system is given by $R = \Delta p/Q_v^2 = 548.18/(5.2)^2 = 20.273$.

Therefore the system characteristic is given by $\Delta p = 20.273 Q_v^2$. This characteristic curve is tabulated as follows:

Q_v	2	2.5	3.0	3.5	4.0	4.5	5.0	5.5
Δp	81.1	126.7	182.5	248.3	324.4	410.5	506.8	613.2

The fan characteristics and the system characteristics are plotted in Figure 23.13. The operating point is observed to be P_1, where

$$Q_v = 4.75 \text{ m}^3/\text{s and } \Delta p = \text{FTP} = 450 \text{ Pa}$$

With the value of P_1, from the table of fan characteristic provided with the example, we find that:

$$\eta = 83\% \text{ and } W = 3.45 \text{ hp} = 2.5737 \text{ kW}$$

The power delivered to air = actual power = $Q_v \Delta p = 4.75(450) \times 10^{-3} = 2.1375$ kW
Fan total efficiency = 2.1375/2.5737 = 83%

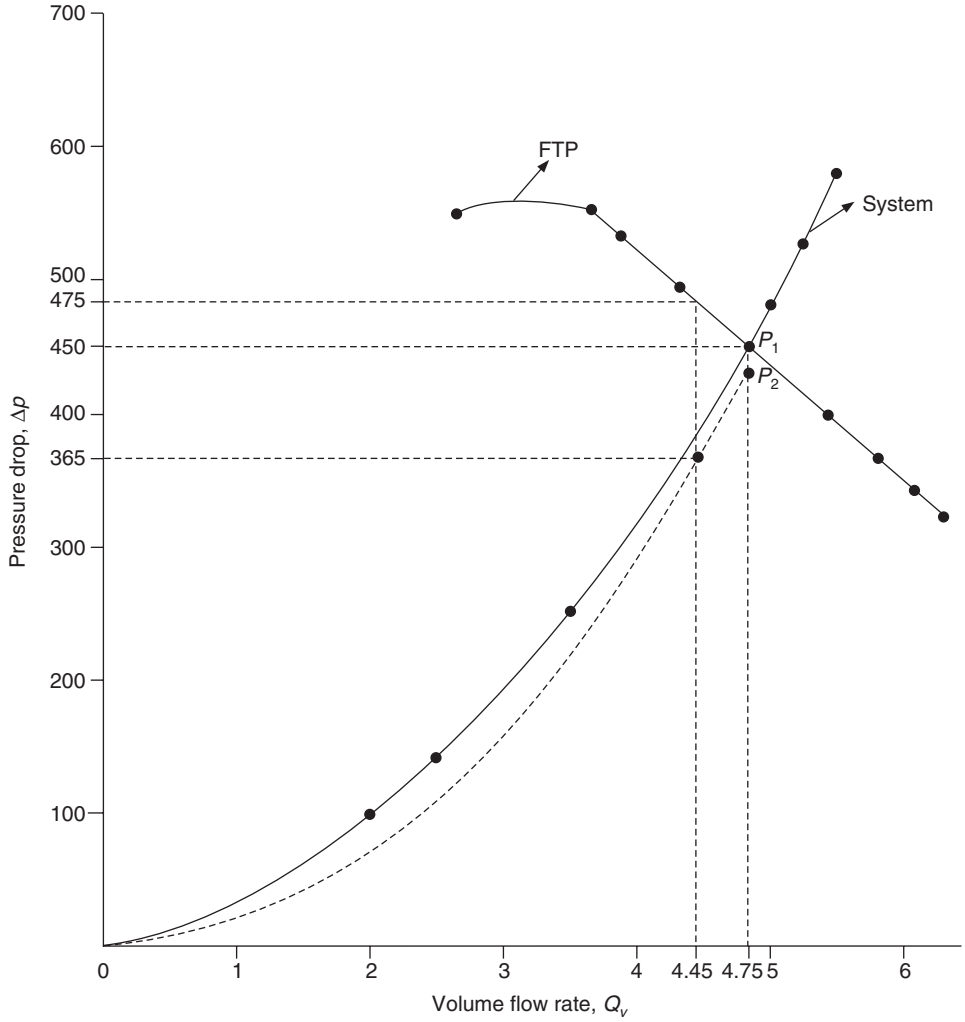

Figure 23.13 Example 23.3.

(b) The FTP at 3 m^3/s is obtained by interpolation in the table. It is (523 + 540)/2 = 531.5 Pa
The system requires a total pressure drop of 182.5 Pa at 3.0 m^3/s.
Therefore the pressure drop in the damper = 531.5 – 182.5 = 349 Pa
Therefore loss in power across the damper = $3(349) \times 10^{-3}$ = 1.047 kW

(c) The system requires a FTP of 548.18 Pa at volume flow rate of 5.2 m^3/s. This is not possible since the fan develops a FTP of 410 Pa at 5.2 m^3/s. One alternative is to increase the speed of the fan to obtain a larger pressure rise. From fan laws it was observed that the FTP is proportional to the square of speed. Hence

$$N_2 = N_2\sqrt{\frac{\Delta p_2}{\Delta p_1}} = 600\sqrt{\frac{548.18}{410}} = 693.78 \text{ rpm}$$

(d) The volume flow rate is proportional to speed. Hence

$$N = 600 \times 5.0/4.75 = 631.6 \text{ rpm}$$

(e) As the air flows through the clogged filter, both the volume flow rate and the pressure drop will change and there is no straight relation governing this. We find the system characteristic in the absence of filter from the given condition that the pressure drop in the filter is 40 Pa.

Pressure drop without filter = 450 – 40 = 410 Pa at volume flow rate of 4.75 m^3/s
Therefore system resistance $R = \Delta p/Q_v^2 = 410/(4.75)^2 = 18.17$
Therefore the system characteristic in the absence of filter is given by $\Delta p = 18.17Q_v^2$. The dashed line in Figure 23.13 shows this. Point P_1 is the design point with clean filter and point P_2 is the point of operation in absence of filter.

To find the design point with dirty filter, we look for a pair of points on the two system lines which have a pressure drop of 110 Pa at the same volume flow rate. A search indicates that:

Without filter at volume flow rate of 4.45 m^3/s, the system pressure drop = 365 Pa.
With filter the fan FTP at volume flow rate of 4.45 m^3/s is 475 Pa.

Therefore at volume flow rate of 4.45 m^3/s the fan develops sufficient pressure to take care of 110 Pa pressure in the dirty filter.

23.11 FAN INSTALLATION

This is an important aspect of the duct–fan system. The fan performance may reduce drastically if the connection with the duct is not proper. The fan should be installed with the duct system such that there should be no abrupt change in velocity at the inlet and outlet. Sometimes the space provided for the fan is limited, as a result the ducts have to be bent and their dimensions changed. This poses a challenge to place the duct in such a manner that excessive pressure drop does not occur.

System effect factors

All pressure losses, frictional and minor like those due to duct friction, fittings, heating coils, dampers and filters, etc. are based upon uniform velocity profile. The velocity profile is usually not uniform at the fan outlet, hence the fittings near the inlet will have larger losses than the rated values.

Fan performance test is carried out with open inlet. In an actual system the presence of inlet duct or some other configuration will change its performance drastically. These are the problems associated with the system and are called *system effect factor*, which gives a pressure correction to be added to the system pressure.

Fan outlet condition

Ideally the duct area and the fan outlet area should be the same. However, good flow conditions may be obtained if the outlet duct area is not greater than 110% and less than 85% of the fan outlet area. In the converging portion of the duct the slope should not be greater than 15° and in the diverging portion it should not be greater than 7°. It takes about a duct length of $0.2V$ diameters after the fan outlet for the flow to become fully developed and to achieve the full pressure developed by the fan. The velocity V is in m/s in this expression. For example, at 15 m/s and 45 m/s velocities, duct lengths of 3 and 9 duct diameters are required. This length is called *one effective length.* For a rectangular duct of width B and height H, the equivalent diameter is defined as $\sqrt{(4BH)/\pi}$. A typical velocity profile in the effective length near the outlet of a centrifugal fan is shown in Figure 23.14.

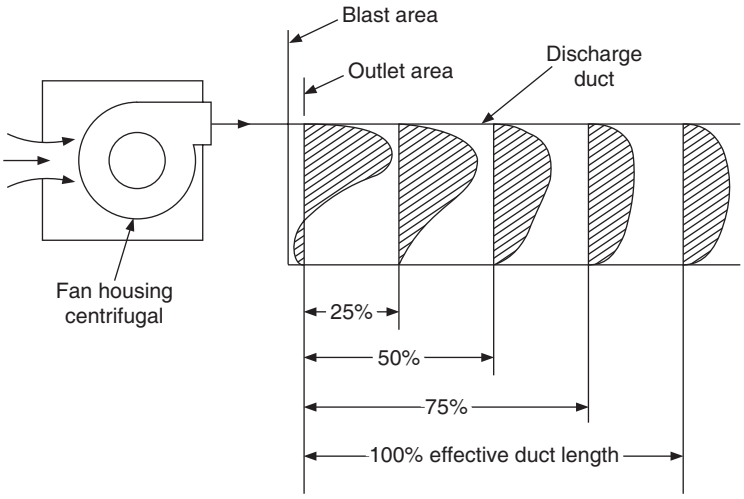

Figure 23.14 Fan outlet velocity profiles.

The first elbow fitting should be at least after this effective length from the fan outlet. If it is not done then it involves additional losses. The damper should also not be close to the fan outlet. Bends and branches should also be at least one effective length away from the fan outlet. Whenever a fan discharges into a plenum, it involves pressure loss. Tables for these losses are available in *ASHRAE Duct Fitting Database*, 1992.

The axial flow fan is better since it has straight-through section without any area change

23.12 FANS FOR VARIABLE VOLUME SYSTEMS

In these systems, the conditioned air is supplied to a large number of zones with volume flow rate controlled according to the load in the zone. The volume flow rate varies between some minimum

value to the full-load value. The minimum volume flow rate at times is as low as 20–25% of the maximum volume flow rate. VAV boxes control the volume flow rate to the zones. The fan should continuously respond to the volume flow rate required by the system to avoid excessive power since volume flow rate is proportional to speed and the power is proportional to the cube of speed. To make the operation economical, many methods are available for speed reduction.

Magnetic couplings referred to as *Eddy Current Drives* are capable of giving continuous adjustment to fan speed.

Adjusting pulley shives can change the diameter of the V-belt driven pulley. This, however, involves high maintenance cost.

The latest method is the adjustable frequency-controlled motor, which gives the best results. This method works with most of the alternating current motors. It is, however, expensive.

The introduction of swirl by vanes at the inlet of the fan also reduces the flow rate. Variable inlet vanes are located in a radial direction in the inlet eye of a centrifugal fan and hinged along a radial centreline. Its inclination to the radial line can be varied. This introduces swirl in the inlet air. The result is not similar to throttling. It just moves the FTP vs. Q_v curve to the dashed line in Figure 23.15. It reduces the volume flow rate to Q_{v2} from the initial value of Q_{v1}. The FTP also decreases in this process.

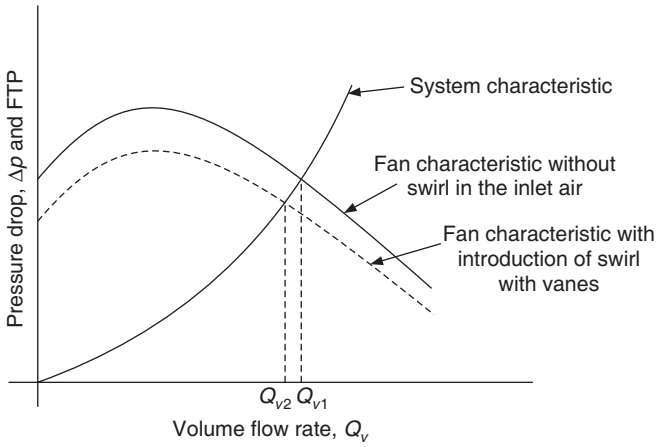

Figure 23.15 Effect of variable inlet vanes in a variable volume system.

Axial flow fans have inlet guide vanes, which work in a manner similar to turning vanes of centrifugal compressor.

Another method used in forward-curved blade fans is to change the effective width of the impeller. A disc mounted on the shaft does this. The location of the disc can be changed from the eye of the impeller to the back plate. If it is near the eye, then virtually no flow would occur through the impeller. On the other hand when the disc is near the back plate, full impeller width is available for flow.

23.13 FANS IN SERIES AND PARALLEL

If two identical fans are connected in series then the air will flow from one fan to the other, as a result the volume flow rate will remain the same. However during its passage through the second fan the fan pressure would increase further by the same amount as it occurred in the first fan,

therefore the total pressure rise will be twice that of a single fan. On the other hand, when the fans are connected in parallel, the pressure rise will be same through each fan while the flow rate of the two fans combined together will be double that of the single fan.

Forward-curved blade fans running near the point of inflection have three possible flow rates, hence the fans can hunt between these flow rates for a given system pressure.

EXAMPLE 23.4 The characteristics of a forward-curved blade fan are as follows:

FTP, Pa	400	425	450	473	463	440	380
Q_v, m^3/s	0	0.5	1.0	2.0	2.5	3.0	3.5

Determine the characteristics when the fans are connected in (a) series and (b) parallel.

Solution:

The characteristics when two such fans are connected in series are as follows:

FTP, Pa	800	850	900	946	926	880	760
Q_v, m^3/s	0	0.5	1.0	2.0	2.5	3.0	3.5

The characteristics when two such fans are connected in parallel are as follows:

FTP, Pa	400	425	450	473	463	440	380
Q_v, m^3/s	0	1.0	2.0	4.0	5.0	6.0	7.0

Figures 23.16 and 23.17 show plots for series and parallel connection.

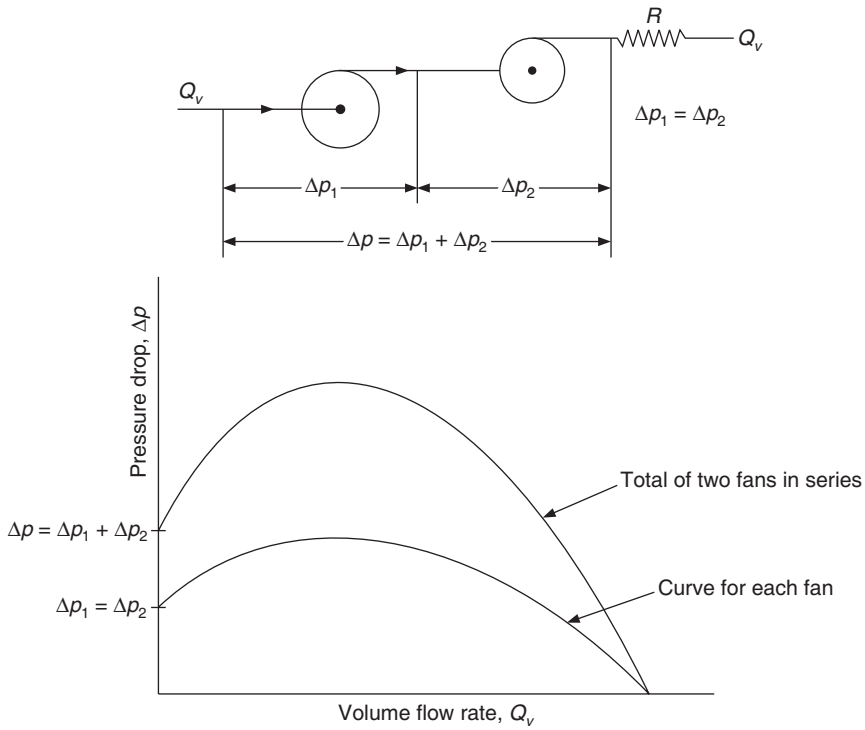

Figure 23.16 The combined characteristic of two fans in series.

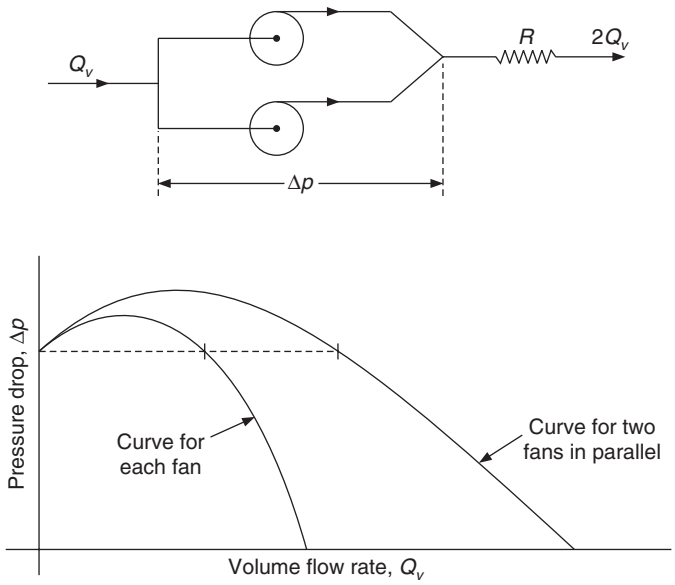

Figure 23.17 The combined characteristic of two fans in parallel.

REFERENCE

ASHARE Handbook of Fundamentals Volume (1993): American Society of Heating, Refrigerating and Air Conditioning Engineers, Inc. Atlanta, G.A.

REVIEW QUESTIONS

1. Discuss the factors governing the performance of fans in air conditioning systems. On the basis of these factor, what are the performance differences between the different types of fans?
2. Compare the characteristics of forward-curved blade and backward-curved blade centrifugal fans.
3. Explain fan laws and discuss their significance.
4. Discuss the factors governing fan selection.
5. Discuss how the fan characteristic is matched with the system characteristics.
6. Discuss the effect of change in fan speed and change in air density on system performance.

Appendix

Table 1 Thermodynamic properties of water and steam at saturation from 0–50°C

Saturation temperature, T (°C)	*Pressure, p* (bar)	*Specific volume of steam, v_g* (m^3/kg)	*Specific enthalpy* (kJ/kg)			*Specific entropy* (kJ/kg-K)		
			Water (h_f)	*Evaporation* (h_{fg})	*Steam* (h_g)	*Water* (s_f)	*Evaporation* (s_{fg})	*Steam* (s_g)
0	0.00611	206.16	0.0	2501.6	2501.6	0.000	9.158	9.158
1	0.00657	192.61	4.2	2499.2	2503.4	0.015	9.116	9.131
2	0.00706	179.92	8.4	2496.8	2505.2	0.031	9.074	9.105
3	0.00758	168.17	12.6	2494.5	2507.1	0.046	9.033	9.079
4	0.00813	157.27	16.8	2492.1	2508.9	0.061	8.992	9.053
5	0.00872	147.16	21.0	2489.7	2510.7	0.076	8.951	9.027
6	0.00935	137.78	25.2	2487.4	2512.6	0.091	8.910	9.001
7	0.01001	129.06	29.4	2485.0	2514.4	0.106	8.870	8.976
8	0.01072	120.97	33.6	2482.6	2516.2	0.121	8.830	8.951
9	0.01147	113.44	37.8	2480.3	2518.1	0.136	8.790	8.926
10	0.01227	106.43	42.0	2477.9	2519.9	0.151	8.751	8.902
11	0.01312	99.909	46.2	2475.5	2521.7	0.166	8.712	8.878
12	0.01401	93.835	50.4	2473.2	2523.6	0.181	8.673	8.854
13	0.01497	88.176	54.6	2470.8	2525.4	0.195	8.635	8.830
14	0.01597	82.900	58.8	2468.5	2527.2	0.210	8.596	8.806
15	0.01704	77.978	62.9	2466.1	2529.1	0.224	8.558	8.8782
16	0.01817	73.384	67.1	2463.8	2530.9	0.239	8.520	8.759
17	0.01936	69.095	71.3	2461.4	2532.7	0.253	8.483	8.736

(Contd.)

Table 1 Thermodynamic properties of water and steam at saturation from 0–50°C (*contd.*)

Saturation temperature, T (°C)	*Pressure, p* (bar)	*Specific volume of steam, v_g* (m^3/kg)	*Specific enthalpy* (kJ/kg)			*Specific entropy* (kJ/kg-K)		
			Water (h_f)	*Evapor-ation* (h_{fg})	*Steam* (h_g)	*Water* (s_f)	*Evapor-ation* (s_{fg})	*Steam* (s_g)
18	0.02062	65.087	75.5	2459.0	2534.5	0.268	8.446	8.714
19	0.02196	61.341	79.7	2456.7	2536.4	0.282	8.409	8.691
20	0.02337	57.838	83.9	2454.3	2538.2	0.296	8.372	8.668
22	0.02642	51.492	92.2	2449.6	2541.8	0.325	8.299	8.624
24	0.02982	45.926	100.6	2444.9	2545.5	0.353	8.228	8.581
26	0.03360	41.034	108.9	2440.2	2549.1	0.381	8.157	8.538
28	0.03778	36.728	117.3	2435.4	2552.7	0.409	8.087	8.496
30	0.04242	32.929	125.7	2430.7	2556.4	0.437	8.018	8.455
32	0.04753	29.572	134.1	2425.9	2560.0	0.464	7.950	8.414
34	0.05318	26.601	142.4	2421.2	2563.6	0.491	7.883	8.374
36	0.05940	23.967	150.7	2416.4	2567.1	0.518	7.816	8.334
38	0.06624	21.627	159.1	2411.7	2570.8	0.545	7.751	8.296
40	0.07375	19.546	167.5	2406.9	2574.4	0.572	7.686	8.258
42	0.08199	17.692	175.8	2402.1	2577.9	0.599	7.622	8.221
44	0.09100	16.036	184.2	2397.3	2581.5	0.625	7.559	8.184
48	0.1116	13.233	200.9	2387.7	2588.6	0.678	7.435	8.113
50	0.1234	12.046	209.3	2382.9	2592.2	0.704	7.374	8.078

Table 2 Saturated dichlorodifluoromethane (CCl_2F_2), R12 datum at −40°C, $h_f = 0$, $s_f = 0$

Saturation temperature, T (°C)	*Pressure, p* (bar)	*Specific volume of steam* (m^3/kg)		*Specific enthalpy* (kJ/kg)		*Specific entropy* (kJ/kg-K)		
		Liquid (v_f)	*Vapour* (v_g)	*Liquid* (h_f)	*Vapour* (h_g)	*Latent* (h_{fg})	*Liquid* (s_f)	*Vapour* (s_g)
−100	0.01185	0.000600	10.1951	−51.84	142.00	193.84	−0.2567	0.8628
−95	0.01864	0.000604	6.6231	−47.56	144.22	191.78	−0.2323	0.8442
−90	0.02843	0.000608	4.4206	−43.28	146.46	189.74	−0.2086	0.8273
−85	0.04254	0.000613	3.0531	−39.00	148.73	187.73	−0.1856	0.8122
−80	0.06200	0.000617	2.1519	−34.72	151.02	185.74	−0.1631	0.7985
−75	0.08826	0.000622	1.5462	−30.42	153.32	183.74	−0.1412	0.7861
−70	0.12298	0.000627	1.1314	−26.12	155.63	181.75	−0.1198	0.7665
−65	0.16807	0.000632	0.8421	−21.81	157.96	179.77	−0.0988	0.7648
−60	0.22665	0.000637	0.6401	−17.48	160.29	177.77	−0.0783	0.7558
−55	0.30052	0.000643	0.4930	−13.14	162.62	175.76	−0.0581	0.7475
−50	0.39237	0.000648	0.3845	−8.78	164.95	173.73	−0.0384	0.7401
−45	0.50512	0.000654	0.3035	−4.39	167.27	171.66	−0.0190	0.7334
−40	0.64190	0.000660	0.2422	0.00	169.60	169.60	0.0000	0.7274
−38	0.70460	0.000663	0.2221	1.76	170.52	168.76	0.0075	0.7251

(Contd.)

Table 2 Saturated dichlorodifluoromethane (CCl_2F_2), R12 datum at −40°C, $h_f = 0$, $s_f = 0$ (*contd.*)

Saturation temperature, T (°C)	*Pressure, p* (bar)	*Specific volume of steam* (m^3/kg)		*Specific enthalpy* (kJ/kg)		*Specific entropy* (kJ/kg-K)		
		Liquid (v_f)	*Vapour* (v_g)	*Liquid* (h_f)	*Vapour* (h_g)	*Latent* (h_{fg})	*Liquid* (s_f)	*Vapour* (s_g)
−36	0.77196	0.000665	0.2040	3.53	171.44	167.91	0.0149	0.7230
−34	0.84421	0.000667	0.1877	5.31	172.36	167.05	0.0224	0.7209
−32	0.92776	0.000670	0.1729	7.08	173.28	166.20	0.0298	0.7190
−30	1.00441	0.000673	0.1596	8.86	174.20	165.34	0.0371	0.7171
−28	1.09311	0.000676	0.1475	10.64	175.11	164.47	0.0444	0.7153
−26	1.18778	0.000678	0.1364	12.43	176.02	163.59	0.0516	0.7135
−24	1.28858	0.000681	0.1265	14.22	176.93	162.71	0.0588	0.7118
−22	1.39581	0.000683	0.1173	16.02	177.83	161.81	0.0660	0.7102
−20	1.50972	0.000686	0.1090	17.82	178.73	160.91	0.0731	0.7087
−18	1.63104	0.000689	0.1090	19.62	179.63	160.01	0.0801	0.7073
−16	1.75963	0.000692	0.1014	21.43	180.53	159.10	0.0871	0.7059
−14	1.89575	0.000695	0.0944	23.23	181.42	159.19	0.0941	0.7045
−12	2.04605	0.000698	0.0880	25.05	182.31	157.26	0.1010	0.7032
−10	2.19172	0.000701	0.0821	26.87	183.19	156.32	0.1080	0.7019
−8	0.35272	0.000704	0.0767	28.70	184.06	155.36	0.1148	0.7007
−6	2.52244	0.000707	0.0717	30.53	184.94	154.41	0.1217	0.6996
−4	2.70116	0.000710	0.0672	32.37	185.80	153.43	0.1285	0.6986
−2	2.88921	0.000713	0.0630	34.20	186.67	152.47	0.1352	0.6975
0	3.08690	0.000717	0.0591	36.05	187.53	151.48	0.1420	0.6965
1	3.18974	0.000719	0.0555	36.98	187.95	150.97	0.1453	0.6961
2	3.29513	0.000720	0.0538	37.90	188.38	150.48	0.1489	0.6956
3	3.40310	0.000721	0.0521	38.83	188.81	149.98	0.1521	0.6951
4	3.51367	0.000723	0.0505	39.76	189.23	149.47	0.1553	0.6947
5	3.62690	0.000725	0.0490	40.69	189.65	148.96	0.1586	0.6943
6	3.74280	0.000727	0.0475	41.62	190.07	148.45	0.1620	0.6938
7	3.86141	0.000729	0.0461	42.56	190.49	147.93	0.1653	0.6933
8	3.98283	0.000730	0.0447	43.50	190.91	147.41	0.1686	0.6929
9	4.10702	0.000732	0.0434	44.43	191.32	146.89	0.1719	0.6925
10	4.23407	0.000734	0.0422	45.37	191.74	146.37	0.1752	0.6921
11	4.36442	0.000736	0.0410	46.31	192.15	145.84	0.1784	0.6917
12	4.49763	0.000738	0.0398	47.26	192.56	145.30	0.1817	0.6913
13	4.63386	0.000739	0.0386	48.20	192.97	144.77	0.1850	0.6909
14	4.77312	0.000741	0.0375	49.15	193.38	144.23	0.1883	0.6906
15	4.91545	0.000743	0.0355	50.10	193.79	143.69	0.1915	0.6902
16	5.06087	0.000745	0.0345	51.05	194.19	143.14	0.1948	0.6898
17	5.20942	0.000747	0.0335	52.00	194.59	142.59	0.1981	0.6894
18	5.36117	0.000749	0.0326	52.95	194.99	142.04	0.2013	0.6891

(Contd.)

Table 2 Saturated dichlorodifluoromethane (CCl_2F_2), R12 datum at −40°C, $h_f = 0$, $s_f = 0$ (*contd.*)

Saturation temperature, T (°C)	*Pressure, p* (bar)	*Specific volume of steam* (m^3/kg)		*Specific enthalpy* (kJ/kg)		*Specific entropy* (kJ/kg-K)		
		Liquid (v_f)	*Vapour* (v_g)	*Liquid* (h_f)	*Vapour* (h_g)	*Latent* (h_{fg})	*Liquid* (s_f)	*Vapour* (s_g)
19	5.51614	0.000751	0.0317	53.91	195.38	141.47	0.2046	0.6888
20	5.67441	0.000753	0.0308	54.87	195.78	140.91	0.2078	0.6884
21	5.83635	0.000756	0.0300	55.83	196.17	140.34	0.2110	0.6881
22	6.00171	0.000758	0.0292	56.79	196.56	139.77	0.2143	0.6878
23	6.17050	0.000759	0.0284	57.75	196.96	139.21	0.2174	0.6875
24	6.34269	0.000761	0.0276	58.73	197.34	138.61	0.2207	0.6872
25	6.51840	0.000764	0.0269	59.70	197.73	138.03	0.2239	0.6868
26	6.69765	0.000766	0.0262	60.67	198.11	137.44	0.2271	0.6865
27	6.88048	0.000768	0.0255	61.65	198.50	136.85	0.2303	0.6862
28	7.06704	0.000770	0.0248	62.63	198.87	136.24	0.2335	0.6859
29	7.25738	0.000772	0.0241	63.61	199.25	135.64	0.2368	0.6856
30	7.45103	0.000775	0.0235	64.59	199.62	135.03	0.2400	0.6853
31	7.64903	0.000777	0.0230	65.58	199.99	134.41	0.2431	0.6850
32	7.85089	0.000779	0.0225	66.57	200.36	133.79	0.2463	0.6847
33	8.05662	0.000782	0.0218	67.56	200.73	133.17	0.2495	0.6845
34	8.26621	0.000784	0.0212	68.56	201.09	132.53	0.2527	0.6842
35	8.48000	0.000786	0.0207	69.56	201.45	131.89	0.2559	0.6839
36	8.69766	0.000789	0.0202	70.55	201.80	131.25	0.2591	0.6836
37	8.91904	0.000792	0.0196	71.55	202.16	130.61	0.2623	0.6833
38	9.14483	0.000794	0.0191	72.56	202.51	129.95	0.2654	0.6830
39	9.37497	0.000796	0.0186	73.57	202.86	129.29	0.2685	0.6828
40	9.60897	0.000799	0.0182	74.59	203.20	128.61	0.2718	0.6825
41	9.84793	0.000802	0.0177	75.61	203.54	127.93	0.2750	0.6822
42	10.09131	0.000804	0.0173	76.62	203.87	127.25	0.2782	0.6820
43	10.33862	0.000807	0.0168	77.65	204.21	126.56	0.2814	0.6817
44	10.59021	0.000810	0.0164	78.68	204.55	125.87	0.2846	0.6814
45	10.84655	0.000813	0.0160	79.71	204.87	125.16	0.2878	0.6811
46	11.10758	0.000815	0.0156	80.75	205.19	124.44	0.2909	0.6808
47	11.37304	0.000818	0.0153	81.79	205.51	123.72	0.2941	0.6805
48	11.64290	0.000821	0.0149	82.83	205.83	123.00	0.2973	0.6802
49	11.91724	0.000824	0.0146	83.88	206.14	122.26	0.3005	0.6800
50	12.19655	0.000827	0.0142	84.94	206.45	121.51	0.3037	0.6797

Table 3 Saturated monochlorodifluoromethane ($CHClF_2$), R22 datum at $-40°C$, $h_f = 0$, $s_f = 0$

Saturation temperature, T (°C)	*Saturation pressure, p* (bar)	*Specific volume of steam* (m^3/kg)		*Specific enthalpy* (kJ/kg)		*Specific entropy* (kJ/kg-K)		
		Liquid (v_f)	*Vapour* (v_g)	*Liquid* (h_f)	*Vapour* (h_g)	*Latent* (h_{fg})	*Liquid* (s_f)	*Vapour* (s_g)
−100	0.02009	0.000643	8.3412	−63.45	203.73	267.18	−0.3144	1.2293
−95	0.03150	0.000647	5.4344	−58.14	206.19	264.33	−0.2843	1.2004
−90	0.04792	0.000652	3.6381	−52.87	208.64	261.51	−0.2550	1.1736
−85	0.07731	0.000656	2.5204	−47.61	211.11	258.72	−0.2269	1.1489
−80	0.10393	0.000661	1.7816	−42.40	213.60	256.00	−0.1989	1.1267
−75	0.14759	0.000666	1.2842	−37.17	216.11	253.28	−0.1721	1.1066
−70	0.20517	0.000672	0.9420	−31.93	218.62	250.55	−0.1461	1.0874
−65	0.27965	0.000677	0.7037	−26.68	221.16	247.84	−0.1206	1.0702
−60	0.37448	0.000683	0.5351	−21.42	223.67	245.09	−0.0959	1.0543
−55	0.49621	0.000689	0.4131	−16.13	226.18	242.31	−0.0712	1.0396
−50	0.64758	0.000696	0.3229	−10.81	228.69	239.50	−0.0473	1.0262
−45	0.83241	0.000702	0.2556	−5.40	231.20	236.60	−0.0234	1.0137
−40	1.05586	0.000709	0.2049	0.00	233.67	233.67	0.0000	1.0024
−38	1.15862	0.000712	0.1882	2.20	234.65	232.45	0.0096	0.9982
−36	1.26910	0.000715	0.1728	4.40	235.65	231.25	0.0188	0.9940
−34	1.38731	0.000719	0.1590	6.58	236.60	230.02	0.0280	0.9902
−32	1.51324	0.000721	0.1465	8.83	237.60	228.77	0.0373	0.9860
−30	1.64690	0.000724	0.1353	11.05	238.55	227.50	0.0464	0.9283
−28	1.78938	0.000727	0.1253	13.29	239.52	226.23	0.0557	0.9785
−26	1.94069	0.000731	0.1161	15.58	240.48	224.90	0.0645	0.9747
−24	2.10207	0.000734	0.1077	17.77	241.41	223.64	0.0733	0.9710
−22	2.27448	0.000738	0.1000	19.99	242.33	222.34	0.0821	0.9676
−20	2.45793	0.000741	0.0930	22.21	243.25	221.04	0.0908	0.9638
−18	2.65310	0.000744	0.0865	24.47	244.17	219.70	0.0996	0.9605
−16	2.85903	0.000748	0.0806	26.72	245.08	218.36	0.01080	0.9576
−14	3.07876	0.000752	0.0752	28.94	245.96	217.02	0.1164	0.9538
−12	3.31172	0.000756	0.0701	31.16	246.84	215.68	0.1248	0.9508
−10	3.55793	0.000759	0.0655	33.40	247.72	214.32	0.1336	0.9479
−8	3.81321	0.000763	0.0612	35.66	248.60	212.94	0.1419	0.9454
−6	4.09172	0.000767	0.0573	37.92	249.46	211.54	0.1503	0.9425
−4	4.37972	0.000771	0.0536	40.19	250.30	210.11	0.1591	0.9396
−2	4.68317	0.000775	0.0503	42.52	251.14	208.62	0.1675	0.9370
0	5.00207	0.000779	0.0471	44.94	251.97	207.03	0.1763	0.9345
1	5.16841	0.000781	0.0457	46.16	252.37	206.21	0.1809	0.9333
2	5.33917	0.000783	0.0443	47.38	252.77	205.39	0.1855	0.9320
3	5.51434	0.000785	0.0429	48.64	253.17	204.53	0.1901	0.9303
4	5.69352	0.000787	0.0416	49.91	253.56	203.65	0.1943	0.9291
5	5.87621	0.000790	0.0403	51.16	253.95	202.79	0.1989	0.9278
6	6.06276	0.000792	0.0391	52.41	254.33	201.92	0.2035	0.9266
7	6.25393	0.000794	0.0379	53.68	254.71	201.03	0.2077	0.9253
8	6.44993	0.000797	0.0368	54.94	255.08	200.14	0.2123	0.9241

(Contd.)

Table 3 Saturated monochlorodifluoromethane ($CHClF_2$), R22 datum at $-40°C$, $h_f = 0$, $s_f = 0$ (*contd.*)

Saturation temperature, T (°C)	*Saturation pressure, p* (bar)	*Specific volume of steam* (m^3/kg)		*Specific enthalpy* (kJ/kg)		*Specific entropy* (kJ/kg-K)		
		Liquid (v_f)	*Vapour* (v_g)	*Liquid* (h_f)	*Vapour* (h_g)	*Latent* (h_{fg})	*Liquid* (s_f)	*Vapour* (s_g)
9	6.65034	0.000799	0.0357	56.22	255.44	199.22	0.2169	0.9228
10	6.85517	0.000801	0.0346	57.52	255.81	198.29	0.2211	0.9216
11	7.06621	0.000803	0.0336	58.80	256.15	197.35	0.2257	0.9203
12	7.27724	0.000805	0.0326	60.07	256.48	196.41	0.2303	0.9190
13	7.49793	0.000808	0.0316	61.38	256.83	195.45	0.2345	0.9178
14	7.72552	0.000810	0.0307	62.72	257.17	194.45	0.2391	0.9165
15	7.95517	0.000813	0.0298	64.02	257.50	193.48	0.2437	0.9152
16	8.18758	0.000815	0.0289	65.32	257.81	192.48	0.2483	0.9140
17	8.42552	0.000817	0.0281	66.63	258.13	191.50	0.2529	0.9127
18	8.63241	0.000820	0.0273	67.95	258.44	190.49	0.2571	0.9115
19	8.91793	0.000822	0.0266	69.27	258.73	189.46	0.2617	0.9102
20	9.17241	0.000825	0.0258	70.59	259.00	188.41	0.2663	0.9089
21	9.43310	0.000827	0.0251	71.93	259.29	187.36	0.2709	0.9077
22	9.69931	0.000830	0.0244	73.31	259.58	186.27	0.2755	0.9065
23	9.97103	0.000833	0.0237	74.66	259.85	185.19	0.2801	0.9052
24	10.24828	0.000835	0.0230	76.04	260.11	184.07	0.2847	0.9039
25	10.53103	0.000838	0.0224	77.39	260.38	182.99	0.2889	0.9027
26	10.81931	0.000841	0.0218	78.79	260.64	181.85	0.2935	0.9014
27	11.11310	0.000844	0.0212	80.16	260.89	180.73	0.2981	0.9002
28	11.41241	0.000846	0.0206	81.54	261.12	179.58	0.3023	0.8989
29	11.69034	0.000849	0.0200	82.96	261.37	178.41	0.3069	0.8977
30	12.03448	0.000852	0.0194	84.38	261.60	177.22	0.3115	0.8964
31	12.35103	0.000855	0.0189	85.77	261.81	176.04	0.3161	0.8948
32	12.67310	0.000858	0.0184	87.17	262.02	174.85	0.3207	0.8935
33	13.00070	0.000861	0.0179	88.57	262.22	173.65	0.3249	0.8922
34	13.33793	0.000864	0.0174	90.00	262.40	172.40	0.3295	0.8909
35	13.68276	0.000867	0.0169	91.43	262.58	171.15	0.3337	0.8893
36	14.03034	0.000870	0.0165	92.85	262.74	169.89	0.3383	0.8880
37	14.38207	0.000874	0.0161	94.24	262.88	168.64	0.3429	0.8868
38	14.74345	0.000877	0.0156	95.63	263.00	167.37	0.3471	0.8851
39	15.11103	0.000881	0.0152	97.03	263.13	166.10	0.3517	0.8838
40	15.48965	0.000884	0.0148	98.44	263.21	164.77	0.3563	0.8822
41	15.86827	0.000887	0.0144	99.82	263.29	163.47	0.3601	0.8809
42	16.25793	0.000891	0.0140	101.24	263.38	162.14	0.3651	0.8797
43	16.65380	0.000894	0.0137	102.68	263.48	160.80	0.3693	0.8780
44	17.05517	0.000898	0.0133	104.12	263.58	159.46	0.3739	0.8767
45	17.46552	0.000902	0.0130	105.58	263.67	158.09	0.3785	0.8755
46	17.88414	0.000906	0.0126	107.04	263.76	156.72	0.3827	0.8738
47	18.30827	0.000910	0.0123	108.51	263.87	155.36	0.3871	0.8723
48	18.73793	0.000914	0.0119	109.98	263.93	153.95	0.3915	0.8709
49	19.12414	0.000918	0.0116	111.42	263.99	152.57	0.3959	0.8694
50	19.61380	0.000922	0.0113	112.86	264.05	151.19	0.4003	0.8680

Table 4 Saturated ammonia (NH_3), R717 datum at −40°C, $h_f = 0$, $s_f = 0$

Saturation temperature, T (°C)	*Saturation pressure, p* (bar)	*Specific volume of steam* (m^3/kg)		*Specific enthalpy* (kJ/kg)		*Specific entropy* (kJ/kg-K)		
		Liquid (v_f)	*Vapour* (v_g)	*Liquid* (h_f)	*Vapour* (h_g)	*Latent* (h_{fg})	*Liquid* (s_f)	*Vapour* (s_g)
−50	0.40896	0.001426	2.6281	−44.43	1373.27	1417.70	−0.1943	6.1603
−48	0.45972	0.001431	2.3565	−35.44	1376.80	1412.24	−0.1551	6.1192
−46	0.51600	0.001436	2.1177	−26.60	1380.20	1406.80	−0.1157	6.0789
−44	0.57710	0.001441	1.9062	−17.81	1383.31	1401.12	−0.0769	6.0394
−42	0.64455	0.001446	1.7196	−8.97	1386.67	1395.64	−0.0384	6.0008
−40	0.71793	0.001451	1.5537	0.00	1390.02	1390.02	0.0000	5.9631
−38	0.79384	0.001456	1.4077	8.97	1393.13	1384.16	0.0381	5.9262
−36	0.88607	0.001462	1.2775	17.81	1396.35	1378.54	0.0758	5.8900
−34	0.98096	0.001467	1.1614	26.84	1399.51	1372.67	0.1131	5.8545
−32	1.08165	0.001472	1.0574	35.68	1402.48	1366.80	0.1506	5.8198
−30	1.19586	0.001477	0.9644	44.66	1405.60	1360.94	0.1876	5.7856
−28	1.31724	0.001483	0.8820	53.68	1408.53	1354.85	0.2242	5.7521
−26	1.44790	0.001488	0.8069	62.61	1411.45	1348.84	0.2607	5.7195
−24	1.58841	0.001494	0.7397	71.73	1414.39	1342.66	0.2970	5.6872
−22	1.73986	0.001500	0.6793	80.76	1417.28	1336.52	0.3330	5.6556
−20	1.90276	0.001505	0.6244	89.78	1420.02	1330.24	0.3984	5.6244
−18	2.07807	0.001511	0.5750	98.76	1422.72	1323.96	0.4043	5.5939
−16	2.26551	0.001517	0.5303	107.83	1425.28	1317.45	0.4397	5.5639
−14	2.46634	0.001523	0.4896	116.95	1427.88	1310.93	0.4747	5.5356
−12	2.68069	0.001529	0.4526	126.16	1430.54	1304.38	0.5096	5.5055
−10	2.90896	0.001536	0.4189	135.37	1433.05	1297.68	0.5443	5.4770
−8	3.15365	0.001541	0.3884	144.35	1435.33	1290.98	0.5789	5.4487
−6	3.41380	0.00548	0.3604	153.56	1437.93	1284.37	0.6139	5.4210
−4	3.69062	0.001554	0.3348	162.77	1440.02	1277.25	0.6473	5.3940
−2	3.98427	0.001561	0.3113	171.98	1442.17	1270.19	0.6812	5.3670
0	4.29586	0.001567	0.2898	181.20	1444.45	1263.25	0.7151	5.3405
1	4.45848	0.001571	0.2798	185.80	1445.49	1259.69	0.7321	5.3277
2	4.62662	0.001574	0.2702	190.40	1446.54	1256.14	0.7487	5.3145
3	4.79931	0.001578	0.2610	195.17	1447.59	1252.42	0.7653	5.3017
4	4.97682	0.001582	0.2521	199.85	1448.63	1248.78	0.7818	5.2888
5	5.15862	0.001585	0.2436	204.46	1449.56	1245.10	0.7989	5.2765
6	5.34745	0.001589	0.2354	209.06	1450.49	1241.43	0.8154	5.2638
7	5.54007	0.001592	0.2276	213.73	1451.54	1237.81	0.8320	5.2513
8	5.73820	0.001595	0.2201	218.50	1452.54	1234.04	0.8487	5.2389
9	5.94186	0.001598	0.2128	223.11	1453.39	1230.28	0.8652	5.2266
10	6.15103	0.001603	0.2060	227.72	1454.22	1226.50	0.8814	5.2141
11	6.36641	0.001607	0.1992	232.53	1455.30	1222.77	0.8979	5.2020
12	6.58731	0.001610	0.1928	237.15	1456.11	1218.96	0.9142	5.1900
13	6.81420	0.001614	0.1866	241.92	1456.96	1215.04	0.9307	5.1780
14	7.04717	0.001617	0.1807	246.60	1457.80	1211.20	0.9470	5.1659
15	7.28276	0.001621	0.1751	251.44	1458.63	1207.19	0.9634	5.1542

(Contd.)

Table 4 Saturated ammonia (NH_3), R717 datum at −40°C, $h_f = 0$, $s_f = 0$ (*contd.*)

Saturation temperature, T (°C)	*Saturation pressure, p* (bar)	*Specific volume of steam* (m^3/kg)		*Specific enthalpy* (kJ/kg)		*Specific entropy* (kJ/kg-K)		
		Liquid (v_f)	*Vapour* (v_g)	*Liquid* (h_f)	*Vapour* (h_g)	*Latent* (h_{fg})	*Liquid* (s_f)	*Vapour* (s_g)
16	7.53104	0.001624	0.1696	256.14	1459.47	1203.33	0.9794	5.1421
17	7.78138	0.001628	0.1643	259.88	1460.24	1200.36	0.9956	5.1302
18	8.03862	0.001633	0.1592	265.54	1460.92	1195.38	1.0118	5.1186
19	8.30551	0.001637	0.1543	270.35	1461.75	1191.40	1.0280	5.1073
20	8.57241	0.001641	0.1496	275.16	1462.60	1187.44	1.0442	5.0956
21	8.85172	0.001645	0.1450	279.77	1463.21	1183.44	1.0604	5.0843
22	9.13655	0.001648	0.1407	284.56	1463.84	1179.28	1.0763	5.0729
23	9.42690	0.001652	0.1365	289.37	1464.63	1175.26	1.0924	5.0616
24	9.72690	0.001656	0.1324	294.19	1465.33	1171.14	1.1083	5.0503
25	10.02760	0.001661	0.1284	298.90	1465.84	1166.94	1.1242	5.0391
26	10.34069	0.001665	0.1246	303.82	1466.59	1162.77	1.1402	5.0279
27	10.66137	0.001669	0.1210	308.63	1467.22	1158.59	1.1563	5.0170
28	10.99172	0.001673	0.1174	313.45	1467.85	1154.40	1.1721	5.0061
29	11.32758	0.001678	0.1140	318.26	1468.45	1150.19	1.1879	4.9951
30	11.66896	0.001682	0.1107	323.08	1468.87	1145.79	1.2037	4.9842
31	12.01655	0.001686	0.1075	327.89	1469.50	1141.61	1.2195	4.9733
32	12.37517	0.001691	0.1045	332.71	1469.94	1137.23	1.2350	4.9624
33	12.74482	0.001695	0.1015	337.52	1470.36	1132.84	1.2508	4.9517
34	13.12137	0.001700	0.0987	342.48	1470.92	1128.44	1.2664	4.9409
35	13.50345	0.001704	0.0960	347.50	1471.43	1123.93	1.2821	4.9302
36	13.89379	0.001709	0.0932	352.29	1471.70	1119.41	1.2978	4.9196
37	14.29517	0.001713	0.0907	357.25	1472.19	1114.94	1.3135	4.9091
38	14.70620	0.001718	0.0882	362.12	1472.45	1110.33	1.3290	4.8985
39	15.12276	0.001723	0.0857	367.11	1472.87	1105.76	1.3445	4.8885
40	15.54483	0.001727	0.0834	371.93	1473.30	1101.37	1.3600	4.8774
41	15.98551	0.001732	0.0811	376.95	1473.50	1096.55	1.3754	4.8669
42	16.43172	0.001738	0.0789	381.79	1473.70	1091.91	1.3908	4.8563
43	16.88344	0.001742	0.0768	386.76	1473.91	1087.15	1.4065	4.8461
44	17.34482	0.001747	0.0747	391.79	1474.12	1082.33	1.4221	4.8357
45	17.81724	0.001752	0.0727	396.81	1474.33	1077.52	1.4374	4.8251
46	18.30070	0.001757	0.0708	401.84	1474.54	1072.70	1.4528	4.8147
47	18.79518	0.001763	0.0689	406.86	1474.68	1067.82	1.4683	4.8045
48	19.29931	0.001768	0.0670	411.89	1474.76	1062.87	1.4835	4.7938
49	19.80965	0.001773	0.0652	416.91	1474.84	1057.93	1.4990	4.7834
50	20.33103	0.001779	0.0636	421.94	1474.92	1052.98	1.5148	4.7732

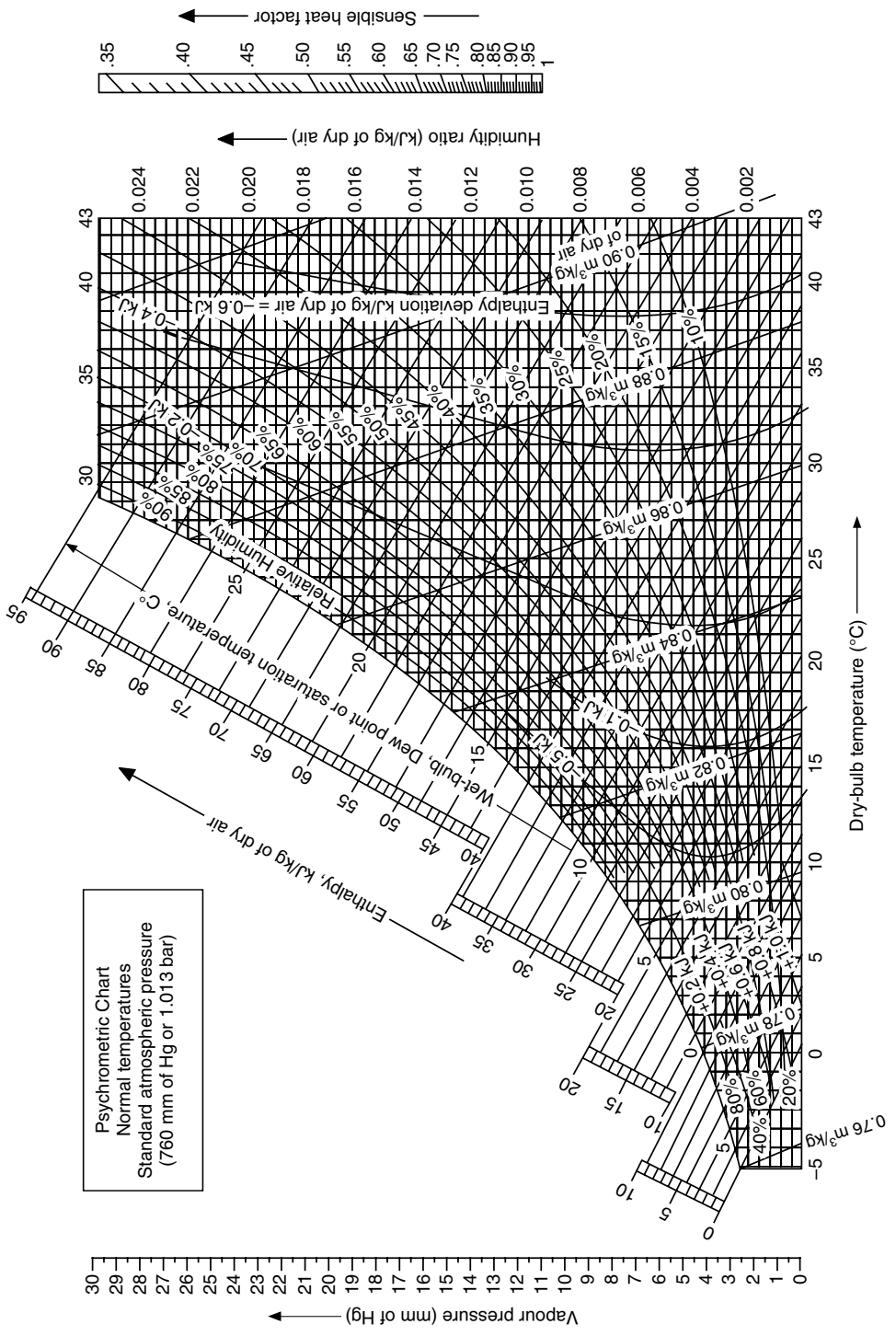
Psychrometric Chart
Normal temperatures
Standard atmospheric pressure
(760 mm of Hg or 1.013 bar)
Sensible heat factor
Humidity ratio (kJ/kg of dry air)
Vapour pressure (mm of Hg)
Dry-bulb temperature (°C)
Enthalpy, kJ/kg of dry air
Wet-bulb, Dew point or saturation temperature, C°
Relative Humidity
Enthalpy deviation kJ/kg of dry air = −0.6 kJ
0.76 m³/kg
0.78 m³/kg
0.80 m³/kg
0.82 m³/kg
0.84 m³/kg
0.86 m³/kg
0.88 m³/kg
0.90 m³/kg of dry air

Index

REFRIGERATION *and* AIR CONDITIONING

RAMESH CHANDRA ARORA

This textbook offers a comprehensive and wide-ranging introduction to theoretical principles and practical aspects of refrigeration and air conditioning systems. Written by an outstanding teacher with 30 years of distinguished career at the Indian Institute of Technology Kharagpur, this work created by late Dr. R.C. Arora (1945–2005) is intended to lead students to a deeper understanding and a firm grasp of the basic principles of this fast-growing and exciting subject area. This text is ideally suited for **undergraduate education in mechanical engineering programmes and specialized postgraduate education in thermosciences**. The book is designed to typically appeal to those who like a more rigorous presentation.

The text begins by reviewing, in a simple and precise manner, the physical principles of *three* pillars of Refrigeration and Air Conditioning, namely thermodynamics, heat transfer, and fluid mechanics. Following an overview of the history of refrigeration, subsequent chapters provide exhaustive coverage of the principles, applications and design of several types of refrigeration systems and their associated components such as compressors, condensers, evaporators, and expansion devices. Refrigerants too, are studied elaboratively in an exclusive chapter.

The second part of the book, beginning with the historical background of air conditioning in Chapter 15, discusses the subject of psychrometrics being at the heart of understanding the design and implementation of air conditioning processes and systems, which are subsequently dealt with in Chapters 16 to 23. It also explains the design practices followed for cooling and heating load calculations.

Each chapter contains several worked-out examples that clarify the material discussed and illustrate the use of basic principles in engineering applications. Each chapter also ends with a set of few review questions to serve as revision of the material learned.

THE AUTHOR

Late Dr. RAMESH CHANDRA ARORA, served as Professor of Mechanical Engineering at Indian Institute of Technology Kharagpur from 1987 to 2005. He joined IIT Kharagpur in 1975 as a lecturer after obtaining his Ph.D. degree in the same year from Case Western Reserve University, Cleveland, Ohio, USA.

Professor Arora was regarded as a highly competent subject matter expert in academia and industry alike. His research areas included fluid mechanics, heat transfer, refrigeration and air conditioning, and alternative refrigerants and thermodynamic cycles.

During his illustrious career, Professor Arora was the recipient of several outstanding teacher awards, national scholarships, merit awards, and graduate fellowship. He is credited with 91 research publications, 8 technical reports, 19 industrial projects and 3 pending patents.

ISBN:978-81-203-3915-6

9 788120 339156

Rs. 495.00

www.phindia.com